GEOLOGICAL SURVEY OF CANADA
OPEN FILE 3058

PROCEEDINGS OF THE OIL AND GAS FORUM '95

ENERGY FROM SEDIMENTS

Editors
J.S. Bell, T.D. Bird, T.L. Hillier, and P.L. Greener

March 28–29, 1995
Calgary, Alberta

INVITATION

The GSC Oil and Gas Forum is held every three years. Since the 1992 Forum the petroleum industry has undergone continued transformation. The GSC, too, has undergone transformation and, with pending government budget cuts, is destined to undergo further transformation. Part of the change in the way the GSC approaches its mandate is a strategic shift toward closer collaboration with industry, and one of the purposes of the 1995 Forum is to garner ideas from clients and partners on how best to consolidate and enhance these collaborations. We'd like to share with you the concepts we've developed and the experience we've gained to date in industrial partnerships and their benefits to both industry and government. As always, however, the main purpose of the Oil and Gas Forum is to illustrate and illuminate our most recent research and survey results on the sedimentary geology of Canada and the resources contained in our sedimentary basins. We've lots of new data and interpretations to share. It's your best chance to catch up on all that the GSC is doing in its mapping and basin analysis work, and it's our best chance to consult with you about new developments. Registration is free. You are cordially invited to attend.

Grant D. Mossop
Director, GSC Calgary

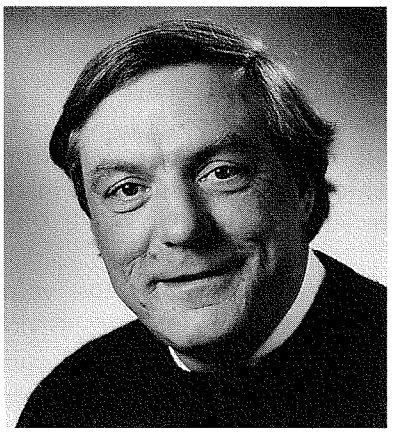

FOREWORD

From the High Arctic to Lake Ontario, from the Grand Banks to the Queen Charlottes, scientists of the Geological Survey of Canada are engaged in a wide range of activities which bear on the extraction of Energy from Sediments, the theme of this year's Oil and Gas Forum. We are delighted to welcome you to this event, our fourth such venture in Calgary. Our intention is to present recent GSC studies and the results of our collaborative research related to Canada's sedimentary basins and the oil, gas and coal resources contained therein. We try to do this in as informal a setting as possible so as to encourage discussion and the exchange of ideas within the earth science community. This community has changed in recent years, as has the Geological Survey of Canada. Our Forum, too, has evolved.

However, one tradition has been maintained. There is no formal registration or charge for attendance. Fellow scientists and clients should feel free to come and go as their schedules permit. As before, the main offering is Posters, with more than one hundred on exhibit. Some twenty Technical Talks will also be presented, as well as three half hour Demonstrations. The latter are a new initiative aimed at involving 20-25 delegates in detailed discussions of specific topics. Each demonstration will be presented twice during the two days of the Forum.

On Tuesday evening, March 28th, we will present a program for the General Public. Starting at 6 pm, the Geological Survey's popular *Pet Rock Clinic* will open its doors and young and old are invited to bring their favourite rocks and fossils for examination and identification by our scientists. At 8 pm, Dr. Alan Hildebrand will present a one hour Public Lecture entitled: *The Comet that killed the Dinosaurs*. This lecture, given by a GSC scientist who is at the forefront of research on the inferred comet impact area in Mexico, will be of interest to everyone who is fascinated by dinosaurs, once the leading citizens of our planet Earth. As with the Pet Rock Clinic, attendance is free.

Another innovation this year is the volume that you hold in your hands. Many attendees asked for handouts at our previous Forums. We hasten to add that these requests were for scientific handouts, or reprints, not the other kind! To meet this need, we have followed the example of many engineering conferences, where a Proceedings Volume is distributed to everyone at the meeting. In this Proceedings Volume, you will find succinct summaries of all the posters on display. Also included are brief descriptions of those GSC facilities that are of interest to the oil, gas and coal industrial communities, as well as the addresses and research activities of the scientists involved in the program. Unfortunately, the Geological Survey of Canada cannot afford to give it away, so the Proceedings Volume is being made available at a nominal charge. Other Geological Survey of Canada publications may be purchased or ordered at the Sales Desk at the front of the Exhibition Hall.

The program for the GSC Oil and Gas Forum '95 includes talks and posters focussed on numerous research activities, some new, others ongoing. These include: recently completed gas assessments in western Canada, the multi-institutional Lithoprobe deep seismic profiling program, and the strategic application of paleontological information. The ongoing NATMAP projects in southern Alberta are part of a new venture for the GSC, the Alberta Mineral Development Agreement reseach projects illustrate evolving Federal-Provincial initiatives, while the comparative studies involving the Barents Sea and the Canadian Arctic typify our international cooperative studies. The new Industrial Partner Program is featured in several posters that relay the results of geophysical, geochemical, hydrodynamic and stratigraphic research which is partially funded in cash or in kind by external clients. Other posters address topical concerns such as production-induced earthquakes, gas hydrates and coal bed methane production, borehole stability and exploration for diamonds. Computer hardware and software advances have made the desktop publishing of sophisticated geological maps a feasible reality and several recent examples are on display. These same techniques are playing a leading role in furthering the GSC's Basin Atlas compilations. Many of the posters are co-authored by scientists working in Universities, federal and provincial institutions and in the private sector, in Canada and abroad. This reflects an increasing external collaboration that is as much required by the demands of today's multi-disciplinary science as it is by the need to operate with ever-shrinking budgets.

The scientists participating in this year's Forum are based all over Canada. GSC staff whose work is being presented come from our offices in Dartmouth, Nova Scotia, from Ottawa, from Calgary, from Vancouver and from Sidney, British Columbia. All of us extend a warm welcome to you, we look forward to discussing our work with you and we will value your comments and reactions.

J.S. Bell and T.D. Bird
Co-Chairmen, Oil and Gas Forum '95

OUR THANKS

We wish to express our gratitude to all the personnel of Natural Resources Canada who have helped put on the Geological Survey of Canada's Oil and Gas Forum '95 – Energy from Sediments. First and foremost, we acknowledge the authors of the many posters and talks presented here. They in turn have been supported by the illustrative material, colour slides and poster titles prepared, edited and reformatted by the Graphics Production Unit, the Photography Department and several technicians at the GSC office in Calgary. We owe a great debt to B.H. Ortman, G.N. Edwards, B.E. Fischer, A. Flood, M. Lazorko, D.A. Lemay, E. Macey, P.J. Neelands, S.D. Orzeck, B.C. Rutley, J.H. Waddell, M.D. Wallace, L.J. Wardle, and P. Wozniak. We are also grateful to H. King, M.L. Jacobs, and L. Cheung for the compilation of the Proceedings Volume. Many essential clerical tasks related to organising the Forum were handled by W. Ell and C. Thompson.

The wide and varied content of the talks, posters and demonstrations testifies to the enthusiastic response of a large number of scientists across the GSC and in associated institutions. The research work presented here has benefitted enormously from the analytical and technical support provided over many years by the GSC's laboratory staff and technicians. Convention decrees that these collaborators are not named as co-authors, but their contributions are as essential as they are valued. Nor could we operate without ready access to the literature, well logs and samples. Our output testifies to the superb services provided by the staffs of our libraries and our sample storage facilities.

Without the dedication of all these people, we would not have been able to present the Oil and Gas Forum '95, or prepare this volume.

J.S. Bell, T.D. Bird, T.L. Hillier, and P.L. Greener (Editors)

FORUM POSTER LIST

BOOKSTORE

The ISPG Bookstore is the largest GSC sales outlet in Western Canada. It sells all Geological Survey of Canada maps and publications on all regions of Canada as well as open files on the Western Canada Sedimentary Basin.

There are four main formats for GSC publications: Papers are preliminary studies of an area, often containing a geological map. Bulletins are intermediate studies often containing paleontological information. Memoirs are complete geological studies of a region and are frequently accompanied by colour geological maps. Open files are either blueline maps, digitally plotted colour maps, computer disks or printed text. They are raw data published without editing to make the information available quickly.

At the beginning of each year, the Survey produces a series of publications entitled "Current Research". These usually consist of four regional volumes of information on field work in progress and a fifth volume covering research in all regions (published later in the year).

One of our newest products is a series of videos detailing the history of the GSC as well as information on mining, oil and gas and natural hazards. A list of the titles and descriptions of the videos is available. GSC pins and key rings are now for sale as well.

EDUCATIONAL MATERIAL

The ISPG Bookstore is your source for a wide variety of educational materials. We distribute free brochures, posters and other materials aimed at a variety of interests and ages. We also sell three types of rock and mineral sample kits aimed at young prospectors, students and enthusiasts.

Catalogues of all our publications are available: paper copies are free; diskette (WP5.1) copies are $15.00.

OTHER SOURCES

In an effort to continue to provide the best possible service to our customers, the Bookstore now stocks selected titles published by the Geological Association of Canada and the Canadian Society of Petroleum Geologists. We also provide an order service for publications of the Alberta Research Council, some of their reports are on display and their free catalogue is available on request.

ONLINE SERVICES

We now have online access to the GEOSCAN database to provide a full reference service for all your geoscience needs. GEOSCAN provides current information on all Canadian geoscience publications including those of the GSC. Demonstrations of the GEOSCAN system will be provided each day at 10:00 am and 3:00 pm during the Oil and Gas Forum at the ISPG Bookstore booth. We will also be demonstrating the GSC's Internet Gopher which provides an online catalogue for GSC publications.

MAKING A PURCHASE

Only a fraction of what we offer can be described here so please take the time to drop by the bookstore and browse through the complete selection. While you are there, you can satisfy your sweet tooth from the bottomless candy dish.

The Bookstore accepts payments in cash, cheque, or money order, or will charge your purchase to Visa, Mastercard or your account. Charged orders can be made by phone or fax 24 hours a day. Prices include postage; express delivery is extra.

Bookstore Hours

Monday–Friday: 9:00–4:00
Phone orders and inquiries: (403) 292-7030
Fax orders: (403) 299-3542

CORE AND SAMPLE REPOSITORY

The Core and Sample Repository at ISPG is maintained by the Geological Survey of Canada and houses cores and unwashed drill cuttings from all lands north of 60; cores from the west coast offshore region; and washed drill cuttings from all lands north of 60, the east and west offshore regions, and the four western provinces. Well history files for lands north of 60 and east coast offshore regions are also available.

EXAMINATION

The public may examine all materials at the Repository. There are 12 examination booths and 5 core tables available for viewing nonconfidential materials and 2 booths and 2 tables available for viewing confidential material. Written permission from the drilling company is required to examine confidential material.

SAMPLING

Policy for sampling cores depends on the condition of the core and the requirements of the proposed analysis. The maximum permitted sample volume is one cubic inch per linear foot and no sample may include a significant fraction of the core diameter of any horizon. Under special circumstances permission may be granted for over-sampling. All requests for sampling that threatens to impair the geological value of the core will be refused.

Requests for cuts of unwashed drill cuttings are on a first-come first-served basis. A maximum of 20 g per sample interval is permitted for each procedure.

A maximum of a 6-8 grains per vial is allowed for washed cuttings, depending on the volume of material in the vial. The remaining contents of each vial must contain essentially the same proportion of constituents present prior to sampling.

All resulting analytical data, petrographic thin sections, recovered macrofossils, microfossils, palynomorph slides and preparations must be returned to the Institute, where they contribute to the inventory of subsurface material. Any unused core material and/or other residues or unprocessed material should also be returned. Except under exceptional circumstances, loans are for a period of 6 months.

Anyone wishing to sample well material should address their requests in writing to the Senior Collections Manager (299-3539), indicating the purpose of the studies, the volume of material required, and the name and intervals of interest for each well. Permission to over-sample requires explanation of the relevance of the work to the geoscientific community. If permission to sample is received, arrangements for sampling can be made by calling the Repository at 292-7057.

The Processed Subsurface Collection is derived mainly from sampling in the Core and Sample Repository. Information about the availability of petrographic thin sections, and macrofossil, microfossil, palynomorph and conodont slides may be obtained by calling 299-3539.

Note: Cores and cuttings are not usually provided ahead of time. Alberta washed cuttings are not available to the public.

Repository Hours

Monday–Friday: 8:00–12:00; 1:00–4:00
Information: (403) 292-7057

LIBRARY

The ISPG Library is the largest geoscience library accessible to the public in Western Canada. It was founded in 1967 with the primary goal of serving the information needs of ISPG researchers. This is still our primary goal but the Library is now open to the public and provides service to the oil and gas industry, the scientific community, academics and students.

The collection covers the geological sciences and related subjects at both the specialized and general levels. Specific subjects include petroleum and coal geology, paleontology, micropaleontology, stratigraphy, structural geology, sedimentary geology, geochemistry, the geology of the Western Canada Sedimentary Basin, and the Arctic. Most materials are in English but many are in other languages, especially Russian, Spanish, Chinese, and French. The Library holds a considerable collection of Russian language materials that have been translated into English.

The library also houses a rare book collection, some of which dates back more than 300 years. This collection includes first edition works by some of the earliest explorers of Canada.

BIBLIOGRAPHIC DATABASES

The Library has online access to GEOSCAN, a bibliographic database of Canadian geoscientific literature concerning the Canadian landmass and offshore regions. GEOSCAN's strength lies in its access to industry assessment reports and its coverage of GSC publications.

Library users may also use the CD-ROM to search databases such as GeoRef, a worldwide bibliographic database of geoscientific literature. Reservations to use the CD-ROM may be made by calling the Reference Desk.

ACCESSING THE LIBRARY COLLECTION

Materials such as journals, books, open files, bulletins, papers, maps, atlases etc. may be consulted in the public reading area. Photocopying facilities are available for a small charge and materials may be photocopied in compliance with copyright law and ISPG Library policy.

Material can be borrowed from the Library through interlibrary loans. These loans are made in compliance with standard interlibrary loan guidelines. GSC open files, reference materials and rare items are not loaned.

Library staff are available to help access the collection on a first come, first served basis. You are encouraged to call ahead to determine how the staff may assist you and to confirm that the material you are seeking is available.

Library Hours

Monday–Thursday: 8:00–12:00; 12:45–4:15
Friday: 8:00–12:00; 12:45–3:30
Reference desk: (403) 292-7165
Fax: (403) 292-5377

GEOPHYSICAL DATA CENTRE

The Geophysical Data Centre (GDC) archives and distributes aeromagnetic and gravity data. These data comprise the National Aeromagnetic and Gravity Data Bases, which also include parameters of the individual surveys. Coverage ranges from regional in focus to site specific detail surveys. The data is available digitally in a wide range of formats and on various output media and as colour plots. A catalogue of services and data is available through the Geophysical Data Centre of any GSC office.

Future initiatives by the GDC include providing online access to the above data sets and operation of an information exchange about data available from industry surveys.

The Geophysical Data Centre can be contacted at:

1 Observatory Crescent
Ottawa, Ontario K1A 0Y3
Tel: 613-995-5326
FAX: 613-992-2787
E-Mail: infogdc@agg.emr.ca

THE COMET THAT KILLED THE DINOSAURS

A free illustrated Public Lecture presented by

Dr. Alan Hildebrand

Research Scientist, Geological Survey of Canada
McLeod Hall A, Calgary Convention Centre
8.00 pm (20.00 hrs)
Tuesday, March 28th, 1995

Fifteen years ago, the unusually high iridium content of a thin distinctive clay layer in a roadcut exposure of the Cretaceous-Tertiary boundary in northern Italy prompted Louis Alvarez, a retired nuclear physicist and Nobel Prize winner from California, his son Walter, a geologist, and two of their colleagues to propose that the iridium had been introduced by a large meteorite. What brought the scientific community to its feet was their suggestion that the inferred meteorite impact produced horrendous climatic changes and that these caused the extinction of the dinosaurs 65 million years ago.

In the intervening years, scientific debate has raged on many fronts as paleontologists, biologists, geologists, geophysicists and astronomers grappled with the implications of this hypothesis and as they spread out far and wide to gather field evidence. Multi-disciplinary science thrived in the heady excitement of rolling back such a major frontier of knowledge. Much supportive evidence emerged, such as shocked mineral grains in the Boundary Clay, but there were also those who disagreed, who interpreted the rock record in favour of the gradual extinction of the dinosaurs, or who believed that volcanic eruptions could generate the anomalous levels of iridium. What was missing was a "smoking gun"; evidence of an impact crater of the appropriate dimensions and the right age.

Now the scar has been found. At Chicxulub, on Mexico's Yucatan Peninsula, there is compelling geological and geophysical evidence for the existence of a huge, now buried, impact crater 170 kilometers in diameter. Studies of crater rocks recovered from oil wells show that their age coincides with the Cretaceous-Tertiary boundary. It is suitably located to have been the source of a 65 million year old layer of ejected material containing shocked minerals, found in many places around the Caribbean. Calculations suggest that the impact would have released an enormous amount of energy over a very short period of time. Moreover, since the target area was a carbonate platform consisting of ancient reefs and sulphate-rich salt deposits, two significant consequences can be inferred. Shock-generated carbon dioxide from the reefs would have caused severe greenhouse warming that could have lasted as long as 100,000 years. Also the impact would have released into the atmosphere large amounts of sulphur dioxide from the salts, possibly enough to induce strong acid rain that would have poisoned the surface layer of the oceans. In combination, such major climatic and chemical disruptions would have killed most large life forms on Earth, including the remaining dinosaurs.

Smaller impacts that are still threatening to our global climate are believed likely to occur approxiately once every half million years. They could be deadly to our civilization and emphasise that it is essential to maintain astronomical vigilance and to develop the technology for deflecting large asteroids and comets.

EXPLORATION AND PRODUCTION IMPLICATIONS OF SUBSURFACE ROCK STRESSES IN WESTERN CANADA

J.S. Bell

Geological Survey of Canada, 3303-33rd Street N.W., Calgary, Alberta T2L 2A7

P.J. McLellan

Advanced Geotechnology Inc., 800, 333-5th Avenue S.W., Calgary, Alberta T2P 3B6

INTRODUCTION

The Western Canada Sedimentary Basin was initiated in Early Mesozoic time as a foreland trough yoked to lithospheric terranes to the west that were then being thickened by overthrusting and subductive underplating. Subsidence and western-sourced sedimentation continued into Mid-Tertiary time, when overthrusting ceased and tectonic rebound began. Since then the basin has been undergoing uplift and erosion. The configuration of its contemporary stress regime is related to the former northeastward overthrusting of the Foothills and Rocky Mountains, but also reflects plate motion drag at the base of the Lithosphere.

Borehole breakouts, together with other types of stress measurements, imply that a simple regional pattern of stress trajectories affects the entire sedimentary column and the underlying basement of the Western Canada Basin. Horizontal stress orientations vary with locality but not with depth. The stress trajectories shown in Figure 1 reflect breakout orientations measured in more than 200 wells.

The stress magnitudes are less well constrained. Magnitudes of the smaller horizontal stress, S_h, have been measured with a few overcoring and micro-frac tests and estimated from numerous mini-frac and leak-off tests. Mini-fracs tend to underestimate S_h because of reservoir depletion, whereas leak-off tests provide upper limits for S_h (Bell et al., 1994). Available data suggests that, at a given depth, S_h decreases in magnitude northeastward across the basin, but there are not enough reliable measurements to confirm or quantify this hypothesis.

APPLICATIONS OF IN SITU STRESS DATA

The Western Canadian Sedimentary Basin has one of the best known stress regimes of any of the World's major hydrocarbon provinces. Its geological history is also excellently documented (Mossop and Shetsen, 1994). This understanding can be exploited in numerous ways to enhance exploration and production activities.

Predicting hydraulic fracture orientation

In what directions will hydraulic fractures propagate? Figure 1 can be used to predict hydraulic fracture orientation. Below approximately 350 m depth, artificially-induced hydraulic fractures will be close to vertical and they will be oriented parallel to S_H. Hydraulic fractures propagate along planes perpendicular to the smallest principal stress at an injection site, so principal stress orientations and relative stress magnitudes are needed for accurate predictions (Fig. 2).

Production from Open Fractures

Where are the best open fractures likely to be found? The stress trajectory map suggests that many subsurface fractures may mimic the S_H trajectories. If we assume that compressive stresses were higher during the period of Mesozoic and Tertiary overthrusting and that overpressures were generated during this time, then they could have dissipated by creating networks of southwest–northeast directed natural hydraulic fractures. One can argue, therefore, that such fractures are likely to be most productive of hydrocarbons where horizontal stresses are the lowest (Enever et al., 1994), namely in the central and eastern parts of the basin. Alternatively, a case can be made that such fractures would exhibit a greater tendency to openness along the western edge of the basin, because horizontal stress magnitudes and stress anisotropy are likely to be relatively greater there. In this scenario, highly permeable open fractures would be those that are oriented close to the plane of S_v and S_H; fractures with

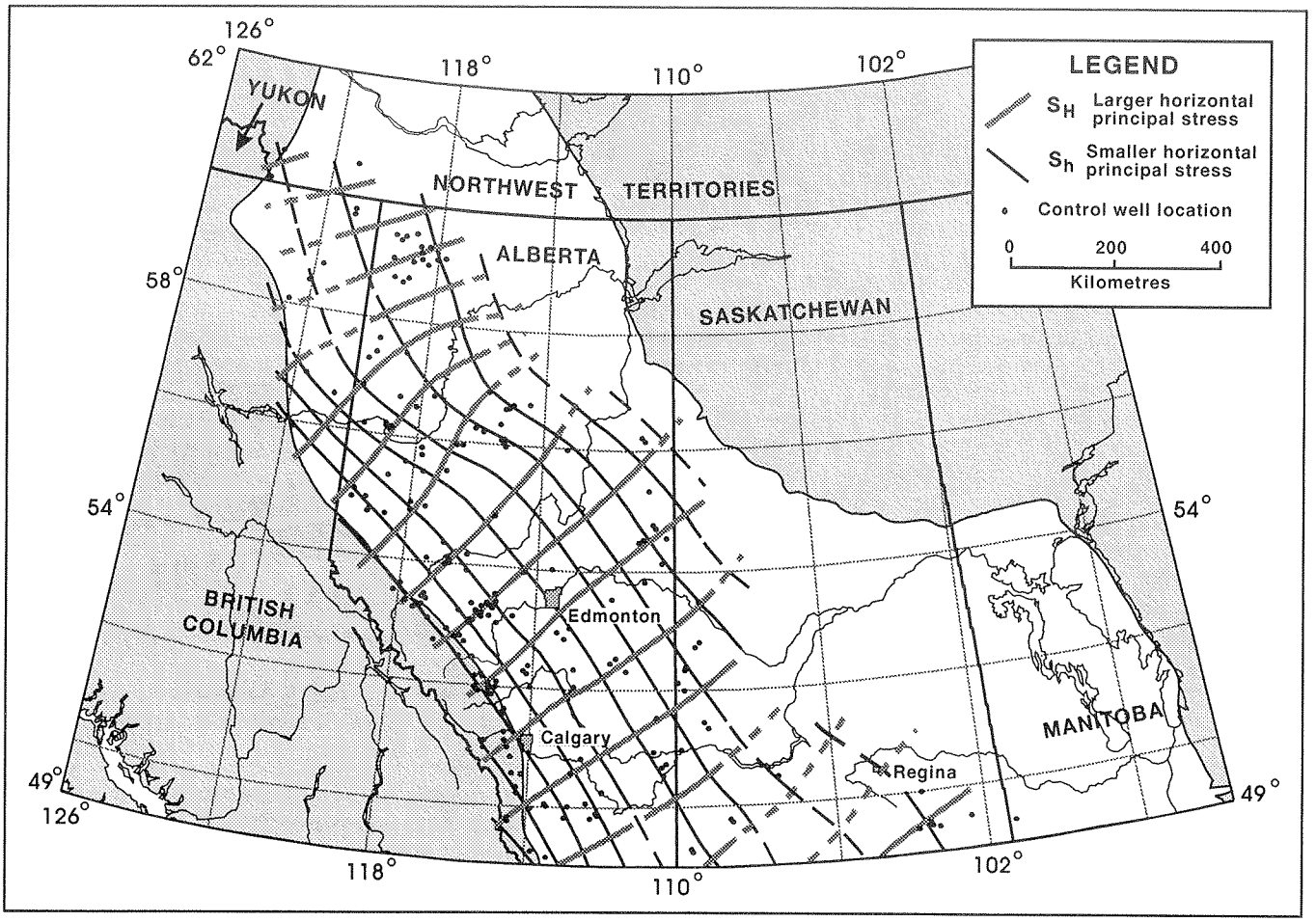

Figure 1. *Horizontal stress orientations for Phanerozoic sediments in the Western Canada Basin, based on breakouts in 209 wells and 22 other indicators. The trajectories shown are very similar to those presented in the Geological Atlas of the Western Canada Sedimentary Basin, but there are modifications in southernmost Alberta and around the Peace River Arch.*

other orientations would tend to close. Tectonic rebound is a complicating factor. The Foothills and adjacent areas have undergone significant uplift and erosion in Late Tertiary time that will have reduced stresses at depth, thereby increasing the permeability of existing fractures and, possibly, creating new ones. Many anticlinal crests exhibit northwest–southeast trending fractures that may have originated in this way, or may be souvenirs of flexure-induced fracturing during thrust plate evolution.

Borehole Stability and Sand Production

Many boreholes collapse because far field stresses are amplified in the rocks immediately surrounding them, and these rocks are not strong enough to resist yielding by brittle fracture or plastic deformation. In Western Canada several types of borehole failure occur depending upon the nature of the rocks, their depth and the magnitude and orientation of the principal stresses (McLellan, 1994). Examples are:

1) Brittle fracture of highly stressed, mechanically anisotropic shales in the Foothills (Wapiabi and Blackstone formations).

2) "Squeezing" of salt sections in the Williston Basin.

3) Time dependent deformation of Upper Cretaceous smectite-rich shales.

4) Spalling of weakly consolidated sandstones at Lloydminster and Cold Lake.

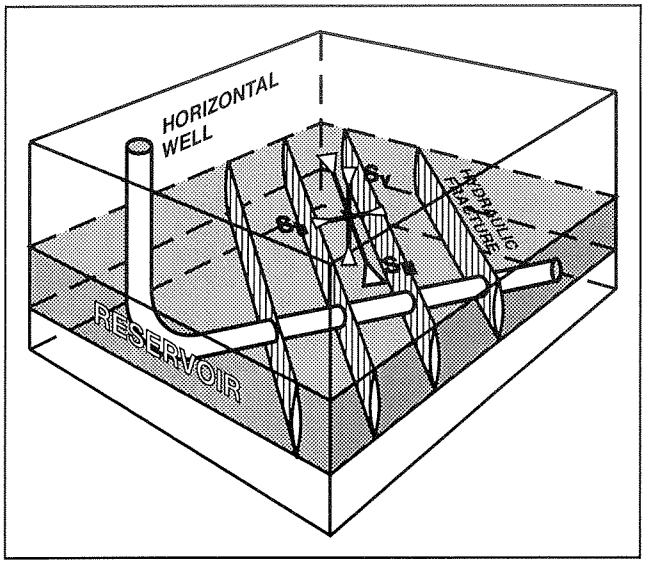

Figure 2. *Relationship between stress orientations and hydraulic fracture propagation directions, as these might apply to a horizontal well drilled into a flat-bedded tabulate reservoir. S_v–vertical principal stress, S_H–larger horizontal principal stress, S_h–smaller horizontal principal stress.*

5) Well bore collapse around cavity completions in coalbed methane wells.

With the advent of new drilling and production technologies such as underbalanced drilling, coiled tubing drilling, jet drilling, horizontal re-entry and multi-branching wells, borehole stability problems are arising more frequently. Knowledge of the local stress regime and of the geomechanical properties of the rocks involved helps to reduce well completion costs as well as to assess whether a particular program is feasible.

Optimum Inclined and Horizontal Well Trajectories

What trajectory is most mechanically stable for a highly inclined well? This depends both on the mean stress level and the in situ stress difference perpendicular to the well trajectory. Hence, the magnitudes and the orientations of all three principal stresses are needed for optimum predictions (Fig. 3). Low angle wells are frequently drilled to intercept open fractures. If the fractures lie in the plane of S_v and S_H (as in Figure 2), a well that intercepts them at 90° should be stable, unless S_H is very much greater in magnitude than S_v, or vice versa.

Steam Stimulation in Oil Sands

Bitumen viscosity in oil sands can be reduced by injecting steam under high pressure. This process may cause the formation to fracture or yield by shear, depending on the in situ stress regime, the steam temperature and the duration of the injection. Oil sands exhibit nonlinear and inelastic behaviour that complicates the mechanics of hydraulic fracturing. For example, field tests and model simulations show that steam injection can promote shear failure in oil sands, and that this can occur at injection pressures lower than those that would initiate classical tensile failure. Furthermore, mini-frac tests in the Athabasca and Cold Lake oil sands have documented high S_h levels with depth, sometimes exceeding S_v. Natural horizontal fracturing has been reported in some localities and it has been postulated that temperature and pore pressures can be varied thereby altering relative stress magnitudes so as to favour the propagation of horizontal fractures (e.g., Dusseault and Simmons, 1982). Hence, a thorough understanding of the stress regime is required to optimize steam injection strategies that take advantage of the geometry of induced fracture networks or of yielded zones.

Causes of Underpressuring

Why are parts of the Deep Basin underpressured? An explanation involving the stress history of the basin is proposed here. Mesozoic rock units are thickest along

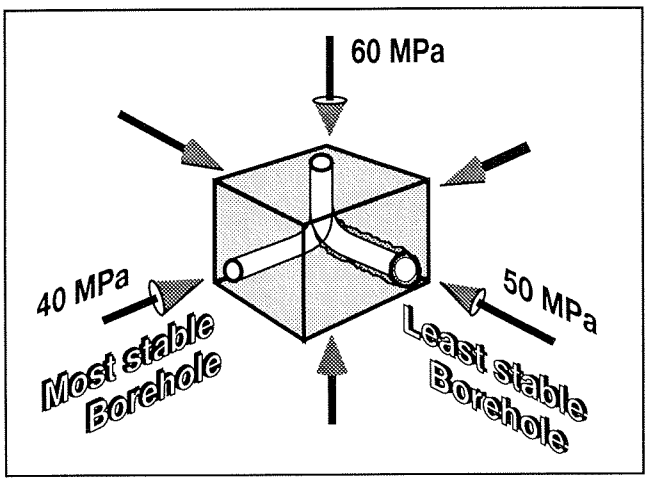

Figure 3. *Block diagram illustrating how borehole stability can be related to stress magnitudes, stress orientations and well trajectory. This figure is schematic but is based partly on experimental studies undertaken by M.A. Addis and others.*

the western edge of the Western Canada Basin. They have been compacted first by the weight of the overburden, then by lateral compression associated with western overthrusting. This two component loading gave rise to high density, low permeability shales and, in association with cementation and diagenesis, to low porosity sandstones. Tertiary rebound and erosion reduced stresses and promoted some dilation of the sandstones that increased their porosity. By contrast, we believe that rebound led to little reversal of shale compaction, so they retained their low permeabilities (Fig. 4). Hence we hypothesize that gas trapped in the sands became underpressured because these rocks were effectively sealed by the shales and this inhibited equilibration with surface fluids.

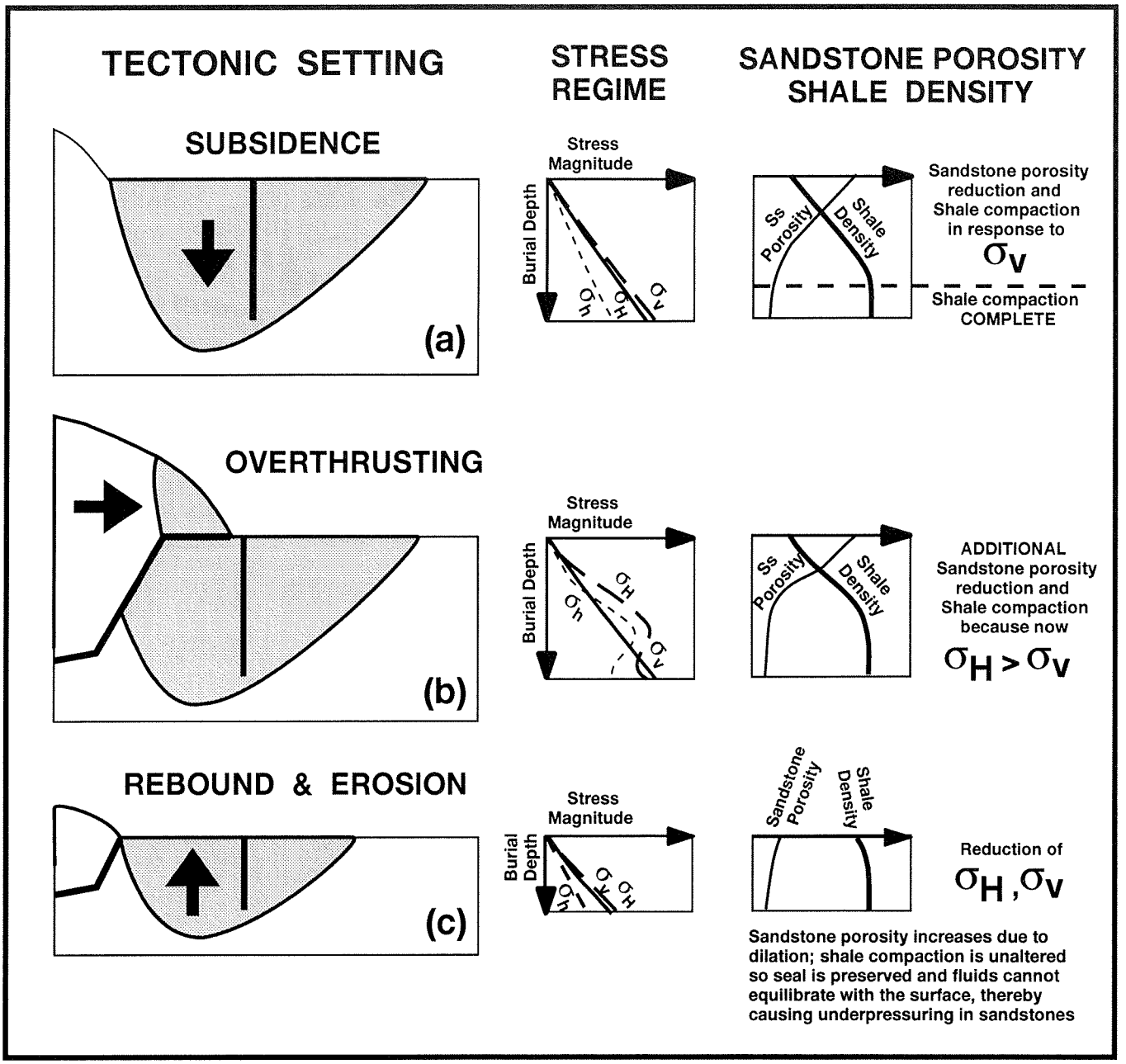

Figure 4. *Qualitative scenario showing how stress regimes may have varied during the Mesozoic and Cenozoic evolution of the Western Canada Sedimentary Basin, and hypothesizing as to how this variation could have controlled shale compaction, sandstone porosity and pore fluid pressures in the area of the Deep Basin.*

CONCLUSIONS

The interplay of basin evolution, stress regime development, overburden erosion, and the geomechanical properties of the sediments controls much subsurface behaviour of rocks that is of economic significance in the Western Canadian Basin. Approaching exploration and production scenarios through consideration of in situ stress measurements and the origin of contemporary stress regimes throws new light on old problems.

REFERENCES

Bell, J.S., Price, P.R., and McLellan, P.J.
1994: In-situ stress in the Western Canada Sedimentary Basin. *In* Geological Atlas of the Western Canada Sedimentary Basin, G. Mossop and I. Shetsen (compilers). Canadian Society of Petroleum Geologists and Alberta Research Council, p. 439–446.

Dusseault, M.B. and Simmons, J.V.
1982: Injection-induced stress and fracture orientation changes. Canadian Geotechnical Journal, v. 19, p. 483–493.

Enever, J.R., Pattison, C.I., McWatters, R.H., and Clark, I.H.
1994: The relationship between in-situ stress and reservoir permeability as a component in developing an exploration strategy for coalbed methane in Australia. *In* Rock Mechanics in Petroleum Engineering, Eurock '94-Proceedings of SPE/ISRM International Conference, 29-31 August 1994, Delft, Netherlands. Pulished by A.A. Balkema, Rotterdam, p. 163–171.

McLellan, P.J.
1994: Assessing the risk of wellbore instability in horizontal and inclined wells. Paper No. HWC94-14 presented at SPE/CIM/CANMET International Conference on Recent Advances in horizontal Well Applications, Calgary, March 20-23, 1994.

Mossop, G.D. and Shetsen, I. (compilers)
1994: Geological Atlas of the Western Canada Sedimentary Basin. Canadian Society of Petroleum Geologists and Alberta Research Council, 510 p.

BENTHIC BIOZONES AS SYSTEMS TRACT AND SEQUENCE SIGNATURES: LOWER CARBONIFEROUS MOUNT HEAD FORMATION, SOUTHWEST ALBERTA AND SOUTHEAST BRITISH COLUMBIA

R.T. Brandley

Richard Brandley Consulting Ltd., Calgary, Alberta, formerly at Department of Geology
The University of Calgary, 2500 University Drive N.W., Calgary, Alberta

F.F. Krause

Department of Geology, The University of Calgary
2500 University Drive N.W., Calgary, Alberta

E.W. Bamber

Geological Survey of Canada, 3303-33rd Street N.W., Calgary, Alberta T2L 2A7

B.L. Mamet

University of Montreal, Montreal, Quebec

INTRODUCTION

The Mount Head Formation is part of the Lower Carboniferous (Mississippian) Rundle Group. It overlies the Turner Valley Formation and is overlain by the Etherington Formation (Fig. 1). The formation was examined in 9 wells and 27 outcrop exposures in the southwest corner of Alberta and the southeast corner of British Columbia (Fig. 2). In its lower part, the Mount Head Formation consists of alternations between silty microcrystalline dolo-mudstone of subtidal sabkha origin (Wileman and Salter members) and coarser grained, carbonate sandstone of wave-swept bank and shoal origin (Baril and Loomis members) (Fig. 3). The upper Mount Head Formation consists of a more complex distribution of silty, microcrystalline dolo-mudstone of subtidal sabkha origin (Marston Member); dense, micritic lime mudstone to packstone of lagoonal origin (Carnarvon Member); carbonate sandstone of wave-swept bank and shoal origin (Loomis Member); and dark, argillaceous, variably sorted lime mudstone to grainstone of open-marine origin (Opal Member) (Fig. 3; Douglas, 1953, 1958; Macqueen and Bamber, 1968; Brandley and Krause, 1992b, 1993; Richards et al., 1993). In addition to vertical variations, the formation also shows significant east–west depositional changes (Fig. 2) (Brandley and Krause, 1992a, c). Deposition occurred on a gently-sloping, westward-deepening ramp in the Mount Head Embayment; a broad embayment in the western North American paleocoastline situated between the Montana Trough and the Peace River Embayment (Brandley et al., 1993; Brandley, 1994).

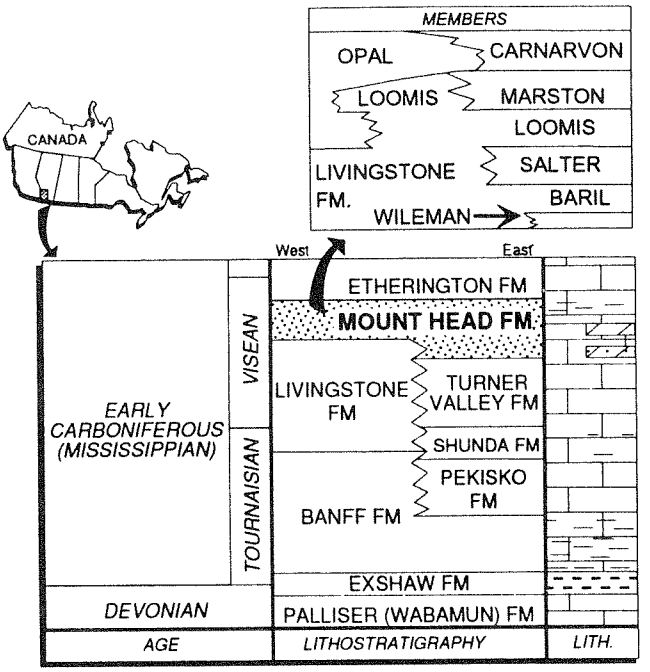

Figure 1. *Stratigraphic correlation chart for part of the Lower Carboniferous of southern Alberta and southeastern British Columbia.*

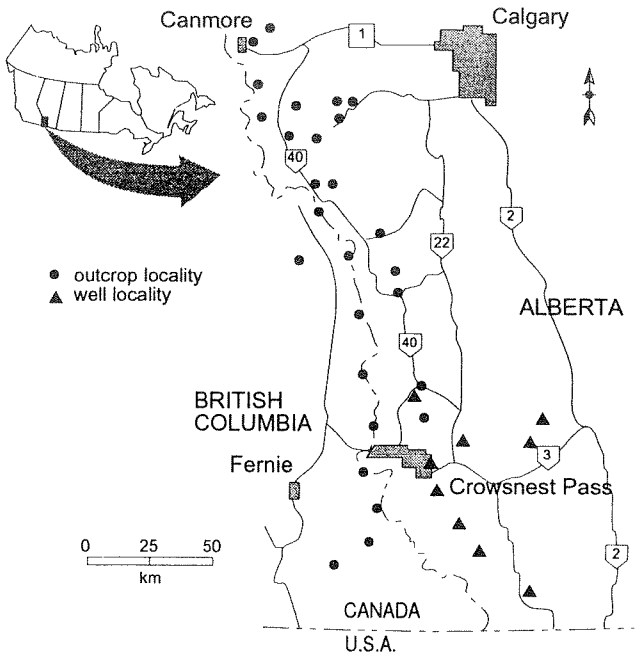

Figure 2. *Index map showing the outcrop and well localities used in this report.*

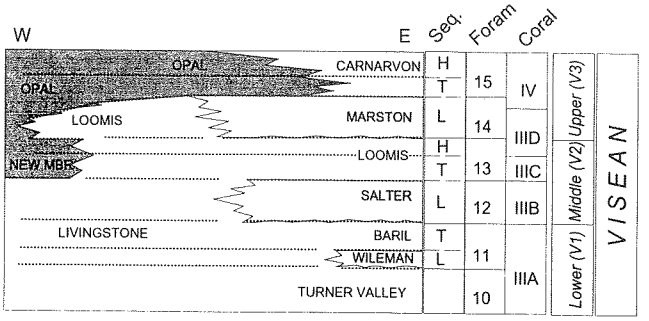

Figure 3. *Stratigraphic correlation chart for the Mount Head, upper Turner Valley, and upper Livingstone formations. The chart shows comparisons between sequence stratigraphic elements and foraminifer and coral zones. Note that in several instances sequence stratigraphic and biozone boundaries are coincident. (L, lowstand deposit, T, transgressive systems tract; H, highstand systems tract; biozones and subzones are indicated by letters and numbers).*

DEPOSITIONAL SEQUENCES

Three depositional sequences are recognized in the Mount Head Formation: the basal Wileman–Baril sequence, the middle Salter–Loomis sequence, and the uppermost Marston–Opal–Carnarvon sequence (Fig. 3; Brandley and Krause, 1992a, c). Each depositional sequence consists of a basal lowstand deposit and an upper transgressive systems tract. In some instances, transgressive systems tracts are capped by highstand systems tracts. Type 2 sequence boundaries, flooding surfaces and, locally, maximum flooding zones are recognized. Sequence stratigraphic trends, with a few important exceptions, are similar to those commonly found in siliciclastic dominated basins. Depositional sequence boundaries bracket an average of 4 Ma of geologic time and individual systems tracts bracket even shorter time intervals (Brandley et al., 1993).

BIOSTRATIGRAPHY

Foraminifers (Mamet zones 11–15) and corals (Sando and Bamber zones IIIA–IIIC, IV) provide a 2–3 Ma chronostratigraphic framework for the formation (Fig. 3; Mamet, 1977; Mamet and Mason, 1968; Mamet and Skipp, 1970a, b; Macqueen and Bamber, 1968; Sando and Bamber, 1985). Comparisons between biostratigraphy and sequence stratigraphy suggest a strong association between biozones, and systems tracts and sequences. The Wileman–Baril depositional sequence is characterized by foraminifer zone 11, and by coral zone IIIA (upper); the Salter–Loomis depositional sequence is characterized by foraminifer zones 12 and 13, and by coral zones IIIB, IIIC and IIID (lower); and the Marston–Opal–Carnarvon depositional sequence is characterized by foraminifer zones 14 and 15, and by coral zones IIID (upper) and IV. In several instances, individual biozones coincide with specific systems tracts within the sequences. The Salter lowstand deposits correspond with foraminifer zone 12 and coral zone IIIB; the Loomis transgressive systems tract corresponds with coral zone IIIC; and the Marston lowstand deposit corresponds with foraminifer zone 14.

DISCUSSION

In both nearshore and offshore settings, coral and foraminifer biozone boundaries appear to be nearly coincident with sequence boundaries, flooding surfaces, and locally, maximum flooding zones. In eastern sections this correlation results, in part, from submarine erosion at flooding surfaces and sequence boundaries. However, the correlation also holds in western sections where submarine erosion is minor to nonexistent. The striking correlations between sequence stratigraphic elements and biostratigraphic zones point to a probable cause and effect relationship between environmental shifts mediated by relative

sea-level fluctuations, and biological changes that lead to biozone recognition. Thus, the benthic biozones in the Mount Head Formation have both a time significance and an environmental significance. The time significance allows them to be used as biostratigraphic tools, and the environmental significance allows them to be used to document shifts in depositional environment. The combination of the two characteristics results in unique biostratigraphic signatures for different sequences and locally, for individual systems tracts. Because of this, benthic biozones can be used to identify and mark shifts in relative sea level even in homogeneous lithologies where sequence boundaries or flooding surfaces are obscure. The strong correlation between benthic biozones and sequence stratigraphic elements contrasts with the character of nektic or planktic faunal biozones that lack associations with sequences, systems tracts, and sequence stratigraphic surfaces. This dual time and environmental utility of Lower Carboniferous biozones should be a particularly powerful tool for exploration for and development of Livingstone Formation reservoirs in the southwest corner of the province. It may also be potentially useful for other Lower Carboniferous units elsewhere in the Western Canada Sedimentary Basin.

REFERENCES

Brandley, R.T.
1994: Mount Head, Upper Livingstone, Turner Valley Project: The Mississippian of the Southern Cordillera. Richard Brandley Consulting Ltd., Consulting Report, Calgary, Alberta, 292 p.

Brandley, R.T. and Krause, F.F.
1992a: Coeval progradation and retrogradation on a carbonate ramp as determined from combined sequence- and biostratigraphic analysis: Lower Carboniferous Mount Head Formation, Southwest Alberta, Southeast B.C., Canada. Geological Society of America, Abstracts with Programs, v. 24, no. 7.

1992b: Mixed carbonate–siliciclastic deposition on a wave-swept carbonate ramp: Lower Carboniferous Mount Head Formation, Southwestern Alberta, Canada. American Association of Petroleum Geologists, 1992 Annual Convention, Official Program, abstract.

1992c: Sequence stratigraphy and biostratigraphy of a mixed carbonate–siliciclastic ramp: Lower Carboniferous Mount Head Formation, Southwest Alberta, Canada. American Association of Petroleum Geologists, 1992 Annual Convention, Official Program, abstract.

1993: Carbonate and siliciclastic deposition on a wave-swept, cold-water, low-latitude ramp: Lower Carboniferous Mount Head Formation, Southwest Alberta and Southeast British Columbia, Canada. Program and Abstracts of the Canadian Society of Petroleum Geologists, Annual Convention (Pangea Conference).

Brandley, R.T., Krause, F.F., Bamber, E.W., and Mamet, B.L.
1993: Benthic biozones as systems tract and sequence signatures: Lower Carboniferous Mount Head Formation, Southwest Alberta, Southeast British Columbia, Canada. Program and Abstracts of the Canadian Society of Petroleum Geologists, Annual Convention (Pangea Conference).

Brandley, R.T., Thurston, J., and Krause, F.F.
1993: Basement-tectonic control on carbonate ramp deposition: Lower Carboniferous Mount Head Formation, southwest Alberta, southeast British Columbia. *In* Alberta Basement Transects Workshop (March 1–2): LITHOPROBE Report no. 31, G.M. Ross (ed.). LITHOPROBE Secretariat, University of British Columbia, p. 98–118.

Douglas, R.J.W.
1953: Carboniferous stratigraphy in the southern foothills of Alberta. Alberta Society of Petroleum Geologists, Guide Book, Third Annual Field Conference, p. 68–88.

1958: Mount Head map-area, Alberta. Geological Survey of Canada, Memoir 291, 241 p.

Macqueen, R.W. and Bamber, E.W.
1968: Stratigraphy and facies relationships of the Upper Mississippian Mount Head Formation, Rocky Mountains and Foothills, southwestern Alberta. Canadian Society of Petroleum Geologists, Bulletin, v. 16, no. 3, p. 225–287.

Mamet, B.L.
1977: Foraminiferal zonation of the Lower Carboniferous: methods and stratigraphic implications. *In* Concepts and Methods of Biostratigraphy, E.G. Kauffman and J.E. Hazel (eds.). Dowden, Hutchinson and Ross, p. 445–462.

Mamet, B.L. and Mason, D.
1968: Foraminifer zonation of the Lower Carboniferous Connor Lakes section, British Columbia. Bulletin of Canadian Petroleum Geology, v. 16, no. 2, p. 147–166.

Mamet, B.L. and Skipp, B.A.
1970a: Lower Carboniferous calcareous foraminifera; preliminary zonation and stratigraphic implications for the Mississippian of North America. International Congress of Carboniferous Stratigraphy and Geology, 6th, Sheffield, 1967, Compte Rendu, v. 3, p. 1129–1146.

1970b: Preliminary foraminifer correlations of Early Carboniferous strata in the North American Cordillera, in Colloque sur la stratigraphie du Carbonifère. Les Congrè et Colloque de l'Université de Liège, v. 55, p. 327–348.

Richards, B.C., Bamber, E.W., Higgins, A.C., and Utting, J.
1993: Carboniferous; Subchapter 4E. *In* Sedimentary Cover of the Craton in Canada, D.F. Stott and J.D. Aitken (ed.). Geological Survey of Canada, Geology of Canada, no. 5, p. 202–271.

Sando, W.J. and Bamber, E.W.
1985: Coral Zonation of the Mississippian System in the Western Interior Province of North America. United States Geological Survey, Professional Paper 1334, 61 p.

LOWER MANNVILLE SYNTHESIS

D.J. Cant and B. Abrahamson

Geological Survey of Canada, 3303-33rd Street N.W., Calgary, Alberta T2L 2A7

INTRODUCTION

This poster presents a newly compiled basin-scale map of the transgressive portion of the Mannville Group (Fig. 1). This map includes the Lower Mannville as well as the transgressive portion of the Middle Mannville (Bluesky, Wabascaw, Cummings) for two reasons: 1) the Lower/Middle Mannville pick is very difficult to identify in places where the Lower Mannville contains marine sediments at its top; and 2) the Lower/Middle Mannville pick is not exactly the same horizon over the entire basin because of minor unconformities. The top of the transgressive portion of the Middle Mannville is the Maximum Flooding Surface throughout the basin, and is more consistently recognizable than any other marker.

The map of the transgressive deposits reflects different features and processes in different areas of the basin. In general however, over much of the craton, it provides a mould of the erosional topography cut on the basal unconformity. Several areas which appear to have distinct isopach patterns can be identified, and each will be discussed separately.

Eastern Basin–The basin extending SE–NW through central Saskatchewan is very shallow over much of its length and deepens toward the Alberta border. This area has generally less than 60 m of transgressive Mannville sediment, and is closely associated with large areas of erosion and nondeposition. The margins of this depositional area can be interpreted as a series of SE–NW and SW–NE trending lineaments. Both the shape and the thickness of the area suggest that it was not undergoing any kind of regional subsidence. This area is directly superimposed over several Devonian-aged evaporites, most notably the Prairie Evaporite. The isopach pattern clearly indicates paleodrainage toward the northwest, into northeastern Alberta, and onto what is now exposed Shield.

Central Basin–This includes most of the depositional areas in the basin. Inspection of the map shows it is dominated by very irregular paleotopography on the basin floor, well documented in the past, and cut during the period of foreland rebound after the Jurassic subsidence episode. The isopach map reveals a well developed NW-oriented drainage system over most of central and northern Alberta which flowed between the well-known Axial and Pembina Highs. The map can be interpreted as indicating that all the drainage flowed northwest, then cut westward in the area of the Peace River Arch.

As noted by several authors, in south-central Alberta, some Upper Jurassic sediments also occur in the bottoms of the valleys, suggesting that the erosion of the valleys originally occurred in the Late Jurassic, and they may have undergone several periods of infill and erosion.

Western Basin–Much of the drainage of the central basin flowed toward the area of abrupt thickening in northwestern Alberta and northeastern B.C. The isopachs can be interpreted as reflecting a) topography on the basal unconformity, most notably the Fox Creek Escarpment; b) some movement on Peace River Arch structures; and c) flexural subsidence as a result of overthrusting to the west. It is believed that this is the only preserved area of substantial flexural subsidence during the transgressive portion of the Mannville. The petrology of the sediments in most areas of the basin confirms that western sources began to play a role in supplying the Mannville only in latest Lower Mannville to early Middle Mannville times.

CROSS-SECTIONS

Several representative cross-sections in different areas are illustrated (Sections 1–6).

Section 1–Southeast Saskatchewan

This section shows the fill of a Lower Mannville valley in the cratonward salt-solution basin. Within the larger valley cut into the Jurassic shales, the fill varies laterally, suggesting several cut-and-fill events. This section can be interpreted in different ways, but it is believed that

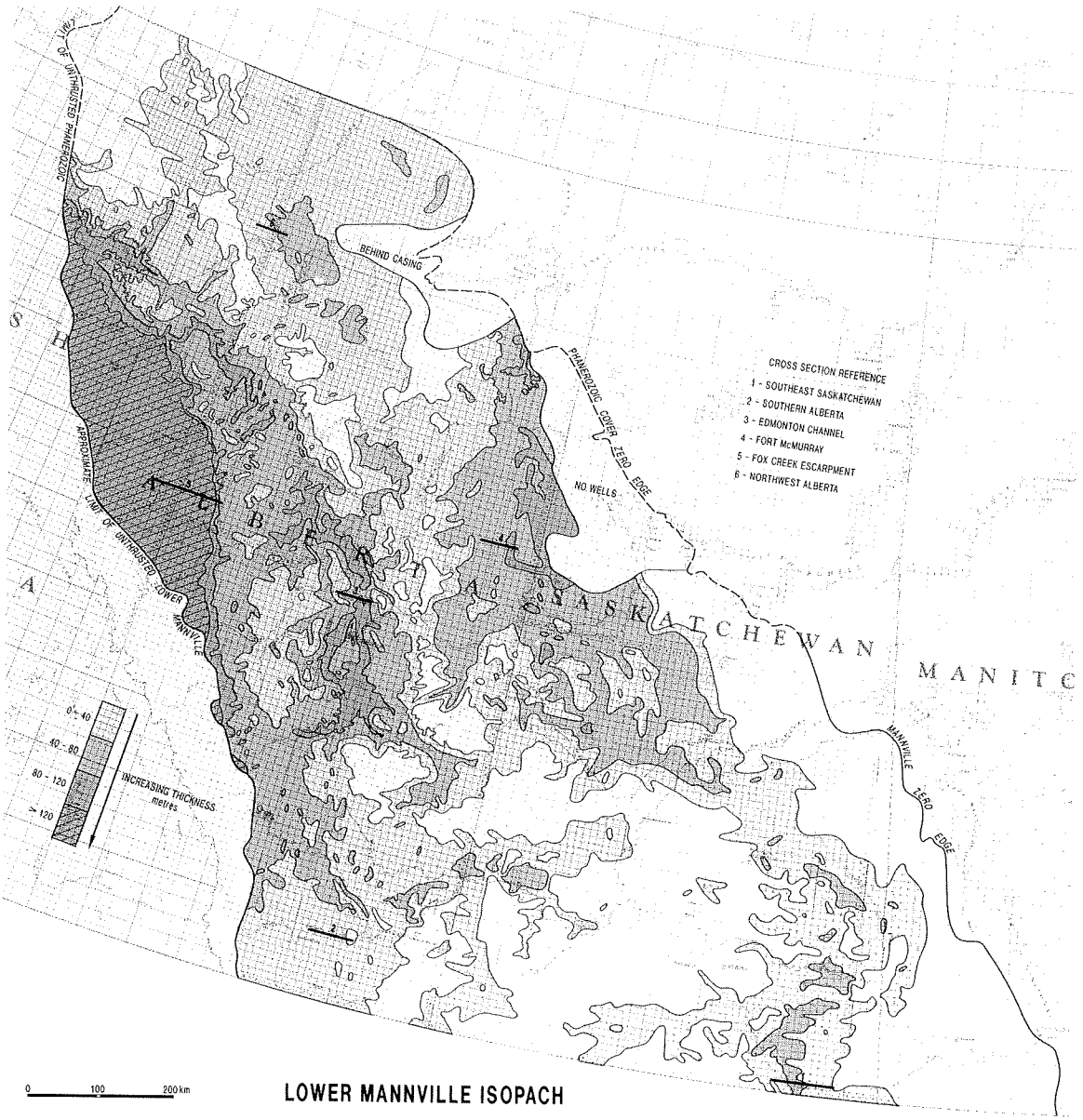

Figure 1. *Isopach map of the lower transgressive portion of the Mannville Group.*

the very thick sand is a later valley fill which removed the sand and shale section preserved in the west. Alternatively, the thick sand could be interpreted as an amalgamation of two sands.

Section 2–Southern Alberta

This section shows the complexity of valley fills in the low subsidence-rate areas of the basin. A portion of the basal valley fill is Jurassic aged, and correlation of this to other areas is entirely the result of log pattern matching. The Cretaceous portion of the fill is dominantly sandy.

Section 3–Central Alberta

Cross-section of the well-developed dendritic drainage system flowing to the northwest. The broad erosional cut was filled in several stages, with a basal sand, itself probably eroded by a later event. The dominantly fine grained sediments of the Ellerslie Formation are in part marine and in part lacustrine as shown by palynological

analysis of cores. The thick sands of the later valley fill are clearly localized by the original valley wall.

Section 4–Northeast Alberta

This east–west section across a thicker valley fill shows a series of sandstones in the McMurray Formation. The stratigraphy is complex, with a number of stages to the valley fill, each of which is interpreted to reflect an episode of incision during McMurray times. The basal sand may be considerably older than the remainder of the Mannville, as judged from some palynological results in the McMurray. The upper part of the unit is finer grained, as a result of increased subsidence rates.

Section 5–West-Central Alberta

This section includes the Cadomin, Gething and Bluesky formations. A basal sand in the Gething, believed to be an unconformity-bounded wedge, is also indicated. The typical fine grained Gething facies is interrupted by thick sandstones (stippled) which are interpreted to be nonmarine valley fills. The lower portions of the section terminate eastward as they onlap against the Fox Creek Escarpment.

Section 6–Northern Alberta

This section shows a much-reduced Lower Mannville infilling the valley cut into the Paleozoics. The only sand lies directly on the unconformity, and is here labelled Gething, but no definitive paleontological evidence or regional correlations exist to confirm this.

LOWER MANNVILLE STRATIGRAPHY

Previously the Lower Mannville was believed to be a continuous unit, with no major breaks. From the evidence of the cross-sections and some biostratigraphic results, it is now believed to contain several unconformities. In western Alberta, where the most complete section occurs, the Cadomin and the Basal Gething Sand are both unconformity-bounded, and the Gething channels are valley fills resulting from base-level falls. Many of these surfaces are not represented in lower subsidence-rate areas because of amalgamation of unconformities.

1

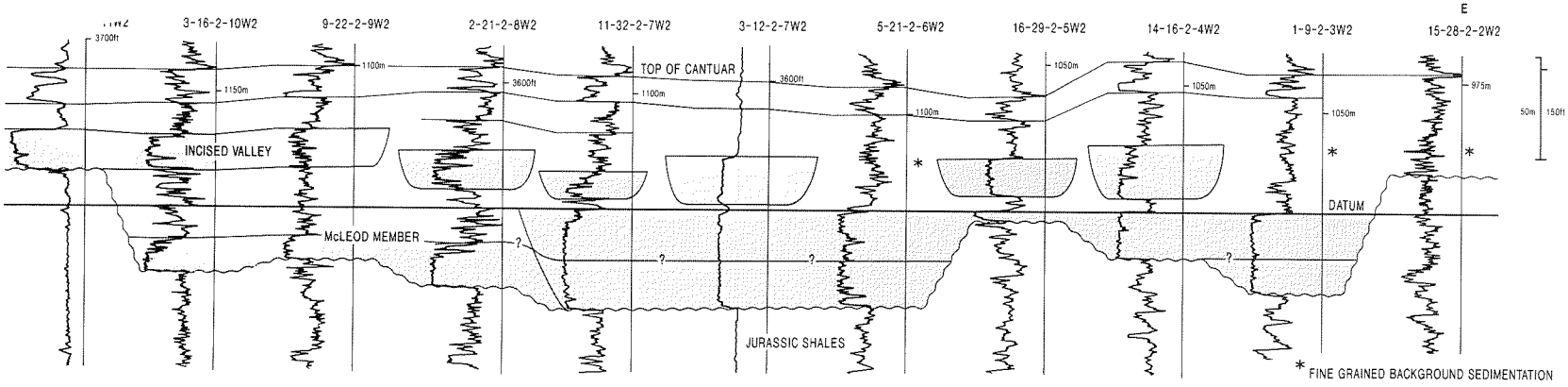

2

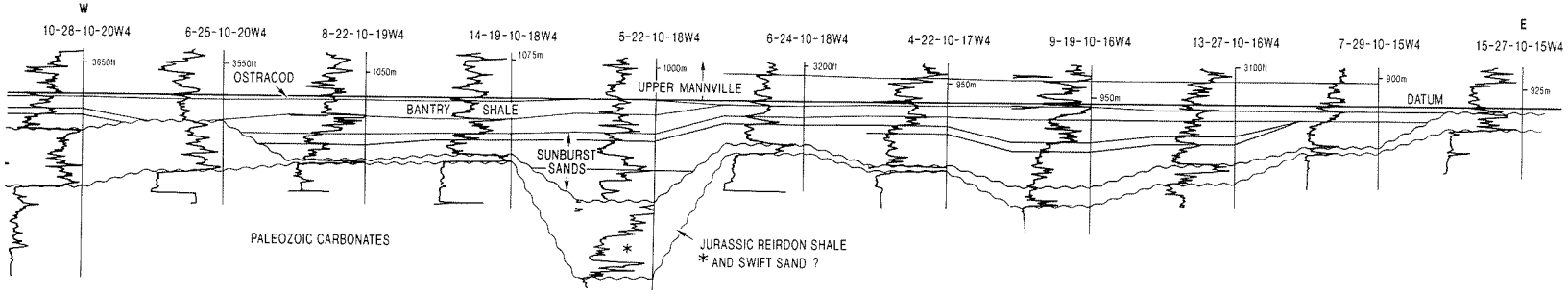

Cross-Sections 1–6

3

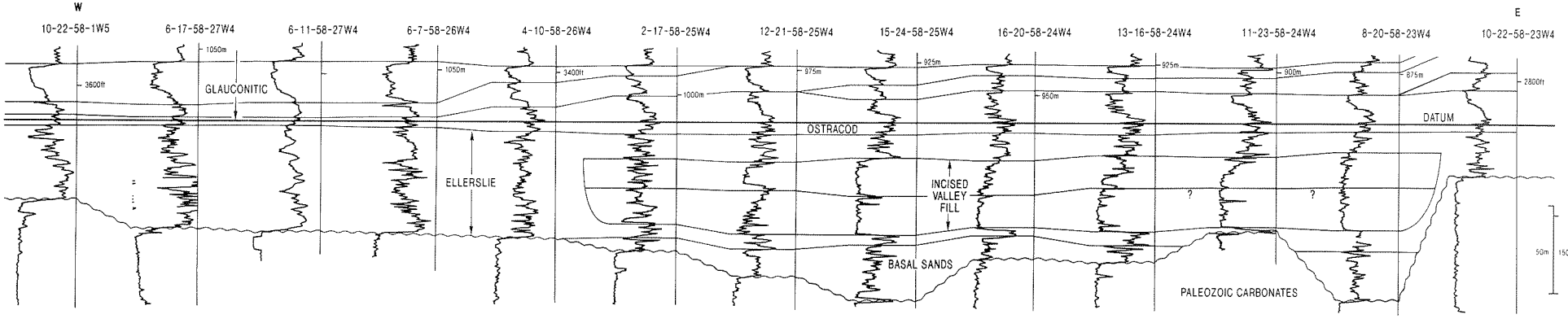

4

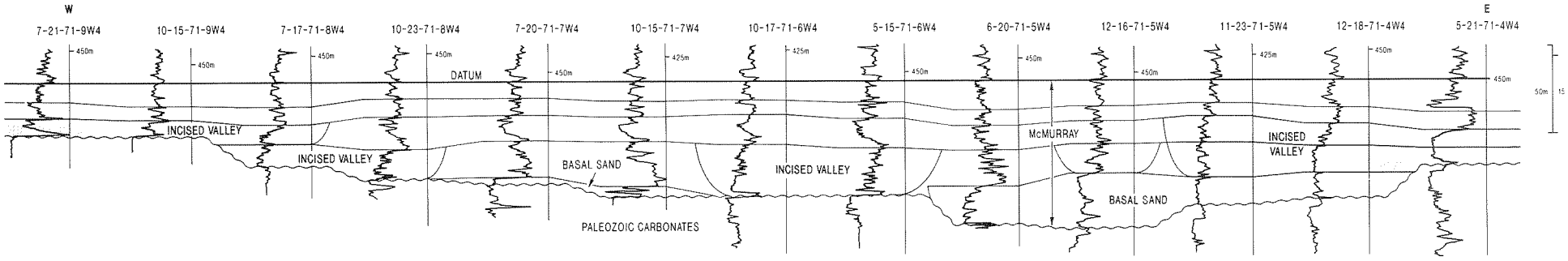
W
7-21-71-9W4
10-15-71-9W4
7-17-71-8W4
10-23-71-8W4
7-20-71-7W4
10-15-71-7W4
10-17-71-6W4
5-15-71-6W4
6-20-71-5W4
12-16-71-5W4
11-23-71-5W4
12-18-71-4W4
5-21-71-4W4
E
DATUM
INCISED VALLEY
INCISED VALLEY
BASAL SAND
PALEOZOIC CARBONATES
INCISED VALLEY
McMURRAY
BASAL SAND
INCISED VALLEY

5

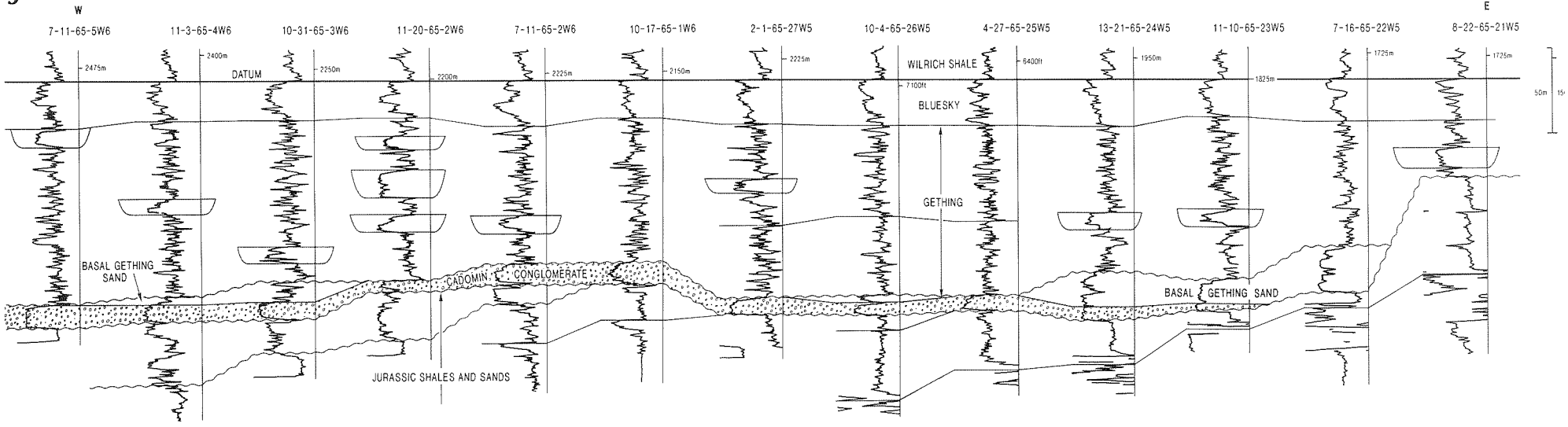
W
7-11-65-5W6
11-3-65-4W6
10-31-65-3W6
11-20-65-2W6
7-11-65-2W6
10-17-65-1W6
2-1-65-27W5
10-4-65-26W5
4-27-65-25W5
13-21-65-24W5
11-10-65-23W5
7-16-65-22W5
8-22-65-21W5
E
DATUM
WILRICH SHALE
BLUESKY
GETHING
BASAL GETHING SAND
CADOMIN CONGLOMERATE
BASAL GETHING SAND
JURASSIC SHALES AND SANDS

6

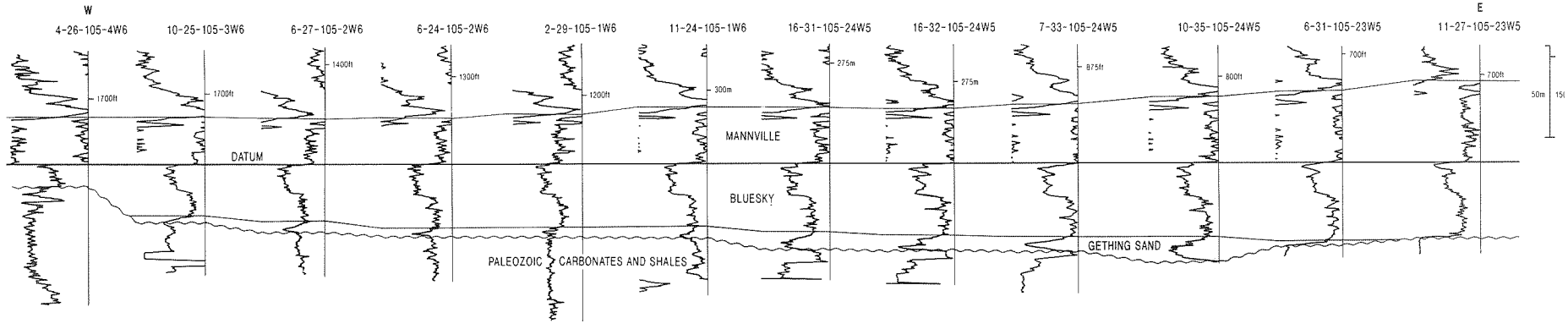
W
4-26-105-4W6
10-25-105-3W6
6-27-105-2W6
6-24-105-2W6
2-29-105-1W6
11-24-105-1W6
16-31-105-24W5
16-32-105-24W5
7-33-105-24W5
10-35-105-24W5
6-31-105-23W5
11-27-105-23W5
E
DATUM
MANNVILLE
BLUESKY
PALEOZOIC CARBONATES AND SHALES
GETHING SAND

PALYNOLOGICAL SUPPORT IN UNDERSTANDING THIRD AND FOURTH ORDER STRATIGRAPHIC CYCLES IN THE UPPERMOST CRETACEOUS/ LOWERMOST TERTIARY, WESTERN CANADA BASIN: AN EXAMPLE OF RECIPROCAL PROXIMAL AND DISTAL STRATIGRAPHIES

O. Catuneanu

Department of Geology, University of Toronto, Toronto, Ontario M5S 3B1

A.R. Sweet

Geological Survey of Canada, 3303-33rd Street N.W., Calgary, Alberta T2L 2A7

J.F. Lerbekmo

Department of Geology, University of Alberta, Edmonton, Alberta T6C 2E3

D.R. Braman

Royal Tyrrell Museum of Palaeontology, Drumheller, Alberta T0J 0Y0

INTRODUCTION

A comprehensive study is in progress on the recognition and correlation of stratigraphic cycles within the marine Bearpaw Formation, its marine and nonmarine correlatives, and nonmarine contiguous strata (OC). As a component of this study, reciprocal proximal and distal stratigraphies have been established for marine and nonmarine Maastrichtian to Paleocene strata on a transect extending from southern Alberta to southwestern Manitoba. Essential information was obtained from the three coreholes completed under the Canadian Continental K-T Drilling Project (CCDP) (Fig. 1, Elkwater, in southwestern Alberta, Wood Mountain in south-central Saskatchewan and Turtle Mountain in southwestern Manitoba). These coreholes supplement an otherwise sporadic stratigraphic latest Cretaceous to Early Paleocene record obtained from outcrops (Fig. 1).

The ages of the disconformity bounded reciprocal stratigraphies are closely constrained by Maastrichtian

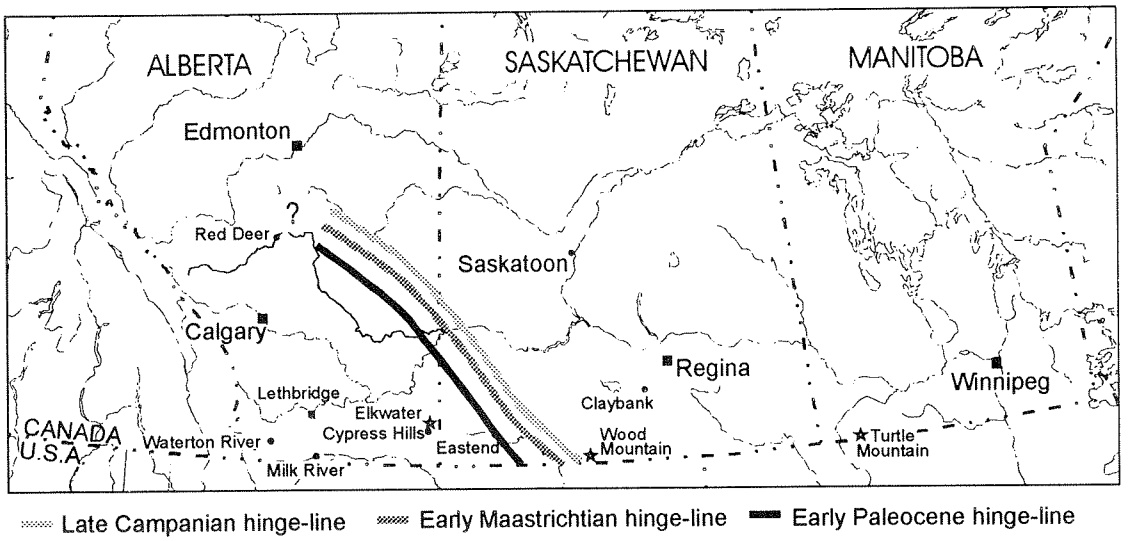

Figure 1. *Reference localities. Stars mark CCDP corehole locations and circles mark outcrop localities.*

and Paleocene palynological biostratigraphies and polarity chronologies (Fig. 2). These can also be used to demonstrate both the time-transgressive and reciprocal nature of proximal and distal depositional trends (i.e., regression of the Bearpaw sea) as predicted by the model of Jordan and Flemings (1991).

RECIPROCAL PROXIMAL AND DISTAL STRATIGRAPHIES

Reciprocal trends are recorded by geophysical logs across the same genetically related packages from proximal and distal parts of the Western Canada Basin within the Bearpaw Formation and its correlatives, and are also reflected in the biostratigraphies of post-Bearpaw strata. Datums defined by these methods have allowed the recognition of the following chronological units within the strata spanned by the CCDP coreholes—late Early Maastrichtian, early Late Maastrichtian, late Late Maastrichtian, and earliest, early to mid and late Early Paleocene—and, in doing so, to identify regional disconformities. In the proximal sector, major stratigraphic gaps correspond to the early Late Maastrichtian and late Early to early Middle Paleocene, but with a relatively continuous record for the Early Maastrichtian, the late Late Maastrichtian and much of the Early Paleocene. In the distal sector, major stratigraphic gaps correspond to the Early Maastrichtian (within the marine strata of the Riding Mountain Formation) and to the late Late Maastrichtian–earliest Paleocene interval, but with an extensive record of the early Late Maastrichtian and parts of the Early Paleocene (Figs. 3, 4).

These results indicate that stages of sediment accumulation (availability of accommodation space and sediment supply) and nondeposition/erosion (lack of accommodation space and/or sediment supply) occurred in both the proximal and distal sectors of the foreland basin. The consistent reciprocal variation in the availability of accommodation space and/or sediment supply on a regional scale implies the active role of tectonic movements in controlling the depositional process. Moreover, proximally, the nonmarine succession is dominated by the fining-

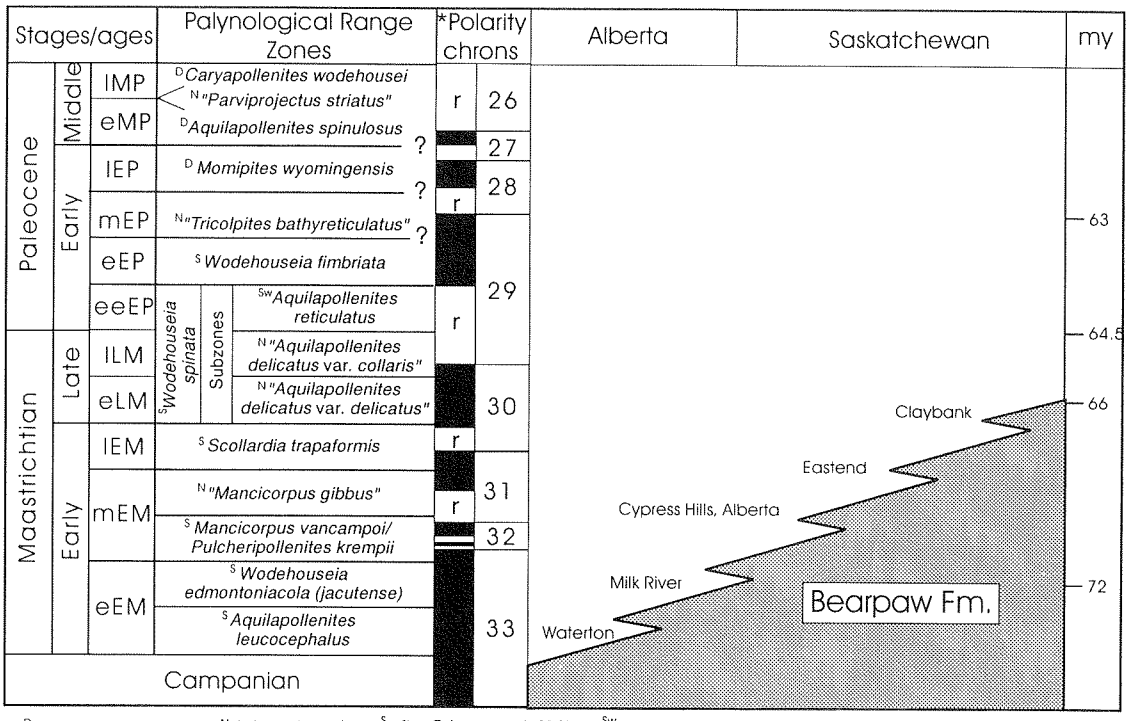

D after Demchuk (1990) N informal zones S after Srivastava (1970) Sw after Sweet (1978)
* after Lerbekmo & Coulter (1985), Lerbekmo (1985) & Lerbekmo et al. (1992)

Figure 2. *Stages/ages, palynologyical range zones, polarity chrons used as datums and their relationship to the regression of the Bearpaw Formation. eEM, early Early Maastrichtian; mEM, middle Early; lEM, late Early; eLM, early Late; lLM, late Late; eeEP, earliest Paleocene; eEP, early Early; mEP, middle Early; lEP, late Early; eMP, early Middle; and lMP, late Middle. Not to vertical scale.*

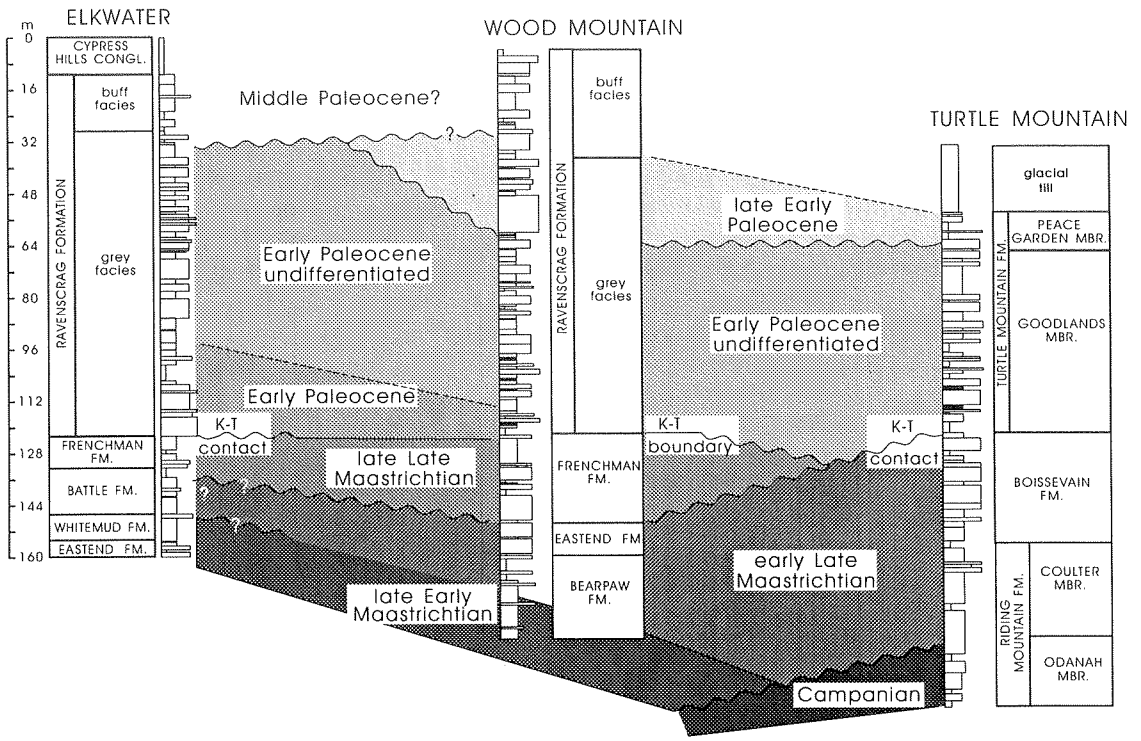

Figure 3. *Stratigraphic correlations established between the three Canadian Continental K-T project coreholes.*

upward sections (which are thicker than the coarsening-upward ones), whereas the situation is reversed distally, where the succession is dominated by the coarsening-upward sections. The recognition of the "proximal-type" and "distal-type" successions, with opposite depositional trends, confirms the existence of the foreland basin hinge-line, which separates sectors with reciprocal stratigraphies. The correlation between proximal and distal disconformities and sedimentary wedges allows us to trace the hinge-line position for the considered stratigraphic interval (Figs. 1, 4). A general orogenward migration tendency is noted, which is consistent with information obtained from the subjacent Bearpaw section.

It is important to emphasize here that two adjacent disconformities, for instance the proximal early Late Maastrichtian disconformity and the distal late Late Maastrichtian one (Figs. 3, 4), should not be considered as parts of a unitary and continuous basin wide disconformity, because such a surface would have a diachroneity of one or two million years, which is unrealistic and not possible to explain both on practical and theoretical grounds: recent research shows that boundary diachronism across the entire basin may reach a maximum 0.5 million years (Plint et al., 1993). Moreover, the absolute value of the stratigraphic gap associated with each disconformity gradually increases from the hinge-line to the peripheral sectors of the basin. This suggests that the reciprocal proximal and distal availability in accommodation space and/or sediment supply is due to reciprocal proximal and distal vertical tectonic movements, with higher amplitudes toward the peripheral sectors of the basin, and symmetrical relative to a point of tectonic equilibrium which corresponds to the hinge-line.

The regional proximal and distal disconformities can be considered to be third order sequence boundaries in the post-Bearpaw nonmarine section, as they bound sequences corresponding to significant stratigraphic intervals, over 1.5 m.y. Vertical lithological profiles show that these boundaries are placed at the top of overall fining-upward sections; therefore, since the disconformities mark episodes of nondeposition, they naturally follow the gradual decrease in depositional energy and sediment supply stages which are responsible for generating fining-upward successions.

Although these large-scale patterns are readily apparent, on a more detailed scale, a precise reciprocal relationship in the timing of sediment accumulation in the proximal and distal sectors did not always exist. Firstly, although major disconformities developed in

both the proximal and distal stages when the lack of accommodation space and/or sediment supply resulted from the depositional surface elevation rising relative to the source of sediment supply, the over generalization of this situation may be misleading. Even when the regional proximal or distal depositional regime is dominated by a general lack of accommodation space and/or sediment supply, over more or less restricted areas such as lacustrine environments or high sinuosity single or multiple channel fluvial systems, a low-rate accumulation of fine sediments may continue. At the same time, under very low sediment supply conditions, coal-generating or pedogenetic processes may develop as well. In all these cases, a continuous fossil record may be preserved in relatively thin strata ("nonmarine condensed sections"), such as lacustrine or fluvial fine clastics, coals or paleosoils, which are time-equivalent with the regional disconformity stratigraphic gap and correlative to the disconformity surface. For instance, in the early Late Maastrichtian, the nonmarine Boissevain Formation, the marginal marine Coulter Member of the Riding Mountain Formation and correlative strata were deposited in the distal sector (Fig. 4). At the same time, either a regional disconformity developed proximally (i.e., between the St. Mary River and Willow Creek formations or the Eastend and Frenchman Formations) or a "condensed section" represented by the Battle Formation, which is described variously as a lacustrine deposit or a paleosoil (Lerbekmo, 1985; unpublished data). The early Late Maastrichtian is presumed to reflect the cessation or slowing of sedimentation proximally during stabilization of the foreland basin following erosional off-loading of the orogenic belt and a corresponding distal subsidence. Similar examples are offered by the work of Wright and Marriot (1993), which also argues that the sequence boundaries may be represented by mature paleo-soils. This concept is important as it explains why reciprocal stratigraphies in nonmarine strata may be represented by either 1) the proximal versus distal presence/absence of strata or 2) a contrast in the nature or thickness of the stratigraphic record across the hinge-line.

Secondly, based on the position of the hinge-line during the Maastrichtian (Fig. 1), the Early Paleocene hinge-line is predicted to have occurred in the vicinity of the Cypress Hills, Saskatchewan, placing both the Turtle Mountain and Wood Mountain coreholes in the distal sector. Both coreholes are similar in the extent of their Early Paleocene records. However, they differ in that there is no representation of the earliest Paleocene in the Turtle Mountain corehole whereas both the latest

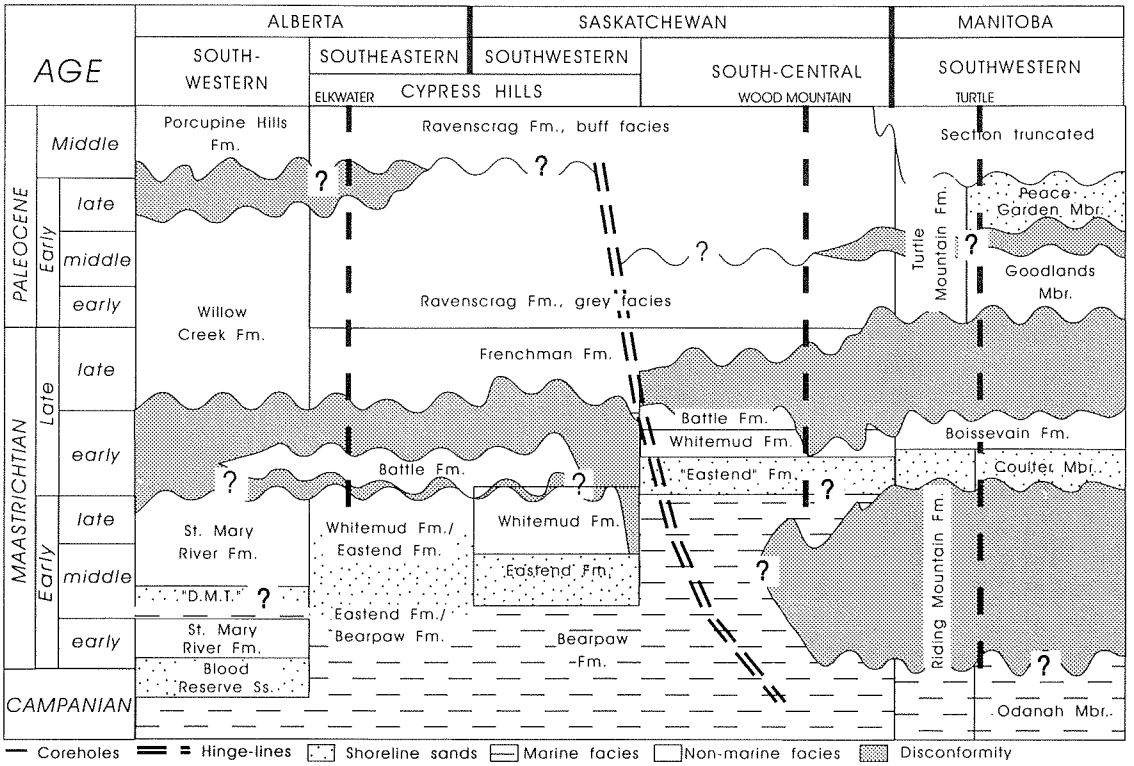

Figure 4. *Preliminary regional lithostratigraphic correlations showing the proposed reciprocal disconformities. Not to vertical scale.*

Maastrichtian and earliest Paleocene (including the actual K-T boundary claystone) occur in the Wood Mountain corehole (Fig. 4).

DISCUSSION

Figure 5 synthesizes the stratigraphy of the nonmarine section along the considered profile, and illustrates the reciprocal correlation between the major proximal and distal disconformities and sedimentary wedges, as well as the position of the foreland basin hinge-line. This model implies that each sedimentary wedge crosses the hinge-line and gets thinner toward the correlative disconformity, both in tems of space and time, until it is completely absorbed by it. Thus, we take into consideration the existence of a "compensation space" in which the correlative regional sedimentary wedges and disconformities gradually change their stratigraphic significance and compensate for each other in such a way that the time they represent is constant. The compensation space for each proximal or distal sedimentary wedge then becomes the distance between the hinge-line and the point where the correlative disconformity replaces entirely the respective strata. On logical grounds, the concept of a compensation space is absolutely necessary when the generation of successive correlative disconformities and sedimentary wedges is not interrupted by stages of simultaneous sediment accumulation across the entire base, since a sedimentary record is preserved in the hinge-line sector as well.

The K-T boundary occurs within the late Late Maastrichtian–earliest Paleocene proximal sedimentary wedge, which correlates to a major distal disconformity. Therefore preservation of the K-T boundary interval in the Wood Mountain corehole, located east of a hinge-line positioned in the Cypress Hills region of Saskatchewan, needs to be explained. The presence of a "compensation space" in the vicinity of the hinge-line in possible combination with subsidence in southwestern and south-central Saskatchewan, in response to Devonian salt solution, as discussed by Broughton (1977, 1988), may be the controlling factors in its preservation.

The interpretation regarding the reciprocal proximal and distal stratigraphies, their tectonic control and the position in space and time of the foreland basin hinge-line is strongly supported by the study of marine Bearpaw strata. The recognition of these generalized patterns on a basin-wide scale is highly important because it allows predictions about the occurrence of packages of strata or major disconformities belonging to less well known stratigraphic intervals within the foreland basin.

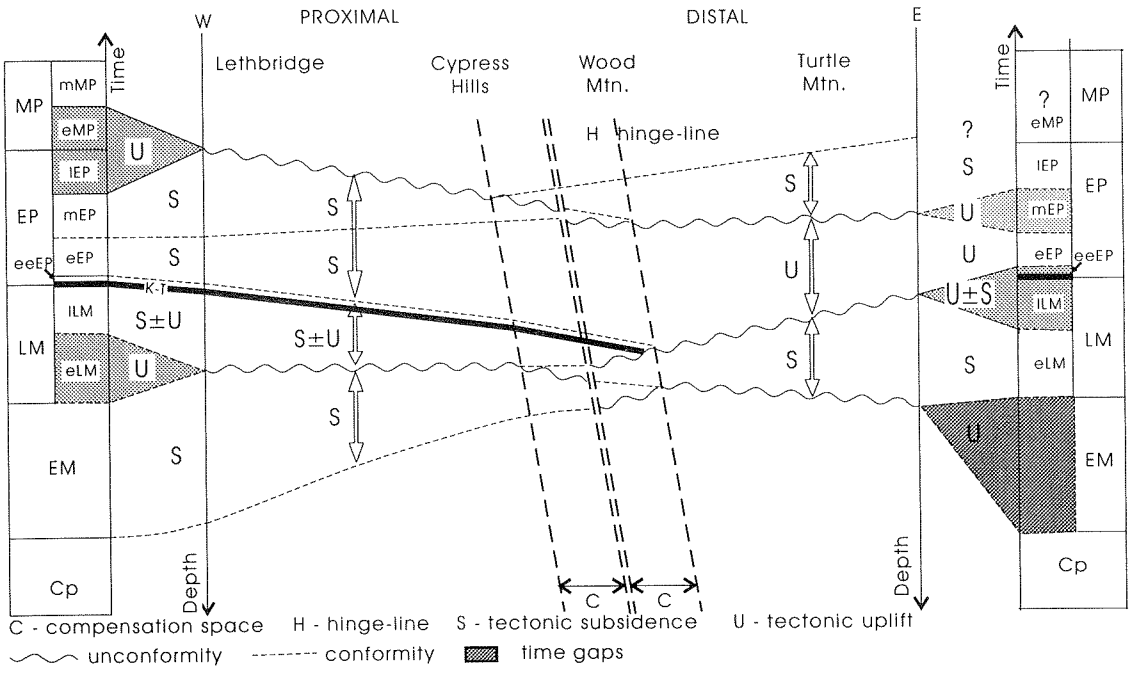

Figure 5. *Southern cross-section through the Western Canada Basin. For time abbreviations, see description for Figure 2. The vertical dimension represents thickness rather than time.*

REFERENCES

Broughton, P.L.
1977: Origin of coal basins by salt solution. Nature, v. 270, p. 420–423.

1988: Formation of Tertiary coal basins in southern Saskatchewan. Saskatchewan Energy and Mines, Open File Report 88–1, 53 p.

Demchuck, T.D.
1990: Palynostratigrahic zonation of Paleocene strata in the central and south-central Alberta Plains, v. 27, p. 1263–1269.

Jordan, T.E. and Fleming, P.B.
1991: Large-scale stratigraphic architecture, eustatic variation and unsteady tectonism: a theoretical evaluation. Journal of Geophysical Research, v. 96, p. 6681–6699.

Lerbekmo, J.F.
1985: Magnetostratigraphic and biostratigraphic correlations of Maastrichtian to Early Paleocene strata between south-central Alberta and southwestern Saskatchewan. Bulletin of Canadian Petroleum Geology, v. 33, p. 213–226.

Lerbekmo, J.F. and Coulter, K.C.
1985: Late Cretaceous to early Tertiary magnetostratigraphy of a continental sequence: Red Deer Valley, Alberta, Canada. Canadian Journal of Earth Sciences, v. 22, p. 567–583.

Lerbekmo, J.F., Demchuk, T.D., Evans, M.E., and Hoye, G.S.
1992: Magnetostratigraphy and biostratigraphy of the continental Paleocene of the Red Deer Valley, Alberta, Canada. Bulletin of Canadian Petroleum Geology, v. 40, p. 24–35.

Plint, A.G., Hart, B.S., and Donaldson, W.S.
1993: Lithosphere flexure as a control on stratal geometry and facies distribution in Upper Cretaceous rocks of the Alberta foreland basin. Basin Research, v. 5, p. 69–77.

Srivastava, S.K.
1970: Pollen biostratigraphy and paleoecology of the Edmonton Formation (Maestrichtian), Alberta, Canada. Paleogeography, Paleoclimatology, Paleoecology, v. 7, p. 221–276.

Sweet, A.R.
1978: Palynology of the Ravenscrag and Frenchman Formations. *In* Coal Resources of Southern Saskatchewan, A model for Evaluation Methodology, S.H. Whitaker, J.A. Irvine, and P.L. Broughton (eds.). Geological Survey of Canada, Economic Geology Report 30, p. 29–38.

Wright, W.P. and Marriott, S.B.
1993: The sequence stratigraphy of fluvial depositional systems: the role of floodplain sediment storage. Sedimentary Geology, v. 86, p. 203–240.

REGIONAL STUDIES OF SEISMIC REFLECTION DATA IN THE EASTERN WILLISTON BASIN–PROJECT REPORT

J.R. Dietrich

Geological Survey of Canada, 3303-33rd Street N.W., Calgary, Alberta T2L 2A7

C. Zhu and Z. Hajnal

Department of Geological Sciences
University of Saskatchewan, Saskatoon, Saskatchewan S7N 0W0

ABSTRACT

Regional aspects of seismic stratigraphy and structure of the Canadian portion of the Williston Basin have previously been investigated through the compilation, reprocessing and analysis of 1350 line-km of industry-donated seismic reflection data across southeastern Alberta, Saskatchewan and southwestern Manitoba (Zhu, 1992; Zhu and Hajnal, 1993). The Geological Survey of Canada and University of Saskatchewan are currently involved in a collaborative project that continues and expands upon seismic-based studies in the Williston Basin. The project includes further analysis of portions of the previously acquired seismic data set and reprocessing/interpretation of an additional 1000 line-km of industry data (recently) donated to the GSC and U of S. Project studies are currently focused on the northeastern flank of the basin, in an area encompassing easternmost Saskatchewan and southwestern Manitoba (Twps. 1–7, Rges. 19–34 W1).

Project objectives include the interpretation and description of regional seismic stratigraphy and structure, evaluation of basement controls on basin development and local depositional history, and general characterisation and assessment of petroleum plays in Lower Paleozoic strata. Project study results will be released (in summary form) through external meeting presentations and journal-published papers.

REFERENCES

Zhu, C.
1992: A seismic study of the northern Williston Basin. Ph.D. thesis, Department of Geological Sciences, University of Saskatchewan.

Zhu, C. and Hajnal, Z.
1993: Tectonic development of the northern Williston Basin: a seismic interpretation of an east-west regional profile. Canadian Journal of Earth Sciences, v. 30, p. 621–630.

T-R SEQUENCE ANALYSIS OF THE TRIASSIC SUCCESSION OF THE WESTERN CANADA SEDIMENTARY BASIN

A.F. Embry and D.W. Gibson

Geological Survey of Canada, 3303-33rd Street N.W., Calgary, Alberta T2L 2A7

Triassic strata of the WCSB are up to 1200 m thick and consist of a variety of siliciclastic and carbonate facies deposited in a shelf-slope setting. T-R sequence analysis has been applied to the succession with sequence boundaries drawn at subaerial unconformities and correlative transgressive surfaces.

The Triassic succession has been divided into five 2nd order T-R sequences by the recognition of six 2nd order sequence boundaries (Fig. 1). These boundaries are characterized by widespread unconformities and by

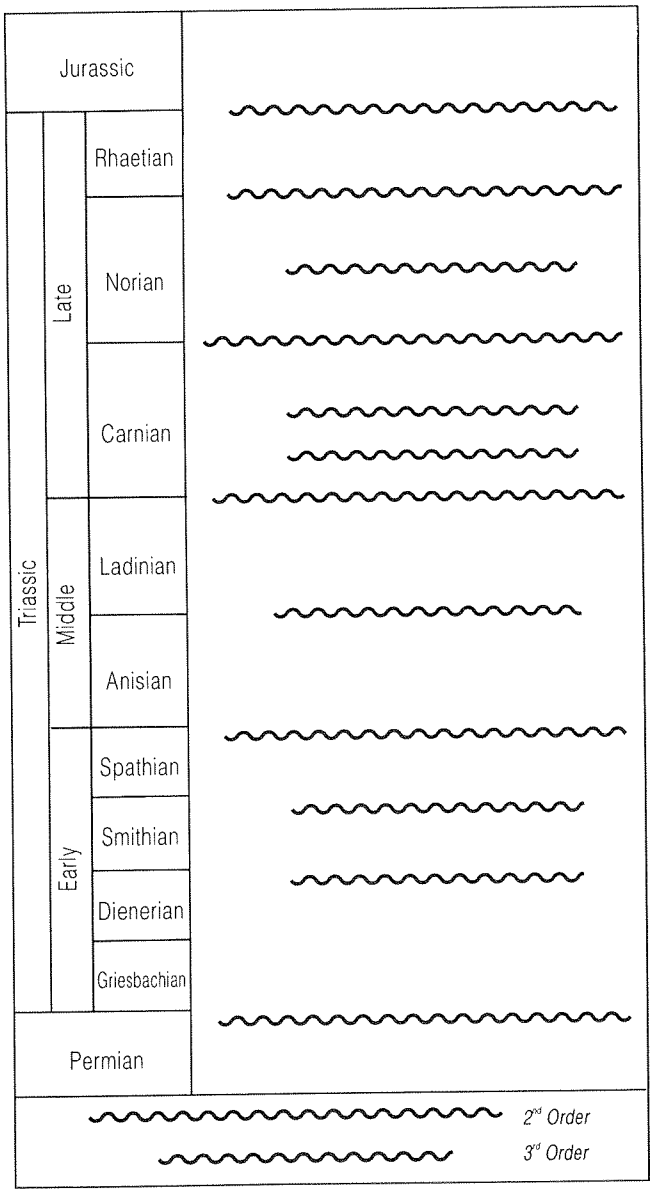

Figure 1. *Triassic second and third order sequence boundaries.*

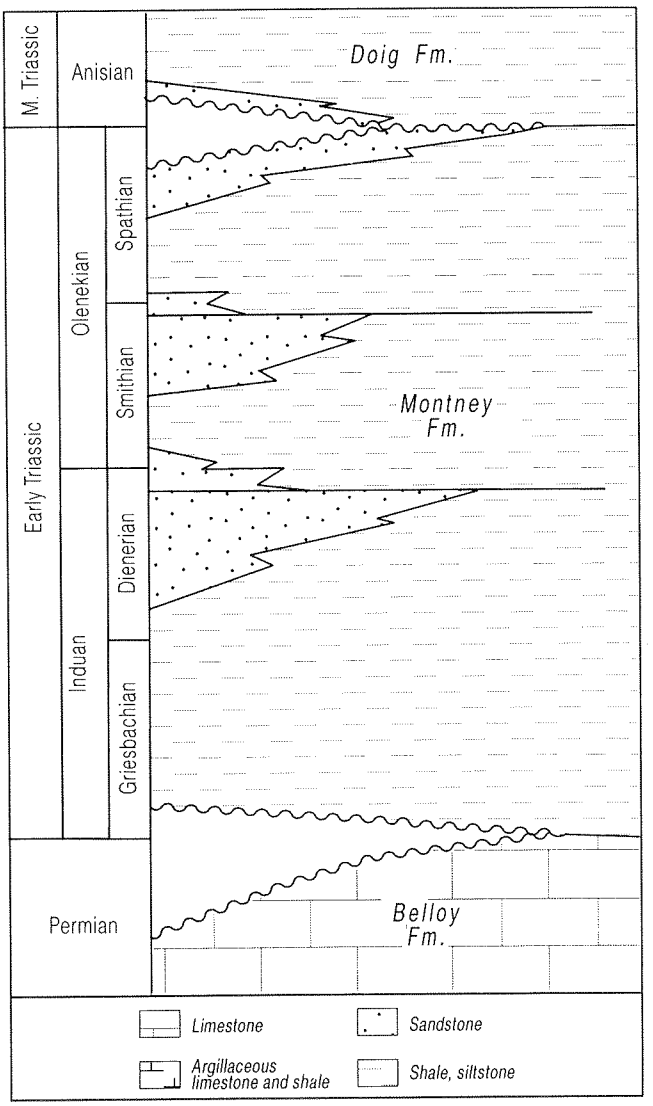

Figure 2. *Lower Triassic stratigraphy, Peace River area.*

major changes of the depositional and subsidence regimes across the boundaries. The stratigraphic levels and ages of these key boundaries are base Montney (latest Permian), base Doig (latest Olenekian), near base Ludington-lower Charlie Lake (latest Ladinian), near top Baldonnel (latest Carnian), base Bocock (latest Norian) and base Fernie (latest Rhaetian) (Figs. 2–5).

Third order T-R sequence boundaries, which are characterized by widespread transgressive surfaces, marginal unconformities and only subtle changes in depositional regime, occur within the second order sequences. These are dated as late Induan, mid-Olenekian, late Anisian, mid-Carnian, late Carnian and mid-Norian and allow the delineation of eleven 3rd order sequences (Figs. 1-5). Numerous fourth and fifth order sequence boundaries, which are mainly transgressive surfaces, are also present but can be correlated only over a portion of the basin.

The second and third order sequence boundaries recognized in Western Canada can be correlated with established Triassic sequence boundaries in other basins in North America, Europe and Asia. The

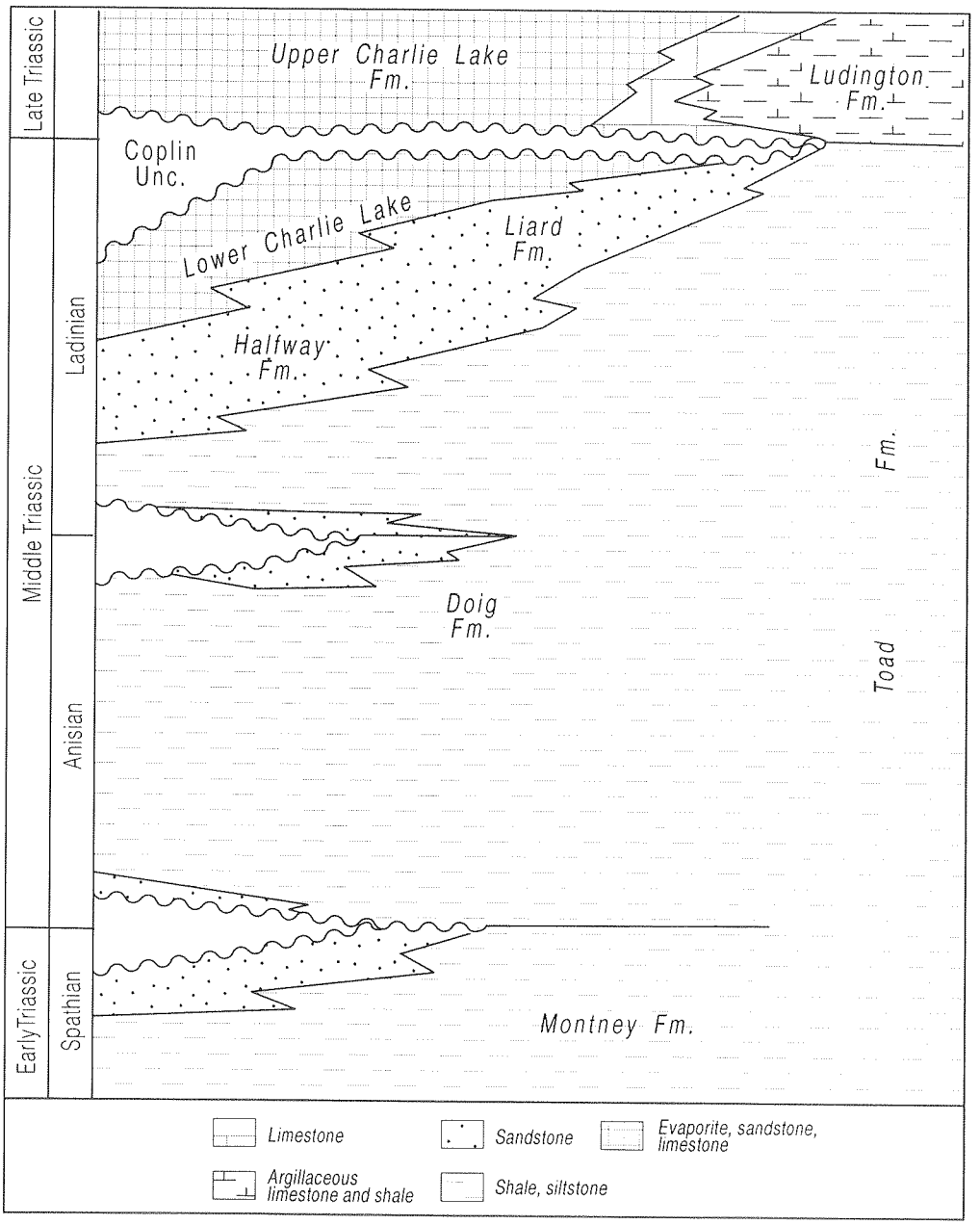

Figure 3. Middle Triassic stratigraphy, Peace River area.

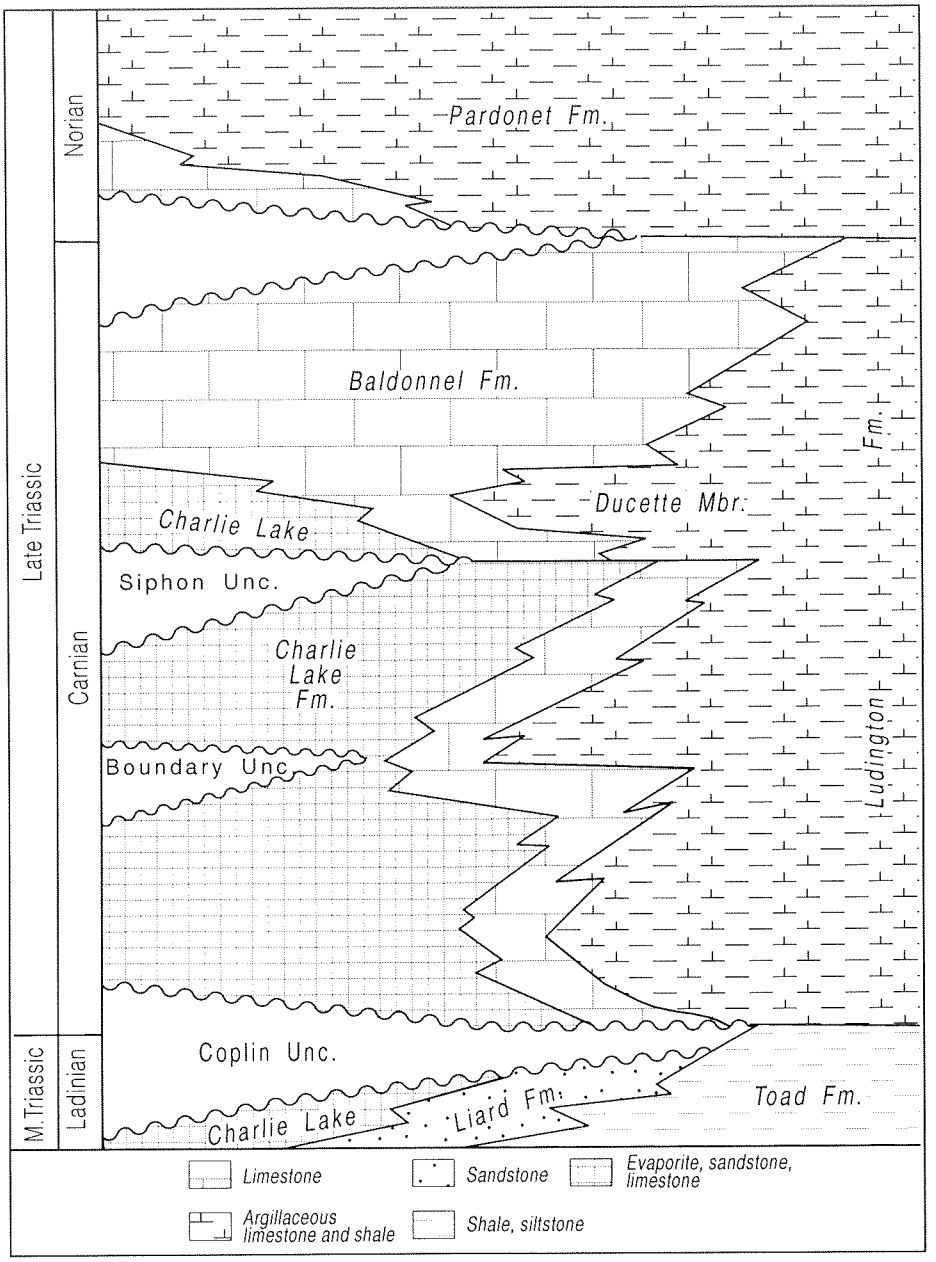

Figure 4. *Carnian stratigraphy, Peace River area.*

boundaries are thus interpreted to reflect plate tectonic reorganizations which induced widespread tectonic and eustatic changes.

The recognition, characterization and correlation of these sequence boundaries provide an excellent stratigraphic framework for facies analysis and for the predication of reservoirs, source rocks, and stratigraphic traps.

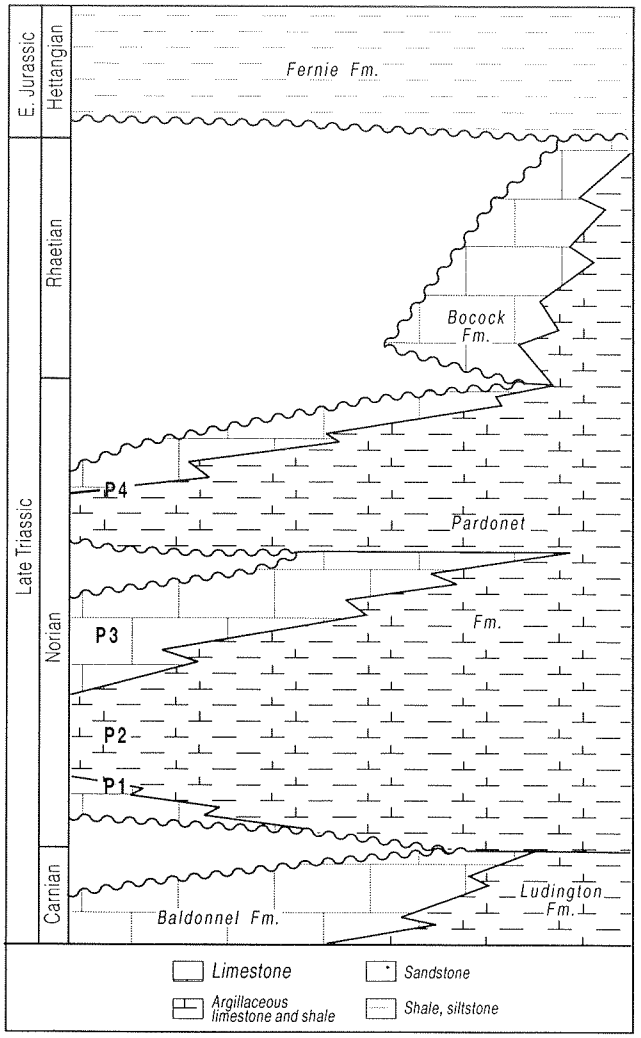

Figure 5. *Norian–Rhaetian stratigraphy, Peace River area.*

DEVONIAN STRATIGRAPHY OF THE ROCKY MOUNTAINS FROM GOLDEN TO HALFWAY RIVER, B.C.

H.H.J. Geldsetzer

Geological Survey of Canada, 3303-33rd Street N.W., Calgary, Alberta T2L 2A7

M.J. Shields

710A - 15th Street N.W., Calgary, Alberta T2N 2B2

INTRODUCTION

More than 50 sections were measured along the Rocky Mountain fold and thrust belt over a distance of about 700 km (Fig. 1). Exact coordinates, number of NTS sheet and a 'local name' referring to the nearest geographical marker on the corresponding NTS sheet are shown for each section on Table 1. Most of the sections are located within a northwest-trending band, about 350 km in length, straddling the Alberta/B.C. boundary. In this area, the provincial boundary more or less coincides with the northern perimeter of the West Alberta Ridge (WAR) which, after having followed a northwesterly trend to the south, swings to the northeast and joins the Peace River Uplift (PRU). Both the WAR and the PRU were prominent but largely passive highs during the Early and Middle Devonian and were gradually flooded during the Late Devonian (Morrow and Geldsetzer, 1988). This tectonic development is indicated by gradual onlap of Early and Middle Devonian sediments from the northwest against the northern perimeter of the WAR and PRU (Fig. 2).

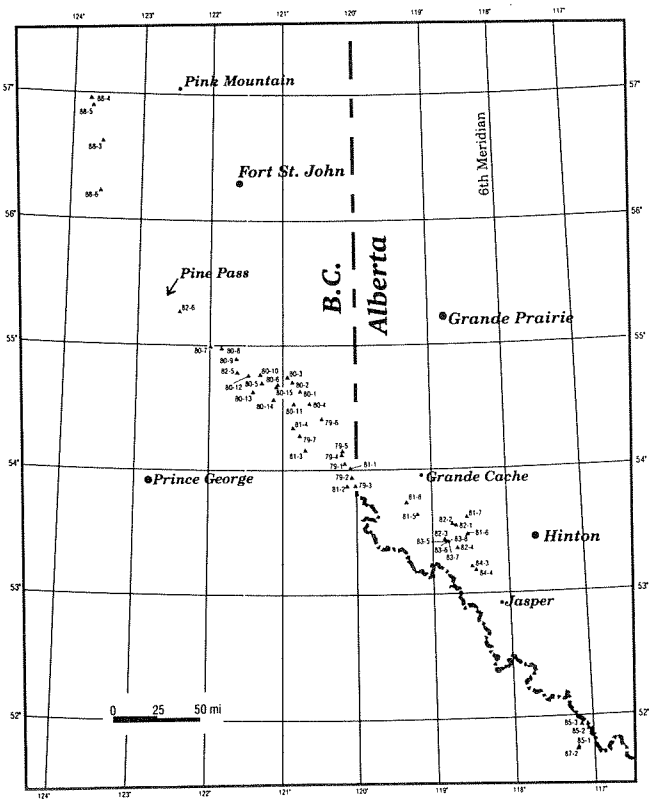

Figure 1. Location map.

Table 1

Geographic coordinates of measured sections

No.	Section	Easting	Northing	Latitude	Longitude	NTS Sheet	Local Name
1	79-1	686000	5993000	54.05	120.16	93 I/1E	St. Andrews Mt., BC
2	79-2	692600	5981000	53.94	120.07	93 H/16	Wallbridge Mt., BC
3	79-3	696000	5973500	53.87	120.02	93 H/16	Bastille Mt., BC
4	79-4	683200	6000700	54.12	120.20	93 I/1E	Mt. Hannington E, BC
5	79-5	683500	6004300	54.16	120.19	93 I/1E	Mt. Hannington N, BC
6	79-6	664400	6032400	54.41	120.47	93 I/8W	Mt. Belcourt, BC
7	79-7	645300	6016700	54.28	120.77	93 I/7W	Herrick Pass W, BC
8	80-1	644300	6056200	54.63	120.76	93 I/10W	Wapiti Lake N, BC
9	80-2	637300	6064000	54.71	120.87	93 I/10W	Bone Mt., BC
10	80-3	632800	6068400	54.75	120.94	93 I/10W	Kinuseo Creek, BC
11	80-4	653200	6045300	54.53	120.63	93 I/10E	Mt. Becker, BC
12	80-5	610300	6062400	54.70	121.29	93 I/11W	Monkman Lake NW, BC
13	80-6	624300	6061500	54.69	121.07	93 I/11E	Windy Peak, BC
14	80-7	564500	6094200	54.99	121.99	93 I/13W	Sentinel Peak N, BC
15	80-8	574300	6092600	54.98	121.84	93 I/13W	Mt. Dudzig N, BC
16	80-9	587600	6083600	54.89	121.63	93 I/13E	Sukunka River W, BC
17	80-10	608700	6070200	54.77	121.31	93 I/14	Hook Lake, BC
18	80-11	639100	6044700	54.53	120.85	93 I/10W	Wapiti Lake SW, BC
19	80-12	598400	6069200	54.76	121.47	93 I/14	Mt. Myhon SE, BC
20	80-13	603000	6054500	54.63	121.40	93 I/10W	Wapiti Lake NW, BC
21	80-14	621100	6048100	54.57	121.13	93 I/11E	Paxton Peak, BC
22	80-15	623100	6059500	54.67	121.09	93 I/11E	Murray River, BC
23	81-1	691000	5989000	54.02	120.08	93 I/1E	Mt. Ruth, BC
24	81-2	688900	5973100	53.87	120.13	93 I/16	Mt. Buchanan, BC
25	81-3	650800	6003900	54.16	120.69	93 I/2E	Ekusquin Mt., BC
26	81-4	639100	6023500	54.34	120.86	93 I/7W	Framstead Creek, BC
27	81-5	354800	5945800	53.64	119.20	83 E/11E	Winnifred Pass, Alta.
28	81-6	398100	5926200	53.48	118.54	83 E/7E	Eagle Nest Pass, Alta.
29	81-7	398200	5941700	53.62	118.54	83 E/10E	Planet Creek, Alta.
30	81-8	345600	5956800	53.74	119.34	83 E/11W	Kvassi Mt., Alta.
31	82-1	388400	5934500	53.55	118.68	83 E/10E	South Berland River, Alta.
32	82-2	385400	5936200	53.56	118.73	83 E/10E	Persimmon Creek, Alta.
33	82-3	377800	5922600	53.44	118.84	83 E/7W	Mount Perce, Alta.
34	82-4	388500	5914500	53.37	118.68	83 E/7W	Blue Creek, Alta.
35	82-5	588500	6071300	54.78	121.62	93 I/13E	Mt. Myhon W, BC
36	82-6	536300	6124900	55.27	122.43	93 / 8	Mt. Hunter, BC
37	83-5	381900	5919600	53.41	118.78	83 E/7W	Noonday Peak, Alta. (SE side of glacier)
38	83-6	381400	5920000	53.42	118.78	83 E/7W	Noonday Peak, Alta. (NW side of glacier)
39	83-7	380600	5920800	53.42	118.80	83 E/7W	Noonday Peak, Alta. (NW side of cirque)
40	83-8	380900	5920200	53.42	118.79	83 E/7W	Noonday Peak, Alta. (SE side of cirque)
41	84-3	400900	5897600	53.22	118.48	83 E/1	Mt. Strange NW, Alta.
42	84-4	404100	5894100	53.19	118.44	83 E/1	Mt. Strange SE, Alta.
43	85-1a	486200	5733600	51.76	117.20	82 N/14	Frigate Mt. E, BC
44	85-1b	485700	5767200	52.87	117.21	82 N/14	Frigate Mt. NE, BC
45	85-1c	485300	5733300	51.75	117.21	82 N/14	Frigate Mt. SE, BC
46	85-1d	486600	5731800	51.74	117.19	82 N/14	Frigate Mt. S, BC
47	85-2a	495400	5749500	51.90	117.07	82 N/14	Icefall Brook Canyon N, BC
48	85-2b	494200	5748000	51.88	117.23	82 N/14	Icefall Brook Canyon W, BC
49	85-2c	495300	5748700	51.89	117.07	82 N/14	Icefall Brook Canyon NW, BC
50	85-3	489500	5753500	51.93	117.15	82 N/14	Lyell Creek, BC
51	87-2a	485300	5732500	51.75	117.21	82 N/11	Frigate Mt. W, BC
52	87-2b	485900	5731500	51.74	117.20	82 N/11	Frigate Mt. SW, BC
53	88-3	465300	6275200	56.62	123.57	94 B/12	lake N of Lapierre Creek, BC
54	88-4	453800	6312600	56.96	123.76	94 B/13	Robb Lake NE, BC
55	88-5	455800	6306300	56.90	123.73	94 B/13	Robb Lake SE, BC
56	88-6	464300	6231400	56.23	123.58	94 B/4	Wicked River, BC

Three composite sections in the southeastern corner of the location map (Fig. 1), about 60 km north of Golden, B.C., are positioned on the southwestern flank of the WAR; four sections in the northwestern corner, the Halfway River map sheet, are near or at the western margin of the stable cratonic area.

STRATIGRAPHY

Lower Devonian

Lower and Middle Devonian sediments are represented by three distinct, unconformity-bounded sequences. The oldest and the middle sequence are characterized by dolomite (Muncho-McConnell Formation) and sandy dolomite (Stone Formation), apparently all shallow-marine and peritidal in nature. The Muncho-McConnell Formation is virtually unfossiliferous except for some very rare brachiopods suggesting a latest Silurian (Pridolian) and earliest Devonian (Gedinnian) age; the Stone Formation has been assigned to the last stage of the Early Devonian (Emsian) on the basis of conodonts and brachiopods. Each formation is about 450 m thick and both sequences thin rapidly against the West Alberta Ridge (WAR) (Fig. 2). Basal sandstones mark the lower contacts, only a few meters thick for the Muncho-McConnell Formation, but up to 59 m for the Stone Formation. In the Halfway River area, 250 km northwest of the WAR and Peace River Uplift (PRU), the contact between the two formations is difficult to identify because the basal clastics of the Stone Formation are very thin or absent.

The two sequences form a massive carbonate platform which is cut by a 30 km wide embayment, the Ospika Embayment (Thompson, 1989), in the northwestern Halfway River area. The embayment extends eastward from the Liard Basin to the west and forms a half-graben with thick basin fill sediments along the northern side and thin sediments along the southern margin. The basin fill sediments are predominantly dark anoxic siltstones with a minimum thickness of 457 m (Thompson, 1989). Fossil assemblages from the siltstones indicate that they are equivalent to the Muncho-McConnell and Stone formations. In the upper part of the siltstones, carbonate blocks occur (Section 88-5) probably derived from the adjacent Muncho-McConnell/Stone platform (Section 88-4).

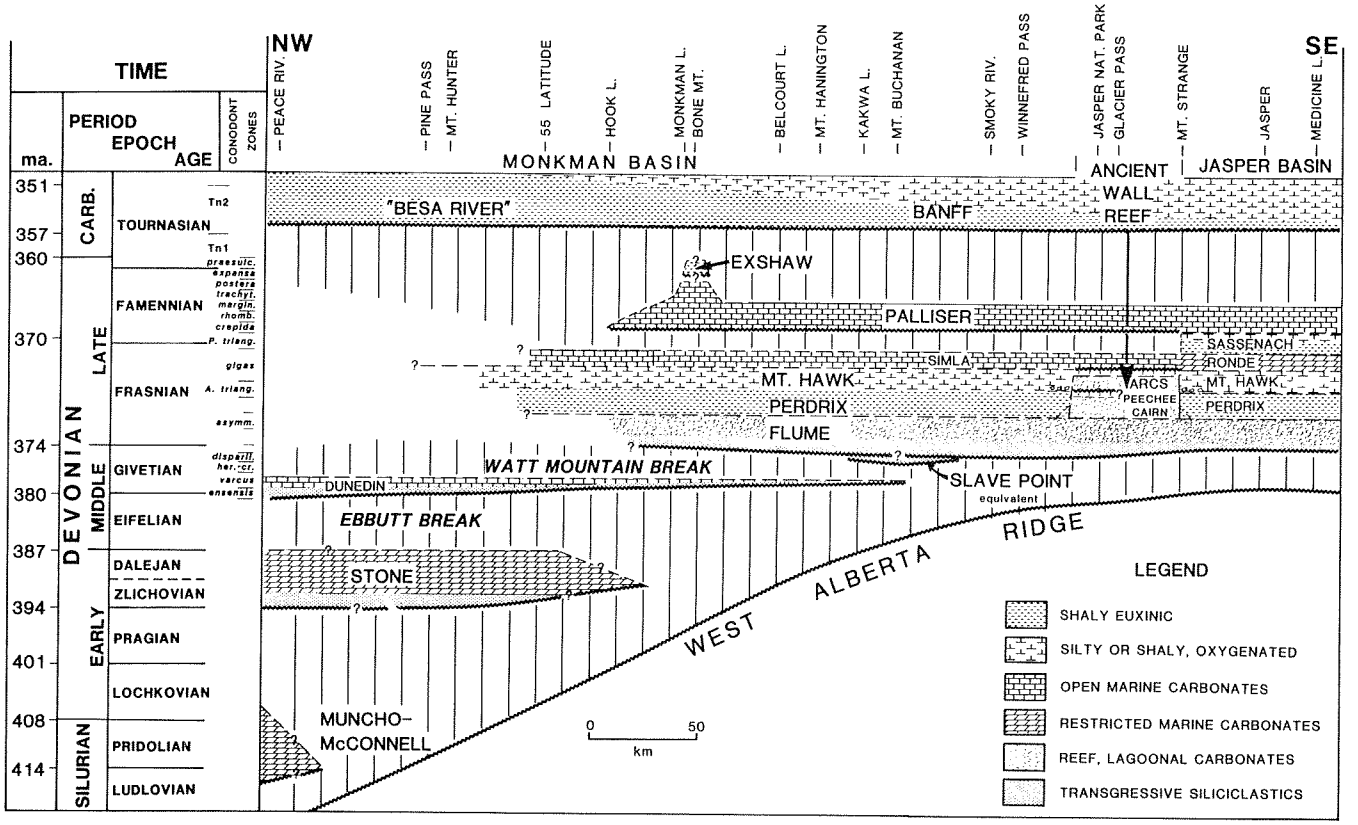

Figure 2. *Devonian time-stratigraphy west of the Peace River Arch and along the northwestern paleosople of the West Alberta Ridge.*

Middle Devonian

The Middle Devonian sequence is represented by open-marine carbonates of the Dunedin Formation. Basal clastics indicate easterly directed paleocurrents suggesting the onset of tectonic activity to the west which increased during the Late Devonian and became very prominent during the Carboniferous. An easterly paleoflow is also supported by current directions from a thick (up to 360 m) quartzose sandstone unit which filled the upper part of the Ospika Embayment (Section 88-5). The sandstone unit is probably equivalent to the lower or entire Dunedin Formation which marks the top of the carbonate platform on both sides of the Ospika Embayment (Sections 88-5 and 88-3). Both the sandstone unit and the Dunedin Formation are overlain by Upper Devonian Besa River black shales.

The Dunedin Formation measures up to 300 m in thickness and pinches out at Mt. Buchanan (Section 81-2) (Fig. 2). The sequence is probably late Eifelian to middle Givetian in age and equivalent to the Keg River Formation to the east. A 462 m thick section occurs in the southern Halfway River area (Section 88-6) within an area occupied by the projected western extension of the Keg River/Presquile barrier reef. It is likely that the upper 192 m of the Dunedin Formation are equivalent to the upper reef complex of the barrier reef, also referred to as the Sulphur Point Formation.

In contrast to the Lower Devonian carbonate sequences, the Middle Devonian carbonate sequence continues to the south along the Golden Embayment which parallels the southwestern flank of the WAR (Morrow and Geldsetzer, 1988). Some of the thick clastics at the base of the Upper Devonian succession of southeastern B.C. (Sections 85-1, 2, 3; 87-2) may be equivalent to Middle Devonian units of the Golden Embayment (Harrogate, Cedared and Burnais formations).

Upper Devonian

Frasnian carbonate platform, reef complexes and interreef basin fill (Flume, Cairn, Peechee, Perdrix, lower Mt. Hawk)

Upper Devonian sediments occur in all areas examined in this report. With the onset of the Upper Devonian, the West Alberta Ridge (WAR) was finally flooded and extensively covered by sediments of the Fairholme Group (Flume to Ronde/Simla) with thicknesses ranging from 350 to 550 m depending upon the location on top of or on the flanks of the WAR.

The topographic relief of the WAR is documented by the thickness of the initial sediments, the carbonate platform of the Flume Formation, ranging from 55 m above the WAR to 160 m along the flanks. The Flume Formation gradually pinches out to the northwest of the WAR (Fig. 2). The basal carbonate platform served as a foundation for the Frasnian reef complexes such as the Ancient Wall Reef Complex (Sections 82-1 to 4; 83-6, 7, 8; 84-3, 4) and the western part of the Southesk-Cairn Reef Complex (Sections 85-2, 3). The reef buildups are 280 m (Sections 82-1, 2) and 360 m (Sections 85-2, 3) thick, respectively. Deposition was continuous from the Flume platform through the lower reef (Cairn) into the lower part of the upper reef (Peechee). Exposure surfaces become very prominent in the upper Peechee and culminate in a major exposure surface at the top of the Peechee, particularly evident in the Ancient Wall Reef Complex (Section 83-5). Solution breccias were produced and probably represented the major contributor of massive debris flows (Section 83-6). Anoxic sediments of the Perdrix Formation (Duvernay of the subsurface) accumulated in the interreef areas during the growth of the reef complexes. Oxygenated sediments of the Mt. Hawk Formation (Ireton of the subsurface) infilled the remaining topography of the reef domain. Both formations contain a substantial amount of terrigenous clastics. To the northwest of the WAR, in the Monkman Basin, the two formations are difficult to differentiate due to the predominantly dark colour of the sediments. The combined thickness ranges from 150 to 300 m.

Frasnian post-reef carbonate banks (Arcs, Grotto, upper Mt. Hawk, Ronde, Simla)

Renewed carbonate deposition started above the former reef complexes with shallow-marine carbonate banks (Arcs, Grotto) prograding outward into adjacent basinal areas as carbonate slope deposits (upper Mt. Hawk Formation) which contain locally bioherms and/or biostromes (Section 81-5). Further out into the Monkman Basin, the carbonate slope sediments grade into nodular limestone and finally into calcareous shale. This interval is equivalent to the Nisku Formation in the subsurface.

Carbonate deposition was again interrupted by a hiatus, affecting only the area of the former reef domain whereas basinal areas continued to be infilled. Renewed deposition above the former reef domain started with easterly derived silts (Calmar of the subsurface) which can be traced into basinal areas. The silts are only a few metres thick and grade upsection into carbonates which are largely peritidal (Ronde) to

the south of the Jasper Basin and more open-marine to the north (Simla) and east (Graminia of the subsurface). Along the northern margin of the Jasper Basin, the Simla Formation consists locally of small overlapping stromatoporoid reefs (Section 82-3). In contrast to the underlying Arc/Grotto interval, the Simla carbonate bank continues to the northwest across the Monkman Basin indicating that the basin had been filled with sediments (Geldsetzer, 1982). The Simla Formation retains a very uniform thickness of about 60 to 70 m over a distance of about 250 km with its northernmost exposure at Section 80-6. The light grey colour and its uniform thickness make the Simla Formation the most visible horizon of the Devonian succession throughout the Monkman Basin.

Famennian clastics and carbonate shelf (Sassenach, Palliser)

The Sassenach Formation is a massive clastic wedge derived from a westerly source. It filled the Jasper Basin and the Sassenach Basin to the south with more than 300 m of siliciclastics during the earliest Famennian (*P. triangularis* conodont zone). Only the upper part of the formation is present in sections bordering the two basins (Sections 84-3, 4 and Sections 85-1, 2, 3). The reef domain east of the basins and the Monkman Basin to the north were above base-level during this time and, thus, no sediments were preserved.

Carbonate deposition (Palliser Formation; Wabamun Formation of the subsurface) was re-established on a regional scale during the next Famennian biozone (*P. crepida* conodont zone). The sediments consist of pelletal mudstones and occasional pelletal grainstones suggesting mostly subwavebase conditions. Thicknesses range from about 200 m above the former reef domain to 300 m in the southern Monkman Basin (Sections 79-6, 80-1, 4) and increase abruptly to 530 m in the Mt. Hannington area (Section 79-4, 5). A similar increase was measured in an area north of Fernie, B.C. The Palliser Formation thins rapidly in the northern Monkman Basin (only 36 m at Section 80-15) due to erosional truncation prior to deposition of the Lower Carboniferous (Tournaisian) Besa River/Banff formations.

Upper Devonian basinal sediments (Besa River Formation)

North of 55° latitude no Upper Devonian carbonate units (Flume, Simla, Palliser) have been identified. A small exposure of calcareous shale at Pine Pass (Fig. 1) yielded Frasnian brachiopods. It appears that all Upper Devonian units north of 55° latitude are represented by an expanded Besa River Formation. This is supported by the stratigraphic relationships of the northern sections where Besa River black shales abruptly overlie carbonates of the Dunedin Formation (Sections 88-3, 4, 6) and quartzose sandstones (Section 88-5) which are mostly likely equivalent to the Dunedin Formation. Conodonts from the base of the Besa River Formation at Section 88-4 are early Frasnian in age (i.e. time-equivalent to the Flume Formation interval of the reef domain to the south). The black shales of the Besa River Formation measure several hundred metres in thickness and can be assumed to represent the entire Late Devonian.

REFERENCES

Geldsetzer, H.H.J.
1982: Depositional history of the Devonian succession in the Rocky Mountains southwest of the Peace River Arch. *In* Current Research, Part C, Geological Survey of Canada, Paper 82-1C, p. 55–64.

Morrow, D.W. and Geldsetzer, H.H.J.
1988: Devonian of the eastern Canadian Cordillera. *In* Devonian of the world, N.J. McMillan, A.F. Embry and D.J. Glass (eds.). Canadian Society of Petroleum Geologists, Memoir 14, p. 85–121.

Thompson, R.I.
1989: Stratigraphy, tectonic evolution and structural analysis of the Halfway River map area (94B), northern Rocky Mountains, British Columbia. Geological Survey of Canada, Memoir 425, 119 p.

STRATIGRAPHIC ARCHITECTURE OF THE CAMPANIAN BELLY RIVER (JUDITH RIVER) GROUP, SOUTHERN ALBERTA PLAINS, SURFACE AND SUBSURFACE

A.P. Hamblin

Geological Survey of Canada, 3303-33rd Street N.W., Calgary, Alberta T2L 2A7

ABSTRACT

The Belly River (Judith River) Group of the southern Plains is underlain by marine shale of the Lea Park Formation and overlain by marine shales of the Bearpaw Formation (Fig. 1). It represents a thick and distinct clastic wedge of predominantly nonmarine and marginal marine deposits, and comprises, in ascending order, the Foremost, Oldman and Dinosaur Park formations (Fig. 2). Each of these units is characterized by a distinct depositional geometry, tectono-stratigraphic implication and hydrocarbon distribution (Fig. 3).

The Foremost Formation is an eastward-thinning wedge of downlapping shoreline-related facies tracts, backed by thick aggradational fluvial deposits. "Basal Belly River" shoreline tracts can be divided into eight

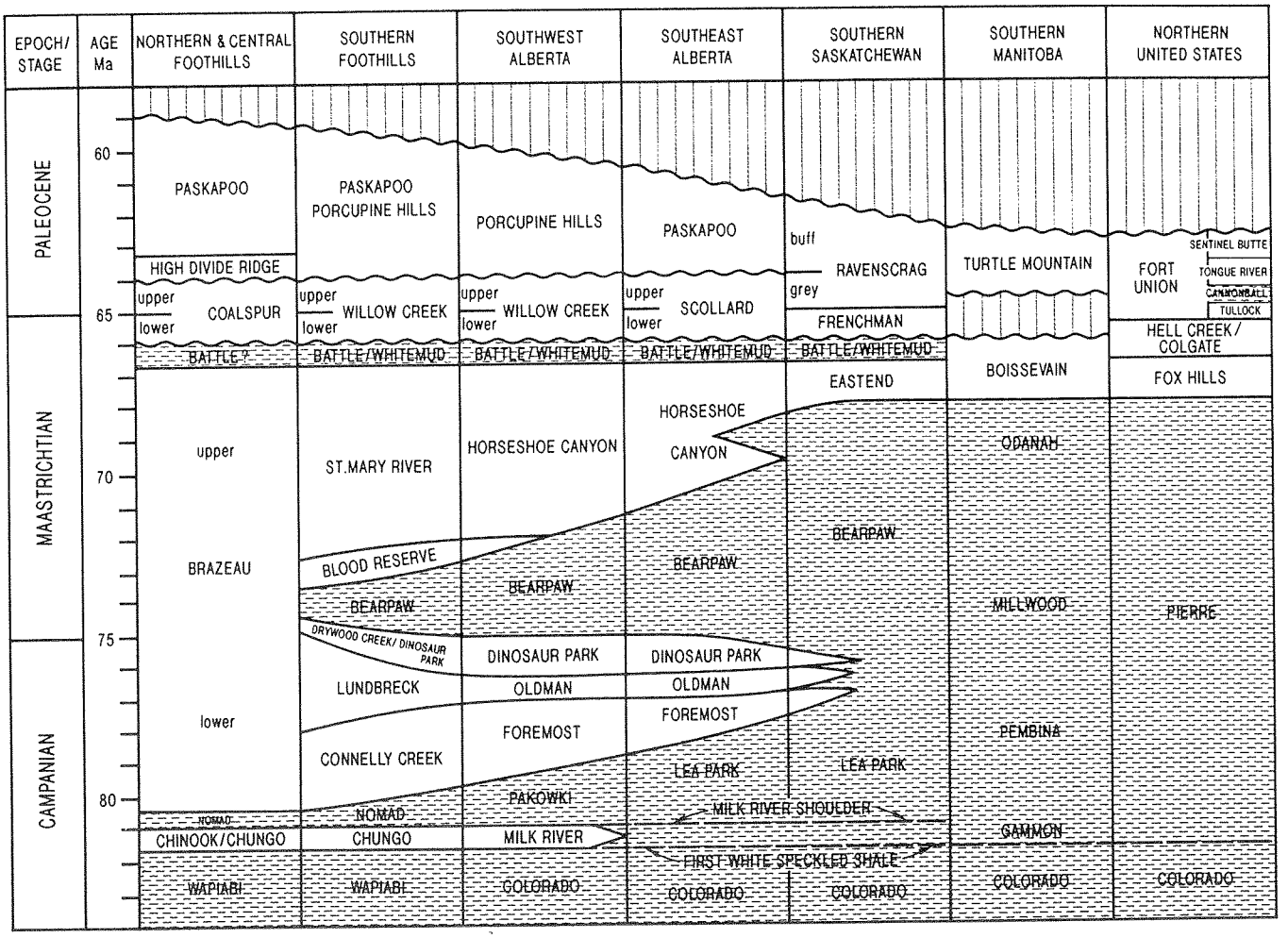

POST - COLORADO SUPERGROUP STRATIGRAPHY

Figure 1. Post-Colorado Supergroup stratigraphy.

stacked composite progradational cycles, separated by marine flooding surfaces, each of which downlaps and shales-out to the east. The locus of sandy deposition of successive cycles is located eastward of, and stratigraphically higher than, the preceding one, indicating that the balance between sediment supply and foreland subsidence allowed eastward, but non-continuous, progradation over more than 400 km into western Saskatchewan during 3–4 Ma.

The Oldman Formation generally thins to the north and northeast and consistently includes the lower "Comrey sandstone" and the upper "siltstone unit". The Comrey sandstone lies on a regional erosional surface and is dominated by linear SW/NE-oriented sandy incised valley fill trends (northeastward paleoflow) composed of stacked lenticular low-sinuosity fining-upward channel units. The overlying siltstone unit is composed of thinly interbedded noncalcareous mudstone and fine sandstone with rooting and pedogenic horizons. Minor evidence from the southeast corner of Alberta suggests it is associated with a minor poorly-known transgression from the southeast. The Oldman sequence may represent an increase in foreland subsidence reflected as an increase in accommodation space, slowing of sedimentation rate and increase in vertical aggradation.

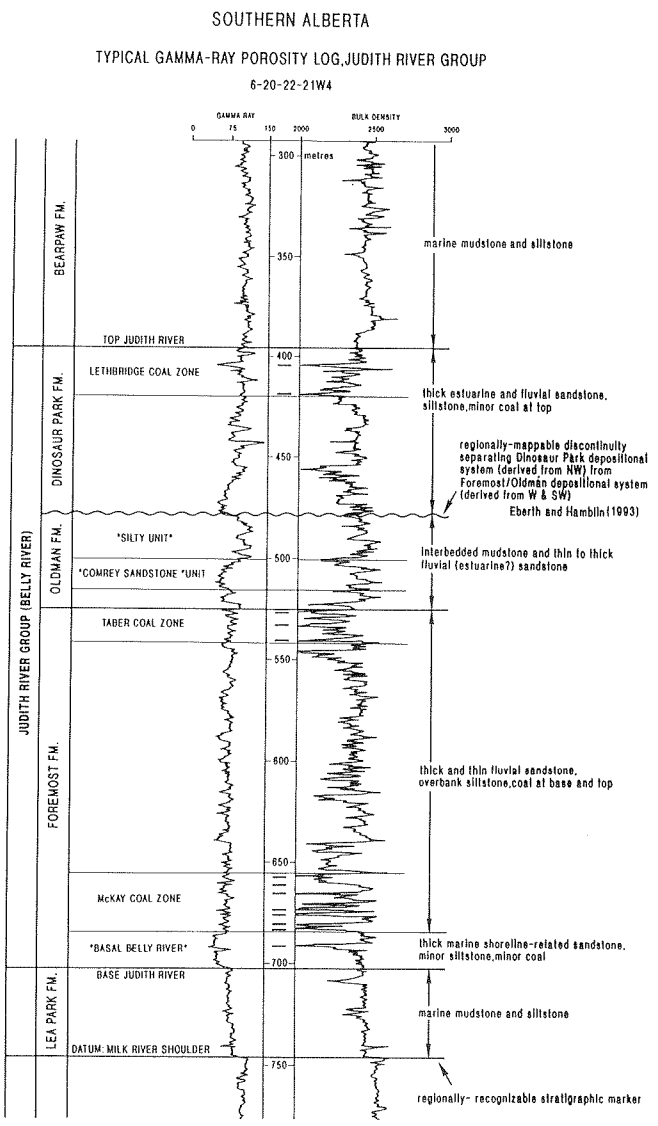

Figure 2. *Southern Alberta typical gamma-ray porosity log, Judith River Group.*

The Dinosaur Park Formation, which lies on a regionally-defineable surface, thins to the southeast and is characterized at its base by sharp-based linear WNW/ESE-trending incised valley fills (east or southeastward paleoflow) comprising thick multi-storied, high-sinuosity fining-upward channel units. These are overlain by interbedded sandstone and siltstone, followed by the Lethbridge Coal Zone and the marine Bearpaw. This regionally consistent upward sequence is interpreted to represent increasing foreland subsidence in southern Alberta, presaging the Bearpaw marine transgression from the southeast.

CONCLUSIONS AND TECTONO-STRATIGRAPHIC INFERENCES

Foremost Formation

1. The Basal Belly River units comprise eight stacked, regionally-identifiable, progradational Cycles, each dominated by shoreline-related sandstones. Each Cycle is actually a composite of several lesser parasequences which typically include reservoirs of both shoreface and channel facies.

2. The locus of clean sandstone deposition of each successive Cycle is located eastward of, and stratigraphically higher than, that of the preceding one: therefore, each Cycle has a specific mapped area of thick shoreline-related clean sandstone, encloses a specific set of gas pools, and has potential for further gas pool discoveries of small to moderate size.

3. Through the later stages of Basal Belly River deposition there was an increasing rate of base level rise/basin subsidence in the Foreland Basin of southern Alberta. This resulted in the vertical stacking of later Basal Belly River shoreline-related

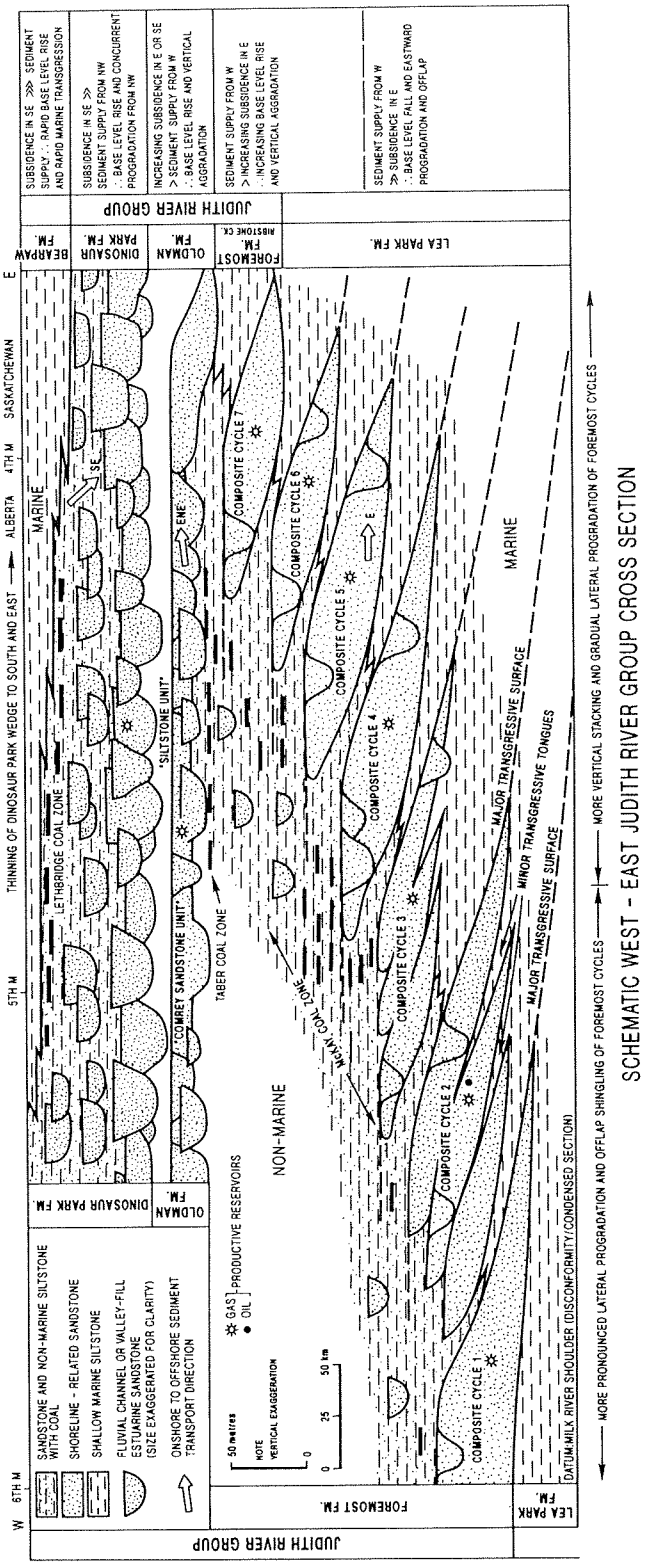

Figure 3. *Schematic west-east Judith River Group cross-section.*

sandstone Cycles in the vicinity of the Alberta–Saskatchewan border.

Oldman Formation

1. The Oldman Formation is thickest to the south and southwest (over 125 m), and gradually thins to the north and northeast (0–40 m), due to both depositional thinning and to increased erosional removal beneath the overlying Dinosaur Park Formation.

2. Two distinct, but previously unrecognized, lithological units are regionally definable: the lower sandstone-dominated Comrey unit, and the upper mudstone-dominated "siltstone unit". The Comrey Sandstone includes SW/NE-oriented linear sandstone-dominated trends, which are sharp-based, and composed of multi-storied individual fining-upward channel sandstone units, interpreted as composite incised valley fills.

3. The regionally consistent upward sequence of Comrey sandstone, to siltstone unit (both supplied from the southwest), to influx of Dinosaur Park deposits from the northwest is interpreted to represent a period of increasing basin subsidence in southern Alberta, possibly presaging the later Bearpaw marine transgression from the southeast.

Dinosaur Park Formation

1. The Dinosaur Park Formation is thickest to the north and northwest (over 125 m), and gradually thins to the south to zero, due to depositional thinning. Complementary thickening of the Oldman Formation results in uniform thickness of strata between the top of the Foremost Formation and the base of the Bearpaw Formation. Sediments of the Dinosaur Park were derived from the north or northwest.

2. Thickness variation of the Dinosaur Park is characterized by relatively narrow, linear sandstone-dominated trends, generally oriented WNW/ESE, which fan out from locii near Rocky Mountain House and Calgary, and result primarily from localized erosional valley-fill geometry at the base of the formation. These overlie a regional discontinuity surface which locally includes erosion of the underlying Oldman Formation. Linear trends are sharp-based, and are overlain by multi-storied

individual fining-upward channel sandstone units, interpreted as composite incised valley fills.

3. The regionally consistent upward sequence of locally erosional base, to thick multi-storied sandstones, to interbedded sandstone and siltstone, to Lethbridge Coal Zone, to Bearpaw marine transgression is interpreted to represent a period of increasing basin subsidence in southern Alberta, possibly presaging the later Bearpaw marine transgression from the southeast.

REFERENCES

Crockford, M.B.B.
1949: Oldman and Foremost Formations of southern Alberta. American Association of Petroleum Geologists Bulletin, v. 33, p. 500–510.

Dawson, F.M., Evans, C.G., Marsh, R., and Richardson, R.
1994: Uppermost Cretaceous and Tertiary strata of the Western Canada Sedimentary Basin. *In* Geological Atlas of the Western Canada Sedimentary Basin, G.D. Mossop and I. Shetsen (compilers). Canadian Society of Petroleum Geologists and Alberta Research Council, p. 387–406.

Dowling, D.B.
1917: The southern plains of Alberta. Geological Survey of Canada, Memoir 93, 200 p.

Jerzykiewicz, T. and Norris, D.K.
1994: Stratigraphy, structure and syntectonic sedimentation of the Campanian "Belly River" clastic wedge in the southern Canadian Cordillera. Cretaceous Research, v. 15, p. 367–399.

McLean, J.R.
1971: Stratigraphy of the Upper Cretaceous Judith River Formation in the Canadian Great Plains. Saskatchewan Research Council, Geology Division, Report No. 11, 96 p.

Nauss, A.W.
1944: Cretaceous stratigraphy of Vermilion area, Alberta, Canada. American Association of Petroleum Geologists Bulletin, v. 29, p. 1605–1629.

Ogunyomi, O. and Hills, L.V.
1977: Depositional environments, Foremost Formation (Late Cretaceous), Milk River area, southern Alberta. Bulletin of Canadian Petroleum Geology, v. 25, p. 929–968.

Power, B.A.
1993: Sedimentology and allostratigraphy of the Upper Cretaceous (Campanian) Lea Park – Belly River transition in central Alberta, Canada. Unpub. PhD thesis, McMaster University, 411 p.

Powers, D.L.
1931: Subsurface study of pale beds and Foremost Formation in Lethbridge-Brooks area of southern Alberta. American Association of Petroleum Geologists Bulletin, v. 15, p. 1197–1213.

Putnam, P.E.
1993: A multidisciplinary analysis of Belly River-Brazeau (Campanian) fluvial channel reservoirs in west-central Alberta, Canada. Bulletin of Canadian Petroleum Geology, v. 41, p. 186–217.

Russell, L.S. and Landes, R.W.
1940: Geology of the southern Alberta plains. Geological Survey of Canada, Memoir 221, 223 p.

Shaw, E.W. and Harding, S.R.L.
1949: Lea Park and Belly River Formations of east-central Alberta. American Association of Petroleum Geologists Bulletin, v. 33, p. 487–499.

Shouldice, J.R.
1979: Nature and potential of Belly River gas sand traps and reservoirs in western Canada. Bulletin of Canadian Petroleum Geology, v. 27, p. 229–241.

Slipper, S.E. and Hunter, H.M.
1931: Stratigraphy of Foremost, Pakowki and Milk River Formations of southern plains of Alberta. American Association of Petroleum Geologists Bulletin, v. 15, p. 1181–1196.

Stott, D. F.
1984: Cretaceous sequences of the Foothills of the Canadian Rocky Mountains. *In* The Mesozoic of Middle North America, Canadian Society of Petroleum Geologists, D.F. Stott and D.J. Glass (eds.). Memoir 9, p. 85–107.

Williams, G.D. and Burk, C.F.
1964: Upper Cretaceous. *In* Geological History of Western Canada, R.G. McCrossan and R.P. Glaister (eds.). Alberta Society of Petroleum Geologists, p. 169–189.

Wood, J.M.
1989: Alluvial architecture of the Upper Cretaceous Judith River Formation, Dinosaur Provincial Park, Alberta, Canada. Bulletin of Canadian Petroleum Geology, v. 37, p. 169–181.

PUBLICATIONS FROM THIS STUDY

Eberth, D.A. and Hamblin, A.P.
1993: Tectonic, stratigraphic and sedimentologic significance of a regional discontinuity in the upper Judith River Formation (Belly River wedge) of southern Alberta, Saskatchewan and northern Montana. Canadian Journal of Earth Sciences, v. 30, p. 174–200.

Hamblin, A.P.

1993: Subsurface tops and thickness data for "Basal Belly River" progradational cycles, Judith River Group, southern Alberta. Geological Survey of Canada, Open File 2752, 40 p.

1994a: The Comrey Sandstone (Oldman Formation) of the Upper Cretaceous Judith River Group (Belly River wedge), subsurface of southern Alberta. Geological Survey of Canada, Open File 2796, 17 p.

1994b: Subsurface tops and thickness data for Comrey Sandstone (Oldman Formation), Judith River (Belly River) Group, southern Alberta. Geological Survey of Canada, Open File 2809, 36 p.

1994c: The Dinosaur Park Formation of the Upper Cretaceous Judith River (Belly River) Group, subsurface of southern Alberta. Geological Survey of Canada, Open File 2831, 17 p.

1994d: Subsurface tops and thickness data for Dinosaur Park Formation, Judith River (Belly River) Group, southern Alberta. Geological Survey of Canada, Open File 2833, 27 p.

Hamblin, A.P., and Abrahamson, B.

1993: Offlapping progradational cycles and gas pool distribution in the Upper Cretaceous "Basal Belly River" sandstones, Judith River Group, southern and central Alberta. Geological Survey of Canada, Open File 2672, 19 p.

A THREE PART SEISMIC STRATIGRAPHY FOR PACIFIC CENOZOIC SEDIMENTS: RESULTS FROM ODP LEG 145, YOKOHAMA TO VICTORIA

T.S. Hamilton

Pacific Geoscience Centre, Geological Survey of Canada
P.O. Box 6000, Sidney, British Columbia V8L 4B2

This poster paper presents selected seismic data acquired on board the JOIDES Resolution during the site occupancy surveys of Ocean Drilling Program (ODP) Leg 145 (north Pacific transect) July-September 1993. High resolution, digital, single-channel seismic profiles provide a regional stratigraphic context for seven drill-sites (881-887) from four locations in the North Pacific. The seismic thickness of the sedimentary section varied from >1 second two way travel-time (s TWT) on the Wayne and Detroit seamount platforms in the northern Emperor Seamount Chain to <0.1 s TWT at the abyssal sea floor Sites 885/886 near the Chinook Trough. The 1 ms data were processed with SIOSEIS receiving mute, deconvolution, gain recovery, and time-varying filters to enhance reflections and correlate to synthetic seismograms generated from downhole logs and physical properties data. The reflection sequence at each site was correlated to the lithostratigraphy and impedance contrasts caused by density and velocity variations with an average mistie of about 3 m over several hundred meters. A three part seismic character was recognized at all locations. The uppermost glacial- and ash-influenced Pliocene–Pleistocene section had high-frequencies and spatial variability characteristic of enhanced hemipelagic sedimentation. Miocene diatom oozes dominate the draping and acoustically transparent middle section. Alternating intervals with discontinuous high-frequency reflections and more widely correlated moderate-amplitude reflections appear as the high-cut and gain are increased. These correspond to alternating intervals of greater and lesser variability in the physical properties. The basal sedimentary section tends to be Paleogene and is characterized by moderate to strong reflections that lap and dip with respect to local basement relief and show evidence of bottom-current influence and downslope slumping and reworking. These near-basement lithologies include claystone, chalk, altered ash and sediment-sill complexes.

The seismic stratigraphy at Site 881 on the Zenkevich rise has folds, unconformities, and faults that cut to the top of the section and show tectonic reactivation on the approach to the Kurile Trench. High-latitude seamount platforms like those sampled by the Detroit sites (882-884) and by Site 887 on the Murray Seamount show great thicknesses and fast rates of middle Tertiary sedimentation. From the high-resolution seismic stratigraphy, the middle Tertiary biosiliceous ooze offers the best prospect for investigations of paleoclimatic and oceanography cyclicity (Figs. 1, 2).

Across the north Pacific, the seismic stratigraphy as calibrated at sites 881 through 887 has a distinctive three-part character. The uppermost seismic facies contains a series of high-frequency reflections that correspond to density and lithology variations in Pliocene–Pleistocene, distal and bathyal, glaciomarine sediments. Tectonic reactivation off the Zenkevitch Rise locally amplifies this part of the section, calibrating the age of the sediment tongue extending offshore from the Kuril Margin (Jacobi and Hayes, 1989; Ludwig and Houtz, 1979). Site 881 gives the best high resolution record of this glacially and volcanically influenced Pliocene–Pleistocene section, and serves as an analog for other high latitude seafloor sites that are influenced by a nearby continental margin.

The middle seismic facies of diatom ooze exhibits drape of underlying units and is only faintly reflective or nonreflective. This facies is well developed seen at the Detroit-Northern Emperor (Lonsdale et al., 1993) sites 882 and 883, the Meiji Drift (Scholl et al., 1977) site 884 and Murray seamount (Bornhold et al., 1989) site (887), where diatom ooze is the dominant sediment. Gain recovery and spiking deconvolution on the processed sections reveal intermittent packages of fine-scale weak reflectors that correlate to slight fluctuations in the density of the diatom ooze. These types of cyclic reflectors are an order of magnitude weaker than those seen in the carbonate oozes of the mid-equatorial Pacific (Bloomer et al., 1994; Mayer, 1991) but, at this latitude, have to little offer in terms of

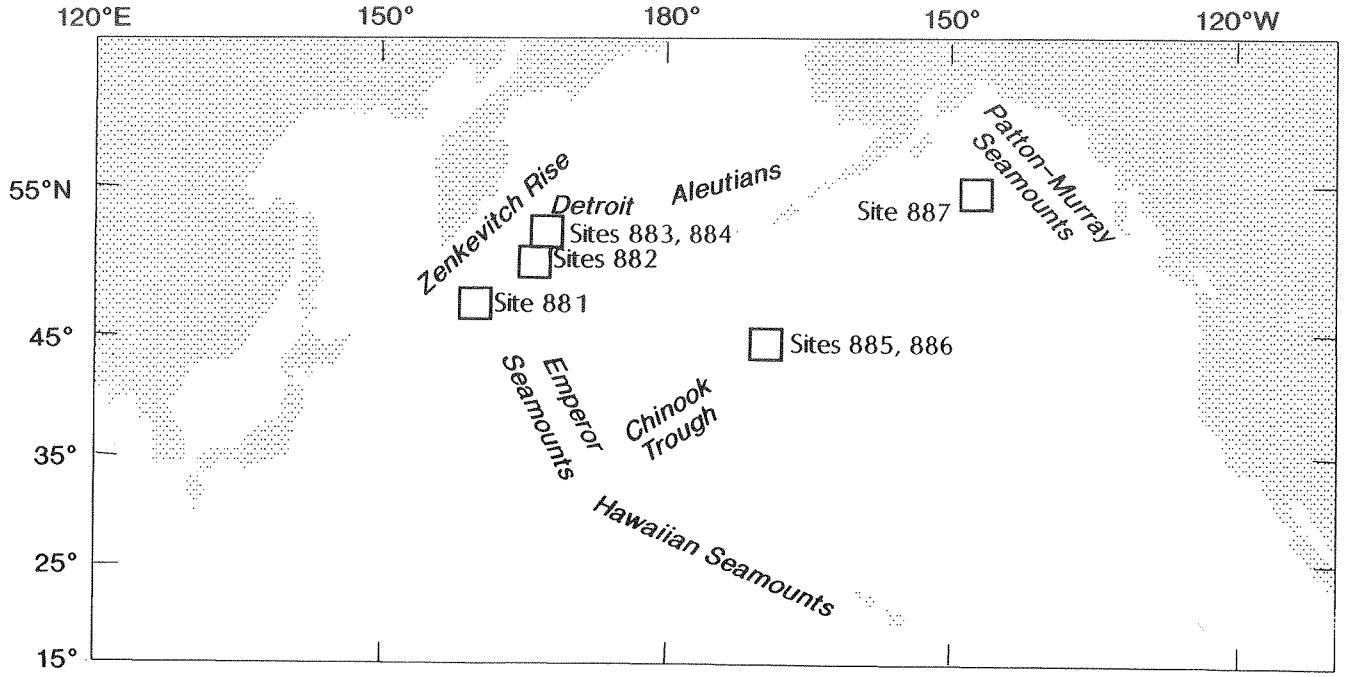

Figure 1. *Location of seismic lines and drill-sites on Leg 145. Boxes mark the location of the drill-sites and seismic profiles shown. Locations of prominent geographic features are labelled for reference.*

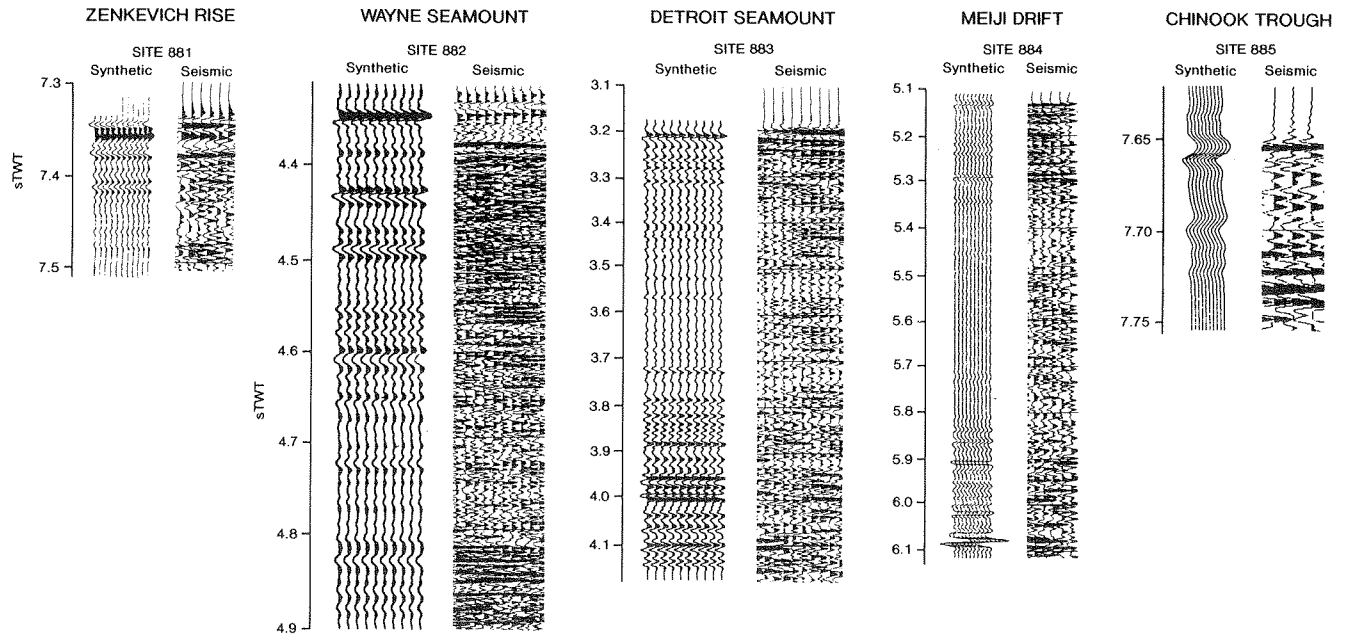

Figure 2. *Synthetic seismograms and processed digital traces near well sites for sites 881, 882, 883, 884 and 885. All vertical scales are annotated in seconds of two-way travel time (sTWT). Synthetic seismograms were calculated from physical properties measurements and a source function digitized from an 80 cu. in. water gun recorded on the* ***Thomas Washington****. Digital seismic traces were filtered back, compared to the seismic profiles, to match the frequency content of the synthetics.*

correlatable cyclic stratigraphy. This middle Tertiary part of the section and underlying units show signs of tectonic deformations that long postdate crustal formation as well as provide evidence of intraplate deformation.

The basal seismic facies are strongly reflective, comparable to the top of the section but at lower frequencies. Their seismic stratigraphy resembles slightly sedimented ridge crest areas like those described by Rohr and Schmidt (1994). These units are unconformable, contain slumps, and show a sense of lap that is highly variable with only local continuity. These facies are best represented on this transect at the deflated abyssal Sites 885/886 near the Chinook Trough.

Recognizing this distinctive sequence of 3 seismic stratigraphic facies can help to calibrate the age of Middle and Upper Tertiary sediments elsewhere in the north Pacific basin. The style of stratigraphic processing utilized to enhance the weakly reflective mid section diatom oozes, serves to bring out correlatable character and cyclic stratigraphy related to paleoceanographic depositional controls and climate forcing.

REFERENCES

Bloomer, S.F., Mayer, L.A., and Moore, T.C.
1994: Seismic stratigraphy of the eastern equatorial Pacific ocean: Paleoceanographic implications. *In* Proceedings ODP, Sci., N.G. Pisias, L.A. Mayer, and T.R. Janecek et al. (eds.). Results, 138, College Station, TX (Ocean Drilling Program).

Bornhold, B.D., Currie, R.G., and Sawyer, B.
1989: Patton-Murray Seamount Group: 3 Maps: Bathymetry, Magnetic Anomaly, Sediment Thickness, 1:250,000. Geological Survey of Canada, Open File 2075.

Hamilton, T.S.
1995: The seismic stratigraphy of Cenozoic sediments from North Pacific seamount platform and deep sea floor drill sites: Leg 145. *In* Proc. ODP. Sci., Results 145, D.K. Rea, I.A. Basov, D.V. Scholl, and J. Allen (eds.). College Station, TX (Ocean Drilling Program), in press.

Jacobi, R.D. and Hayes, D.E.
1989: Sedimentary effects of interplay between the Kuroshio extension and Pacific Plate motions. Geological Society of America Bulletin., v. 101, p. 549–560.

Lonsdale, P., Dieu, J., and Natland, J.
1993: Post Erosional Volcanism in the Cretaceous part of the Hawaiian Hotspot Trail. Journal of Geophysical Research, v. 3, p. 4081–4098.

Ludwig, W.J. and Houtz, R.E.
1979: Isopach map of Sediments in the Pacific Ocean Basin and marginal sea basins. American Association of Petroleum Geologists, Map Ser. 647.

Mayer, L.A.
1991: Extraction of high-resolution carbonate records for paleoclimatic reconstruction. Nature, v. 352, p. 148–150.

Rea, D.K., Basov, I.A., Janacek, T.R., Palmer-Julson, A., et al.
1993: Proc. ODP, Init. Repts., 145: College Station, TX (Ocean Drilling Program).

Rohr, K.M.M. and Schmidt, U.
1994 Seismic structure of Middle Valley near Sites 855-858, Juan de Fuca Ridge. *In* Proc. ODP. Sci., Results 139:3-17, M.J. Mottl, E.E. Davis, A.T. Fisher and J.F. Slack (eds.). College Station, TX (Ocean Drilling Program).

Scholl, D.V., Hein, J.R., Marlow, M., and Buffington, E.C.
1977: Meiji sediment tongue: North Pacific evidence for limited movement between the Pacific and North America plates. Geological Society of America Bulletin, v. 88, p. 1567–1576.

LITHO- AND BIOSTRATIGRAPHY OF CAMBRIAN AND ORDOVICIAN STRATA IN THE SUBSURFACE OF THE WESTERN CANADA BASIN IN CENTRAL ALBERTA

F.J. Hein

Department of Geology and Geophysics, University of Calgary, Calgary, Alberta T2N 1N4

G.S. Nowlan, B.S. Norford, and W.H. Fritz

Geological Survey of Canada, 3303-33rd Street N.W., Calgary, Alberta T2L 2A7

R. Wicander

Department of Geology, Central Michigan University, Mount Pleasant, Michigan 48859

LITHOSTRATIGRAPHY

The lowermost Gog-equivalent Sauk I successions are absent in the subsurface east of the Rocky Mountains (Fig. 1). Later, as the Middle Cambrian sea transgressed eastward, it emplaced the diachronous Sauk II mixed clastic and carbonate succession that onlaps the craton and occurs within the subsurface of Alberta (Aitken, 1968, 1989). Within the Alberta subsurface most workers consider the lowermost deposits of the Sauk II succession (the Basal Sandstone) to be equivalent to the Mount Whyte Formation exposed in the southern Cordillera.

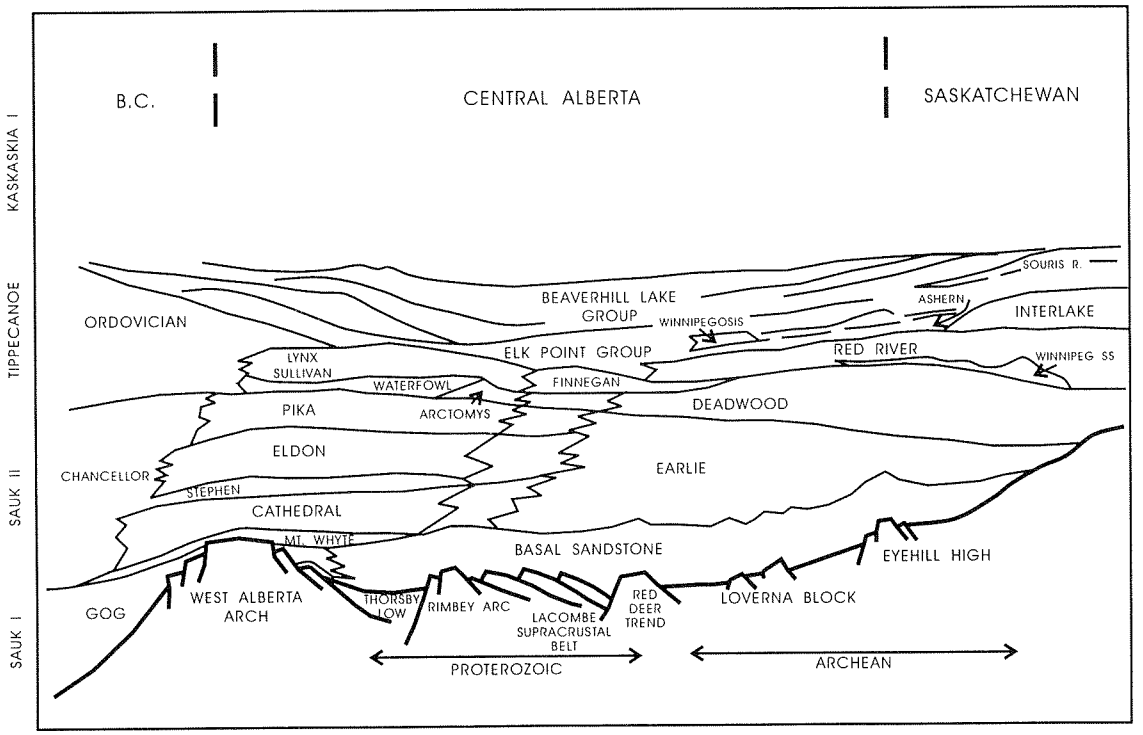

Figure 1. *Schematic cross-section from west to east across the Alberta Basin, showing general relationships between the Lower Paleozoic sedimentary cover and the underlying basement domains (modified from A. Hamblin, pers. comm., 1993).*

In the eastern part of the Alberta subsurface, the shales and carbonates of the Mount Whyte to Eldon formations change eastward into the more clastic-dominated shale and sandstone of the Earlie Formation. A prominent geophysical log marker, the Pika Marker, occurs at the top of this argillaceous succession in the eastern subsurface of Alberta. The Earlie Formation includes all those shaly clastic successions below the Pika Marker and above the Basal Sandstone (Fig. 1). The top of the Pika is cut by a regional disconformity. Above this disconformity are the younger transgressive clastics of the Deadwood Formation, and the overlying interbedded clastics/carbonates of the Finnegan Formation (Fig. 1). The stratigraphic relationships of the Deadwood and Finnegan formations are poorly understood (Pugh, 1971; Aitken, 1989; Osadetz and Haidl, 1989). The Finnegan Formation may be assigned to part of the younger Sauk III Sequence (Aitken, 1989). In the northwestern part of the study area, the carbonate-dominated Eldon Formation is replaced by one or two sandstone-dominated successions, that were sourced from the Peace River–Athabasca Arch.

PETROGRAPHIC ANALYSES AND FORMATION DIFFERENTIATION

Differentiation of many of the clastic-dominated successions in the eastern subsurface of Alberta is difficult, particularly in those areas where the geophysical log markers are less pronounced. However, many of these successions are potential Cambrian reservoir units, occurring locally as structural and/or stratigraphic traps. For this reason, a detailed petrographic study was conducted on selected potential reservoir units within the Cambrian subsurface; and, in the following section, only these units are discussed.

Basal Sandstone Unit

The quartz grains of the Basal Sandstone are, in general, yellowish with pink to maroon-red (hematitic) staining, and well rounded. Sorting of individual beds is poor to very poor, and locally the sandstones are pebbly or conglomeratic. The sandstone has good to excellent porosity, except in a band south and southeast of Edmonton (Twps. 36–52, Mer. 4 to Mer. 5) where there is a kaolinitic cement in the pink sandstone (cf. Pugh, 1971). Petrographically, the Basal Sandstone samples examined in the present study are quartz arenites and orthoquartz arenite, with minor amounts of strained and polycrystalline quartz; and very minor plagioclase and K-feldspar grains, igenous and metamorphic rock fragments. Cement is quartz. In constrast with the overlying younger Eldon sandstones, the Basal Sandstone generally lacks polycrystalline quartz grains and feldspar.

Eldon Formation

The Eldon Formation throughout most of the central Alberta subsurface is characteristically a dolostone, locally fenestral, silty or sandy. In the eastern subsurface, where it is indistinguishable from other clastics beneath the Pika Marker, it is mapped as part of the Earlie Formation. To the northwest, the Eldon becomes a sandstone.

Where the Eldon sandstone is best developed, it is a medium to coarse-grained sandstone, with good to excellent porosity. During the present study, petrographic samples of the Eldon sandstone were only examined in the Gulf Swanson 10-16-38-10W4 well. Here the Eldon sandstone is a quartz arenite, with strained and polycrystalline quartz grains, feldspar and metamorphic rock fragments. Sand grains are less mature than in the underlying Basal Sandstone unit.

Earlie Formation

In the present study area, the coarser sandstone and siltstone interbeds of the Earlie Formation have fair to good porosity. With the exception of the PCP Killam well, all of the samples from the Earlie sandstones are greensands, consisting of very glauconitic quartz arenite, with accessory components including green lithic rock fragments, very angular quartz grains, micaceous carbonate matrix, and carbonate clasts. In general, the Earlie sandstones are less feldspathic and lack the strained and polycrystalline quartz grains that are more typical of sandstones within the Eldon Formation and the Basal Sandstone unit.

Pika Formation

Deiss (1939) separated the upper shaly part of the Eldon Formation into the Pika Formation, which is more shaly and lithologically varied, with a more prominent bedding-style than the underlying Eldon. The Pika is in gradational contact with the underlying Eldon to the west, and with the Earlie Formation to the east (Fig. 1). In the type section (near Castle Mountain in the Rocky Mountain Main Ranges), the Pika is a thin bedded micrite, with dolomitized partings. To the east, the Pika laterally grades into glauconitic and fine grained clastics.

Lynx Formation and Group

In the subsurface, the Lynx Group comprises "cyrstalline" dolostones (cf. Pugh, 1971) and limestones, with siltstone and shale interbeds. Locally, thin interbeds of dolomitic edgewise breccias occur. To the north of the present study area, Pugh (1971) mentions the occurrence of a very porous, honeycombed textured dolostone, with significant intercrystalline porosities and oil-staining in successions both at the top and base of the upper Lynx Group.

Deadwood Formation

In the present study area, the coarser sandstone and siltstone interbeds of the Deadwood Formation have fair to good porosity. Petrographically, the Deadwood sandstone samples examined are glauconitic to very glauconitic quartz arenites/quartzose calcarenite, with accessories including strained quartz and very angular feldspar grains, and green lithic fragments, most likely igneous or metamorphic rock fragments.

Finnegan Formation

During the present study, many of the limestone interbeds within the Finnegan Formation were observed to be resedimented, edgewise limestone (dolostone) breccias. Lithologies of the limestone clasts within these breccias are identical to limestone/dolostone beds of the upper Lynx Group, suggesting that, in part, some of the Finnegan Formation may have been derived by reworking of the upper Lynx Group carbonate. The sandstones associated with the Finnegan carbonate breccias are greensands, consisting of very glauconitic quartz arenites, with resedimented limestone clasts, and minor carbonate matrix. The coarser green sandstones and limestone breccias of the Finnegan Formation have fair to good porosity.

SEDIMENTATION HISTORY

Preliminary facies analysis indicates that the Cambrian successions within the subsurface of the Alberta Basin were emplaced as mixed clastic and carbonate ramps, carbonate banks or reefs, and marine shoals within a shallow-marine embayment, called the Lloydminster Embayment of the Western Canada Sedimentary Basin. Monadnocks of basement rock disrupted sedimentation patterns and locally supplied coarse-clastic detritus to the marine embayment. During Middle Cambrian time, a transgressive flooding event occurred within an intracratonic, clastic-dominated tidal embayment, overlying Archean basement with a regional unconformity, and flanking basement highs. At this time, the Basal Sandstone Unit was deposited as coarse grained shoreline fan-delta and nearshore marine successions with an onlap and overstep relationships with a series of Precambrian basement highs. Following this initial transgression, shallow marine carbonate banks and ramps grew above the present location of the West Alberta Ridge, which flanked an inboard mixed carbonate and clastic embayment during the Cambrian, becoming more shaly and lithic dominated toward the east. During post-Pika Middle Cambrian time a major hiatus occurred, now recorded by a disconformity, locally an unconformity, between the Pika and the overlying Sullivan Formation. Late Cambrian time was marked by shallow carbonate bank and oolitic shoals, mainly preserved to the west as the Sullivan and Lynx formations. Post-Lynx Late Cambrian time was a major hiatus, marked by disconformities and hardgrounds, local karstification and dissolution of the Lynx and locally Sullivan carbonates. Following this a major transgression from the south occurred, with deposition of the Deadwood clastic-dominated succession, sourced from the south, with local sedimentation continuing into late Early Ordovician time at least. This was followed by a major period of erosion. The next transgression was marked by the reworking of eroded carbonate of the Lynx and Sullivan formations, with emplacement of these reworked carbonates as edgewise carbonate breccias within a mixed clastic glauconitic greensand and carbonate shelf-ramp succession comprising the Finnegan Formation. Post-Finnegan Early Ordovician time was a period of nondeposition, marked by an hiatus and disconformity, with more substantial erosion occurring in Devonian time.

BIOSTRATIGRAPHY

Prior to this study, Cambrian faunas had been reported from only five wells in the Alberta subsurface, all are trilobites of Middle to Late Cambrian age. No reports of Ordovician fossils from the study area were available prior to this study.

Three approaches have been used for biostratigraphy in this study. Firstly, all macrofossils encountered in the cores have been examined. While relatively few of the macrofossils have proven useful for biostratigraphy, as most are too fragmentary to be identified with sufficient precision, some have provided key data. Secondly, carbonate units encountered in cores have been sampled for conodonts. Over 200 samples have been

processed and about 62% of the samples have produced indentifiable conodonts. A total of 7500 specimens have been recovered. Thirdly, fine grained clastic units encountered in the core have been sampled for palynology. To date 69 samples have been examined from Cambrian strata. Recovery of acritarchs from the Cambrian has been sparse, but some valuable data have been gained.

Macrofossils

Trilobites assignable to the Middle Cambrian *Glossopleura* Zone have been recovered from the Stephen Formation in PCI et al. Windfall (12-36-59-15W5). Coral faunas from the Red River Formation in Gulf Spiers (11-15-34-15W4) include specimens of *Catenipora* and possible *Paleofavosites* in an interval that is dated on the basis of conodonts as Edenian to Maysvillian age (Fig. 2). Higher in the same well specimens of the corals *Bighornia* and *Deiracorallium*, Richmondian age occur in an interval interpreted to be Stony Mountain Formation. In this interval conodonts are less abundant and less biostratigraphically

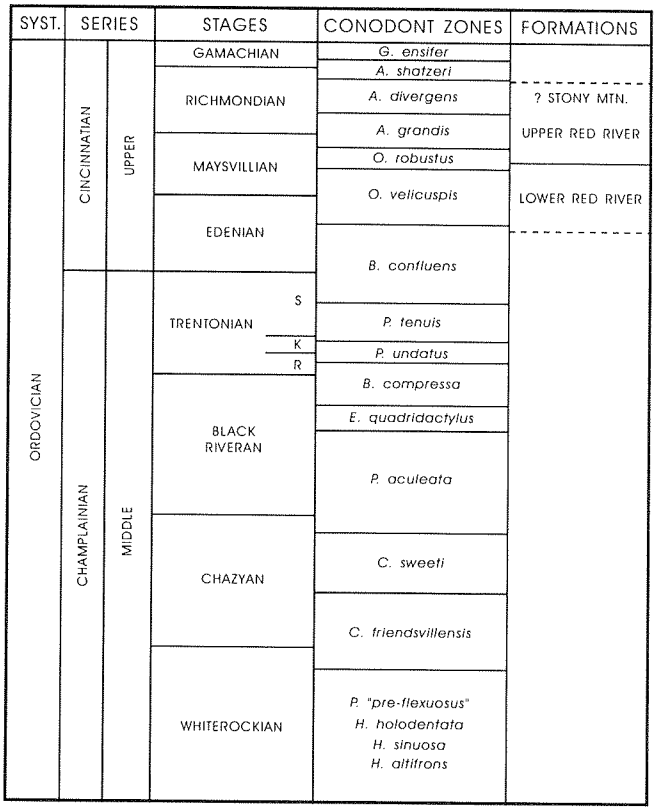

Figure 2. *Correlation chart for the Middle and Upper Ordovician; conodont zones after Sweet (1982). R = Rocklandian, K = Kirkfieldian, S = Shermanian.*

diagnostic. Specimens of *Bighornia* and the brachiopod *Megamyonia nitens* of Maysvillian to Richmondian age have been recovered from presumed Stony Mountain Formation in Calstan Pacific Marwayne (14-29-52-2W4).

Conodonts

Conodonts are rare in most of the Cambrian formations sampled. A few Middle to Late Cambrian forms are present in the Eldon Formation in Rio Bravo Ronald (1-6-38-15W4). Fragments of possible Cambrian age have been recovered from the Lynx Formation in Fina Amoco Sundance (15-29-55-17W5). Conodonts of Late Cambrian to earliest Ordovician age have been recovered from the Finnegan Formation in five wells: Socony Craigmyle (12-32-32-16W4), Chevron Link (14-35-34-17W4), Rio Bravo Ronald (1-6-38-15W4), PCP Provost (11-35-38-10W4), and Suncor Strome (11-16-44-16W4). Specimens of *Furnishina* sp., *Phakelodus* sp. and *Proconodontus* sp. representing the Late Cambrian *Proconodontus* Zone occur well below the top of the Finnegan Formation. Conodonts of the succeeding Late Cambrian *Eoconodontus* Zone occur in higher parts of the Finnegan Formation and indicate the youngest part of the Finnegan in most wells. However, younger conodonts including specimens of *Cordylodus* have been recovered from Suncor Strome indicating an age close to the Cambro–Ordovician boundary (Fig. 3).

Early Ordovician conodonts have been recovered from Devonian strata in three wells: Gulf Spiers (11-15-34-15W4), Imperial H.B. Joffre (9-8-39-26W4), and Chevron Gilby (4-5-41-2W5). Extremely diverse faunas including *Cordylodus* sp., *Diaphorodus* sp., *Oepikodus communis* (Ethington and Clark) and *Rossodus manitouensis* Repetski and Ethington have been recovered. These represent a wide variety of ages in the Early Ordovician ranging from the earliest Ordovician Skullrockian Stage through the *Oepikodus communis* Zone the early Blackhillsian Stage (Fig. 3). This material indicates that Lower Ordovician rocks were being eroded at the time of deposition of the Middle Devonian.

Sections of the Red River Formation have been sampled in cores in seven wells: Socony Craigmyle (12-32-32-16W4), Gulf Spiers (11-15-34-15W4), Chevron Link (14-35-34-17W4), PCI Provost (6-4-37-16W4), PCP Provost (11-35-38-10W4), Suncor Strome (11-16-44-16W4), and Calstan Pacific Marwayne (14-29-52-2W4). Collectively these wells have yielded over 7000 conodont specimens of Late Ordovician age. The faunas are numerically dominated

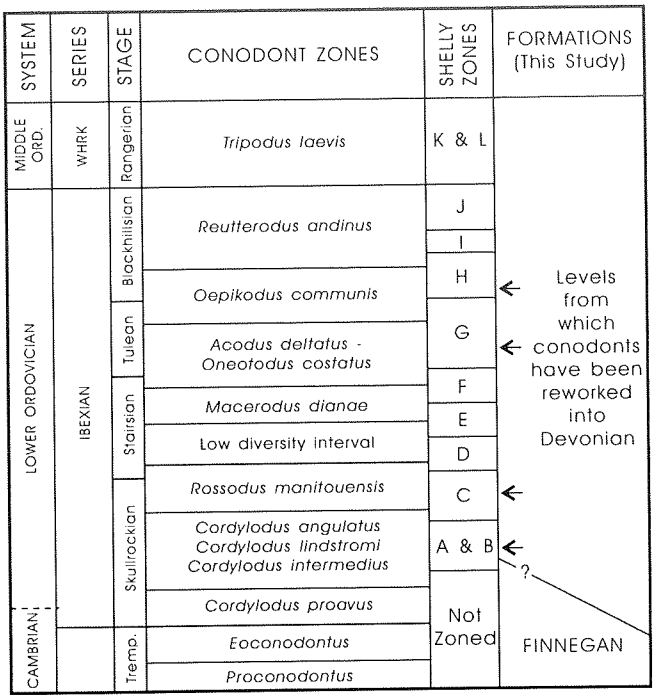

Figure 3. *Correlation chart for the Upper Cambrian and Lower Ordovician; stages and conodont zones after Ross et al. (1993).*

by species of *Panderodus*, a long-ranging genus, but several other biostratigraphically useful forms are present. The faunas represent shallow water forms of Midcontinent Province affinity.

All wells contain evidence of conodonts of early to middle Late Ordovician (Edenian–Maysvillian) age, characterized by the presence of *Culumbodina penna*. A correlation with the Selkirk Member of the lower part of the Red River Formation is suggested for these intervals. The presence of specimens similar to *Oulodus rohneri* in the highest samples in some wells probably indicate that the upper part is exclusively Maysvillian. In four wells, the conodont abundance and diversity drops off considerably in the uppermost part of the Ordovician interval. In one well this interval is dated as late Late Ordovician (Richmondian) by macrofossils. It is considered that this interval may represent the upper part of the Red River Formation or the Stony Mountain Formation (Fig. 2).

Palynomorphs

Only the Cambrian part of the interval has been sampled for palynomorphs. Most of the 63 samples collected from strata of supposed Cambrian age contained sufficient kerogen or palynomorphs to determine a Thermal Alteration Index (TAI) and to characterize the kerogen. Analysis of the kerogen palynofacies indicates that all of the Cambrian samples are probably marine in origin. The samples contained acritarchs, leiospheres, or botryoidal-shaped kerogen indicating a nearshore marine environment.

In terms of the palynomorphs recovered, preservation precluded identification to the species level in all but a few cases. However, many of the genera are restricted to the Cambrian (*Adara, Retisphaeridium, Timofeevia* and *Trunculumarium*), or Cambrian–Early Ordovician (*Goniosphaeridium*). In addition, colonial botryoidal-shaped algal colonies were recovered from many of the samples. These are very similar to those reported in the literature from other Cambrian localities. There were also very distinct specimens of *Leiosphaeridia* that have been reported elsewhere from the Cambrian. In addition, there are several samples in which sheaths are abundant. These are similar to sheaths reported in the literature from Cambrian deposits. These sheaths are found only in samples dated as Cambrian and may prove useful for correlation in this area. Identifiable specimens have been recovered from the Basal Sandstone, Earlie, Stephen, Eldon, Deadwood and Finnegan formations.

REFERENCES

Aitken, J.D.
1989: The Sauk Sequence–Cambrian to Lower Ordovician miogeocline and platform. *In* Western Canada Sedimentary Basin, A Case History, B.D. Ricketts (ed.). Canadian Society of Petroleum Geologists, Chapter 7, p. 105–119.

Deiss, C.F.
1939: Cambrian formations of southwestern Alberta and southeastern British Columbia. Bulletin of the Geological Society of America, v. 50, p. 951–1019.

Osadetz, K.G. and Haidl, F.M.
1989: Tippecanoe Sequence: Middle Ordovician to Lowest Devonian vestiges of a great epeiric sea. *In* Western Canada Sedimentary Basin, A Case History, B.D. Ricketts (ed.). Canadian Society of Petroleum Geologists, Chapter 8, p. 121–137.

Pugh, D.C.
1971: Subsurface Cambrian stratigraphy in southern and central Alberta. Geological Survey of Canada, Paper 70–10, 33 p.

1975: Cambrian stratigraphy from western Alberta to northeastern British Columbia. Geological Survey of Canada, Paper 74–37.

Ross, R.J. Jr., Hintze, L.F., Ethington, R.L., Miller, J.F., Taylor, M.E., and Repetski, J.E.
1993: The Ibexian Series (Lower Ordovician), a replacement for "Canadian Series" in North American chronstratigraphy. United States Geological Survey, Open File Report 93-598, 75 p.

Sweet, W.C.
1982: Graphic correlation of upper Middle and Upper Ordovician rocks, North American Midcontinent Province, U.S.A. *In* Aspects of the Ordovician System, Paleontological Contributions from the University of Oslo, Norway, no. 295, p. 23–35.

SOME REMARKS ON THE SURFACE MAPPING OF THE SOUTHERN CORDILERRAN FOOTHILLS IN ALBERTA AS A TOOL IN HYDROCARBON EXPLORATION

T. Jerzykiewicz

Geological Survey of Canada, 3303-33rd Street N.W., Calgary, Alberta T2L 2A7

INTRODUCTION

The prime target of the exploration for hydrocarbons in the Southern Cordilleran Foothills of Alberta are Paleozoic carbonates. These rocks are brought to the surface on a series of large thrust sheets, and in most of the Foothills they are covered by Mesozoic clastic rocks. The Mesozoic strata of the Fernie-Kootenay, Blairmore, Alberta Group, and Belly River clastic wedges are imbricated and folded in a very complex way, masking the simpler geometry of the carbonate thrust sheets. While the indentification of the structure of the Paleozoic carbonates in the subsurace can be interpreted from seismic reflection sections, the definition of the shallow subsurface and surface structure of the Mesozoic strata is best accomplished by a combination of surface mapping with seismic data and wireline logs.

The purpose of these remarks is to endorse a poster entitled "Belly River strata in the footwall of the Livingstone Thrust: an insight into stratigraphy, sedimentation and structure of the Southern Foothills" as an example of application of recently developed stratigraphy for mapping a 1:50 000 Blairmore map sheet (i.e., the area of an intensive exploration for hydrocarbons).

STRATIGRAPHY

The bulk of the bedrock in the area of the imbricate thrust faults and folds of the Southern Foothills between the Livingstone Thrust and the Triangle Zone consists of the Upper Cretaceous post-Wapiabi (Colorado) strata. Lower post-Wapiabi strata up to the contact with the Bearpaw shale, which are more than 1000 m thick on the Crowsnest River, have been subdivided recently into several mappable lithostratigraphic units (Jerzykiewicz and Norris, 1994). According to this new classification, the succession of strata between the Wapiabi and Bearpaw shale, which had been previously mapped as the "Belly River Formation", contains the uppermost Alberta Group (Lees Lake, Burmis and Pakowki formations) and the Belly River Group (Connelly Creek, Lundbreck and Drywood Creek formations) (Fig. 1).

The purpose of this new stratigraphy is three-fold: (1) to establish a base for the correct correlation of the "Belly River" clastic wedge; (2) to provide a framework for the interpretation of sedimentary environments within the "Belly River" clastic wedge; and (3) to demonstrate how mapping of the established stratigraphic units may help in the interpretation of structure of the underlying imbricate thrust and fold belt.

STRUCTURE

The formations mentioned (Fig. 1) are currently being utilized for remapping the 1:50 000 scale Blairmore map sheet. New interpretations of thrusts and folds shown on the poster include the imbricate stack in the footwall of the Livingstone Thrust, the Tetley Thrust, plus the Todd Creek, Lundbreck and Tower anticlinal structures.

For example: (1) An imbricate stack of the Burmis Formation in the footwall of the Livingstone Thrust has been mapped between Crowsnest River at Burmis to the south, and Centre Peak of the Livingstone Range to the north (Twps. 7 and 8, Rge. 3) at the Dupret Ranch. There, the cliff-forming Burmis sandstone, with a magnetite-rich marker bed near the top and the distinctive Lees Lake turbidites at the base, is repeated by faults and forms an imbricate stack up to 250 m thick (Figs. 2, 3). (2) The new stratigraphy can be used to calculate displacement on the Tetley Thrust in the railway track outcrops some 4 km northeast of Burmis. There, the Tetley Thrust brings the upper part of the Burmis Formation (overlain by the basal channel of the Connelly Creek Formation) into contact with folded Lundbreck and Drywood Creek formations in the footwall. Identification of the Burmis sandstone on the

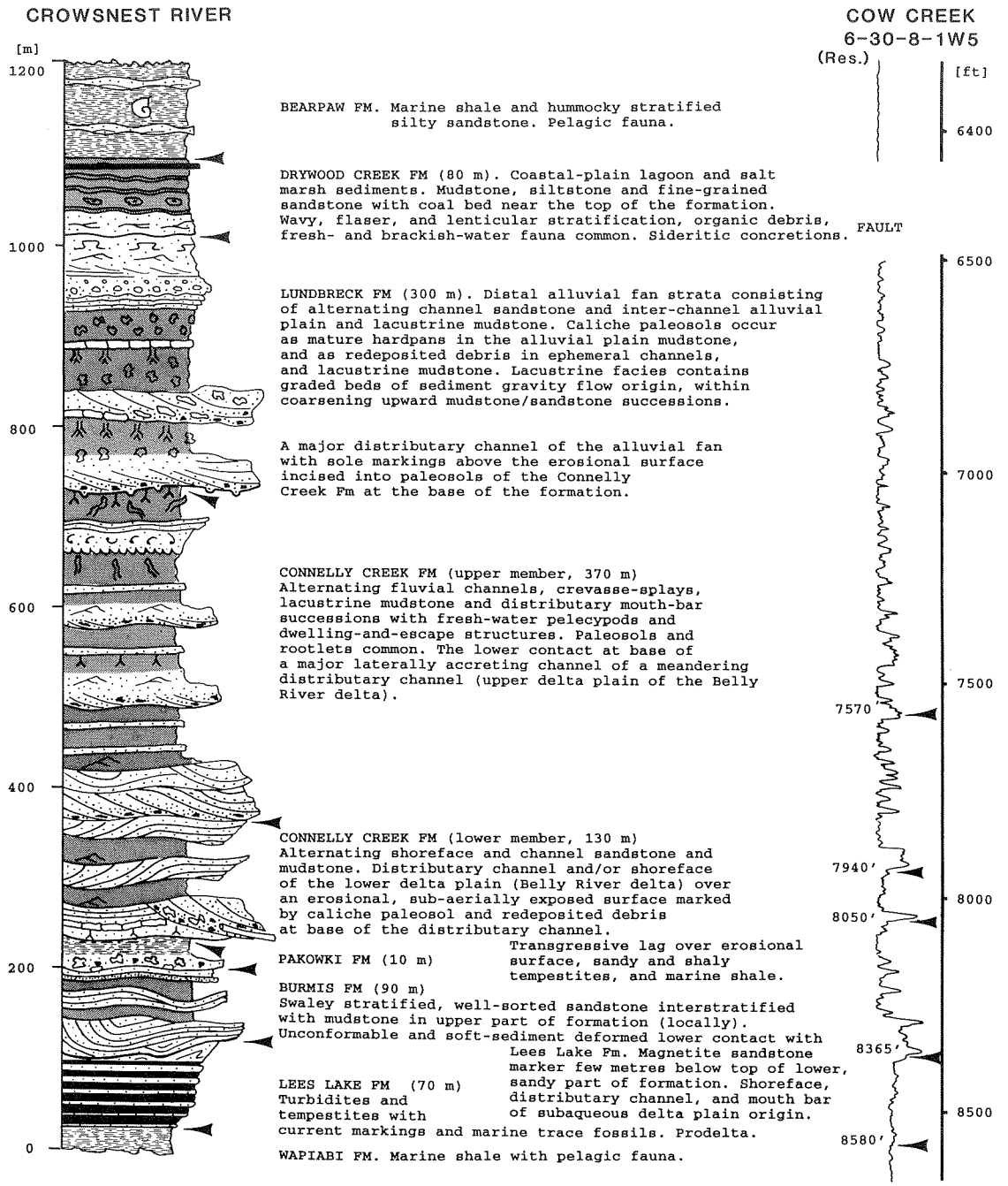

Figure 1. *Lithostratigraphic units and diagnostic sedimentary structures of the Belly River and contiguous strata on Crowsnest River and in the wire log of the Cow Creek well. Southern Cordilleran Foothills, Blairmore map sheet.*

hanging wall of the thrust, and the Lundreck strata folded with the Drywood Creek strata in the footwall, documents stratigraphic separation of approximately 900 m (for thickness of the formations cf. Fig. 1). The displacement on the steep west dipping (~70°) Tetley Thrust is therefore in the order of 1 km.

Other examples of structures illustrated on the poster include the Todd Creek, Lundbreck and Tower anticlines which were recognized and mapped in outcrops of Burmis, Pakowki, Connelly Creek and Lundbreck formations.

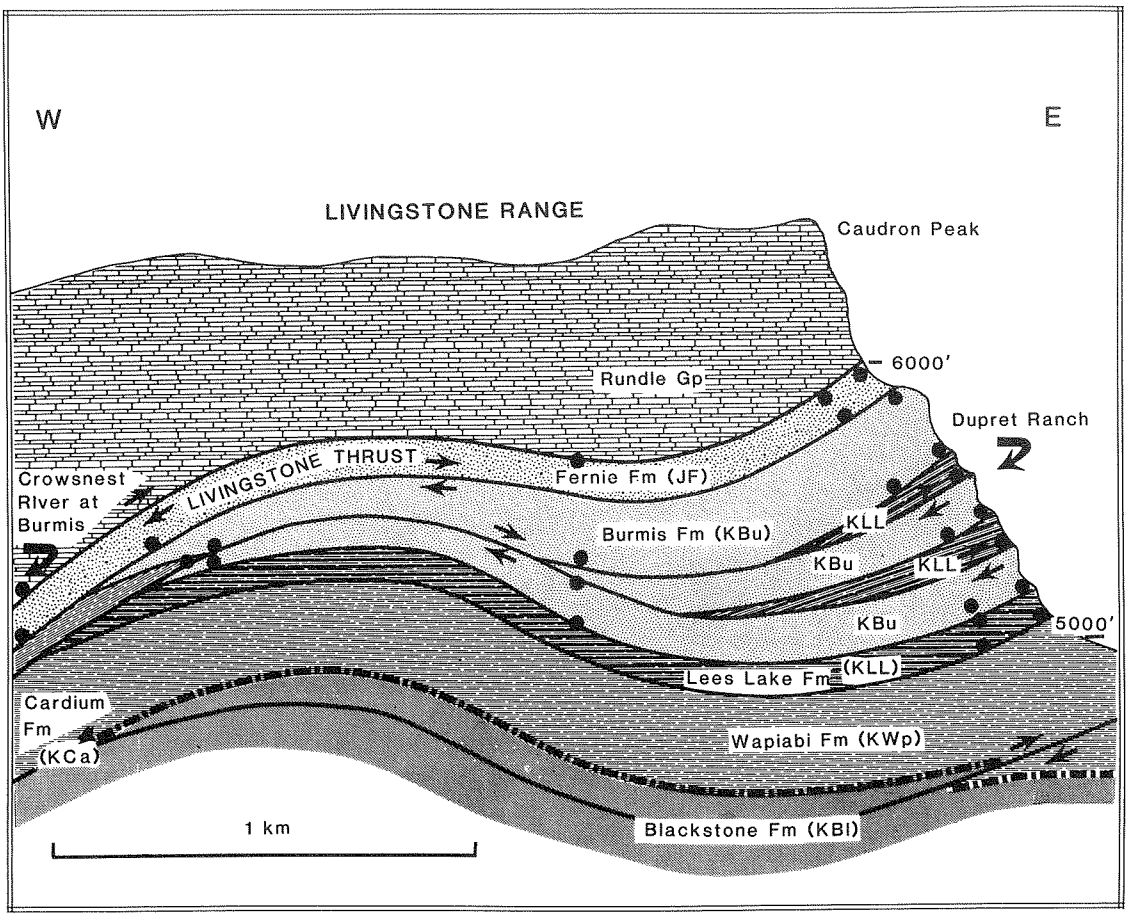

Figure 2. *Imbricate stack of the Burmis and Lees Lake formations in the footwall of the Livingstone Thrust at the Dupret Ranch. The thickness relations and contacts between formations are based on surface mapping of outcrops marked by large black dots on the section.*

CONCLUSIONS

The refinement of the stratigraphy of the Belly River and contiguous rocks in the Cordilleran thrust and fold belt in this area helps in: (1) recognition, definition and mapping of some poorly understood or otherwise overlooked structures; (2) correct definition of the UZA-3/UZA-4 sequence boundary in the Foothills at the base of the Connelly Creek Formation; and (3) reconstruction of the succession of sedimentary environments developed during and after the Colorado Sea regression from the Crowsnest Embayment as a response to the orogenic activity in the Cordillera.

REFERENCES

(A complete list of relevant references is published in the listed publications which are available from the author at the poster booth)

Jerzykiewicz, T.
1994: Significance of the Pakowki Formation to mapping in the deformed belt of the southern Canadian Cordillera, Alberta. *In* Current Research 1994-E; Geological Survey of Canada, p. 95–100.

Jerzykiewicz, T. and Norris, D.K.
1994: Stratigraphy, structure and syntectonic sedimentation of the Campanian "Belly River" clastic wedge in the southern Canadian Cordillera. Cretaceous Research, v. 15, p. 367–399.

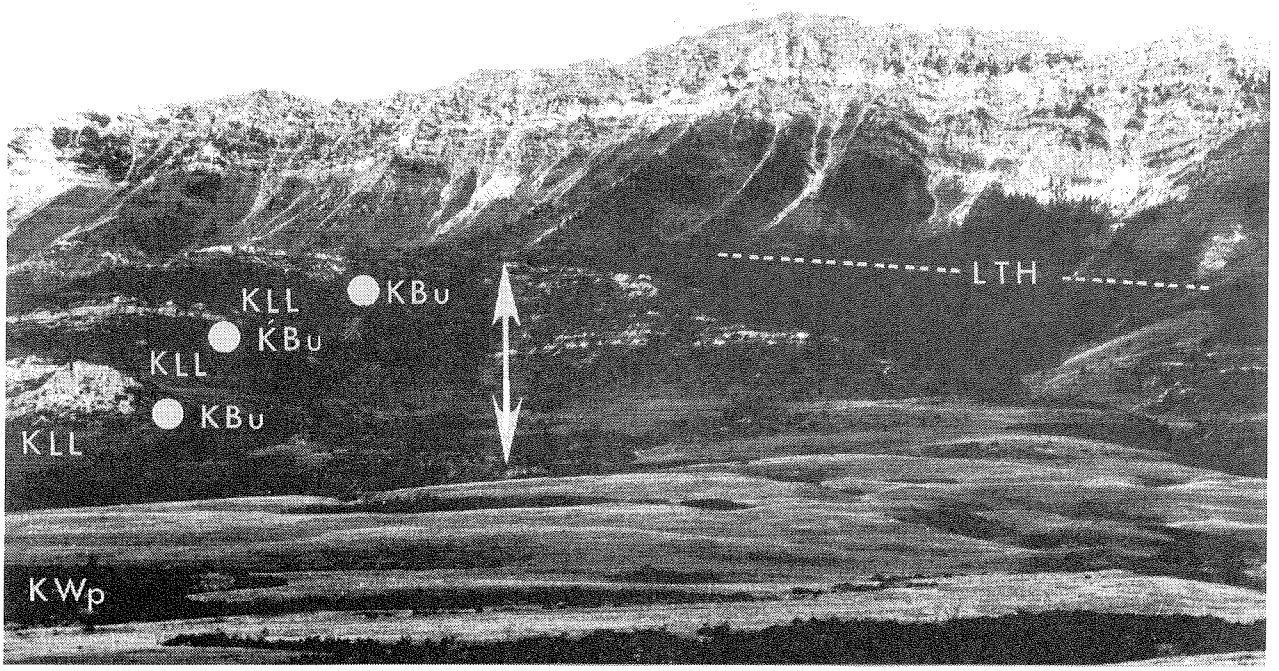

Figure 3. *Imbricate stack of the Burmis (KBu) and Lees Lake (KLL) formations in the footwall of the Livingstone Thrust (LTH). View from the Burmis road over a plateau formed by the Wapiabi shale (KWp) toward the west at the imbricate stack (marked by white arrows), and the Livingstone Range in the background. Note the fault-repeated, cliff-forming Burmis sandstone (marked by white dots and symbols KBu).*

GEOLOGY AND CROSS-SECTION, WATERTON LAKES MAP AREA, ALBERTA (82H/4), SOUTHERN ALBERTA NATMAP PROJECT

D. Lebel

Geological Survey of Canada, 3303-33rd Street N.W., Calgary, Alberta T2L 2A7

INTRODUCTION

Bedrock mapping of the Waterton Lakes area was conducted as part of the second year of research associated with the Southern Alberta Foothills NATMAP project (see Lebel, this volume). This five-year project (1993-1998) will produce a new digital geoscience database for the eastern edge of the Cordillera in southern Alberta, comprising new bedrock geological maps (Lebel, Douglas and Norris, 1994; Lebel and Williams, 1994) and new cross-sections of subsurface structure established in cooperation with the petroleum industry using proprietary seismic information.

The Waterton Lakes map area (NTS 82 H/4) overlaps the southern Alberta Foothills and the Rocky Mountain Front Ranges geological divisions and lies immediately north of the Canada–U.S.A. border. The western part of the area is marked by the Lewis thrust sheet (Mesoproterozoic Purcell Supergroup) and the Foothills belt in the eastern part (only Upper Cretaceous strata are exposed at the surface). The northeastern corner of the map is within 5 km of the edge of the Foothills thrust belt (triangle zone). This paper discusses results of field work during the 1993 and 1994 field seasons which focussed on the remapping of the Mesozoic strata found in the Foothills to apply the new stratigraphic units within the Alberta and Belly River groups recognized recently by Jerzykiewicz and Norris (1994) for the Crowsnest Pass (Blairmore) area. Quaternary deposits are extensive in the area, and relief generally is less than 300 m in the Foothills. Good exposures are found along the banks of the Waterton and Belly rivers and Lee Creek (Fig. 1).

The area was previously mapped in detail locally by Williams (1949, Lee Creek area) and as a whole by Douglas (1952). In addition to the revision of the Upper Cretaceous stratigraphy, remapping of the area was required to utilize recent petroleum industry seismic and well data, to construct cross-sections, to create a new digital geological database and to apply new notions of thrust tectonics. Geological mapping was conducted for two weeks in the summer of 1993 and six weeks in 1994. Three important gas fields (Waterton, Pincher Creek and Lookout Butte) exploit deep subsurface reservoirs situated in Mississippian thrust sheets (Gordy et al., 1977).

STRATIGRAPHY

In the Foothills of the area, only Upper Cretaceous rocks are exposed (Fig. 1). Regional mapping has confirmed the southern extension of several new Upper Cretaceous stratigraphic units recently defined in the Crowsnest Pass area. Six new stratigraphic units defined by Jerzykiewicz and Norris (1994) are used herein. The six new units overlying the Wapiabi Formation are, in stratigraphic order: the Lees Lake, Burmis and Pakowki formations (upper Alberta Group, Campanian), and the Connelly Creek, Lundbreck and Drywood Creek formations (Belly River Group, Campanian). Four other formations overlie the Belly River Group: the Bearpaw Formation (Uppermost Campanian), the Blood Reserve Formation and the St. Mary River Formation (Lower to Mid-Maestrichtian) (Fig. 1). Previously, Douglas (1952) used the base of the Lees Lake Formation for the base of his Belly River Formation which ranged to the base of the Bearpaw Formation.

STRUCTURAL GEOMETRY OF THE FOOTHILLS

The Foothills of the eastern part of the Waterton Lakes area consist of a series of closely spaced southwest-dipping, northeast-verging thrust faults deforming Upper Cretaceous strata (Fig. 1). These are extensions of other faults mapped in the Cardston area (Lebel and Williams, 1994). No southwest-directed, northeast dipping thrust fault (backthrust) was mapped in the area. However some northeast-directed, northeast-dipping folded thrust faults were observed locally and are interpreted to extend over a wide area in the interior part of the Foothills of the area (Fig. 1).

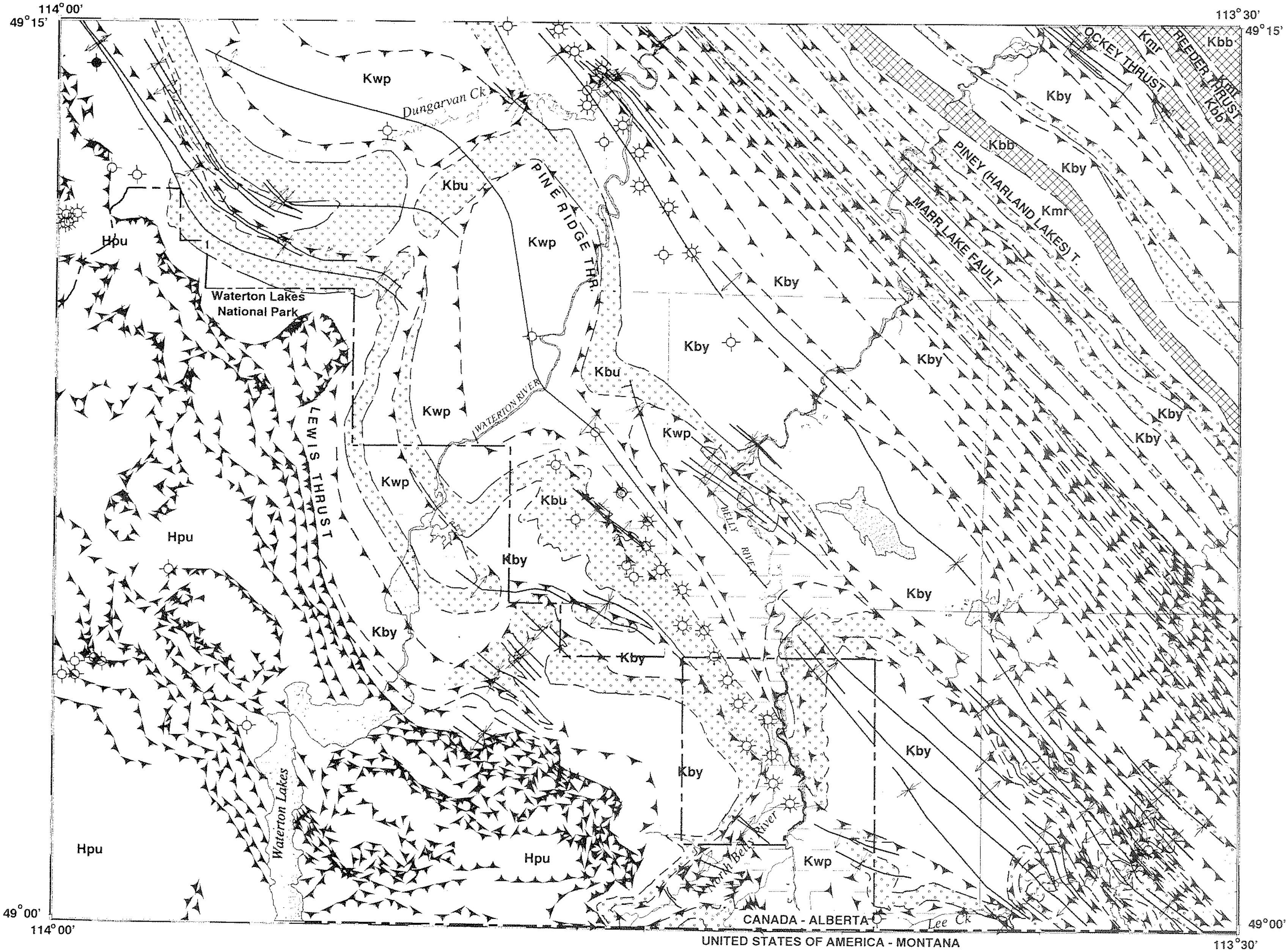
114°00'
49°15'
113°30'
49°15'
Kbb
REEDER THRUST
Kmr
OCKEY THRUST
Kby
Kbb
PINEY (HARLAND LAKES) T.
Kmr
MARR LAKE FAULT
Kwp
Dungarvan Ck
Kbu
PINE RIDGE THR.
Waterton Lakes
National Park
LEWIS THRUST
WATERTON RIVER
BELLY RIVER
Kwp
Kbu
Kby
Hpu
Waterton Lakes
North Belly River
Lee Ck
CANADA - ALBERTA
UNITED STATES OF AMERICA - MONTANA
49°00'
114°00'
49°00'
113°30'

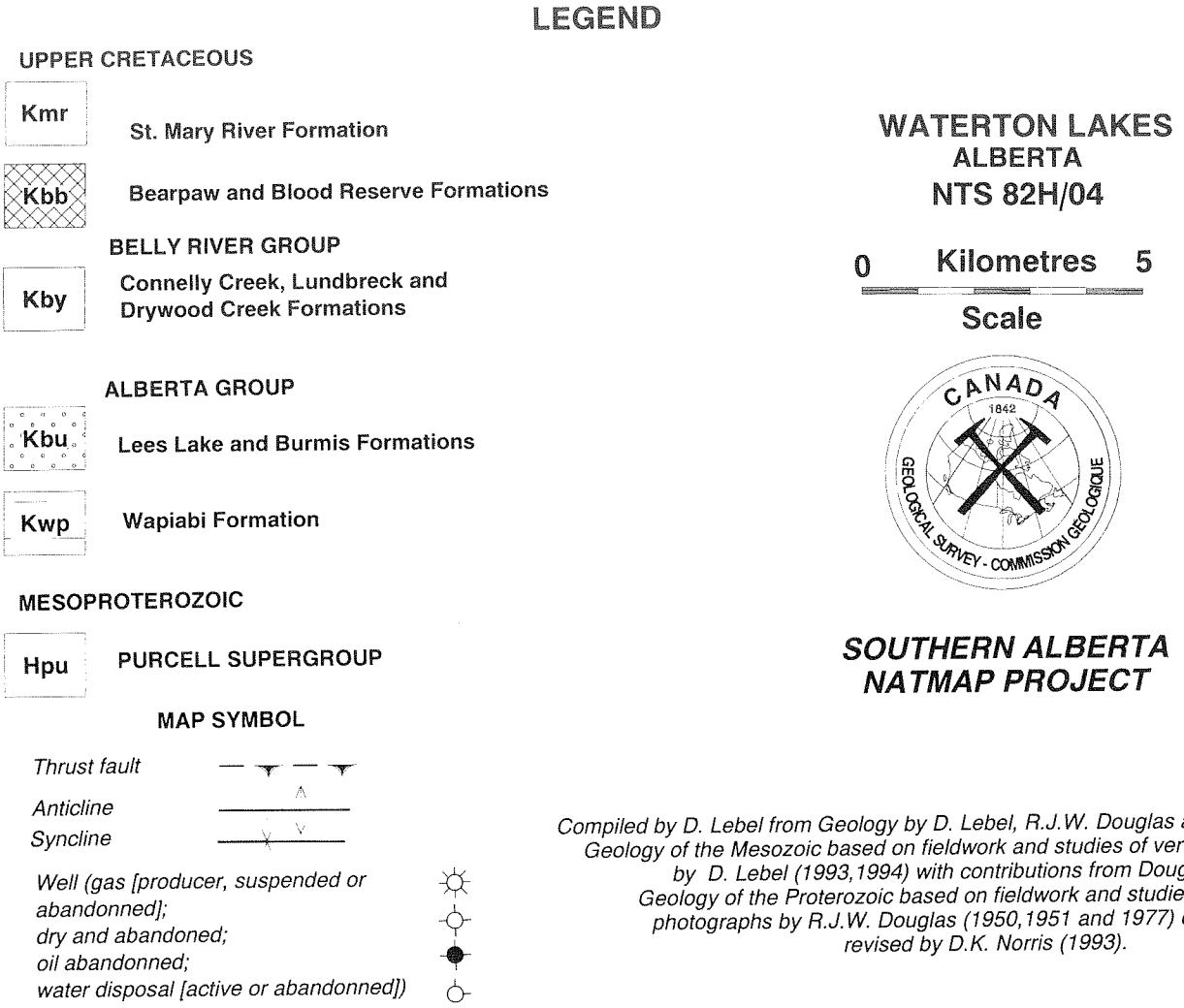

Figure 1. *Simplified geological map of the Waterton Lakes map area (NTS 82 H/4).*

Structure of the Outer Foothills

Structure of the outer Foothills is largely inferred from two relatively well exposed outcrop sections across the structure, along Lee Creek in the southeast part of the area and along the Belly River (Fig. 1). In between these two sections, few outcrops are present and only a few sandstone ridges can be traced through an area of relatively low relief (Lebel et al., 1994 for exact representation of the exposure and relief). The section along Lee Creek shows a series of structural repeats of the Lundbreck, Connelly Creek, Burmis and Lees Lake formations. Most strata are moderately inclined and make thrust sheets striking northwest–southeast, up to an area in Lee Creek situated about 5 km north from the international border where strata are broadly folded. A few of the sandstone ridges of the Burmis Formation can be traced throughout the outer Foothills to the Belly River and the Waterton River. These ridges provide a basis for inferring extensions to the northwest of the structures mapped in the southeast along Lee Creek. Preliminary assessment of seismic data obtained from Amoco Canada suggests that most of these thrust faults are restricted to within 1 km of the surface and join with a décollement near or below Upper Cretaceous rocks that separate these rocks from older ones. Only a few of the surface faults can be traced lower in the subsurface, where they cut through Lower Cretaceous and older rocks.

Structure of the Interior Foothills

Interpretation of air photographs, and re-evaluation of the structure of several critical sections allows for a substantially different representation of the structure of the interior Foothills of the Waterton Lakes area than that of Douglas (1952). A few, broadly folded thrust sheets compose the overall surface structure of the area. Beneath these thrust sheets, the Wapiabi Formation is

more deformed locally and generally by extension (Lebel et al., 1994).

In the upstream portion of the Lee Creek section, strata and faults display generally low attitudes and are involved in broad folds (Fig. 1). Along the escarpments situated on both sides of the valley of the head of the Belly River, the Burmis Formation is nearly flat lying, cut by no significant thrust fault. In contrast, in exposures along the North Belly River (west branch of the headwaters of the Belly River), the underlying Wapiabi Formation is significantly more folded and faulted, cut and duplicated by a series of moderately to steeply inclined, southwest dipping thrust faults. To explain the discrepancy in shortening observed between these two stratigraphic units, a décollement horizon is interpreted near the top of the Wapiabi Formation.

In the north-central portion of the area, northeast-directed, northeast-dipping folded thrust faults were observed locally along Dungarvan Creek. One of these faults, the Piney Ridge thrust is interpreted to underlie most of a prominent sandstone ridge (Burmis Formation) crossing the central part of the Waterton Lakes area from north-northwest to south-southeast. This fault is interpreted to be folded and join with the décollement inferred in the North Belly River area. The exact relationship between the various faults will be reassessed in the near future in light of seismic data provided by the oil industry.

REFERENCES

Gordy, P.L., Frey, F.R., and Norris, D.K.
1977: Geological guide for the CSPG 1977 Waterton-Glacier Park Field Conference. Canadian Society of Petroleum Geologists, Calgary, Alberta, Canada, 93 p.

Douglas, R.J.W.
1952: Waterton. Geological Survey of Canada, Preliminary Map 52-10.

Jerzykiewicz, T. and Norris, D.K.
1994: Stratigraphy, structure and syntectonic sedimentation of the Campanian 'Belly River' clastic wedge in the southern Canadian Cordillera. Cretaceous Research, v. 15, p. 367–399.

Lebel, D., Douglas, R.J.W., and Norris, D.K.
1994: Waterton Lakes (82H/4), Alberta–Geology (preliminary). Geological Survey of Canada, Open File 2855, scale 1:50 000.

Lebel, D. and Williams, E.P.
1994: Geology, Cardston (82H/4), Alberta. Geological Survey of Canada, Open File 2854, scale 1:50 000.

Williams, E.P.
1949: Preliminary Map, Cardston, Alberta. Geological Survey of Canada, Paper 49-3.

GEOLOGICAL MAP AND CROSS-SECTIONS, ATHABASCA–BRAZEAU AREA, ALBERTA

D. Lebel

Geological Survey of Canada, 3303-33rd Street N.W., Calgary, Alberta T2L 2A7

E.W. Mountjoy

Department of Earth and Planetary Sciences, McGill University
3600 University Street, Montreal, Quebec H3A 2A7

INTRODUCTION

Regional mapping (Fig. 1; Mountjoy, Price and Lebel, 1992; Douglas and Lebel, 1993), the study of seismic data, deep petroleum exploration wells and the construction of a series of cross-sections through the Athabasca–Brazeau portion of the central Canadian Rocky Mountain thrust-fold belt (Lebel, 1993) outline three types of first order décollement within or along the border of the present orogenic wedge: basal décollement, intermediate or internal décollement and an upper décollement (Fig. 2). The evolution of these different structural elements appears to have been intimately interrelated and influenced by the overall geometry of the orogenic wedge. The presence of a prominent upper décollement and low-taper triangle zone (Jones, 1982) suggest a specific sequence of structural events in this area.

MULTIPLE DÉCOLLEMENTS IN THE ATHABASCA–BRAZEAU AREA

Basal and internal décollements

The basal décollement changes stratigraphic position both laterally and toward the foreland and has two ramps: one from the base of the stratigraphic pile to a slippage zone in the Devonian and another from this flat to another flat in the Upper Cretaceous. This last flat corresponds to the upper décollement above which a southwest-verging panel overrides the foreland portion of the orogenic wedge. Internal décollements are recognized by layer-parallel glide horizons that correspond to extensive flat segments above a ramp. These ramps link each internal décollement to the basal décollement situated in the more hinterland area of the orogenic wedge. Basal and internal décollements are similar in geometry in that several imbricate fault systems emanate from each. In the study area, five extensive layer-parallel glide horizons are recognized: the Sassenach-basal Palliser formations (basal décollement); the Fernie Group, the upper portion of the Nikanassin Formation, and the Blackstone Formation (internal décollements) and the Wapiabi Formation (upper décollement). Successive forward shifts of the basal décollement to deeper levels within the stratigraphic pile led to the formation of internal décollements. These internal décollements are in some cases cross-cut by younger faults rising from deeper and more northeastward décollements.

The Upper Décollement

In the Cardinal River area, northeast-verging and southwest-dipping faults that cut through the Brazeau and Paskapoo formations, are present at the surface northeast of the Brazeau thrust. These faults indicate that part of the upper décollement was carried by younger, deeper thrusts during the late stages of deformation. Seismic data recently accessed through Husky Oil suggest that the upper décollement panel is substantially larger than previously described in the cross-section by Douglas and Lebel (1993). A revision of that cross-section will have to show little or no shortening within the Upper Cretaceous and Tertiary stratigraphic pile.

It is suggested that the evolution of the upper décollement combined with underlying thrust sheet emplacement prevented further underthrusting of the orogenic wedge along the basal-upper décollement conjugate surface. This provoked a rise of the critical taper angle of the orogenic wedge. Renewed internal deformation within the wedge eventually led to a downward shift of the basal décollement and allowed for renewed foreland accretion along a new basal décollement until another cycle of basal décollement abandonment occurred. The presence of several

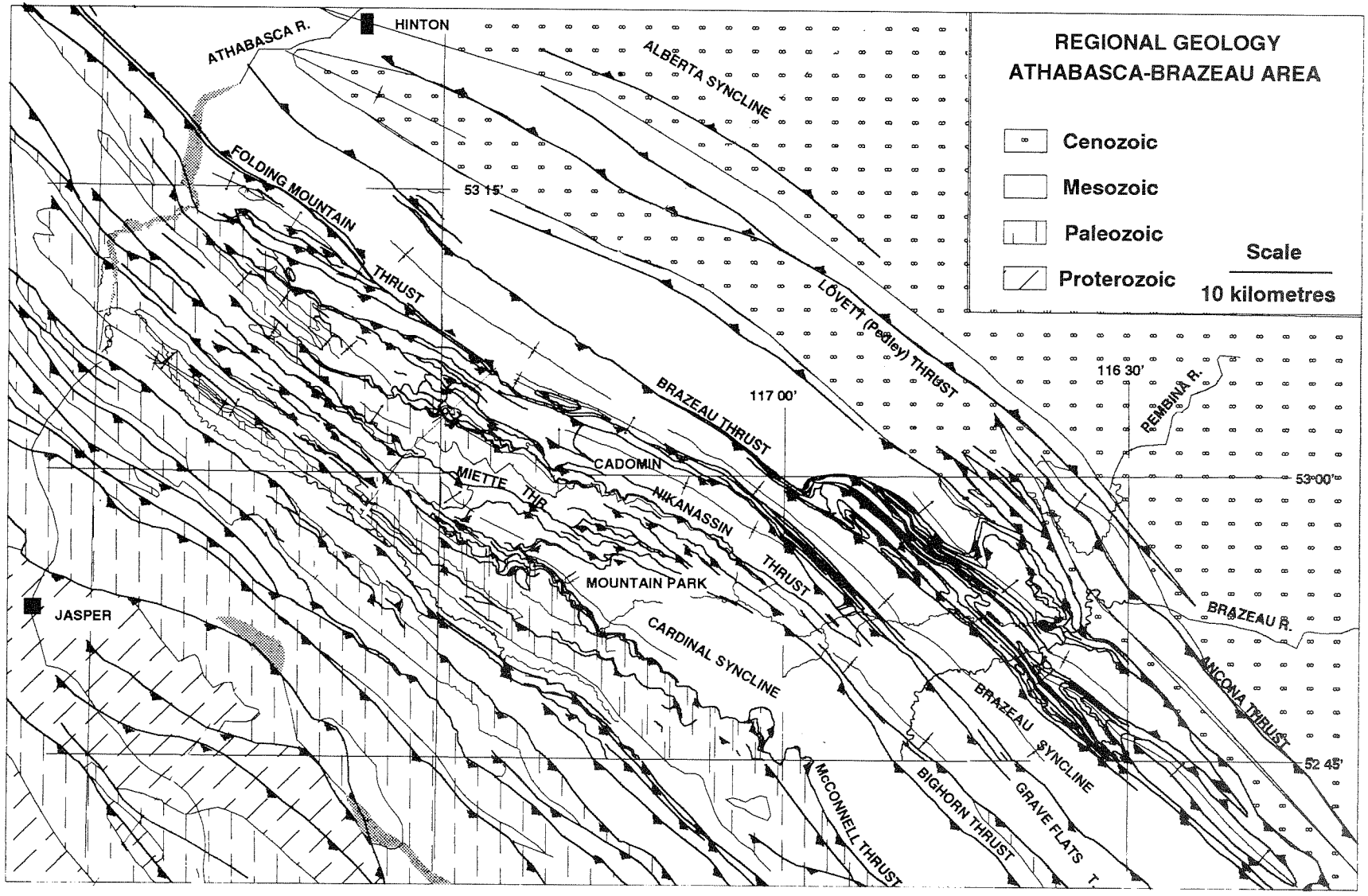

Figure 1. *Regional geological map of the Athabasca–Brazeau area. Sharp contrast in structural style exists between the NW and SE parts of the area. The upper décollement forms a large panel broken into several large backthrust sheets of Upper Cretaceous and Tertiary strata in the NW part; in contrast, a series of closely spaced foreland directed thrust faults breaks through the same stratigraphic interval in the SE area.*

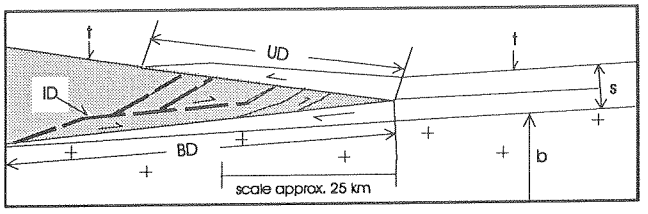

Figure 2. *Structural position of observed décollements in the outer part of the central Canadian Rocky Mountains foreland thrust belt. BD, basal décollement; UD, upper décollement; ID, internal décollement; other surfaces and volumes include: t, topographic surface; b, crystalline basement; s, sedimentary stratigraphic pile.*

internal decollements in the study area also signifies that conventional section balancing using relative bed lengths must be done for the entire Foothills to produce valid cross-sections and must take into consideration possibly large discrepancies between shortening values observed above and below the upper décollement.

REFERENCES

Jones, P.B.
1982: Oil and gas beneath east dipping underthrust faults, Alberta Foothills. *In* Geologic studies of the Cordilleran Thrust Belt, R.B. Powers (ed.). Rocky Mountain Association of Geologists, p. 61–74.

Mountjoy, E.W., Price, R.A., and Lebel, D.
1992: Geology and structure cross-sections, Mountain Park, Alberta. Geological Survey of Canada, Map 1830A, NTS 83C/14, scale 1:50 000.

Douglas, R.J.W. and Lebel, D.
1993: Geology and structure cross-section, Cardinal River, Alberta. Geological Survey of Canada. Map 1828A, NTS 83C/15, scale 1:50 000

Lebel, D.
1993: Geometry, kinematics and computer simulations of thrust faulting, central Canadian Rocky Mountains, Alberta. Unpublished Ph.D. thesis, McGill University, 155 p.

GEOLOGY AND CROSS-SECTION, CARDSTON MAP AREA, ALBERTA (82H/3), SOUTHERN ALBERTA NATMAP PROJECT

D. Lebel

Geological Survey of Canada, 3303-33rd Street N.W., Calgary, Alberta T2L 2A7

INTRODUCTION

Bedrock mapping of the Cardston area represents one of the initial geological mapping projects of the new Southern Alberta Foothills NATMAP project (Fig. 1). This five-year project (1993-1998) will produce a new digital geoscience database for the eastern edge of the Cordillera in Southern Alberta, comprising new bedrock geological maps (Lebel et al., 1994; Lebel and Williams, 1994) and new cross- sections of subsurface structure established in cooperation with the petroleum industry using proprietary seismic information.

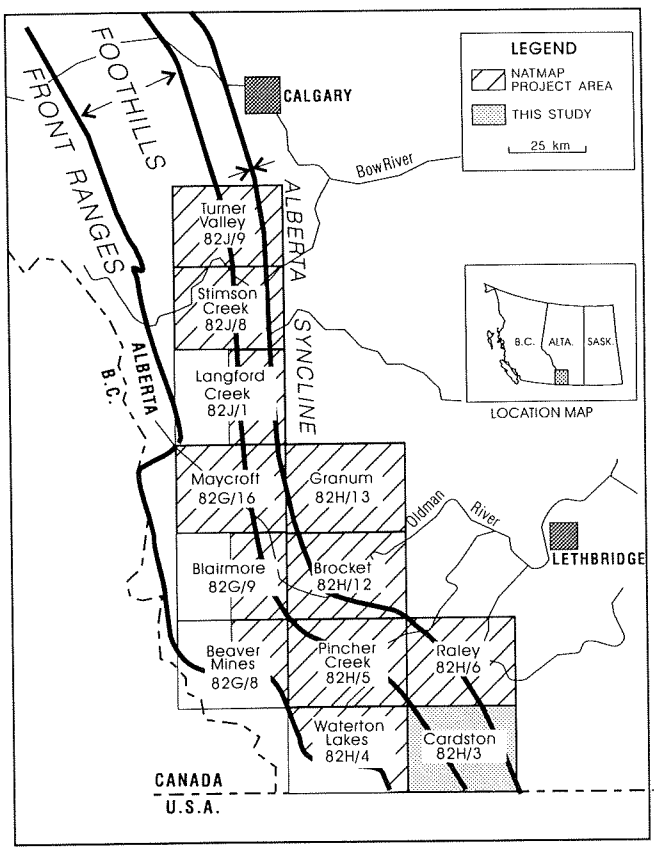

Figure 1. *Location of the study area and the Southern Alberta bedrock mapping NATMAP project.*

The Cardston map area (NTS 82 H/3, Fig. 1) overlaps the Southern Alberta Foothills and Alberta Plains geological divisions and lies immediately north of the Canada–U.S.A. border. The eastern part of the area is marked by the Alberta Syncline and the western flank of the Bow Island (Sweetgrass) Arch. Quaternary deposits are extensive in the area, and relief generally is less than 300 m. Good exposures are found along the banks of the St. Mary River and Lee Creek (Fig. 2).

The Foothills belt in the western part of the area was previously mapped in detail (1:31 680) by Williams (1949). Remapping of the area was required: to apply the new stratigraphic units within the Alberta and Belly River groups recognized recently by Jerzykiewicz and Norris (1993, 1994) for the Crowsnest Pass (Blairmore) area to the north; to utilize recent petroleum industry seismic and well data; to construct cross-sections to create a new digital geological database; and to apply a modern kinematic framework. Geological mapping was conducted for two months in the summer of 1993. Observations were plotted on air photographs (1:30 000 scale) and all data were compiled on a 1:50 000 digital topographic base map. Available well and seismic data will be used in the future to outline the structure of the area at depth.

STRATIGRAPHY

Upper Cretaceous to Tertiary rocks are exposed in the Cardston map area (Fig. 2). Regional mapping has recognized the southern extension of several new Upper Cretaceous stratigraphic units recently defined in the Crowsnest Pass area. The lower part of this segment of the regional stratigraphic column has been revised and redefined by Jerzykiewicz and Norris (1994). Their six new stratigraphic units are used herein. The six new units overlying the Wapiabi Formation are, in stratigraphic order: the Lees Lake, Burmis and Pakowki formations (upper Alberta Group, Campanian), and the Connelly Creek, Lundbreck and Drywood Creek formations (Belly River Group, Campanian). Four other formations overlie the Belly River Group: the Bearpaw

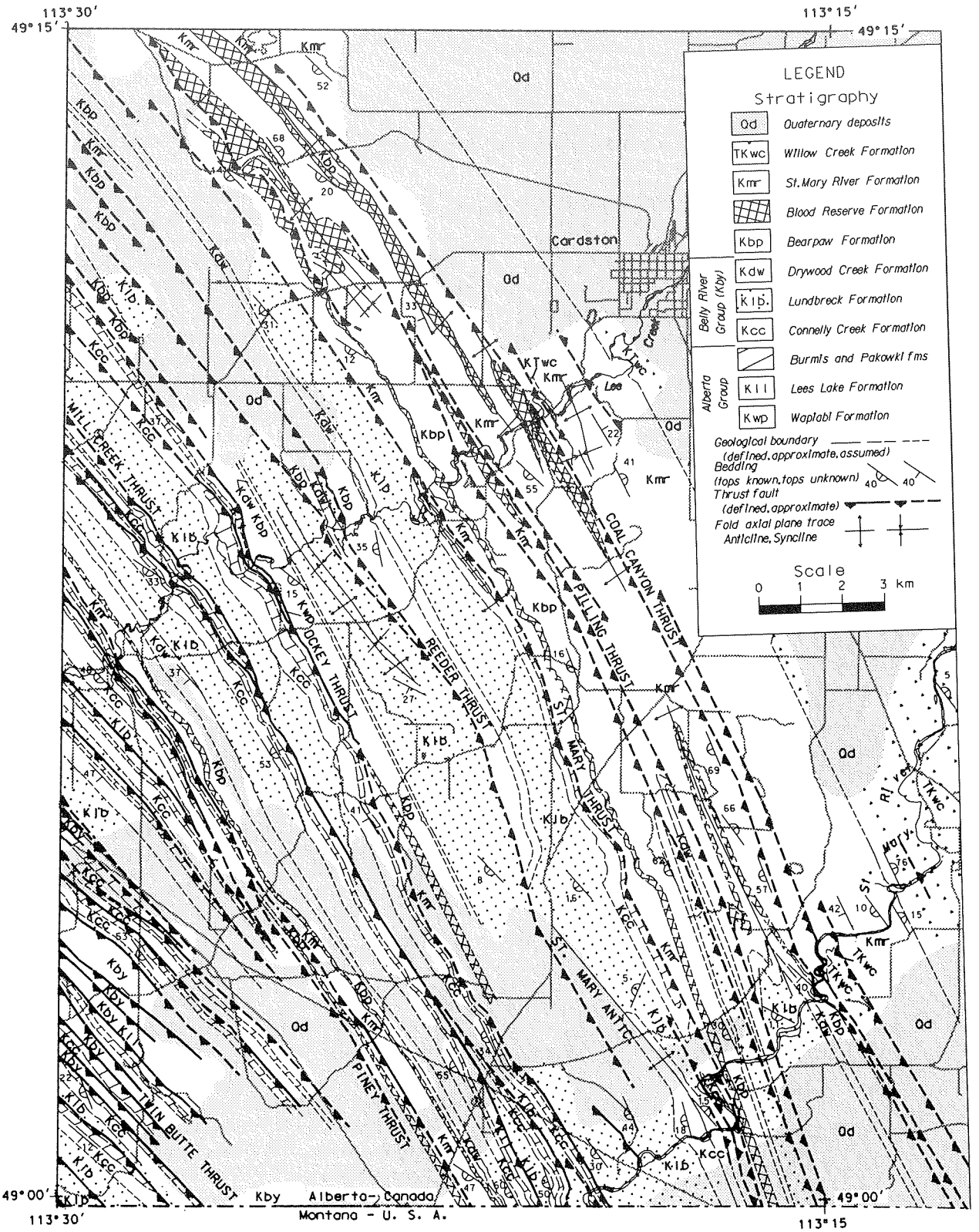

Figure 2. *Geological map of the west half of the Cardston map area (NTS 82 H/3).*

Formation (Uppermost Campanian), the Blood Reserve Formation and the St. Mary River Formation (Lower to Mid-Maestrichtian), and the Willow Creek Formation (Upper Maestrichtian to Lower Paleocene) (Figs. 2, 3). Previously, Williams (1949) used the base of the Burmis Formation for the base of his Belly River Formation which ranged to the base of the Bearpaw Formation.

STRUCTURAL GEOMETRY OF THE FOOTHILLS FROM SURFACE GEOLOGY

The eastern edge of the Rocky Mountain Foothills underlies the Cardston area. The Foothills in this area consist of a series of southwest-dipping, northeast-verging thrust faults deforming Upper Cretaceous strata (Fig. 2). Although no major southwest-verging thrust fault was mapped near the edge of the Foothills belt, structural relationships observed on some outcrops and at the regional scale suggest the presence of a triangle zone with a complex kinematic history.

Geometry of the Frontal Zone

For most of the Foothills of the Canadian Cordillera, a triangle zone is usually recognized, where a west-verging panel overlies the edge of the deformed belt along an upper décollement (Jones, 1982; MacKay, 1991). In the Cardston area and further south in Montana (Mudge et al., 1983) no such triangle zone has been discussed or recognized to date in the scientific literature. At the eastern edge of the Foothills belt in the Cardston area, most important faults are northeast-verging and only a few west-verging backthrusts occur with relatively small displacement. Only a few kilometers to the northwest of the Cardston map area, cross-sections presented by Gordy et al. (1977, Figs. 11b, 14) and Hiebert (1992) based on well and seismic data interpretation, suggest that the triangle zone still exists there, with an upper décollement panel showing significant displacement. One of the backthrusts has been traced from the Pincher Creek area and appears to decrease in displacement toward the south. Seismic data provided by Amoco Canada and crossing the Cardston area outlines the presence of a backthrust cutting through the Willow Creek Formation, a few kilometers northeast of Cardston, now obscured by Quaternary deposits. Field observations suggest that some backthrusts located in the interior part of the Foothills are cross-cut by east-verging faults.

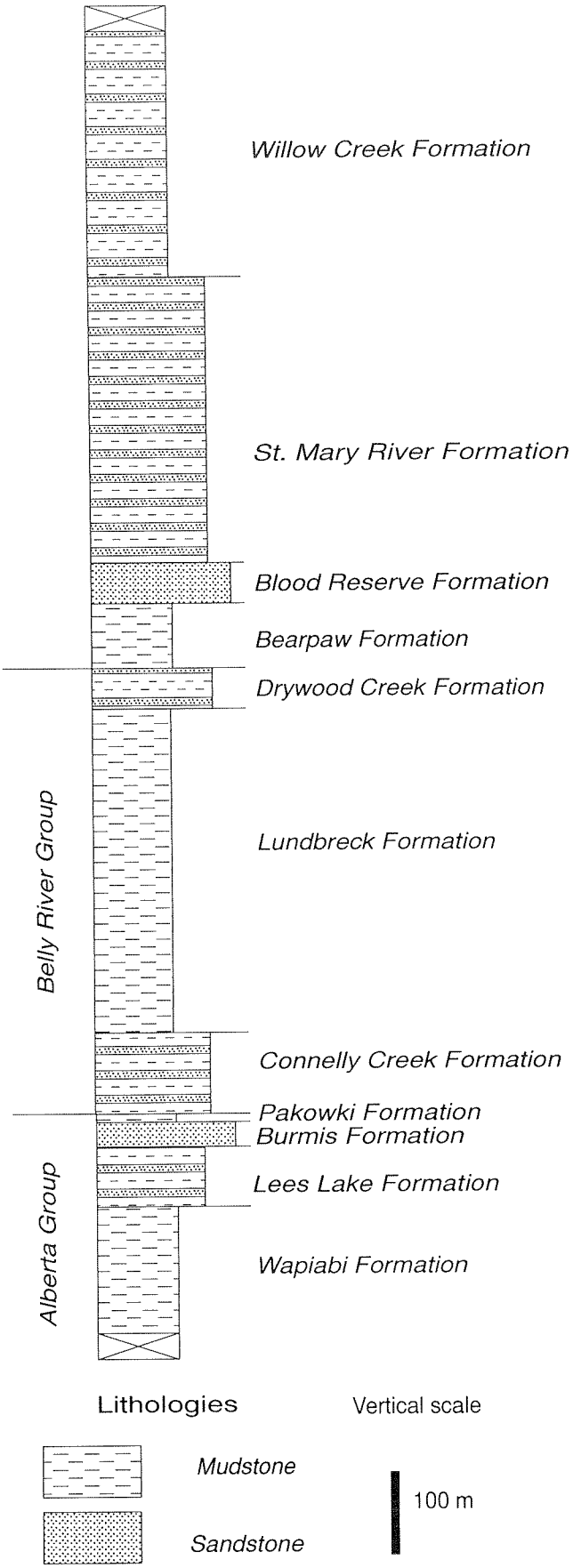

Figure 3. *Schematic stratigraphic column of the Cardston area.*

THE CRETACEOUS MCDOUGAL–SEGUR CONGLOMERATE: BLAIRMORE GROUP, ROCKY MOUNTAIN FOOTHILLS AND ADJACENT SUBSURFACE, ALBERTA, CANADA

D.A. Leckie

Geological Survey of Canada, 3303-33rd Street N.W., Calgary, Alberta T2L 2A7

L.F. Krystinik

Union Pacific Resource Company, P.O. Box 7, Fort Worth, Texas 76101-0007

INTRODUCTION

Lenses of Cretaceous igneous- and metamorphic-clasts occur within one stratigraphic unit — the McDougal–Segur Conglomerate — in the Rocky Mountain Foothills and Front Ranges of southwestern Alberta, northern Montana, and westernmost interior plains of Alberta. The purpose of this study is to document the occurrence of these igneous-clast conglomerate bodies, up to 60 m thick and 3 km wide, in outcrop and subsurface. The economic significance of the McDougal–Segur Conglomerate lies in their potential as hydrocarbon reservoirs in the subsurface (Cox, 1993; ERCB, 1994). Our observations in outcrop point to the McDougal–Segur Conglomerate having considerably more potential as a subsurface reservoir target in the Rocky Mountain Foothills and Interior Plains. Igneous-clast conglomerate from the correlative Bow Island Formation contains an estimated 775 x $10^6 m^3$ (ERCB, 1994). The conglomerates will be described with respect to their dimensions, geometry, petrography, economic potential and tectonic significance.

Thirty-five outcrops were measured in the Rocky Mountain Foothills and Main Ranges in southwestern Alberta. During the summer of 1991, each thrust sheet of the Rocky Mountain Foothills was flown by helicopter from the Montana border to west of Calgary, to identify, map and describe the distribution of McDougal–Segur conglomerate bodies within the Blairmore Group.

The stratigraphic position of the McDougal–Segur Conglomerate is not precisely known for all occurrences. In the Crowsnest Pass area, the conglomerate occurs near the top of the Blairmore Group and within the Bruin Creek Member (Fig. 1) of the Mill Creek Formation. A reference section for the McDougal–Segur Conglomerate has been designated at the type section for the Bruin Creek Member at Bruin Creek. The McDougal Segur Conglomerate occurs within the Beaver Mines and Mill Creek formations which are latest Early Albian or early Middle Albian, and middle Middle Albian or late Middle Albian age respectively. A late Middle Albian age for these rocks is supported by radiometric K/Ar ages of 99 and 101 Ma from the overlying Crowsnest volcanics on Mill Creek (Folinsbee et al., 1961). The McDougal–Segur Conglomerate does not represent a single fluvial event but was deposited at different times at different positions along the basin.

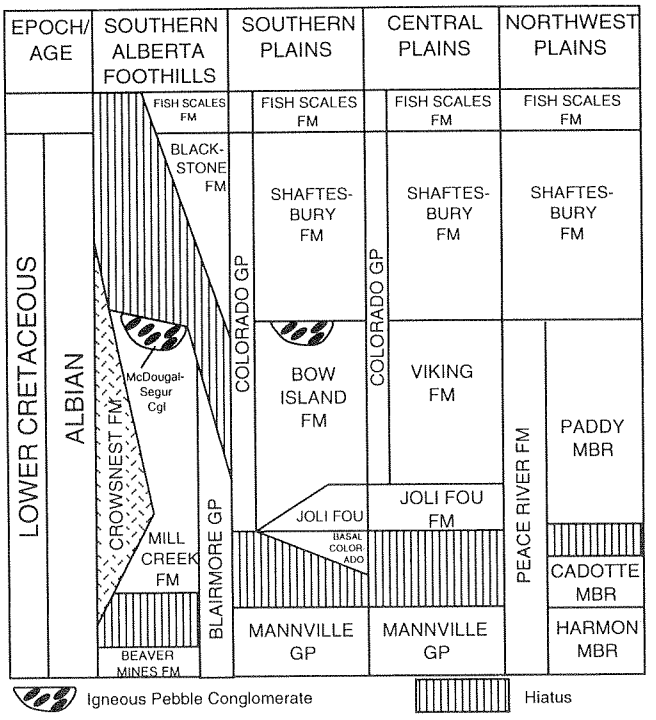

Figure 1. *Stratigraphic position of McDougal–Segur Conglomerate and equivalent igneous-pebble conglomerate in the subsurface Bow Island Formation.*

GENERAL DESCRIPTION OF THE CONGLOMERATE

The McDougal–Segur conglomerate consists of multiple channeled occurrences of pebble- to cobble-size sediment which fill scours cut up to 60 m into underlying sediments of the Mill Creek or Beaver Mines formations. In outcrop, the conglomerate can be traced laterally for 220 to 3000 m. Underlying sediment consists of very fine to medium grained, grey to green sandstone and siltstone, with no igneous pebbles. The conglomerate is overlain by sandstone with no evidence of igneous-clast conglomerate.

The conglomerate is predominantly clast-supported, with a medium to coarse grained sandstone matrix. Local occurrences of open-work gravel occur. Clast size varies from 1 to 30 cm. Maximum clast size of 30 cm occurs near Crowsnest Pass; elsewhere the maximum clast size is generally 15 to 20 cm. Individual strata vary from poorly to well sorted; some beds contain clasts decimetres in size which are abruptly overlain by beds containing centimetre-sized clasts. In most outcrops, other than the occurrence of large intraformational clasts (up to 2 m in size) at the base of the conglomerate, there is no discernible vertical grain size variation. At Bruin Creek, the top 4.5 m of the conglomerate consists of interbedded sandstone and conglomerate with beds 0.25 to 1 m thick. All pebbles are rounded to well rounded and are typically well imbricated, with clasts aligned transverse to paleoflow. Fractured pebbles and pressure solution pits at point contacts are characteristic of the conglomerate in outcrop. Erosively-based horizons of cobble-sized material, 1 to 3 clasts thick, that can be traced for several tens of metres, occur throughout the conglomerate. Tree casts occur but are rare. Stratification consists of crude to well-stratified, parallel bedding with bed sets up to 40 cm. Planar-tabular crossbedded conglomerate, with sets up to 50 cm thick, are defined by clasts lying on foresets. Medium grained, chloritic sandstone occurs as eroded, pebbly lenses up to 1.5 m thick, pinching out over a few metres to 20 m, and as the matrix for most of the conglomerate deposits. The sandstone is trough crossbedded and parallel laminated.

At most outcrops, the McDougal–Segur Conglomerate is overlain by medium to coarse grained, arkosic sandstone up to 40 m thick. At Bruin and Dutch creeks, this sandstone is about 8 m thick and contains minor burrowing and possibly roots.

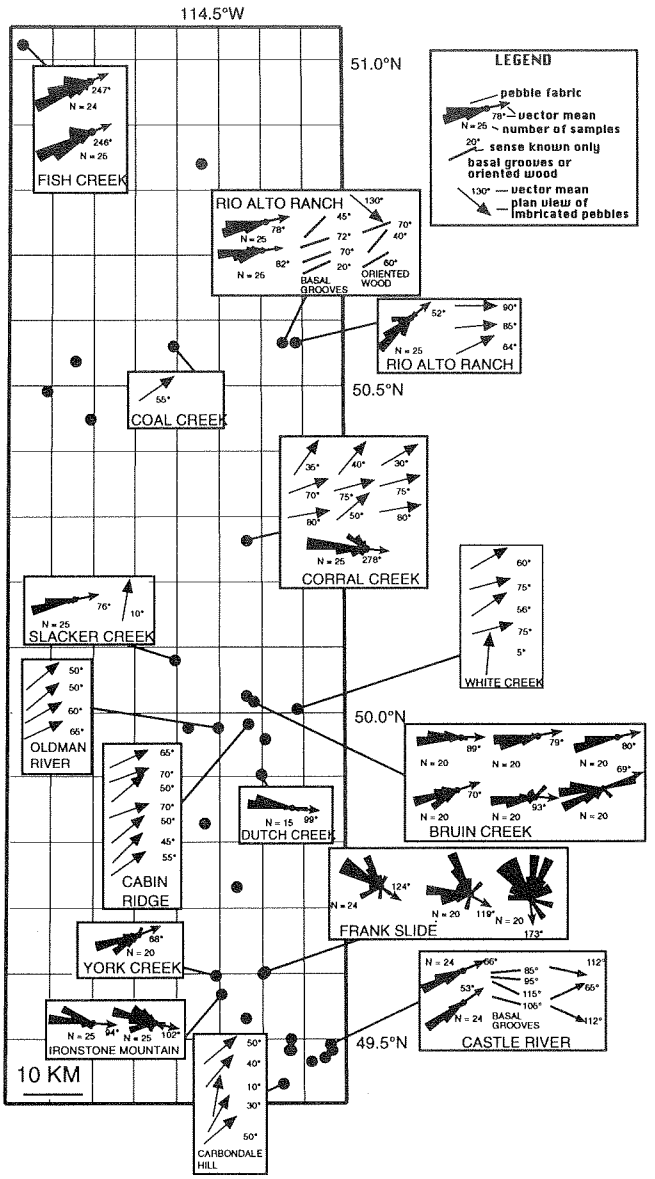

Figure 2. *Paleocurrent data for the McDougal–Segur Conglomerate.*

The McDougal–Segur Conglomerate consists of pebble to boulder-sized clasts of granite and mafic volcanics, chert, quartzite, and argillite.

PALEOCURRENTS

Paleocurrent data from imbricated clasts, basal channel grooves and oriented wood debris is plotted in Figure 2. An east–northeastward paleoflow dominates the data sets with the spread of vector means from pebble fabrics ranging from northeast to south. The

paleocurrent data shows considerable variability within individual outcrops and between adjacent outcrops (e.g., compare Frank Slide and Castle River). The east to northeastward trend is confirmed by occurrences of the conglomerate on multiple separate thrust slices along the Rocky Mountain Foothills. There is considerable range in the azimuths of the imbrication vector means, reflecting the local variability within the inferred braided channels, caused by local water-flow directions in the channel and by clasts near channel banks being obliquely oriented to the main channel.

The imbricated pebbles are predominantly aligned so that their long axes are oriented transverse to the paleoflow indicating transport by traction currents on the bed. Some pebbles align with their long axes parallel to the paleoflow.

CHANNEL SYSTEMS OF THE MCDOUGAL–SEGUR CONGLOMERATE

Four major channel systems — Highwood, Sentinel, Bruin, and Crowsnest channels — and five smaller channels — Lusk, Fish Creek, Racehorse, Vicary, and Carbondale channels — are identified from outcrop occurrences (Fig. 3). A sixth smaller channel — Sheep Channel— is defined from subsurface data. Delineation of the channels is based on the distribution of the conglomerate and how it pinches out to the north and south into finer-grained sediments. The east–west orientation of the channels is based on paleocurrent data and repeated occurrences of conglomerate on adjacent thrust slices.

The McDougal–Segur Congomerate outcrops were brought to the surface by, and can be traced laterally in multiple thrust sheets of the Rocky Mountain Front Ranges and Foothills. For example, Figure 4 shows conglomerate occurrences on thrusts of the Coleman Fault, east of the McConnell Thrust Fault and on the Livingstone Fault Thrust. The conglomerates on the different thrust sheets, align to define the east-trending Bruin Channel (Fig. 4). The Bruin Channel, up to 52 m thick, is defined by ten occurrences of conglomerate on the three different thrust sheets (Fig. 4). At the northern and southern margins of Bruin Channel, the conglomerate thins to about 2 m. Conglomerate making up the Highwood Channel is up to 38 m thick and occurs on several different thrust slices. The conglomerate at Rio Alto Ranch occurs on two adjacent thrust slices, 0.75 km apart, but is not present in the Highwood River, 1 km to the south. Crowsnest

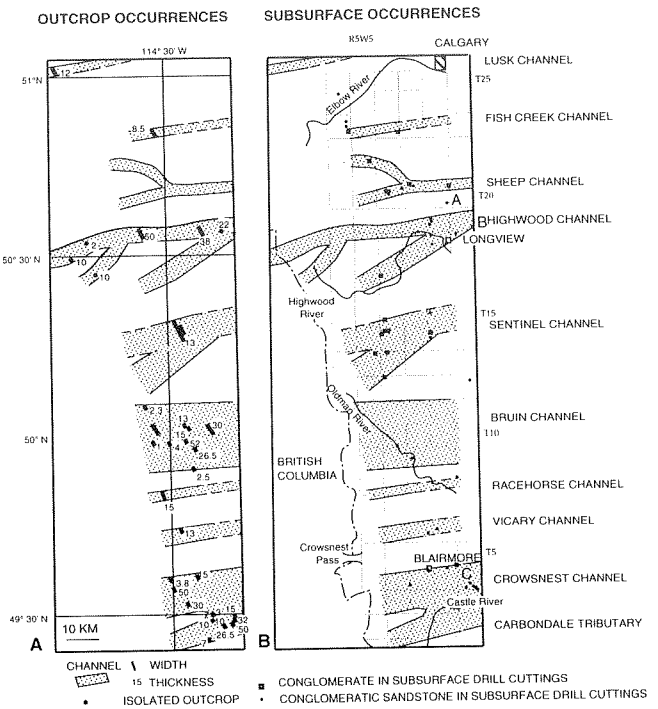

***Figure 3. A.** Outcrop occurrences of McDougal–Segur Conglomerate and channel distribution. **B.** Subsurface occurrences of igneous-pebble conglomerate and channel distribution.*

Channel, up to 50 m thick, is defined by 13 conglomerate occurrences on 7 to 8 thrust sheets including Coleman, Mutz, Turtle Mountain and other unnamed faults. Carbondale tributary is delineated from Crowsnest Channel by nonconglomeratic lithologies occurring between the two channels and a slightly different paleocurrent trend than Crowsnest Channel. Channel widths vary from 220 m wide at Screwdriver Creek to the ~22 km wide Bruin and Crowsnest channels.

The conglomerates on the different thrust sheets can be palinspastically restored 2 to 154 km west of their present outcrop positions (Urbatt, 1988; McMechan and Thompson, 1993). Based on this reconstruction, outcrop occurrences of the conglomerate indicate channels at least 25 to 400 km long (Leckie and Craw, in press).

SUBSURFACE

In the Turner Valley area, several wells drilled in the 1930s yielded hydrocarbon shows. Scout tickets indicate "possible gas sand", "40 ft. mud, 120 ft.

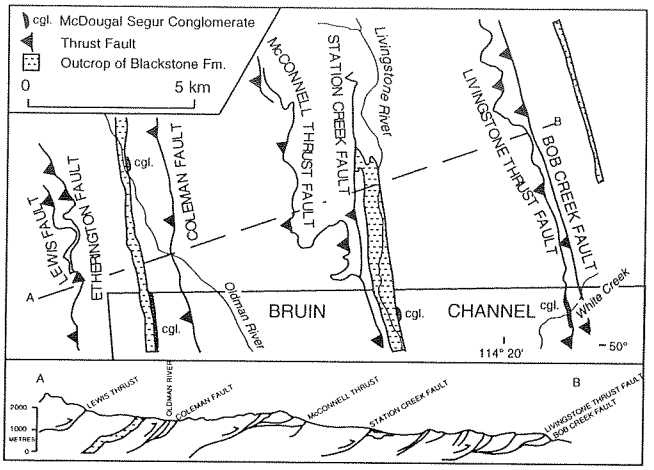

Figure 4. *Conglomerate occurrences on thrusts of the Coleman Fault, east of the McConnell Thrust Fault, and on the Livingstone Thrust Fault, to provide the mapping and trend of Bruin Channel. Note that the conglomerate occurs on multiple thrust slices.*

condensate", "oil in Blackstone, 34 MCF gas to surface" from middle Mannville units and McDougal–Segur sandstone.

The only known hydrocarbon production from igneous pebble conglomerate equivalent to the McDougal–Segur conglomerate is from the uppermost Bow Island Formation in the Blood–Magrath, Lethbridge–Chin Lakes, and Keho–Barons fields in southern Alberta (Fig. 5). Cox interpreted these as the deposits of a braided river and an "estuarine channel complex". Although Cox (1993) shows a north–south trending estuarine channel up to 30 m thick in the Blood–Magrath area, his data indicates a more northeastward-trending channel. Cox (1993) demonstrated that density–velocity variations of the conglomeratic could be used on seismic to identify and map the channels on a local basis. Cox's data suggest that the channel trends northeastward to a northwest-oriented shoreline.

The distribution of east–northeast directed channels of the McDougal–Segur Conglomerate in the Rocky Mountain Foothills (Leckie and Craw, in press) and adjacent subsurface is shown in Figure 5. The distribution of McDougal–Segur channels coincides and lines up with a system of preglacial, gravel-filled, buried valleys of the Saskatchewan Gravels and Sands (Stalker, 1961a). The close correspondence of Early Cretaceous and late-Tertiary to Quaternary channels suggests a possible underlying structural control or continuous superposition of channels across the Rocky Mountain Foothills and Main Ranges.

CONCLUSIONS

1. The McDougal–Segur Conglomerate is an igneous-clast braided-fluvial deposit which flowed east–northeast, perpendicular to the mountain front, into the foreland basin from a source terrain in batholiths of the Omineca Crystalline Belt.

2. Nine subparallel channels, up to 22 km wide and 60 m deep, have been identified flowing into foreland basin. The channels can be traced along easterly trends for up to 66 km in several thrust slices in the Rocky Mountain Foothills.

3. There is no indication in the underlying or adjacent sediment to herald the introduction of the conglomerate into the basin. After its deposition, sediment sedimentation returned to medium grained sandstone or finer detritus. The pulses of conglomerate are inferred to be related to shifting of the headwaters of drainage basins and stream capture in the Omineca Belt.

4. McDougal–Segur Conglomerate may have reservoir potential in the subsurface of the Rocky Mountain Foothills and western Interior Plains, particularly when sourced from the Second White Specks Formation. Porosity may be enhanced in the Foothills by the common crushing and fracturing of pebbles.

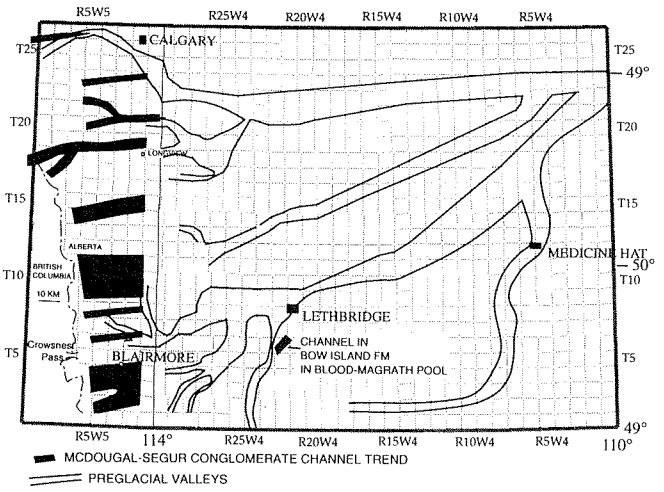

Figure 5. *Map showing alignment and correspondence of McDougal–Segur Conglomerate from outcrop in the Rocky Mountain Foothills (Leckie and Craw, in press) and from late Tertiary to early Quaternary preglacial valleys (Stalker, 1961) in southwestern Alberta. The subsurface channel from the middle Cretaceous Bow Island Formation is from Cox (1993).*

REFERENCES

Cox, J.
1993: The stratigraphy and sedimentology of the Bow Island Formation, south–west Alberta. Unpublished Ph.D. thesis, Dept. of Geology and Petroleum Geology, University of Aberdeen, 172 p.

ERCB (Energy Resources Conservation Board)
1994: Alberta's reserves of crude oil, oil sands, gas and natural gas liquids and sulphur. ERCB ST 94–18, Variably paginated.

Folinsbee, R.E., Baadsgaard, H., and Lipson, J.
1961: Potassium – Argon dates of Upper Cretaceous ash falls, Alberta, Canada. New York Academy of Science, Annals, v. 91(2), p. 352–363.

Leckie, D.A. and Craw, D.
in press: Westerly-derived Early Cretaceous gold paleoplacers in the Western Canada foreland basin: tectonic and economic implications.

McMechan, M.E., and Thompson, R.I.
1993: The Canadian Cordilleran Fold and Thrust Belt south of 66°N and its influence on the Western Interior Basin. *In* Evolution of the Western Interior Basin. W.G.E. Caldwell and E.G. Kauffman (eds.). Geological Association of Canada, Special Paper 39, p. 73–90.

Stalker, A. MacS.
1961: Buried valleys in central and southern Alberta. Geological Survey of Canada, Paper 60–32, 13 p.

Urbatt, R.R.
1988: Provenance of the Lower Cretaceous (Albian) McDougall–Segur Conglomerate, southwestern Alberta. Unpublished B.Sc. Thesis, University of Calgary, 85 p.

CRATER FACIES AND WAVE-REWORKED KIMBERLITE OF THE ALBIAN COLORADO GROUP–SMEATON NO. 169, FORT À LA CORNE FIELD, SASKATCHEWAN, CANADA

D.A. Leckie

Geological Survey of Canada, 3303-33rd Street N.W., Calgary, Alberta T2L 2A7

B.A. Kjarsgaard

Geological Survey of Canada, 601 Booth Street, Ottawa, Ontario K1A OE8

The Fort à la Corne kimberlite field in central Saskatchewan contains more than 70 geophysical targets of which more than 40 have been confirmed by drilling. The kimberlites consist of crater facies, and fluvial and wave-reworked material. Mineralogically, the kimberlites are classified as Group I. Age constraints on basement rocks in the area are poor, but they are inferred to be of Trans-Hudson vintage (Paleoproterozoic), consistent with zircon ages from kimberlite-derived lower crustal xenoliths. The geology of the Fort à la Corne area is represented by nonmarine Cretaceous sandstone, siltstone and shale (Mannville Group) overlain by marine shale (Westgate Formation of the Colorado Group), which in turn is overlain by 90 to 130 m of glacial till. The kimberlites were emplaced syn- to post-Mannville and pre- to syn-Westgate, consistent with available radiometric age determinations (102 to 96 Ma). This paper presents petrology and sedimentology of Smeaton kimberlite No. 169, based on detailed studies of 132 m of drill core through Cretaceous strata. Five distinct lithological units are distinguished.

The base of the core (unit 1), consists of 4.5 m of trough-crossbedded, matrix-supported kimberlite conglomerate fining upward to a carbonaceous pebbly olivine sandstone, representing deposition in a meandering-river point bar. This is overlain by ≈20 m of interbedded siltstone and sandstone. Siltstone beds (massive, rippled and laminated) are carbonaceous and rooted. Foraminifera indicate localized, stressed, brackish-water conditions. This unit is interpreted as deposited in a low-energy, nonmarine to delta-plain setting associated with the upper Mannville Group. An early episode of kimberlite emplacement was reworked by fluvial processes in this setting. Tentative correlations would indicate reworking during the Albian which would be younger than 108 to 105 Ma.

Unit 2 consists of 38 m of kimberlite lapilli dominated tuffs of variable grain size. The more than 50 individual normal graded beds (10 cm to 1 m scale) contain more lapilli than olivine. Some beds grade from coarse grained lapilli-rich bases to fine grained olivine-rich tops and contain large (metre-scale) shale clasts. This unit is interpreted as being dominated by pyroclastic airfall deposits, with agglutinated lapilli tuffs and welded spatter suggestive of mildly explosive Strombolian type volcanism. Rare reverse-graded beds (with outsize clasts) are interpreted as slumps or debris flows related.

Unit 3 is 45.5 m thick and consists of six normal-graded beds 3 to 13 m thick. The base of each bed is rich in dominantly poorly-sorted, coarse grained olivine, kimberlite lapilli, mantle xenocrysts and xenoliths plus country rock xenoliths. Each bed grades upward into well-sorted medium to very fine grained deposits (with minor internal stratification) dominated by olivine crystals with very rare, coarse grained kimberlite lapilli. This unit is interpreted as an airfall crystal-tuff deposit; the very high proportion of olivine and depletion in matrix ash requires aeolian sorting (i.e., a high eruption cloud consistent with highly-explosive phreatomagmatic vulcanian-type volcanism).

Unit 4 consists of 12 m of micaceous, fine grained, parallel-bedded sandstone fining upward to shaley siltstone; this in turn is overlain by a 10 m, coarsening-upward succession of shale grading to very-coarse olivine + mantle xenocryst-rich sandstone. Sedimentary structures indicate reworking by waves in an coarsening-upward shoreline succession of reworked and concentrated kimberlitic material overlain by a transgressive lag deposit. Unit 4 is interpreted as flooding and burial of kimberlite by the Colorado Sea and shallow-marine/shoreface reworking of kimberlite detritus. Heavy minerals and diamonds have the potential to be concentrated in the shoreface and transgressive lag deposits.

The top of the core (unit 5), consists of 12 m of black marine shale with light to moderate bioturbation. Foraminifera place the shale in the upper Albian Westgate Formation of the Colorado Group, below the Fish Scales Formation.

CANADA/ALBERTA PARTNERSHIP ON MINERALS (MINERAL DEVELOPMENT AGREEMENT) – PROJECTS AND PROGRESS

R.W. Macqueen

Geological Survey of Canada, 3303-33rd Street N.W., Calgary, Alberta T2L 2A7

INTRODUCTION

Mineral Development Agreements (MDAs; known as Economic Development Agreements in Yukon and NWT) are contractual arrangements between the Canadian Federal Government and a particular province or territory, to undertake specific, mineral-related studies over 3 to 4 year time periods and with agreed-upon levels of funding. All provinces and territories except Prince Edward Island hold or have held MDAs. The idea is to conduct and publish studies that will encourage mineral exploration and production in Canada. Alberta's first MDA, known also as the "Canada–Alberta Partnership on Minerals", covers the period 1992–95 with a wrap-up year 1995–96. Over the four year period of the Alberta MDA, 1992–1996, a total of about $8.6 million will have been spent by both levels of government, with federal funding about $4.7 million and the Province of Alberta the remainder. Activities and levels of funding (considering federal and provincial expenditures together) include Geoscience (~65%), Mining and Minerals Technology (~16%), Technology Development (~9%), Economic Development (~2%), Public Information (~3%) and Program Administration (~5%). The heavy weighting of expenditures on geoscience studies is based on advice from the mining industry and experience elsewhere: sound geoscience studies including up-to-date geological maps is generally agreed to be the best exploration investment/stimulus governments can make. Studies in geoscience, mining and minerals technology, etc. as noted above are undertaken by government scientists and contractors; a general requirement is that all work must reach the public domain for the use of all. A significant part of the geoscience work is conducted by collaborative studies involving personnel of the Geological Survey of Canada and the Alberta Geological Survey.

GEOSCIENCE STUDIES

Provincially-funded geoscience studies number more than 20, with nearly half of these conducted by private contractors. Included are studies on mineral potential of the Southern Alberta Rift, hydrogeochemistry of Northern Alberta, potential for co-production of minerals/metals in Oil Sand deposits, mineral potential of northeastern Alberta, limestones of Alberta, commodity profiling of minerals, etc. Results of many of these studies have already been released as Open Files.

On the federal side, 13 projects are underway within six subprograms (northeastern minerals, southwestern minerals, diamonds, industrial minerals, orientation studies, and coordination), highlights follow. Much of the work is conducted by Geological Survey of Canada geoscientists based in Ottawa and Calgary; some studies are contracted (e.g., lake sediment geochemistry). Figure 1 shows the location of the 12 field-based studies in Alberta, and references listed at the end of this contribution indicate some of the findings and progress to date.

NORTHEASTERN MINERALS

Tectonic evolution of the Precambrian Shield of Northeastern Alberta (IA), M.R. McDonough, GSC Calgary. All or parts of 14 1:50 000 scale maps in NTS 74 are being geologically mapped to modern standards, with emphasis on the tectonic evolution of the region and the mineral potential of all units especially including shear zones. Radiometric dating is a key part of this new work. All map data are being acquired digitally in FIELDLOG and AutoCad and all maps are being produced digitally and in hard copy versions. Many new occurrences of gossans/alteration zones/breccia sites have been found and sampled for base and precious metals. More than half of the geological maps have been released as GSC Open Files.

Metallogenic studies for U-polymetallic mineralization of the Athabasca Basin and adjacent area (IB), V. Ruzicka, GSC Ottawa. The Proterozoic-aged Athabasca

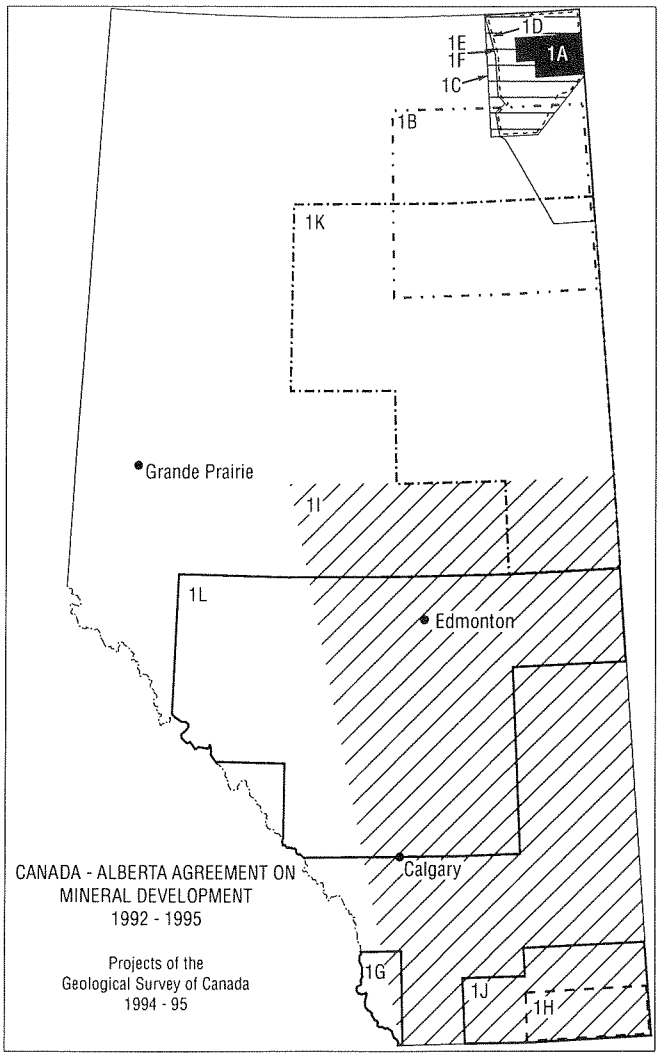

Figure 1. Map showing the study areas of Federal MDA projects currently underway in Alberta.

Basin of Saskatchewan is one of the richest uranium-bearing basins in the world: this project deals with the extension of this basin into Alberta. Work to date confirms the similarity of the area with Saskatchewan, and therefore the favourability of the basement and the overlying Athabasca Group sediments in Alberta for monometallic and polymetallic mineralization. Lenses of massive pitchblende and coffinite are known from basement and cover rocks, especially along the sub-Athabasca unconformity. Elevated amounts of certain metals occur in the area, including nickel, arsenic, uranium, molybdenum, boron and chromium, and traces of gold are found in all units.

Quaternary geology and till geochemistry (IC), J. Bednarski, GSC Calgary. This project is designed to aid mineral exploration on the Canadian Shield of Alberta by providing a comprehensive map of the surficial geology. Emphasis is on the nature and provenance of the glacially-derived materials, and on mineral enrichment in these materials. The mapping also provides an inventory of granular materials and a resource for land-use planning. There is a need for the surficial data provided by this project, given the high level of interest in the possible occurrence of diamond-bearing kimberlites in Alberta and their recognition by diamond indicator minerals.

Airborne gamma-ray spectrometer-magnetics-VLF plus interpretation and follow-up (ID), B.W. Charbonneau, GSC Ottawa. This project is now almost complete with the production of 12 colour maps at 1:250 000 scale (8 radiometric, 2 magnetic, and 2 VLF plus), including a

complete set of stacked profiles. The data are available as two open files: one digital, and one hard copy with coloured maps (see selected references, below). The airborne survey produced a set of well-defined geophysical patterns. A novel aspect of the survey was the ability to calibrate and interpret airborne data using geochemical analyses derived from the analysis of 694 widely-spaced samples collected by personnel of the Alberta Geological Survey in the 1960s and 1970s. It is expected that the survey will generate significant economic interest.

Geochemical surveys (IE), P.W.B. Friske, GSC Ottawa. A reconnaissance lake sediment and water geochemical survey was carried out during the summer of 1993, to National Geochemical Reconnaissance standards. The survey covered 21 400 km^2, and consists of samples from 1160 sites. These data are now available in digital and hard copy form, as GSC open files (see references below). There is considerable interest on the part of mining companies in the southern part of the area covered by this survey. Work elsewhere in Canada demonstrates that regional geochemical surveys of lake sediments and waters are a cost-effective means of quickly evaluating the mineral potential of an area.

Data Integration (IF), C.F. Chung, GSC Ottawa. The goal of this project is to use data from all of the projects noted above to produce mineral potential maps for northeastern Alberta. These maps will integrate all spatial data, and will attempt to indicate the likelihood of occurrence of particular commodities based on probabilities.

SOUTHWESTERN MINERALS

Mineral potential, metamorphism and petrogenesis of the Crowsnest Volcanics (IG), T. Peterson, GSC Ottawa. Field studies and analytical data derived from this project indicate that the Crowsnest volcanics originated by partial melting of lower crustal rocks; no mantle-derived mafic melts were involved except perhaps as a source of heating for melting. The distribution of base metal concentrations in both fresh and metamorphosed epiclastic rocks of the Crowsnest volcanics indicates that no mobility of metals was induced, and no anomalous metal concentrations have been observed. Studies carried under this project suggest that the potential for precious and base metal mineralization in these rocks is low. Zeolites and garnets also occur in these rocks, but the amounts and distributions appear to be subeconomic.

DIAMONDS

Kimberlite mineralogy, petrology and geochemistry (IH), B.A. Kjarsgaard, GSC Ottawa. Much of Alberta has been staked in diamond exploration programs, based on the occurrence of diamondiferous kimberlites in the Fort a la Corne area of central Saskatchewan and on the Canadian Shield in the Lac de Gras area of the Northwest Territories. Intrusive rocks of Eocene age are known in the Milk River area of southernmost Alberta as part of the Sweet Grass intrusive suite of the Montana Alkaline Province. Mineralogical and chemical studies of these rocks demonstrate that they are minettes and are similar to other minettes from the Montana alkaline province. Although the potential for these minettes to be diamond-bearing is considered to be low, this does not rule out the possibility of occurrence of diamond-bearing kimberlites or lamproites in the adjacent Medicine Hat crustal block of Archean age. Minettes may have some potential for the occurrence of gold or platinum group elements, and this study will also evaluate this potential.

Geochemical and mineralogical reconnaissance (IJ), L.H. Thorleifson and R.G. Garrett, GSC Ottawa. Because prospecting for diamonds via diamond indicator minerals is of much interest to industry, this study is designed to provide regional background data on the provenance, chemical composition and heavy mineral content of till and soils of the Canadian prairies. Sample design was based on a study carried out in 1991; the main survey, completed under contract in 1993, involved samples from more than 300 sites in southern Alberta. Broad, regional trends are present in drift provenance and geochemical data. Diamond indicator minerals were obtained from the 25 kg samples collected. Three GSC open files have been released on these data. These data significantly influence private sector mineral exploration programs. The geochemical data from this survey are also of interest in terms of the trace element compositions of soils and agricultural crops grown on these soils.

Aeromagnetic Survey (IK), P. Stone, GSC Ottawa. This survey was completed under contract in 1992–1993, with maps and digital data being released in 1993 (see references below). The maps and digital data are of continuing value to those in the geological and geophysical exploration community who are attempting to detect kimberlites, intrasedimentary anomalies and basement structure of importance to hydrocarbon and structural framework studies. The data are of very high quality, and are attracting favourable comments from industry users.

INDUSTRIAL MINERALS

Brine resources of Alberta (IL), H.J. Abercrombie, GSC Calgary. This study began with a focus on calcium- and magnesium-rich brines within Middle Devonian units of the central Alberta subsurface, but the discovery of anomalous amounts of gold in the Fort McKay region of Alberta necessitated a change in emphasis from brines to gold. Recent work centers around the identification of anomalous gold and platinum group element mineralization and on analytical methods development. The presence of micron-sized disseminated gold has been confirmed, but important questions remain on the distribution and possible economic significance of this find. The work is supported by industry contributions and involves GSC, the Alberta Geological Survey and mining exploration companies. Significant staking activity was generated in the spring of 1994 based on data from this project.

ORIENTATION STUDIES

Orientation Studies (IL), S.B. Ballantyne, GSC Ottawa. It has been known for some years that Tertiary and Quaternary gravels in central Alberta commonly have small amounts of placer gold and platinum group elements. This study is designed to identify the nature, amounts and sources of these and other elements of possible economic significance in heavy mineral concentrates from gravels. Scanning electron microscopy and electron probe identification are major means of identifying and classifying precious and native elements in this study. Work to date indicates that hot (mantle-sourced) and cold (brine-transported) models of gold, platinum group elements and native metals may apply in Alberta. Considering the widespread distribution in alluvial drainages of fine gold, platinum group elements and native metals and alloys in Alberta as demonstrated in this project, the sedimentary mineral potential of Alberta may be significant, and is yet to be exploited.

COORDINATION

Coordination and Publication (IM), R.W. Macqueen, GSC Calgary. The objective of this project is to encourage the completion of high-quality research of specific benefit to the mineral industry, and to foster the public release of the results of MDA-funded work in a timely fashion and a suitable format. Plans are underway to produce a GSC Bulletin in 1995 for release in 1996 summarizing all of the above projects and including certain provincially-funded projects.

REFERENCES

Bednarski, J.M.
in press: Surficial Geology, Andrew Lake, Alberta, Saskatchewan, NWT. Geological Survey of Canada, Open File 2982, 1:50 000 scale.

Davis, W.J. and Kjarsgaard, B.A
1994: A Rb-Sr phlogopite – whole rock isochron age for olivine minette from the Milk River area, southern Alberta. *In* Radiogenic Age and Isotopic Studies: Report 8, Current Research 1994-F. Geological Survey of Canada, p. 11–14.

Feng, R. and Abercrombie, H.J.
1994: Disseminated Au-Ag-Cu mineralization in the Western Canada Sedimentary Basin, Forth MacKay, Northeast Alberta: A new gold deposit type. *In* Current Research 1994-E. Geological Survey of Canada, p. 121–132.

Friske, P.W.B., McCurdy, M.W., Day, S.J., Gross, H., Balma, R.G., Lynch, J.J., and Durham, C.C.
1994: Regional Lake Sediment and Water Geochemical Data, Northeastern Alberta. Geological Survey of Canada, Open File 2856, Parts of NTS 74E, 74L and 74M.

Garrett, R.G.
1994: The distribution of cadmium in A horizon soils in the prairies of Canada and adjoining United States. *In* Current Research, 1994-B. Geological Survey of Canada, p. 73–82.

Garrett, R.G. and Thorleifson, L.H.
1993: Prairie kimberlite study – soil and till geochemistry and mineralogy, low density orientation survey traverses, Winnipeg–Calgary–Edmonton–Winnipeg, 1991. Geological Survey of Canada, Open File 2685, one diskette.

Harris, D.C. and Ballantyne, S.B.
1994: Characterization of gold and PGE-bearing placer concentrates from the North Saskatchewan River, Edmonton, Alberta. *In* Current Research 1994-E. Geological Survey of Canada, p. 133–139.

Hetu, R.J., Holman, P.B., and Charbonneau, B.W.
1994: Multiparameter airborne geophysical survey of northeastern Alberta, NTS 75L/14, 15; 74M/1–3, 6–11, 14–15. Geological Survey of Canada, Open File 2807.

Kjarsgaard, B.A.
1994: Potassic magmatism in the Milk River area, southern Alberta: Petrology and Economic Potential. *In* Current Research, 1994-B. Geological Survey of Canada, p. 59–68.

Kjarsgaard, B.A. and Davis, W.J
1994: Eocene magmatism in the Sweet Grass Hills and its tectonic significance. *In* Lithoprobe Alberta Basement Transects Workshops (Feb 14–15), G.M. Ross (ed.). Lithoprobe Report No. 37, Lithoprobe Secretariat, University of British Columbia, p. 234–237.

McDonough, M.R. and Abercrombie, H.J.
1995: Mineral occurrences in Middle Devonian carbonates, salt River and Stony Islands (Slave River) areas, northeastern Alberta. *In* Current Research 1995-B. Geological Survey of Canada, p. 125–130.

McDonough, M.R., Cooley, M.A., and Schetselaar, E.M.
1994: Geology, Hay Camp, Alberta (74M/11). Geological Survey of Canada, Open File 2832, 1:50 000 scale.

McDonough, M.R., Grover, T.W., McNicoll, V.J., Cooley, M.A., Schetselaar, E.M., and Robinson, N.N.
1994: Geology, Cornwall Lake, Alberta (74M/10). Geological Survey of Canada, Open File 2896, 1:50 000 scale.

McDonough, M.R., Grover, T.W., McNicoll, V.J., Lyndsay, D.D., Kelly, K.L., and Guerstein, P.G.
1994: Revised Geology, Mercredi Lake, Alberta (74M/15). Geological Survey of Canada, Open File 2904, 1:50 000 scale.

1994: Revised Geology, Andrew Lake, Alberta (74M/16). Geological Survey of Canada, Open File 2905, 1:50 000 scale.

1994: Geology, Tulip Lake, Alberta (East half, 74M/14). Geological Survey of Canada, Open File 2820, 1:50 000 scale.

McDonough, M.R., Plint, H.E., McNicoll, V.J., and Grover, T.W.
1994: 40Ar/39Ar and K-Ar age constraints on shear zone evolution, southern Taltson magmatic zone, northeastern Alberta. *In* Lithoprobe Alberta Basement Transects Workshop (Feb. 14–15), G.M. Ross (ed.). Lithoprobe Report No. 37, Lithoprobe Secretariat, University of British Columbia, p. 254–266.

Peterson, T.D. and Currie, K.L.
1993: Analcite-bearing igneous rocks from the Crowsnest Formation, southwestern Alberta. *In* Current Research, Part B. Geological Survey of Canada, Paper 93-1B, p. 51–56.

Ross, G.M., Mariano, J., and Dumont, R.
1994: Was Eocene Magmatism Widespread in the Subsurface of Southern Alberta? *In* Alberta Basement Transects Workshop (Feb. 14, 15), G.M. Ross (ed.). Lithoprobe Report No. 37, Lithoprobe Secretariat, University of British Columbia, p. 240–249.

Ruzicka, V.
1994: Metallogenic Features of the Athabasca Basin, Alberta (abstr.). *In* "Program and Abstracts, The Calgary Mining Forum, February 10–11". Calgary Mineral Exploration Group Society, Calgary, p. 31, 45.

Stone, P.E.
1993: High Resolution Aeromagnetic Total Field Survey of the Cypress Hills Area, Alberta, 6 sheets (black and white) scale 1:100 000, released May 7, 1993. Geological Survey of Canada, Open File 2588. Maps are: map 1 – 82H/NE (south half); map 2 – 72E/NW; map 3 – 72E/NE; map 4 – 82H/SE; map 5 – 72E/SW; map 6 – 72E/SE.

1993: Coloured maps: aeromagnetic residual Total Field Colour Interval Maps with Line Contours, Cypress Hills area, southern Alberta, scale 1:100 000. 82H/NE (south half) – map C9865G; 72E/NW – map C9866G; 72E/NE – map C9867G; 82H/SE – map C9868G; 72E/SW – map C9869G; 72E/SE – map C9870G.

Thorleifson, L.H. and Garrett, R.G.
1993: Prairie kimberlite study – till matrix geochemistry and preliminary indicator mineral data. Geological Survey of Canada, Open File 2745, one diskette.

DIAGNOSING NATURAL AND DRILLING-INDUCED FRACTURES WITH BOREHOLE IMAGES OF WESTERN CANADIAN WELLS

R.E. McCallum

R.E.M. Consulting 1447-19th Avenue S.W., Calgary, Alberta T2T 0J1

J.S. Bell

Geological Survey of Canada, 3303-33rd Street N.W., Calgary, Alberta T2L 2A7

INTRODUCTION

Strenuous efforts are being made today within the oil industry to document and quantify fracture networks in reservoirs in order to develop optimum hydrocarbon recovery scenarios. Traditionally, fractures have been identified on core samples, or inferred indirectly from acoustic and density logs. New logging technology now permits earth scientists to directly image fractures on borehole walls. This information is currently recorded by Formation MicroScanners (FMS), Formation Micro-Imagers (FMI) and Borehole Televiewers (BHTV). FMS and FMI tools measure microresistivity contrasts, whereas BHTVs record variations in acoustic velocity. In this paper, we present and discuss FMI images of fractured reservoirs in Western Canada. The concepts presented rely on geometry and are fully applicable to FMS and BHTV log interpretation.

FORMATION MICRO-IMAGER

A Formation Micro-Imager gathers its data with 8 pads that are fitted with numerous electrodes (Fig 1). The pads are hydraulically pressed against the sides of the well as the tool is raised. Variability in surface resistivity is recorded where the pads are in contact with the wall. Interpretive software converts the digital microresistivity contrasts into brown-yellow tones or shades of grey. Dark colors indicate high conductivity and light colors indicate low conductivity (Bourke et al., 1989). The images are displayed as unravelled resistivity maps of the borehole walls. Open fractures become filled with drilling mud and exhibit low resistivity (dark colours). Cemented fractures are more resistive compared to the matrix and are seen as white traces (Heliot et al., 1990). If the borehole wall has rough surface topography, the pads will be unable to make close contact with the formation and an unfocussed image will be recorded (Fig. 2).

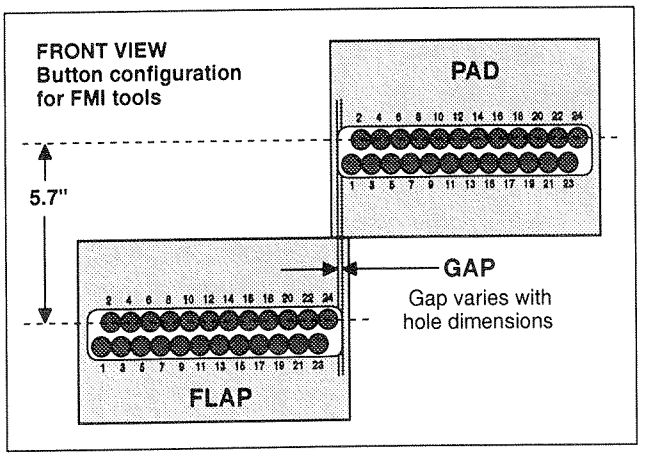

Figure 1. *Sketch of the FMI pad configuration. The flapper pads positioned below and offset from each of the regular pads allow for excellent hole coverage (80% in 8 in. holes). The button electrodes detect electrical currents and provide the raw data that is processed to yield high resolution (0.2 in.) images of the borehole wall.*

Micro-imaging tools must be run in open holes filled with conductive drilling muds. They cannot operate in holes containing oil-based muds, or record data through casing.

NATURAL FRACTURES vs. DRILLING-INDUCED FRACTURES

When an inclined fracture intercepts a well, its trace forms a sine wave loop wrapped around the inside of the hole (Fig. 3). The fracture's relative resistivity, compared to the formation, indicates whether it is open or cemented. Identifying such features on FMI/FMS logs as fractures is straightforward and interactive software is used to determine their orientations and assess

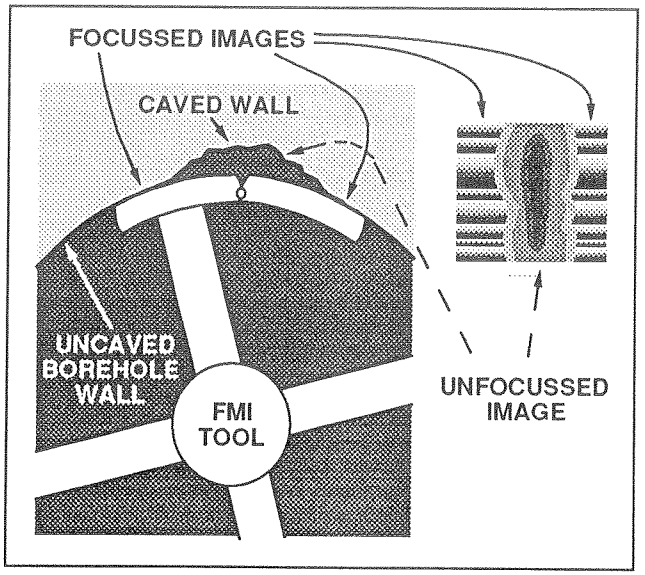

Figure 2. *Schematic of an FMI image in ovalized borehole conditions. The tool pads are unable to make firm contact with the formation in the spalled zones and a diffuse, unfocussed image results.*

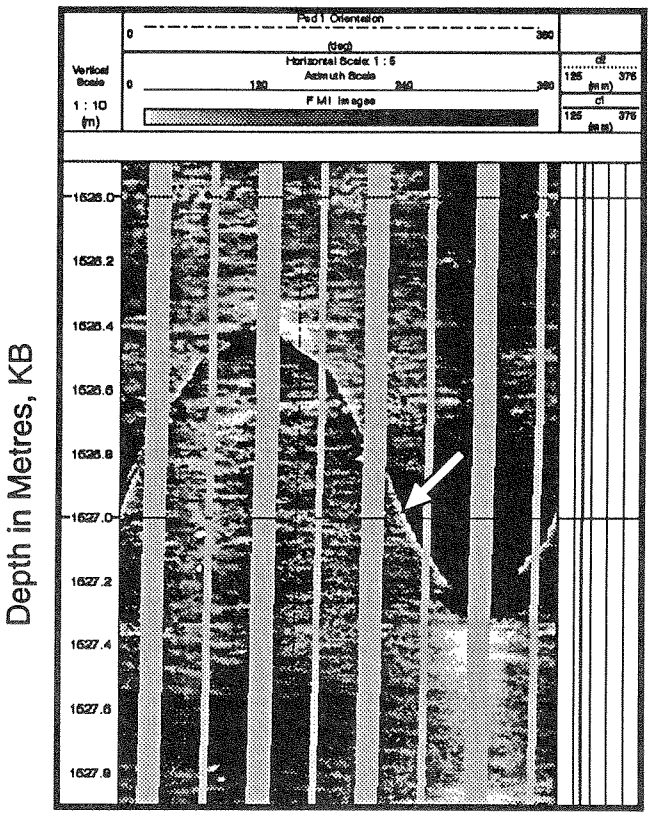

Figure 3. *FMI image of an inclined fracture that intersects the borehole wall. Its trace forms a sine wave loop wrapped around the inside of the hole.*

hydraulic properties. Difficulties arise, however, during fracture analysis, because some of the fractures recorded by borehole-imaging tools are not natural pre-existing features. They are induced by the drilling process itself and involve cracks that are present only in rocks close to the wellbore.

HOW CAN DRILLING-INDUCED FRACTURES BE RECOGNISED?

Figure 4 portrays a semicontinuous open fracture that intersects the borehole wall along its length. It follows the well trajectory which, in this case, is approximately vertical. This fracture occurs near the top of the open hole section (i.e., beneath the casing shoe), where the rocks are least consolidated. Moreover, its strike azimuth is 035°, which we know from breakouts in

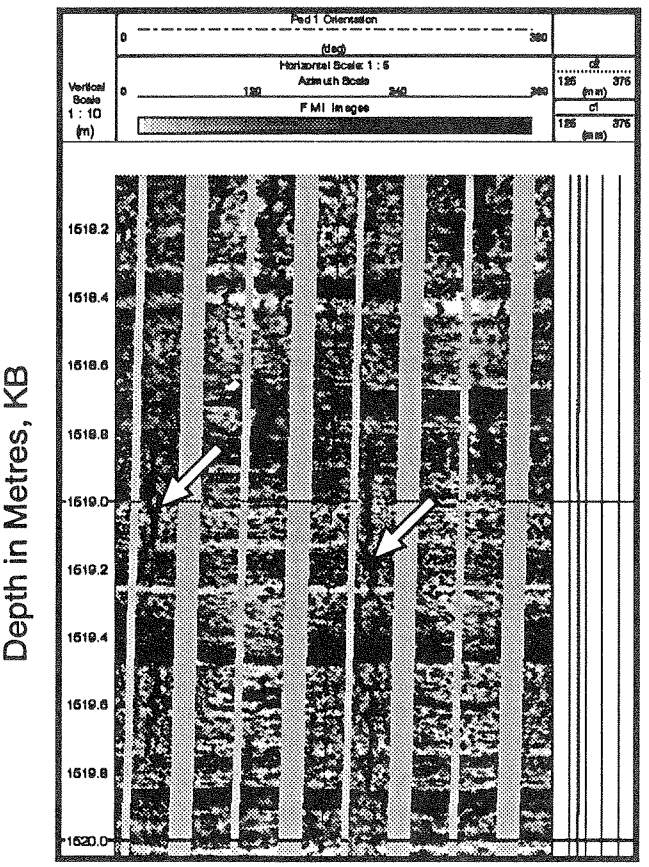

Figure 4. *FMI image of a drilling induced semi-continuous open fracture that intersects the borhole wall along its length. This fracture parallels borehole trajectory (approximately vertical in this instance). Its strike azimuth is 035° and parallels the direction of* S_{Hmax}*, the larger principal stress acting on these rocks.*

nearby wells is approximately parallel to S_{Hmax}, the larger horizontal principal stress acting on these rocks (Bell et al., 1994). These considerations make it probable that the feature evolved by hydraulic fracturing during drilling, or during the running-in of drill pipe on a trip. At such times the drillpipe can act as a piston and raise the pressure of the mud in the well sufficiently to initiate fractures. Well-parallel, open fractures that lie in the plane of the larger two principal stresses (S_v and S_{Hmax}) and occur near the top of an open hole interval (where in-situ stresses are the least) are best explained as drilling-induced.

Figure 5 is an FMI image of open fractures that trace a series of coalescing arcs on the borehole wall. The mean trends of the traces follow the well trajectory. Such fractures typically occur in facing pairs 180° apart on opposite sides of the well. The arcuate traces indicate that these fractures are inclined at low angles to the borehole wall. The fractures surround flakes that are poised to spall away from the wall (Plumb, 1989). The flakes are centered at azimuths 130° and 310°, which corresponds to the axis of S_{Hmin} at the well site (Bell et al., 1994). In fact, they represent the first signs of breakout ovalisation. These fractures are caused by shear fracturing of the borehole wall that results from localized stress amplification aligned with S_{Hmin} (Bell and Gough, 1979). The arcuate fractures, therefore, are not natural features at all; they merely testify to the presence of anisotropic far field stresses and to the low cohesive strength of the rocks involved. They exist because an open cylinder has been created in a suitable geomechanical setting.

The third category of what we interpret as drilling-induced fractures is more enigmatic. A typical example is shown in Figure 6. According to the FMI record, these features appear to be discontinuous en échélon open fractures that are concentrated on opposite sides of the borehole, and occur within a narrow azimuthal

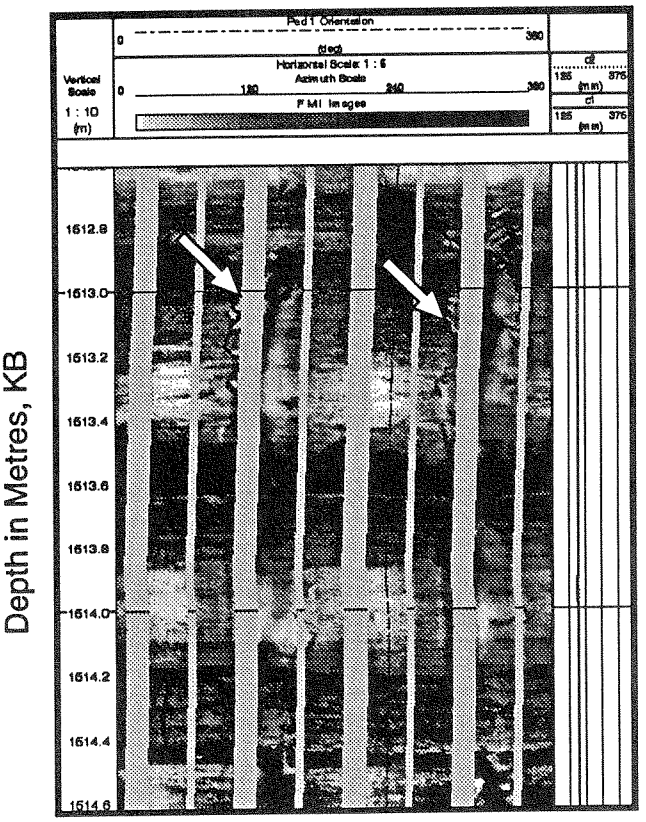

Figure 5. *FMI image representing incipient borehole ovalisation. The thin open fractures trace a series of coalescing arcs on the borehole wall that occur in facing pairs 180° apart centered at azimuths of 130° and 310°. This orientation is parallel to* S_{Hmin}. *The fractures surround flakes that are poised to spall off the borehole wall. The calipers to the right of the image show no borehole ovalisation at this point.*

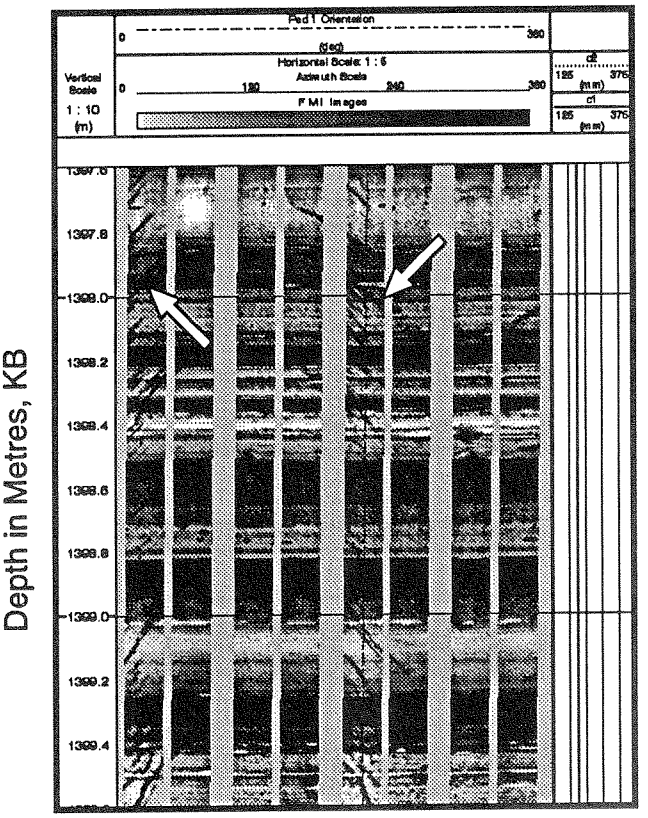

Figure 6. *FMI image showing open, discontinuous, en échélon fractures that occur in a narrow azimuthal band. We term these features "chatter fractures" and suspect that they are drilling-induced.*

band. We term these features "chatter fractures". Dips usually exceed 50° and remain remarkably constant within an individual well. Azimuthal distribution is also constant. To date, we have only observed these features in Foothills wells. Some interpreters suspect that they are open natural fractures that are not fully recorded by the imaging tool (P.W. Heffernan, pers. comm., 1992).

Because of the regularity of the occurrence of these fractures, the wellbore-parallel arrays and their orientational coincidence with S_{Hmax} directions, we suspect that these fractures are drilling-induced features. In several wells, en échélon fractures are ubiquitous in the reservoir section, yet production is nonexistent, suggesting that they are not part of an extensive fluid conduit.

We can envisage two possible explanations. The en échélon fractures may represent natural closed fractures that have been opened slightly in the plane of S_{Hmax} (Heliot et al., 1990) by drilling fluid pressures. Alternatively, they may be drilling-induced hydraulic fractures that are diagnostic of principal stress axes aligned obliquely to the drillhole trajectory (Aadnoy, 1990). The latter possibility is currently under investigation.

SUMMARY

These examples indicate that care needs to be taken when attempting to identify natural fractures on borehole imagery logs. Just as core recovery can induce stress-release fractures, so drilling procedures can generate open fractures in the rocks surrounding a well. It is necessary to remove drilling-induced features from consideration before analysing natural fractures. Identification of drilling-induced phenomena depends on knowledge of the local in situ stress trajectories. If the latter are known, relationships can be recognised between stress directions and suspect features.

REFERENCES

Aadnoy, B.S.
1990: In-situ stress directions from borehole fracture traces. *In* Journal of Petroleum Science and Engineering, v. 4, p. 143–153.

Bell, J.S. and Gough, D.I.
1979: Northeast-southwest compressive stress in Alberta: evidence from oil wells. *In* Earth and Planetary Science Letters, v. 45, p. 475–482.

Bell, J.S., Price, P.R., and McLellan P.J.
1994: In-situ stress in the western Canada sedimentary basin. Chapter 29. *In* Geological Atlas of the Western Canada Sedimentary Basin, G.D. Mossop and I Shetsen (compilers). Canadian Society of Petroleum Geologists, p. 439–446.

Bourke, L., Delfiner, P., and Fett, T.
1989: Using Formation Microscanner images. *In* The Technical Review, v. 37, no. 1, p. 16–40.

Heliot, D., Etchecopar, A., and Cheung, Ph.
1989: New developments in fracture characterization from logs. *In* Rock at Great Depth, V. Maury and D. Fourmaintraux (eds.), p. 1471–1478.

Plumb, R.A.
1989: Fracture patterns associated with incipient wellbore breakouts. *In* Rock at Great Depth, V. Maury and D. Fourmaintraux (eds.), p. 761–768.

APATITE FISSION TRACK AND ^{40}AR–^{39}AR ANALYSIS OF THE EXTERNAL ZONE OF THE CANADIAN ROCKIES NEAR JASPER, ALBERTA: IMPLICATIONS FOR THERMAL MATURITY

M.R. McDonough, G.S. Stockmal, and D.R. Issler

Geological Survey of Canada, 3303-33rd Street N.W., Calgary, Alberta T2L 2A7

A.M. Grist and M. Zentilli

Dalhousie University, Fission Track Research Laboratory
Department of Earth Science, Halifax, Nova Scotia B3H 3J5

D.A. Archibald

Queen's University, Department of Geological Sciences, Kingston, Ontario K7L 3N6

The southern Canadian Rocky Mountains at the latitude of Jasper, Alberta are divisible into Main Ranges, Front Ranges and Foothills belts, forming the external zone of the fold thrust belt (Fig. 1). The rocks of the thrust belt west of the Foothills are conventionally regarded to have been heated to temperatures in excess of the oil window and therefore are nonprospective for hydrocarbons, but few quantitative studies of the thermal and cooling history of the thrust belt have been undertaken. The best constraints on the burial and exhumation history of the thrust belt come from stratigraphic and coal rank studies from the Foothills

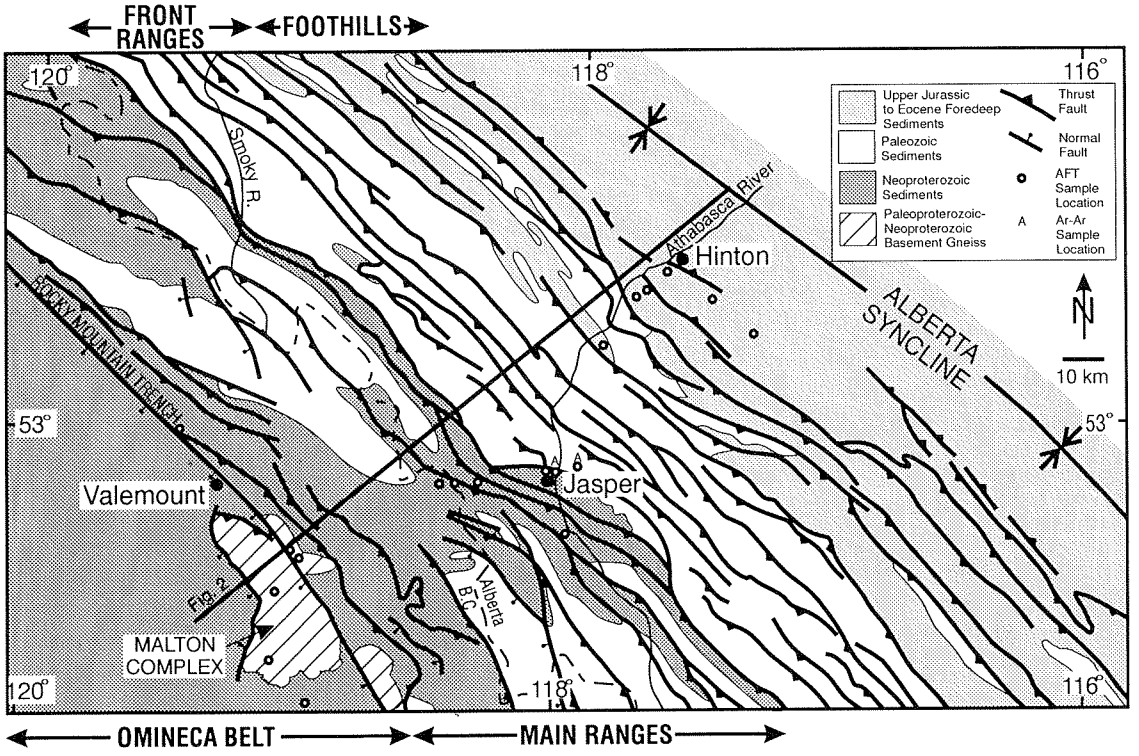

Figure 1. *Generalized geological and sample location map for the Jasper transect (modified from McMechan and Thompson, 1989).*

(Kalkreuth and McMechan, 1988; Dawson and Kalkreuth, 1994), and from bottomhole temperatures from Foothills hydrocarbon penetrations (Majorowicz et al., 1985).

We constrain the low temperature thermal and exhumational history of the Rockies in a transect from the Hinton, Alberta, area through the Jasper, Alberta, area (Fig. 1) using fission track analysis of apatite (AFT) and ^{40}Ar-^{39}Ar step heating experiments on K-feldspar. Figures 2 and 3 illustrate the crustal geometry of the internal and external zones of the orogen, and summarize AFT and "closure" (see below) ages, and ^{40}Ar-^{39}Ar ages for the Jasper transect.

AFT AGES AND FISSION TRACK LENGTH RESULTS

AFT ages increase from west to east in the external zone of the Rocky Mountain Belt (Figs. 2, 3). Main Ranges samples give 46-30 Ma AFT ages, and Front Ranges and Foothills samples yield AFT ages of 73-52 Ma. The oldest ages are from the easternmost part of the transect. Confined fission track length data for the transect are summarized in Figure 4. Mean track length for Exshaw and Brazeau samples ranges from 13.05 to 13.85 μm (Fig. 4). The small 10-15% reduction from the maximum theoretical mean track length (15.2 μm) indicates heating to temperatures in excess of 120°C during burial to fully anneal the fission tracks in apatite, followed by cooling during exhumation. This information, combined with the AFT ages and late Campanian palynomorph ages from the Brazeau Formation near Hinton (80-75 Ma; Sweet, 1983), suggest rapid burial (heating) and partial exhumation (cooling) of the Brazeau within 2-7 m.y. of deposition. The Entrance conglomerate has a mean track length of 12.81 μm, which suggests 3 to 4 km of burial followed by significant exhumation within 2 m.y. of its deposition. Alternatively, it may record detrital apatite derived from Cordilleran volcanic sources active during

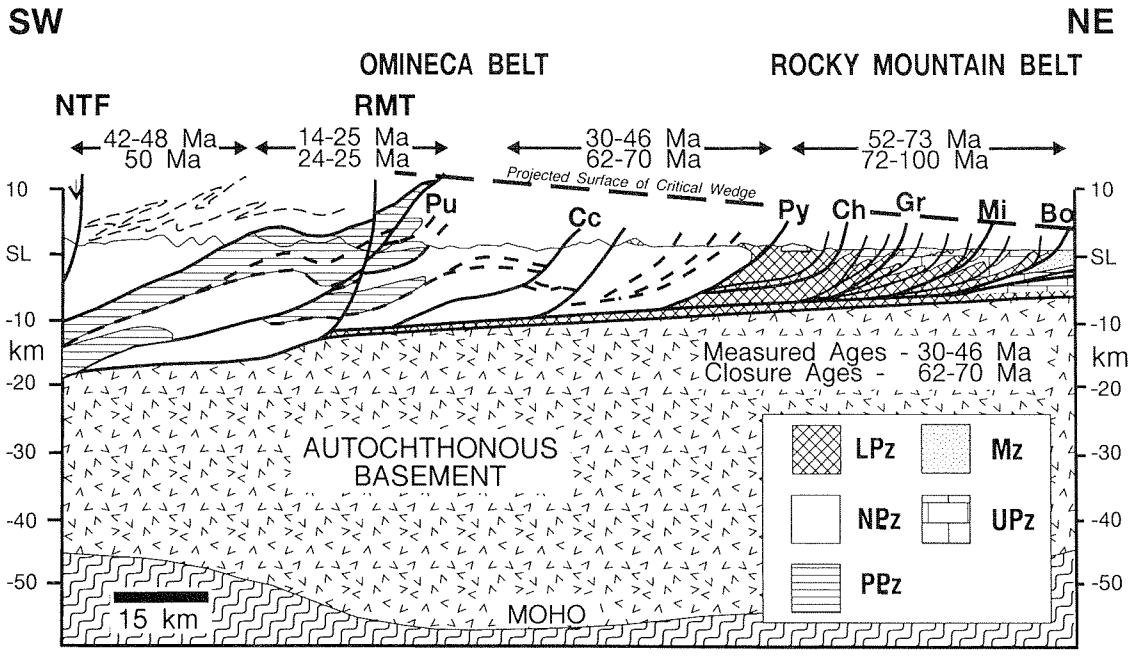

Figure 2. *Crustal section showing the range in AFT ages (upper set of numbers) for the Foothills and Front Ranges, Main Ranges, and the Omineca belt. The corresponding range in closure ages are given beneath the AFT age ranges. Three sets of faults that feed into a basal décollement above autochthonous Laurentian basement are illustrated: (1) Jurassic to Early Cretaceous thrust faults that carried sheets of crystalline basement into the proto-Rocky Mountain and have little or no bearing on the low-temperature cooling and exhumation history; (2) Late Cretaceous to Paleocene thrust faults, which are probably in-sequence in the Front Ranges, but are out-of-sequence in the Main Ranges; and (3) Tertiary normal faults. Only the two sets of younger structures are linked to the cooling/exhumation history of the thrust belt through the temperature intervals addressable by AFT and $^{40}Ar/^{39}Ar$ analysis. An estimate of the depth of thrust burial is given using a critical opening angle of 8° to approximate the geometry of the thrust wedge.*

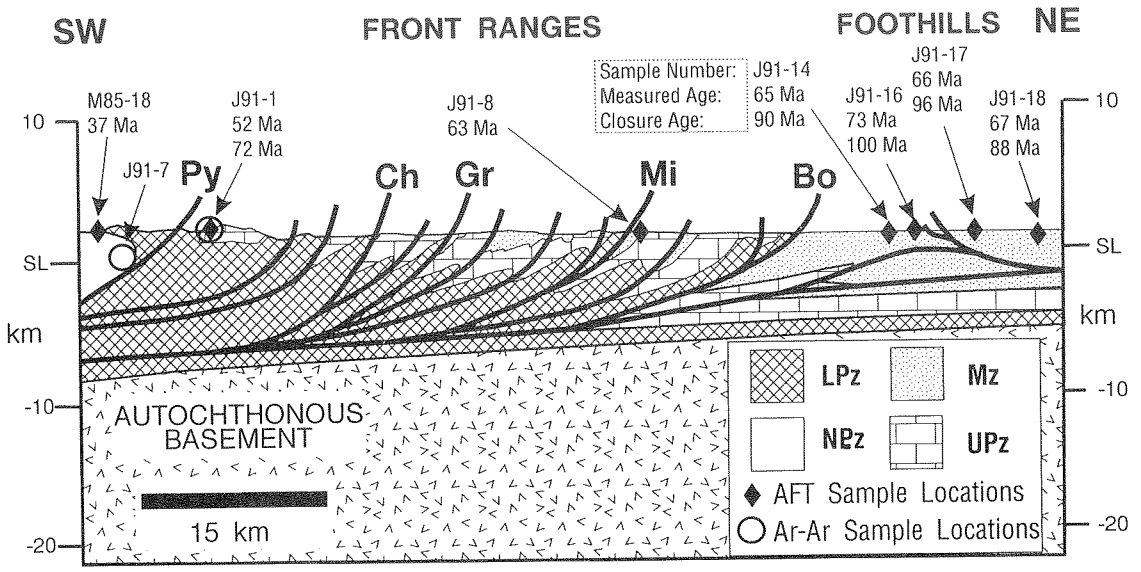

Figure 3. *Cross section for the Foothills and Front Ranges part of the transect. Seismic data (courtesy of Shell Canada Ltd.) were used to constrain the geometry of the eastern part of the section.*

upper Brazeau time, which is consistent with low vitrinite reflectance values of 0.57–0.65% for the Entrance syncline (Rmax; Dawson and Kalkreuth, 1994; see Arne and Zentilli, 1994).

^{40}AR–^{39}AR RESULTS

Figure 5 shows the age spectra for ^{40}Ar-^{39}Ar step heating experiments for K-feldspar. Samples J91-1 (sanidine from Exshaw tuff; Front Ranges) and J91-7 (microcline from Jasper member of Miette Group; Main Ranges) each have disturbed K-feldspar spectra that give minimum ^{40}Ar-^{39}Ar ages of about 170 Ma, indicating heating to less than 200°C. Thus, K-feldspars in the external zone were not fully reset during Cretaceous thrust burial. However, the disturbed spectra indicate partial resetting due to heating to about 150–170°C, which provides an upper temperature limit for thermal modelling.

THERMAL MODELS

Model time–temperature paths derived from inversion of confined fission track length data (see Issler et al. 1990; Ravenhurst et al. 1994; Issler and Stockmal, this volume) are given in Figure 6. The Chetamon thrust sheet (Fig. 6a) entered the annealing window (AW; 120–70°C) at about 60 Ma and cooled to 70°C at 35 Ma, yielding a linear cooling rate of 2°C/m.y., with a maximum instantaneous cooling rate of about 3°C/m.y. Model temperature histories for the Foothills are also concave-up, yielding cooling rates that range from 1.0 to about 1.75°C/m.y. (Fig. 6b, c, d). The time of fastest model cooling in Figures 6a and d is Maastrichtian to Eocene, which overlaps with the waning stages of thrusting derived from stratigraphic arguments (Porter et al., 1982; McMechan and Thompson, 1989). Main Range models were constrained to cool only, therefore the model envelopes are narrow and convex up (Fig. 6e, f). The resultant model cooling rates through the AW are very slow, 1–1.25°C/m.y. during Paleocene to Miocene times.

IMPLICATIONS FOR EXHUMATION AND HYDROCARBON GENERATION

Although the fission track age and length information indicate relatively slow cooling and exhumation that overlaps with the waning stages of thrust uplift in the external zone, the resultant slow erosion could have been accomplished entirely by isostatic processes. The ^{40}Ar-^{39}Ar K-feldspar analyses indicate maximum paleotemperatures of about 150–170°C for the Front Ranges in the Cretaceous. Thus, although the fission track data indicate that the entire Front Ranges and Foothills probably experienced temperatures high enough to crack hydrocarbons (>120°C), most of the external zone of the thrust belt remained in the wet gas window and probably remains prospective for natural gas.

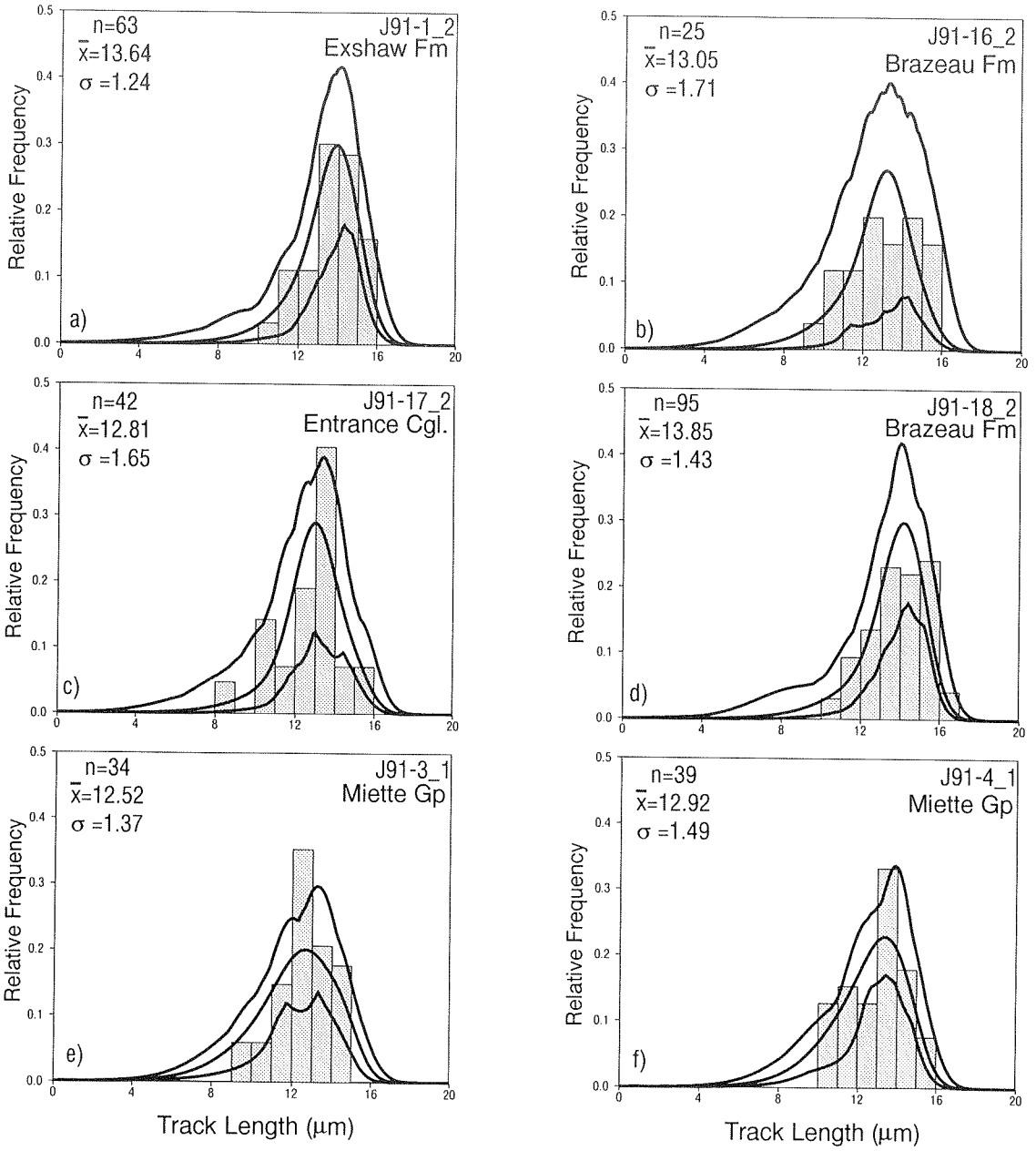

Figure 4. *Confined fission track length histograms for apatite (shaded), and model track length solutions with envelopes from track length inversion: a) Front Range sample; b), c) and d) Foothills samples; e) and f) Main Ranges samples. Sample numbers with a suffix of __1 are modelled by cooling only (Main Ranges); a suffix of __2 indicates heating and cooling.*

REFERENCES

Arne, D. and Zentilli, M.
1994: Apatite fission track thermochronology integrated with vitrinite reflectance: A review. *In* Vitrinite Reflectance as a Maturity Parameter, P.K. Mukhopadhyay and W.G. Dow (eds.). American Chemical Society, Washington, D.C., p. 249-268.

Dawson, F.M. and Kalkreuth, W.
1994: Coal rank and coalbed methane potential of Cretaceous/Tertiary coals in the Canadian Rocky Mountain Foothills and adjacent Foreland: 1. Hinton and Grande Cache areas, Alberta. Bulletin of Canadian Petroleum Geology, v. 42, p. 544–561.

Issler, D.R., Beaumont, C., Willett, S.D., Donelick, R.A., Mooers, J., and Grist, A.
1990: Preliminary evidence from apatite fission-track data concerning the thermal history of the Peace River Arch region, Western Canada Sedimentary Basin. Bulletin of Canadian Petroleum Geology, v. 38A, p. 250–269.

Kalkreuth, W. and McMechan, M.
1988: Burial history and thermal maturity, Rocky Mountain Front Ranges, Foothills and Foreland, east-central British Columbia and adjacent Alberta, Canada. American Association of Petroleum Geologists, Bulletin, v. 72, p. 1395–1410.

Majorowicz, J., Rahman, M., Jones, F., and McMillan, N.
1985: The paleogeothermal and present thermal regimes of the Alberta basin and their significance for petroleum occurrences. Bulletin of Canadian Petroleum Geology, v. 33, p. 12–21.

McMechan, M.E. and Thompson, R.I.
1989: Structural style and history of the Rocky Mountain fold and thrust belt. *In* Western Canada Sedimentary Basin: A Case History, B.D. Rickets (ed.). Canadian Society of Petroleum Geologists, Calgary, p. 47–71.

Porter, J.W., Price, R.A., and McCrossan, R.G.
1982: The Western Canada Sedimentary Basin. Philosophical Transactions of the Royal Society of London, v. A305, p. 169–182.

Ravenhurst, C.E., Willett, S.D., Donelick, R.A., and Beaumont, C.
1994: Apatite fission track thermochronometry from central Alberta: Implications for the thermal history of the Western Canada Sedimentary Basin. Journal of Geophysical Research, v. 99, p. 20 023–20 041.

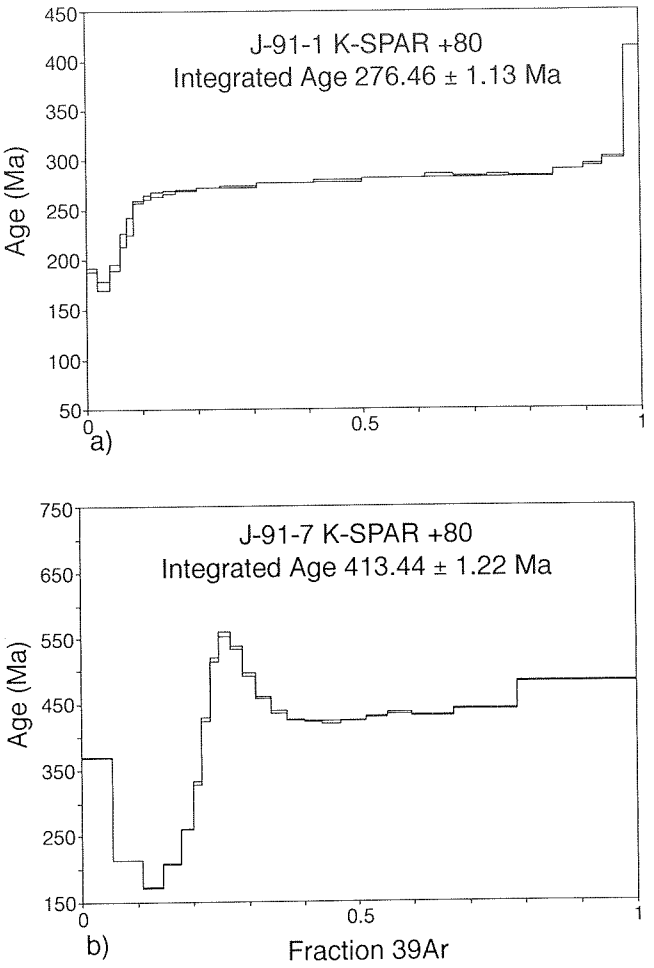

Figure 5. *$^{40}Ar/^{39}Ar$ age spectra for K-feldspar mineral separates from the Jasper transect: a) sample J91-1 (Exshaw bentonite); b) sample J91-7 (Jasper member of the Miette Group).*

Sweet, A.R.
1983: Biostratigraphic framework for the Entrance and High Divide conglomerates. Geological Survey of Canada, Miscellaneous Report No. 8-ARS-1983.

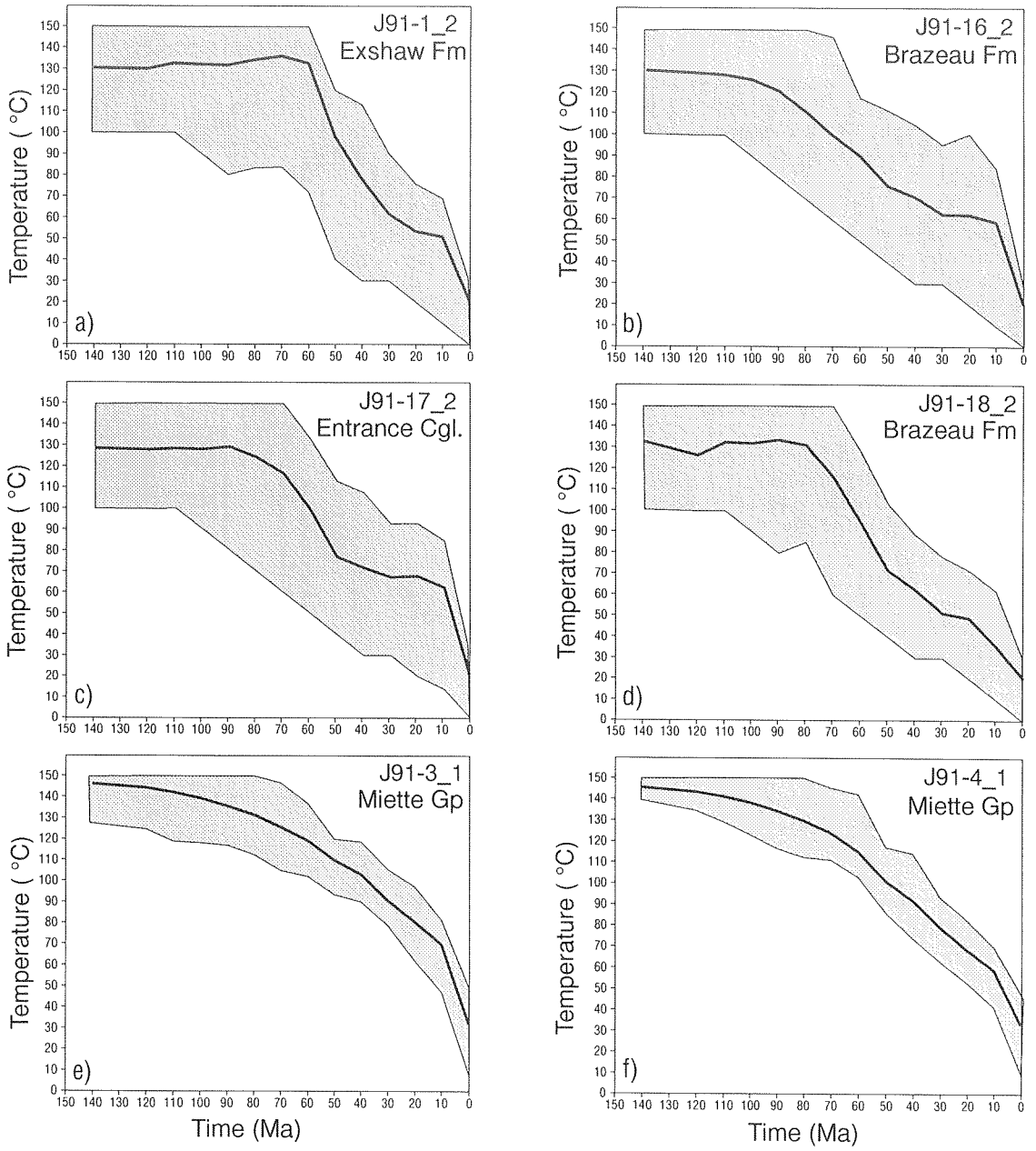

Figure 6. *Model time-temperature solutions from inversion of confined fission tracks in apatite: a) Front Range sample; b), c) and d) Foothills samples; e) and f) Main Ranges samples. Sample numbers with a suffix of __1 are modelled by cooling only (Main Ranges); a suffix of __2 indicates heating and cooling.*

STRUCTURE OF THE FOOTHILLS AND FRONT RANGES – SMOKY RIVER TO PEACE RIVER, ALBERTA AND BRITISH COLUMBIA

M.E. McMechan

Geological Survey of Canada, 3303-33rd Street N.W., Calgary, Alberta T2L 2A7

INTRODUCTION AND SUMMARY

Bedrock mapping between 53°45′ (Smoky River) and 56°N (Williston Lake/Peace River; Fig. 1) was undertaken as part of regional geologic studies to better define the structure, stratigraphy and resource potential of this 340 km long segment of the Canadian Rocky Mountain Foreland Belt. Bedrock maps are being published by the Geological Survey of Canada at 1:50 000 scale for the southern part of this area (NTS 83E/13, 14; 83L/3, 4, 5; 93H/15; 93I/1, 7, 8) and at 1:250 000 scale for the northern part of the area (Dawson Creek 93P; Pine Pass, 93O). Regional cross-sections constrained by surface geology, petroleum exploration wells and interpretation of proprietary seismic data, illustrate the subsurface geology in the Smoky River, Narraway River, Sukunka River and Carbon Creek areas (Fig. 1).

Folds dominate the surface structural style in the Foothills and Front Ranges at these latitudes. At Smoky River exposed Foothills folds conceal a thrust belt of Paleozoic and Triassic strata. In contrast, at Carbon Creek exposed Foothills folds conceal more complex, smaller wavelength faulted fold structures in Carboniferous and Triassic strata. This change in subsurface structural style is largely attributed to the influence of stratigraphic changes. The increased thickness and proportion of incompetent Upper Devonian to Lower Cretaceous units to the north resulted in more detachment horizons, more (initial) folding and greater disharmony at these stratigraphic levels in the subsurface. The greater than 50% reduction in estimated Foothills shortening from about 40 km at Smoky River in the south to about 15 km at Sukunka River in the north enhanced the stratigraphically induced changes in structural style. Centrifuge models (Lui and Dixon, 1990) suggest that even if greater shortening had occurred to the north, the increased structural disharmony would remain.

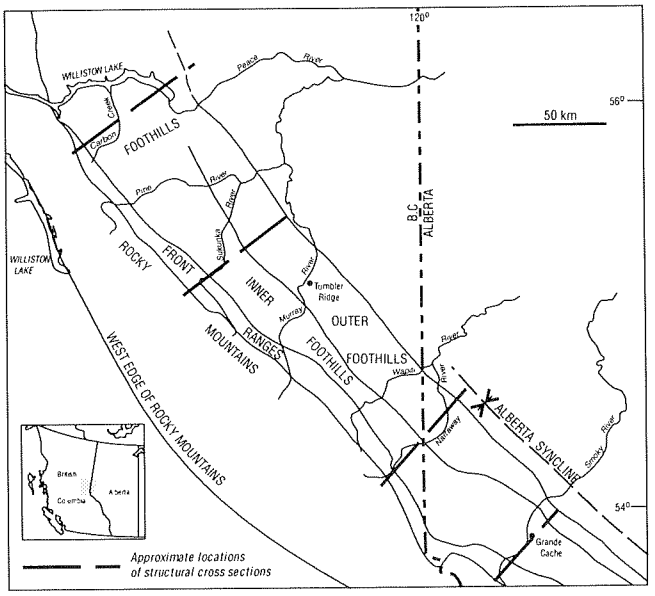

Figure 1. *Major drainages and structural subprovinces of the Rocky Mountain Foreland Belt in the Smoky River to Peace River area, Alberta and British Columbia. The regional structural cross-sections form the basis of the subsurface structural discussion in the text and will be displayed at the poster session.*

STRATIGRAPHY

The character of the deformed stratigraphic section has greatly influenced the structural style observed in the Foothills and Front Ranges of the study area. Upper Cretaceous sandstone and shale form the main level of exposure in the Outer Foothills, whereas Jurassic and Lower Cretaceous sandstone, shale and conglomerate form the predominant level of exposure in the Inner Foothills. Upper Devonian, Carboniferous and Triassic shale and carbonate form the predominant level of exposure in the Front Ranges. The entire stratigraphic succession above a Cambrian to Devonian 'platform' is characterised by alternating successions of incompetent (shale rich) and competent (carbonate or sandstone rich) strata (Fig. 2). Important detachments occur at several levels in the stratigraphic section. Consequently, folds tend to dominate the surface structural geometry,

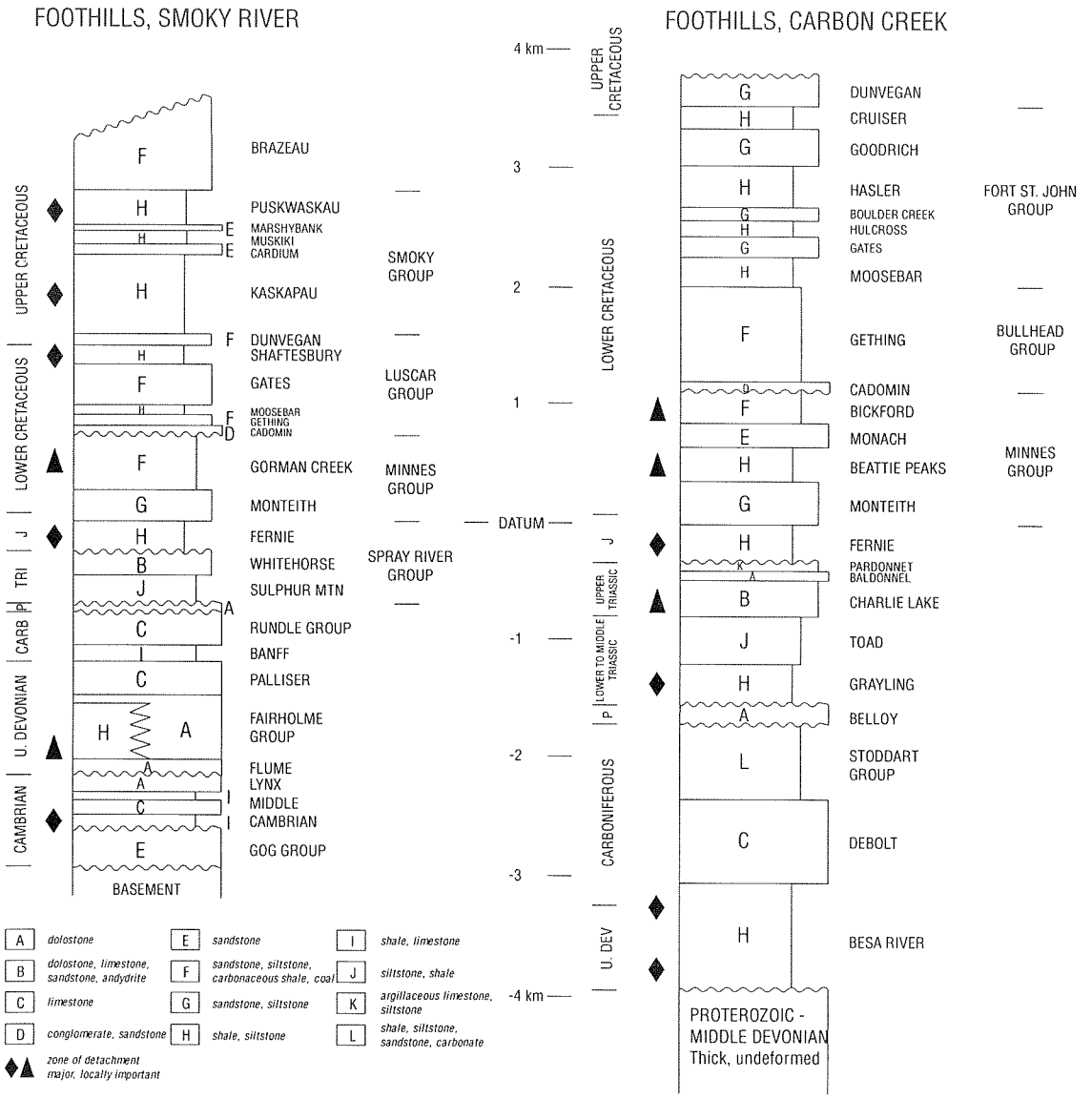

Figure 2. *Generalized stratigraphy of the Foothills in the Smoky River and Carbon Creek areas.*

and thrust faults through Upper Devonian to Triassic strata tend to be of smaller displacement and more closely spaced than in the Foothills and Front Ranges of southern Alberta. The thickness and proportion of incompetent Upper Devonian to Lower Cretaceous strata increases to the northwest from Smoky River to Carbon Creek, and thrust faults become even more discontinous. Near Williston Lake (Peace River), the thickness of Carboniferous, Permian and Lower Cretaceous strata appears to decrease markedly across north-side-up basement structures. In the Sukunka River and Carbon Creek area, the Sukunka Uplift (Richards et al., 1994) is reflected by a reduced Carboniferous section in the Front Ranges. Reliable estimates of stratigraphic thickness are essential for the estimation of shortening of less competent units using the area balancing method.

STRUCTURAL GEOMETRY

At Smoky River, chevron and box folds dominate the surface structural style of the Foothills. Detachments in three thick Cretaceous shale units (Shaftesbury, Kaskapau, Puskwaskau formations; Fig. 2) separate folds of different wavelengths and amplitudes developed in the under- and overlying more competent sandstone dominated packages (Luscar Group; Dunvegan Formation; Cardium, Marshybank formations; Brazeau Formation). The Outer Foothills form a very narrow

zone along the eastern edge of deformation (Fig. 1). Across the Inner Foothills an important detachment in Jurassic shale of the Fernie Formation separates the exposed folds from simply deformed thrust sheets of Paleozoic and Triassic strata. In the east where the Minnes or Nikanassin interval is thin, these strata deform with the overlying Luscar Group. In the west where the interlayered sandstone, siltstone and carbonaceous shale of the upper Minnes (Gorman Creek Formation; Fig. 2) are over about 500 m thick, they become an important detachment zone characterized by small scale folds and faults. This detachment zone separates folds of different wavelengths and amplitudes developed in underlying Monteith sandstone (lower Minnes) and overlying Luscar Group sandstone and conglomerate. Middle Cambrian strata are interpreted to be involved in thrusting across most of the Inner Foothills. Shortening at the top of the Carboniferous is estimated at almost 40 km across the Foothills (or 50%) in the Smoky River area. This is accomplished on numerous small displacement thrusts with 2 to 8 km spacing at the level of the Carboniferous.

At Smoky River, the Front Ranges comprise thrust sheets of Upper Devonian to Triassic strata that plunge out to the north where they are replaced at surface by large exposures of fault-repeated Fernie Formation. Displacement on the thrust fault underlying the spectacularly folded Carboniferous and Triassic strata at Llama Mountain (Front Ranges, Smoky River) must go into the Fernie Formation as a blind thrust.

North from Smoky River, the Foothills Belt widens considerably. The Inner Foothills widen to the northwest because of the northward plunging out of Front Ranges structures. In contrast, the Outer Foothills widen to the northwest because the out-of-sequence Muskeg Thrust no longer brings Lower Cretaceous strata to surface. The Outer Foothills also expand to the northeast because fault and fold structures deform Carboniferous and younger strata about 15 km further to the northeast. This deformation at depth is reflected by broad surface structures developed in the Upper Cretaceous Brazeau (Wapiti) Formation. West-vergent, upper detachment faults no longer break to surface from about Kakwa River north.

At Narraway River (Fig. 1) the Front Ranges widen at the expense of the Inner Foothills. The Front Ranges comprise folded Upper Devonian to Triassic strata with subsidiary faults. These folds are detached from underlying thick thrust sheets carrying competent quarztite and carbonate strata at a major detachment in shale of the Upper Devonian Perdrix Formation. The Jurassic and Lower Cretaceous Minnes Group is thick across the Inner Foothills, and the upper Minnes forms a prominent detachment. Cambrian strata probably become involved in Foothills structures near the western edge of the Inner Foothills. Subsurface thrusts in the Paleozoic and Triassic are still of small displacement and, with the exception of the easternmost structures in the Outer Foothills, are closely spaced. Estimated shortening across the Foothills at Narraway River is about 25 km (top Carboniferous), about two thirds of that for Smoky River. Interestingly, estimated shortening across the relatively narrow Inner Foothills is still 50%.

At Sukunka River, the Outer Foothills, characterized by gently folded Upper Cretaceous strata at surface, forms a broad belt 25 km wide. Underlying Triassic and Lower Cretaceous strata appear to deform as one structural unit with a few kilometres of fault-related shortening. The Upper Cretaceous Kaskapau shales appear to form a detachment zone. Lower Cretaceous Minnes, Bullhead and Fort St. John group strata form the dominant level of exposure in the Inner Foothills. Major detachments in the Fernie and Minnes separate exposed chevron and box folds in the Cadomin to Boulder Creek formations from faulted folds in the Triassic Baldonnel and Pardonet formations. Fractured dolomitized carbonate strata in these folds make excellent reservoirs and form the principal exploration target of the Sukunka–Bullmoose gas play (Barrs and Montadon, 1981; Cooper et al., 1992; Morrison and Cooper, 1992). Detachments in Triassic evaporitic and shale units are interpreted to separate these structures from underlying structures developed in Carboniferous and Permian strata. Across the Inner Foothills, shortening of the Minnes Group appears to be greater than that of the overlying Cadomin to Boulder Creek strata. In addition, Minnes shortening appears to be greater than that of the underlying Triassic. This excess shortening is probably linked to structures that deformed the Triassic further to the west. I interpret the great thickening (more than 3 times) of the Fernie/ Minnes in this area to be largely of structural rather than stratigraphic origin. Estimated shortening across the Foothills is about 15 km (top Triassic) or just over half the estimate at Narraway River to the south.

The term "Front Ranges" is a bit of a misnomer at the latitude of Sukunka River. The northeastern part of the "Front Ranges" consists of kilometre-scale folds and associated faults in Carboniferous to Triassic strata. These folds formed above a major detachment in Upper Devonian and Carboniferous Besa River shales. The Merrick Thrust brings Carboniferous to Triassic strata to surface and appears to be the only significant

displacement (>5 km) fault through the Carboniferous and Triassic carbonates in the Foothills and "Front Ranges" at this lattitude. The northeastern part actually forms ranges. The rest of the "Front Ranges" is topographically low. In the southwest part the Rundle Group has been completely cut out by sub-Permian erosion. Permian carbonate and Triassic shale outline a few folds. The central part of the belt is underlain by complexly folded and faulted Upper Devonian and Carboniferous shale and minor carbonate of the Perdrix, Mount Hawk and Besa River formations. Simple thrust sheets of Cambrian to Middle Devonian carbonate and quartzite underlie the Front Ranges structural belt.

In the Carbon Creek area near Peace River (Fig. 1) the Dunvegan Formation is the only Upper Cretaceous unit preserved in the Foothills and adjacent Plains. The Foothills consist of a broad eastern part characterized by large, flat bottomed synclines outlined by Lower Cretaceous Bullhead and Fort St. John group strata, separated by complex anticlines. Large scale folded Upper Triassic, Fernie and lower Minnes strata outcrop in the western Foothills. The "Front Ranges" structural belt exposes faulted folds of Carboniferous carbonate, spiculite and sandstone and Permian chert in the east, and complexly deformed Besa River shale in the west. The folds outlined by competent Carboniferous strata formed above simple thrust sheets of Cambrian to Middle Devonian carbonate and quartzite. The folds have a very different geometry than those outlined by overlying Cretaceous strata. On the basis of surface structural geometries, particularly those from north of Williston Lake and well data, I proposed (McMechan, 1985) that there was also a major detachment in the Lower Triassic Toad–Grayling Formation. Using area balancing calculations, I proposed that there was 10 km more shortening at the Upper Devonian to Lower Triassic level than at the exposed Upper Triassic to Cretaceous level across the Foothills. Modern deep seismic reflection profiles across the wide eastern part of the Foothills suggest there is somewhat greater shortening at the Carboniferous level but not as much as I previously estimated. The seismic data confirm the Besa River as the principal basal detachment zone, and show the Lower Triassic as the principal upper detachment zone in the east. However, from Carbon Peak west, the Minnes appears to become the main upper detachment zone. Comparison of the old and new strucutral interpretations illustrates the importance of original stratigraphic thickness on area balancing calculations and the difficulty of estimating thicknesses in an area of more complex thickness changes without seismic control.

REFERENCES

Barss, D.L. and Montandon, F.A.
1981: Sukunka–Bullmoose gas fields: models for a developing trend in the southern Foothills of northeast British Columbia. Bulletin of Canadian Petroleum Geology, v. 29, p. 293–333.

Cooper, M.A., Green, R., Becker, G., Bogle, E.W., Macey, G., Morrison, M.L., and Reid, J.
1992: The Sukunka–Bullmoose Playtrend in the Foothills of northeast British Columbia. American Association of Petroleum Geologists, 1992 Annual Convention, Official Program, p. 23.

Liu, S. and Dixon, J.M.
1990: Centrifuge modelling of thrust faulting: strain partitioning and sequence thrusting in duplex structures. *In* Deformation Mechanisms, Theology and Tectonics, R.J. Knipe and E.H. Rutter (eds.). Geological Society Special Publication, no. 54, p. 431–444.

McMechan, M.E.
1985: Low-taper triangle-zone geometry: an interpretation for the Rocky Mountain Foothills, Pine Pass–Peace River area, British Columbia. Bulletin of Canadian of Petroleum Geology, no. 33, p. 31–38.

Morrison, M.L. and Cooper, M.A.
1992: The control of fracturing on reservoir quality and productivity within the Sukunka–Bullmoose Playtrend of the northeast British Columbia Foothills. American Association of Petroleum Geologists, 1992 Annual Convention, Official Program, p. 91.

Richards, B.C., Barclay, J.E., Bryan, D., Hartling, A., Henderson, C.M., and Hinds, R.C.
1994: Chapter 14 – Carboniferous strata of the Western Canada Sedimentary Basin. *In* Geological Atlas of the Western Canada Sedimentary Basin, G.D. Mossop and I. Shetson (compilers). Canadian Society of Petroleum Geologists and Alberta Research Council, p. 221–250.

PARASEQUENCES AND FORAMINIFERAL DISTRIBUTIONS IN THE CAMPANIAN FOREMOST FORMATION OF SOUTHERN ALBERTA

D.H. McNeil and J.H. Wall

Geological Survey of Canada, 3303-33rd Street N.W., Calgary, Alberta T2L 2A7

D.A. Eberth

Royal Tyrrell Museum of Palaeontology, Drumheller, Alberta T0J 0Y0

INTRODUCTION

The Foremost Formation of southeasternmost Alberta is an 80 m thick clastic unit that forms the lower part of the regressional phase of the Judith River Group and overlies open-marine shales of the Pakowki Formation. It was deposited approximately between 78 and 79Ma in a series of coarsening-upward cycles that pinch out laterally into the marine Pakowki Formation to the east (Fig. 1).

In this paper we examine marine-influenced micropaleontological characteristics of these cycles from outcrop data in the Milk River Valley of southeastern Alberta (Pinhorn Ranch section, see Fig. 2). Parasequence stratigraphic concepts are applied and foraminiferal distributions are used to define marine flooding events in the section. We also compare the parasequence stratigraphy in the Milk River valley with the Princess core from Alberta Research Council core hole 1-83 situated 190 km to the northwest near Dinosaur Provincial Park (Fig. 2). The comparison demonstrates stratigraphy in two contrasting depositional settings. The Milk River section shows significant marine influence; the Princess section is terrestrially dominated (coal measures) with minor marine influence.

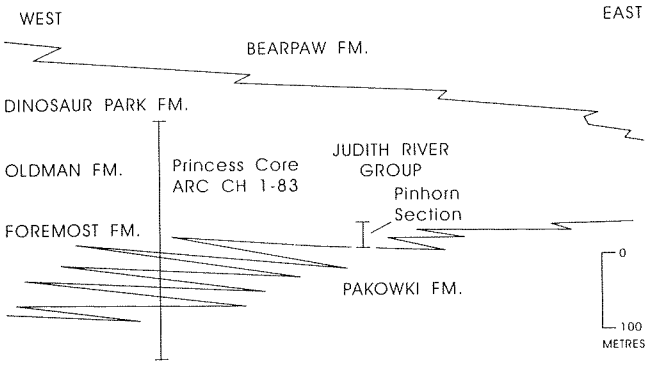

Figure 1. *Schematic regional cross-section of Pakowki, Foremost, and overlying formations in southern Alberta.*

SEQUENCE TERMINOLOGY

Sequence stratigraphy focuses on the subdivision of the stratigraphic record into genetically related sedimentary packages that are bound by significant subaerial erosional unconformities, or their correlative

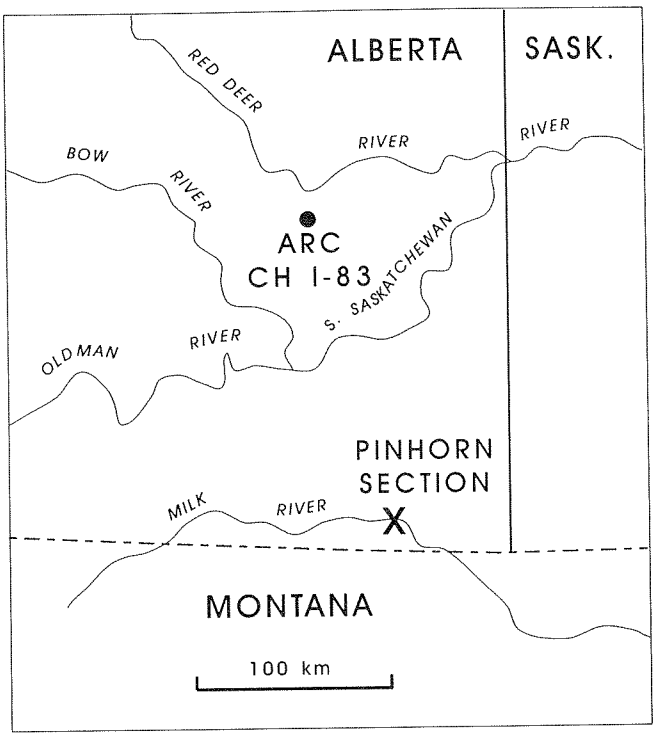

Figure 2. *Location of Pinhorn Ranch outcrop and Alberta Research Council (ARC) core hole 1-83.*

conformities (Van Wagoner et al., 1988). Parasequences are subdivisions of sequences. They are relatively conformable successions of genetically related beds bounded by marine-flooding surfaces and their correlative surfaces (Van Wagoner et al., 1988).

Parasequences are the focus of this paper, and they are particularly well-developed in the marginal marine cycles of the Foremost Formation. In Foremost strata, flooding surfaces can be recognized by transgressive lags overlain by foraminiferal rich marine mudstones. Paleontological data assists in tracing unconformities and flooding surfaces more widely across sedimentary basins.

THE PINHORN RANCH SECTION

The Foremost Formation crops out in the Milk River valley of southeastern Alberta. An 84 m thick section, referred to as the Pinhorn Ranch section (7-21-2-7W4), is exposed in the valley and was measured by D.A. Eberth in 1992 (Fig. 3). The Pinhorn section can be divided into three major units. The lower unit consists of fluvial, foreshore, and shoreface sands. It is overlain by a predominantly mudstone section that includes three coarsening-upward cycles each capped by pebbly lag deposits. The upper unit consists of fluvial and paralic deposits with several coaly units. The Foremost Formation in the Milk River valley has been studied previously by Ogunyomi and Hills (1977) who interpreted the succession in terms of offshore/barrier-island/lagoonal cycles. Re-interpretation of the Foremost Formation in southeastern Alberta and southwestern Saskatchewan by Kwasniowski (1993) focused on the recognition of regional discontinuity horizons marked by lag deposits and controlled by fluctuations in relative sea level. In this context, the Pinhorn Ranch succession could be interpreted in terms of simple transgressive–regressive cycles or parasequences. We examined the foraminiferal content of the mudstones in the Foremost succession, therefore, to assess marine influence and document flooding events.

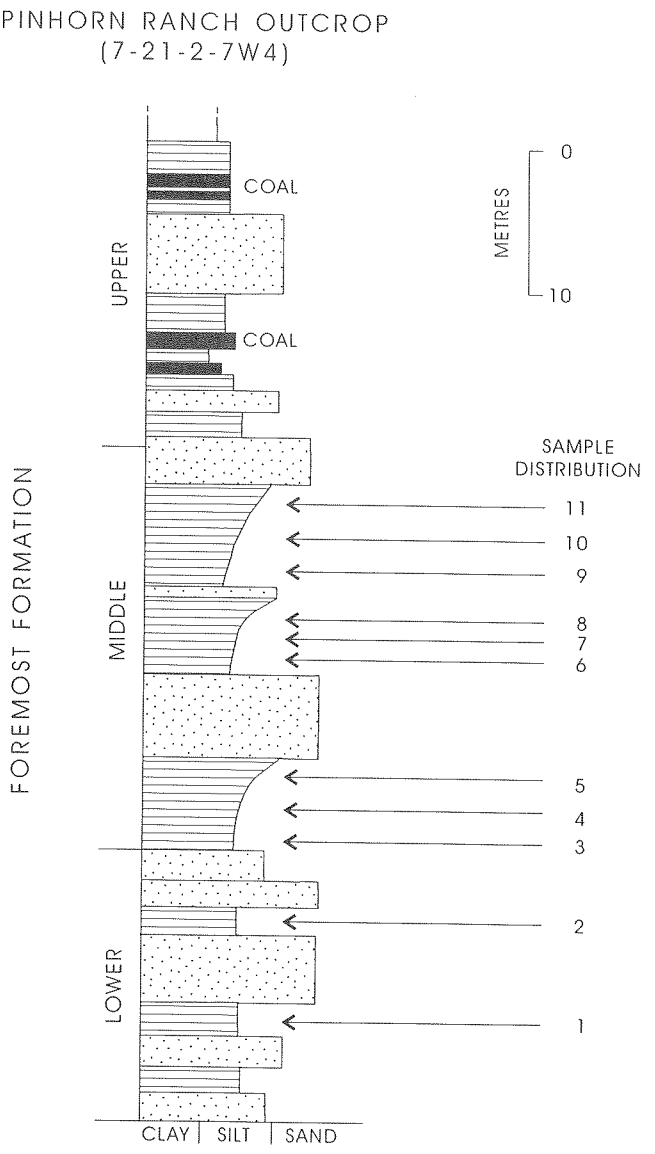

Figure 3. *Outcrop section of Foremost Formation at Pinhorn Ranch, Milk River, southeastern Alberta. Numbers 1 to 11 indicate horizons sampled for microfossils.*

Eleven samples were examined from the Pinhorn section and the distribution of microfossils is illustrated in Figure 4. The foraminiferal recovery indicates a cyclical pattern with three marine pulses (samples 3, 6, and 9) and four nonmarine pulses (1, 5, 7, and 11). The foraminiferal assemblages are composed exclusively of agglutinated benthic species dominated by *Haplophragmoides* cf. *H. rota* Nauss and *Pseudoclavulina*? sp. (Fig. 4). Rare specimens of *Bathysiphon* sp., *Saccammina* spp., and *Trochammina* sp. complete the assemblages. The foraminifers clearly indicate marine influence, but the assemblages alone might not adequately discriminate between a variety of potential marginal marine environments. Some marginal marine environments, however, can by ruled out. The Pinhorn Ranch assemblage is not typical of a marsh since *Ammobaculites*, *Ammotium*, *Trochammina*, and *Jadammina* are absent. Neither is a lagoonal or estuarine environment likely in view of the absence of *Ammobaculites*, *Ammotium*, *Eggerella*, and

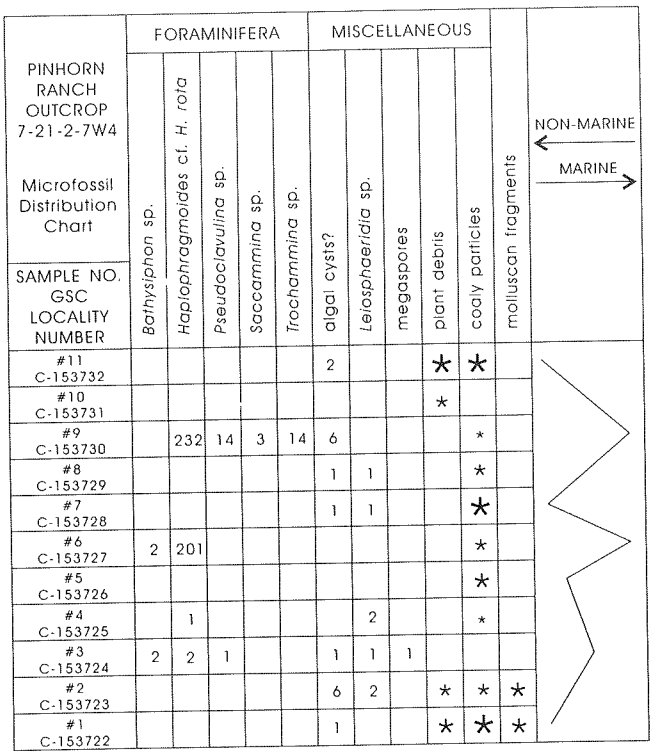

Figure 4. *Distribution of microfossils in the mudstone units of the Formemost Formation at Pinhorn Ranch in Milk River valley.*

Miliammina. When viewed in context with more complete foraminiferal successions in the Pakowki and Foremost formations, however, the interpretation of the Pinhorn assemblage becomes more obvious.

THE PRINCESS CORE

The Alberta Research Council core hole 1-83 (1-2-20-12W4), drilled in 1983, is situated near Princess, Alberta, 190 km northwest of the Pinhorn Ranch section (Fig. 2). The cored section included 61.8 m of Pakowki Formation overlain by a complete 141.5 m-thick section of the Foremost. Two hundred and nine samples were analyzed for micropaleontological content. Detailed foraminiferal occurrences cannot be illustrated here, but the overall abundance profile illustrated in Figure 5 quantitatively demonstrates the microfaunal trend.

The Pakowki Formation contains an abundant microfauna that includes agglutinated and calcareous benthic foraminifers. Open marine conditions of sedimentation are indicated by a minor influx of planktonic species in the upper part of the Pakowki Formation (Fig. 5). The overlying Foremost Formation contains a much different foraminiferal assemblage consisting of low diversity *Trochammina–Pseudobolivina* associations typical of low salinity, restricted, marginal marine environments. These microfaunas were controlled by cyclical deposition in a coal measures sequence resulting in a different species composition than at Pinhorn Ranch. Although less diverse, the Pinhorn Ranch assemblage compares much more closely with assemblages in the upper part of the Pakowki Formation at the Princess site. The distinctive *Haplophragmoides* cf. *H. rota*, for example, occurs in association with calcareous benthic and planktonic foraminifers in the Princess core. Extrapolation of this association to the Pinhorn site strongly suggests that the microfossiliferous mudstone units in the Pinhorn section represent a direct marine incursion.

PARASEQUENCE MODELS AND FORAMINIFERAL DISTRIBUTIONS

Sedimentological and foraminiferal data indicate that the Foremost Formation is developed in distinctly different facies at Pinhorn Ranch and at the Princess core hole. These differences are summarized in two parasequence models illustrated in Figures 6 and 7.

At the Pinhorn Ranch site (Fig. 6), the parasequence boundary is drawn at a pebble lag deposit interpreted as the initial flooding surface. Mudstone beds immediately above the lag deposits yield an abundant foraminiferal assemblage representing rapid transgression and maximum flooding. The regressive phase of the cycle is marked by an influx of turbid sediment carrying an increasingly abundant supply of terrestrial debris which displaced the marine microfauna basinward. The regressive phase was completed with the deposition of hummocky cross-stratified sand overlain by foreshore sands.

In the more complex coal measures facies of the Foremost Formation at the Princess locality a simple parasequence model is not as easily derived. Nonetheless, Figure 7 is a preliminary illustration of a typical succession. Further work will be necessary to fully resolve parasequence boundaries in these facies. The succession shown in Figure 7 shoals upward and begins with stacked shoreface sands of a barrier island overlain by foreshore deposits. The first foraminiferal assemblage is found in tidal flat deposits and consists of *Pseudobolivina rollaensis*, *Trochammina* sp. and a distinctive thin-walled flattish *Trochammina* sp. which likely grew attached to shallow water plants on the tidal

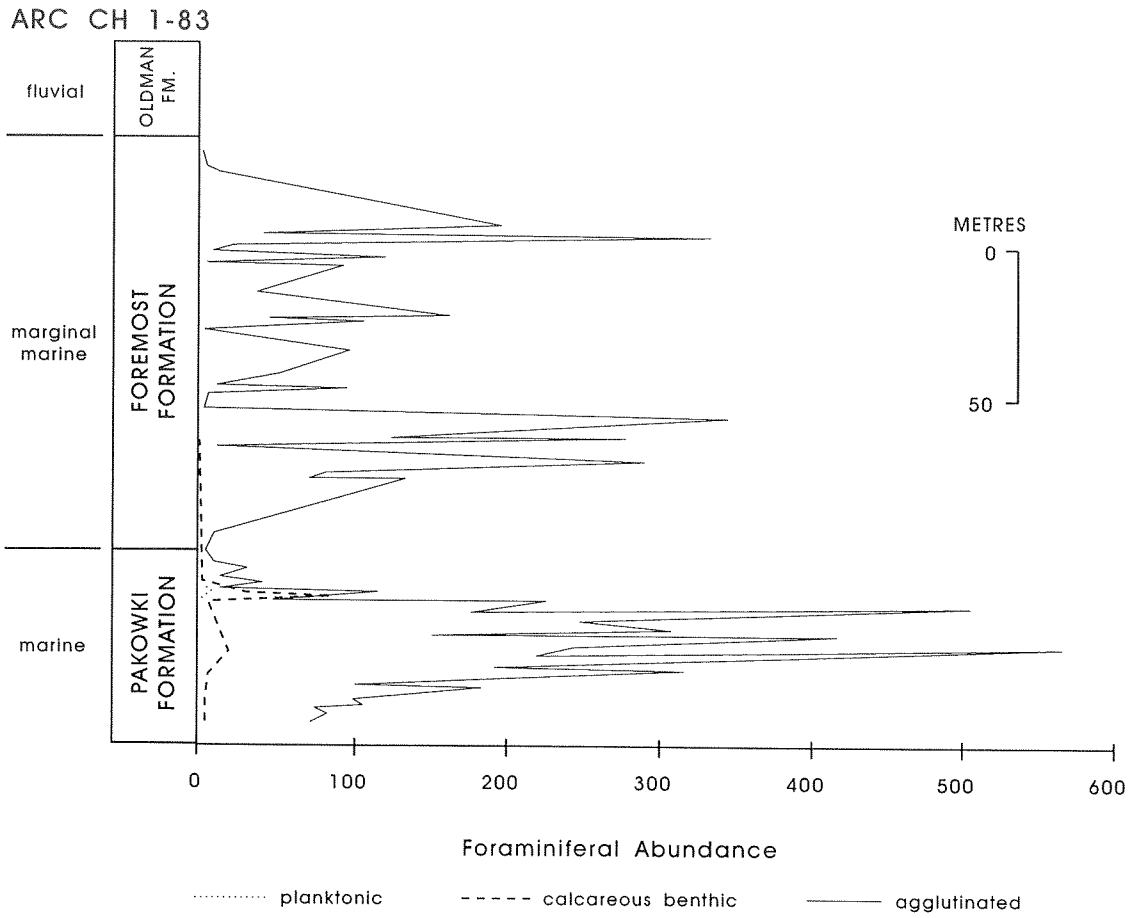

Figure 5. *Graphic illustration of foraminiferal abundance trends in the Pakowki and Foremost formations in the Princess core located near Princess, Alberta.*

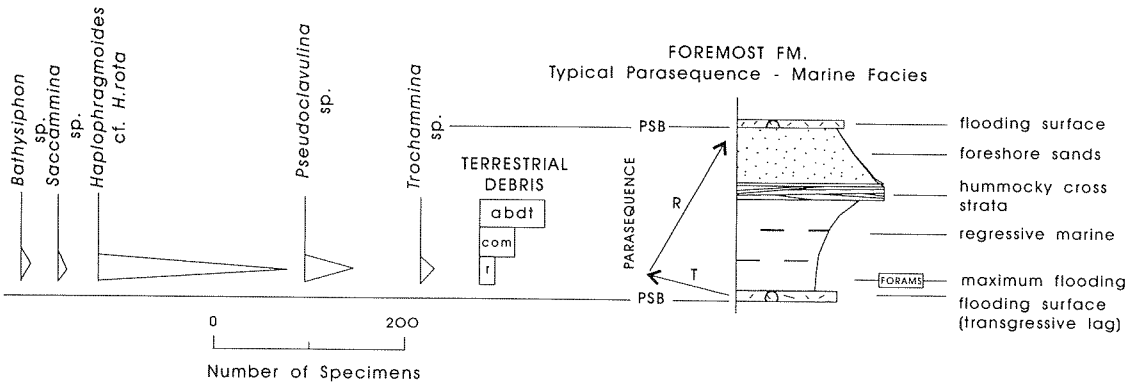

Figure 6. *Parasequence model of sedimentary features and microfossil distributions in shallow marine facies of the Foremost Formation, Milk River area, Alberta.*

flat. Coals above the tidal deposits mark the end of the regressive phase and a parasequence boundary is indicated above the coals by a pebble lag deposit. Marine influenced mudstone deposits (lagoonal?) containing the foraminifers *Ammotium, Pseudobolivina rollaensis, Trochammina albertensis,* and *Trochammina* sp. mark the maximum flooding phase of the new parasequence.

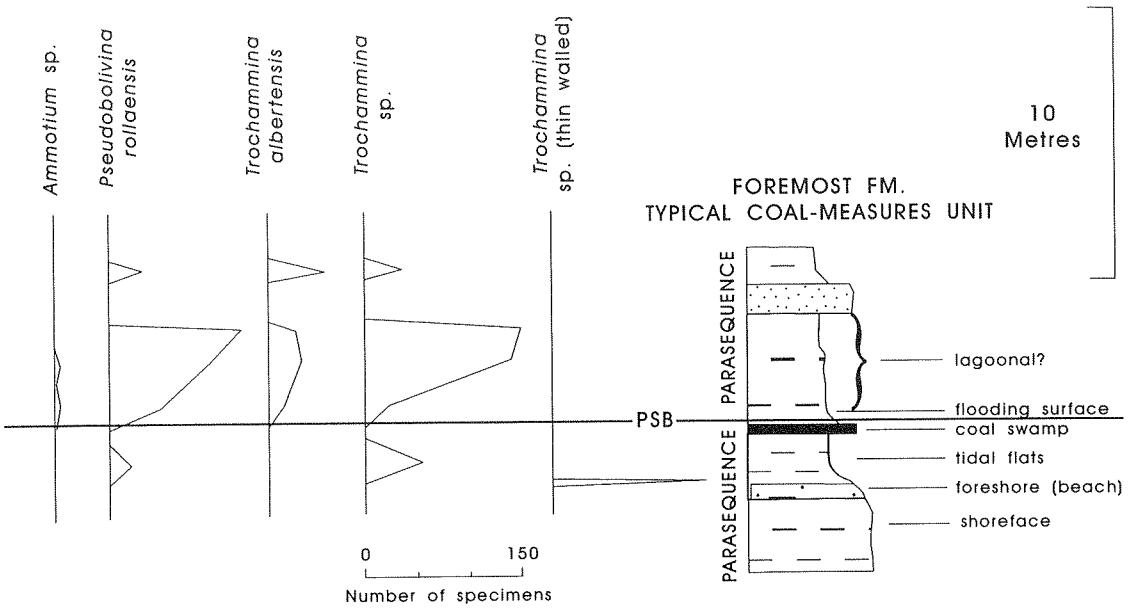

Figure 7. *Preliminary parasequence model showing stratigraphy and microfossil distributions in coal measures facies of the Foremost Formation based on data from the Princess core (ARC CH 1-83).*

SUMMARY

Foraminiferal distributions in mudstone-sandstone cycles of the Foremost Formation in the Milk River valley of southern Alberta play an important role in sequence analysis. The stratigraphic position and nature of foraminiferal assemblages can provide evidence to document maximum marine flooding events and determine parasequence boundaries. The composition of the foraminiferal assemblage assists in determining the depositional environment. At the Pinhorn Ranch section, an assemblage dominated by *Haplophragmoides* cf. *H. rota* and *Pseudoclavulina* sp. indicates maximum marine flooding. This conclusion is based on these species occurring in association with planktonic species and a more diverse benthic assemblage in the open marine upper Pakowki Formation near Princess, Alberta. The absence of typical lagoonal foraminifers such as *Ammotium*, *Miliammina*, and *Trochammina* at the Pinhorn Ranch locality suggests that lagoonal deposits are not present. In contrast to the marine influenced Pinhorn locality, the Foremost Formation is developed in a terrestrially dominated coal measures succession in the Princess core 95 km to the northwest. The foraminiferal assemblages are dominated by *Trochammina* and *Pseudobolivina* with minor occurrences of *Ammotium* and *Miliammina*. These assemblages indicate restricted marginal marine environments such as lagoons and tidal flats. Maximum marine flooding events are more difficult to recognize in the coal measures facies but *Trochammina–Pseudobolivina* bearing mudstones (lagoonal?) overlying pebble lag deposits on coaly beds probably signify maximum marine events.

REFERENCES

Kwasnioski, S.M.
1993: Effects of sea level variation on the Upper Cretaceous (Campanian), Foremost Formation in southeastern Alberta and southwestern Saskatchewan. Geological Association of Canada, Annual Meeting, 1993, Program and Abstracts, p. A55.

Ogunyomi, O. and Hills, L.V.
1977: Depositional environments, Foremost Formation (Late Cretaceous), Milk River area, southern Alberta. Bulletin of Canadian Petroleum Geology, v. 25, no. 5, p. 929–968.

Van Wagoner, J.C., Posamentier, H.W., Mitchum, R.M., Vail, P.R., Sarg, J.F., Loutit, T.S., and Hardenbol, J.
1988: An overview of the fundamentals of sequence stratigraphy and key definitions. *In* Sea-Level Changes: An Integrated Approach, C.K. Wilgus, B.S. Hastings, C.G.St.C. Kendall, H.W. Posamentier, C.A. Ross, and J.C. Van Wagoner (eds.). Society of Economic Paleontologists and Mineralogists, Special Publication 42, p. 109–124.

THE DEVONIAN GRAMINIA FORMATION IN CENTRAL ALBERTA

N.C. Meijer Drees, M.G. Fowler, and L.D. Stasiuk

Geological Survey of Canada, 3303-33rd Street N.W, Calgary, Alberta T2L 2A7

D.I. Johnston

P.O. Box 1700, Centre for Earth and Ocean Research
University of Victoria, Victoria, B.C. V8W 2Y2

INTRODUCTION

In order to increase our knowledge of the subsurface geology in Alberta it is necessary to periodically review new information from recently completed drilling ventures of the oil and gas industry. If such a review incorporates the use of new concepts and new analytical methods, it may clarify some geological problems. Thus we combine, in this preliminary report on the Graminia Formation, a study of the new litho-stratigraphic information obtained by the petroleum industry, with the results of a biostratigraphic study of conodonts and a geochemical analysis of potential source rocks. The integration of new data provides us with a much better definition of the Frasnian–Famennian boundary, a better understanding of the Upper Devonian sedimentary framework and a second look at the hydrocarbon potential of the Graminia Formation.

PREVIOUS WORK

The Devonian succession in the subsurface of central Alberta is formally subdivided into five groups (Grayston et al., 1964; Belyea, 1964), with each group including a number of formations. These groups are named in ascending order: Elk Point, Beaverhill Lake, Woodbend, Winterburn and Wabamun.

The Graminia Formation, descibed in this report, was introduced as a member by the Geological Staff of Imperial Oil Ltd. (1950), and forms the upper part of the Winterburn Group. It includes the boundary between the Frasnian and Famennian stages (Mound, 1968; Switzer et al., 1994). In the type section (Pyrcz 12-25-50-26W4), the Graminia Formation consists of anhydrite, dolostone and siltstone. The Graminia overlies the Calmar Formation and is overlain by the Wabamun Group.

The Graminia Formation is widely distributed in the subsurface of central Alberta and is penetrated by a large number of boreholes. The formation was recently mapped in the Geological Atlas of the Western Canada Sedimentary Basin (Switzer et al., 1994) and described as a carbonate ramp deposit that includes carbonates, evaporites and clastics. The correlations in the atlas suggest that the boundary between the Frasnian and Famennian stages lies somewhere in the upper part of the formation. This boundary was interpreted as an erosional unconformity that represents a sequence boundary in the Western Canada Sedimentary Basin (Morrow and Geldsetzer, 1989).

Choquette (1955) reported on the Graminia Formation in the area northwest of Edmonton. He subdivided the formation into a lower Blue Ridge Member and an upper Graminia Silt member. The Blue Ridge Member was described from drill cuttings as being composed of very fine crystalline, locally porous dolostone overlain by dense, slightly silty dolostone. The informal Graminia Silt member was described as consisting of argillaceous siltstone.

PRESENT WORK

Since Choquette (1955) published his report on the Graminia Formation, a number of cores were obtained in the type area of the Blue Ridge Member (Twp. 85-8W5). Hence it is now possible to describe the upper part of the Blue Ridge Member and the overlying Graminia Silt in much greater detail than previously. From the present work it is apparent that the Graminia Formation includes four, rather than two, mappable units. Thus a subdivision is proposed that includes lower, middle and upper Blue Ridge submembers in addition to the Graminia Silt member (Fig. 1).

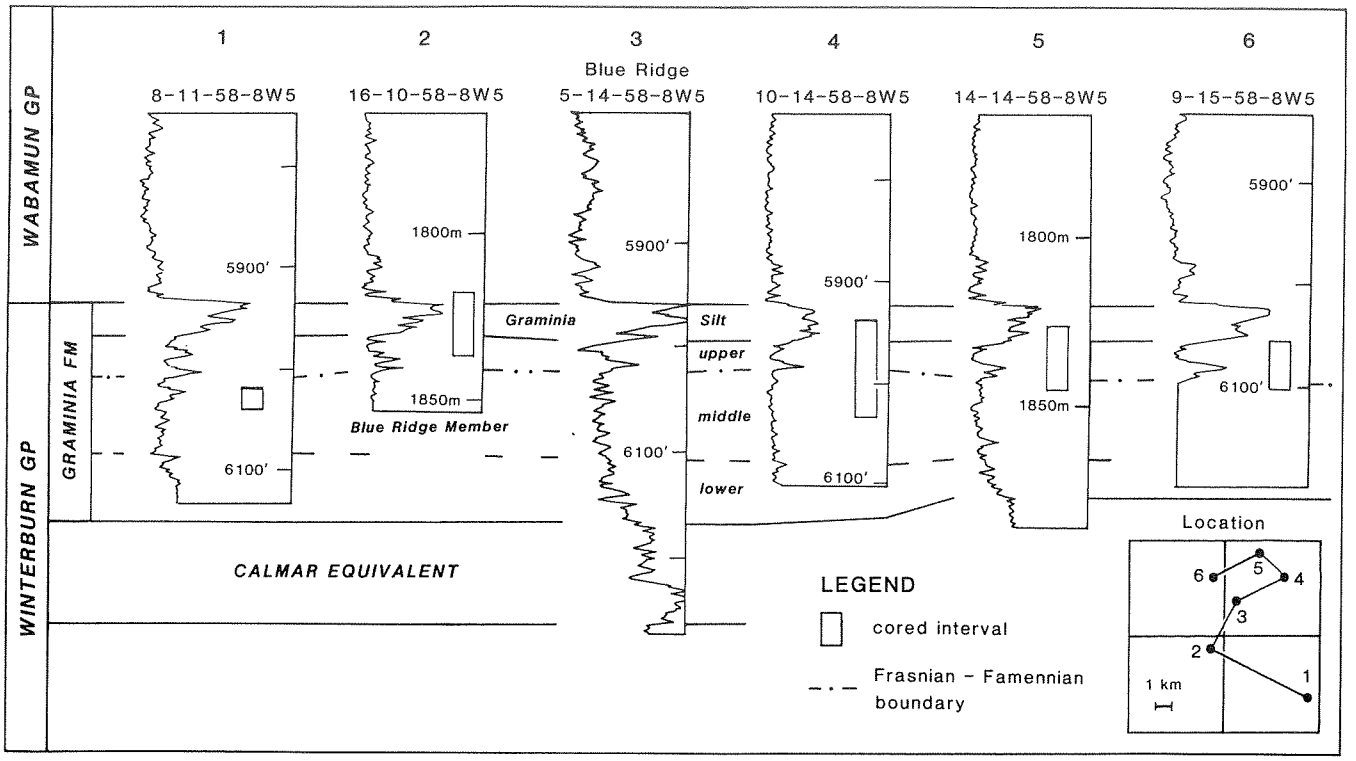

Figure 1. *The proposed subdivision of the Graminia Formation is shown by means of gamma-ray correlations between the Blue Ridge type section and nearby sections that include cored intervals.*

Stratigraphy

The lower Blue Ridge submember overlies the shaly beds equivalent to the Calmar Formation with a gradational boundary. It consists of argillaceous and silty dolostone that (in Majeau 4-29-57-3W5) has a massive, bioturbated aspect and locally includes fragments of crinoids and brachiopods.

The middle Blue Ridge submember overlies the lower submember with a gradational contact and is composed of porous, very fine to fine crystalline dolostone, including scattered, poorly preserved corals and brachiopods. Reefal beds including colonial corals are locally present. The vuggy porosity is partly or completely filled with coarsely crystalline calcite or anhydrite. The fossiliferous dolostone is interbedded with very dark grey, bituminous shale partings that range in thickness between 0.1 and 0.5 cm.

The upper Blue Ridge submember overlies the middle submember with a sharp contact that is marked by a 0.2 to 0.5 cm thick, very dark grey, bituminous shale bed. It is an interbedded unit of nonporous, silty and locally stromatolitic dolostone; porous, peloidal dolostone and nonporous, brecciated, locally anhydritic dolostone including a sandy matrix. Some dolostone breccias beds are regolith-like and truncated by an erosional surface. Other breccias are rubble deposits and overlie an erosional surface.

The Graminia Silt member overlies the Blue Ridge Member with a fairly sharp boundary and consists of interbedded green and greenish grey, dolomitic sandstones, siltstones and shales. The member is easily identified on the gamma-ray curve of geophysical borehole logs because of its radioactivity, and forms a well defined marker bed in central Alberta below the Wabamun Group (Fig. 1).

Environment of deposition

Several geologists have commented on the succession of rock types of the Graminia Formation in terms of a progradational depositional sequence within a carbonate ramp setting (Moore, 1989; Morrow and Geldsetzer, 1989; Switzer et al., 1994; Meijer Drees et al., 1994). According to these geologists, the carbonates accumulated during the Frasnian Stage along the margin of a shallow basin that succeeded the West Pembina Shale basin (Exploration Staff, Chevron Standard, 1979), centered in west central Alberta.

Thus the fossiliferous carbonates of the lower and middle Blue Ridge submembers may be interpreted as transgressive, marine, shallow water deposits, which accumulated in a semi-restricted coastal embayment. The embayment may have been deep enough to provide space for the establishment of small reefs analogous to the "Ronde/Simla (Blue Ridge) patch reefs" described by Shields and Hedinger (1990) from the Whitehorse Creek area near Cadomin.

The peloidal and stromatolitic carbonates and overlying carbonate rubble deposits, that constitute the upper Blue Ridge submember, may be interpreted to represent peritidal and subsequent terrestial conditions of deposition. These deposits may be contemporaneous with the Graminia anhydrite deposits present in the Gold Creek area of west-central Alberta.

The interbedded clastics and carbonates of the Graminia Siltstone member are interpreted as a basal transgressive deposit of the overlying sedimentary sequence belonging to the Famennian Stage.

The transgressive-regressive boundary

In a paper on eustatic sea level fluctuations during the Devonian Period, Johnson et al. (1985) recognized at least 14 transgressive-regressive (T-R) sedimentation cycles in the Devonian rocks of North America. They placed the boundary between T-R cycle IId and IIe at the base of the Sassenach Formation.

From the discussion about the environment of deposition, it is evident that the start of T-R cycle IIe coincides with the base of the upper Blue Ridge submember. The boundary between the middle and upper Blue Ridge submembers is sharp but does not represent an erosional unconformity. However, several erosional surfaces are present in the upper part of the upper Blue Ridge submember. One of these may correlate with the erosional unconformity (interpreted as a sequence boundary) that is locally present in the Rocky Mountains at the base of the Sassenach Formation (Morrow and Geldsetzer, 1989, Fig. 15).

Biostratigraphy

The colonial corals in the lower and middle Blue Ridge submembers of the Blue Ridge area (at 14-14-58- 8W5, 1840–1845 m) are dolomitized and poorly preserved. Colonial corals found at other locations (Wanham 12-20-77-3W6, 8992-9000 ft.; Asplund 4-22-66-23W5, 9299 ft.) in limestone beds equivalent to the lower part of the Graminia Formation are "probably part of the youngest pre-Frasnian/Famennian extinction coral fauna" (Pedder, 1994). Solitary corals indicative of a Givetian to Frasnian age range are present at 10-14-58-8W5 (5989 ft.), 9-15-58-8W5 (6100–6105 ft.), 10-15-56-11W5 (7640-7668 ft.), 4-12-59-3W5 (4509 ft.), 4-29-57-3W5 (5073 ft.) and 7-31-67-5W6 (11625 ft.).

Upper Frasnian conodonts were extracted from limestone beds of the Graminia Formation including corals and stromatoporoids. The faunas collected at Wanham 12-20-77-3W6 between 8993 and 9000 ft. and at Gold Creek 7-31-67-5W6 between 11617 and 11705 ft. belong to the Upper *rhenana* Zone.

The carbonates of the upper Blue Ridge submember are devoid of significant megafossils. They commonly include hemispherical stromatolites and rarely include stromatoporoids that may belong to the genus *Labechia*. The absence of corals and the paucity of stromatoporoids suggest a Famennian age. Conodonts obtained from peloidal limestone beds between 10507.5 and 10521 ft. in the upper Blue Ridge submember at Bigstone 6-19-60-21W5 are questionably assigned to the Middle to Upper *crepida* zones.

The carbonates and clastics of the Graminia Siltstone member are unfossiliferous. We did not attempt to process samples from the Siltstone member for conodonts in the Blue Ridge area because of a lack of suitable limestone interbeds.

Johnston and Meijer Drees (1993) reported the presence of early Famennian conodonts from sandy and peloidal limestone beds in the upper part of the Winterburn Group at Baseline 10-25-65-27W5. Correlations in the subsurface suggest that these beds may be equivalent to the Graminia Siltstone member.

The Frasnian–Famennian boundary

The above information indicates that in central Alberta the Frasnian–Famennian boundary more or less coincides with the boundary between the middle and upper submembers of the Blue Ridge Member (Fig. 1). It is clear that the faunal extinction that marks the end of the Frasnian Stage in central Alberta is related to a change in the environment of deposition due to a regression or due to excessive evaporation.

In west central Alberta, the Frasnian–Famennian boundary beds reflect a different depositional setting. At Gold Creek 7-31-67-5W6 the coraliferous and stromatoporoidal (Frasnian) carbonates equivalent to the middle Blue Ridge submember are sharply overlain

by a peloidal grainstone of the Wabamun Group which includes gastropods, Labechiid stromatoporoids and Famennian conodonts (Johnston and Meijer Drees, 1993). Here the change in the environment of deposition across the Frasnian–Famennian boundary is from normal to semi-restricted marine.

At Wanham 12-20-77-3W6 the Frasnian reefal limestone is erosionally overlain by a peloidal grainstone, including at the base, reworked fragments of Frasnian corals. Here the change in the environment of deposition across the boundary is also from normal to semi-restricted marine.

Geochemistry of potential source rocks

Samples were collected from the dark grey, bituminous shale interbeds and partings in the lower and middle Blue Ridge submembers to determine if they could generate hydrocarbons. The analysis by Rock-Eval pyrolysis indicates that the total organic carbon content of the shale partings ranges between 0.5 and 11.83 per cent; the Hydrogen index lies between 59 and 289 and the level of thermal diagenesis of the organic material ranges between marginally mature and mature. This suggests that the shale partings are potential source rocks.

The potential source rocks are in close contact with the porous and locally vuggy dolostone of the middle Blue Ridge submember and underlie the vuggy, peloidal dolostone beds of the upper Blue Ridge submember. The potential reservoir beds are regionally overlain by anhydritic carbonates of the Wabamun Group that form a seal. Because the porous dolostone beds of the Blue Ridge change to anhydrite in east-central Alberta it is possible that the hydrocarbons have migrated updip and are trapped along this lateral facies change.

REFERENCES

Belyea, H.R.
1964: Woodbend, Winterburn and Wabamun Groups, Part II, Chapter 6. *In* Geological History of Western Canada, R.G. McCrossan and R.P. Glaister (eds.). Alberta Society of Petroleum Geologists, Calgary, p. 66–88.

Choquette, A.L.
1955: The Blue Ridge Member of the Graminia Formation. Journal of the Alberta Society of Petroleum Geologists, v. 3, p. 70–73.

Exploration Staff, Chevron Standard Ltd.
1979: The geology, geophysics and significance of the Nisku reef discoveries, west Pembina area, Alberta, Canada. Bulletin of Canadian Petroleum Geology, v. 27, p. 326–359.

Geological Staff, Imperial Oil Ltd.
1950: Devonian nomenclature in Edmonton area, Alberta, Canada. American Association of Petroleum Geologists, Bulletin 34, p. 1807–1825.

Grayston, L.D., Sherwin, D.F., and Allan, J.F.
1964: Middle Devonian, Chapter 5. *In* Geological History of Western Canada, R.G. McCrossan and R.P. Glaister (eds.). Alberta Society of Petroleum Geologists, Calgary, p. 49–59.

Hedinger, A. and Shields, M.
1990: Fairholme stratigraphy and sedimentology, nothern margin of the Southesk-Cairn carbonate complex, Alberta. Fieldtrip Guide, 1990 Annual Convention Basin Perspectives, Canadian Society of Petroleum Geologists, Calgary.

Johnson, J.G., Klapper, G., and Sandberg, C.A.
1985: Devonian eustatic fluctuations in Euramerica. Geological Society of America Bulletin, v. 96, p. 567–587.

Johnston, D.I. and Meijer Drees, N.C.
1993: Upper Devonian conodonts in west central Alberta and adjacent British Columbia. Bulletin of Canadian Petroleum Geology, v. 41, p. 139–149.

Meijer Drees, N.C., Johnston, D.I., and Fulmer, E.G.
1994: Devonian stratigraphy and depositional history across Peace River highland, west-central Alberta. Geological Survey of Canada, Open File 2851.

Moore, P.F.
1989: Devonian geohistory of the western interior of Canada. *In* Devonian of the world, v. I, N.J. McMillan, A.F. Embry and D.J. Glass (eds.). Canadian Society of Petroleum Geologists, Memoir 14, p. 67–83.

Morrow, D.W. and Geldsetzer, H.H.J.
1989: Devonian of the eastern Canadian Cordillera. *In* Devonian of the world, v. I, N.J. McMillan, A.F. Embry and D.J. Glass (eds.). Canadian Society of Petroleum Geologists, Memoir 14, p. 85-121.

Mound, M.C.
1968: Upper Devonian conodonts from southern Alberta. Journal of Paleontology, v. 42, p. 444–524.

Pedder, A.E.H.
1994: Report on two lots of Upper Devonian corals and associated faunas from the subsurface of Iosegun Lake map sheet, Alberta. Unpublished Paleontological report, Geological Survey of Canada, No. NCMD-173-AEHP-94.

Switzer, S.B., Holland, W.G., Christie, D.S., Graf, G.C., Hedinger, A.S., McAuley, R.J., Wierzbicki, R.A., and Packard, J.J.
1994: Devonian Woodbend-Winterburn Strata of the Western Canada Sedimentary Basin, Chapter 12. *In* Geological Atlas of the Western Canada Sedimentary Basin, G. Mossop and I. Shetsen (compilers). Canadian Society of Petroleum Geologists, Calgary, p. 165–201.

PETROLEUM GEOLOGY OF THE MIDDLE DEVONIAN WINNIPEGOSIS AND PRAIRIE FORMATIONS IN EAST-CENTRAL ALBERTA

N.C. Meijer Drees, B.C. Palmer, M.G. Fowler, L.D. Stasiuk, and G.S. Nowlan

Geological Survey of Canada, 3303-33rd Street N.W., Calgary, Alberta T2L 2A7

D.C. McGregor

Geological Survey of Canada, 601 Booth Street, Ottawa, Ontario K1A 0E8

INTRODUCTION

This report and the poster display are the result of work done during the first year (1993–94) of a two year cooperative project involving the oil and gas industry and the Geological Survey of Canada under the Industrial Partners Program. The principal objective of the program involves a study into the petroleum potential of the Lower Paleozoic rocks. We report here only on the work that was done on the Middle Devonian rocks.

The Middle Devonian rocks in the subsurface of east-central Alberta have been penetrated by many boreholes. Most of the subsurface data and material obtained from the boreholes is available in one form or another from the Alberta Energy and Resources Conservation Board (AERCB). Thus, B.R. Palmer has manipulated, culled and augmented by computer the geological information in the AERCB data files and transformed them into maps and cross-sections. N.C. Meijer Drees described the Middle Devonian rock succession and collected samples from cored intervals in 9 boreholes stored at the AERCB Core Reseach Centre. M.G. Fowler and L.D. Stasiuk analysed the source rock potential of the Devonian succession and G.S. Nowlan and D.C. McGregor studied the microfossils obtained from the core samples.

REGIONAL GEOLOGY

The Middle Devonian carbonates described here belong to the Elk Point Group, an interbedded succession of fine and coarse grained clastics, redbeds, evaporites and carbonates that accumulated in a paleotopographic basin (the Elk Point Basin of Grayston et al., 1964). During the late Silurian to early Devonian period of uplift and erosion a large part of the Lower Paleozoic rocks was removed from the region now represented by southwestern Saskatchewan and Alberta. Thus, in central Alberta the basal clastics of the Elk Point Group overlie and onlap rocks ranging in age from Precambrian to Late Ordovician.

The clastics, redbeds and evaporites in the lower part of the Elk Point Group accumulated in the deeply eroded parts of the Central Alberta Subbasin while the carbonates and evaporites in the upper part extend across the entire Elk Point basin (Grayston et al., 1964; Meijer Drees, 1994).

In the subsurface between Mannville (Alberta) and Meadow Lake (Saskatchewan), the lower Elk Point strata onlap an east–west trending, paleotopographic escarpment (the Meadow Lake Escarpment of van Hees, 1958) that marks the erosional edge of a highland in southern Saskatchewan underlain by resistant, Late Ordovician carbonates (see Norford et al., 1994; Fig. 9-22). On the isopach map of the Elk Pont Group (Meijer Drees, 1994; Fig. 10-3) the escarpment changes character in the west because the upper part, composed of the erosional edge of the Upper Ordovician Red River carbonates curves southward and trends toward Hanna (see Norford et al., 1994, Fig. 9-22), while the lower part, composed of less resistant Ordovician and Cambrian clastics, continues westward to Edmonton.

Upper Elk Point strata

The clastics, carbonates and evaporites in the upper part of the Elk Point Group onlap and overlie the more elevated parts of the pre-Devonian paleotopography. This is shown schematically on a southwest-northeast trending cross section (Fig. 1).

Here stratigraphic relationships within the upper part of the Elk Point Group suggest a gentle onlap of the Ashern and Winnipegosis formations against a pre-Devonian highland composed of Upper Ordovician carbonates. The transgressive onlap is marked by an

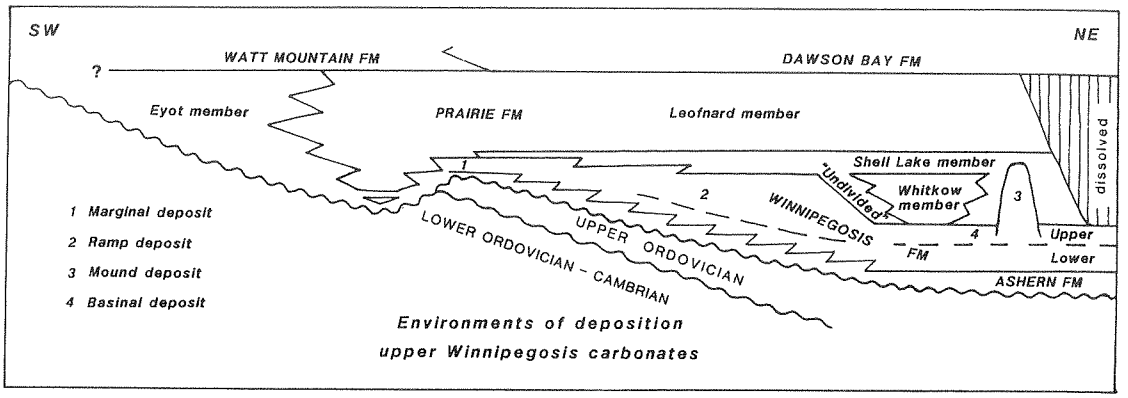

Figure 1. *Schematic cross-section including the pre-Devonian unconformity and the onlap-stratigraphy of the Upper Elk Point strata in central Alberta and west-central Saskatchewan.*

upward change in lithology from fine grained clastics (Ashern Formation) to fossiliferous carbonates (Winnipegosis Formation).

The greenish grey, dolomitic shales and siltstones of the Ashern Formation form a basal transgressive deposit. Along the east flank of the highland they interfinger with and grade laterally into the overlying carbonates of the Lower Member of the Winnipegosis Formation (Jones, 1965).

The Winnipegosis Formation (Baillie, 1953) and its equivalents (the Keg River and Methy formations) are widely distributed in southwestern Manitoba, southern Saskatchewan and Alberta. Jones (1965) introduced a subdivision of Lower and Upper members in the subsurface of southern Saskatchewan.

The Lower member overlies the Ashern with a transitional contact and forms a widely ditributed unit composed of argillaceous dolostone or limestone that ranges in thickness between 0 and 15 m. It includes, in the upper part, interbeds of marlstone rich in pelagic tentaculitids and crinoidal debris. In southwestern Saskatchewan and southeastern Alberta, the Lower member decreases in thickness to zero because of a lateral facies change with the Ashern (Jones, 1965).

The distribution of the Upper Member of the Winnipegosis Formation extends beyond the depositional boundaries of the Lower member and includes four facies: 1) a marginal evaporitic carbonate facies; 2) a bioclastic carbonate ramp and platform facies; 3) a biostromal mound facies which locally overlies the platform facies; and 4) a basinal, bituminous, laminated and locally anhydritic carbonate facies (Jones, 1965; Wardlaw and Reinson, 1971; Meijer Drees, 1986). The relationships between the four facies are shown schematically on Figure 1.

Regional work on the formations in the upper part of the Elk Point Group by Bebout and Maiklem (1973) and Meijer Drees (1985), indicates that the upper boundary of the Winnipegosis and its equivalents (the Keg River and Methy formations) represents a depositional surface with considerable relief (up to 68 m), due to the presence of shallow channels, shoals, biostromal mounds and reefal deposits.

This situation suggests that deposition of carbonate sediment in the Elk Point basin could only locally keep up with the relative rise in sea level, so that the water depth in the embayment increased locally. It has been further suggested that the formation of a barrier reef at the entrance of the Elk Point embayment, followed by a relative sea level fall, changed the circulation pattern in the embayment and decreased the production of carbonates (Maiklem, 1971; Bebout and Maiklem, 1973).

In southern Saskatchewan and eastern Alberta, the carbonates of the Winnipegosis Formation are overlain by salt deposits of the Prairie (Evaporite) Formation (Baillie, 1953), by means of intervening deposits of interbedded anhydritic carbonates and anhydritic shale (the Ratner, Shell Lake and "Undifferentiated Shell Lake-Whitkow" members of Reinson and Wardlaw, 1972).

The complex stratigraphic relationships between the members of the Prairie Formation (the Whitkow, Shell Lake and Leofnard members) and the four facies units of the Winnipegosis Formation are shown schematically on Figure 1.

The anhydritic deposits of the Shell Lake Member and the salt beds of the Leofnard Member pass laterally into the Eyot member. The Eyot (Meijer Drees, 1994) constitutes an interbedded succession of argillaceous carbonates, anhydritic carbonates, silty shales and bituminous shales, which onlaps the eastern flank of the Western Alberta Ridge, a pre-Devonian highland situated in southwestern Alberta (Grayston et al., 1964).

PETROLEUM GEOLOGY

Of prime interest to the petroleum geologist are the two Middle Devonian oil discoveries in east-central Alberta at Spiers and Rich. The oil discovered at Spiers 16-16-34-15W4 (interval 1925.5–1927.5 m) and Spiers 11-15-34-15W4 (intervals 1923–1926.5 and 1928.5–1929.5 m) occurs in fractured and brecciated, Upper Ordovician Red River carbonates (including mid-Edinian conodonts) which underlie the pre-Devonian unconformity.

The oil at Spiers is trapped at the erosional edge of the Upper Ordovicoan succession along the southwestern extension of the Meadow Lake Escarpment in a paleotopographically and structurally high location (Fig. 1).

The oil at Rich 7-25-34-21W4 (API 23.2) is produced from a unit below the Middle Devonian salt beds consisting of interbedded porous dolostone and nonporous dolomitic anhydrite (intervals 2246.5–2249.5 and 2251.3–2253.3 m). These lithologies are typical for the marginal deposits of the Winnipegosis Formation or the Shell Lake member. The oil at Rich occurs in a stratigraphic onlap trap at the west flank of the southwestern extension of the Meadow Lake Escarpment (Fig. 1).

Of secondary interest to the petroleum geologist is the information obtainable from drill stem tests performed on porous Middle Devonian rocks. They indicate that in east-central Alberta the bioclastic ramp deposits of the Winnipegosis Formation (Fig. 1) constitute an important aquifer that may be considered as a possible reservoir facies. The postulated presence of ancient grainstone shoals and sediment-filled channels in the upper part of the ramp deposits, and the irregular nature of the (secondary) anhydritization in the overlying Shell Lake carbonates suggest the possible presence of stratigraphic traps. The expected closure of the stratigraphic traps at the top of the ramp deposits in the Winnipegosis Formation could range between 3 and 10 m. The porosity distribution within the expected traps is difficult to predict. If we use the reservoir facies at Provost 11-35-38-10W4 as an example, the expected maximum permeability may range between 6.37 and 45.3 mD and the porosity between 1.21 and 11.38 per cent.

Geochemistry

The Middle Devonian rocks that underlie the salt beds of the Prairie (Evaporite) Formation and are in contact with the Upper Ordovician carbonates, include the Ashern, the marginal deposits of the Winnipegosis, and the Shell Lake and Eyot members of the Prairie Formation (Fig. 1). These map units include dark grey, bituminous shale partings and beds as thick as 1 cm.

These shales are generally high in organic carbon content. Values of up to 20 per cent Total Organic Carbon (TOC) were measured by Rock-Eval pyrolysis. Many of the samples also show high Hydrogen Indices (up to 600–650). The high T-max and vitrinite reflectance values indicate that the shales are marginally mature and may have generated hydrocarbons in the deeper part of the basin (west of Range 20W4).

The geochemical characteristics of the oil found in the Rich and Spiers fields are similar and indicate that both oils originated from the same or similar source rocks. Although work on the extracts of bituminous core samples of nearby boreholes is not complete, it is already apparent that the biomarker distributions of these oils are similar to those found in the extracts of some of the Middle Devonian shales.

The above information suggests that the oil in the Rich and Spiers fields was generated from mature organic material present in the Middle Devonian strata farther downdip and migrated updip below the salt beds into adjacent porous Middle Devonian or Upper Ordovician carbonates.

Micropaleontology

Several bituminous shale samples of the Ashern Formation contain scolecodonts, chitonozoans, small acritarchs and leiospheres. These microfossils are believed to have lived in a marine environment. The presence of well preserved Middle Devonian, trilete spores, associated with marine palynomorphs, in one sample (Provost 11-35-38-10W4, 1672 m) point to a mixed terrestial and marine origin for the organic material. Samples from the marginal deposits of the Winnipegosis Formation contain leiospheres, poorly

preserved marine acritachs and poorly preserved Middle Devonian spores. A sample from the beds just below the Prairie salt deposits at Spiers 11-15-34-15W4 (1914.75 m) yielded an assemblage of spores that is correlated with the late Givetian *optivus-triangulatus* Zone of Richardson and McGregor (1986). The absence of acritarchs and the presence of spores in the Eyot member suggest a terrestial environment of deposition. Abundant and well preserved trilete spores were recovered at Bashaw 16-36-41-23W4 (depth 2273.34 m) at the top of the Eyot. Here several species of spores are indicative of Givetian age.

Organic facies

It is possible to recognize three paleoenvironments of deposition in the bituminous shale deposits based on microfossils, the particulate organic (maceral) composition of the bituminous shales and the textural relationships between the organic and inorganic particles. Broadly defined, these include: 1) terrestial paleoenvironments with a marine influence, 2) marine paleoenvironments with a terrestial influence, and 3) wholly marine paleoenvironments of deposition.

In the Shell Lake member at Provost 11-35-38-10W4 (interval 1664.1–1647.7 m), the bituminous interbeds change upward from marine-influenced, vitrinite-sporinite-rich terrestial coals, to sporinite- and *Botyrococcus* alginite-rich lacustrine shales, to evaporitic lagoonal shales that include cyanobacteria-like stromatolites and marine acritarchs. The mixed marine and lagoonal, evaporitic facies is also present in the evaporitic, marginal deposits of the Winnipegosis at Spiers 11-15-34-15W4 and Rich 15-30-34-20W4, but includes significantly more terrestial material.

REFERENCES

Bailie, A.D.
1953: Devonian system of the Williston Basin area. Manitoba Mines Branch, Publication 52-5.

Bebout, D.G. and Maiklem, W.R.
1973: Ancient anhydrite facies and environments, Middle Devonian Elk Point Basin, Alberta. Bulletin of Canadian Petroleum Geology, v. 21, p. 287–343.

Grayston, L.D., Sherwin, D.F., and Allan, D.F.
1964: Middle Devonian, Chapter 5. *In* Geological History of Western Canada, R.G. McCrossan and R.P. Glaister (eds.). Alberta Society of Petroleum Geologists, Calgary, p. 49–59.

Jones, L.J.
1965: The Middle Devonian Winnipegosis Formation of Saskatchewan. Saskatchewan Department of Mineral Resources, Report no. 123.

Maiklem, W.R.
1971: Evaporite drawdown - a mechanism for waterlevel lowering and diagenesis in the Elk Point Basin. Bulletin of Canadian Petroleum Geology, v. 19, p. 485–503.

Meijer Drees, N.C.
1986: Evaporitic deposits of Western Canada. Geological Survey of Canada, Paper 85–20.

1994: Elk Point Group in the Western Canada Sedimentary Basin, Chapter 10. *In* Geological Atlas of the Western Canada Sedimentary Basin, G.D. Mossop and I. Shetsen (eds.). Canadian Society of Petroleum Geologists, Calgary, p. 129–147.

Norford, B.S., Haidl, F.M., Bezys, R.K., Cecile, M.P., McCabe, H.R., and Paterson, D.F.
1994: Middle Ordovician to Lower Devonian strata of the Western Canada Sedimentary Basin, Chapter 9. *In* Geological Atlas of Western Canada Sedimentary Basin, G.D. Mossop and I. Shetsen (eds.). Canadian Society of Petroleum Geologists, Calgary, p. 109–127.

Reinson, G.E. and Wardlaw, N.C.
1972: Nomenclature and stratigraphic relationships, Winnipegosis and Prairie Evaporite formations, central Saskatchewan. Bulletin of Canadian Petroleum Geology, v. 20, p. 301–320.

Richardson, J.B. and McGregor, D.C.
1986: Silurian and Devonian spore zones of the Old Red Sandstone Continent and adjacent regions. Geological Survey of Canada, Bulletin 364.

van Hees, H.
1958: The Meadow Lake Escarpment - its regional significance to Lower Paleozoic stratigraphy. North Dakota Geological Society, Second International Williston Basin Symposium, p. 70–78.

Wardlaw, N.C. and Reinson, G.E.
1971: Carbonate and evaporite deposition and diagenesis, Middle Devonian Winnipegosis and Prairie Evaporite formations of south-central Saskatchewan. American Association of Petroleum Geologists Bulletin, v. 55, p. 1759–1786.

THE LOWER PALEOZOIC: A NEW FRONTIER IN THE WESTERN CANADA BASIN

G.S. Nowlan, M.G. Fowler, N.C. Meijer Drees, B.R. Palmer, and L.D. Stasiuk

Geological Survey of Canada, 3303-33rd Street N.W., Calgary, Alberta T2L 2A7

F.J. Hein

Department of Geology and Geophysics, University of Calgary, Calgary, Alberta T2N 1N4

INTRODUCTION

The Lower Paleozoic, Cambrian to Middle Devonian, strata of the Western Canada Sedimentary Basin in Alberta have been little studied. A project has been designed to gain a clearer understanding of the sedimentary packages that lie between Precambrian basement and the base of the Devonian Beaverhill Lake Formation. It encompasses a study of Cambrian to earliest Ordovician clastic, Upper Ordovician carbonate and basal Devonian clastic, carbonate and evaporitic strata. In the area delimited for the first year of this project (Fig. 1) a total of 135,000 wells have been drilled; of these only 187 penetrate Cambrian and 61 penetrate basement. Cores and cuttings from many of these wells have been examined and analyzed for petrography, biostratigraphy, organic petrology, and organic geochemistry. A schematic cross-section from west to east across the Alberta part of the basin (Fig. 2) shows the general relationships between the Lower Paleozoic sedimentary cover and the underlying basement domains. A table of formations considered in the present study is provided as Figure 3.

The project was conducted under the Industrial Partners Program of the Geological Survey of Canada (GSC) in which projects that are successful in attracting industry funds are eligible to receive matching funds up to $50,000 from GSC. The principal purposes of the program are to foster closer working relationships between GSC staff and industry and to enhance GSC's response to the needs of its industrial clients.

CAMBRIAN

The following stratigraphic units have been examined: the Basal Sandstone unit; the Earlie, Mount Whyte, Cathedral, Stephen, Eldon, Pika, Arctomys, Waterfowl,

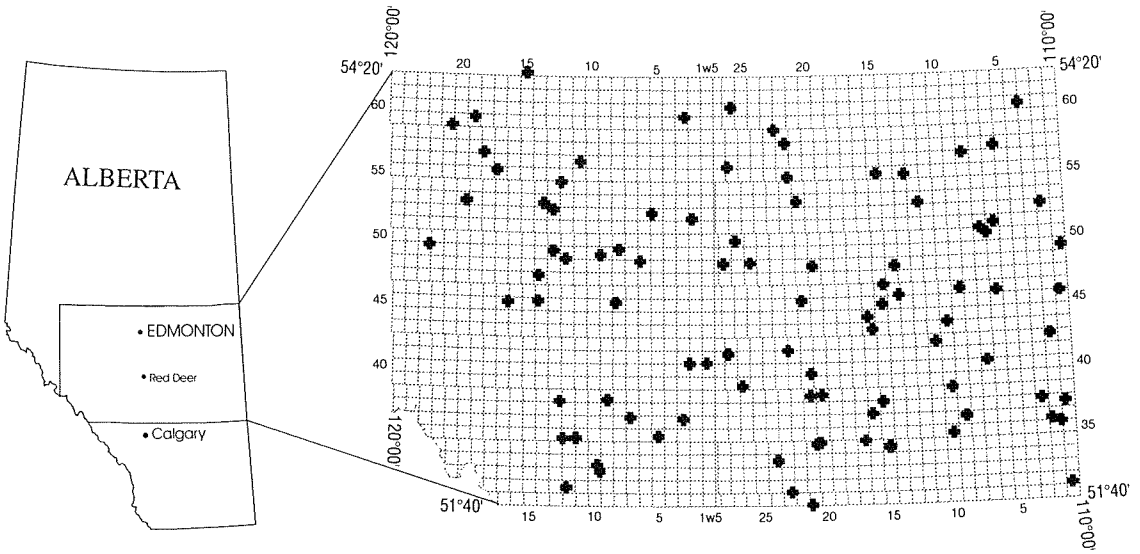

Figure 1. *Location map of study area. Dots indicate wells with Cambrian penetrations.*

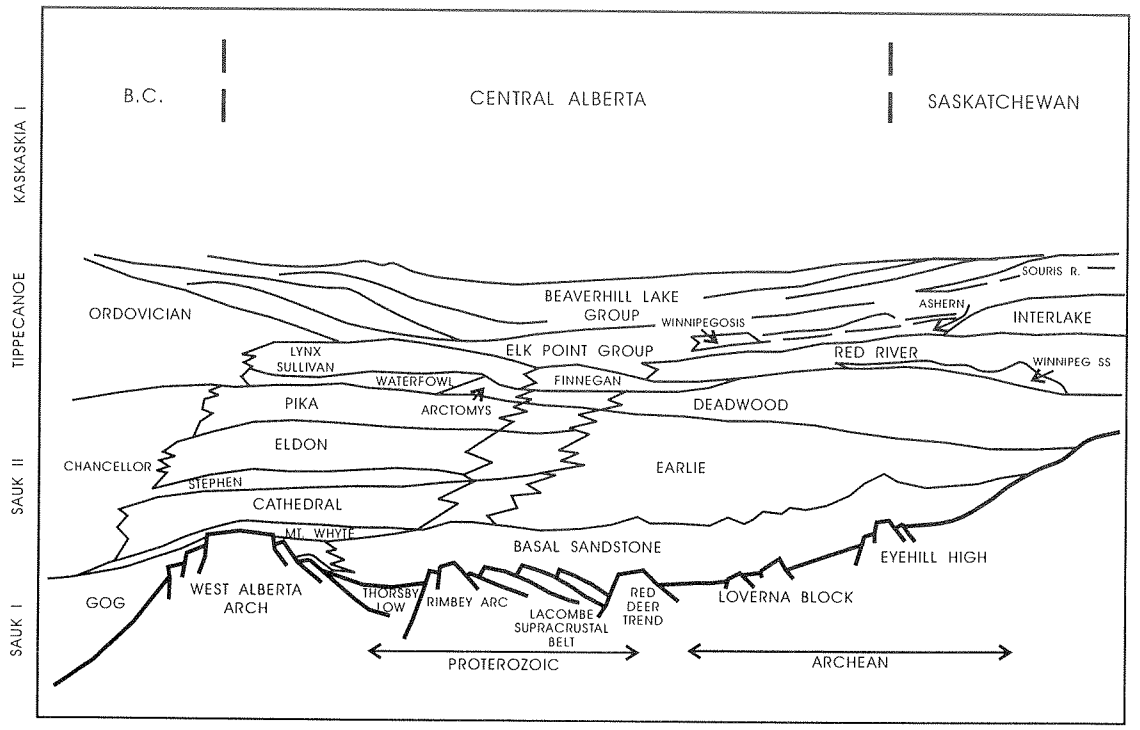

Figure 2. *Schematic cross-section from west to east across the Alberta Basin, showing general relationships between the Lower Paleozoic sedimentary cover and the underlying basement domains (modified from A. Hamblin, pers. comm., 1993).*

Sullivan and Lynx formations and, for uppermost Cambrian, the Finnegan and Deadwood formations. They comprise the Sauk II subsequence. In Alberta the shale and carbonate succession from the Mount Whyte to Eldon formations changes eastward to argillaceous rocks of the Earlie Formation (Fig. 2). The Earlie Formation is overlain by the Pika marker, the top of which is cut by a regional disconformity and succeeded by the transgressive clastics of the Deadwood Formation, and the overlying interbedded clastics and carbonates of the Finnegan Formation. The relationship of the Deadwood and Finnegan to other units of the Sauk II succession are poorly understood and the Finnegan Formation might be assignable to the Sauk III subsequence. In the northwestern extremity of the study area, the carbonates of the Eldon Formation are replaced by sandstone-dominated successions, derived from the northwest, presumably from the Peace River–Athabasca Arch area.

Preliminary facies analysis indicates that the Cambrian successions were emplaced as mixed clastic and carbonate ramps, carbonate banks or reefs, and marine shoals within a shallow-marine embayment. Monadnocks of basement rock disrupted sedimentation patterns and locally supplied coarse-clastic detritus to a marine embayment, known as the Lloydminster Embayment.

In Middle Cambrian time, the Basal Sandstone Unit represents a transgressive flooding event within a deep, clastic-dominated tidal embayment that includes coarse grained shoreline fan-delta and nearshore marine successions. The unit overlies Precambrian basement with a regional unconformity and flanks basement highs. The flooding surface of the Cambrian seaway was not flat, particularly in the east where a series of Precambrian basement highs pierce the platformal succession. The succeeding Eldon Formation represents shallow marine carbonate banks and ramps, that were replaced by clastic tidal deltas and fan-deltas toward the northwest, in areas influenced by the Peace River–Athabasca Arch. The overlying Pika Formation represents a shallow marine carbonate bank to the west, with a mixed carbonate/clastic embayment, more argillaceous toward the east, where it merges with fine grained, low-energy clastics of the Earlie Formation. After deposition of the Pika there is an hiatus that results in a disconformity with the Sullivan and Deadwood formations to the east.

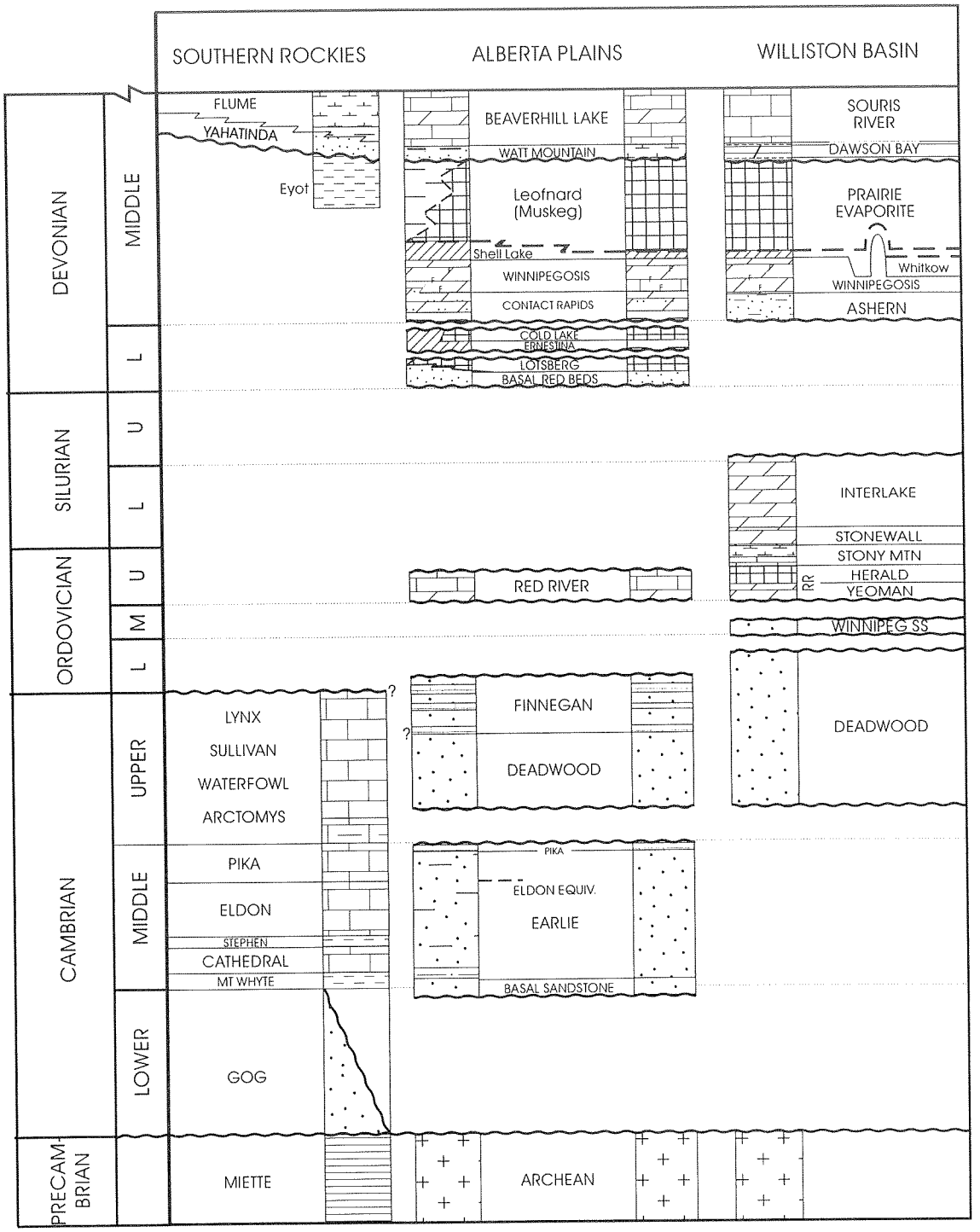

Figure 3. *Table of formations and their correlation.*

In the Late Cambrian the Sullivan and Lynx formations represent shallow carbonate banks and oolitic shoals, mainly preserved to the west. The Lynx Formation has internal disconformities and hard-grounds; local karstification and dissolution of the carbonates has occurred. The Deadwood Formation represents a transgressive clastic-dominated shelf-ramp succession locally capped by a disconformity although in some areas deposition continued into late Early Ordovician time at least. During this hiatus, reworking of the Lynx carbonate platformal succession occurred toward the east where the Finnegan Formation

represents a transgressive mixed clastic and carbonate shelf-ramp succession. Deposition of the Finnegan Formation is followed by an hiatus and disconformity, although the more substantial erosion may not have occurred until Devonian time.

The Cambrian part of the sequence is characterized by good to excellent porosity in many units but potential source rocks are rare. Samples have been screened for hydrocarbon source potential by Rock-Eval/Total Organic Carbon (TOC) analysis. The TOC content of Cambrian rocks are low, none exceeding 1%. In terms of organic facies, the dominant macerals of the Cambrian samples are unicellular and coccoidal alginite, acanthomorphic and sphaeromorphic acritarchs and chitinozoans. Distinctive algal mat textures have been noted in micro-interlaminated marls and carbonates in one well.

Analysis of the kerogen palynofacies indicates that all 63 samples of Cambrian strata analyzed are marine in origin. The samples contain acritarchs, leiospheres, or botryoidal-shaped kerogen indicating a nearshore marine environment. Palynomorphs are poorly preserved and preclude identification at the specific level in all but a few cases. However, many of the genera are restricted to the Cambrian (*Adara*, *Retisphaeridium*, *Timofeevia* and *Trunculumarium*) or Cambrian-Early Ordovician (*Goniosphaeridium*).

Conodonts of latest Cambrian to earliest Ordovician age have been recovered from the Finnegan Formation in several wells. Specimens assignable to the *Proconodontus*, *Eoconodontus* and *Cordylodus proavus* zones have been recovered. Conodonts are rare in the Eldon and Lynx formations. Trilobites of the *Glossopleura* Zone have been recovered from the Stephen Formation.

ORDOVICIAN

The Upper Ordovician carbonates in the subsurface of southeastern Alberta form the western edge of a much thicker platformal succession of carbonates (the Tippecanoe Sequence) that is more completely preserved in the Williston Basin, centred in North Dakota. The Tippecanoe Sequence overlies Cambrian and Early Ordovician rocks with an erosional unconformity and includes, in the central part of the Williston Basin, a basal unit of shale and sandstone (the Winnipeg Formation). This unit is overlain by carbonates of the Big Horn and Interlake groups which, along the northern margin of the Williston Basin, were uplifted and truncated prior to the Devonian Period in the region northwest of the Meadow Lake Escarpment. Thus, the western limit of the Upper Ordovician carbonate succession in Alberta is an erosional edge (Fig. 2). The Upper Ordovician Bighorn Group in the subsurface of the southern Interior Plains includes the Red River, Stony Mountain and Stonewall formations, however only the Red River and Stony Mountain formations have been identified from the Alberta subsurface.

Conodonts are abundant in the Red River Formation, indicating a mid-Edenian to mid-Maysvillian age. Conodonts of late Maysvillian age are rare in the upper part of the Red River. Faunal abundance and diversity drops dramatically in the Stony Mountain Formation, however, the diagnostic Richmondian coral *Bighornia* has been recovered from the Stony Mountain Formation in a few wells.

Oil shows from two wells have been examined. Organic geochemistry indicates that these are similar to Winnipegosis-sourced oils known from the Williston Basin. The oil from Big Valley Rich (7-25-34-21W4, 2231-2234 m), hosted in the Winnipegosis Formation, is slightly more mature than organic matter in the Virago et al. Rich well (15-30-34-20W4) which is a few kilometres to the east. Hence, there is a possibility that the oil is locally sourced. The hydrocarbons at Gulf Spiers (11-15-34-15W4), hosted in the Red River Formation, are significantly less mature than the oil at Big Valley Rich, but much more mature than organic-rich units in the overlying Winnipegosis. Therefore they must presumably have migrated some distance from more mature rocks to the west, possibly near the Virago et al. Rich well.

DEVONIAN

The Middle Devonian Elk Point Group, an interbedded succession of fine and coarse grained clastics, redbeds, evaporites and carbonates accumulated in a paleotopographic basin named the Elk Point Basin, centred in east-central Alberta. The Elk Point Group forms the lower part of a much thicker succession of strata, the Kaskaskia Sequence that includes carbonates of Late Devonian and Carboniferous age. During the Late Silurian to Early Devonian period of uplift and erosion that separates the Tippecanoe from the Kaskaskia sequence, the Silurian and a large part of the Ordovician and Cambrian were removed from the region. Thus, in central Alberta the basal Elk Point Group overlies rocks ranging in age between Precambrian and Late Ordovician. The group onlaps paleotopographic relief of about 600 m which had a

major influence on the distribution of the Early to early Middle Devonian clastics and salt deposits in the Elk Point Basin.

The oldest Devonian deposits consist of coarse grained clastics that pass upward and basinward into redbeds and into the Lower and Upper salt members of the Lotsberg Formation. These units accumulated in the central part of the Elk Point Basin and are confined to east-central Alberta and western Saskatchewan (Fig. 3). The carbonates and anhydrite deposits of the Ernestina Lake Formation overlie continental redbeds and salt beds and pass laterally into the Basal Red Beds unit. The redbeds and clastics in the lower part of the overlying Contact Rapids Formation represent the marginal facies and the redbeds and salt deposits of the coeval Cold Lake Formation represent the facies in the centre of the Elk Point Basin. The lateral change from salt to redbeds is controlled by transgressive onlap.

The early Middle Devonian transgression is represented by southward onlap of the upper Contact Rapids, Ashern and Winnipegosis formations against the Meadow Lake Escarpment. Lithologically the transgression is marked by an upward change from fine grained clastics to fossiliferous carbonates. The carbonates of the Winnipegosis Formation overlie shaly beds of the Ashern and Contact Rapids formations with a gradational contact. The lower member changes laterally into the Ashern Formation along the southwestern margin of the Elk Point embayment. The Upper member includes four facies: 1) a marginal, evaporitic carbonate facies; 2) a bioclastic carbonate platform facies; 3) a biostromal mound facies which locally overlies the carbonate platform; and 4) a basinal, laminated and locally anhydritic carbonate facies. The upper boundary of the Winnipegosis represents a depositional surface with considerable local relief (up to 68 m) due to the presence of shallow channels, shoals, biostromal mounds and reefal deposits.

Carbonates of the Winnipegosis Formation are overlain by salt deposits of the Prairie Formation through an intervening unit of interbedded anhydritic carbonate and anhydritic shale, the Shell Lake member. The Shell Lake member and the overlying salt deposits of the Leofnard Member pass laterally into an interbedded succession of argillaceous and anhydritic carbonate, and bituminous and silty shale of the Eyot Member which onlaps the eastern flank of the Western Alberta Arch.

Middle Devonian, probably Givetian, spores are locally abundant and diverse in samples of the Elk Point Group. Spores of land-based plants were obtained from the Contact Rapids, Ashern, and Winnipegosis formations and from the Shell Lake and Eyot members of the Prairie Formation. In addition to spores, the Winnipegosis and Ashern formations and (in one well) the Eyot Member of the Prairie Formation contained acritarchs and/or other palynofossils indicating marine conditions of deposition.

Based on maceral composition and organic-inorganic textural relationships, several organic facies have been defined for organic-rich intervals in the Winnipegosis Formation. Organic facies broadly defined include: (i) terrestrial paleoenvironments with marine influence; (ii) marine paloenvironments with terrestrial influence; and (iii) wholly marine paleoenvironments.

A detailed examination of core from Pan Canadian Provost 11-35-38-10W4 revealed 8 samples with TOC values greater than 1% and 4 greater than 10%. The more organic-rich samples are either Type I-II consisting mostly of algal/bacterial organic matter that accumulated in a lagoonal environment with anoxic bottom waters or Type III containing predominantly terrestrial-derived organic matter such as vitrinite, inertinite and sporinite (thin coal). While these potential source rock intervals tend to be thin, some have an extremely high hydrocarbon potential including one sample that has a TOC content of 17.2% and a hydrogen index of 626.

The Winnipegosis Formation in the PCP Provost well is immature with respect to hydrocarbon generation and cannot be the source of commercial quantities of liquid hydrocarbons. However, the biomarker distributions of some samples with higher hydrocarbon potential show some source characteristics similar to those of the Big Valley Rich oil and the Gulf Spiers oil shows. Thus it is probable that the source rocks of the oils were also deposited in restricted lagoonal to nearshore, restricted platform environments.

THERMAL MATURITY

Preliminary assessment of Cambrian conodont CAI, palynomorph TAI and reflectance data (%Ro) suggests that a substantial portion of the Cambrian is within the oil to late condensate stage of thermal maturity. For the Middle Devonian, a preliminary thermal maturity plot shows that the eastern portion of the study area is immature to marginally mature and that peak maturity is in the central part of the region. The northwest corner is near the oil window and the southwest corner is within the condensate–wet gas zone.

THE 1:1 000 000 GEOLOGICAL ATLAS OF CANADA: BEDROCK GEOLOGY OF THE LETHBRIDGE MAP AREA (NM–12–G)

A.V. Okulitch

Geological Survey of Canada, 3303-33rd Street N.W., Calgary, Alberta T2L 2A7

INTRODUCTION TO THE ATLAS PROGRAM

The Geological Atlas of Canada program is a continuing activity designed to produce, in paper and digital form, compilations of the bedrock geology of Canada, displayed on maps and geotectonic correlation charts. Map and chart sets, which also include descriptive notes, supplementary maps of physiography, tectonostratigraphic elements, and as appropriate, metamorphism, dyke swarms, mineral occurrences, oil and gas fields etc., provide, in addition, a map and extensive lists of data sources. The general aim is to provide a thorough introduction to the geology of each area and direction for additional information.

The compilation process is used by the GSC to resolve regional geologic problems, to emphasise areas needing new work and to study major geologic elements, plate tectonic features, etc. The map and chart sets serve as valuable teaching aids and as tools for delineating research study areas at universities. They enable mining and exploration companies to plan regional prospecting proposals and to target broad areas of economic interest. They form the basis for numerous derivative studies of economic assessment and development, land-use planning, wildlife research and others. The digital files are structured into an elementary geographic information system accessable within the AutoCAD drafting program used for compilation and cartography, and they can be readily imported into other systems such as Arc Info.

CURRENT STATUS OF THE ATLAS PROGRAM

The current status of the program is illustrated on the accompanying map. About 100 map areas cover the continental and marine regions of Canada and adjacent nations. Thirteen map and chart sets have been published in the past 15 years (4 in the past 2 years). Three sets are under production at present. The Maguse River area (NP 15–16) central to Canada, west of Hudson Bay, contains the Ennadai–Rankin Greenstone Belt, an area of significant exploration activity during the past few years. The compilation brings together for the first time the results of new mapping and current regional interpretations. Preliminary compilations have been made available to companies active in the region.

The Halifax area (NL–20), has been compiled with the cooperation of geologists at three GSC offices, Acadia University and two provincial departments of mines. It is the first new compilation of Nova Scotia in 15 years and the very first compilation to integrate sea floor geologic data with on-land mapping. It incorporates a comprehensive set of up-to-date 1:50 000 scale digital maps compiled by Nova Scotia and New Brunswick geologists. The compilation is also being used to produce a 1:500 000 scale map of Nova Scotia.

The Lethbridge area (NM–12) covers a substantial part of the hydrocarbon-rich Interior Plains/Great Plains region of southern Alberta, southwestern Saskatchewan and northwestern Montana. The compilation utilizes new mapping and compilations of plains areas by staff of the Montana Bureau of Mines, new mapping and stratigraphic studies of part of the Cretaceous succession by GSC staff in Calgary and incorporates recently published maps of the Glacier/Waterton parks area by GSC, USGS and Montana Bureau of Mines staff.

GEOLOGY OF THE LETHBRIDGE MAP AREA

The Lethbridge map area extends between latitudes 48° and 52° north, from the Bearpaw and Little Rocky mountains uplifts in north–central Montana to the southern plains of Alberta, and from the Lewis Thrust sheet in Waterton and Glacier national parks, across the Sweetgrass Arch to the latest Tertiary strata of the Cypress Hills. A stratigraphic succession that spans the entire Phanerozoic lies unconformably on Archean and Paleoproterozoic (Aphebian) crystalline basement of the buried western Canadian Shield. The shield has been "mapped" by isotopic dating and petrographic studies of well cores integrated with interpretations of

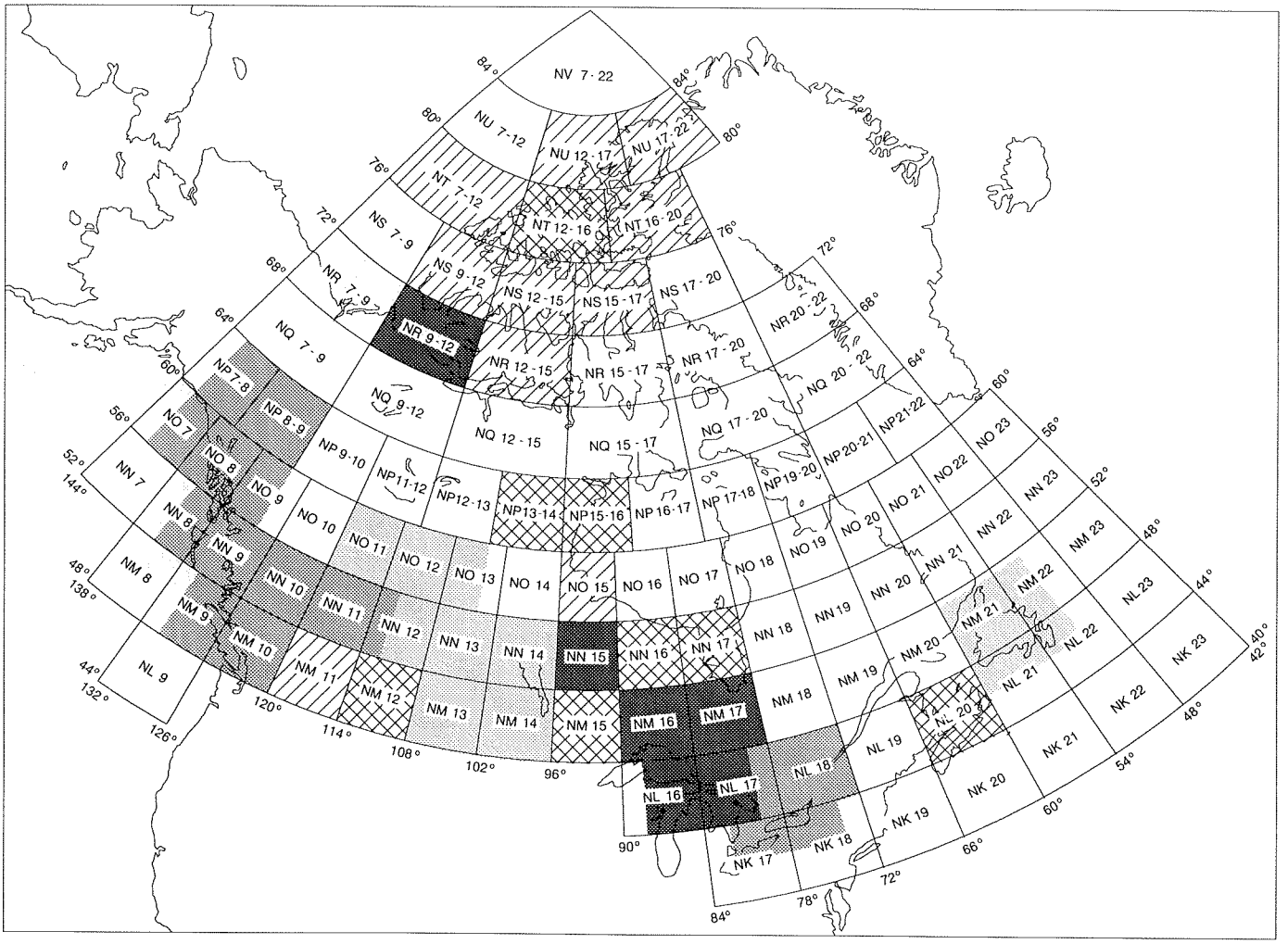

Publiée en / published 1994

THE NATIONAL ATLAS SERIES / SÉRIE NATIONALE DES SCIENCES DE LA TERRE

THE 1:1 000 000 SCALE GEOLOGICAL ATLAS / ATLAS GÉOLOGIQUE, ÉCHELLE: 1/1 000 000

GEOLOGY / GÉOLOGIE

GENERAL CO-ORDINATOR / COORDONNATEUR GÉNÉRAL: A.V.OKULITCH

DECEMBER 1994 DÉCEMBRE

Copies of this map may be obtained
from the Geological Survey of Canada:

On peut obtenir des exemplaires de cette carte
auprès de la Commision géologique du Canada:

601 Booth Street, Ottawa, Ontario K1A 0E8
3303-33rd Street N.W., Calgary, Alberta T2L 2A7
100 West Pender Street, Vancouver, B.C. V6B 1R8

Computer cartography by A.V. Okulitch,
Geological Survey of Canada

Cartographie automatique par A.V. Okulitch,
Commission géologique du Canada

Published; over 20 years old
Publié; il y a plus de 20 ans

Published; 10 - 20 years old
Publié; entres 10 - 20 ans

Published; under 10 years old
Publié; depuis 10 ans

Compiled; in cartography or editing
Compilé; en cartographie ou rédaction

Under compilation
En compilation

aeromagnetic and gravity data and extrapolations from exposed shield terranes to the northeast. This basement is exposed only in the core of the Little Rocky Mountains Uplift.

In the southwestern part of the map area, the Lewis Thrust and accompanying folds and thrusts of the Rocky Mountains Fold Belt, carry Mesoproterozoic (Helikian) strata of the Belt/Purcell Supergroup over Paleozoic and Mesozoic units of the Cordilleran miogeocline. Much of the supergroup was deposited initially in a failed rift environment which evolved into a large inland sea or lake between about 1500 and 1300 million years ago. Middle Cambrian sediments unconformably overlie the Belt Supergroup in the thrust belt east of and structurally below the Lewis Thrust, and are in turn unconformably overlain by Devonian and Carboniferous strata.

The Interior/Great Plains portion of the map area is also underlain by Paleozoic rocks which are predominantly carbonates with lesser clastic and evaporitic units. The thin cratonal succession was deposited in the inter-cratonic Williston Basin (whose northwesternmost portion lies in the southeast corner of the map area), across the Sweetgrass Arch (which extends north-northeastward through the south-central part of the map area) and the continental terrace wedge west of the Arch. The terrace wedge was influenced in its inception by an Early Cambrian landmass, Montania, in the southwestern part of the map area. The succession is interrupted by numerous disconformities, predominantly at or near system boundaries, which can be related to Ordovician, Devono-Carboniferous and Permian tectonism west of the map area and reactivation of cratonal elements such as Montania and the Sweetgrass and Peace River arches. Carboniferous strata are followed by a thin, unconformably overlying Jurassic clastic succession. This, and the underlying Paleozoic strata only occur in the subsurface in the Lethbridge map area.

Cretaceous clastic units form the predominant outcrops of the plains region and record a complex interaction among eustatic sea-level changes, mild intracratonic tectonism and pronounced compression, uplift, erosion, migration of the Continental drainage divide and crustal loading caused by the Late Jurassic to Paleogene evolution of the Columbian Orogen to the west. Final stages of orogenesis influenced deposition of Paleogene strata presently exposed in the Cypress Hills and just east of the Foothills fold belt, and deposited in extensional half-grabens in the southwest corner of the map area. Morphogenic uplift continued throughout much of the Tertiary, resulting in several kilometres of erosion of the Cretaceous and Tertiary succession and its redeposition as fans and terraces at successively lower elevations.

COMPARATIVE DIAGENESIS OF THE SWAN HILLS AND LEDUC CARBONATES, DEVONIAN "DEEP BASIN" AREA OF WEST-CENTRAL ALBERTA

H. Qing and J. Wendte

Geological Survey of Canada, 3303-33rd Street N.W., Calgary, Alberta T2L 2A7

INTRODUCTION AND SCOPE OF STUDY

This paper summarizes the results of part of an ongoing investigation of Devonian dolomites in the structurally "deep-basin" area of west-central Alberta (Fig. 1). Devonian strata in this area include shallow-water carbonates of the Swan Hills, Leduc, and Nisku formations and the overlying Upper Winterburn and Wabamun successions, and intervening deeper water shales and limestones (Fig. 2). The Leduc, Nisku, and Upper Winterburn carbonates are predominantly dolomite, whereas the Swan Hills and Wabamun carbonates contain varying proportions of limestone and dolomite. In the Devonian Deep Basin, these successions occur at a present burial depth between 2500 and 5000 m. This deep depth of burial reflects rapid subsidence as a result of tectonic loading during the formation of the Cretaceous foreland basin succession.

Hydrodynamic studies of Devonian strata in the Devonian Deep Basin indicate one widespread flow system linking the shallow-water carbonates of the Swan Hills, Leduc, Nisku, Upper Winterburn, and Wabamun successions. Fluids in this system are normally pressured and contain moderate to high H_2S contents. The occurrence of this flow system corresponds to areas with common to pervasive amounts of dolomites. Some isolated Leduc reefs in this area are isolated from this flow system. These reefs are geopressured, predominantly limestone, and lack any appreciable H_2S.

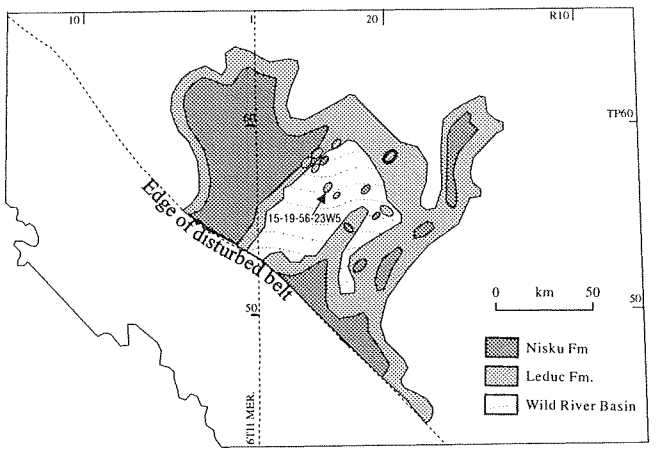

***Figure 1.** Schematic geological map for the Leduc and Nisku formations in the Devonian Deep Basin.*

This paper focuses on the dolomitization and associated diagenesis of the Swan Hills and Leduc carbonates near the centre of the Wild River Basin (Fig. 1). In this area, two abnormally high pressured (>0.90 PSI/Foot), isolated limestone reefs of the Leduc Formation occur at a depth in excess of 4000 m and overlie a normally pressured Swan Hills carbonate platform with varying proportions of limestone and dolomite (Figs. 1, 2). Thermally overmature, organic-rich source beds of the Duvernay Formation juxtapose these reefs (Fig. 2). In this study, Leduc reefal carbonates from the overpressured 15-19-56-23W5 well and the normally pressured Swan Hills carbonates from surrounding 10-17-57-23W5, 10-9-57-24W5, and 4-32-55-21W5 wells were examined by petrographic and isotopic techniques.

The Swan Hills and Leduc formations in this area were selected for study because phases of diagenesis could be timed with respect to the onset of overpressuring in the 15-19 Leduc reef complex. Petrographic relationships indicate the collapse of some stromatoporiods and corals following the formation of dolomite and calcite cements. Comparable limestones at shallower depths (2400–2800 m) northeast of the Devonian Deep Basin area are normally pressured and totally lack the collapse features that occur in the 15-19 Leduc reef complex. This relationship indicates that the collapse features in the Leduc reef formed at deep burial depths (>2800 m) as a result of rapid loading and subsidence during Cretaceous time. Because overpressuring counteracts lithostatic pressure and reduces the effective burial stress, the formation of

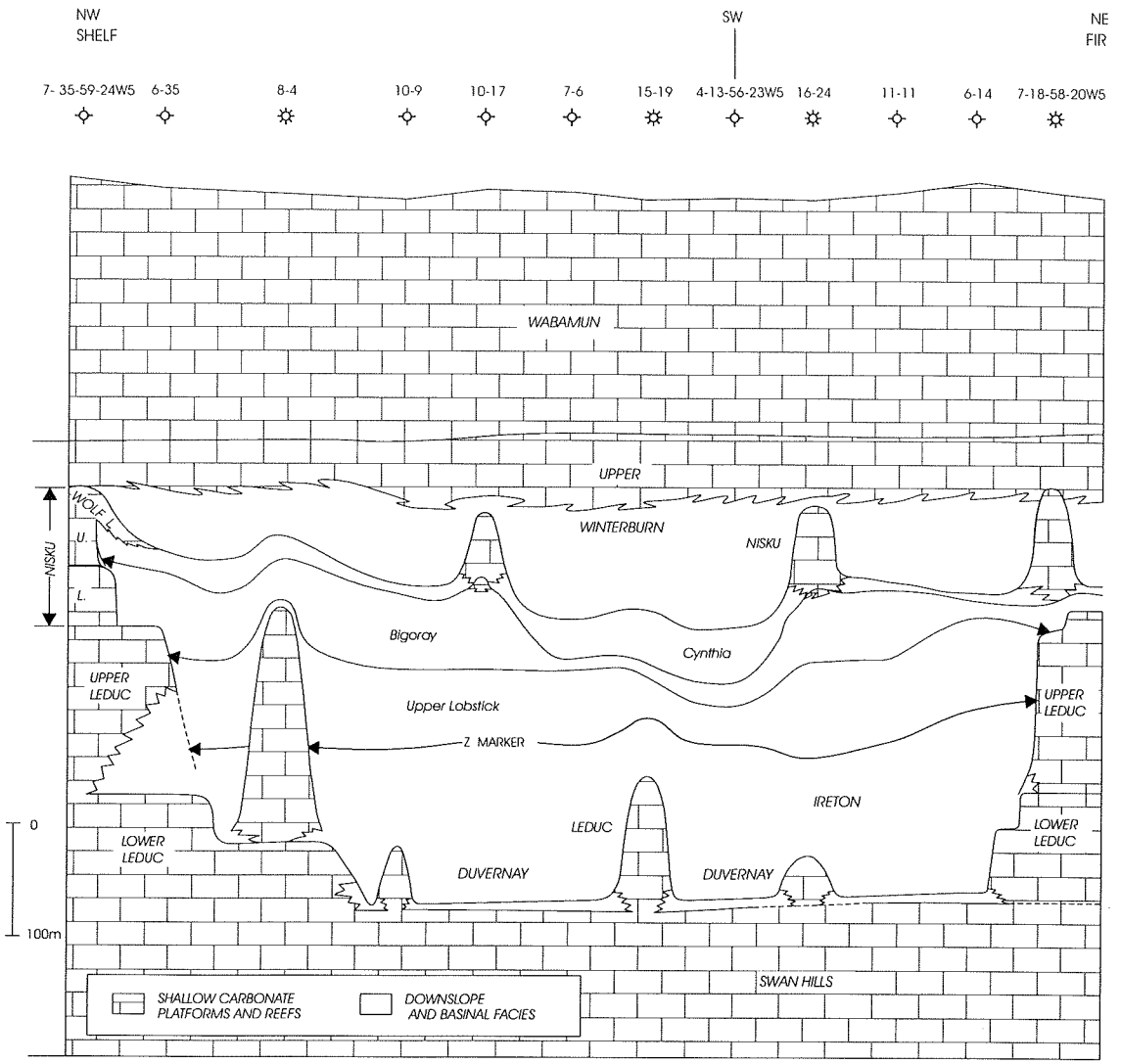

(Unpublished Section, J.C.Wendte, 1992)

Figure 2. *Stratigraphic cross-section across the Devonian Deep Basin.*

these collapse features must precede the onset of overpressuring. Therefore, the onset of overpressuring occurred as a result of rapid burial during Cretaceous time and corresponds to the infusion of gas generated from the immediately adjacent Duvernay source beds as well as the formation of bottom, lateral, and top seals.

DIAGENETIC PRODUCTS

Diagenetic products in the Swan Hills and Leduc formations are divided into those that precede and postdate overpressuring the 15-19 Leduc reef complex. Diagenetic products in the Swan Hills and Leduc formations that precede the onset of overpressuring include, in sequence of formation, fine-equant non-ferroan calcite cements, coarse-equant non-ferroan and zoned non-ferroan to ferroan calcite cements, replacive dolomites, saddle dolomite cements, and coarse-equant ferroan and possibly non-ferroan calcite cements. Only macrocrystalline, non-ferroan calcite cements in the Swan Hills Formation postdate the onset of overpressuring in the Leduc reef complex.

OXYGEN AND CARBON ISOTOPIC ANALYSIS

Figures 3, 4, and 5 show the $\delta^{18}O$ and $\delta^{13}C$ signatures of the coarse-equant non-ferroan and zoned calcite

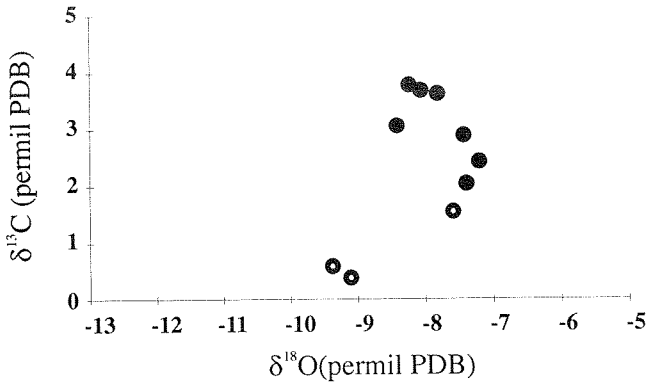

Figure 3. *Oxygen and carbon isotopic values for coarse-equant and ferroan zoned calcite cements in the Swan Hills Formation (open circles) and Leduc Formation (solid dots).*

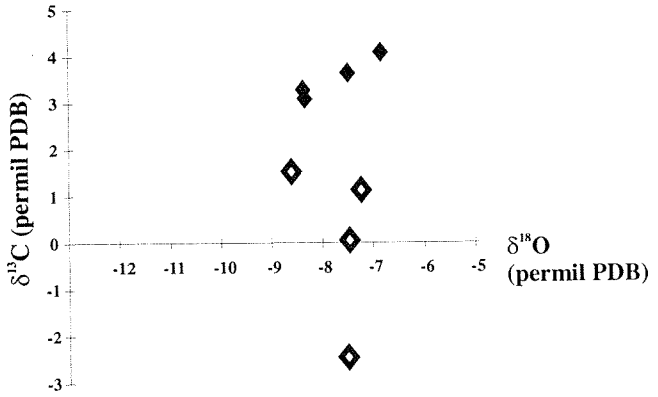

Figure 4. *Oxygen and carbon isotopic values for replacive dolomites in the Swan Hills Formation (open diamonds) and Leduc Formation (solid diamonds).*

cements, replacive dolomites, and saddle dolomite cements, respectively. Each of these components have similar ranges of $\delta^{18}O$ in both the Swan Hills and Leduc formations, suggesting comparable temperatures of formation. In addition, the $\delta^{18}O$ values of saddle dolomite cements are lower (1-2 permil) than replacement dolomite in both the Swan Hills and Leduc formations, suggesting higher temperature of formation for the saddle dolomite cements.

$\delta^{13}C$ values of each of these three components are systematically lower in the Swan Hills Formation than in the Leduc Formation [approximately 2 permil for

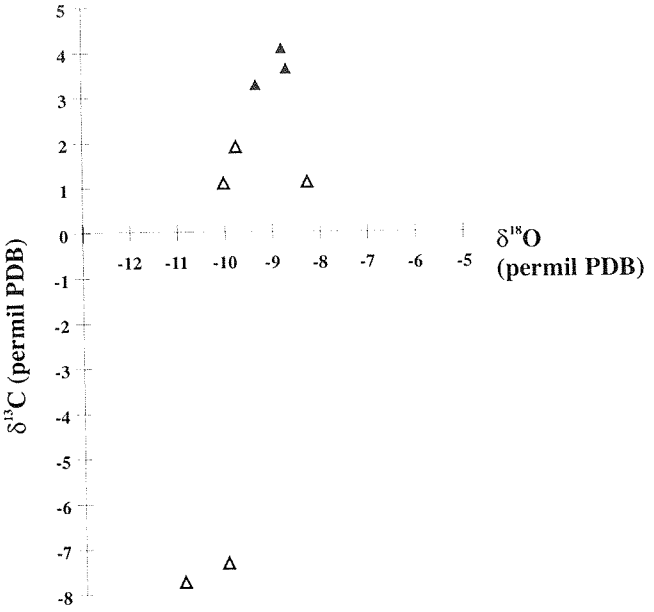

Figure 5. *Oxygen and carbon isotopic values for saddle dolomite cements in the Swan Hills Formation (open triangles) and Leduc Formation (solid triangles).*

coarse-equant calcite cements (Fig. 3), 2 to 6 permil for replacement dolomites (Fig. 4), and 2 to 10 permil for saddle dolomite cements (Fig. 5)]. These relationships suggest that fluids with organic carbon derived from thermal maturation may have played a more significant role in the formation of these components in the Swan Hills Formation than in the Leduc Formation.

Macrocrystalline calcite cements occur only in the Swan Hills Formation and are interpreted to postdate the onset of overpressuring in the 15-19 Leduc reef complex. The $\delta^{13}C$ values of these cements vary from -10 to -24 permil, indicating a very significant input of organic carbon derived from thermal maturation (Fig. 6).

SUMMARY

Petrographic relationships indicate that coarse equant calcite cements, replacive dolomites, and saddle dolomite cements in both of the Swan Hills and Leduc formations formed prior to the onset of overpressuring in the 15-19 Leduc reef complex. These diagenetic products formed from fluids that were part of a regional flow system. However, the systematic shift toward lighter carbon isotopes in each of these components in

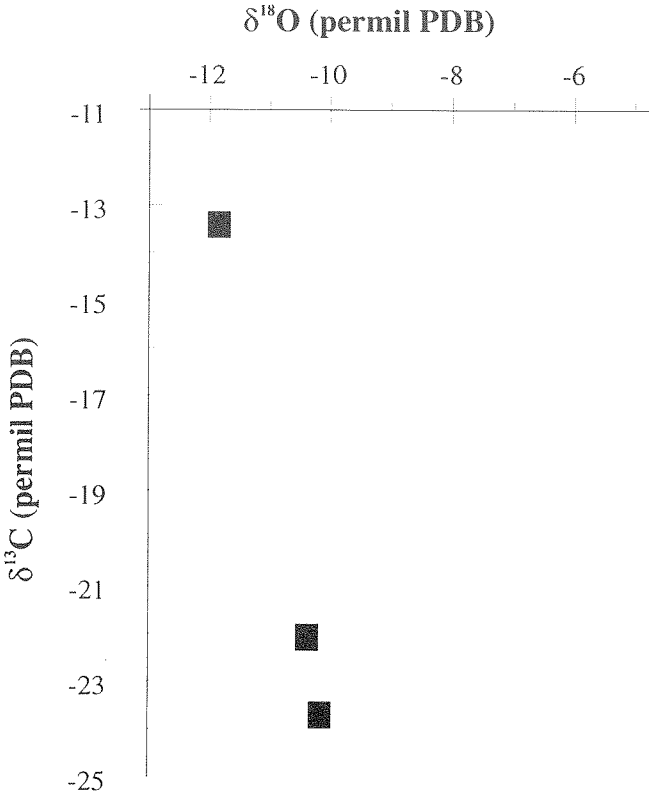

Figure 6. *Oxygen and carbon isotopic values for late-stage macrocrystalline calcite cements in the Swan Hills Formation.*

the Swan Hills Formation than in the Leduc Formation may suggest a tenuous or limited connection between the regional Swan Hills platform and the overlying Leduc reef complex. Gas generation and the subsequent onset of overpressuring halted diagenesis in the reef complex. During the same period, fluids continued to flow through the regional Swan Hills platform, resulting in the formation of macrocrystalline calcite cements. The remarkably light $\delta^{13}C$ values of these cements suggest significant input of organic carbon, probably derived from thermal sulphate reduction (TSR). TSR also explains the considerably higher H_2S content in the Swan Hills Formation than in the isolated, overpressured limestone reefs of the Leduc Formation.

ACKNOWLEDGMENTS

We are indebted to Dr. Art Saller at the Unocal Research Lab of Brea California for oxygen and carbon isotopic analyses. We also thank Canadian Hunter Exploration in Calgary for the loan of thin sections from the Leduc Formation in the 15-19-56-23W5 well.

CONTINENTAL DRAINAGE AND PROVENANCE EVOLUTION OF THE CORDILLERAN MIOGEOCLINE: CONSTRAINTS FROM NEODYMIUM ISOTOPIC STUDIES

G.M. Ross

Geological Survey of Canada, 3303-33rd Street N.W., Calgary, Alberta T2L 2A7

N.D. Boghossian, P.J. Patchett, and G.E. Gehrels

Department of Geosciences, University of Arizona, Tucson, AZ 85721

We report on the neodymium (Nd) isotopic composition of clastic sedimentary rocks in the Cordilleran miogeocline that range in age from ~650 Ma (Windermere Supergroup) to 80 Ma (Belly River Group). Isotopes of samarium (Sm) and neodymium (Nd) are a parent-daughter system that is relatively unfractionated by most crustal processes. The Nd isotopic composition of the crust and mantle of western Canada, and North America in general, is relatively well known and this allows the application of isotopic measurements Sm and Nd in sedimentary rocks as a means of tracking the evolution of provenance signatures. The measured isotope ratios are a mixture of different components and thus are not a unique fingerprint but provide an excellent perspective on the broad-scale patterns of sedimentation and source area evolution. The goals of this study were: 1) to develop a North American miogeoclinal reference for Nd isotopes and to provide a baseline for continental input to the terranes of the Canadian Cordillera, 2) to constrain the importance of proximal and distal North American basement sources for these sediments, and 3) to constrain the timing of juvenile terrane accretion at the Cordilleran margin.

All samples were collected from the Bow Corridor (Icefield Parkway, Trans-Canada Highway and Kananaskis Country) from well characterized stratigraphic units. Each sample was analyzed for bulk mineralogy and chemistry and leaching experiments were conducted to examine the effects of diagenesis and high concentrations of carbonate within shales on isotopic values. In as many cases as possible, sample pairs of sandstone and shale were collected from each unit in order to assess the potential fractionation due to grain sorting or lithology-dependent diagenesis. Nd isotopic data are reported in standard ϵ notation with calculated values given for the time of sedimentation. A total of 34 samples were analyzed which, given the stratigraphic thickness and complexity of the Cordilleran sediment wedge, should be considered a reconaissance level study. Nonetheless consistent and, in some cases, surprising isotopic signatures were obtained.

ϵNd values calculated for the time of sedimentation for Neoproterozoic (Windermere Supergroup) to Upper Ordovician (Mount Wilson Quartzite) rocks of the wedge range from -20.7 to -14.3 and are easily explained by derivation of sediment from proximal sources within the crystalline basement of Alberta. A positive shift of 6 ϵNd units occurs in the Upper Devonian Sassenach Formation (-9.5) and persists until foreland basin sedimentation in the Upper Jurassic. The Devonian to Triassic (Whitehorse Formation) ϵNd values vary only slightly from -9.5 to -6.7. A single subsurface sample from the Duvernay Formation in western Alberta has the same isotopic composition as the Devonian of the miogeocline. Foreland basin sediments of Upper Jurassic (Fernie Formation) to Cretaceous age (Belly River; Chungo Member) show marked heterogeneity but appear to diverge in terms of ϵNd values. Some samples tend toward more evolved signatures (negative ϵ values) whereas others appear to tend toward more primitive (positive ϵ) signatures. This is interpreted to reflect the relative proportions of detritus derived from erosion of pre-Devonian strata in the thrust belt, characterized by negative Nd signatures, and volcanic detritus, likely derived from the southern Coast Belt of southwestern Canada or possibly terranes west of the Omineca Belt, characterized by relatively juvenile (positive) Nd signatures.

The change from relatively evolved signatures in the Neoproterozoic to Upper Ordovician to more primitive signatures in the Devonian through Middle Jurassic cannot be explained by diagenetic alteration and likely reflects a fundamental change in source area, beginning in the Devonian. Any hypothesis to explain this pattern must address not only the isotopic composition but

homogeneity of values over a significant interval of sedimentation. The composition and persistence of isotopic change from the Devonian to Triassic is puzzling and can be approached in three different ways.

The first hypothesis suggests that the juvenile signature is the result of sediment input from fringing island arcs and back-arc basins such as Quesnellia and Slide Mountain Terrane, respectively, to the west of the miogeocline. These tectonic elements were intitiated following Devono–Mississippian Antler orogenic activity which also marks the initiation of basin reorganization in western Canada and deposition of sediment derived from western sources (e.g., Black Clastic unit of Prophet Trough and Selwyn Basin). The change in the isotopic patterns in the sediments overlaps with the Antler event and therefore derivation of sediment from juvenile sources to the west would have contaminated the Shield signature characteristic of pre-Devonian samples. This component could, in part, be volcanic material introduced by airborne ash or pelagic processes or erosion of primitive arc material. However this explanation is untenable for several reasons. First volcanism of Devono–Mississippian age, although widespread in the southern Cordillera, including the Exshaw bentonites, is isotopically too evolved to have caused the observed shift. Possibly, volcanic material was derived from primitive, mantle-derived arc magmas of Quesnellia which were active from late Devonian through early Jurassic and coincide with the timing of the observed Nd shift. However, typical arc magmas, such as basaltic andesite, have much lower Nd concentrations than does continental crust (10 ppm vs. 35 ppm, respectively) and mass balance calculations suggest that more than 50% of the material in the samples we analyzed would have to be volcanic in origin. This is difficult to reconcile with quartzose composition of many of the units (Sassenach, Rocky Mountain Group etc.).

A second model suggests that the Devonian is being fed by sediment derived from the Appalachian orogen of eastern North America. The Nd isotopic composition of Devonian through Triassic sediments of western Canada are virtually identical with the composition of sediments of Silurian through Pennsylvanian age in the Ouachita trough and intracratonic basins (Illinois and Forest City basins). In the Appalachian foreland, this reflects the prevalence of Grenville age basement in the orogenic source area. A major problem with this scenario for western Canada is the persistence of the TransContinental Arch in the central plains, a major topographic arch that would have impeded sediment transport and divided continental drainage.

A third model holds that sediment of this interval was derived from Ellesmerian sources in the Canadian Arctic. Although little is known of the Nd isotopic composition of Ellesmerian foreland sediments of the Canadian Arctic, it is known to comprise one of the largest orogenic sediment wedges in the world. It is possible that distal facies of the Ellesmerian foreland, formed during Caledonide convergence, could have covered the Canadian Shield and supplied sediment to the Cordilleran miogeocline. If true, this is supported by the work of Oliver and Cowper (1963) for example, who suggested that the terrigenous component in the Ireton was derived from the northeast, based on the geometry of clinoforms in the shales. This model can be tested by analysis of Devonian sediments of the Ellesmerian foredeep. If correct it would suggest that substantial sediment transport persisted as an Arctic source supplied terrigenous detritus to what must have been a largely covered Canadian Shield throughout the late Paleozoic and early Mesozoic.

In conclusion Nd isotopes provide a unique perspective on provenance evolution and a novel means of evaluating avenues of sediment dispersal at the continental scale.

REFERENCES

Oliver, T.A. and Cowper, N.W.
1963: Depositional environments of the Ireton Formation, central Alberta. *In* Bulletin of Canadian Petroleum Geology, v. 11 , p. 183–202.

LITHOPROBE CRUSTAL SEISMIC PROFILES IN CENTRAL ALBERTA: NEW REFLECTIONS ON THE EVOLUTION OF THE ALBERTA BASIN

G.M. Ross

Geological Survey of Canada, 3303-33rd Street N.W., Calgary, Alberta T2L 2A7

D.W. Eaton and B. Milkereit

Geological Survey of Canada, 1 Observatory Crescent, Ottawa, Ontario K1A 0Y3

E.R. Kanasewich

Department of Physics, University of Alberta, Edmonton, Alberta T6G 2J1

The crystalline basement beneath the Western Canada Sedimentary Basin is composed of crustal domains delineated on the basis of aeromagnetic signatures and U-Pb zircon geochronology of drill core recovered by the petroleum industry. Using analogies from the Canadian Shield, the mosaic of crustal domains is inferred to have formed during continental collision and accretionary events during the interval of 1.78–2.0 Ga. A long-standing uncertainty in basin evolution and formulation of exploration strategies by the petroleum industry has been the degree of control of sedimentary and diagenetic patterns by antecedent basement structures. In order to examine this problem and elucidate the Precambrian tectonic evolution of western Canada, LITHOPROBE acquired more than 500 km of crustal scale (18 sec.) seismic reflection data along a transect through central Alberta. The profile extends from the Archean Hearne Province (Alberta–Saskatchewan border) northwestward into the Rae Province (west of Edmonton) and crosses a number of Phanerozoic features including hydrocarbon production trends such as the Pembina field, Rimbey–Meadowbrook trend and Bashaw reef trend. It also crosses the Snowbird Tectonic Zone, a remarkable geophysical discontinuity that can be traced from beneath the Cordilleran Foothills across the Canadian Shield to Hudson Bay.

Prominent reflections have been observed throughout the entire thickness of the crust (35–45 km) beneath the sedimentary section and sole into reflective lower crust, the base of which is characterized by a dramatic loss in reflectivity (12–14 sec.) which is interpreted as reflection Moho. Many of the reflections are geometrically suggestive of compressional deformation and delineate a broad region of crustal-scale thrust imbrication. The eastern 300 km shows evidence for a west-northwest-verging thrust belt that shows a corresponding increase in depth to Moho and metamorphic grade into the inferred hinterland region. A prominent positive step in the gravity field in the western part of the transect is associated with an inferred reversal in vergence and possibly a crust-penetrating offset of Moho formed during late stages of collision along the Snowbird Tectonic Zone. Available geochronologic constraints suggest contemporaneity of crustal imbrication observed in the Alberta basement with that documented in the Trans-Hudson Orogen to the east (1.78–1.81 Ga). This implies that a region of continental crust was undergoing shortening across strike for more than 1000 km during assembly of this part of the Canadian Shield.

Consistent acquisition and processing parameters, coupled with the unusual length and continuity of this transect, provide a unique regional seismic perspective from which to address the question of basement control on basin evolution. In general, basement control over sedimentary patterns is subtle but three distinct styles of basement influence have been observed: 1) sedimentary drape over paleogeographic highs on the basal unconformity; 2) intersections of strong dipping reflections (faults?) with the base of the sedimentary section; and 3) seismic sedimentary facies transitions that are spatially associated with basement domain boundaries. In general the long-wavelength relief of the basement surface is the result of Laramide flexure but is punctuated by local paleotopographic features that range in scale from tens of metres to 50 km. A long wavelength basement high near Stettler, Alberta, underlies the Leduc southern Alberta shelf edge and was an area of positive relief from Upper Cambrian to as late as Devonian. Evidence for the second class of

interaction is provided by a series of strong, east-dipping reflections in the uppermost basement beneath central Alberta that are continuous with regional compressional reflection fabric in the basement and thus may represent faults in the basement. Relationships with the sedimentary cover suggest, within the limits of seismic resolution, that these structures affected Middle Cambrian or older strata.

An example of the third class of basement influence is particularly evident beneath the Rimbey–Meadowbrook reef trend which overlies a major basement suture zone marked by a belt of granitic rocks (Rimbey granites) in the basement. In map view there is an imperfect alignment of the magnetic fabric of the basement and the reef trend, suggesting that, if basement structures controlled the reef orientation, such control must have been indirect in nature. However, juxtaposition of seismic images from opposite sides of the reef trend, accomplished by removal of that segment of the seismic section disturbed by the velocity pull-up associated with the reef trend, reveals a series of abrupt facies changes within Middle Cambrian to Middle Devonian strata that directly overlie the basement structure. In addition, the top-of-basement reflection is less coherent in this area and is preceded by a high-amplitude localized basement precursor event in the sediments. Deep-seated controls over the orientation of the reef foundation, and possibly over diagenetic fluid circulation patterns, could explain the coincidence of these elements in the seismic profile.

Future seismic reflection programs under the aegis of Lithoprobe include a regional profile across the Peace River Arch (recorded in the summer of 1994) and southern Alberta , including the enigmatic Vulcan Low (a.k.a. the southern Alberta graben), slated for acquisition in 1995. When complete, the Lithoprobe program will provide a coherent seismic reflection transect from northeastern British Columbia south to the U.S. border, and provide an unparalleled opportunity to examine the regional geometric relationships within a cratonic sedimentary basin.

CYCLIC AND DEPOSITIONAL CONTROLS ON ORGANIC FACIES AND ORGANIC CARBON CONTENTS, UPPER DEVONIAN DUVERNAY FORMATION, REDWATER ALBERTA

L.D. Stasiuk and J.C. Wendte

Geological Survey of Canada, 3303-33rd Street N.W., Calgary, Alberta T2L 2A7

INTRODUCTION

The Duvernay Formation encompasses a widespread succession of basinal limestones and shales of Frasnian age in Alberta. In the East Shale Basin, the upper organic rich unit of the Duvernay Formation grades upslope and intertongues with shallow water carbonates of isolated Leduc reefs and more areally extensive platform carbonates of the Grosmont Complex (Stoakes, 1980, 1992; Switzer et al., 1994). These relationships indicate coeval deposition of an upper organic rich interval of the Duvernay Formation and an intermediate portion of the Leduc reefs (Stoakes, 1992; Switzer et al., 1994). The potential hydrocarbon source rocks of the Duvernay Formation (Creaney et al., 1994) are finely laminated deposits with variable clay and quartz content and with total organic carbon contents (TOC) of commonly 4 to 5 per cent when thermally mature (Stoakes and Creaney, 1985). Stoakes (1980) postulated deposition of these deposits in anoxic waters generally in excess of 100 m in a vertically stratified basin. Upslope these laminites grade into organic lean dysoxic bioturbated calcareous shales and, further shelfward, into oxic argillaceous lime wackestones. Stoakes (1980) and Stoakes and Creaney (1985) attributed the high TOCs to the anoxic bottom conditions and to low rates of sedimentation. In this paper, organic facies and TOCs are related to depositional cycles and lithofacies of Duvernay deposits along the northeast margin of the Redwater reef complex.

RESULTS AND DISCUSSION

Organic Facies (OF)

Incident light microscopic (white and ultraviolet light) analysis of primary macerals (alginites, acritarchs, dinoflagellates and terrestrial sporinites) has been used to define organic facies for 85 samples from the 10-27-57-21W4 and the 12-28-57-21W4 well. The morphology, relative state of preservation and phyletic affiliation of these macerals can provide a snapshot of the water column phytoplanktonic population and organic matter degradation processes. The distribution of specific alginite and acritarchs in marine settings are controlled by nutrient supply and water agitation, which in turn is related to the position above the sea floor. Thus a change in a phytoplanktonic assemblage can potentially be used for interpreting the degree of agitation of the upper water column and the profile at the sea floor. Figure 1, based largely on the work of Dorning (1987) but modified for the Duvernay, provides a model that explains the distribution of phytoplanktonic assemblages from bank to basin during a phase of normal productivity. The model used for this study is divided into 3 main regions or organic facies based on maceral assemblages (Fig. 1). The main maceral components of each organic facies in the Duvernay are as follows:

(i) Organic Facies A represents the most basinal maceral assemblage and is dominated by small, thin-walled Prasinophyte-like alginite (mainly <10 μm). Larger (up to 180 μm), thick-walled Prasinophytes are relatively rare as are acanthomorphic acritarchs.

(ii) Organic Facies B represents an "intermediate" maceral assemblage containing Prasinophyte alginite similar to those in OF A, but in addition, OF B contains abundant acanthomorphic acritarchs; sporinites may or may not be present.

(ii) Organic Facies C accumulated in the most proximal position and contains a maceral assemblage similar to OF B with the addition of coccoidal alginite colonies and sporinites.

STRATIGRAPHIC SUCCCESSION AT REDWATER

Organic-rich Duvernay facies and foreslope Leduc facies intertongue in an embayment that extends into the northeastern periphery of the Redwater reef

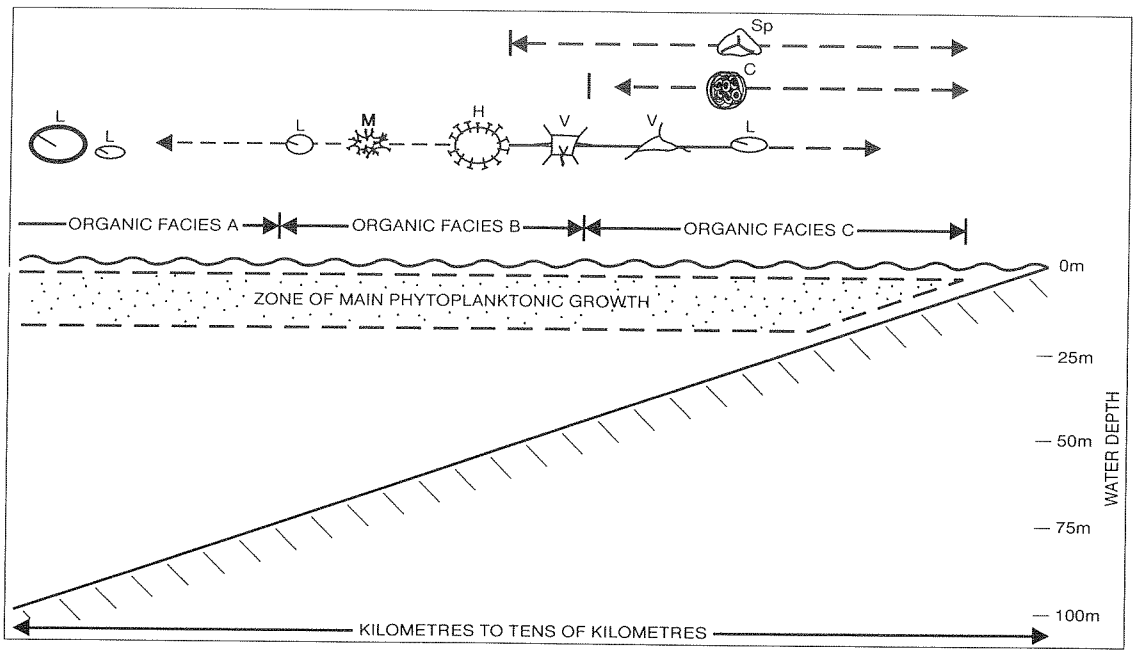

Figure 1. *Model of Duvernay organic facies at Redwater 10-27-57-21W4 based on recorded maceral abundance and position relative to the sea floor; based largely on the work of Dorning (1987).*

complex (Fig. 2). A number of shoaling–upward cycles were identified along the northeast periphery of the reef complex and correlated downslope into coeval Duvernay successions. The cycles are grouped into informal lower, middle and upper Leduc members (Fig. 2). The upper member postdates the organic-rich Duvernay successions and is not discussed in this summary.

Lower Leduc Member

This member represents a ramp-like reef to basin foreslope succession, with a poorly developed reef margin (Fig. 2). The lagoonal portion consists of a predominantly well-circulated subtidal succession. Tidal-flat accumulations are only commonly developed at or near the top of this unit (Fig. 2). The more basinal wells (16–28 and 10–27) are dominated by a peloidal carbonate sand foreslope succession. Estimated water depth at the top of this member at 10-27 is approximately 38 m. In the most basinal well (10-27; Fig. 2) laminites are confined to the lower half of the member and exhibit minor bioturbation. TOCs are relatively high (5.8–6.8%) and correspond to samples with OF A with mixtures of either OF C or OF B (Fig. 3).

Middle Leduc Member

This member encompasses an overall transgressive–regressive succession in a shallow-water reef setting (Fig. 2) and corresponds to the initial development of a well-zoned reef complex, with distinct foreslope, margin and peritidal backreef facies. The margin consists of a *Renalcis* stromatoporoid boundstone that built up to sea level, thereby restricting circulation and creating a more restrictive and less diverse lagoonal succession consisting of subtidal *Amphipora* rudstones and floatstones and tidal-flat cryptalgal laminites and fenestral limestones.

Five major cycles (ML1–ML5) are grouped into a lower transgressive, an intermediate aggradational and an upper regressive phase. The transgressive portion corresponds to the backstepped ML1 succession in the 1–22 and 5–36 wells (Fig. 2). In the 5–36 well this cycle consists of a progradational succession of facies grading from reef margin to debris up through peritidal deposits. Coeval downslope facies are peloidal foreslope carbonate sands and muds shed from the reef. The more basinal 16–28 and 10–27 wells consist of two subcycles (ML1A and ML1B) dominated by bioturbated unfossiliferous lime mudstones. The evolution from the underlying lower Leduc foreslope peloidal sands to lime muds in these wells reflects a

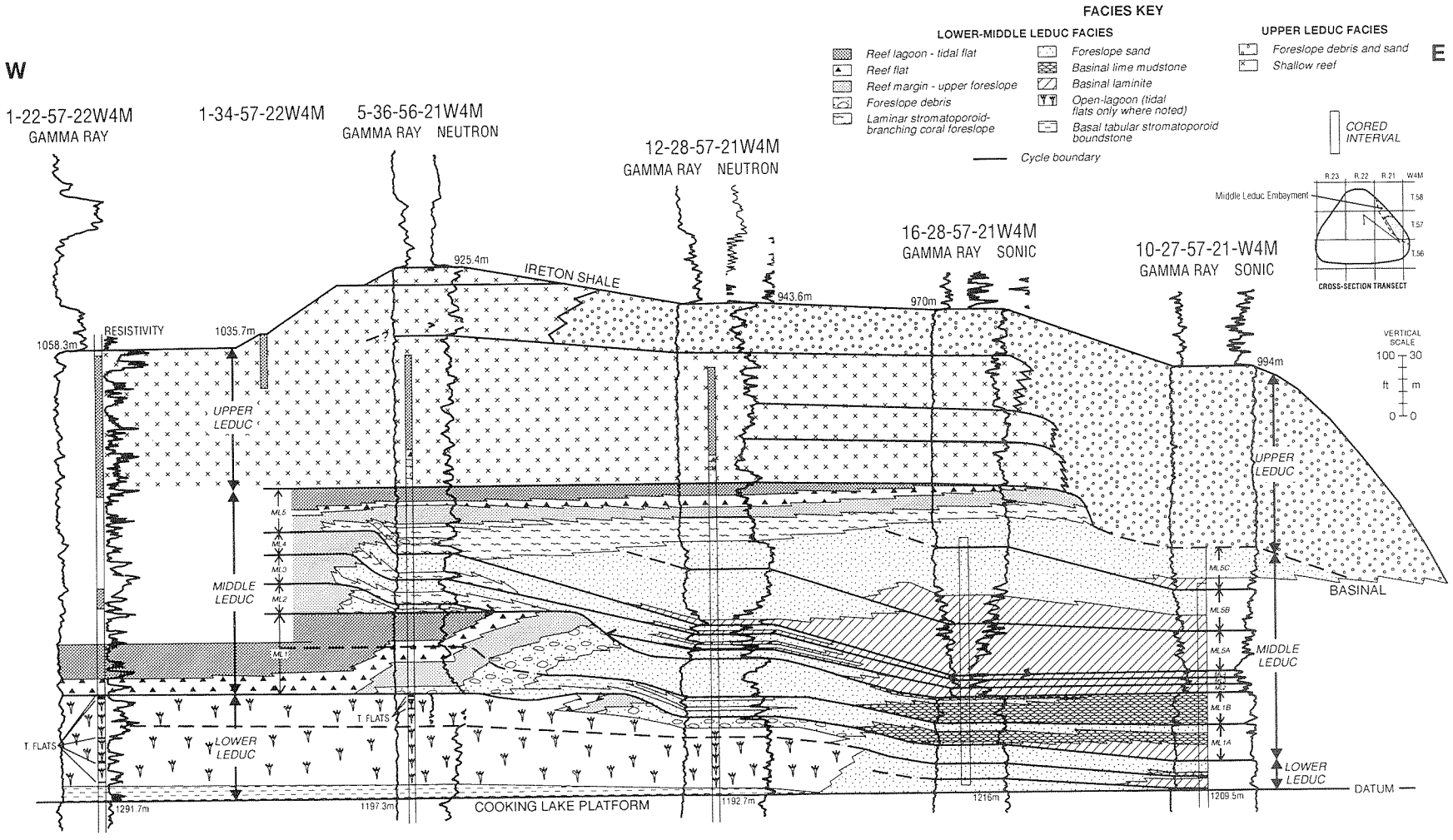

Figure 2. *Stratigraphic and depositional facies cross-section of Redwater reef complex, Alberta.*

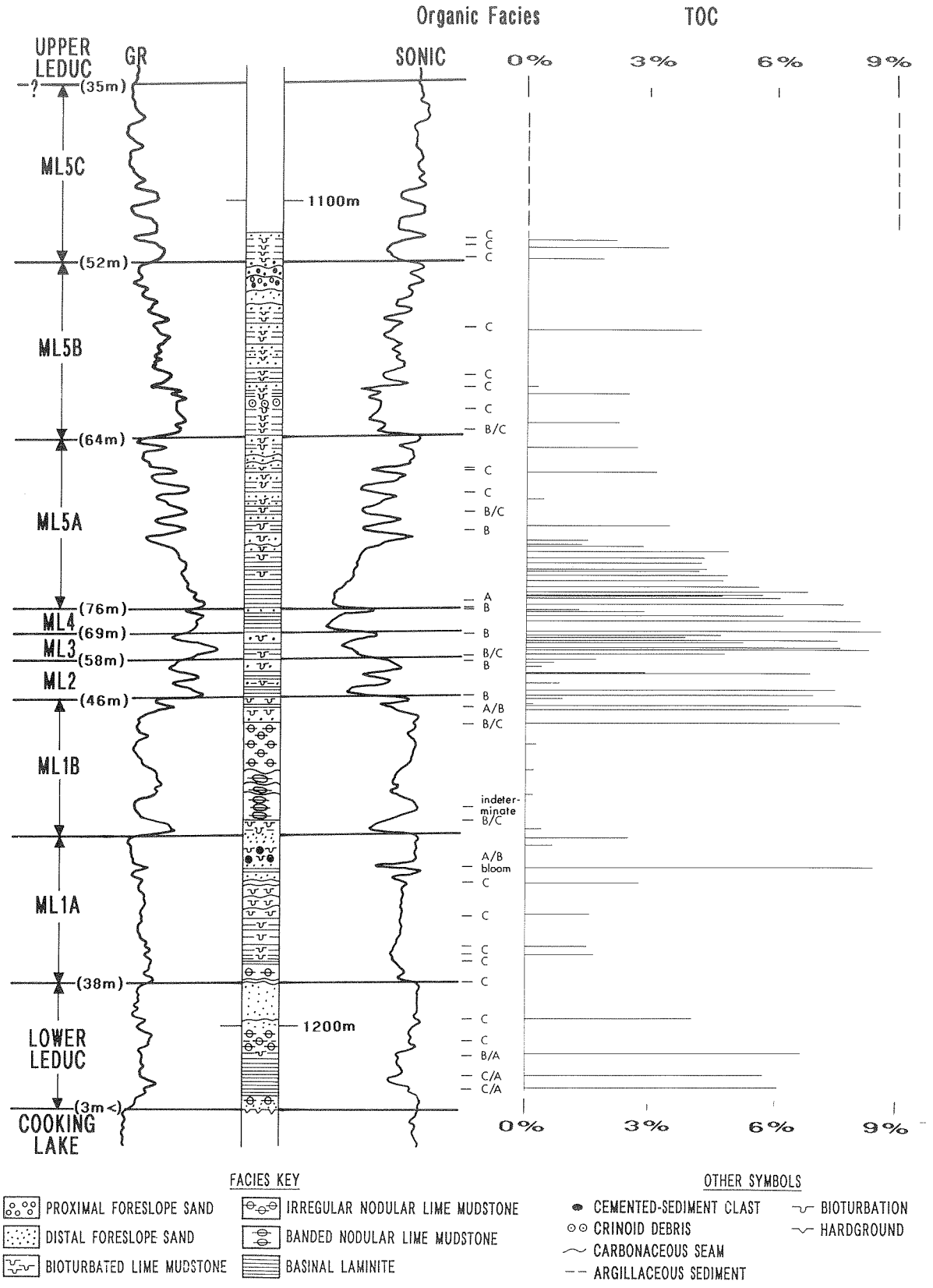

Figure 3. Detailed section of depositional facies, laminite occurrence, organic facies and total organic carbon contents for the Duvernay Formation at 10-27-57-21W4.

backstepping reefal succession (Fig. 2). Estimated water depth at the top of the ML1 unit at 10–27 is 46 m.

Laminites in the ML1A cycle form a relatively thick basal succession in the most basinal 10–27 well and thin upslope toward the 16–28 well (Fig. 2). These laminites are moderately to extensively bioturbated. TOCs are generally low (1.5–2.8%) and correspond to samples with OF C (Fig. 3). Thin intervals of laminites also occur in the overlying ML1A and ML1B successions. These laminites are characterized by only very minor bioturbation. TOCs are high (6–9%) and correspond to mainly OF B and OF A (Fig. 3).

The intermediate aggradational phase includes the ML2, ML3 and ML4 cycles (Fig. 2). In an upper foreslope setting (5–36), these cycles consist of either a foreslope reef debris (ML2) or an in situ deep-water reef succession (ML3 and ML4) grading up into shallower water foreslope peloidal lime grainstones. Coeval downslope accumulations are foreslope carbonate sands and organic-rich laminites. In the most basinal 16–28 and 10–27 wells, these cycles grade from laminites into bioturbated peloidal-skeletal sands (Fig. 2). The onset of "anoxic" water laminite formation resulted from increased water depths and further backstepping with less sediment dilution. Estimated water depths at the top of the ML2, ML3 and ML4 cycles in the 10–27 well show increasing values of 58 m, 69 m and 78 m, respectively.

The laminites in the ML2–ML4 successions of the more basinal 16–28 and 10–27 wells are very finely laminated with only very minor burrow traces and high TOCs (6–9%) and correspond to samples with OF B (Fig. 3). Upslope the laminites occur interbedded with foreslope carbonate sands in 12–28 (Fig. 2). These laminites have only slightly lower TOCs (4–6%) than coeval deposits in the 10–27 well and contain almost exclusively samples with OF B. Laminites are virtually absent in the ML2 cycle at 12–28 and initially occur just above the base of the ML3 cycle. Calculated water depth for the basal part of ML2, prior to anoxia, is 36 m and for the basal part of ML3, after the onset of anoxia, is 47 m. An estimation of 41.5 m for the onset of anoxia is similar to the 42 m water depth computed for laminites in the Lower Leduc interval. However, bioturbated lime mudstones at the very top of the ML1 cycle at 10–27 have an estimated water depth of 46 m, indicating dysoxic conditions at somewhat deeper depths. The onset of anoxia may therefore vary between cycles, but probably occurs between 40 to 50 m of water depth.

The regressive ML5 phase corresponds to an initial deepening followed by progradation of the reef margin (Fig. 2). Coeval downslope deposits are allochthonous foreslope sands and laminites. In the most basinal 16–28 and 10–27 wells, the ML5 can be subdivided into three distinct subcycles (Fig. 2). Estimated water depths for the top of each of these subcycles show decreasing values of 64 m, 52 m and 35 m, respectively, reflecting outgrowth of the reef. Very finely laminated laminites dominate in the lower one-half of ML5A in the more basinal 16–28 and 10–27 locations, and grade up into foreslope sands. The laminites in the basal portion of the ML5A cycle have only very minor horizontal burrow traces, TOCs up to 8% and a dominance of OF A. These deposits are the deepest water accumulations at Redwater, with estimated water depths at 10–27 of 88 m. Overlying laminites in the ML5B succession are moderately to extensively bioturbated and have common to abundant transported bioclasts. TOCs in these laminites range from 1.5 to 4.0%, and correspond mainly to samples with OF C (Fig. 3). Laminites in the basal part of the ML5B cycle consist of OF B and OF C, a departure from the dominance toward OF C in the underlying laminites of the ML5A cycle.

Cycle, Depositional Facies, Organic Facies and TOC Relationships

Two general trends are apparent in the relationship between cycles, depositional facies, organic facies, and TOCs at the 10–27 well. Firstly, laminites with only minor bioturbation correspond to samples with high TOCs (>5%) and OF B to A. TOCs decrease and organic facies shift to a dominance of C with increasing bioturbation. Moderately to extensively burrowed laminites have intermediate TOCs (1.5–4.0%) and correspond mainly to OF C. Completely bioturbated lime mudstones and nodular lime mudstones have low TOCs (<1.0%) and correspond to OF C. TOCs (<0.5–5.0%) and organic facies (OF C to OF B) in bioturbated distal foreslope peloidal sands are more variable. We interpret these relationships similar to that of Stoakes and Creaney (1985), who attributed almost identical relationships between lithofacies and TOCs elsewhere in the Duvernay Formation to variations in bottom water oxygen levels and the degree of bioturbation. Furthermore, the correlation between organic facies and the degree of bioturbation suggests a shared hydrodynamic control. A shallower zone of increased wave agitation corresponds to both OF C and a high level of bottom oxygenation. Conversely, a deeper zone of decreased wave agitation corresponds

to OF B or OF A and a relatively low level of bottom oxygenation.

Secondly, variations in TOC and organic facies closely approximate the cyclical shifts in facies belts. TOCs are generally higher in lower portions of cycles, and decrease upward. Similarly, OF C becomes dominant in the upper part of cycles except for ML2, ML3 and ML4 where OF B is exclusive. Furthermore, TOCs and organic facies vary between cycles. The highest TOCs occur in the laminites in the ML2, ML3, ML4 and the lowermost part of the ML5A cycle and correspond to the highest frequency of OF B (ML2, ML3, ML4) and OF A (lower ML5A). These occurrences correspond to the estimated deepest water conditions (56–88 m) and to the furthest backstepped positions of the reef margins. Overlying successions in the ML5 cycle show an overall decreasing trend in TOC and a shift to OF C dominance, corresponding to overall shallowing and to increasing amounts of foreslope peloidal sands. Deep water depths, sufficient for anoxia to develop, and slow rates of sediment dilution appear to be the two primary controls on TOC values and organic facies distribution.

The amount of sediment dilution, rather than the degree of bioturbation related to the oxygenation level, appears to explain the slightly lower TOCs in the lower Leduc cycle (5–7%) than in the ML2, ML3 and ML4 cycles (5–9%) in the 10–27 well. The evidence suggests that once anoxia is developed, all other controls being equal (including sediment dilution), TOCs should remain constant as water depths increase. A measure of sediment dilution can be approximated by the ratio of sediment thickness in the more basinal 10–27 well to the cycle thickness or accommodation space created on the shallower water reef. The ratio for the highly organic rich ML2–ML4 succession is 0.3, compared to 0.8 for the underlying ML1 cycle and to 3.0 for the highly regressive ML5 cycle. These variations in dilution indices correspond to the position and shifts of the reef margins. The lowest degree of dilution therefore corresponds to the more proximal position of the reef margin, and the highest degree to the more basinal position of the reef margin.

Water depths and degree of sediment dilution, however, do not explain all variations in TOC. At 10–27, bioturbated peloidal sands with TOCs typically $<2\%$ overlie laminites with TOCs commonly between 6 and 9% in the ML2, ML3 and ML4 cycles (Fig. 3). Both the laminites and bioturbated peloidal sands contain maceral elements of OF B. These bioturbated peloidal sands were deposited in water depths estimated to be between 58 and 78 m, far deeper than the 42 m depth calculated for the onset of anoxia. As well, an increase in sediment dilution rate alone does not explain the bioturbated aspect of these deposits. A correspondence does, however, exist in the nature of the ML2, ML3 and ML4 cycles between the more basinward 10–27 well and the more proximal 5–36 well (Fig. 2). The cycles in the 5–36 well suggest an initial aggradational reef phase, with comparatively little sediment shed downslope, and an upper progradational reef phase with basinward shedding of peloidal foreslope sands. The deeper water aggradational portion of the cycles in the 5–36 well are interpreted to correspond to deposition of the laminites at the base of each cycle in the 10–27 well and mark times of very slow sediment dilution. The accumulation of the peloidal foreslope sands in the upper parts of the cycles in the 5–36 well are interpreted to be coeval with the bioturbated zones at the top of the cycles in the 10–27 well. It is postulated that storm generated waves acting on the peloidal foreslope sand apron intermittently triggered either sediment-gravity flows or tractional bottom flows. These flows travel down the reef foreslope, temporarily disrupting the stratified water column and introducing oxygenated conditions to the sea floor at deep depths adjacent to the reef. The resulting oxygenated conditions fostered times of prolific bioturbation, thereby reducing the TOC. The occurrence of OF B in both the laminites and peloidal sands supports the interpretation for intermittent, short-lived sediment gravity flows that temporarily disrupted the anoxia of the water column. Longer periods of disruption should promote a change in phytoplanktonic population toward OF C.

REFERENCES

Creaney, S., Allan, J., Cole, K.S., Fowler, M.G., Brooks, P.W., Osadetz, K.G., Macqueen, R.W., Snowdon, L.R., and Riediger, C.L.
1994: Petroleum generation and migration in the Western Canada Sedimentary Basin. *In* Geological Atlas of the Western Canada Sedimentray Basin, G. Mossop and I. Shetsen (compilers). Canadian Society of Petroleum Geologists and the Alberta Research Council, p. 455–468.

Dorning, K.J.
1987: The organic paleontology of carbonate environments. *In* Micropaleontology of carbonate environments, M.B. Hart (ed.). The British Micropaleotological Series, p. 256–265.

Stoakes, F.A.
1980: Nature and control of shale basin fill and its effect on reef growth and termination: Upper Devonian Duvernay and Ireton formations of Alberta, Canada. Bulletin of Canadian Petroleum Geology, v. 28, p. 234–410.

1992: Woodbend megasequence. *In* Devonian-Early Mississippian Carbonates of the Western Canada

Sedimentary Basin: A Sequence-Stratigraphic Framework, J.C. Wendte, F.A. Stoakes and C.V. Campbell (authors). Society for Sedimentary Geology, Short Course No. 18, p. 183–206.

Stoakes, F.A. and Creaney, S.
1985: Controls on the accumulation and subsequent maturation and migration history of a carbonate source rock. Society of Economic Paleontologists and Mineralogists, Core Workshop Proceedings, Golden, Colorado, U.S.A., August, 1985, p. 343–376.

Switzer, S.B., Holland, W.G., Christie, D.S., Graf, G.C., Hedinger, A.S., McAuley, R.J., Wierzbicki, R.A., and Packard, J.J.
1994: Devonian Woodbend-Winterburn Strata of the Western Canada Sedimentary Basin. *In* Geological Atlas of the Western Canada Sedimentary Basin, G. Mossop and I. Shetsen (compilers). Canadian Society of Petroleum Geologists and the Alberta Research Council, p. 165–202.

Tyson, R.V.
1991: Palynofacies analysis. *In* Applied micropaleontology, D.G. Jenkins (ed.). Kluwer Academic, Netherlands, p. 153–191.

SOUTHERN ALBERTA NATMAP MAPPING IN MAYCROFT (82G/16) (WHALEBACK RIDGE AREA): PROGRESS TO DATE

G.S. Stockmal

Geological Survey of Canada, 3303-33rd Street N.W., Calgary, Alberta T2L 2A7

INTRODUCTION AND PREVIOUS WORK

New structural mapping in the Maycroft (82G/16) map area was initiated in 1993 as a component of the GSC's Southern Alberta NATMAP project (see location, Fig. 1). The principal products stemming from this five-year project will be twelve new 1:50 000 scale bedrock map sheets (eleven full-sheets and one half-sheet, Fig. 1) and attendant cross-sections, in traditional as well as digital format including databases. The Maycroft map sheet straddles the structural front of the Cordilleran orogen, encompassing most of the west flank of the Alberta syncline, the triangle zone, and east-vergent foothills structures.

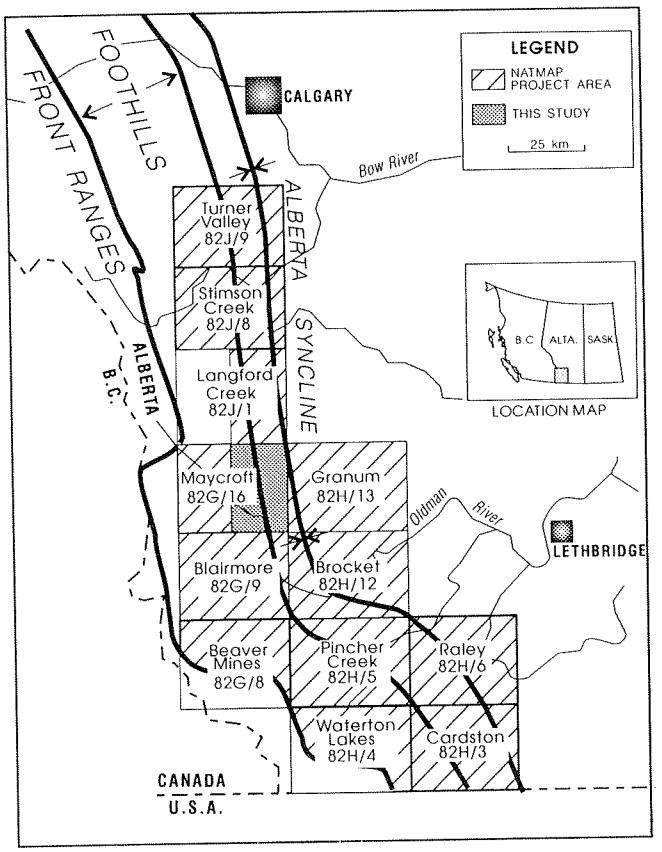

Figure 1. *Location map, southern Alberta, showing locations of 1:50 000 scale map sheets encompassed by the Southern Alberta NATMAP project, and the location of this study.*

Initial results from the Maycroft area indicated substantial differences in interpretation in comparison with those of earlier workers [compare Stockmal and MacKay (1994) and Lawton et al. (1994) with Price (1981) and Douglas (1950)]. Notable among these differences are: (1) the identification of the upper detachment of the triangle zone at a deeper stratigraphic level (within the Bearpaw Formation) and therefore in a more westerly geographic position; (2) documentation of substantial deformation in the hanging wall of the triangle zone upper detachment (the Oldman River triangle zone is **not** a "passive roof duplex"); and (3) the recognition of at least two "nested" triangle zones or tectonic wedges. New structural and stratigraphic observations coupled with the availability of seismic data, through cooperation with industry and academia, were crucial to these new interpretations (MacKay et al., 1994, p. 25; Stockmal and MacKay, 1994; Lawton et al., 1994). Mapping undertaken during the 1994 field season indicated that some structural and stratigraphic revisions of the initial results were required, although these affect the surface and subsurface interpretations in detail only.

A new stratigraphic subdivision of the upper Alberta Group and the former Belly River Formation has been proposed by Jerzykiewicz and Norris (1994; Fig. 2). In their six-fold subdivision, the upper Alberta Group, above the Wapiabi Formation, comprises the Lees Lake, Burmis, and Pakowki formations, whereas the Belly River Group (*sensu stricto*) comprises the Connelly Creek, Lundbreck, and Drywood Creek formations. The utility of this subdivision, developed in the Crowsnest Pass area immediately to the south, was demonstrated in the Maycroft area by an increase in map-scale structural detail based upon observations along the Oldman River (e.g., Stockmal and MacKay, 1994, fig. 3). However, application of the proposed subdivisions of the Belly River Group to 1:50 000 scale mapping has proven to be difficult because exposure of

the shale-dominated facies, crucial to correct stratigraphic identification of the bulk of the group, is rarely adequate in areas away from river exposures.

NEW OBSERVATIONS AND INTERPRETATIONS

Observations of the Belly River Group, made along a number of measured sections along the Oldman River (Stockmal, GSC Current Research, in prep.), suggest that differentiation of the group as suggested by Jerzykiewicz and Norris (1994) may not be applicable within the Maycroft map area. This is due to the presence of more varied facies associations than those described in the type-areas, in strata probably equivalent to both the Connelly Creek and Lundbreck formations. A clear change in grain size, sedimentology, and colour of the sandstone facies occurs approximately 100 m above the base of the Belly River Group. Sandstone units dominated by fine grained, dark grey, medium bedded and current-rippled strata are superseded by sandstone dominated by medium to coarse grained, light to very light grey, thickly to very thickly bedded and trough crossbedded strata. Caliche hardpans and nodules in association with the shale-dominated facies, considered diagnostic of the Lundbreck Formation when abundant (Jerzykiewicz and Norris, 1994), occur throughout much of the Belly River Group exposed along the Oldman River. Although they occur in the lowermost 100 m, they do not become prominent until more than 200 m above the base of the group, stratigraphically well above the transition in the sandstone facies. Furthermore, facies considered diagnostic of the Connelly Creek Formation, including dark grey to coaly shale and abundant redeposited fresh-water bivalves and "dwelling-and-escape structures" (Jerzykiewicz and Norris, 1994), occur at a variety of levels throughout the Belly River Group.

The uppermost proposed formation of the Belly River Group, the mudstone-dominated Drywood Creek Formation (Fig. 2), is extremely recessive and is only known to be exposed in the Maycroft area in one locality on the Oldman River where its measured thickness is approximately 80 m (the type-section thickness is only 55 m; Jerzykiewicz and Norris, 1994). Its thinness, recessive nature, and stratigraphic position between two recessive units strongly limit the utility of the Drywood Creek Formation as a mappable unit.

For the purposes of 1:50 000 scale structural mapping, the transition in sandstone facies of the Belly River Group at ~100 m above the base is most useful. Unfortunately, the thinness of this unit (Connelly Creek

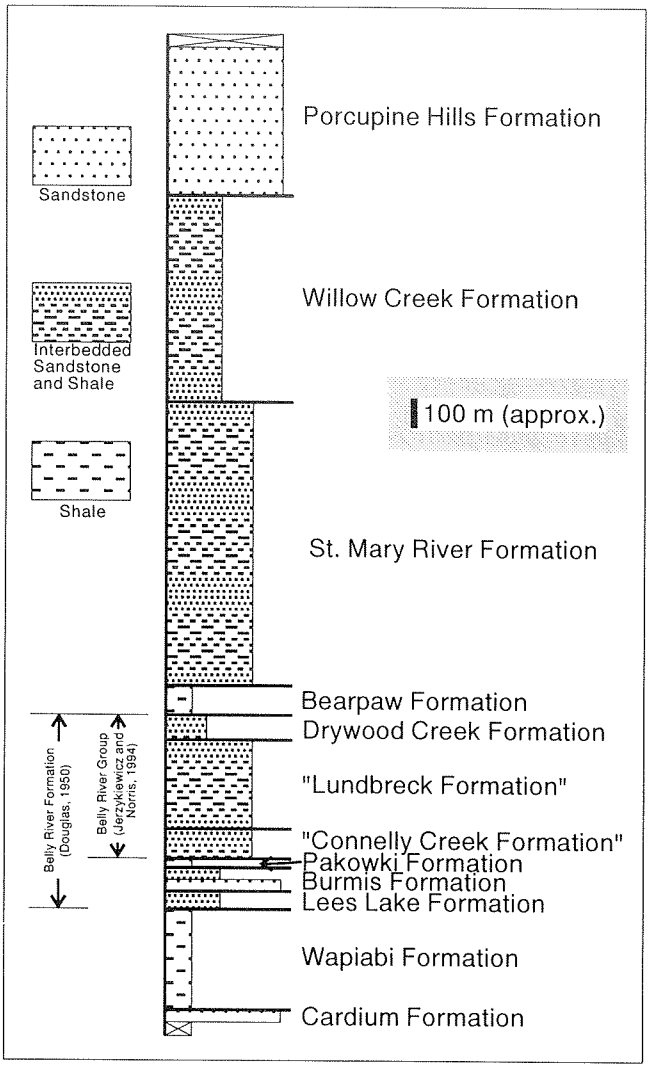

Figure 2. *Schematic stratigraphic column for Maycroft (east-half). Thicknesses are approximate. Those units encompassed by the new definition of the Belly River Group and the upper Alberta Group (Jerzykiewicz and Norris, 1994) and those encompassed by the usage of Douglas (1950) are indicated. Names in quotations indicate an uncertainty of the application of the formation names in this area.*

equivalent?), coupled with limited exposures away from the Oldman River, makes it difficult to map this boundary regionally.

The three newly-defined formations of the upper Alberta Group (Fig. 2; marine to marginal-marine/deltaic/shoreline facies) can usually be mapped over broad areas by virtue of the thick (ca. 40 m) and resistant trough crossbedded lower sandstone unit of the Burmis Formation (Fig. 2; Jerzykiewicz and Norris,

1994; Stockmal, GSC Current Research, in prep.). The basal sandstone of the Belly River Group is very similar to the Burmis Formation in the Maycroft area, where it is known to be up to 17 m thick; therefore caution must be exercised away from river exposures to not confuse these units.

The six formations proposed by Jerzykiewicz and Norris (1994; Fig. 2) can therefore be mapped in practice as two distinct packages in the Maycroft area: (1) the Lees Lake/Burmis/Pakowki interval (upper Alberta Group), approximately 175 m total thickness (from measured sections); and (2) the Connelly Creek/Lundbreck/Drywood Creek interval (Belly River Group, *sensu stricto*), probably on the order of 450 m total thickness (estimated from composite sections and limited well control). It is important to note that this two-fold subdivision represents a significant improvement over the mapping of Douglas (1950), which treated the Belly River Formation (which included units now placed in the Alberta Group) as a single entity.

MAP AND CROSS-SECTION

The two-fold subdivision (and locally three-fold, where the sandstone-facies transition can be mapped) of the former Belly River Group has afforded mapping of faults not previously recognized, and improved the resolution of stratigraphic offset. A digital 1:50 000 scale map of results to date in the Maycroft east-half map sheet will be presented at the Forum, with one of two planned balanced and restored cross-sections (see also Stockmal et al., in prep.).

SUMMARY

New structural mapping and interpretation in the Maycroft map-area, southern Alberta Foothills, has provided a modern view of the triangle zone and related structures. The timely nature of the NATMAP project and its focus was demonstrated by the three-session Triangle Zones Symposium organized for the 1994 Joint Convention of the CSEG and the CSPG, and the special issue of the Bulletin of Canadian Petroleum Geology planned for 1995, stemming from the symposium. Cooperation with industry and academia for access to seismic data was essential for the interpretation in the Maycroft area, and will be essential for all NATMAP map sheets.

REFERENCES

Douglas, R.J.W.
1950: Callum Creek, Langford Creek, and Gap map-areas, Alberta. Geological Survey of Canada, Memoir 255, 124 p.

Jerzykiewicz, T. and Norris, D.K.
1994: Stratigraphy, structure and syntectonic sedimentation of the Campanian 'Belly River' clastic wedge in the southern Canadian Cordillera. Cretaceous Research, v. 15, p. 367–399.

Lawton, D.C., Stockmal, G.S., and Spratt, D.A.
1994: Seismic definition of the triangle zone east of Maycroft, Alberta. *In* Current Research, Part E, Geological Survey of Canada, p. 109–116.

MacKay, P.A., Spratt, D.A., Soule, G., and Lawton, D.C.
1994: The triangle zone of southern Alberta – geometry, lateral variations and associated oil and gas fields. Field-Trip Guidebook, (PR-2), Canadian Society of Exploration Geophysicists–Canadian Society of Petroleum Geologists, 1994 Joint National Convention, Calgary, Alberta, 105 p.

Price, R.A.
1981: The Cordilleran foreland thrust and fold belt in the southern Canadian Rocky Mountains. *In* Thrust and Nappe Tectonics, N.J. Price and K.R. McClay (eds.). Geological Society of London, Special Publication No. 9, p. 427–448.

Stockmal, G.S. and MacKay, P.A.
1994: Triangle zone and foothills structures along and adjacent to the Oldman River, southwestern Alberta. *In* Current Research, Part E, Geological Survey of Canada, p. 101–108.

Stockmal, G.S., MacKay, P.A., Lawton, D.C., and Spratt, D.A.
in prep.: The triangle zone and foothills structures adjacent to the Oldman River, southwestern Alberta: seismic definition and implications of new structural mapping. Bulletin of Canadian Petroleum Geology.

THE MANNVILLE GROUP OF SOUTHWESTERN SASKATCHEWAN: NEW MAPS, PERSPECTIVES AND POTENTIAL

N.A. Vanbeselaere

Rocky Mountain Consultants
445-35th Avenue N.W., Calgary, Alberta T2K 0C2

D.A. Leckie

Geological Survey of Canada, 3303-33rd Street N.W., Calgary, Alberta T2L 2A7

D.P. James

Wascana Energy Ltd.
2500, 205-5th Avenue S.W., Calgary, Alberta T2P 2V7

The Mannville Group in the Western Canada Sedimentary Basin contains large volumes of highly-economic light and medium oils and gas, in addition to billions of barrels of heavy oil. Because of the value of this resource and the relatively shallow drilling depths in many areas, the Mannville Group has been and remains a highly competitive and successful target. However, despite thousands of well penetrations, no consistent regional stratigraphic framework has emerged. Nomenclature from the Alberta Foothills differs from that employed in British Columbia, and in the Plains. Terminology employed in the Lloydminster area is not the same as that used in southwestern Saskatchewan. With all these terms, it is little wonder stratigraphic chaos has evolved.

This study presents results of the first phase of a multi-year, regional stratigraphic study which will extend from southwestern Saskatchewan to the Foothills. The objectives are to 1) construct an integrated regional framework across the Western Canada Sedimentary Basin; 2) provide sedimentological and paleogeographical interpretations of the area; 3) to provide a sequence stratigraphic framework for the interval; and 4) to provide a suite of regional maps for each of the unconformity-bounded successions. The first phase of this study (Twps. 1 to 20, Rges. 13 to 22 W3), and the subject of this poster session is located in the producing trend of southwestern Saskatchewan, an area characterized by a large number of wells with good core control. The poster session presents regional maps resulting from the study.

In southern Saskatchewan, Mannville-equivalent sediments are termed the Pense, Cantuar and Success (S2) formations (Fig. 1). The strata range from Oxfordian/Kimmeridgian for the Success (S1) to middle Albian for the Pense Formation. The interval, which is up to 100 m thick, was deposited over 40 to 50 million years, and is riddled with unconformities and weathered horizons. Stratigraphic correlations using well logs are difficult, imprecise and highly suspect unless corroborated by core control.

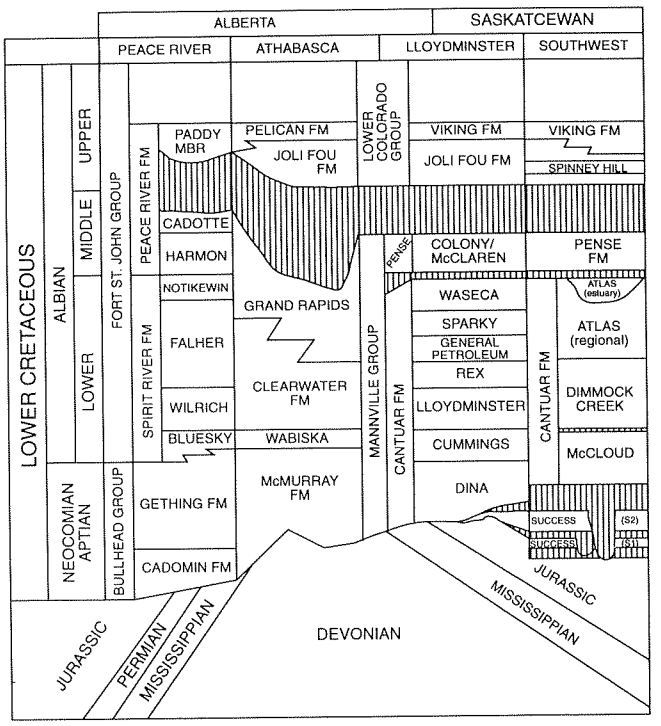

Figure 1. *Stratigraphic nomenclature (modified from Christopher, pers. comm., 1994).*

Jurassic Success S1 sediment was deposited in a restricted shallow-marine or lacustrine environment. The top of the S1 is extremely weathered indicating a long hiatus. The S2 was deposited as a sheet of quartzose, braided-fluvial sandstone that unconformably cuts into the S1. S2 sediments extended across the southern prairies. Contrary to existing thought, there was minimal relief at the base of the S2, which is the Sub-Cretaceous unconformity. The top of the S2 is commonly a deeply-weathered, thick paleosol overlain by coal and carbonaceous shale.

The Cantuar Formation consists of dominantly lithic sandstone, siltstone, and shale overlying a basal quartzose unit. The base of the Cantuar Formation has high local relief and in places has eroded long wide valleys into the Success and older Jurassic strata (Masefield, Roseray and Rush Lake formations). Regional maps show that the regional Cantuar valley system trended north–south with up to 74 m of relief. Remnants of Success sediment are preserved as isolated, buried cuestas on the margins of the valley

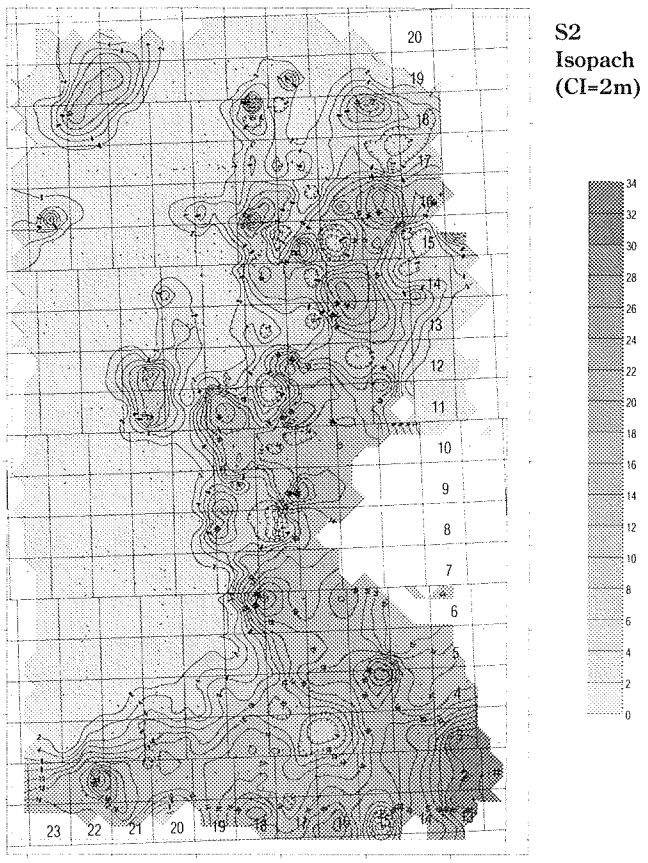

Figure 2. *Isopach map of the Success (S2) Formation.*

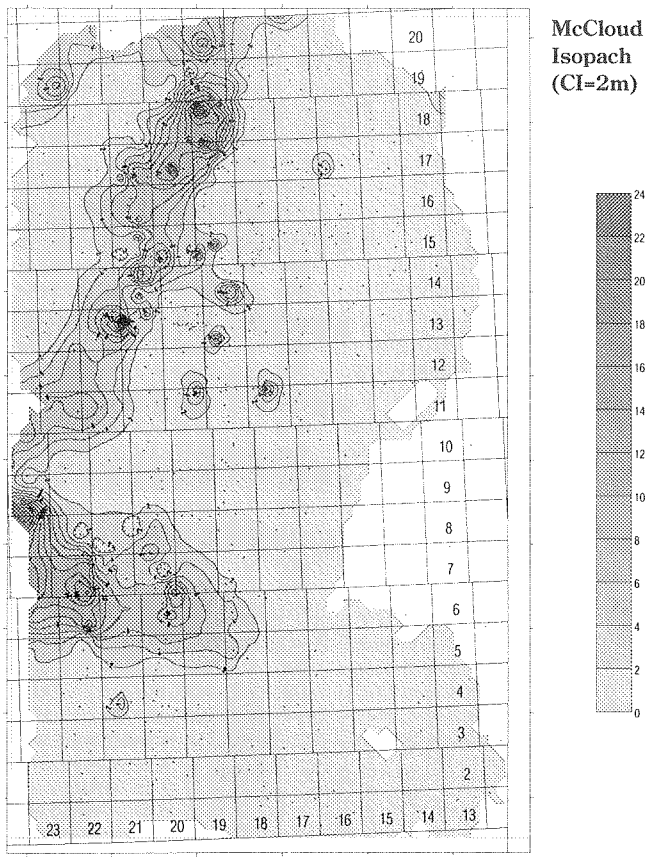

Figure 3. *Isopach map of the McCloud Member, of the Cantuar Formation.*

walls (Fig. 2). Cantuar valley fill (Fig. 3) is dominantly nonmarine, with the basal quartzose sediment of McCloud Member (equivalent to the lower Mannville in southern Alberta) overlain by lithic–feldspathic sediments of the Dimmock Creek and Atlas Members (equivalent to the Upper Mannville). Cantuar sediments represent the infill of the extensive valley system. The fill was from meandering streams with abundant paleosols, shallow lacustrine, and splay deposits.

The top of the Atlas Member (Fig. 4) is represented by chert and quartzose sandstones deposited in a north–south trending estuarine system with several tributaries. The onset of Pense sedimentation (Fig. 5) is represented by a transgressive surface of erosion overlain by the marine condensed section of the IHACM marker. The Pense Formation consists of up to seven upward-coarsening cycles deposited in a shallow-marine basin which thickened eastward. The Pense transgression variably overlies either Cantuar or Success sediments.

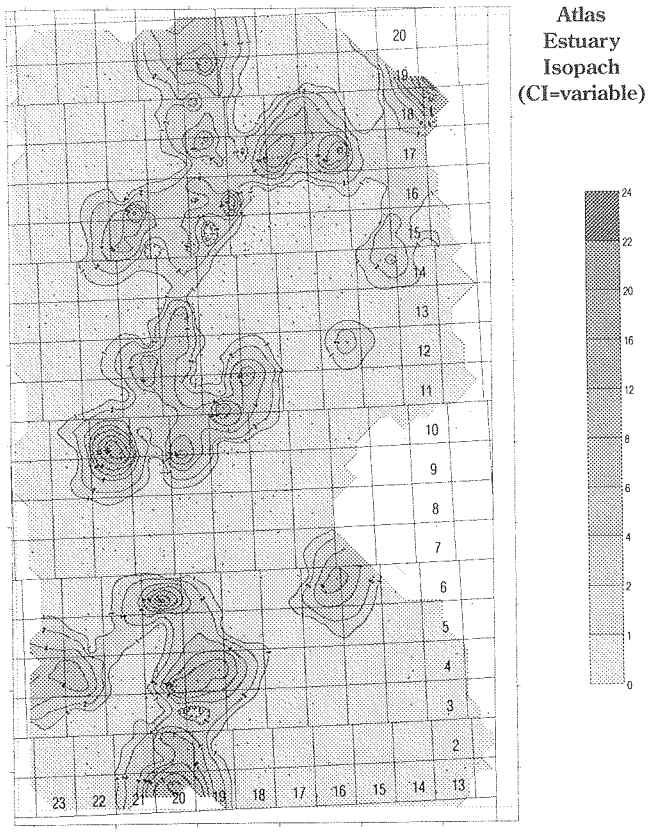

Figure 4. *Isopach map of the Atlas estuary facies.*

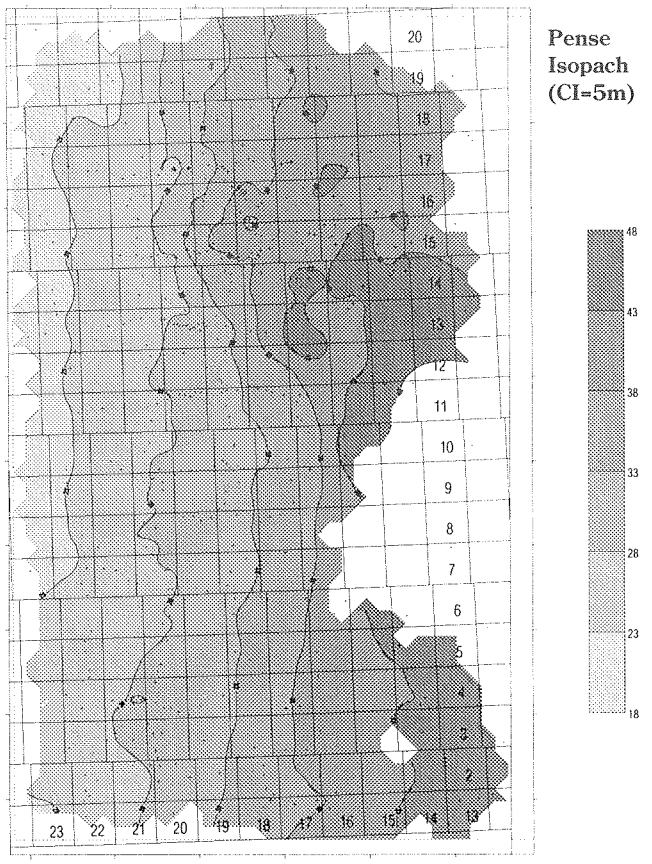

Figure 5. *Isopach map of the Pense Formation.*

The study has important economic considerations because of the hydrocarbons produced from several of these stratigraphic units, most noticeably from the S2 and quartzose, estuarine sandstones of the Atlas Member. Play types (Fig. 6) are dominantly stratigraphic and include: 1) Pense shelfal sandstone; 2) Pense transgressive sandstone; 3) estuary sandstone of the Atlas Member; 4) point bar sandstone of the Atlas Member; 5) preserved remnants of the S2 braid plain; and 6) thin-bedded marine/lacustrine? sandstone of the S1.

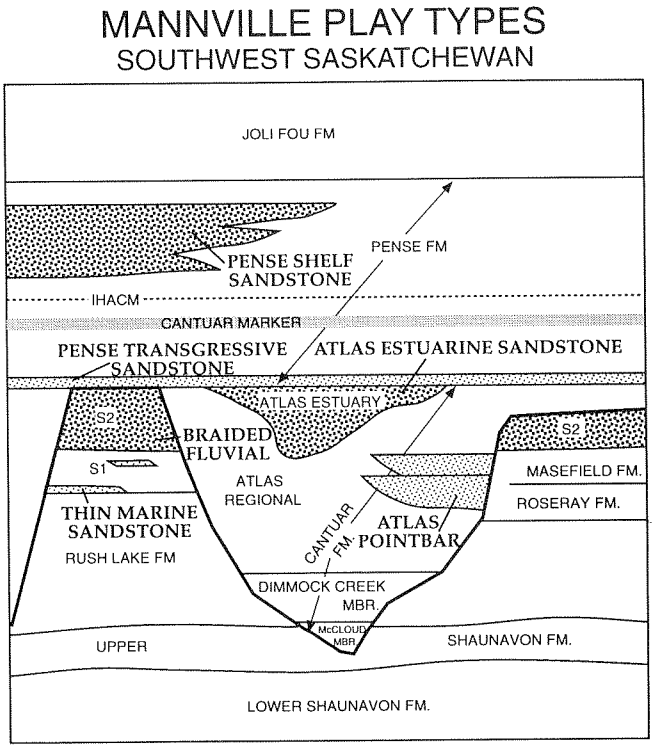

Figure 6. *Play types of the Mannville Group in southwestern Saskatchewan.*

PHYSICAL STRATIGRAPHY AND CONODONT BIOSTRATIGRAPHY OF THE BEAVERHILL LAKE GROUP, LATE MIDDLE TO EARLY LATE DEVONIAN, EAST-CENTRAL ALBERTA

J.C. Wendte, T.T. Uyeno, and B. Abrahamson

Geological Survey of Canada, 3303-33rd Street N.W., Calgary, Alberta T2L 2A7

INTRODUCTION

The Beaverhill Lake Group in east-central Alberta consists predominantly of limestones and dolostones, up to slightly over 200 m thick. These carbonate strata overlie coastal plain shales and dolostones of the Watt Mountain Formation, and are overlain by shallow-water carbonates of the Cooking Lake Formation. The term Beaverhill Lake was erected by the Geological Staff of Imperial Oil Ltd. (1950), with the type section well in central Alberta (Anglo-Canadian Beaverhill Lake No. 2, located at 11-11-50-17W4M). There, it consists of, in ascending order, the Fort Vermilion, Slave Point, and Waterways formations. In northeastern Alberta, Crickmay (1957) subdivided the Waterways Formation into, in ascending order, the Firebag, Calumet, Christina, Moberly, and Mildred members. This paper summarizes the results of an integrated study of conodont biostratigraphy, physical stratigraphy and sedimentology of the Beaverhill Lake Group in east-central Alberta, extending from Townships 24 to 71, and from the Alberta-Saskatchewan border to western Alberta.

PHYSICAL STRATIGRAPHY

The Beaverhill Lake Group was divided into nine, predominantly upward-shoaling cycles (termed A to H, with A subdivided into Lower and Upper parts), that were correlated throughout, or almost throughout, the study area. Figure 1 is an east-west cross-section of the

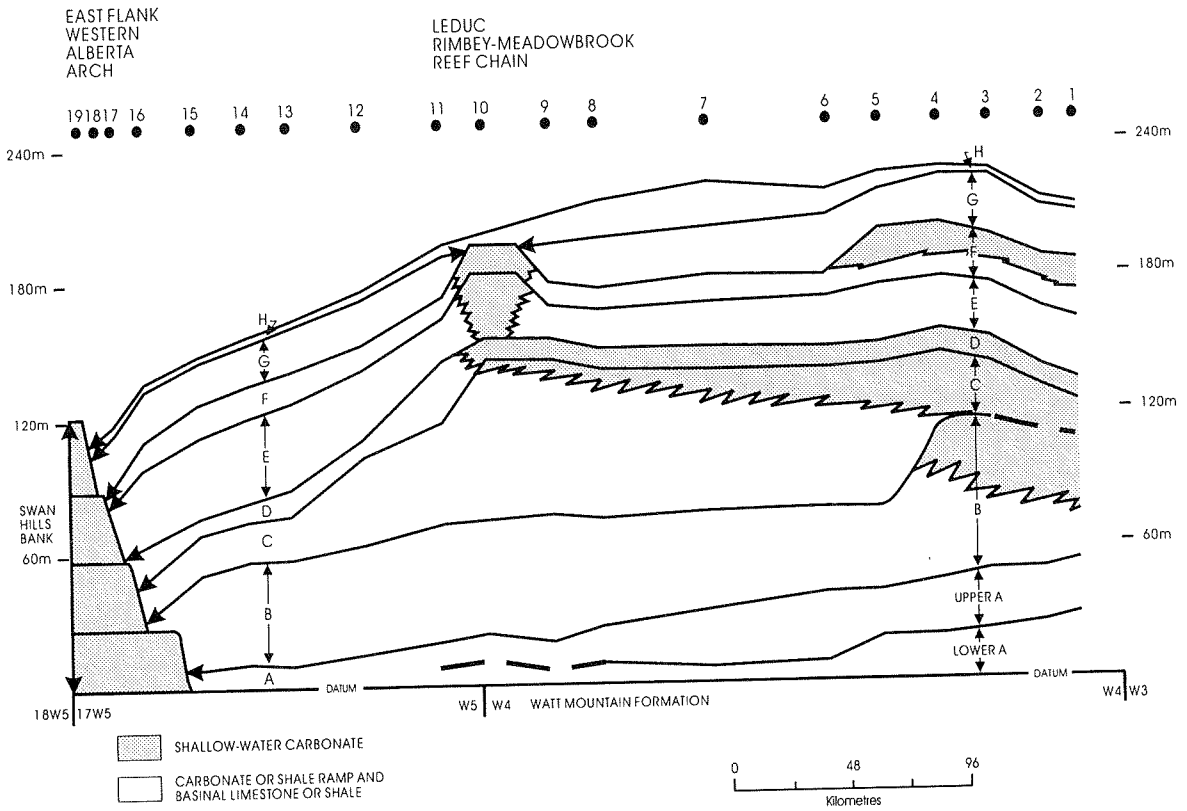

Figure 1. *Stratigraphic cross-section of the Beaverhill Lake Group at the latitude of Townships 50 to 52.*

group across the Alberta Basin, at the latitude of Townships 50 to 52. On the eastern side of the basin, shallow-water lithofacies are mainly limited to an area east of the Fifth Meridian. Deeper-water facies of this succession dip toward the west, and downlap onto a much thinner bank complex of the Swan Hills Formation, located along the eastern flank of the Western Alberta Arch. The strata on the eastern side of the basin comprise two major transgressive-regressive (T-R) successions.

The Lower T-R succession extends from the base of the group to the top of Cycle D. The transgressive phase of this succession includes shales and relatively deep water limestones of the Lower and Upper A cycles, and the basalmost part of Cycle B. The regressive phase culminates in progradation of shallow-water, platformal carbonates of cycles C and D to approximately the Fifth Meridian.

The Upper T-R succession consists of the ramp carbonates of cycles E and F, and the shaly limestones or calcareous shales of cycles G and H. The phase of maximum transgression corresponds to a level approximately at the middle of Cycle G. Argillaceous strata in the upper part of Cycle G and Cycle H sigmoidally prograde to the west. To the east of Well 7, the top of the Beaverhill Lake Group is unconformable, but is conformable to the west of it.

Shallow-water carbonates of cycles E and F occur in isolated shoals that commonly occur along the Fifth Meridian. These carbonates are capped by a *Tripinites*-bored, submarine hardground and are covered by the sigmoidally prograding argillaceous deposits of Cycle H. These shoals helped to localize the margin of the overlying platformal carbonates of the Cooking Lake Formation and, in turn, the occurrence of the overlying reef complexes of the Leduc Formation.

CONODONT BIOSTRATIGRAPHY

Figure 2 summarizes the correspondence between the depositional successions identified in this investigation, and the stratigraphic units of the Waterways Formation as established in the Bear Biltmore No. 1 well (7-11-87-17W4M, the Standard Subsurface Reference Section; Weihmann, 1990), and the conodont zones determined in this study.

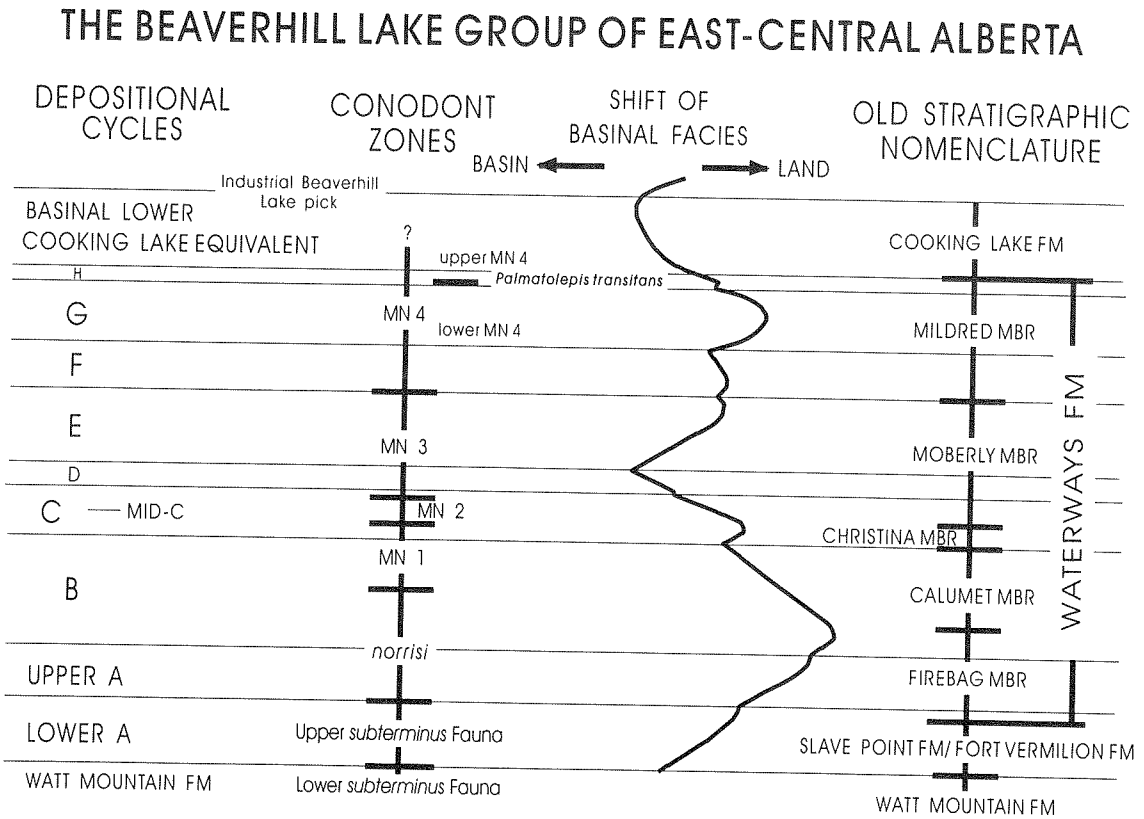

Figure 2. *Summary diagram showing correspondence of depositional successions, conodont zones, and previous stratigraphic nomenclature.*

Six conodont zones are recognized in the Beaverhill Lake Group. The lower two, the Upper *subterminus* Fauna and the *norrisi* Zone, are of late Givetian age (late Middle Devonian); the upper four, Montagne Noir (MN) zones 1 to 4, are of early Frasnian age (early Late Devonian) (Fig. 3). Regionally at least, the uppermost zone, MN 4, can be informally subdivided into lower and upper parts, with the base of the upper part marked by the first occurrence of *Palmatolepis transitans*. The bases of the zones are based on the first occurrences of diagnostic taxa. The Middle-Upper Devonian boundary falls within a conformable succession in Cycle B. It is interesting to observe that the most rapid zonal changes appear to correspond to the regressive phase of the Lower T-R succession.

The start of the Lower T-R succession coincides with the start of T-R Cycle IIa-2 of Day et al. (in press), and that of the Upper T-R succession with the start of T-R Cycle IIb-2 of Day et al. (in press). These cycles are modifications of those proposed by Johnson and others (1985). Elsewhere, the start of Cycle IIa-2 marks the deposition of the Allochthonous Beds in the Powell Creek area, District of Mackenzie, and of the Argillaceous limestone beds of the Souris River Formation of southern Manitoba (Uyeno, 1979; Uyeno *in* Norris et al., 1982; Muir et al., 1984; Muir, 1988). The start of Cycle IIb-2 is at the base of the Dolomitic limestone member of the Souris River Formation in southern Manitoba, and is probably within the Allochthonous Beds in the Powell Creek area. At Cold Sulphur Spring, Jasper National Park, the base of the Flume Formation probably coincides with the start of Cycle IIa-2 (Uyeno *in* Norris and Pedder, 1985).

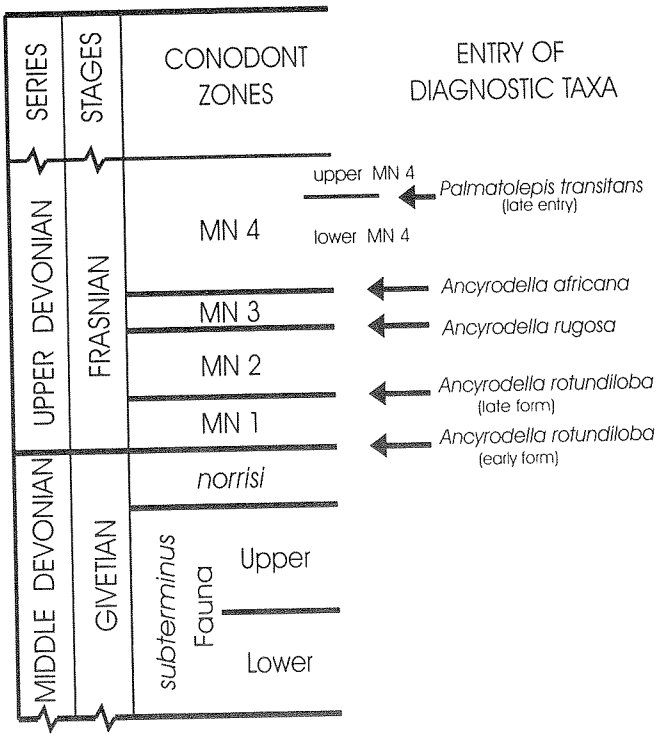

Figure 3. *Conodont zonation (after Klapper, 1989, pers. comm., 1994; Klapper and Johnson in Johnson, 1990). MN = Montagne Noire. Note that the entry of Palmatolepis transitans is considered to be late in the area under study.*

SUMMARY

The development of the Beaverhill Lake Group in east-central Alberta records the interactive influences of sea level, tectonic and environmental controls. The basin-wide cycles correspond to changes in the relative sea level. Areas of slow subsidence, such as along the Western Alberta Arch, helped to localize the occurrence of carbonate platforms. The prevailing northeasterly trade winds created a wind-wave dominated regime, which resulted in the westerly shedding and clinoforming of carbonate muds off the carbonate platforms located east of the Fifth Meridian.

The Beaverhill Lake Group spans six conodont zones, the uppermost one of which can be subdivided locally into two parts. These zones correlate in a consistent manner with the depositional cycles throughout the study area.

REFERENCES

Crickmay, C.H.
1957: Elucidation of some western Canada Devonian formations. Published by the author, Calgary, 15 p.

Day, J., Uyeno, T.T., Norris, A.W., Witzke, B.J., and Bunker, B.J.
in press: Middle-Upper Devonian relative sea level histories of central and western North American interior basins. *In* Paleozoic Cratonic Sequence Stratigraphy, North American Perspectives, B.J. Bunker, G.A. Ludvigson, and J. Day (eds.). Geological Society of America, Special Paper.

Geological Staff, Imperial Oil Limited, Western Division
1950: Devonian nomenclature in Edmonton area, Alberta, Canada. Bulletin of American Association of Petroleum Geologists, v. 34, p. 1807–1825.

Johnson, J.G.
1990: Lower and Middle Devonian brachiopod-dominated communities of Nevada, and their position in a biofacies-province-realm model (with a section on revision of Middle Devonian conodont zones, by G. Klapper and J.G. Johnson). Journal of Paleontology, v. 64, p. 902–941.

Johnson, J.G., Klapper, G., and Sandberg, C.A.
1985: Devonian eustatic fluctuations in Euramerica. Geological Society of America Bulletin, v. 96, p. 567–587.

Klapper, G.
1989: The Montagne Noire Frasnian (Upper Devonian) conodont succession. *In* Devonian of the World, Proceedings of the Second International Symposium on the Devonian System, N.J. McMillan, A.F. Embry and D.J. Glass (eds.). Paleontology, Paleoecology and Biostratigraphy, Vol. III, Canadian Society of Petroleum Geologists, Memoir 14, p. 449–468 (imprint 1988).

Muir, I.D.
1988: Devonian Hare Indian and Ramparts formations, Mackenzie Mountains, N.W.T.: basin-fill, platform and reef development. Unpublished Ph.D. dissertation, University of Ottawa, Ottawa, 593 p.

Muir, I., Wong, P., and Wendte, J.
1984: Devonian Hare Indian – Ramparts (Kee Scarp) evolution, Mackenzie Mountains and subsurface Norman Wells, N.W.T.: basin-fill and platform-reef development. *In* Carbonates in Subsurface and Outcrop, L. Eliuk (ed.). 1984 C.S.P.G. Core Conference, Canadian Society of Petroleum Geologists, p. 82–101.

Norris, A.W., Uyeno, T.T., and McCabe, H.R.
1982: Devonian rocks of the Lake Winnipegosis-Lake Manitoba outcrop belt, Manitoba. Geological Survey of Canada, Memoir 392, 280 p.

Norris, A.W. and Pedder, A.E.H. (eds.)
1987: Devonian of Alberta Rocky Mountains between Banff and Jasper, a field trip guidebook. Subcommission on Devonian Stratigraphy, Geological Survey of Canada, Calgary, 85 p.

Uyeno, T.T.
1979: Devonian conodont biostratigraphy of Powell Creek and adjacent areas, western District of Mackenzie. Geological Association of Canada, Special Paper 18, p. 233–257.

Weihmann, I.
1990: Waterways Formation (Beaverhill Lake Group). *In* Lexicon of Canadian Stratigraphy, v. 4, D.J. Glass (ed.). Canadian Society of Petroleum Geologists, p. 676–677.

IMPORTANCE OF MICROFOSSILS FOR IDENTIFYING CRETACEOUS ROCK UNITS IN THE CALIFORNIA STANDARD C. & E. COW CREEK 6–30–8–1W5 WELL: IMPLICATIONS FOR STRUCTURAL SECTIONS IN THE TRIANGLE ZONE, SOUTHERN ALBERTA

J.H. Wall

Geological Survey of Canada, 3303-33rd Street N.W., Calgary, Alberta T2L 2A7

D.K. Norris

Geological Consultant, Kelowna, British Columbia

ABSTRACT

The California Standard C. & E. Cow Creek well is located at the apex of the Triangle Zone along the eastern boundary of the Alberta Foothills. It penetrated 14 382 ft. (4 384 m) of Cretaceous and Jurassic rocks before reaching autochthonous Mississippian carbonates with no hydrocarbon shows to a total depth of 14 905 ft. (4 543 m).

Microfossils, chiefly foraminifera, are utilized to confirm identification of Upper Cretaceous marine rock units. The Bearpaw Formation is present from 6035 to 6 470 ft. (1 839–1 972 m) overlying a normal section of the Belly River Formation to 8 482 ft. (2585 m), within which the Pakowki Formation or equivalent is recognized between 7 940 and 8 010 ft. (2 420 and 2 441 m). The Belly River is underlain by a thin section of the Wapiabi Formation to 9 010 ft. (2 746 m), where the first of two thin thrust repeats of the Belly River is encountered. The second Wapiabi over Belly River thrust is recorded at 10 050 ft. (3 063 m), below which the sequence appears normal, including a nearly complete section of the Alberta Group as documented by the succession of microfossil assemblages.

The basal detachment for Foothills deformation and the Triangle Zone occurs in the basal Belly River and in the upper Wapiabi, as illustrated in a revised regional structure section.

INTRODUCTION

The California Standard C. & E. Cow Creek 6–30–8–1W5 well, about 60 mi. (100 km) west of Lethbridge and 6 mi. (10 km) north of Lundbreck, was drilled at the apex of the Triangle Zone along the boundary between the Foothills (Disturbed) Belt and the Interior Plains (Fig. 1). It was abandoned in 1965 at a total depth of 14 905 ft. (4 543 m) in Mississippian carbonates with no hydrocarbon shows. This paper provides data to supplement a previous abstract by the authors (Wall and Norris, 1992).

Cow Creek is considered a key well because it provided vital stratigraphic and structural information at a location equivalent to that of the oilfield at Turner Valley. Further, it was deemed important that the stratigraphy of the well be accurately determined as a

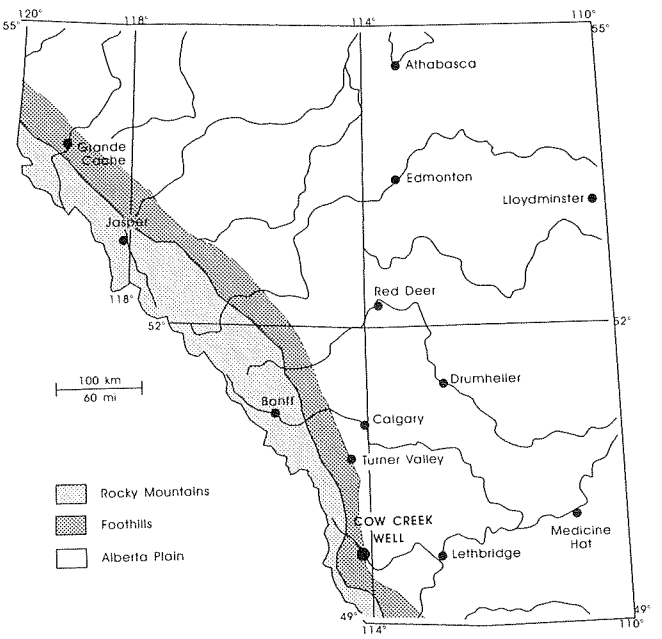

***Figure 1.** Map of southern Alberta showing location of the Cow Creek 6-30-8-1W5 well with reference to the major physiographic divisions.*

Table 1

Stratigraphic succession in the Cow Creek 6-30-8-1W5 well

Rock Units	Depth	
	ft.	(m)
California Standard C. & E. Cow Creek 6-30-8-1W5 Well Elevation K.B.: 3978 ft. (1212.5 m)		
Willow Creek Fm.	at surface	
St. Mary River Fm.	150?	(45.7)
Coal beds	5 502	(1 677)
Bearpaw Fm.	6 035	(18 39.5)
Belly River Fm.	6 470	(19 72.1)
Pakowki Fm. or equivalent	7 940–8 010	(24 20.1–2 441.4)
Alberta Group		
Wapiabi Fm.		
Hanson(?), Thistle members	8 482	(2 585.3)
Belly River Fm. (fault)	9 010	(2 746.2)
Pakowki Fm. or equivalent	9 050–9 120	(2 758.4–2 779.8)
Alberta Group		
Wapiabi Fm.		
Hanson(?), Thistle members	9 580	(2 920)
Belly River Fm. (fault)	10 050	(3 063.2)
Alberta Group		
Wapiabi Fm.		
Hanson(?), Thistle members	10 483	(3 195.2)
Dowling Member	11 025?	(3 360.4)
Marshybank Member	11 330?	(3 453.4)
Muskiki Member	11 535?	(3 515.9)
Cardium Fm. or equivalent	11 710	(3 569.2)
Blackstone Fm.		
Opabin Member	11 740	(3 578.4)
Haven Member	11 895	(3 625.6)
Vimy Member	12 105?	(3 689.6)
Sunkay Member	12 230	(3 727.7)
Grit Bed	12 339	(3 760.9)
Blairmore Group		
Mill Creek, Beaver Mines fms. undifferentiated	12 346	(3 763.1)
Home Sand	13 668	(4 166)
Gladstone Fm.		
Calcareous (Ostracod) Mbr.	13 737	(4 187)
Kootenay Group		
Morrisey Fm.	13 915	(4 241.3)
Fernie Fm.		
Passage Beds	14 002	(4 267.8)
Green Beds	14 040	(4 279.4)
Grey Beds	14 070	(4 288.5)
Rundle Group		
Mount Head Fm.	14 382	(4 383.6)
Livingstone Fm.	14 644	(4 463.5)
Total Depth	14 905	(4 543)

prerequisite to the completion and balancing of structure sections down to the undeformed Paleozoic sedimentary succession of the foreland and westward in the deformed rocks of the Cordilleran Orogen. To meet this objective, a microfaunal study of the well was undertaken to resolve conflicting interpretations of the Upper Cretaceous stratigraphy, which were assumed to have been based on electrolog and lithologic data alone. An updated version of the stratigraphic succession is presented integrating log, sample and microfossil evidence (Table 1, Fig. 2). The thrust repeats recognized in the well have been incorporated into a structure section across the Triangle Zone (Fig. 3) in the Cowley map-area (Hage, 1945).

STRATIGRAPHY

In the illustrations and following discussion, the terms Belly River Formation and Alberta Group are used in the sense of Stott (1963) and others prior to the revised nomenclature of Jerzykiewicz and Norris (1994). In that study, the Belly River is raised to group status and is restricted to the nonmarine interval between the top of the Pakowki Formation and the base of the Bearpaw Formation, which is divided into three new formations designated as Connelly Creek, Lundbreck and Drywood Creek in ascending order. The Alberta Group is extended above the Wapiabi Formation to include in ascending order the newly named, predominantly marine Lees Lake and Burmis formations, formerly regarded as informal members in the lower part of the Belly River Formation, and the Pakowki Formation.

Microfossils, chiefly foraminifera, are crucial for the proper assignment of marine shales in faulted Cretaceous subsurface sections of the Alberta Foothills. Recognition of the first marine unit at 6 035 ft. (1 839.5 m) as the Bearpaw Formation (Fig. 2A), based on comparison of its microfauna with that from the Lundbreck outcrop section studied by Rosene (1972), is pivotal to the correct designation of the contiguous formations. Earlier misidentification of this unit as the older Wapiabi Formation resulted in an erroneous interpretation of the stratigraphy and structure.

Within the first or normal section of the Belly River Formation (Fig. 2B), arenaceous foraminifera at 7 940–8 010 ft. (2 420.1–2 441.4 m) indicate a marine incursion correlative with the Pakowki Formation of the Plains, as discussed by Jerzykiewicz and Norris (1994, p. 382). The same fossils are encountered downhole at 9 050–9 120 ft. (2 758.4–2 779.8 m) in the first thrust repeat of the Belly River at the same position relative to the base of the formation.

The first two blocks of the Alberta Group (Fig. 2B, C) carry assemblages characteristic of the upper part of the Wapiabi Formation [Hanson(?), Thistle mbrs.], whereas the third block, immediately beneath the lower detachment of the Triangle Zone (Fig. 2C, D), reveals a nearly complete succession of microfaunas through the

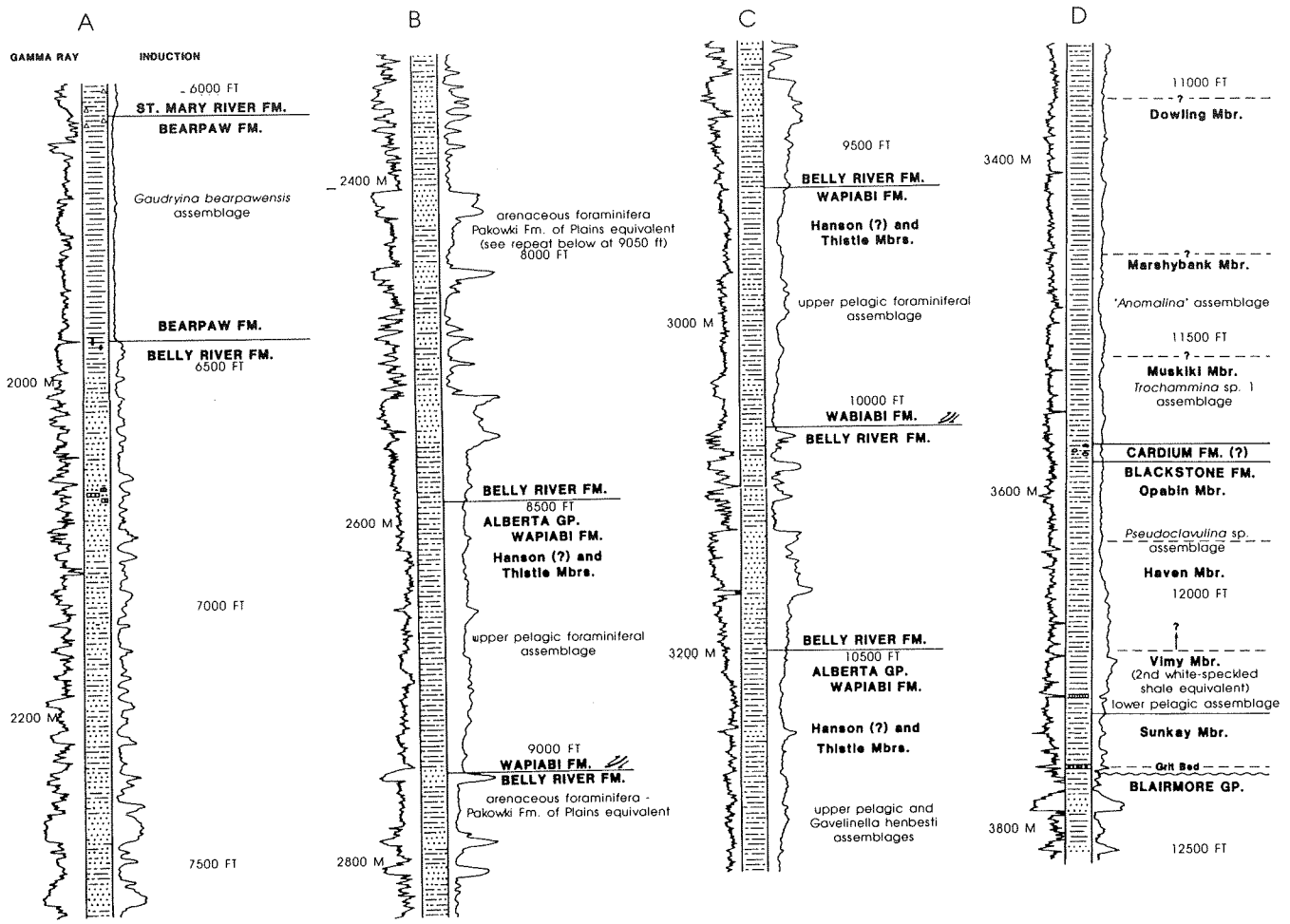

Figure 2. *Integration of geophysical, lithological and microfaunal data through Upper Cretaceous strata in the Cow Creek 6-30-8-1W5 well. Note Wapiabi/BellyRiver fault contacts at 9 010 and 10 050 ft.*

Wapiabi and Blackstone formations, as established for the area by Wall (1967) and Wall and Rosene (1977). The position of the medial Cardium Formation in the third block is indicated by a concentration of chert pebbles and by foraminifera associated with the basal Wapiabi and uppermost Blackstone. The occurrence of the lower or second white-speckled shale equivalent of the Alberta Plain is confirmed by the identification of the lower pelagic assemblage of Wall (1967) [= *Hedbergella loetterlei* Zone of Caldwell et al. (1978) and Bloch et al. (1993)] in the Vimy Member of the Blackstone (Fig. 2D).

STRUCTURAL GEOLOGY

The Triangle Zone at the Cow Creek well lies in the structural reentrant between the Highwood River and Clark Range salients of the eastern margin of the Cordilleran Orogen. It was pierced by the Cow Creek well almost exactly at its apex so that its fault-bounded, trigonal geometry is clearly revealed. The west-verging Waldron Fault defines its east flank, the east-verging Bridge Fault its west flank, and two unnamed, east-verging thrusts provide its basal detachment (Fig. 3). The Triangle Zone is, therefore, allochthonous with offsets at the Belly River/Bearpaw contact indicating approximately 20 000 ft. (6 km) of displacement eastward relative to the foreland. Anomalous thicknesses of Upper Cretaceous formations at the apex of the Triangle Zone appear to be due in part to acute folding and in part to marked variations in depositional and erosional thickness of the formations involved.

The Triangle Zone is a regional feature resulting directly from orogenic transpression at the leading edge of the Laramide deformation front. However, it is not

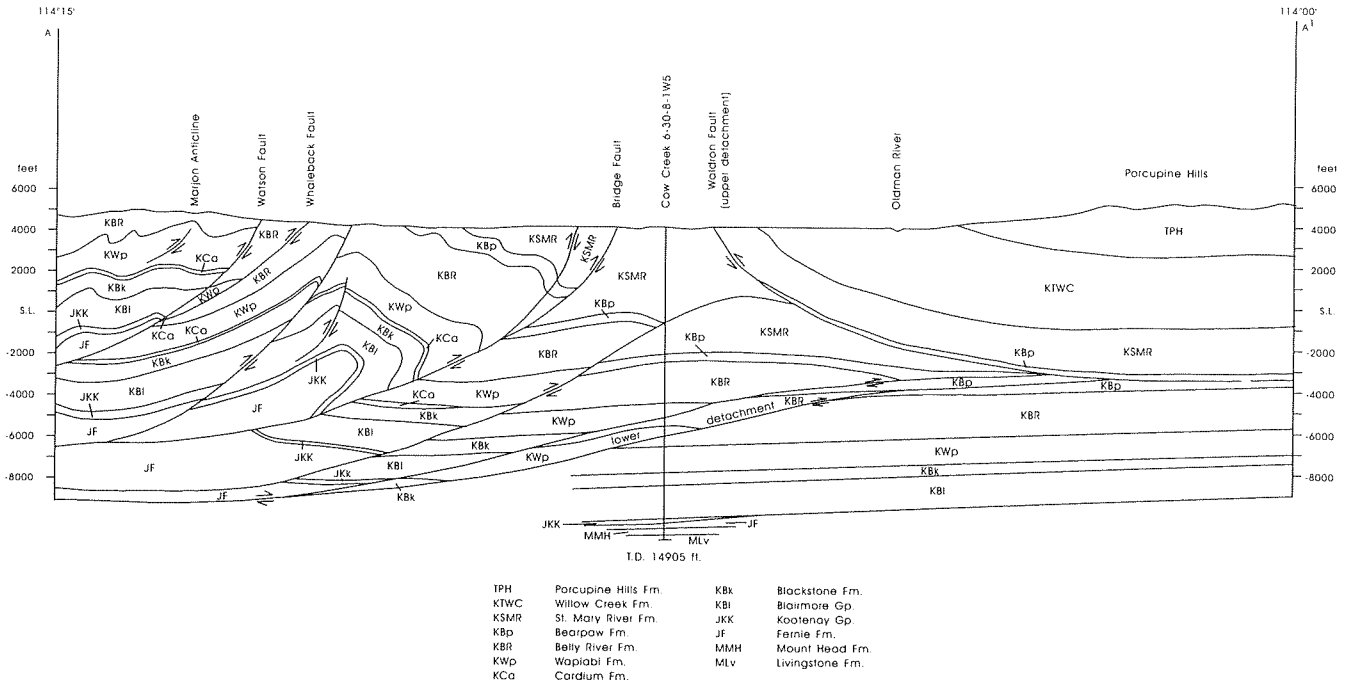

Figure 3. *Schematic structure section through the Cow Creek 6-30-8-1W5 well (latitude 49°40'25").*

unique to the eastern margin of the Foreland Thrust and Fold Belt. It began as a curvilinear uplift, reflecting the primeval shape of the Cordilleran Miogeocline, west of the Rocky Mountain Trench in the Late Cretaceous (Campanian). Geometrically, it probably was not unlike the Triangle Zone we see today associated with the uplifted Porcupine Hills. The Zone migrated haltingly but progressively northeastwardly from the Late Cretaceous into the Paleocene and played a major role in the tectonization of the craton as the migrating deformation front encroached upon it to generate the Foreland Thrust and Fold Belt.

ACKNOWLEDGMENTS

The samples on which the study is based were supplied through the courtesy of Chevron Canada Resources Limited by N.H. Schultheis and B.G. Van Helden. The microfossils were prepared for examination by J.J. Labadi and D.R. Then. Final drafting and manuscript processing were handled by D.R. Then. Consultation on log interpretation and stratigraphic topics was provided by D.W. Gibson, T. Jerzykiewicz, C.J. Klep, D.A. Leckie and M. Staniland. The authors express their gratitude to all of these individuals for their cooperation.

REFERENCES

Bloch, J., Schröder-Adams, C., Leckie, D.A., McIntyre, D.J., Craig, J., and Staniland, M.
1993: Revised stratigraphy of the lower Colorado Group (Albian to Turonian), Western Canada. Bulletin of Canadian Petroleum Geology, v. 41, no. 3, p. 325–348.

Caldwell, W.G.E., North, B.R., Stelck, C.R., and Wall, J.H.
1978: A foraminiferal zonal scheme for the Cretaceous System in the Interior Plains of Canada. *In* Western and Arctic Canadian Biostratigraphy, C.R. Stelck and B.D.E. Chatterton (eds.). Geological Association of Canada, Special Paper 18, p. 495–575.

Hage, C.O.
1945: Cowley, Alberta. Geological Survey of Canada, Map 816A.

Jerzykiewicz, T. and Norris, D.K.
1994: Stratigraphy, structure and syntectonic sedimentation of the Campanian "Belly River" clastic wedge in the southern Canadian Cordillera. Cretaceous Research, v. 15, no. 4, p. 367–399.

Rosene, R.K.
1972: Micropaleontology of the Bearpaw Formation, southwestern Alberta Foothills. Unpublished M.Sc. thesis, University of Alberta, Edmonton.

Stott, D.F.
1963: The Cretaceous Alberta Group and equivalent rocks, Rocky Mountain Foothills, Alberta. Geological Survey of Canada, Memoir 317, 306 p.

Wall, J.H.
1967: Cretaceous foraminifera of the Rocky Mountain Foothills, Alberta. Research Council of Alberta, Bulletin 20, 185 p.

Wall, J.H. and Norris, D.K.
1992: Microfossil-based Upper Cretaceous stratigraphy of the California Standard C. & E. Cow Creek 6–30–8–1W5 well: Implications for structural sections in the Triangle Zone, southern Alberta. American Association of Petroleum Geologists, 1992 Annual Convention Program and Abstracts, p. 136–137.

Wall, J.H. and Rosene, R.K.
1977: Upper Cretaceous stratigraphy and micropaleontology of the Crowsnest Pass–Waterton area, southern Alberta Foothills. *In* Cordilleran Geology of Southern Alberta and Adjacent Areas, M.S. Shawa (ed.). Bulletin of Canadian Petroleum Geology, v. 25, no. 4, p. 842–867.

SEQUENCE STRATIGRAPHY OF COAL WITH EXAMPLES FROM THE MANNVILLE GROUP IN CENTRAL ALBERTA

I. Banerjee and W.D. Kalkreuth

Geological Survey of Canada, 3303-33rd Street N.W., Calgary, Alberta T2L 2A7

E.H. Davies

Branta Biostratigraphy Ltd., #4, 4640 Manhattan Road S.E., Calgary, Alberta T2G 4B5

INTRODUCTION

Sequence stratigraphy, which analyses stratigraphic framework in terms of sea level cycles, can be directly applied to the interpretation of coal formation in the paralic environment. In paralic coals three aspects of sequence stratigraphy are relevant:

1. The effect of transgression-regression (TR) cycles in peat accumulation and preservation.

2. The effect of global sea level cycles in coal formation.

3. Location of areas of maximum development of coal within the sequence stratigraphic framework.

TRANSGRESSION-REGRESSION CYCLES AND COAL FORMATION

As discussed by Diessel (1992), peat accumulation in coastal areas is controlled by: i) the ratio of clastic vs. organic accumulation, and ii) rise or fall of the water table which is directly controlled by the sea level.

The water table in the coastal areas can be equated with the sea level. During periods of low sea level (water table) plant debris cannot accumulate because of oxidation or erosion. Peat will accumulate with the rise of the sea level, but with continuing rise peat accumulation ultimately ceases with the drowning of the mire. During regression, peat accumulation and preservation are only possible if subsidence keeps pace with peat formation so that peat growth takes place under or close to the water table.

GLOBAL SEA LEVEL CYCLES

The rate of changes in sea level within global cycles of various orders can be compared with the rates of peat accumulation (0.1–1.0 m/ka) or more appropriately, the coal formation. It seems that the third-order glacio-eustatic cycles (Haq et al., 1988) are too fast (10–100 m/ka) and second order tectono-eustatic cycles are too slow (0.01–0.1 m/ka) to accommodate peat accumulation (Diessel, 1992). A combination of the two could result in a rate of sea level change just right for coal formation. Many coal seams are time-transgressive and therefore, their formation also depends upon rates of progradation rather than simply sea level changes.

MAXIMUM COAL DEVELOPMENT WITHIN THE SEQUENCE STRATIGRAPHIC FRAMEWORK

The most important aspect of the sequence stratigraphy of coal is predicting the position of maximum likelihood of occurrence of thick seams in a cluster. Within a Type 1 sequence, such positions have been identified as within the lowstand systems tract (LST) and both highstand systems tract (HST) and transgressive systems tract (TST) on either side of the maximum flooding surface (MFS). In a Type 2 sequence such a position has been located in the shelf margin systems tract (SMST) (Diessel, 1992).

SEQUENCE STRATIGRAPHIC MODEL OF COAL DEVELOPMENT

Summarizing studies related to Cretaceous coals from the Western Interior Seaway, Cross (1988) presented a sequence stratigraphic model (Fig. 1) of coal formation. Major coal seams are concentrated at two turnaround points: 1) maximum regression to transgression (LST), and 2) maximum transgression (MFS) to regression (HST). Recently, Hamilton and Tadros (1994) found that the Permo-Carboniferous coal seams of Australia are located at sequence boundaries, as defined by Galloway (1989). However, according to the Exxon terminology (Van Wagoner et al., 1990), these are

maximum flooding surfaces. The MFS being hiatal surfaces marking the ends of depositional episodes (Frazier, 1974), record periods of nondeposition of clastics (Fig. 2), and are ideal times for peat accumulation. Diessel (1992) constructed a sequence stratigraphic model (Fig. 3) of coal from major coal occurrences around the world. The model not only shows favourable locations of coal seams within a sequence, but also, on a smaller scale, their position within individual parasequences.

Major features of the sequence stratigraphy of coal are the following:

1) Maximum development of coal takes place at or near the MFS because during change-over from maximum transgression to regression the movement of the shoreline is slow enough for accumulation of thick seams within vertically stacked parasequences.

2) Within a parasequence, coals may form both at the base (transgression) or at the top (regression). Two parasequences might share a seam formed during a minor TR cycle.

3) The same seam, followed landward or seaward, might be successively overlain by marine, transitional and continental roof rocks.

4) Seams formed within the TST are more likely to have marine roof rocks than those formed within the HST.

TRANSGRESSIVE AND REGRESSIVE (TR) COAL SEAMS

The effects of TR cycles on coal seams are documented by coal seam splits and chemical, petrological and palynological characteristics which are distinctive for transgressive and regressive settings. Coal seam splits form whenever there is a change-over from transgression to regression or regression to transgression. Minor splits might also occur within a parasequence recording higher order TR cycles.

Transgressive and regressive seams also differ by their typical signatures in a vertical profile of chemical and petrological properties. Ratios of H/C, Vitrinite/Inertinite, S%, Tissue Preservation Index (TPI) and Gelification Index (GI) are major indicators. Palynology also records the succession of flora within a coal seam and might indicate salinity changes in the environments which would be distinctive for transgressive and regressive seams. Detailed stratigraphic analysis integrated with chemical, petrological and palynological profiles of coal seams are therefore essential tools for sequence stratigraphy of coal seams.

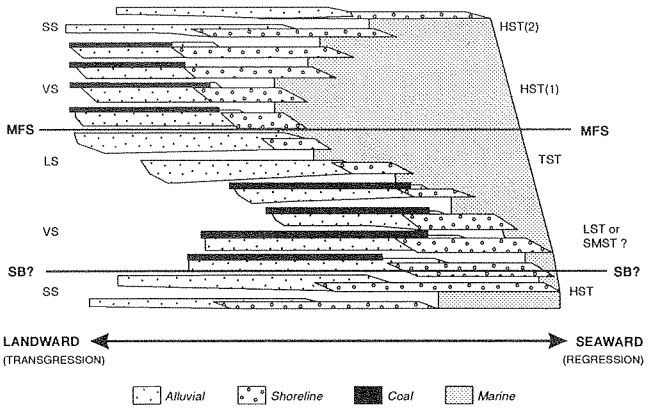

Figure 1. *Coal seams in a sequence stratigraphic framework (modified from Cross, 1988). In his original diagram, Cross only related coals to stacking patterns such as: SS, seaward-stepping; LS, landward stepping; and VS, vertically stacked. The following sequence stratigraphic terminology was put in by the present author: MFS, maximum flooding surface; SB, sequence boundary; LST, lowstand systems tract; SMST, shelf margin systems tract; TST, transgressive systems tract; and HST, highstand systems tract.*

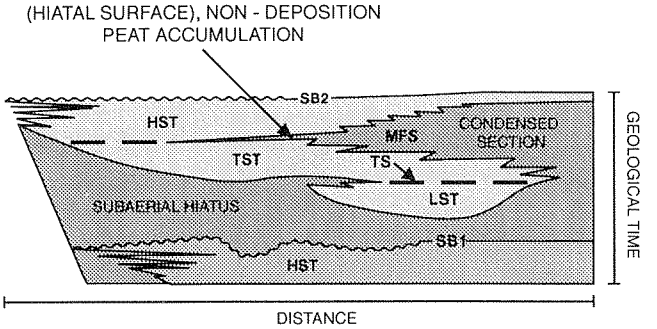

Figure 2. *Relation between the maximum flooding surface (MFS), peat accumulation, clastic nondeposition and condensed section based on the model of Frazier (1974) and Galloway (1989). Legend same as in Figure 1.*

THE MANNVILLE CASE STUDY

The Medicine River (MR) coal seam belonging to the Lower Cretaceous Mannville Group was chosen for this study as a part of the Coal Bed Methane project of the

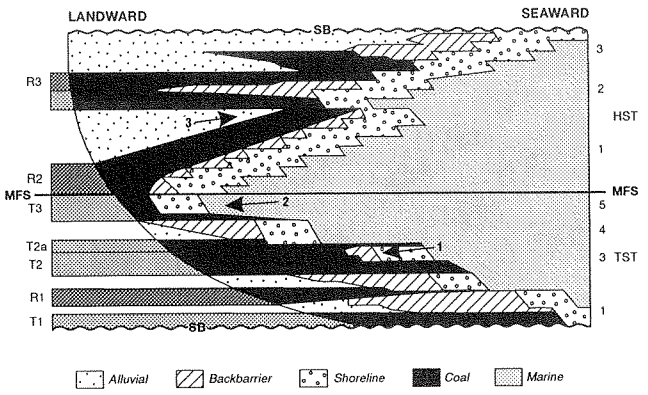

Figure 3. *Diessel's (1992) summary of sequence stratigraphic relations of paralic coals within a Type 1 sequence. Numbers 1 to 5 against the TST and the HST columns refer to individual parasequences. R1 to R3 and T1 to T3 are regressive and transgressive coals within a parasequence. Numbered arrows are location of coal seam splits: 1) within a parasequence: transgression–transgression; 2) within a sequence: transgression–regression; and 3) within a parasequence: regression–transgression. Note that a coal seam (T2a) may be successively overlain by alluvial, back barrier and marine roof rocks as it is traced seaward.*

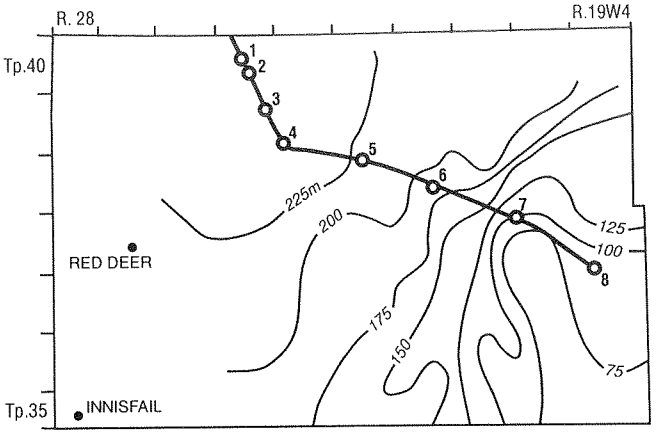

Figure 4. *Isopach map of the Mannville Group in the study area. Note the southeastward thinning trend toward a paleotopographic high.*

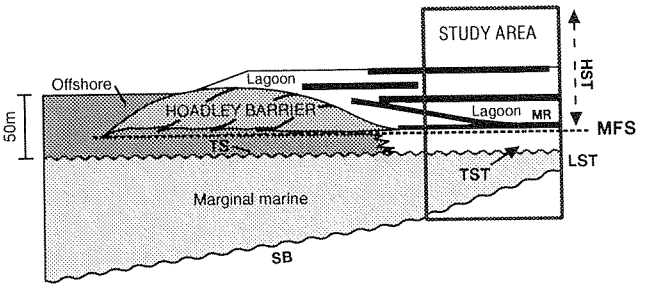

Figure 5. *Paleoenvironmental setting of the study area shown in a NW–SE cross-section with a sequence stratigraphic interpretation. MR is the Medicine River coal seam. Compare the boxed area to the stratigraphic cross-section shown in Figure 6.*

Geological Survey of Canada in the target area (Twp. 35-40, R19W4-R25W4) near Red Deer. Mannville strata in this area thin toward the southeast (Fig. 4) approaching a paleo-topographic high. Paleoenvironmentally, the area is located behind the Hoadley barrier bar (Fig. 5) in a coastal swamp-lagoon-tidal flat setting. A stratigraphic cross-section (Fig. 6) reveals that the MR coal seam, which splits into two toward the northwest, is located above the MFS which overlies a succession of coarsening-upward parasequences with a retrogradational stacking pattern forming the transgressive part of the sequence lying above the regional sub-Cretaceous unconformity or the sequence boundary. These parasequences onlap onto the paleohigh toward the southeast. The marine influence in the shale split which contains the brackish dinoflagellate *Balmula* and pyritized *Skolithos* burrows suggests that the upper MR seam is regressive and the lower one is transgressive. A thinner coal seam, called the "Glauconitic Coal", forms the basal transgressive part of a parasequence.

Cored intervals of both the upper regressive and the underlying transgressive MR seams and the transgressive Glauconitic coal seam in three wells were analyzed in detail for their chemistry, maceral content (Fig. 7) and palynology.

COAL SEAM CHARACTERISTICS

Upper Medicine River Coal

The seam was sampled in thirteen 30 cm thick intervals from Well 4 (Fig. 6) representing the entire coal/shale interval of the upper Medicine River coal zone. Petrographic analysis indicates a detrital nature of the coal, where macerals such as vitrodetrinite and inertodetrinite account for more than 50 Vol%, except at the very base of the coal zone. Alternating coal and shale intervals in this regressive seam indicate fluctuating water levels during peat accumulation. The preserved organic matter was subjected to severe degradation as evidenced by very low tissue preservation indices and high values of vitrodetrinite and inertodetrinite, indicating oxidation and erosion near the surface.

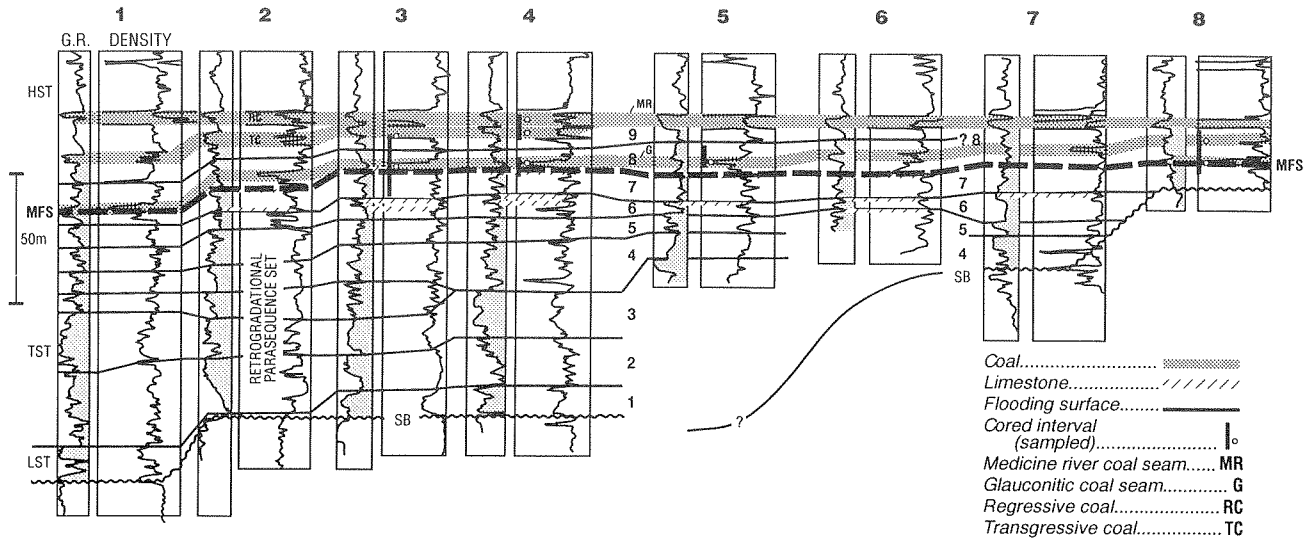

Figure 6. *Stratigraphic cross-section of the Mannville Group containing the Medicine River coal seam in the study area. Location of the line of cross-section is shown in Figure 4. Well locations: 1) 16-21-41-25W4; 2) 16-15-41-25W4; 3) 10-25-25-40-25W4; 4) 6-7-40-24W4; 5) 10-33-39-23W4; 6) 10-20-39-22W4; 7) 8-36-38-21W4; and 8) 6-6-38-19W4.*

The palynomorphs in this seam demonstrate an initial regressive succession (Fig. 8A) back to dry and wet marshes alternating with ponding intervals. This is overlain by forested swamp and then brackish pond environments followed by a restricted marine shale.

Lower Medicine River Coal

Only the lower 1 m of the seam was cored and was sampled in 17 consecutive column samples from Well 3 (Fig. 6) to study the petrographic and chemical variations from the base upward. The lithotype-log shows frequent changes in the brightness of the coal (Fig. 7A). Dull lithotypes indicate a larger input of mineral matter (Dm) and/or inertinite (Di), which are low in the brighter lithotypes (BB, B) (Fig. 7A). During accumulation of the peat, five major episodes of flooding occurred, which resulted in a significant influx of mineral matter (Fig. 7A). The vitrinite/inertinite-ratio, a relative measure of the height of the water table during accumulation of the peat, is highly variable throughout the seam. The top of the investigated interval is characterized by an initial low ratio above the parting, and much wetter conditions near the top. Proportions of structured to detrital macerals and corresponding tissue preservation indices (Diessel, 1992) determined for individual lithotypes are highly variable (0.1–4.3). The sulphur distribution within the Lower Medicine River coal seam is also variable. The values range from 0.13 to 3.45 wt.%. The lowest sulphur values were recorded in intervals rich in mineral matter, suggesting a predominantly organic affinity of the sulphur. Hydrogen Indices derived from Rock-Eval pyrolysis are highly variable throughout the seam ranging from 114 to 297 mg hydrocarbons/g TOC.

Although stratigraphic analysis indicates this seam to be transgressive, petrographic and chemical parameters are highly variable without showing any typical transgressive signature. It should be noted, however, that only the lower one-quarter of the seam was available for analysis. The high sulphur value at the base of the seam may indicate brackish conditions during peat accumulation.

The palynomorphs in this seam demonstrate a transgressive succession (Fig. 8B) from periodically dry *Gleichenia* marsh, through *Taxodium* swamps, to freshwater marsh with zygnemataceous algae, and finally to a restricted marine incursion in a shale parting.

Glauconitic Coal

The seam was sampled in 7 consecutive column samples from Well 3 (Fig. 6). The lithotype log shows a high variability in dull and bright bands throughout the seam (Fig. 7B). The lower part of the seam (approximately 10 cm above base) is characterized by the predominance of vitrinite macerals and high vitrinite/inertinite ratios (Fig. 7B). The top part of the

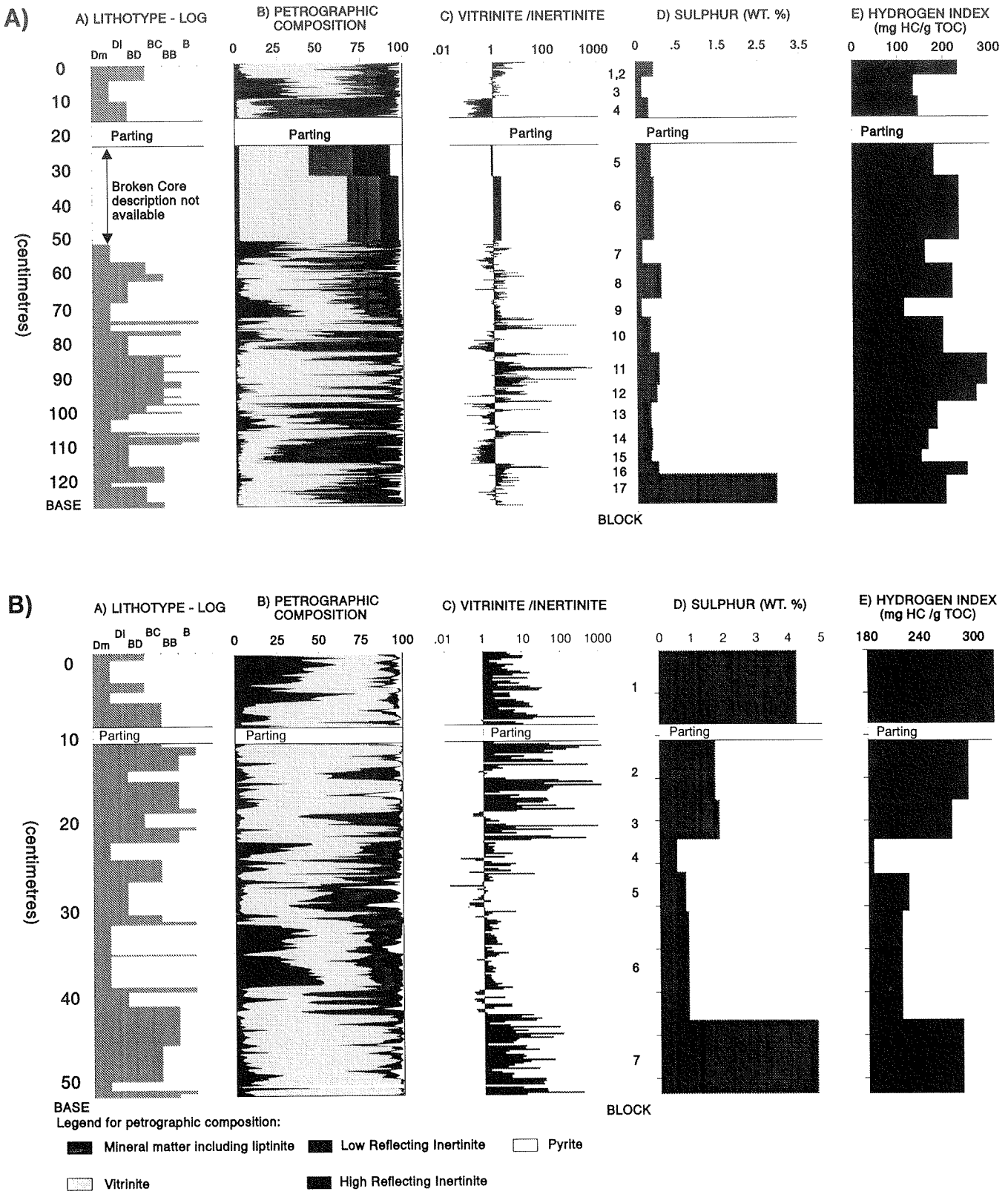

Figure 7. *Chemical and petrological profiles of the coal seams studied from cored intervals:* ***A)*** *Basal part of the Medicine River (MR) coal seam in Well 3 in Figure 6. This seam has been interpreted as a transgressive seam;* ***B)*** *The entire thickness of the Glauconitic coal seam in Well 3 in Figure 6. The sulphur content, hydrogen index and the vitrinite/inertinite ratios show a typical transgressive signature.*

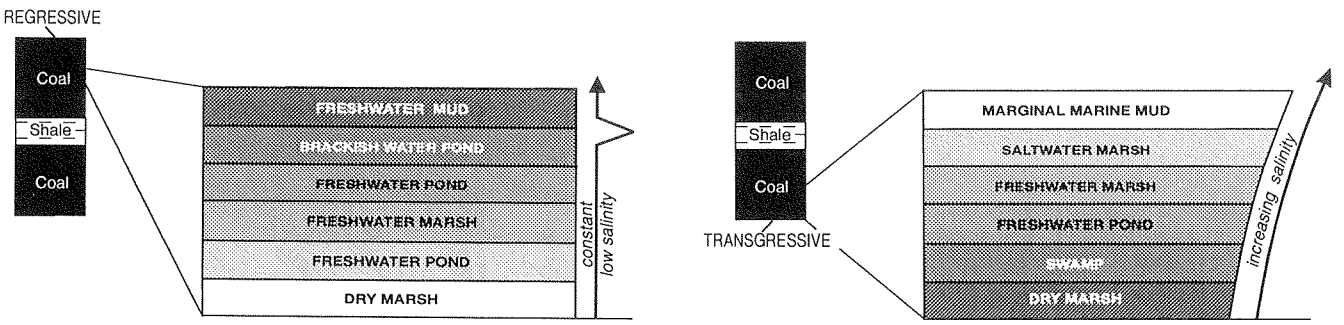

Figure 8. *Sequence of floral development in the Medicine River coal seam as inferred from palynological assemblages:* ***A)*** *Regressive coal in Well 4;* ***B)*** *Transgressive coal in Well 3.*

seam (0–10 cm) shows a large influx of mineral matter and a high vitrinite/inertinite ratio prior to the drowning of the mire (Fig. 7B). Sulphur contents are highest in seam intervals close to the top and base (4.2 and 4.8 wt.%, respectively, Fig. 7B), indicating a brackish/marine influence during initial peat accumulation and due to the drowning of the mire. Lowest sulphur content (0.54 wt.%) occurs in the center portion of the seam (Fig. 7B). Hydrogen Indices show a similar pattern (Fig. 7B). Highest values occur at base and top of the seam reflecting the higher overall vitrinite contents in these seam intervals. Lowest hydrogen indices occur in the central portion of the seam, where larger concentrations of inertinite macerals indicate a somewhat drier depositional environment.

As the entire thickness of this transgressive seam was available for analysis, the typical transgressive signature of the seam is revealed by the following parameters which increase toward the top of the seam: sulphur, pyrite, vitrinite and hydrogen (hydrogen index).

The aquatic palynological assemblages throughout this seam are highly impoverished. The terrestrial assemblages are marked predominantly by two forms, the gymnosperm *Taxodium* and the fern *Gleichenia*, dividing the coal into two similar successions changing from periodically dry *Gleichenia* marsh to *Taxodium* swamps with anemiacean ferns. This suggests a trend toward a warmer and more humid climate. Near the top of the coal, high abundances of freshwater algal cysts suggest a wet marsh environment.

ACKNOWLEDGMENTS

The authors wish to acknowledge contributions from the following personnel of the Institute of Sedimentary and Petroleum Geology (ISPG): M. Tomica and K. Pratt of the coal and organic petrology laboratories for sample preparation and image analysis; Dr. D.A. Leckie for critically reading the manuscript; and Dr. V. Stasiuk for his useful comments. The coals were analyzed by Dr. D. Marchioni of Petro-Logic services.

REFERENCES

Cross, T.A.
1988: Controls on coal distribution in transgressive-regressive cycles, Upper Cretaceous, Western Interior, U.S.A. *In* Sea level change: an integrated approach, C.K. Wilgus, B.S. Hastings, C.G. Kendall, H.W. Posamentier, C.A. Ross, and J.C. Van Wagoner (eds.). Society of Economic Paleontologists and Mineralogists, Special Publication 42, p. 371–380.

Diessel, C.F.K.
1992: Coal-bearing deposition systems. Springer-Verlag, Berlin, Germany, 721 p.

Frazier, D.E.
1974: Depositional episodes: their relationship to the Quaternary stratigraphic framework of the northwestern portion of the Gulf Basin. University of Texas at Austin, Bureau of Economic Geology, Geological Circular 74-1.

Galloway, W.E.
1989: Genetic stratigraphic sequences in basin analysis I: architecture and genesis of flooding-surface bounded depositional units. American Association of Petroleum Geologists Bulletin, v. 73, p. 125–142.

Hamilton, D.S. and Tadros, N.Z.
1994: Utility of coal seams as genetic stratigraphic sequence boundaries in nonmarine basins: an example from the Gunnedah Basin, Australia. American Association of Petroleum Geologists Bulletin, v. 78, p. 267–286.

Haq, B., Hardenbol, J., and Vail, P.R.
1988: Mesozoic and Cenozoic chronostratigraphy and cycles of sea level change. *In* Sea level change: an integrated

approach. C.K. Wilgus, B.S. Hastings, C.G. Kendall, H.W. Posamentier, C.A. Ross, and J.C. Van Wagoner (eds.). Society of Economic Paleontologists and Mineralogists, Special Publication 42, p. 71–108.

Van Wagoner, J.C., Mitchum, R.M., Campion, K.M., and Rahmanian, V.D.
1990: Siliciclastic sequence stratigraphy in well logs, cores and outcrops. American Association of Petroleum Geologists, Methods in Exploration, No. 7.

ORIGIN AND ENGINEERING IMPLICATIONS OF DEEP ICE-BEARING PERMAFROST, CANADIAN BEAUFORT SHELF

S. Blasco

Geological Survey of Canada, P.O. Box 1006, Dartmouth, Nova Scotia B2Y 4A2

The late Neogene to Holocene Beaufort–Mackenzie sedimentary basin consists of a succession of sediments deposited in ever decreasing water depths. At the basin depocentre located at mid shelf water depths, this succession, identified as the Iperk Sequence, exceeds 3500 m in thickness (Fig. 1). The upper 1000 m of this Sequence is of Quaternary age and consists primarily of delta front to delta top sediments which spatially constitute a broad coastal plain section. This coastal plain section thins significantly east, west, north and south across the Beaufort Shelf (Blasco et al., 1990).

For the eastern shelf area, the upper 50 m of this thick coastal plain section consists of laterally extensive regressive fluvial outwash sands overlain by thin transgressive interbeds of sand, silt and clay and thin surficial marine muds at seabed (Blasco et al., 1990). The regressive fluvial sands were deposited subaerially in a paralic environment. The source was sediment laden meltwaters discharging from the stagnant or retreating late Wisconsinan ice front further to the south. Rapid deposition of the sands was accompanied by the contemporaneous aggradation of permafrost. Pore ice, ice lenses, veins and layers formed in the sands during deposition. Rising Holocene sea level truncated and eroded the ice-bearing sand plain, generated a well defined regional unconformity and deposited the thin marine transgressive interbeds and surficial marine muds. Warm Mackenzie river waters partially degraded the ice-bearing permafrost in the fluvial sands.

This ice-bearing fluvial sand/marine interbed and mud sequence separated by a transgressive unconformity represents a typical regressive/ transgressive cycle associated with glacial/interglacial (or stadial/ interstadial) periods for the Beaufort shelf. Successive ice advances and retreats in the western Arctic from late Pliocene to Holocene would lead to the deposition of a series of these regressive/transgressive cycles at the depocentre of the subsiding Beaufort–Mackenzie sedimentary basin. The thick coastal plain section referred to above would represent the net accumulation of a sequence of regressive fluvial sand deposits and transgressive marine mud deposits.

In 1988, Gulf Canada Resources Limited completed a 500 m deep borehole in 32 m of water near the basin depocentre (Fig. 1). Chilled drilling muds were used with a wireline drilling system to recover ice-bearing sediment samples with minimal thermal and sediment disturbance. The GSC participated in the borehole logging program on site and was provided with a suite of recovered samples (maintained at approximately in situ temperature) for ice fabric analysis, porewater salinity and geochemistry (oxygen and hydrogen

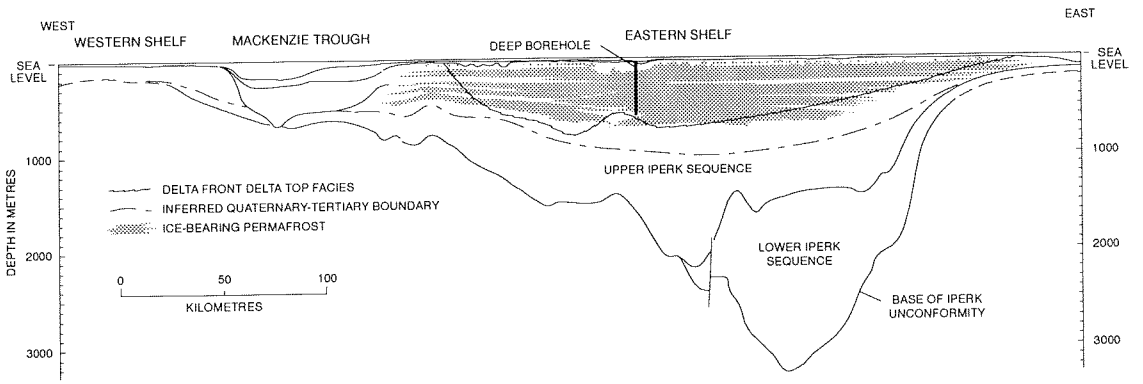

Figure 1. *Schematic east-west cross-section of the Canadian Beaufort Shelf: seabed to base of Iperk Sequence.*

isotopes), sedimentology, biostratigraphy and macrofossil analysis. As the deep borehole sampling started at the top of the ice-bearing permafrost zone and not at the seabed, an engineering borehole collected previously at the site by Gulf Canada was used to complete the shallow section of the shelf stratigraphy.

Based on the field logs and results of the above analyses of borehole samples, 8 regressive/transgressive fluvial sand/marine mud cycles with associated unconformities were recognized downcore (Fig. 2). Sand units showed primary fluvial sedimentary structures, low salinities, fluvial-sourced porewaters, freshwater pollen assemblages, terrestrial macrofossils at base, and generally high ice contents (as pore ice, lenses, layers, and vein ice). The mud units exhibited both uniform and interbedded lithologies, higher salinities, estuarine to shallow marine pollen and microfossil assemblages, and low to high ice contents (as pore ice, lenses, layers and vein ice). Porewater geochemistry indicated a marine source. Ice fabric analysis for both the sand and mud units suggest nearsurface formation processes for the segregation ice, similar to growth processes observed in the modern subaerial Mackenzie delta today. In addition, the ice fabric indicated rapid formation with no subsequent deformation.

Using the known stratigraphy of the upper 50 m of sediment as a model representing the most recent late Wisconsinan–Holocene regressive/transgrressive glacial/interglacial cycle, the 8 sand/mud sediment sequences observed downcore may represent a succession of regressive/transgressive glacial/interglacial or stadial/interstadial deposits.

During the extensive periods of subaerial exposure of the aggrading and prograding regressive fluvial sand deposits, negative isotherms -10° to -15°C (J. Brigham-Grette, pers. comm., 1994) migrated downward, freezing the sands and the underlying marine interbeds and muds. During high sea level stands (interglacials or interstadials) the shelf was flooded. Negative seabottom temperatures (-1°C) insulated bottom sediments and inhibited degradation of the ice-bearing sediments at depth. Successive glaciations and stades resulted in repeated subaerial exposure and successive cycles of permafrost aggradation across the shelf. Ice-bearing sediments accumulated on the shelf layer by layer to a thickness of 700 m (Fig. 1), and are preserved through time. Low heat flow from below through the Beaufort–Mackenzie Tertiary sedimentary basin (11 000 m of sediment) has yet to melt the ice in the upper 700 m of the shelf.

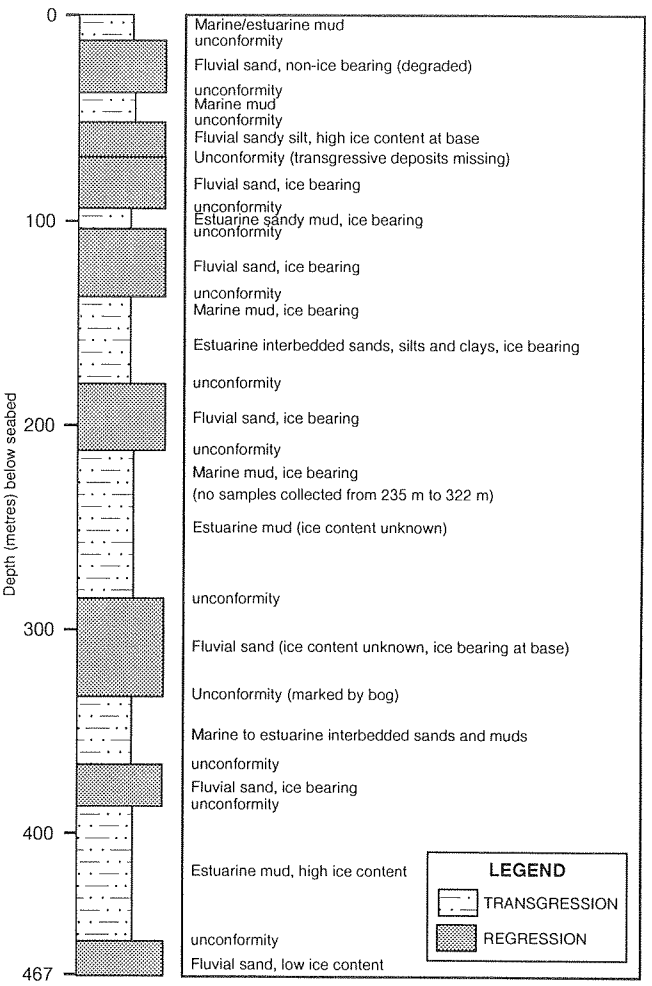

Figure 2. *Interpreted shelf stratigraphy.*

From an engineering geology perspective, the above stratigraphy and permafrost history is, in contrast to present assumptions, feeding design concepts for oil production through thick ice-bearing permafrost. Present engineering models regard the Quaternary sediment wedge as a single thick layer consisting of a fine grained saline sediment unit deposited in a marine environment. This wedge was normally consolidated, then subsequently subaerially exposed to permafrost aggradation. These factors combine to generate low sediment ice contents. Such a geological history would suggest that under thawing conditions around a production well (caused by the flow of hot oil), the amount of thaw settlement would be minimal.

However, current understanding of the shelf stratigraphy and origin of deep permafrost suggests this engineering design model to be incorrect. The thick Quaternary sediment wedge consists of layers of

ice-bearing sands interlayered with low to high ice-bearing muds to depths greater than 500 m below seabed. Rapid deposition of the sand units with contemporaneous aggradation of permafrost would suggest that these sands are underconsolidated and may have high ice contents. This multilayered ice-bearing permafrost model suggests significant vertical as well as lateral variations in ice content. At the basin depocentre, significant differential thaw settlement may occur around a production well. East and west of the depocentre, sediment units thin out and ice contents are reduced.

The above discussion represents a summary of research results to date. Borehole sample analyses, data synthesis and interpretation are presently being completed to finalize the project. Contributors to the 500 m deep borehole study include: E. Davies (palynology, macrofossils), A. Bertie (macrofossils), H. Helenes and C. Schroeder (foraminifera), K. Edwardson (sedimentology), W. Pollard (ice fabric), F. Michel (porewater salinity and geochemistry), and P. Harrison (compilations). EBA Engineering Consultants Ltd. conducted the borehole logging and sampling program including permafrost descriptions and laboratory testing. Chris Graham provided access to borehole data and samples and helpful advice.

REFERENCE

Blasco, S.M., Fortin, G., Hill, P.R., O'Connor, M.J., and Brigham-Grette, J.

1990: The late Neogene and Quaternary stratigraphy of the Canadian Beaufort continental shelf. *In* The Arctic Ocean Region, A. Grantz, L. Johnson and J.F. Sweeney (eds.). The Geology of North America, v. L, p. 491–502.

STRATIGRAPHY AND STRUCTURE OF MEIGHEN ISLAND, CANADIAN ARCTIC ARCHIPELAGO

T.A. Brent and A.F. Embry

Institute of Sedimentary and Petroleum Geology, Geological Survey of Canada
3303-33rd Street N.W., Calgary, Alberta T2L 2A7

INTRODUCTION

Meighen Island is a small (750 km^2) island located west of Axel Heiberg Island. The island is on the margin of the Arctic Continental Terrace Wedge and the bedrock consists entirely of unconsolidated clastics of the Pliocene Beaufort Formation. In the early 1970s Dome Petroleum shot 500 km of seismic reflection on the island and drilled one well, Dome Crocker I-53, to a depth of 3570 m (Fig. 1). The seismic data were recently reprocessed and interpreted in conjunction with the well data as part of a regional study of the northeast portion of the Arctic continental shelf. This extended abstract presents the preliminary interpretations of the seismic and well data.

STRATIGRAPHY

Crocker I-53

Crocker I-53, drilled on northeast Meighen Island, encountered 2575 m of conglomerate, sandstone and carbonaceous siltstone and shale assigned to the Beaufort Formation and Eureka Sound Group overlying 625 m of shale, siltstone and very fine grained sandstone of the Kanguk Formation. These strata represent the edge of the continental terrace wedge and range in age from Pliocene to Late Cretaceous. Beneath the Kanguk Formation, 400 m of shale, siltstone and very fine grained sandstone of the Carnian (Upper Triassic) Hoyle Bay Formation were drilled. Diabase

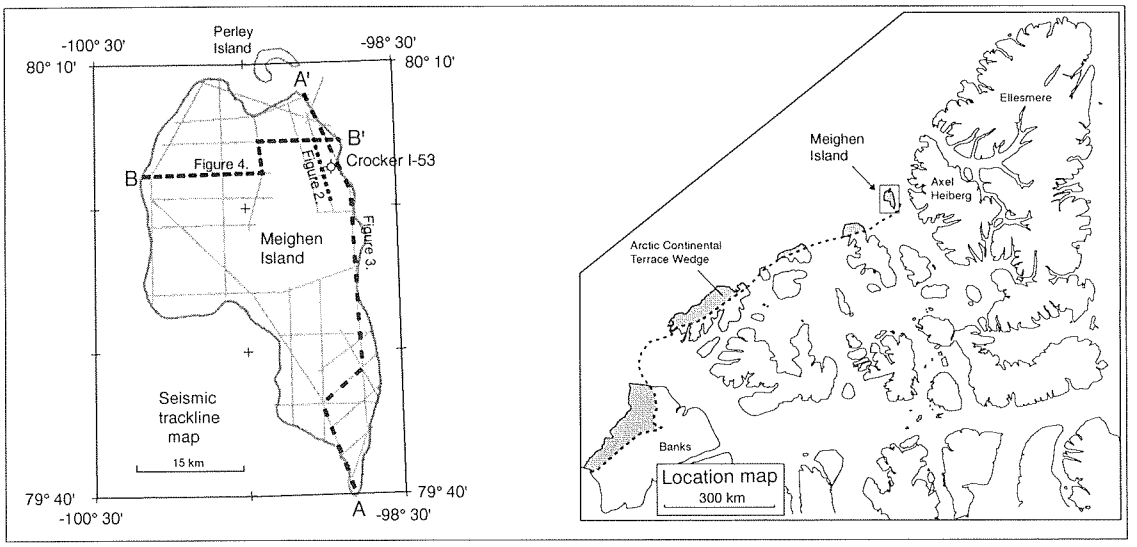

Figure 1. *Seismic trackline and location maps of Meighen Island.*

sills of Early Cretaceous age intrude the Hoyle Bay strata which were deposited on the northwest flank of the Sverdrup Basin. The seismic data of the line on which the well is located are of poor quality due to an on-strike normal fault so a nearby dip line has been used to tie the seismic to the well data (Fig. 2). It is interpreted that the contact between the Kanguk Formation and the underlying Triassic strata in the well is a fault rather than an unconformity (Fig. 2).

Seismic sequences

Figures 2, 3, and 4 show where three seismic sequence boundaries have been recognized on seismic data, allowing the succession to be divided into four seismic sequences. Sequence 1 comprises the oldest strata and includes the intruded Carnian Hoyle Bay Formation encountered in Crocker I-53. This sequence likely comprises thick Triassic shales and siltstones of the Blind Fiord (Lower Triassic), Murray Harbour (Middle Triassic) and Hoyle Bay (Upper Triassic) formations. On southern Meighen Island, sequence 1 exhibits a seismic character that includes discontinuous high amplitude events (Fig. 3) interpreted as Cretaceous diabase sills within the Triassic strata.

The sequence boundary which caps sequence 1 is distinguished by the occurrence of onlapping beds and, in a few cases, angular truncation of strata below the

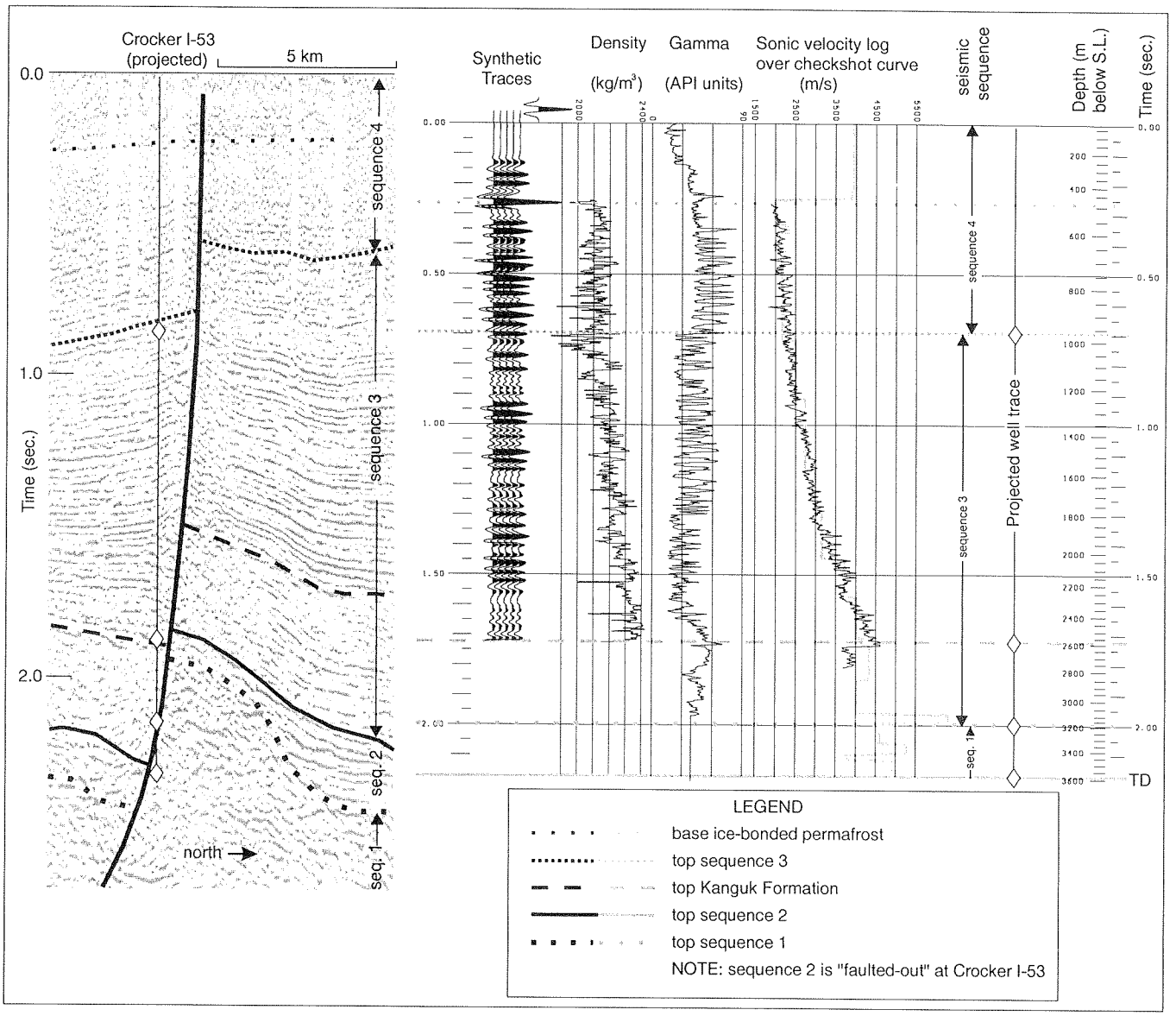

Figure 2. *Dome Arctic Ventures Crocker I-53, well data and correlation to dip line to west.*

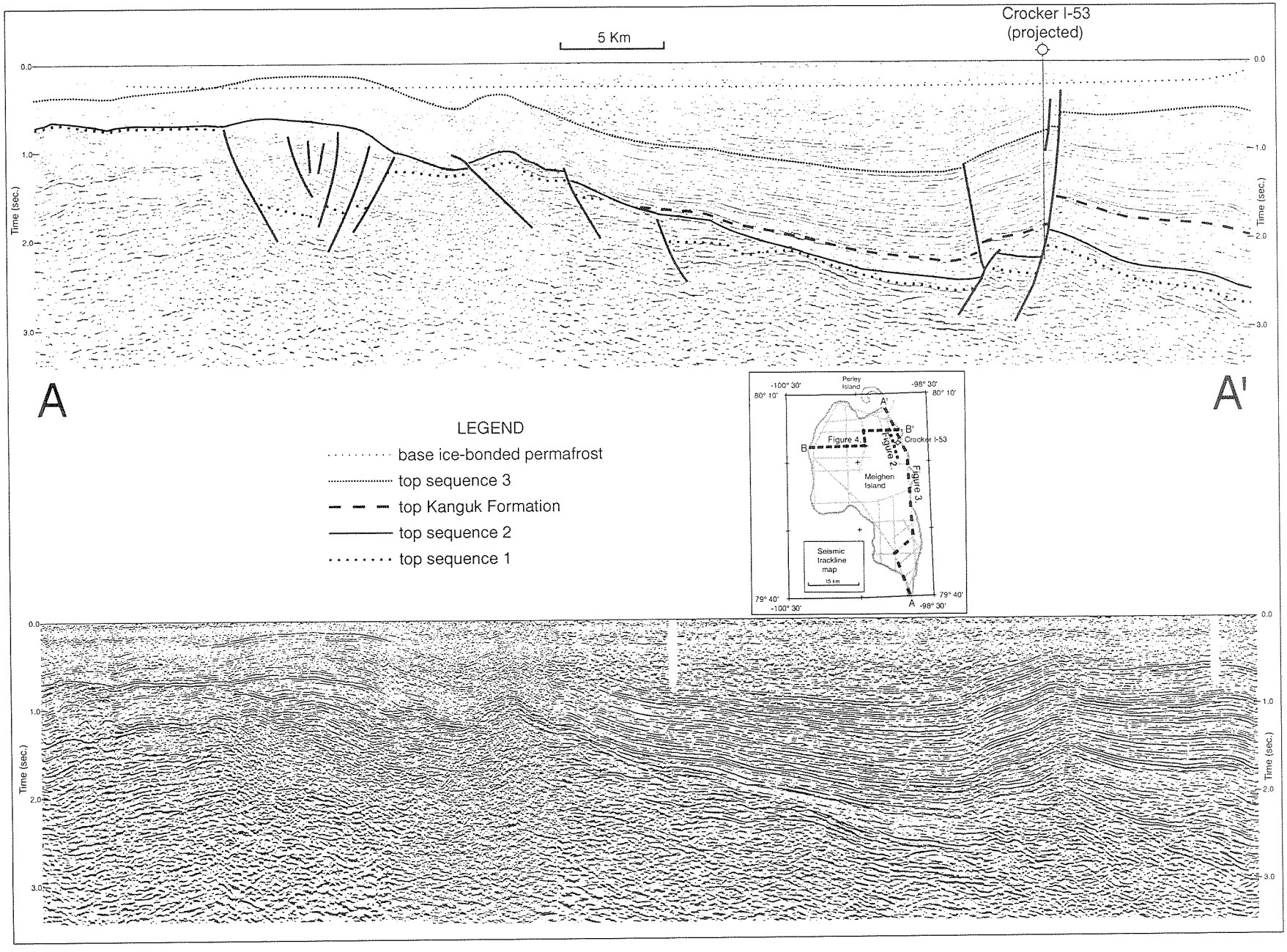

Figure 3. *Interpreted and uninterpreted migrated seismic profiles.*

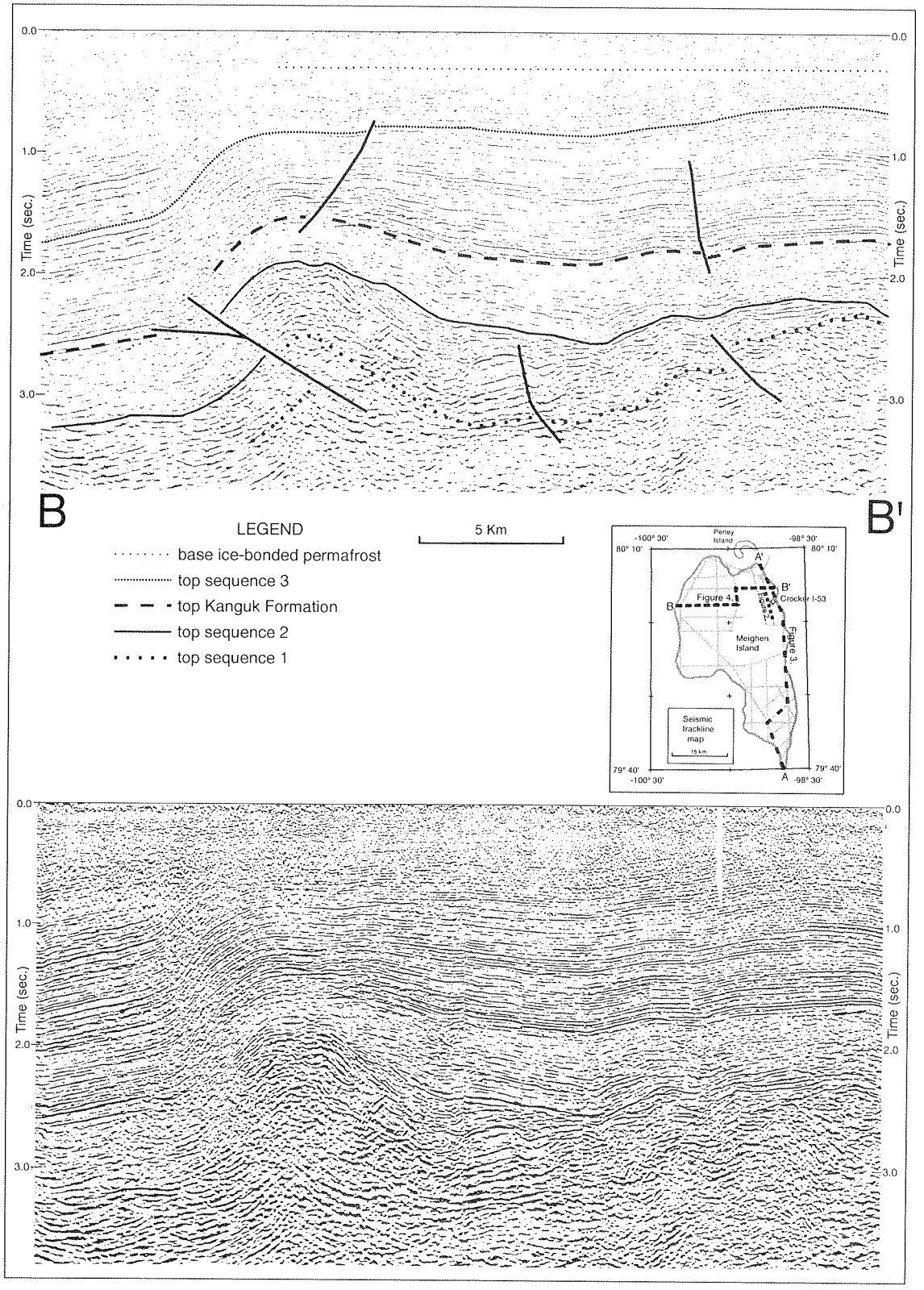

Figure 4. *Interpreted and uninterpreted migrated seismic profiles.*

boundary. The age of the sequence boundary is not well established because it was not penetrated in the well due to faulting (Fig. 2). Presently we interpret the boundary as the base Norian (Upper Triassic) sequence boundary, a widespread 2nd order sequence boundary which exhibits onlap and truncation on the flanks of the Sverdrup Basin (Embry, 1991).

Sequence 2 is generally seismically reflective and is up to 2100 m thick. These strata are interpreted as the uppermost Triassic to Lower Cretaceous succession of the Sverdrup Basin which are up to 3000 m thick on adjacent northwestern Axel Heiberg Island. The main lithologic units of this sequence are the argillaceous Barrow Formation, the arenaceous Heiberg Formation, the argillaceous Savik Group, and Mackenzie King Formation, the arenaceous Isachsen Formation, and the argillaceous Christopher Formation. The thickness of this sequence varies greatly over the island (Figs. 3, 4, 5) due to truncation and some of the thickest occurrences are located in grabens on southern Meighen (Fig. 3).

The upper boundary of sequence 2 is a major unconformity which exhibits angular discordances and the truncation of numerous normal faults (Figs. 3, 4). This sequence boundary can be confidently correlated with the widespread mid-Cenomanian (mid-Cretaceous) 1st order sequence boundary which marks the end of seafloor spreading in the adjacent oceanic Canada Basin (Embry and Dixon, 1994).

Sequence 3 consists of two seismic units. The lower unit is characteristically reflection free and can be correlated with the argillaceous Kanguk Formation (Figs. 2, 3, 4). This unit thins and eventually pinches out on southern Meighen (Fig. 3). The upper unit is very reflective and correlates with the interbedded sandstone, siltstone and shale of the Eureka Sound Group (uppermost Cretaceous–Eocene?). Sequence 3 ranges in thickness from 460 m in the south to 3200 m in the north (Fig. 5).

The upper boundary of sequence 3 shows both truncation below and onlap above. The age of the boundary is not well known and is tentatively correlated with the mid-Eocene 1st order sequence boundary of eastern Axel Heiberg Island (Ricketts, 1994). The strata of sequence 4 consist mainly of fluvial sandstones and conglomerates with thin siltstone and shale units and are assigned to the Buchanan Lake Formation (Eocene) and the Pliocene Beaufort Formation. This sequence thickens northwestward to a maximum of 2700 m (Fig. 5).

STRUCTURE

Normal faults cut sequences 1 and 2 and are commonly truncated at the mid-Cenomanian unconformity. The faults trend east–west to northeast–southwest and likely developed during the Lower Cretaceous when rifting and volcanism were occurring in the Sverdrup Basin. A final episode of faulting and widespread uplift occurred in earliest Late Cretaceous. A few of the normal faults extend up through sequence 3 into sequence 4. A north-plunging anticline, cored by a westward-directed thrust fault, occurs on central Meighen and coincides with a mid-Cretaceous high (Fig. 4). Portions of sequence 3 and 4 thin on the crest of the structure indicating growth during the early Tertiary. A similar timing of tectonic uplift of southern Meighen can be inferred from thinning and onlap patterns (Fig. 3). This deformation, which culminated during deposition of sequence 4, is part of the Eurekan Orogeny (Paleocene–Oligocene).

REFERENCES

Embry, A.F.
1991: Mesozoic history of the Arctic Islands. *In* Innuitian Orogen and Arctic Platform: Canada and Greenland, H.P. Trettin (ed.). Geology Survey of Canada, Geology of Canada No. 3, p. 369–433.

Embry, A.F. and Dixon, J.
1994: The age of the Amerasian Basin. *In* Proceedings of the 1992 International Conference on Arctic Margins, D.K. Thurston and K. Fujita (eds.). United States Mineral Management Service Report 94–0040, p. 389–294.

Ricketts, R.D.
1994: Basin analysis, Eureka Sound Group, Axel Heiberg and Ellesmere islands, Canadian Arctic Archipelago. Geological Survey of Canada, Memoir 439, 119 p.

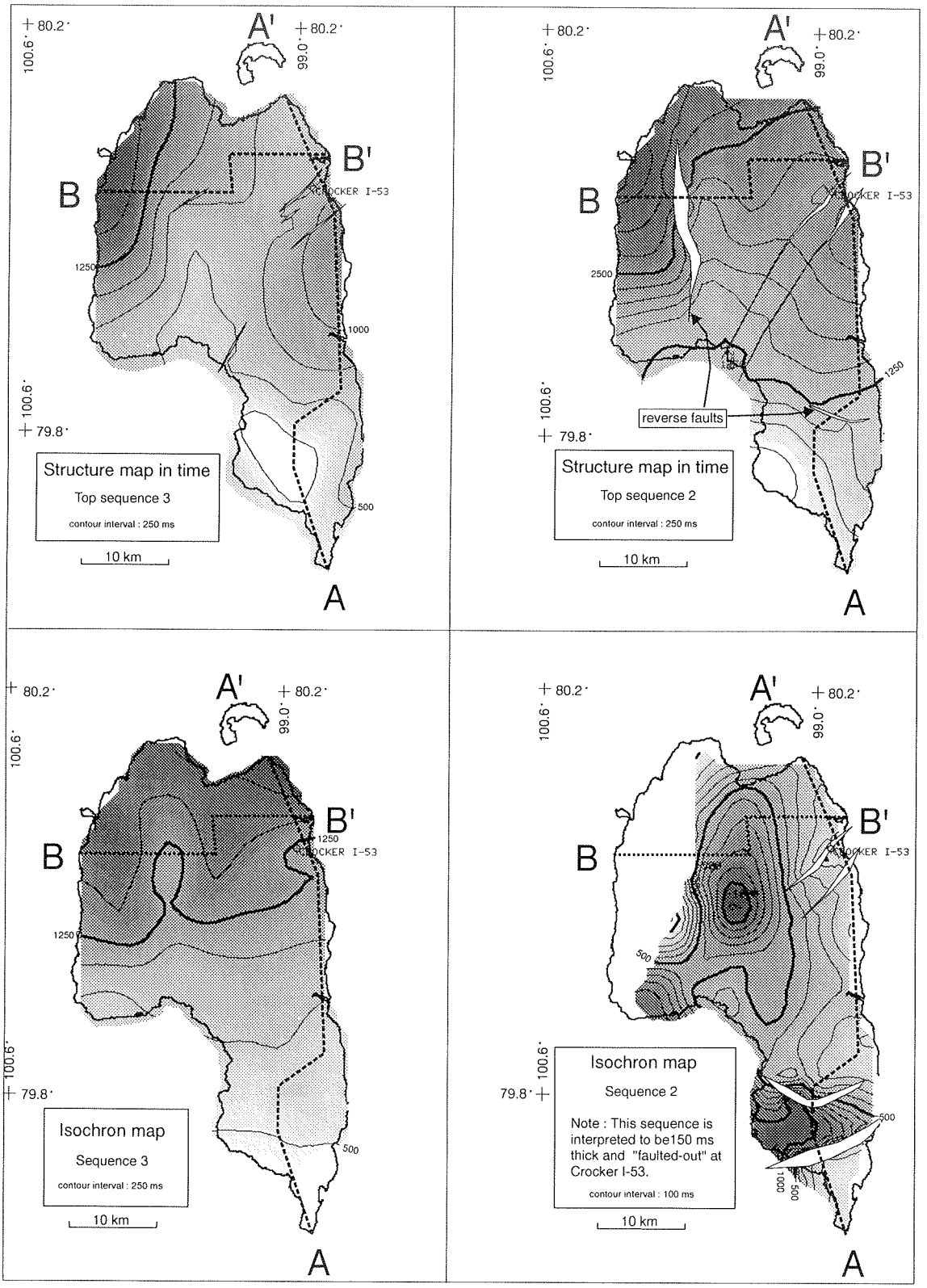

Figure 5. *Generalized subsurface maps in time for Meighen Island. Faults are normal, except where noted.*

TECTONIC INVERSIONS AND THEIR RELATIONSHIP TO HYDROCARBONS IN THE COLVILLE HILLS REGION, N.W.T.

D.G. Cook and B.C. MacLean

Geological Survey of Canada, 3303-33rd Street N.W., Calgary, Alberta T2L 2A7

INTRODUCTION

Seismic data from the Colville Hills region (Fig. 1) record three types of tectonic inversion. Of two that affect only Precambrian strata, one involves extensional half-grabens inverted as thrust faults, and the other involves a synclinal basin inverted as an anticline. The latter is truncated by the sub-Cambrian unconformity and has high risk hydrocarbon potential. A third type, of which the gas-bearing Tweed Lake anticline is an example, comprises a sort of double-inversion (compression to extension to transpression).

PETROLEUM POTENTIAL

The main exploration play in the Colville hills has been the basal Cambrian sands of the Mount Clark Formation. Three gas pools, Tedji Lake, Tweed Lake, and Bele (Fig. 1) have been discovered. Tweed Lake gas has a peculiar composition (mainly methane and nitrogen) and includes some condensate (Bever and MacIlreath, 1992). The National Energy Board (Price, 1993) reports recoverable reserves, calculated at 50% probability, as follows: Tedji Lake, 1014 M m^3 (36 BCF), Tweed Lake, 5055 M m^3 (179 BCF), and Bele, 4768 M m^3 (169 BCF). Bever and MacIlreath (1992) report 112 BCF in Tweed Lake.

Thermal maturation studies of Proterozoic well samples in the Northwest Territories revealed a 75 m shale interval in Mobil Belot Hills M-63 containing up to 1.4% organic carbon content at a maturity beyond the oil window but within the gas generation phase (Snowdon and Williams, 1986, p. 6). Although this shale was correlated with strata of the Mackenzie Mountains Supergroup (Aitken and Pugh, 1984), our current correlations would place it in much older strata, equivalent to the Dismal Lakes Group which is known to be older than the 1267 Ma Coppermine basalts and younger than the 1663 Ma Hornby Bay Group.

At present the relationship of hydrocarbons to inversions is purely geometric with no evidence of any genetic linkage. In fact two gas discoveries, Tedji K-24 and Bele O-35, are on structures which are products of simple reactivation, rather than inversion. Consequently we present the various types of inversion primarily as a contribution to our understanding of the geological history of the sedimentary basin. Nonetheless, the history of the gas-bearing Tweed Lake anticline and the development of long-wavelength anticlines truncated by the sub-Cambrian unconformity may interest hydrocarbon explorers.

STRATIGRAPHY AND TECTONIC HISTORY

Informal Precambrian subsurface assemblages (Hornby Bay, Dismal Lakes, and Copper Creek) are correlated (Cook and MacLean, in press) with formal units (Hornby Bay, Dismal Lakes, and Copper Creek groups) mapped on Coppermine Homocline (Ross and Kerans, 1989). Hornby Bay Assemblage is subdivided into three informal units (Basinal, Platformal, and Syntectonic) which are correlated with the surface Lady Nye, East River, and Kaertok formations. The region has been subjected to a number of compressional, extensional, transpressional, and epeirogenic events but a full discussion of the regional tectonic history and correlation rationale is beyond the scope of this paper and the reader is referred to Cook and MacLean (1992; in press) and MacLean and Cook (1992).

A number of events germane to this paper warrant special mention. Half grabens formed during Basinal Unit deposition were inverted during the Forward Orogeny. This orogeny generated structures in Hornby Bay and older rocks which were subsequently truncated by regional erosion and buried by sediments of the Dismal Lakes Assemblage. Post-Dismal Lakes extension produced half-grabens, some of which negatively inverted steeply dipping Forward Orogeny thrust faults. Some of those half-grabens were themselves mildly inverted by Laramide transpression to form certain faulted anticlines of the Colville Hills. At least one syntectonic synclinal basin, filled during the Forward Orogeny, was inverted as an anticline during Post-Copper Creek Assemblage long-wavelength folding.

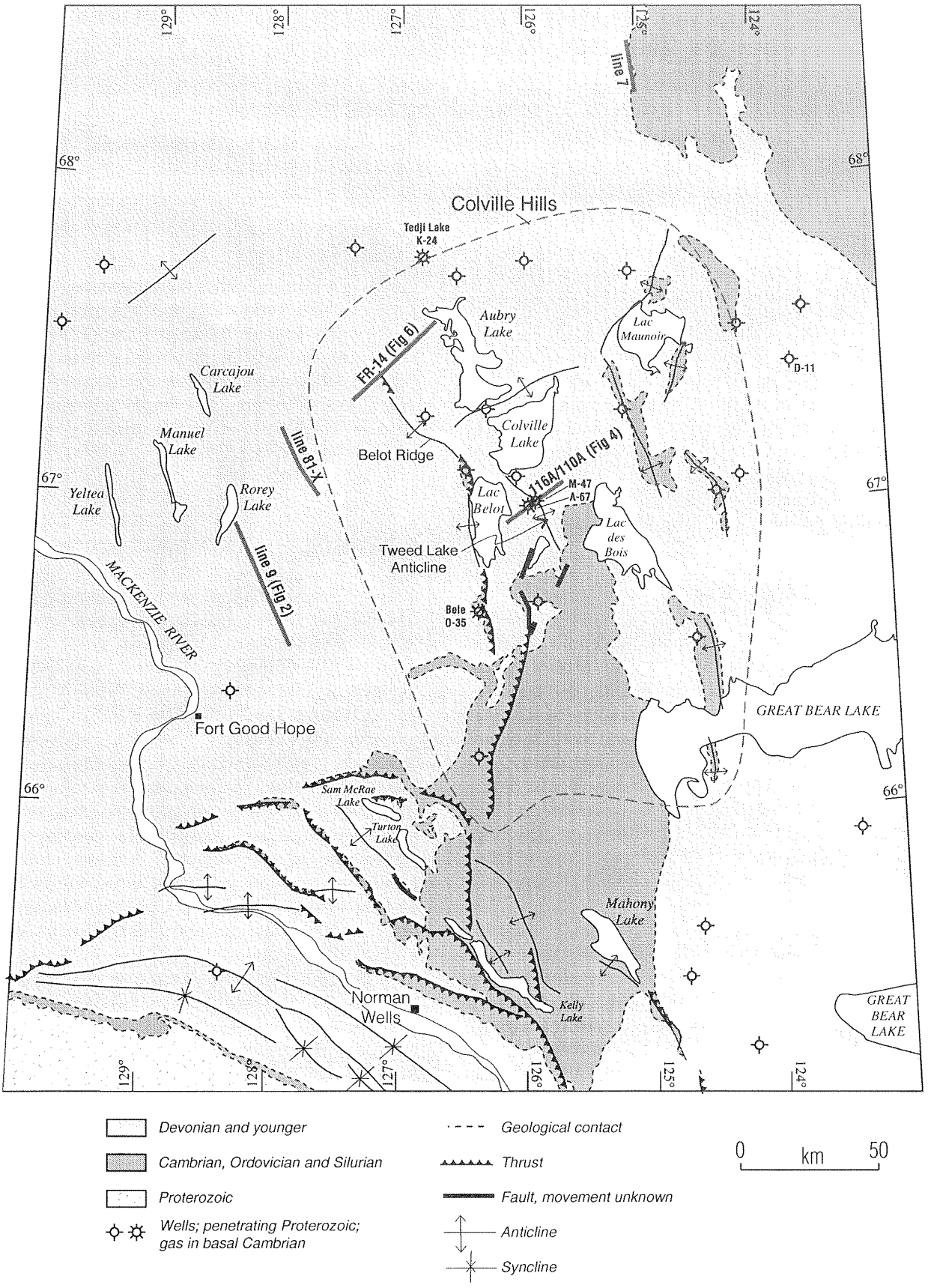

Figure 1. *Location map.*

INVERSIONS

Half Grabens Inverted during Forward Orogeny

A number of half-graben growth faults were generated during deposition of the Basinal Unit of the Hornby Bay Assemblage and at least one was subsequently inverted during Forward Orogeny compression. That structure (a classical positive inversion as defined by Williams et al., 1989) is discussed and illustrated in Cook and MacLean (in press). Half grabens appear on Petro-Canada Line 81X and HBOG Line 7 (Fig. 1) which are included in a poster display at the 1995 GSC Oil and Gas Forum but, as they have no obvious economic potential, are not illustrated here.

Syncline inverted as an anticline

Dismal Lakes strata occurring in a broad anticlinal uplift about 30 km across with about 4 km of structural relief are unconformably truncated by basal Cambrian strata (Fig. 2a). The Precambrian arch represents an inversion of a synclinal depositional basin that had developed during the Forward Orogeny. The synclinal trough, detectable in the variably thick strata of the Hornby Bay Syntectonic Unit, is better illustrated by restoring the sub-Dismal Lakes unconformity to horizontal (Fig. 2b). The basin lies between two Forward Orogeny uplifts and was filled during orogenesis as marked by lozenge-shaped unconformity-bounded sequences. Unlike most inversions, both the negative basin-forming phase (Forward Orogeny) and the positive basin-uplift phase (long-wavelength folding) apparently were compressional. This huge anticline, composed as it is of strata interpreted to be older than 1267 m.y., is a high risk exploration target but cannot be entirely discounted. Very limited thermal maturity data (Snowdon and Williams, 1986) indicate that some Proterozoic strata in the region, although overmature, are still in the gas generation range. Moreover, if reservoir conditions exist, the mechanism by which Phanerozoic gas migrated into the basal Cambrian sands may also have charged Proterozoic beds immediately below the unconformity.

Double Inversions, Tweed Lake Anticline

Tweed Lake anticline contains an estimated 112 BCF of recoverable gas trapped in basal Cambrian sands of the Mount Clark Formation (Bever and McIlreath, 1992). Our interpretation of this structure is modified from a previous one (Cook and MacLean, 1992; MacLean and Cook, 1992), and departs fundamentally from earlier interpretations (see Cook and Coflin, 1990; Sevigny

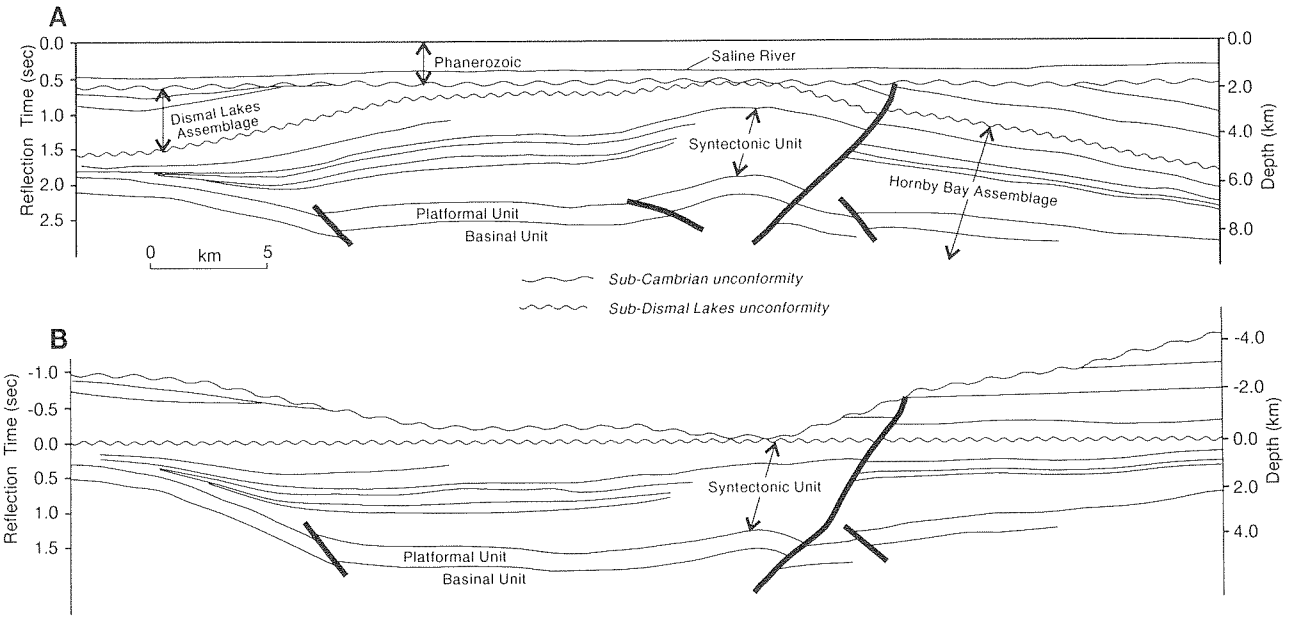

Figure 2. *Inverted syncline. a) Line drawing based on 1975 Dome Petroleum Line 9, Rond Lake (stacked), illustrating a broad anticlinal arch truncated by the sub-Cambrian unconformity. An antecedent, pre-Dismal Lakes, synclinal trough is recorded in a broad lozenge of Syntectonic Unit. For location, see Figure 1. b) Figure 2a flattened on sub-Dismal Lakes unconformity as datum to illustrate antecedent synclinal trough. Unconformity bounded depositional wedges in Syntectonic Unit record progressive uplift, during Forward Orogeny, of flanks of the synclinal basin.*

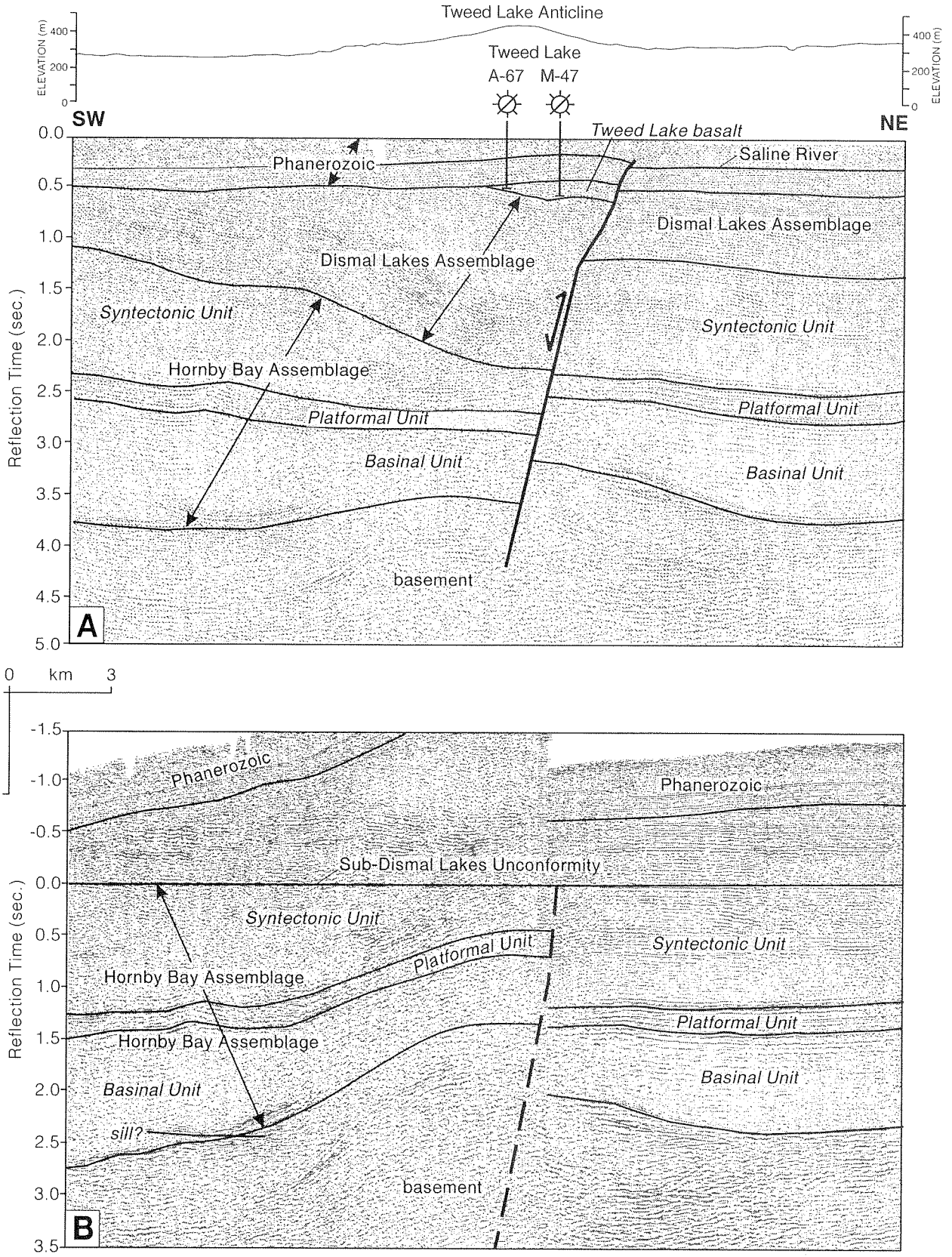
Tweed Lake Anticline
ELEVATION (m)
400
200
0
Tweed Lake
A-67
M-47
SW
NE
Tweed Lake basalt
Saline River
Phanerozoic
Dismal Lakes Assemblage
Dismal Lakes Assemblage
Syntectonic Unit
Syntectonic Unit
Hornby Bay Assemblage
Platformal Unit
Platformal Unit
Basinal Unit
Basinal Unit
basement
Reflection Time (sec.)
0.0
0.5
1.0
1.5
2.0
2.5
3.0
3.5
4.0
4.5
5.0
A
0
km
3
3
km
0
Phanerozoic
Phanerozoic
Sub-Dismal Lakes Unconformity
Syntectonic Unit
Syntectonic Unit
Platformal Unit
Hornby Bay Assemblage
Hornby Bay Assemblage
Platformal Unit
Basinal Unit
Basinal Unit
sill?
basement
Reflection Time (sec.)
-1.5
-1.0
-0.5
0.0
0.5
1.0
1.5
2.0
2.5
3.0
3.5
B

Figure 3. Structure of Tweed Lake anticline. a) Annotated 1979 Petro-Canada Line 110A/116A (migrated). Thrust fault flanking Tweed Lake anticline is interpreted to root into an underlying normal fault zone. The thrust is considered to be due to transpressional inversion of the normal fault. The normal displacement was itself a negative inversion of a Forward Orogeny steeply dipping thrust. For location, see Figure 1. b) Figure 2a flattened on sub-Dismal Lakes unconformity as datum to illustrate the ancestral Forward Orogeny thrust block. In the computer restoration all adjustments were vertical, and the curved thrust fault is schematic.

et al., 1991). The structure is here interpreted to be a product of Laramide transpressional inversion of a Proterozoic half-graben, itself a result of inversion of a Forward Orogeny thrust fault. The structure is recorded on a number of seismic lines, one of which, 1979 Petro-Canada Line 116A/110A (Fig. 3a), passes through the gas discovery well, Tweed Lake M-47.

The anticline (Figs. 1, 3a) lies directly above a Proterozoic fault zone. A small west-dipping Laramide thrust fault offsets the east limb and must root into the underlying steeply dipping ancestral fault because no westward dipping detachment from which it might splay can be detected crossing prominent east-dipping stratigraphic reflections. Two ancestral stages of deformation preceded the Laramide: the first was compressional (Forward Orogeny) and the second extensional. The more obvious extensional stage (Fig. 3a) saw the development of a half-graben with about 3.7 km of normal-fault offset of the sub-Dismal Lakes unconformity. The normal displacement more or less balanced, and therefore masked, the older compressional phase the magnitude of which is revealed (Fig. 3b) by removing the effects of the half-graben extension by restoring the sub-Dismal Lakes unconformity to horizontal. This structure is thus the product of two tectonic inversions: the first, a negative inversion, was an extensional reversal of the original Forward Orogeny thrust; the second, positive, was a transpressional inversion of the normal fault zone.

At least two other "double-inversion" structures have been found in the region. The northern part of Belot Ridge anticline (Fig. 4), like Tweed Lake anticline, resulted from transpressional reactivation of a post-Dismal Lakes half-graben, which was itself an extensional inversion of a Forward Orogeny compressional thrust fault. Similarly, Maunoir Ridge (not illustrated here) was, at least in part, developed as a consequence of compression-extension-transpression double inversion. Belot and Maunoir ridges were tested by Belot Hills M-63 and Colville D-45 respectively, both dry holes.

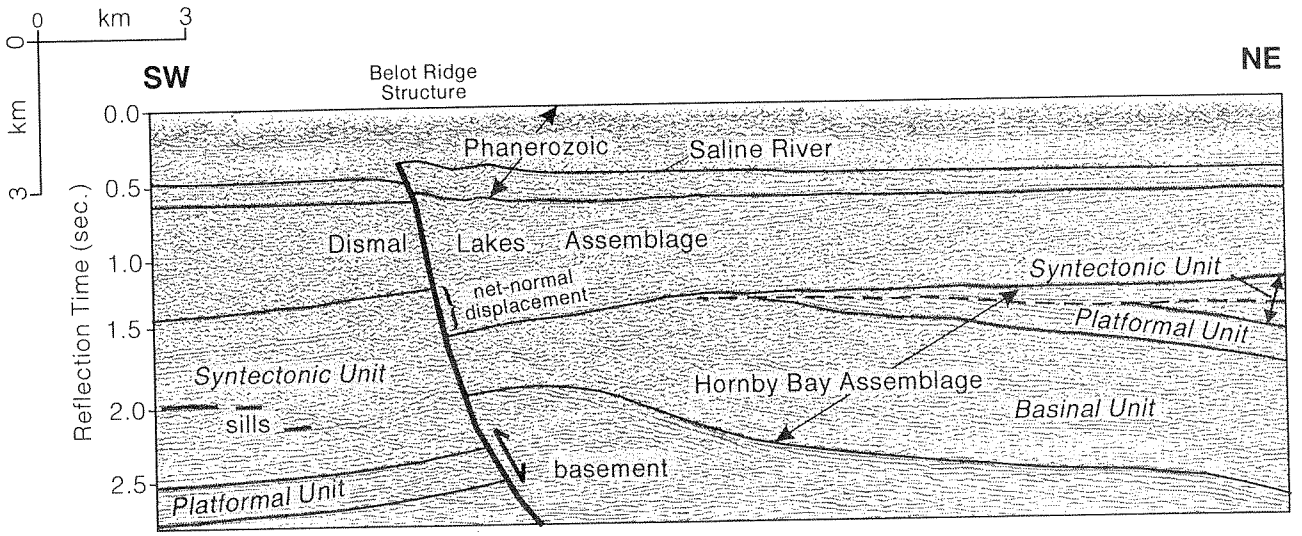

Figure 4. Annotated Forward Resources Line FR-14 (migrated). Structural history was: first, compressional displacement on a stepply dipping thrust fault to generate a large tilted fault block; second, peneplanation of the structure followed by deposition of Dismal Lakes Assemblage strata; third, negative inversion of the thrust to form a small half-graben; and fourth, transpressional inversion of the half-graben to form the Belot Ridge Laramide structure. For location, see Figure 1.

SUMMARY

The gas-bearing Tweed Lake Anticline was generated by a double inversion, positive to negative to positive (compression-extension-transpression). The northern part of Belot Ridge, and Maunoir Ridge have similar double inversion histories, but the central part of each ridge has been tested by dry holes (Belot Hills M-63 and Colville D-45).

Two types of Precambrian negative to positive inversion are important primarily for understanding the pre-Phanerozoic tectonic framework. One, occurring as large anticlinal structures capped by Phanerozoic strata, may have high-risk hydrocarbon potential.

REFERENCES

Aitken, J.D. and Pugh, D.C.
1984: The Fort Norman and Leith Ridge structures: Major, buried, pre-Cambrian features underlying Franklin Mountains and Great Bear and Mackenzie Plains. Bulletin of Canadian Petroleum Geology, v. 32, p. 139–146.

Bever, J.M. and McIlreath, I.A.
1992: (abstract) The Early Cambrian Tweed Lake gas field and related gas occurrences, Northwest Territories, Canada. American Association of Petroleum Geologists, 1992 Annual Convention, Official Program, p. 8, 9.

Cook, D.G. and MacLean, B.C.
1992: Proterozoic thick-skinned intracratonic deformation, Colville Hills region, Northwest Territories, Canada. Geology, v. 20, p. 67–70.

in press: The intracratonic Early Proterozoic Forward Orogeny, and implications for regional correlations, Northwest Territories, Canada. Canadian Journal of Earth Sciences.

Cook, F.A. and Coflin, K.C.
1990: Reactivation tectonics in the Arctic of Western Canada. Marine Geology, v. 93, p. 303–316.

MacLean, B.C. and Cook, D.G.
1992: The influence of Proterozoic structures on the development of Laramide age structures, Northwest Territories, Canada. Bulletin of Canadian Petroleum Geology, v. 40, p. 207–221.

Price P.R.
1993: NEB releases new estimates of oil and gas resources in Canada's north. National Energy Board News Release 93/46.

Ross, G.M. and Kerans, C.
1989: Geology, Hornby Bay and Dismal Lakes groups, Coppermine Homocline, district of Mackenzie, Northwest Territories. Geological Survey of Canada Map 1663A, scale 1:250 000.

Sevigny, J.H., Cook, F.A., and Clark, E.A.
1991: Geochemical signature and seismic stratigraphic setting of Coppermine basalts drilled beneath the Anderson Plains in northwest Canada. Canadian Journal of Earth Sciences, v. 28, p. 184–194.

Snowdon, L.R. and Williams, G.K.
1986: Thermal maturation and petroleum source potential of some Cambrian and Proterozoic rocks in the Mackenzie Corridor. Geological Survey of Canada, Open File 1367, 14 p.

Williams, G.D., Powell, C.M., and Cooper, M.A.
1989: Geometry and kinematics of inversion tectonics. *In* Inversion Tectonics, M.A. Cooper and G.D. Williams (eds.). Geological Society Special Publication No. 44, p. 3–15

STRATIGRAPHIC CONTROLS ON POTENTIAL HYDROCARBON AND MINERAL ACCUMULATIONS OF CENTRAL ELLESMERE ISLAND

T. de Freitas, J.C. Harrison, U. Mayr, and R. Thorsteinsson

Geological Survey of Canada, 3303-33rd Street N.W., Calgary, Alberta T2L 2A7

INTRODUCTION AND EXPLORATION HISTORY

Hydrocarbon and mineral exploration parties first entered the Arctic Islands in about 1959, but by 1960 such parties were widespread. A significant lead zinc discovery on Little Cornwallis Island by J.C Sproule and Associates during these early field investigations led to the development of Canada's most northern mine, the Polaris Mine of Cominco Ltd. Fourteen years later, Panarctic Oils Ltd. drilled two wells in southern Bjorne Peninsula (Panarctic ARCO et al., Blue Fiord E-46 and Panarctic Tenneco et al. CSP Eids M-66; Fig. 1; Uyeno, 1990; Mayr et al., 1994) to access potential oil pools in Ordovician and Silurian carbonates. The Eids well pierced the basinal succession, but the Blue Fiord well penetrated a large pinnacle reef structure (Figs. 2, 3). The well yielded considerable quantities of oil-flecked

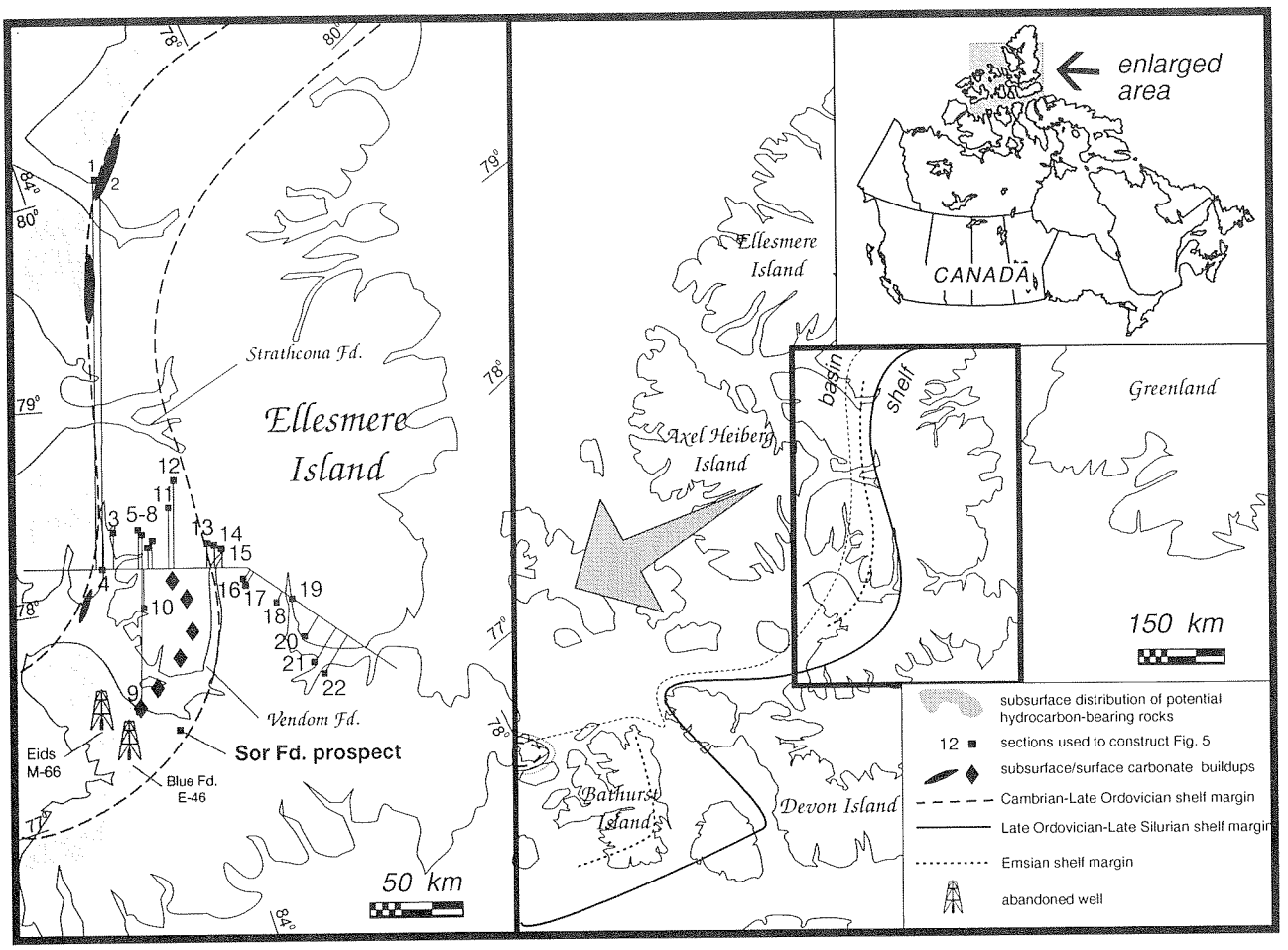

Figure 1. *Location map. Line of section (stratigraphic section localities 1-22) is shown in Figure 5. Two wells, Panarctic ARCO et al. Blue Fiord and Panarctic Tenneco et al. Eids M-66 well are indicated, and additional lithology and thermal maturity data are shown in Figures 2 and 3.*

water indicating good porosity, and the adjacent source rock sustained burial depths for peak hydrocarbon generation (Fig. 3); however, exploration was discontinued as Panarctic focused its exploration effort in the Sverdrup and Franklinian basins in the western

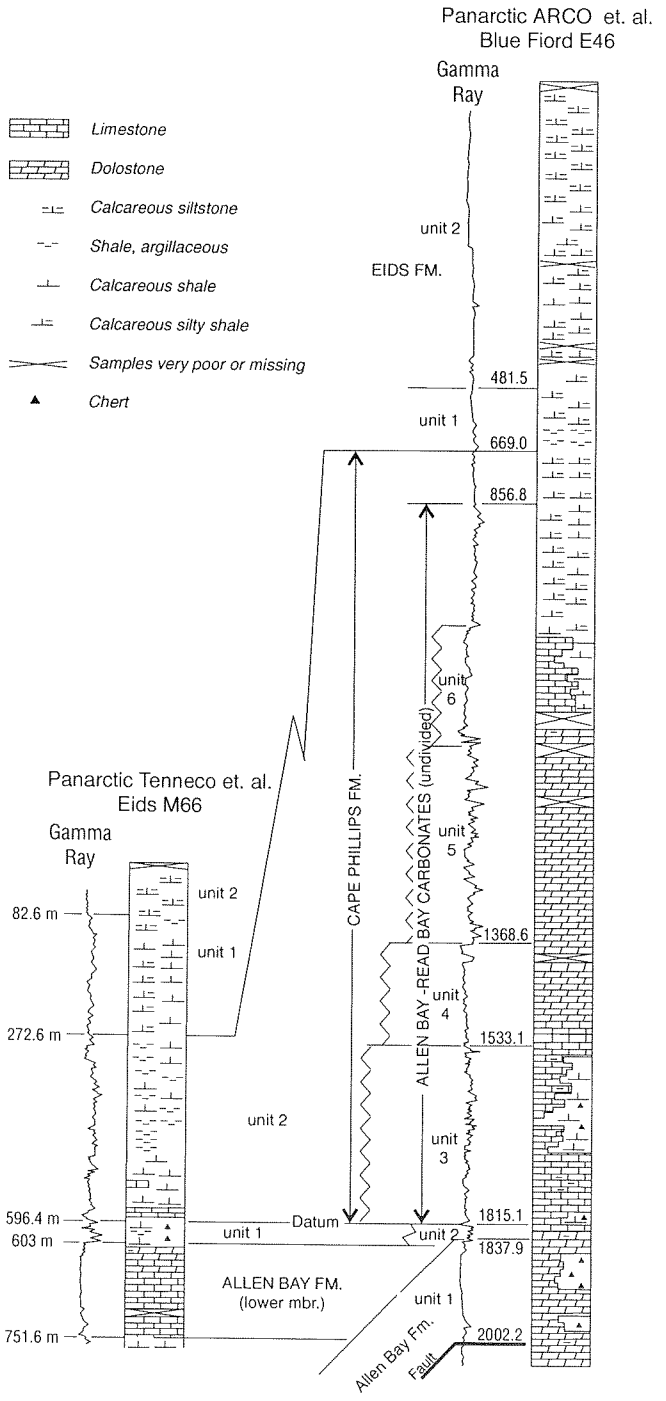

Figure 2. *Lithological and gamma ray profile of the two wells in southern Ellesmere Island. See Figure 1 for location. Data adapted from Mayr (in Uyeno, 1990).*

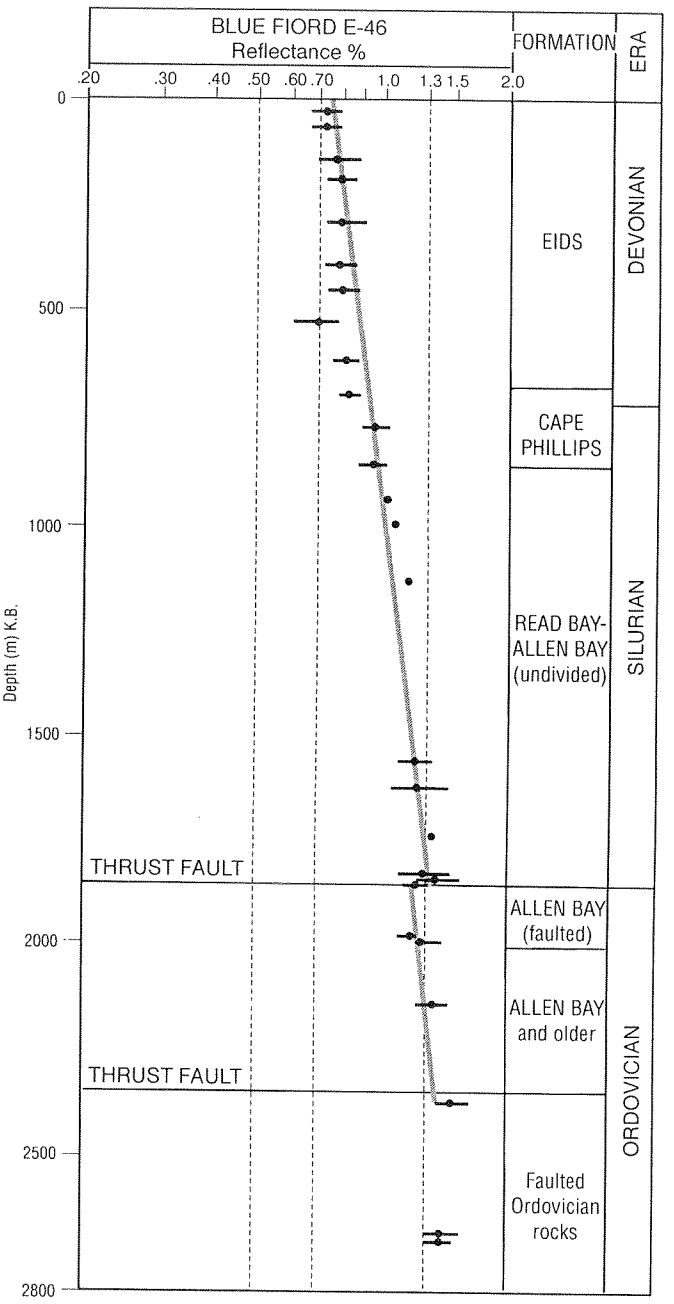

Figure 3. *Vitrinite and bitumen reflectance and its relationship to depth below the surface in the Panarctic ARCO et al. Blue Fiord well, southern Ellesmere Island. See Figure 1 for location. The area between the dashed vertical lines at 0.5% and 0.7% represents the initiation of significant hydrocarbon generation of type II and type III kerogen, respectively. The end of oil generation is indicated by the dashed line at 1.3%, and the zone of wet gas condensate generation is represented by the area between the lines at 1.3% and 2.0% (from Mayr et al., 1994). Comparable information on the Panarctic Tenneco et al. Eids M-66 is available in Mayr et al. (1994).*

Arctic Islands. This move was successful, because Panarctic discovered the Bent Horn oil field in Lower Devonian, Blue Fiord Formation carbonates in Cameron Island. However, Panarctic was again attracted to southwestern Ellesmere Island by potentially large oil pools in Ordovician–Silurian carbonates. The Sor Fiord prospect (Fig. 1) was one of several exploration agreements signed by Panarctic Oils in 1982 that covered most of the subsurface distribution of the Ordovician–Silurian shelf-to-basin transition (Rayer, 1981). Although closure was demonstrated within the Sor Fiord prospect, extreme company down-sizing and lack of demand for Sverdrup Basin gas discouraged further investment by the exploration partners, and thus, ideal hydrocarbon traps, with updip seals, have not been adequately explored.

Recent geological investigations in the vicinity of Vendom and Strathcona fiords by the Geological Survey of Canada has yielded a wealth of stratigraphic and structural information suggesting economically significant accumulations of hydrocarbons and minerals in central Ellesmere Island. For example, abundant bitumen is observed in surface exposures that are correlatives with the Bjorne Peninsula subsurface hydrocarbon prospects, and several mineral occurrences indicate potential base metal accumulations in central Ellesmere Island.

NEW FINDINGS

The summary cross-sections in Figures 4 and 5 outline the main, lower Paleozoic stratigraphic features in the Strathcona Fiord and Vendom Fiord map areas and form part of a larger field-based study to better understand the geology of this part of the Arctic Islands (also see companion reports by Gentzis et al. and Harrison et al. in this publication). The more than 9 km thick stratigraphic succession is subdivided in to five stages on the basis of commonalities in tectonic setting, sedimentology, and stacking pattern of transgressive-regressive (T-R) sequences. Main features of these are summarized below (Figs. 4, 5 for stratigraphic ranges of the 5 stages).

STAGE I
(Early Cambrian? to Late Cambrian)

- basin initiation
- mixed clastic carbonate units
- high rates of sedimentation along a growth faulted (faults in Melville Island) trailing continental margin; at least 4-5 km of strata may occur beneath the cross-section, based on measured thicknesses of correlative rock units in northern Ellesmere Island

STAGE II
(Late Cambrian to Middle Ordovician)

- lesser, more uniform subsidence rates than Stage I
- deposition of extensive, shelf evaporites and a microbial boundstone rim (e.g., Baumann Fiord, Bulleys Lump formations)
- condensed organic chert-mudrock basinal sequence (Hazen Formation)

STAGE III
(Late Ordovician to Late Silurian)

- termination of microbial rim and evaporitic shelf in most areas
- platform backstepping and development of distally steepened platform with chert and organic mudrock (Hazen Formation) in deepest part of basin; mudrock, carbonate, chert, and large reefs deposited on drowned shelf (Cape Phillips Formation)
- basin begins to fill with Caledonian orogen-derived flysch (Danish R. Formation)

STAGE IV
(Late Silurian to Early Devonian)

- basement uplifts (Bache and Boothia uplifts) influence sequence architecture (upper member of Goose Fiord Formation, Vendom Fiord Formation, Blue Fiord Formation)
- increased rates of deep marine sediment accumulation
- flysch oversteps drowned shelf, and large parts of basin fill to sea level

STAGE V
(late Early to Late Devonian)

- foreland basin sedimentation
- termination of most carbonate shelf sedimentation

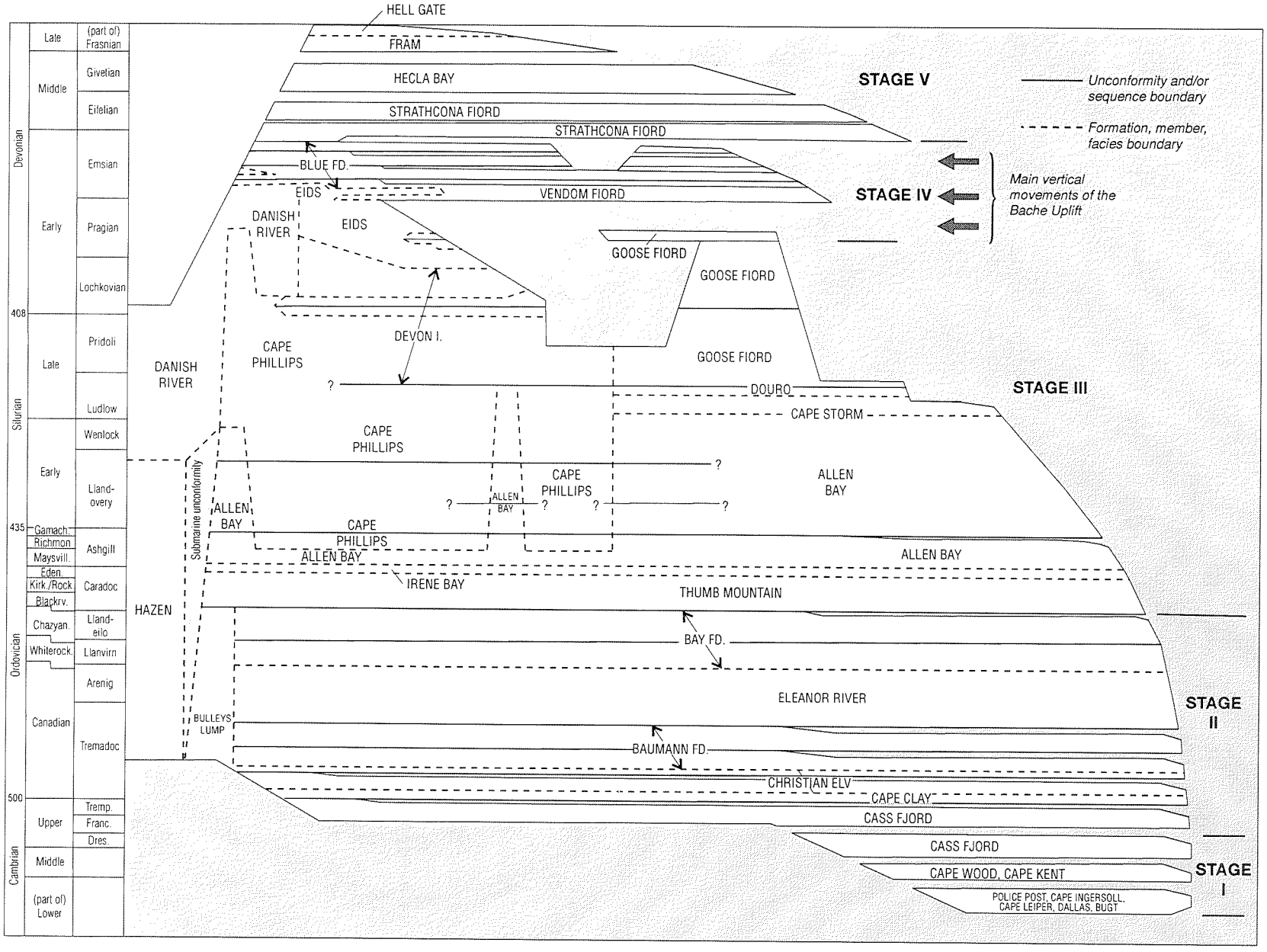

Figure 4. *Ages of the formations shown in Figure 5. Some biostratigraphic information is from Uyeno (1990) and Trettin (1978, 1979).*

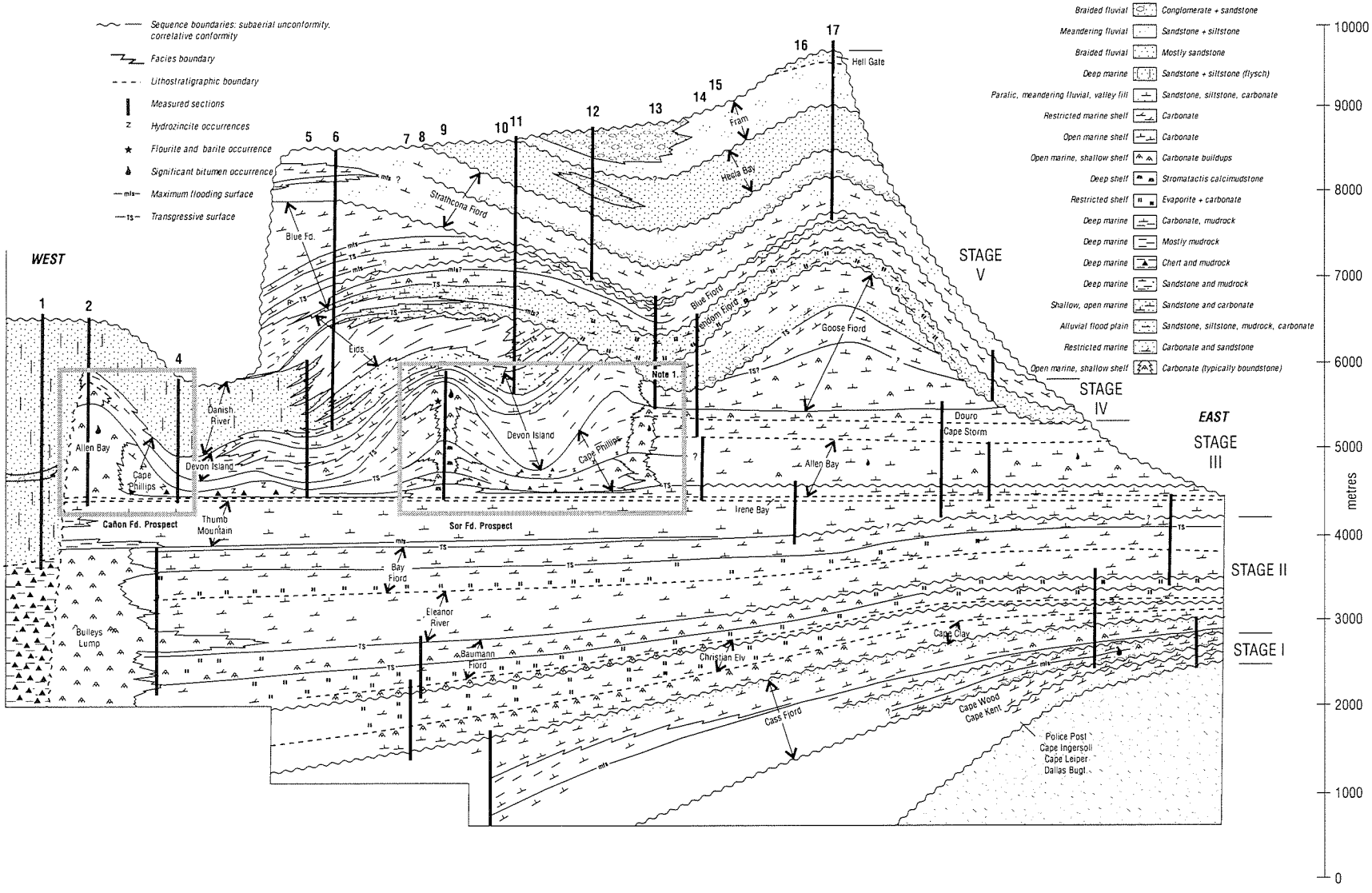

Figure 5. *Stratigraphic cross-section of the Lower Cambrian to Upper Devonian succession, central Ellesmere Island. Most data are previously unpublished, but data for localities 1 and 11 are based partly on Trettin (1979, 1978). Although strata beneath the Cass Fjord and Bulleys Lump formations in the western part of the section are not exposed, it may be assumed that an additional 4 to 5 km of Lower Cambrian strata exists beneath these units. This assumption is based on measured sections in northern Ellesmere Island (Trettin, 1994). Note 1: The Lower Devonian unconformity in the upper part of the Goose Fiord Formation is a feature restricted to the vicinities of localities 13 and 14, Figure 1. South of the cross-section and in the subsurface of the Sor Fiord prospect, the shelf edge is in a conformable sequence.*

- continental sediments deposited over most of the Arctic Islands and extensive subaerial unconformities bound many sequences

- clinoforms in seismic profiles and outcrops

The Bjorne Peninsula subsurface hydrocarbon prospects are exposed to the north, and consist primarily by shelf-margin boundstone and grainstone and isolated pinnacle reefs in the Allen Bay (reservoir) and Cape Phillips–Devon Island (source) formations (Fig. 5, boxed area) . Reef structures are composed of stromatoporoid boundstone and coral microbial boundstone that are locally dolomitized with porosity values up to 20%. In at least one exposure, the oil-water contact occurs about 200 m below the updip seal (Devon Island Formation), in a reef structure that is more than 1 km thick and about 5 km long. A comparable subsurface structure has been identified in southern Ellesmere Island (Sor Fiord prospect, Fig. 1), and numerous others are likely, because reefs are abundant in the correlative outcrop belt farther north (Fig. 1). In support of the reef prospects, graptolite reflectance studies (Gentzis et al., this volume) indicate that the source rocks (Cape Phillips and Devon Islands formations) were buried to depths of peak hydrocarbon generation (also see Harrison et al., this volume, for a discussion of structural aspects of this area).

In addition to these large isolated reefs, the drowned Ordovician shelf edge (Cañon Fiord Prospect, Fig. 5) harbours more than 1 km thick reef successions that have not been considered in past hydrocarbon exploration programs. Exposed examples of these large structures occur in several areas in central and northern Ellesmere Island, and further examples may occur in the subsurface, in areas to the northwest and west of southern Ellesmere Island (Fig. 1). In the vicinity of Cañon Fiord, the carbonate apron deposits of one of these reef structures contains abundant bitumen and locally good moldic and vuggy porosity, and the adjacent Cape Phillips and Hazen formations contain significant thicknesses of organic-rich shales (Trettin, 1979).

Further plays include basinal sandstone bodies and platformal carbonates of Devonian age, which locally contain good porosity and an interfingering relationship with source rocks that have a comparable thermal maturity with those adjacent to the older reef structures.

Other than these hydrocarbon prospects, the area hosts potential base metal deposits (lead, zinc, and copper): Silurian carbonates near Bay Fiord contain disseminated galena; a single reef structure west of Vendom Fiord contains extensive, fracture-filling barite and fluorite; and hydrozincite occurs extensively in basinal rocks that are correlatives of the mineral-bearing reefs. Although some of these mineral showings are not associated with base metal mineralization, their presence warrants further investigation.

REFERENCES

Gentzis, T., de Freitas, T., Goodarzi, F., Melchin, M.J., and Lenz, A.C.
this volume: Thermal maturity of lower Paleozoic sedimentary succession, Arctic Canada.

Harrison, J.C., de Freitas, T., and Thorsteinsson, R.
this volume: Structural controls on potential hydrocarbon accumulations in central Ellesmere Island.

Mayr, U., Goodarzi, F., and Stewart, K.R.
1994: Economic geology. *In* The Phanerozoic geology of southern Ellesmere and North Kent Island, Canadian Arctic Archipelago, U. Mayr, J.J. Packard, Q.H. Goodbody, A.V. Okulitch, R.J. Rice, F. Goodarzi, and K.R. Stewart (eds.). Geological Survey of Canada, Bulletin 470, p. 138–144.

Rayer, F.G.
1981: Exploration prospects and future petroleum potential of the Canadian Arctic Islands. Journal of Petroleum Geology, v. 3, p. 367–412.

Trettin, H.P.
1978: Devonian stratigraphy, west-central Ellesmere Island. Geological Survey of Canada, Bulletin 302, 119 p.

1979: Middle Ordovician to Lower Devonian deep-water succession at southeastern margin of Hazen Trough, Cañon Fiord, Ellesmere Island. Geological Survey of Canada, Bulletin 272, 84 p.

1994: Pre-Carboniferous geology of the northern part of the Arctic Islands. Geological Survey of Canada, Bulletin 430, 248 p.

Uyeno, T.T.
1990: Biostratigraphy and conodont faunas of Upper Ordovician through Middle Devonian rocks, eastern Arctic Archipelago (with contributions by U. Mayr and R.F. Roblesky). Geological Survey of Canada, Bulletin 401, 211 p.

GEOLOGICAL ATLAS OF THE BEAUFORT–MACKENZIE AREA

Edited by

J.D. Dixon

Geological Survey of Canada, 3303-33rd Street N.W., Calgary, Alberta T2L 2A7

The Geological Atlas of the Beaufort–Mackenzie Area was conceived and designed for exploration geologists, although others will find it equally useful. It is oriented more towards the presentation of data in a graphical form (maps, charts, diagrams, etc.), although some explanatory text is included. The base-map has a 1:1 000 000 scale, with other scales used less frequently. Twenty-seven geoscientists contributed to the atlas involving not only GSC scientists but also university and consulting geologists and geophysicists, and staff of the National Energy Board. The area covered by the atlas extends from latitutde 68° to 72°N, longitude 128° to 142°W, the bulk of which falls in the Beaufort Sea.

One hundred and eight figures are used to present data on regional setting, stress regime, seismicity, geothermal regime, stratigraphy, biostratigraphy, organic geochemistry, thermal maturity, compaction, and examples of the major oil and gas discoveries. Although the total geological setting is addressed, much of the data is restricted to the Jurassic to Tertiary succession. This reflects the abundance of data available for these rocks. A comprehensive bibliography is included in the atlas.

Printing is anticipated to be in 1995.

TIME-SLICE THERMAL MATURATION DATA FOR MAINLAND YUKON AND NORTHWEST TERRITORIES

B.J. Dougherty

Geological Survey of Canada, 601 Booth Street, Ottawa, Ontario K1A 0E8

INTRODUCTION

In 1989, the Geological Survey of Canada initiated a program to compile and coordinate, in a digital format, thermal maturity information generated from various rock analyses. These analyses had been conducted at the Institute of Sedimentary and Petroleum Geology in Calgary. The main focus of the project was to provide a central access to thermal maturity information and to produce standard format reports or data files.

The area of mainland Canada north of 60°N was selected for the pilot database development because levels of thermal maturity vary across the area (Dougherty and Uyeno, 1989; Feinstein et al., 1989; Utting, 1989; Link and Bustin, 1989; Morrow, et al., 1993), and the geology is reasonably well known (Pugh, 1983; Norris, 1985; Gabrielse and Yorath, 1991). The initial phase of the project correlated the relationship between thermal maturity indices (Dougherty et al., 1991). The work showed that the pattern of thermal maturation is primarily produced from regional geological factors and generally is not related to localized thermal anomolies.

The final stage of the project is to release the information in a format that can be used in sedimentary basin analysis. The maps which are at the Oil & Gas Forum '95 show thermal maturation patterns through the Phanerozoic. These maps will form the basis for a chapter—dealing with the organic component of the sedimentary rocks—to be published in the up-coming Geologic Atlas of Northern Mainland Canada.

DATABASE DESIGN

The maps show data which has been plotted from the Thermal Maturation database. The database was developed using a commercially available, PC-based, relational database software package. The database was designed to facilitate access to information which comes from a variety of sources and to produce outputs in a flexible format. The main focus of the database is thermal maturity, but a side benefit has been that the database provides a window to work in the pilot project area: who has been working in the area, when the work was conducted, and where to find the results.

A series of tables were created in the database. These tables relate the geographic, stratigraphic, and publication information to individual samples which were analysed for thermal maturity.

The outputs from the system can be either ASCII files for export to other digital software, such as a Geographic Information System (GIS), or written reports which highlight the interrelationships within the data. The relational nature of the database means that the report formats need not be pre-established and can be tailored to answer questions on an as-needed basis. A few pre-set queries have been designed to answer more commonly asked questions such as: What is the thermal maturation pattern for a given age or geologic unit? What is the relationship between different thermal maturity indices? What is the relationship of thermal maturation to depth in a given location?

When evaluating regional thermal maturity over varied lithologies and facies, it is important that several types of maturity indices be used, as no single index produces valid results in all circumstances (Utting et al., 1989). Studying the geochemistry and optical properties of organic material provides information about the physical and chemical nature of the material, while fossils containing organic material can provide a biostratigraphic framework to augment the thermal maturation data derived from the fossils. Combining multiple indices will provide a more complete analysis of maturation patterns in a region (Gentzis and Goodarzi, 1993; Gentzis et al., 1993).

The thermal maturity indices which have been incorporated in the database are conodont Colour Alteration Index (CAI), palynomorph Thermal Alteration Index (TAI), geochemistry of organic material (Rock-Eval and Tmax), and analysis of reflectance of dispersed organic matter (Ro).

The thermal maturity indices of CAI and TAI were taken from published sources (Dougherty and Uyeno, 1989; Utting, 1989; Norford et al., 1993; Dodds et al., 1993), but data was also included from unpublished internal ISPG reports. Biostratigraphic information, which was available for many of the these samples, has been included in the database to allow selection of information based on geologic age. If biostratigraphic interpretation is not available, then the geologic age of the sample can be determined from the stratigraphic details provided for each. If the stratigraphic and biostratigraphic age differs substanially, then the more constrained age is used. Sometimes both interpretations are used jointly to obtain a more precise age.

The organic geochemical and petrologic data were taken from published sources, either Open Files (e.g., Feinstein et al., 1989; Snowdon, 1990) or more formal publications (e.g., Dougherty et al., 1991; Feinstein et al., 1991; Morrow et al., 1993). Interpretations of the thermal maturity, as given by the original authors, were preserved in the database. Uninterpreted thermal maturity data were taken from some Open Files; interpretations of these data are based on the critera outlined by Peters (1986) and Wright (1980). The geologic age was determined from stratigraphic or depth information associated with each sample.

The strengths of the system which was designed for handling the thermal maturity data at the GSC are:

1. Broad regional trends in the data can be detected;

2. The geographic and stratigraphic details for a large number of samples from a wide region makes database output ideal for GIS applications;

3. Large volumes of varied data are easily accommodated;

4. The availablity of information is not age or lithology dependent;

5. Gaps in one data set may be filled by information contained in another set. If doubts arise concerning the data and the interpretation of the information, corroborating analyses are readily available.

6. The system is flexible and fairly detailed answers to some difficult questions can be answered quickly.

REFERENCES

Dodds, C.J., Campbell, R.B., Read, P.B., Orchard, M.O., Tozer, E.T., Bamber, E.W., Pedder, A.E.H., Norford, B.S., McLaren, D.J., Harker, P., McIver, E., Norris, A.W., Ross, C.A., Chatterton, B.D.E., Cooper, G.A., Flower, R.H., Haggart, J.W., Uyeno, T.T., and Irwin, S.E.B.
1993: Macrofossil and conodont data from: SW Kluane Lake [115G & F(E 1/2)], Mount St. Elias [115B & C(E 1/2)], SW Dezadeash (115A), NE Yakutat (114O) and Tatshenshini River (114P) map areas, southwestern Yukon and northwestern British Columbia. Geological Survey of Canada, Open File 2731.

Dougherty, B.J. and Uyeno, T.T.
1989: A conodont-based thermal maturation study of some Lower and Middle Devonian rocks, northwestern District of Mackenzie and Yukon Territory. *In* Current Research, Part G. Geological Survey of Canada, Paper 89–1G, p. 37–42.

Dougherty, B.J., Abercrombie, H.J., Achab, A., Bertrand, R., Goodarzi, F., Snowdon, L.R., and Utting, J.
1991: Correlation of thermal maturity indicators for the Tenlen A-73, Crossley Lake South K-60, and Kugaluk N-02 wells in northern District of Mackenzie, Northwest Territories. *In* Current Research, Part E. Geological Survey of Canada, Paper 91–1E, p. 197–202.

Feinstein, S., Brooks, P.W., Gentzis, T., Goodarzi, F., Snowdon, L.R., and Williams, G.K.
1989: Thermal maturity in the Mackenzie Corridor, Northwest and Yukon Territories, Canada. Geological Survey of Canada, Open File 1944.

Feinstein, S., Williams, G.K., Snowdon, L.R., Goodarzi, F., and Gentzis, T.
1991: Thermal maturation of organic matter in the Middle Devonian to Tertiary section, Fort Norman area (central Mackenzie Plain). Canadian Journal of Earth Sciences, v. 28, p. 1009–1018.

Gabrielse, H. and Yorath, C.J.
1991: Introduction, Chapter 1. *In* Geology of the Cordilleran Orogen in Canada, H. Gabrielse and C.J. Yorath (ed.). Geologcial Survey of Canada, no. 4, p. 3–11.

Gentzis, T. and Goodarzi, F.
1993: Regional thermal maturity in the Franklinian Mobile Belt, Melville Island, Arctic Canada. Marine and Petroleum Geology, v. 10, p. 215–230.

Gentzis, T., Goodarzi, F., and Snowdon, L.R.
1993: Variation of maturity indicators (optical and Rock-Eval) with respect to organic matter type and matrix lithology: an example from Melville Island, Canadian Arctic Archipelago. Marine and Petroleum Geology, v. 10, p. 507–514.

Link, C.M. and Bustin, R.M.
1989: Organic maturation and thermal history of Phanerozoic strata in Northern Yukon and northwestern District of Mackenzie. Bulletin of Canadian Petroleum Geology, v. 37, p. 266–292.

Morrow, D.W., Potter, J., Richards, B., and Goodarzi, F.
1993: Paleozoic burial and organic maturation in the Liard Basin Region, Northern Canada. Bulletin of Canadian Petroleum Geology, v. 41 p. 17–31.

Norford, B.S., Orchard, M.O., Norris, A.W., Uyeno, T.T., Cecile, M.P., Abbott, J.G., Jackson, D.E., Fritz, W.H., Hofmann, H.J., Nowlan, G.S., and Tipnis, R.S.
1993: Paleontological identifications and correlations Niddery Lake map-area N.T.S. 105 O and immediately adjacent map-areas. Geological Survey of Canada, Open File 2682.

Norris, D.K.
1985: Eastern Cordilleran foldbelt of northern Canada: its structural geometry and hydrocarbon potential. American Association of Petroleum Geologists, Bulletin, v. 69, p. 788–808.

Peters, K.E.
1986: Guidelines for evaluating source rock using programmed pyrolysis. American Association of Petroleum Geologists, Bulletin, v. 70, p. 318–329.

Pugh, D.C.
1983: Pre-Mesozoic geology in the subsurface of Peel River map area, Yukon Territory and District of Mackenzie. Geological Survey of Canada, Memoir 401, 61 p.

Snowdon, L.R.
1990: Rock-Eval/TOC Data for 55 Northwest and Yukon Territories Wells (60° to 69°N). Geological Survey of Canada, Open File 2327.

Wright, N.J.R.
1980: Time, Temperature and Organic Maturation–the evolution of rank within a sedimentary pile. Journal of Petroleum Geology, v. 2 p. 411–425.

Utting, J., Goodarzi, F., Dougherty, B.J., and Henderson, C.M.
1989: Thermal maturity of Carboniferous and Permian rocks of the Sverdrup Basin, Canadian Arctic Archipelago. Geological Survey of Canada, Paper 89–19.

T-R SEQUENCE – THE PRACTICAL GENETIC UNIT FOR STRATIGRAPHIC ANALYSIS

A.F. Embry

Geological Survey of Canada, 3303-33rd Street N.W., Calgary, Alberta T27 2A7

INTRODUCTION

Sequence analysis provides an excellent genetic stratigraphic framework for undertaking a detailed characterization of a reservoir and for predicting lateral and vertical changes in the reservoir on both a field and a fairway scale. However, over the past decade five different types of sequences have been defined and used for genetic stratigraphic analysis. Consequently exploration and development geologists are faced with the question of what type of sequence is most practical for the task at hand - be it the efficient development of a field, recommending stepout locations, or finding new fields along a fairway.

Vail et al. (1977) defined a sequence as "a stratigraphic unit composed of genetically related strata bounded at the top and bottom by unconformities and their correlative conformities". This definition provided us with a genetic stratigraphic unit which has unconformities, across which significant changes in the depositional regime commonly occur, on the boundaries rather than within. It also defined a unit which can be mapped over any size study area, from a single field to an entire basin. For the purposes of establishing a stratigraphic framework for detailed facies analysis, a sequence has obvious advantages over a standard, lithostratigraphic unit (formation, member) which may contain significant unconformities, which can be mapped only over a portion of a basin, and which commonly has very diachronous boundaries.

Five different types of sequences have sprung from Vail et al's seemingly straight forward definition. Each type is bounded by a unique combination of a specific type of unconformity and a specific correlative conformity. Thus the term sequence now embraces a family of genetic units which are related to each other by having unconformities as boundaries. Unfortunately this proliferation of sequence types has caused some confusion and has made sequence analysis more difficult and chaotic than it needs to be.

It is essential that the practitioner understand the nature of each of the five sequence types. Such understanding allows the geologist to evaluate the various types and to select the sequence type most appropriate for the development or exploration project being undertaken.

EVENT STRATIGRAPHY AND SEQUENCE TYPES

One way of achieving a good understanding of the various sequence types is to relate each unique type of sequence boundary to the various stratigraphic responses which occur during a base level transit cycle (Figs. 1, 2). Four different types of unconformities are developed during a cycle and these form during specific intervals of the cycle. The subaerial unconformity and the regressive surface of erosion are generated during base level fall. In contrast, the ravinement surface and the offshore marine surface of erosion form during the early part of base level rise (when transgression is occurring) (Fig. 1). Whereas the unconformable surfaces form over relatively long time intervals during a cycle, the correlative conformity surfaces are developed over short time intervals. These surfaces can be related to specific "events" which occur during a base level cycle. The events, their stratigraphic responses, the surfaces generated by the responses, and the resulting types of sequence boundaries are described below. The stratigraphic relationships of these surfaces are illustrated in Figure 3.

1. ***Start of Base Level Fall*** – This event is coincident with the cessation of coastal onlap and the start of seaward migration of the subaerial unconformity. The conformable surface equivalent to this event is a hypothetical time line which has no lithological expression. Some authors have used either the regressive surface of erosion or the conformable base of a sandstone-dominant interval to represent this event. Such contacts are highly diachronous boundaries and are not suitable approximations of this event. The combination of the subaerial unconformity and the hypothetical time line form the boundary for a Depositional Sequence Type III as recently discussed by Posamentier et al. (1992) and Jervey (1993).

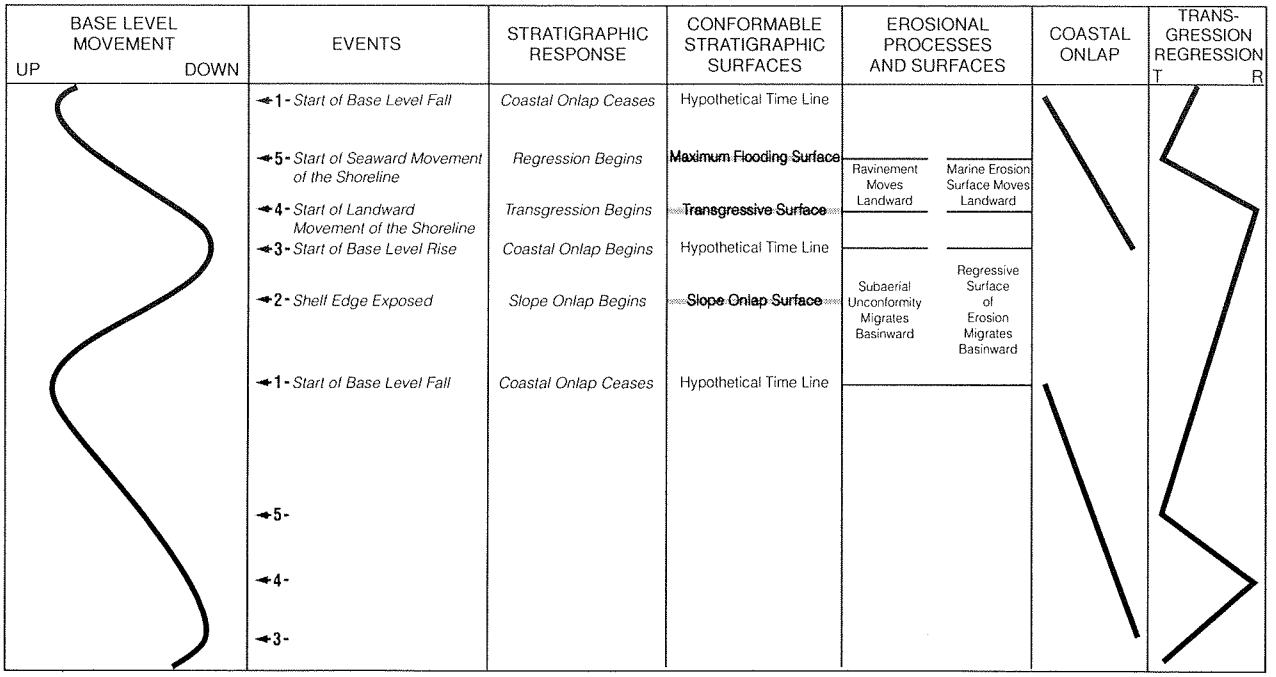

Figure 1. *The relationship of the various types of unconformities and correlative conformities to a base level transit cycle. The unconformities develop during specific intervals (e.g., base level fall) of the cycle whereas the correlative conformities are stratigraphic responses to specific events (e.g., Shelf edge exposed).*

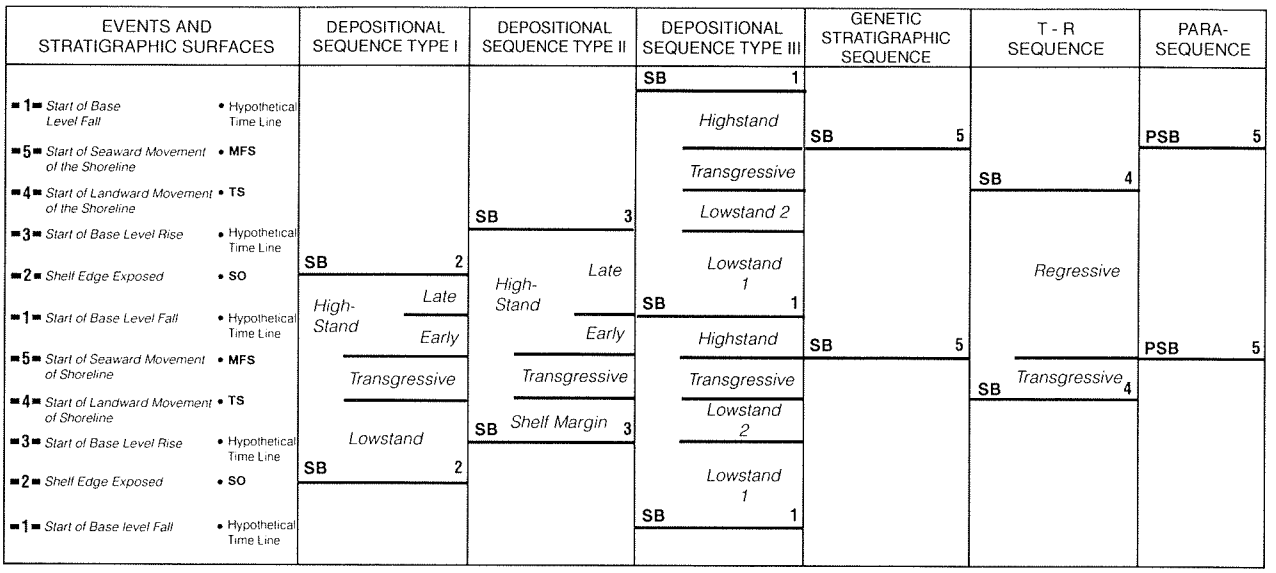

Figure 2. *Each of the five different types of sequences uses one of the five different correlative conformities which are generated during a base level transit cycle. MFS–maximum flooding surface, TS–transgressive surface, SO–slope onlap surface, SB–sequence boundary, PSB–parasequence boundary.*

2. ***Shelf Edge Exposed*** – When the subaerial unconformity migrates near or to the shelf edge there is a significant change in sedimentation pattern with the sediments being channelled mainly down submarine canyons. This results in sediment starvation over much of the slope and eventually the slope is onlapped by expanding, channel-fed sediments. This generates the slope onlap surface and this surface, in combination with the updip subaerial unconformity, is used as the boundary for a Depositional Sequence Type I (Jervey, 1988; Posamentier et al., 1988).

3. ***Start of Base Level Rise*** – At the time of this event the subaerial unconformity has reached its maximum basinward extent and it begins to be onlapped by coastal sediments. The equivalent conformable surface is a hypothetical time line with no lithologic expression. The combination of the subaerial unconformity and the hypothetical time

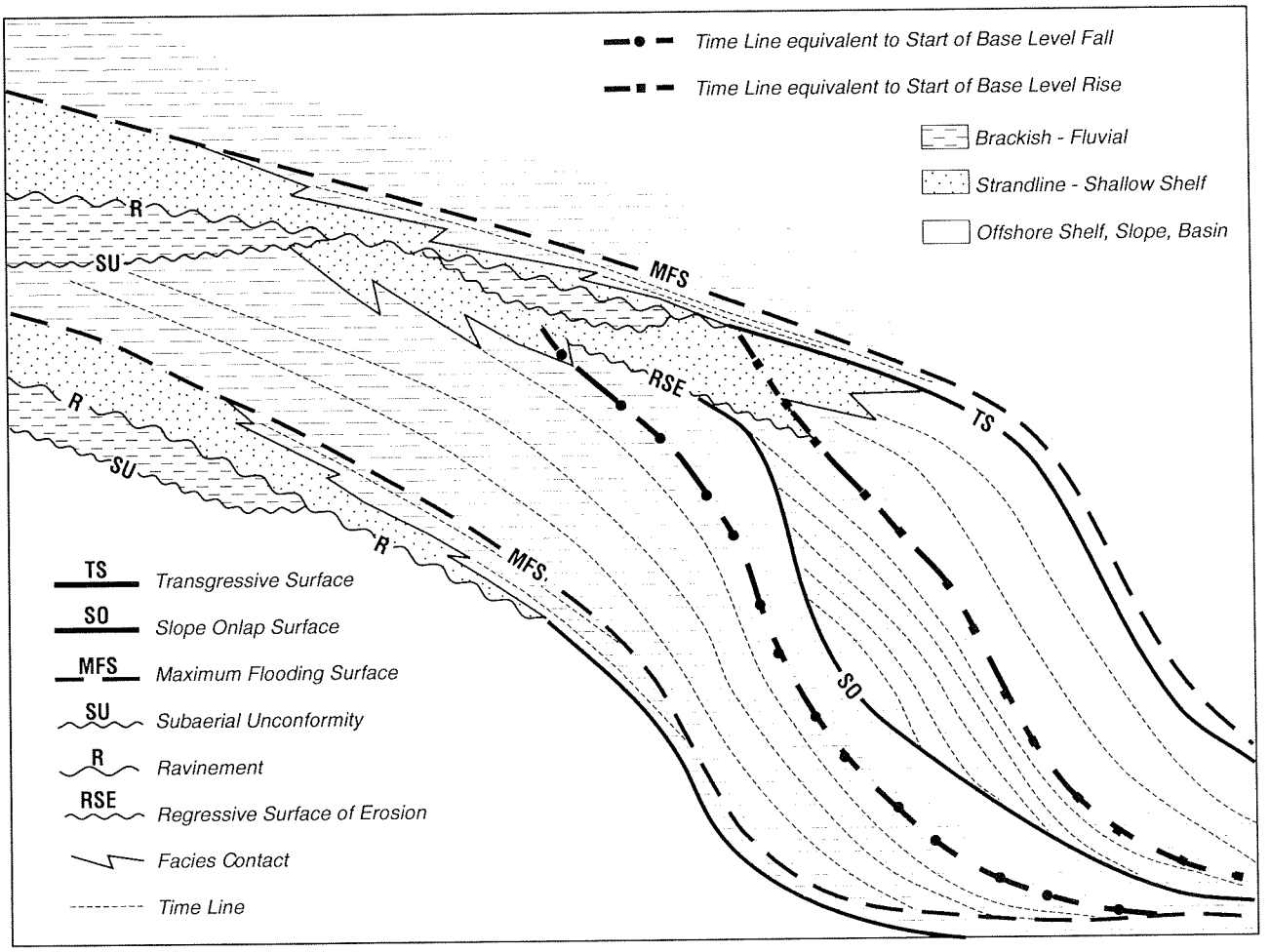

Figure 3. *A schematic stratigraphic cross-section which shows the relationship between the six surfaces of sequence stratigraphy–subaerial unconformity, ravinement surface, regressive surface of erosion, transgressive surface, maximum flooding surface and slope onlap surface and clastic facies. The cross-section was constructed using a constant supply of sediment to a basin with a distinct shelf/slope break and a cycle of base level rise and fall. Using various surfaces or hypothetical time lines as unit boundaries five main types of sequences have been defined. These are: (1) Depositional Sequence Type II bounded by a subaerial unconformity and/or a ravinement surface, and the time line equivalent to start of base level rise (end of base level fall) (Jervey, 1988). (2) Depositional Sequence Type III bounded by a subaerial unconformity and/or a ravinement surface and the time line equivalent to the start of base level fall (Jervey, 1993). (3) Depositional Sequence Type I bounded by a subaerial unconformity and/or a ravinement surface and a slope onlap surface. (4) Genetic Stratigraphic Sequence bounded by maximum flooding surfaces (Galloway, 1989). (5) T-R Sequence bounded by a subaerial unconformity and/or a ravinement surface and a transgressive surface (Embry, 1993).*

line forms the boundary for a Depositional Sequence Type II (Jervey, 1988; Posamentier et al., 1988).

4. ***Start of Landward Movement of the Shoreline*** – This event is the start of transgression and the subaerial unconformity continues to be onlapped. The erosive shoreface ravinement surface begins to migrate landward at this time and often erodes through portions of the underlying onlapping sediments and the subaerial unconformity. In the marine area a conformable transgressive surface, which separates shallowing-upward, regressive sediments from deepening-upward, transgressive sediments, is generated. The combination of the subaerial unconformity and/or the ravinement surface and the conformable transgressive surface is used for the boundary of a T-R Sequence (Embry, 1993).

5. ***Start of Seaward Movement of the Shoreline*** – This event is the start of regression and represents the time of maximum landward extent of the shoreline. The stratigraphic surface generated at this time is the maximum flooding surface which is the stratigraphic surface which separates transgressive strata from overlying regressive strata. The surface varies from being conformable to being unconformable where submarine scour results in net sediment loss at this time (offshore marine surface of erosion). The Genetic Stratigraphic Sequence of Galloway (1989) has maximum flooding surfaces as boundaries. Parasequences, as used by Van Wagoner et al. (1990), also have maximum flooding surfaces for boundaries in most cases.

EVALUATION OF SEQUENCE TYPES

When trying to decide what sequence type is appropriate for a given study, it is useful to consider the ease and objectivity of boundary recognition over the study area and the relationship of the sequence to the geological history. In regard to the second point, the T-R Sequence and the three types of Depositional Sequence are all very useful in areas where subaerial unconformities are present. In contrast, the Genetic Stratigraphic Sequence is not recommended for such situations. The reason for this is that depositional and tectonic changes commonly occur across subaerial unconformities and it is essential that such surfaces not be included within a genetic unit (e.g., Genetic Stratigraphic Sequence).

In areas where the sequence boundaries are conformities the T-R Sequence and the Genetic Stratigraphic Sequence are most practical to use because they have readily recognizable boundaries. Depositional Sequence Type II and Type III are very difficult to employ in such settings because they have unrecognizable correlative conformities (hypothetical time lines). Depositional Sequence Type I has the slope onlap surface as the correlative conformity and thus can be used only in areas where this surface is generated. This type of sequence is not practical in shallow marine ramp settings.

In study areas where both unconformities and conformities are present, the T-R Sequence is most practical. It has unconformities on the boundaries and has readily recognizable correlative conformities. All other sequence types have at least one major drawback which diminishes their value in such a setting.

REFERENCES

Embry, A.F.
1993: Transgressive-regressive (T-R) sequence analysis of the Jurassic succession of the Sverdrup Basin, Canadian Arctic Archipelago. Canadian Journal of Earth Sciences, v. 30, p. 301–320.

Galloway, W.E.
1989: Genetic stratigraphic sequences in basin analysis I: architecture and genesis of flooding-surface bounded depositional units. American Association of Petroleum Geologists, Bulletin, v. 73, p. 125–142.

Jervey, M.T.
1988: Quantitative modeling of siliciclastic rock sequences and their seismic expression. *In* Sea level changes: an integrated approach, C.K. Wilgus et al. (eds.). SEPM Special Publicaton 42, p. 47–70.

1993: Siliciclastic sequence development in foreland basins, with examples from Western Canada Foreland Basin. *In* Foreland basins and fold belts, R.W. Macqueen and D.A. Leckie (eds.). American Association of Petroleum Geologists, Memoir 55, p. 47–80.

Posamentier, H.W., Jervey, M.T., and Vail, P.R.
1988: Eustatic controls on clastic deposition I - conceptual framework. *In* Sea level change: an integrated approach, C.K. Wilgus et al. (eds.). SEPM Specical Publication 42, p. 109–124.

Posamentier, H.W., Allen, G.P., James, D.P., and Tesson, M.
1992: Forced regressions in a sequence stratigraphic framework: concepts, examples and exploration significance. American Association of Petroleum Geologists, Bulletin, v. 76, p. 1687–1709.

Vail, P.R., Mitchum, R.M., and Todd, R.G.
1977: Seismic stratigraphy and global changes in sea level. *In* Seismic stratigraphy – applications to hydrocarbon exploration. American Association of Petroleum Geologists, Memoir 26, p. 49–212.

Van Wagoner, J.C., Mitchum, R.M., Campion, K.M., and Rahmanian, V.D.
1990: Siliciclastic sequence stratigraphy in well logs, cores and outcrops. Methods in Exploration. American Association of Petroleum Geologists, no. 7.

GEOLOGY AND RESOURCE POTENTIAL OF PRINCE PATRICK AND EGLINTON ISLANDS REGION, CANADIAN ARCTIC ISLANDS

J.C. Harrison and T.A. Brent

Geological Survey of Canada, 3303-33rd Street N.W., Calgary, Alberta T2L 2A7

INTRODUCTION

Hydrocarbon exploration on Prince Patrick and Eglinton islands (including the intervening marine channels) was carried out by Husky (Elf), Esso, Panarctic and Triad (BP) from 1971 to 1976. Targets, including Silurian shelf edge carbonate buildups, Tertiary anticlinal culminations, and Jurassic and Triassic basin margin sandstones were assessed with a reconnaissance grid of seismic data and eight exploratory wells. Results proved to be disappointing and exploration in the area was abandoned. The present report provides an introductory reassessment of hydrocarbon and mineral resources from revised bedrock geological maps (Harrison, 1993) and reprocessed seismic data.

SURFACE GEOLOGY (Figure 1)

Exposed strata range from Middle Devonian to Pliocene in age. Devonian strata include various formations of an extensive Middle and Upper Devonian foreland clastic wedge. Vitrinite data indicate that these latter rocks range from oil window in the Famennian to thermally overmature in older strata (Embry, 1988; Goodarzi, pres. comm., 1994). Paleozoic strata are broadly folded about northwestward-trending lines and are overlain with profound angular unconformity by Upper Triassic to Lower Cretaceous strata of the Sverdrup Basin and Upper Jurassic to Upper Cretaceous strata of Eglinton Graben. Faulted outliers of Middle Jurassic to Lower Cretaceous strata are also known in a belt of northward-trending horsts and grabens located between Green Bay and Walker Inlet on southern Prince Patrick Island. Folds of probable early Tertiary age are mapped throughout the region. However, the magnitude of shortening is insignificant. The western two-thirds of Prince Patrick Island is mantled by a continuous near-flat-lying and unconformable blanket of Pliocene sand (Beaufort Formation).

SUBSURFACE GEOLOGY (Figures 2-4)

Seismic mapping has defined an extensive belt of northward- and northwestward-trending thrust anticlines and synclines expressed within both the Devonian clastic wedge and in underlying Silurian and older shelf carbonate strata. Intensity of shortening is most pronounced beneath Mesozoic and older cover of northeastern Eglinton and Prince Patrick islands. Important detachments are documented at two levels in the Cambrian and at the base of the Devonian clastic wedge. The Devonian clastic wedge is extensively and deeply eroded below the northeastern fold belt. In contrast, Devonian clastics range to 5500 m thick within a regional syncline that extends from southwestern Prince Patrick Island to southern Eglinton Island.

Upper Paleozoic and Mesozoic strata on seismic profiles present a northeastward thickening wedge of relatively undeformed strata. Upper Paleozoic strata are overstepped to the southwest in the subsurface by the Triassic and are therefore only found northeast of the Intrepid and Jameson Bay wells. Overstep relationships are documented at numerous other levels in this succession.

An important recent discovery is the documentation of: 1) a previously unreported sedimentary basin ("Tullett Point basin") beneath western Prince Patrick Island, and 2) a subsurface rift zone extending from Mould Bay northward to the Cape Discovery area on the north coast of the Island ("Cape Discovery graben"). The east side of the rift is defined by a horst block of Devonian "basement" rocks centred on Green Bay. Both the basin and rift zone remain untested. However, seismic correlation and surface geological constraints indicate Middle Jurassic (Bajocian) through mid-Early Cretceous (Albian) phases of rifting and sediment accumulation. Sediment thickness in "Tullett Point basin" and "Cape Discovery graben" ranges to 1300 m and 2100 m, respectively.

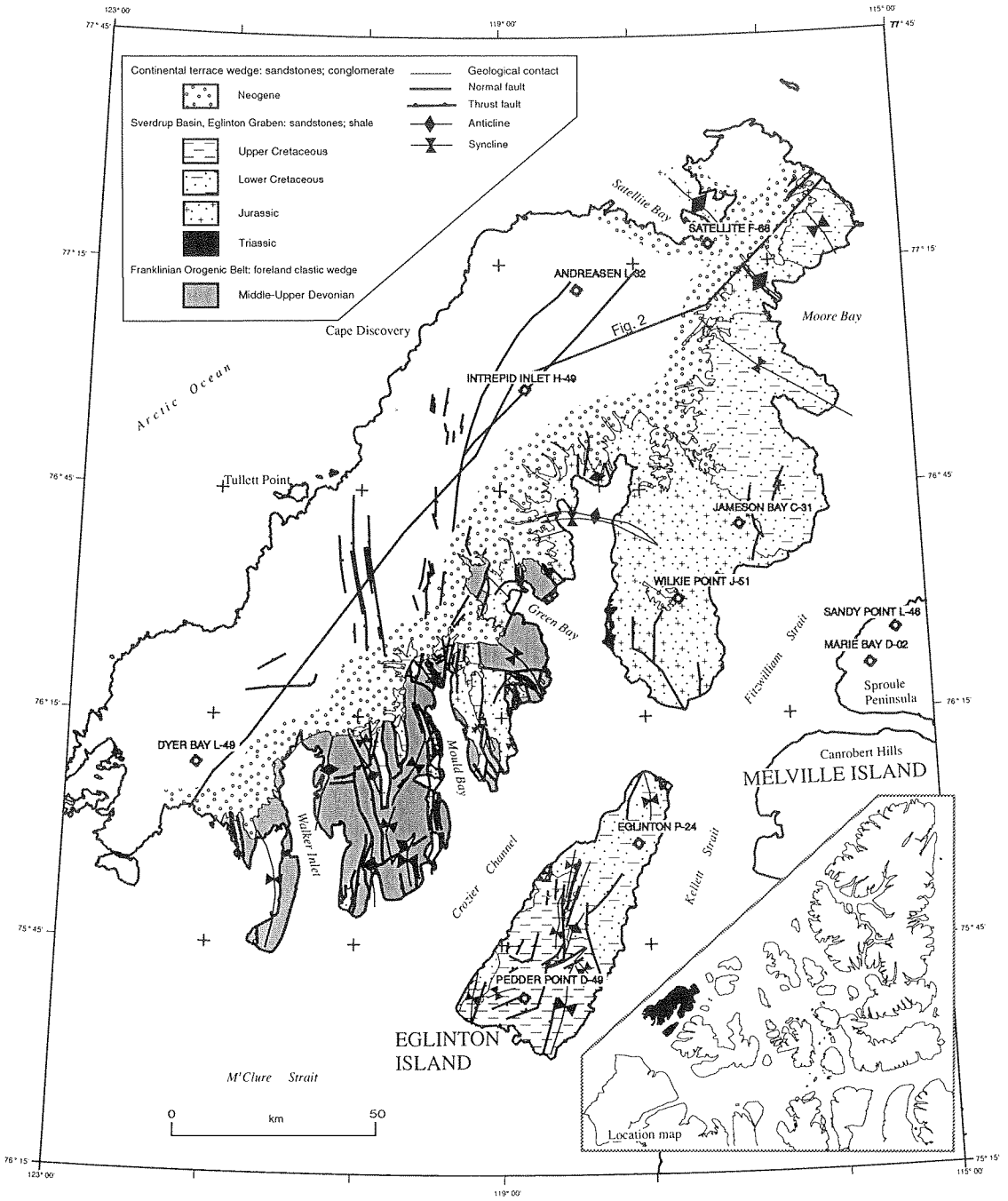

Figure 1. *Bedrock geology of Prince Patrick and Eglinton islands, western Canadian Arctic Islands (simplified from Harrison et al., 1994).*

RESOURCE POTENTIAL

Lower Paleozoic. Potential source rocks lie in a widespread Early Devonian condensed interval. Middle Devonian slope shales may also possess some source potential. Silurian shelf edge and forereef carbonates (tested at two locations), and Middle to Upper Devonian marine sandstones provide the best potential reservoir rocks. However, vitrinite and related organic matter indicates widespread thermally overmature conditions for Middle Devonian and older strata of the Prince Patrick and Eglinton islands.

Sverdrup Basin. Contained organic matter ranges from fully mature in the upper Paleozoic and deeper Mesozoic to immmature in the younger and shallower

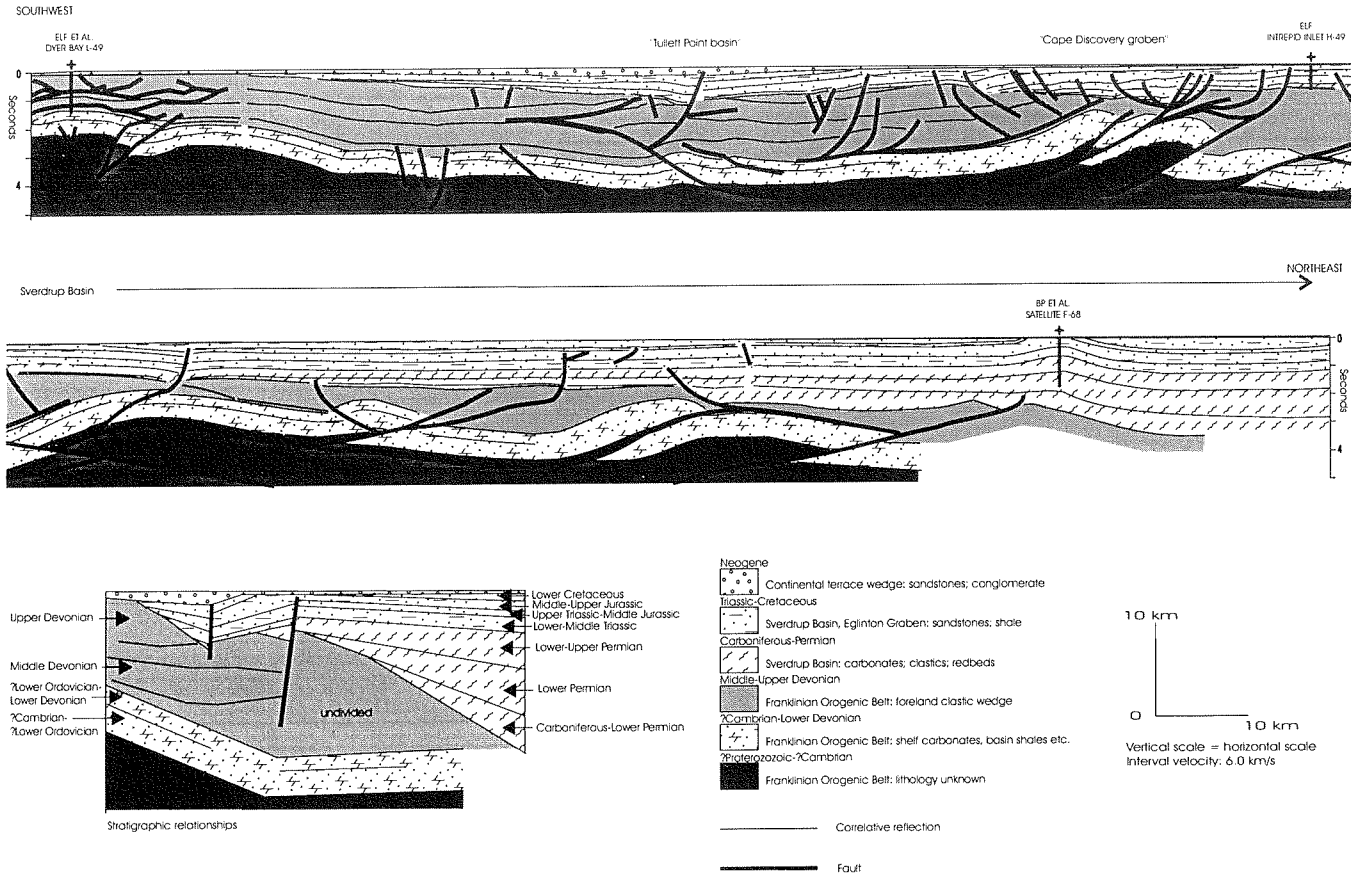

Figure 2. *Time-structure cross-section of Prince Patrick Island as provided by migrated seismic reflection profiles. Vertical exaggeration ranges from approximately 2.6 for the youngest and slowest Mesozoic strata (est. 2.3 km s^{-1}) to 1.0 for the fastest lower Paleozoic strata (est. 6.0 km s^{-1}).*

Mesozoic. Known source rocks of the western Sverdrup Basin occur in the Middle and Upper Triassic and Lower Jurassic (Embry et al., 1991). Stratigraphic traps (updip pinch out of reservoir sands) have significant potential but remain difficult and risky targets. Larger structural traps, including the Moore Bay anticline, have been drilled. However, the location and extent of closure on this structure remains unknown. Smaller anticlinal closures remain untested.

Eglinton Graben. Two structures have been drilled and found to be barren. Numerous small traps remain untested. Thick and widespread accumulations of bedded oolitic manganese (rhodochrosite) have been identified at surface in the Eglinton Member of the Kanguk Formation (Upper Cretaceous). Thin coal seams occur near the north end of the island in the Lower Cretaceous.

"Tullett Point basin" and "Cape Discovery graben". Source and reservoir potential is unknown. This entire area remains untested and seismically underexplored. Lignite grade coal has been noted in the graben immediately east of the Mould Bay weather station.

REFERENCES

Embry, A.F.
1988: Middle-Upper Devonian sedimentation in the Canadian Arctic Islands and the Ellesmerian Orogeny. *In* Devonian of the World - Proceedings of the Second International Symposium on the Devonian System, N.J. McMillan, A.F. Embry, and D.J. Glass (eds.). Canadian Society of Petroleum Geologists, Memoir 14, p. 15–28.

Embry, A.F., Powell, T.G., and Mayr, U.
1991: Petroleum resources, Arctic Islands. *In* Chapter 20 of Innuitian Orogen and Arctic Platform: Canada and Greenland, H.P. Trettin (ed.). Geological Survey of Canada, Geology of Canada No. 3, p. 263–279.

Harrison, J.C.
1993: Geology of Prince Patrick and Eglinton islands, Canadian Arctic Archipleago. Geological Survey of Canada, Open File 2654, scale 1:125 000 (five sheets).

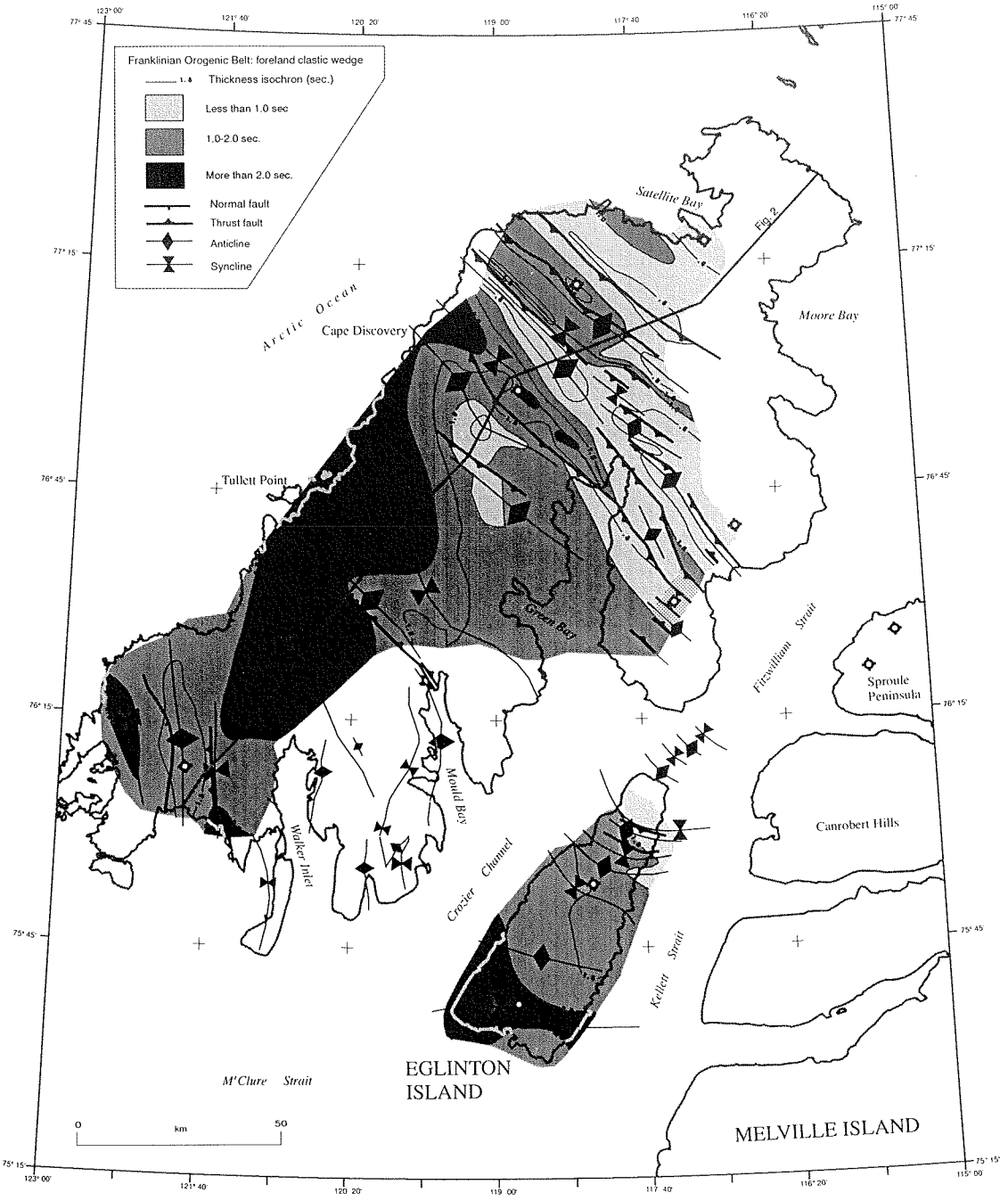

Figure 3. *Time-thickness and structure of the upper Paleozoic and Mesozoic strata of Prince Patrick and Eglinton islands. Positions of faults have been plotted as located on seismic profiles at the base of this succession whereas fold traces may extend to surface.*

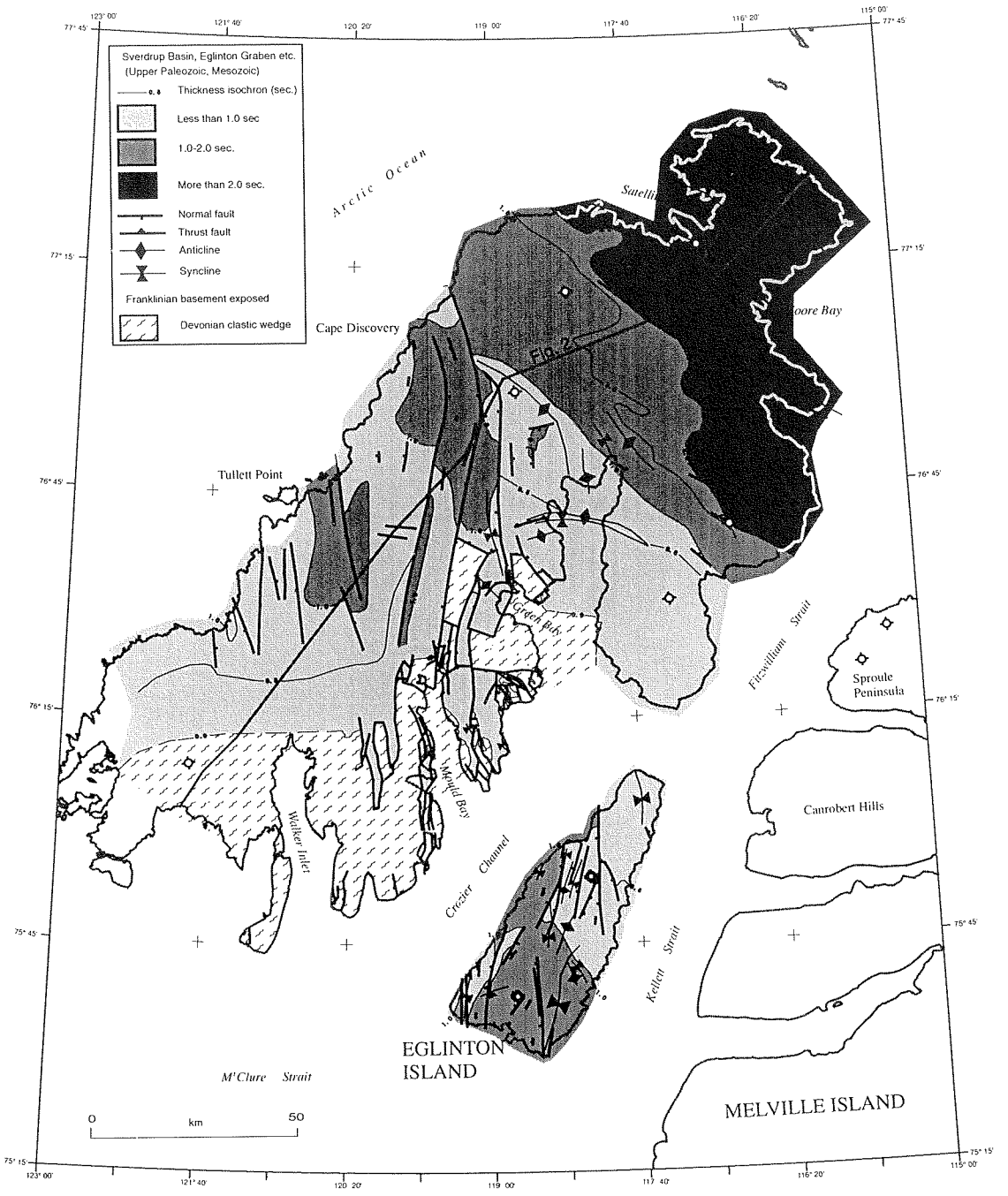

Figure 4. *Time-thickness and structure of the Devonian clastic wedge of Prince Patrick and Eglinton islands. Folds and faults have been plotted as located on seismic profiles at the base of this succession but are plotted at surface in the belt of Devonian outcrops on southern Prince Patrick Island.*

STRUCTURAL CONTROLS ON POTENTIAL HYDROCARBON ACCUMULATIONS OF CENTRAL ELLESMERE ISLAND

J.C. Harrison, T. de Freitas, and R. Thorsteinsson

Geological Survey of Canada, 3303-33rd Street N.W., Calgary, Alberta T2L 2A7

The resource exploration history and stratigraphic setting for potential hydrocarbon accumulations of central Ellesmere Island are summarized by de Freitas et al., this volume. The present paper summarizes the tectonic history, and identifies potential structural traps.

TECTONIC HISTORY

Early Cambrian to Early Devonian (Figs. 1–3)

- Stable platform carbonate, siliciclastic and, in the Ordovician, evaporite deposition (Trettin et al., 1991; de Freitas et al., this volume).
- The shelf to deep-water basin transition displays large fluctuations in position through time.
- Common Silurian and Lower Devonian (reservoir) reefs deposited on central Ellesmere Island (de Freitas et al., this volume).
- Phases of movement on the Bache uplift are indicated by syntectonic redbed clastic wedges and some faulting (Pragian–Emsian).

Middle–Upper Devonian (Figs. 2–4)

- Deposition of a northerly- and westerly-derived foreland clastic wedge more than 2000 m thick (Middle–Upper Devonian; Embry, 1991).
- Southward- to southeastward-directed folding and thrusting related to the plate convergence of Pearya with ancestral North America (Okulitch, 1991).

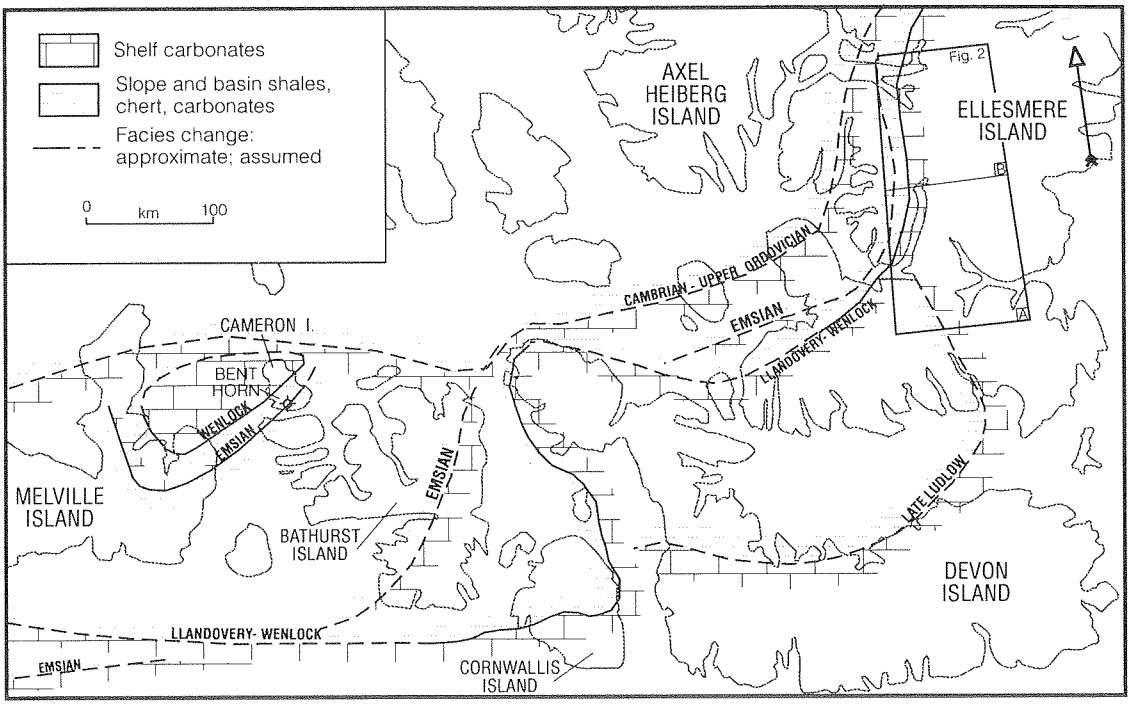

Figure 1. Location map and Cambrian to Devonian shelf edge facies fronts of the eastern Arctic Islands (modified from Trettin et al., 1991).

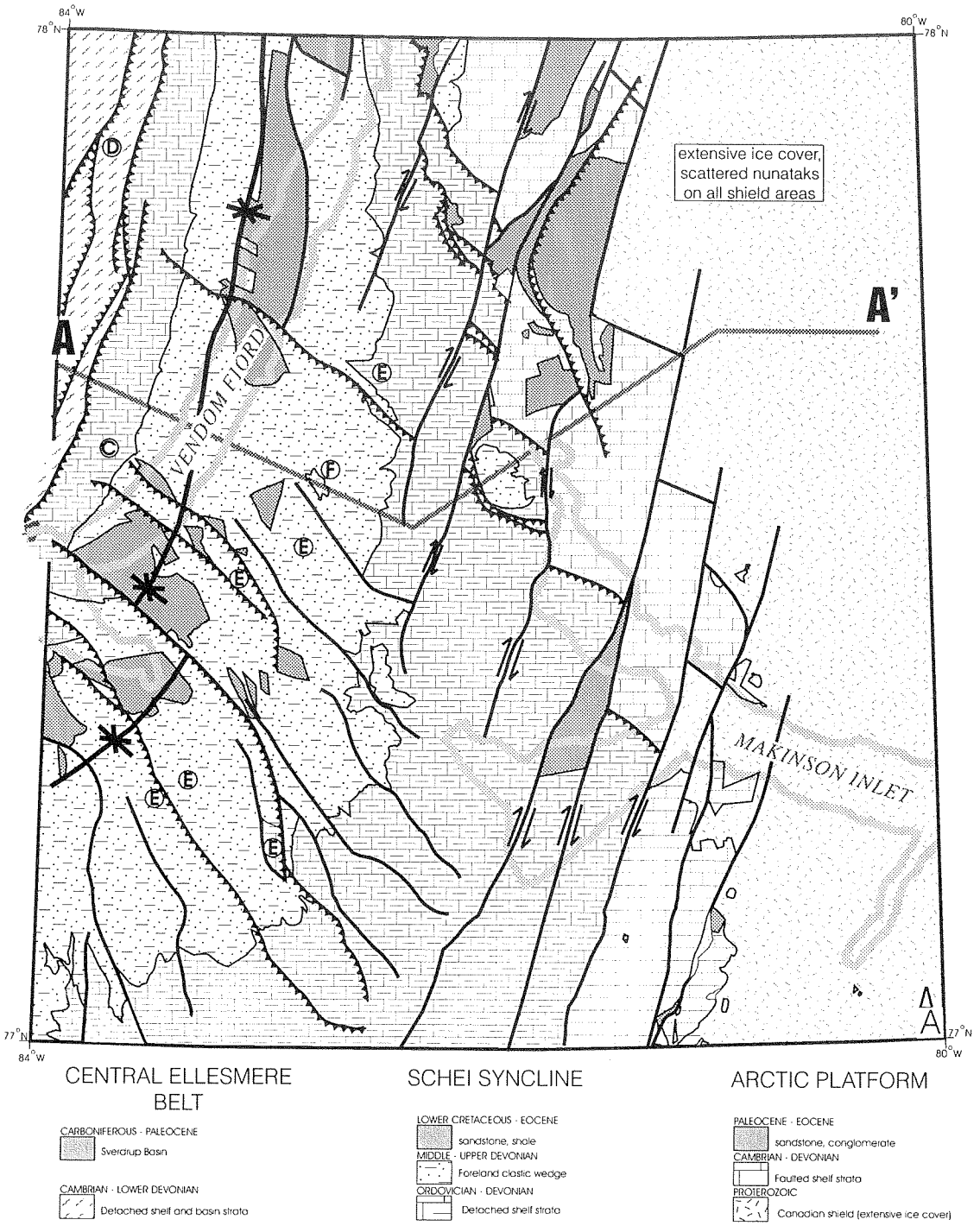

Figure 2a. *Geology of Vendom Fiord map area (adapted from Thorsteinsson et al., 1994).*

- Thrusts extend to the east side of the Schei Syncline within a décollement riding in Ordovician evaporites (Thorsteinsson et al., 1994; Harrison et al., 1994).
- The western limb of the Schei Syncline lies above a major thrust ramp linking a possible Lower Cambrian detachment to Ordovician evaporites.
- Other thrusts link the evaporite detachment to an upper detachment in Lower Devonian slope shales.

Early Carboniferous–Jurassic

- Rifting and passive subsidence of the Sverdrup Basin (Stephenson et al., 1987).

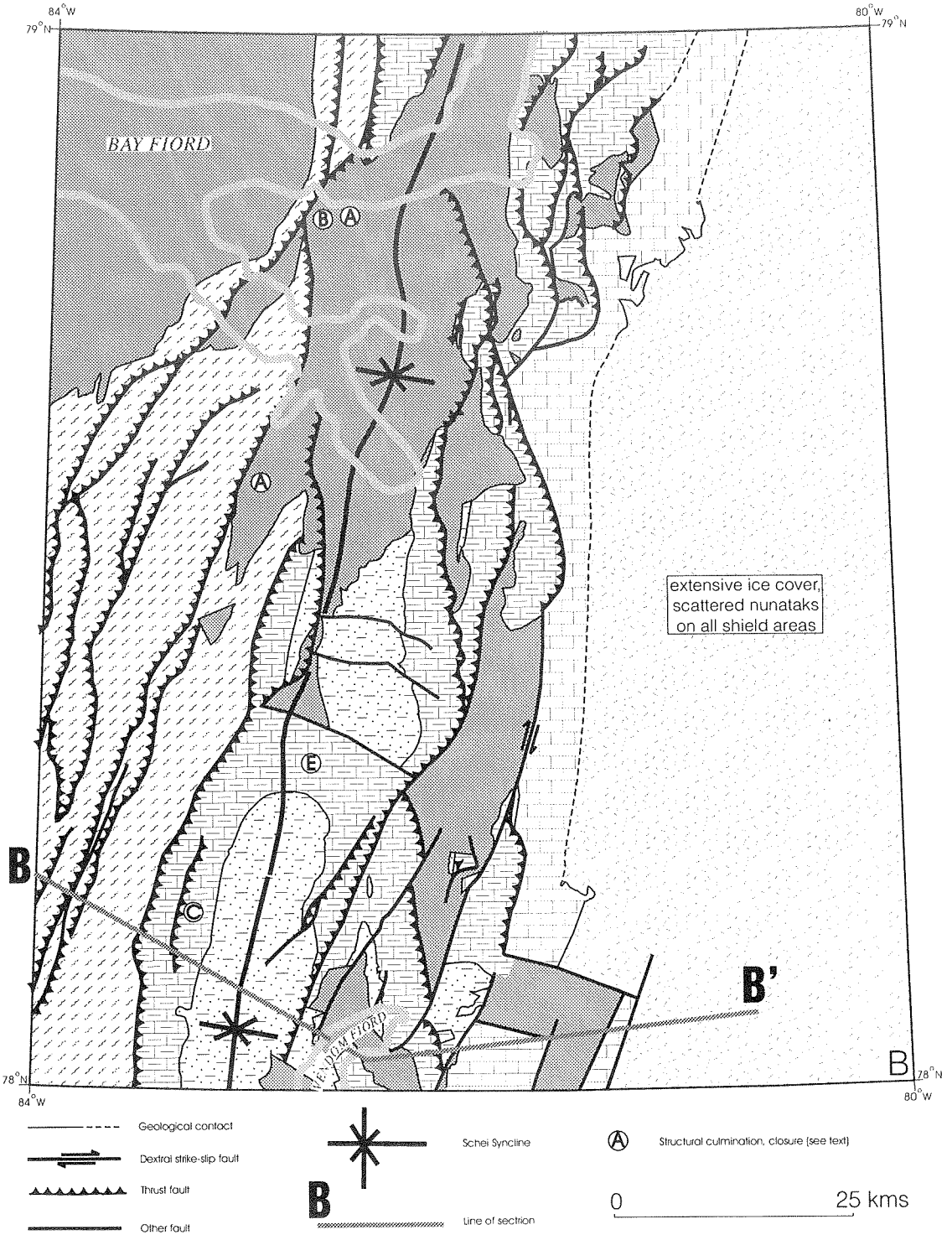

Figure 2b. *Geology of Strathcona Fiord map area (adapted from Harrison et al., 1994).*

Early Cretaceous–Paleocene (Figs. 2, 3, 5)

- Incipient rifting in Baffin Bay and southeastern Ellesmere Island produces northwestward striking normal faults and northward striking strike-slip faults throughout the Schei Syncline (Trettin and Okulitch, 1991).

- Intrusion of gabbro dyke swarm(s) on Axel Heiberg and northern Ellesmere islands.

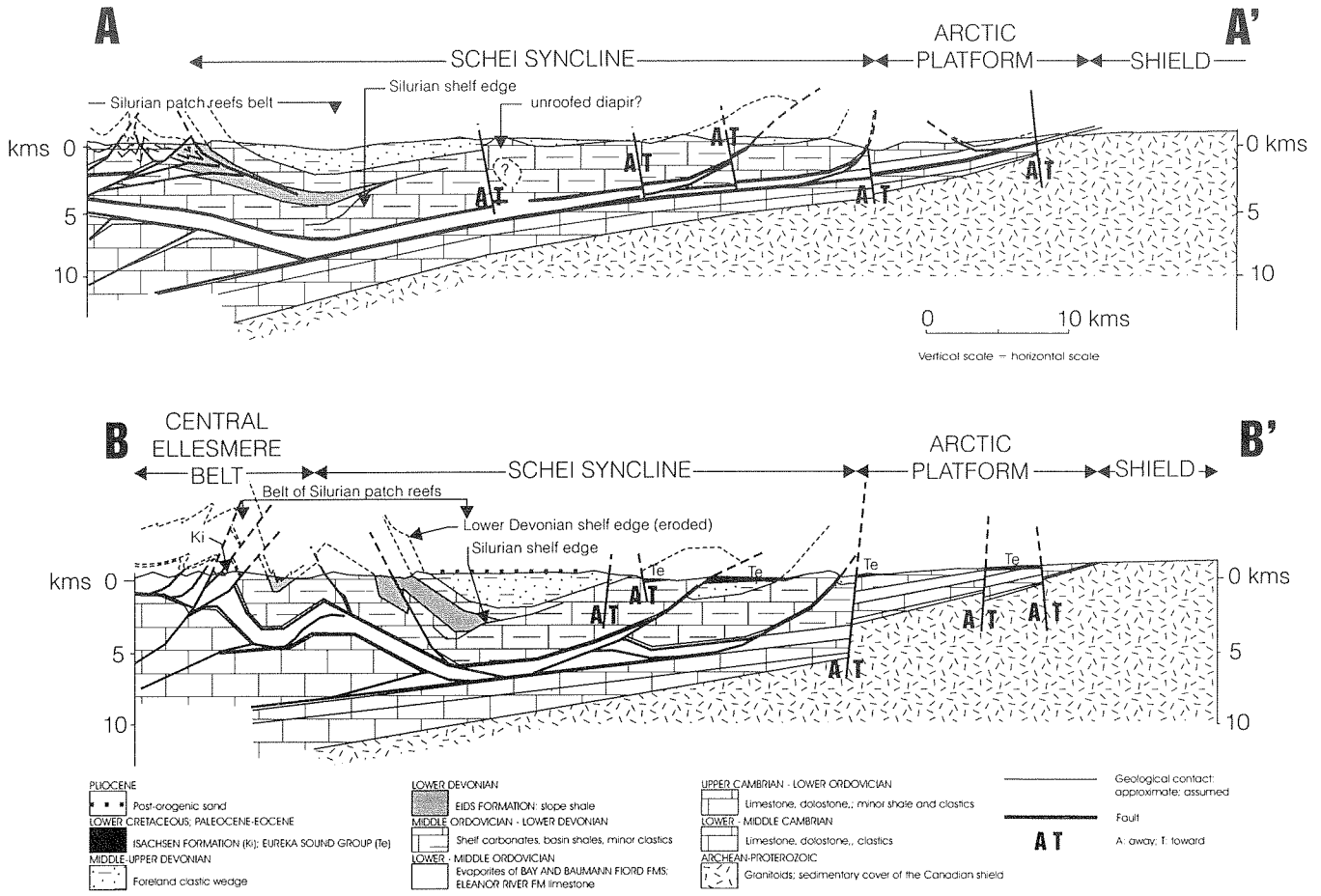

Figure 3. *Schematic structural cross-sections of central Ellesmere Island. Depth to detachments and gross structure under Schei Syncline is based on data obtained from unmigrated seismic profiles of southwestern Ellesmere Island. Lines of sections are shown on Figure 2.*

Eocene–Oligocene (Figs. 2, 3, 6)

- Convergence of the ancestral Greenland tectonic plate (including southeastern Ellsemere Island) with the Arctic Islands during partly coeval oceanic spreading in Baffin Bay and Labrador Sea (Trettin and Okulitch, 1991).

- Northwestward-striking thrusts and northerly-striking dextral strike-slip faults on central Ellesmere Island (Thorsteinsson et al., 1994; Harrison et al., 1994).

- Ordovician thrust over Tertiary on east side of Schei Syncline.

- Reactivation and refolding of many prexisting Ellesmerian structures.

- Inversion of Cretaceous-Tertiary normal faults.

- Unroofing of the Canadian shield in the early Eocene indicated by deposition of syntectonic conglomerates (Thorsteinsson et al., 1994; Harrison et al., 1994).

PETROLEUM POTENTIAL

Source rocks. Silurian and Lower Devonian basin facies shales (de Freitas et al., this volume).

Reservoir rocks and oil shows. Dolomitized Silurian and Lower Devonian shelf edge and offshore build-ups and forereef breccias — identified at surface and potentially discovered with additional seismic data and testing; Lower Devonian basinal sandstones (de Freitas et al., this volume).

Seals. Lower Devonian slope shales; Ordovician evaporites.

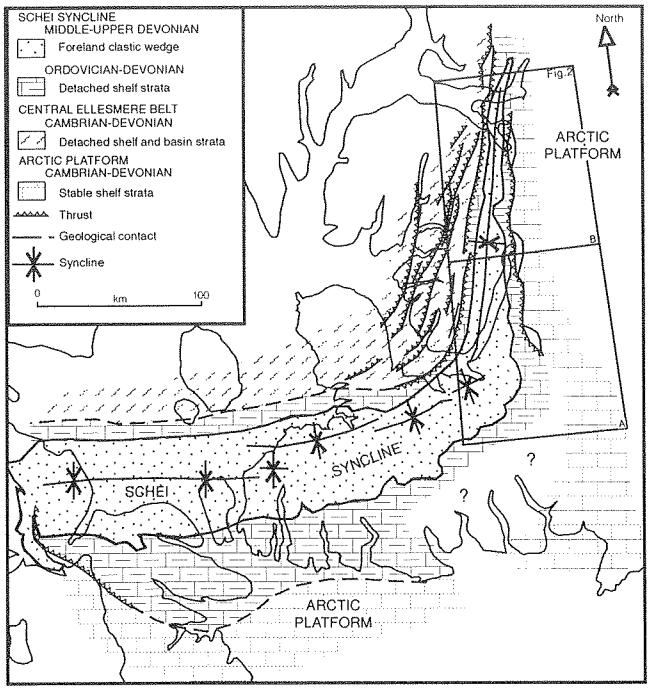

Figure 4. *Major tectonic elements of the Ellesmerian Orogeny (latest Devonian-early Carboniferous), central Ellesmere Island (modified from Trettin et al., 1991).*

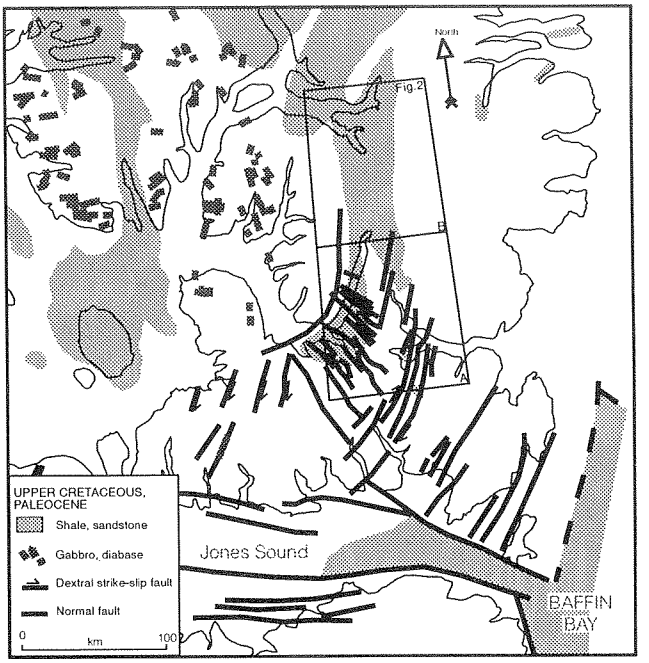

Figure 5. *Late Cretaceous and Paleocene paleogeography, igneous rocks and tectonic elements of central Ellesmere Island (modified from Trettin and Okulitch, 1991).*

Thermal maturity. Oil window for source and reservoir rocks throughout central Ellesmere (de Freitas et al., this volume).

Potential structural traps (lettered examples located on Figs. 2, 3)

A. Northward-trending Tertiary anticlinal culminations in Tertiary and older strata of Schei Syncline.

B. Northward-trending Tertiary anticlinal culminations in Devonian and older strata of Schei Syncline.

C. Tertiary and/or mid-Paleozoic anticlinal culminations in Devonian and older strata of Schei Syncline.

D. Tertiary and/or mid-Paleozoic anticlinal culminations within the central Ellesmere thrust-fold belt.

E. Hangingwall of northwestward-striking thrusts in Schei Syncline.

F. Semicircular culmination in Schei Syncline (above unroofed evaporite diapir?).

REFERENCES

Embry, A.F.
1991: Middle–Upper Devonian clastic wedge of the Arctic Islands. *In* Innuitian Orogen and Arctic Platform: Canada and Greenland, H.P. Trettin (ed.). Geological Survey of Canada, Geology of Canada No. 3, p. 263–279.

Harrison, J.C., Thorsteinsson, R., and de Freitas, T.A.
1994: Phanerozoic geology of Strathcona Fiord map area (NTS 49E and part of 39F), District of Franklin, Northwest Territories. Geological Survey of Canada, Open File 2881, scale 1:125 000 (1 sheet).

Okulitch, A.V.
1991: Late Devonian–Early Carboniferous deformation of the central Ellesmere and Jones Sound fold belts. *In* Innuitian Orogen and Arctic Platform: Canada and Greenland, H.P. Trettin (ed.). Geological Survey of Canada, Geology of Canada No. 3, p. 318–320.

Okulitch, A.V. and Trettin, H.P.
1991: Late Cretaceous–Early Tertiary deformation, Arctic Islands. *In* Innuitian Orogen and Arctic Platform: Canada and Greenland, H.P. Trettin (ed.). Geological Survey of Canada, Geology of Canada No. 3, p. 469–489.

Stephenson, R.A., Embry, A.F., Nakiboglu, S.M., and Hastaoglu, M.A.
1987: Rift-initiated Permian to Early Cretaceous subsidence of the Sverdrup Basin. *In* Sedimentary basins and basin-forming mechanisms, C. Beaumont and A.J. Tankard (eds.). Canadian Society of Petroleum Geologists, Memoir 12, p. 213–231.

Thorsteinsson, R., Harrison, J.C., and de Freitas, T.
1994: Phanerozoic geology of Vendom Fiord map area (NTS 49D), District of Franklin, Northwest Territories. Geological Survey of Canada, Open File 2880, scale 1:125 000.

Trettin, H.P., Mayr, U., Long, G.D.F., and Packard, J.J.
1991: Cambrian to Early Devonian deposition, Arctic Islands. *In* Innuitian Orogen and Arctic Platform: Canada and Greenland, H.P. Trettin (ed.). Geological Survey of Canada, Geology of Canada No. 3, p. 163–237.

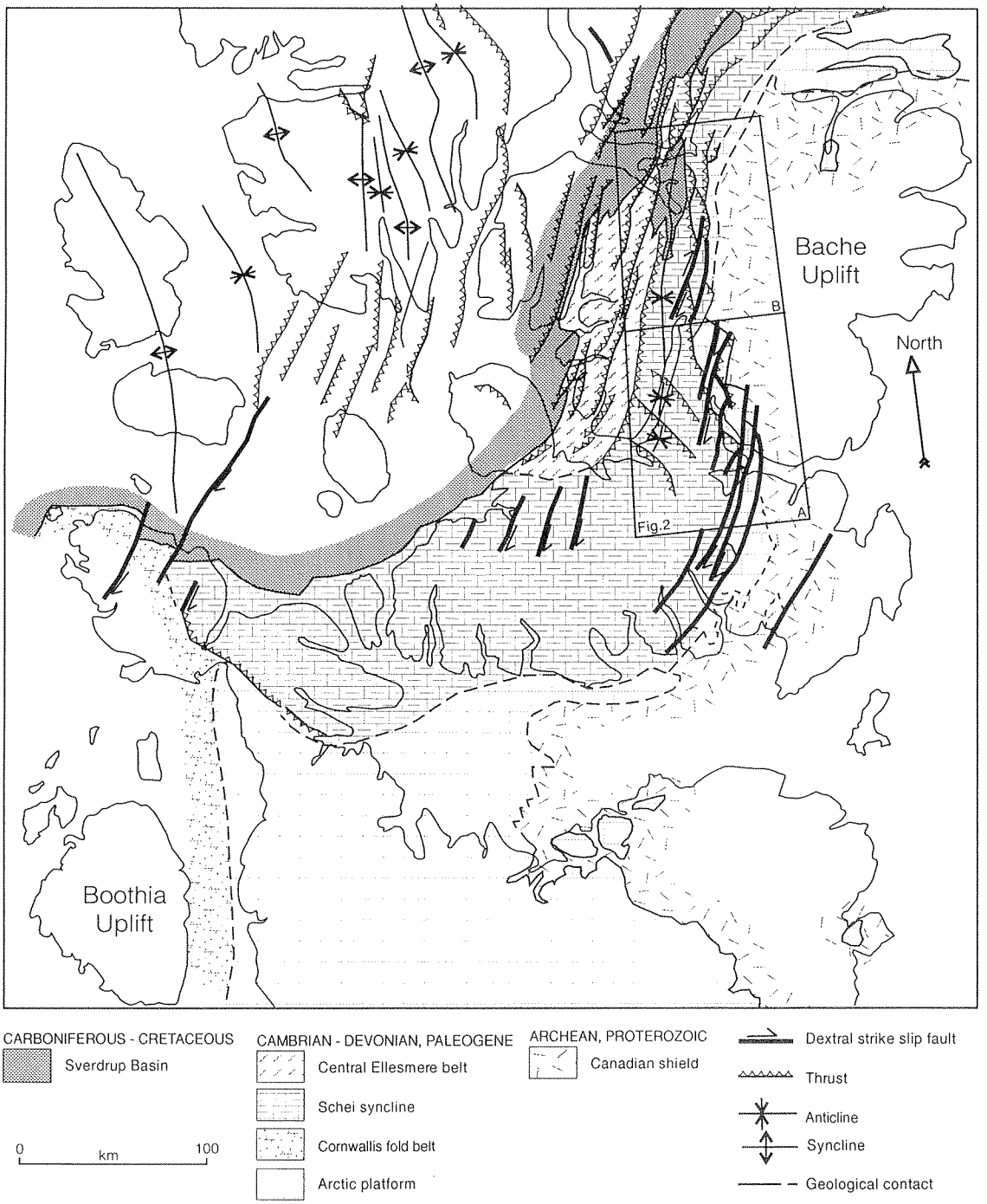

Figure 6. *Major tectonic elements of the Eurekan Orogeny (Eocene-Oligocene) of the eastern Arctic Islands (modified from Trettin and Okulitch, 1991).*

AN OVERVIEW OF FOSSIL FUNGAL ASSEMBLAGE FROM THE ICEBERG BAY FORMATION, EUREKA SOUND GROUP, AT KANGUK PENINSULA, AXEL HEIBERG ISLAND, NORTHWEST TERRITORIES

R.M. Kalgutkar

Geological Survey of Canada, 3303-33rd Street N.W., Calgary, Alberta T2L 2A7

ABSTRACT

This preliminary progress report illustrates an assemblage of well-preserved and noteworthy fungal remains containing spores and fruiting structures encountered during the palynological investigation of the area. Controlled oxidation technique was applied to samples from Section RAK-83-27 to secure recovery of fungal palynomorphs. A total of 34 genera and 79 species of fungal spores are being investigated and will be subsequently described for publication. The entire assemblage was characterized by wide morphological diversity in the fungal population and is supported by the Floristic Similarity Index. Preliminary examination of pollen and fungal floras infer an age range of Late Paleocene to Early Eocene and a mesothermal humid climate with swamp conditions for the Iceberg Bay Formation at Kanguk Peninsula.

INTRODUCTION

The distribution of plant microfossils, and their abundance in subsurface and well samples where other fossils are not available for correlation purposes, have made palynology an important hydrocarbon and mineral exploration tool. Among the various types of plant microfossils, the study of fungal spores and fruiting bodies in biostratigraphy (mycostratigraphy) and paleoclimatic interpretations is the newest and the least well known.

In recent years, however, information on fossil fungi has increased rapidly, providing not only significant data on the diversity of fungi in the fossil record but also on the potential relationships that exist among the major groups of fungi (Taylor and White, 1989).

Because of their universal distributions, fungal palynomorphs commonly occur in samples in which other fossils useful for age determinations or paleoenvironmental considerations are not present. In other samples, they provide independent and sometimes more precise, age control than is otherwise available. The application of fossil fungi in biostratigraphy has increased with discoveries of characteristic and unique spores having limited stratigraphic ranges. Distinctive fungal spores like *Pesavis* and *Ctenosporites* are used more than often by palynologists as index fossils to substantiate age determinations. Kalgutkar and Sweet (1988) documented the first occurrence of *Pesavis* in the Maastrichtian from northwestern Canada. The stratigraphic usefulness of *Pesavis* was further developed by Kalgutkar and Sweet with the documentation of a phylogenetic lineage starting in the Maastrichtian with *P. parva* (Pl. 1, fig. 10) and extending into the Eocene with *P. tagluensis* (Pl. 1, fig. 11). Fossil microthyriaceous fructifications and helicosporous fungi are generally considered as reliable indicators of paleoenvironmental conditions.

Fossil fungi are receiving greater attention in the studies concerning the boundary events. Visscher and Brugman (1986) and Visscher (1988) reported the noteworthy and dominant assemblage of fungal remains at the Permian-Triassic (P-T) boundary in the southern Alps and visualized the plant world of the western part of the Tethys realm at the very end of Paleozoic dying as a result of a polluted atmosphere and decaying as a result of extreme fungal activity. The exclusive presence of fungal spores in the Permian–Triassic boundary horizon in Israel with existence of no pollen and other spores is inferred as indicative of a strong ecological stress during the transition from the Permian to the Triassic which resulted in the extinction of most Permian flora and the expansion of the fungal activity that replaced the extinct vegetation (Eshet, 1989).

Remains of fossil fungi are also an important source of information for interpreting past environments if their affinities to extant species have been determined. It is now widely accepted that an emphasis on the combined studies of fossil and living fungi is necessary to realize the full potential of fossil palynomorphs as

predictors of past environments (Kalgutkar and McIntyre, 1991).

An assemblage of fossil dispersed fungal palynomorphs was recovered from the Iceberg Bay Formation, Eureka Sound Group at Kanguk Peninsula, Axel Heiberg Island, Northwest Territories (Fig. 1). Thirteen of 35 samples from Section RAK-83-27 yielded a noteworthy and well preserved population of fungal spores and fructifications after reprocessing them by controlled oxidation technique.

RESULTS

Occurrence

A total of 34 genera and 79 species of fungal spores and fruiting bodies were recorded. Twenty-one new species will be subsequently described. An entire assemblage was characterized by the presence of distinctive spores such as *Ctenosporites eskerensis* (Pl. 1, fig. 1), *Dictyosporites eccentricus* (Pl. 1, fig. 2), *Diporicellaesporites pluricellus* (Pl. 1, fig. 3), *Psilodiporites krempii* (Pl. 1, fig. 4), *Diporisporites anklesvarensis* (Pl. 1, fig. 5), *Helicoon-Helicodendron*-type (Pl. 1, fig. 8), *Helicosporium*-type (Pl. 1, fig. 9), *Palaeocirrenalia oligoseptatum* (Pl. 1, fig. 6), *Pesavis tagluensis* (Pl. 1, fig. 11) and microthyriaceous ascocarps (fructifications) of *Callimothallus pertusus* (Pl. 1, fig. 13), *Euthythyrites oleinites* (Pl. 1, fig. 14), *Microthallites lotusus* (Pl. 1, fig. 16), *Paramicrothallites canadensis* (Pl. 1, fig. 17), *Paramicrothallites* sp. (Pl. 1, fig. 18), *Phragmothyrites eocaenica* (Pl. 1, fig. 19), *Plochmopeltinites masoni* (Pl. 1, fig. 21), *P. cooksoni* (Pl. 1, fig. 20), and species of *Trichothyrites* (Pl. 1, fig. 15).

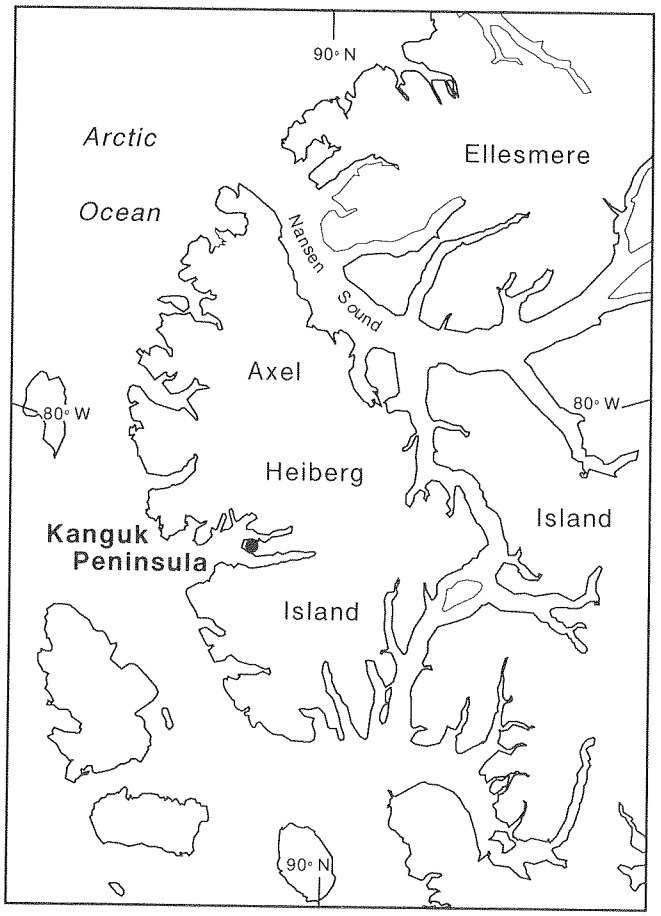

Figure 1. *Location of Section RAK-83-27 in the Iceberg Bay Formation, Kanguk Peninsula, Axel Heiberg Island.*

The total flora of Section RAK-83-27 contained species which are restricted to one sample each and species very limited in their distribution (Fig. 2). This indicates floral diversity in the fungal population of the Iceberg Bay Formation and is supported by the values of the Coefficient of Similarity Index (Fig. 3).

Age

Preliminary examination of pollen flora indicates an age range of Late Paleocene to Early Eocene for the Iceberg Bay Formation at Kanguk Peninsula. The presence of helicosporous fungi and other fungi such as *Dicellaesporites* sp. (Pl. 1 , fig. 7), *Phragmothyrites eocaenica*, *Plochmopeltinites cooksoni* suggest an Early Eocene age based on the comparison with the known fungal flora of the Early Eocene in the Iceberg Bay Formation at Strand Fiord. The presence of *Ctenosporites eskerensis*, *Diporicellaesporites pluricellus*, and *Diporisporites anklesvarensis*, which are mainly restricted to the Eocene of the Arctic, also favour an Eocene age for the samples.

Paleoenvironment

The presence of diversified and remarkable fungal population in the Iceberg Bay Formation at Kanguk Peninsula is indicative of an environment ideal and conductive to the flourishing of these fungi. The fungal spores were generally found to be related to the types belonging to extant Hyphomycetes and Ascomycetes. This suggests that the depositional environments of the Iceberg Bay Formation strata favoured the growth of both saprophytic and parasitic forms along with epiphyllous fungi.

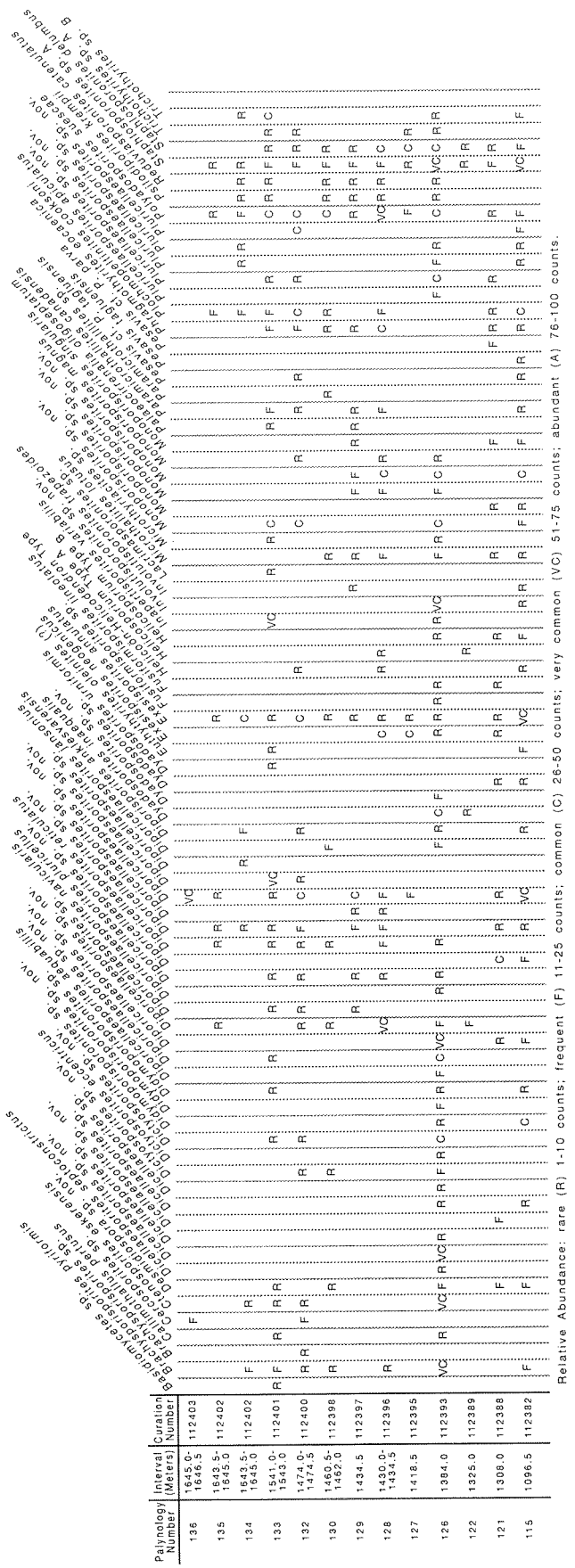

Distribution of various microthyriaceous fungi combined with common occurrences of hyphomycetous taxa of saprophytic nature suggests a mesothermal humid climate during deposition of the Iceberg Bay Formation at Kanguk Peninsula. The dominance of pollen of Taxodiaceae and the number of coal samples suggest the existence of swamp forest conditions with dominant vegetation consisting of coniferous trees. The presence of helicosporous fungi represented by *Helicoon-Helicodendron*-type, *Helicosporium*-type, species of *Involutisporonites* (Pl. 1, fig. 12) and *Palaeocirrenalia oligoseptatum*, which typically have been found in fossil aquatic habitats with open, marshy and waterlogged areas (Ramanujam and Srisailam, 1978; Kalgutkar and McIntyre, 1991), indicates a similar depositional climate in the Iceberg Bay Formation at Kanguk Peninsula. Ricketts (1991) has concluded that the extensive coal-bearing strata from this part of the Iceberg Bay Formation are of delta-plain origin. Swamp forest would most likely be a major vegetation type in such an environment.

A Coefficient of Similarity Index was applied to the spore assemblages from each sample to determine the degree of floristic affinity between samples. The Sörensen Coefficient (K) expresses degree of floristic similarity and gives a good indication of the affinity between two floras. The "K" values obtained for fungal assemblages differed significantly from each of their fungi, thereby suggesting a floral diversity in the fungal population of the Iceberg Bay Formation.

Sample Numbers	115	121	122	126	127	128	129	130	132	133	134	135	136
115		58	10	47	23	44	44	36	44	45	40	28	5
121			14	33	40	43	43	43	31	37	27	40	8
122				14	33	29	17	32	12	11	11	33	0
126					21	39	26	38	42	48	35	14	4
127						40	38	38	34	32	29	57	20
128							71	59	59	48	43	47	15
129								48	43	52	36	38	9
130									43	44	50	48	12
132										61	38	40	13
133											44	26	12
134												48	12
135													20
136													

Figure 3. *Coefficient of similarity (K-values)–between samples.*

Figure 2. *Distribution and relative abundance of fungi in Iceberg Bay Formation.*

REFERENCES

Eshet, Y.
1990: The palynostratigraphy of the Permian-Triassic boundary in Israel: Two approaches to biostratigraphy. The Weizmann Science Press of Israel, v. 39, p. 1–15.

Kalgutkar, R.M. and McIntyre, D.J.
1991: Helicosporous fungi and early Eocene pollen flora, Eureka Sound Group, Axel Heiberg Island, N.W.T. Canadian Journal of Earth Sciences, v. 28, p. 364–371.

Kalgutkar, R.M. and Sweet, A. R.
1988: Morphology, taxonomy and phylogeny of the fossil fungal genus *Pesavis* from northwestern Canada. Contributions to Canadian Paleontology, Geological Survey of Canada, Bulletin 379, p. 117–133.

Ramanujam, C.G.K. and Srisailam, K.
1978: Fossil fungal spores from the Neogene beds around Cannanore in Kerala State. Botanique, v. 9, p. 119–138.

Ricketts, B.D.
1991: Delta evolution in the Eureka Sound Group, Western Axel Heiberg Island: The transition from wave-dominated to fluvial-dominated deltas. Geological Survey of Canada, Bulletin 402, 72 p.

Taylor, T.N. and White, J.F., Jr.
1989: Fossil fungi (Endogonaceae) from the Triassic of Antarctica. American Journal of Botany, v. 76, p. 389–396.

Visscher, H.
1988: A dramatic floral event at the Permian-Triassic junction. 7th International Palynological Congress, Brisbane, Australia, Abstracts, 174 p.

Visscher, H. and Brugman, W.A.
1986: The Permian-Triassic boundary in the southern Alps: A palynological approach. Memorie della Societa Geologica Italiana, v. 34, p. 121–128.

PLATE 1

In the explanation of figures, all figured photographs were taken using a Carl Zeiss transmitted light microscope with attached camera. All photographs x1000, unless otherwise indicated.

Fungal Spores

Figure 1. *Ctenosporites eskerensis*
Figure 2. *Dictyosporites eccentricus* x500
Figure 3. *Diporicellaesporites pluricellus*
Figure 4. *Psilodiporites krempii*
Figure 5. *Diporisporites anklesvarensis*
Figure 6. *Palaeocirrenalia oligoseptatum*
Figure 7. *Dicellaesporites* sp. nov.
Figure 8. *Helicoon-Helicodendron*-type
Figure 9. *Helicosporium*-type
Figure 10. *Pesavis parva*
Figure 11. *Pesavis tagluensis*
Figure 12. *Invoutisporonites trapezoides*

Microthyriaceous Ascocarps

Figure 13. *Callimothallus pertusus*
Figure 14. *Euthythyrites oleinites* x500
Figure 15. *Trichothyrites* sp.
Figure 16. *Microthallites lutosus* x500
Figure 17. *Paramicrothallites canadensis*
Figure 18. *Paramicrothallites* sp. x500
Figure 19. *Phragmothyrites eocaenica* x500
Figure 20. *Plochmopeltinites cooksoni* x500
Figure 21. *Plochmopeltinites masoni* x500

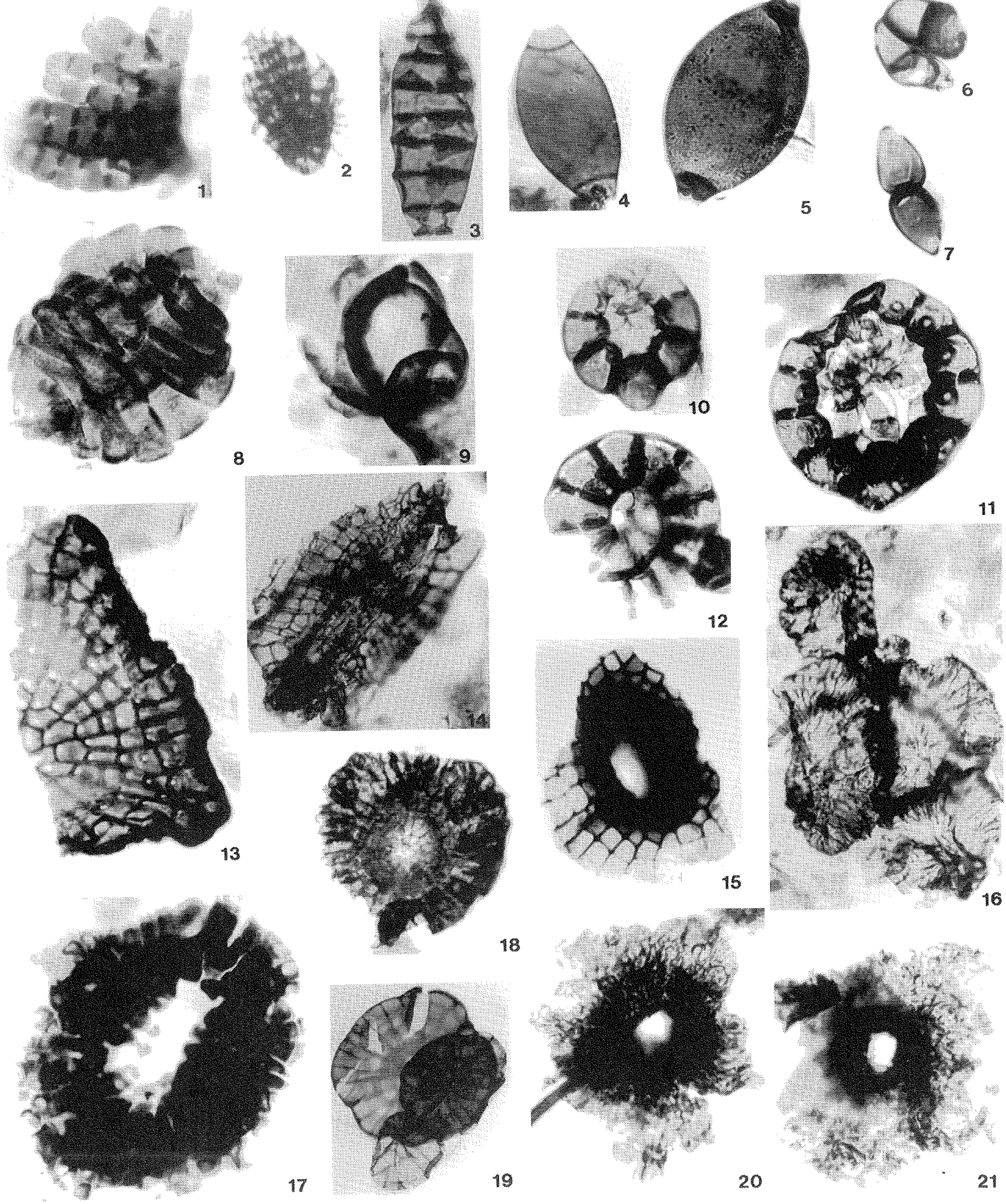
1
2
3
4
5
6
7
8
9
10
11
12
13
14
15
16
17
18
19
20
21

SHALE PORE-STRUCTURE EVOLUTION UNDER VARIABLE SEDIMENTATION RATES IN THE BEAUFORT–MACKENZIE BASIN

T.J. Katsube

Geological Survey of Canada, 601 Booth Street, Ottawa, Ontario K1A 0E8

J. Bloch

Scealu Modus, 2617 Cutler Avenue N.E., Albuquerque, New Mexico 87106

D.R. Issler

Geological Survey of Canada, 3303-33rd Street N.W., Calgary, Alberta T2L 2A7

ABSTRACT

Petrophysical characteristics of shales from a range of depths (0.9–4.5 km) and areas with different sedimentation rates in the Beaufort–Mackenzie Basin are being studied to obtain a better understanding of shale compaction and abnormal pressure development processes. As a result, pore-structure evolution models for increasing depth of burial and varied sedimentation rate have been developed. Shale pore-structure is characterized by a unimodal pore-size distribution. In normally compacted zones, both porosity and pore-size mode decrease with depth. In zones with higher sedimentation rates, porosity decreases with increasing burial depth, but with essentially little or no change in the pore-size modes. The study of shale pore-size distributions may provide important clues concerning the mechanisms for overpressure generation (e.g., disequilibrium compaction, hydrocarbon generation) and the timing of overpressure development in relation to the sediment burial history.

INTRODUCTION

Petrophysical characteristics of shales from areas with different sedimentation rates (depths: 0.9–4.5 km) in the Beaufort–Mackenzie Basin are being studied (e.g., Issler and Katsube, 1994; Katsube and Issler, 1993; Katsube and Best, 1992) to obtain a better understanding of shale compaction and abnormal pressure development processes. Results indicate that porosity (ϕ) and permeability (k) decrease with increasing burial depth and approach minimum values (ϕ = 5–15%, k = 10^{-21}–10^{-20} m^2) at the critical depth of burial (CDB; Katsube and Williamson, 1994a, b), at approximately 2.5–3.5 km. This trend may be reduced or reversed at greater depths. At the CDB, most of the mechanical compaction and permeability reduction is complete with pore-size modes approaching minimum values. High sedimentation rates tend to increase the CDB (Issler and Katsube, 1994) as indicated in Figure 1. Shale pore-size distribution changes with depth and sedimentation rate (Katsube and Issler, 1993). In this paper, we present pore structure evolution models for burial depth, sedimentation rate, overpressure development, and discuss the shale texture changes involved in these processes.

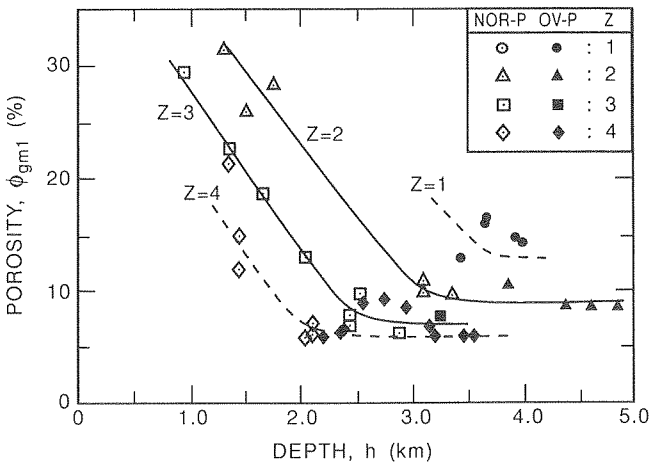

Figure 1. *Mercury porosity (ϕ_{gm1}) as a function of depth (h) for Beaufort–Mackenzie Basin shale samples from four compaction zones with different time-averaged Pliocene- Pleistocene sedimentation rates (Issler and Katsube, 1994). Z–zone; NOR-P–normally pressured; OV-P–overpressured. Sedimentation rates decrease from zone 1 to zone 4. Sedimentation has been effectively continuous in zones 1 to 3 whereas zone 4 has experienced erosion (<1 km).*

BASIC SHALE PORE STRUCTURE MODEL

Nano-pores, in the range of 3 to 14 nm, constitute the main pore throats (Katsube et al., 1991, 1992) or fluid flow paths of tight shales, and are the reason for extremely low shale permeabilities of 10^{-22}–2 x $10^{-20}m^2$. These nano-pores are characterized by unimodal distributions of 0.3–60 nm (solid curve; Fig. 2) with mean pore-sizes or modes, d_{np}, of 2.7–11.5 nm (Katsube, 1992); values representing some of the smallest known pore-sizes for rocks. Pore-sizes above 25 nm do exist but do not significantly contribute to the flow paths, although they may be part of the interconnected pore-structure network. Pore-size distribution analysis for a suite of tight shale samples (Katsube, 1992; Katsube et al., 1992) has shown that the contribution to porosity from nano-pores (ϕ_{np}) is 1.5–10.2%, which is about 83±4% of their effective porosity (ϕ_E).

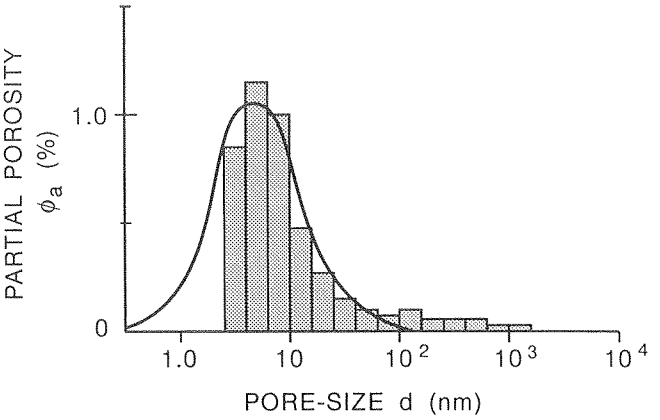

Figure 2. *Unimodal distribution of nano-pores (0.3–60 nm) characterizing tight shales (Katsube, 1992). The sum of partial porosity (ϕ_a) values contributed by each pore-size class (d) equals the effective porosity (ϕ_E) for the shale sample.*

EVOLUTION MODELS

Model (I): Effect of burial

Shales are characterized by unimodal pore-size distributions, with modes and porosities decreasing from approximately 200–400 nm and 30%, respectively, at approximately 1000 m depth, to 10–20 nm and 5–15% at the CDB and at greater depth (Issler and Katsube, 1994; Katsube and Issler, 1993) as a result of normal compaction. Figure 3 shows the porosity (ϕ_{gml}) and mean pore-size (d_{hg}) decrease (left-hand side) and pore-size distribution change (right-hand side) with increasing depth for Beaufort–Mackenzie Basin shale samples (Katsube and Issler, 1993) from a normally compacted zone with a time-averaged Pliocene–Pleistocene sedimentation rate of 40–190 m/m.y. (zone 3 of Issler, 1992). The shaded horizontal lines (left-hand side) indicate sample locations for pore-size distributions displayed on the right. Permeabilities (k) of samples at depths of 2.46 and 2.88 km have already reached extremely low values of 3 x 10^{-21} and 2 x $10^{-22}m^2$, respectively. This variable, depth-dependent pore-size distribution (Fig. 3) is also shown in Figure 4, where the distributions are represented by normal distribution-like curves (solid lines) that shift to the left-hand side of the diagram as depth increases. The corresponding depths (h) and effective porosities (ϕ_E in brackets) for these solid curves (indicated by arrows) are displayed at the top of the diagram.

Model (II): Effect of sedimentation rate

High sedimentation rates tend to delay the porosity decrease with depth and increase the CDB (Issler and Katsube, 1994), as previously indicated (Fig. 1). Pore-size distributions at similar depths (2.9–4.0 km) for zones of different sedimentation rate are compared in Figure 5. The time-averaged Pliocene- Pleistocene sedimentation rates for these zones (zones 1, 2 and 3) are 380–660 m/m.y., 190–380 m/m.y. and 40–190 m/m.y., respectively (Issler 1992). Except for one sample (2.88 km; zone 3), pore-size modes remain essentially constant whereas maximum porosity decreases sequentially from zone 1 to zone 3 (Fig. 5). Samples at 3.67 and 4.01 km depth (zone 1) and at 3.25 km depth (zone 3) are overpressured. Unlike the normally compacted region of zone 3, where pore-size modes decrease with depth (Figs. 3, 4), a mode of 20–50 nm (equivalent depth of approximately 1.6 km in zone 3) is maintained to greater depths of 3–4 km in zones of higher sedimentation rate (zones 1 and 2). This trend is illustrated in Figure 4 by the normal distribution-like curves (broken lines). The numbers above those in the brackets at the upper left-hand side of Figure 4 represent the depth (km) and porosity (%) for these curves. Subscripts at the lower right of the brackets represent the zone of compaction. The curve representing 3.7 km and 16% porosity in zone 1 is overpressured, probably as a result of disequilibrium compaction in this zone of high sedimentation rate.

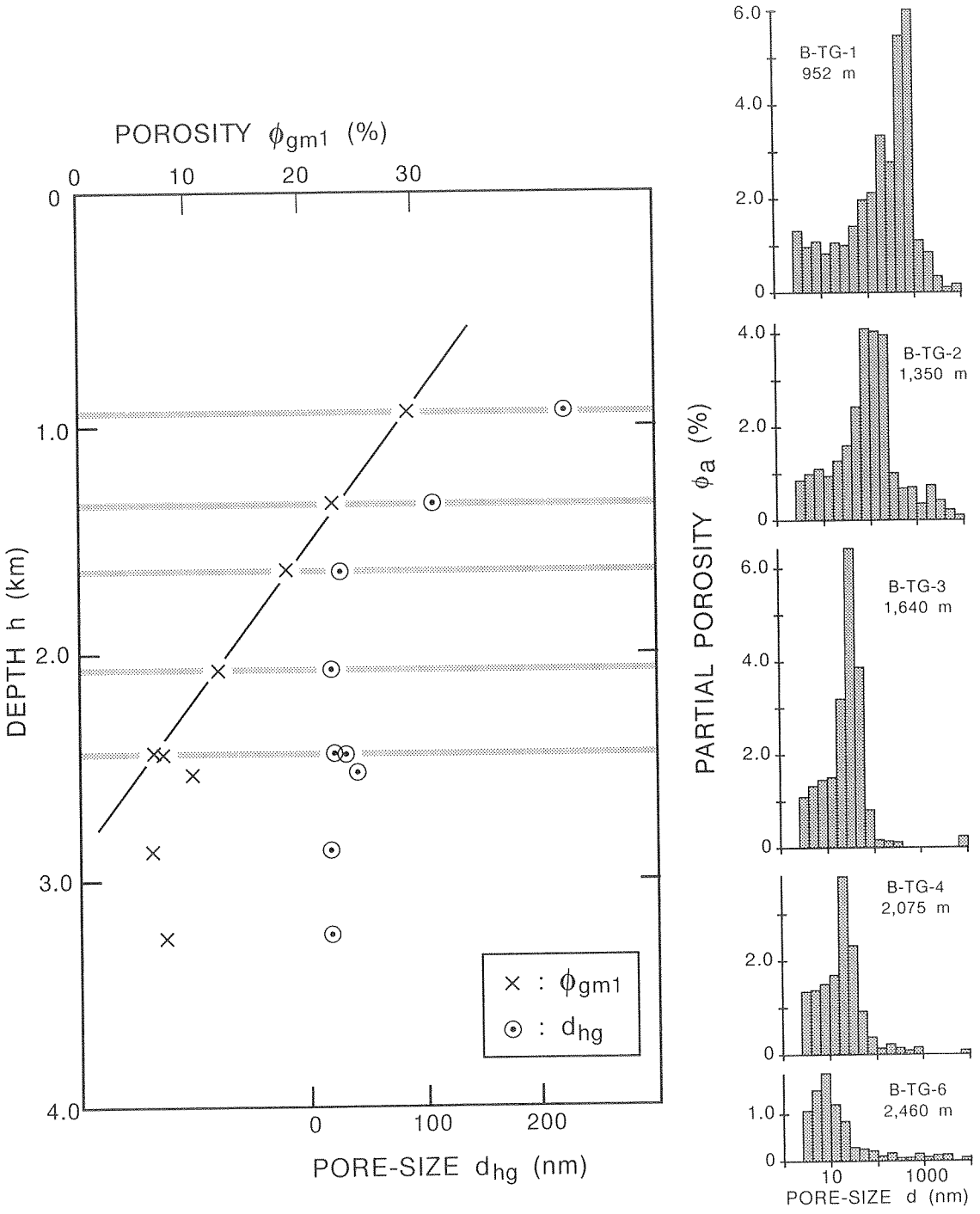

Figure 3. *Porosity (ϕ_{gm1}) and mean pore-size (d_{hg}) as a function of burial depth for samples from the three Taglu wells (zone 3) in the Beaufort–Mackenzie Basin (Katsube and Issler, 1993). Pore-size distributions for normally compacted shales are shown to the right of the porosity-depth plot and the shaded horizontal lines indicate the location of these samples.*

Model (III): Effect of overpressure

The contribution of certain pore-sizes (e.g., 30 nm) to the overall porosity is more pronounced in overpressured zones underlain by normally compacted strata (i.e., zones 3, 4 and 5 of Issler, 1992). The curve expressed by the shaded line in Figure 4 represents such a case. These type of pore-size distributions may be related to overpressure associated with disequilibrium compaction. Alternatively, if overpressures developed after maximum vertical compaction, these pore-size distributions may reflect other processes (e.g., hydrocarbon generation, change in regional stress field). Work is currently underway to determine whether pore-size distribution data can be used to discriminate between competing mechanisms of overpressure generation.

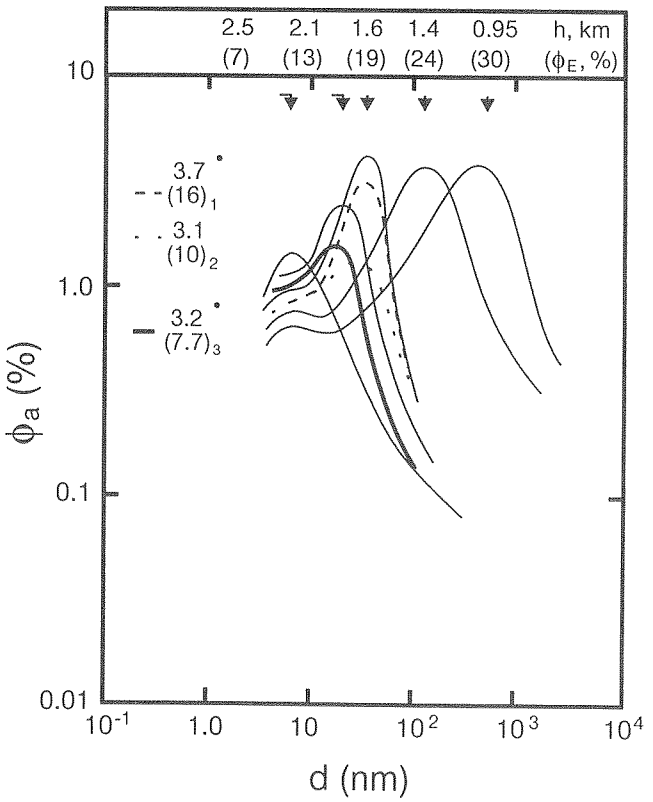

Figure 4. *Variation in pore-size distribution with depth. Sample depths are shown above corresponding effective porosity values (brackets). Subscripts adjacent to brackets refer to different compaction zones in the Beaufort–Mackenzie Basin. Solid lines: normally compacted zone (zone 3, Fig. 1). Broken lines: under compacted zones (zones 1 and 2). Shaded line: overpressured zone (zone 3, depth >3.2 km).*

SHALE TEXTURE EFFECTS

Petrographic data indicate that shales from normally compacted zones have well sorted fabrics with low silt contents. In contrast, shales from zones with high sedimentation rates have poorly sorted fabrics and high silt contents; a characteristic of rapid deposition. These textural features significantly influence the petrophysical properties of the shales. For example, the normally pressured shales generally develop significant compaction fabrics, including grain reorientation and concavo-convex contacts, at depths of approximately 2.5 km. This corresponds to the minimum CDB. In contrast, shales from zones with high sedimentation rates do not develop significant compaction fabrics until a depth of 3.5 km or the upper limit of the CDB. A high silt content yields a framework supported fabric which inhibits matrix compaction. This partially explains why high sedimentation rates delay the decrease of ϕ, k and d with depth.

SUMMARY

Shale pore-structure is characterized by a unimodal pore-size distribution, as described in Figures 2 and 3. The pore-structure evolution for increasing depth of burial, increased sedimentation rates and overpressure development are described in Figure 4. The pore-size distributions represented by normal distribution-like curves (solid lines) shift to the left-hand side of the diagram as burial depth increases. This is represented by a pore-size mode decrease with depth. At higher sedimentation rates, porosities decrease with burial depths (Fig. 1), similar to normal compaction conditions, but with essentially little or no change in the values of the pore-size modes. Further studies are needed to determine whether pore-size distributions can be used to distinguish between different overpressure mechanisms.

REFERENCES

Issler, D.R.
1992: A new approach to shale compaction and stratigraphic restoration, Beaufort–Mackenzie Basin and Mackenzie Corridor, Northern Canada. American Association of Petroleum Geologists Bulletin, v. 76, p. 1170–1189.

Issler, D.R. and Katsube, T.J.
1994: Effective porosity of shale samples from the Beaufort–Mackenzie Basin. *In* Current Research, Part B. Geological Survey of Canada, Paper 94–1B, p. 19–26.

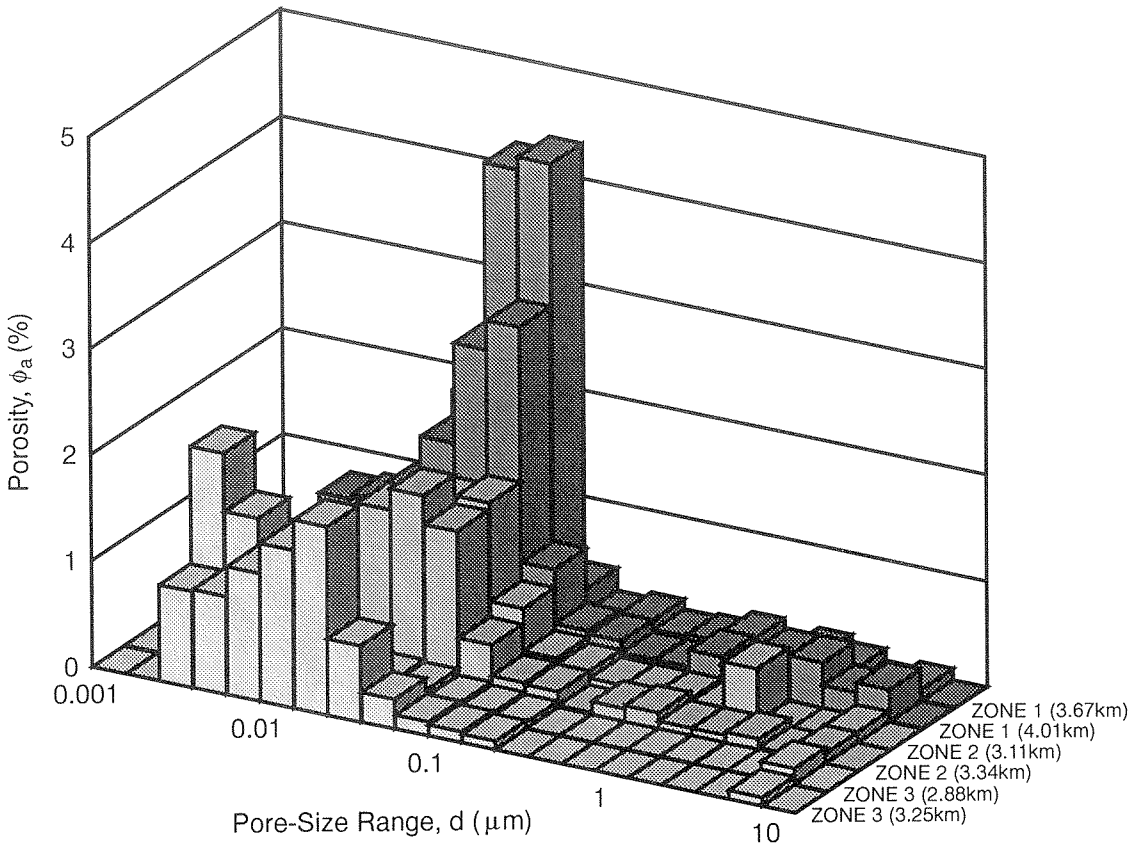

Figure 5. *Pore-size distribution for shale samples from different depths in the Beaufort–Mackenzie Basin. Time-averaged Pliocene–Pleistocene sedimentation rate decreases from zone 1 to zone 3. Zone 1 samples and a zone 3 sample (3.25 km) are overpressured.*

Katsube, T.J., Best, M.E., and Mudford, B.S.
1991: Petrophysical characteristics of shales from the Scotian Shelf. Geophysics, v. 56, p. 1681–1688.

Katsube, T.J.
1992: Statistical analysis of pore-size distribution data of tight shales from the Scotian Shelf. *In* Current Research, Part E. Geological Survey of Canada, Paper 92–1E, p. 365–372.

Katsube, T.J., and Best, M.E.
1992: Pore structure of shales from the Beaufort–Mackenzie Basin, Northwest Territories. *In* Current Research, Part E. Geological Survey of Canada, Paper 92–1E, p. 157–162.

Katsube, T.J., Williamson, M., and Best, M.E.
1992: Shale pore structure evolution and its effect on permeability. *In* Symposium Volume III of the Thirty-Third Annual Symposium of the Society of Professional Well Log Analysts (SPWLA). The Society of Core Analysts Preprints, Oklahoma City, Oklahoma, June 15-17, 1992, Paper SCA–9214, p. 1–22.

Katsube, T.J., and Issler, D.R.
1993: Pore-size distribution of shales from the Beaufort-Mackenzie Basin, northern Canada. *In* Current Research, Part E. Geological Survey of Canada, Paper 93–1E, p. 123–132.

Katsube, T.J. and Williamson, M.A.
1994a: Shale petrophysics and basin charge modelling. *In* Current Research, Part D. Geological Survey of Canada, Paper 94–1D, p. 179–188.

Katsube, T.J. and Williamson, M.A.
1994b: Effects of diagenesis on shale nano-pore structure and implications for sealing capacity: in press for "Proceedings of the Conference on Diagenesis, Overpressuring and Reservoir Quality", 25-26 March, 1993, Cambridge, England, U.K.

A NEW 3-STAGE MODEL FOR THE EVOLUTION OF THE WESTERN ARCTIC OCEAN

L.S. Lane

Geological Survey of Canada, 3303-33rd Street N.W., Calgary, Alberta T2L 2A7

ABSTRACT

Reinterpretation of the kinematic evolution of Canada Basin is required by new data on Beaufort Sea continental margin structure. At least three kinematic stages were required to produce the Canada and Makarov basins. Stage One produced the western Makarov Basin and an area adjacent to Arctic Alaska. Stage Two produced most of Canada Basin and the rifting of Chukchi Borderland northwestward, away from the Beaufort–Mackenzie region. Stage Three resulted from a ridge jump and fragmentation of the Arctic Ocean plate and produced a rectangular region in southern Canada Basin where spreading was oriented nearly east–west. Northern Canada Basin continued to spread northwestward, requiring an accommodation zone north of Chukchi Borderland.

INTRODUCTION

Numerous simple models have been proposed for the plate tectonic evolution of Canada Basin (reviewed in Lawver and Scotese, 1990). The most popular model invokes 66° of counterclockwise rotation of Arctic Alaska and Chukotka away from the Canadian Arctic Islands (Grantz et al., 1990a). That model is widely accepted on the basis of limited paleomagnetic data and the fit of geologic trends on such a rotation (Embry, 1992). Although those trends generally permit such an interpretation, they do not preclude alternatives.

Conversely, the following data conflict with the rotation hypothesis, casting doubt on its viability. The Alaska margin is 30 m.y. older than its supposed conjugate on the Canadian side. Chukchi borderland and the Russian continental shelf overlap onto the Canadian Arctic Islands by as much as 600 km on restoration of 66° of rotation (Fig. 1). The rotation model requires a hypothetical arcuate transform fault along which Chukotka was translated 2600 km (Fig. 1). The interpreted aeromagnetic anomalies in the southern Canada Basin do not fan sufficiently to validate the rotation hypothesis. Mantle velocity anisotropy indicates an opening direction nearly perpendicular to that required by the rotation hypothesis (Mair and Lyons, 1981).

The Frontier Geoscience Program of the Geological Survey of Canada funded geological, potential field, crustal-refraction and deep crustal-reflection seismic studies designed to provide new data for the crustal structure and geological evolution of the Beaufort Sea continental margin. Stephenson et al. (1994) synthesized those regional data into a well-constrained crustal model (Fig. 2). This paper summarizes the plate-kinematic implications of that synthesis (Lane 1994).

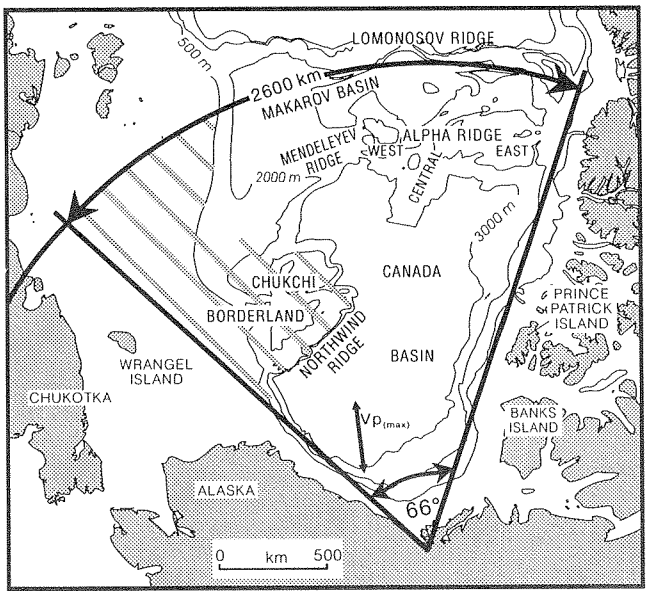

Figure 1. *Bathymetric map of the Arctic region showing 66° of rotation on a hypothetical transform fault adjacent to Lomonosov Ridge (Grantz et al., 1990a, b). Hachured area is continental overlap resulting from restoration of that rotation. Overlap area would increase using a less conservative estimate of the continent-ocean transition. Vpmax is the direction of maximum mantle P-wave velocity from Mair and Lyons (1981).*

NEW ARCTIC MODEL

The new Beaufort synthesis has a direct implication for the tectonic evolution of the Arctic Ocean. An offset in the continental margin near longitude 136°W is defined by the simultaneous, abrupt termination of both the continental margin gravity high and a linear magnetic low previously identified as marking the continent-ocean transition farther northeast (Fig. 2). The offset is interpreted as a fracture zone and is therefore a direct constraint on the kinematics of ocean opening in this part of the basin.

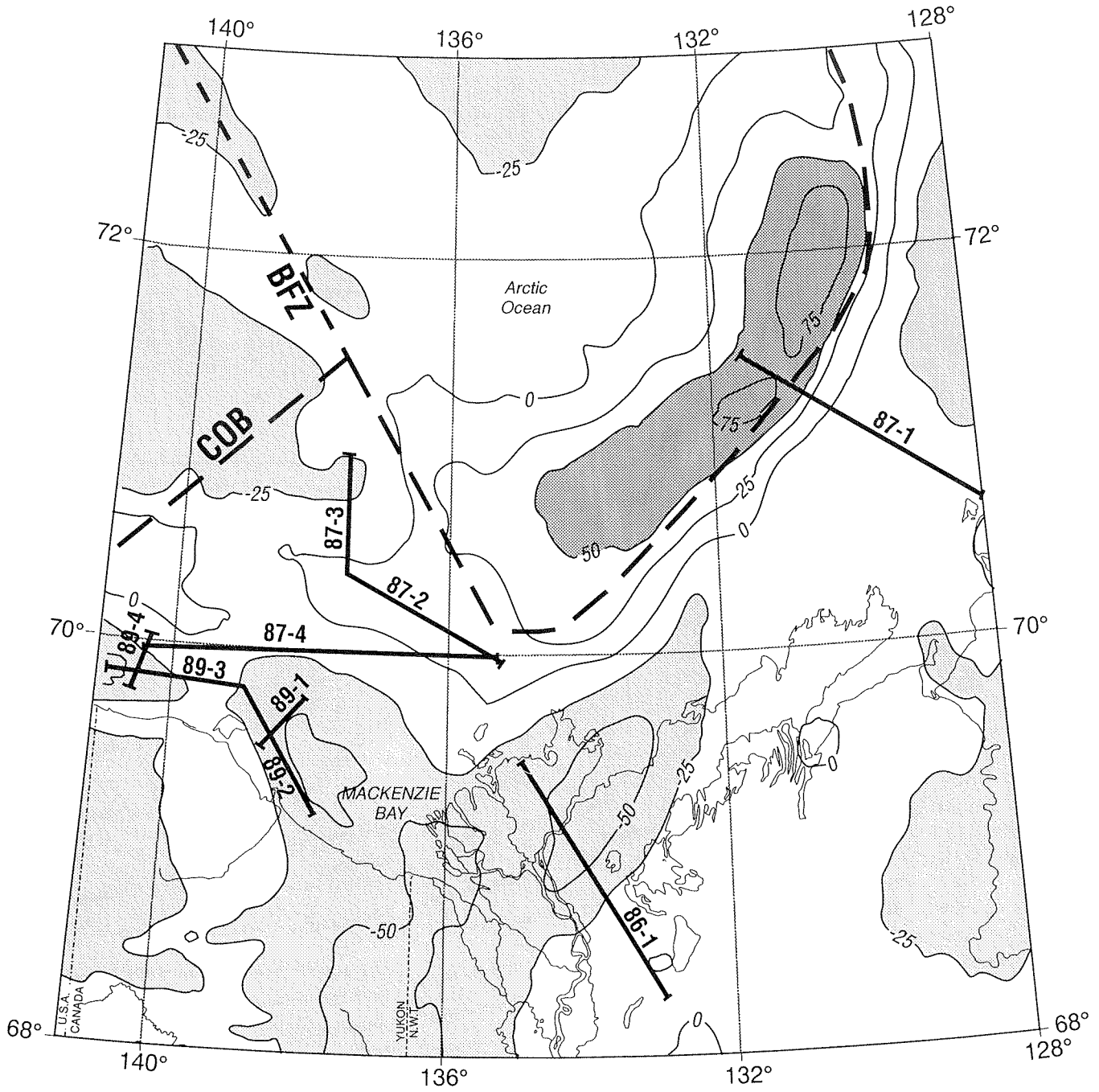

Figure 2. *Location of continent–ocean boundary (COB) in the Beaufort–Mackenzie Basin (modified from Stephenson et al., 1994) superimposed on the gravity map of the Beaufort Sea (Bouguer onshore, free-air offshore, 25 mgal contour interval). The offset of the COB is projected northwestward along a linear gravity low, and defines the Beaufort fracture zone (BFZ). Numbered solid lines are FGP seismic reflection profiles.*

Three stages of oceanic crust formation are proposed. The first is the formation of the western Makarov Basin as well as oceanic crust along the Arctic Alaska continental margin. The second and best-defined stage is based on bathymetry, potential field data and known crustal structure from localities throughout Canada Basin. The final stage produced a rectangular zone in the centre of the southern Canada Basin and contains a few north-south trending magnetic anomalies. This stage resulted from a decoupling of the southern part of the basin from the northern part in the Late Cretaceous, possibly due to a ridge jump caused by the initiation of the Alpha Ridge plume.

Stage 1

Four lines of evidence support an early stage of basin formation (Fig. 3). First is the seismically well-defined evidence for Jura-Cretaceous extension followed by a Late Hauterivian (Early Cretaceous) age of the rift-drift transition along the Arctic Alaska continental margin (e.g., Grantz et al., 1990c). At least some oceanic crust probably formed there in the Early Cretaceous. Second, Chukotka accreted to the Omolon massif and east Siberian continental collage in the Early Cretaceous, following closure of the South Anyuy ocean basin at the convergent South Anyuy suture. The Chukotka data suggest a Late Jurassic to Early Cretaceous age because the formation of Arctic Ocean crust is assumed to be contemporaneous with the closure of the South Anyuy Ocean (Zonenshain et al., 1990). Third, when the Arctic Ocean is closed to a pre-Stage 2 position, significant ocean basin remains. Fourth, the Blow trough in northern Yukon is an extensional basin containing greater than 5 km of early Albian siltstones and turbidites (Lane, 1988), indicating that Arctic Alaska was indeed moving with respect to cratonic North America in early Albian time.

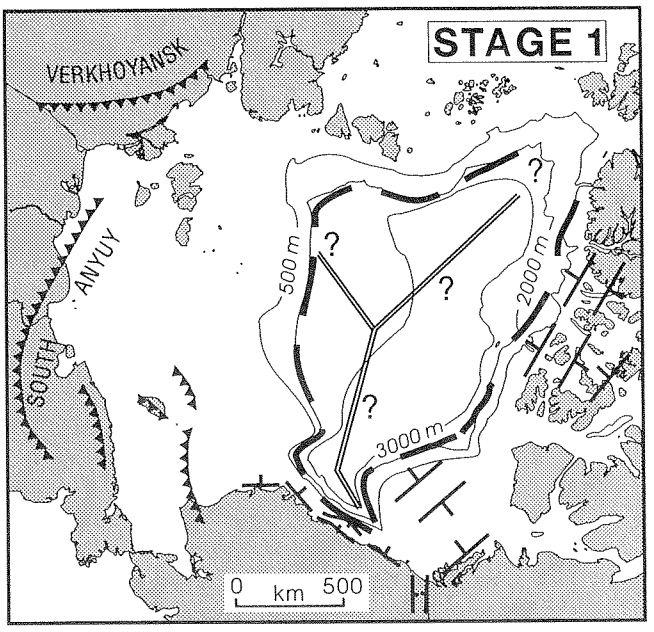

Figure 3. Speculative geometry at the end of Stage 1 spreading. Early Cretaceous convergence in Chukotka, and extension and igneous activity across the European shelf probably accommodated seafloor spreading. Heavy lines are continent-ocean boundary, double lines represent speculative spreading axes.

Stage 2

This stage is supported by data from throughout Canada Basin. The most definitive is the offset of the continent-ocean transition on the Beaufort Fracture Zone (Fig. 4). Both the location and orientation of the offset are well-defined (Fig. 2). Because fracture zones parallel the relative trajectory of conjugate plates, the conjugate of the eastern Beaufort Sea margin must have rifted to the northwest. The fracture zone appears to project northwestward along a diffuse linear gravity low to near 73°N and 141°W. Also, the valley and ridge geometry of Chukchi Borderland is nearly parallel with the eastern Beaufort Sea margin near the Mackenzie Delta, and also with the Canadian polar margin north of Prince Patrick Island (Fig. 4).

Aeromagnetic anomalies in Canada Basin are locally useful as corroborating evidence for Stage 2 kinematics (Fig. 4). A few linear anomalies occur in the adjacent basin parallel to Northwind Ridge (Fig. 4). Also, a succession of linear anomalies occur in the basin, beginning approximately 300 km northwest of Prince Patrick Island (Fig. 4). They are parallel to the adjacent Canadian polar margin, parallel to Northwind Ridge and its adjacent magnetic anomalies, and perpendicular to the Beaufort fracture zone (Lane, 1994). These alignments among widely dispersed physiographic and magnetic features in Canada Basin argue against a fortuitous alignment, and strongly for a genetic correlation.

Stage 3

Evidence for Stage 3 is found in southern Canada Basin, within an area defining a north-south elongate rectangle. The few linear magnetic anomalies that can be interpreted there have trends which vary about

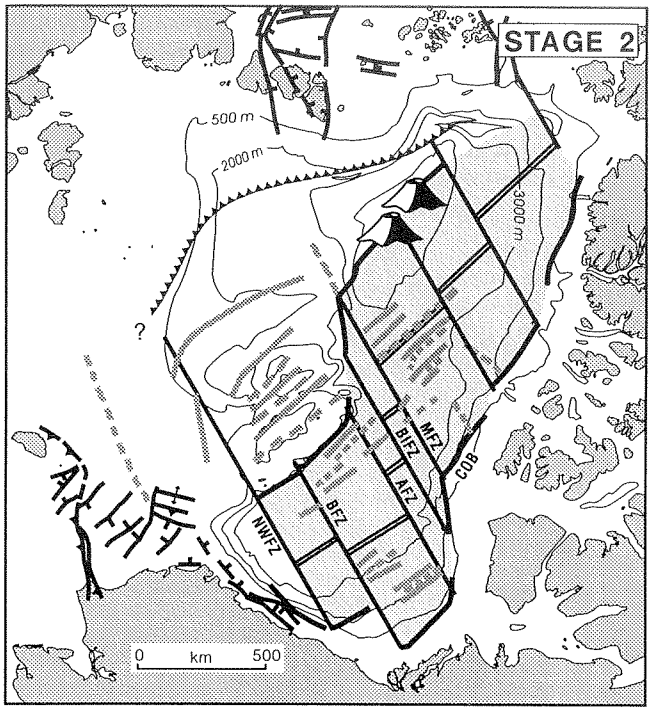

Figure 4. *Canada Basin at the end of Stage 2 spreading. Chukchi borderland physiography and magnetic anomalies support northwestward extension (Lane, 1994). Fracture zones: BFZ, Beaufort Fracture Zone; NWFZ, Northwind Fracture Zone; AFZ, Amundsen Fracture Zone; BIFZ, Banks Island Fracture Zone; MFZ, M'Clure Fracture Zone. Seafloor spreading may have been accommodated by convergence beneath the Russian Arctic shelf. Double lines are spreading axes, single lines are fracture zones (Stephenson et al., 1994). The COB has been repeated and displaced to the northwest to bracket the area of Stage 2 oceanic crust (shaded). The volcanoes on the linear submarine plateau (future Mendeleyev and Central Alpha ridges) represent the incipient Alpha Ridge plume. Solid and dashed grey lines are magnetic anomaly trends (positive and negative respectively) pertinent to Stage 2 (principally from Kovacs et al., 1990; P.G.O. Sevmorgeologia, unpublished).*

north–south, suggesting a broadly east–west spreading direction (Fig. 5).

The west boundary of the Stage 3 area is locally constrained between magnetic anomalies trending north–south and those parallel to Northwind Ridge (Fig. 5). The east boundary is approximately constrained by the termination of the Beaufort Fracture Zone gravity anomaly, and has been extrapolated northward parallel to the Stage 3 anomaly trend. The northern boundary of the Stage 3 area is a line between northern Prince Patrick Island and the northern edge of Chukchi Borderland. North of this line the magnetic stripes of Stage 2 origin are prominent features of the magnetic anomaly field (Fig. 4). This line includes a fracture zone but is clearly more complex. Accordingly it has been labelled as the Prince Patrick Lineament (Fig. 5). The Stage 2 magnetic anomalies trending northeast from the Prince Patrick Lineament indicate that the northward-trending Stage 3 anomalies are confined to the south of it.

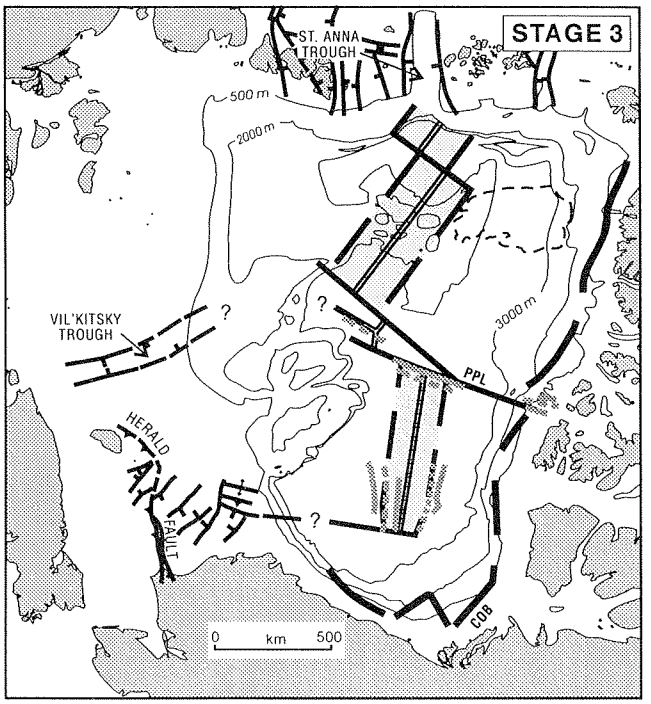

Figure 5. *East–west Stage 3 spreading in southern Canada Basin, synchronous with NW–SE spreading in northern Canada Basin. Triple junction in the central basin is schematic, representing a geometrically required zone accommodating differing simultaneous displacements. Continental accommodation in bordering regions is speculative but consistent with available data (Thurston and Theiss, 1987; Grantz et al., 1990b, c; Zonenshain et al., 1990). The Prince Patrick Lineament (PPL) is shown, double lines are spreading axes, and long dashed lines bracket Stage 3 oceanic crust (shaded). Dashed outline in northern Canada Basin is the site of the future post-accretionary Alpha Ridge.*

Geometric requirements suggest that Stage 3 opening in the south was connected through an extensional transform zone, shown schematically in Figure 5, to continued northwestward spreading farther north.

CONCLUSIONS

Existing data require a multistage kinematic evolution. Most of the preserved Canada and eastern Makarov basins formed by northwestward Stage 2 spreading away from Arctic Canada. Constraints include the Beaufort Fracture zone, the bathymetry of western Alpha Ridge and Chukchi borderland, the continent–ocean transition of parts of the Canadian polar margin, and aeromagnetic anomaly trends in both northern and southern Canada Basin. Stage 3 in southern Canada Basin is based on several north–south trending magnetic anomalies that truncate Stage 2 anomalies in both southern and northern Canada Basin. East–west Stage 3 spreading is confined to southern Canada Basin and occurred while northwest–southeast spreading continued in northern Canada Basin. Fragmentation and divergent spreading of the two Arctic oceanic microplates were presumably accommodated in a complex zone north of Chukchi Borderland. Stage 1 evolution is poorly defined, but is required to accommodate the timing of Alaska margin formation and Chukotkan deformation.

REFERENCES

Embry, A.F.
1990: Geological and Geophysical evidence in support of the hypothesis of anticlockwise rotation of northern Alaska. Marine Geology, v. 93, p. 317–329.

Grantz, A., May, S.D., Taylor, P.T., and Lawver, L.A.
1990a: Chapter 22: Canada Basin. *In* The Arctic Ocean Region, A. Grantz, L. Johnson, and J.F. Sweeney (eds.). Geological Society of America, The Geology of North America, v. L, p. 379–402.

Grantz, A., May, S.D., and Hart, P.E.
1990c: Chapter 16: Geology of the Arctic continental margin of Alaska. *In* The Arctic Ocean Region, A. Grantz, L. Johnson, and J.F. Sweeney (eds.). Geological Society of America, The Geology of North America, v. L, p. 257–288.

Grantz, A., Green, A.R., Smith, D.G., Lahr, J.C., and Fujita, K.
1990b: Plate 11: Major phanerozoic tectonic features of the Arctic Ocean region. *In* The Arctic Ocean Region, A. Grantz, L. Johnson, and J.F. Sweeney (eds.). Geological Society of America, The Geology of North America, v. L, 1 sheet, 1:6 000 000 scale.

Kovacs, L.C., Johnson, G.L., Srivastava, S.P., Taylor, P.T., and Vogt, P.R.
1990: Plate 4: Residual magnetic anomaly chart of the Arctic Ocean region. *In* The Arctic Ocean Region, A. Grantz, L. Johnson, and J.F. Sweeney (eds.). Geological Society of America, The Geology of North America, v. L, 1 sheet, 1:6 000 000 scale.

Lane, L.S.
1988: The Rapid fault array: A foldbelt in Arctic Yukon. *In* Current Research, Part D. Geological Survey of Canada, Paper 88–1D, p. 95–98.

1994: A new plate kinematic model of Canada Basin evolution. *In* Proceedings of the 1992 International Conference on Arctic Margins, D.K. Thurston and K. Fujita (eds.). U.S. Department of the Interior, Minerals Management Service, Anchorage, Alaska, p. 283–288.

Lawver, L.A. and Scotese, C.R.
1990: Chapter 31: A review of tectonic models for the evolution of the Canada Basin. *In* The Arctic Ocean Region, A. Grantz, L. Johnson and J.F. Sweeney (eds.). Geological Society of America, The Geology of North America, v. L, p. 593–618.

Mair, J.A. and Lyons, J.A.
1981: Crustal structure and velocity anisotropy beneath the Beaufort Sea. Canadian Journal of Earth Sciences, v. 18, p. 724–741.

Stephenson, R.A., Coflin, K.C., Lane, L.S., and Dietrich, J.R.
1994: Crustal structure and tectonics of the southeastern Beaufort Sea continental margin. Tectonics, v. 13, p. 389–400.

Thurston, D.K. and Theiss, L.A.
1987: Geologic report for the Chukchi Sea planning area, Alaska. U.S. Department of the Interior, Minerals Management Service, Anchorage, Alaska, OCS Report MMS 87–0046.

Zonenshain, L.P., Kuzmin, M.I., and Natapov, L.M.
1990: Geology of the USSR: A plate-tectonic synthesis. Geodynamic Series Volume 21, American Geophysical Union, Washington, D.C., 242 p.

GEOMETRY AND TECTONICS OF EARLY TERTIARY TRIANGLE ZONES, NORTHEASTERN EAGLE PLAIN, YUKON TERRITORY

L.S. Lane

Geological Survey of Canada, 3303-33rd Street N.W., Calgary, Alberta T2L 2A7

ABSTRACT

Two deformation fronts are observed in archival Chevron seismic reflection profiles in northeastern Eagle Plain. Preliminary interpretation of the subsurface data provides new insight into the structural evolution of the northern Cordillera.

The most clearly defined zone occurs at the southeast front of the Dave Lord Mountains. The Dave Lord triangle zone trends east-northeast in the vicinity of Porcupine River and involves rocks of the Eagle Plain Group of Late Cretaceous age. The tip of the décollement zone appears to lie within the Jurassic–Early Cretaceous succession. A generally north–south trending frontal zone marks the west flank of the Richardson Mountains. Definition of its frontal zone is complicated by facies changes, more complex structural geometry, and poorer seismic signal. The principal décollement zone appears to detach within Imperial Formation in the Richardson Mountains deformation front, ramping through the Mesozoic only near the tip.

Regional east–west shortening was driven by the eastward convergence of Arctic Alaska against the craton, reflected by north–south striking structures in the Richardson and northern Ogilvie mountains, and in Eagle Plain. The Dave Lord range strikes northeast and links shortening accommodated by the northern Ogilvie mountains with shortening accommodated farther northeast in the northern Richardson mountains. The highly deformed zones are shale troughs or basins with attenuated basement, which have been tectonically inverted. The less-deformed Eagle Plain is underlain by a thick succession of early Paleozoic competent platform carbonates. As the deformation progressed onto the platform, the more competent rocks were relatively resistant and deformed less intensely.

INTRODUCTION

Eagle Plain is an intermontane basin underlain by Cretaceous sandstone and shale, and rimmed concentrically by upper and lower Paleozoic strata uplifted in the surrounding mountain ranges. Bell Basin comprises the northeast corner of Eagle Plain, between the converging trends of the Dave Lord and Richardson mountain ranges (Fig. 1). Eagle Plain and the

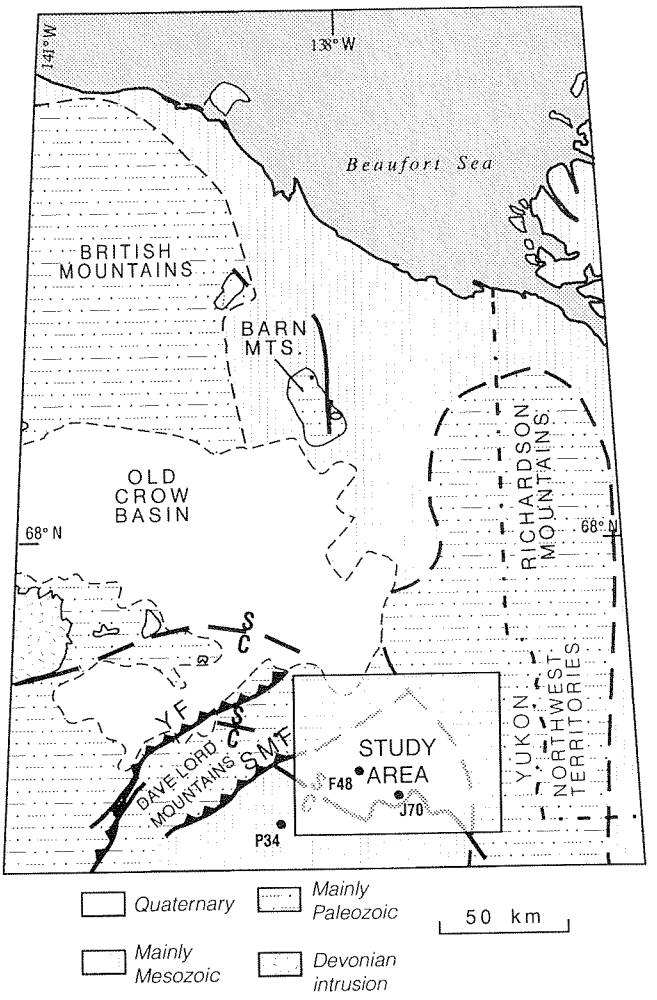

Figure 1. *Location map showing the study area and surrounding mountain ranges. YF, Yukon Fault; SMF, Sharp Mountain Fault. Early Paleozoic carbonate shaleout (C/S) is interpreted as having been telescoped by eastward Tertiary thrusting.*

surrounding ranges have been mapped at reconnaissance scale (e.g., Norris, 1981, 1985). The Upper Cretaceous stratigraphy, constituting the poorly exposed subcrop strata of Bell Basin, has been studied by Dixon (1992).

Eagle Plain is a known petroleum-bearing basin, with five oil and gas discoveries occurring in Carboniferous and Permian units in southern Eagle Plain (Hamblin, 1990). The exploration history of Eagle Plain includes 9952 km of seismic reflection profiles shot since the early 1950s (NEB statistic, 1994). Much of those data consists of 6-fold data shot by Chevron Canada Resources during 1970–72. Record lengths of 4 s (TWT) result in seismic penetration through the Paleozoic in most areas. This study employs some of the Chevron data, delineates the geometry of Laramide (Early Tertiary) triangle zones, and discusses their implications for Early Tertiary tectonics.

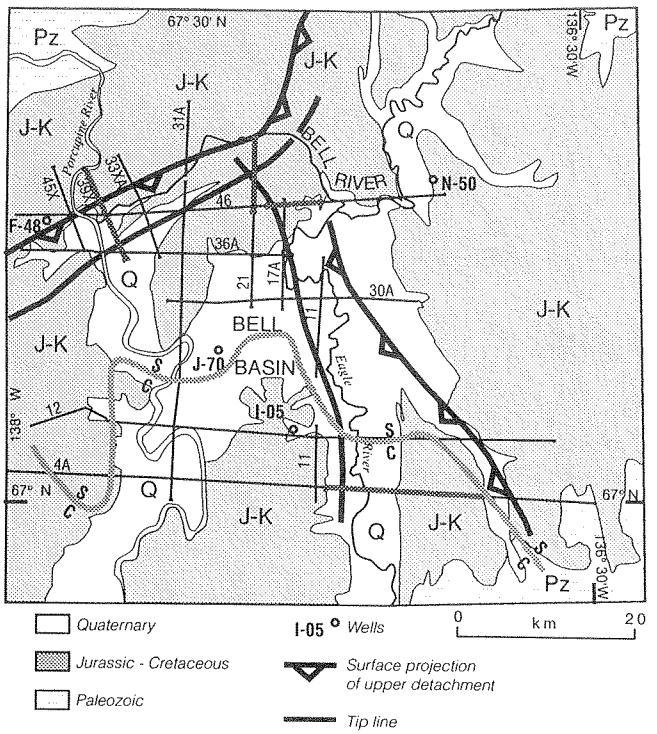

Figure 2. *Detailed map of Bell Basin with locations of local wells, seismic lines used, and smoothed tip lines and surface projections of upper detachment surfaces. The parts of lines 39X, and 4A shown in Figures 3 and 4 are shown by thicker line widths. Also shown is the generalized position of the Silurian carbonate (C)–shale (S) facies transition (unpublished NEB file 45-6-2-112).*

STRATIGRAPHY

Regional and local stratigraphies are known from reconnaissance surface mapping and stratigraphic studies (e.g., Norris, 1981, 1985; Dixon, 1992), and from subsurface studies (e.g., Pugh, 1983). The regional pre-Mesozoic stratigraphy of Eagle Plain correlates with equivalent strata of the Mackenzie Platform east of the Richardson Mountains. Also, a regionally important facies change from platform carbonate to deeper water shale is well documented by surface mapping and subsurface studies (Fig. 2; Lenz, 1972; Pugh, 1983).

Bell Basin is underlain by Upper Cretaceous sandstone and shale of the Eagle Plain Group (Dixon, 1992). Parkin Formation, a shale-dominant unit of Cenomanian age, lies unconformably on the Albian Whitestone River Formation. It is gradationally overlain by the Fishing Branch Formation of interbedded sandstone, siltstone and shale. Its age is poorly documented, but a Cenomanian age has been suggested (Dixon, 1992, p. 38). The Burnthill Creek Formation is a shale-dominant unit, locally containing considerable siltstone and sandstone, and generally fining toward the west and northwest. The youngest unit exposed in the area is the Cody Creek Formation, consisting of interbedded sandstone and shale.

TIMING OF DEFORMATION

The maximum age of deformation for rocks in Bell Basin is limited by the age of the youngest rocks involved. Those rocks are the Cody Creek Formation, inferred to be as young as Campanian in age. Thus, the folding and thrusting observed in the Dave Lord and Richardson ranges adjacent to Bell Basin are essentially Maastrictian or younger in age. A post-Cody Creek age for deformation is further supported by the lack of depositional evidence for uplift of the Bell Basin area during Cody Creek deposition (Dixon, 1992).

The deformation age is further refined by the regional context: the Bell Basin triangle zones developed as part of regional tectonism involving the adjacent Yukon north slope and offshore Beaufort foldbelt. There, deformation climaxed in the Late Paleocene to Middle Eocene in nearshore and onshore areas (e.g., Lane and Dietrich, 1995). This interpretation is supported by Late Paleocene to Early Eocene apatite fission track cooling ages from various localities across the Yukon north slope (e.g., McMillen and O'Sullivan, 1990).

SEISMIC INTERPRETATION

Seismic interpretation was carried out on unmigrated reflection profiles shot between 1970 and 1972, and provided to the author by Chevron Canada Resources Limited (Fig. 2). The present interpretation concentrates on tracing two regionally important unconformities, the sub-Mesozoic and mid-Cretaceous (post-Albian) unconformities. The resulting three-fold seismic stratigraphy consisting of Paleozoic, Jurassic to Lower Cretaceous and Upper Cretaceous units provides an adequate and reliable basis for illustrating triangle zone geometries, and their variations along strike.

DAVE LORD TRIANGLE ZONE

The Dave Lord triangle zone trends east-northeastward (Figs. 2, 3). The frontal syncline is clearly imaged in Upper Cretaceous strata of the autochthon. The basal décollement lies within the Jurassic–Lower Cretaceous succession at the thrust tip, but ramps downward into the Paleozoic succession about 7 km toward the northwest, and shows 4 km of displacement based on the interpreted positions of the sub-Mesozoic unconformity in the hanging wall and footwall. Other structures are not constrained by cutoffs, but the overlying thrust sheet has been displaced by a minimum of 3 km. Reconnaissance mapping (Norris, 1981) shows that dated, flat-lying Jurassic strata are exposed along Porcupine River adjacent to the north end of this section, and are underlain by Permian strata farther north.

RICHARDSON TRIANGLE ZONE

The Richardson Mountains frontal structure is more complex and variable than the Dave Lord triangle zone, and less well imaged seismically (Fig. 4). Consequently, less can be said about its internal geometry. However, visible structures occur at two levels. One deep thrust fault offsets the Paleozoic carbonate succession by nearly 1 km. Other structures include two small Jura-Cretaceous normal faults, and two thrust faults, one of which is hinterland-directed. Both thrust faults root in the Imperial Formation but it is impossible to identify a master fault linking them to each other, or eastward to the deformed belt. The master thrust shown (Fig. 4) is schematic, with the acknowledgement that the shortening represented by the imaged thrusts actually may be accommodated by distributed deformation within the Imperial Formation. The (east-verging) back-thrust which projects to the surface near the east end of the profile (Fig. 4) is probably the same structure as the one mapped as a northwest- striking normal fault juxtaposing Imperial Formation on the southwest against Whitestone River Formation on the northeast (Norris 1985). However, the seismic data show clearly that the structure is a thrust fault that offsets Upper Cretaceous strata at this locality.

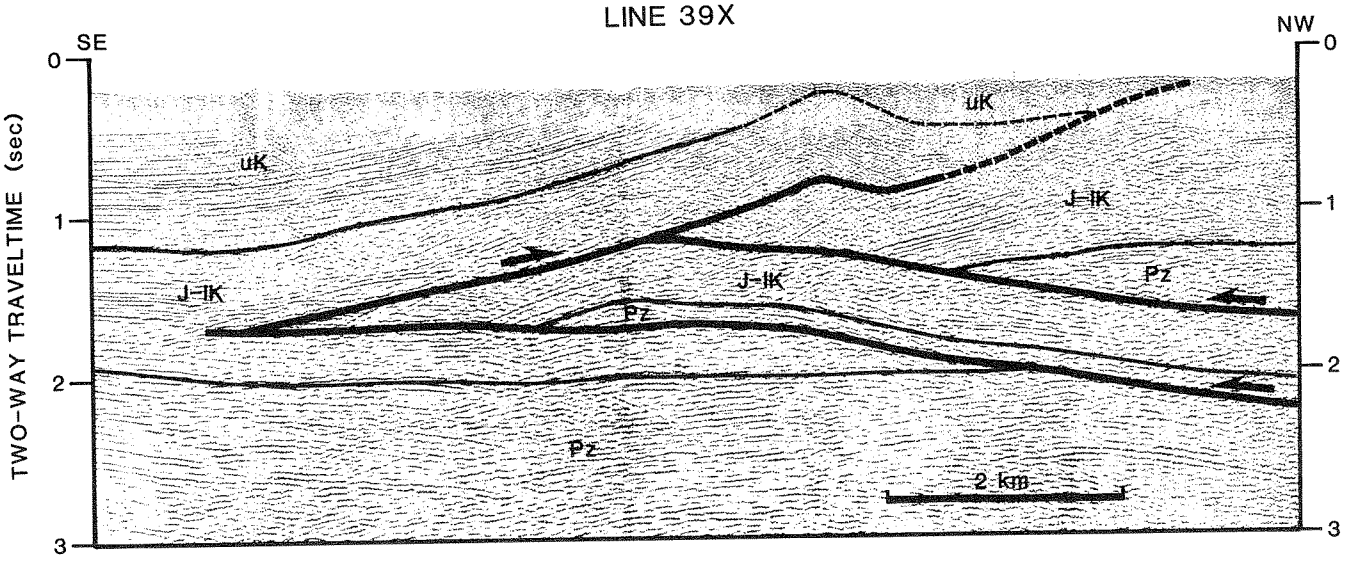

Figure 3. Interpreted seismic line 39X, showing Dave Lord Mountains frontal zone. This and the following profile are unmigrated Chevron data. Horizontal exaggeration is 28% for a seismic velocity of 3.5 km/s (approximate velocity of the Mesozoic succession).

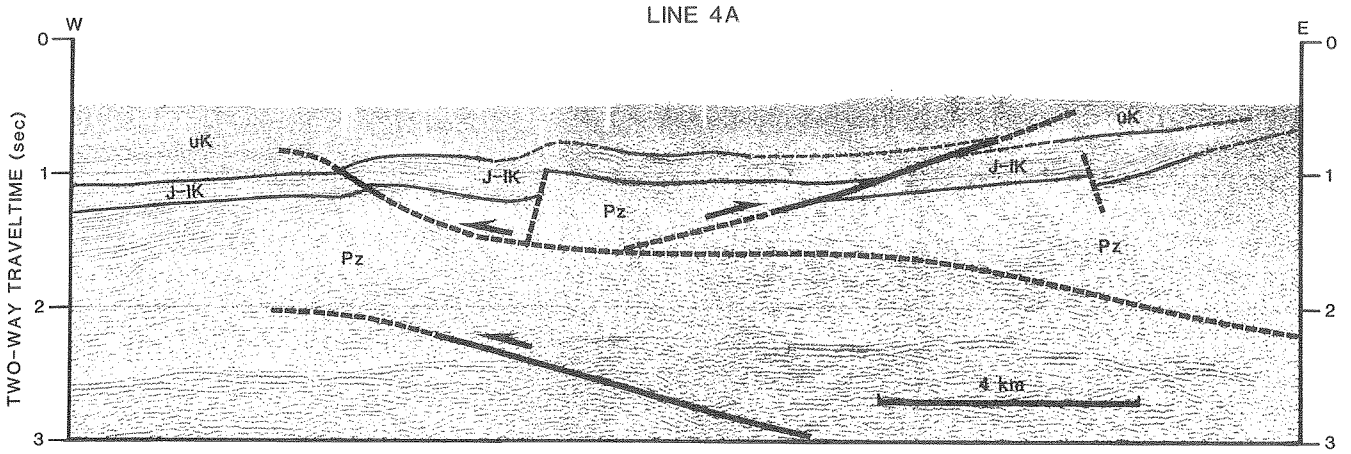

Figure 4. *Interpreted seismic line 4A, showing part of the Richardson frontal zone. High-amplitude reflections within the Paleozoic succession near 2.5 s (TWT) represent the top of the lower Paleozoic carbonates.*

TECTONIC SETTING

The geographic and stratigraphic positions of the triangle zones are partly controlled by the carbonate-shale facies transition in the lower Paleozoic succession. Although the carbonate shale-out position varies through time, in general it trends northward beneath eastern Eagle Plain and swings westward through Bell Basin (Fig. 2), marking the boundary between the Porcupine Platform and the Richardson and British–Barn mountains troughs (e.g., Lenz, 1972). The shaleout position is only broadly constrained by surface exposures across the Dave Lord Mountains, but the distribution is consistent with an original west-northwest trend which has been telescoped eastward by the Tertiary thrusting (Fig. 1).

The tectonic setting of Early Tertiary deformation in northern Yukon reflects North America–Eurasia convergence at the same time as the north Atlantic spreading system migrated across the Arctic. Arctic Alaska was displaced eastward on the Kaltag and other faults to produce east–west shortening of eastern Alaska and northern Yukon against the North American craton.

CONCLUSIONS

The Dave Lord Mountains are bordered by a narrow, shallow triangle zone trending east-northeast, with a basal décollement that ramps upward toward the east, from the Jurassic–Lower Cretaceous succession near Porcupine River, to within the Upper Cretaceous succession. The frontal syncline is well imaged throughout the length of the structure.

The western frontal zone of the Richardson Anticlinorium is not a well-formed triangle zone, but consists of a more complex arrangement of discrete, well-imaged structures, rooting in a zone in which discrete structures are not apparent. This zone trends north–south, but swings northwest approaching the Dave Lord Mountains. Farther north the two deformed belts merge to form the northern Richardson Mountains. The principal décollement zone appears to be within the Devonian Imperial succession, although specific structures are not clearly defined. A deeper incipient structure is locally imaged, which could have caused the deformed belt to step farther westward if the deformation had evolved further.

The tectonic setting is one of regional east–west shortening, driven by the eastward convergence of Arctic Alaska against the craton during Early Tertiary time. The Dave Lord Mountains strike northeast to east-northeast and link the shortening accommodated by the northern Ogilvie mountains with shortening accommodated farther north in the northern Richardson Mountains.

REFERENCES

Dixon, J.
1992: Stratigraphy of Mesozoic strata, Eagle Plain area, northern Yukon. Geological Survey of Canada, Bulletin 408, 58 p.

Hamblin, A.P.
1990: Upper Paleozoic petroleum geology and potential, southern Eagle Plain, Yukon Territory. Geological Survey of Canada, Open File 2286.

Lane, L.S. and Dietrich, J.R.
1995: Tertiary structural evolution of the Beaufort Sea–Mackenzie Delta region, Arctic Canada. Bulletin of Canadian Petroleum Geology, in press.

Lenz, A.C.
1972: Ordovician to Devonian history of northern Yukon and adjacent District of Mackenzie. Bulletin of Canadian Petroleum Geology, v. 20, p. 321–361.

McMillen, K.J. and O'Sullivan, P.B.
1990: Tectonic and Eustatic origin of regional unconformities, northeast Alaska and northwest Canada: comparison of fission track cooling ages and subsurface data. Program with Abstracts, Geological Association of Canada, Mineralogical Association of Canada, Joint Annual Meeting, Vancouver, B.C., v. 15, p. A88.

Norris, D.K.
1981: Geology, Bell River Yukon Territory–Northwest Territories. Geological Survey of Canada, Map 1519A, 1 sheet, 1:250 000 scale.

1985: Geology of the northern Yukon and northwestern District of Mackenzie. Geological Survey of Canada, Map 1581A, 1 sheet, 1:500 000 scale.

Pugh, D.C.
1983: Pre-Mesozoic geology in the subsurface of Peel River map area. Yukon Territory and District of Mackenzie. Geological Survey of Canada, Memoir 401, 61 p.

DEEP GAS RESERVOIRS OF THE MANETOE DOLOMITE: INSIGHTS FROM OUTCROP

D.W. Morrow and T.D. Bird

Geological Survey of Canada, 3303-33rd Street N.W., Calgary, Alberta T2L 2A7

INTRODUCTION

The 'Manetoe Facies' or 'Manetoe Dolomite' has been recognized from the late 1950s as a very distinctive rock type in the southern parts of the Northwest and Yukon Territories. Thick masses of Manetoe Dolomite within the central region of the Liard Basin are hosts to several large producing gas fields (Beaver River, Kotaneelee and Pointed Mountain; Fig. 1). Petrographically, this dolomite resembles the better known Presqu'ile Dolomite of the Pine Point region in that they are both diagenetic white "sparry" dolomites developed within Devonian carbonates. Also, like the Presqu'ile Dolomite, the Manetoe Dolomite is not confined to a small region. Although the Manetoe Dolomite is best known as the host for the Devonian gas fields in Liard Basin, it also extends laterally across about 8000 km^2 of the southern Northwest and Yukon territories (Fig. 2). The Manetoe Dolomite in the gas fields is distinctive because of its great vertical extent through strata equivalent to the Arnica up to the top of the Nahanni (Fig. 3).

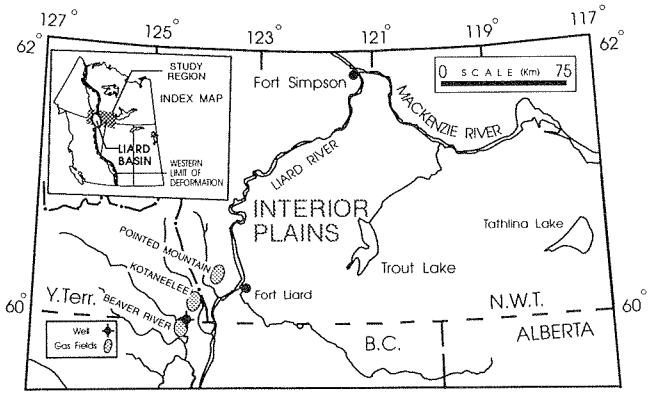

Figure 1. *Index map and location of Liard Basin. Manetoe Dolomite gas fields are within this basin.*

OUTCROP EXAMPLES

Similar occurrences of Manetoe Dolomite also with considerable vertical extent occur at a few outcrop localities. One outcrop locality with large scale vertical developments occurs close to the southern flank of the Funeral Shale Embayment northeast of Nahanni National Park near Ram Plateau (locality 3; Fig. 2). The Manetoe Dolomite is co-extensive with the southern part of the lower Paleozoic Mackenzie Shelf sequence and extends northward from 60° to 63°N latitude. The western limit of the Manetoe Dolomite (Fig. 2) coincides almost exactly with the shelf-to-basin transition of Lower Devonian carbonates to the basinal

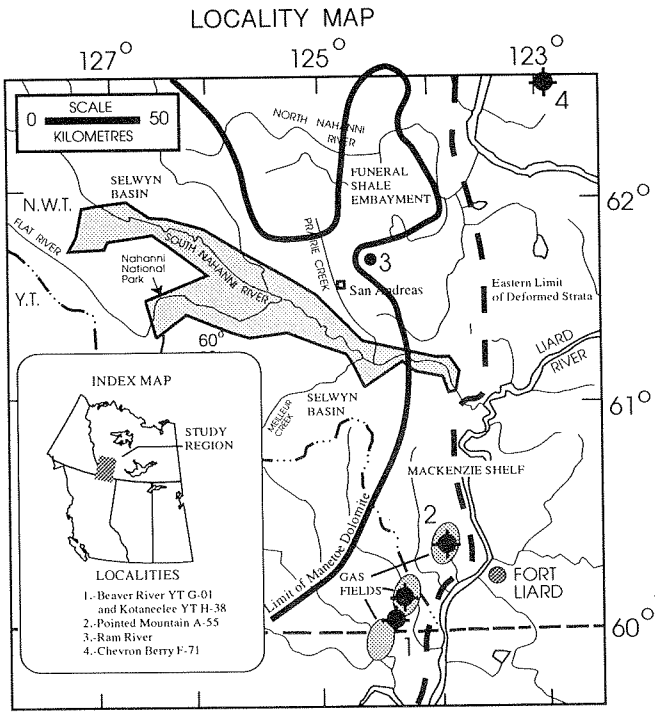

Figure 2. *Index map of Manetoe Dolomite localities. Localities 1, 2 and 4 are well sections. Locality 3 is a spectacular outcrop locality near Ram Plateau. The Manetoe Dolomite extends across the entire eastern part of this region.*

shales of the Selwyn Basin. The region of the Funeral Shale Embayment is an exception in that the Manetoe Dolomite is absent beneath the Funeral shale sequence that fills the embayment but is present as a generally stratiform body throughout the lower Devonian part of the Mackenzie Shelf sequence to the east. The Manetoe is particularly thick along a trend subparallel to the southern margin of the Funeral Embayment where it extends upward from the Arnica Formation to the base of the argillaceous limestones of the Headless Formation (Fig. 3). Throughout most of the Mackenzie Shelf, the Manetoe is about 50 m thick, but at locality 3 where the Manetoe passes abruptly basinward to Funeral shale, large mound-shaped masses of Manetoe Dolomite extend above the Headless shaly limestones into the overlying biostromal limestones of the Nahanni Formation. It is not known if these intra-Nahanni dolomite masses extend to the top of the Nahanni at locality 3 in Figure 2. Several dolomite bodies at this locality extend variable distances up into the Nahanni.

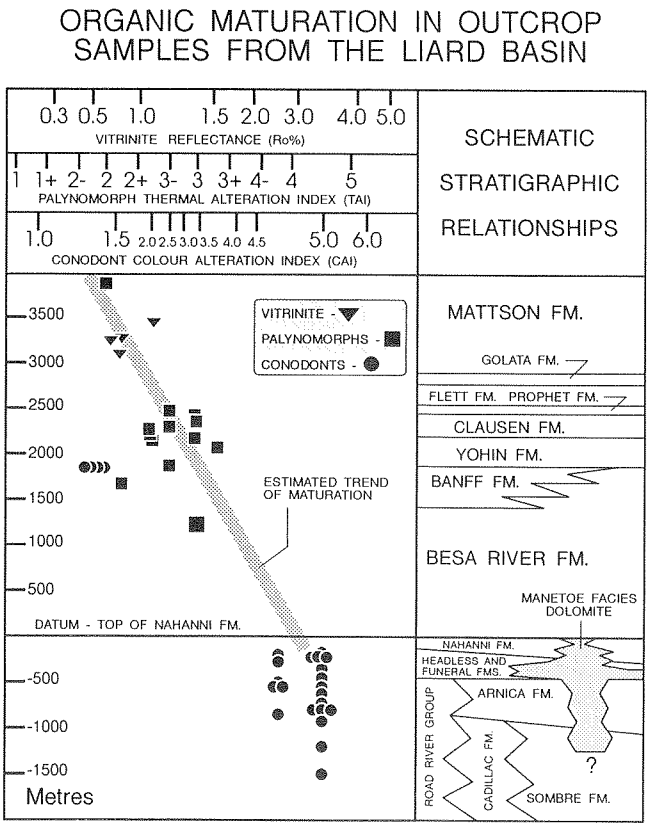

Figure 3. *Schematic cross-section on the right side shows disposition of the Manetoe Dolomite within Devonian strata. In the Liard gas fields and a few outcrop localities, the Manetoe extends up into the Nahanni. The left side shows the rapid downward increase in maturation from the top of the Carboniferous Mattson to the top of the Nahanni.*

Typically, these dolomite bodies are several hundred metres broad and fifty to one hundred metres thick within the Nahanni and tend to be elongate parallel to the shelf edge along the southern margin of the Funeral Shale Embayment. Nahanni Butte at the confluence of the South Nahanni and Liard Rivers is another outcrop locality where the Manetoe Dolomite extends upward into the Nahanni Formation above its usual stratigraphic level. At Nahanni Butte, masses of Manetoe Dolomite extend upward from the stratiform Manetoe at the level of the Landry Formation to the top of the Nahanni. Interestingly, solid bitumen is present as a coating on centripetal dolomite cements in vugs in Manetoe Dolomite at Nahanni Butte in a manner similar to bitumen vug-fillings within the Manetoe Dolomite of the Liard Basin subsurface gas fields. At other localities, such as locality 3 and 4 in Figure 2, where the Manetoe probably does not extend to the top of the Devonian carbonates, there is little, if any, bitumen present. This is consistent with the perception that the hydrocarbons migrated into the Manetoe Dolomite only in places where it was in direct contact with the overlying Besa River organic-rich shales. Thus, the time of hydrocarbon emplacement constrains the age of origin of the Manteoe Dolomite

TIMING OF OIL GENERATION

In Liard Basin a thick sequence of late Paleozoic, primarily Carboniferous, shale-dominated sediments overlies Devonian carbonates (Morrow et al., 1990, 1993, Figs. 3, 4). This thick wad of late Paleozoic sediment thins northward and eastward and in the Interior Plains, Cretaceous strata rest directly on Devonian shales (Fig. 4). Early work from outcrop showed that there is a rapid downward increase in organic maturation from low values of about 0.4 to 0.5%R_o (vitrinite reflectance) at the top of the Carboniferous Mattson Formation to values of 4.5%R_o at the top of the Devonian carbonates. Later, more detailed vitrinite reflectance profiles through Liard Basin wells verified this perception of a rapid downward increase in organic maturation within the upper Paleozoic (Fig. 5). Simulations of the thermal history for strata in these wells, based upon their burial history and upon generalized heat flow histories, were used to model the maturation of their organic material (i.e., vitrinite). In general, heat flow models involving high late Paleozoic heat flow (>120 mW/m^2) and incorporating decreasing heat flow to the present day value of 80 mW/m^2 generate calculated vitrinite reflectances that match the observed profiles of vitrinite reflectances in these wells more closely than do heat flow models which incorporate high heat flows in Cretaceous–

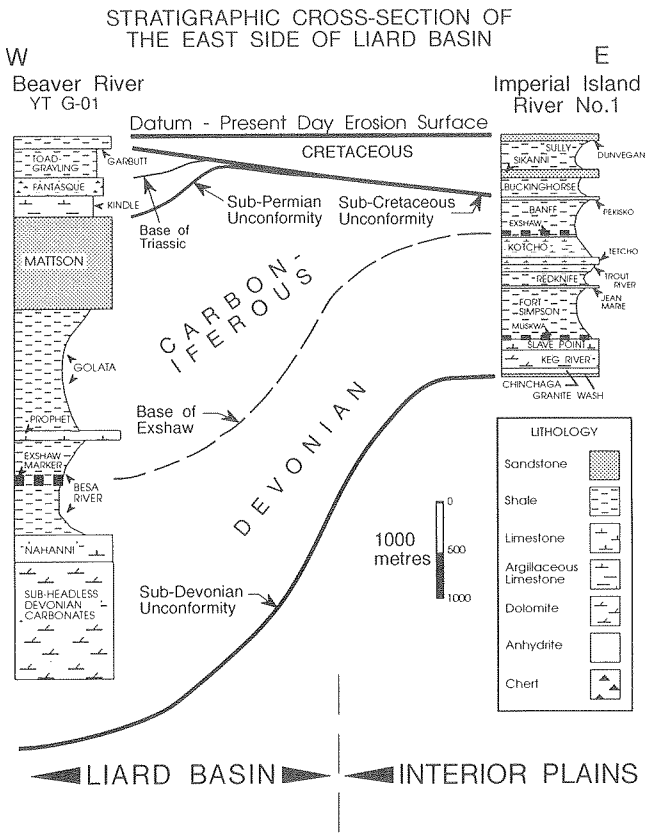

Figure 4. *Stratigraphy in Liard Basin versus that in Interior Plains farther east. Deposition of thick Carboniferous Liard Basin sequence caused early maturation and generation of hydrocarbons in that basin.*

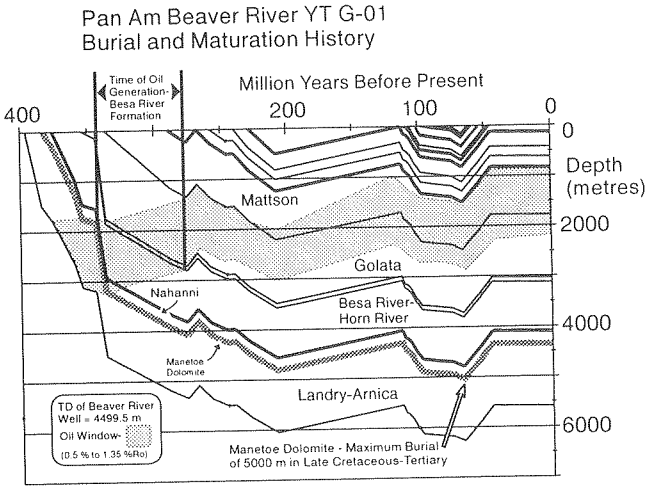

Figure 5. *Burial history or 'geohistory' plot of the post-Silurian sequence at the Pan Am Beaver River YT G-01 well (60.0069°N/124.2633°W). Oil generation in the Besa River organic-rich shales occurred in late Paleozoic time.*

Tertiary time. Regardless of which type of heat flow model is adopted, the inescapable conclusion is that hydrocarbon generation occurred in late Paleozoic time in the most probable source beds for the gas phase hydrocarbons in the Liard Basin Manetoe Dolomite gas fields, the overlying Besa River shales. This is also consistent with the observation that bitumen emplacement postdates dolomite cementation (Morrow et al., 1990).

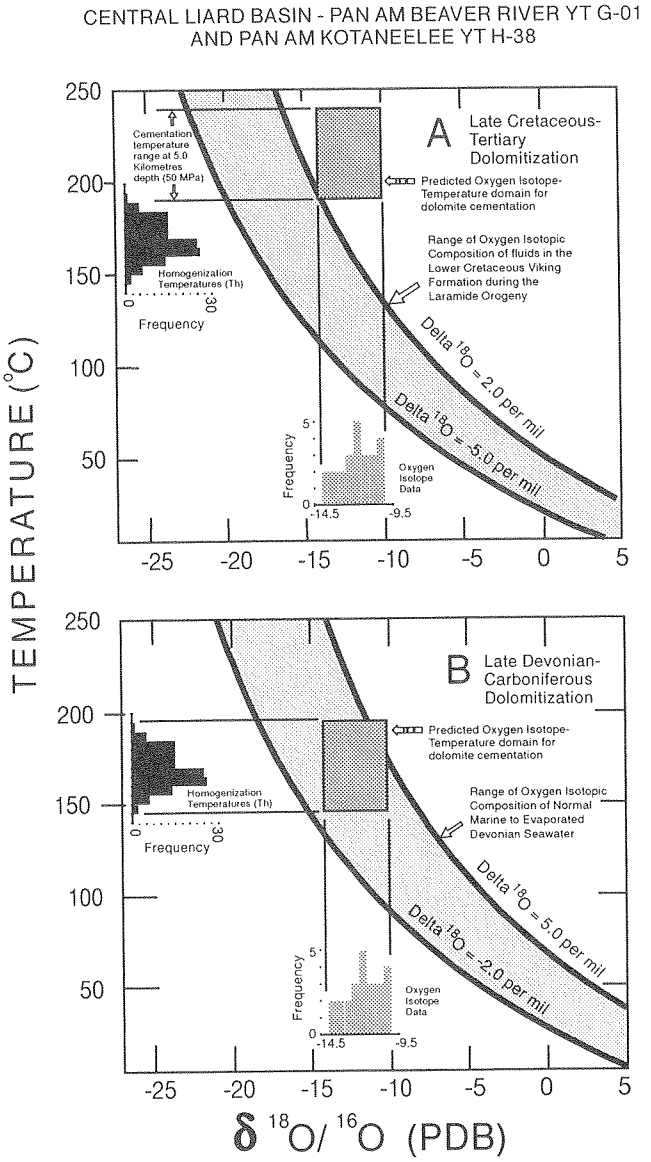

Figure 6. *Plots of fluid inclusion homogenization temperatures versus $\delta^{18}O$ values of Manetoe Dolomite cements from localities 1 and 2 in Figure 2. Pressure corrections for paleoburial depths have been applied for late Paleozoic versus Late Cretaceous–Tertiary dolomite cementation.*

ISOTOPIC AND FLUID INCLUSION EVIDENCE

Evidence for the time of origin of the Manetoe Dolomite comes also from fluid inclusion and oxygen isotope data (Fig. 6). Temperatures of precipitation for Manetoe dolomite cements calculated from the estimated $\delta^{18}O$ values of paleosolutions that may have precipitated these dolomites provide a much closer match to their observed $\delta^{18}O$ values and their fluid inclusion temperatures if a Late Devonian to Carboniferous age of dolomite cementation is assumed (see also Aulstead et al., 1988). This type of comparison may be made at all four outcrop and subsurface localities shown in Figure 2.

CONCLUSION

The Manetoe Dolomite clearly predated the emplacement of hydrocarbons from the overlying Besa River shales. Correlation of oxygen isotopic data with fluid inclusion data from the Manetoe dolomite cements is most consistent with a Late Devonian to Carboniferous time of origin for the Manetoe Dolomite in agreement with the late Paleozoic time of oil generation for organic material.

REFERENCES

Aulstead, K.L., Spencer, R.J., and Krouse, H.R.
1988: Fluid inclusion and isotopic evidence on dolomitization, Devonian of Western Canada. Geochimica and Cosmochimica Acta, v. 52, p. 1027–1035.

Morrow, D.W., Cumming, G.L., and Aulstead, K.L.
1990: The gas-bearing Devonian Manetoe Facies, Yukon and Northwest Territories. Geological Survey of Canada, Bulletin 400, 54 p.

1993: Paleozoic burial and organic maturation in the Liard Basin region, northern Canada. Bulletin of Canadian Petroleum Geology, v. 41, no. 1, p. 17–31.

GEOLOGICAL ATLAS OF THE NORTHERN CANADIAN MAINLAND SEDIMENTARY BASIN

D.W. Morrow and D.G. Cook

Geological Survey of Canada, 3303-33rd Street N.W., Calgary, Alberta T2L 2A7

INTRODUCTION

This new geological atlas was begun in the fall of 1993 under the joint sponsorship of the Geological Survey of Canada and the Department of Energy, Mines and Petroleum Resources of the Government of the Northwest Territories at the invitation of the Government of the Northwest Territories. The region covered by the Northern Canadian Mainland Sedimentary Basin Atlas falls between the Western Canada Sedimentary Basin Atlas (Mossop and Shetsen, 1994) to the south and the Beaufort Sea Atlas (Dixon, in press) to the north and is centered on the Mackenzie Corridor, the main tranportation corridor through northern Canada. Like the Western Canada Atlas of the Canadian Society of Petroleum Geologists, the Northern Canada Atlas is a major undertaking that is focussed on the autochthonous sedimentary cover of the Interior Plains and the Cordillera. It extends from longitude 110° westward to the Alaska border excluding the region southwest of the Tintina Trench. This is an area close to 2 000 000 km^2 (Fig. 1).

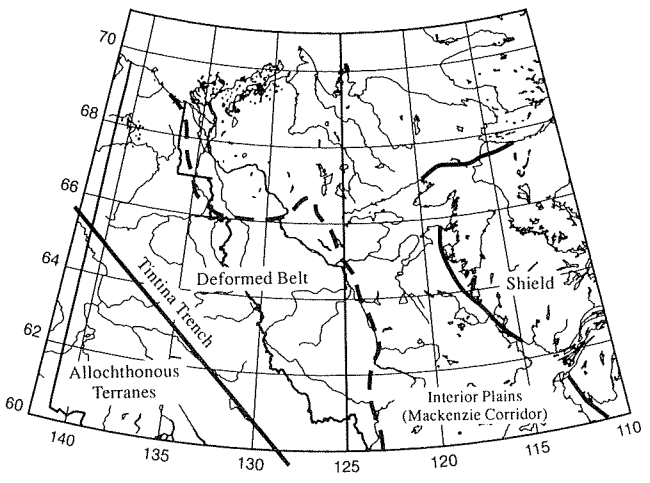

Figure 1. *Base map for the Geological Atlas of the Northern Canadian Sedimentary Basin. This base is the same scale and projection as that of the Geological Atlas of the Western Canadian Sedimentary Basin.*

The subsurface Upper Proterozoic to Phanerozoic sequence of northern Canada is thinner and less well known than its counterpart in western Canada south of 60° and has been far less studied. The number of wells is more than an order of magnitude lower than for western Canada (about 1500 wells). On the other hand the deformed belt is far broader than down south and has been the object of many regional stratigraphic studies, mainly, although not exclusively, by the Geological Survey of Canada. The Northern Cordillera also contains a number of large, upper Paleozoic to Cretaceous, hydrocarbon-bearing basins, such as the Eagle Plain and Liard basins, which have few counterparts in the narrower deformed belt of the western Canadian Cordilleran deformed belt to the south. Recent interest by the petroleum industry in these northern basins as well as in the Mackenzie Corridor itself points to the acute need for a regional compilation in the form of a geological atlas. The map base for the Atlas is a Lambert Conic Conformal projection at a scale of 1:5 000 000 extending from 60° to 71°N latitude and from 110° to 141°W longitude (Fig. 1). It is at the same scale and projection as the Western Canada Atlas Base Map. Thus, it will be possible to join these maps along their common boundary at 60° latitude. The print scale for this base, and the northern Canada Atlas itself will be 11 inches by 17 inches, or tabloid size.

ATLAS ORGANIZATION

The atlas will be divided into three chapter types – a set of **introductory chapters** followed by **time slice** and **theme chapters**. The introductory chapters will deal with the present day geography, the existing mineral and hydrocarbon resource base as well as the transportation network including roads and oil and gas pipelines. They will also deal with the regional geological and geophysical setting and will include generalized maps of bedrock geology and tectonic

provinces and geophysical maps showing the regional gravity and magnetic fields. Distribution of publicly available seismic lines will also be shown as part of the introductory chapters.

The time slice chapters, like the time slice chapters of the Western Canada Atlas, divide the sedimentary column into natural subdivisions most of which are unconformity bounded. These correspond approximately to Sloss Sequences, particularly for the lower Paleozoic which extends uninterrupted across most of the Atlas area. Unlike most of western Canada, however, shelf-to-basin transitions are well developed in lower Paleozoic strata of northern Canada and have a complex plan view geometry. These complex shelf-to-basin transitions may have provided opportunities for the entrapment of hydrocarbons in more porous shelf margin facies.

In contrast, upper Paleozoic and lower Mesozoic sequences tend to be confined to local areas, between which it is more difficult to draw correlations. Consequently, the Permian, Triassic and Jurassic are treated together as part of the same chapter. Each of these chapters will be in turn subdivided into a number of subchapters that reflect abrupt changes in the tectono-sedimentologic regimes within major sequences or chapters. Each time slice chapter will include a discussion of its contained mineral and hydrocarbon resources and the events which led to the emplacement of these resources.

Theme chapters will deal with non-temporal topics, such as organic maturation and petroleum potential, derived primarily from ROCK-EVAL data. Other theme chapters will deal with groundwater chemistry and metallic element contents of shale masses, such as the Road River Shales, and with hydrothermal dolomitization and its association with mineralization and as reservoir formers for the emplacement of hydrocarbons. Figures 2 and 3 show the database and preliminary geothermal gradient maps that will be included in the theme chapter concerning heat flow in the north. These types of maps and data provide essential information concerning the present day subsurface temperature distribution that may be utilized in modelling studies dealing with maturation of hydrocarbons.

Most information will be displayed on this standard base map but different scale maps will be included to highlight special regions, such as the dense concentrations of gold and diamond deposits in the Precambrian Slave Province and the regions around the Norman Wells Oil Field and the Kotaneelee–Pointed Mounted Gas Fields of Liard Basin.

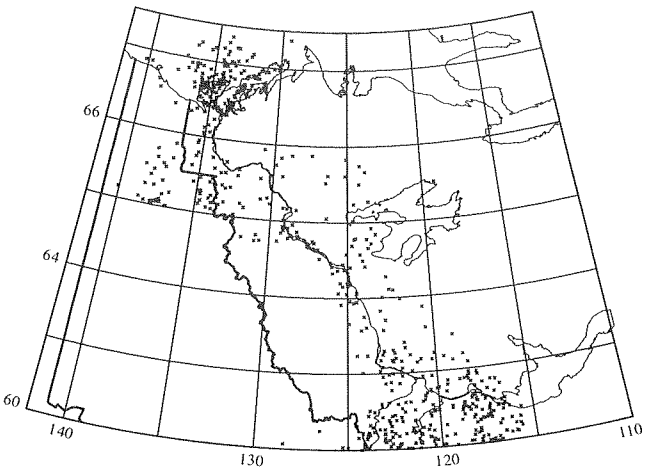

Figure 2. *Well control for the present day heat flow and thermal conductivity maps for the northern Canada Atlas. This map will be included in the theme chapter dealing with heat flow.*

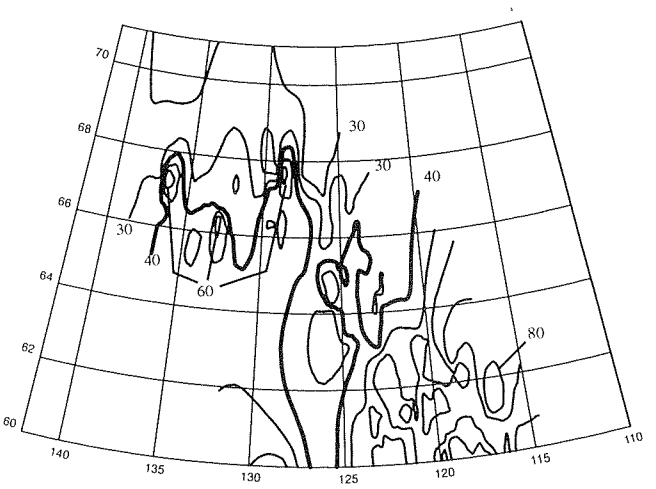

Figure 3. *Geothermal gradient map of the northern Canadian mainland. Contours are in C°/Km. The shield area tends to be a region with high geothermal gradients.*

Contract work in progress or completed include geothermal studies (J. Majorowicz), Precambrian studies (J.D. Aitken), Quaternary studies (A. Duk-Rodkin) and a mineral resource inventory (M. Senkiw). One additional comment that could be made is that this atlas project will benefit, and will benefit from, the SNORCLE lithoprobe transect that will extend across the southern Interior Plain.

CONCLUSION

Why embark on this project? The reasons are essentially those in favour of any regional compilation; that it assists the explorationist to place the geology of his particular area of interest in the proper context of a clear regional picture in the form of maps and cross sections. It will also provide governments at all levels with a reference document for decisions concerning the regulation of oil and gas and mineral industry activity.

REFERENCES

Dixon, J.
in press: Geological Atlas of the Beaufort–Mackenzie Area. Geological Survey of Canada, Miscellaneous Report.

Mossop, G.D. and Shetsen, I. (compilers)
1994: Geological Atlas of the Western Canada Sedimentary Basin. Calgary, Canadian Society of Petroleum Geologists and Alberta Research Council, 510 p.

PALYNOSTRATIGRAPHIC CORRELATION OF UPPER PERMIAN ROCKS OF THE CANADIAN ARCTIC, SOUTHERN BARENTS SEA AND VOLGA/URALS, RUSSIA

J. Utting

Geological Survey of Canada, 3303-33rd Street N.W., Calgary, Alberta T2L 2A7

N. Esaulova

Kazan University, Kazan, Russia

M. Grigoriev

VIIOkeangeologiya, St. Petersburg, Russia

ABSTRACT

Upper Permian rocks (Trold Fiord Formation) in the Sverdrup Basin of the Canadian Arctic Archipelago may be correlated reliably by marine faunas with the Wordian (Guadalupian) of Texas. Correlation of the Wordian with the Russian stratotypes in the Volga/Urals area is less certain due to the scarcity or lack of marine fauna in the latter, although many workers have correlated the Wordian with parts of the Kazanian. Palynomorphs occur in abundance in the Trold Fiord Formation, in the Kazanian stratotype, and in Kazanian/Tatarian rocks of the southern Barents Sea. Assemblages from the Canadian Arctic and the southern Barents Sea have many features in common, but those from the Kazanian stratotype are very different.

INTRODUCTION

Correlation of Permian rocks throughout the world is based partly on comparisons with stratotype sections located in and near the Urals, Russia. Lower Permian stages are well defined by their abundant marine faunas (Asselian, Sakmarian and Artinskian), but more problematical are the partially marine younger stages with their sparse marine faunas (Kungurian, Ufimian and Kazanian) and the essentially nonmarine Tatarian Stage.

Of considerable importance to the Permian of North America is the correlation of the stratotypes of the Guadalupian Series (Roadian, Wordian and Capitanian stages) of Texas with the Ufimian and Kazanian stratotypes of Russia (Fig. 1). The stratotypes of the

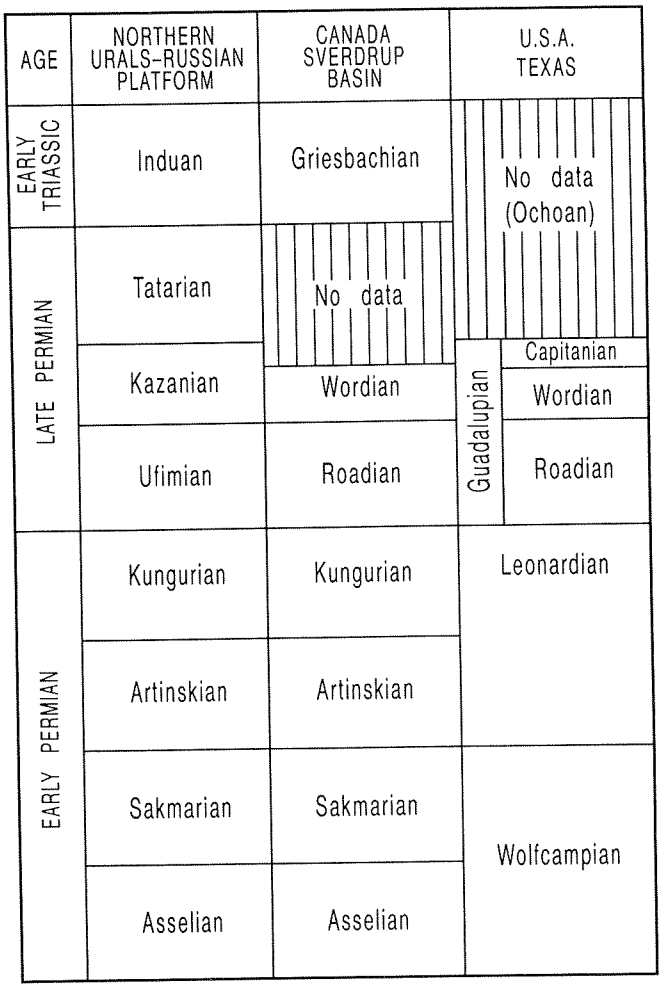

Figure 1. *Tentative correlation of stages between Northern Urals and Russian platform (Russia), Sverdrup Basin (Canada), and Texas (U.S.A.).*

Wordian Stage and part of the Capitanian Stage (Upper Permian in the sense historically used in the Urals) have been correlated by many workers (e.g., Dickins, 1992; Jin Yu-gan et al., 1994) with the Kazanian stratotype near Kazan, Russia (Fig. 2). These correlations are uncertain because, although the dominantly carbonate Guadalupian stratotype contains a rich diverse fauna of conodonts, brachiopods, fusulinaceans and ammonoids (Wardlaw et al., 1994), the Kazanian stratotype contains only a sparse marine fauna of brachiopods and bivalves and a nonmarine fauna of bivalves, ostracods, and conchostracans (Solodukho et al., 1993). Direct palynostratigraphic comparisons between Guadalupian stratotypes and the type Kazanian are not possible because palynomorphs have yet to be found in the former, although abundant well preserved pollen and spores occur in the latter. Thus, to establish palynostratigraphic correlations, detailed palynological information is required from the Wordian. This is available in the Sverdrup basin of the Canadian Arctic (Fig. 2) where rocks (Trold Fiord Formation) dated as Wordian by ammonoids (Nassichuk, in press), brachiopods (Waterhouse *in* Thorsteinsson, 1974) and conodonts (Henderson, 1981; Henderson, pers. comm.) contain well preserved, diverse assemblages of pollen and spores (Utting, 1994).

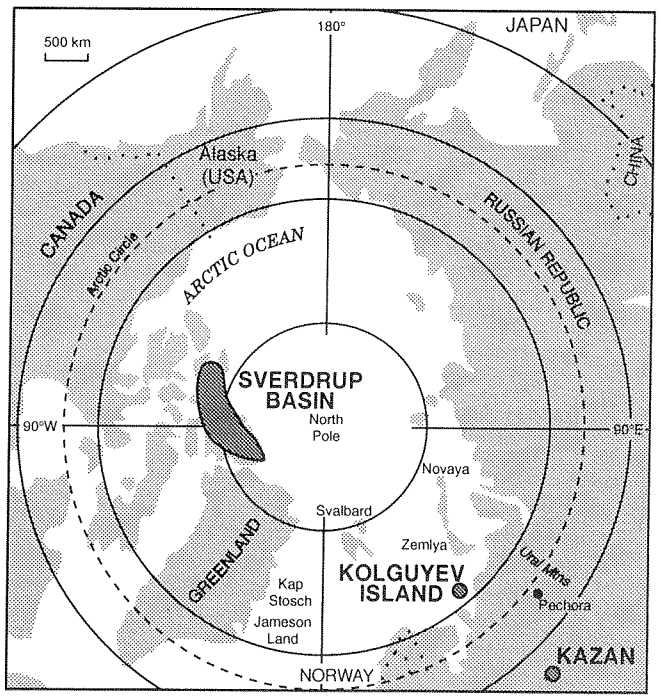

Figure 2. *Location of Sverdrup basin (Canada), Kolguyev Island, southern Barents Sea (Russia), and Kazan (Russia).*

PALYNOLOGICAL ASSEMBLAGES

One might anticipate that if the Wordian and Kazanian are approximately time equivalent, as suggested by the marine faunas, then pollen and spore assemblages should be similar. However, this does not appear to be true. In Wordian strata of the Canadian Arctic, trilete spores and non-taeniate, taeniate, and polyplicate pollen are common to abundant, and monosaccate pollen and acanthomorph acritarchs are rare. In contrast, trilete spores are rare in Kazanian stratotype material, although other suprageneric groups are present in comparable proportions. There are also differences in the taxa present. For example, the distinctive species *Scutasporites nanuki, Ahrensisporites thorsteinssonii, A. multifloridus,* and *Hamiapollenites erebi,* which all have their earliest occurrence in the Wordian of the Canadian Arctic, are, with the possible exception of *H. erebi,* absent from the Kazanian stratotype. *Limitisporites monstruosus* and *Crucisaccites ornatus* are present in the Kazanian stratotype, but both are absent from the Wordian of the Canadian Arctic, although the former occurs in the Artinskian.

In view of the significant differences between palynomorph assemblages in Wordian strata of the Canadian Arctic and Kazanian strata in the Volga/Urals area, material was also studied from rocks of Kazanian/Tatarian age (based on bivalves and brachiopods) from the subsurface of Kolguyev Island, southern Barents Sea. Kolguyev Island is situated geographically between the Canadian Arctic and the Kazanian stratotype (Fig. 2) and is an area where oil and gas exploration is currently active. In many respects, Kolguyev assemblages resemble the Wordian of the Canadian Arctic, but they also show some affinities to species from the Kazanian stratotype. Like the Canadian material, they contain abundant trilete spores, but unlike the Canadian material they contain only minor amounts of non-taeniate and taeniate disaccate and monosaccate pollen. Assemblages containing *Scutasporites nanuki, Ahrensisporites thorsteinssonii,* and *A. multifloridus* resemble the Wordian of Canada and the presence of *Limitisporites monstruosus* is reminiscent of the Kazanian stratotype.

DISCUSSION

If strata at these three localities are approximately time equivalent, then the differences in the assemblages may be caused by differences in one or more of the following factors: floral province, paleoenvironment, facies, paleoclimate, latitude, and relative position on the continent of Pangea. Paleofloristic data for all three

localities are sparse, but all three probably fall within the Sub-Angara province (Meyen, 1982, 1987; Esaulova, 1991; Utting and Piasecki, in press). Deposition at all three localities was mainly shallow marine to terrestrial, but rock types are different. For example, the Wordian of Arctic Canada contains glauconitic sandstone and shale as well as limestone, whereas the Kazanian/Tatarian of Kolguyev Island consists mainly of sandstone, shale and siltstone. At the Kazanian stratotype, rock types include limestone, dolomite, marlstone with siltstone intercalations, and claystone. The paleoclimate, undoubtedly influenced by latitude and relative positions on Pangea, was probably different in all three localities. That of the Canadian Arctic was probably cool as suggested by the presence of glacial dropstones (Beauchamp, 1994). It was probably arid with periods of humidity; taeniate disaccate and polyplicate pollen are abundant, but also trilete spores are common in some samples (Utting 1994). The Kolguyev climate was humid (coaly beds locally present; abundance of trilete spores), whereas the climate of the Kazanian stratotype was hot and arid (gypsiferous limestone sometimes present; abundance of polyplicate and taeniate disaccate pollen). Climatic differences of this magnitude would have resulted in significant vegetational differences between the three localities. The Canadian Arctic and the southern Barents Sea occupied similar latitudes in the Late Permian, and probably a similar position in Pangea relative to the continental margin (Lottes and Rowley, 1990). The Volga/Urals area on the other hand was probably situated further south and further from the continental margin.

REFERENCES

Beauchamp, B.
1994: Permian climatic cooling in the Canadian Arctic. *In* Pangea: Paleoclimate, Tectonics and Sedimentation During Accretion, Zenith and Break-up of a Supercontinent: Boulder, Colorado, G.O. Klein (ed.). Geological Society of America, Special Paper 288, p. 229–246.

Dickins, J.M.
1992: Permian geology of Gondwana countries. International Geology Review, v. 34, no. 10, p. 986–1000.

Esaulova, N.K.
1994: Flora of the Kazanian stage in the Kama River Region: Stratigraphic and phytogeographic position. Permian System of the World. Program and abstracts, IPC, Perm August, 1991, A24.

Henderson, C.M.
1981: Conodont paleontology of the Permian Sabine Bay, Assistance and Trold Fiord formations, northern Ellesmere Island, Canadian Arctic Archipelago. Unpublished M.Sc. thesis. University of British Columbia, 135 p.

Jin, Y., Glenister, B.F., Kotlyar, G.V., and Sheng, J.
1994: An operational scheme of Permian Chronostratigraphy. *In* Palaeontology and Stratigraphy, Vol 1, Permian Stratigraphy, Environments and Resources, Y. Jin, J. Utting and B. Wardlaw (eds.). Palaeoworld, v. 4, p. 1–13.

Lottes, A.L. and Rowley, D.B.
1990: Reconstruction of the Laurasian and Gondwana Segments of the Permian Pangaea. *In* Palaeozoic Palaeogeography and Biogeography, W.S. McKerrow and C.R. Scotese (eds.). Geological Society Memoir No. 12, p. 383–395.

Meyen, S.V.
1982: The Carboniferous and Permian floras of Angaraland (a synthesis). International Publishers Lucknow (India), 109 p.

1987: Fundamentals of Palaeobotany. Chapman and Hall Ltd., London, 432 p.

Nassichuk, W.W.
in press: Permian ammonoids in the arctic regions of the world. *In* The Permian of Northern Pangea, P.A. Scholle, T.M. Peryt, and D.S. Ulmer-Scholler (eds.). Springer Verlag, v. 1 (Paleogeography, Paleoclimates, Stratigraphy).

Solodukho, M.G. et al.
1993: Permian System: Guides to Geological Excursions in the Uralian Type localities. Part 5 – Volga Region, Occasional Publications ESRI, New Series, v. 10, p. 269–303.

Thorsteinsson, R.
1974: Carboniferous and Permian stratigraphy of Axel Heiberg Island and Western Ellesmere Island, Canadian Arctic Archipelago. Geological Survey of Canada, Bulletin 224, 115 p.

Utting, J.
1994: Palynostratigraphy of Permian and Lower Triassic rocks, Sverdrup Basin, Canadian Arctic Archipelago. Geological Survey of Canada, Bulletin 478, 107 p.

Utting, J. and Piasecki, S.
in press: The palynology of the Permian of Northern Continents: a review. *In* The Permian of Northern Pangea, P.A. Scholle, T.M. Peryt, and D.S. Ulmer-Scholler (eds.). Springer Verlag, v. 1 (Paleogeography, Paleoclimates, Stratigraphy), 62 ms pages, 7 figs.

Wardlaw, B.R., Grant, R.E., and Rohr, D.M.
1994: Preliminary proceedings of the Guadalupian Symposium including abstracts to all chapters. U.S. Department of the Interior, U.S. Geological Survey, Open File Report 94–000, 33 p.

SEQUENCE STRATIGRAPHIC ANALYSIS OF THE LATE CRETACEOUS–PALEOGENE FORMATIONS IN THE JEANNE D'ARC BASIN, OFFSHORE EASTERN CANADA

A. Agrawal, M.A. Williamson, K.C. Coflin, K. Dickie, J. Shimeld, K.D. McAlpine, B. Altheim, F.J. Thomas, T. Semper, and V. Pascucci

Atlantic Geoscience Centre, P.O. Box 1006, Dartmouth, Nova Scotia B2Y 4A2

BACKGROUND

The stratigraphic framework and depositional systems of Late Cretaceous–Paleogene units of the central Jeanne d'Arc basin are being characterized with respect to relative sea-level variations. An improved understanding of the stratal geometry, facies variations and reservoir continuity of these sedimentary units fulfils, in part, objectives of the Hydrocarbon Charge Modelling Project (HCMP). For example, depositional facies analysis of the South Mara lowstand unit (fan/turbidite complex) will assist in further assessment of this hydrocarbon play. Similarly, the observed biodegradation of the hydrocarbons in shallow reservoirs is probably related to the characteristics of invading fluids, that are in turn controlled by aquifer hydrogeology and reservoir facies variation. Resolution of the stratigraphic complexities preserved within these units is key to the refinement of existing 2-D models of fluid-migration and reservoir-seal system evolution (Williamson et al., this volume). Analyses of stratal geometry, reflection characteristics and lithology are in progress using digital seismic, and log and core data from wells (Fig. 1).

DEPOSITIONAL SEQUENCES AND FEATURES

This ongoing study has revealed two unconformity-bound sequences, a Late Cretaceous sequence and a Paleogene sequence (Fig. 2, Table 1). The Late Cretaceous sequence overlies a regional Mid-Cretaceous (Albian/Cenomanian) unconformity and its correlative conformity, and is bounded above by the base-Tertiary unconformity. This sequence consists of a lower shaly unit (Eider sand and equivalent Nautilus shale), overlain by the Petrel Member, and the Otter Bay unit (which includes a deltaic feature). The overlying Paleogene sequence lies between the base-Tertiary and Middle Eocene unconformities (Fig. 2, Table 1), and it is divided into a lower South Mara unit, and overlying transgressive and highstand shale units.

Depositional processes led to development of the following features:

Otter Bay delta. The Otter Bay unit of the Dawson Canyon Formation lies between the Petrel Member and the base-Tertiary unconformity (Table 1). A distinctive deltaic feature (Fig. 2) is observed in this interval near the western margin of the basin, south of the Hibernia oil field. Several sedimentary lobes are observed in the depocentre to the east (see stippled areas in Fig. 3) that may have accumulated from the sediments shed during

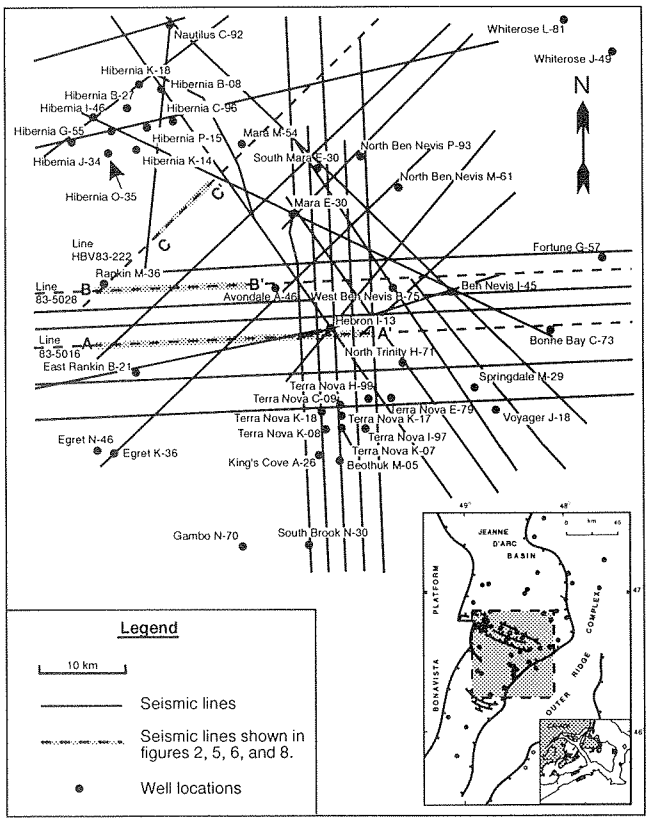

***Figure 1.** Map showing the location of the seismic lines and wells used in this study.*

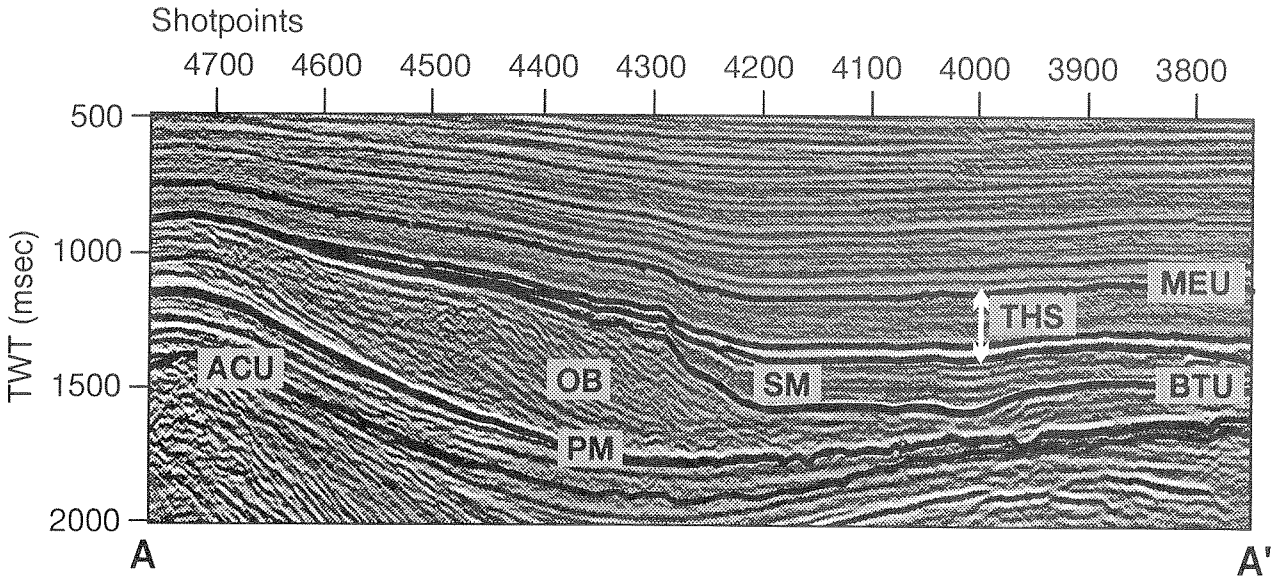

Figure 2. *West–east seismic profile (Fig. 1, part of line Chevron 83-5016) showing general stratigraphic section, and unconformities. ACU, Albian/Cenomanian unconformity; BTU, Base Tertiary unconformity; MEU, Middle Eocene unconformity; PM, Petrel Member top; OB, Otter Bay unit; SM, South Mara unit; THS, transgressive/highstand units.*

Table 1

Depositional framework of the Late Cretaceous–Paleozoic rock units in the southern part of the Jeanne d'Arc Basin

Stratigraphic Units	Systems Tracts
Middle Eocene unconformity	*Sequence Boundary*
Unnamed shaly unit	Transgressive Systems Tract/ Highstand Systems Tract
South Mara unit	Lowstand Systems Tract
Base Tertiary unconformity	*Sequence Boundary*
Otter Bay unit	Highstand Systems Tract
Petrel Member	
Eider sand / Nautilus Shale formations	Transgressive Systems Tract
Albian/Cenomanian unconformity	*Sequence Boundary*

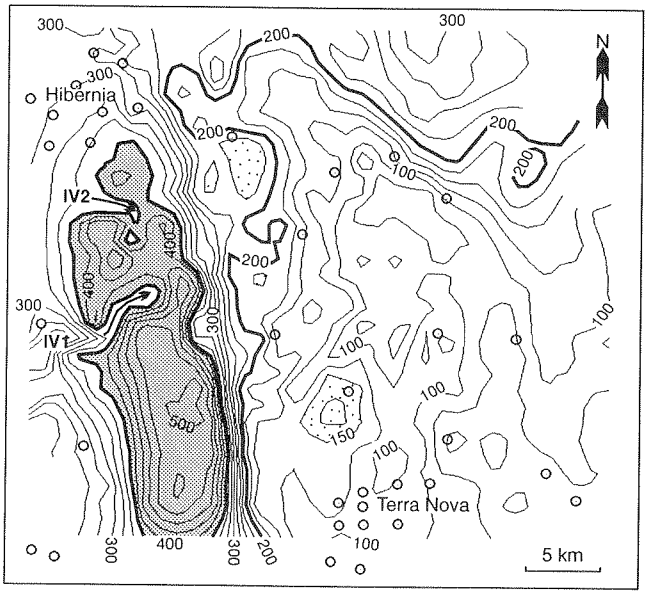

Figure 3. *Isochron map of the Otter Bay unit (in milliseconds). Shaded area thickness is more than 375 ms (~500 m). Two incised valleys erode the delta after entering the area from the west. IV1 and IV2 indicate locations of the two incised valleys. Stippled area: sedimentary lobes (refer to text).*

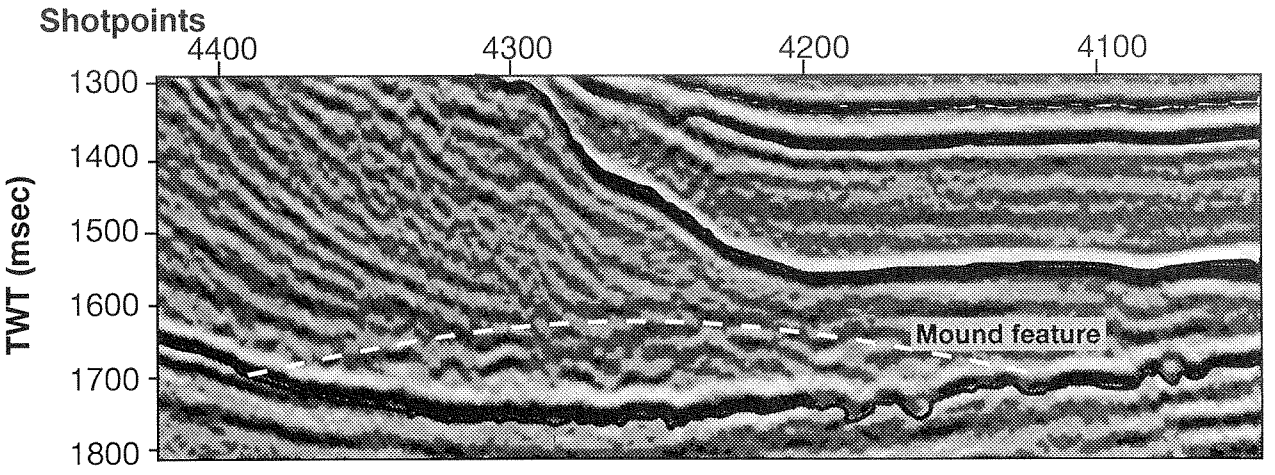

Figure 4. *West–east section (part of line Chevron 83-5016 shown in Fig. 2) showing a feature with mounded cross-section and chaotic/subparallel reflections. The mounded feature shown is interpreted as synchronous debris-flow accumulations shed from the delta during its growth.*

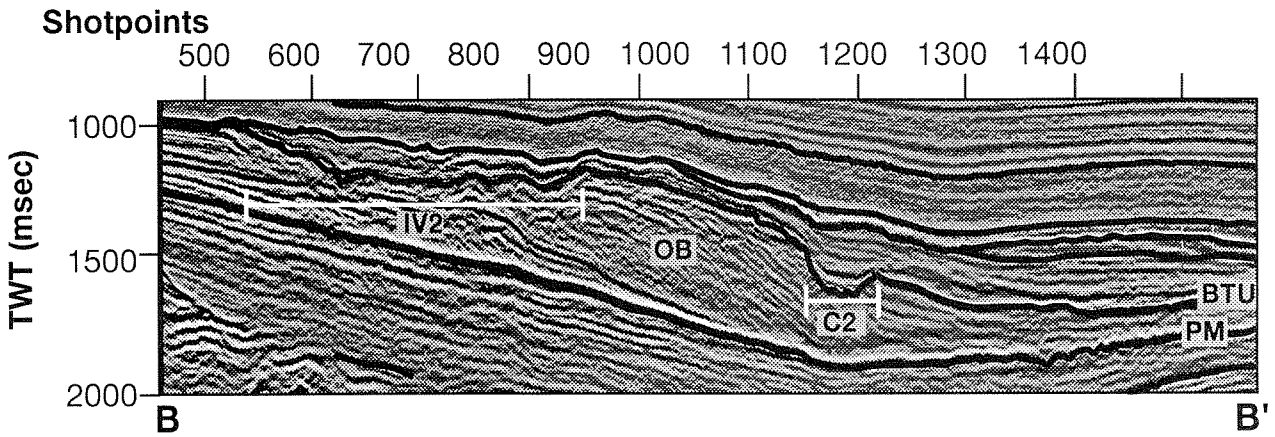

Figure 5. *West–east seismic section (part of line Chevron 83-5028 shown in Fig. 1) showing an incised valley (IV2, see Fig. 3) and a canyon (C2). See Figure 7 for location of the two canyons. The incised valleys connect to the canyons on the delta slope. PM, Petrel Member top; OB, Otter Bay unit; BTU, Base Tertiary unconformity.*

growth of the delta. The thicker part of the feature has not been drilled yet. The delta is much less developed in the Hibernia oil field to the north where it has been penetrated by several wells.

Debris flow/Turbidite complex. Depositional features that show mounded cross-sections and chaotic/subparallel reflections (Fig. 4) are preserved in the distal part of the delta. Such features may be a result of disorganized debris flow shed due to episodic mass-transport activity during delta growth. As defined here, the facies has not been penetrated by wells. Detail mapping of this facies is in progress.

Incised Valleys. The base-Tertiary unconformity represents an erosional surface over the shelf (deltaic) region. The development of two wide incised valleys (Figs. 5, 6) is quite spectacular on the northern half of the shelf and have eroded into the underlying Otter Bay unit. The Otter Bay unit isochron map (Fig. 3) reveals that the incised valleys enter from the western side of the study area, merge further downgradient and drain

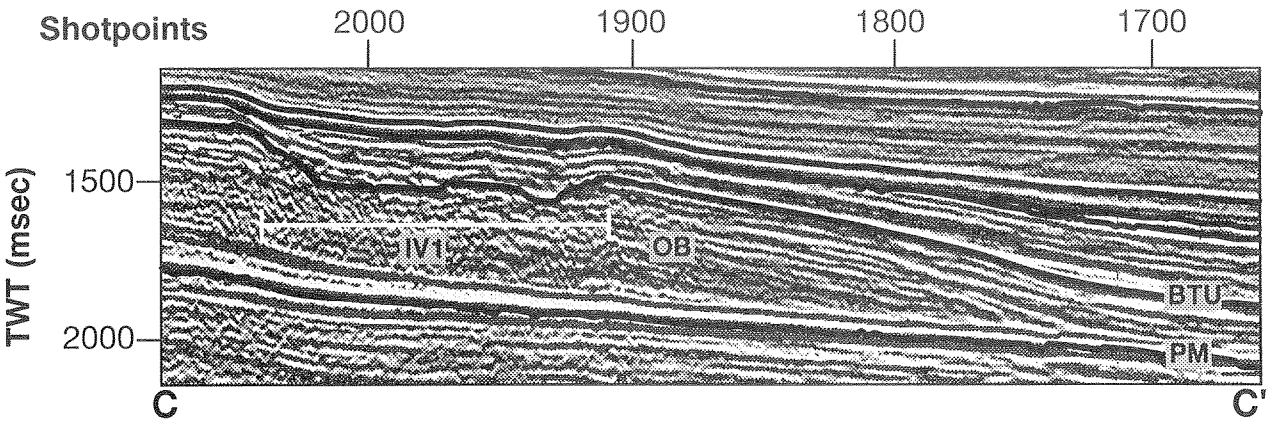

Figure 6. North–south seismic section (part of line HBV 83-222 shown in Fig. 1) showing an incised valley (IV1, see Fig. 3) that erodes part of the underlying Otter Bay unit (OB). The base of the incised valley corresponds to the Base Tertiary unconformity (BTU). PM, Petrel Member top.

eastward into separate canyons on the delta slope. Proximity and merging of the two incised valleys on the shelf may indicate significant lateral channel migration, switching and avulsion.

Channel-Levee complex. The South Mara unit overlies the base-Tertiary unconformity and comprises a thick unit occupying the depression adjacent to the delta (Fig. 7), and is bounded above by an onlap (transgressive) surface. This unit may be divided into several thin subunits with variable contacts (Fig. 8) that accumulated in the depocentre largely as aggradational packages. Most of the subunits appear to consist of channel-levee features separated by interchannel areas based on their stratal geometry and reflection characters (summarized by Weimer, 1990). The unit has been penetrated by several wells (Fig. 7). Detailed characterization of the unit in terms of evolution of channel-levee depositional systems and facies variation is in progress.

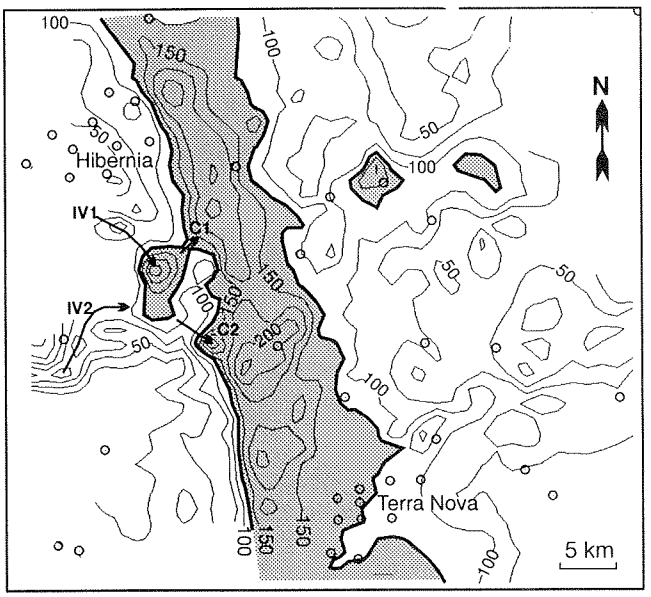

Figure 7. Isochron map of the South Mara unit (in milliseconds). Shaded area has a thickness of more than 125 ms (~150 m). C1 and C2 are locations of canyons connected to the incised valleys on the delta. Arrows indicate the positions of the two incised valleys, IV1 and IV2.

DEPOSITIONAL SEQUENCE ANALYSIS

The Late Cretaceous in the Jeanne d'Arc Basin generally represents a period of relative sea-level rise that allowed deposition of a 200 m or more thick shale unit followed by deepening and accumulation of Petrel Member limestone. The ensuing Otter Bay delta accumulated near the western margin of the basin (Fig. 3) due to subsidence and accommodation during a relative sea-level highstand. The overlying base-Tertiary unconformity is an important erosional surface over the delta (incised valleys) as it corresponds to a period of major sediment bypass over the shelf during an Early Paleocene relative sea-level fall/lowstand. The South Mara (Paleocene to earliest Eocene) unit was deposited during the relative sea-level fall/lowstand, and preserves several phases of channel-levee complex development in the depression situated basinward of the delta. The South Mara unit was sourced from the west through

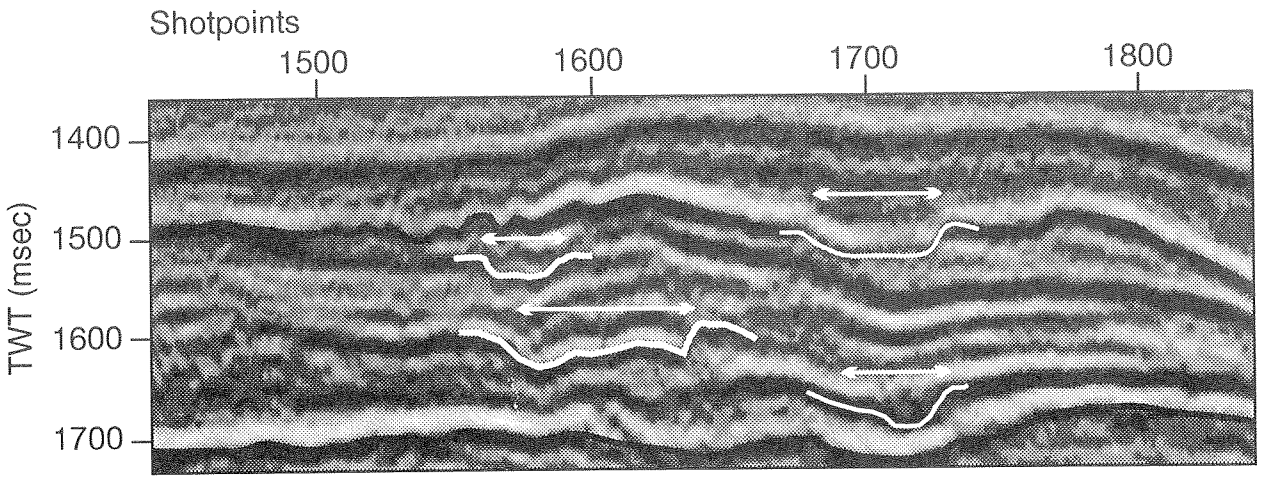

Figure 8. *Seismic section of part of the South Mara unit showing aggradational/stacked channel-levee systems. Horizontal arrows indicate approximate extent of individual channel-levee systems.*

two west–east incised valleys that developed south of the Hibernia oil field. The early Eocene transgressive and highstand shaly units overlying the South Mara unit represent a period of rapid relative sea-level rise and copious sediment accumulations.

REFERENCE

Weimer, P.
1990: Sequence stratigraphy, facies geometry, and depositional history of the Mississippi Fan, Gulf of Mexico. American Association of Petroleum Geologists Bulletin, v. 74, p. 425–453.

THE EAST COAST BASIN ATLAS SERIES GOES ON-LINE!

J.L. Bates, K.D. McAlpine, and P.N. Moir

Atlantic Geoscience Centre, Geological Survey of Canada
Bedford Institute of Oceanography, P.O. Box 1006, Dartmouth, Nova Scotia B2Y 4A2

INTRODUCTION

The East Coast Basin Atlas Series (ECBAS) is a synthesis of research undertaken by the Atlantic Geoscience Centre (AGC) of the Geological Survey of Canada (GSC). The Series provides a current overview of the sedimentary basins of offshore Eastern Canada for a national and international user community. The Labrador Sea and Scotian Shelf volumes are published and are available as printed volumes and individual maps (Fig. 1). The third volume of the Series, Grand Banks of Newfoundland, is in production at the AGC. This Atlas is expected to be published on-line, available for purchase on Internet through the AGC World Wide Web Mosaic site as on-demand printed copies and digital files. A CD-ROM of the volume is also under consideration.

EAST COAST BASIN ATLAS SERIES

The ECBAS is a synthesis of all geological, geophysical, geochemical, and geotechnical data collected on the sedimentary basins of Eastern Canada. These data, provided by industry and government, include seismic reflection and refraction data as well as surficial, geotechnical, magnetic, gravity, and well data.

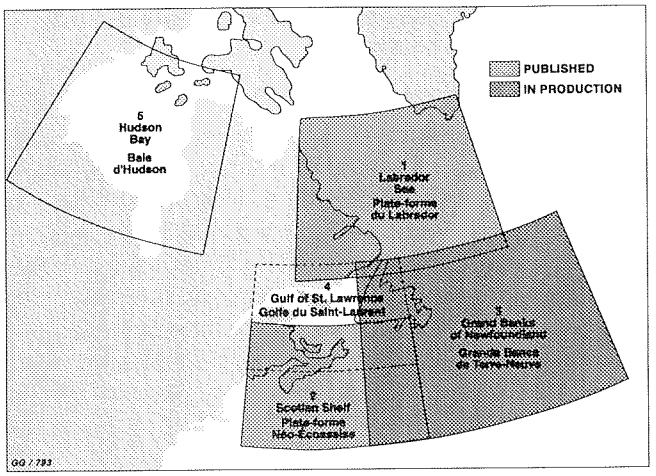

***Figure 1.** Specific volume areas, published and in production.*

A series of standard maps (1:2 000 000 scale, Lambert Conformal projection with standard parallels at 45°N and 66°W) form the basis of the East Coast Basin Atlas Series and allow for compatibility of data between maps of the different volumes. When applicable, other scales are used to portray regional or local features. These maps in combination with illustrations, charts, plots, and descriptive text attempt to define the surficial geology, stratigraphy, structure, and sedimentology of each study area.

GRAND BANKS OF NEWFOUNDLAND BASIN ATLAS

A passive continental margin that formed during the opening of the North Atlantic Ocean during the Mesozoic and Cenozoic provides the regional geological setting for the Grand Banks of Newfoundland. Triassic to Early Jurassic redbeds and evaporites, Jurassic carbonates and shales, and Cretaceous marine clastics comprise the Mesozoic basin sequences. A peneplain separates these sediments from Upper Cretaceous and Cenozoic clastics and chalky limestones. The petroleum resources are found mainly in the Cretaceous and older rocks.

The Grand Banks of Newfoundland Basin Atlas assimilates much of the industry and Geological Survey of Canada data available on this region. Both petroleum exploration and academic interests will favour this compendium of maps and panels displaying Quaternary and bedrock geology, structure, stratigraphy, geotechnics, geophysics and hydrocarbon potential. Table 1 provides a tentative listing of the contents of the Atlas. Figure 2 is an example of the preliminary Atlas map panels.

Table 1
Preliminary Content of Grand Banks of Newfoundland Basin Atlas

1.0 Introduction
- 1.1 Bathymetry and physiographic features
- 1.2 Well location map
- 1.3 Seismic coverage

2.0 Quaternary Geology and Modern Sedimentary Processes
- 2.1 Quaternary geology control
- 2.2 Regional surficial geology
- 2.3 Surficial geology–Hibernia area
- 2.4 Deep-water surficial geology
- 2.5 Surficial features map
- 2.6 Subsurface Quaternary features
- 2.7 Hibernia area–sidescan mosaic
- 2.8 Coastal geology
- 2.9 Stratigraphy and physical properties (index map)
- 2.10 Stratigraphy and physical properties (Halibut Channel)
- 2.11 Stratigraphy and physical properties (NE Grand Banks–Hibernia)
- 2.12 Stratigraphy and physical properties (St. Pierre Slope and Laurentian Fan)
- 2.13 Stratigraphy and physical properties (Flemish Pass)
- 2.14 Stratigraphy and physical properties (Southeast Grand Banks)
- 2.15 Stratigraphy and physical properties (Innershelf–Burgeo and Rose Blanche)
- 2.16 Icebergs and iceberg scouring
- 2.17 Tidal range, wave height, ice cover
- 2.18 Sediment transport potential (1 year event)
- 2.19 Sediment transport potential (10 year event)
- 2.20 Sediment transport potential (32 year event)
- 2.21 Sediment transport potential (100 year event)
- 2.22 Paleo-oceanography and paleoglaciology

3.0 Bedrock Geology
- 3.1 Bedrock geology map
- 3.2 Pre-Mesozoic basement and volcanic occurrences

4.0 Lithostratigraphy
- 4.1 East coast stratigraphic charts
- 4.2 Review and type sections
- 4.3 Cross-sections AA' (Cormorant-Flying Foam) and BB' (Hibernia-Ben Nevis)
- 4.4 Cross-section CC' (Spoonbill-Baccalieu)
- 4.5 Cross-sections EE' (Pelican-Heron) and FF' (Coot-Osprey)
- 4.6 Cross-section FF' (Narwhal-Spoonbill)

5.0 Biostratigraphy
- 5.1 Biostratigraphic zonations
- 5.2 Tabulated zonation data
- 5.3 to 5.6 Correlation of stratigraphic zones
- 5.7 to 5.10 Biostratigraphic zonation and maturation data
- 5.11 Visual kerogen data

6.0 Seismic Expression
- 6.1 Interpreted seismic sections–East Newfoundland Basin (Orphan Basin)
- 6.2 Interpreted seismic sections–Jeanne d'Arc Basin
- 6.3 Interpreted seismic sections–Flemish Pass and Jeanne d'Arc Basins
- 6.4 Interpreted seismic sections–Whale Basin and South Whale Subbasin
- 6.5 Interpreted seismic sections–Jeanne d'Arc, Carson and Horseshoe Basins

7.0 Structure and Isopach
- 7.1 Near base Tertiary depth map
- 7.2 Petrel Marker depth map
- 7.3 Near base Upper Cretaceous depth map
- 7.4 Near base Cretaceous depth map
- 7.5 Near pre-Mesozoic basement depth map
- 7.6 Post Cretaceous isopach
- 7.7 Late Cretaceous isopach
- 7.8 Early Cretaceous isopach
- 7.9 Jurassic and Late Triassic iospach
- 7.10 "B" Marker, Jeanne d'Arc Basin time map
- 7.11 Intra Paleozoic Marker–Bonavista Platform
- 7.12 Tectonic elements map

8.0 Isopach and Facies
- 8.1 Selected iospach and facies maps of the Jeanne d'Arc Basin

9.0 Paleogeography
- 9.1 Regional Paleogeographies of the Triassic, Early Jurassic and Middle Jurassic
- 9.2 Regional Paleogeographies of the Late Jurassic, Early Cretaceous and Late Cretaceous

10.0 Geochemistry
- 10.1 Geothermal gradients
- 10.2 Organic geochemistry and source rocks
- 10.3 Overpressure

11.0 Hydrocarbons
- 11.1 Hydrocarbon occurrences and fields–part 1
- 11.2 Hydrocarbon occurrences and fields–part 2

12.0 Geophysics
- 12.1 Magnetic anomaly map
- 12.2 Gravity anomaly map
- 12.3 Regional transect–introduction
- 12.4 Regional transect 84-3 (part A)
- 12.5 Regional transect 84-3 (part B)
- 12.6 Regional transect 85-3 and 87-3 (part A)
- 12.7 Regional transect 85-3 and 87-3 (part B)
- 12.8 Regional transect 85-4 (part A)
- 12.9 Regional transect 85-4 (part B)
- 12.10 Regional transect 85-1&2 (part A)
- 12.11 Regional transect 85-1&2 (part B)
- 12.12 Regional transect 87-5
- 12.13 Crustal stress, earthquakes, and crustal thickness

13.0 Seafloor Spreading History
- 13.1 & 13.2 Magnetic anomalies along track
- 13.3 Plate reconstructions, bathymetry
- 13.4 Plate reconstructions, gravity and magnetic anomalies
- 13.5 Plate reconstructions, closure bathymetry
- 13.6 Plate reconstructions, closure gravity anomaly
- 13.7 Plate reconstructions, closure magnetic anomaly
- 13.8 Depth to basement

14.0 Cited References

The Grand Banks of Newfoundland Basin Atlas will be published as an on-line/on-demand publication contrast to the first two atlases that were published as bound printed volumes. Individuals interested in purchasing the volume contents will be able to view the maps and panels on AGC's WWW Mosaic site (http://agcwww.bio.ns.ca) and then either download the required digital files and/or request on-demand print copies. In addition, a CD-ROM of the complete atlas is under development.

You are encouraged to browse the AGC Mosaic site for the current status of the ECBAS and other science activities at AGC.

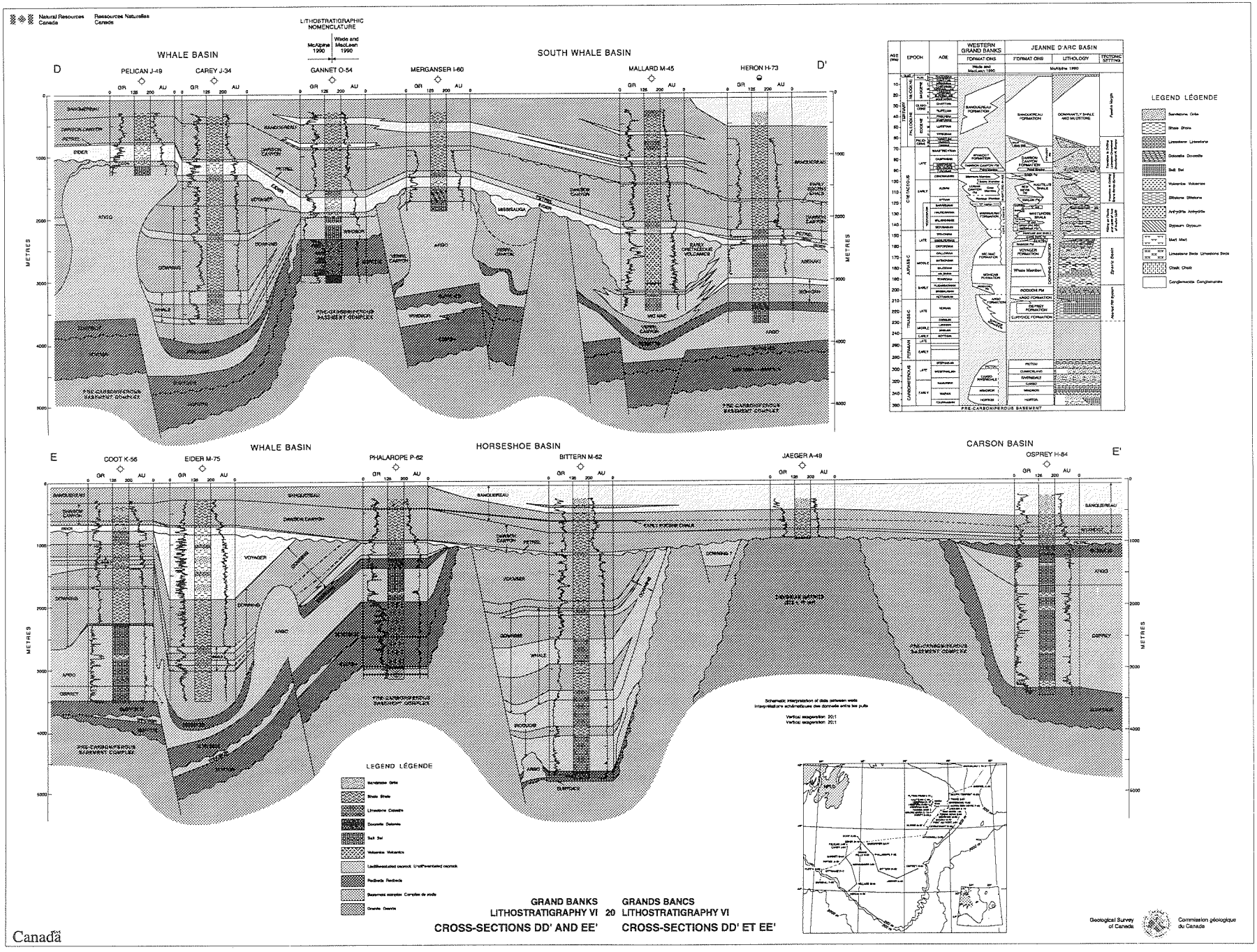

Figure 2. *Example of the preliminary Atlas map panels.*

SHALE PROPERTIES AND THEIR SIGNIFICANCE IN SEDIMENTARY BASIN MODELLING

M.E. Best

Pacific Geoscience Centre, Geological Survey of Canada
P.O. Box 6000, Sidney, B.C. V8L 4B2

D.R. Issler

Geological Survey of Canada, 3303-33rd Street N.W., Calgary, Alberta T2L 2A7

T.J. Katsube

Mineral Resources Division, Geological Survey of Canada
601 Booth Street, Ottawa, Ontario K1A 0E8

INTRODUCTION

Shales play an important role in basin processes. They make up a significant portion of the sediment within a basin and also have unique chemical and physical properties. For example, they have much lower porosities and permeabilities (often orders of magnitude) than carbonates and sandstones because of their microscopic structure and packing of the mineral grains (Katsube et al., 1991). Shales therefore tend to form reservoir seals and zones of restricted flow within a basin.

The petroleum industry has shown little interest in shales because they were perceived to have no direct economic value due to their nonreservoir properties. Consequently their physical properties are not as well documented as those of carbonates and sandstones. Recent interest in basin modelling and methane production from organic-rich shale source rocks is changing industry's perception of the role shales play in basin processes. The Geological Survey of Canada (GSC) recognized the important role of shales in basin processes in the late 1980s and established a long term research program to investigate shale properties (Mudford, 1988; Mudford and Best, 1989). In particular the GSC noted the need for accurate values of shale permeability and porosity for quantitative basin modelling (Williamson, 1992; Williamson and Smyth, 1992). Since that time, the program has expanded to include pore-size distribution and formation resistivity measurements plus detailed analysis of sonic and other downhole logging tools (Issler, 1992).

In this paper we report on progress to date and attempt to illustrate how the research has impacted on our capability to model basin evolution and fluid migration.

SHALE PROPERTIES AND BASIN PROCESSES

An attempt to link shale properties to basin processes is illustrated in Figure 1. The inner circle of the diagram

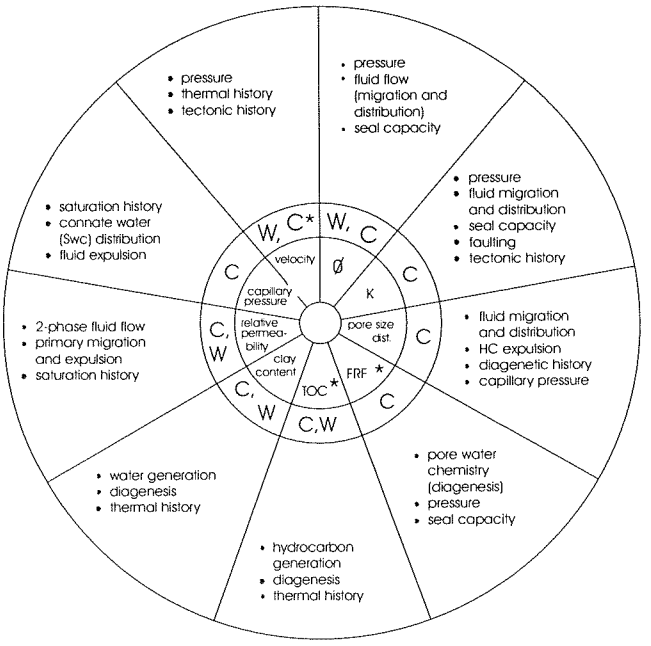

* C = core measurement
TOC = total organic content
W = log measurement in well
FRF = formation resistivity factor

Figure 1. Schematic illustration of the relation of shale properties to basin processes.

represents shale core. It is surrounded by a number of properties separated from each other by radial spokes. The next circular region indicates the measurement scale (core or log) commonly used to obtain the parameters associated with a particular property. Finally, the outer circle lists several basin processes that are influenced by that shale property. The list of properties and processes is not meant to be complete. In this paper we shall restrict our discussion to permeability, porosity and pore-size distribution obtained from core measurements and analysis of sonic logs to investigate overpressure.

PERMEABILITY MEASUREMENTS

Permeability is one of the most important shale properties because of its influence on the distribution, migration and pressure evolution of fluids within a basin over geological time scales. It is also an important parameter for determining shale seal capacity, pressure buildup and faulting.

As part of the GSC's shale program, permeability measurements have been made on samples obtained from two Canadian basins (Katsube et al., 1991; Katsube and Coyner, 1994) using the transient pulse technique (e.g., Katsube and Coyner, 1994). Measured permeabilities for tight shales from depths of 4–6 km in the Venture Gas field (offshore Nova Scotia) and 2–4 km in the Beaufort–Mackenzie Basin (northern Canada) range between 0.1–300 nano-darcies (10^{-22}-3×10^{-19} m^2). These are some of the lowest permeability values measured for rocks, being 6–11 orders of magnitude lower than those for sandstones.

Examples of shale permeability versus effective pressure P_e (overburden pressure minus pore pressure) are shown in Figure 2. As expected, the permeability decreases as effective pressure increases. We believe that this permeability-pressure behaviour can be represented by several different exponential curves, each taking the form (Katsube and Coyner, 1994)

$$k_i = k_{oi}\exp(-\alpha_i P_e), \quad i = 1, \ n \text{ where } n = 2 \text{ or } 3 \quad (1)$$

where k_{oi} is the permeability at atmospheric pressure for the ith curve, P_e is the effective pressure and α_i is the slope of the ith curve (Fig. 2). A three curve system is proposed for the data illustrated in Figure 2a. A two-curve system, easily recognized even when measurement errors (vertical bars) are relatively large, is shown in Figure 2b.

We believe that the three curve system (Fig. 2a) represents (from low to high pressures) closure of micro-fractures developed as a result of stress-release during sample removal, closure of micro-fractures opened as a result of overpressure development, and

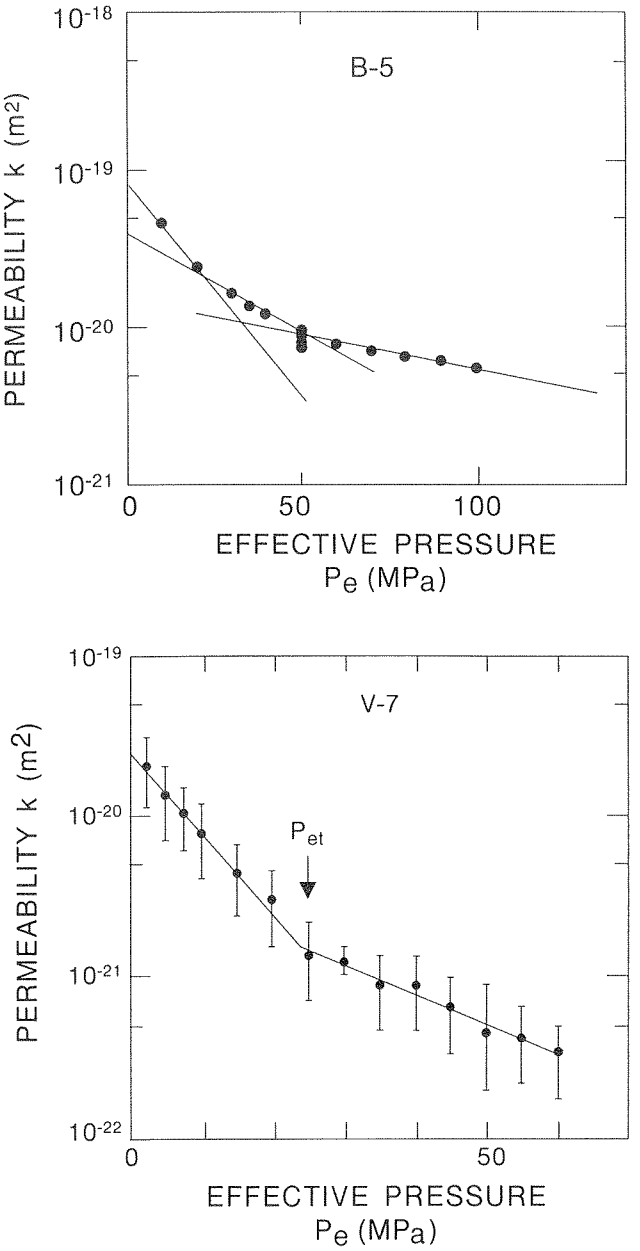

Figure 2. *Absolute permeability versus effective pressure. (Top) Sample B-5 from the Beaufort-Mackenzie Basin at a depth of 3760 m (Katsube and Coyner, 1994). (Bottom) Sample V-7 from the Venture Field, offshore Nova Scotia at a depth of 5272 m (Best and Katsube, 1993). The exponential defined by the equation in the text is different for values of P_e above and below the transition point P_{et}.*

compaction of the shale sample as lab pressures exceed the maximum burial pressure (Katsube and Coyner, 1994). This process is schematically illustrated in Figure 3 (Best and Katsube, 1995). As the sediments are buried, permeability decreases with depth of burial to the present day in situ effective pressure P_{et}. The dashed line represents the increase in permeability, due to pressure release, as a core is brought to the surface from the present day depth of burial. When a sample from that core is pressurized in the laboratory, the permeability decrease with increased pressure follows the two solid straight lines: (1) one line to P_{et}, as the pores that developed as a result of decompression are closed; and (2) the other line above P_{et}, where the matrix of the sample is being compressed at these pressures for the first time. As depicted in the diagram, the permeability curve for P_e values less than P_{et} does not have the same shape as that of the burial curve.

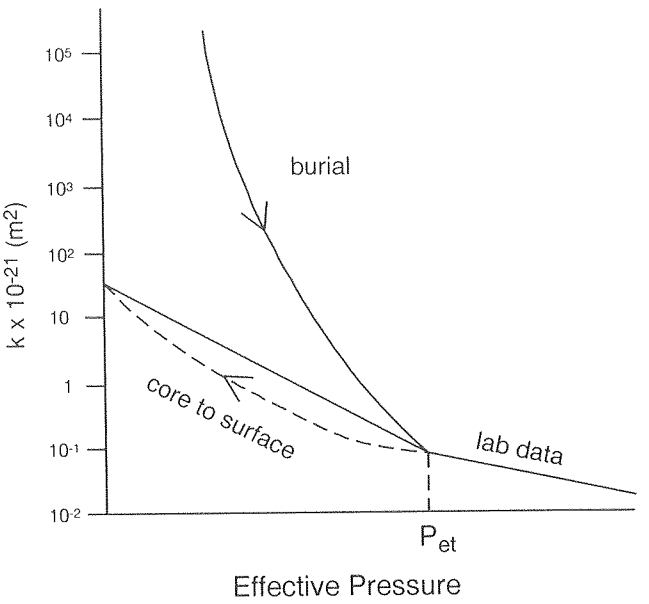

Figure 3. *Schematic illustrating how permeability is related to the stress release caused by bringing the sample to the surface (Best and Katsube, 1995).*

PERMEABILITY AND POROSITY CHANGE WITH DEPTH

The dependence of shale permeability on depth is an important parameter because it affects how the pore pressure evolves within a basin during sediment deposition. An empirical relationship is generally used to describe the dependence of permeability on depth for model studies because measured permeability values have generally been lacking. Permeability and porosity (ϕ) are usually related by a power law of the form $k = a\phi^m$, with porosity an exponential function of depth $\phi = \phi_o \exp(-bz)$ so that

$$k = k_o \exp(-\beta z) \qquad (2)$$

with $k_o = a\phi_o^m$ and $\beta = bm$. The values of ϕ_o, m, b and a are determined empirically from log and core data where available (Mudford and Best, 1989; England et al., 1987).

What do shale permeability measurements carried out by the GSC tell us about the permeability/depth relationship? Predicted permeabilities (Mudford and Best, 1989) are compared with measured values (Katsube and Coyner, 1994) in Figure 4. The data points for the measured permeabilities are corrected for their in situ depth, using plots similar to those in Figure 2. Whereas these measured permeabilities are in the range (10^{-21}–$10^{-20}m^2$) required to generate the present day overpressures observed in the Venture gas field (Mudford, 1988; Mudford and Best, 1989), they are generally larger than the corresponding empirical values (solid line). Why is this? According to the "critical depth of burial" (CDB) concept (Katsube and Williamson, 1994), permeabilities and porosities which were 10^{-14}–$10^{-11}m^2$ and 70–80% at the ocean floor decrease continuously with depth, approaching values of $10^{-21}m^2$ and 5%, respectively, at the CDB (2.5–3.5 km depth). At depths greater than the CDB, permeability and porosity decrease at a reduced rate or may even show a slight increase with depth (Figs. 4, 5). The permeability and porosity changes are due mainly to mechanical compaction at depths less than the CDB, and mainly to diagenesis at greater depths. In addition, many of these measurements are on shale samples from overpressured areas, which appear to increase the permeability and porosity values. Indeed, if the measured rather than the empirically determined permeability values were used to model the pore pressure history for the Venture area, the model pressures would be lower. Therefore, it is necessary to consider these and other factors when predicting permeabilities.

PERMEABILITY AND ITS RELATION TO PORE-SIZE

Why are compacted shale permeabilities so low? Pore-size distribution analysis obtained using mercury porosimetry (Katsube et al., 1991) indicates that tight Venture shales have a unimodal distribution of extremely small pores which are mainly concentrated

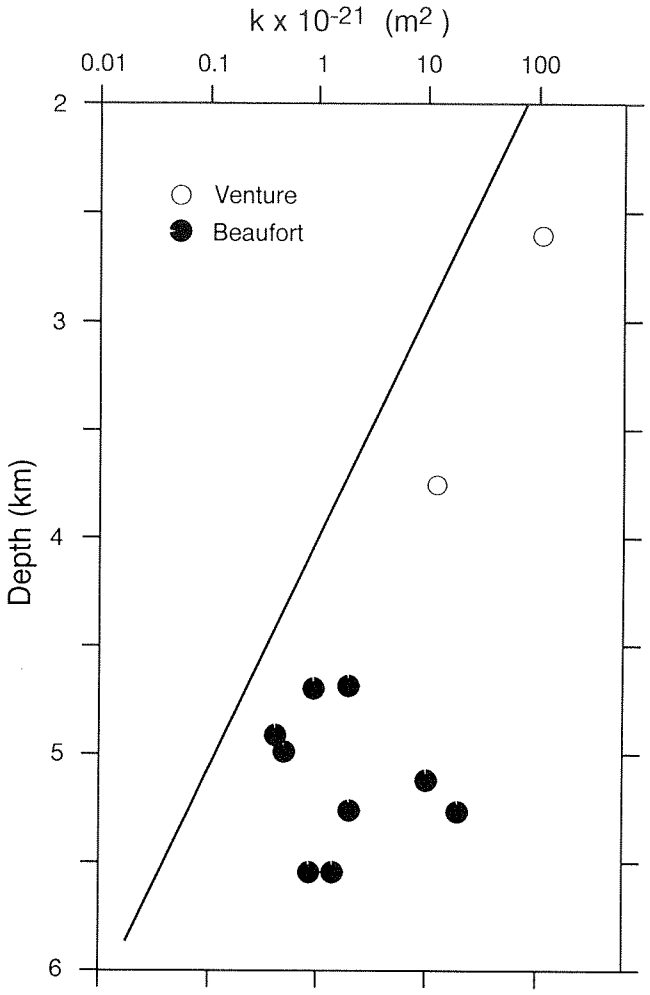

Figure 4. *Graph of permeability versus depth for samples from the Venture Field and the Beaufort–Mackenzie Basin. The permeabilites were obtained from curves similar to those in Figure 2 where the effective pressure that was used is equal to the in situ value. The straight line is from the empirical equation described in Mudford and Best (1989) with* $m = 8$, $b = 0.00028\ m^{-1}$, $\phi_o = 0.46$ *and* $a = 4 \times 10^{-15} m^2$ ($k_o = 8.02 \times 10^{-18} m^2$, $\beta = 0.00224\ m^{-1}$).

in the 0.3–60 nm size range (Fig. 6); values representing some of the smallest known pore-sizes for rocks. The modes (3–12 nm) of these distributions appear to represent the pore-sizes of the main fluid-flow paths of these shales, thus providing a qualitative explanation for the observed low permeabilities. Continuing studies suggest that it may be possible to obtain a more quantitative explanation for low shale permeabilities.

Shales generally display a unimodal pore-size distribution with modes and porosities decreasing with depth (Fig. 5) (Katsube and Best, 1992). Sedimentation rates and overpressure conditions also affect the pore-size distributions (Issler and Katsube, 1994; Katsube and Issler, 1993).

What does the measurement of pore-size distributions tell us about shale properties? Light hydrocarbon molecules such as methane, ethane, butane and propane have C-C bond lengths around 1.5 Angstroms (0.15 nm) and C-H bond lengths around 0.11 nm, with corresponding molecular dimensions in the 0.1 to 0.5 nm range. How do these and larger molecules, with dimensions not much different than the measured mean pore-sizes, move within a shale? These measurements have forced us to ask these fundamental questions and to re-examine the basis of fluid movement and expulsion in shales.

MAPPING POROSITY WITH SONIC LOGS

Sonic log transit-time measurements, calibrated using shale core porosity data, have been used to map shale compaction trends in Upper Cretaceous-Tertiary strata of the Beaufort-Mackenzie Basin (Issler, 1992). The equation (first proposed by Chapman, 1981),

$$\phi = 1-(\Delta t_{ma}/\Delta t)^{1/x} \qquad (3)$$

where Δt is the mean sonic transit-time from well logs ($\mu s/m$), Δt_{ma} is the shale matrix transit-time (220 $\mu s/m$) and x is the acoustic formation-factor exponent (2.19), was used to convert sonic transit-time values to porosity. Five compaction zones were defined on the basis of porosity-depth trends, and thickness changes in Pliocene-Pleistocene strata. Shale porosity-depth trends are strongly correlated with Pliocene–Pleistocene sedimentation rates, overpressure and the magnitude of erosion.

Figure 7a shows a plot of mean sonic transit-time versus depth for shales from a representative well (Nerlerk M-98) in compaction zone 1 of the Beaufort–Mackenzie Basin. Compaction zone 1 is characterized by high Pliocene–Pleistocene sedimentation rates (>380 m/m.y.) and highly undercompacted, overpressured shales. Superimposed on this plot are pore pressure data (drillstem test data) from nearby wells in zone 1. The top of overpressure (approx. 1.2 km) can be estimated by comparing the sonic trends in zone 1 with sonic data from normally compacted, hydrostatically pressured shales (zone 3). Although fluid pressures below 1.2 km are greater than hydrostatic, the major increase in pore pressure coincides with an abrupt increase in sonic transit-time

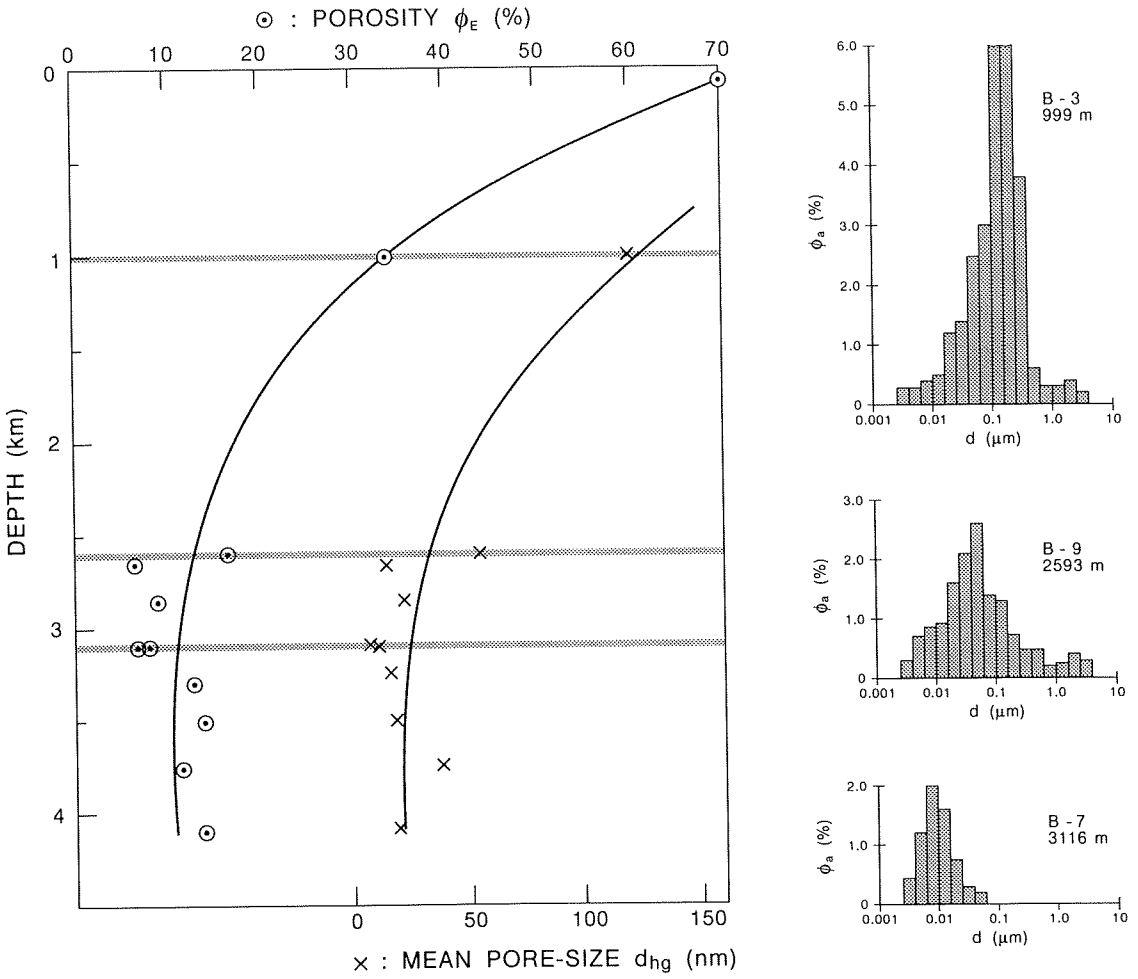

Figure 5. *Pore structure change with depth for shale samples from the Beaufort-Mackenzie Basin (Katsube and Best, 1992) showing effective porosity ϕ_E and mean pore-size (x) decreasing and pore-size distribution changing with increasing depth. The thicker horizontal lines (left-hand side) indicate sample locations for pore-size distributions displayed on the right. The partial porosity, ϕ_a, is the contribution of each pore-size to the total effective porosity.*

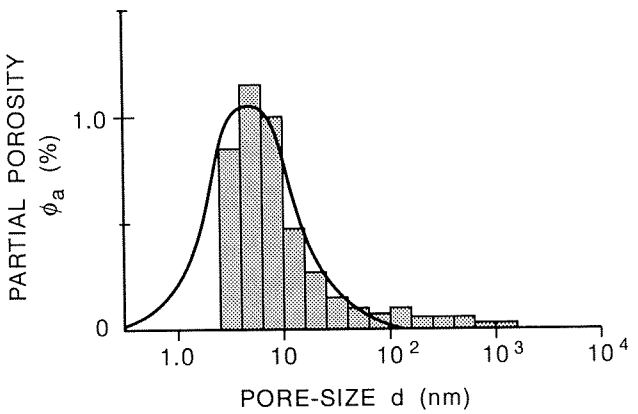

Figure 6. *Typical example of the pore-size distribution of a tight shale (Katsube, 1992). The sum of partial porosity (ϕ_a) values equals the effective porosity of the sample.*

near the base of the Pliocene–Pleistocene Iperk sequence at approximately 2.8 km (Fig. 7a).

A simple effective pressure model (Fig. 7b) was used to calculate pore pressure (P_f) variation with depth for compaction zone 1. Although the model underestimates the deeper pressure data by 10 to 15%, it reproduces the major pressure trends, which is encouraging, given the uncertainties in the underlying assumptions. Effective pressure [$P_e(\phi)$] was estimated as a function of porosity using the normal shale compaction curve of zone 3. The total overburden pressure (P_o) was calculated using compaction curves from zone 1 and assumed sediment grain densities. These results support the concept that disequilibrium compaction is the major mechanism controlling overpressure in this region.

SUMMARY AND OUTLOOK

The processes that form a basin over geological time determine the present day distribution of porosity, permeability and fluids within that basin. During the past few years, industry has begun to appreciate the role that shales play in these processes and the importance of shales in the generation, migration and entrapment of hydrocarbons. In the past, shales have largely been ignored because they had little economic interest.

Shale permeability is a controlling factor in fluid migration and entrapment and in overpressure development. The Geological Survey of Canada recognizes the importance of shales and has put a program in place to study the petrophysical properties

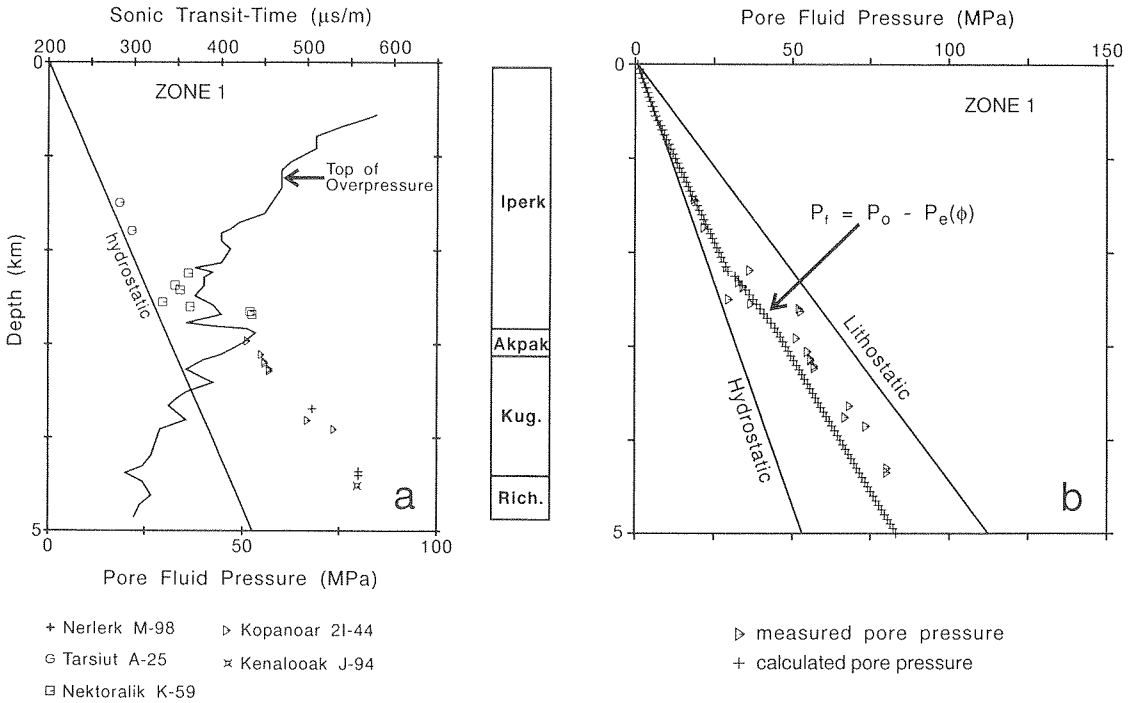

Figure 7. *(a) Shale sonic transit-time and pore pressure versus depth for compaction zone 1 of the Beaufort-Mackenzie Basin. The solid curve shows shale sonic transit-time variation with depth for a representative well (Nerlerk M-98) from zone 1. The stratigraphic column to the right shows the major Tertiary sedimentary sequences at the Nerlerk M-98 well location. Pressure data are from drillstem tests taken in nearby wells within zone 1. (b) A comparison of calculated and observed pore pressure (P_f) versus depth for compaction zone 1 of the Beaufort-Mackenzie Basin. $P_e(\phi)$–effective pressure as a function of porosity; P_o–total overburden pressure.*

of shales and to understand the relationships between these properties. These studies include the effects of burial and diagenesis on the petrophysical characteristics. More research is needed to characterize shales and to understand the quantitative effects they have on basin processes. The present research effort, though very limited, is a step along this path.

REFERENCES

Best, M.E. and Katsube, T.J.
1993. Possible effects of overpressure on shale permeability. Society of Exploration Geophysicists, Expanded Abstract, 63rd Annual Meeting, Washington, p. 1237–1240.

Best, M.E. and Katsube, T.J.
1995: Shale permeability and its significance in hydrocarbon exploration. The Leading Edge, Feb., Society of Exploration Geophysicists.

Chapman, R.E.
1981: Geology and Water - An Introduction to Fluid Mechanics for Geologists. Martinus Nijhof/Dr. W. Junk, The Hague, 228 p.

England, W., Mackenzie, W., Mann, D., and Quigley, T.
1987: The movement and entrapment of petroleum fluids in the subsurface. Journal of the Geological Society, London, v. 144, p. 327–347.

Issler, D.R.
1992: A new approach to shale compaction and stratigraphic restoration, Beaufort-Mackenzie Basin and Mackenzie Corridor, northern Canada. American Association of Petroleum Geologists Bulletin, no. 76, 1170–1189.

Issler, D.R. and Katsube, T.J.
1994: Effective porosity of shale samples from the Beaufort-Mackenzie Basin and Mackenzie Corridor, Northern Canada. *In* Current Research, Part B. Geological Survey of Canada, Paper 94–1B, p. 19–26.

Katsube, T.J.
1992: Statistical analysis of pore-size distribution data of tight shales from the Scotian Shelf. *In* Current Research, Part E. Geological Survey of Canada, Paper 92–1E, p. 365–372.

Katsube, T.J. and Best, M.E.
1992: Pore structure of shales from the Beaufort–Mackenzie Basin, Northwest Territories. *In* Current Research, Part E. Geological Survey of Canada, Paper 92–1E, p. 157–162.

Katsube, T.J., Best, M.E., and Mudford, B.S.
1991: Petrophysical characteristics of shales from the Scotian Shelf. Geophysics, v. 56, p. 1681–1689.

Katsube, T.J. and Coyner, K.
1994: Determination of permeability(k)-compaction relationship from interpretation of k-stress data for shales from eastern and northern Canada. *In* Current Research, Part D. Geological Survey of Canada, Paper 94–1D, p. 169–177.

Katsube, T.J. and Issler, D.R.
1993: Pore-size distributions of shales from the Beaufort-Mackenzie Basin, northern Canada. *In* Current Research, Part E. Geological Survey of Canada, Paper 93–1E, p. 123–132.

Katsube, T.J. and Williamson, M.A.
1994: Shale petrophysics and basin charge modelling. *In* Current Research, Part D. Geological Survey of Canada, Paper 94–1D, p. 179–188.

Mudford, B.S.
1988: Modelling the occurrence of overpressure on the Scotian Shelf, offshore eastern Canada. Journal of Geophysical Research, v. 93, p. 7845–7855.

Mudford, B.S. and Best, M.E.
1989: Venture Gas Field, Offshore Nova Scotia: a case study of overpressuring in region of low sedimentation rate. American Association of Petroleum Geologists Bulletin, v. 73, p. 1383–1396.

Williamson, M.A.
1992: The subsidence, compaction, thermal and maturation history of the Egret Member source rock, Jeanne d'Arc Basin, offshore Newfoundland. Bulletin of Canadian Petroleum Geology, v. 40, p. 136–150.

Williamson, M.A. and Smyth, C.
1992: Timing of gas and overpressure generation in the Sable Basin offshore Nova Scotia. Bulletin of Canadian Petroleum Geology, v. 40, p. 151–169.

FLYING FOAM STRUCTURE, JEANNE D'ARC BASIN, GRAND BANKS OF NEWFOUNDLAND

K.C. Coflin

Atlantic Geoscience Centre, P.O. Box 1006, Dartmouth, Nova Scotia B2Y 4A2

On the western edge of the Jeanne d'Arc Basin, in Jurassic and Cretaceous sediments, is a large anticlinal feature known as the Flying Foam structure or anticline. As imaged on reflection seismic data, the Flying Foam structure is an excellent example of a feature resulting from a synthetic overlapping transfer zone and concomitant fault movement over a stepping detachment.

The Jeanne d'Arc Basin is one of a number of Mesozoic basins separated by Paleozoic highs on the Grand Banks of Newfoundland. This basin has been extensively studied by industrial organizations because of its proven hydrocarbon resource. The Geological Survey of Canada and LITHOPROBE have also collected data in the basin with the aim to place it in the larger tectonic setting (Enachescu, 1987; Keen et al., 1987; Tankard and Weisink, 1987; Edwards, 1990; Grant and McAlpine, 1990).

It is generally agreed that the Jeanne d'Arc Basin opened during three distinct periods of rifting, producing the broad "V" shaped basin. The first stage of rifting occurred in the Late Triassic to Early Jurassic creating an evaporatic basin resulting in the deposition of thick salt units (Osprey and Argo formations). These salt units have had a significant impact on the development of the basin, creating several large diapiric features which have been the focus of exploration interest. The second phase of rifting occurred in the Early Cretaceous with the resulting depocenter being filled with thick clastic units. These sediments contain the traps for the basin's oil and gas accumulations including the giant Hibernia oilfield. The final stage of rifting occurred during Aptian–Albian time. From this final stage to the present, thermal subsidence has been taking place, deepening the basin. At present there are over 20 km of syn- and postrift sediments deposited in the depocenter of the Jeanne d'Arc Basin.

Along the western margin of the basin north of Hibernia field, the Flying Foam structure (Fig. 1) is imaged on a dense network of reflection seismic data. An example of one of these profiles is show in Figure 2. The Flying Foam structure was formed during the last

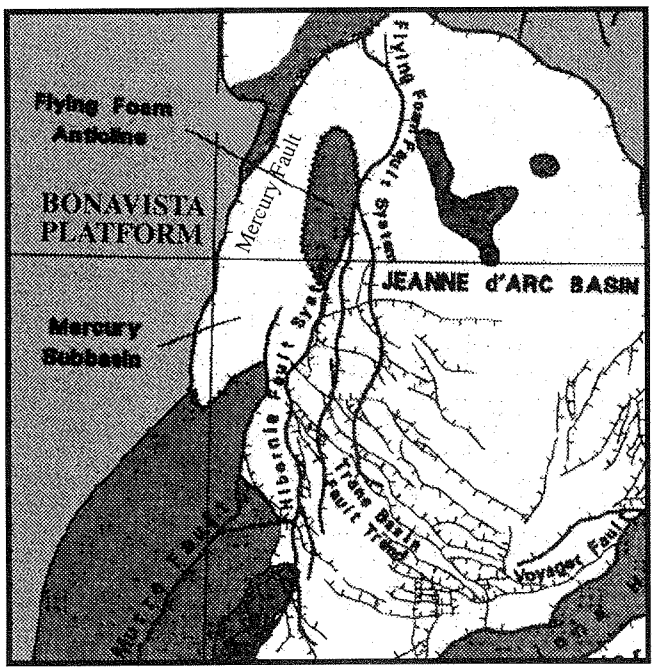

Figure 1. *Generalized fault map for part of the western edge of the Jeanne d'Arc Basin.*

stage of rifting on the Grand Banks. This structure consists of rotated Paleozoic basement, Jurassic and Early Cretaceous sediments. There is obvious growth faulting during Aptian–Albian time producing a basin (Mercury Subbasin, Fig. 1), with greater than 4 km of sedimentary fill on its western edge. The culmination of the structure was eroded during the final stages of rotation, exposing Jurassic rocks. The structure has a strike length of over 50 km.

The key to understanding the structure is the relationship between the major faults in the area. Figure 3 shows that two faults, the Flying Foam and the Mercury, bracket the structure. The northern extent of the structure is closely related to the disappearance of the Flying Foam Fault. The proposed location of a transfer fault between the Murre and Mercury faults defines the southern end. The Murre and Mercury faults are inferred to be basin bounding faults (Enachescu, 1987).

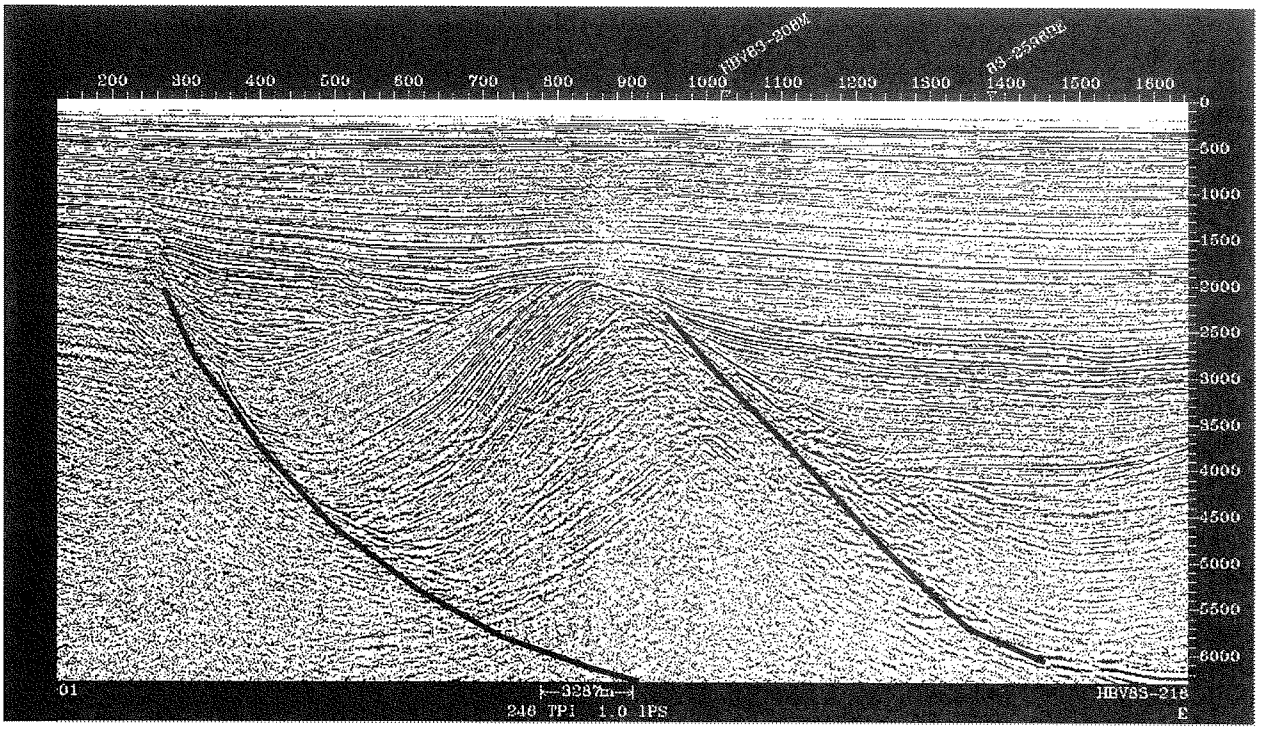

Figure 2. *Example seismic line crossing the Flying Foam Anticline. The Mercury and Flying Foam faults are identified. The west dipping reflections between shot points 300 and 900, below 2500 ms define the western limb of the anticline. Examination of these reflections show that shallower events are syn-rotational while the deeper ones were deposited before deformation.*

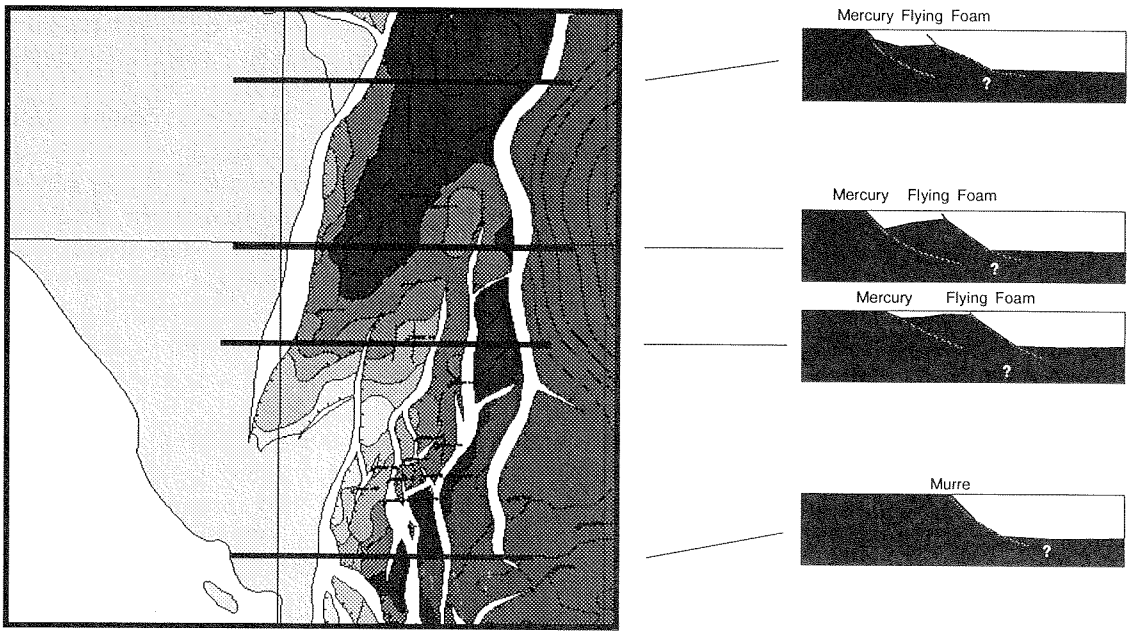

Figure 3. *Simplified structure map for a near base Cretaceous event (the colours become darker with increased depth). The four schematic sections show the relationships of the major faults along the strike of the feature.*

Prior to Aptian–Albian time the location of the basin bounding fault was near the present location of the Flying Foam Fault (Enachescu, 1987). West of this older basin bounding fault there was a relatively minor paleo-Mercury Fault. Between the basin bounding fault and the early Mercury Fault was an area of minor fault rotation. This displacement is demonstrated by thin Early Cretaceous and Jurassic rocks occurring between the faults. In pre-Aptian/Albian time, this area could be characterized as being a step up from the deep basin onto a minor platform, at the present location of the Mercury Subbasin, and then up to the Bonavista Platform.

At the southern end of the Flying Foam Structure is the junction of the Murre, Flying Foam and Mercury faults. A problem posed during mapping of the basin is the relationship between these faults. The Murre Fault can be projected into a major crustal listric reflection that has been imaged on 20 s reflection seismic profiles crossing the basin (Keen et al., 1987). A similar nature had been implied for the Mercury Fault. Tankard and Weisink (1987) interpreted the existence of a transfer or tear fault connecting the two present bounding faults. Enachescu (1987) did not identify a tear fault and more detailed mapping by Edwards (1990) also failed to find such a fault but instead showed the Mercury Fault losing displacement to the south, with the Flying Foam Fault losing displacement to the north and merging into the Murre Fault to the south near Hibernia oilfield.

The question arises therefore: how was the displacement on the Mercury Fault transferred to the Murre Fault? The data are interpreted as showing that most of the displacement on the old basin bounding fault was transferred to the Mercury Fault during the latest period of rifting by the stepping back toward the Bonavista Platform. The geometry of the Mercury Fault beneath the Mercury Subbasin caused at least part of the anticlinal nature of the Flying Foam structure. As the Cretaceous sediments were displaced toward the basin, space considerations rotated them to their present location. It is possible that the structure was later amplified by salt movement.

The displacement on the Mercury Fault was transferred to the Murre Fault in a synthetic overlapping transfer zone near the southern end of the Flying Foam structure producing a fault pattern similar to Figure 4 (Morely et al., 1990). This type of displacement does not require a tear or connecting fault but instead has the displacement take place at depth. This interpretation places the Hibernia field at the position of the transfer which may have also been the site of a transfer zone pre-Aptian–Albian.

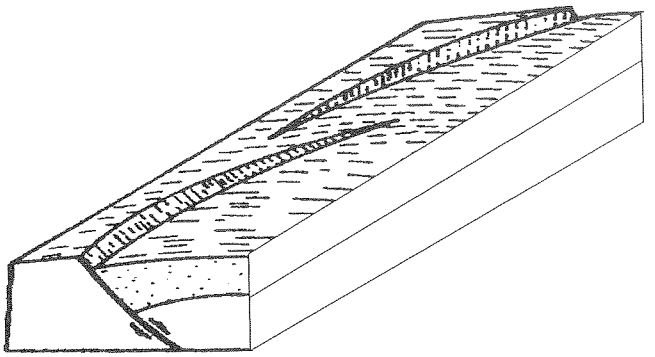

Figure 4. *Schematic isometric diagram showing a idealized overlapping transfer zone (modified from Morley et al., 1990). The two faults in this case would be the Murre and Mercury.*

REFERENCES

Edwards, A.
1990: The western margin of the Jeanne d'Arc Basin offshore Newfoundland (Eastern Canada). *In* The Potential of Deep Seismic Profiling for Hydrocarbon Exploration, B. Pinot and C. Bois (eds.), p. 161–173.

Enachescu, M.E.
1987: Tectonic and structural framework of the northeast Newfoundland continental margin. *In* Sedimentary Basins and Basin Forming Mechanisms, C. Beaumont and A. Tankard (eds.). Canadian Society of Petroleum Geologists, Memoir 12, p. 117–146.

Grant, A.C. and McAlpine K.D.
1990: The continental margin around Newfoundland: Chapter 6. *In* Geology of the Continental Margin of Eastern Canada, M.J. Keen and G.L. Williams (eds.). Geological Survey of Canada, Geology of Canada, no. 2, p. 239–292.

Keen, C.E., Boutilier, R., de Voogd, B., Mudford, B., and Enachescu, M.E.
1987: Crustal geometry and extensional models for the Grand Banks, eastern Canada: constraints from deep seismic reflection data. *In* Sedimentary Basins and Basin Forming Mechanisms, C. Beaumont and A. Tankard (eds.). Canadian Society of Petroleum Geologists, Memoir 12, p. 101–115.

Morely, C.K., Nelson, R.A., Patton T.L., and Munn, S.G.
1990: Transfer zones in the East African Rift system and their relevance to hydrocarbon exploration in rifts. American Association of Petroleum Geologists Bulletin, v. 74, no. 8, p. 1234–1253.

Tankard, A.J. and Welsink, H.J.
1988: Extensional tectonics, structural styles and stratigraphy of Mesozoic Grand Banks of Newfoundland. *In* Triassic-Jurassic rifting; Amsterdam, W. Manspeizer (ed.), Elsevier, p. 129–156.

MEASUREMENT AND ANALYSIS OF PERMEABILITY TRANSITIONS: MARINE CLAYS TO SHALES

K. Desroches

Department of Earth Sciences, Dalhousie University, Halifax, Nova Scotia B3H 3J5

K. Moran

Atlantic Geoscience Centre, P.O. Box 1006, Dartmouth, Nova Scotia B2Y 4A2

M.A. Williamson and T.J. Katsube

Geological Survey of Canada, 601 Booth Street, Ottawa, Ontario K1A 0E8

BACKGROUND

An understanding of the characteristic permeability of sedimentary formations is necessary for many applications, including those in hydrogeology, geotechnical engineering, engineering geology and petroleum geology. Since Terzaghi (1943) first presented his theory of one-dimensional consolidation, it has been known that permeability is the primary control on the rate of gravitational compaction; thus, this parameter is also a key component in sedimentary basin evolution. Results of basin modelling suggest that the consolidation processes of clays and clay shales are crucial to the study of sealing efficiencies and migration pathways of hydrocarbon-bearing fluids. Permeability is also an important control on the timing and nature of primary fluid migration in shale source rocks (Williamson, 1992). Although permeability is important to all of these studies, it is the sediment and rock property that is least known. With increasing interest in developing reservoirs within clay shales, it is essential to better characterize the permeability of these sedimentary systems.

In the field of geotechnical engineering, permeability is a critical parameter for all design problems associated with clay foundations. Because of this, a large data base of clay permeabilities has developed. In addition, test methods specific to fine-grained materials have been developed. The results of these tests show a consistent log-linear relationship between clay permeability, in terms of hydraulic conductivity, and porosity (e.g., Silva et al., 1981) where the slope of the relationship varies with clay mineral type.

In comparison, due in part to the difficulty in measuring, the permeability of low porosity sediments consists of a much smaller data base. The geotechnical-type tests (low pressure) cover a wide, but high range of porosity (50–95%); while test results (high pressure) from clay shales are from a smaller range of very low porosity (<20%). This study is designed to bridge the gap between these two disparate data sets so that the larger geotechnical data base can be applied to clay shales in hydrocarbon systems. Two clay-rich samples from the Scotian Shelf have been split to provide material for high and low pressure permeability testing. The combined results provide a more comprehensive relationship between compaction-driven porosity and permeability.

PROCEDURE

Two samples were split to provide sediment for both low gradient/low pressure and high gradient/high pressure analyses. High pressure measurements were made using the transient pressure method of Brace et al. (1968) to determine permeability in the low porosity range. In this method, a fluid reservoir is pressurized at each end of the sample and the entire system is placed under a confining pressure. The fluid pressure in one reservoir is reduced by a small amount, resulting in the imposition of a pressure gradient across the sample. This gradient induces flow through the sample, from which the permeability is derived.

Permeability of high porosity fine-grained sediment cannot be measured using high gradient methods because the relationship between flow rate and hydraulic gradient is nonlinear under these conditions (Silva et al., 1981). The nonlinearity is likely due to

disruption of the clay fabric induced by the pressure gradient. Consequently, low gradient tests were performed on the samples to determine permeability in the high porosity range.

Low gradient measurements were performed using a back-pressured consolidometer, equipped with a multi-speed low flow pump permeameter. The advantage of this arrangement is that the constant back pressure maintains a fully saturated sample throughout the experiment. The flow pump technique allows permeability measurements to be made more quickly and at lower fluid gradients than with conventional falling- and constant-head methods. The design and operation of the flow pump system is described by Olsen et al. (1988) and the operation of the back-pressured oedometer by Silva et al. (1981).

RESULTS

Low gradient tests follow Darcy's Law, providing good quality test results. An example of this behaviour is shown for Sample 88010-002 (Fig. 1). The slope of this curve defines the hydraulic conductivity (K) or Darcy's coefficient of permeability, defined as follows:

$$v = Ki \qquad \text{Equation 1}$$

where v is the fluid flow velocity and i is the pressure gradient. Hydraulic conductivity is dependent on both the intrinsic permeability (k) of the sediment and the properties of the fluid in the sediment. Hydraulic conductivity is converted to intrinsic permeability (k) as follows:

$$k = K\mu/\rho g \qquad \text{Equation 2}$$

where μ is fluid viscosity, ρ is fluid density, and g is gravitational acceleration.

Low gradient flow tests were run on both samples under four porosities. Different porosities were achieved by consolidating the samples to incrementally higher effective stresses. Permeability results are plotted as a function of porosity (Fig. 2). Low gradient results (solid dots) show a consistent log-linear trend. Preliminary results for one duplicate sample tested under high gradients follows the log-linear porosity/ permeability function for sample 88010-02 (Fig. 3) with a slightly different slope.

SUMMARY

This preliminary comparison of high pressure permeability tests with low pressure, low gradient tests shows promise. Additional, future test results will provide improved correlation and, perhaps, a comprehensive relationship for fine-grained sediment over a full range of porosity, from clays to shales.

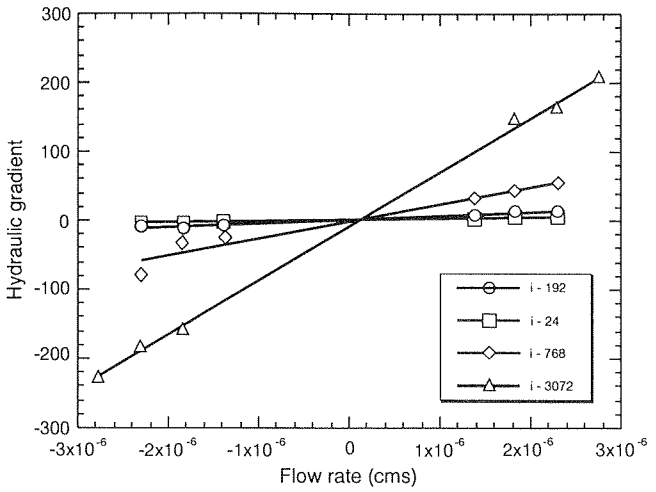

Figure 1. *Results of low gradient permeability tests for sample 88010-02. Each symbol represents a series of flow measurements at a different effective stress, labelled in the key, in units of kPa.*

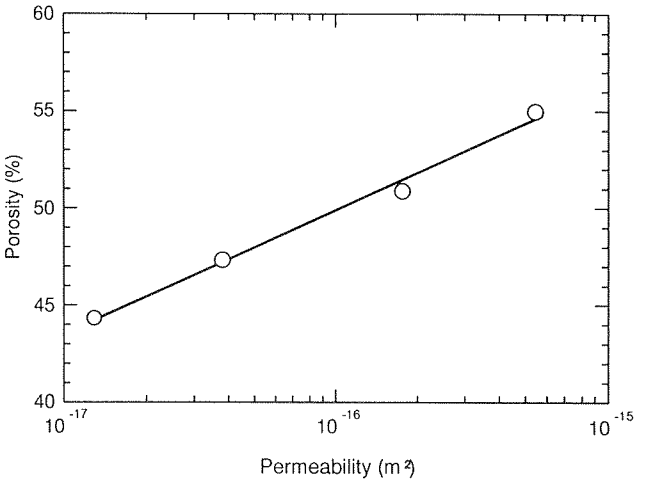

Figure 2. *Porosity plotted against permeability for sample 88010-02 tested under low gradient conditions. The relationship is log-linear.*

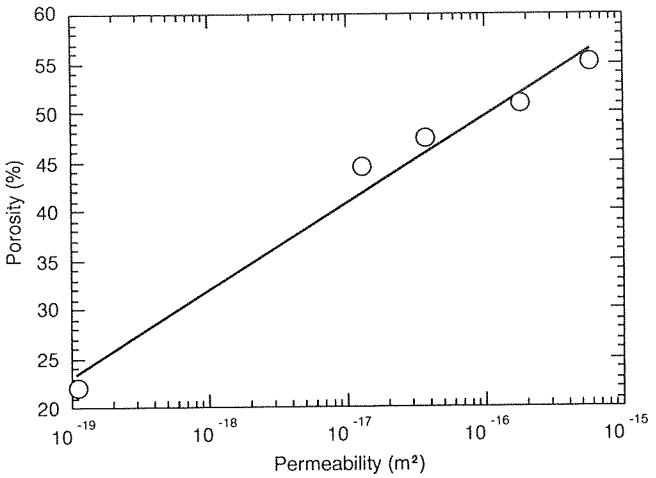

Figure 3. *Porosity plotted against permeability for sample 88010-02. The higher permeability measurements (>10-17) are low gradient results and the low permeability measurement is from high gradient/high pressure tests. The relationship is log-linear, similar to Figure 2, but has a slightly higher slope.*

REFERENCES

Brace, W.F., Walsh, J.B., and Frangos, W.T.
1968: Permeability of granite under high pressures. Journal of Geophysical Research, v. 73, p. 2225–2236.

Olsen, H.W., Morin, R.H., and Nichols, R.W.
1988: Flow Pump Applications. *In* Triaxial Testing, Advanced Testing of Soil and Rock, ASTM STP 977, R.T. Donaghe, R.C. Chaney, and M.L. Silver (eds.). American Society for Testing and Materials, Philadelphia, p. 68–81.

Silva, A.J., Hetherman, J.R., and Calnan, D.I.
1981: Low-gradient permeability testing of fine-grained marine sediments. *In* Permeability and Groundwater Containment Transport, ASTM STP 746, T.O. Zimmie, C.O. Riggs (eds.). American Society for Testing and Materials, p. 121–136.

Tavenas, F., Leblond, P., Jean, P., and Leroueil, S.
1983: The permeability of natural soft clays. Part I: Methods of laboratory measurement. Canadian Geotechnical Journal, v. 20, p. 629–644.

Terzaghi, K.
1943: Theoretical Soil Mechanics. New York, John Wiley and Sons, 510 p.

Williamson, M.A.
1992: The subsidence, compaction, thermal and maturation history of the Egret Member source rock, Jeanne d'Arc Basin, offshore Newfoundland. Bulletin of Canadian Petroleum Geology, v. 40, no. 2, p. 136–150.

CENOZOIC BIOSTRATIGRAPHY AND PALEOECOLOGY OF THE JEANNE D'ARC BASIN, OFFSHORE EASTERN CANADA

R.A. Fensome, F.C. Thomas, and G.L. Williams

Atlantic Geoscience Centre, P.O. Box 1006, Dartmouth, Nova Scotia B2Y 4A2

The study involves amalgamation of micropaleontological and palynological data for wells in the Jeanne d'Arc Basin, offshore eastern Canada. The fossil groups involved are foraminifera, radiolaria, dinoflagellates and spores and pollen. This amalgamation will allow for refined age-dating and paleoecological analysis of the sediments, and thus input vital control data into hydrocarbon charge models. Detailed micropaleontological analyses are already available for several wells, and palynological analyses (involving dinoflagellates, spores and pollen) are underway at the time of writing. Hence, in this extended abstract, emphasis will be placed on micropaleontological results. As the project progresses the data will be analyzed using graphic correlation – incorporating all data in the same plots – and sequence stratigraphic techniques.

The Cenozoic sections of 16 wells in the Jeanne d'Arc Basin have been studied for foraminiferal content. Since this work is based on cuttings, reliance has been placed primarily on stratigraphic tops.

Types of benthic assemblages can be used to approximate paleodepths and tend to show a gradual shoaling from middle bathyal to neritic depths near the edges of the structure through the Tertiary, with deeper water facies in central sites. Faunal events (e.g. pyritization, appearance of agglutinated assemblages, radiolarian abundances) in some cases are traceable over large portions of the basin. Some of these phenomena may be related to seismic horizons and oceanographic events (i.e., changes in circulation) during the Tertiary. (Seismic lines in the basin show almost the whole Cenozoic to be composed of flat-lying, parallel and even traces. A few stronger reflectors appear to represent the seismic traces of these oceanographic events.)

Rapid clastic deposition of the so-called South Mara unit in the deeper parts of the basin (500-1000 m paleodepth) occurred during the Paleocene and earliest Eocene, somewhat diluting benthic foraminiferal faunas, but permitting widespread preservation of large, spherical to ovoid radiolarians.

Later in the Early Eocene, a more pelagic sedimentation regime produced a rich calcareous benthic foraminiferal assemblage in much of the basin. Toward the end of this interval and continuing through the Middle Eocene, the bottom was overlain by water poor in oxygen and calcite, and agglutinated "flysch-type" benthic faunas became established. Simultaneously, an incursion of warm surface waters from the south brought low-latitude keeled planktics to the area. During the Early and Middle Eocene, continuing erosion of a Mesozoic outcrop, probably in the western Bonavista Platform, continued to contribute Late Cretaceous foraminifera to the record. The Late Eocene saw a return to cooler surface waters and better oxygenation at depth resulted in re-establishment of largely calcareous benthic faunas. Continuing regional subsidence during the Paleogene kept the bottom environment in upper bathyal depths. Planktic assemblages in this interval contain some elements common in coeval Scotian Shelf strata and cooler indicators as seen in northern Grand Banks sites.

The regional Oligocene sea level drop and offlap, probably coupled with the Late Oligocene oxygen minimum resulted in a marked decline in benthic foraminiferal productivity, perhaps exacerbated by changes in sedimentary dynamism. The net sedimentation rate in the basin is reduced relative to the Eocene, and water depths probably remained in the upper bathyal range. In the Miocene, enough shoaling had occurred for a variety of outer neritic benthic assemblages to become established, their diversity probably reflecting local ecological variations (Fig. 1).

EPOCH		ZONATION	Sedimentary Events	Faunal Events	Oceanographic Events		Sea level and tectonic events
					Bottom Water	Surface Water	
MIOCENE	L	*Asterigerina gurichi*	Reduced net deposition (?erosion)	establishment of variety of benthic assemblages			water depths reduced to ?100-300 m
	M	*Spiroplectammina carinata*					
	E						
OLIGOCENE	L	*Turrilina alsatica*		local pyritization localized diminution of benthic faunas, near disappearance of planktics	?increase in currents (dynamision)		sea level drop, coastal offlap
	E					temperate conditions	
EOCENE	L	*Reticulophragmium amplectens* - *Limacina canadensis*	Reworked older Paleogene in some sites Reworked Cretaceous material in western sites pyritization South Mara Member deltaic turbidites sands	re-establishment of calcareous benthic fauna; cool and warm water planktics keeled planktics agglutinated benthic fauna calcareous benthic fauna, radiolarians dilution of benthics by deltaic sedimentation	bottom waters re-aerated	mix of warm and cool surface regions	water depths in mid-upper bathyal range 500-1000 m
	M	*Spiroplectammina spectabilis*			reduced O_2 "stagnation"	incursion of warm low-latitude waters	
	E	Megaspore sp. 1					
PALEOCENE	L	*Gavelinella beccariformis* - *Rzehakina epigona*					
	E						

Figure 1. *Chart showing synthesis of sedimentary, faunal, and oceanographic events as determined by micropaleonotological biostratigraphy in the Cenozoic of the Jeanne d'Arc Basin. Sea level and tectonic events are also shown.*

CAMBRO-ORDOVICIAN HYDROCARBON POTENTIAL OF ONSHORE AND NEARSHORE WESTERN NEWFOUNDLAND

A.P. Hamblin and M.G. Fowler

Geological Survey of Canada, 3303-33rd Street N.W., Calgary, Alberta T2L 2A7

D. Hawkins and I. Knight

Department of Mines and Energy, Government of Newfoundland and Labrador
P.O. Box 8700, St. John's, Newfoundland A1B 4J6

ABSTRACT

Hydrocarbon seeps throughout Lower Paleozoic rocks of western Newfoundland have been known since 1812, and sporadic exploration has proceeded for 125 years, including active exploration during the present drilling season. A brief review of the very complex tectonic and depositional history combined with recent geochemical studies provides understanding and encouragement that this "frontier" basin has significant potential.

A thick Late Proterozoic/Cambrian/Ordovician sedimentary succession includes shallow marine platformal clastic and carbonate facies and coeval deep marine mudstone-dominated facies, deposited on the Lower Paleozoic passive margin of North America. Taconian, Salinic and Acadian plate convergence and deformation telescoped, and juxtaposed, excellent source rocks with potential reservoir rocks in the onshore and nearshore area (Figs. 1–3).

This study integrates extensive new geochemical data from oils and organic-rich rocks with all previous geological and geochemical information to more effectively assess the hydrocarbon potential of the area. All samples of oils collected from old wells, organic-rich shales, and other bituminous rocks have similar geochemical characteristics (Fig. 4). Chemistry of the oils implies a pre-Devonian clastic source rock containing Type I/II organic matter of mostly algal (*Gloeocapsomorpha prisca*) origin. Widespread shales of the Cambro–Ordovician Green Point Formation, and probable equivalents, include excellent source rock intervals (TOC up to 10.35%, HI up to 759) and, through biomarker comparisons, are correlated directly to the oils obtained from seeps and wells. Tmax values range from 434 to 443, indicating the source rocks at surface are marginally mature to mature. Two maturity trends are evident in western Newfoundland: increasing maturity from the Port au Port area in the south to the Gros Morne area in the north, and increasing maturity from west to east across the Port au Port area.

Equally widespread, and partly coeval, Cambro–Ordovician dolomitized platform/shelf carbonates (now being tested) and deeper marine clastics and carbonates (previously-proven) offer abundant good potential reservoir facies. Complex structural deformation allows numerous possibilities for thrust repetition of source rocks, juxtaposition of source and reservoir rocks, abundant trap situations and significant hydrocarbon accumulations at depth.

This study is a timely demonstration that significant exploration opportunities exist in previously-ignored, but easily-accessible sedimentary basins of Canada.

CONCLUSIONS AND IMPLICATIONS FOR FUTURE EXPLORATION

1) Hydrocarbon exploration in western Newfoundland has a long history of successful, but sporadic, subsurface exploration from 1867 to 1965. Many of these wells, primarily in the Gros Morne and Port au Port areas, still seep oil today. Through recent land issuance cycles, exploration permits/leases are now held for many onshore and offshore areas.

2) Oils and bitumens from western Newfoundland show characteristics implying they have a similar source rock, probably a Lower Paleozoic clastic interval. Some material that occurs in Cambro–Ordovician sediments, described by previous workers as "bituminous", is inorganic.

3) Data from this and previous studies indicate that the Green Point Formation shales are the best

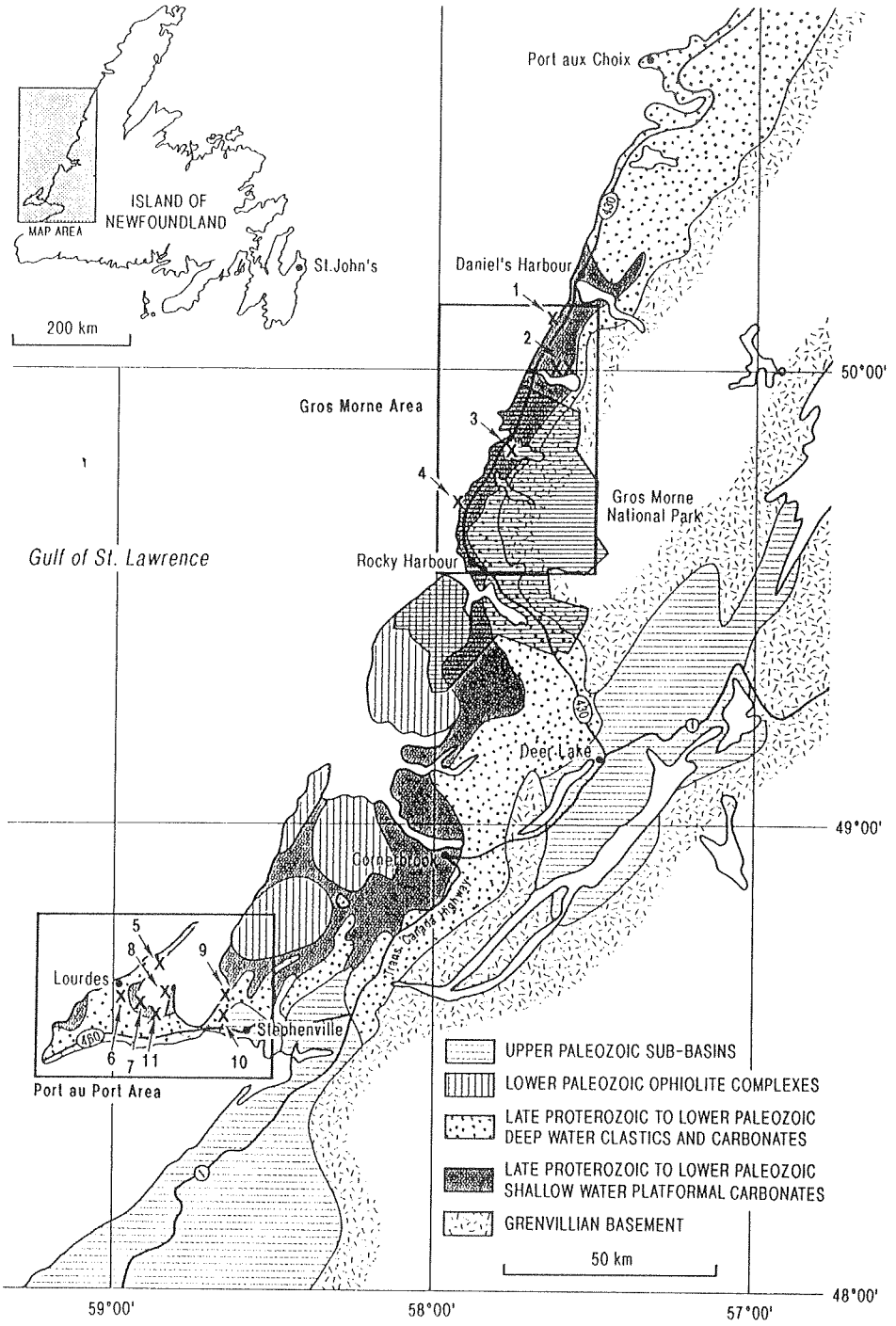

1 - ARCHES

2 - PARSON'S POND
oil smpls 757, 1317, 1582, 1587 to 1589
rock smpls 7780, 8022, 8023 Green Pt. Fm.

3 - ST.PAUL'S INLET
oil smpls 1328, 1580, 1581, 1583

4 - GREEN POINT
rock smpls 7775, 6502

5 - LONG POINT
rock smpls 7985 to 7988 Lourdes Fm.

6 - LOURDES QUARRY
rock smpls 6501, 8027 to 8029 Mainland Fm.

7 - WEST BAY
rock smpls 7984, 8024 to 8026 ?Green Pt. Fm.?

8 - SHOAL POINT
oil smpls 1444,1456

9 - TWO GUT POND
bitumen smpls 7981,7982

10 - TABLE MTN.
rock smpl 7990

11 - HINK'S QUARRY
bitumen smpls 6504,8030

Figure 1. *Generalized geology for the area of interest in this study and sample locations.*

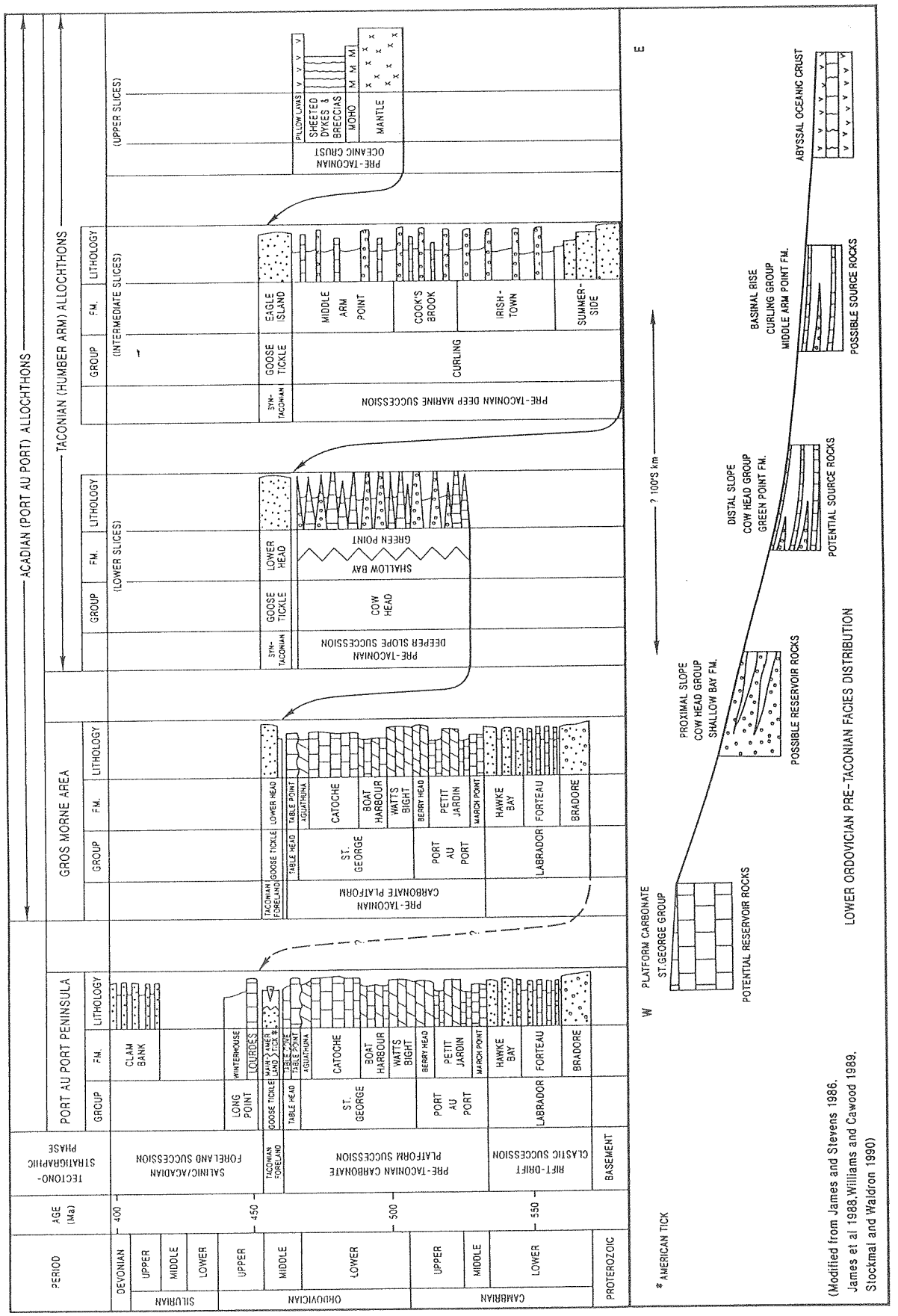

Figure 2. *Lower Paleozoic tectono-stratigraphic chart for western Newfoundland. Modified from the following workers: James and Stevens (1986), James et al. (1988), Williams and Cawood (1989), and Stockmal and Waldron (1990).*

Lower Paleozoic source rocks in western Newfoundland. Oil-source correlations indicate these shales are the major source of the western Newfoundland oils. Table Head Group sediments also have some potential to generate hydrocarbons and could feasibly contribute to some oils.

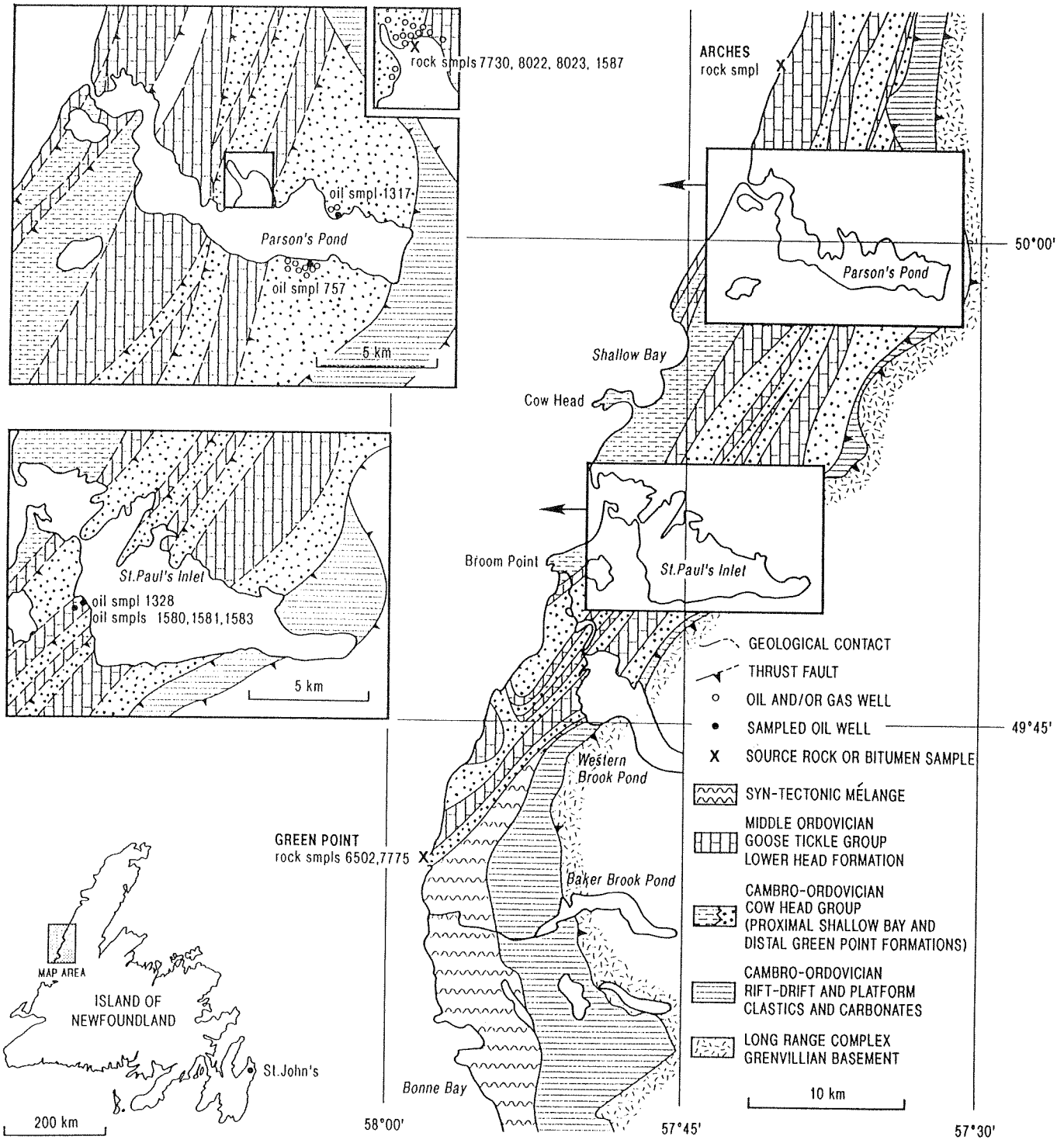

Figure 3. *Generalized lower Paleozoic geology, well and sample locations for the Gros Morne area. Modified from Williams and Cawood (1989), Government of Newfoundland and Labrador (1982), and Fleming (1970).*

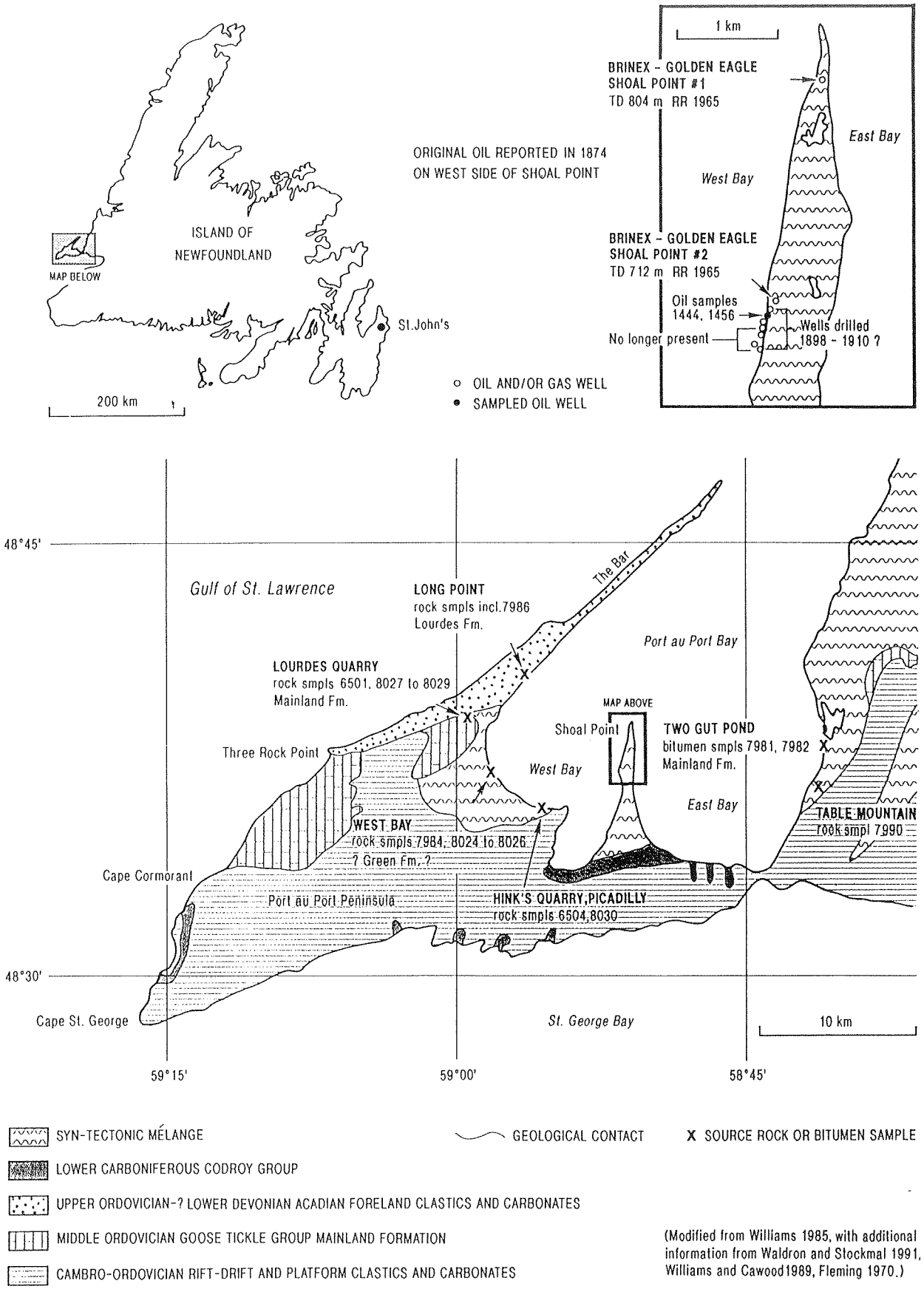

Figure 4. *Generalized lower Paleozoic geology, well and sample locations for the Port au Port area. Modified from Williams (1985) with additional information from Fleming (1970), Williams and Cawood (1989), and Waldron and Stockmal (1991).*

4) Two maturity trends are evident: a) increasing maturity from south to north, from Shoal Point to Parson's Pond; and b) increasing maturity from west to east across Port au Port Bay. Almost all samples studied here are thermally mature and fall within the "oil window". Several are marginally mature.

5) The occurrence of oil shows at Shoal Point and Two Gut Pond suggests that more mature equivalents of the (?)Green Point Formation shales that outcrop at West Bay occur in the subsurface across Port au Port Bay. Hence there is a possibility of significant hydrocarbon accumulations in the offshore part of Port au Port Bay, if suitable reservoirs, traps and seals are available.

REFERENCES

Fleming, J.M.,
1970: Petroleum exploration in Newfoundland and Labrador. Newfoundland Department of Mines, Agriculture and Resources, Mineral Resources Report, no. 3, 118 p.

Fowler, M.G., Hamblin, A.P., Hawkins, D., Stasiuk, L.D., and Knight, I.
1995: Petroleum geochemistry and hydrocarbon potential of Cambrian and Ordovician rocks of western Newfoundland. Bulletin of Canadian Petroleum Geology, v. 43 (June '95 issue).

Government of Newfoundland and Labrador
1982: Onshore/Offshore Western Newfoundland, Prospects for Petroleum. Petroleum Directorate, Special Report PD 82-1, 85 p.

1989: Hydrocarbon potential of the western Newfoundland onshore area. Department of Energy, 20 p.

James, N.P. and Stevens, R.K.
1986: Stratigraphy and correlation of the Cambro–Ordovician Cow Head Group, western Newfoundland. Geological Survey of Canada, Bulletin 366, 143 p.

Waldron, J.W.F. and Stockmal, G.S.
1991: Mid-Paleozoic thrusting at the Appalachian deformation front: Port au Port Peninsula, western Newfoundland. Canadian Journal of Earth Sciences, v. 28, p. 1992–2002.

Weaver, F.J. and Macko, S.A.
1988: Source rocks of Western Newfoundland. Organic Geochemistry, v. 13, 411–421.

Williams, H.
1984: Miogeoclines and suspect terranes of the Caledonian–Appalachian Orogen: tectonic patterns in the North Atlantic region. Canadian Journal of Earth Sciences, v. 21, p. 887–901.

PERMEABILITY PREDICTION USING A COMPUTER NEURAL NETWORK: APPLICATION IN THE VENTURE GAS FIELD, OFFSHORE NOVA SCOTIA

Z. Huang, J. Shimeld, and M. Williamson

Atlantic Geoscience Centre, P.O. Box 1006, Dartmouth, Nova Scotia B2Y 4A2

T.J. Katsube

Geological Survey of Canada, 601 Booth Street, Ottawa, Ontario K1A 0E8

BACKGROUND

Among the computer-based numerical techniques introduced during the last five years, the geological application of expert systems, computer neural networks (CNNs) and fuzzy set logic, which belong to the field broadly defined as artificial intelligence, has seen rapid development (e.g., Simann and Aminzadeh, 1989; Baldwin et al., 1990; Pulli and Dysart, 1990; Rogers et al., 1992; Wang, 1992; Osborne, 1992). This growth has been due to several distinct advantages over traditional statistical and deterministic approaches. Over the last year, we have applied the CNN approach to problems posed by the Hydrocarbon Charge Modelling Project carried out at the Atlantic Geoscience Centre (Williamson et al., 1993; Huang et al., 1994).

Computer neural networks (CNNs) are an information processing technique inspired by studies of the brain's nervous systems (Stephen, 1990). A CNN is "trained" with a series of examples (e.g., patterns and definitions). Information acquired from training is represented by a set of connection weights. The nature of neural network memory leads to efficient network responses (i.e., giving answers) when presented with previously unseen inputs. Advantages of a CNN approach over conventional approaches include less need of *a priori* information, the fact that a problem is modelled directly and in a more sophisticated way, and increased tolerance to noisy data.

One of the most popular types of CNN learning algorithms is known as back-propagation (BP-CNN) (Rumelhart et al., 1986), which takes a supervised training approach. A variation of BP-CNN, known as Quickprop (Fahlman, 1988), is used in our study. A BP-CNN always has an input layer containing several input elements, an output layer containing one or more output elements and at least one hidden layer which contains several processing elements (neurons) (Fig. 1). The elements of different layers are interconnected by weights, but there is no interconnection among elements in the same layer for a BP-CNN. Upon exposure to training examples, the network automatically adjusts the weights until a best generalization has been achieved. Information about relationships between all variables is represented by the final values of the connection weights. Once trained and tested, a BP-CNN can be used for solving problems that are similar in nature to those presented in the training stage.

PERMEABILITY PREDICTION IN THE VENTURE GAS FIELD, SABLE BASIN

Permeability is an important parameter in seal/reservoir characterization and basin modelling. However, the estimation of permeability in uncored wells or intervals is a difficult petrophysical problem as there is no direct

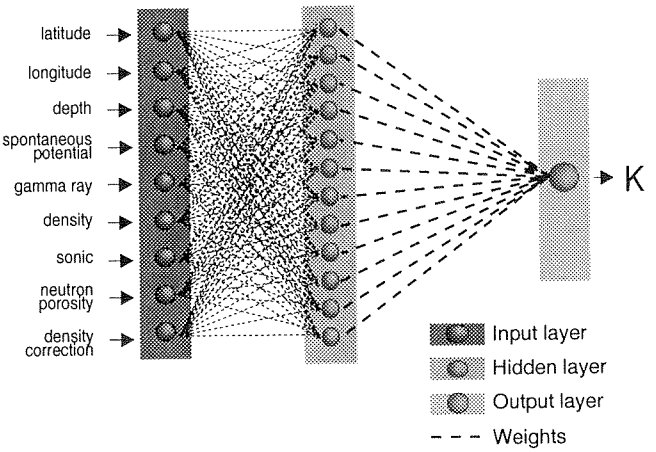

Figure 1. *The structure of the BP-CNN used for modelling.*

method of estimating permeability from well logs. For example, simple porosity–permeability relationships do not offer reliable permeability estimations in most cases since they are only directly applicable in unconsolidated sand and homogeneous rocks (Beard and Weyl, 1973; Bos, 1982).

The interrelationships between permeability, porosity, and other rock properties such as grain size, type and amount of cement etc., are very complex and area-specific. In general though, well log responses are functions of lithology, pore-fluid composition and porosity. Similarly, permeability is also a function of lithology and porosity. Therefore, with an adequate data set, correlations between permeability and several well log responses can be used to estimate permeability. For example, a predictive equation can be built from well logs and core measurements using multiple linear regression (MLR) to estimate permeability in uncored intervals (Wendt et al., 1986). However, the fundamental assumption of linear relationships among well logs and rock permeability may not be valid, and this limits the usefulness of this approach.

As an alternative to conventional methods, we use CNN techniques to model relationships among well logs and permeability in reservoir intervals of the Venture Gas Field in the Sable Subbasin (Grant et al., 1986), offshore eastern Canada. Our data are from five wells in this field (Venture B-13, Venture B-43, Venture B-52, Venture H-22 and Venture C-62). The permeability data set also includes a few measurements on low permeability shale published by Katsube et al. (1991). The well logs and measured permeability data were preprocessed to address such problems as shifts between recorded well log depths and sample depths, the difference in spatial resolution between well logs and core samples, uneven distribution of core measurements and so on.

Data from the first four wells were divided into CNN training and supervising data sets. Each example in the data set consists of permeability measurements with corresponding well log readings and spatial information. Data from Venture C-62 were retained as a totally independent data set to test the performance of the trained BP-CNN.

The network is given nine input values, from which it calculates one value (permeability) as the output. The number of nodes in the hidden layer was chosen after a series of trials with networks of different architecture. One network found to have a good generalization ability has 12 nodes in the hidden layer. For comparison, we built a predictive equation with the same training data set using the MLR approach (Davis, 1986).

The slope of the best-fit line, determined using the reduced matrix axis (RMA) method (Davis, 1986), on the cross-plot of the measured permeability and the BP-CNN predicted permeability of the supervising data set is 45.3° and the correlation coefficient is 0.8 (Fig. 2a). The slope of the RMA on the cross-plot of measured permeability and MLR equation predicted permeability of the supervising data set is 28° and the correlation coefficient is 0.65 (Fig. 2b). These results indicate that the predictive equation from MLR analysis is less successful than the trained BP-CNN.

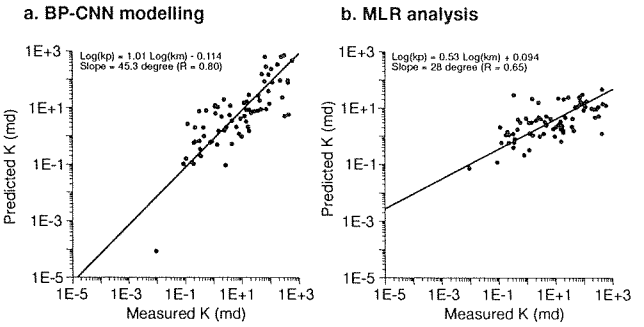

Figure 2. *Crossplot of measured permeability from CNN modelling (a), and from MLR analyses (b).*

The trained BP-CNN was applied to the independent Venture C-62 data set. Comparison between the calculated permeability profile and measured values in the reservoir interval (4788–5230 m) at this well is impressive, considering that the BP-CNN was trained with data sets that do not include any information from the C-62 well (Fig. 3).

Given the good performance of the trained BP-CNN, we calculated continuous permeability curves at the four Venture wells over the interval from 4400 m to 5800 m. With the aid of gamma ray logs, we correlated high permeability zones (sandstone and siltstone intervals) and low permeability zones (shale and limestone intervals) between the Venture wells. Correlation of the CNN-derived permeability curves reveals the relative importance of various seals in terms of their thickness, lateral continuity, and the predicted permeability. This detailed information on the distribution of low and high permeability zones within reservoir intervals can serve as a useful platform, in conjunction with pressure and flow test data, for

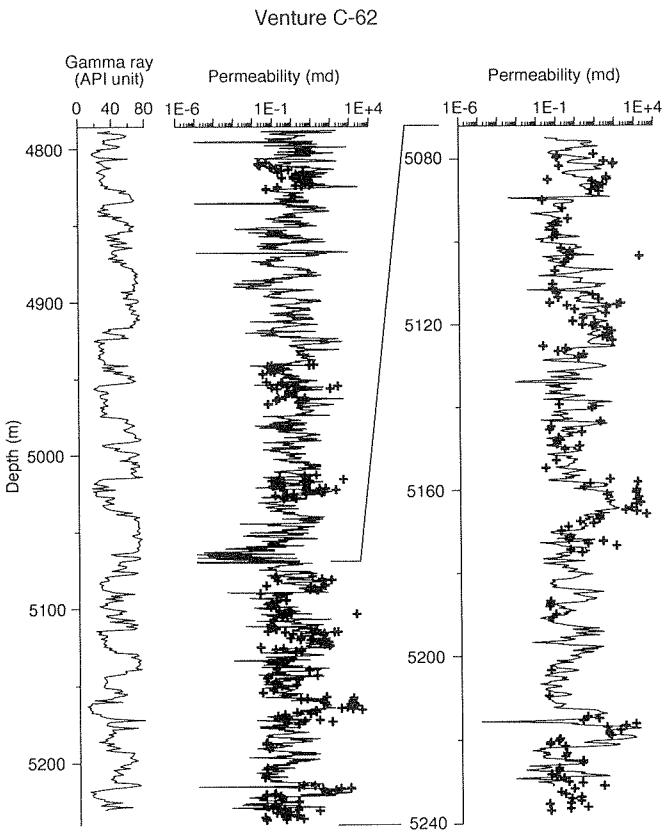

Figure 3. *Continuous predicted permeability (curve) and measured permeability values (crosses) at Venture C-62.*

analysis of producing zone potential and connectivity. The level of detail would not be possible if we had only used unevenly distributed permeability measurements (preferentially sampled from sandy intervals), or if we only had used one or two well logs indirectly related to permeability.

SUMMARY

Our work with a BP-CNN illustrates its usefulness in geologic applications. The example shows how further quantitative information can be extracted from old data sets. Further CNN studies include: (1) Experimentation with other CNN algorithms; (2) Use and calibration of the method with well data sets from the Western Canada Sedimentary Basin where permeability and core data are more readily available; and (3) Construction of a more comprehensive database to include as much information as possible for the Sable and other eastern Canada offshore basins to develop CNN models applicable for large areas.

REFERENCES

Baldwin, J.L., Otte, D.N., and Wheatley, C.
1990: Application of neural network to problem of mineral identification from well logs. The Log Analyst, v. 3, p. 279–293.

Beard, D.C. and Weyl, P.K.
1973: Influence of texture on porosity and permeability of unconsolidated sand. American Association of Petroleum Geologists Bulletin, v. 57, p. 349–369.

Bos, M.R.E.
1982: Prolific dry oil production from sands with water saturation in excess of 50%, a study of a dual porosity system. Paper BB in SPWLA Transactions.

Davis, J.C.
1986: Statistics and data analysis in geology. Second Edition, New York, John Wiley, 646 p.

Fahlman, S.E.
1988: Fast learning variations on back–propagation: an empirical study. *In* Proceedings 1988 connectionist models summer school, D.S. Touretzky, G. Hinton, and T. Sejnowski (eds.). Morgan Kaufmann Publishers, San Mateo, California, p. 38–51.

Grant, A., McAlpine, D., and Wade, J.
1986: The continental margin of eastern Canada—geological framework and petroleum potential. *In* Future petroleum provinces of the world. M.T. Halbouty (ed.). American Association of Petroleum Geologists Memoir 40, p. 177–205.

Huang, Z., Shimeld, J., and Williamson, M.A.
1993: Application of computer neural network and fuzzy set logic to petroleum geology, offshore eastern Canada. *In* Current Research, 1994–E. Geological Survey of Canada, p. 243–250.

Katsube, T.J., Mudford, B.S., and Best, M.E.
1991: Petrophysical characteristics of shales from the Scotian shelf. Geophysics, v. 56, p. 1681–1689.

Osborne, D.A.
1992: Neural networks provide more accurate reservoir permeability. Oil and Gas, September 28, p. 80–83.

Pulli, J.J. and Dysart, P.S.
1990: An experiment in the use of trained neural networks for regional seismic event classification. Geophysical Research Letters, v. 17, p. 977–980.

Rogers, S., Fang, J.H., Karr, C.L., and Stanley, D.A.
1992: Determination of lithology from well logs using a neural network. American Association of Petroleum Geologists Bulletin, v. 76, p. 731–739.

Rumelhart, D.E., Hinton, G.E., and Williams, R.J.
1986: Learning internal representations by error propagation. *In* Parallel distributed processing, v. 1 foundations, D.E. Rumelhart and J.L. McClelland (eds.). The MIT Press, Cambridge, Massachusetts, p. 318–362.

Simaan, M. and Aminzadeh, F. (eds.)
1989: Artificial intelligence and expert systems in petroleum exploration: advances in geophysical data processing, v. 3. JAI Press Inc., Greenwich, Connecticut.

Stephen, J.J.
1990: Neural network design and the complexity of learning. The MIT Press, Cambridge, Massachusetts, 150 p.

Wang, L.X.
1992: A Neural detector for seismic reflectivity sequences. IEEE Transaction on Neural Networks, v. 3, p. 338–340.

Wendt, W.A., Sakurai, S., and Nelson, P.H.
1986: Permeability prediction from well logs using multiple regression. *In* Reservoir Characterization, L.W. Lake and H.B. Carroll, Jr. (eds.). Academic Press, San Diego, California, p. 181–221.

Williamson, M.A., Katsube, T.J., Huang, Z., Fowler, M., McAlpine, K.D., Thomas, F.C., and Avery, M.P.
1993: Hydrocarbon charge history of east coast offshore basins: modelling geological uncertainty. *In* Current Research, Part E. Geological Survey of Canada, Paper 93–1E, p. 299–306.

PETROPHYSICAL, GEOCHEMICAL AND DEPOSITIONAL FEATURES OF THE EGRET MEMBER (KIMMERIDGIAN) OIL SOURCE ROCK, JEANNE D'ARC BASIN, OFFSHORE EASTERN CANADA

Z. Huang, M.A. Williamson, and K.D. McAlpine

Atlantic Geoscience Centre, P.O. Box 1006, Dartmouth, Nova Scotia B2Y 4A2

J.A. Bateman

Department of Earth Sciences, Dalhousie University, Halifax, Nova Scotia B3H 3J5

M.G. Fowler

Geological Survey of Canada, 3303-33rd Street N.W., Calgary, Alberta T2L 2A7

BACKGROUND

The Egret Member of the Rankin Formation is the major oil source rock in the Jeanne d'Arc Basin, offshore eastern Canada. In the absence of core samples of this interval we have to make use of geochemical cuttings analysis and petrophysical log information to answer such questions as: How and where is the organic matter distributed within the gross source rock interval? What is the nature of the interbedded nonorganic matter rich material? Does the variability of the source rock provide clues regarding the deposition and preservation of organic matter? Characterization of the source rock in this way provides clues to oil volume and expulsion efficiency and is a vital part of our broader research effort that attempts to map the basin's dynamic hydrocarbon charge history.

Several methods assist us in the detailed characterization of the source interval. Extensive Rock-Eval profiles (at 10 m intervals) have recently been supplemented by detailed cuttings examination. Our application of the ΔlogR method of Passey et al. (1990) allowed us to derive TOC (Total Organic Carbon) and S2 (amount of material volatized and/or cracked to hydrocarbons between 300°C and 600°C) profiles for the source rock. Most recently we have applied a CNN (Computer Neural Network) modelling technique that integrates information from both well logs and cutting samples to construct TOC profiles. The combination of these methods, coupled to the use of gamma ray logs to determine source variability, indicates that the Egret Member exhibits a Milankovitch-type cyclicity. Examination of these cyclic sequences provide important time constraints useful in our attempts to understand the deposition and preservation of organic matter within the Egret Member.

DETAILED ORGANIC RICHNESS CHARACTERIZATION ΔLOGR METHOD

The ΔlogR technique (Passey et al., 1990) is derived from a basic consideration of the difference between source rocks and nonsource rocks in their solid and fluid components and observations on their responses to different logs. It overlays a porosity log (sonic, density or neutron porosity) on to a resistivity log (at an appropriate scale) and uses the separation of the two logs together with information about maturity and kerogen type, to calculate TOC and S2 values.

Twenty wells penetrated or reached the Egret Member in the study area (Fig. 1). TOC and S2 profiles for the 17 wells were calculated where sufficient data were available. The relative level of maturation at the well sites was ranked according to Rock-Eval, vitrinite reflectance (R_o) data, extraction data and biomarker distributions. The level of maturity (LOM) at each well location was determined using the scale described in Hood et al. (1975).

Most of the wells show a fairly good fit between cutting measurements and TOC and S2 values computed using the ΔlogR method (Fig. 2). Correlation coefficients for the average measured values and the average computed values for TOC and S2 in the Egret Member are 0.93 and 0.89, respectively. Detailed variations in organic richness (e.g., existence of nonsource layers) are revealed by the calculated TOC and S2 curves. We used the gamma ray log for high resolution correlations between the calculated TOC and S2 values for individual lithological layers. For immature areas, higher TOC and S2 peaks are correlatable to high gamma ray readings, and low TOC and S2 to low gamma ray responses. In mature areas,

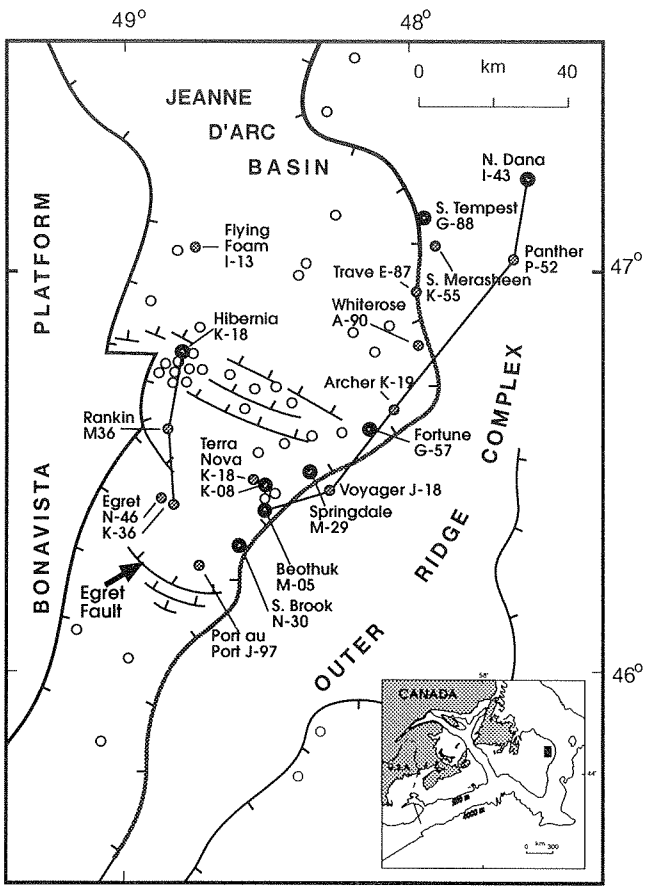

Figure 1. *The Jeanne d'Arc Basin study area. Shaded dots indicate wells which penetrated or reached the Egret Member. The bold rims indicate that these wells also contain oil reservoirs.*

most of the higher TOC and S2 peaks also correlate to high gamma ray readings, although at some levels, the higher TOC peaks correlate with low gamma ray readings. Further Rock-Eval analysis on four lithological groups from the Egret Member (dark-brown laminated shale, light brown to grey shale, marlstone/limestone and claystone, and sandstone) indicates that TOC decreases from the first group to the last one. Therefore, we conclude that in the Egret Member, the organic-rich layers are the more shaly layers while the nonsource rock layers seem to be limestone/marls to the south, and siltstone/sandstone to the north. Some of the calcareous or sandy intervals (low gamma ray intervals) corresponding to the higher TOC peaks in the mature area may be an indication of oil/gas migration.

CNN MODELLING

The ΔlogR method is limited by its dependence on maturation information and on the accuracy of assumed well log baselines. For immature areas, this dependency could result in substantial errors in calculated TOC and S2. Therefore, we devised a data and knowledge based approach to accurately map oil source rock character. This approach makes use of computer neural network (CNN) modelling and is composed of four steps. The first step is to extract examples using an empirical relationship between TOC and gamma-ray, resistivity, and sonic logs. An example consists of a measured TOC value from a composite cutting sample over a 10 m interval, which represents the interval's average TOC, a suite of well log readings which yields the median of the pseudo-TOC values from the empirical relationship in the corresponding interval, and spatial information. The second step identifies and deletes false examples using a measured TOC and pseudo-TOC median crossplot. The third step performs pattern recognition using CNN modelling. A particular variation of the back-progradation algorithm known as Quickprop (Fahlman, 1988) combined with the Dynamic Node Creation scheme of Ash (1989) was used for efficient modelling. Examples selected from 12 wells were divided into training and supervising sets. Examples from another 3 wells were retained as an

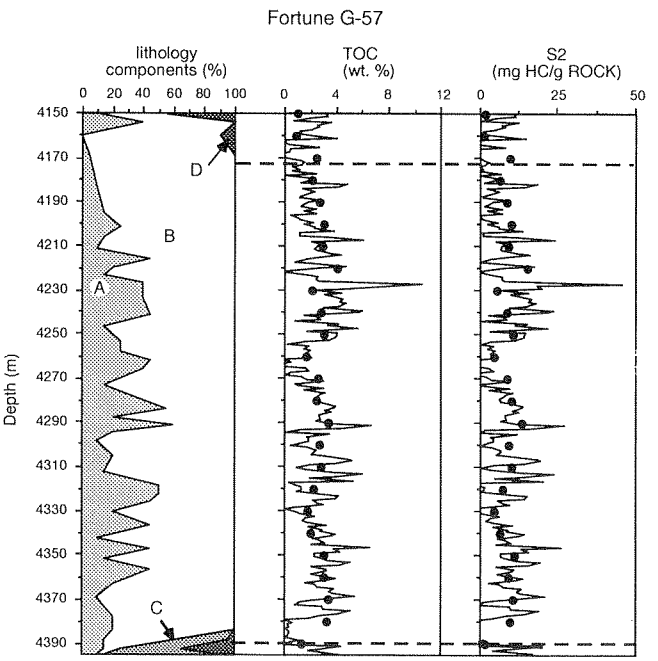

Figure 2. *Lithology (A, carbonate, B, Shale/claystone, C, siltstone, and D, sandstone, percentage from cutting sample examination), calculated TOC and S2 with ΔlogR method (Passey et al., 1990), and measured TOC and S2 (circles) at Fortune G-57. The dashed lines mark the upper and lower boundaries of the Egret Member.*

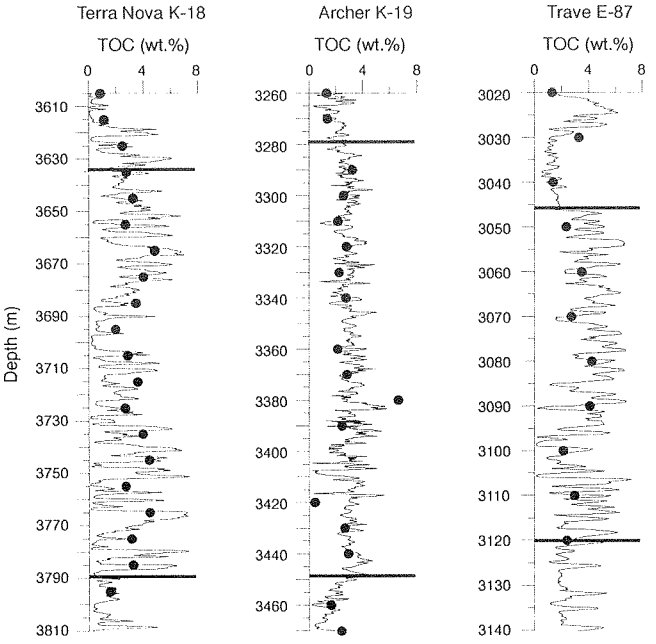

Figure 3. *CNN predicted TOC curves and TOC measurements on cuttings (circles) for three wells. The information from these wells was not included in the examples to train the CNN. The boundaries of the Egret Member are shown as thick horizontal lines.*

independent data set to test the trained CNN (Fig. 3). In the last step, the trained CNN was used to construct TOC curves from well logs. The utility of this approach is maximized when there are Rock-Eval measurements on cutting samples only (usually collected over 10 m intervals) and few well logs.

CYCLICITY AND DEPOSITION PROCESS OF THE EGRET MEMBER

The Egret Member source rock is highly variable in organic richness and geochemical parameters, and the variations appear cyclic. Rock-Eval analysis on selected cuttings of different lithologies indicates that the variations seen on TOC curves are primarily related to lithological changes. Therefore, we used gamma ray logs as indicators of lithological change to investigate the cyclicity in the Egret Member. Detailed examination reveals three different orders of cycles. The large and medium scale cycles are correlatable among wells. Four large scale cycles can be found in most of the wells (Fig. 4). Usually a large scale cycle contains four medium scale cycles and a medium scale cycle has five small scale cycles. The cyclicities are estimated semi-quantitatively according to relationships among the three orders of cycles and the approximate time span of the Egret Member from published geological time scales. The large-scale cyclicity is estimated to be about 413 ky, the medium-scale cycles about 100 ky and the small-scale cycles about 20 ky. We interpret that the depositional cycles are caused by orbitally forced sea level and climatic changes and that the Egret Member was deposited in at least 1.65 million years. Using chronological information drawn from sedimentary cycles, we examine both spatial and vertical (temporal) variations in sedimentation rate for the member. The sedimentation rate for the Egret Member varies from 3.8 cm/ky to 14.7 cm/ky. Low sedimentation rates correlate with relatively high total organic content values in this basin. Environmental Scanning Electron Microscope examination reveals that in organic-rich samples euhedral pyrite, which is indicative of extensive anoxia, is more abundant than framboidal pyrite, whereas in organic-lean samples framboidal habits are more common. It is probable that the organic-rich layers were deposited during periods of high sea-level stand and warmer climate.

SUMMARY

We have used two techniques for detailed source rock characterization in the Jeanne d'Arc Basin. The results reveal the variation of TOC in the Egret Member source rock and its cyclic nature. Detailed correlation of gamma ray logs indicates that the cyclicity is of

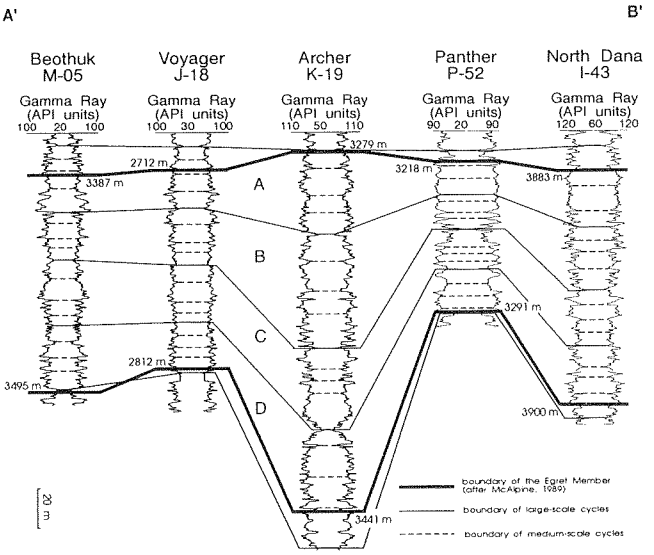

Figure 4. *Correlation of Egret Member sedimentary cycles in Beothuk M-05, Voyager J-18, Archer K-19, Panther P-52, and North Dana I-43, in Figure 1. Large scale cycles are labelled A, B, C, and D.*

Milankovitch-type. Information from sedimentary cycles combined with new geochemical information from cuttings have enhanced our understanding of the deposition and preservation process of organic matter in the Egret Member.

REFERENCES

Ash, T.
1989: Dynamic node creation in backpropagation networks. Institute of Cognitive Science Report 8901, University of California, San Diego, La Jolla, California, 11 p.

Fahlman, S.E.
1988: Fast learning variations on back-propagation: an empirical study. *In* Proceedings 1988 connectionist models summer school, D.S. Touretzky, G. Hinton, and T. Sejnowski (eds.). Morgan Kaufmann Publishers, San Mateo, California, p. 38–51.

Hood, A., Gutjahr, C.C.M., and Heacock, R.L.
1975: Organic metamorphism and the generation of petroleum. American Association of Petroleum Geologists, v. 59, p. 986–996.

Passey, Q.R., Creaney, S., Kulla, J.B., Moretti F.J., and Stroud, J.D.
1990: A practical model for organic richness from porosity and resistivity logs. American Association of Petroleum Geologists, v. 74, p. 1777–1794.

CRITICAL DEPTH OF BURIAL OF SUBSIDING SHALES AND ITS EFFECT ON ABNORMAL PRESSURE DEVELOPMENT

T.J. Katsube

Geological Survey of Canada, 601 Booth Street, Ottawa, Ontario K1A 0E8

M.A. Williamson

Atlantic Geoscience Centre, P.O. Box 1006, Dartmouth, Nova Scotia B2Y 4A2

ABSTRACT

As muds subside and are transformed into tight shales, there appears to be a "critical depth of burial" (CDB), about 2.5–3.5 km, at which the mode of compaction due to burial changes (Fig. 1; Katsube and Williamson, 1994a, b). Mud and shale porosities (ϕ_E) decrease with burial depth from 60–80% at the ocean floor surface to 5–15% at the CDB or greater. Permeabilities (k) decrease from 10^{-14}–$10^{-11}m^2$ to 10^{-21}–$10^{-20}m^2$ at the same depths, a 7 to 11 orders of magnitude decrease. Following a rapid ϕ_E and k decrease with depth to the CDB, the rate of decrease is reduced considerably and both parameters may even increase at greater depths (Katsube and Best, 1992). The rapid ϕ_E and k decrease at the initial stage is mainly due to mechanical compaction, during which shale bulk density (δ), ϕ_E and k values approach critical values of 2.6, 5.0% and $10^{-21}m^2$, respectively (Katsube and Williamson, 1994a, b). At depths greater than the CDB, the diagenetic influence is greater than that of the mechanical compaction (Katsube and Williamson, 1994b). At these depths, shales with cemented (CM) pores show only a slight reduction of k and ϕ_E with depth, due to a tendency for preservation of both pore throats and storage pores under compaction. Shales with dissolution (DS) pores show a more rapid reduction of k and ϕ_E, due to the collapse of both pore throats and storage pores. This implies, that although shales with cemented pores are generally less permeable than those with well developed secondary dissolution pores, this relationship could be reversed at greater depth (Katsube and Williamson, 1994b). These mechanisms have a significant effect on abnormal pressure development, such as allowing overpressures to develop at depths less than the CDB, tendencies for early stage excess pore pressure pulses for CM-shales and delayed pulses for DS-shales.

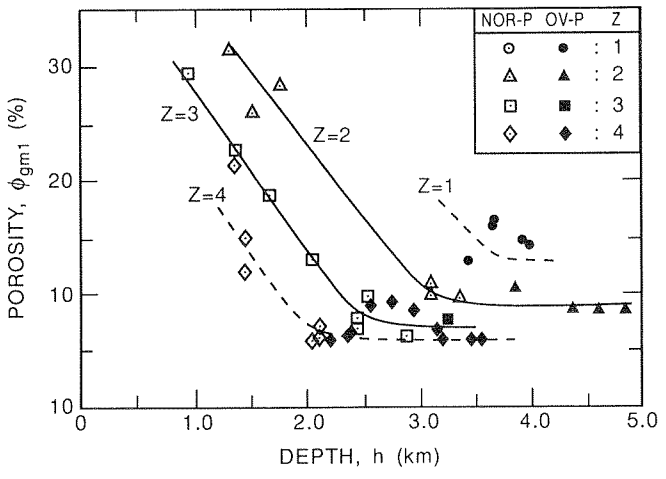

Figure 1. *Porosity as a function of depth (h) for 4 different compaction zones with different sedimentation rates (Issler, 1992). Z, zone; NOR-P, normally pressured; OV-P, overpressured; ϕ_{gm1}, porosity measured by mercury porosimetry.*

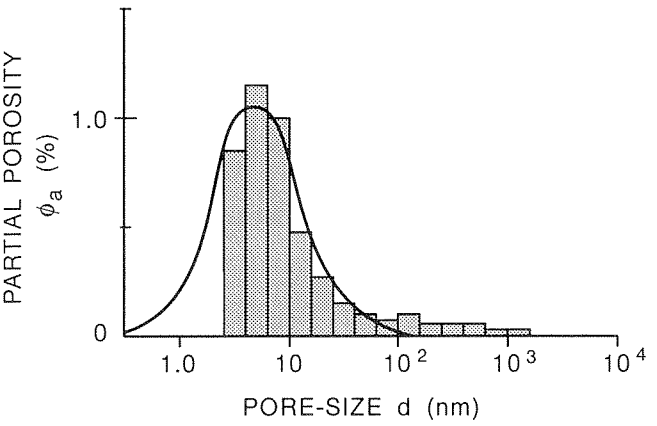

Figure 2. *Pore-Size Distribution Model (Katsube, 1992). Partial porosity (ϕ_a) is the porosity for each pore-size cell along the horizontal axis, and d is the pore-size.*

SHALE PORE STRUCTURE

Tight shale pore structure is characterized (Katsube et al., 1991a) by nano-pores of 0.3–60 nm with a unimodal pore-size distribution (Fig. 2) and modes, d_{np}, in the range of 2.7–11.5 nm (Katsube, 1992), values representing some of the smallest known pore-sizes for rocks. Nano-pores, in the range of 3 to 14 nm (Fig. 2), constitute the main pore throats or fluid flow paths of tight shales, and are the reason for extremely low shale permeabilities of 10^{-22}–2 x $10^{-20}m^2$ (Katsube et al., 1991a). Pore-sizes above 25 nm do exist but do not significantly contribute to the flow paths, although they may be part of the inter-connected pore-structure network. They are either few in number or are blind (or pocket) pores.

EXPERIMENTAL EVIDENCE SUPPORTING THE CDB CONCEPT

Porosity-depth relationships

Figure 1 shows a plot of porosity versus depth for samples from four different compaction zones in the Beaufort–Mackenzie Basin. The sedimentation rates for these zones (Z = 1, Z = 2, Z = 3 and Z = 4) are 380–660 m/Ma, 190–380 m/Ma, 40–190 m/Ma and <40 m/Ma, respectively (Issler and Katsube, 1994). These porosities were obtained from laboratory helium porosity measurements. The solid and dashed curves illustrate general trends in the data. Porosity generally decreases with increasing depth as previously indicated (Katsube and Best, 1992) for samples from this area. However, the rate of porosity decrease with depth is dramatically reduced or reversed within overpressured zones at depths greater than CDB (2.5–3.2 km) across the study area. In addition, porosity values are highest in regions with the highest sedimentation rates (Z = 1), and decrease toward regions with the lowest sedimentation rates (Z = 4). These porosity-depth trends support the relationship between shale compaction, pore fluid pressure and sedimentation rate, as determined by Issler (1992) on the basis of sonic logs.

The porosity-depth relationship displayed in Figure 3 also supports the CDB concept. The porosity decreases with compaction and burial depth, and reaches a value of 30% at 1000 m, and then continues to decrease to 5–15% at greater depths (2.5–4.1 km). This data was obtained by laboratory mercury porosimetry measurements (Katsube and Best, 1992). The pore-structure generally shows a unimodal pore-size distribution, with a mean pore-size (d_{hg}) of about 120 nm at 1.0 km, which decreases to 10–20 nm at

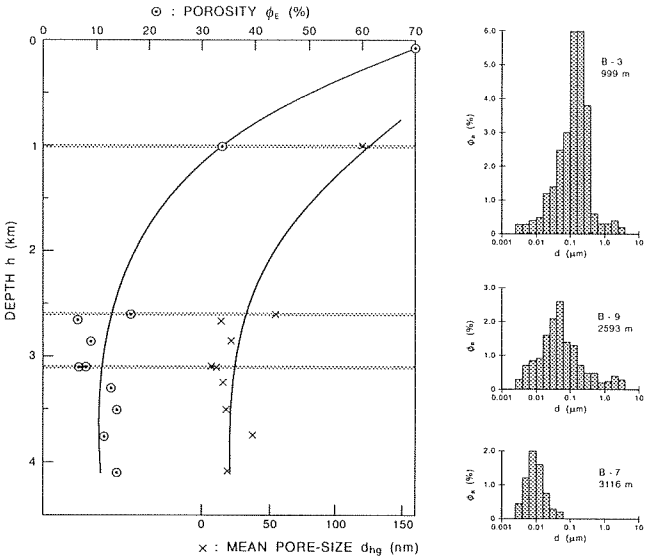

Figure 3. *Pore-size distribution variation with depth for the Beaufort–MacKenzie shale samples (Katsube and Best, 1992), showing effective porosity (ϕ_E) and mean pore-size (d_{hg}) decreasing (left-hand side) and pore-size distribution changing with increasing depth (right-hand side). The shaded lines (left-hand side) indicate sample locations for pore-size distributions displayed on the right.*

greater depths. The porosity value for the minimum depth (5–10 m) in this figure is obtained from Katsube et al. (1991b). Following the porosity decrease with depth to about 2.5–2.8 km, there are indications that there might be a slight increase in porosity with depth from about 2.8 km to greater depths.

Shale and mud permeabilities

The k values of 10^{-14}–$10^{-11}m^2$ (Katsube et al., 1991b) at the ocean floor surface decrease to 10^{-22}–$10^{-21}m^2$ at 2.4–2.9 km depths, values similar to those seen at depths greater than the CDB (Table 1). This is a 7 to 11 orders of magnitude decrease. At depth greater than the CDB, diagenetic phases of cementation (CM) and dissolution (DS) play a major role in determining the petrophysical characteristics of compacting shales. The data in Table 1 suggests that there could be a permeability (k) increase with depth at these depths, if the effect of dissolution pores are dominant (Katsube and Williamson, 1994b).

The permeability-stress (k-P_e) relationship for two unconsolidated mud samples from the ocean floor are illustrated in Figure 4. The rate of permeability (k)

decrease with depth for one of them approaches the 10^{-20} m^2 level at an effective stress (P_e) of about 50 MPa. That stress is equivalent to the overburden stress of about 3 km, a depth within that of the CDB.

IMPLICATIONS OF CDB CONCEPT

Mudford and Best (1989) indicated that shale seals of 10–20 m in thickness require permeabilities (k) of 10^{-21}–$10^{-20}m^2$ for the disequilibrium compaction process to generate the present day overpressures observed in the Venture gas field, offshore Nova Scotia. The sedimentation rate in that area has been about 100–150 m/Ma for the last 5 Ma (Williamson and Smyth, 1992). The permeabilities of the shale samples from that area are actually in the required range of values (Table 1). The experimentally compacted samples also approach these k values (Fig. 4).

The CDB concept implies that overpressures could be generated at depths less than the CDB (2.5–3.2 km, Katsube and Williamson, 1994b), since permeabilities of subsiding shales rapidly decrease as they approach the minimum k (10^{-22}–$10^{-20}m^2$) at the CDB. The greater the sedimentation rate, the smaller is the required depth for generating overpressure. In the Beaufort–Mackenzie Basin, the sedimentation rate can be as high as 660 m/Ma (Issler, 1992), implying that overpressure could be generated at depths considerably less than the CDB.

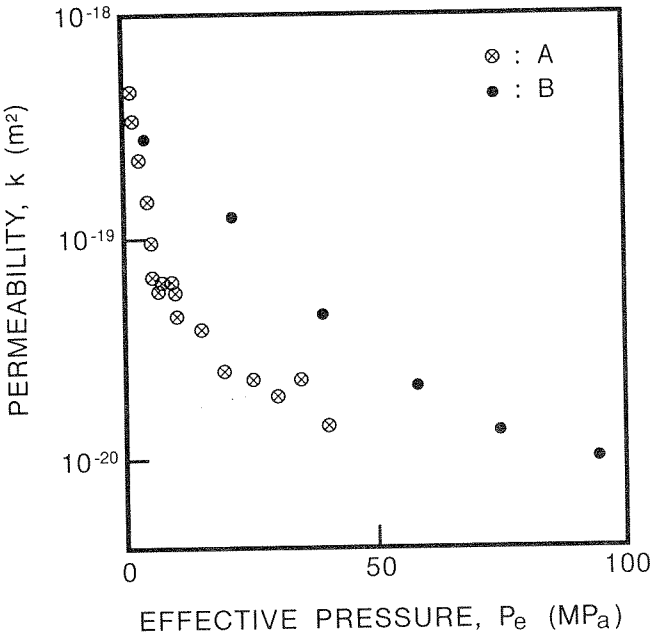

Figure 4. *Permeability-stress (k-P_e) relationship for two unconsolidated mud samples (A and B) from the ocean floor, offshore Nova Scotia.*

At depths greater than the CDB, the shale seals have been mechanically compacted to their maximum degree of compaction, with minimum k (10^{-22}-$10^{-20}m^2$) already reached. At these depths, the diagenetic history of the shale formation determines whether today's permeabilities will be above or below the minimum permeabilities (Katsube and Williamson, 1994b). The expected effects of diagenesis on shale seal characteristics are shown diagrammatically in Figure 5. At constant subsidence rates, shales with dissolution pores are characterized by high permeabilities that rapidly decrease. Shales with cemented pores are characterized by low permeabilities with smaller rates of decrease under compaction. This implies a possible reverse of permeabilities at greater depth, resulting in a tendency for an early stage excess pore pressure pulse for shales with cemented pores, and a delayed pulse for shales with dissolution pores.

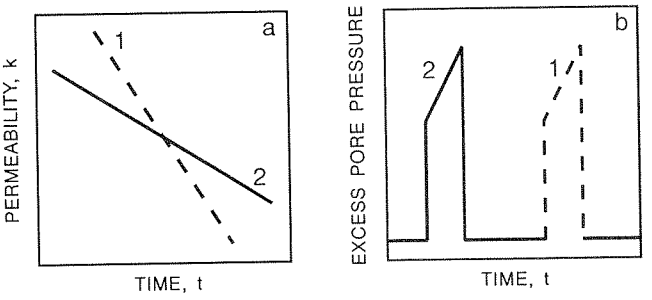

Figure 5. *Influence of diagenesis on timing of excess pore pressure (Katsube and Williamson, 1994b).* ***a.*** *Typical k-P_e curves for shales with dissolution pores (DS) and shales with cemented pores (CM).* ***b.*** *Excess pore pressure pulses for CM and DS shales.*

REFERENCES

Issler, D.R.
1992: A new approach to shale compaction and stratigraphic restoration, Beaufort–Mackenzie Basin and Mackenzie Corridor, Northern Canada. American Association of Stratigraphic Palynologists, v. 76, p. 1170–1189.

Issler, D.R. and Katsube, T.J.
1994: Effective porosity of shale samples from the Beaufort–MacKenzie Basin. *In* Current Research, Part B. Geological Survey of Canada, Paper 94–1B, p. 19–26.

Katsube, T.J., Best, M.E., and Mudford, B.S.
1991a: Petrophysical characteristics of shales from the Scotian Shelf. Geophysics, v. 56, p. 1681–1688.

Katsube, T.J., Wires, K., Cameron, B.I., and Franklin, J.M.
1991b: Porosity and permeability of ocean floor sediments from the Middle Valley Zone in the northeast Pacific: Borehole PAR90-1. Geological Survey of Canada, Paper 91–E, p. 91–97.

Katsube, T.J.
1992: Statistical analysis of pore-size distribution data of tight shales from the Scotian Shelf. *In* Current Research, Part E. Geological Survey of Canada, Paper 92–1E, p. 365–372.

Katsube, T.J. and Best, M.E.
1992: Pore structure of shales from the Beaufort–MacKenzie Basin, Northwest Territories. *In* Current Research, Part E. Geological Survey of Canada, Paper 92–1E, p. 157–162.

Katsube, T.J. and Coyner, K.
1994: Determination of permeability(k)-compaction relationship from interpretation of k-stress data for shales from Eastern and Northern Canada. *In* Current Research, Part D. Geological Survey of Canada, Paper 94–1D, p. 169–177.

Katsube, T.J. and Williamson, M.A.
1994a: Shale petrophysics and basin charge modelling. *In* Current Research, Part D. Geological Survey of Canada, Paper 94–1D, p. 179–188.

Katsube, T.J. and Williamson, M.A.
1994b: Effects of diagenesis on shale nano-pore structure and implications for sealing capacity; in press for "Proceedings of the Conference on Diagenesis, Overpressuring and Reservoir Quality", 25-26 March, 1993, Cambridge, England, U.K.

Katsube, T.J., Bloch, J., and Issler, D.R.
1995: Shale pore structure evolution under variable sedimentation rates in the Beaufort–MacKenzie Basin; this Volume.

Loman, J.M., Katsube, T.J., Correia, J.M., and Williamson, M.A.
1993: Effect of compaction on porosity and formation factor for tight shales from the Scotian Shelf, offshore Nova Scotia. *In* Current Research, Part E. Geological Survey of Canada, Paper 93–1E, p. 331–335.

Mudford, B.S. and Best, M.E.
1989: Venture Gas Field, offshore Nova Scotia: case study of overpressuring in region of low sedimentation rate. American Association of Petroleum Geologists Bulletin, v. 73, p. 1383–1396.

Williamson, M.A. and Smyth, C.
1992: Timing of gas and overpressure generation in the Sable Basin offshore Nova Scotia. Bulletin of Canadian Petroleum Geology, v. 40, no. 2, p. 151–169.

Table 1

Shale permeabilities at various depths

Depth (m)	Region (I.D.)	Porosity (%)	Permeability (m^2)	References
0.3–7.7	NP	72–80	4×10^{-15}–10^{-11}	Katsube et al., 1991b
2460	BMB		3×10^{-21}	Katsube et al., 1995
2880	BMB		2×10^{-22}	Katsube et al., 1995
3760	BMB (B-5)		$(5\text{-}8) \times 10^{-21}$	Katsube and Coyner, 1994
4700–5600	VTR			
CM	(V6, 9)	0.3–1.5	$(0.3\text{–}3.6) \times 10^{-21}$	Katsube and Coyner, 1994 Katsube and Williamson, 1994b Loman et al., 1993
DS	(V-4, 10)	0.1–12	$(0.1\text{–}30) \times 10^{-21}$	Katsube and Coyner, 1994 Katsube and Williamson, 1994b Loman et al., 1993

Regions: NP, north Pacific; BMB, Beaufort–Mackenzie (Northwest Territories); VTR, Venture Gas Field (offshore Nova Scotia). Diagenetic Phases (Katsube and Williamson, 1994b): CM, late-stage cementation; DS, late-stage dissolution.

INTEGRATING GEOSCIENTIFIC DATA, KNOWLEDGE AND INTERPRETATION FOR THE EAST COAST BASINS OF CANADA

P.N. Moir, M.A. Williamson, and S. King

Atlantic Geoscience Centre, P.O. Box 1006, Dartmouth, Nova Scotia B2Y 4A2

INTRODUCTION

The Atlantic Geoscience Centre (AGC) uses diverse computer software programs and databases while mapping, visualizing, evaluating and interpreting the numerous subsurface geoscientific features of Canada's east coast frontier basins. No reliance is placed on any single turnkey system; the emphasis is placed on the ability to move data freely between computer programs and computer platforms using standard interchanges and data models. In this way the scientific synthesis, modelling, and interpretations can be performed using the software/platform most suited to the task.

Relational databases, geographical information systems, scientific visualization, 2- and 3-D seismic interpretation and basin modelling software are used for the subsurface mapping of petroliferous basins as they are currently configured and as they were at key times in the past. The intent of this note is to give an up to date snapshot of the type of data contained within AGC's BASIN and BASIN_GIS databases, as well as the arsenal of computer programs that are used for basin mapping and modelling. Examples demonstrate the flow of data between databases and applications.

DATABASES

BASIN

BASIN is a digital database containing a wealth of geological, geophysical and engineering information related to 25 years of petroleum exploration of basins offshore eastern Canada. BASIN contains both raw and interpreted information for all exploration wells and a large number of seismic surveys. Data have been gathered from many sources including well histories and drilling reports, to purchased proprietary data sets containing electrical log traces and rock cutting descriptions, to interpretive data such as formation picks, age determinations and vitrinite reflection values. Most of the data is contained within one relational database constructed using Oracle™ software. Raw seismic reflection data that are part of the National Digital Geoscience Data Library (NDGDL), are maintained on thousands of magnetic tapes. Figure 1 depicts categories of information that make up BASIN and serves to highlight the type of data that make up the database. These categories are largely historical rather than functional, reflecting the fact that until recently most of the information was contained on several computer platforms using diverse database software.

To make effcient and effective use of the data, AGC is commited to the Epicentre/Public Petroleum Data Model (PPDM) relational data model as a route to standardize and organize the BASIN database. The PPDM association is a nonprofit organization dedicated to the ongoing definition of a standard data model for petroleum exploration and production needs. Presently the PPDM data model and the Petrotechnical Open Software Corporation (POSC) Epicentre data model are undergoing a merger process that will see a single industry standard model. This will provide oil and gas organizations, including AGC, with methods to manage and to support integrated multidisciplinary projects. Adhering to a standard database structure and naming convention allows for ease of data transfer between the

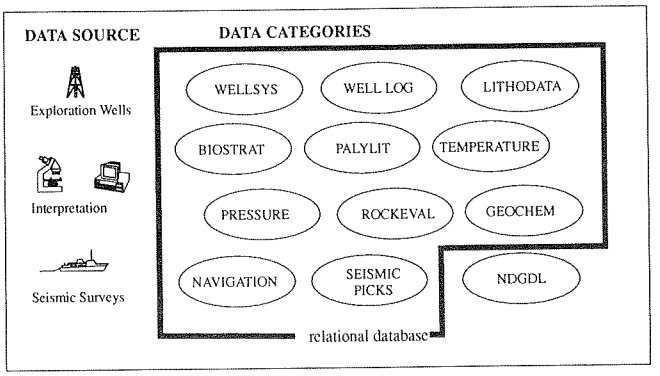

Figure 1. *Depiction of source and categories of data contained in the BASIN database.*

database and applications. Many petroleum industry software programs will be able to directly access a database based on this model.

BASIN_GIS

The use of CARIS™ software, a geographic information system (GIS), started at AGC in 1987. It has been used very successfully to digitize, manipulate and produce maps, most notably for the Basin Atlas Series. One of the advantages of using a GIS to capture the mapped data is the creation of a digital map database that can be used for multiple purposes beyond any originally projected use. Figure 2 depicts a location map for the Heavy Oil project that was created from Jeanne d'Arc structure maps that are a part of the Basin Atlas for the Grand Banks of Newfoundland. These digital maps, referred to here as BASIN_GIS, form an extension to the BASIN database for vector based data. This database is a collection of over 200 individual GIS, vector based maps.

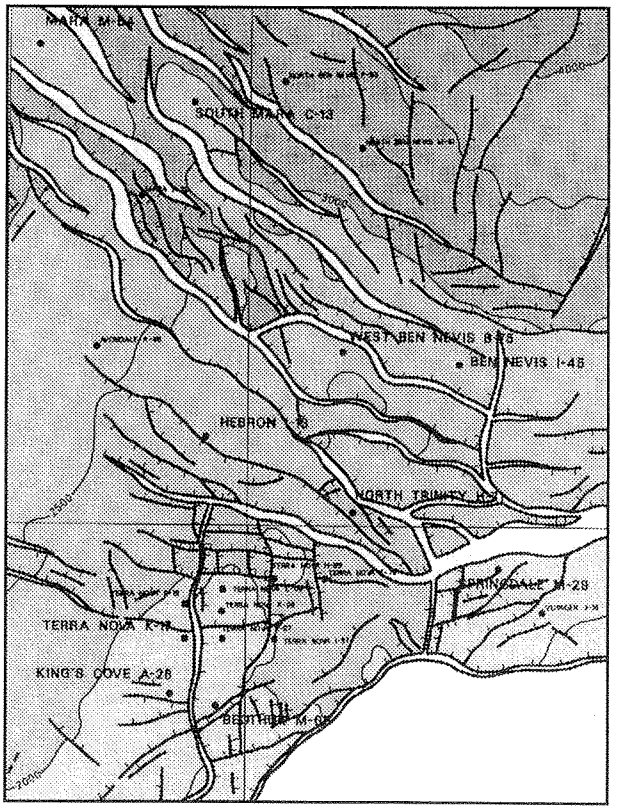

Figure 2. *Heavy oil project study area, Jeanne D'Arc basin.*

APPLICATION SOFTWARE

Scientific syntheses of these data through basin anaysis, interpretation and modelling are aided by a variety of software and the computer platforms most suited to the task. The ability to move data freely between the databases and the application software is very important, and is continually undergoing refinement. The crux of this is the use of standard data models and interchange formats, and efficiently networked workstations, based on open computer systems. Application software must import and export data in a common format, or at least as ASCII text files. Figure 3 characterizes the flow of data from data bases to application software. Basin mapping in this figure refers to mapping of all present day parameters including geometry, stratigraphy and physical properties of the rocks and fluids.

The table below is a list of major software programs and a brief description of the function of the software as it pertains to basin analysis at AGC.

Software name	Software function in basin analysis at AGC
Oracle™	relational database
Epicentre/PPDM™	data model (projected) for relational database
CARIS™	geographic information system (GIS) and 3-D visualization
BasinMod™	1- and 2-D basin modelling Landmark™
Seisworks™	seismic interpretation
Stratworks™	stratigraphic interpretation and correlation
Z-Map Plus™	mapping, gridding, contouring and visualisation
MATLAB™	high performance numeric computation and visualization

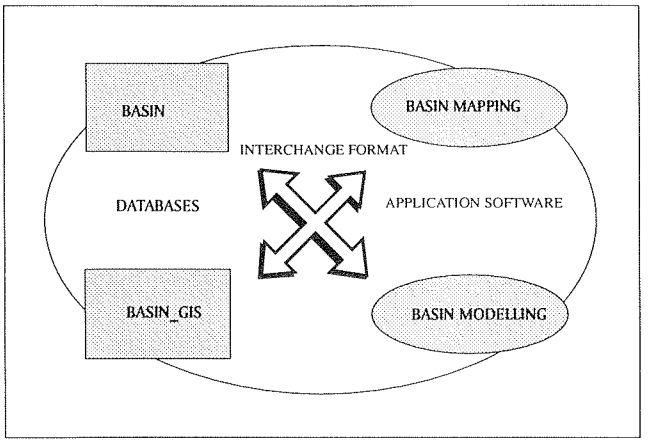

Figure 3. *Characterization of the bi-directional flow of data between databases and applications.*

Khoros™	scientific visualization
Surface III™	contouring and 3-D visualization
CorelDraw™	illustrations and poster creation
World Wide Web server	on line (internet) access to AGC information

EXAMPLES

Figure 4 shows a 3-D shaded relief image of the 'B' marker horizon for the Terra Nova area of the Jeanne d'Arc basin. The 'B' marker was picked by Shimeld (1994), using Landmark's Seisworks software. The picked horizon was exported as an ASCII text file and imported into the GIS software CARIS. The 3-D digital terrain model was created and used to make the 3-D shaded relief image. Well locations were added from an existing digital Basin Atlas map in BASIN__GIS. Besides the use of two powerful application software packages, this example also demonstrated the scientific visualization. The difference between scientific visualization and presentation graphics is that the latter is primarily concerned with communication of information and results that are already understood. In scientific visualization we are seeking to understand the data (Earshaw and Wiseman, 1992).

Figure 5 shows modelled volumes of generated oil from the Hibernia Drainage Area calibration study (Williamson et al., 1994). In this example data, many of which are contained in BASIN, were used in the BasinMod™ software to model oil generation at well locations and pseudo-wells. Basin structure and horizon geometry from BASIN__GIS are used to constrain and contour the hydrocarbon generation.

REFERENCES

Earshaw, R.A. and Wiseman N.
1992: An Introduction Guide to Scientific Visualization. Springer-Verlag, 156 p.

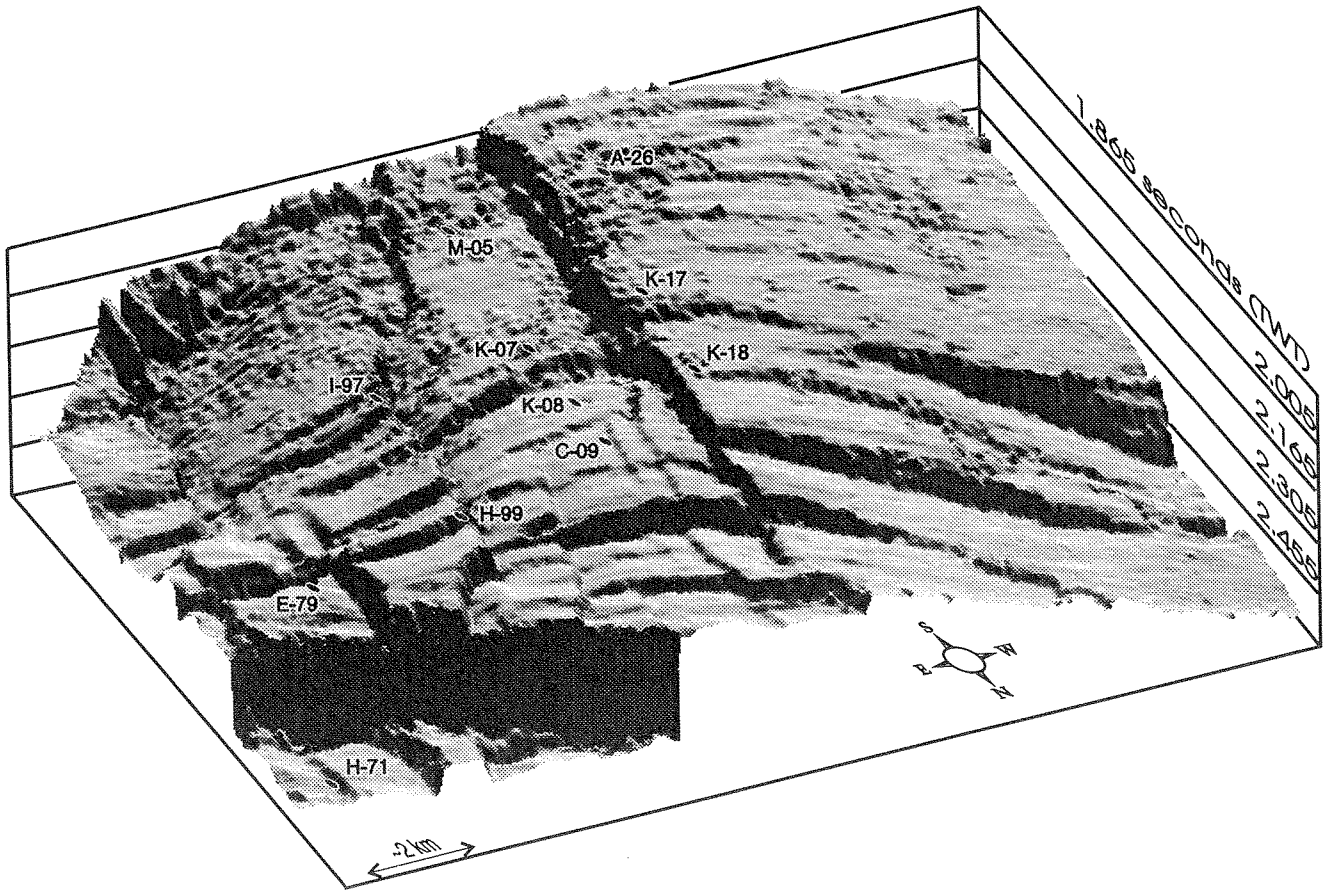

Figure 4. 3-D shaded relief image of the 'B' marker horizon. Sun angle = 225°/65° (azimuth/dip).

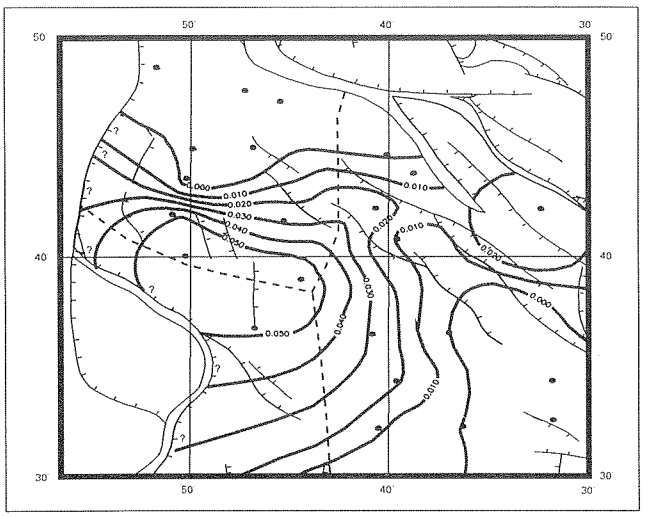

Figure 5. *Hibernia drainage area: modelled generation of hydrocarbons (m^3 oil per m^3 of source rock).*

Shimeld, J.W.
1994: Development of an Algorithm to Detect Subsurface Fractures Using Conventional Wells Logs and Fuzzy Inference: Practical Application at the terra Nova Oil Field, Offshore Newfoundland. M.Sc. thesis, Dalhousie University, 148 p.

Williamson, M.A., Coflin, K.C., King, S., Desroches, K., Moir, P.N., McAlpine, K.D., and Wray, A.
1994: A Hydorcarbon charge model of the Hibernia drainage area, Jeanne d'Arc Basin, Offshore Newfoundland. *In* Energy Exploration and Exploitation, v. 12, no. 4.

STRATIGRAPHIC CORRELATION AND PETROLEUM GEOLOGY OF THE CENTRAL MARITIMES BASIN, EASTERN CANADA

T.A. Rehill and M.R. Gibling

Department of Earth Sciences, Dalhousie University, Halifax, Nova Scotia B3H 3J5

M.A. Williamson

Atlantic Geoscience Centre, P.O. Box 1006, Dartmouth, Nova Scotia B2Y 4A2

BACKGROUND

The Maritimes Basin of Atlantic Canada (Fig. 1) (Williams, 1973) covers approximately 150 000 km^2, but, with 67% of the basin's area lying beneath the Gulf of St. Lawrence, relatively little is known about regional stratigraphy, tectono-stratigraphic history and hydrocarbon potential.

The presence of oil seeps in coeval onshore strata, sourced from the Early Carboniferous Horton Group, led to the drilling of 20 exploration wells in the Central Maritimes Basin (CMB). Most of the wells had gas shows (Fig. 5), but all were classified dry and abandoned, except the East Point E-49 gas discovery.

The discovery and subsequent mapping of a thick Upper Carboniferous coal-bearing package underlying much of the Gulf of St. Lawrence (Grant and Moir, 1992), provoked a renewed look at the resource potential of the basin. Recent studies suggest that these coal measures have the potential to source hydrocarbons (Mossman, 1992). Traditionally the depositional setting of most of the offshore strata was thought to be fluviolacustrine (Howie and Barss, 1975). However, studies of agglutinated foraminifera now indicate that sections of the coal measures were deposited in marine influenced environments, enhancing the possibility of sourcing hydrocarbons from type II and III kerogens (Wightman et al., 1994). The detection of marine foraminfera within the coal measures also supports recent suggestions of cyclothemic deposition in the Maritimes Basin (Grant, 1994).

PROBLEMS

The CMB is a large, little explored frontier basin (Fig. 2) with ample indications of hydrocarbon charge (East Point E-49, well history report). However, few studies explain why the exploration wells drilled in the CMB did not encounter significant hydrocarbons. The CMB has not been an active area of exploration for the petroleum industry since the late 1970's. To help renew interest in this area, it will be necessary to explain the past failures, develop new plays and address questions regarding the basins hydrocarbon generation and migration history. It will also be necessary to quantify the principle risks associated with additional exploration in the basin.

Over the past 147 years, stratigraphic classification of the onshore strata has utilized combinations of biostratigraphy, chronostratigraphy and litho-stratigraphy. A recent revision of Cumberland subbasin stratigraphy focuses on lithostratigraphy with emphasis on the formation component (Ryan et al., 1991). The proposed revisions only apply to the Upper Carboniferous to Lower Permian strata in the Cumberland Basin but do suggest applicability to the regional Maritimes Basin (Ryan et al., 1991). In fact, with no formal stratigraphic nomenclature existing specifically for the Maritimes Basin, any detailed stratigraphy of the offshore portion of the Maritimes Basin was restricted to areas of interest to the petroleum industry and published primarily in company well history reports.

SCOPE

Geological studies have traditionally focused on the onshore portions of the Maritimes Basin. As work progresses onshore, it has become clear that the CMB database must be addressed to advance our understanding of the geological framework of the regional Maritimes Basin. The basin analysis project reported here addresses the CMB database, and comprises three main components: stratigraphic correlation, sedimentology and hydrocarbon generation

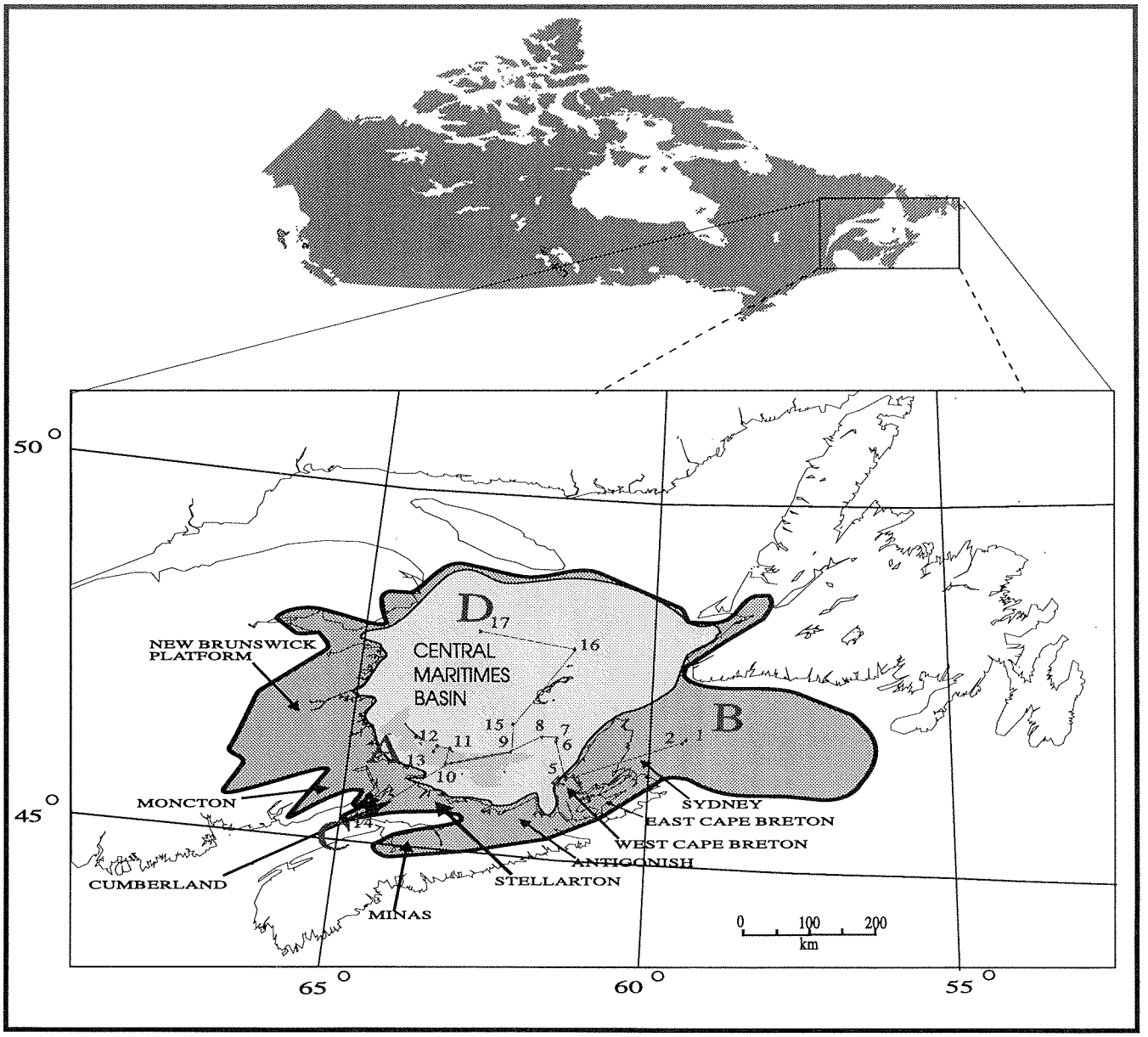

Figure 1. *The Maritimes Basin (dark grey) of Atlantic Canada, with subbasin locations, is one of North America's largest preserved Late Paleozoic depocentres. The Central Maritimes Basin (CMB) is outlined in light grey. Locations of study cross-sections (A–B, C–D) are shown.*

modelling. The stratigraphic component of the project is discussed here.

An important question is whether the Maritimes Basin's onshore exposures are representative of what underlies the Gulf of St. Lawrence. The stratigraphic and sedimentological relationships between the offshore and onshore sedimentary rock packages are important aids to tracing stratigraphic units under the Gulf. Ryan et al. (1991) and Hacquebard (1986) attempted to tie onshore Maritimes Basin stratigraphy to the offshore CMB fill using changes in lithologic colour and coal spores, respectively. Both studies correlated large stratal packages (500–1000 m) of representative onshore sections with the isolated exploration wells in the Gulf of St. Lawrence and on Prince Edward Island.

The study involves the reconnaissance of Cape Breton Island, Prince Edward Island, northern Nova Scotia and southern Newfoundland exposures, the

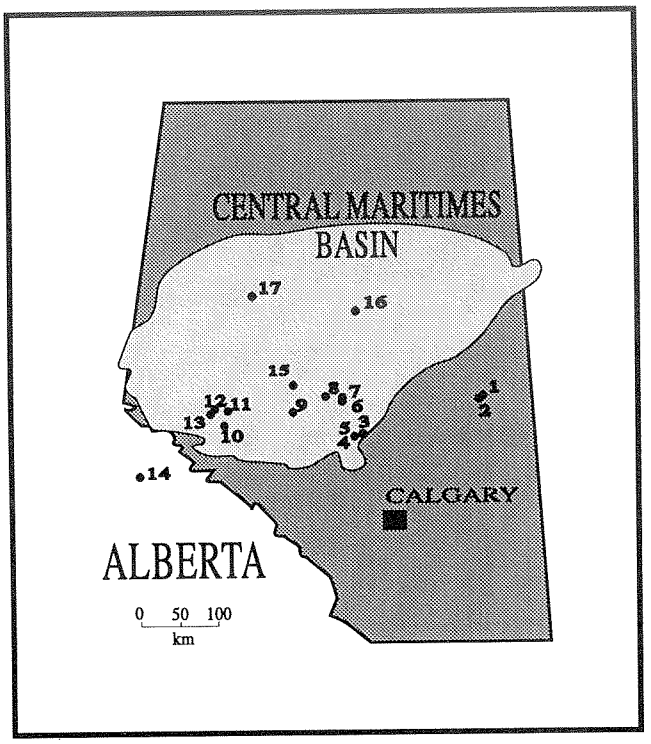

***Figure 2.** More than a third the size of Alberta, the Central Maritimes Basin has a well spacing of 1 well/5400 km².*

linking of key stratal units and isolated wells to seismic data, and addresses well logs for lithology, correlation and sedimentological trends. In addition the study has also correlated stratal units from the CMB wells to representative onshore sections, which may assist in establishing a regional stratigraphic framework for the Maritimes Basin.

STRATIGRAPHY

Thirteen CMB wells, which intersect the coal-bearing package underlying the Gulf of St. Lawrence and Prince Edward Island, and two offshore Sydney Basin wells have been considered for correlation using a Westphalian B–Westphalian C datum (Fig. 4). The datum (Top Unit 2) was defined using digital well logs and is supported by micropaleontological, seismic and representative onshore section data. The datum lies stratigraphically above a thick (>300 m) sand body, occasionally referred to as the Lower Riversdale sandstones (East Point E-49 well history report; North Sydney P-05 well history report). This sand package, underlying the datum in all the study wells, is hypothesized to be the lateral equivalent of the Ragged Reef Formation (Ryan et al., 1991), found in the Cumberland subbasin (Fig. 3), and the Sydney Mines Formation, found in the Sydney subbasin.

The sand package mentioned above is the second of three coarse grained sand packages (Unit 1, Unit 2, Unit 3) which typify the Late Carboniferous Maritimes Basin fill (Fig. 3). This unit contains the marine agglutinated foraminifera. Each coarse grained package forms the basal unit of a large scale fining upward sequence. At the base of each fining upward sequence are regionally recognizable surfaces (S1, S2, S3).

The identification of regionally extensive stratigraphic units and surfaces, evidence of marine influence during the deposition of Units 2 and 2A, biostratigraphic age data, well log signatures and seismic data support a Braidplain fan delta depositional environment (Fig. 6) for each coarse grained clastic unit, followed by a low energy environment.

FUTURE DIRECTIONS

The interpretation and refinement of detailed and large scale Central Maritime Basin stratigraphic cross-sections will establish a regional stratigraphic framework for the Maritimes Basin. To put the CMB cross-sections into a regional context, it will be necessary to incorporate representative onshore stratigraphic section into the cross-section. Interpretive gamma logs will be constructed using documented onshore sections; this

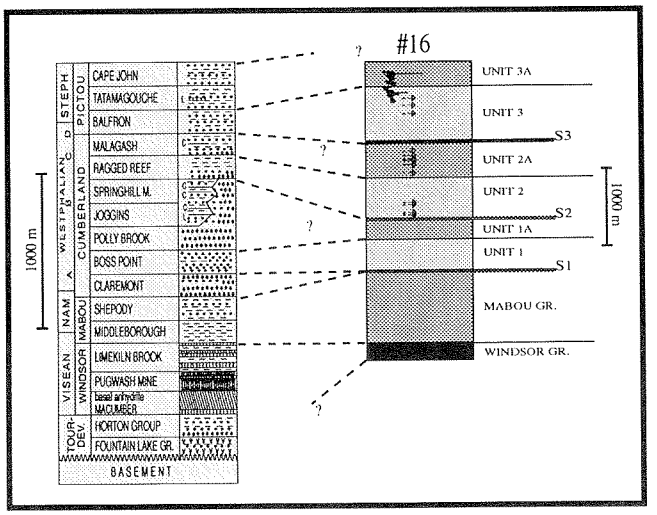

***Figure 3.** A typical well in the CMB (right) with the fining-upward sequences and surfaces outlined. The proposed correlation of units with the Cumberland Subbasin lithostratigraphy (Ryan et al., 1991) (left) is shown.*

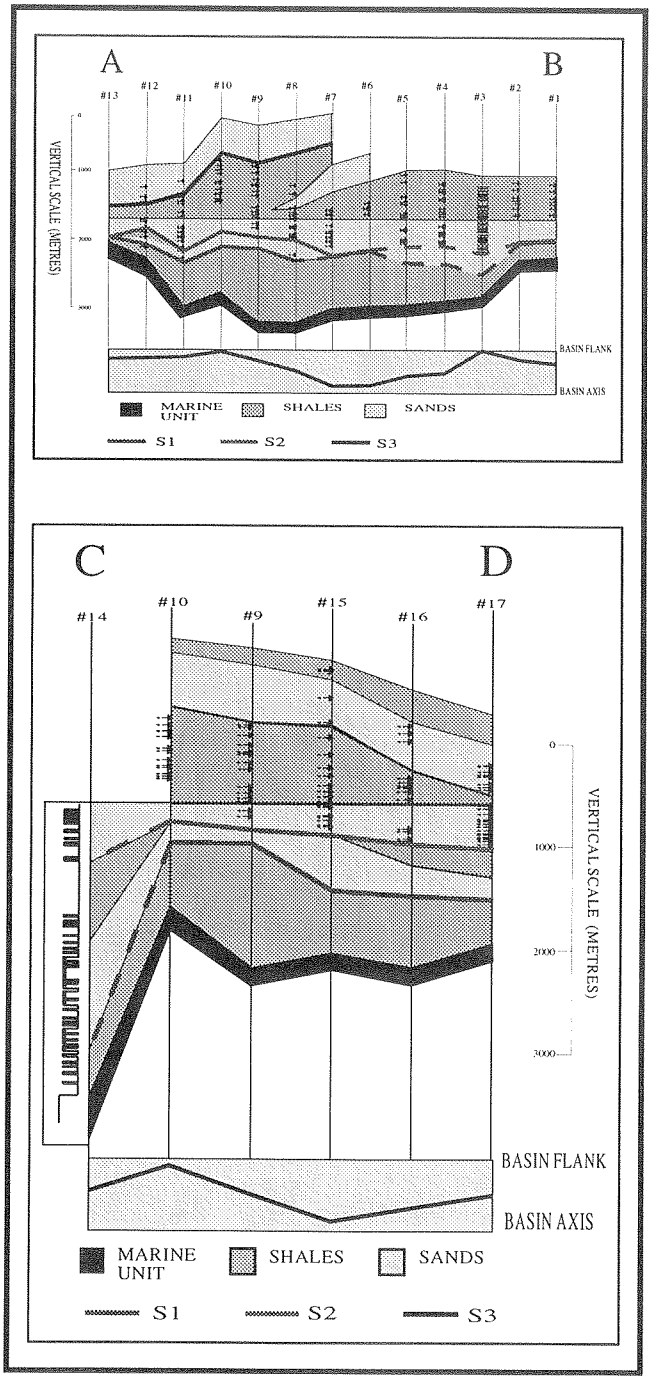

Figure 4. *Stratigraphic cross-sections across (Section A–B) and down (Section C–D) the axis of the basin. Both indicate that the coarse clastic units (1, 2, 3) are regionally extensive. The cross-sections also indicate that at the base of each coarse clastic unit lies a regionally identifiable surface. The black arrows along the wells indicate the locations of coals.*

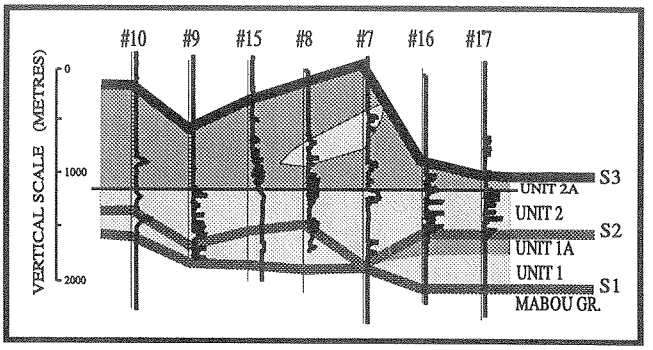

Figure 5. *Gas kicks from 7 CMB wells, as indicated on mud logs, are superimposed on a correlation of Units 1, 1A, 2, 2a and the East Point sand. The majority of the gas kicks are found within Units 2 and 2A (modified after Grant and Moir, 1992).*

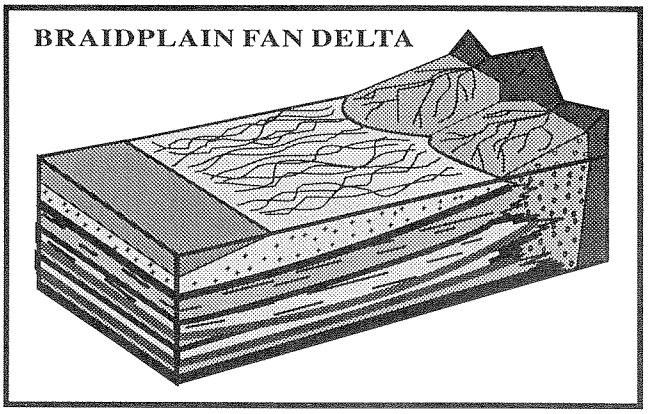

Figure 6. *The identification of regionally extensive stratigraphic units and surfaces, evidence of marine influence during the deposition of Units 2 and 2A, biostratigraphic age data, well log signatures, and seismic data support the interpretation of a "Shelf Type" braidplain fan delta depositional environment for each coarse clastic unit followed each time by low energy environments.*

will help with the correlation of offshore well logs to the onshore sections. Well log data from onshore New Brunswick and Nova Scotia will be incorporated into the CMB database to help complete the regional picture.

This project will result in the construction of a detailed stratigraphic correlation of CMB wells tied to

representative onshore sections and seismic data, resulting in a regional basin lithostratigraphic framework. The CMB work will also develop a provisional basin depositional model with analogues to other basins based on sedimentological, stratigraphical, seismic, micropaleontological and tectonic data.

REFERENCES

Grant, A.C.
1994: Aspects of seismic character and extent of Upper Carboniferous Coal Measures, Gulf of St. Lawrence and Sydney Basin. Paleogeography, Paleoclimatology, Paleoecology, v. 106, p. 271–285.

Grant, A.C. and Moir, P.N.
1992: Observations on coalbed methane potential, Prince Edward Island. Geological Survey of Canada, Paper 92–1E, p. 269–278.

Hacquebard, P.A.
1986: The Gulf of St. Lawrence Carboniferous Basin: the largest coalfield of eastern Canada. Canadian Institute of Mining Bulletin, v. 79, p. 67–78.

Howie, R.D. and Barss, M.S.
1975: Upper Paleozoic rocks of the Atlantic Provinces, Gulf of St. Lawrence, and adjacent continental shelf. Geological Survey of Canada, Paper 74–30, v. 2, p. 35–50.

Mossman, D.J.
1992: Carboniferous source rocks of the Canadian Atlantic margin. *In* Basins on the Atlantic Seaboard: Petroleum Geology, Sedimentology and Basin Evolution, J. Parnell (ed.). Geological Society Special Publication, no. 62, p. 25–34.

Ryan, R.J., Boehner, R.C., and Calder, J.H.
1991: Lithostratigraphic revisions of the upper Carboniferous to lower Permian strata in the Cumberland Basin, Nova Scotia and the regional implications for the Maritimes Basin in Atlantic Canada. Bulletin of Canadian Petroleum Geology, v. 39, no. 4, p. 289–314.

Wightman, W.G., Grant, A.C., and Rehill, T.A.
1994: The Westphalian Coal Measures of the Gulf of St. Lawrence–Sydney Basin Region, Canada: Paleontological evidence for marine influence during deposition. *In* Current Research, Part D. Geological Survey of Canada, Paper 94–1D, p. 41–49.

Williams, E.P.
1973: St. Lawrence Lowlands, Gaspé and Gulf of St. Lawrence area. *In* The Future Petroleum Provinces of Canada: Their Geology and Potential, R.G. McCrossan (ed.). Canadian Society of Petroleum Geologists, Memoir 1, p. 561–587.

FRACTURE MAPPING USING 3D SEISMIC DATA AND CONVENTIONAL WELL LOGS IN THE TERRA NOVA OIL FIELD, OFFSHORE NEWFOUNDLAND

J.W. Shimeld, Z. Huang, and P.N. Moir

Atlantic Geoscience Centre, P.O. Box 1006, Dartmouth, Nova Scotia B2Y 4A2

INTRODUCTION

Of the 260 wells drilled offshore Eastern Canada by 1986, only 7100 m of core, comprising less than 1% of the total drilled depth, were recovered (Keen and Piper, 1990). Furthermore, most East Coast wells were drilled before modern borehole imaging tools such as Schlumberger's Formation MicroScanner™ saw widespread application. Therefore, in practically all East Coast wells, including those of the Terra Nova oil field (located in the Jeanne d'Arc Basin, 350 km southeast of St. John's), seismic and conventional well log data are the only sources of information about fracturing. 3-D seismic data at Terra Nova allow detailed mapping of fault geometries, while well log data provide a high resolution estimate of fracture intensity, known as the fracture index, down the length of individual boreholes (Shimeld, 1994). Information from both sources is integrated in this study to provide a comprehensive description of fracturing at Terra Nova.

MAPPING FAULT GEOMETRIES AT TERRA NOVA USING 3-D SEISMIC DATA

The 3-D seismic data were collected for Petro-Canada in 1985 and cover a 17 by 23 km area centred over Terra Nova. Shotpoint spacing is 25 m in the inline direction and 50 m in the crossline direction, which provides high lateral resolution even at depths of several kilometres. To image faults in the greatest possible detail, a number of horizons were interpreted on roughly every tenth inline and crossline of the survey. Arbitrary lines and horizontal timeslices were used to check and improve the continuity of interpretations in highly faulted areas. Then, an "auto-picking" routine was used to extend the interpretations throughout the entire dataset. Harsh parameters were chosen for the auto-picking routine so that the manually picked horizons would be closely honoured wherever seismic reflections could be easily followed, and so that gaps would be left wherever reflections were highly discontinuous. The auto-picked horizons were examined and troublesome areas resolved through further manual interpretation. During this iterative process, calculation of complex seismic trace attributes, such as instantaneous phase and frequency, proved useful in identification of subtle faults and in correlating events (Taner et al., 1979).

A vector-based Geographic Information System called CARIS™ was used for 3-D visualisation of the interpreted horizons. Figure 1 is a shaded relief, northeast view of the 'B' Marker (Early Cretaceous) horizon. The image clearly shows a series of north–south trending faults related to formation of the keystone graben at Terra Nova, and a series of east–west trending faults related to formation of the Trans-Basin Fault Trend of the Jeanne d'Arc Basin (Grant and McAlpine, 1990). The southeasternmost portion of the horizon is "spiky" in nature due to the proximity of the Outer Ridge Complex, a complexly deformed and eroded paleo-high of Jurassic sediments. Figure 1 demonstrates that the fault mapping procedure used in this study can resolve faults with throws of as little as 10 ms.

USING CONVENTIONAL WELL LOG DATA TO MAP FRACTURES

Conventional well logs (such as the resistivity, sonic, density correction, and photoelectric effect logs) often exhibit abnormal values in response to fractured zones, although no single log response is diagnostic of fracturing. Indeed, for a specific log, it is difficult to quantitatively define what response might be expected in the presence of a fracture.

Fuzzy inference, a formalized logic based on the concept of a fuzzy set (Zadeh, 1965), provides one method of addressing these difficulties in a consistent and rational manner.

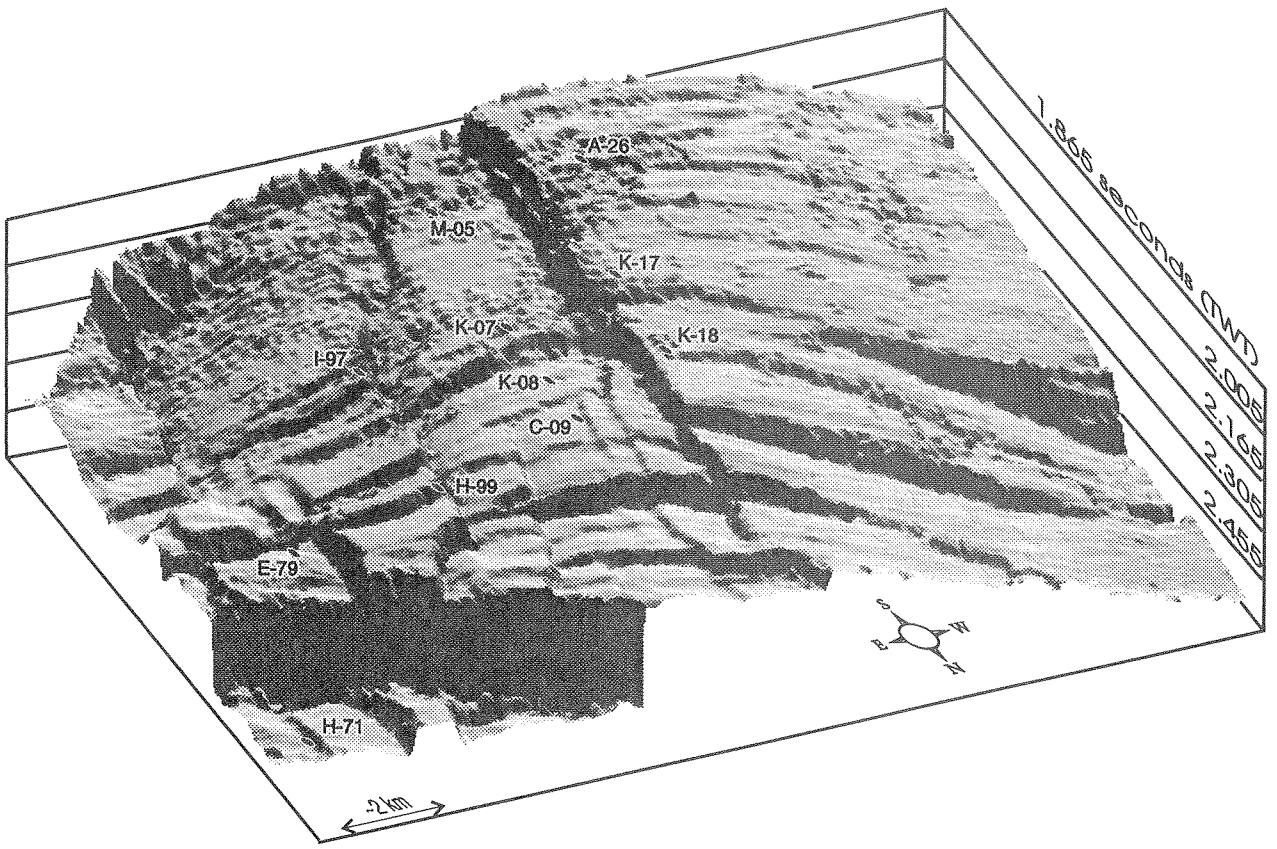

Figure 1. *3-D shaded relief image of the 'B' marker horizon. Sun angle = 225°/65° (azimuth/dip).*

The fuzzy inference algorithm first preprocesses well log data to statistically evaluate the deviation of a given log response from the local averaged response. Preprocessed results are used to construct membership functions for a number of fuzzy sets which express various grades of "fracture relatedness". For example, the "fracture relatedness" of a given log response might be 75% high, 31% medium, and 12% low. A database of rules translates the preprocessed log grades for a given depth into the fracture index. The rules are created in a manner which reflects "rule of thumb" petrophysical knowledge. For example, one rule could be: If the resistivity log is high, and the sonic log is high, and the density correction log is high, then the fracture index is high. Although we are currently using petrophysical knowledge found in the literature for the identification of fractures, design of the rule database need not be purely empirical. A line of future research might be to incorporate the use of a neural network to optimise the rules for a particular dataset.

The magnitude of the fracture index is an indication of the number of logs that exhibit fracture-like signatures; the higher the fracture index, the more extensive the fractured zone is likely to be. Figure 2 is an example of the fracture index results at K-18, where core happens to intersect a fault zone. In general, peaks in the fracture index curve tend to be 2 to 4 m wider than the corresponding fracture zones observed in core (or on the Formation MicroScanner when it is available). This is because the fracture index calculations are based on conventional well logs that have radii of investigation up to several metres beyond the borehole wall. This is a useful property of conventional well logs that, under ideal conditions, allows extensive natural fracture systems to be distinguished from shallow, drilling induced fractures.

Figure 3 summarises the fracture index results at Terra Nova and places them within a lithostratigraphic context. Some large scale trends are apparent between various lithostratigraphic units. For instance, in all wells except C-09, it is possible to recognize the South Mara Unit by the quiet nature of the fracture index log signature. This is significant considering that the specific well logs available for fracture mapping are not

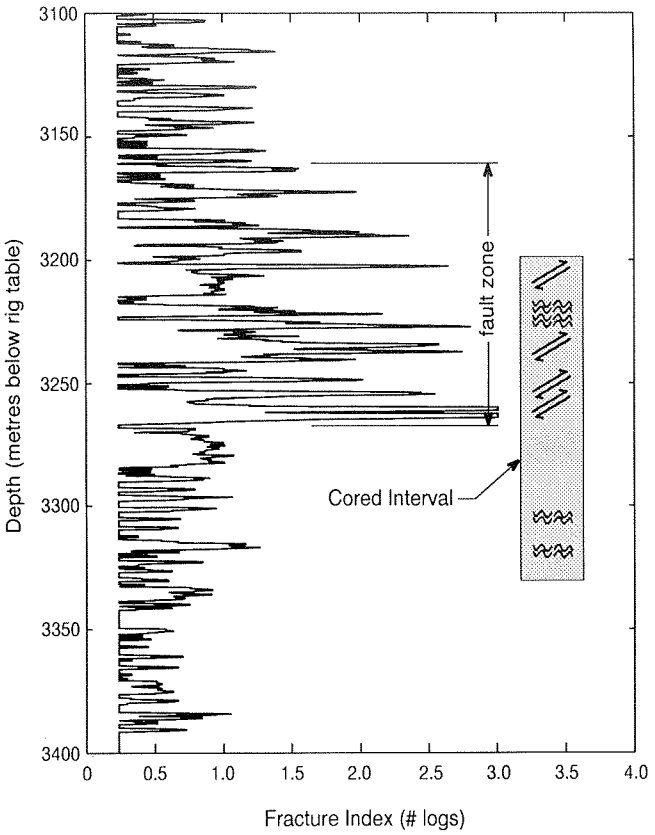

Figure 2. *Comparison of fracture indices with core information at Terra Nova K-18. Double arrows represent slickensides, and wavy lines represent fractures.*

the same at every well. In most cases, though, peaks in the fracture index log continue across lithologic boundaries and, with a few exceptions, exhibit no obvious dependency on small scale lithologic changes. Interestingly, many of the known oil accumulations at Terra Nova coincide with elevated fracture indices. Since fracture indices are calculated using as many as seven different well logs, most of which are insensitive to the presence of hydrocarbons, it is not likely that the oil itself is the cause of the fracture index peaks.

INTEGRATION OF 3-D SEISMIC DATA AND FRACTURE INDICES

Comparison between the 3-D seismic data and the fracture indices is provided by Figure 4. In most cases, fault zones imaged with the seismic data correlate with elevated fracture indices at the well. For instance, the faults and fractures contained in the core at K-18 (Fig. 2) correspond to the lower fault zone that intersects K-18 in Figure 4. At most wells, it appears that open fractures are currently associated with faults at Terra Nova.

Further work is being conducted to study the fracture index signature within selected seismic reflection packages. For example, the strongly positive, continuous reflection 80 ms above the Petrel horizon at K-18 (Fig. 4) becomes hummocky and discontinuous toward E-79. The fracture index signature, though, remains remarkably consistent. While the continuity and structure of the seismic reflector changes dramatically across the study area, the fracture content does not. This suggests that the fracturing is post-diagenetic.

SUMMARY

In areas where core and modern borehole imaging logs are unavailable, seismic and conventional well log data can provide useful information about the distribution and intensity of fracturing. Integration of the seismic and well log data provides corroborative evidence of fracturing in an area where very little direct evidence exists.

REFERENCES

Keen, M.J. and Piper, D.J.W.
1990: Chapter 1: Geological and Historical Perspective. *In* Geology of the Continental Margin of Canada, M.J. Keen and G.L. Williams (eds.). Geological Survey of Canada, Geology of Canada, no. 2, p. 5–30.

Taner, M.T., Koehler, F., and Sheriff, R.E.
1979: Complex Seismic Trace Analysis. Geophysics, v. 44, no. 6, p. 1041–1063.

Grant, A.C. and McAlpine, K.D.
1990: Chapter 6: The Continental Margin around Newfoundland. *In* Geology of the Continental Margin of Canada, M.J. Keen and G.L. Williams (eds.). Geological Survey of Canada, Geology of Canada, no. 2, p. 239–292.

Shimeld, J.W.
1994: Development of an Algorithm to Detect Subsurface Fractures Using Conventional Well Logs and Fuzzy Inference: Practical Application at the Terra Nova Oil Field, Offshore Newfoundland. M.Sc. thesis, Dalhousie University, 148 p.

Zadeh, L.
1965: Fuzzy Sets. Information and Control, v. 8, p. 338–353.

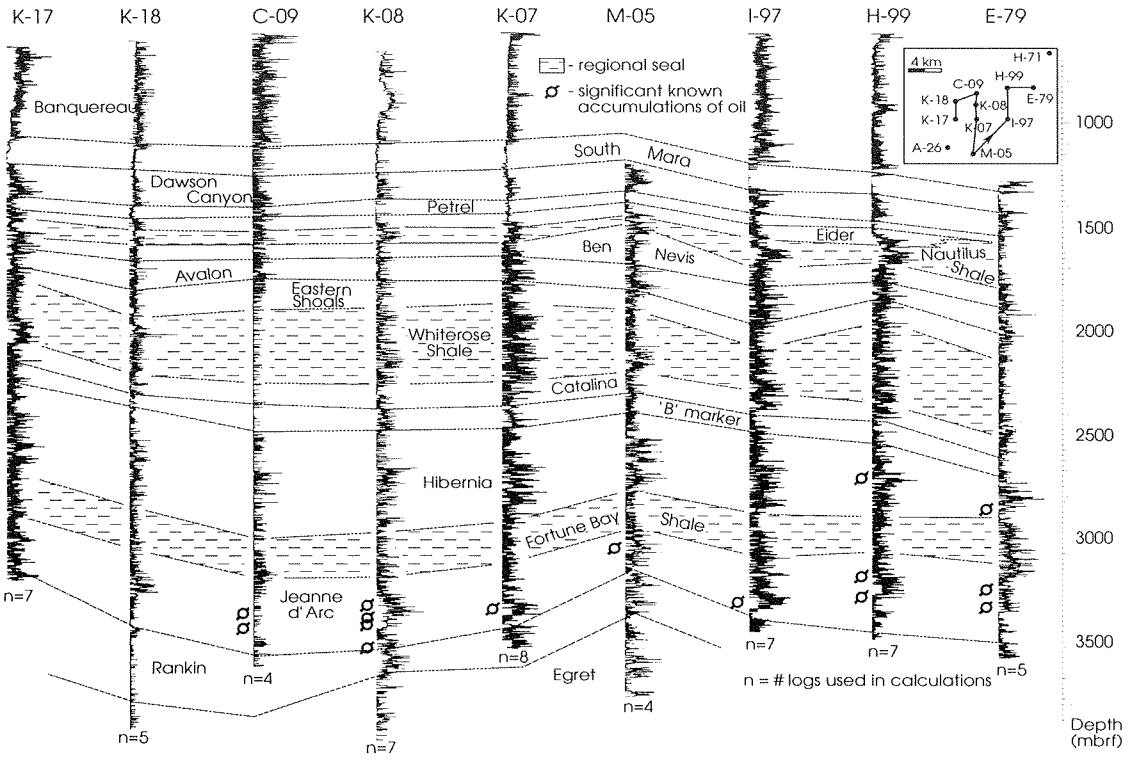

Figure 3. *Summary of fracture indices at Terra Nova.*

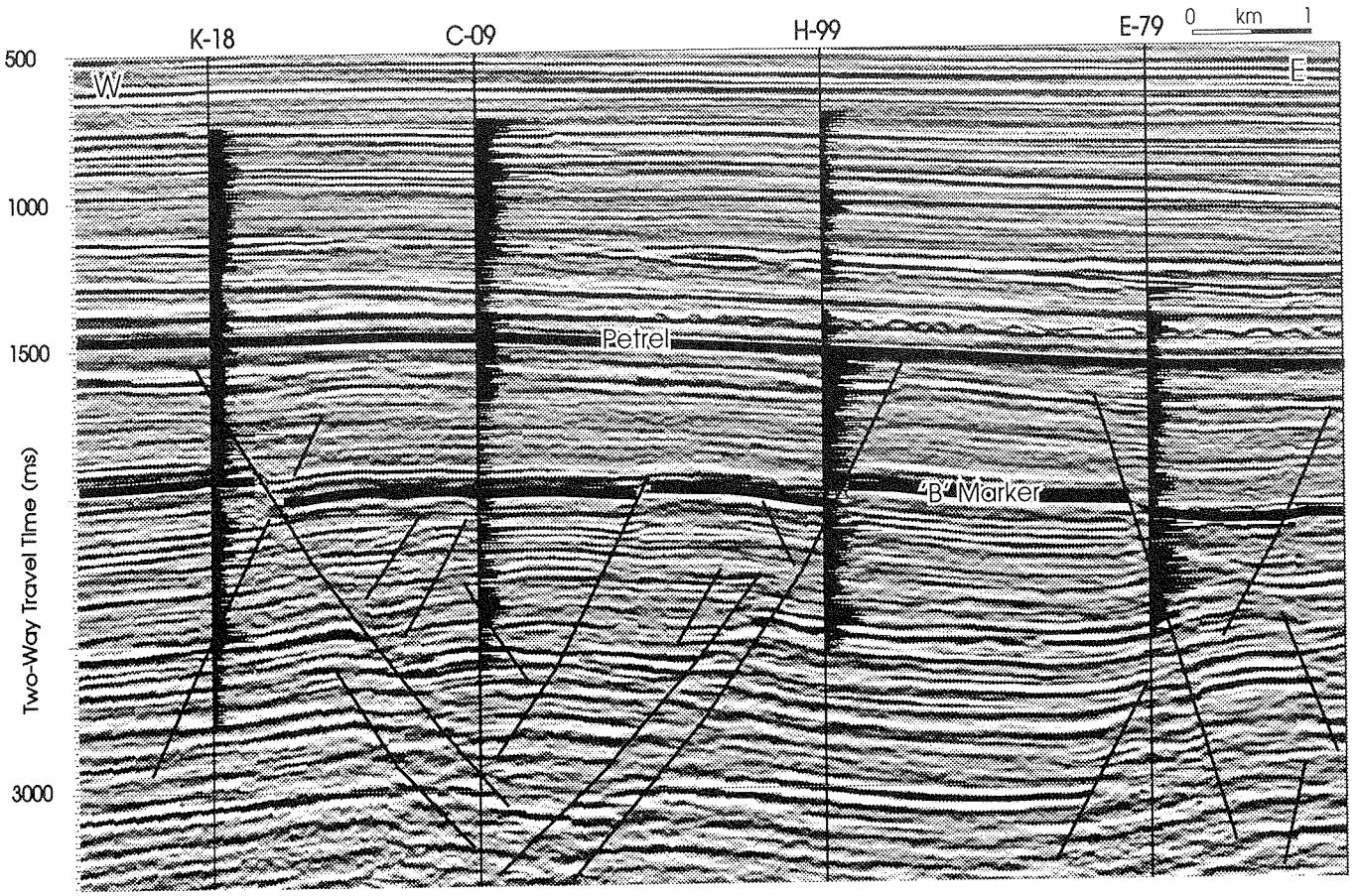

Figure 4. *Integrating fracture indices with seismic data, K-18 to E-79. West to east section across Terra Nova (see Figure 1 for well locations).*

MATURATION MODELLING FOR KINEMATICS OF HYDROCARBON GENERATION AND PREDICTION OF HYDROCARBON COMPOSITION: EXAMPLES FROM THE JEANNE D'ARC BASIN

D.N. Skibo and J.S. Bell

Geological Survey of Canada, 3303-33rd Street N.W., Calgary, Alberta T2L 2A7

INTRODUCTION

A detailed study of hydrocarbon generation has been compiled for the HIBERNIA K-18 and TERRA NOVA K-08 wells that are located on opposite flanks of the Jeanne d'Arc basin. Each well penetrates a major oil accumulation. Four topics were considered: 1) source rock characterization, 2) source rock maturation, 3) hydrocarbon generation, and 4) hydrocarbon expulsion.

METHODOLOGY

The results from GSC and other studies (well log measurements, biostratigraphic and chronostratigraphic studies, Rock Eval pyrolysis, GC/MS, %Ro vitrinite reflectance) were summarized and integrated with the above items. Subsidence histories were re-evaluated using porosity and thermal conductivity parametric systematics calculated from well-log and lithologic data and then compared to results calculated using Basin-Mod software.

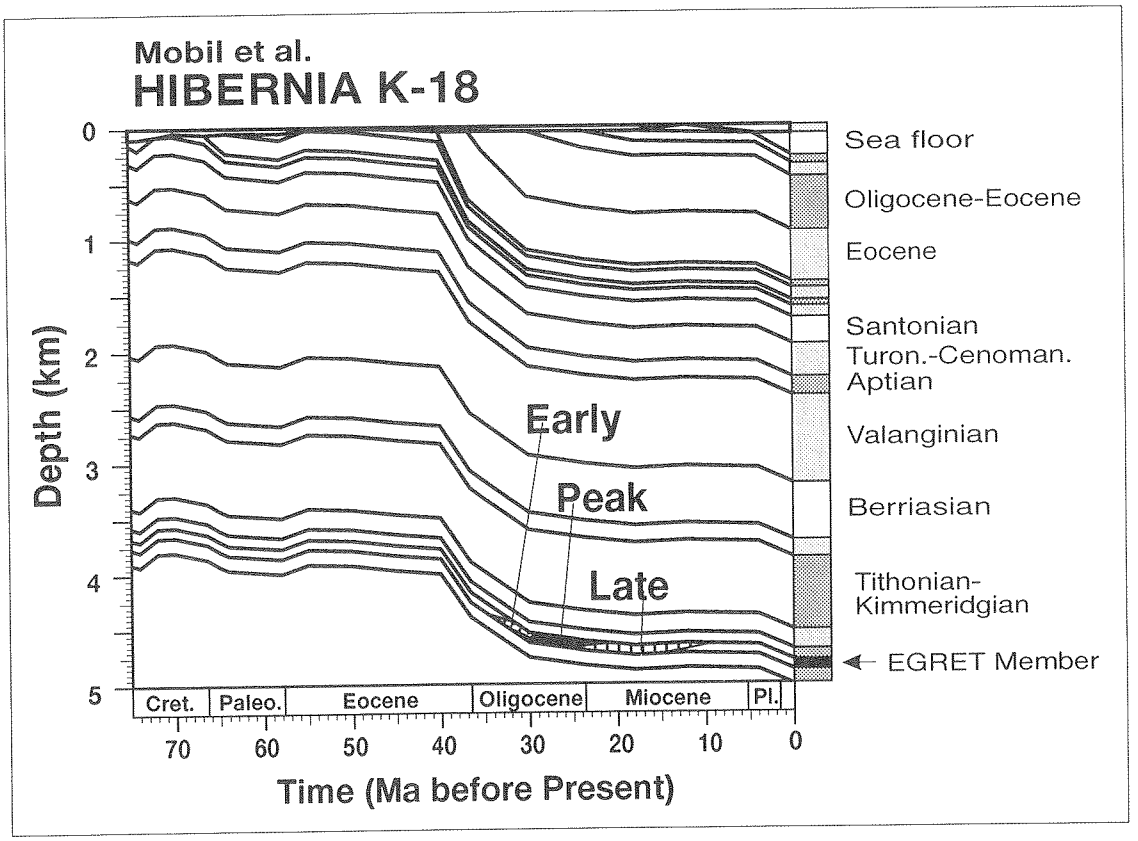

Figure 1. Subsidence and maturation history of Hibernia K-18 modelled with BASIN-MOD.

Kinetic models of hydrocarbon generation were derived from published hydrous pyrolysis studies on Type II (and some Type I) kerogen sources. Secondary reaction kinetics were obtained from models fitted through least-squares analyses to published hydrous pyrolysis experimental data.

Quantity and timing of source rock hydrocarbon expulsion was calculated and the results were compared for two models of overpressuring and hydrocarbon expulsion. Where possible, analogue studies (including deeper sections modelled seismically) were made from results for hydrocarbon generation history from these two wells. Some uncertainties exist in the model calculations of hydrocarbon generation (quantities, type and timing) due to biostratigraphic imprecision and limitations in knowledge of the chemical, physical and geological processes involved in basin evolution.

RESULTS

The subsidence and maturation history of the Egret member at the Hibernia K-18 well site is shown in Figure 1. Vitrinite Reflectance levels and subsurface temperatures for Hibernia K-18 are shown in Figure 2, as are modelled pressure profiles which coincide closely with measured values. Figure 3 presents modelled pressure and temperature history through time for a horizon at the base of the Egret member source rock.

Figure 4 shows the predicted composition of the hydrocarbons generated from the Egret member at the Hibernia K-18 well site. As Table 1 shows, there is significant correspondence between the modelled values for the composition of oil that would be expelled at the present time and those measured on actual samples. This lends credence to the validity of the

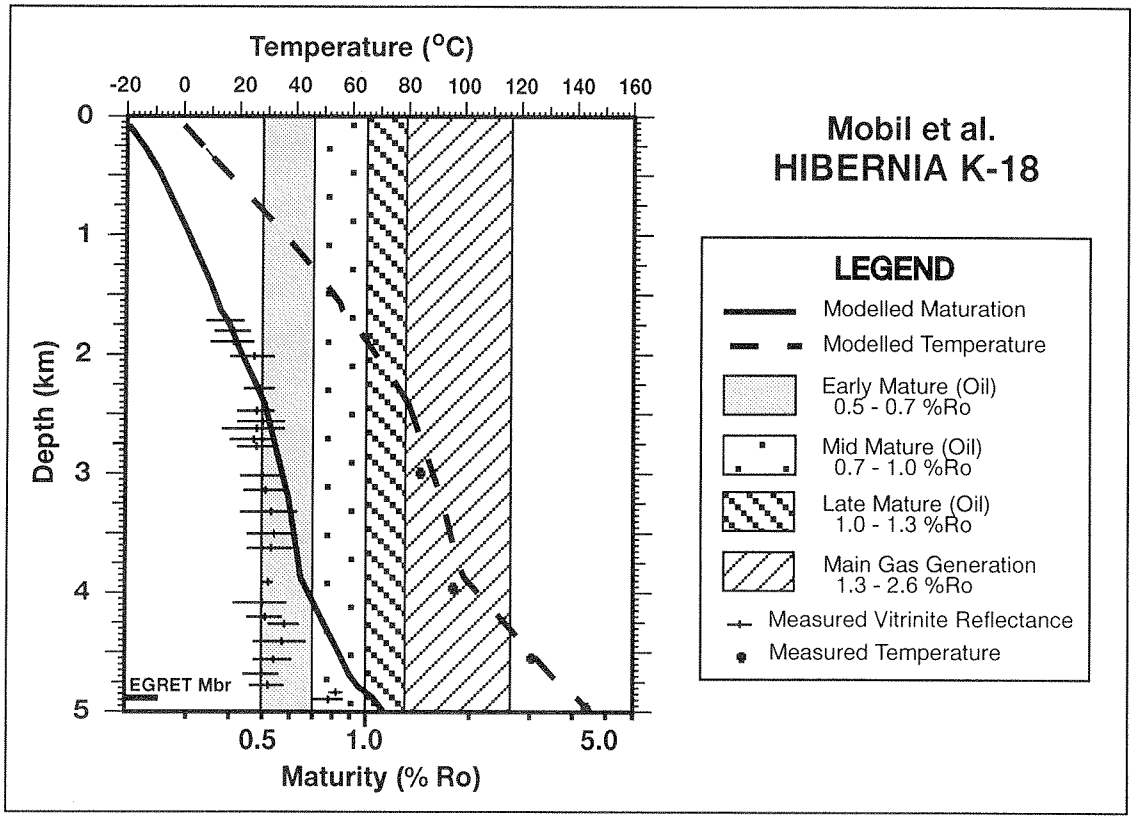

Figure 2. Measured subsurface temperatures and vitrinite reflectance values at Mobil et al. Hibernia K-18, compared to modelled values of these parameters.

proposed new kinematics. However, there is some discrepancy. This could be due to the effects of overpressuring, which were not taken into account during compositional modelling. On the other hand, if maturation proceeded slightly further than modelled here, the predicted compositions would be more nearly in accord with those that are observed. This scenario would be feasible if the oil recovered from Hibernia K-18 was generated from the Egret Member in a downdip site and migrated up to its present location. From a structural point of view, this is highly likely to have occurred.

If it proves feasible to predict the level of hydrocarbon maturation and the composition of any oil present prior to drilling, it will not only assist exploration, but it will also make it possible to assess the economics of refining any discovered oils.

Table 1

Comparison of Solvent Extract/Liquid Chromotography on Hibernia K-18 (sample 4890 m) with calculated composition of present day oil (Fig. 4)

Component	mg/g TOC observed	Calculated mg/g TOC at Present Day
Total Extract Yield	513.3	–
% Hydrocarbons	69.1	70.0
% C15+ Components	18.2	25.0
% C6–C15	40.3	30.0
% C2–C5	28.8	28.0

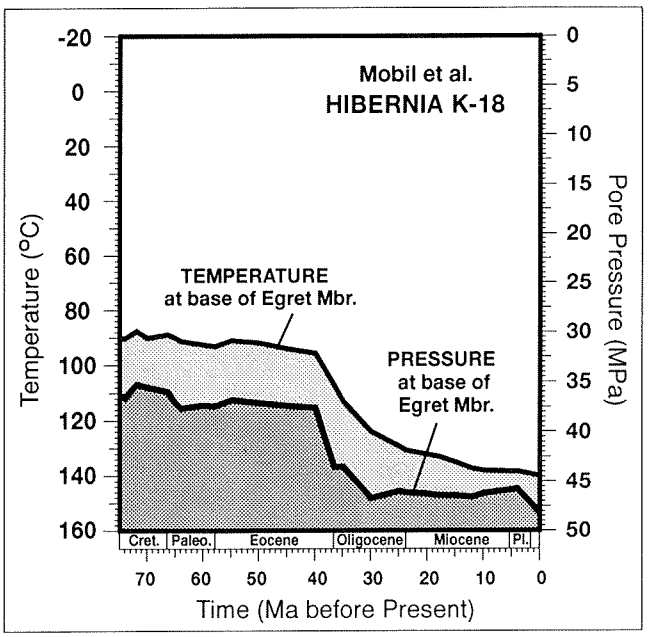

Figure 3. *Modelled pressure and temperature changes between Late Cretaceous time and the Present at the Hibernia K-18 well site.*

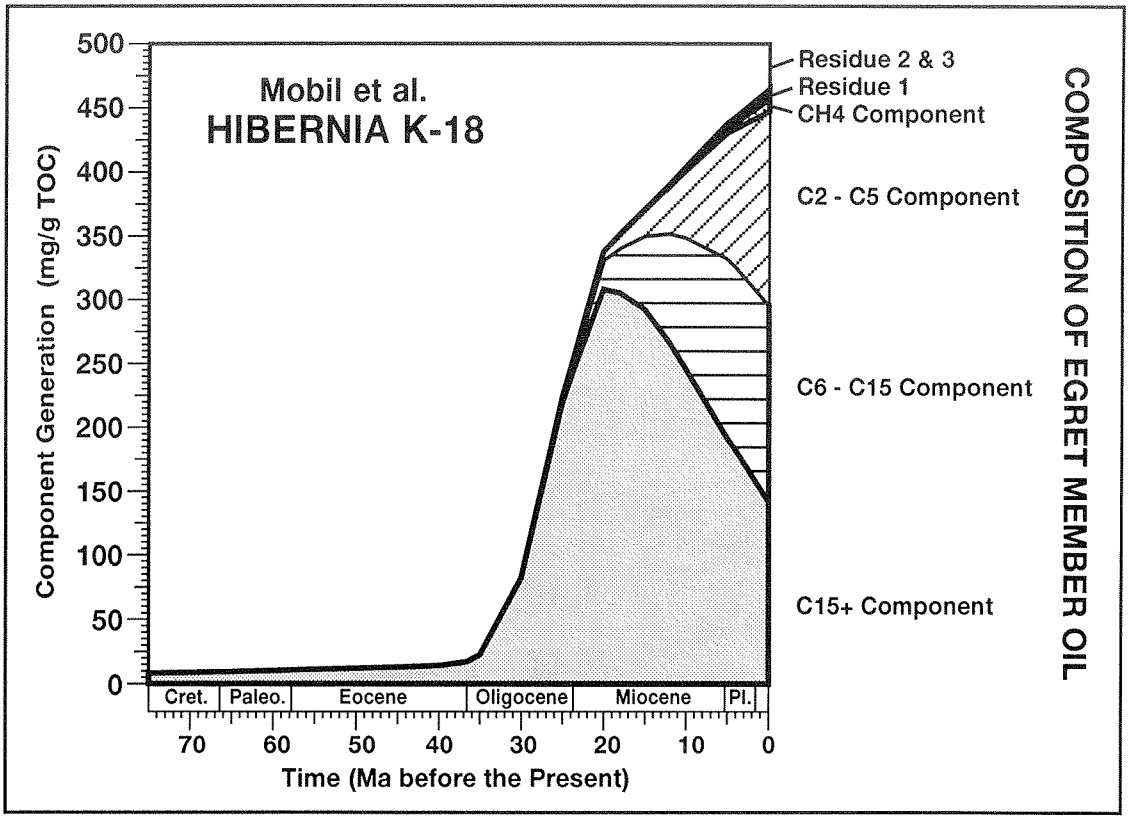

Figure 4. *Variation in composition of oils expelled from Egret Member source rocks at Hibernia K-18, based on kinematic modelling.*

HYDROCARBON CHARGE MODELS FOR EAST COAST BASINS: A STATUS REPORT

M.A. Williamson

Atlantic Geoscience Centre, P.O. Box 1006, Dartmouth, Nova Scotia B2Y 4A2

BACKGROUND

The Hydrocarbon Charge Modelling Project (HCMP) is a multidisciplinary effort to quantify the dynamic interaction of physical, chemical, geological and oceanographic processes that have controlled the distribution of hydrocarbons within Canada's offshore east coast frontier basins (Fig. 1).

The program of research is executed through an association between the Geological Survey of Canada, Atlantic Geoscience Centre (AGC) and Institute of Sedimentary and Petroleum Geology (ISPG), several petroleum exploration and production companies, Dalhousie University Department of Earth Sciences and NSERC. This association involves several joint research ventures supported through industry and government funding.

The development of genetic models of the generation, expulsion, migration and accumulation of petroleum will assist in efforts to assess the remaining undiscovered resource and define the major geological risks and uncertainties associated with further frontier exploration and production.

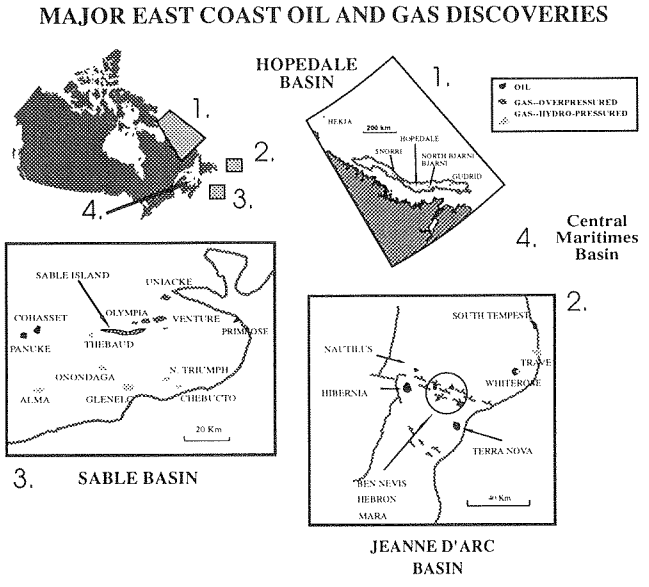

Figure 1. *Schematic view of major east coast oil and gas discoveries.*

WHY?

It might appear that the objective of the HCMP is the prediction of what we already know!!, i.e., that in both the Jeanne d'Arc and Sable basins, a prolific hydrocarbon charging system has been in operation and has worked. So what is the point of developing sophisticated models to show that this has been the case? This view would be credible if the HCMP was tasked only to reconstruct regional charge models, if charge modelling was restricted to reconstruction of source rock systems alone and if every wildcat drilled into the basin had been successful.

Regional charge models will inevitably fall out of the research process, however the HCMP is specifically focussed on resolving practical exploration issues in the basins of interest and by definition requires the reconstruction of the interplay between source rock, reservoir (secondary migration conduits) and seal systems.

A selection of these practical issues include:

- Origin of heavy, biodegraded oil accumulations in Jeanne d'Arc Basin.
- Risk of shallow targets containing biodegraded accumulations.
- Total basin resource estimates–proportion lost to degradation.
- Post-mortem model review of instances where the charging system has failed, i.e., dry and abandoned wells.

- Source rock potential and charge history of the area to the west of the Flying Foam structure.
- Reservoir potential and charging mechanisms of the Cretaceous–Cenozoic delta-turbidite-fan depositional complex, Jeanne d'Arc Basin.
- Generation timing in Jeanne d'Arc Basin depocentre (Adolphus area), salt as vertical migration conduits.
- Timing of and potential for long distance lateral migration from Jeanne d'Arc Basin depocentre to the south where the source rock has not matured.
- Nature and origin of overpressures in the Sable Basin.
- Overpressured versus hydropressured gas reserves to be discovered in the Sable Subbasin.
- Charge origin and history of Panuke/Cohasset type oils, Sable Subbasin.
- Regional sequence and seismo-stratigraphic framework of the Central Maritimes Basin (CMB).
- Regional source rock, reservoir and seal dynamics in the CMB.
- Reservoir potential in CMB.
- New play potential in the CMB.

THE GEOSCIENTIFIC SCOPE

In order to develop charge solutions to some of the problems outlined above, the HCMP conducts research on geologic processes that occur on the molecular to basin scales. In the development of quantitative, integrated models we are faced with making numerous assumptions about the nature of the physical and chemical processes controlling hydrocarbon generation and migration and about the lithostratigraphic framework of the basins within which the fluids have moved and accumulated. Much of the research effort put into the HCMP is designed to better constrain certain of these key unknowns or subsurface parameters.

During our efforts to better constrain many of these assumptions, we inevitably develop tools and/or concepts of potential use in other basins or in other geoscientific fields of endeavour. An example of this is our general use of petrophysical well log information coupled to computer learning algorithms (fuzzy inference and neural network modelling) to extract detailed information about a formation's permeability profile, source rock geochemistry, and fracture distribution (see Huang et al. and Shimeld et al., this volume).

The research approach employed in the HCMP is very much an iterative one. It involves the development of a series of initial models from which we gain insight into the sensitivity of the results to specific subsurface parameters and or process assumptions. We also derive clues regarding the nature and extent of the actual physical and chemical interactions. These clues also point out weaknesses in our numerical treatment of such processes. This then becomes the basis for further parameter research, the results of which ultimately find their way into later generation models.

In essence, all aspects of the HCMP's assumptions regarding basin processes and/or specific geological parameter assumptions are constantly under review. Table 1 captures the scope of such review.

TOWARDS SOLUTIONS

The activities carried out under the HCMP umbrella integrate information, data and knowledge from a broad range of disciplines (Fig. 2). The following lists several of these activities (and are detailed elsewhere in this volume) each of which is annotated with a review of the contribution of the particular activity to the broader HCMP.

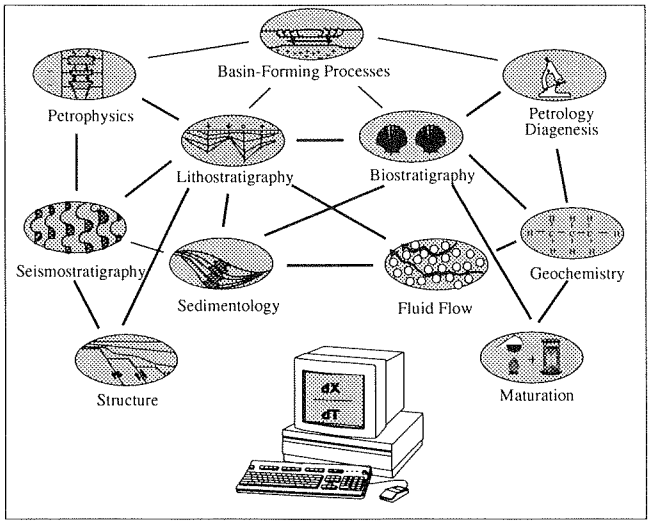

***Figure 2.** Hydrocarbon charge modelling at AGC. An integration of disciplines, knowledge and data.*

Table 1

Common parameter assumptions used in modelling	HCMP efforts to constrain assumptions
Compaction Processes: Porosity–Permeability Fluid Flow mechanisms Thermal Processes: Steady state vs. Transient Conductivities Maturation Processes: Vitrinite Geochemistry Expulsion Processes: Efficiency/Yield Timing Secondary Migration Processes: Aquifer geometry Porosity/Permeability Faults Entrapment Processes: Seal Properties Degradation	Measurements of k Permeability prediction Compaction experiments: mud ► shale Physical and chemical properties of shales Matrix conductivity from logs Reflectance measurements Biostratigraphic resolution Fission track data Fluid inclusion data Activation energies Biomarker data Source rock mineralogy Source rock lithofacies Source rock chemofacies Source rock cyclicity/deposition Reservoir mapping Fault plane sections 1-D to 2-D fluid migration Intergrated log ► faults

PETROPHYSICAL, GEOCHEMICAL AND DEPOSITIONAL FEATURES OF THE EGRET MEMBER (KIMMERIDGIAN) OIL SOURCE ROCK, JEANNE D'ARC BASIN, OFFSHORE EASTERN CANADA

In the absence of core or outcrop, we really know very little about the detailed nature of the source rock system in the Jeanne d'Arc Basin, particularly those features of the system that control expulsion efficiencies etc. This project was designed to add to the Rock-Eval screening of cutting samples for the 19 well penetrations of the Egret. The project maximizes our knowledge of the operating source rock system through detailed petrophysical log and cutting examination and neural network modelling. A complete characterization of the source rock is important for estimation of expulsion efficiencies and genetic potential.

PRELIMINARY 2-D MODELS OF HYDROCARBON MIGRATION IN THE JEANNE D'ARC AND SABLE BASINS, OFFSHORE EASTERN CANADA

Preliminary 2-D models of hydrocarbon migration in the Jeanne d'Arc and Sable basins, offshore eastern Canada represents our effort to understand the interplay among the evolving source rock, reservoir and seal systems. The timing of 3 phase (water, oil, gas) migration events at select areas in the Jeanne d'Arc and Sable basins is being examined in an effort to reproduce specific pool filling histories. These sophisticated 2-D 3 phase migration models use much of the information and data generated by other projects in the study and are constructed using the BasinMod™ 2-D software by Platte River Associates.

MEASUREMENT AND ANALYSIS OF PHYSICAL PROPERTY TRANSITIONS: MARINE CLAYS TO SHALE

At many stages in the charge modelling process, particularly the 2-D migration modelling, assumptions are made regarding the clay to shale compaction process. How we model compaction impacts reconstructions of an areas thermal, fluid pressure and subsidence history. This project is providing basic experimental data on how to represent clay to shale compaction in our basin reconstructions. The emphasis here is on the early history of clay compaction (i.e., from deposition to about 800 m depth).

CRITICAL DEPTH OF BURIAL OF SUBSIDING SHALES AND ITS EFFECT ON ABNORMAL PRESSURE DEVELOPMENT

As for the project above, this research activity is geared to better constrain seal compaction models. The emphasis however is on the deeper compaction and diagenetic processes (i.e., 800 m to more than 6000 m). This project has included a systematic petrophysical characterization of the east coast shale seal formations and contributes broadly to the HCMP modelling/ compaction assumptions.

MINERALOGY AND GEOCHEMISTRY OF THE EGRET MEMBER SOURCE ROCK, JEANNE D'ARC BASIN, OFFSHORE NEWFOUNDLAND

This project contributes to our knowledge set regarding the specific inorganic mineral character for the Egret source interval. The project aids the general effort (see above) to reconstruct the source rock deposition/ preservation history.

THE RISK OF ENCOUNTERING HEAVY DEGRADED CRUDES IN THE JEANNE D'ARC BASIN: AN EVALUATION

This is a site specific charge model project that combines detailed structural and stratigraphic mapping together with organic and inorganic geochemistry and migration modelling to reconstruct the pool filling and post fill degradation histories of heavy oil accumulations. The project also draws upon others in the series that are defining the nature of the precise subsurface parameters.

PERMEABILITY PREDICTION USING COMPUTER NEURAL NETWORKS: APPLICATIONS IN THE VENTURE GAS FIELD, OFFSHORE NOVA SCOTIA

Our 2-D 3 phase fluid migration models are very dependant on estimates of lateral and vertical formation permeability. In the general absence of hard data (i.e., measurements) on formation permeability, particularly for the less permeable strata (e.g., shales and silts), this project is applying innovative, computer neural network modelling technologies to compute permeability-depth profiles.

FRACTURE MAPPING USING CONVENTIONAL WELL LOGS AND 3-D SEISMIC DATA IN THE TERRA NOVA OIL FIELD, OFFSHORE NEWFOUNDLAND

Faults and fractures represent important fluid migration pathways, yet we know little about their fluid transmissive capacities through time. This project uses fuzzy inference technology to detect fractures in and around well bores using conventional well log data. This then is merged to 3-D seismic data to establish the distribution of the more important fracture/fault conduits.

SEQUENCE STRATIGRAPHIC ANALYSIS OF THE LATE CRETACEOUS–PALEOGENE ROCK UNITS IN THE JEANNE D'ARC BASIN, OFFSHORE NEWFOUNDLAND

This stratigraphic interval preserves a complex delta-fan-turbidite depositional complex comprising numerous, unconformity bound units. This project is developing a depositional model to assist reservoir/seal prediction in the interval and to facilitate efforts to reconstruct post charging tectonic history of heavy oil accumulation. This will help model the paleo-hydrodynamics of such accumulations and contribute to efforts to understand the degradation phenomenon.

STRATIGRAPHIC CORRELATION AND PETROLEUM GEOLOGY OF THE CENTRAL MARITIMES BASIN, EASTERN CANADA

This project is developing a detailed sequence-seismo stratigraphic framework for the basin within which to fully consider the context of the numerous gas shows (and one discovery) encountered during previous drilling activity (1960s and 1970s). Coupled to a modelling component, this project will assess the basins further potential and principal risks.

INTEGRATING GEOSCIENTIFIC DATA, KNOWLEDGE AND INTERPRETATIONS FOR EAST COAST BASINS

Underpinning all our research efforts within the HCMP is access to a vast, good quality and comprehensive well, and seismic database. The interchangeable and portable nature of these databases is key to the efficient execution of the projects contributing to the HCMP.

Other activities contributing to the HCMP, but not reported in this volume, include the application of Fission Track analysis to constrain thermal history; detailed biostratigraphic syntheses of the Cenozoic intervals; and, log and sample based thermal conductivity modelling to constrain thermal modelling.

The success of the project is entirely due to the teamwork and scientific contributions of several Geological Survey of Canada, Dalhousie University and contracted staff including: A. Agrawal, B. Altheim, J. Bateman, K. Coflin, K. Desroches, K. Dickie, R. Fensome, M. Fowler, M. Gibling, A. Grant, Z. Huang, J. Katsube, S. King, G. Li, D. McAlpine, P. Moir, K. Moran, V. Pascucci, C. Ravenhurst, T. Rehill, T. Semper, J. Shimeld, C. Smyth, F. Thomas, J. White, G. Williams, M. Williamson, A. Wray, M. Zentilli.

We are grateful to the many companies, institutes and organizations that have provided support (i.e., funding, in kind or intellectual) to the project. These include: Mobil Canada, Amoco Canada, LASMO Nova Scotia, Norcen Energy, Chevron Canada, Petro-Canada, Husky Oil International, Shell Canada, UNOCAL of California, Chevron USA Research, Platte River Associates Denver, The Office of Energy Research and Development (OERD, Ottawa), NSERC, and the Geological Survey of Canada.

THE RISK OF ENCOUNTERING BIODEGRADED CRUDES IN THE JEANNE D'ARC BASIN

M.A. Williamson, K.C. Coflin, A. Agrawal, Z. Huang, K. Dickie, and K.D. McAlpine

Atlantic Geoscience Centre, P.O. Box 1006, Dartmouth, Nova Scotia B2Y 4A2

M.G. Fowler

Geological Survey of Canada, 3303-33rd Street N.W., Calgary, Alberta T2L 2A7

BACKGROUND

In the decade following the discovery of the Hibernia field in 1979, 16 further oil discoveries were made in the Jeanne d'Arc Basin, several of which included, in their shallower sections, pools of heavy (API less than 20°) crude oil. Subsequent chemical analyses determined that these heavy oils were due to extensive biodegradation of varying degrees of severity (see Table 1, Fig. 1). Although geochemical data are not available for all heavy oil accumulations, some 12 individual pools of biodegraded oil have been documented. Table 1 indicates *heavy oil* wells, with depth ranges, reservoir temperatures, stratigraphic occurrence and API gravity.

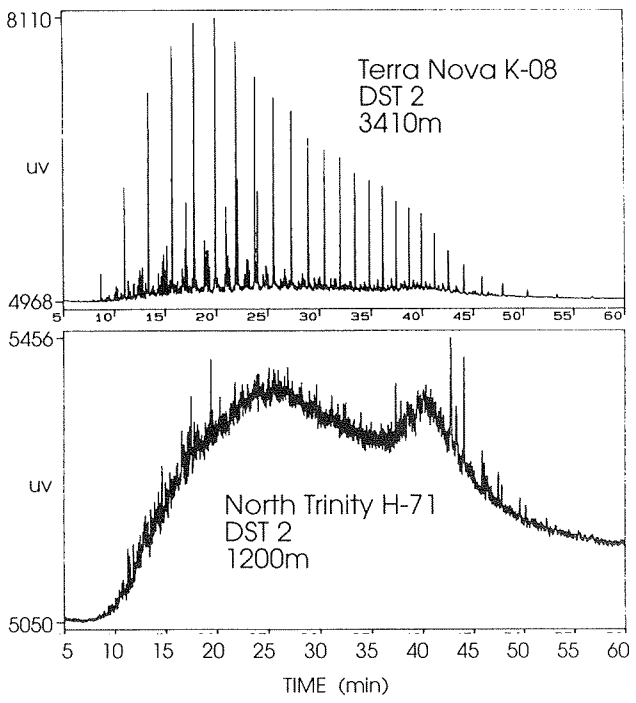

Figure 1. *Saturate gas chromatogram of an unbiodegraded oil from Terra Nova K-08 (DST 2) and a biodegraded oil from North Trinity H-71 (1200 m). Note the large unresolved hump of compounds in the biodegraded oil.*

In the absence of a genetic model to explain the occurrence of biodegraded (heavy) oil in the Jeanne d'Arc Basin, exploration of shallow (less than 2300 m) targets remains a high risk activity. It is possible that the biodegradation is the result of processes operating uniformly throughout the basin at depths shallower than 2300 m (temperatures less than 80°C). However, several occurrences of undegraded crudes at shallow depths counter a uniform biodegradation model. At Hibernia O-35 for example, 8 DST tests from 2005 to 2538 m recovered normal, high gravity crudes (30° API). At the West Ben Nevis B-75 location, heavy degraded crudes were encountered at 2445 m and regular crudes were recovered from as shallow as 2002 m. The Mara M-54 location preserves a mixed, biodegraded and nondegraded crude accumulation at 2704 m. These occurrences suggest that the degradation process operating within the basin has been selective and is likely due to a combination of factors linked to the specific post fill hydrodynamic history of the locations in question. The Mara accumulation in particular has been explained as a result of local Cenozoic tectonics (associated with unconformities and late fault movements) that breached the local reservoir system allowing ingress by degrading fluids.

In order to establish genetic models of the biodegradation process operating throughout the basin, the Atlantic Geoscience Centre, the Institute of Sedimentary and Petroleum Geology and several oil companies have combined in a collaborative project to place each biodegraded occurrence into a firm and detailed structural and stratigraphic context and to develop a dynamic understanding of the pool filling

Table 1

Biodegraded Heavy Oil: Jeanne d'Arc Basin

Well Name	Depth (m) Top	Base	Temp °C	Formation	Test#	API	Biodegraded
East Rankin H-21*	1357	1394		Eastern Shoals	DST2	~17.6°	yes
	1444	1450		Eastern Shoals	DST1	~17.6°	NA
Hebron I-13	1866	1876	50	Ben Nevis	DST10	19°	yes
	1905	1915	51	Ben Nevis	DST9	13.6°	yes
	2722	2735	73	Catalina	DST8	16.9°	NA
Kings Cove A-26	1245			Dawson Canyon			yes
	1535			Ben Nevis			yes
	1540	1550		Ben Nevis	DST4	13–18°	NA
	1559			Ben Nevis	RFT1	12.1°	NA
Mara M-54	1851	1857	58	South Mara Unit	DST3	22°	yes
	2403	2408	73	Dawson Canyon	DST2	20.5°	yes
	2704	2708	79	Avalon	DST1	11°	yes
North Trinity H-71	1200		36	Banquereau			yes
	1412		42	South Mara Unit	RFT2	11.9°	NA
	2830			Ehiterose Shale			yes
South Brook N-30*	819	840		Banquereau	DST2	13.7°	NA
	1462	1467		Jeanne d'Arc	DST1	~13.7°	NA
Terra Nova K-17	1543	1562		Ben Nevis	DST2	14.6°	NA
West Ben Nevis B-75	2445	2465	82	Eastern Shoals	DST6	22.8°	yes

NA–not analysed
*–wells drilled with oil-based mud

history and post filling hydrodynamics of each accumulation. Models derived from this should be able to explain the occurrence of biodegradation at shallow depths and the occurrence of regular crudes at similar depths. Such models will be used to assist in the detailed risk assessment of shallow targets/plays and in the production of basin wide resource estimates that fully discount estimates of the total resource potential of the basin for losses due to biodegradation.

BIODEGRADATION

Biodegradation of crude oils is generally considered to occur in shallow reservoirs under aerobic conditions. Some recent work has suggested that anaerobic bacteria may also be responsible, but this mechanism remains controversial. Certain conditions that appear to be needed for biodegradation to take place include an incursion of fresh meteoric water containing nutrients into reservoirs at relatively low temperatures. While some bacteria can live at higher temperatures, 80°C appears to be the maximum temperature at which biodegradation can occur and the process is most severe between 20 and 60°C. Bacteria live in the aqueous phase and hence biodegradation takes place at the water-oil interface. From a chemical standpoint, biodegradation of hydrocarbons is a bio-oxidation process with alkanes and aromatics being transformed first into oxygen-containing derivatives with these likely being attacked subsequently by anaerobic bacteria. The biodegradability of C_{15+} hydrocarbons is well known and is commonly used to rank oils as to the extent of their biodegradation. Water-washing typically accompanies the biodegradation of petroleum and results in the selective loss of lighter hydrocarbons, especially aromatics.

STRUCTURE AND STRATIGRAPHY

The structure and stratigraphic mapping component of this project is detailing the geometry of each occurrence with particular emphasis on features that might have been able to provide ingress of circulating fluids into the local reservoir system. This includes faults, down cutting channel systems and unconformities. It is understanding the nature and extent of the numerous Late Cretaceous–Late Eocene unconformities that is thought to be key to any model that requires the periodic breaching of an oil wet reservoir

system. Increasing our level of understanding of these unconformities, and post fill Cenozoic (charge) tectonics in general, is the focus of this part of the study.

GEOCHEMISTRY AND MIGRATION MODELLING

Biodegraded oils in the Jeanne d'Arc Basin are generally found in shallow reservoirs indicating that degradation is most likely associated with the incursion of meteoric waters into these zones. At Mara M-54 there is evidence of mixing between biodegraded and more mature undegraded hydrocarbons. One scenario that has been proposed to occur at Mara is that there were two phases of oil generation/migration with the earlier oil being biodegraded within the reservoir and the later oil entering when the reservoir was more deeply buried, when conditions were not conducive for microbial activity (von der Dick et al., 1989). In wells such as Kings Cove A-26 and South Brook N-30, degraded hydrocarbons are found at depths where it is feasible to assume that biodegradation is occurring today.

Organic geochemical analyses have determined the degree and extent of biodegradation for most occurrences of heavy oil (Table 1, Fig. 1). Furthermore, extract analysis shows that the oil emplaced in the pools prior to biodegradation was generated from the Late Jurassic Egret Member (i.e., the same source-rock responsible for most of the other, nondegraded crudes discovered in the basin). A permeability versus oil saturation plot (Fig. 2) show high degrees of oil saturation in the permeable as well as in the less permeable zones of the reservoir at Hebron I-13. Since it is hard to envisage the migration of biodegraded and relatively viscous heavy hydrocarbons into the lower permeability zones of the reservoir, Figure 2 leads us to believe that the pools were initially charged with regular crudes and suffered post-filling, in situ geochemical alteration due to microbial activity.

The hydrocarbon charge history of the heavy oil accumulation at Hebron I-13 has been simulated with a 2-dimensional numerical model, using BasinMod™ software, based on detailed structural and stratigraphic mapping in the area. The example given (Fig. 3) shows simulated oil saturation at 20 Ma in a cross-section from the Hebron fault block through to the Ben Nevis area (for more details of our 2-D migration modelling in the area, see Williamson, Huang and Moir, this volume).

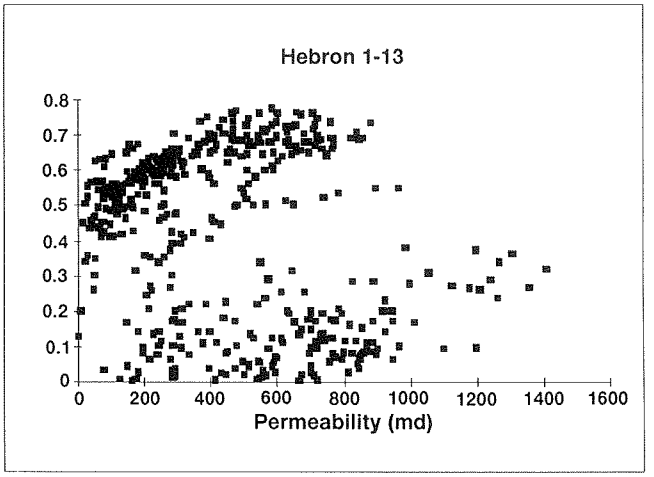

Figure 2. *Oil saturation versus permeability for the 1860–1970 m interval of Hebron I-13 (sampled at 0.2 m interval).*

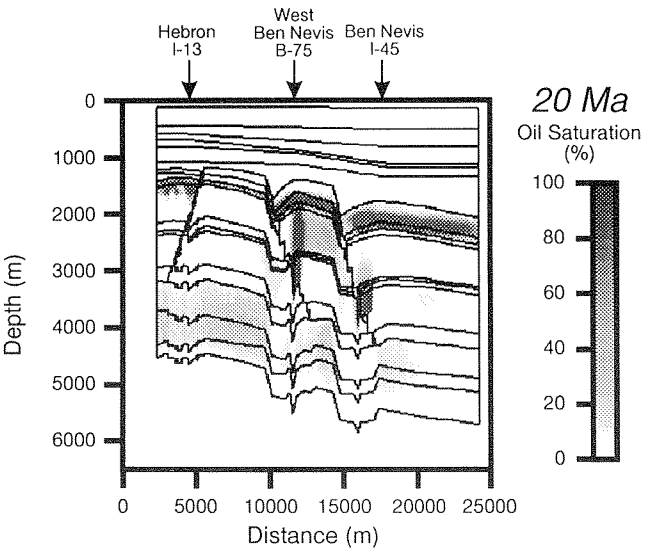

Figure 3. *Two dimensional migration model for the Hebron to Ben Nevis area (see Williamson et al., this volume).*

Migration models for the Hebron location indicate that the pool underwent two episodes of charging with hydrocarbons prior to biodegradation. The first migration phase occurred following oil generation deeper in the basin as early as 80 Ma with petroleum migrating essentially vertically, but focused primarily along fault conduits. Such hydrocarbons pooled under a regional shale seal, and moved up-dip to the Hebron accumulation. More recently, oil has been generating directly beneath the Hebron location and has charged the shallower pools through the Hebron fault. This

pool-filling history is supported by fluid inclusion analyses of the Hebron heavy oil reservoirs which indicate an initial hydrocarbon accumulation during a period of quartz overgrowth/cementation, followed by a later phase of accumulation during a subsequent interval of kaolinite growth and quartz fracture/annealing.

RESEARCH IN PROGRESS

Biodegradation mechanisms are being investigated in the light of the distinct fluid-rock interactions and secondary mineral cementation that one would expect to be preserved. Petrographic, SEM, and XRD analyses of the reservoir rocks and isotopic studies of the authigenic cements are in progress to characterize the bio-geochemical processes that affected degradation of hydrocarbons. Ultimately it will be this organic and inorganic geochemistry database, and the structural and stratigraphic framework placed into a dynamic context through fluid migration modelling that will allow us to choose a preferred biodegradation model. Once established, such a model will be used to interpret the nature and apparent selectivity of the degrading mechanisms in the basin.

Models that explain the occurrence of biodegradation within the basin will not only assist in the definition of the risk of encountering heavy oils in further exploration but also in assessing the volume of the basin's total hydrocarbon resource that has been lost to degradation processes.

REFERENCES

von der Dick, H., Meloche, J.E., Dwyer, J., and Gunther, P. 1989: Source rock geochemistry and hydrocarbon generation in the Jeanne d'Arc Basin, Grand Banks, offshore eastern Canada. Journal of Petroleum Geology, v. 12, p. 51–68.

DEPOSITIONAL AND ECONOMIC ASPECTS OF UPPER CARBONIFEROUS COAL MEASURES, MAGDALEN BASIN – SYDNEY BASIN REGION, EASTERN CANADA

A.C. Grant

Atlantic Geoscience Centre, P.O. Box 1006, Dartmouth, Nova Scotia B2Y 4A2

ABSTRACT

Coal seams intersected by exploratory wells in the Magdalen Basin – Sydney Basin region coincide with a "Coal Measures" seismic facies mappable over an area of more than 60 000 km^2. The volume of coal indicated by the extent of this facies could contain more than 70 TCF of coalbed methane. Beneath central Prince Edward Island (P.E.I.) this facies is in the depth range from which coalbed methane is exploited in the United States.

The Coal Measures seismic facies is interpreted as evidence of cyclothem deposition, with depositional cycles that included marine incursions. Evidence for such incursions (agglutinated foraminifera) has been reported from the Sydney Coalfield and from offshore exploratory wells. These findings present the possibility of Upper Carboniferous marine source rocks for conventional hydrocarbon generation. The depocentre for these rocks may have coincided with the zone of evaporite tectonism in Magdalen Basin, where resultant structures form potential traps for hydrocarbons.

INTRODUCTION

Hacquebard (1986) correlated Upper Carboniferous coal zones in exploratory wells with coals in the Mabou and Inverness coalfields on the west coast of Cape Breton Island (Fig. 1). He concluded that the Carboniferous Basin in the Gulf of St. Lawrence is the largest coalfield of eastern Canada. Grant and Moir (1992) proposed that the coal zones coincide with a regionally mappable seismic facies. Grant (1994) interpreted the wide extent of this facies as evidence of cyclothem deposition, including marine incursions. The following brief review notes possible economic implications of these interpretations. Details and background references are contained in the papers cited above.

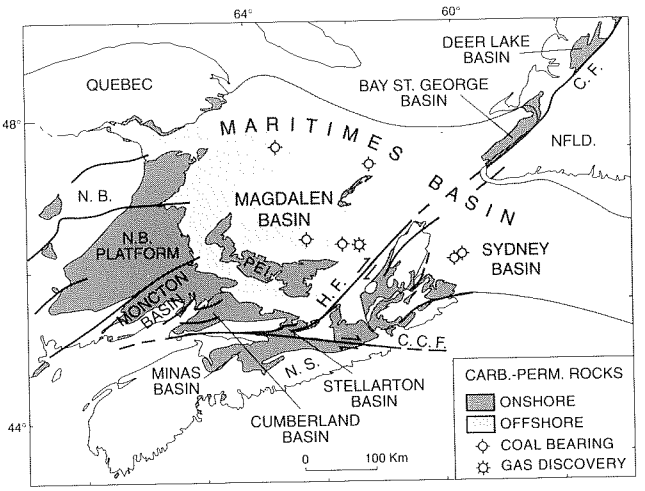

Figure 1. *Distribution of Carboniferous and Permian rocks and major faults in the Maritimes Basin region of Atlantic Canada.*

Geological background

The Magdalen and Sydney basins (Fig. 1) lie within the Permo-Carboniferous Maritimes Basin of Atlantic Canada, a successor basin on Lower Paleozoic rocks deformed by the Taconic and Acadian orogenies. The stratigraphic units in the Maritimes Basin (Fig. 2) generally comprise a relatively flat-lying suite of coarse and fine grained terrestrial siliciclastics with subordinate shallow marine clastics, carbonates and evaporites. Initial stages of sedimentation (Late Devonian–Early Carboniferous) were largely controlled by differential movement of basement blocks within and bordering the basin. In a subsequent phase of gradual subsidence (mid-late Carboniferous) depositional basins expanded and progressively onlapped basement.

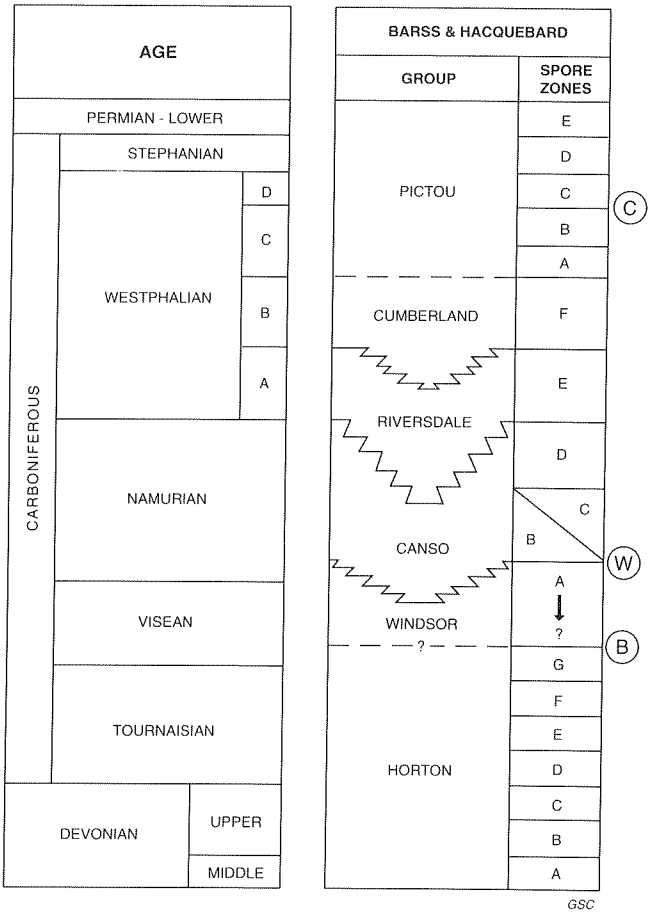

Figure 2. *Stratigraphic diagram for Upper Paleozoic rocks in eastern Canada. Circled letters denote regional seismic markers.*

Data

Interpretations reviewed in this paper are based mainly on multichannel seismic data shot by industry from the late 1960s to early 1980s (ca. 100,000 km; Fig. 3). Subsurface geologic control is available from exploratory wells at 10 offshore locations, and 12 boreholes on P.E.I. (Fig. 4).

MAP OF COAL MEASURES

Grant and Moir (1992) mapped a "Coal Measures" seismic facies over more than 60 000 km^2 (Fig. 4). The character of this facies is illustrated by a seismic record from the Cable Head well site (Fig. 5). There, about a dozen coal seams, ranging in thickness from 0.3–2.4 m, occur over an interval of 500 m at a depth of 2500 m.

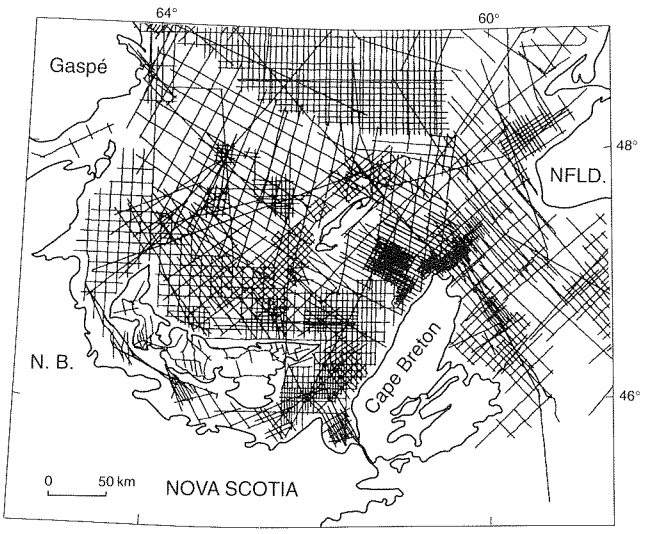

Figure 3. *Industrial multichannel seismic coverage used in this study.*

The coal seams are not resolved individually, but yield a band of reflections of variable amplitude and continuity.

Figure 6 illustrates lateral waxing and waning of the Coal Measures seismic facies, as inferred from development of shallower and deeper bands of similar reflections. Figure 6b is a line drawing of principal reflectors on the entire seismic line, showing shallower and deeper markers with Coal Measures seismic character. This diagram illustrates two points: First, the deeper and shallower markers may indicate deeper and shallower coal seams. These extra seams occur in a structural low (Fig. 4) trending eastward toward the zone of evaporite tectonism. This may indicate that the principal depocentre of the Coal Measures lay within that zone. Second, this section indicates lateral continuity of the Coal Measure seismic facies for over 120 km; the map (Fig. 4) shows continuity for over 400 km.

DISCUSSION

Implications re. coalbed methane

The product of the mapped area of the Coal Measures seismic facies (Fig. 4), and average thickness and number of coal seams intersected by wells, yields an estimate of the coal resource. Grant and Moir (1992) used this volume of coal to evaluate the potential

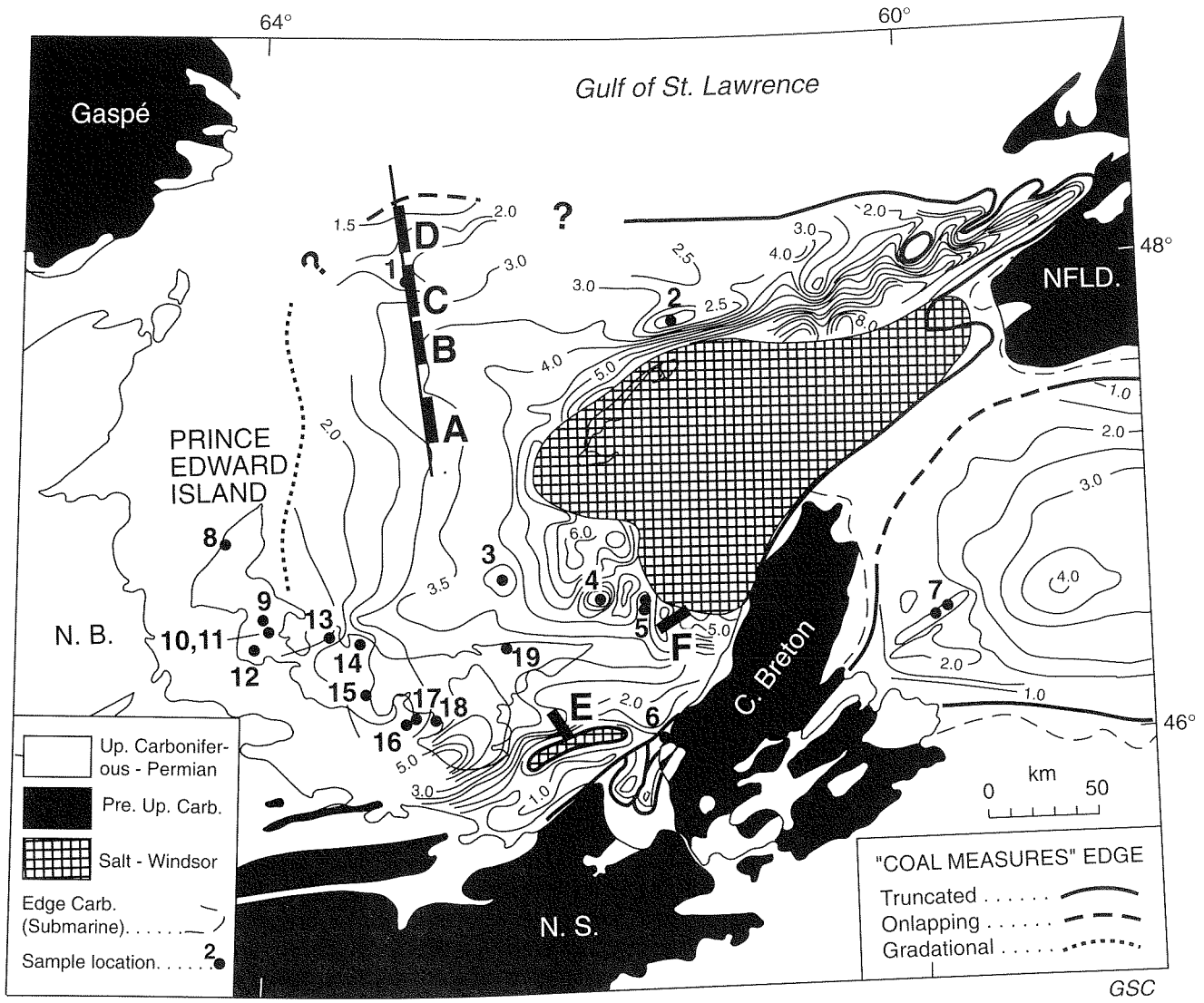

Figure 4. *Map of extent and depth of Coal Measures seismic facies. Contour interval 1 km. Black dots mark wells, heavy lines locate seismic sections. Crosshatching denotes areas of evaporite tectonism. From Grant and Moir (1992).*

resource of coalbed methane (CBM), and showed that even conservative assumptions of methane content yield astonishingly large numbers (e.g., more than 70 TCF). Ten per cent of this resource could lie beneath central and eastern P.E.I. In the United States CBM is produced from the depth range of coal deposits beneath central P.E.I.

The inferred offshore coalfields are larger than coalfields on land, by 2–3 orders of magnitude (Fig. 7). The coalfields in Cape Breton appear to be peripheral parts of two offshore basins that may originally have connected across Cape Breton.

Implications re. marine source rocks

Grant (1994) speculated that the regional continuity of the Coal Measures seismic facies (Fig. 4) expresses cyclothem deposition, including marine incursions. This interpretation is supported by reports of marine forams in Sydney Basin and in offshore wells, and of cyclothem deposits in Sydney Basin. The significance of possible Upper Carboniferous marine deposits in the Magdalen Basin lies in the potential for marine source rocks for hydrocarbons. Such rocks might occur in the original depocentre of the basin, now occupied by the zone of evaporite tectonism. There, the numerous

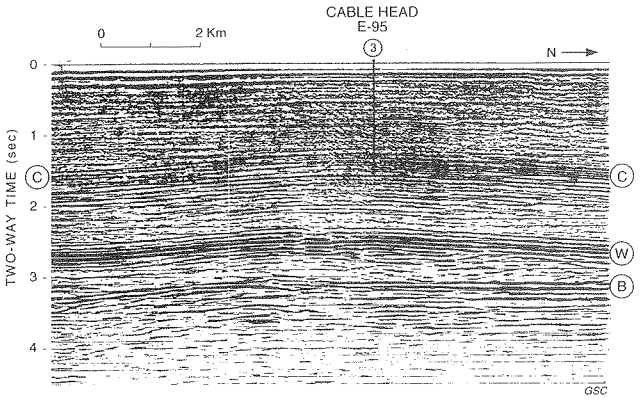

Figure 5. *Industry seismic record through Cable Head E-95 well site (Fig. 4). Letters denote seismic markers; C, Coal Measures (Fig. 2). Chevron Standard Ltd. Line 82-49-11. From Grant and Moir (1992).*

structures provide potential trapping mechanisms. These comments are speculative, as no oil shows were reported from any wells in the Coal Measures. However, none of the wells were necessarily very close to the original depocentre.

CONCLUSION

Evidence exists for a large resource of CBM in the Magdalen Basin – Sydney Basin region. Evidence for Upper Carboniferous marine rocks in the Maritimes Basin presents the possibility of source rocks for oil, which may be trapped in structures related to evaporite tectonism.

ACKNOWLEDGMENTS

This work benefited from input by associates in the Geological Survey of Canada, the Nova Scotia Department of Mines and Energy, and in industry. I particularly thank my colleague Art Jackson for much help in this work.

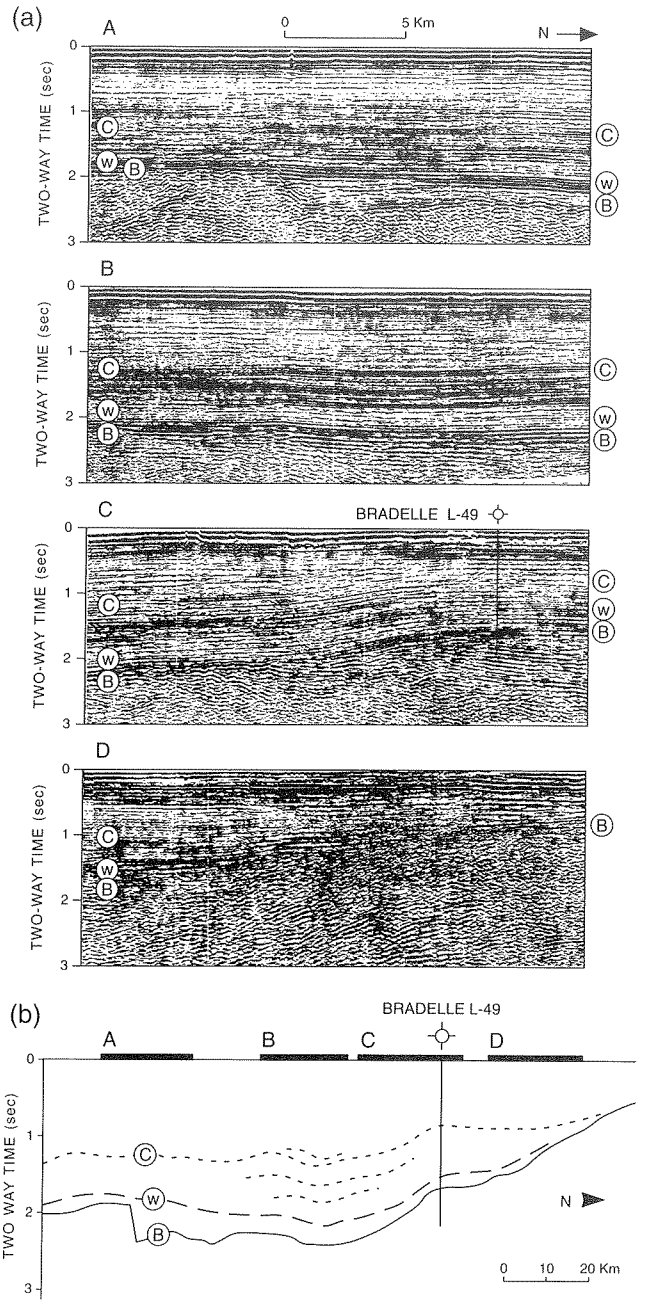

Figure 6. ***a)*** *Segments (A-D) of N–S seismic line through Bradelle L-49 well site (Fig. 4) illustrating lateral change in character of Coal Measures seismic facies. Chevron Standard Ltd. Line 81-25-11MX.* ***b)*** *Line drawing of principal reflectors on seismic line shown in segments in 6a; C = Coal Measures. Horizontal scale compressed 4X. From Grant (1994).*

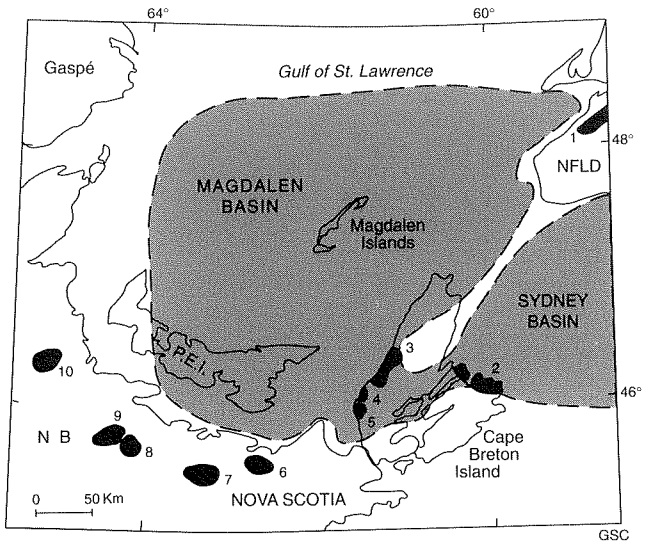

Figure 7. *Speculative map of minimum original extent of the Coal Measures seismic facies (stippled) compared to coalfields (black areas) on land. From Grant (1994).*

REFERENCES

Grant, A.C.
1994: Aspects of seismic character and extent of Upper Carboniferous Coal Measures, Gulf of St. Lawrence and Sydney basins. Palaeogeography, Palaeoclimatology, Palaeoecology, v. 106, p. 271–285.

Grant, A.C. and Moir, P.N.
1992: Observations on coalbed methane potential, Prince Edward Island. *In* Current Research, Part E, Geological Survey of Canada, Paper 92–1E, p. 269–278.

Hacquebard, P.A.
1986: The Gulf of St. Lawrence Carboniferous Basin: the largest coalfield of Eastern Canada. Bulletin of Canadian Institute of Mining and Metallurgy, v. 79, p. 67–78.

Poster 68 can be found on page 515.

CARBONIFEROUS AND PERMIAN GAS RESOURCES OF WESTERN CANADA SEDIMENTARY BASIN, INTERIOR PLAINS

Geological Play Analysis and Resource Assessment

J.E. Barclay

Hardy Oil and Gas Canada Ltd., 530 - 8th Avenue S.W., Calgary, Alberta T2P 3S8

P.J. Lee

Geological Survey of Canada, 3303-33rd Street N.W., Calgary, Alberta T2L 2A7

R.I. Campbell

PanCanadian Petroleum Ltd., 150 - 9th Avenue S.W., Calgary, Alberta T2P 2S5

G.D. Holmstrom

G.H. Consulting, 2016-26th Avenue N.W., Calgary, Alberta T2M 2G4

G.E. Reinson

Petrel Robertson Ltd., 2801-18th Street N.W., Calgary, Alberta T2E 7K5

ABSTRACT

This paper describes the discovered gas resources of the major Carboniferous and Permian gas plays in the Interior Plains of Western Canada and presents a prediction based on geological and statistical analysis for their undiscovered gas resources (Fig. 1). The results of this analysis represent part of the Geological Survey of Canada Western Canada Gas Assessment Project that is now essentially complete and being documented in various publications (see the following list).

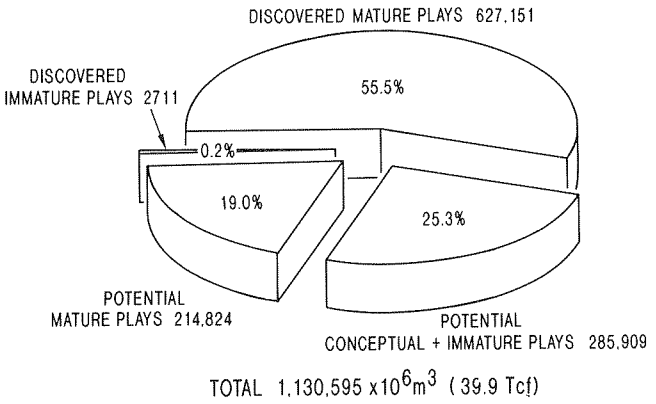

Figure 1. *Relation between discovered gas-in-place resource for mature and immature plays and undiscovered gas-in-place resource (potential) for mature plays and conceptual plus immature plays.*

In the Plains, 587.208 x 10^9m^3 (20.8 TCF) or 53% of the Carboniferous and Permian Plains plus Foothills discovered in-place gas total occurs in 5 Carboniferous established mature Plains plays in 241 fields with 883 pools. The predicted expected potential of Carboniferous initial volume in-place gas in the 5 established mature Plains plays is 142.041 x 10^9m^3 (5.0 TCF) predicted within 3177 undiscovered pools. Thus, 19% of the Carboniferous (Plains) gas-in-place resource in mature plays remains to be discovered. There are 4 immature plays identified for the Carboniferous in the Plains and they contain 2.711 x 10^9m^3 (0.1 TCF) initial volume in-place gas in 10 gas fields each consisting of one pool. Immature play potential was incorporated in the conceptual play analysis.

For the Permian in the Plains, 39.943 x 10^9m^3 (1.4 TCF) or 96% of the Permian in-place Plains plus Foothills total occurs in 48 fields with 93 pools in 1 established mature play. The expected potential of Permian initial volume in-place gas in the Plains is predicted to be 72.783 x 10^9m^3 (2.6 TCF) contained within 907 undiscovered pools. The total number of discovered and undiscovered Permian pools (Plains) is thus 1000. Almost 65% of the Permian gas-in-place

resource in the Plains therefore remains to be discovered. No immature Permian plays were identified.

The predicted expected potential for Carboniferous and Permian conceptual and immature plays is 285.909 x 10^9m^3 (10.1 TCF). This statistical analysis predicts about 22 plays to exist in the Carboniferous and Permian and this number should represent the 6 mature plays, the 4 immature plays and thus 12 purely conceptual plays remain to be discovered in the Carboniferous and Permian. For comparison, at least 5 to 10 purely conceptual plays were suggested and predicted on the basis of our regional geological analysis.

The Carboniferous and Permian (Plains) discovered initial volume in-place gas for all mature and immature established plays is 629.862 x 10^9m^3 (22.4 TCF) within 296 fields and 986 pools. The total initial volume in-place gas resource (discovered and undiscovered) for all Carboniferous and Permian Plains mature, immature and conceptual plays is 1130.595 x 10^9m^3 (40.1 TCF), predicted to occur in 5070 discovered and undiscovered pools belonging to mature plays plus an undetermined number of undiscovered pools in the conceptual and immature plays. The expected potential of 500.733 x 10^9m^3 (17.8 TCF) for all mature, immature and conceptual plays thus represents an undiscovered 44% of the total Plains Carboniferous and Permian gas resource.

SUMMARY

Total discovered Western Canada Basin Carboniferous in-place gas in the Interior Plains and Rocky Mountain Foothills and Front Ranges is 1108.507 x 10^9m^3 (39.3 TCF) in 322 gas fields with 1064 pools.[1] Approximately 702 x 10^9m^3 (24.9 TCF) or 63% of this in-place gas is marketable and represents about 16% of the total Western Canada Basin Plains plus Foothills marketable gas reserves in all strata.

The total discovered initial volume in-place gas in the mainly Permian Belloy Formation and equivalent strata in the Plains and Foothills occurs within 51 gas fields and 96 pools and is 41.706 x 10^9m^3 (1.5 TCF) of which approximately 29.8 x 10^9m^3 (1.1 TCF) is marketable gas and represents about 0.8% of the total Western Canada marketable gas reserves.

In-place gas for the Carboniferous and Permian plays in the study area, which includes the Plains portion but not the Rocky Mountain Thrust Belt, is 629.862 x 10^9m^3 (22.4 TCF) discovered in 986 pools within 6 major mature exploration plays. The undiscovered resource (expected potential) for these mature plays is estimated to be 214.824 x 10^9m^3 (7.6 TCF) predicted to occur in 4084 pools of varying sizes, including numerous small pools many of which may be uneconomic to produce. In addition to the 6 mature plays, 4 immature plays were identified that have only 10 discovered single-pool fields. Also, 12 conceptual plays are predicted for the Carboniferous and Permian. The predicted undiscovered resource (potential) for the conceptual and immature plays is 285.909 x 10^9m^3 (10.1 TCF).

Regional geological analysis provided criteria to group the 893 discovered Carboniferous pools into two main groups of established, mature and immature, geologically defined plays: 1) subcrop plays which contain the bulk of the discovered gas, and 2) stratigraphic and structural plays which have less discovered gas but have significantly more potential than the subcrop plays. The 93 mainly Permian Belloy Formation pools were grouped into one major established play that consists mainly of pools in structural traps but also has many pools with significant control by internal and external unconformities. Quantitative methods based on the exploration discovery histories of pools and their sizes within the geologically-defined plays were used to assess play potentials.

For the Carboniferous only, marketable gas reserves in the cratonic Interior Platform (within the Interior Plains) and the Rocky Mountain Thrust Belt (mainly within the Rocky Mountain Foothills) are approximately 702 x 10^9m^3 (24.9 TCF) occurring in 322 fields with 1064 pools representing about 16% of total Western Canada Basin marketable gas reserves in all strata. The total volume of discovered gas-in-place volume is 1108.507 x 10^9m^3 (39.3 TCF; Carboniferous Plains plus Foothills), of which 587.208 x 10^9m^3 (20.8 TCF) or 53% of the total occurs in the Plains in 5 mature plays and an additional 2.711 x 10^9m^3 (0.1 TCF) occurs in 4 immature Plains plays.

The Plains Carboniferous has 5 mature established plays with 241 fields comprised of 883 pools and 4 immature established plays with 10 single-pool gas fields. The expected potential of Carboniferous gas-

[1] In this paper gas resources are given as initial volume in-place (i.e., gross volume of raw natural gas) unless noted otherwise as marketable. Associated, non-associated and solution gas are included and aggregated in this analysis.

in-place in the Plains mature plays is predicted to be 142.041 x 10^9m^3 (5.0 TCF) contained within 3177 undiscovered pools. Thus the total number of discovered and undiscovered Carboniferous pools in Plains mature established plays is 4060. The total discovered plus Undiscovered Carboniferous gas resource in established mature plays is 729.249 x 10^9m^3 (25.9 TCF) gas-in-place of which 19% remains to be discovered.

The mature play with the largest Discovered gas -in-place volume and second largest gas-in-place potential is the Mississippian Subcrop–Edson/ Harmattan play with 499.115 x 10^9m^3 (17.7 TCF) gas-in-place in 597 Discovered pools and an Expected potential of 52,351 x 10^6m^3 (1.9 TCF) predicted to occur in 343 Undiscovered pools. The play contains 80% of the discovered Carboniferous and Permian gas-in-place volume in the Plains mature plays and 24% of the Expected potential.

The established mature Carboniferous and Permian plays, ordered by gas-in-place Expected potential (10^6m^3) are as follows:

Belloy Peace River Structural–Eagle Play
Expected potential (Undiscovered): 72,783[1] (2.6 TCF)
Discovered gas-in-place volume: 39,943 (1.4 TCF)
% Undiscovered: 65%
Largest undiscovered pool: 1,644 (58 BCF)
Discovered pools: 93
Undiscovered pools: 907
% of Carboniferous–Permian mature play potential: 34%

Kiskatinaw Clastics–Pouce Coupe Play
Expected potential (Undiscovered): 54,322 (1.9 TCF)
Discovered gas-in-place volume: 29,015 (1.0 TCF)
% Undiscovered: 65%
Largest undiscovered pool: 581 (21 BCF)
Discovered pools: 115
Undiscovered pools: 1085
% of Carboniferous–Permian mature play potential: 25%

Mississippian Subcrop–Edson/Harmattan Play
Expected potential (Undiscovered): 52,351 (1.9 TCF)
Discovered gas-in-place volume: 499,115 (17.7 TCF)
% Undiscovered: 9%
Largest undiscovered pool: 1893 (70 BCF)
Discovered pools: 597
Undiscovered pools: 343
% of Carboniferous–Permian mature play potential: 24%

Peace River Carbonates–Dunvegan Play
Expected potential (Undiscovered): 16,640 (0.6 TCF)
Discovered gas-in-place volume: 48,895 (1.7 TCF)
% Undiscovered: 25%
Largest undiscovered pool: 2900 (103 BCF)
Discovered pools: 90
Undiscovered pools: 130
% of Carboniferous–Permian mature play potential: 8%

Bakken Stratigraphic/Subcrop–Loverna Play
Expected potential (Undiscovered): 12,233 (0.4 TCF)
Discovered gas-in-place volume: 3,290 (0.1 TCF)
% Undiscovered: 79%
Largest undiscovered pool: 341 (12 BCF)
Discovered pools: 37
Undiscovered pools: 1063
% of Carboniferous Permian mature play potential: 6%

Rundle Sweetgrass Structural–Black Butte Play
Expected potential (Undiscovered): 6,495 (0.2 TCF)
Discovered gas-in-place volume: 6,893 (0.2 TCF)
% Undiscovered: 49%
Largest undiscovered pool: 306 (11 BCF)
Discovered pools: 44
Undiscovered pools: 556
% of Carboniferous–Permian mature play potential: 3%

The total discovered plus Undiscovered gas-in-place volumes for each of the 6 Carboniferous and Permian mature plays (Plains) were used as data points for a statistical prediction of the Undiscovered initial volume gas-in-place resource contained in conceptual plays. The predicted conceptual play potential would be assumed to include the predicted potential for the 4 established immature Carboniferous plays which were excluded as data points because they have inadequate discovered resources and no directly predicted potential. The predicted gas-in-place potential for conceptual plays (those with no Discovered pools but predicted to exist on the basis of geological and statistical analyses) and immature plays in the Carboniferous and Permian Plains plays is 285.909 x 10^9m^3 (10.1 TCF). The Carboniferous and Permian Plains gas resources comprise 841.975 x 10^9m^3 (29.9 TCF) discovered plus potential gas-in-place for the established mature plays in 5060 pools plus the 285.909 x 10^9m^3 (10.1 TCF) potential in an unknown number of Undiscovered pools predicted for the conceptual and immature plays plus 2.711 x 10^9m^3 (0.1 TCF) for the immature play Discovered gas-in-place in 10 pools for an aggregate total of 1130.595 x 10^9m^3 (40.1 TCF) gas-in-place in more than 5070 pools.

[1]gas-in-place reported in 10^6m^3; largest undiscovered pools reported at their median values being the best estimate of their predicted size.

In addition to the 6 Carboniferous and Permian established mature plays and 4 established immature plays, we predict on the basis of a geological analysis, at least 5 Carboniferous and/or Permian geologically-predicted conceptual plays and possibly up to 10 conceptual plays if the major conceptual play is split into 5 sub-plays. This geologically-based prediction of play numbers is similar to and provides credibility to the 12 statistically-predicted conceptual plays. The geologically-predicted conceptual play thought to have the most potential is the Rundle down-dip stratigraphic play in which hydrocarbons are trapped by facies or diagenetic changes down-dip from the subcrop edge.

Carboniferous potential is suggested by continuing drilling activity and significant gas and oil discoveries in the stratigraphic and structural plays such as at Alces, Bilawchuk, Boundary Lake, Craigmyle/Michichi, Desan, Doe, Ghost Pine, Goodwater, Hoosier, Mica and Pouce Coupe. Although relatively thin and areally restricted in comparison to most Carboniferous deposits, Permian gas potential is indicated by a significant gas discovery at Boundary Lake in 1987. We feel that our predicted potential for the Carboniferous and Permian provides additional justification for continued exploration in these units.

CONCLUSIONS

1. Five established mature plays with 883 Discovered pools and four established immature plays with 10 Discovered pools were identified in Carboniferous strata within the Interior Plains portion of the Western Canada Basin. One established mature play with 93 pools was identified in Permian Plains strata. No immature Permian plays were identified. Twelve conceptual plays (i.e., with no Discovered pools) were predicted for the Carboniferous and Permian.

2. The five established mature Carboniferous Plains plays and their discovered resources and potential (respectively and ordered by discovered resources) are:

   i) Mississippian Subcrop–Edson Harmattan Play, 499,115/52,351 (discovered/Undiscovered, 10^6m^3 gas-in-place)

   ii) Peace River Carbonates–Dunvegan Play, 48,895/16,640

   ii) Kiskatinaw Clastics–Pouce Coupe Play, 29,015/54,322

   iv) Rundle Sweetgrass Structural–Black Butte Play, 6,893/6,495

   v) Bakken Stratigraphic/Subcrop–Loverna Play, 3,290/12,233.

   The Permian established mature play is the Belloy Peace River Structural-Eagle Play which has a Discovered gas-in-place resource of 39,943 x 10^6m^3 and a predicted potential of 72,783 x 10^6m^3. The four Carboniferous immature established plays have discovered resources of 2.711 x 10^9m^3 and their potential was included but unspecified in the conceptual play analysis. The Belloy and Kiskatinaw plays have the greatest predicted potentials. The largest predicted Undiscovered pool occurs in the Peace River Carbonates-Dunvegan Play and is 2,900 x 10^6m^3 gas-in-place in size.

3. Total Discovered gas-in-place resources for the Carboniferous mature and immature plays is 589.919 x 10^9m^3 and the Undiscovered resource (potential) for the mature plays only is 142.041 x 10^9m^3. The Permian discovered resource is 39.943 x 10^9m^3 and potential is 72.783 x 10^9m^3. Potential for the Carboniferous and Permian conceptual and immature plays is 285.909 x 10^9m^3. Of the total Carboniferous and Plains resource of 1130.6 x 10^9m^3, 500.7 x 10^9m^3 or 44% remains to be discovered. Of the total resource, 19% remains to be found in the Undiscovered pools of the mature plays.

4. The discovered resources of the Carboniferous and Permian plays are concentrated in the Mississippian Subcrop-Edson/Harmattan Play in fields along several major Carboniferous erosional edges yet the gas potential in Carboniferous–Permian plays appears to be concentrated in structural or stratigraphic traps downdip of those edges. The potential is predicted to occur in 4084 pools in the mature plays and in an unknown but probably large number of pools in the conceptual and immature plays.

5. The Carboniferous-Permian Plains plays comprise 9.7% of the total Western Canada Basin Discovered gas-in-place resources and 7.7% of the total Undiscovered resource.

REFERENCES

Barclay, J.E., Holmstrom, G.D., Lee, P.J., Campbell, R.I., and Reinson, G.E.
in prep.: Carboniferous and Permian gas resources of Western Canada Sedimentary Basin, Interior Plains: Geological play analysis and resource assessment. Geological Survey of Canada, Bulletin.

Bird, T.D., Barclay, J.E., Campbell, R.I., Lee, P.J., Waghmare, R.R., Dallaire, S.M., and Conn, R.F.
1994: Triassic gas resources of the Western Canada Sedimentary Basin, Interior Plains. Geological Survey of Canada, Open File 2911, 91 p.

Holmstrom, G., Reinson, G.E., and Lee, P.J.
in prep.: Jurassic gas resources of Western Canada Sedimentary Basin, Interior Plains. Geological Survey of Canada, Bulletin.

Osadetz, K.G., Hannigan, P., and Lee, P.J.
in prep.: Gas resources of the Canadian Cordillera. Geological Survey of Canada, Bulletin.

Reinson, G.E., Lee, P.J., Warters, W., Osadetz, K.G., Bell, L.L., Price, P.R., Trollope, F., Campbell, R.I., and Barclay, J.E.
1993: Devonian gas resources of the Western Canada Sedimentary Basin. Geological play analysis and resource assessment. Geological Survey of Canada, Bulletin 452.

Reinson, G.E., Lee, P.J., Barclay, J.E., Bird, T.D., and Osadetz, K.G.
1993: Western Canada basin conventional gas resource estimated at 232 TCF. Oil and Gas Journal, Oct. 25, v. 91, no. 43, p. 92–97.

PRELIMINARY ESTIMATES OF ECONOMICALLY RECOVERABLE GAS (FUTURE RESERVE ADDITIONS) FROM UNDISCOVERED NATURAL GAS RESOURCES IN THE WESTERN CANADA SEDIMENTARY BASIN

R.F. Conn, R.R. Waghmare, L. Roux, and S.M. Dallaire

Energy Sector, Natural Resources Canada, 580 Booth Street, Ottawa, Ontario K1A 0E4

ABSTRACT

This presentation provides a preliminary estimate of economically recoverable resources (reserve additions) of raw gas from undiscovered natural gas resources estimated to exist in the Western Canada Sedimentary Basin (WCSB). A brief description of the methodology used to prepare these estimates is provided. Supply curves, estimating the relationship between the plant-gate price and economic resource potential, are shown for completed studies on the Devonian, Triassic, and Permian–Carboniferous systems. Supply curves for the most important plays within each of these systems are also presented. The results from these completed studies are then used to prepare a preliminary estimate of future reserve additions of natural gas from future discoveries in all strata in the WCSB, at $1.00 and $3.00 per MCF.

BACKGROUND

Estimates of Canada's undiscovered oil and gas resources are prepared by Natural Resources Canada. The Institute of Sedimentary and Petroleum Geology (ISPG) is responsible for the resource assessment. These resource estimates exclude the impact of economic or technical constraints (Lee, 1993). Estimates of the portion of the undiscovered resource base which can be expected to be economic to find, develop and produce are prepared by the Energy Sector of Natural Resources Canada.

Natural Resources Canada is currently updating the natural gas resource estimate for the WCSB. Geological Survey of Canada, Bulletins 452 and 483 provide the results for the Devonian and Triassic systems, respectively. Other studies are in various stages of completion. Part II of these publications provided estimates of supply prices for undiscovered pools under different sets of geological, technical and economic assumptions.

Supply price, or marginal cost, refers to the plant gate price of natural gas and coproducts required to recover all costs, including a minimum discounted cash flow rate-of-return on investment. Supply prices are prepared for the full-cycle and half-cycle cases. The *full-cycle* analysis includes all exploration, development and production costs, including overhead, while the *half-cycle* analysis excludes all predevelopment costs. In some cases, a *weighted supply price* (a weighted average of the full-cycle and half-cycle supply prices) is provided. This estimate is appropriate when plays are superimposed, in whole or in part, on one another, and oil and gas resources in shallower plays may be discovered with wells drilled to targets in deeper plays. *Economic potential*, at a given price, is the sum of recoverable resources with estimated supply prices less than or equal to the given price. The supply price/economic potential relationship is defined as the *supply curve* or marginal cost curve.

The methodology used to estimate supply prices is presented, along with several major and minor changes dictated by geological differences, available infrastructure to support exploration and development, and changing company practices. More complete descriptions are provided in Geological Survey of Canada, Bulletins 452 and 483 (Dallaire, Waghmare and Conn, 1993; Waghmare, Dallaire and Conn, 1994).

RESULTS OF COMPLETED WORK

Supply curves for the Devonian, Triassic and Permian–Carboniferous systems are provided. For comparison, both full- and half-cycle supply curves are shown. For the Triassic and Permian–Carboniferous systems, weighted supply curves are also provided.

Supply curves for individual plays within these geological systems are also displayed in order to demonstrate the significant variation between plays (Waghmare, 1994). This work also shows that a handful of plays contain the bulk of the economically recoverable resources.

ESTIMATES OF FUTURE RESERVE ADDITIONS

The ISPG's resource assessment for gas in the WCSB provides estimates for both mature plays and immature and conceptual plays. Figure 1 shows the ISPG's preliminary estimate of total in-place undiscovered natural gas potential of 232 TCF for the WCSB (Reinson et al., 1993). Figure 2 shows the portion of this estimate which can be expected to be economic at $1 and $3 per MCF. These estimates have been prepared by extrapolating the results of completed studies to the ISPG's total estimate, and incorporating the expected increases in economic potential as a result of cost reductions arising from technological improvements, infrastructure development, and improved exploratory success (Conn, 1994; Armstrong and Calantone, 1990; Fisher, 1994).

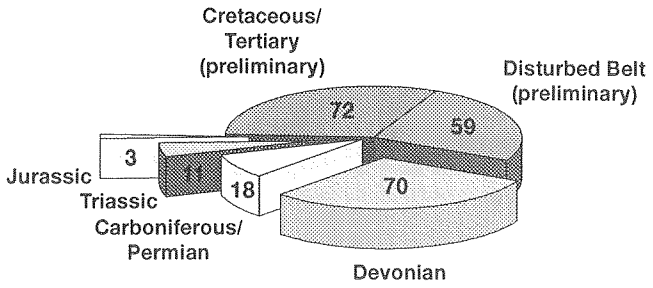

Figure 1. Mean estimates of raw in-place undiscovered natural gas resources for the Western Canada Sedimentary Basin. Total undiscovered resource is 232 TCF. See Reinson et al., Oil and Gas Journal, October 25, 1993, p. 92–94.

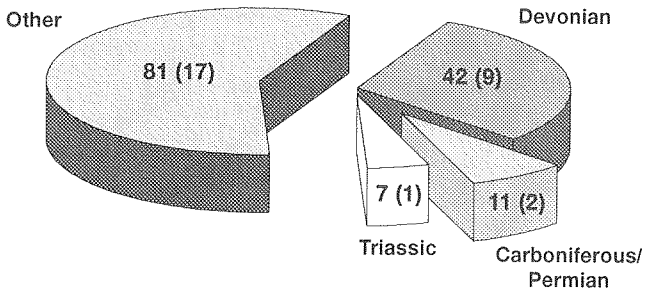

Figure 2. Mean estimates of economically recoverable undiscovered natural gas resources for the Western Canada Sedimentary Basin assuming a plant gate price of $3.00/MCF ($1.00/MCF). Total undiscovered recoverable potential at $3.00 and $1.00 are 140 TCF and 30 TCF, respectively (1993 Canadian dollars).

REFERENCES

Armstrong, D.E. and Calantone, C.
1990: Submission to the National Energy Board in support of the ANG EXPANSION PROJECT and in Response to Information Request in letter dated 1 November.

Conn, R.F.
1994: The economic potential of Western Canada's conventional undiscovered gas resources. Presented at the CERI North American Natural Gas Conference.

Dallaire, S.M.
1994: A methodology for handling exploration risk and constructing supply curves for oil and gas plays when resources are stacked. Bulletin of Canadian Petroleum Geology, v. 42, no. 3, p. 392–403.

Dallaire, S.M., Waghmare, R.R., and Conn, R.F.
1993: Devonian gas resources of the Western Canada Sedimentary Basin (Part II: Economic Analysis). Geological Survey of Canada, Bulletin 452.

Fisher, W.L.
1994: How technology has confounded U.S. gas resource estimators. Oil and Gas Journal, v. 92, no. 43 , p.100–107.

Lee, P.J.
1993: Two decades of Geological Survey of Canada petroleum resource assessments. Canadian Journal of Earth Sciences, v. 30, p. 321–332.

Reinson, G.E., Lee, P.J., Barclay, J.E., Bird, T.D., and Osadetz, K.G.
1993: Western Canada basin conventional gas resource estimated at 232 Tcf. Oil and Gas Journal, v. 91, no. 43, p. 92–95.

Waghmare, R.R.
1994: The economics of the Devonian gas resources of the Western Canada Sedimentary Basin – Further analysis. Presented to the Canadian Society of Economic Geology and Canadian Society of Petroleum Geologists, Joint National Convention (Exploration Update '94).

Waghmare, R.R., Dallaire, S.M., and Conn, R.F.
1994: Triassic gas resources of the Western Canada Sedimentary Basin, Interior Plains (Part II: Economic Analysis). Geological Survey of Canada, Bulletin 483.

PETROLEUM RESOURCE POTENTIAL OF THE QUEEN CHARLOTTE BASIN REGION, WEST COAST, CANADA

J.R. Dietrich

Geological Survey of Canada, 3303-33rd Street N.W., Calgary, Alberta T2L 2A7

ABSTRACT

Ten onshore and 8 offshore petroleum exploration wells have been drilled in the Queen Charlotte Basin region of Canada's west coast (Fig. 1), as part of a number of industry exploration programs dating from 1913 to 1984. No oil or gas fields were discovered, but drilling and surface mapping revealed the presence of

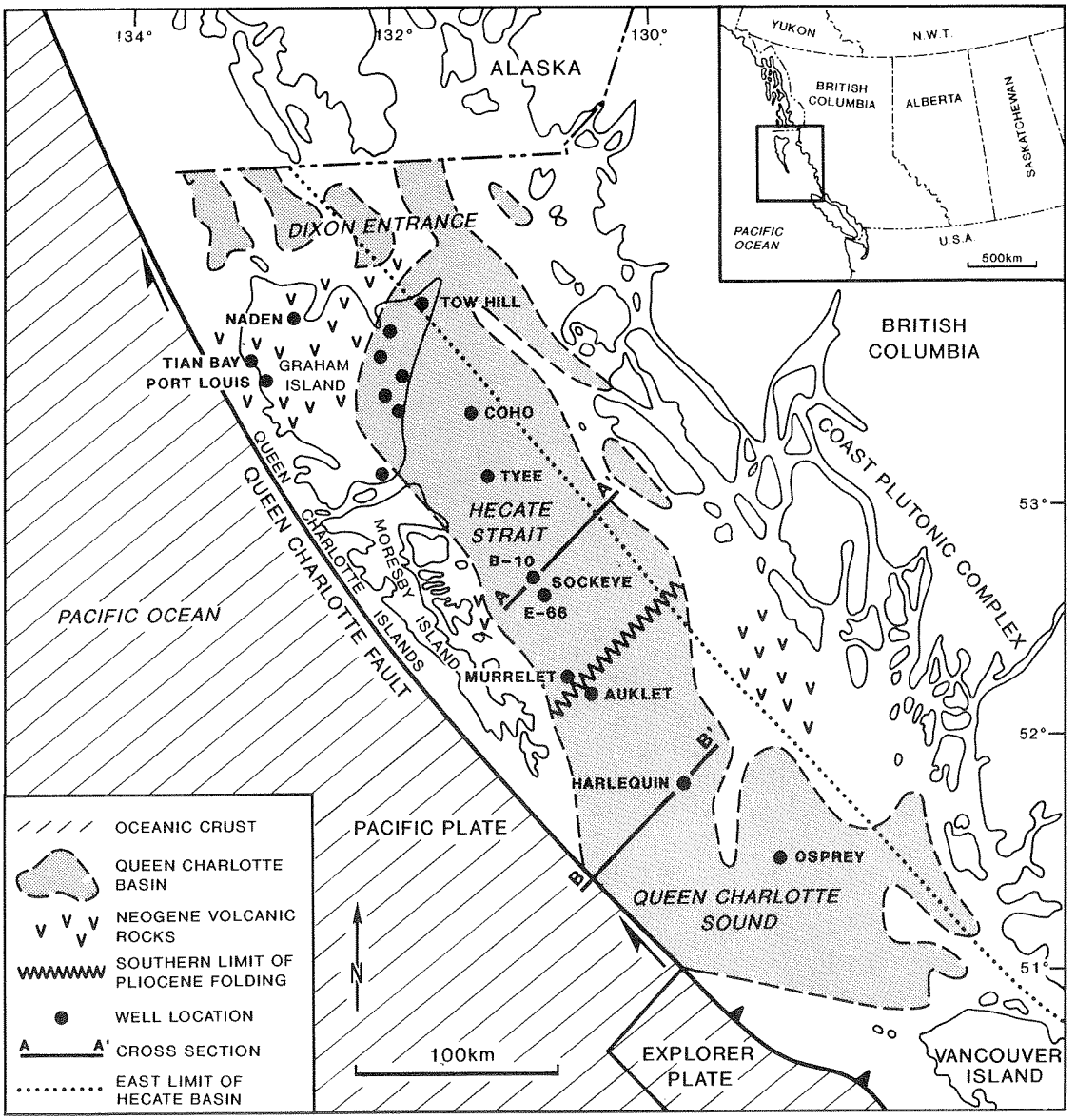

Figure 1. *Geographic and geologic setting of the Queen Charlotte Basin.*

reservoir and source rocks and oil and gas shows within the region, indicating significant potential for petroleum accumulations. Some of the most prospective parts of the region occur offshore where an exploration moratorium has been in effect since 1972. Although petroleum exploration has been limited since the moratorium onset, regional basin analysis studies have continued through various government and academic institution programs (e.g., Woodsworth, 1991). Recent studies have included a quantitative assessment of petroleum potential in the region (Dietrich, 1994), the results of which will contribute to a resource information framework for future government policy decisions on exploration moratoriums and land-use planning.

The assessment involved analysis of regional-scale petroleum plays within Mesozoic forearc and Tertiary strike-slip basins that developed along Canada's active Pacific continental margin. The most prospective plays

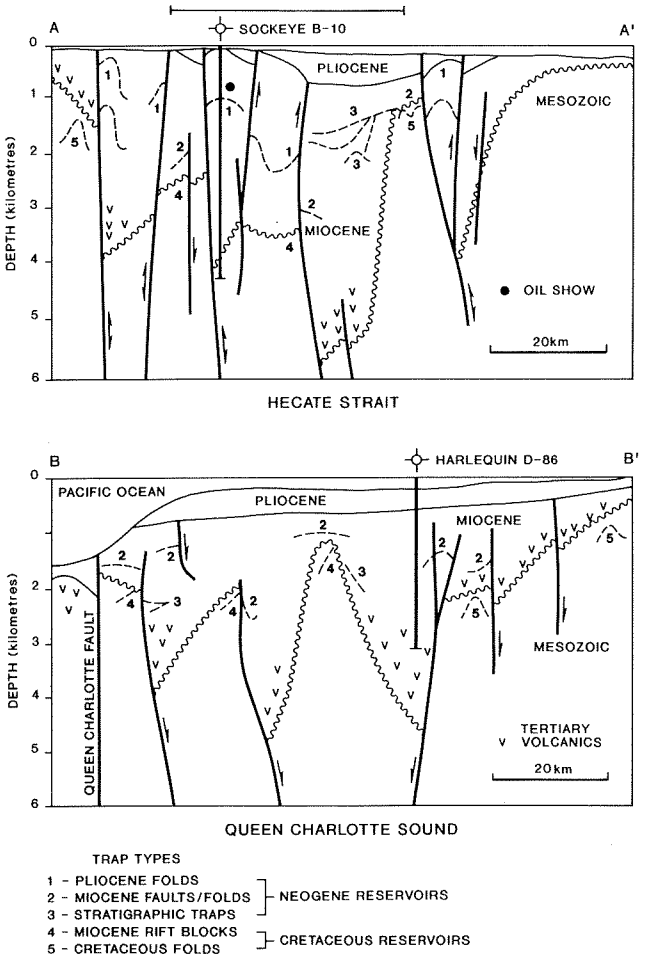

Figure 2. *Petroleum plays within and beneath the Neogene Queen Charlotte Basin.*

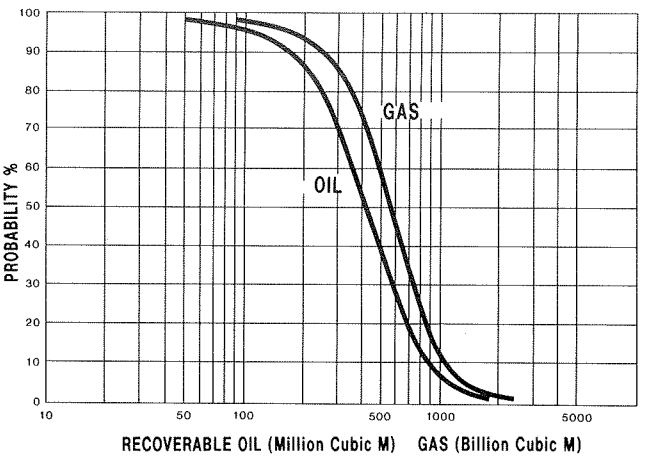

Figure 3. *Total oil and gas potential, Queen Charlotte Basin region.*

are associated with Neogene sandstones and conglomerates within the strike-slip Queen Charlotte Basin, predominantly in offshore areas of Hecate Strait and Queen Charlotte Sound (Figs. 1, 2). Median value estimates of the region's total petroleum potential (from all plays) are 414 x $10^6 m^3$ (2.6 Bbbl) of recoverable oil and 565 $10^9 m^3$ (20 TCF) of recoverable gas (Fig. 3). The largest (undiscovered) individual fields within the region are estimated (at median values) to contain 70 $10^6 m^3$ (440 Mbbl) of recoverable oil and 77 $10^9 m^3$ (2.7 TCF) of recoverable gas (Fig. 4). The total potential and field size estimate numbers provide an optimistic view of the petroleum resource potential in the Queen Charlotte Basin region.

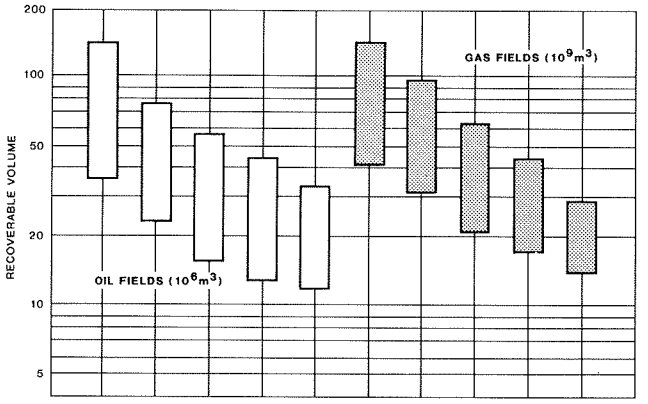

Figure 4. *Estimates of region's 5 largest oil and gas fields (Boxes = 25 to 75% probability ranges).*

REFERENCES

Dietrich, J.R.
1994: Petroleum resource potential of the Queen Charlotte Basin and Environs, west coast Canada. Bulletin of Canadian Petroleum Geology.

Woodsworth, G.J. (ed.)
1991: Evolution and hydrocarbon potential of the Queen Charlotte Basin, British Columbia. Geological Survey of Canada, Paper 90–10.

ASSESSMENT OF UPPER CRETACEOUS–TERTIARY GAS RESOURCES, POST-COLORADO STRATA, WCSB

A.P. Hamblin and P.J. Lee

Geological Survey of Canada, 3303-33rd Street N.W., Calgary, Alberta T2L 2A7

ABSTRACT

The uppermost Cretaceous (Campanian-Maastrichtian) post-Colorado Group strata comprise the youngest preserved bedrock units in the Western Canada Sedimentary Basin. Although commonly ignored in hydrocarbon exploration, these strata comprise up to 25% of the basin fill and represent an additional opportunity for discoveries. A total of 14 productive shallow gas plays encompassing 1405 known gas pools have been identified, described and assessed, using Petrimes, as part of the ongoing Gas Assessment activity. Discovered reserves total 556 304 x 10^6m^3 (19.8 TCF), 82% of which resides in the Southeast Alberta Gas System Milk River and Medicine Hat formations. However, an additional total expected potential of 132 985 x 10^6m^3 (4.7 TCF) may be present in undiscovered pools of all 14 plays through central and southern Alberta (Table 1).

The defined plays span the Milk River/Medicine Hat and equivalents (1 play), Judith River/Belly River Group (10 plays), Edmonton Group (2 plays), and Scollard Formation (1 play) and include targets undergoing presently active exploration.

Milk River/Medicine Hat marine sandy shale to siltstone reservoirs (including the Alderson Member) have discovered reserves of 455 000 x 10^6m^3 in 25 pools in a large stratigraphic and/or hydrodynamic trap. A small expected potential is estimated at 4 862 x 10^6m^3 spread through about 600 undiscovered pools.

"Basal Belly River" gas reservoirs are separated into 7 mappable offlapping shoreline-related sandy cycles of the Foremost Formation across southern Alberta into southwestern Saskatchewan. Because these cycles represent strata which are stratigraphically and geographically distinct on a regional scale, each is treated as a single play, with separate play areas, associated reserves and potential. However, each cycle also is a composite of individual small-scale cycles which include both shoreface and estuarine channel sandstone reservoir facies. In total, discovered reserves are 67 925 x 10^6m^3 in 713 pools in stratigraphic traps. Expected total potential is estimated at 52 819 x 10^6m^3 in about 2400 pools. In particular, Cycles 2, 3, 4 and 5 may present more attractive potential due to the presence of oil in Cycle 2 (Pembina area) and the geographic location of these cycles over the crest of the Sweetgrass Arch and underlying Paleozoic trends, where subtle structural drape may enhance trap possibilities and size.

Fluvial channel sandstones of the Foremost Formation, behind the shoreline-related trends, have discovered reserves of 23 252 x 10^6m^3 in 453 small pools, and expected potential of 18 547 x 10^6m^3 in an additional 830 pools. Stacked multistorey channel sandstones of the overlying Oldman Formation (primarily in the Comrey Member) account for a discovered reserve of 3 179 x 10^6m^3 in 43 known small pools, with an expected undiscovered resource of 15 691 x 10^6m^3 scattered through about 950 additional pools. Estuarine valley-fills in the lower portion of the newly-defined Dinosaur Park Formation include 137 known pools with reserves of 4 686 x 10^6m^3. Expected undiscovered gas resources of 25 283 x 10^6m^3 could be present in up to 1860 pools in the large play area.

Extensive marine shoreline-related sandstones at the base of the Edmonton Group (Bearpaw-Horseshoe Canyon transition) in central Alberta include 18 known pools with reserves of 1 237 x 10^6m^3. Modest expected potential of 9 949 x 10^6m^3 should be scattered through up to 600 additional pools. Fluvial channel sandstones of the middle and upper Edmonton Group, behind these shorelines, have so far yielded reserves of 532 x 10^6m^3 in 17 shallow pools in central Alberta, but are attributed expected resources of 5 834 x 10^6m^3 in up to 600 additional small pools.

Thick fluvial sandstones overlying the disconformity at the base of the shallow Scollard Formation currently enclose a single pool assigned reserves of 29 x 10^6m^3, but this play was not further assessed.

Whereas the known reserves and potential of plays are modest, their shallow depth, relative predictability, large play areas and bypassed nature of pay make them attractive targets for smaller explorers.

Table 1

Summary of the Upper Cretaceous Assessments

Play Name	UAI	Discovered Resource 10^6m^3	Potential Expected	Potential Probable	n/N	β	μ	σ^2
Edmonton Group								
Fluvial	C5119405	532	5 834	5 834	17/600	0.8	0.777	1.900
Marine	C5129405	1 237	9 949	10 342	18/600	1.6	2.226	1.307
Belly River								
Dinosaur Park	C4819404	4 686	25 283	26 502	137/2000	0.3	2.235	1.280
Oldman Fm–Fluvial	C4829404	3 179	15 691	15 691	43/1000	0.8	2.212	1.280
Foremost Fm–Fluvial	C4839404	23 252	18 547	22 812	452/1280	0.9	2.496	2.000
Foremost Fm–Shoreline	C4849404	67 925	52 819	86 532				
Cycle 1	C5519406	116	3 446	5835				
Cycle 2	C5529406	19 997	4 404	15 267	104/280	0.7	3.119	2.800
Cycle 3	C5539406	12 295	6 615	14 180	96/360	0.9	2.625	2.900
Cycle 4	C5549406	21 537	20 194	26 484	235/840	0.8	2.660	2.500
Cycle 5	C5559406	6 147	5 088	7 114	141/320	0.5	2.736	1.700
Cycle 6	C5569406	4 281	3 406	6 109	90/380	0.9	1.592	3.000
Cycle 7	C5579406	3 552	6 666	11 543	46/280	0.4	1.896	3.600
Milk River/Medicine Hat	C4529310	455 493	4 862	4 862	25/600	1.2	1.315	1.926
Total		**556 304**	**132 985**	**172 575**				
		19.8 TCF	4.7 TCF	6.1 TCF				

CONTRASTS BETWEEN THE GSC AND CPGC PROCEDURES FOR ESTIMATING UNDISCOVERED GAS RESOURCES

P.J. Lee, K. Olsen-Heise, and H.P. Tzeng

Geological Survey of Canada, 3303-33rd Street N.W., Calgary, Alberta T2L 2A7

The Geological Survey of Canada's (GSC) PETRIMES procedure has been used for the past decade in petroleum resource evaluation (Lee, 1993; Lee and Tzeng, 1993). Recently, the Canadian Gas Potential Committee (CPGC) adapted modules from PETRIMES to its planned Western Canada gas assessment procedure. The objective of this paper is to contrast the procedures based on the following five factors: (1) play definition; (2) input data used; (3) statistical assumptions and methods used; (4) output from the analyses; and (5) comparison of estimates.

All relationships between the two procedures described in this paper are based on the CSPG technical talk presented by Mr. Meneley (1994). His presentation dealt exclusively with the Swan Hills–Kaybob South gas play which had previously been evaluated by the ERCB (1992) and the GSC (Reinson et al., 1993).

Assessments provided by the GSC are used by a variety of different sectors for purposes of formulating policy. Consequently, during the assessment, the process tends to minimize subjective interpretations in order to: (1) produce data-driven estimates; (2) maintain the same level of uncertainty throughout all plays; and (3) maintain impartiality.

Contrasts between the GSC and CPGC procedures are summarized as follows:

1. The definition of the Swan Hills–Kaybob South gas play differs between the GSC and the CPGC in that: (1) the GSC definition includes nonassociated, associated, and solution gases. Only the non-associated gas is included in the CPGC definition. (2) according to the GSC stratigraphic correlations, the McLeod and Wild River pools included in the CPGC play belong to Leduc plays; and (3) the Hanlan Swan Hills and the Caroline Swan Hills pools were not included in the GSC definition because they are not in the vintage of the pool data base used by the GSC. The differences are summarized in Table 1.

Table 1

Gas pools used in the GSC and CPGC assessments

Field & pool name	Pool type[1]	Play defined by GSC	Play defined by CPGC
Kaybob South, BHL A	NA	Swan Hills	Swan Hills
Caroline, BHL A	NA	Swan Hills	Swan Hills
Hanlan, BHL A	NA	Swan Hills	Swan Hills
Blackstone, BHL A	NA	Swan Hills	Swan Hills
Minehead, BHL A	NA	Swan Hills	Swan Hills
Minehead, BHL	NA	Swan Hills	Swan Hills
Rosevear, BHL A	NA	Swan Hills	Swan Hills
Rosevear, BHL B	NA	Swan Hills	Swan Hills
Kaybob, BHL C	NA	Swan Hills	Not used
Hanlan, BHL C	NA	Swan Hills	Swan Hills
Fox Creek, BHL	S	Swan Hills	Not used
Kaybob, BHL B	A&S	Swan Hills	Not used
Chickadee, Swan Hills	NA	Swan Hills	Not used
Kaybob South, BHL	NA	Swan Hills	Swan Hills
Sakwatamau, Swan Hills	NA	Swan Hills	Not used
McLeod, BHL	NA	Leduc play[2]	Swan Hills
Wild River, BHL	NA	Leduc play[2]	Swan Hills
Caroline, Swan Hills	NA	Swan Hills[3]	Swan Hills
Hanlan, Swan Hills	NA	Swan Hills[3]	Swan Hills

Note 1. Pool type: NA, nonassociated; S, solution; A, associated gas.
Note 2. These two pools are grouped into two Leduc plays by the GSC.
Note 3. These pools were not used by the GSC assessment because they were not available in the 1990 data base.

2. The GSC procedure recognizes the fact that estimates can be derived from the discovery sequence resulting from selective drilling programs (Fig. 1A). This procedure is based on statistical principles and the results are supported by geological interpretation.

   The CPGC procedure uses the lognormal probability plot to obtain the mean and variance of a population, which implies that the discoveries are made randomly (Fig. 1B). The procedure requires that the value of N be given at the beginning of the assessment, and that other assumptions are brought into assessments. For example, how the value of

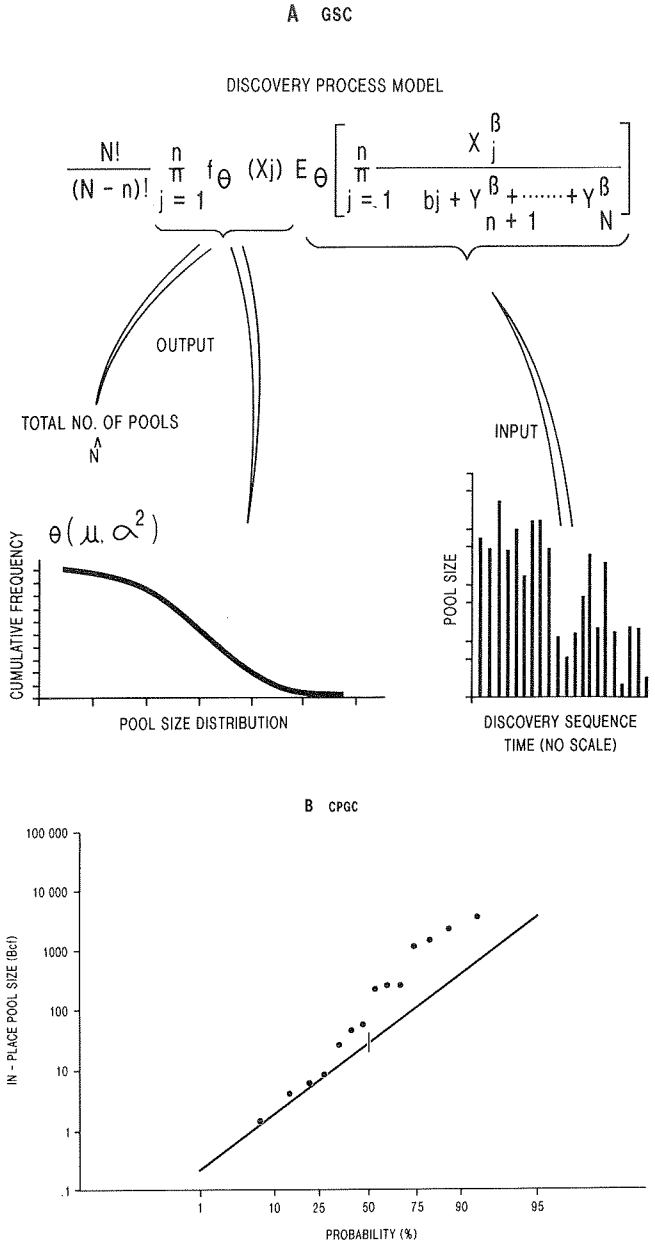

Figure 1. A. *Diagram showing the GSC discovery process model concept. The discovery sequence is the input to the discovery process model and the pool size distribution and the total number of pools are the output from the models. x_j is the pool size; β is the exploration efficiency (the larger the value, the greater the exploration efficiency); N is the total number of discovered and undiscovered pools in the play; and n is the number of discovered pools. The f_θ represents the pool size distribution to be estimated; the E_θ represents the discovery sequence as input data.* ***B.*** *The CPGC's procedure to estimate μ and σ^2 by moving the largest pools toward the right-hand side (After Meneley, 1994, Fig. 9).*

$\hat{N} = 100$ was not addressed. The lognormal probability plot was provided by PETRIMES to examine possible mixed populations and to discern if a given set of discoveries may be lognormally distributed. The application of the lognormal probability plot to predict undiscovered resources was invented by the CPGC.

3. The CPGC procedure uses the smallest pool size among the discovered pools as the starting point in the lognormal probability plot. This will underestimate the number of small pools. According to their estimates, there are only 5 pools with sizes less than 1 BCF. This number cannot stand the close examination of the drill-stem tests.

4. The geological and statistical meanings of the CPGC estimates are not defined. Mr. Meneley did not explain the statistical or geological meaning of their estimates during his presentation. The reliability and the level of uncertainty of the estimates are unknown.

5. As an option, PETRIMES matches discovered pool sizes to the median in the GSC method (Fig. 2A). Geologists can, however, match the Minehead and Rosevear A and B pools to ranks, for example, as low as 7, 8, and 9 (Fig. 2B). In such a situation geological judgement is appropriate. The undiscovered pool sizes can then be re-estimated from the matching output (i.e., the pool sizes and their rankings as shown in Fig. 3). The expected potential is the summation of all the undiscovered pool sizes (only the first 20 pool ranks are displayed in Fig. 2A). The expected potential for the match displayed in Figure 2A is 52 541 $10^6 m^3$, whereas the expected potential for the match displayed in Figure 2B is 69 340 10^6 m^3 . On the other hand, the probable potential for the Swan Hills case, for example, is 246 883 $10^6 m^3$ and does not rely on the Matching Process (e.g., Fig. 2A or 2B). Furthermore, this probable value is at a lower probability level. The probability levels of the expected and probable potentials, are respectively 0.60 and 0.18, for example (Fig. 4). The GSC's expected values may be considered equivalent to the ERCB's Category 2, whereas the probable values may be considered equivalent to the sum of the ERCB's Categories 2 and 3 (Table 2).

6. It is a mistake to compare the CPGC estimate with the sum of all three ERCB Categories, which includes the pool boundary expansion (Category 1). Further, the GSC estimates are derived by a data-driven procedure, whereas the CPGC

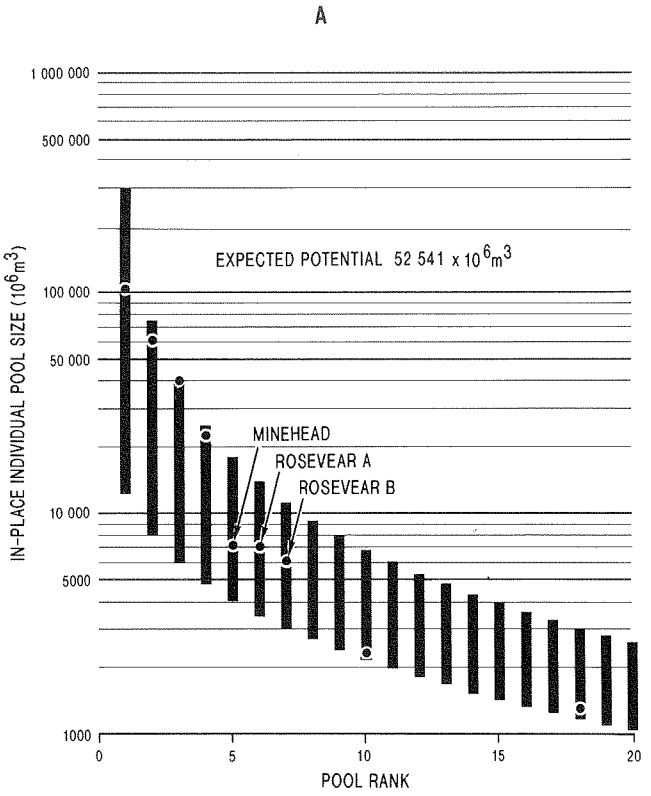

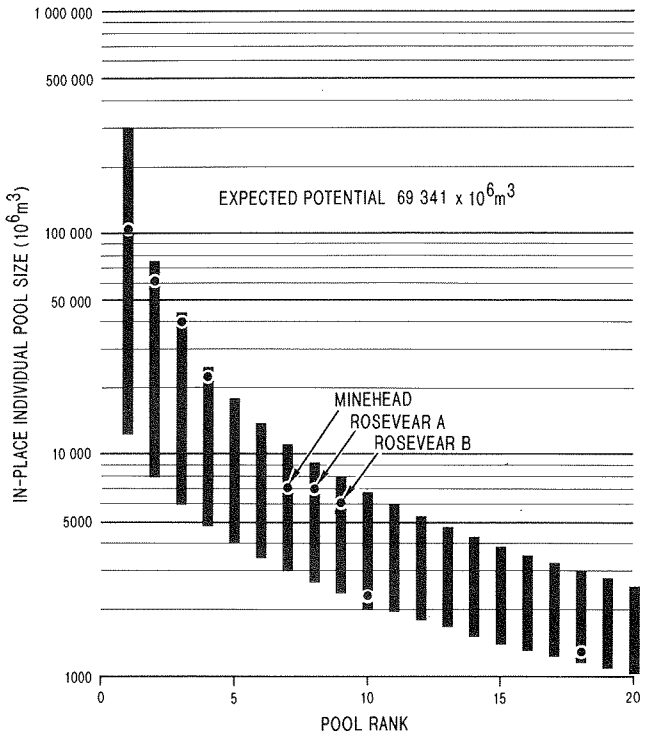

Table 2

Contrasts of the ERCB, GSC and CPGC gas resource estimates for the Swan Hills–Kaybob South play (Discovered & potential resources expressed in 10^6m^3)

Estimated by	Definitions	Estimates	Discovered resource
GSC	Expected	52 541	
	Probable	246 803[1]	254 453
ERCB	Category 1	43 520[2]	
	Category 2	47 150[3]	
	Category 3	249 520[4]	250 300
CPGC	Statistical and geological meanings unknown	6.2 Tcf (174 679[5])	9 494.8 Bcf (267 506[6])

Note 1. For the Devonian plays, only the summation of all play probable values was published.

Note 2. Category 1: "describes areas where the geology and historical drilling suggest that future discoveries of in-place gas will be realized as a result of pool boundary expansion, primarily due to step out drilling." (ERCB, 1992, p. 3–9).

Note 3. Category 2: "describes areas where the geology and historical drilling indicates that future discoveries of in-place gas will be made primarily as a result of new pools being discovered on trend with proven pools." (ERCB, 1992, p. 3–9).

Note 4. Category 3: "describes the remaining areas within the boundaries of a defined play area where a generally limited amount of historical drilling has resulted in minimal established reserves. In these areas reserve additions are expected to be made as a result of true exploratory type discoveries." (ERCB, 1992, p. 3–9).

Note 5. The original values were converted from the British unit into 10^6m^3 by the authors.

Note 6. Difference in discovered reserve values are due to different vintages and different play definitions.

Figure 2. *The GSC pool-size-by-rank plots for the Swan Hills–Kaybob South play.* ***A.*** *Pools are matched to the median values by PETRIMES. The box represents the prediction interval (0.9 probability) and the dot indicates the in-place pool size. The top 20 pools are shown on these plots.* ***B.*** *The Minehead and Rosevear A and B pools are matched to the lower ranks by geological interpretations.*

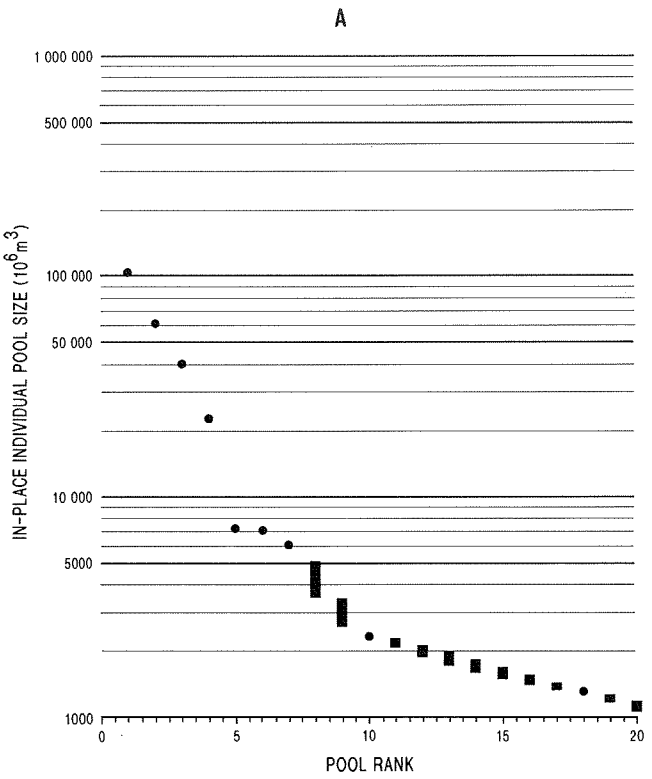

Figure 3. *The GSC pool-size-by-rank plot for the Swan Hills–Kaybob South play. The undiscovered pool sizes were conditioned according to the matching process (Fig. 2A). The dots indicate the discovered pools, whereas the bars indicate the prediction interval (0.9 probability). The expected potential is the sum of all undiscovered pools.*

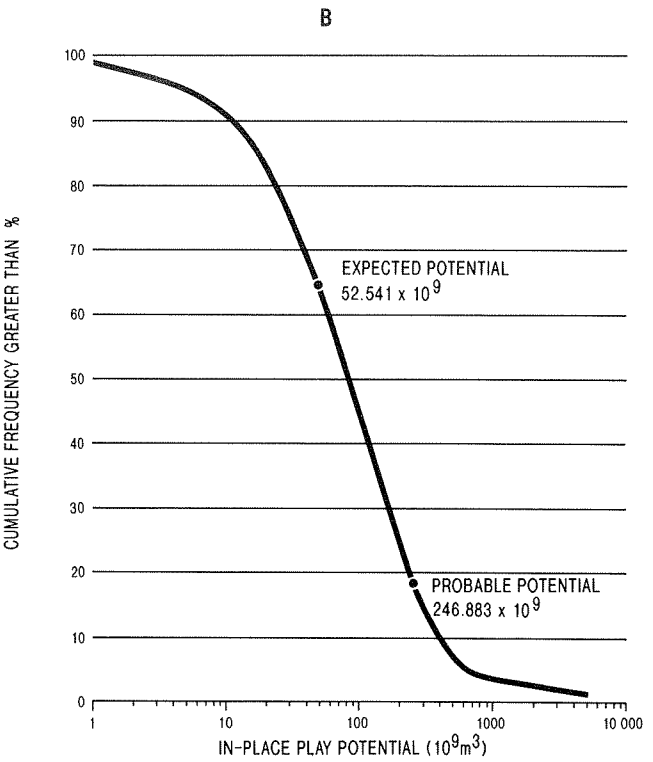

Figure 4. *The play potential distribution was conditioned according to the sum of discovered reserves to obtain the probable potential.*

estimates are derived by a subjective procedure. It is likewise a mistake to compare the estimates derived by these two procedures.

The CPGC procedure is highly dependent on judgement and has a limited basis in statistical theory. It implies that a random drilling process is used in exploration. On the contrary, the GSC procedure is highly dependent on data used, involves a minimal number of assumptions, and has a firm basis in statistical science. A direct comparison of resource estimates of these two methods is inappropriate.

ACKNOWLEDGMENTS

The authors would like to thank Jack McMillan, Wendy Warters, and Kirk Osadetz for their comments and suggestions.

REFERENCES

ERCB
1992: Ultimate potential and supply of natural gas in Alberta. Energy Resources Conservation Board Report 92–A.

Lee, P.J.
1993: Two decades of Geological Survey of Canada petroleum resource assessments. Canadian Journal of Earth Sciences, v. 30, p. 321–332.

Lee, P.J. and Tzeng, H.P.
1993: The Petroleum Exploration and Resource Evaluation System (PETRIMES) – Working Reference Guide. Geological Survey of Canada, Open File 2703, 168 p.

Meneley, R.A.
1994: The Swan Hills gas play, an example of an assessment methodology to be used by the Canadian Potential Gas Committee. Presented before the Canadian Society of Petroleum Geologists Technical Program on September 7, 1994.

Reinson, G.E., Lee, P.J., Warters, W., Osadetz, K.G., Bell, L.L., Price, P.R., Trollope, F., Campbell, R.I., and Barclay, J.E.
1993: Devonian gas resources of the Western Canada Sedimentary Basin – Part I: Geological play analysis and resource assessment. Geological Survey of Canada Bulletin 452, 127 p.

EFFECTS OF APPRECIATION AND/OR DEPRECIATION OF GAS POOLS ON PETROLEUM RESOURCE ASSESSMENTS

P.J. Lee and H.P. Tzeng

Geological Survey of Canada, 3303-33rd Street N.W., Calgary, Alberta T2L 2A7

Pool reserve is one of the variables used in assessing petroleum resources. Gas pool reserves, however, may be appreciated and/or depreciated from their time of discovery. In this paper, the effect of gas pool reserve changes on petroleum resource assessment is examined.

The Jumping Pound Rundle gas play of the Western Canada Sedimentary Basin (Ozadetz et al., 1994) was chosen for this study. The following procedure was used:

1. The play data, comprising 94 discoveries in the 1991 database, were divided into four time windows: pre-1966 (Fig. 1A, 14 discoveries); pre-1974 (Fig. 1B, 25 discoveries); pre-1978 (Fig. 1C, 59 discoveries); and pre-1991 (Fig. 1D, 94 discoveries).

2. The data sets for the four time windows were evaluated using PETRIMES (Lee and Tzeng, 1993). The pool reserves used in the study were the values reported by the ERCB at the end of 1965 (ERCB,

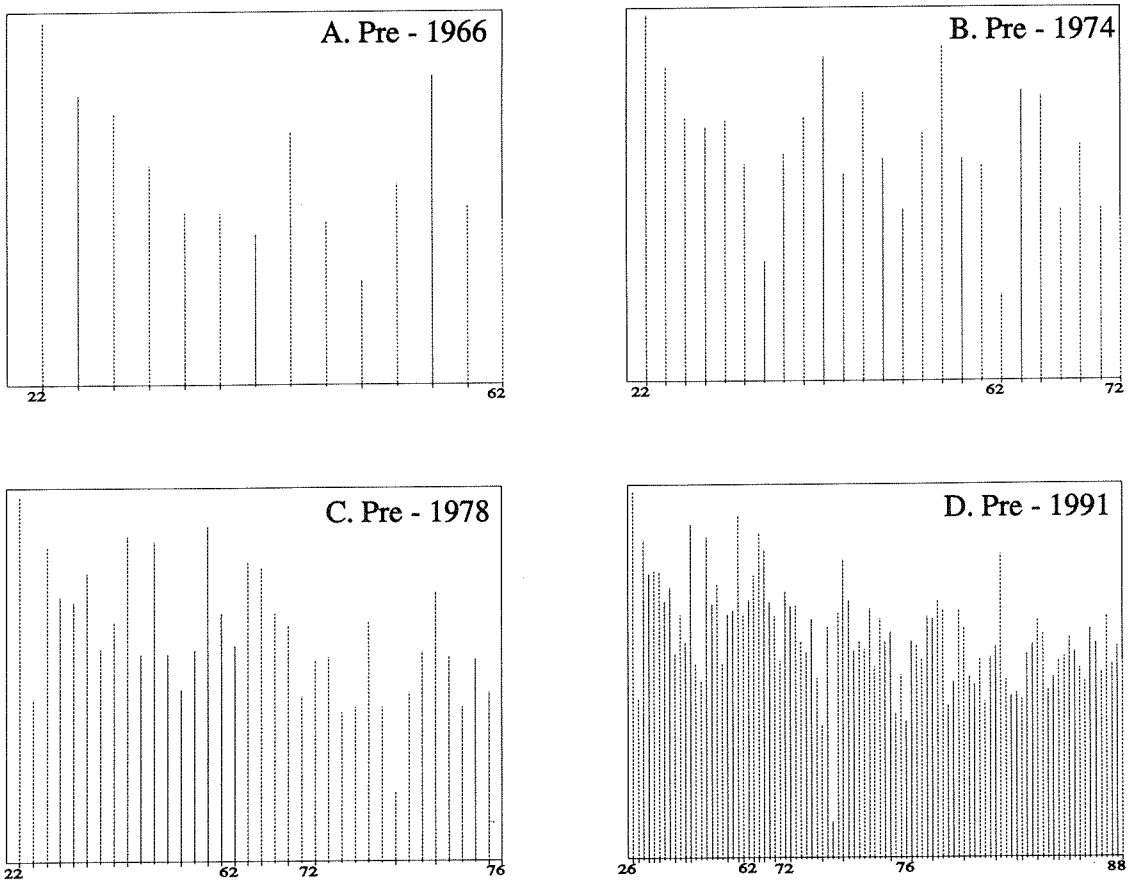

Figure 1. *Discovery sequences of the four time windows, Jumping Pound Rundle gas play.* ***A.*** *Pre-1966;* ***B.*** *Pre-1974;* ***C.*** *Pre-1978; D: Pre-1991.*

1966), 1973 (ERCB, 1974), 1977 (ERCB, 1978), and 1990 (ERCB, 1991).

3. The following estimates from the four time windows were compared:

   (1) Number of pools to be discovered in each pool size class;
   (2) Largest yet-to-be discovered pool size;
   (3) Play resource distribution;
   (4) Play potential distribution;
   (5) Total number of pools in the play;
   (6) Pool size distribution; and
   (7) Growth of individual pool reserves.

This approach allows us to examine the growth behaviour of pool reserves as well as the effect of appreciation and/or depreciation on the results of petroleum resource evaluations.

The effects of appreciation and/or depreciation of gas pools on resource assessments can be tentatively summarized as follows (Tables 1–3):

1. In this case, the play resource was appreciated and depreciated in the four time windows (Table 1).

2. The most severe impact on resource assessments due to appreciation and/or depreciation of the reserves is evident in estimation of the total number of pools, N. On the other hand, the effect on the resource distribution estimation is minimal, as can be seen from the similarity in the resource distributions for all time windows (Table 2).

3. The sums of the discovered and expected potential values are more or less the same for all time windows. If the sums are compared to the 1991 value (Table 3), one sees that the maximum difference is 16% for the 1966 time window, decreasing gradually to 3% for the 1978 time window.

4. The largest pool predicted for the 1966 time window is the Quirk Creek Rundle A pool discovered in 1967. The largest pool predicted for the 1974 time window is Clearwater Rundle A pool discovered in 1980.

REFERENCES

Energy Resources Conservation Board (ERCB)

1966: Reserves of crude oil, gas, natural gas liquids and sulphur, Province of Alberta at December 31, 1965. Alberta Energy Resources Conservation Board, Calgary, Alberta, OGCB Report 66–18, Table I–2.

1974: Reserves of crude oil, gas, natural gas liquids and sulphur, province of Alberta at December 31, 1973. Alberta Energy Resources Conservation Board, Calgary, Alberta, ERCB 74–18, Table 4–1.

1978: Alberta's reserves of crude oil, gas, natural gas liquids and sulphur at 31 December 1977. Alberta Energy Resources Conservation Board, Calgary, Alberta, p 4–1 to 4–166.

1991: Alberta's reserves of crude oil, oil sands, gas natural gas liquids and sulphur at December 1990: Alberta Energy Resources Conservation Board, Calgary, Alberta, Table 4–5.

Lee, P.J. and Tzeng, H.P.

1993: The Petroleum Exploration and Resource Evaluation System (PETRIMES) – Working Reference Guide. Geological Survey of Canada, Open File 2703, 168 p.

Ozadetz, K.G., Lee, P.J., Hannigan, P.K., and Olsen-Heise, K.

1994: Natural gas resources of the foreland belt of the Cordilleran orogen in Canada. Manuscription in preparation.

Table 1

Summary of the appreciation and/or depreciation of the gas pools in the Rundle play (All reserve and potential values are expressed in 10^6m^3)

Time window	No. of pools discovered	Reserve at the time window	Reserve at 1990	Appreciation and/or depreciation
1966	14	175 412	194 113	+10%
1974	25	261 536	243 091	-8%
1978	59	330 461	272 258	-21%
1991	94	355 082	355 082	–

Table 2

Summary of the Retrospective Study
(All reserve and potential values are expressed in $10^6 m^3$)

Time window before	Total no. of pools estimated	Expected potential	Resource distribution estimated*	Resource distribution estimated	Largest pool predicted*
1966	110	145 130	195 200–468 120	304 134	11 148–15 177
1974	100	63 366	182 520–730 370	376 326	6 910–10 930
1978	160	42 963	173 140–967 240	432 813	4 565–5 830
1991	173	27 794	210 020–630 020	366 373	4 611–5 883

*0.9 probability prediction interval.

Table 3

Comparisons between various time windows
(All reserve and potential values are expressed in $10^6 m^3$)

Time window	Sum of the discovered and the expected potential	Difference relative to 1991 Resource	Difference relative to 1991 N^	Difference relative to 1991 Mean
1966	320 542	-16%	-36%	-17%
1974	324 902	-15%	-42%	+3%
1978	373 424	-3%	-8%	+18%
1991	382 876			

NATURAL GAS RESOURCES OF THE FORELAND BELT OF THE CORDILLERAN OROGEN IN CANADA

K.G. Osadetz, P.J. Lee, P.K. Hannigan, and K.D. Olsen-Heise

Geological Survey of Canada, 3303-33rd Street N.W., Calgary, Alberta T2L 2A7

INTRODUCTION

The Foreland Belt of the Cordilleran orogen contains a raw initial gas-in-place (RIGIP) reserve of 908 749 x $10^6 m^3$ in 682 pools. Gas occurs primarily in anticline traps, formed during the deformation and shortening of North American miogeocline and foreland strata as they were accreted to allocthonous terranes that collided with the craton during the interval Late Jurassic to Paleogene. Two major characteristics of this gas province are:

- a northward decrease in both proven reserve and inferred potential, that parallels a northward decrease in the amount of Laramide tectonic shortening, and
- a fundamentally different stratigraphic distribution of gas reserves and resources, compared to that in the undeformed strata of the Interior Platform geological province.

Exploration of this hydrocarbon province began prior to the turn of the century. The first economically significant discoveries were made 90 years ago. Yet, important discoveries and developments continue to be made, often in plays identified years to decades earlier. The long, rational exploration history and anticlinal mode of accumulation make the Foreland Belt gas resources a most suitable target for analysis using the "Discovery History Process Model" of the Geological Survey of Canada's PETRIMES Resource evaluation system.

PLAY DEFINITION

Plays analyzed by "Discovery History Process" are defined by a combination of geographic (structural) and stratigraphic features that unify a set of hydrocarbon pools. Many features of the Foreland Belt, including structural style and hydrocarbon pool characteristics are controlled by north–south stratigraphic changes along the Foreland Belt. These changes result in three regions of distinctive structural style and stratigraphic succession commonly named the southern, central and northern segments of the Rocky Mountains and Foothills, with the boundaries of the central segment being defined approximately by the Athabasca and Peace rivers. Within the southern segment a marked change in structure and stratal succession occurs northward between portions of the Front Range with stratal successions characteristic of "Montania" versus those of the "Western Alberta Ridge" (Fig. 1). In the southernmost region immediately east of the triangle zone, there are other structures, many of which may have formed wholly or partly in response to Tertiary motions on the western flank of the Sweetgrass Arch that are also considered in our assessment. Likewise, profound differences in stratigraphy and structure naturally subdivide the northern segment into "Liard" and "Halfway-Sikkani" regions at about the latitude of Fort Nelson.

Overlain on the transverse stratigraphic variations are changes in the stratigraphic succession that control the position of reservoirs, source rocks, and which, through the structure, control the leading edge of deformation in any prospective reservoir horizion. Individual plays are, therefore, defined by using combinations of geographic region, structural style, and reservoir stratal horizon. Plays are subdivided into "mature" and "immature" plays (Table 1). "Mature" plays are those to which the "Discovery History Process" analysis could be easily applied. "Immature" plays are those whose play potential was determined by a "Discovery History Process" analysis of the total set of "mature" Foreland Belt plays. Individual pool sizes for immature plays were then determined using a play analogy in the set of mature plays.

GAS OCCURRENCE AND EXPLORATION HISTORY

Within the Foreland Belt, the major stratigraphic horizion for the largest accumulation of natural gases occurs in the highest strata below the most effective

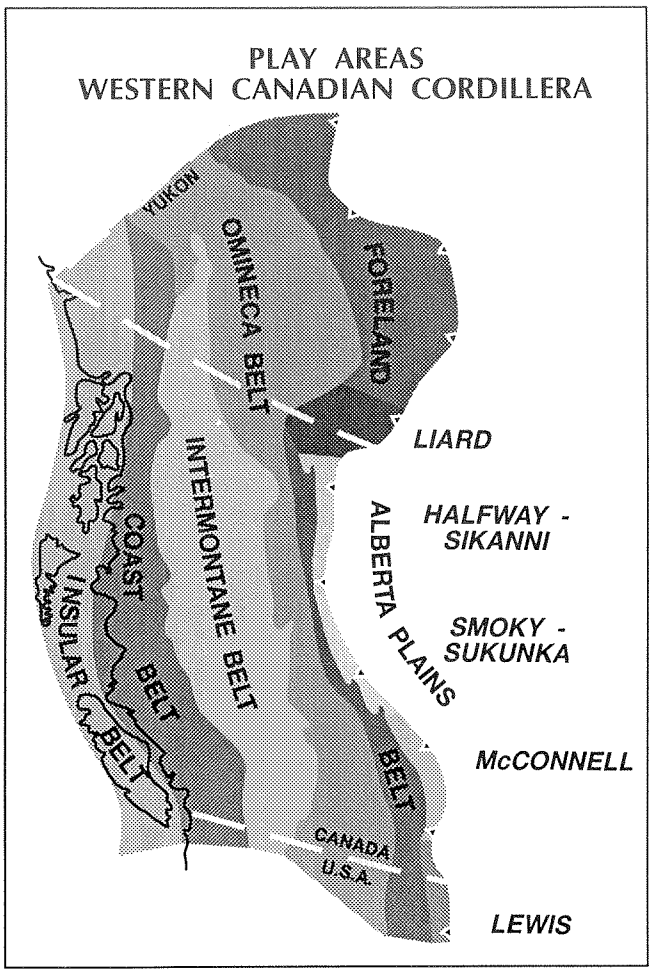

Figure 1. *Geographic assessment areas.*

regional seal. Throughout most of the geographic regions, the major seal occurs at the base of the Foreland Basin succession, while the highest porous zone changes northward due to the progressive preservation of higher Paleozoic and, ultimately, lower Mesozoic strata below the Foreland succession. In the Liard geographic area, the major regional seal appears to be the Devonian–Carboniferous shale succession overlying Manetoe lithofacies dolostones. The internal reserves of the Mesozoic Foreland successions are small compared with those in the underlying Paleozoic and Lower Mesozoic miogeoclinal succession. This is a marked contrast to the stratigraphic distribution of gases in the Interior Platform, and it suggests that the process of hydrocarbon generation, migration and entrapment history in the Foreland Belt is significantly different than that of the Plains. The origin and details of these differences are not understood, but they are accommodated with the play definitions used in this assessment.

Since the discovery of natural gas at Turner Valley, now 90 years ago, there has been a progressive and efficient exploration of the Foothills and Front Ranges. The cross plot of Exploratory Success Rate vs. Return on Your Dollar (Fig. 2), in fact, the rate of finding gas per metre of exploratory well drilled, illustrates this efficiency. Historical analysis of plays reinforces the validity and applicability of the "Discovery History Process" analysis.

RESULTS

The analysis of natural gas resources in the Foreland Belt of the Cordilleran orogen suggests that mature plays, with reserves of 675 149 x 10^6m^3 RIGIP in 626 pools, suggests that an additional 799 356 x 10^6m^3 RIGIP will be found in ~4981 undiscovered pools (Fig. 3, Table 1).

Many plays, including the Waterton Rundle/Wabamun play, are affected by political, economic, technical and conceptual restrictions that have prevented free exploration of the play area. For example, the Waterton Rundle/Wabamun play (220 687 x 10^6m^3 RIGIP), extends into the United States where various factors have prevented free exploration. Thus, the family of mature plays was subjected to a "Discovery History Process" analysis from which the size of immature and conceptual plays was predicted. By relying on a stratigraphic ordering of potential, empirical relationships between exploration stage and proportion of resource discovered, and constrained by the size of mature plays, we distinguished immature from conceptual plays. The Waterton Rundle/Wabamun

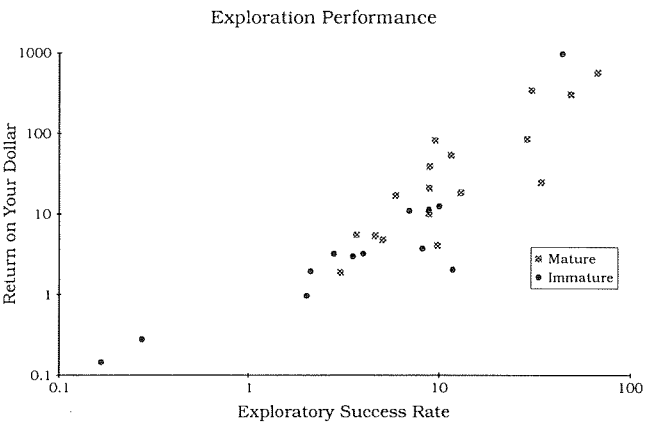

Figure 2. *Exploration risk vs. Return on Your Dollar.*

immature play is suggested to have an undiscovered expected resource of 530 910 x 10^6m^3 RIGIP, probably lying largely in the United States. The other 12 immature plays are inferred to have an additional undiscovered expected resource 581 253 x 10^6m^3 RIGIP for a total undiscovered expected resource in immature plays of 1 112 163 x 10^6m^3 RIGIP in approximately 3900 undiscovered gas pools. Conceptual plays are expected to contain 440 190 x 10^6m^3 RIGIP in an unknown number of pools. Details of the analysis appear in Table 1.

The analysis also predicts the size of undiscovered pools (Table 1, Fig. 4), a feature probably of greater interest to explorationists than the total resource, since pools are roughly equivalent to prospects. Figure 4 shows that greatest potential for large pools lies in the immature plays. The outlying pool to the far right is a large undiscovered pool in the Waterton Rundle-Wabamun Play. It is however possible that the Waterton Sheet Three pool is the largest pool in this play, but reserves underlying Waterton National Park have not been considered. Regardless, the analysis suggests that a very large pool, comparable to or larger than Waterton Sheet Three remains undiscovered in this play, although it probably lies in the United States of America.

The next three largest undiscovered pools are expected in the Chinook Ridge Permo-Carboniferous Play of the Central Foothills, the Carboniferous play in the Liard Basin and in the Del Bonita Rundle/Madison play (Table 1), immediately updip of the large Waterton Rundle/Wabamun Play. All three plays are immature, but all are expected to yield a large pool between 0.5 and 1.0 TCF.

Table 1

Play by play results

PLAY NAME	DISCOVERED E6 m3	EXPECTED E6 m3	Total Res. E6 m3	disc. #	undisc. #	largest E6 m3	Exp risk %	bang4$ E3(E6m3/m)
MATURE PLAYS								
Brazeau Belly River	3389	19357	22746	29	871	456.56	3.02	1.88
Ricinus Cardium	33446	3369	36815	94	66	739.55	12.91	18.48
Ricinus Viking	6337	4413	10750	15	85	456.39	3.66	5.57
Turner Valley Blairmore	2910	12143	15053	41	359	718.55	9.76	4.13
Nordegg Triassic	3003	84443	87446	8	292	1575.40	8.79	10.07
Jumping Pound Rundle	355082	27794	382876	94	79	5207.70	29.94	343.15
Burnt Timber Wabamun	18500	46084	64584	12	108	2326.40	8.89	38.84
Ansell Cardium	23189	39179	62368	42	158	3901.30	8.82	20.96
Jackpine Paddy/Cadotte	2278	9878	12156	10	190	571.37	5.08	4.79
Grizzly Blairmore	15066	15474	30540	67	523	524.00	33.67	24.72
Sukunka Triassic	84125	183960	268085	42	258	11684.00	48.28	308.71
Jedney Blairmore	6210	13583	19793	19	381	2107.40	5.90	16.98
Jedney Baldonnel	34288	162370	196658	29	381	6625.10	9.45	82.03
Jedney Charlie Lk.	2375	19539	21914	13	537	265.64	4.63	5.40
Jedney L. Triassic	23127	13762	36889	31	119	2236.20	11.48	53.84
Jedney Permo-Carb.	28004	41258	69262	46	184	4958.50	28.40	85.71
Beaver River Devonian	33820	102750	136570	10	390	5064.00	66.67	570.59
Total Mature Plays	675149	799356	1474505	602	4981			
IMMATURE PLAYS								
Waterton Rundle/Wabamun	220687	530910	751597	28	172	290900.00	43.75	973.20
Waterton Colorado	199	27405	27604	2	210	6607.20	2.02	0.97
Waterton Mannville	459	34076	34535	3	115	1303.90	3.53	2.99
Del Bonita Colorado	150	5036	5186	4	36	2334.80	8.16	3.72
Del Bonita Madison	780	54813	55593	3	23	27555.00	6.98	10.91
Limestone Fairholme	4586	73870	78456	10	132	6035.20	10.00	12.45
Lawrence 2WS	257	32664	32921	1	252	7323.00	0.17	0.15
Red Rock Belly River	1772	17865	19637	11	754	702.00	2.11	1.94
Hinton Dunvegan	1979	34242	36221	9	1402	948.00	4.00	3.22
Findley Nordegg	952	59552	60504	3	204	1470.00	2.80	3.20
Chinook Ridge P-Carb	1449	92634	94083	3	41	39022.00	8.82	11.24
Edson 2WS	246	31130	31376	1	240	7120.00	0.27	0.28
Beaver River Carboniferous	84	117966	118050	2	325	16717.00	11.76	2.04
Total Immature Plays	233600	1112163		80				
Total Mature and Immature	908749	1911519						
Conceptual Plays		440190						

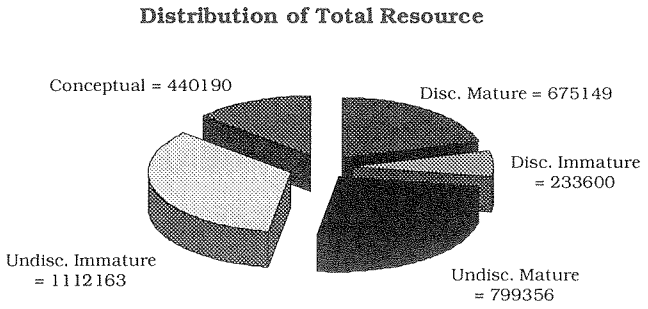

Figure 3. *Distribution of resources.*

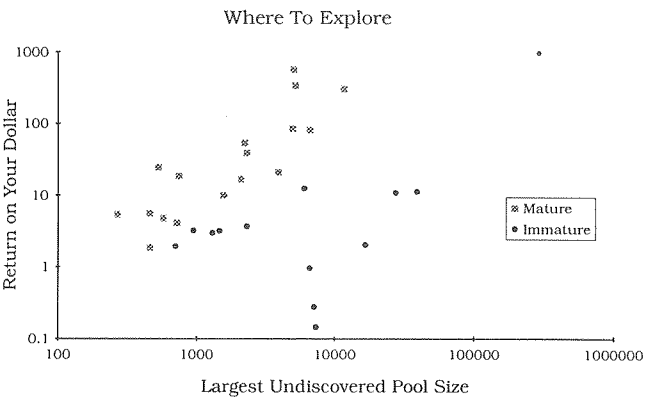

***Figure 4.** Undiscovered pools size vs. Return on Your Dollar.*

Smaller pools, approximately 0.5 TCF and smaller are expected to remain in the three most prospective and efficiently exploitable mature plays that occupy the upper centre of Figure 4. These include the Triassic Sukunka, Jumping Pound Rundle and Beaver River Devonian plays.

In summary, the analysis of mature and immature plays in the Foreland Belt using the "Discovery History Process" not only shows a significant undiscovered potential, but it points to the existence of very large undiscovered pools. Very large undiscovered pools occur among the currently more difficult to explore immature plays, yet significant undiscovered potential and attractive pools remain undiscovered in the more facile mature plays.

OIL AND GAS EXPLORATION PLAYS OF MAINLAND NORTHWEST TERRITORIES AND YUKON

T.D. Bird

Geological Survey of Canada, 3303-33rd Street N.W., Calgary, Alberta T2L 2A7

P.R. Price

National Energy Board, 311-6th Avenue S.W., Calgary, Alberta T2P 3H2

M.C. Fortier

Indian and Northern Affairs Canada, Ottawa, Ontario K1A 0H4

G. Cave

P & NG, 2410-10th Avenue S.W., Calgary, Alberta T3C 0K6

Oil and gas exploration of the northern extension of the Western Canada Sedimentary Basin in the mainland portion of the Northwest Territories and eastern Yukon has identified 27 significant discoveries of hydrocarbons (Table 1). At least 6 petroleum systems are suggested by these discoveries in ten stratigraphic intervals found between 60° and 68°N (Fig. 1). This area has been penetrated by fewer than 700 exploratory wells drilled sporadically since the 1920s. Discovered oil resources (mean recoverable) total almost 39 x 10^6m^3 (245 x 10^6 bbl) in three discoveries of which 21 x 10^6m^3 have been produced from the Norman Wells field. Discovered gas resources (mean recoverable) of over 35 x 10^9m^3 (almost 1.3 x 10^{12} cu. ft.) are distributed in the remaining discoveries. Cumulative total gas production is 10.6 x 10^9m^3 (0.4 x 10^{12} cu. ft.) from the Pointed Mountain, Kotaneelee, and Beaver River fields, all located in the Liard area.

Gas and oil discoveries, in plays defined as very immature, occupy 5 areas, broadly defined by physiographic region (Fig. 2). These are, beginning in the southwest:

1) Liard (site of Pointed Mountain and Kotaneelee fields),

2) Great Slave Plain – South Slave (which includes more than 12 discoveries and recent activity at Cameron Hills and Arrowhead),

3) Mackenzie Plain (site of the Norman Wells oilfield which produces oil out of the Middle Devonian Kee Scarp member of the Ramparts Formation),

4) Colville Hills (where 4 pools have been identified in Cambrian aged strata), and

5) Eagle Plain (where oil and gas have been encountered in Permian, Carboniferous and Cretaceous strata).

Other physiographic regions with no known discoveries include the sparsely drilled Great Bear, Anderson and Peel Plains.

The historical trend for relatively low levels of exploration activity in the entire area is due, in part to difficult operating conditions and remoteness from petroleum development in Alberta and British Columbia, as well as a hiatus in land rights issuance due to native land claims. For the first time in 25 years, starting in mid-1994, large areas have been opened to exploration. In December 1994, 6 companies bid a total of $22 million for eight parcels in the Liard and western Slave regions. Five more parcels in the central Mackenzie Valley are open for bids until April 24, 1995.

With exploration companies trying to expand a shrinking reserve base in more conventional areas to the south, this area, with its comparitively sparse drilling, is likely to become the focus for more exploration activity in the near future.

Work done in collaboration with National Energy Board and Indian and Northern Affairs Canada forms the basis for an appraisal of undiscovered resources as part of the continuing Western Canada assessment program.

Table 1. Mainland Northwest Territories and Yukon Discovered Resources by Play Type

Significant Discovery	Mean Recoverable Volume in Million Cubic Metres	Mean Recoverable Volume in Billion Cubic Feet	Producing Zone(s)	Play Type	Map Ref.
Gas					
Liard					SW 1
Pointed Mountain (field total)	10200	360.2	Middle Devonian Nahanni (Manetoe facies dolomite)	structural (anticlinal traps) with diagenetic influence (Manetoe facies dolomite)	
Beaver River (Yukon portion only)	218.22	7.7	Nahanni (Manetoe)	" "	
La Biche	1771	62.5	Nahanni (Manetoe)	" "	
Liard	958.71	33.9	Arnica (Manetoe)	" "	
Kotaneelee- N. Beaver River (field total)	5012.35	177.0	Nahanni, Arnica (Manetoe)	" "	
subtotal	18160.28	641.3			
South Slave					
Bovie Lake J-72	178.2	6.3	Devonian Keg River (Presqu'ile facies dolomite)	stratigraphic- diagenetic with structural overprint	SW 2
Arrowhead G-69	120	4.2	Keg River	stratigraphic - Middle Devonian carbonate bank edge	SW 2
Arrowhead B-41	291.9	10.3	Lwr. Cretaceous Clastics	stratigraphic- channel sands with structural overprint	SW 2
Netla N-07	625.1	22.1	Devonian Slave Point (Presqu'le facies dolomite)	stratigraphic - diagenetic - M. Dev. carbonate bank edge	SW 2
Celibeta H-78	148.8	5.3	Slave Point	stratigraphic -M. Dev. carbonate bank edge	SW 2
S. Island River M-41	51.44	1.8	Slave Point	" "	S 2
Trainor Lake C-39	32.89	1.2	Slave Point	" "	S 2
Grumbler G-63	37.66	1.3	Slave Point	" "	
Rabbit Lake O-16	334.34	11.8	Slave Point	" "	SE 3
Tathlina N-18	73.2	2.6	Slave Point	" "	SE 3
Cameron Hills M-31, F-51(confidential wells not included)	106.67	3.8	Slave Point, Sulphur Point and Keg River	stratigraphic with structural overprints	SE 3
subtotal	2000.2	70.6			
Colville Hills					N 4
Tedji Lake K-24	1147	40.5	Cambrian Mount Clark	structural/stratigraphic - sandstone reservoirs in fault bounded structures superimposed on large domal features	
Tweed Lake M-47	5697	201.2	Cambrian Mount Clark	" "	
" "	409	14.4	Cambrian Mount Cap	" "	
Bele O-35	5344	188.7	Cambrian Mount Clark	" "	
subtotal	12597	444.9			
EAGLE PLAIN					NE 6
Blackie	725	25.6	Permian Jungle Creek	sandstone reservoirs - Laramide folds	
Birch (field total)	283	10.0	Carboniferous (Miss.) Chance, Tuttle	sandstone reservoirs - Laramide folds	
Chance (field total)	1666	58.8	Lower Cretaceous Fishing Branch, Carboniferous (Miss.) Chance, Canoe River, Tuttle	structural/stratigraphic- sandstone reservours Carboniferous limestone -Laramide folds	
subtotal	2674	94.4			
TOTAL GAS	**35431.48**	**1251.2**			
Oil	mean recoverable in-place volume in million cubic meters	mean recoverable in-place volume in Million Barrels			
Norman Wells	37.50	235.88	Middle Devonian Ramparts Formation, Kee Scarp Member	Stratigraphic reef, with structural overprint	N 5
Eagle Plain - Chance (field total)	1.49	9.37	Carboniferous Chance, Canoe River	Mississippian sandstones, limestone- structural and stratigraphic	NE 6

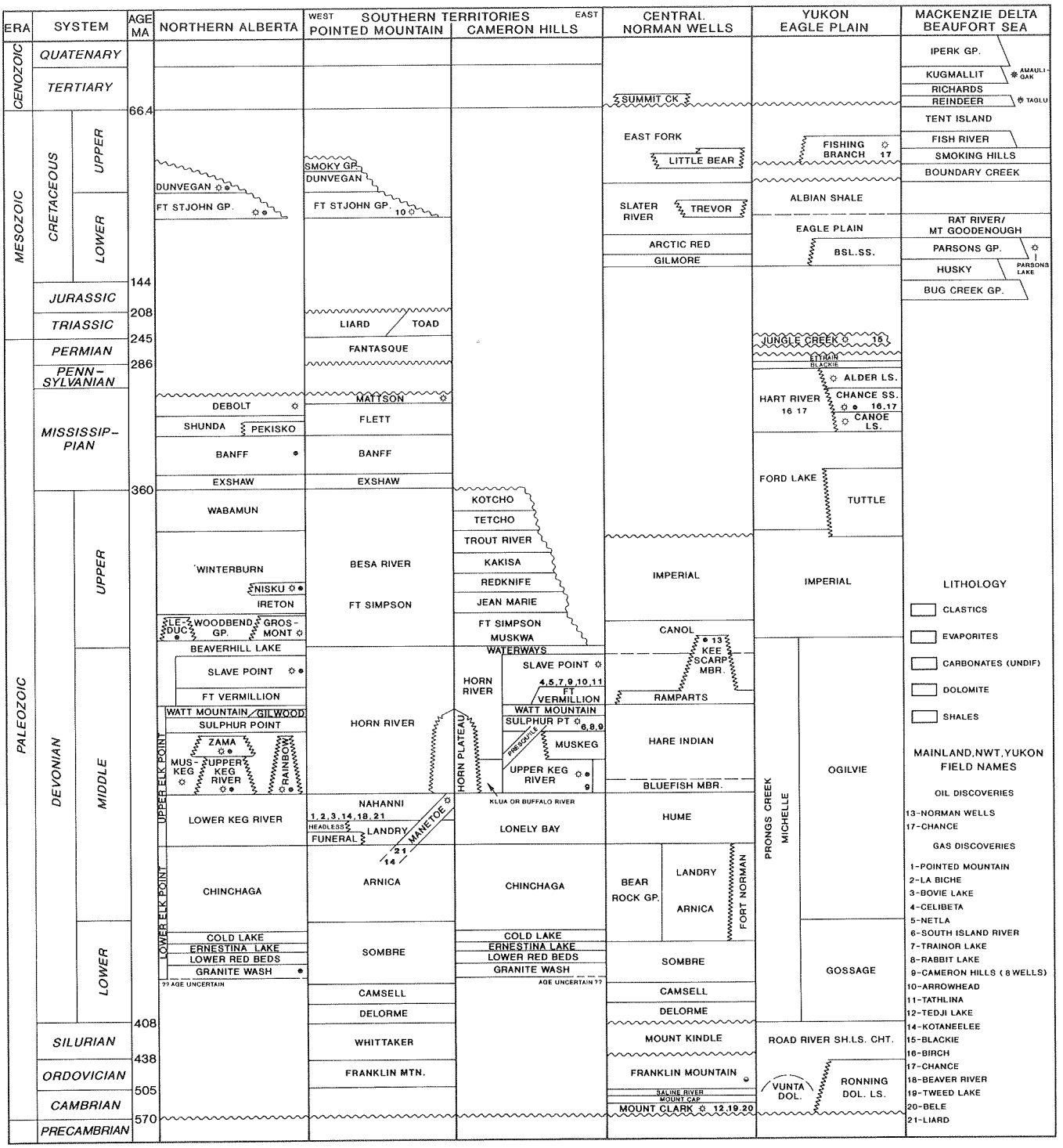

Figure 1. *Stratigraphic column showing significant discoveries by zone.*

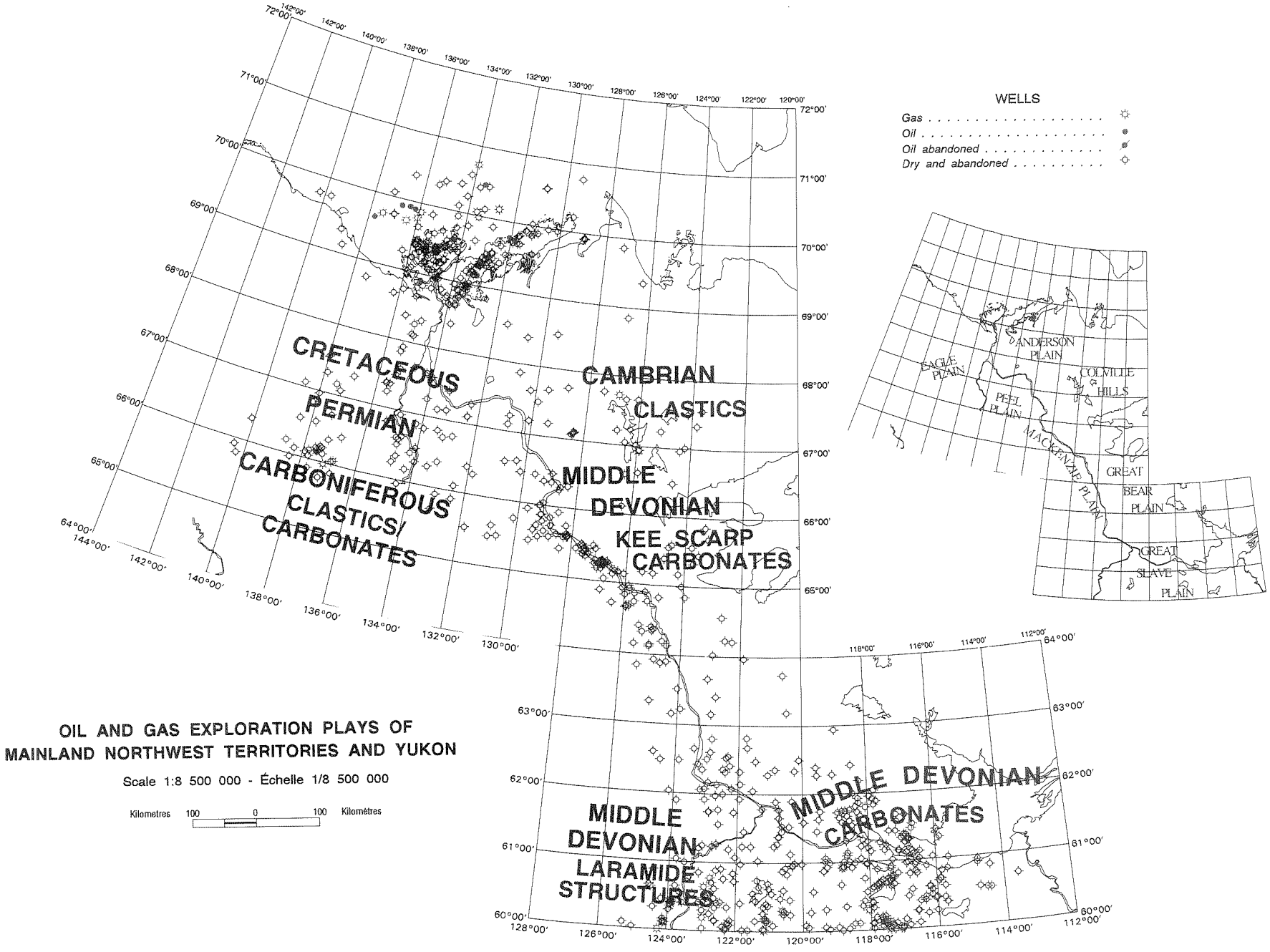

Figure 2. *Oil and gas exploration plays of mainland Northwest Territories and Yukon.*

PETROLEUM RESOURCES OF THE LIARD PLATEAU AREA, SOUTHERN YUKON TERRITORY, CANADA

P.R. Price

National Energy Board, 311-6 Avenue S.W., Calgary, Alberta T2P 3H2

EXECUTIVE SUMMARY

The Liard Plateau is an immaturely explored area with proven middle Devonian gas potential. Potential exists for further discoveries in Devonian, Mississippian, Permian and lower Cretaceous portions of the stratigraphic section.

Basin Age	lower Paleozoic to Cretaceous; Quaternary cover
Basin Area (Yukon Territory)	8553 km^2 (3302 mi^2)
Depth to Target Zones	middle Devonian Targets: 3500 to 5000 m (11 500 to 16 400 ft.); Mississippian Targets: 2250 to 3000 m (7380 to 9840 ft.); lower Cretaceous Targets: 600 to 800 m (1960 to 2625 ft.)
Maximum Basin Thickness	over 6000 m; up to 3600 m of Mesozoic rocks
Hydrocarbon Shows	Surface: None Subsurface: *Gas:* Mississippian Prophet Formation, Devonian Besa River, Nahanni and Arnica formations *Oil:* None
First Discovery	Canadian Southern et al. North Beaver R. TY I-27 (R.R. 12-Apr-64; Manetoe facies–Nahanni Formation; sour, acid gas)
Discovered Resources	*Gas* (Initial Gas In-place): 5230 x 10^6m^3 *Gas* (Rec. Resources; median value): 1171 x 10^6m^3 *Oil:* None
Production	*Gas* (to 06/03/93): 1256 x 10^6m^3 *Oil:* None
Undiscovered Potential Resources	*Gas:* Mean Value: 1.99 TCF @ 38.6% Probability
(Study Area Totals)	*Oil*: Mean Value: 0.01 Mmbbls @ 41.7% Probability
Basin Type	Paleozoic: Epiric Sea on a stable platform; Mesozoic to Recent: Foreland Basin
Depositional Setting	Paleozoic: Carbonate Shelf, Bank and Slope; Mesozoic: Fluvial, Deltaic and shallow Shelf clastics
Potential Reservoirs	*Gas:* Cretaceous Fort St. John Group clastics, Permian fractured cherts, Mississippian Mattson clastics and Prophet Formation cherts, Devonian Besa River fractured shales, Middle Devonian Nahanni, Landry and Arnica formations (Manetoe facies dolomites) *Oil*: basal Cretaceous clastics
Regional Structure	Northwestward, northward and northeastward trending Laramide folded Anticlines, high-angle reverse faults and thrust faults; Northeastward Laramide and post-Laramide normal faults formed along pre-existing structural zones of Paleozoic age.
Seals	Cretaceous Targets: Shales of the Buckingshorse, Lepine, Sully and Garbutt formations; Permian Targets: Triassic and Cretacoue shales; Mississippian Targets: Mississippian Etanda shales, Triassic and Cretaceous shales; Manetoe Facies Targets: Devonian Shales and tight limestones
Source Rocks	Cretaceous shales; Triassic shales; Middle Devonian Besa River Shales
Depth to Oil/Gas Window	Top: surface to 1200 mKb (Cretaceous to Mattson Strata); Base: 500 to 2500 mKb (in the Golata shales)
Wells in Study Area	11 (6 gas wells; 5 dry and abandoned)
Released Seismic Coverage	2-D: more than 850 line kilometres (6% post 1975) 3-D; 0 line kilometres (0% post 1975)
Pipelines	West Coast Pipeline–Kotaneelee/Pointed Mountain (10 inch line; maximum capacity 300 x 10^6m^3/day; percentage utilization 20% (July 94); Gas processed at Fort Nelson, B.C., Plant (about 100 x 10^6m^3 in spare capacity at the plant (July 94))
Area under Licence	145.1 km^2

INTRODUCTION

A study of the petroleum resources of the Yukon Territorial portion of the Liard Plateau was undertaken in response to a request from the Yukon Territorial Government. The study fulfils the National Energy Board's (the "Board") requirements under the Yukon Accord for technical support of the Territorial Government leading up to the transfer of oil and gas regulation under the terms of the Yukon Accord. Assessment of petroleum resource potential is important for the formation of regulatory policy with respect to these resources and to provide a basis for planing an issuance of exploration rights.

The objective of the study was to investigate the petroleum resource potential and endowment of the Liard Basin region under the jurisdiction of the Yukon Territory. The study area is located in the southeastern portion of the Yukon Territory between the Yukon and Northwest Territorial border and longitude 126°W and latitudes 60° to 61°N (Fig. 1). This region lies within the Canadian Cordillera west of the northern portion of the Western Canadian Interior Plains and is bordered by the Rocky Mountains to the south and the Mackenzie and Franklin Mountains to the north. The area is marked by a complex landscape of rugged anticlinal mountains and plateaus with elevations up to 1500 m. The terrain is deeply dissected by more or less parallel, northward-trending, wide intermontaine valleys with elevations ranging from 450 to 600 m.

REGIONAL GEOLOGICAL SETTING

The study area occupies an area of 8553 km^2 (3302 sq. mi.) and is situated in the vicinity of the boundaries of the province of British Columbia, and the Yukon and Northwest Territories. It is bounded to the north and east by the Yukon Territory–Northwest Territory border, to the south by the British Columbia–Yukon Territory border and to the west by longitude 126° (the approximate eastern margin of the Hyland Plateau). The study area includes the following present day physiographic elements; the Liard Plateau and the portions of the southern Mackenzie and Franklin Mountains (Fig. 2).

The Liard Plateau lies between the Rocky Mountains to the south and the Mackenzie and Franklin Mountains to the north and includes the Tlogotsho Plateau in the Northwest Territories. To the east of the Liard Plateau lies a vast area of low relief called the Great Slave Plain (an extension of the Interior Plains of North America) that is largely underlain by Cretaceous to Paleozoic strata and is generally below 300 m in elevation. To the West of the Liard Plateau lies a well timbered low relief area called the Hyland Plateau.

In the eastern part of the study area lie the Liard and Nahanni ranges, while to the west lie the more rugged Sunblood, Sombre, Arnica, Manetoe and Funeral ranges. Overall the study area is rugged and mountainous with local elevations above 1500 m. The plateau is deeply dissected with the more or less parallel resistant Paleozoic cored anticlinal ridges trending northward and separated by wide synclinal Mesozoic cored valleys, at elevations of 450 to 600 m, that are partially covered by alluvium. Two major rivers dissect the Plateau and drain eastward into the Liard River: the Beaver River and the Nahanni River. The central portion of the study area is composed of the fairly flat topped Nahanni and Tlogostsho Plateaus which are dissected by the canyon of the Nahanni River. To the southwest lies the more gentle rolling heavily timbered country around the Beaver River Anticline including Spruce Lake, Fantasque Lake and Larsen Lake.

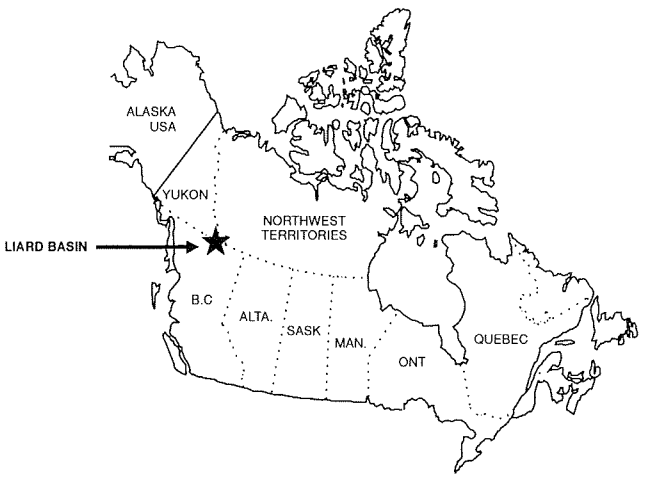

Figure 1. *Location map.*

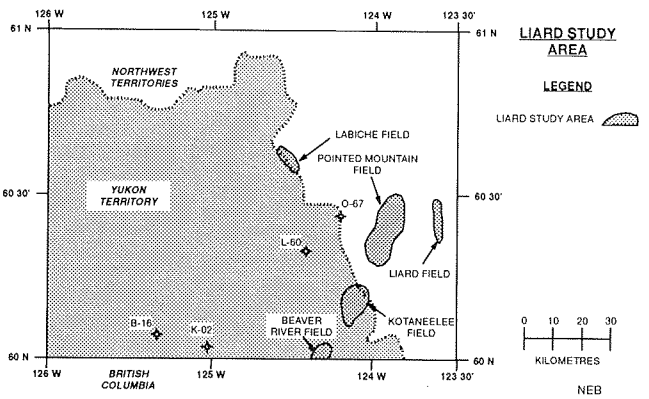

Figure 2. *Liard Plateau study area.*

Underlying the sedimentary cover of the study area and forming the effective basement is a melange of meta-sedimentary, metamorphic and igneous rocks of Precambrian age. These rocks are generally overlain by Miogeoclinal Paleozoic strata characterized by marine carbonates and shales. Deposition of Mesozoic strata was characterized by predominantly fine and medium grained clastics derived from the erosion of the emerging Cordillera in the west and to a minor extent from the Canadian Shield to the east.

Surface exposures of Devonian and older rocks is confined mainly to the northwest half of the study area, while Mississippian and Cretaceous rocks are exposed in the southeast half of the study area. Cretaceous rocks lie directly upon rocks of Permian age. No Pennsylvanian or Jurassic strata are present in the study area.

Access to the area is via the Alaska Highway (approximately 20 to 60 miles to the south), by boat or barge on the Liard River to the east and on the Nahanni River downstream from Virginia Falls, by float plane on Larsen Lake, Spruce Lake and Fantasque Lake or by fixed wing plane from the airstrips at Fort Liard or Nahanni Butte, Northwest Territories. The presence of muskeg in the low lying valleys, windfall and burnt dead-fall makes any surface summer travel through the study area away from the main river courses extremely difficult.

PETROLEUM GEOLOGY

Six petroleum plays were identified within the study area (5 gas and 1 gas with potential oil): one play can be considered established, the Middle Devonian Manetoe facies Dolomite sour gas play, as it has both proven discoveries and gas production; the other five significant have shows from analogues in adjacent areas and are considered immature. These plays include: the Lower Cretaceous Chinkeh Clastics Play (sweet gas and oil shows in N.W.T. and B.C.), the Permian Fantasque Fractured Chert Play (sweet gas show in B.C.), the Permo-Carboniferous Mattson Clastics Gas Play (sweet gas show in B.C.), the Mississippian Prophet/Flett Carbonate Play (sour(?) gas show in B.C.), and the Middle Devonian Muskwa/Besa River Fractured Shale Play (sour (?) gas show in B.C.). The current analysis yields the following results for the undiscovered marketable resources within the study area (Table 1).

REFERENCES

Leckie, D.A., Potocki, D.J., and Visser, K.
1991: The Lower Cretaceous Chinkeh Formation: a Frontier-Type Play in the Liard Basin of Western Canada. American Association of Petroleum Geologists Bulletin, v. 75, no. 8, p. 1324–1352 (25 refs.).

Morrow, D.W., Cumming, G.L., and Aulstead, K.L.
1990: The Gas-Bearing Devonian Manetoe Facies, Yukon and Northwest Territories. Geological Survey of Canada, Bulletin 400.

Morrow, D.W., Potter, J., Richards, B., and Goodarzi, F.
1993: Paleozoic Burial and Organic Maturation in the Liard Basin Region, Northern Canada. Bulletin of Canadian Petroleum Geology, v. 41, no. 1, p. 17–31 (44 refs.).

National Energy Board
1993: Probabilistic Estimates of Hydrocarbon Volumes. *In* Northern Canadian Frontier Discoveries. National Energy Board News Release no. 93/46.

1994: Natural Gas Resource Assessment, Northeast British Columbia. National Energy Board Working Document.

Table 1

Marketable Product Volume	Value at a Probability of 95%	Value at a Probability of 50%	Value at a Probability of 5%	Value at the Mean	Probability of Mean
Lower Cretaceous Gas (BCF)	.46	1.13	2.46	1.24	41.7
Lower Cretaceous Oil (mmbbl)	0.005	0.013	0.031	0.015	41.7
Permian Fantasque Gas (BCF)	0.22	0.59	1.83	0.76	39.8
Mattson Gas (BCF)	55.41	148.13	359.54	170.0	41.9
Prophet/Flett Gas (BCF)	28.0	67.0	153.0	76.5	41.7
Muskaw/Besa River Gas (BCF)	36	149	472	191.9	36.4
Manetoe Gas (BCF)	295	1201	3830	1548	36.9
Total Gas Immature Plays (BCF)	92	327	1163	440.4	38.4
Total Oil Immature Play (mmbbl)	0.005	0.013	0.031	0.015	41.7
Total Gas Mature Play (BCF)	295	1201	3830	1548	36.9
Total Oil Mature Play (mmbbl)	0	0	0	0	0
Total Gas (BCF)	383	1439	5394	1987.3	38.6
Total Oil (mmbbl)	0.005	0.013	0.031	0.015	41.7

PETROLEUM RESOURCES ASSESSMENT OF THE EAGLE PLAIN BASIN, YUKON TERRITORY, CANADA

J.A. Davidson

National Energy Board, 311-6th Avenue S.W., Calgary, Alberta T2P 3H2

A.P. Hamblin and J. Dixon

Geological Survey of Canada, 3303-33rd Street N.W., Calgary, Alberta T2L 2A7

EXECUTIVE SUMMARY

The Eagle Plain Basin is an immaturely explored area with proven Cretaceous, Permian, Mississippian and Devonian gas and oil potential. Potential exists for further gas and oil discoveries in these and lower portions of the stratigraphic section.

Basin Age	Lower Paleozoic to Cretaceous; Quaternary cover
Basin Area	20 608 km^2 (8050 sq. miles)
Depth to Target Zones	Middle Devonian targets: 1000 to 2000 m (3300–6400 ft.); Mississippian targets: 800 to 1500 m (2600–5000 ft.); lower Cretaceous targets: 600 to 1000 m (1960–3300 ft.)
Maximum Basin Thickness	5800 m
Hydrocarbon Shows	Surface: None Subsurface: *Gas:* In several wells, from Silurian–Ordovician Ronning Group to Lower Cretaceous Fishing Branch Formation *Oil:* In several wells, from Mississippain Chance Sand to Permian Jungle Creek Formation
First Discovery	Western Minerals Chance Y.T. No. 1 M-08 (Rig Release 25, May, 60; Fishing Branch Formation gas, Chance Sand Member gas and oil, Canoe River Limestone Member gas and oil, Tuttle Sand gas
Last discovery	Socony Mobil Western Minerals Birch B-34 (Rig release 8, June, 65; Chance Sand Member gas, Tuttle Sand gas)
Discovered Resources	Gas: 2376 x 10^6m^3 (83.7 BCF) Oil: 1.5 x 10^6m^3 (9.5 mmbbls)
Production	No production to date
Undiscovered Potential	Gas: Mean 28 478 x 10^6m^3 (1005.7 BCF) @ 45% probability Oil: Mean 4.5 x 10^6m^3 (28.2 mmbbls) @ 45% probability
Basin Type	Shallow marine shelf (Paleozoic to early Mesozoic); intermontane compressional (Cretaceous to Recent)
Depositional Setting	Shallow water carbonate and clastic shelf
Potential Reservoirs	Carbonate reefal mounds and facies fronts; fractured carbonates; unconformity traps and discontinuous marine clastic lenses
Regional Structure	Long wavelength folds at surface; detachment with thrust folds within deeper strata; contraction and minor relaxation faulting
Seals	Cretaceous Targets: Shales of the Whitestone River Formation. Permian Targets: Cretaceous Shales of the Whitestone River Formation. Carboniferous Targets: Lower Carboniferous Alder Member limestones or Upper Carboniferous Blackie Formation shales. Devonian Targets: Lower Carboniferous Ford Lake Formation shale, Upper Devonian Imperial and Canol Formation shales or Middle Devonian carbonates. Silurian–Ordovician Targets: Road River Formation shales or Ronning carbonates
Source Rocks	Cretaceous shales; Carboniferous shales; Devonian shales
Depth to Oil/Gas Window	1900 to 3100 m
Wells in Study Area	30 (2 gas wells; 1 gas and oil well, 2 oil wells and 25 dry and abandoned)
Released Seismic Coverage	2-D: 9952 line km (8% post 1975); 3-D: 0 line km
Pipelines	None
Area under Licence	8900 ha (0.4% of the basin)

INTRODUCTION

A study of the petroleum resources of the Yukon Territory's Eagle Plain Basin was undertaken in response to a request from the Yukon Territorial Government. The study is part of the National Energy Board's (the "Board") requirements under the Yukon Accord for technical advisory support to the Territorial Government in leading up to the transfer of oil and gas regulation. Assessment of petroleum resource potential is important for the formation of regulatory policy with respect to these resources and to provide a basis for the planning and issuance of exploration rights.

The objective of this study was to investigate the petroleum resource potential and endowment of the Eagle Plain basin (Fig. 1). This study is only intended to provide an overview of the geology and petroleum potential of this basin. The study area is located in the north central portion of the Yukon Territory between Latitudes 65°and 68° North and Longitudes 135°and 140° West and covers an area of approximately 20 608 km^2 or 8050 sq. miles (Fig. 2). The Arctic Circle essentially bisects the surface area of the basin. Physiographic features within the study area include the Eagle Plains bounded by surrounding mountain ranges including the Dave Lord and Nahoni Ranges of the Richardson Mountains and the Ogilvie Mountains.

Regional Geological Setting

The study area includes the present day physiographic elements of the Eagle Plain and its surrounding mountain ranges (Fig. 2). The Eagle Plain Basin is an intermontane compressional basin with a maximum sediment thickness of 5800 m. The basin is outlined by outcrops of Mesozoic sediments in the surrounding mountain ranges. Recent alluvium covers much of the Basin's surface area. The present Eagle Plain surface consists of low rolling hills with elevations varying between 400 and 800 m. The southern plains are lightly forested with the amount of forestation thinning to the north. Tundra conditions exist in both the northern areas and at higher elevations in the southern areas. Access to the basin is available via the Dempster Highway which straddles the plains and is open to traffic for most of the year.

Petroleum Geology

Twelve petroleum plays were identified within the study area (7 gas and 5 gas and oil): seven plays can be considered established as they have yielded proven discoveries; the other five have shows in this basin or in other basins and are considered immature. The plays in the study area are outlined in the following table.

These estimates of undiscovered resources are based on limited data, especially for the immature plays and for the stratigraphic plays. There is considerable uncertainty involved both in the play analysis and in the play assessment (Table 1).

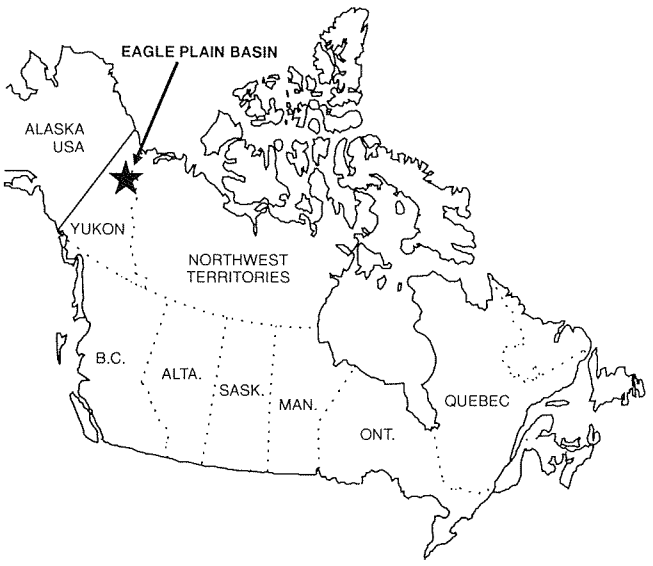

Figure 1. Location map.

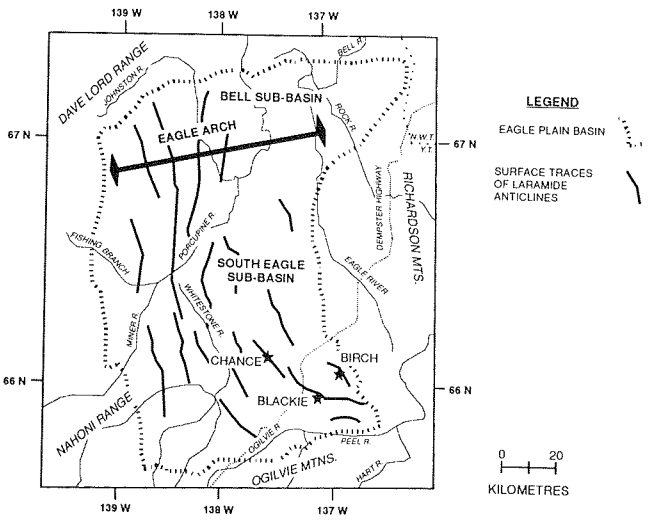

***Figure 2.** Physiographic features of Eagle Plain Basin.*

Table 1

Established Plays	Potenital
Cretaceous Fishing Branch Sand–Laramide folds	gas
Permian Jungle Creek Sand–Laramide Folds	gas and oil
Mississippian Chance Sand–Laramide folds	gas and oil
Mississippian Chance Sand–Structural and Stratigraphic	gas and oil
Mississippian Chance Sand–Stratigraphic	gas and oil
Mississippian Canoe River Limestone–Stratigraphic	gas and oil
Lower Carboniferous Tuttle Sand–Stratigraphic	gas
Immature Plays	
Cretaceous Sands–Triangle Zone Structure	gas
Upper Carboniferous Ettrain Limestone–Stratigraphic	gas
Devonian Ogilvie/Gossage Carbonates–Stratigraphic	gas
Devonian Ogilvie/Gossage Carbonates–Antiformal Structures	gas
Ordovician/Silurian Ronning Group–Stratigraphic	gas

DISCUSSION OF RESULTS

The probability charts for the total undiscovered marketable gas and for total undiscovered recoverable oil are shown on the following pages for the Eagle Plain Basin (Table 2). For gas, the range is from 9.0 x 10^9m^3 (316 BCF) at 95 per cent probability to 63.6 x 10^9m^3 (2.24 TCF) at 5 per cent probability with a mean of 28.5 x 10^9m^3 (1.01 TCF) at a probability of 45 per cent. For oil, the range is from 1.11 x 10^6m^3 (7 MMBbls) at 95 per cent probability to 11.13 x 10^6m^3 (70 MMBbls) at 5 per cent probability, with a mean of 4.5 x 10^6m^3 (28.2 MMBbls) at 45 per cent probability. In addition, the program generates values for by-products. At the mean gas value, there are estimated to be 2.4 x 10^6m^3 (14.9 MMBbls) of natural gas liquids.

REFERENCES

Dixon, J.
1992: Stratigraphy of Mesozoic Strata, Eagle Plain Area, Northern Yukon. Geological Survey of Canada, Bulletin 408.

Hamblin, A.P.
1990: Upper Paleozoic Petroleum Geology and Potential, Southern Eagle Plain, Yukon Territory. Geological Survey of Canada, Open File 2286.

National Energy Board
1994: Natural Gas Resource Assessment, Northeast British Columbia. National Energy Board, Working Document.

1994: Petroleum Resources Assessment of the Eagle Plain Basin, Yukon Territory, Canada. National Energy Board, Working Document.

Table 2

Total Discovered Resources – Eagle Plain

EAGLE PLAINS - UNDISCOVERED RESOURCES							
		RECOVERABLE OIL		MARKETABLE GAS		LIQUID BY-PRODUCTS	
AGE	PLAY_NAME	MEAN	STD_DEV	MEAN	STD_DEV	MEAN	STD_DEV
LOWER CRETACEOUS	FISHING BRANCH SS	0.00	0.00	54.28	30.64	0.30	0.17
PERMIAN	JUNGLE CREEK	0.12	0.08	30.01	15.00	0.02	0.01
CARBONIFEROUS	ETTRAIN	0.00	0.00	18.05	14.65	0.15	0.13
CARBONIFEROUS	CHANCE SS LARAMIDE	1.29	0.73	90.82	37.57	1.93	0.82
CARBONIFEROUS	CHANCE SS STRUCT/STRAT	13.38	8.56	79.63	39.10	2.86	1.43
CARBONIFEROUS	CHANCE SS STRAT	12.37	7.07	56.16	28.81	1.53	0.81
MISSISSIPPIAN	CANOE CARBONATE	1.02	0.97	55.75	47.17	2.21	1.92
CARBONIFEROUS	TUTTLE SS	0.00	0.00	75.73	51.34	1.29	0.91
DEVONIAN	DEVONIAN CARB STRAT	0.00	0.00	262.87	184.30	3.14	2.30
DEVONIAN	DEVONIAN ANTIFORMS	0.00	0.00	98.74	84.57	1.17	0.99
CRETACEOUS	TRIANGLE ZONE	0.00	0.00	46.51	33.61	0.26	0.19
ORD-SIL	RONNING CARB	0.00	0.00	137.50	129.22	0.03	0.02
	TOTALS	28.17	MMB	1006.04	BCF	14.90	MMB
	CHANCE SS	27.04		226.61		6.33	
	CARBONIFEROUS	28.05		376.13		9.98	
	DEVONIAN			361.61		4.31	
	LOWER PALEOZOIC			545.62		4.60	
	CRETACEOUS			100.79		0.56	

RESOURCE ASSESSMENT OF THE CADOTTE PLAINS AND DEEP BASIN GAS

K. Olsen-Heise and P.J. Lee

Geological Survey of Canada, 3303-33rd Street N.W., Calgary, Alberta T2L 2A7

G.E. Reinson

Petrel Robertson Ltd.
2801-18th Street N.E., Calgary, Alberta T2E 7K5

The Cadotte sandstones contain a discovered resource of 24 872 m^3 gas (878 BCF) trapped in 107 pools. As well as stratigraphic and structural traps, a deep basin trap type has also been proposed. To investigate whether the deep basin type should be considered a separate play for resource assessment utilizing PETRIMES, the Cadotte play was divided into a Deep Basin play and a Plains play (Fig. 1). The deep basin region encompasses both pools identified as deep basin by Davis (1984) and pools in which initial pressures are clearly below the regional water gradient (Fig. 2).

Assessment of the Cadotte as one play or as two plays gave similar estimates of the expected potential. Discounting that the comparable results are merely fortuitous, this similarity indicates that either:

1) the deep basin mechanism is not a controlling play factor, or

2) definition of the Deep Basin play needs further refinement.

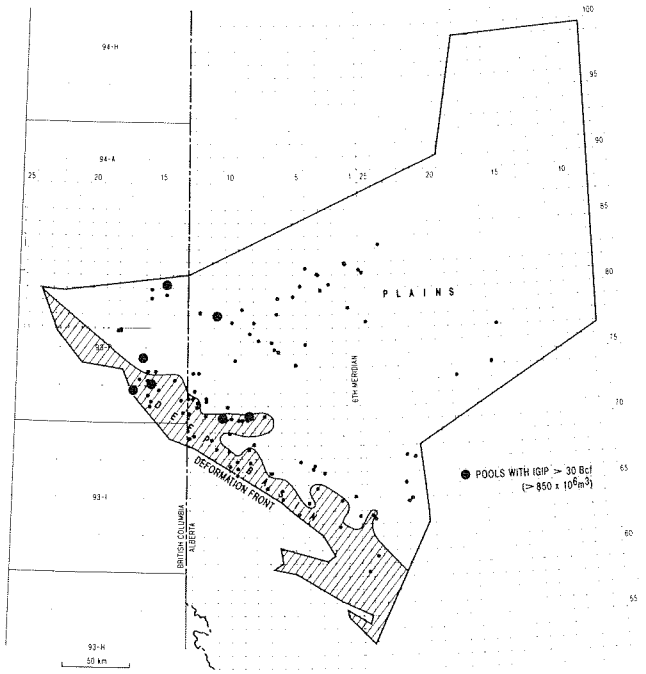

Figure 1. *Cadotte deep basin and plains regions. Location of the discovery well for each Cadotte pool is indicated by the dots.*

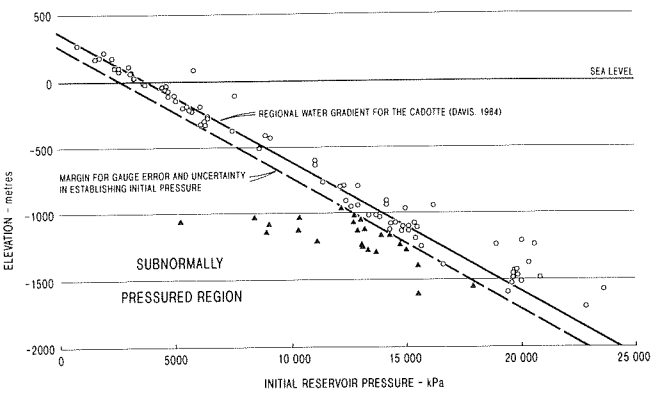

Figure 2. *Initial reservoir pressure versus elevation, Cadotte gas pools.*

REFERENCE

Davis, T.B.
1984: Subsurface pressure profiles in gas-saturated basins. *In* Elmworth – case study of a Deep Basin gas field, J.A. Masters (ed.). American Association of Petroleum Geologists, Memoir 38, p. 189–203.

GEOLOGICAL PLAY DEFINITIONS AND GAS RESOURCES, LOWER CRETACEOUS COLORADO GROUP, WESTERN CANADA INTERIOR PLAINS

G.E. Reinson

Petrel Robertson Ltd., 2801-18th Street N.E., Calgary, Alberta T2E 7K5

P.J. Lee, K. Olsen-Heise, R.I. Campbell, G. Holmstrom, and R.J. Gault

Geological Survey of Canada, 3303-33rd Street N.W., Calgary, Alberta T2L 2A7

The assessment of the Lower Cretaceous Colorado Group gas potential in the Interior Plains of the Western Canada Sedimentary Basin involved the geological delineation and statistical evaluation of twelve established mature plays and one immature play. The plays were defined on the basis of geological criteria, primarily litho- and sequence stratigraphic controls. Undiscovered gas potential for each play was determined using a statistical assessment technique termed the **discovery process model**, which is part of the PETRIMES resource evaluation system developed by the Geological Survey of Canada (Lee and Tzeng, 1993).

The thirteen Lower Cretaceous Colorado gas plays are as follows: Viking/Bow Island regressive, Viking/Bow Island transgressive, Viking/Bow Island channel, Paddy, Cadotte, Basal Colorado, Cardium, Base of Fish Scales, Dunvegan, Doe Creek, Second White Specks shallow marine, Second White Specks fracture, and Spinney Hill. All plays except the Spinney Hill were subjected to statistical analysis using the discovery process model. The potential of the immature Spinney Hill play was evaluated indirectly using the other plays as the "pool" population (Reinson et al., 1993).

Results of the assessment of undiscovered gas expected potential are summarized in Figures 1 and 2. The discovered in-place gas resource for the Colorado Group is $812 \times 10^9 m^3$ (29 TCF) and the analysis suggests that about 27% of the total source remains to be discovered (Fig. 1). Examination of undiscovered resource on a play by play basis (Fig. 2) indicates that the Viking/Bow Island transgressive and Cadotte plays have the most potential. Of the total resource remaining to be discovered, about 43% and 14% are contained within the Viking/Bow Island transgressive and Cadotte plays, respectively. Comparison of the discovered resource with the undiscovered potential predicted for each play (Fig. 2) emphasizes the relative exploration immaturity and high upside potential of the Paddy and Cadotte plays relative to all other plays except that of the Viking/Bow Island transgressive play.

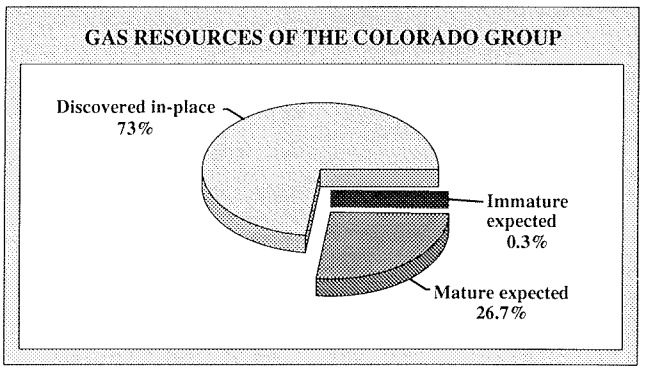

Figure 1. *Distribution of total gas resources in the Lower Cretaceous Colorado Group.*

REFERENCES

Lee, P.J. and Tzeng, H.P.
1993: The petroleum exploration and resource evaluation system (PETRIMES) working reference guide, Version 3.0 (PC Version). Geological Survey of Canada, Open File 2703.

Reinson, G.E., Lee, P.J., Warters, W., Osadetz, K.G., Bell, L.L., Price, P.R., Trollope, F., Campbell, R.I., and Barclay, J.E.
1993: Devonian gas resources of the Western Canada Sedimentary Basin–Part I: Geological play anlaysis and resource assessment. Geological Survey of Canada, Bulletin 452, 128 p.

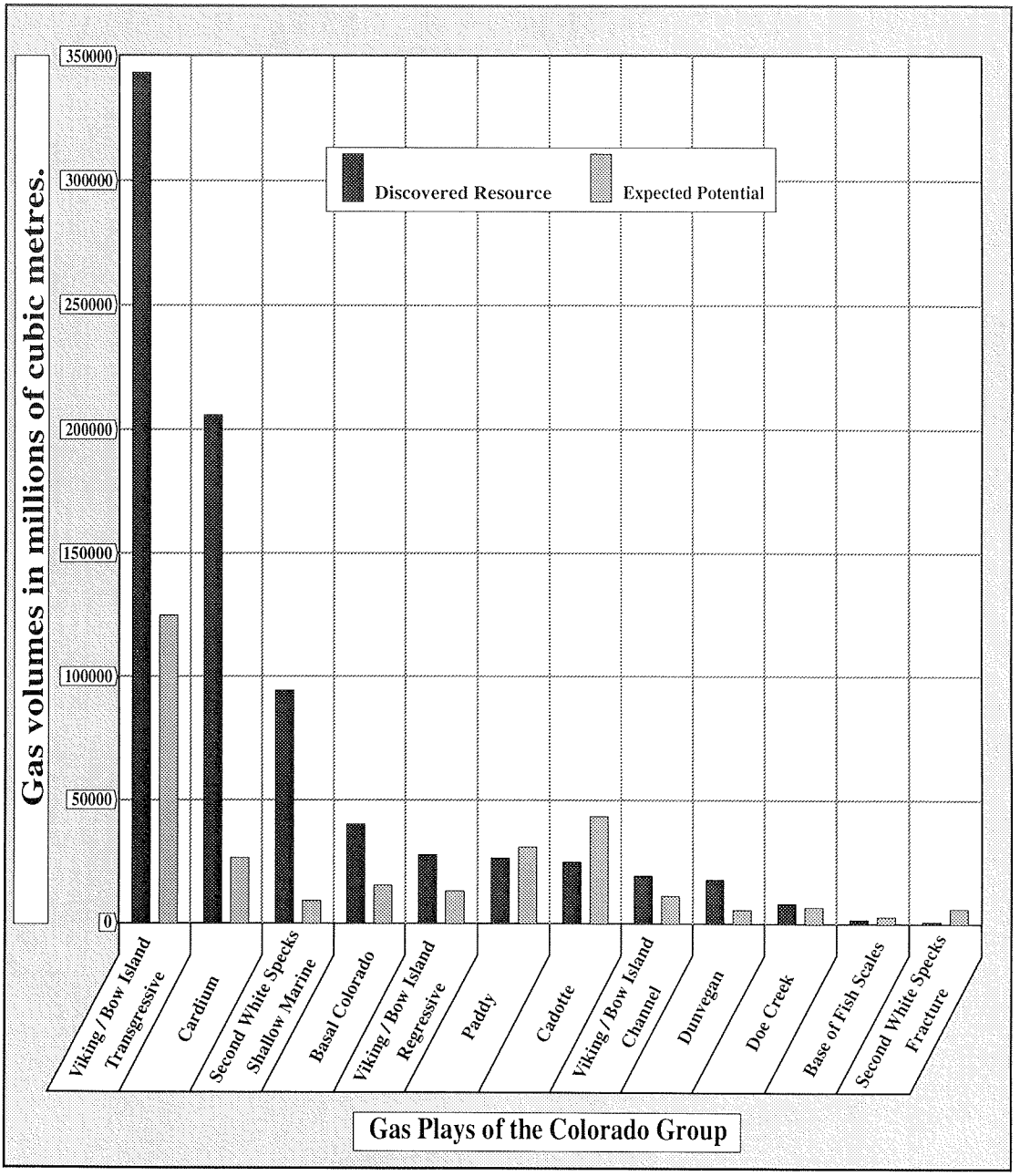

Figure 2. *Discovered and potential gas resources in mature Colorado Group plays.*

MANNVILLE GAS RESOURCES OF THE WESTERN CANADA SEDIMENTARY BASIN

Geological Play Definition and Resource Assessment

W.J. Warters, D.J. Cant, H.P. Tzeng, and P.J. Lee

Geological Survey of Canada, 3303-33rd Street N.W., Calgary, Alberta T2L 2A7

Natural gas resource potential of the Mannville Group, and its equivalent strata, in the Western Canada Sedimentary Basin (excluding the Foothills Belt) was evaluated based on geological play analysis and statistical estimation (Table 1).

The Western Canada Sedimentary Basin was divided for assessment purposes into six geographic areas: 1) northwestern Alberta and B.C., 2) Athabasca, 3) Lloydminster, 4) central Alberta, 5) southern Alberta, and 6) Saskatchewan. Each area was further subdivided based on the stratigraphy of the Mannville Group. The lower Mannville Group is characterized by continental deposits, with the lowermost unit being the alluvial plain and braided river deposits of the Cadomin Formation. These were followed by the fluvial and lacustrine deposits of the Basal Quartz/Ellerslie, Gething, Cutbank/Sunburst, Dina, and McMurray formations that grade upward into marginal marine deposits. With continued southward transgression of the Boreal Sea, a series of transgressive shorelines were deposited, which include the Bluesky, Wabiskaw, and Cummings formations. At this point there was a major change in the depositional style from the lower transgressive Mannville Group to upper regressive Mannville Group. The progradational shoreline deposits of the Glauconite and Clearwater formations mark this change. These, in turn, are followed by a further progradation represented by the Spirit River Formation, Grand Rapids Formation, and the Upper Mannville Group. Each of these stratigraphic divisions in a given geographic area of the Western Canada Sedimentary Basin was considered as a play.

Seventeen plays were defined in this assessment, the total number of pools discovered and the total gas-in-place and primary reserves are tabulated below. The natural gas resource potential of each play was estimated by PETRIMES (Petroleum Exploration and Resource Evaluation System), which utilizes the pool volume and its date of discovery to estimate the total play potential and size range of the undiscovered pools. The total potential gas resource for the Mannville Group in the Western Canada Sedimentary Basin is estimated to have an expected value of 957,491 x $10^6 m^3$ gas in-place. Based on this estimate, 39 per cent of the total gas resource of the Mannville Group remains to be discovered.

Table 1

Mannville gas plays and reserves

Play Name	No. of Pools	Gas-In-Place 10^6m^3	Potential Resource (Expected Value) 10^6m^3
Deep Basin			
Spirit River	275	102,582	28,888
Bluesky	304	105,478	48,585
Gething/Dunlevy	693	140,681	22,151
Cadomin	178	45,691	100,010
Athabasca			
Upper Mannville	1275	87,535	55,060
Wabiskaw	219	53,957	21,776
McMurray	565	45,450	13,413
Lloydminster			
Upper Mannville	3791	212,535	87,008
Cummings	198	5,216	2,160
Dina	230	11,102	13,283
Central Alberta			
Upper Mannville	2335	315,572	91,411
Ostracod	297	38,084	16,677
Ellerslie/Basal Quartz	2451	257,755	67,399
Southern Alberta			
Upper Mannville	280	38,642	30,312
Lower Mannville	386	30,508	12,005
Saskatchewan			
Cantaur	4	2,434	Immature Play
Alberta/Saskatchewan			
Detrital	193	11,432	33,563
Immature & Conceptual Plays			313,790
TOTAL	**13,674**	**1,504,655**	**957,491**

Compiled from:

1) Reservoir Annual 1990, Saskatchewan Energy and Mines.
2) Alberta's Reserves of crude oil, oil sands, gas, natural gas liquids and sulphur, Dec. 1990, Energy Resources Conservation Board Report ST91-18.
3) Hydrocarbon and by-product reserves in British Columbia, Dec. 1990, Province of British Columbia, Ministry of Energy, Mines and Petroleum Resources.

HYDROGEOLOGICAL AND HYDROCHEMICAL ATLAS OF THE WESTERN CANADA SEDIMENTARY BASIN

H.J. Abercrombie

Geological Survey of Canada, 3303-33rd Street N.W., Calgary, Alberta T2L 2A7

D. Barson, K. Rakhit, and G. Fullmer

Rakhit Petroleum Consulting Ltd., 230, 309-2nd Avenue S.W., Calgary, Alberta T2P 0C5

INTRODUCTION

The information and knowledge base of the potential for flow and compositions of fluids in the Western Canada Sedimentary Basin (WCSB) has increased significantly since the publication of the last basin scale compilation of hydrochemistry and hydrogeology (Hitchon, 1964), part of the first geological atlas of the WCSB (McCrossan and Glaister, 1964). The recently published Geological Atlas of the Western Canada Sedimentary Basin (Mossop and Shetsen, 1994) provides updated and expanded references to the stratigraphic architecture of the WCSB. However, hydrogeology and hydrochemistry are not included in the newest atlas. The objective of this project is to produce a basin scale compilation and synthesis of the hydrogeology and hydrochemistry of the WCSB.

The hydrogeological and hydrochemical atlas project is a joint research partnership involving GSC Calgary and Rakhit Petroleum Consulting Ltd. (RPCL). It is partly funded by the GSCs Industrial Partners Project and a number of industrial partners, and includes participation by Digitech Information Services Ltd. (Digitech) and Alberta Geological Survey. Compilation, verification, and synthesis of hydrogeological and hydrochemical data is being done by RPCL with technical review and advice provided by geoscientists in university, government, and industry.

DATA

One of the basic requirements for large scale mapping across the WCSB is access to data, preferably in digital format. Provincial governments have archived much of the necessary stratigraphic, pressure, and water composition data, and have made some of these data available digitally. Most of the data used in the present study, however, has been digitized and verified by private data vendors. Detailed discussion of the methods of verification and mapping is beyond the scope of this paper.

Stratigraphic data are required for two purposes: to determine the regional slopes of confining surfaces, and to check for the correct assignment of well data to stratigraphic units. Formation tops data provided with the Geological Atlas of the WCSB (Mossop and Shetsen, 1994) were used for the former purpose (i.e., to characterize regional slopes). A total of 20 stratigraphic surfaces have been defined and mapped at basin scale. The Geological Atlas used an average sample density of one well per township which is equal to the node spacing (10 x 10 km) used in this project for determining the dip of confining surfaces. For the second purpose, checking for correct assignment of well data to stratigraphic units, the density of Geological Atlas control wells was found to be inadequate. The objective is to remove any data obtained from a test interval that straddles stratigraphic boundaries. The generalized surfaces constructed from the Geological Atlas formations tops were not of sufficient accuracy to reliably locate formation boundaries in wells other than the control wells, so the more abundant formation tops data from Digitech were used. Culling was done by cross-checking the depth interval for each pressure measurment and water sample against Digitech formation tops that defined the base and top of the stratigraphic unit for that well. Any data for which the the reported test interval did not wholly lie within the relevant formation boundaries was rejected.

The balance of information needed for hydrogeological and hydrochemical mapping originates from drill stem (DST) and production tests, and includes pressure transient analyses and water compositions. Digital pressure data are available from Digitech (the former Canadian Institute of Formation Evaluation database). Verification of pressure data is designed to remove erroneous pressure measurements and the

effects of production induced drawdown (PID). Use of Digitechs production database permits automated culling of pressure data by calculating an interference index (Toth and Corbett, 1986) for each DST pressure. The interference index increases with the number of active production wells within a user defined radius of the DST well, their production lifetime prior to the DST date, and their proximity to the DST well. Pressure data are rejected if pumping from one or more nearby wells removed significant volumes of fluids before the DST was conducted. Nearest neighbour comparisons facilitate identification and rejection of erroneous pressure data. Water compositions have been coded in the DWAF (digital water analysis file) which is available commercially from RPCL. The codes reflect criteria that have been developed to identify incomplete and erroneous analyses, and to identify samples unrepresentative of natural formation waters, such as those contaminated by drilling, stimulation, and other fluids.

METHODS

Hydrogeology

Construction of hydraulic potential maps is complicated in sedimentary basins that contain waters of variable density. In previous analyses of hydraulic potentials in the WCSB (e.g., most recently, Bachu and Undershulz, 1993), head calculations have been made assuming unit water density. This is sufficient to accurately map (contour) potentiometric surfaces in areas of near-freshwater composition, and will produce the correct disposition of isopotential lines in areas of higher, but constant, water density (although the head value of these lines will be incorrect). In regions of changing and elevated water densities, the unit density calculation is inadequate to accurately represent the true driving force for water. Other methods have been used in an attempt to correct head calculations for variable density and may be applicable in some situations. For example, environmental head (Lusczynski, 1961) has been used in unconfined coastal aquifers that contain waters ranging from freshwater to seawater. It is impossible to use this approach in a sedimentary basin because the requirement of an unconfined aquifer is, in general, not met. In fact, potentiometric surfaces are incapable of representing the driving forces for fluid flow in situations of variable density because under these conditions a single, unique potential cannot be defined (Hubbert, 1940).

An alternate method for representing flow in variable density systems is to explicitly calculate the fluid flow force field. Figure 1 is a schematic cross-section

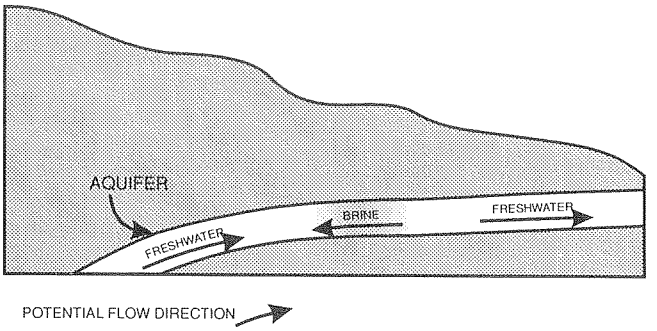

Figure 1. *Heavy brine in a dipping aquifer has a tendency to flow downdip. Accurate evaluation of the force field for fluid flow must account for aquifer dip and true formation water density, as well as hydraulic head.*

showing the situation for a slug of dense brine in a dipping aquifer where freshwater heads indicate updip flow. The negative buoyant force tends to drive the brine downdip along the basal confining layer and against the upward directed freshwater head gradient. This situation cannot be adequately represented using fluid potential calculations alone. As an alternative, the force acting upon the fluid at any point can be depicted by a vector calculated as the resultant of two independent components: buoancy and the freshwater hydraulic gradient (Fig. 2). As depicted in Figure 2, regional freshwater head, water density, and structure surfaces must all be constructed in order to calculate the fluid force vector.

Standard mapping procedures are used to calculate freshwater head, density, and structure from the verified datasets. Once these surfaces are constructed, the fluid flow force vector is calculated. In regions of constant

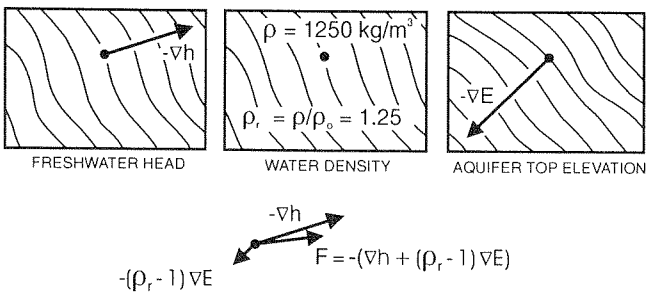

Figure 2. *Schematic illustration of the calculation of the fluid flow force field vector, F. The fluid flow force vector represents the combined effects of hydraulic head, density, and slope of the confining surface (Barson, 1993).*

density, the fluid flow force vector is aligned perpendicular to freshwater head equipotential lines and its magnitude is proportional to the gradient of the freshwater potential field. In regions where densities vary over relatively short distances, the fluid flow force vector will not necessarily be aligned perpendicular to freshwater head equipotential lines (Fig. 2). In areas with low hydraulic gradients, force vectors may be directed against the calculated freshwater gradient. In practise, the fluid flow force vectors are calculated at grid node points and are then superimposed as a separate layer on maps of the freshwater potentiometric surface.

Hydrochemistry

The construction of hydrochemical maps is straightforward and involves gridding and contouring of verified data. Basic maps include salinity (total dissolved solids), chlorinity, and resistivity for each of 20 hydrostratigraphic units. Other parameters, however, are useful for developing insights into chemical and physical controls on water compositions. Selected parameters will be available for each hydrostratigraphic unit and will be incoporated into later publications on regional controls on water compositions.

ATLAS PRODUCTS

The atlas will be released at various scales and in a number of formats over a period of three years. It will first be made available to industry participants in 1995 as a catalogue of 1:750 000 scale maps produced by RPCL. This will become publicly available in 1996. The GSC will prepare a 1:5 000 000 scale digital version of the hydrogeological and hydrochemical atlas surfaces for release in 1998, and will join with the Hydrogeology Division of the Canadian Society of Petroleum Geologists to produce a thematic volume on the hydrogeology and hydrochemistry of the WCSB.

REFERENCES

Bachu, S. and Undershultz, J.R.
1993: Hydrogeology of formation waters, northeastern Alberta Basin. American Association of Petroleum Geologists Bulletin, v. 70, p. 1745–1768.

Barson, D.
1993: The hydrogeological characterization of oilfields in north-central Alberta for exploration purposes. Ph.D. thesis (unpublished), University of Alberta, Edmonton.

Hitchon, B.
1964: Formation Fluids. *In* Geological History of Western Canada, R.G. McCrossan and R.P. Glaister (eds.). Alberta Society of Petroleum Geologists, p. 201–217.

Hubbert, M.K.
1940: The theory of ground-water motion. Journal of Geology, v. 48, p. 785–944.

Lusczynski, N.L.
1961: Head and flow of ground water of variable density. Journal of Geophysical Research, v. 66, p. 4247–4256.

McCrossan, R.G. and Glaister, R.P. (eds.)
1964: Geological History of Western Canada. Calgary, Alberta Society of Petroleum Geologists, 232 p.

Mossop, G.D. and Shetsen, I. (compilers)
1994: Geological Atlas of the Western Canada Sedimentary Basin. Canadian Society of Petroleum Geologists and Alberta Research Council, Calgary, 510 p.

Toth, J. and Corbet, T.
1986: Post-Paleocene evolution of regional groundwater flow-systems and their relation to petroleum accumulations, Taber area, southern Alberta, Canada. Bulletin of Canadian Petroleum Geology, v. 34, p. 339–363.

MINERALOGICAL AND GEOCHEMICAL TRAITS OF THE EGRET MEMBER SOURCE ROCK, JEANNE D'ARC BASIN, OFFSHORE NEWFOUNDLAND, CANADA

J.A. Bateman

Department of Earth Sciences, Dalhousie University, Halifax, Nova Scotia B3H 3J5

M.A. Williamson

Atlantic Geoscience Centre, P.O. Box 1006, Dartmouth, Nova Scotia B2Y 4A2

BACKGROUND

One challenge to our understanding the Egret source rock system in the Jeanne d'Arc Basin is the lack of outcrop or cores. To address this, we have prepared a detailed characterization of the source rock utilizing a comprehensive suite of petrophysical, organic, and inorganic geochemical data. We report here on elements of the source rock mineralogy and geochemical characteristics. Other studies contributing to a broader definition of the source rock in this region include Huang et al. (in press., and this volume) in which petrophysical log data and geochemistry are integrated to characterize the Egret Member in terms of its organic richness, lithofacies, and cyclicity. Collectively, these studies have been useful to our attempts to understand the depositional and environmental conditions responsible for the observed features of the source interval.

Of the 20 wells that penetrate the Egret Member within the Jeanne d'Arc Basin, we have chosen Rankin M-36, Port au Port J-97, Voyager J-18, Fortune G-57, and Trave E-87 for detailed examination (Fig. 1). Not only do these wells provide basin-wide coverage and variable thicknesses, they are also representative of diverse present-day geologic regimes that vary in depth and thermal maturity. A multidisciplinary approach is followed to provide a comprehensive data set and encompasses many of the perspectives typically considered in shale investigations. Detailed Rock-Eval and Inductively Coupled Plasma (ICP) chemical analyses, integrated with x-ray diffraction (XRD) and Environmental Scanning Electron Microscope (ESEM) techniques were performed on well cutting samples from throughout the Egret Member. All cuttings samples were obtained from 10 m intervals; wells drilled using oil-based muds were not studied.

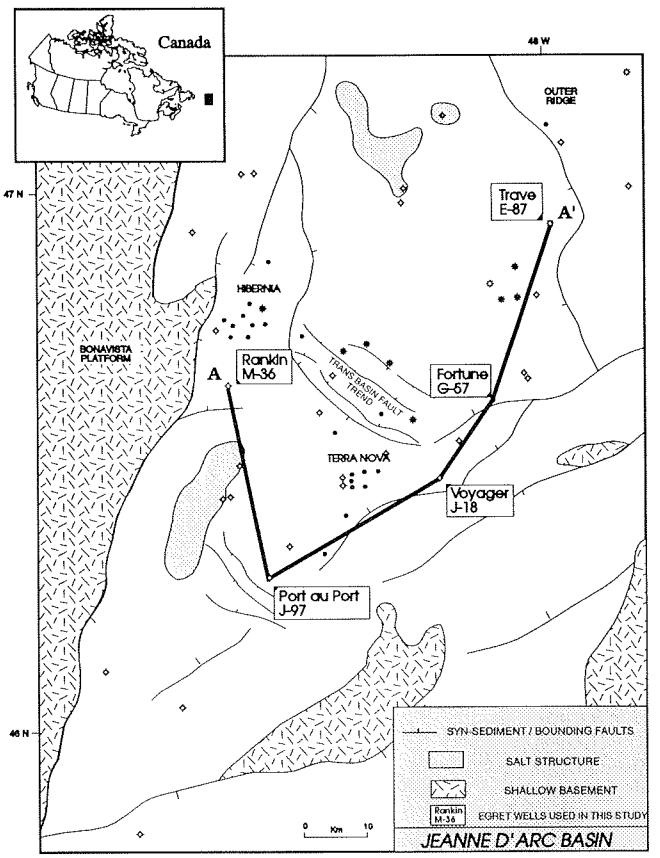

Figure 1. *Location map of the Jeanne d'Arc Basin. Wells that penetrate the Egret Member are labelled, wells considered in this study are highlighted in boxes.*

MINERALOGICAL AND GEOCHEMICAL CHARACTERIZATION BULK (NON-CLAY) AND CLAY MINERALOGY

The bulk-rock mineralogy of the Egret Member was investigated using crushed well cutting samples from each of the study wells. The >30 μm fraction was analyzed for non-clay components using a nonoriented mounting technique and semiquantified following methods outlined in Cook et al. (1975). Figure 2 illustrates the minerals identified and their relative abundances with respect to depth in each well. Quartz and calcite typically comprise the dominant mineralogy, with quartz being most abundant in the deeper wells; calcite is most common in shallow samples. Mica, feldspar, and pyrite are all present in subordinate amounts amongst the wells.

The clay components within the Egret were identified from the <2 μm fraction. Quantitative estimates of each clay component are reported in relation to a 5 wt% internal talc standard following methods outlined in Stoffyn-Egli et al. (1992). Figure 3 illustrates the clay abundances with respect to depth in each well. Five clay species have been identified in the Egret Member. Illite is present in amounts typically less than 20 wt% in each well, however there are no apparent trends with depth. Kaolinite is also common, with greater abundances present in more shallow wells. Chlorite is also present, however, a mixed-layer chlorite/vermiculite species is dominant in the Port au Port J-97 well. The most abundant clay species identified, which typically represents 45% of the total clay component, is a mixed-layer illite/smectite. This species usually contains a <10% smectite component, however, the smectite component reaches approximately 40% in Port au Port J-97. No free-swelling smectites have been identified within the Egret Member.

The presence and abundance of the bulk minerals identified are interpreted as depositional in origin with diagenetic processes controlling the clay mineralogy. The mineral assemblages identified are consistent with present-day maturation levels of the interval. The abundance of chlorite in shallow samples and the presence of a mixed-layer chlorite/vermiculite in Port au Port J-97 suggest a high detrital iron component, perhaps from a volcanic source in this vicinity.

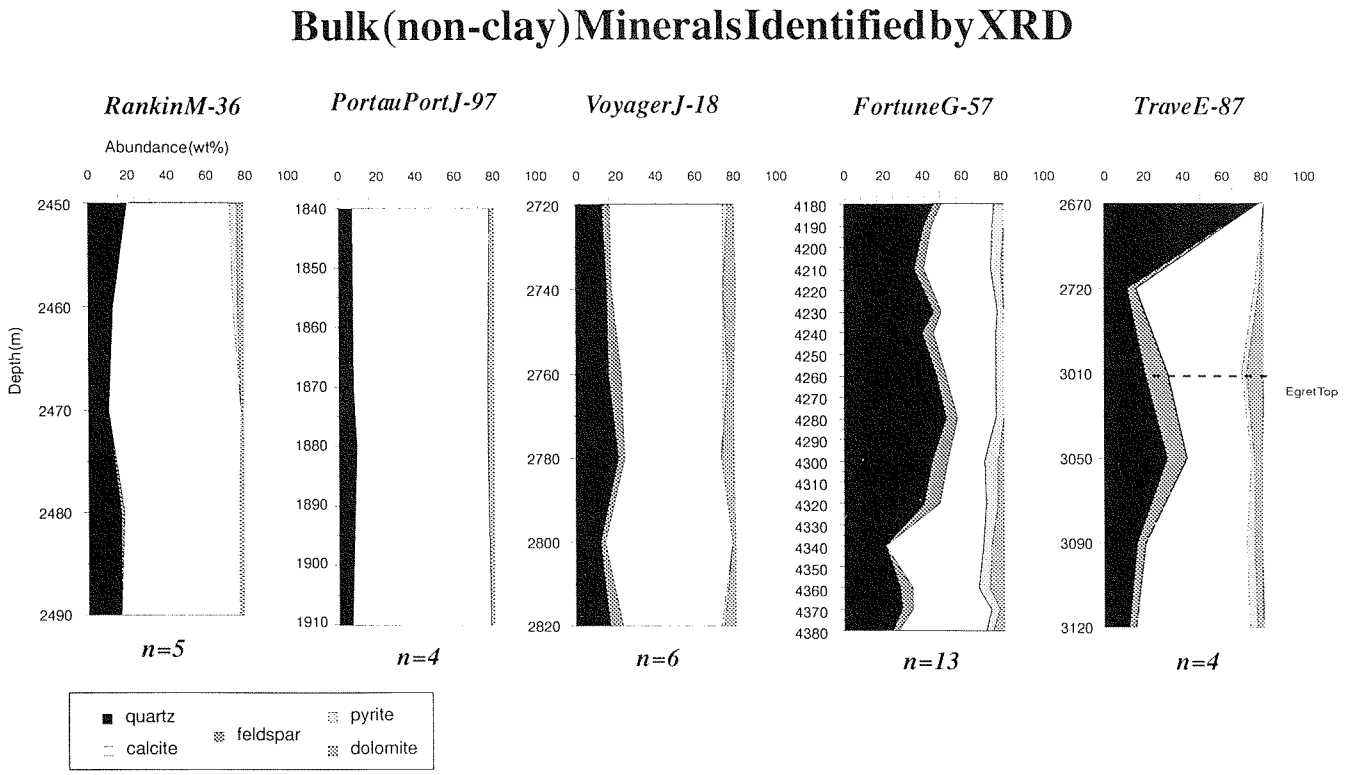

Figure 2. *Bulk (non-clay) minerals identified by XRD. Semiquantitative abundances are after Cook et al. (1975). Number of samples analyzed in each well are indicated by n = 6.*

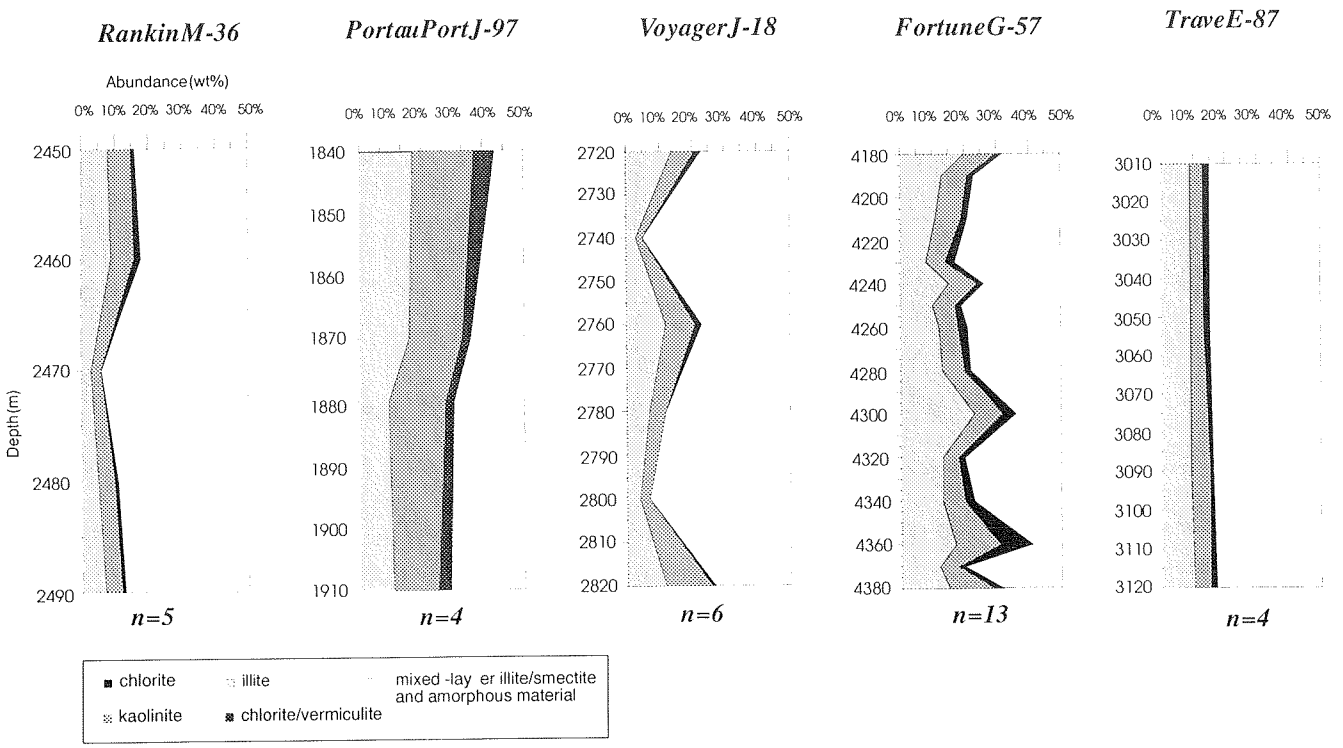

Figure 3. *Clay minerals identified by XRD. Quantitative abundances are after Stoffyn-Egli et al. (1992). Number of samples analyzed in each well are indicated by n = 6.*

CARBON-SULFUR-IRON SYSTEMATICS

Primary production and subsequent recycling of organic matter are ubiquitous processes characteristic of organic-rich shales. The abundance and availability of organic matter, sulphate, and iron are closely related to depositional environment and early diagenetic processes and have been used to interpret depositional environments of ancient sediments. An examination of the carbon, iron, and sulfur systematics of Egret shales has clarified the paleoceanographic conditions that have facilitated the preservation of organic matter and the precipitation of authigenic pyrite, and gives some clues regarding the paleosalinity conditions and oxygen distribution in the basin.

Bulk-rock carbon, sulfur, and iron abundances for the Egret Member in the wells considered in this study are presented in Figures 4 and 5. Figure 4 shows the relationship between total sulfur and iron. Figure 5 displays total sulfur versus TOC. In Figure 4, samples show an unrestricted range of values that all plot above the trend for stoichiometric pyrite. This indicates that iron is in excess in these sediments relative to stoichiometric pyrite, but that pyrite controls the iron/sulfur ratio. The broad dispersal of data amongst the wells is indicative of heterogeneous distribution that reflects episodic sedimentation in specific areas of the basin. The elevated iron values in Fortune G-57 reflects the presence of diagenetic ferroan carbonate minerals (i.e., ankerite) identified from ESEM within the interval. The abundance and trend of iron in the data suggests that iron was not a limiting factor for sulphate reduction, rather a function of water salinity or alternatively, organic carbon reactivity in various parts of the basin. High iron retention associated with reduced sulfur contents may suggest a more proximal environment of deposition, this is likely the case in the vicinity of Fortune G-57.

In Figure 5, samples show elevated sulfur values with respect to "normal marine" values as defined by Berner and Raiswell (1984). The data generally plots parallel to, and above the "normal marine" trend. Elevated sulfur values have been interpreted to be indicative of euxinic conditions; any variance from the

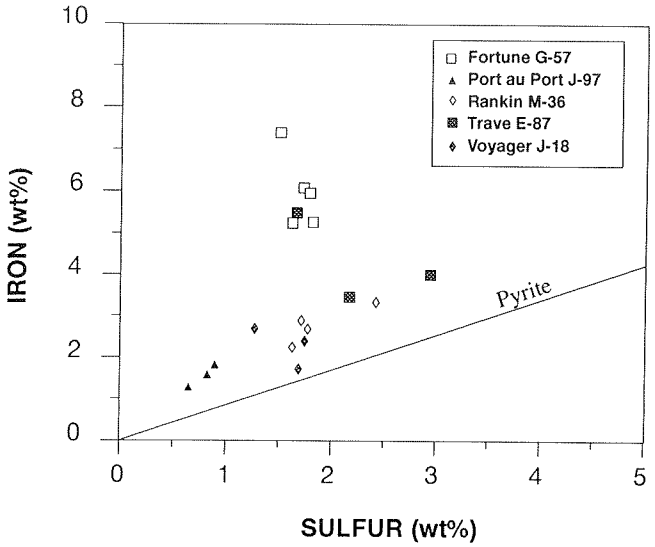

Figure 4. *Total sulfur versus iron for selected wells in the Jeanne d'Arc Basin. Pyrite line represents stoichiometric pyrite (Fe = 0.87 S). (After Berner and Raiswell, 1983.)*

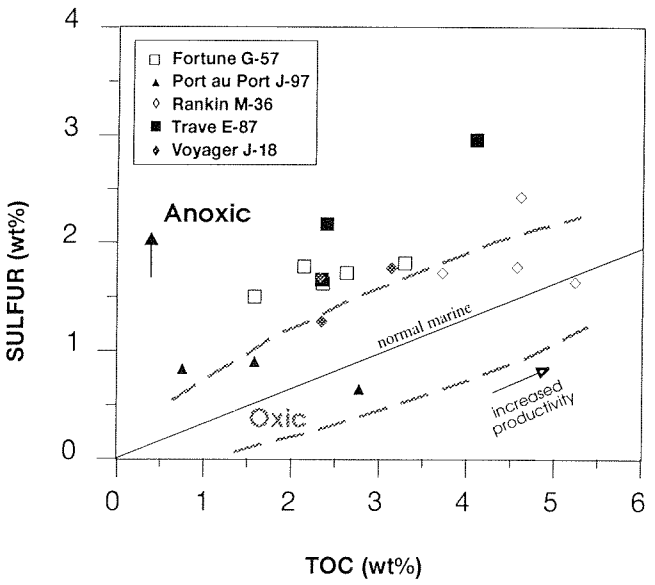

Figure 5. *Total sulfur versus TOC for selected wells in the Jeanne d'Arc Basin. Normal marine line is after Berner and Raiswell (1983). (After Leventhal, 1983.)*

"normal marine" carbon-sulfur relationship occurs in euxinic environments where H_2S exists in the water column. This allows for the precipitation of authigenic pyrite in the water column and/or at the water/sediment interface. The identification of both euhedral and framboidal pyrite in organic-rich and organic-lean Egret samples respectively, indicates that diagenetic processes were active early in the paragenetic sequence of the sediments. Euhedral pyrite is thought to be indicative of drastic levels of anoxia suggesting that the Egret Member experienced more reducing conditions episodically in the past. Individual samples from Port au Port J-97 and Rankin M-36 that plot on or just below the "normal marine" trend (Fig. 5) suggest a low reactivity of organic matter, perhaps from a terrestrial source in the proximity. This further supports the interpretation that the depositional environment was a major factor affecting the chemical composition of the organic matter contained within the Egret Member.

HAND-PICKED LITHOLOGIES AND ROCK-EVAL/TOC

In order to determine the physical and chemical nature of the lithologic components responsible for the observed variabilities in the interval evident from well log signatures, individual lithologies were separated from well cuttings using visual discrimination techniques and a binocular microscope. Four rock-types have been identified; in order of abundance, they include: 1) a dark brown laminated shale; 2) a grey to grey-brown shale; 3) a light brown marlstone/limestone; and 4) a fine grained sandstone and siltstone. Rock-Eval/TOC characteristics of each of the identified rock-types suggest that each lithology contributes differentially to the interval's overall organic character and generation potential, and may serve to control expulsion efficiencies within the source system (Table 1). The shales clearly represent the hydrocarbon generating component of the Egret Member, whereas the marl/limestone and sand/siltstone may have acted as carrier beds to enhance primary migration of generated hydrocarbons from within the source interval. In Trave E-87, for example, the dark-brown shales have the highest potential to generate oil with organic characteristics of marine-derived Type I/II kerogen,

Table 1

Rock Type	Dominant Features	HI (mg HC/g TOC)	TOC (wt%)	Tmax (°C)	Kerogen Type	Generation potential
Dark-Brown Laminated Shale (40-60%)	laminated to interlaminated with carbonaceous shale and limestone, part slightly to very calcareous	591-687	6.61-10.82	426-431	Type I/II	High
Grey-brown Shale	unlaminated, calcareous, carbonaceous, grade to marlstone locally	422-595	0.75-3.77	424-429	Type II	Low
Marlstone	grey to light-brown, shaley to silty, calcareous, locally pyritic, often grade to limestone, locally microcrystalline	53-400	0.90-1.58	422-429	Type II/III	None
Sandstone	very fine to medium grained, subrounded, poorly to well sorted, calcareous to slightly dolomitic, traces of pyrite and oolites locally	15-248	0.09-0.64	428-433	Type III	None

elevated hydrogen indices (HI), and rich organic carbon levels reaching over 10 wt% locally. On the other hand, marlstone and sandstone lithologies have no generation potential evident from their low TOC levels, reduced HIs and terrestrial-derived Type III kerogen configuration (Table 1). Although the source rock at Trave E-87 is good, maturation indicators (i.e., T_{max} and R_o) suggest that the Egret is immature with respect to oil generation at this locality.

EGRET MEMBER DEPOSITIONAL MODEL

Collectively, the data and interpretations presented above support the supposition that the deposition and preservation of Egret Member shales throughout the Jeanne d'Arc Basin were controlled by fluctuating bottom water oxygen levels which are interpreted to be in response to orbitally-controlled sea level and climatic changes during the Kimmeridgian (Huang et al., in press). A depositional model in which bottom water anoxia correlates with periods of high sea level, warm climatic conditions, and sluggish oceanic convection, is favoured to explain the enhanced organic matter preservation in the Egret Member (Demaison and Moore, 1980; Huang et al., in press). Figure 6 illustrates the depositional model proposed for the Egret Member. The setting of the Jeanne d'Arc Basin in the late Jurassic is typified by a restricted, relatively shallow (<200 m) silled basin occupied by an early pseudo-Atlantic Ocean (McAlpine, 1990). The development of a stratified water column is initiated by restricted vertical mixing largely controlled by water circulation locally, and regional climate (Fig. 6a) (Demaison and Moore, 1980). The vertical cyclic variation in the sediment lithology and organic character, appears to be related to the vertical movement of the oxic-anoxic interface upward through the sediment column, and the sediment-water interface in the bottom waters. During periods of high sea level and warm climatic conditions, deposition was characterized by organic-rich laminated shales, and slow pelagic sedimentation of marine organisms in a basinal setting (Fig. 6a). Unlaminated, organic-lean shales are deposited somewhat faster, in a more proximal environment during a lowering of sea level and a colder climate, characterized by dysaerobic conditions capable of supporting limited benthic infauna (Fig. 6b). Similarly, marlstones and claystones are deposited during lowstands of sea level in an oxic environment capable of hosting calcareous organisms. During periods of low sea level stand, organic matter incorporated into the sediments is dominantly terrestrial-derived. Sandstone deposition is likely periodic via turbidity flows that transport slope and shelf sediments into more distal, basinal environments.

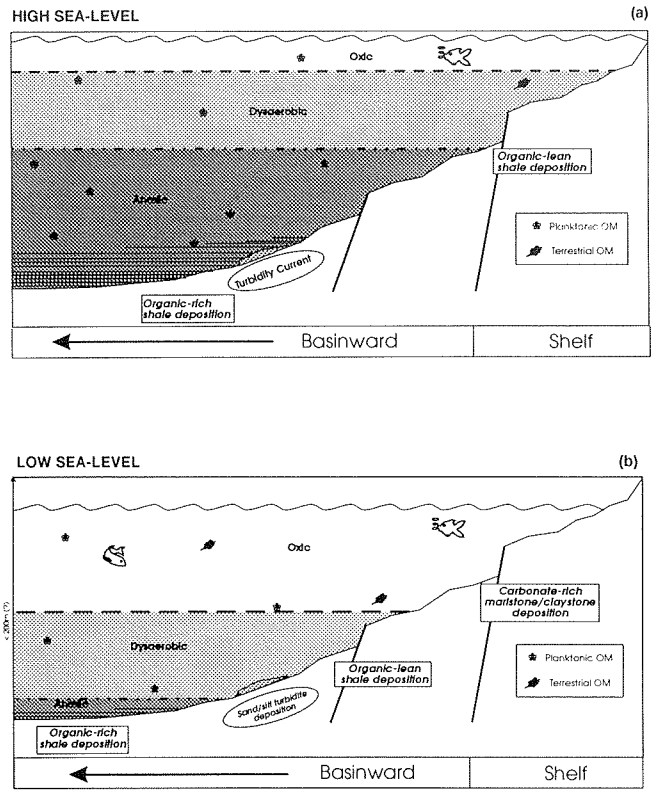

Figure 6. *Depositional model proposed to account for the observed variabilities in the Egret Member. The setting is one of a restricted, silled basin, occupied by a stratified water column in which orbitally-controlled sea level fluctuation regulates deposition. During periods of high sea-level (a), anoxic conditions dominate favouring the deposition of organic-rich, laminated shales characterized by marine-derived organic matter. During periods of low sea-level (b), more oxic conditions prevail, favouring the deposition of organic-lean shales and carbonate-rich marlstones in a more proximal setting. (After Demaison and Moore, 1980; Huang et al., in press.)*

REFERENCES

Berner, R.A. and Raiswell, R.
1983: Burial of organic carbon and pyrite sulfur in sediments over Phanerozoic time: A new theory. Geochimica et Cosmochimica Acta, v. 47, p. 855–862.

Cook, H.E., Johnson, J.G., Matti, J.G., and Zemmels, I.
1975: Methods of sample preparation and x-ray diffraction data analysis, X-ray Mineralogy Laboratory, D.S.D.P., University of California, Riverside. *In* Initial Reports of the Deep Sea Drilling Project, v. XXVII, Washington, D.C., p. 999–1007.

Demaison, G.J. and Moore, G.T.
1980: Anoxic Environments and Oil Source Bed Genesis. American Association of Petroleum Geologists, Bulletin, v. 64, p. 1179–1209.

Huang, Z., Williamson, M.A, Bateman, J.A., McAlpine, K.D., and Fowler, M.G.
in press: Cyclicity In The Egret Member (Kimmeridgian) Oil Source Rock, Jeanne d'Arc Basin, Offshore Eastern Canada. Marine and Petroleum Geology.

Leventhal, J.S.
1983: An interpretation of carbon and sulfur relationships in Black Sea sediments as indicators of environments of deposition. Geochimica et Cosmochimica Acta, v. 47, p. 133–137.

McAlpine, K.D.
1990: Mesozoic stratigraphy, sedimentary evolution, and petroleum potential of the Jeanne d'Arc Basin, Grand Banks of Newfoundland. Geological Survey of Canada, Paper 89–17, 50 p.

Stoffyn-Egli, P., Sonnichsen, G.V., and Zawadski, A.
1992: Clay-size minerals and near-surface stratigraphy on the northeastern Grand Banks of Newfoundland. *In* Current Research, Part E. Geological Survey of Canada, Paper 92–1E, p. 323–331.

THE EFFECTS OF THE USE OF OIL-BASED DRILLING MUDS AND OTHER ORGANIC ADDITIVES ON ORGANIC GEOCHEMICAL ANALYSIS OF SAMPLES FROM THE JEANNE D'ARC BASIN, OFFSHORE EASTERN CANADA

M.G. Fowler

Geological Survey of Canada, 3303-33rd Street N.W., Calgary, Alberta T2L 2A7

INTRODUCTION

The Jeanne d'Arc Basin is situated in the northeastern Grand Banks area, off the east coast of Newfoundland. Since 1979, several large hydrocarbon discoveries have been made in this basin of which the largest are Hibernia, Terra Nova and Whiterose. Offshore drilling is expensive, and moreover this area is prone to extreme weather and natural hazards (e.g., icebergs) which can cause serious disruption to drilling. Amongst the techniques used to enhance borehole stability, reduce drilling time and hence cut costs is the use of oil-based drilling muds (OBM). Many of the wells drilled with OBM in the Jeanne d'Arc Basin used Biovert. Biovert is an invert mud (an "inverted-emulsion" of water and oil) which differs from conventional OBM because instead of toxic diesel oil, a non-toxic "mineral oil" is used as the base. This mineral oil is a high paraffinic, low aromatic (less than 2%) low molecular weight cut. Biovert was developed for use in environmentally sensitive areas such as the Grand Banks.

In the Jeanne d'Arc Basin, the problems caused by the use of OBM and other additives are compounded by the lack of core taken. For example, at least 22 wells penetrated the main source rock in the basin, the Kimmeridgian-aged Egret Member of the Rankin Formation, but not one of them cored this unit. Only cuttings samples, usually taken over 10 m intervals are available. The object of this presentation is to demonstrate the effects of OBM and other organic drilling additives on the organic geochemistry of samples from the Jeanne d'Arc Basin. Although this a commonly encountered problem, many organic geochemists appear to be ignorant of the use of these materials and the problems they can cause.

RESULTS AND DISCUSSION

Amongst the wells drilled in the Jeanne d'Arc Basin using OBM is Whiterose A-90. This well is significant from a source rock viewpoint because it is the only well that penetrated the Egret Member in the vicinity of the Whiterose field. When the cuttings were washed to remove the drilling mud, prior to analysis, it was observed that they were extremely oily. An initial reconnaissance Rock-Eval/TOC study of samples from this well indicated that they had high S1 and PI (S1/S1 + S2) values, obviously related to the use of OBM which could be partially alleviated by leaving the samples in an oven at 45°C overnight (Fowler et al., 1990). Because the interval above the Egret Member in this well is organic-lean it was still possible to pick the top of the source rock interval which agreed with that obtained from down hole logs. The effect of the base oil from the OBM was examined in more detail in six of these samples, from high and low TOC intervals.

As in the preliminary study, the initial samples showed high S1 and PI values. However, the PI values were on average about 50% less than the original samples indicating that from the time when they were washed six months previously, much of the base oil had evaporated. Drying in an oven at 30°C for 36 hours further lowered the PI by about an additional 10%. The results from Rock-Eval analyses of Egret Member samples were less influenced by use of the OBM than non-source intervals. Tmax values were not changed by drying or extraction, but as they suggest a higher maturity than indicated by biomarkers, this parameter may be affected by the use of OBM. This has been confirmed in other wells.

Drying in the oven reduces the extract and hydrocarbon yields, the % hydrocarbons and the saturate/aromatic ratio. Once again this is more evident for the non-source intervals. The greater proportional decrease in saturate hydrocarbons is because of the low proportion of aromatics in Biovert OBM.

The saturate fraction gas chromatograms (SFGCs) of all the samples are dominated by C_{13}-C_{16} n-alkanes on a hump of unresolved compounds (Fig. 1). This indicates that the base oil was still present in all samples including those dried in the oven. Drying reduced the size of the hump and moved the centre of the hump to a slightly higher retention time (i.e. C_{14}->C_{15}) This was most evident for the non-source intervals. The pr/ph ratio was higher than normally observed for Egret Member extracts suggesting that this ratio was affected. Aromatic fraction gas chromatograms showed no hump and appear to be less affected by the use of OBM.

Biomarkers ratios did not appear to be influenced by the use of OBM and are those expected for Egret Member extracts. They indicate that the Egret Member extracts from Whiterose A-90 are considerably less mature than the Whiterose oils which, rather than being locally sourced, may have migrated some distance from the west.

Another example of the use of organic drilling additives in the Grand Banks area, is that of "Superlube" at Lancaster F-70. This represents from an (organic geochemists viewpoint) a worse case scenario. Rock-Eval/TOC logs indicate that for samples below 3380 m, the PI started to rise as OBM was used. Contamination from drilling additives became even more of a problem below 4430 m depth where high amounts of a lubricant called "Superlube" was used. "Superlube" is gilsonite, a biodegraded heavy oil which is used with a light base oil as a solvent. Over the depth range where this material was used, samples often resembled road asphalt after washing and drying and were unsuitable for geochemical analysis. Attempts to improve sample quality by hand-picking or washing with detergents were unsuccessful. Samples have high TOC, S1 and S2 values, and lower than expected Tmax values. The S2 values may be affected by the gilsonite because it is not volatile enough to be measured by the S1 peak. The SFGCs of samples that were extracted show a hump of unresolved compounds under the C_{14}-C_{17} n- alkanes (presumably from the base oil), a low abundance of C_{22+} n-alkanes and a high abundance of higher molecular weight biomarkers. These latter include β-carotane which is not found in extracts from any other well in the area. Other biomarker characteristics are also constant for samples from different

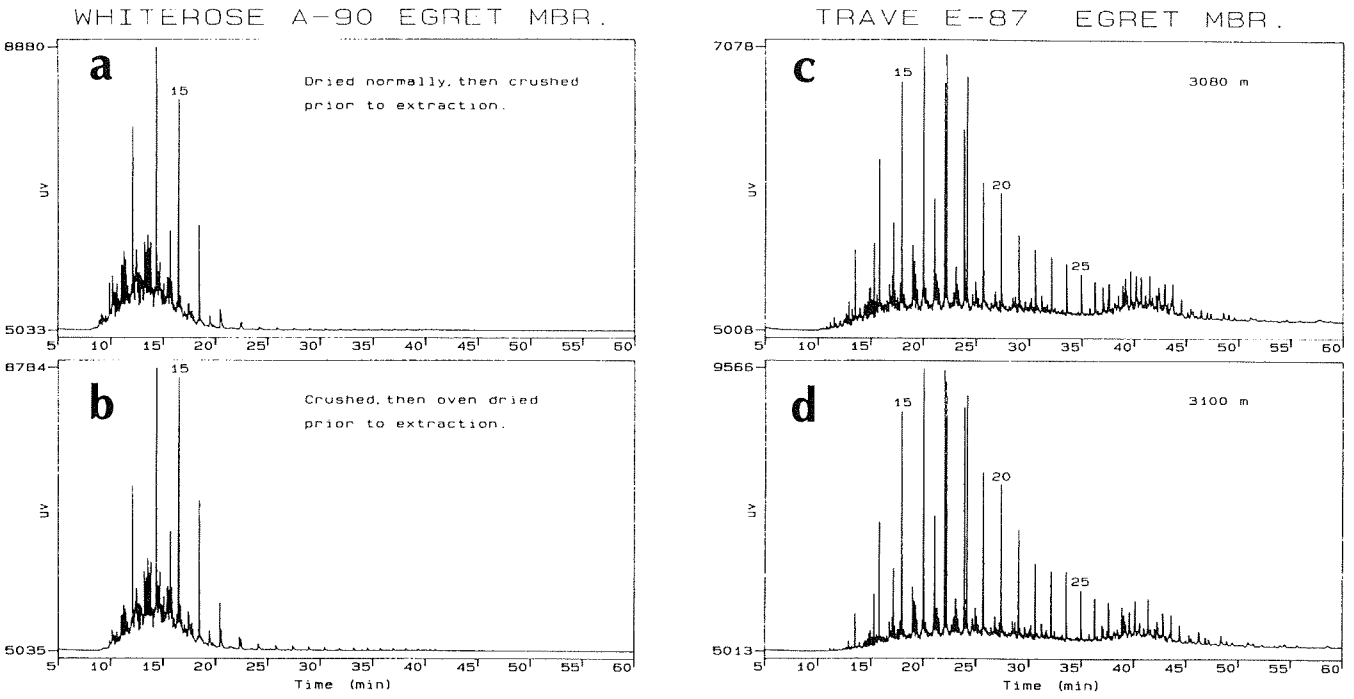

Figure 1. *Saturate fraction gas chromatograms of the extracts of cutting samples from; (a, b) a high TOC Egret Member interval from Whiterose A-90 (2950 m), that is contaminated by OBM base oil, before and after drying; (c, d) two high TOC Egret Member extracts where OBM was not used. 15, 20 and 25 are the C_{15}, C_{20} and C_{25} n-alkanes.*

Table 1

Rock-Eval extract data from two cutting samples from Whiterose A-90

	TOC%	PI	HI (mg HC/g Org C)	HC Yield (mg HC/g Org C)	%HC	Sat/Arom
Whitehorse A-90 2860 m (low TOC example)						
original sample*	0.75	0.93	62			
washed sample 6 months later	0.40	0.52	372	669	57.1	6.42
dried sample	0.35	0.47	331	482	47.1	2.32
sample after extraction	0.13	0.00	120			
dried sample after extraction	0.14	0.00	193			
Whitehorse A-90 2950 m (high TOC example)						
original sample*	3.91	0.54	361			
washed sample 6 months later	3.29	0.27	518	222	59.6	11.98
dried sample	3.19	0.24	535	167	48.4	6.75
sample from extraction	2.34	0.00	564			
dried sample after extraction	2.46	0.00	576			

*Nb The "original sample", although from the same cuttings interval is not the exact same material as used in the later experiments.

depths and suggest that they are derived from gilsonite. In summary, no useful organic geochemical data could be obtained from the cuttings from Lancaster F-70 over the lower part of the well where "Superlube" was used.

Another problem associated with the use of OBM is that it can affect the physical properties of hydrocarbons produced during Drill Stem Tests. A heavy oil may flow like a less biodegraded sample if the base oil acts as a solvent. This occurred for an oil from East Rankin H-21. The SFGC of this sample shows a large hump of unresolved compounds with the only resolved peaks being the lower molecular weight n-alkanes and acyclic isoprenoids, and the 17α(H)-hopanes. It resembles a chromatogram obtained where there is mixing between biodegraded and unbiodegraded hydrocarbons, as occurs in some parts of this basin. This also occurred at East Rankin but the undegraded hydrocarbons were derived from OBM. This should be taken into account when measuring a physical property such as specific gravity (e.g., API gravity) on a DST fluid taken from a well where OBM was used.

CONCLUSIONS

In summary, the use of OBM can affect organic geochemical analyses. Examination of well logs are recommended to find out possible causes of contamination that may have occurred during drilling. It is still possible to observe source rocks using Rock-Eval/TOC logs, although the value of parameters such as TOC and HI are affected. Tmax does not appear to be affected. Saturate fraction gas chromatograms are badly affected but because of the limited molecular weight range of the base oils, biomarker distributions such as those of steranes and terpanes are not. Aromatic hydrocarbons are less affected where Biovert OBM is used. When heavier oils are used, organic geochemical analyses can become almost impossible. While these materials may cut down on drilling costs, they can severely reduce the amount of information (not only geochemical) that be obtained from these wells.

REFERENCES

Fowler, M.G., Snowdon, L.R., Stewart, K.R., and McAlpine, K.D. 1990: Rock Eval/TOC data from nine wells located offshore Newfoundland. Geological Survey of Canada Open File 2271.

BIOMARKER CHARACTERISTICS OF MIDDLE DEVONIAN OILS FROM NORTHWESTERN ALBERTA, CANADA

M.G. Fowler

Geological Survey of Canada, 3303-33rd Street N.W., Calgary, Alberta T2L 2A7

INTRODUCTION

Although at least ten oil families are known to occur in the Western Canada Sedimentary Basin (Creaney et al., 1994), there have been few detailed descriptions of the composition of these families. From a biomarker perspective, some of the most interesting oils are those thought to be sourced and reservoired within Middle Devonian Elk Point Group sediments in the Rainbow/Zama/Shekile subbasins of northwestern Alberta. Despite a claim to the contrary (Clark and Philp, 1989), the general consensus is that a convincing oil-source correlation has not been demonstrated for these oils, probably because of lack of core through the putative source rock units (Creaney et al., 1993). These are thought to be intervals within the Muskeg and Keg River formations. While some aspects of the biomarker compositions of oils from this area have been considered by previous workers (Summons and Powell, 1987; Clark and Philp, 1989; Allan and Creaney, 1991), this present study easily represents the most comprehensive both in terms of the number of samples considered and the classes of compounds examined. Here we present the data from the analysis of saturate and aromatic biomarkers in 35 oils from Middle Devonian reservoirs in northwestern Alberta. The unusual biomarker distributions of these oils are used to group them and to comment on the nature of their source rocks.

SATURATED HYDROCARBON BIOMARKERS

Most of the oils have similar gross compositions and saturate fraction gas chromatograms, including a high saturate/aromatic ratio, similar n-alkane distribution and low pristane to phytane ratio (<1.0). However, some oils from the Zama Subbasin have a higher sulphur content, lower saturate/aromatic ratio and a greater concentration of C_{20+} acyclic isoprenoids and polycyclic biomarkers than other oils. Only one oil in the sample set showed evidence of biodegradation.

Despite the above noted similarities, the oils show considerable variation both in their saturate and aromatic biomarker distributions. This allows them to be divided into at least three families, a "Rainbow" type, a "Zama" type and an intermediate group. The end member oils of the Rainbow and Zama groups have a more restricted geographical distribution than the intermediate oils.

Rainbow oils show m/z 191 mass fragmentograms (Fig. 1) with four dominant peaks corresponding to the C_{23} tricyclic terpane, the C_{24} tetracyclic terpane, Ts and the C_{29} 18α(H)- neohopane (C_{29}Ts). The 17α(H)-hopanes are in very low abundance in these oils. The predominant terpane compounds are 8,14-secoho panes. The m/z 123 mass fragmentograms show a complicated distribution of these compounds with at least two series of C_{27}, C_{29}-C_{35} 8,14-secohopanes being present. In contrast, the m/z 191 mass fragmentograms of the Zama oils (Fig. 1) are dominated by 17α(H)-hopanes with the 8,14-secohopanes present in only very low abundance. The extended C_{31}-C_{35} hopanes are in high relative abundance with $C_{35}>C_{34}$. Gammacerane is also in high abundance and the Ts/Tm ratio is much less than one. All oils have much higher concentrations of terpanes than steranes suggesting a considerable bacterial contribution to the organic matter of the source rock.

The m/z 217 mass fragmentograms show less variation among the different oil families. All the oils have similar carbon number distributions of the regular C_{27}:C_{28}:C_{29} steranes and in most oils there are low amounts of diasteranes compared to regular steranes. One major difference is the relative abundance of the C_{21} sterane which is the largest peak in all the Rainbow oils but is in lesser abundance in the Zama oils. An unusual characteristic of the Rainbow and intermediate group oils is the high values (most in the 1.2-1.5 range) for the ratio of the 20S/20R 5α(H),14α(H), 20α(H) C_{29} steranes. The ratio of the 5α(H),14β(H),17β(H) to 5α(H), 14α(H), 17α(H) steranes is also very high. These

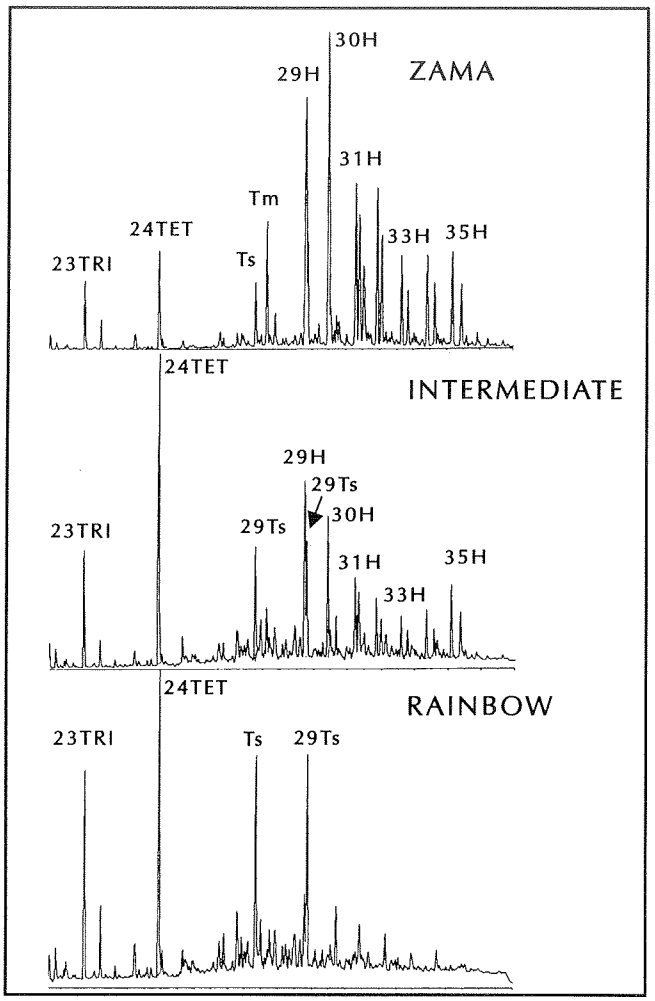

Figure 1. *Three m/z 191 mass fragmentograms of oils from Rainbow and Zama subbasins. 29-35H = 17α(H)-hopanes, Tm = 17α(H)-trisnorhopane, Ts = 18α(H)-trisnorhopane, 29Ts = C_{29} 18α(H)-hopane, 23T = C_{23} tricyclic terpane, 24 TETRA = C_{24} tetracyclic terpane.*

observations have previously been reported for extracts and oils derived from carbonates deposited under high salinity conditions (ten Haven et al., 1986). While all the oils are thought to be fully mature, their relative maturities cannot be determined using conventional biomarker parameters.

The most abundant steroidal-derived compounds in Rainbow oils are tricyclic compounds that show a major fragment of m/z 219 and are probably "seco-steranes" (Jiang et al., 1990). These compounds and the 8,14-secohopanes are the polycyclic biomarkers in highest concentrations in the Rainbow oils. In one sample where these compounds were abundant, regular steranes could not be detected using GC-MS analysis. The carbon number distribution of the C_{27}-C_{29} members of this series parallels that of the regular steranes.

Carotenoid-derived compounds such as β-carotane and 1, 1, 3-trimethyl-2-alkylcyclohexanes were also detected in some samples using GC-MS analysis.

AROMATIC HYDROCARBON BIOMARKERS

The aromatic fractions of these oils also show considerable variation. Aryl isoprenoids and their parent C_{40} diaromatic compounds are present in higher concentrations relative to other compounds in the aromatic fractions of Zama oils than in Rainbow oils. All oils have a high abundance of n-alkylbenzenes with an odd carbon number preference. The C_{15}-benzene is the most abundant, with some oils showing an enormous predominance of this compound compared to its homologues. This has been previously noted for a Michigan Basin oil (Williams et al., 1988) and in extracts from hypersaline sediments (Connan et al., 1986). The C_{25} and C_{27} n-alkylbenzenes are also often in elevated abundance.

The C_{32}-C_{35} benzohopanes occur in the Zama oils but not in the Rainbow oils (Fig. 2). All the oils contain the monoaromatic 8, 14-secohopanes and a series of "8, 14-benzosecohopanes". These latter comprise a series of C_{32}-C_{35} compounds with a base fragment of m/z 123 and are particularly abundant in the Rainbow oils. To our knowledge this is their first reported occurrence in oils or sediments. There is a strong predominance of the C_{28} over the C_{26} and C_{27} triaromatic steroids in the Zama oils. Triaromatic steroids were not detected in the Rainbow oils.

DISCUSSION

From the above it is apparent that there are at least two families of oils ("Rainbow" and "Zama") and hence two source rocks operating in this area. Many of the oils show intermediate characteristics which at present we interpret as mixing of these end members. This is being further investigated. In addition, some oils such as one from the Amber field in the west of the Zama Subbasin, have characteristics that suggest somewhat different facies of these source rocks may be contributing in some locations. The unusual characteristics of the oils are almost certainly related to the depositional environments of their source rocks. The Zama oils are likely sourced from a carbonate deposited under high salinity conditions, while the source of the Rainbow

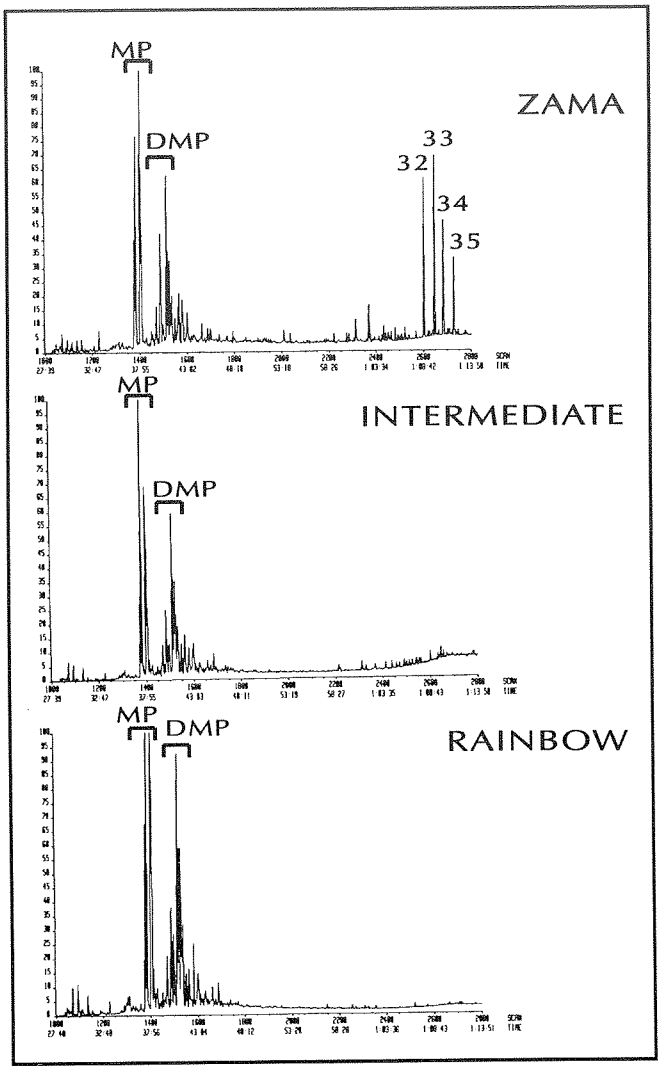

Figure 2. *Three representative aromatic fraction m/z 191 mass fragmentograms showing the distributions of the methylphenanthrenes (MP), dimethylphenanthrenes (DMP) and the C_{32}-C_{35} benzohopanes (32–35). Note these latter compounds are absent in the Rainbow and Intermediate oil.*

oils was deposited in a hypersaline environment. These conditions would not be incongruous with those occurring during the deposition of the Keg River and Muskeg formations.

REFERENCES

Allan, J. and Creaney, S.
1991: Oil families of Western Canada Basin. Bulletin of Canadian Petroleum Geology, v. 39, p. 107–122.

Connan, J., Bourollec, J., Dessort, D., and Albrecht, P.
1986: The microbial input in carbonate-anhydrite facies of a sabkha palaeoenvironment from Guatemala: A molecular approach. Organic Geochemistry, v. 10, p. 29–50.

Creaney, S., Allan, J., Cole, K., Fowler, M.G., Brooks, P.W., Osadetz, K.G., Macqueen, R.W., Snowdon, L.R., and Riediger, C.L.
1993: Petroleum generation and migration in the Western Canada Sedimentary Basin. Chapter 31. *In* Geological Atlas of the Western Canada Sedimentary Basin, G. Mossop and I. Shetsen (compilers), p. 455–468.

Clark, J.P. and Philp, R.P.
1989: Geochemical characterization of evaporite and carbonate depositional environments and correlation of associated crude oils in the Black Creek Basin, Alberta. Bulletin of Canadian Petroleum Geology, v. 37, p. 401–416.

Jiang, Z.S., Fowler, M.G., Lewis, C.A., and Philp, R.P.
1990: Polycyclic alkanes in biodegraded oil from the Kelamayi oilfield, northwestern China. Organic Geochemistry v. 15, p. 35–46.

Summons, R.E. and Powell, T.G.
1987: Identification of aryl isoprenoids in source rocks and crude oils. Biological markers for green sulphur bacteria. Geochimica et Cosmochimica Acta, v. 51, p. 557–566.

ten Haven, H.L., de Leeuw, J.W., Peakman, T.M., and Maxwell, J.R.
1986: Anomalies in steroid and hopanoid maturity indices. Geochimica Cosmochimica Acta, v. 50, p. 853–855.

Williams, J.A., Dolcater, D.L., Torkelson, B.E., and Winters, J.C.
1988: Anomalous concentrations of specific alkylaromatic and alkylcycloparaffin components in West Texas and Michigan crude oils. Organic Geochemistry, v. 13, p. 47–59.

SOURCE ROCK QUALITY, PALEOENVIRONMENTS AND OIL-SOURCE CORRELATION OF MIDDLE DEVONIAN ELK POINT GROUP, EAST CENTRAL ALBERTA

M.G. Fowler, L.D. Stasiuk, and N.C. Meijer Drees

Geological Survey of Canada, 3303-33rd Street N.W., Calgary, Alberta T2L 2A7

INTRODUCTION

The only proven Lower Paleozoic petroleum source rocks in Western Canada south of 60°N occur in the Upper Ordovician Yeoman and Middle Devonian Winnipegosis formations of the Williston Basin (Osadetz et al., 1992). Oil reservoired in Middle Devonian rocks in the Rainbow/Zama/Shekile subbasins of northwestern Alberta is also believed to have a Middle Devonian source (e.g., Fowler and Brooks, 1993). Oil-source rock correlations have linked oil from Winnipegosis reefal rocks in southwestern Saskatchewan to a Type II marine kerogen preserved within inter-reef anoxic paleoenvironments of the Winnipegosis Formation (Osadetz et al., 1992). No oils from central or southern Alberta have previously been shown to have a Middle Devonian source (e.g., Creaney et al., 1994).

Here we present preliminary results of source rock and oil studies for the Elk Point Group in east central Alberta, concentrating on samples from four wells (PCP Provost 11-35-38-10W4, Gulf Spiers 11-35-34-15W4, Virago Rich et al. 15-30-34-20W4 and Big Valley 7-25-34-21W4). The data include: (i) Rock-Eval/TOC analysis and organic facies petrography for potential source rocks; and (ii) gas chromatography (gc) and gc-mass spectrometry (gc-ms) of source rock extracts, oil-stained rocks and oils.

SOURCE ROCK QUALTITY

Over 160 Middle Devonian samples from central Alberta were screened by Rock-Eval/TOC analysis. Many Winnipegosis and Prairie Formations or equivalent units have high TOC contents and hydrogen index (HI) values (up to 600-650 mgHC/g TOC)), indicating that they have good to excellent source potential. A Winnipegosis Formation core from Provost was examined in detail between 1647.15 and 1674.0 m depth (Fig. 1). Eight samples have TOC contents greater than 1% and four greater than 10%. On an oxygen index (OI) versus HI plot, the more organic-rich samples plot either in the Type I-II area or in the Type III area, reflecting deposition in different

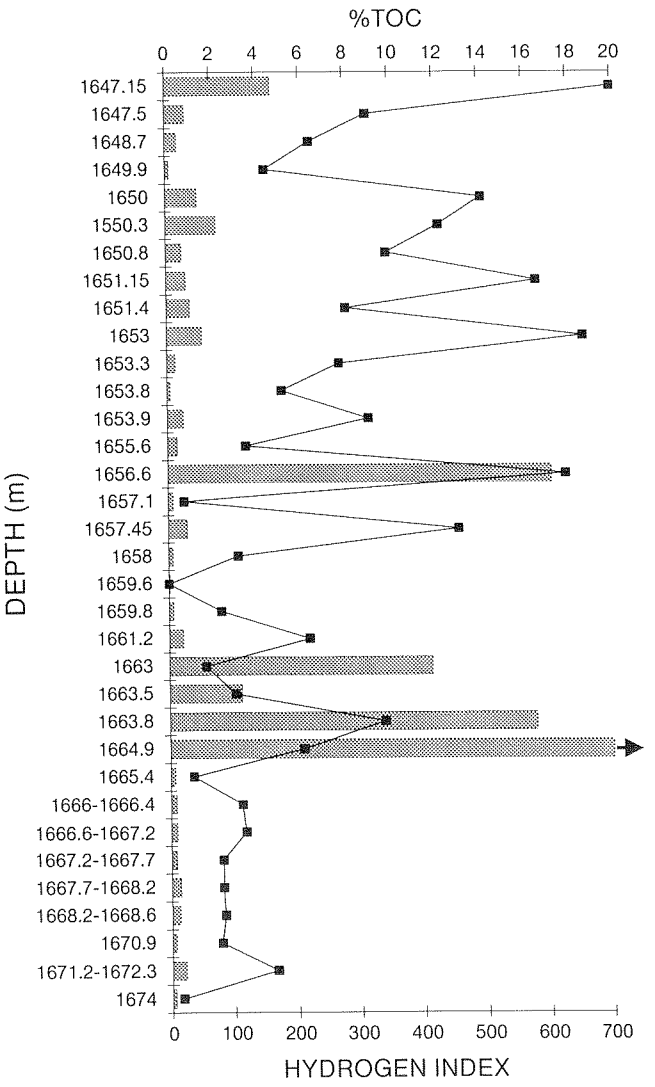

Figure 1. *Plot of total organic carbon (TOC, bars) and hydrogen index versus depth for Winnipegosis core samples from PCP Provost 11-35-38-10W4. Note the TOC content of the sample from a depth of 1664.9 m is off scale at 57.49%.*

environments. As discussed below, the former probably accumulated in a lagoonal environment with anoxic bottom waters, while the latter includes a sample from a thin coal (1664.9 m; Fig. 1) that has a TOC content of 57.5%. Although most of the Type II-I kerogen potential source rock intervals tend to be thin, some, such as at 1656.6 m, have an extremely high hydrocarbon potential (TOC 17.2%; HI 626). The uppermost sample (1647.15 m; Fig. 2) also shows good source rock potential (TOC 4.8%; HI 700) and may be part of a more extensive interval that was not fully cored. The maturity of the Winnipegosis Formation in this area varies from immature at Provost to marginally mature at Virago et al. Rich, 54 km to the west.

ORGANIC FACIES

Based on maceral composition and organic-inorganic textural relationships (Stasiuk, 1993), several organic facies-paleoenvironments have been defined for potential source rock intervals in the Winnipegosis and Prairie formations (Fig. 2). Broadly defined organic facies include: (i) terrestrial paleoenvironments with marine influence, (ii) marine paloenvironments with terrestrial influence, and (iii) wholly marine paleoenvironments. The Elk Point in the Provost core exhibits a spectrum of paleoenvironments through a transgressive source rock transition (1664.9–1647.7 m), where organic facies change from a marine-influenced, vitrinite-sporinite-rich terrestrial coal facies, to a sporinite- and *Botyrococcus* alginite-rich lacustrine interval, to a marine evaporitic (displacive anhydrite), lagoonal interval dominated by stromatolitic filamentous alginite with minor marine acritarchs (Fig. 2). Similar marine lagoonal organic facies, but with significantly more terrestrial macerals and less restricted conditions (indication of periodic normal platformal marine conditions), also characterize organic-rich intervals at Gulf Spiers and Virago et al. Rich.

SOURCE ROCK OIL CORRELATION

Oil shows from two wells in the area are of significance for this study. One is a Middle Devonian oil (23.2 °API) produced from the Big Valley well (2231–2234 m). Two closely spaced but separate oil shows were sampled in an uppermost Ordovician core unconformably underlying the Winnipegosis in the Gulf Spiers (1923.74–1923.76 m and 1928.50–1928.53 m). All three of these samples have similar geochemical characteristics indicating that they have the same or similar source rocks (Fig. 3). Characteristics that support this conclusion include: a low pristane/phytane ratio,

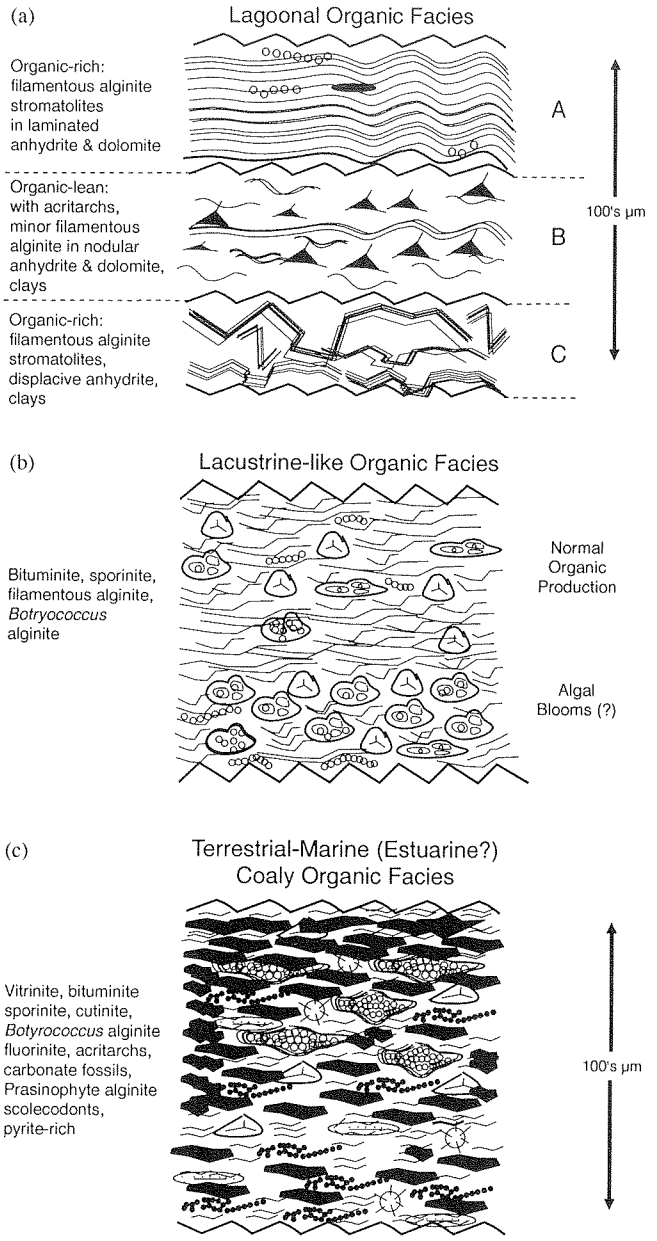

Figure 2. *Summary of vertical changes in Winnipegosis organic facies at 11-35-38-10W4. (a) Restricted, mat-forming lagoonal organic facies (1650.0 m, 1649.9 m and 1647.7 m). (b) Lacustrine-like* ***Botryococcus*** *alginite- and sporinite-rich organic facies (1656.6 m). (c) Coaly organic facies with marine influence (1664.9 m).*

relatively high concentrations of acyclic isoprenoids and polycyclic biomarkers, unusual C_{31}-C_{35} hopane distribution with the C_{34} in higher abundance than the C_{33} and C_{35} members, C_{24} tetracyclic terpane in much higher abundance than the tricyclic terpanes, a large predominance of C_{29} over C_{27} and C_{28} steranes, and a

low abundance of diasteranes relative to regular steranes. When compared to oils further east from the Williston Basin (e.g., Osadetz et al., 1992), these samples are similar to Winnipegosis-sourced oils.

The oil from Big Valley is slightly more mature than organic matter from the Winnipegosis Formation in the Virago et al. Rich well which is a few kilometres to the east. Hence, there is a possibility that the oil is locally sourced. The hydrocarbons at Gulf Spiers are significantly less mature than the oil at Big Valley Rich, but much more mature than organic-rich units in the overlying Winnipegosis. Therefore they must presumably have migrated some distance from more mature rocks to the west, possibly in the vicinity of the Virago et al. Rich well.

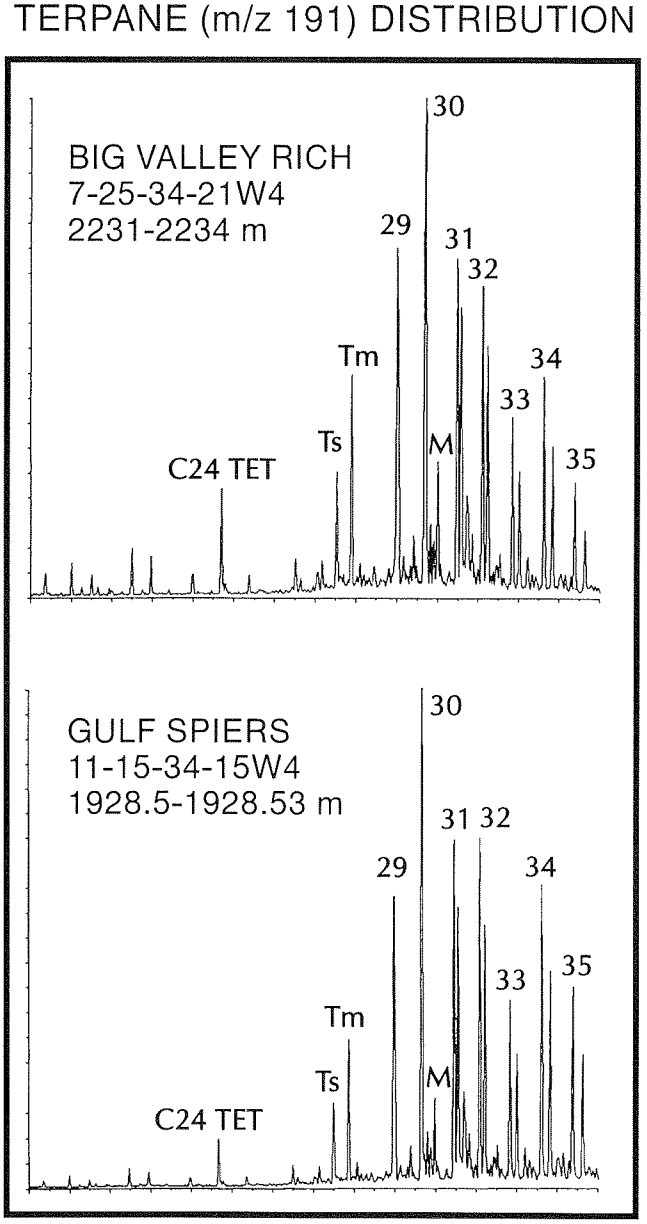

Figure 3. *Terpane (m/z 191) distributions for Winnipegosis oil from Big Valley Rich 7-25-34-24W4 and Gulf Spiers 11-15-34-15W4.*

The Winnipegosis and Prairie formations in the Provost well is immature with respect to hydrocarbon generation. However, the biomarker distributions of some samples with higher hydrocarbon potential (e.g., 1647.15 m) show source characteristics similar to those of the Big Valley Rich oil and the Gulf Spiers oil (Fig. 3) shows suggesting that the source rocks of the oils were also deposited in a restricted lagoonal to nearshore, restricted platform environment.

CONCLUSIONS

Organic geochemical and organic petrological techniques have shown that organic-rich intervals within the Middle Devonian Elk Point Group of east central Alberta were deposited in a wide range of paleoenvironments. Although, to date, only one economic discovery and oil shows in another well have been correlated to the Winnipegosis Formation in the area, it is expected that ongoing studies will demonstrate that it has sourced several other hydrocarbon pools, thus confirming the presence of an additional petroleum system in this part of the Western Canada Sedimentary Basin.

REFERENCES

Creaney, S., Allan, J., Cole, K., Fowler, M.G., Brooks, P.W., Osadetz, K.G., Macqueen, R.W., Snowdon, L.R., and Riediger, C.L.
1994: Petroleum generation and migration in the Western Canada Sedimentary Basin. *In* Western Canada Basin Sedimentary Basin Atlas, G. Mossop and I. Shetson (compilers), Chapter 32, p. 455–468.

Fowler, M.G. and Brooks, P.W.
1993: Biomarker characteristics of Middle Devonian oils from northwestern Alberta. *In* Organic Geochemistry, Poster sessions from the 16th International Meeting on Organic Geochemistry, Stavanger, 1992, K. Oygard et al. (eds.), p. 105–108.

Osadetz, K.G., Brooks, P.W., and Snowdon, L.R.
1992: Oil families and their sources in Canadian Williston Basin, (southeastern Saskatchewan and southwestern Manitoba). Bulletin of Canadian Petroleum Geology, v. 40, p. 254–273.

Stasiuk, L.D.
1993: Algal bloom episodes and the formation of bituminite and micrinite in hydrocarbon source rocks; evidence from the Devonian and Mississippian, northern Williston Basin. International Journal of Coal Geology, v. 24, p. 195–210.

REGIONAL MATURITY IN ARCTIC CANADA USING GRAPTOLITE REFLECTANCE

T. Gentzis

Alberta Research Council, P.O. Box 8330, Edmonton, Alberta T6H 5X2

T. de Freitas and F. Goodarzi

Geological Survey of Canada, 3303-33rd Street N.W., Calgary, Alberta T2L 2A7

METHOD

Graptolitic shale and carbonate samples were collected from 25 sections in Arctic Canada. Reflectance of 78 graptolites was measured (both Ro_{max} and Ro_{min}) using a Zeiss MPM II microscope. Samples were prepared and polished according to the method of Goodarzi and Stasiuk (1987).

RESULTS

Interpretation and depositional history

The platform configuration, prior to the onset of synorogenic siliciclastic sedimentation, is a necessary consideration for interpreting graptolite reflectance data. Through most of the Arctic Islands, the carbonate shelf-to-basin transition was a static feature for at least 80 Ma, beginning in about Late Cambrian time. During this time interval, sediment accumulation rates in the starved basin (Hazen and Ibbett Bay formations, Figs. 1a, b, c) were much less than in the coeval carbonate-evaporite shelf, and a submarine edifice, with relief of 1.6 to 2.0 km formed at the facies transition (Trettin et al., 1991; Trettin, 1994). A shelf step-back occurred in Late Ordovician time (Figs. 1a, b, c), and graptolitic mudrock, chert, and carbonate (Cape Phillips Formation) were deposited over the drowned shelf (de Freitas et al., this volume). However, sediment accumulation rates in the Hazen-Ibbett Bay basin and on the drowned Cape Phillips shelf were slow, and the carbonate edifice remained an important submarine feature until the onset of Silurian and Devonian synorogenic clastic deposition. Clastic sedimentation was highly diachronous, commencing in Early Silurian time in Ellesmere Island (Danish River Formation; Figs. 1a, b) and Middle Devonian time in Melville Island (Blackley, Cape de Bray, Weatherall, Hecla, Beverley Inlet, and Parry Islands formations, Fig. 1c; Embry, 1991). The oldest clastics to arrive in any of the transects (Figs. 1a, b, c) encountered the pre-existing submarine topography. Clastics accumulated first in the topographically lowest areas, such as over the Ibbett Bay and Hazen formations, but once this depression was filled, siliciclastics overstepped, and accumulated on, the drowned shelf. Important depocentres thus formed in areas previously occupied by the Ibbett Bay (Fig. 1c) and Hazen (Figs. 1a, b) formations which were also areas closer to the inferred flexural downwarp in front of the Devonian mountain belt (Fig. 1a). High thermal values in these areas suggests clastic wedge thicknesses of up to 11 km.

Graptolite reflectance values are lower on the drowned shelf, such as in eastern Melville Island (Fig. 1c) and are attributed to burial by more than 5.5 km of clastics, which are about half that interpreted for the western part of the island. This distribution of reflectance values is due to the following: the lower Palaeozoic passive margin sequence beneath the Devonian clastic wedge in eastern Melville Island is thicker, and water depths at the onset of clastic deposition were considerably less than that of the adjacent deep water basin (Ibbett Bay Formation), as mentioned above. The thick crustal sequence created greater flexural rigidity, and thus the area experienced lesser subsidence due to the application of vertical (sediment and tectonic) load. In addition, the basinward crustal sequence beneath the Ibbett Bay Formation was thinner, topographically lower, less rigid, and closer to the crustal downwarp adjacent to the northern mountain belt (Fig. 1a).

In drowned shelf areas of Bathurst Island, graptolite reflectance values are less than those of eastern Melville Island, and thus present burial thicknesses, about 5 km, are nearly complete, but farther east, on Cornwallis Island, substantially lower thermal maturity values are attributed to a very thin clastic wedge. In addition to resting on the drowned shelf, this area contains

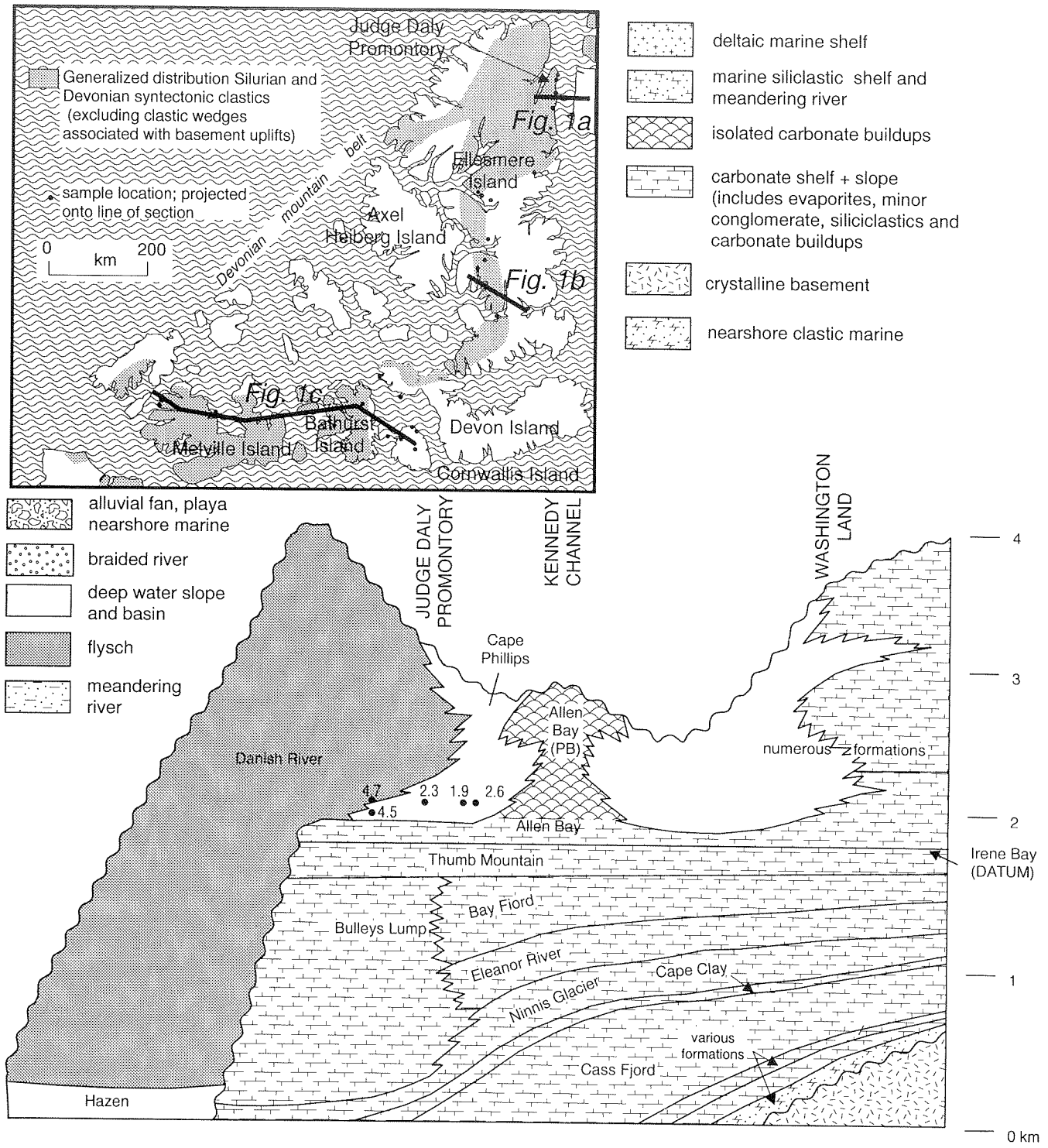

Figure 1a. *Schematic stratigraphic cross-section, Judge Daly Promontory (Ellesmere Island) to Washington Land (North Greenland).*

widespread evidence for a Late Silurian–Lower Devonian basement uplift event that featured coarse, syntectonic sedimentation (Prince Alfred and Snowblind Bay formations, Fig. 1c) and abrupt continental-to-marine facies transitions. Although most structural relief formed prior to deposition of the Devonian clastic wedge, Middle and Upper Devonian facies and formation thicknesses indicate that the uplift

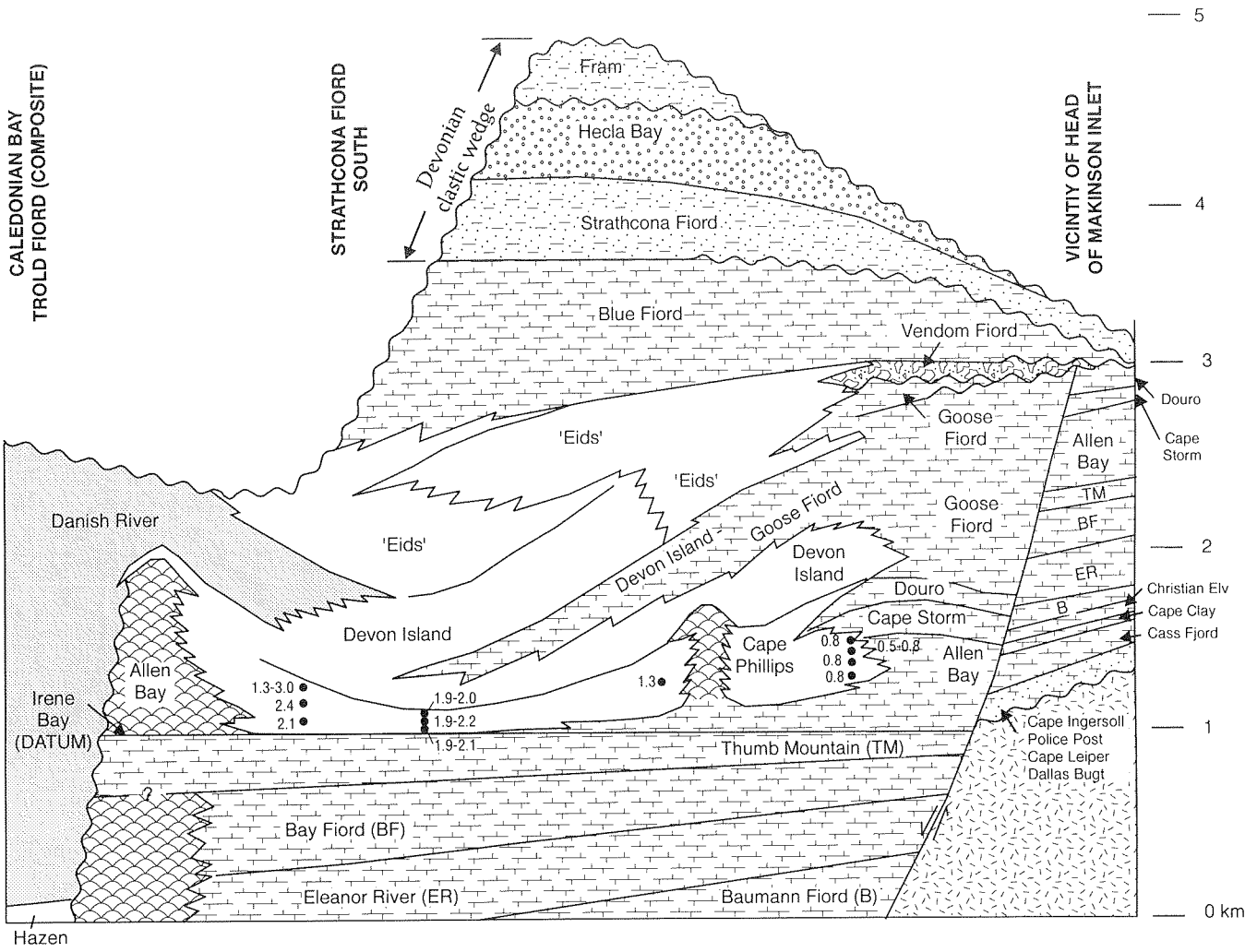

Figure 1b. *Schematic stratigraphic cross-section, central Ellesmere Island.*

subsided with lesser rates than in areas adjacent to the uplift. Because of this, some Devonian siliciclastic map units are absent locally over the Boothia Uplift, or they are much thinner than in Bathurst and Melville islands (Fig. 1c).

Thermal maturity trends in the Ellesmere Islands are similar to those in Melville Island (Fig. 1b). The Danish River Formation represents the initial synorogenic siliciclastics deposits of the area. As described above, the detritus encountered a substantial submarine edifice and thus accumulated initially west of the shelf-to-basin transition. The Danish River Formation siliciclastics were covered by more than 3 km of Middle and Upper Devonian clastics and carbonates, and graptolitic rocks were thus buried by about 4 km of strata. However, reflectance values indicate burial by at least 6.5 km of strata, and thus, about 2.5 km of strata has been eroded. An easterly decrease in graptolite reflectance is attributed to a thinner sequence of Middle and Upper Devonian clastics. The eastern part of the cross-section includes a prominent, Lower Devonian, topographic–structural basement culmination which is associated with at least 3 km of structural relief and with contraction and extension faults (de Freitas et al., this volume; Harrison et al., this volume). During the Middle and Upper Devonian, the thickened crustal succession perhaps subsided at lesser rates than the adjacent basinal areas beneath the Hazen Basin and outer shelf carbonates. In addition, crustal areas beneath outer shelf and basinal areas may have been deflected downward due to the southeastward advance of the overthrust belt and associated syntectonic sedimentary wedge (Fig. 1a).

In Judge Daly Promontory, reflectance values in the drowned shelf transect are greater than those of the basinal Ibbett Bay Formation in Melville island (Fig. 1c), indicating that this area accommodated a sedimentary column that was at least 9 km thick, which is far greater

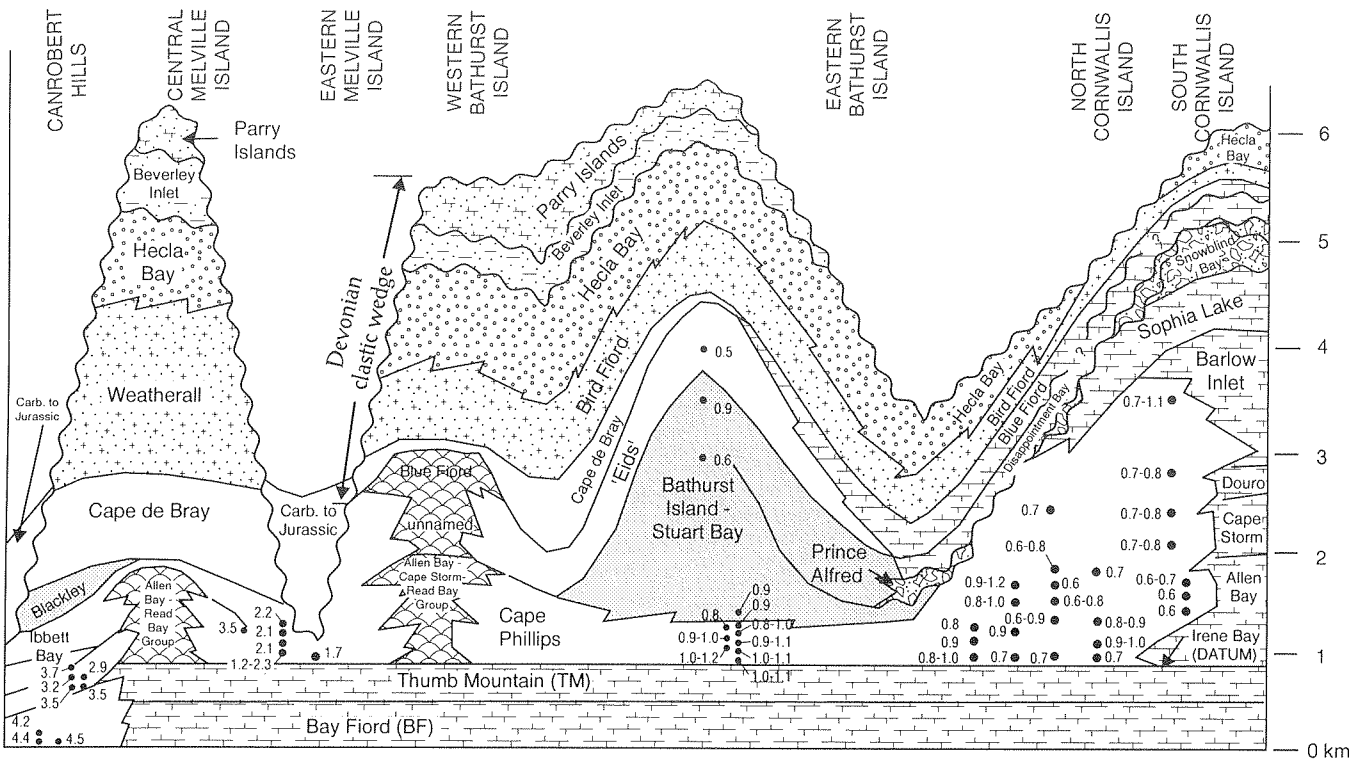

Figure 1c. *Schematic stratigraphic cross-section, Cornwallis, Bathurst, and Melville islands.*

than the thickness values interpreted for the drowned shelf in central Ellesmere Island (Figs. 1a, b). An additional 2 km should be added to this value to account for the initial sedimentation west of the submarine carbonate edifice, described above, and thus, an estimated 11 km of clastics accumulated in the Hazen deep water basin.

Reflectance values are very high in Judge Daly Promontory, but they also show abrupt lateral variation, a feature interpreted tentatively as due to the tectonic downflexing of an inhomogeneous crust. Recent studies have demonstrated that orogenic belts obducted across older passive margins are influenced substantially by pre-existing thermal and structural characteristics of the crust. We speculate that the imposed load on the Cambro–Ordovician passive margin reactivated older extension faults, developed during Late Proterozoic–Early Cambrian continental breakup, and caused the abrupt lateral variation in sediment thicknesses and thus the observed graptolite reflectance values. In support of this interpretation, Greenland workers in the adjacent and correlative outcrop belt have stressed the importance of growth faults, rooted in the basement, for controlling the location of the lower Palaeozoic, high relief, shelf-to-basin transition (Soper and Higgins, 1990, and references therein).

PRESENCE OF BITUMEN AND IMPLICATIONS FOR HYDROCARBONS

Bitumen is often associated with graptolites. Bitumen morphology ranges from low-reflecting (%Ro = 0.15–0.5%) and rounded to high-reflecting (%Ro_{max} = 2.0), granular, and angular, resembling "reservoir" bitumen. An intermediate bitumen type, indicative of the transition from nongranular to granular bitumen, is present in some graptolite-bearing samples. In areas with graptolite Ro_{max} of 1.5 or less, liquid hydrocarbons are the main product expected. On the contrary, only gases are expected at maturity levels greater than 2.0% Ro_{max} of graptolites. The presence of bitumen populations points to hydrocarbon generation and migration through the successions.

The presence of two populations of bitumen, along with their morphology, texture and reflectance indicate hydrocarbon generation and migration through the graptolite-bearing successions. Gaseous hydrocarbons are expected in areas with graptolite Ro_{max} of >2.0%, while liquid hydrocarbons could be generated in areas showing %Ro_{max} <1.5%. This study demonstrates the significance of reflectance of graptolites in pre-Devonian sedimentary strata in interpreting thermal maturity variations on a regional scale.

REFERENCES

de Freitas, T., Harrison, J.C., Mayr, U., and Thorsteinsson, R.
this volume: Stratigraphic controls on potential hydrocarbon and mineral accumulations of central Ellesmere Island.

Embry, A.F.
1991: Middle-Upper Devonian clastic wedge of the Arctic Islands, Chapter 10. *In* Geology of the Innuitian Orogen and Arctic Platform of Canada and Greenland, H.P. Trettin (ed.). Geological Survey of Canada, Geology of Canada, no. 3, p. 263–279.

Goodarzi, F. and Stasiuk, L.D.
1987: Graptolite preparation for reflected light microscopy, a technical note. Geological Survey of Canada, Paper 87–1A, p. 317–322.

Harrison, J.C., de Freitas, T., and Thorsteinsson, R.
this volume: Structural controls on potential hydrocarbon accumulations of central Ellesmere Island.

Soper, N.J. and Higgins, A.K.
1990: Models for the Ellesmerian mountain front in North Greenland: a basin margin inverted by basement uplift. Journal of Structural Geology, v. 12, p. 83–97.

Trettin, H.P.
1994: Pre-Carboniferous geology of the northern part of the Arctic Islands: Hazen Fold Belt and adjacent parts of central Ellesmere Fold Belt, Ellesmere Island. Geological Survey of Canada, Bulletin 430, 248 p.

Trettin, H.P., Mayr, U., Long, G.D.F., and Packard, J.J.
1991: Cambrian to Early Devonian basin development, sedimentation, and volcanism, Arctic Islands; Chapter 8. *In* Geology of the Innuitian Orogen and Arctic Platform of Canada and Greenland, H.P. Trettin (ed.). Geological Survey of Canada, Geology of Canada, no. 3, p. 165–238.

REGIONAL MATURITY OF ROCK FROM THE TRIASSIC OF THE CANADIAN ARCTIC ISLANDS

K.R. Stewart

Arctic Geochem Consultants, Calgary, Alberta T3J 1T2

T. Gentzis

Alberta Research Council, P.O. Box 8330, Edmonton, Alberta T6H 5X2

F. Goodarzi and A.F. Embry

Geological Survey of Canada, 3303-33rd Street N.W., Calgary, Alberta T2L 2A7

INTRODUCTION

Middle to Upper Triassic source rocks are widespread in the Sverdrup Basin. They are present in the Cape Caledonia Member of the Murray Harbour Formation and the Eden Bay and Cape Richards members of the Hoyle Bay Formation. The organic petrology and geochemistry has been studied extensively (Brooks et al., 1992; Goodarzi et al., 1989; Goodarzi et al., 1992; Gentzis and Goodarzi, 1993). In this paper, regional variations in the level of thermal maturity of organic-rich Triassic shales and their hydrocarbon generating potential will be described and interpreted using isoreflectance contour maps and Rock-Eval/TOC pyrolysis data.

RESULTS AND DISCUSSION

Regional variations in organic maturity

The Schei Point Group and its lateral equivalent, the Blaa Mountain Group, comprise most of the Middle to Upper Triassic succession in the Sverdrup Basin. On the flanks of the basin, the Schei Point Group contains five formations which are widespread in the subsurface of the western Sverdrup Basin. These are: Murray Harbour, Roche Point, Hoyle Bay, Pat Bay and Barrow (Embry 1984a). In the basin center, equivalent deep water shales are assigned to the Blaa Mountain Group which consists of the following formations in order of decreasing age: Murray Harbour, Hoyle Bay and Barrow (Fig. 1).

Organic-rich, highly oil-prone source beds containing Type II or an admixture of Type II-I (marine algal) kerogen are present in the lower portion of the Cape Caledonia Member of the Murray Harbour Formation and in the lower portions of the Eden Bay and Cape Richards members of the Hoyle Bay Formation (Fig. 1).

Regional variations in the level of organic maturity attained by Schei Point source rocks were assessed primarily from vitrinite reflectance data. Initially, log %Ro versus depth graphs were compiled for 82 Sverdrup Basin boreholes. These graphs were used to establish visual best-fit maturation gradients for each borehole and, ultimately, to determine the level of organic maturity at selected stratigraphic levels.

Regional variation in the degree of organic maturity at the base of the Cape Caledonia and Eden Bay members is illustrated by isoreflectance contour maps (Figs. 2, 3), respectively. The maps indicate that maturity increases from immature to marginally mature (0.50–0.70% Ro), along relatively narrow belts parallel to the southern and northern basin margins, to mature to slightly overmature in the southwestern depocenter. In the area of the main depocenter, near central Ellef Ringnes Island, the Blaa Mountain Group shales have maximum burial depths in excess of 4500 m and are overmature (Powell, 1978). Diabase dykes and sills intrude this area and, undoubtedly, contributed to the high thermal maturation of the Blaa Mountain Group. The isoreflectance contour map for the base of the Cape Caledonia Member is restricted to the southwestern Sverdrup, due to lack of control points in the eastern and northeastern parts of the basin.

Along the basin axis of the southwestern Sverdrup Basin, Middle to Upper Triassic shales have maximum burial depths of less than 3700 m. Dykes and sills do not occur in the Mesozoic over most of this area. Consequently, highly oil-prone source rocks within the Schei Point Group are in the mature oil to early wet

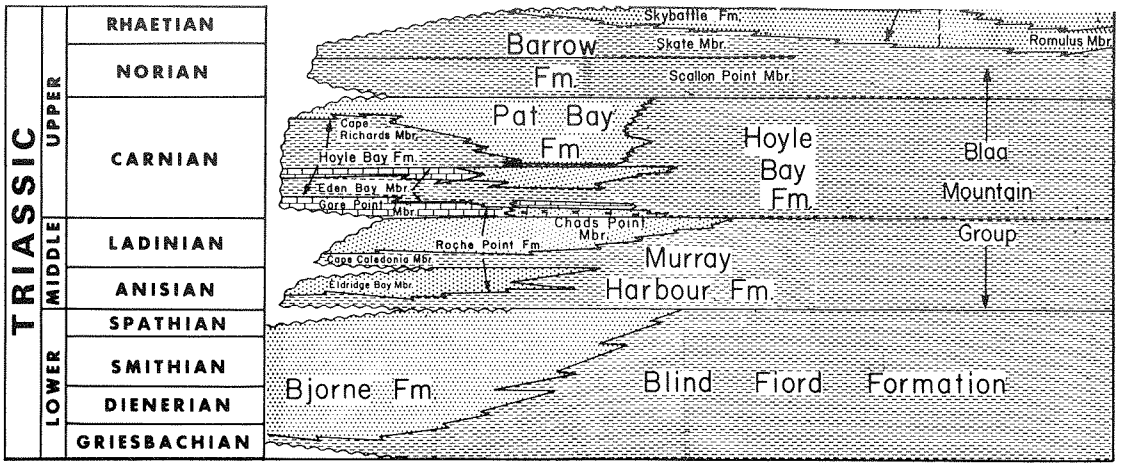

Figure 1. *Triassic stratigraphic nomenclature–Sverdrup Basin.*

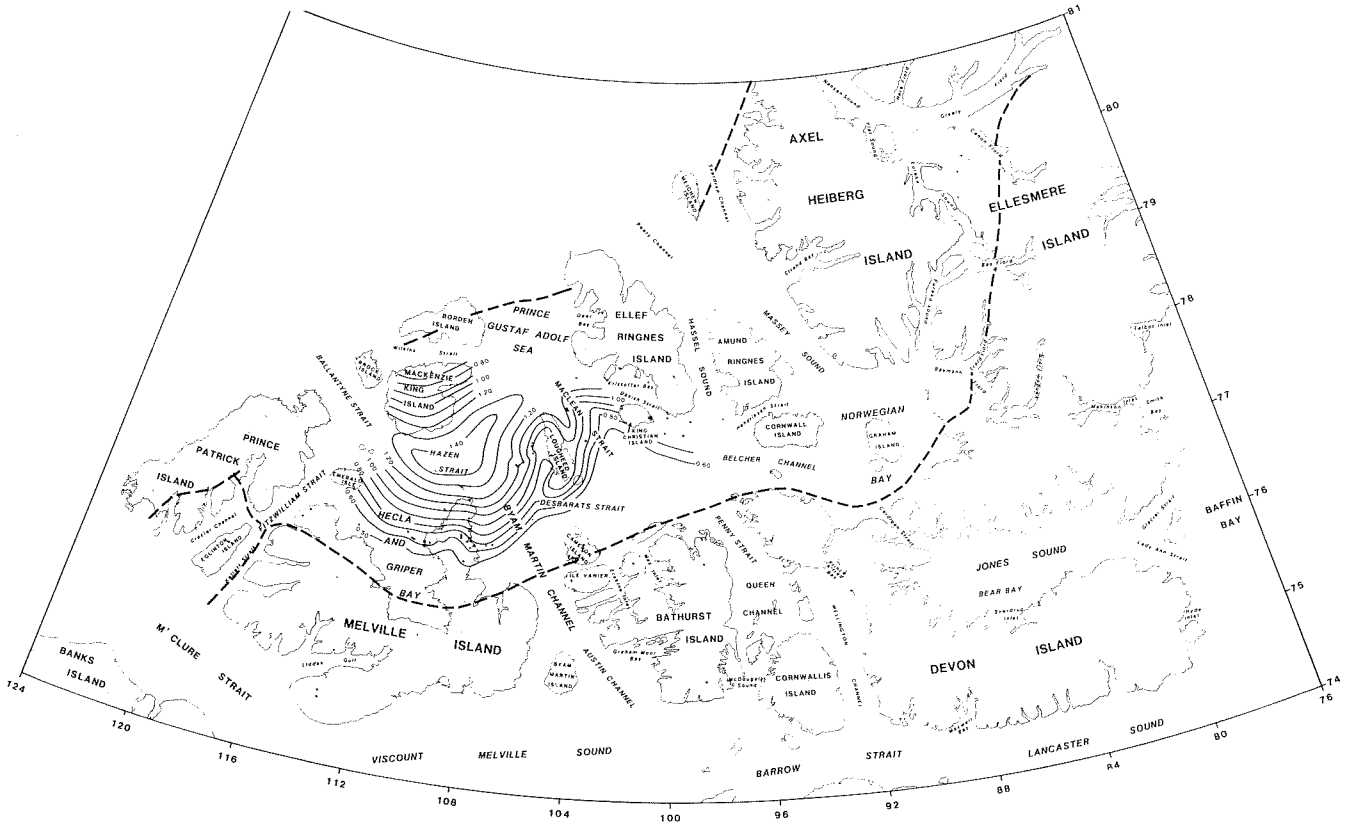

Figure 2. *Isoreflectance contour map of the Cape Caledonia Member, Murray Harbour Formation.*

gas-condensate stages of maturation, throughout a relatively broad symmetrical area about the basin axis (Figs. 2, 3).

The isoreflectance contour pattern for the base of the Eden Bay Member (Fig. 3) is similar to that of the Cape Caledonia Member (Fig. 2). However, a sufficient number of control points are available for the former to vaguely define the relatively high maturation levels attained by Schei Point sediments in the main depocenter area, located near central Ellef Ringnes Island (Fig. 3).

With some notable exceptions, the isoreflectance contour patterns on both maps are similar to the regional isopach of Mesozoic strata (Embry, 1991). This suggests that maturation levels are largely controlled by burial depth. Exceptions are the north-northwest trending arch of low isoreflectance contours around Lougheed Island as indicated in the isoreflectance map for the base of the Eden Bay Member (Fig. 3). Another exception is a similar trend of low isoreflectance contours between Ellef Ringnes and Amund Ringnes (Fig. 3). This pattern may reflect the highly biased nature of the well control in this area. The control points are all on the crests or large scale salt-cored structures, whose intermittent growth rates maintained relatively shallow burial depth and hence low levels of organic maturity (Stewart et al., 1992).

Many of the boreholes evaluated in this study are high-relief, salt-cored structures. Salt has a relatively high thermal conductivity, therefore, these features may represent anomalous high heat flow areas. Accordingly, extrapolation of maturity trends measured on these structural highs and across intervening deep synclinal areas may be misleading.

Factors influencing maturity of the Mesozoic succession

Factors, other than normal heating rates associated with burial depth, appear to have influenced the thermal history of the Mesozoic succession, as vitrinite reflectance depth trends are nonlinear, for several boreholes in or near the western depocenter. The three main factors that control geothermal gradients are:

a) differences in the primary heat flow related to tectonic phenomena;

b) differences in the thermal conductivity of the different rock types in the stratigraphic sequence; and

c) subsurface water circulation.

These factors also control source rock maturity, to a large extent, because organic maturation is mainly dependent on temperature. The Sverdrup Basin was generated by extension and it has a long-lasting history of diapiric intrusions by evaporites, magmatic invasion

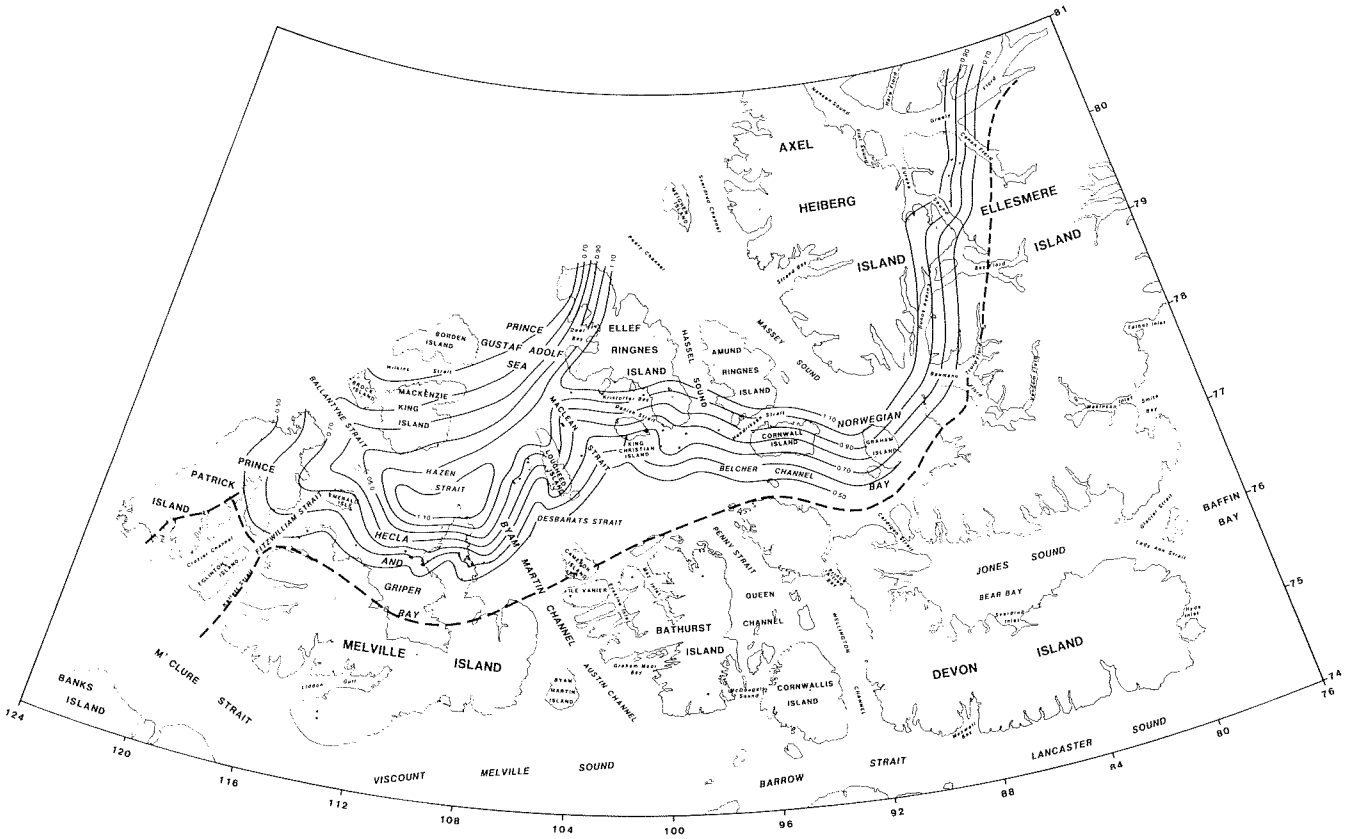

Figure 3. *Isoreflectance contour map of the Eden Bay Member, Hoyle Bay Formation.*

in rift zones and highly variable subsidence and sedimentation rates, all of which could be accompanied by significant heat flow variations. It is, therefore, unlikely that either heat flows or geothermal gradients have been invariant with time. Another possible cause of nonlinear vitrinite reflectance gradients is paleo-overpressured zones that may have developed due to the generation of hydrocarbons within mature, highly oil-prone source rocks of the Schei Point Group. The presence of oil and gas as pore fillers in organic-rich fine grained source rocks that are largely oil-wet decreases the thermal conductivity of the source rock resulting in an increase of the geothermal gradient and faster generation of hydrocarbons from the kerogen. Currently there is no evidence of abnormally pressured zones in the Sverdrup Basin. However, since the geothermal gradient leaves a permanent record on the organic matter of sedimentary rocks, the vitrinite reflectance technique can recognize past changes in geothermal gradients and can recognize corresponding paleo-abnormally pressured zones that may be normal today (Hunt, 1979). Higher heat flows due to changing thermal conductivity structure controlled by salt diapirism underlying certain structures provide another reason for believing in heat flow variations. Thus, it is tentatively concluded that variations in conductivity structure appear to be the most significant cause of vitrinite reflectance gradient variations.

Regional variations in distribution of Schei Point Group source rocks

The areal extent of organic-rich, oil-prone source rocks deposited during Ladinian to Carnian times, varies in response to the direction of clastic influx from the margins of the basin. Areas containing the best quality source rocks can be correlated to areas which were distal to their associated prograding clastic successions. During the Anisian and Ladinian, sediment influx was mainly from the south. Anoxic conditions prevailed over much of an offshore marine shelf, mainly in the north and northeast, during Ladinian time. As a result, dark brown bituminous shale accumulated in the lower portion of the Cape Caledonia Member during and directly following a major transgression. During early Carnian time, the main direction of sediment source shifted to the north. This major shift in sediment source direction resulted in the development of an anoxic offshore marine shelf in the south and southwest, where during and directly following major transgressions, dark brown bituminous shale accumulated in the lower portions of both the Eden Bay and Cape Richards Members (Brooks et al., 1992). Thus, highly oil-prone source rocks are widespread, particularly in the western Sverdrup Basin, although their areal extent and degree of organic maturity varies greatly from area to area. Highly oil-prone source rocks of the Cape Richards Member are immature with respect to oil generation, hence, these potential oil source rocks will not be discussed further in this paper.

Regional variation in hydrocarbon generating potential

The hydrocarbon generating potential of the Schei Point Group source rocks was evaluated primarily from Rock-Eval/TOC pyrolysis data obtained from both bulk and handpicked samples of drill cuttings. A total of (275) composite handpicked samples were analyzed and the sample suite includes samples from nearly all boreholes that were drilled deep enough to encounter Schei Point source rocks. The handpicked samples were collected from selected intervals from 35 boreholes. In addition, Rock-Eval/TOC data were obtained for bulk samples of drill cuttings, at a sampling frequency of between 3 to 10 m, for 11 boreholes in the vicinity of Lougheed Island. The visible portion of the organic matter in a number of handpicked samples was also characterized using reflected/UV light microscopy techniques. The results indicate that the organic matter in the Cape Caledonia and Eden Bay member is similar consisting of a mixture of autochthonous marine algal cysts (Leiosphaeridia, Nostocopsis, Tasmanites, Petrosphaeridia), dinoflagellates, acritarchs, bituminite and very little vitrinite and inertinite (Goodarzi et al., 1989; Gentzis and Goodarzi, 1993).

Rock-Eval/TOC data indicate that the vast majority of immature to marginally mature handpicked samples have TOC values ranging between 2 and 6 wt.%, with associated HI values ranging between 500 and 650 mgHc/g TOC. A few samples have TOC contents in excess of 8.0 wt.% and HI values in excess of 750 mgHc/g TOC. Such values are indicative of source rocks containing Type II or an admixture of Type II-I marine kerogens, which have a good to excellent oil-generative potential at optimum maturation levels.

Hydrocarbon generation is particularly evident from the decrease of HI values with increasing maturity. In the western depocenter, most of the HI values for mature to late mature samples range between 50 and 300 mgHc/g TOC. This drop in HI values is a consequence of high conversion rates of the kerogen into hydrocarbons, which are known to be in the 60 to 80 per cent range for hydrogen-rich kerogens similar to those encountered in the Schei Point Group.

At any given location, vertical variations in source rock richness and quality follow that pattern expected of transgressive marine shales. There also appear to be considerable differences in the TOC content and HI values for samples from the Cape Caledonia and Eden Bay members from different boreholes. Much of this variation is attributable to differences in thermal maturity, however, there remains a considerable variation suggesting possible lateral changes in organic facies. The most likely cause for lateral changes in organic facies and source bed thickness is syn-sedimentary diapiric growth. Locally, this may have resulted in less reducing conditions over the crest of structures that were diapirically active during the time of source bed deposition.

CONCLUSIONS

Organic-rich highly oil-prone source rocks consisting mainly of Type II kerogen are present in the lower portion of the Cape Caledonia Member and in the lower portions of the Eden Bay and Cape Richards members. The source rocks are widespread, particularly in the western Sverdrup Basin, although their areal extent, thickness and degree of organic maturity varies greatly from area to area.

In the depocenter region of the southwestern Sverdrup Basin, oil-prone source rocks of the Cape Caledonia and Eden Bay members are in the mature oil to early wet gas-condensate stages of hydrocarbon generation, throughout a relatively broad symmetrical area about the basin axis. Factors other than normal heating rates associated with burial depth appear to have influenced the thermal history of the Mesozoic stratigraphic succession. Variations in conductivity structure appear to be the most significant cause of vitrinite reflectance gradient variations.

REFERENCES

Brooks, P.W., Embry, A.F., Goodarzi, F., and Stewart, R.
1992: Organic geochemistry and biological marker geochemistry of Schei Point Group (Triassic) and recovered oils from the Sverdrup Basin (Arctic Islands, Canada). Bulletin of Canadian Petroleum Geology, v. 40, p. 173–187.

Embry, A.F.
1984a: The Schei Point and Blaa Mountain groups (Middle–Upper Triassic), Sverdrup Basin, Canadian Arctic Archipelago. *In* Current Research, Part B. Geological Survey of Canada, Paper 84-1B, p. 327–336.

1984b: Stratigraphic subdivision of the Roche Point, Hoyle Bay and Barrow formations (Schei Point Group), western Sverdrup Basin, Arctic Islands. *In* Current Research, Part B. Geological Survey of Canada, Paper 1984-1B, p. 275–283.

1991: Mesozoic history of the Arctic Islands. *In* Geology of the Innuitian Orogen and Arctic Platform of Canada and Greenland, Chapter 14, H.P. Trettin (ed.). Geological Survey of Canada, Geology of Canada, no. 3; (also Geological Society of America, The Geology of North America, v. E).

Gentzis, T. and Goodarzi, F.
1993: Maturity studies and source-rock potential in the southern Sverdrup Basin, Arctic Canada. International Journal of Coal Geology, v. 24, p. 141–177.

Goodarzi, F., Davies, G.R., Nassichuk, W.W., and Snowdon, L.R.
1987: Organic petrology and Rock-Eval analysis of Lower Carboniferous Emma Fiord Formation in Sverdrup Basin, Canadian Arctic Archipelago. Marine and Petroleum Geology, v. 4, p. 132–145.

Goodarzi, F., Brooks, P.W., and Embry, A.F.
1989: Regional maturity as determined by organic petrography and geochemistry of the Schei Point Group (Triassic) in the western Sverdrup Basin, Canadian Arctic Archipelago. Marine and Petroleum Geology, v. 6, p. 290–302.

Goodarzi, F., Gentzis, T., Embry, A.F., Osadetz, K.G., Skibo, D.N., and Stewart, K.R.
1992: Evaluation of maturity and source rock potential in the Lougheed Island area of the central Sverdrup Basin, Arctic Canada. *In* Arctic Geology and Petroleum Potential, T.O. Vorren (ed.). NPF Special Publication 2, Elsevier, Amsterdam, p. 147–157.

Goodarzi, F., Snowdon, L.R., Gentzis, T., and Pearson, D.E.
1994: Petrological and chemical characteristics of liptinite-rich coals from Alberta, Canada. Marine and Petroleum Geology, v. 11, p. 307–319.

Hunt, J.M.
1979: Petroleum Geochemistry and Geology. W.H. Freeman and Company, San Francisco, p. 617.

Powell, T.G.
1978: An assessment of the hydrocarbon source rock potential of the Canadian Arctic Islands. Geological Survey of Canada, Paper 78-12, 82 p.

Stewart, K.R., Embry, A.F., Goodarzi, F., and Skibo, D.N.
1992: Evaluation of organic maturity and hydrocarbon source potential of the Ringnes Formation, Sverdrup Basin, Arctic Canada. Organic Geochemistry, v. 18, p. 317–332.

OIL FAMILIES AND SOURCE ROCKS OF SOUTHWESTERN ONTARIO, CANADA

M. Obermajer

Department of Earth Sciences, University of Western Ontario, London, Ontario N6A 5B7

M.G. Fowler, F. Goodarzi, and L.R. Snowdon

Geological Survey of Canada, 3303-33rd Street N.W., Calgary, Alberta T2L 2A7

SUMMARY

Three stratigraphically defined oil families occur in southwestern Ontario. These are Cambro–Ordovician, Silurian and Devonian reservoired oils. Detailed organic petrological and geochemical studies of potential source rocks in the study area suggest discontinuous organic rich laminae occurring within the Trenton carbonates as the principle source for Cambro–Ordovician oils. A hydrocarbon contribution from marginally mature to mature Upper Ordovician Blue Mountain and Collingwood shales is also possible. The Devonian oils show similarities with the Ordovician oils indicating their possible genetic relationship with Ordovician source rocks. However, geological evidence and low maturity of the Devonian oils require a stratigraphically younger and less mature source. The Silurian oils have very distinctive geochemical characteristics, especially in the distribution and concentration of their saturated hydrocarbon biomarkers. They show a close geochemical relationship with extracts from the Eramosa dolostones. The maturity of Silurian strata is sufficient for this unit to be a source rock.

INTRODUCTION

Sedimentary rocks in southern Ontario represent almost flat-lying sequences belonging to the Michigan and the Appalachian basins, and range in age from Late Cambrian to Late Devonian (Fig. 1). Hydrocarbons in southwestern Ontario are known to occur in more than a dozen stratigraphic units and have been commercially exploited since the middle of the 19th century. About 75% of the annual production of oil (1.6×10^6 bbl) comes from dolomitized platformal carbonates (Treton–Black River Group). The remaining 25% comes from Silurian pinnacle reefs (Guelph Formation) and Devonian dolomitized domes (Lucas and Dundee formations). By the end of 1993, total cumulative hydrocarbon production in Southern Ontario had reached $10.9 \times 10^6 m^3$ (68.5×10^6 bbl) of oil and $30.5 \times 10^9 m^3$ (1 TCF) of gas. Although these quantities represent only a fraction of the growing hydrocarbon consumption in Ontario, local petroleum resources are still attracting the attention of the industrial and scientific communities. The occurrence of organic-rich strata in southwestern Ontario corresponds to the stratigraphic levels of the hydrocarbon reservoirs. The Ordovician (Treton, Blue Mountain, Collingwood), Silurian (Eramosa) and Devonian (Marcellus, Kettle Point) strata all contain sufficient amounts of oil-prone organic matter to be considered as possible source rocks. Numerous studies documented that equivalent units in the Michigan and Appalachian Basins are hydrocarbon source rocks. However, in Ontario only Cambrian–Middle Ordovician sediments have been defined as being mature with respect to hydrocarbon generation (Legall et al., 1981). Collingwood shales and Eramosa dolostones have been positively correlated with Cambro–Ordovician and Silurian oils respectively (Powell et al., 1984).

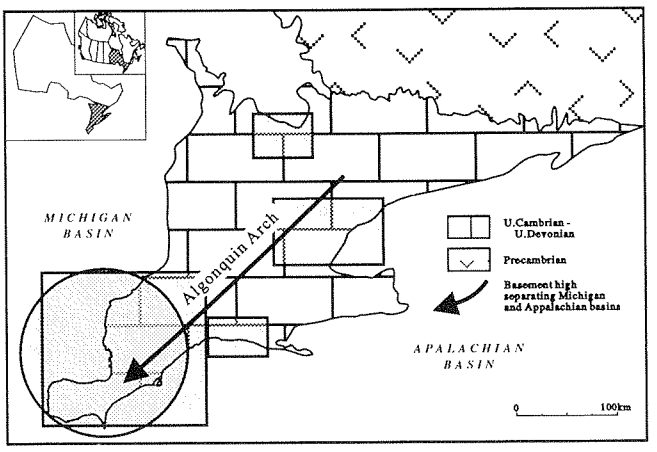

Figure 1. *Location map showing the area of sample collection (circle–oils; rectangle–rocks), main structural geological elements and simplified geology of southwestern Ontario.*

EXPERIMENTAL

A total of 35 oil samples were analyzed as part of this study. They were obtained from hydrocarbon producing wells and represent all major producing horizons in southwestern Ontario (Devonian-8, Silurian-8, Ordovician-15, Cambrian-1). Over 600 rock samples from Ordovician (Trenton, Blue Mountain, Collingwood), Silurian (Eramosa) and Devonian (Marcellus, Kettle Point) organic-rich strata were screened for hydrocarbon potential. Most of these samples were collected from scientific and petroleum exploration wells (drill cores and cuttings), except for Silurian samples that were collected from an outcrop.

Oil samples were distilled and the fraction boiling below 210°C was removed. The >210°C fraction was deasphalted, and then fractionated using open column liquid chromatography. Saturate fractions were anlayzed by gas chromatography on a Varian 3700 FID gas chromatography. Saturate fractions were analyzed by gas chromatography on a Varian 3700 FID gas chromatograph. Gas chromatography-mass spectrometry was performed on a VG 7070 mass spectrometer with a gas chromatograph attached directly to the ion source. Rock samples were pulverized and screened by Rock-Eval/TOC analysis. Samples were selected for petrographic study and solvent extraction analyses based on these results. Using a Zeiss UMSP 50 microscope, the samples were examined under reflected white light and UV light, in oil and water immersion respectively. Organic matter was soxhlet extracted for 24 hours with chloroform:methanol (87:13) and the resulting extracts were fractionated and analyzed following the same procedure as for oils.

RESULTS AND DISCUSSION

Oils from southwestern Ontario can be distinguished into three families based on their geochemical characteristics. All 35 oils contain a high proportion of hydrocarbons ranging from 71% to 97%. The Cambro–Ordovician (referred herein as Ordovician) and Devonian oils have the highest concentrations (saturates: Ord-70%, Dev-58%; aromatics: Ord-25%, Dev-34%), whereas Silurian oils reach lower values (sat-43%, arom-43%), being more aromatic and containing more resin and asphaltenes (15%). Saturate fraction gas chromatograms of Ordovician and Devonian oils show some compositional affinities. Both types have n-alkane distributions centered at C_{15}–C_{17}, with a strong odd carbon number predominance in the range C_{11}–C_{27}. Concentrations of C_{20+} n-paraffins are low (slightly higher in Devonian oils). Simiarly the relative abundance of pristane (Pr) and phytane (Ph) relative to n-alkanes is low for both types although somewhat higher for the Devonian oils. However, Pr/Ph ratio is almost identical for both Ordovician and Devonian oils. Silurian oils are characterized by a broad n-alkane distribution, high concentrations of acyclic isoprenoids (i.e., Pr and Ph) with a predominance of phytane over pristane (Table 1). The n-alkanes show maxima at C_{15} and $C_{23\text{-}25}$, possibly due to a contribution from algal and bacterial OM respectively, no pronounced odd or even carbon number predominance.

The distinctive character of the Silurian oils, as compared to the Ordovician and Devonian, is further shown by the distribution of steranes and terpanes. C_{29} and C_{30} hopanes are dominant in all the oils (Table 1, Fig. 2). However, a predominance of Tm over Ts, a high concentration of gammacerane, the distribution of C_{31}–C_{35} homohopanes, low concentrations of the C_{23} tricyclic relative to C_{24} tetracyclic terpane and lower

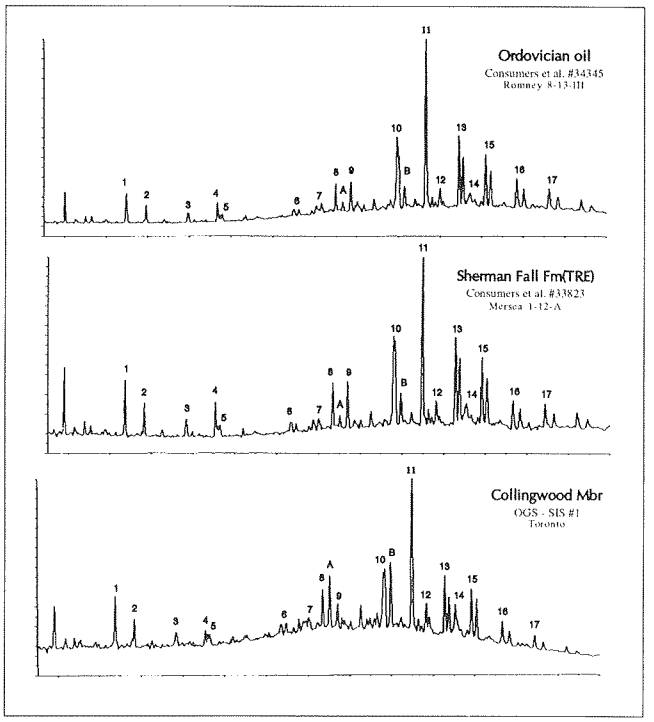

1 C_{23} tricyclic terpane
2 C_{24} tricyclic terpane
3 C_{25} tricyclic terpane
4 C_{24} tetracyclic terpane
5 C_{26} tricyclic terpane
6 C_{28} tricyclic terpane
7 C_{29} tricyclic terpane
8 18α(H),22,29,30-trisnorhopane (Ts)
9 17α(H),22,29,30-trisnorhopane (Tm)
10 17α(H),21β(H)-30-norhopane
11 17α(H),21β(H)-hopane
12 17β(H),21α(H)-moretane
13 17α(H),21β(H)-homohopanes
14 gammacerane
15 17α(H),21β(H)-bishomohopanes
16 17α(H),21β(H)-trishomohopanes
17 17α(H),21β(H)-tetrakishomohopanes
A unknown (?C_{35} tricyclic)
B 17α(H)-diahopane

Figure 2. *Representative m/z 191 mass fragmentograms of Ordovician oils and source rock extracts.*

amounts of rearranged steranes make a distinction of a separate Silurian oils family very easy. Mass fragmentograms of Ordovician and Devonian oils show very subtle differences. Terpanes ratios are almost identical, with Ts being dominant over Tm, low gammacerane concentrations and a higher C_{23} tricyclic/C_{30} hopane ratio compared with Silurian oils. The sterane fingerprint shows abundant C_{29} and C_{27} diasteranes. The distribution of C_{27}, C_{28} and C_{29} regular steranes (C_{29} being dominant) clearly separates Silurian oils from Ordovician and Devonian. Isomerization of C_{29} steranes, and hence maturity, increases from Devonian through Silurian reaching equilibrum in Ordovician oils. These may reflect maturity of source rocks during the time of hydrocarbon generation or can be related to reservoir depths and post-migrational maturation of oils in their reservoirs ("aging"). Similarly the ratio of C_{30} hopane to C_{29} $\alpha\alpha\alpha$R sterane is the highest for Ordovician oils and decreases through Silurian to Devonian oils (Table 1). This pattern may indicate increasing contribution of algal material in source rocks. However, a similar trend has been observed for the extracts with the hopane/sterane ratio increasing with increasing maturity (e.g., Collingwood: marginally mature-21.7, mature-7.46). Thus the relative concentration of hopanes and steranes is defined not only by the character of the original biological input, but also by maturity. The composition of the studied oils is typical for oils derived from marine organic matter. Their geochemical character (i.e., relative amounts of rearranged to unrearranged hopanes and steranes) indicates a carbonate source rock deposited in a strongly reducing environment for the Silurian oils, and a clastic source for the Cambro–Ordovician and Devonian oils.

The Rock-Eval/TOC results display a high organic carbon content in all the sampled rock formations. Tmax and Production Indices indicate that, with the exception of the Kettle Point Formation, all the studied lithostratigraphic units are within the "oil window". Based on consistently high Hydrogen and low Oxygen Indices the organic matter is mainly type II. These data are in agreement with microscopical observations that unstructured, amorphous marine kerogen is the dominant component of the organic matter. Unicellular alginite (varying proportions of telalganite and lamelaganite) is a primary maceral in the Ordovician and Silurian samples, whereas sieve-like bituminite (type III) is most abundant in the Devonian samples. Minor inertinite occurs in Silurian and Devonian samples, and rare sporinite in the Kettle Point samples. The bulk of the kerogen is hydrogen-rich, as indicated by a highly fluorescing groundmass. Based on optical thermal maturity indicators (fluorescence of *Tasmanites* and *Leiosphaeridia* telalganite, reflectance of chitinozoa) the Trenton and Blue Mountain samples are defined as mature, the Collingwood, Eramosa and Marcellus samples are marginally mature to mature and the Kettle Point is immature.

Extract data (HC yield, %HC in extract) agree with the optical results showing good to excellent source rock potential and a higher degree of thermal maturity for most of the Ordovician samples. As shown by saturate fraction gas chromatograms, the Silurian extracts are characterized by abundant C_{17}–C_{32} n-alkanes, and the presence of a conspicuous "base line hump", while the Ordovician and Devonian extracts show smooth n-parraffins distribution with low concentrations of C_{20+} compounds. The distribution of steranes in the extracts is in agreement with the level of thermal maturity defined by Rock-Eval/TOC, extract and optical data.

Comparison of oils and extracts indicates a positive oil-source correlation between the Ordovician oils and Ordovician organic matter. Thin (few mm to few cm) discontinous organic-rich laminae within the Trenton carbonates are believed to be the principle source because of their sufficient thermal maturity, stratigraphic position (below the oil reservoirs) and geographic location (proximity to oil pools). This explanation is more plausible because if the Ordovician oils were considered to be sourced from Collingwood and Blue Mountain shales, a long-range and possibly down-dip migration would have to be assumed. The Devonian oils show similar geochemical characteristics to the extracts of the Marcellus shales. However, the Marcellus shales occurring in the study area are yet to enter the main stage of oil generation. Many similarities the Devonian oils share with the Ordovician oils may indicate their possible genetic relationship with Ordovician source rocks. Subtle differences in their saturate biomarker distribution occur as a result of different maturities of these two oil families. Therefore, strong affinities of these two oil families may be explained either by a common source or similar organic matter and depositional environment of their sources. Although it is possible to picture cross-stratigraphic migration through a fracture system within Salina evaporites, none of the studied Devonian oils shows evidence of mixing, which must have occurred as Ordovician-generated hydrocarbons would have come into contact with Silurian oils or source rocks. Hence, the migration from mature Devonian sources located outside of the area of study and having similar geochemical composition to the Ordovician source rocks cannot be excluded. The Silurian extracts show a close geochemical relationship with the Silurian oils. Therefore sources in this interval are likely.

Table 1

Biomarker ratios of southwestern Ontario oils and possible source rocks

Sample	Steranes			Terpanes						
	$C_{29}S/(R+S)$[1]	$C_{29}\alpha\beta\beta/\alpha\alpha\alpha+\alpha\beta\beta$[2]	$C_{27}diaS/\alpha\alpha\alpha R$[3]	C_{27} Ts/Tm[4]	C29/C30[5]	gamm/C_{30}[6]	$C_{32}22S/22R+22S)$[7]	C_{23} tri/C_{30}hop[8]	Hop/C_{29}Ster[9]	Pr/Ph[10]
Oil										
Devonian	0.46	0.56	2.05	1.26	0.62	0.10	0.60	0.40	3.89	1.32
Silurian	0.50	0.67	1.22	0.94	0.46	0.24	0.60	0.13	6.14	0.56
Ordovician	0.54	0.67	4.81	1.12	0.59	0.10	0.61	0.47	8.09	1.24
Extract										
Kettle Point Fm.	0.29	0.33	0.65	0.40	0.67	0.09	0.52	0.55	0.48	2.11
Marcellus Fm.	0.48	0.50	1.72	1.11	0.48	0.09	0.59	0.34	1.73	1.40
Eramosa Mbr.	0.49	0.66	1.95	0.70	0.63	0.13	0.59	0.28	5.50	1.27
Collingwood Mbr.[a]	0.40	0.38	1.23	0.66	0.56	0.09	0.59	0.21	2.17	1.57
Collingwood Mbr.[b]	0.51	0.66	5.93	1.59	0.43	0.18	0.59	0.63	7.46	1.59
Blue Mountain Fm.	0.51	0.61	4.93	1.06	0.47	0.15	0.60	0.58	4.47	1.51
Trenton Group	0.51	0.56	3.35	1.08	0.66	0.09	0.63	0.52	7.57	1.52

[a]Collingwood Mbr immature
[b]Collingwood Mbr mature
[1]5α(H),14α(H),17α(H)20S/(20S+20R) - C_{29} sterane
[2]5α(H),14β(H),17β(H)/5α(H),14α(H),17α(H)+5α(H),14β(H),17β(H) - C_{29} sterane
[3]10α(H),13β(H),17α(H) 20S-diacholestane/5α(H),14α(H),17α(H) 20R-cholestane
[4]18α(H)-trisnorhopane/17α(H)-trisnorhopane
[5]17α(H),21β(H)-norhoapne/17α(H),21β(H)-hopane
[6]gammacerane/17α(H),21β(H)-hopane
[7]17α(H),21β(H) 20S/(20S+20R) - bishomohopane
[8]C_{23} tricyclic terpane/17α(H),21β(H)-hopane
[9]17α(H),21β(H)-hopane/5α(H),14α(H),17α(H) 20R-stigmastane
[10]pristane/phytane

REFERENCES

Legall, F.D., Barnes, C.R., and Macqueen, R.W.
1981: Thermal maturation, burial history and hotspot development, Paleozoic strata of southern Ontario, Quebec, from conodont and acritarch colour alteration studies. Bulletin of Canadian Petroleum Geology, v. 29, p. 492–539.

Powell, T.G., Macqueen, R.W., Barker, J.F., and Bree, D.G.
1984: Geochemical character and origin of Ontario oils. Bulletin of Canadian Petroleum Geology, v. 32, p. 289–312.

THE LOWER CRETACEOUS OSTRACODE ZONE, ITS SOURCE-ROCK POTENTIAL AND RELATIONSHIP TO OILS FROM THE PROVOST AREA, EASTERN ALBERTA

C.L. Riediger

Department of Geology and Geophysics, University of Calgary, Calgary, Alberta T2N 1N4

M.G. Fowler and L.R. Snowdon

Geological Survey of Canada, 3303-33rd Street N.W., Calgary, Alberta T2L 2A7

INTRODUCTION AND METHODS

The Lower Cretaceous Ostracode Zone (Mannville Group) in southern and central Alberta comprises predominantly dark grey to black, interbedded calcareous mudstone and fossiliferous limestone. The study area is bounded by Twps. 13 to 55, and Rges. 1W4 to 13W5 (Fig. 1). Within this area, the Ostracode Zone ranges in thickness from about 25 m in the western part of the study area to a zero edge close to the fourth meridian (Alberta–Saskatchewan border). Sedimentological, stratigraphic and paleontological studies suggest that the Ostracode Zone was deposited in a shallow, brackish, locally stagnant embayment (e.g., Banerjee and Davies, 1988; Leckie and Smith, 1992; Barclay and Smith, 1992). In this paper, we investigate the hydrocarbon source rock potential of this unit.

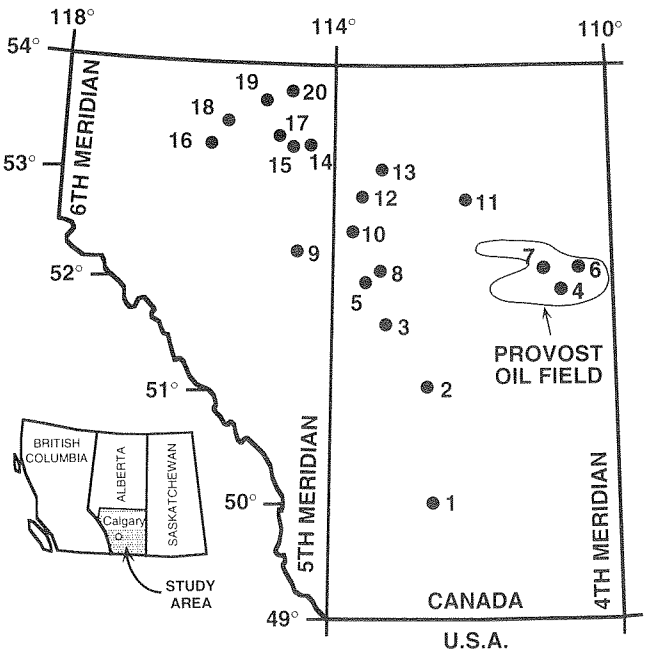

CORE LOCATIONS

1. 16-5-13-19W4
2. 10-5-25-19W4
3. 8-29-30-23W4
4. 2-11-35-6W4
5. 6-33-35-25W4
6. 11.27-37-4W4
7. 5-18-37-7W4
8. 7-1-37-24W4
9. 13-32-38-4W4
10. 11-8-41-24W4
11. 1-14-44-15W4
12. 14-32-44-25W4
13. 15-21-47-23W4
14. 6-32-49-3W5
15. 6-34-49-5W5
16. 10-35-49-13W5
17. 6-5-51-6W5
18. 9-8-52-11W5
19. 6-18-54-7W5
20. 6-22-55-5W5

Figure 1. *Map showing the location of the Provost oil field (shaded), and the cores sampled (solid dots).*

Rock-Eval/TOC analysis was performed on 192 samples from 22 core locations (Fig. 1), followed by saturate fraction gas chromatography (GC), GC-mass spectrometry (GC-MS) and organic petrographic examination (reflected white light/UV irradiation) of 20 selected samples. The effectiveness of the Ostracode Zone as an oil source rock is demonstrated by comparison of the saturate fraction biomarker data from the Ostracode Zone extracts with several oils from the Provost area of eastern Alberta (Twps. 35–42; Rges. 1–12W4).

RESULTS AND DISCUSSION

Rock-Eval/TOC Analysis

The Ostracode Zone contains a mixture of Type I and Type III kerogen. This is indicated by HI-TOC and S2-TOC cross-plots showing two distinct kerogen end-member types, with some samples showing intermediate compositions that are interpreted as a mixture of the two kerogen types. The cluster of points along the Type II curve on the Hydrogen Index (HI) vs. Oxygen Index (OI) diagram (Fig. 2) indicates either maturation of Type I organic matter, or a high concentration of terrestrial spore material. The latter interpretation is supported by petrographic investigations (see below). Total organic carbon (TOC) values for Ostracode Zone samples range from less than 1% to 11.6 wt. %, and average 2.5 wt. %. In a stratigraphic

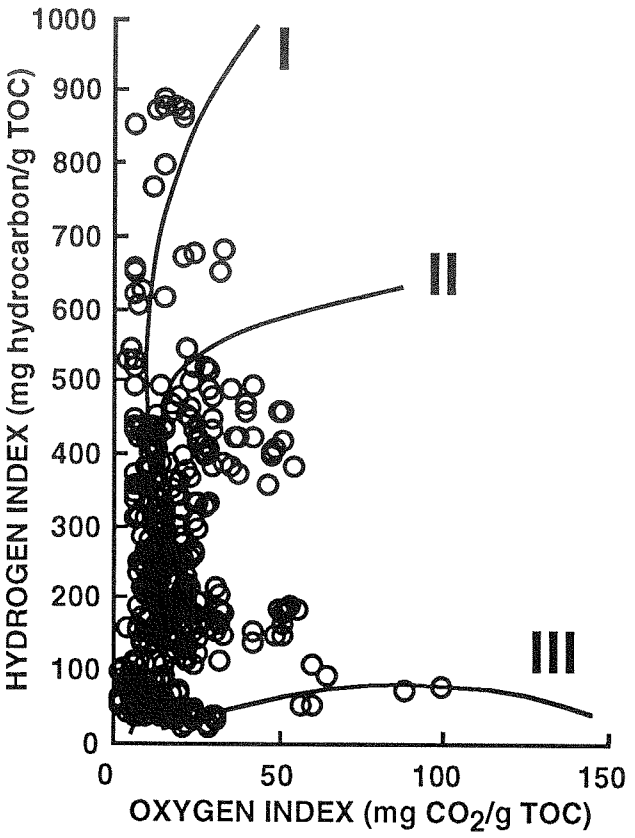

Figure 2. *Hydrogen Index vs. Oxygen Index cross-plot, Ostracode Zone.*

sense, samples with moderate TOC and high HI values (suggesting a greater contribution of Type I kerogen) are interbedded with samples yielding moderate to high TOC and low HI values (which contain more Type III (woody) material) (Fig. 3). The samples with highest HI and moderate TOC values (i.e., dominantly Type I kerogen) commonly have Tmax values that are higher than the average Tmax for adjacent samples (Fig. 3). Thus the Rock-Eval/TOC data suggests that the Ostracode Zone comprises an interbedded succession of organic-rich, fine grained sediments, which alternately contain dominantly Type I or Type III organic matter, with lesser amounts of Type II kerogen.

Tmax values range from 429 to 464°C, however the variable mixtures of kerogen types in the Ostracode Zone suggest that Tmax may not be a reliable thermal maturation index for this unit. Tmax values vary between about 442°C and 450°C for the samples with highest HI values, which is typical of Type I kerogen (Espitalié, 1986). Nonetheless, the Rock-Eval/Tmax values generally increase from east to west, a trend which is consistent with the thermal maturity pattern indicated by vitrinite reflectance data from overlying Mannville Group coals.

Organic Petrology

Organic petrographic investigations of samples from the Ostracode Zone indicate that the organic matter comprises variable mixtures of sporinite, alginite and vitrinite, with minor amounts of inertinite and amorphous material. No obvious marine alginite has been observed in samples from the Ostracode Zone. Bright yellow fluorescing *Botryococcus braunii*, a type of algae which thrives in lacustrine to brackish water environments, is the only alginite observed in these samples. The generally good to excellent preservation of the sporinite and alginite in these samples indicates selective preservation of the more resistant bio-macromolecules. Low oxygen levels in the environment of deposition is suggested to account for the preservation of organic matter in these samples.

Very little pyrite is observed in samples examined from the Ostracode Zone. The abundance of clay minerals in these sediments suggests that the formation of pyrite was not iron limited, but may have been limited by low sulphur availability. Unlike fully marine

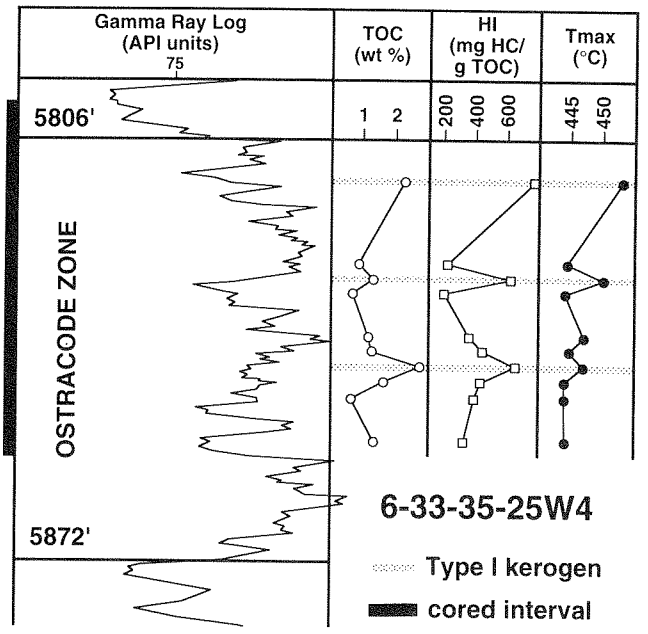

Figure 3. *Example of the gamma ray geophysical log for the Ostracode Zone, with Rock-Eval pyrolysis data for samples from this well. Intervals dominated by Type I kerogens show high TOC, Hydrogen Index (HI) and Tmax values.*

depositional environments, lacustrine to brackish environments have low salinity, and thus low abundance of sulphate.

Interpretation of depositional environments

Paralic to restricted marine (brackish) conditions are indicated by palynological data from Ostracode Zone cores in the area of this study (Banerjee and Davies, 1988). This is confirmed by the predominance of mixed Type I/III kerogen and the low pyrite content in the Ostracode Zone. The greater abundance of Type I (mainly sporinite and freshwater alginite) kerogen relative to Type III kerogen in some beds in the southernmost part of the study area, suggests paralic depositional environments, and is consistent with the interpretation of Lower Mannville paleogeography proposed by Barclay and Smith (1992) and Leckie and Smith (1992). In this interpretation, the area of this study lies within a restricted marine embayment (Edmonton Embayment) extending south from the more open marine Clearwater–Moosebar Sea. Organic geochemical data and petrographic observations indicate increasing freshwater influence toward the south, resulting in the formation of organic-rich sediments dominated by Type I kerogen.

Biomarker analysis and oil-source correlations

Pristane/phytane and pristane/nC_{17} ratios show wide variations, ranging from 1.16 to 5.35 and 0.10 to 2.07, respectively. Most samples exhibit an odd/even predominance in the range C_{23} to C_{29}. Hopane/sterane ratios greater than 15 are consistent with the inferred freshwater influence during deposition of some intervals within the Ostracode Zone.

The m/z 217 mass fragmentograms for a mature extract of the Ostracode Zone and a Provost oil are provided in Figure 4. The sterane C_{27} to C_{29} carbon number distribution (using 5α(H), 14β(H), 17β(H) isomers) shows a predominance of the C_{29} sterane in most samples, further indicating the nonmarine origin of the organic matter. The ratio of C_{27} diasterane to C_{27} regular sterane is variable (<1.0 to 4.8), and likely reflects local variations in the environment of deposition. The m/z 191 mass fragmentograms (not shown) indicate low abundance of tricyclic terpanes and low ratios of 18α(H)-trisnorneohopane/ 17α(H)-trisnorhopane in all samples. Hopane is the dominant terpane peak, and the extended hopane series to C_{35} is observed. Some samples show a C_{35}/C_{34}-hopane ratio >1.

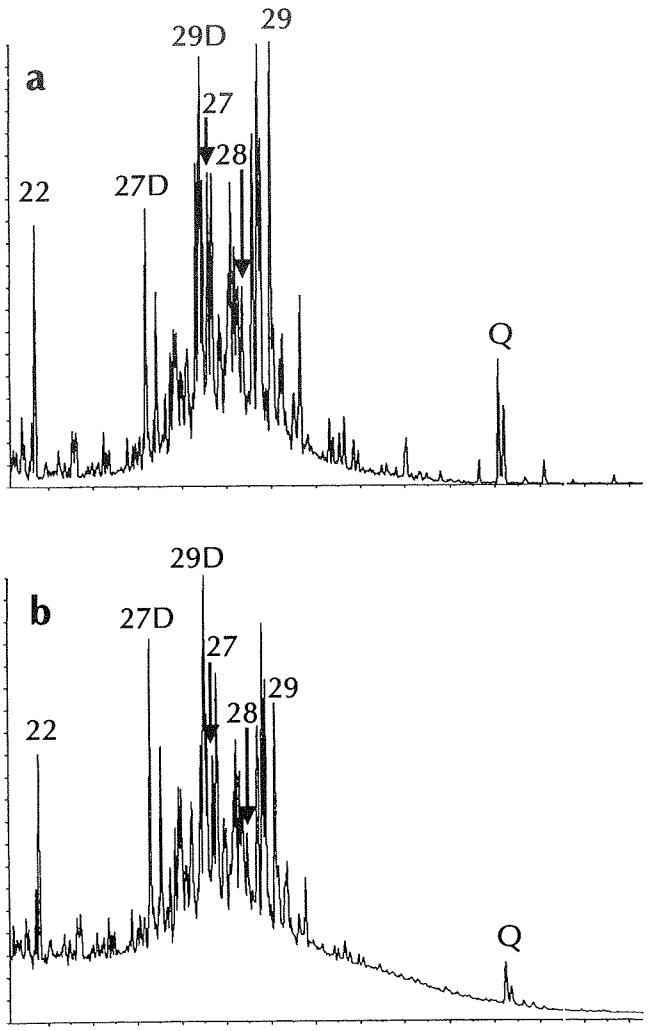

Figure 4. *m/z 217 mass fragmentograms for* ***(a)*** *Ostracode Zone extract, 4299 ft. (1310.3 m), 15-21-47-23W4; and* ***(b)*** *Provost oil, Dina Formation, 931.5–936.5 m, 16A-2-37-7W4. 22 = C_{22} sterane; 27D, 29D = C_{27}, C_{29} diasteranes; 27, 28, 29 = Cl_{27}, C_{28}, C_{29} 5α(H), 14α(H), 17α(H) 20R steranes; Q = unknown compounds.*

Unknown C_{34} hexacyclic compounds (identified by Q in Figure 4) are present in all of the extracts (often in high abundance), which yield major mass fragment ions m/z 217, 191, 285, 259, 451 and 466. These compounds have also been detected in several Lower Cretaceous Mannville Group oils from the Provost area, and thus have proven to be important for local oil-source correlations in southern and eastern Alberta. An attempt to identify these compounds is currently underway.

REFERENCES

Banerjee, I. and Davies, E.H.
1988: An integrated lithostratigraphic and palynostratigraphic study of the Ostracode Zone and adjacent strata in the Edmonton Embayment, Central Alberta. *In* Sequences Stratigraphy, Sedimentology: Surface and Subsurface, D.P. James and D.A. Leckie (eds.). Canadian Society of Petroleum Geologists, Memoir 15, p. 261–274.

Barclay, J.E. and Smith, D.G.
1992: Western Canada Foreland Basin oil and gas plays, Chapter 7: *In* Foreland Basins and Foldbelts: Part I - Type Basin - Western Canada Mesozoic-Cenozoic clastic wedge, R.W. Macqueen and D.A. Leckie (eds.). American Association of Petroleum Geologists, Petroleum Basin Series, p. 191–227.

Espitalié, J.
1986: Use of Tmax as a maturation index for different types of organic matter. Comparison with vitrinite reflectance. *In* Thermal Modelling in Sedimentary Basins, J. Burrus (ed.). 1st IFP Exploration Research Conference, Editions Technip, Paris, p. 475–496.

Leckie, D.A. and Smith, D.G.
1992: Regional setting, evolution, and depositional cycles of the Western Canada Foreland Basin, Chapter 1. *In* Foreland Basins and Foldbelts: Part I - Type Basin - Western Canada Mesozoic-Cenozoic clastic wedge, R.W. Macqueen and D.A. Leckie (eds.). American Association of Petroleum Geologists, Petroleum Basin Series, p. 9–46.

MULTIPHASE SYSTEMS AND OVERPRESSURE

L.R. Snowdon

Geological Survey of Canada, 3303-33rd Street N.W., Calgary, Alberta T2L 2A7

ABSTRACT

Subsurface fluid flow in response to a pressure differential follows Darcy's Law such that it increases with an increase in the pressure applied and with the permeability of the matrix, and decreases as a function of the viscosity of the fluid. Overpressure is considered to be caused by either mechanical means (dis-equilibrium compaction due to rapid sediment loading or the horizontal equivalent, tectonic stress) or by fluid volume expansion due to geothermal heating, kerogen conversion to bitumen or mineral transformation. An additional factor that has not been considered as a cause of overpressure is the reduction of effective permeability. Total or effective permeability (as opposed to theoretical or intrinsic permeability) of a rock (the sum of relative permeabilities of all of the separate fluid phases) decreases rapidly in response to the introduction of immiscible fluid phases. Familiar two-phase relative permeability diagrams indicate that effective or total permeabilities drop to one third of intrinsic permeability as the saturation of the nonwetting phase increases. Experimental results in three-phase systems (oil, gas, water) suggest that effective permeability will fall by a factor of more than four when all three phases are present in significant concentrations. A reduction of the effective or total permeability of a rock by a factor of four would be expected to be balanced by a decrease in the fluid flow rate and simultaneous increase in the pressure. The simple algebra of Darcy's Law requires that the pressure/fluid flow rate would also have to change by a factor of four. For example, the pressure might double to near lithostatic values while the fluid flow rate halves (2/.5 = 4). The significance of these simple observations is that the introduciton of one or more immiscible, nonaqueous phases into a water saturated system, that is, hydrocarbon generation, could make a significant contribution to the development of overpressure merely by virtue of the introduction of the additional phases. In addition it is apparent that, contrary to conventional wisdom or intuition, if permeability changes are more or less equally accommodated through increases in pressure and simultaneous decreases in flow rate, flow dynamics and hence petroleum source potential may not be attenuated by more than a factor of two or three relative to normally pressured systems, until lithostatic failure increases the effective permeability (Fig. 1).

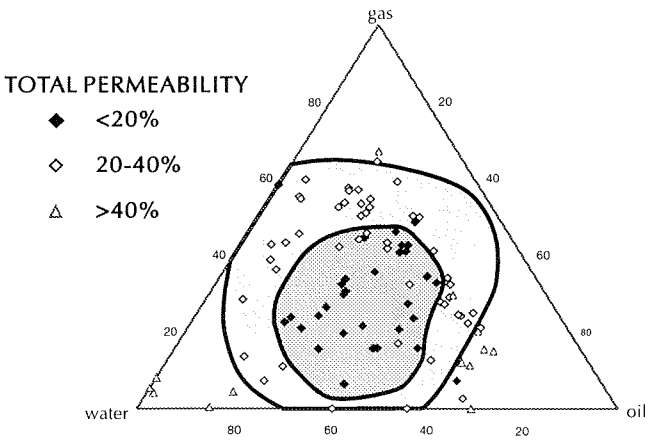

Figure 1. *Total permeability as a function of the relative concentration of gas, oil and water using data from Leverett and Lewis (1941).* K_t *(total relative permeability)* $= K_{water} + K_{oil} + K_{gas}$ *is contoured. The data points are plotted according to the relative saturation level for the three phases at the start of the experiment.*

REFERENCES

Leverett, M.C. and Lewis, W.B.
1941: Steady flow of gas-oil-water mixtures through unconsolidated sands. Transactions of the American Institute of Mining and Metallurgical Enqineers, v. 142, p. 107–116.

GEOCHEMISTRY AT THE INSTITUTE OF SEDIMENTARY AND PETROLEUM GEOLOGY: NEW DIRECTIONS AND TECHNOLOGY

L.R. Snowdon, M.G. Fowler, and H.J. Abercrombie

Geological Survey of Canada, 3303-33rd Street N.W., Calgary, Alberta T2L 2A7

NEW DIRECTIONS

Organic geochemistry research at ISPG has shifted out of an almost exclusive mandate of petroleum exploration in Canadian frontier basins and into: 1) oil sources in the Western Canada Sedimentary Basin (WCSB) including both the Canadian Williston (e.g., Osadetz and Snowdon, 1986a, b, c, 1994; Osadetz et al., 1989, 1991, 1992, 1994; Brooks et al., 1987a, b, 1988) and Alberta basins (e.g., Brooks et al., 1989a, b; Riediger et al., 1990a, b, c, 1995; Riediger, 1994; Creaney et al., 1994); 2) environmental geochemistry of fossil fuels and related hydrocarbons (e.g., Fowler et al., 1994); and 3) engineering applications of geochemistry to oil production (Brooks et al. unpublished work on Hangingstone heavy oil project). Inorganic geochemistry research has shifted away from an emphasis on theoretical, experimental and natural clay diagenesis and mineralogy toward hydrochemistry in the WCSB, reservoir diagenesis and organic/inorganic interactions in sedimentary systems (Davidson, 1993).

Oil Source Systems

Petroleum systems that have been studied in the Canadian portion of the Williston Basin include those derived from Ordovician, Middle Devonian, Upper Devonian/Mississippian, Mississippian and Cretaceous source rocks. Identification and characterization of these systems has lead to a basic understanding of probable migration routes, determination of hydrocarbon generation timing and a semi-quantitative estimation of undiscovered resources (for some of the systems) on the basis of volumetric and maturity based calculations.

Similarly, the "Nordegg" member has been investigated as a potential source in the vicinity of the Peace River Arch. The character of the expected petroleum product and the potential for production directly from the Nordegg via horizontal wells has been considered.

Current projects include an investigation of the differences in oil quality from closely spaced wells for various Mannville reservoirs, an investigation of the possibility of Lower Paleozoic source rocks and oil or gas plays in east central Alberta, and a study of Permian/Triassic discoveries in northwestern Alberta and northeastern British Columbia. Preliminary screening studies of thermal maturity and petroleum source potential are also ongoing for various parts of southern Alberta. This work entails the analysis of drill cuttings using a Rock-Eval/TOC pyrolysis apparatus (Snowdon, 1994a, b; Snowdon and Riediger 1995a, b).

In general, our approach has been one of analyzing crude oil and condensate samples using an array of analytical tools (see below) and interpreting the results both on the basis of their fundamental chemistry and via comparison and contrast with crude oil data already in our library. Source rock analyses use similar analytical techniques applied to bitumen extracted from core samples that have been selected on the basis of well logs and Rock-Eval/TOC screening.

Environmental geochemistry of fossil fuels and related hydrocarbons

Environmentally motivated studies have been centred on our analytical capability and interpretation expertise, both in the context of an extensive library of crude oil data. For example, ISPG geochemists have participated in the characterization of acute oil spills. The first of these was the bunker oil derived from the Nestucca barge which sank off Washington State and washed ashore on central Vancouver Island. In another case, about 100 barrels of crude oil recovered from Rainbow Lake was determined to be unlike any of our approximately thirty library samples from that region and also unlike the oil residue in a truck suspected as a possible perpetrator.

Also of potential interest to the oil and gas exploration and production community is a long term

objective to determine and publish pre-anthropogenic (that is, natural or background) levels of petroleum-like hydrocarbons in and around existing or proposed exploration, production and transportation facilities. To this end, opportunistic samples will be analyzed for the concentrations and characteristics of petroleum compounds either before any industrial infrastructure is in place or through using well dated recent sediment cores so that pre-anthropogenic hydrocarbon levels can be estimated. To date, a number of core samples from surface to a few hundred metres depth on the Mackenzie Delta have been obtained and analyzed. The samples contain variable amounts of hydrocarbons (up to several tens of parts per million) with characteristics ranging from those of modern biological to very immature or marginally mature petroleum-like material.

Another project involves a long term study of the evolution of creosote compounds in a near surface aquifer in cooperation with a range of university and corporate partners (Fowler et al., 1994). This project will shift from a passive or monitoring phase to one of active remediation. ISPG expertise in this project includes both the analysis and interpretation of high molecular weight hydrocarbon data as well as some background in natural degradation of petroleum compounds in near surface environments.

Engineering applications of geochemistry

In a highly experimental study, closely spaced samples of a bitumen saturated reservoir core were extracted and the character of the bitumen mapped as a vertical profile. Variations in the chemistry were then compared with a heavy oil sample produced from the well after steam soaking in order to determine if the produced material was coming from any particular stratigraphic interval in the reservoir. The project was quite successful in that the geochemical character was useful to conclude that hydrocarbons were mobilized from only a portion of the reservoir.

Another engineering application made use of our oil-oil and oil-source correlation work. In this case, a gas well that had been subjected to reservoir stimulation (fracture job) began to produce oil. Because deep and shallow resource rights were not held by one company, it was important in this example to know where the oil was being produced from. Similarly, in another case oil was seeping to the surface outside of the casing and it was important to be certain of the source of the oil before remediation of the leakage was undertaken.

Inorganic geochemistry

Inorganic geochemistry laboratories at ISPG fulfill both research and service functions in basin analysis, sedimentary diagenesis, environmental and mineral exploration geochemistry, and stratigraphic studies. The labs are equipped with leading edge instrumentation for analysis of major to ultra-trace element compositions of a wide range of solid and liquid inorganic and organic materials, and for quantitative analysis of the mineralogy and textures of sedimentary rocks and studies of airborne particulate matter. A full range of statistical, mapping, and geochemical modelling software is available to assist in data synthesis and interpretation. Organizational integration with organic geochemistry has led to growing analytical capabilities and expertise in the study of organic- inorganic linkages in sedimentary basin analysis and environmental geochemistry.

Inorganic geochemical analyses are carried out in the lab and the field. Field sampling and analysis of waters is routinely done to ensure sample integrity and to produce comprehensive analyses of the highest quality. Measurement of volatile and transient species in the field is critical for environmental work, and for studies of deep formation waters and co-produced waters in secondary and tertiary recovery where water-rock interactions may significantly affect reservoir performance. Routine field analytical procedures include ultra-filtration, analysis of pH, dissolved gases, acid and base neutralizing capability, and preservation for a wide variety of inorganic and organic, chemical and stable isotope analyses.

Research is conducted in areas of low temperature water-rock interactions in natural and artificial sedimentary diagenesis (Abercrombie, 1991; Hutcheon et al., 1993; Abercrombie et al., 1994; de Caritat et al., in press a), with particular attention paid to the identification of natural diagenetic processes. Work done by Bloch and co-workers (Bloch et al., 1993; de Caritat et al., in press b) on shales of the Colorado Group relied to a great extent on quantitative analyses of compositions and mineralogy of bulk rocks and clay extracts provided by the inorganic geochemistry laboratories. Work in progress on regional controls of water compositions of the Mannville Group in the WCSB has utilized new capabilities for ICP-MS (Inductively Coupled Plasma–Mass Spectrometry) and IC (Ion Chromatography) analysis of major to ultra-trace elements and low molecular weight volatile fatty acids in waters. Environmental research has involved hydrochemical and hydrogeological analysis of the potential impact of coalbed methane development in

southeastern B.C. (Harrison et al., 1994, 1995) and has led to new insights into the nature of hydrogeological flow systems in mountainous terrain.

Through the GSCs Industrial Partners Program (IPP) and other cost-shared arrangements, the inorganic geochemistry laboratory has become increasingly active in the development of joint research projects with industry. This has included work on the petrology and geochemistry of deep gas reservoirs in northeastern B.C. (Qing et al., 1994), and work in progress on the hydrogeological and hydrochemical atlas of the WCSB (Abercrombie et al., 1995). As well, a joint industry-government project based on the discovery of disseminated Au-Ag-Cu mineralization in northeast Alberta (Abercrombie and Feng, 1994; Feng and Abercrombie, 1994) may lead to the development of new opportunities for mineral exploration across the WCSB.

TECHNOLOGY

The above examples of the types of research undertaken in the ISPG geochemistry group are all predicated on the availability of a world class analytical facility. Instrumentation includes a full spectrum of organic and inorganic analytical tools. Organic analysis equipment includes: gas chromatography (GC) with both flame ionization (hydrocarbons) and flame photometric (sulfur compounds) detectors, Purge-and-Trap GC (volatile compounds), pyrolysis-GC (bitumen and biodegraded samples), GC-mass spectrometry (GC-MS, polycyclic biological marker compound analysis including polyaromatic hydrocarbons), GC-MS-MS, Rock-Eval/TOC (source rock screening and kinetics analysis), and hydrous pyrolysis (oil generation simulation experiments). Inorganic geochemical facilities include: X-ray Diffraction (mineral determination), X-ray Fluorescence (elemental analysis), Thermogravimetric-Fourier Transform Infrared Spectroscopy (mineral as well as organic characterization and kinetics studies), Laser Ablation-Inductively Coupled Plasma-Mass Spectrometry (trace element analysis of rocks, water, oils), Scanning Electron Microscopy-Energy Dispersive X-ray analysis (microphotography, micro-elemental analysis), and Ion Liquid Chromatography (speciation of sulfate, nitrate, carbonate and organic acids in water samples). Related groups at ISPG house reflectance, fluorescence and fluid inclusion stage microscopes required in support of thermal maturity and organic matter characterization studies. The ISPG also houses a wide array of different computer systems operating in support of our research efforts.

REFERENCES

Abercrombie, H.J.
1991: Reservoir processes in steam-assisted recovery of bitumen, Leming pilot, Cold Lake, Alberta, Canada: compositions, mixing and sources of co-produced waters. Applied Geochemistry, v. 6, p. 495–508.

Abercrombie, H.J., Bloch, J.D., Hutcheon, I.E., and de Caritat, P.
1994: Silica activity and the smectite-illite reaction. Geology, v. 22, p. 539–542.

Abercrombie, H.J. and Feng, R.
1994: Gold and PGE anomalies in Phanerozoic sedimentary rocks, northeastern Alberta - potential for new deposits? Program and Abstracts, Calgary Mining Forum, Calgary Mineral Exploration Group Society, p. 51.

Abercrombie, H.J., Barsons, D., Fullmer, G., and Rakhit, K.
1995: Hydrogeological and hydrochemical atlas of the Western Canada Sedimentary Basin. This volume.

Bloch, J., Schröder-Adams, C., Leckie, D.A., McIntyre, D.J., Craig, J., and Staniland, M.
1993: Revised stratigraphy of the lower Colorado Group (Albian to Turonian), western Canada. Bulletin of Canadian Petroleum Geology, v. 41, p. 327–341.

de Caritat, P., Bloch, J.D., Hutcheon, I., Longstaffe, F.J., and Abercrombie, H.J.
in press a: Waiting for diagenesis. Geology.

de Caritat, P., Bloch, J.D., Hutcheon, I.E., and Longstaffe, F.J.
in press b: Compositional trends of a Cretaceous foreland basin shale (Belle Fourche Formation, Western Canada Sedimentary Basin): diagenetic and depositional controls. Clay Minerals.

Brooks, P.W., Osadetz, K.G., and Snowdon, L.R.
1988: Geochemistry of Winnipegosis discoveries near Tablelands Saskatchewan. Geological Survey of Canada, Current Research, Paper 88–1, p. 11–20.

1987a: Origin of compositional differences amongst oils from the Hummingbird Field (Paleozoic), Southeast Saskatchewan. Geological Survey of Canada, Paper 87–1A

Brooks, P.W., Snowdon, L.R., and Osadetz, K.G.
1987b: Families of oils in southeastern Saskatchewan. Fifth International Williston Basin Symposium Proceedings, v. 9, p. 253–264.

Brooks, P.W., Fowler, M.G., and Macqueen, R.W.
1989a: Biomarker geochemistry of Cretaceous oils sands, heavy oils and Paleozoic carbonate trend bitumens, Western Canada Basin. *In* Fourth UNITAR/UNDP International Conference on Heavey Crude and Tar Sands, R.F. Meyer and E.J. Wiggins (eds.). v. 12, AOSTRA, p. 594–606.

Brooks, P.W., Fowler, M.G., and Macqueen, R.W.
1989b: Use of biomarkers, including aromatic steroids, to indicate relationships between oil sands/heavy oils/bitumens and conventional oils, Western Canada Basin. *In* Proceedings

of Eastern Oil Shale Symposium, Institute for Mining and Minerals Research, University of Kentucky, p. 104–111.

Creaney, S., Allan, J., Cole, K.S., Brooks, P.W., Fowler, M.G., Macqueen, R.W., Osadetz, K.G., Snowdon, L.R., and Riediger, C.L.
1994: Petroleum generation and migration in the Western Canada Sedimentary Basin, G.D. Mossop (ed.). Western Canadian Sedimentary Basin Atlas, Chapter 31.

Davidson, R.A.
1993: Water soluble organic acids from the hydrous pyrolysis of an immature, organic-rich shale from the Western Canada Sedimentary Basin and their diagenetic implications. M.Sc. thesis, University of Waterloo, 157 p.

Feng, R. and Abercrombie, H.J.
1994: Disseminated Au-Ag-Cu mineralization in the Western Canada Sedimentary Basin, Forth MacKay, Northeast Alberta: A new gold deposit type. *In* Current Research, 1994–E. Geological Survey of Canada, p. 121–132.

Fowler, M.G., Brooks, P.W., Northcott, M., King, M.W.G., Barker, J.F., and Snowdon, L.R.
1994: Preliminary results from a field experiment looking at the fate of some higher molecular weight components of creosote in a natural aquifer. Organic Geochemistry, v. 22.

Harrison, S.M., Abercrombie, H.J., and Barker, J.F.
1994: Hydrochemical and hydrogeological investigation of a potential coalbed methane area, southeastern British Columbia. *In*, Current Research, 1994–E. Geological Survey of Canada, p. 117–120.

Harrison, S.M., Abercrombie, H.J., Barker, J.F., Rudolph, D., and Aravena, R.
1995: Hydrochemical and hydrogeological investigation of a potential coalbed methane area, southeastern British Columbia. This volume.

Hutcheon, I.E., Shevalier, M., and Abercrombie, H.J.,
1993: pH buffering by metastable mineral-fluid equilibria and evolution of carbon dioxide fugacity during burial diagenesis. Geochimica et Cosmochimica Acta, v. 57, p. 1017–1028.

Osadetz, K.G. and Snowdon, L.R.
1986a: Speculation on the petroleum source rock potential of portions of the Lodgepole Formation (Mississippian) of southern Saskatchewan. Geological Survey of Canada, Paper 86–1B, p. 647–651.

1986b: Petroleum source rock reconnaissance of southern Saskatchewan. *In* Current Research, Geological Survey of Canada, Paper 86–1A, p. 609–617.

1986c: Petroleum source rock reconnaissance of southern Saskatchewan. Geological Association of Canada, Mineralogical Association of Canada, Canadian Geophysical Union, Joint Annual Meeting Program with Abstracts, v. 11, p. 110.

1994: Significant Paleozoic petroleum source rocks, their distribution, richness and thermal maturity in Canadian Williston Basin (southeastern Saskatchewan and southwestern Manitoba). Geological Survey of Canada, Bulletin 487.

Osadetz, K.G., Snowdon, L.R., and Stasiuk, L.D.
1989: Association of enhanced hydrocarbon generation and crustal structure in the Canadian Williston Basin. Geological Survey of Canada, Current Research, Paper 89–1D, p. 35–47.

Osadetz, K.G., Snowdon, L.R., and Brooks, P.W.
1991: Relationships amongst oil quality, thermal maturity and post-accumulation alteration in Canadian Williston Basin (southeastern Saskatchewan and southwestern Manitoba). *In* Proceedings of the Sixth International Williston Basin Symposium, J.E. Christopher and F.M. Haidl (eds.). Regina, p. 293–311.

Osadetz, K.G., Brooks, P.W., and Snowdon, L.R.
1992: Oil families and their sources in Canadian Williston Basin, (southeastern Saskatchewan and southwestern Manitoba). Bulletin of Canadian Petroleum Geology, v. 40/3, p. 254–273.

Osadetz, K.G., Snowdon, L.R., and Brooks, P.W.
1994: Oil families in Canadian Williston Basin (southwestern Saskatchewan). Bulletin of Canadian Petroleum Geology, v. 42/2, p. 155–177.

Qing, H., Teare, M., Abercrombie, H.J., Reimer, J., and Riediger, C.L.
1994: Diagenetic paragenesis of Middle Devonian Presqu'ile Barrier, northeastern British Columbia. Geological Survey of Canada, Current Research, 1994–B, p. 43–48.

Riediger, C.L.
1990: Rock-Eval/TOC data from the lower Jurassic Nordegg Member, and the lower and middle Triassic Doig and Montney formations, Western Canada Sedimentary Basin, Alberta and British Columbia. Geological Survey of Canada, Open File 2308, 27 p.

1994: Migration of "Nordegg" oil in the Western Canada Basin. How much and how far? Bulletin of Canadian Petroleum Geology, v. 42/1, p. 63–73.

Riediger, C.L., Fowler, M.G., Brooks, P.W., and Snowdon, L.R.
1990a: Triassic oils and potential Mesozoic source rocks, Peace River Arch area, Western Canada Basin. Organic Geochemistry, v. 16, p. 295–305.

Riediger, C.L., Brooks, P.W., Fowler, M.G., and Snowdon, L.R.
1990b: Lower and Middle Triassic source rocks, thermal maturation and oil source correlations in the Peace River Embayment area, Alberta and British Columbia. Bulletin of Canadian Petroleum Geology, v. 38a, p. 218–235.

Riediger, C.L., Fowler, M.G., Snowdon, L.R., Goodarzi, F., and Brooks, P.W.
1990c: Source rock analysis of the Lower Jurassic Nordegg Member and oil-source correlations, northwestern Alberta and northeastern British Columbia. Bulletin of Canadian Petroleum Geology, v. 38a, p. 236–249.

Riediger, C.L., Fowler, M.G., and Snowdon, L.R.
1995: Organic geochemistry of the Lower Cretaceous Ostracode Zone, a brackish/nonmarine source for some lower Mannville oils in southern Alberta. Mannville Symposium Volume, Canadian Society of Petroleum Geology.

Snowdon, L.R. and Osadetz, K.G.
1988: Gasoline range (C5 to C8) and C15+ saturate fraction gas chromatograms for the crude oils from the southeastern portion of the Williston Basin. Geological Survey of Canada, Open File 1785, 261 p.

1988: Geological processes interpreted from gasoline range analyses of southeast Saskatchewan and Manitoba oils. Geological Survey of Canada, Current Research, Paper 88–1D, p. 33–40.

Snowdon, L.R., Osadetz, K.G., and Brooks, P.W.
1987: Analysis of gasoline range hydrocarbons in southern Saskatchewan. Geological Association of Canada, Mineralogical Association of Canada, 1987 Joint Annual Meeting, Program with abstracts, 1987, v 12, p. 90.

Snowdon, L.R.
1994a: Rock-Eval/TOC data for 13 south-central Alberta wells (Townships 36 to 59, Ranges 3 to 21W5). Geological Survey of Canada, Open File 2935, 87 p.

1994b: Rock-Eval/TOC data for ten southwest Alberta wells (Townships 16 to 30, Ranges 2 to 10W5). Geological Survey of Canada, Open File 2916, 114 p.

Snowdon, L.R. and Riediger, C.L.
1995a: Rock-Eval/TOC data for 10 eastern Alberta wells (Townships 25-33, Ranges 1-10W4). Geological Survey of Canada, Open File 2989, 44 p.

1995b: Rock-Eval/TOC data for 19 southern Alberta wells (Townships 7 to 41, Ranges 15W4 to 3W5). Geological Survey of Canada, Open File 2990, 125 p.

CRUDE OIL AND HYDROCARBON FLUID INCLUSION FLUORESCENCE MICRO-SPECTROMETRY: APPLICATION TO THE STUDY OF OIL MIGRATION

L.D. Stasiuk

Geological Survey of Canada, 3303-33rd Street N.W., Calgary, Alberta T2L 2A7

ABSTRACT

The fluorescence properties of oils are currently being evaluated for their potential use in studying petroleum migration (e.g., carrier bed identification, thermal maturity and the relationship between migration and reservoir diagenetic events). The relative and absolute intensity of crude oils and hydrocarbon fluid inclusion (**hcfi**) fluorescence are measured between 400 and 700 nm using an incident light microscopic and micro-spectrometric system. The spectral character of reservoired crude oils within the petroleum system being studied provide a "signature" for identifying similar oils trapped as hydrocarbon inclusions, oils adsorbed onto clay minerals, or oils trapped as intercrystalline globules. Two examples are presented to illustrate the potential of utilizing micro-fluorescence. Petroleum migration pathways are being mapped in the Upper Devonian Birdbear Formation, southeast Saskatchewan. At least three oils have been identified. Fluorescence spectra of hcfi and free oils (Type D1A and Type D1B) from carrier beds, stylocumulates, fracture zones and organic-rich lithologies from the Birdbear Formation, match well with spectra obtained from Family D1 (Osadetz et al., 1992) crude oils produced from the Birdbear. In addition, a population of very high maturity oil has been recognized in the Birdbear. The fluorescence spectra of crude oils from Late Jurassic and Early Cretaceous sandstone reservoirs, Jeanne d'Arc basin, offshore Newfoundland, are compared with the spectra of hcfi from the same reservoir sandstones. A relatively low maturity oil (Type A) trapped in quartz cements/overgrowths and a high maturity oil (Type B) trapped in annealed fractures and kaolinite characterize most of the reservoirs. The hcfi spectra are different from the spectra of the crude oils suggesting that the later is a mixture of a low and high maturity oil.

INTRODUCTION AND METHOD

The spectral distribution of auto fluorescence emitted from hydrocarbons is a direct function of the gross chemical composition (saturate, aromatic, asphaltene and resin) which in turn is controlled by thermal maturity, and in some oils, the degree of bio-degradation (e.g., Van Gijzel, 1981; Bertrand et al., 1986; Hagemann and Hollerbach, 1986; Khorasani, 1987). The fluorescence properties of crude oils and hydrocarbon fluid inclusions (**hcfi**) can be conveniently characterized between 400 and 700 nm with an incident light micro-spectrometric system equipped with an ultra-violet light source. The shape of the spectral curve from "oil" fluorescence, wavelength of maximum emission intensity (Lmax), Red/Green quotients ($Q = Intensity_{650nm}/Intensity_{500nm}$) and de convoluted spectra are useful for defining oil groups and providing a basis for correlation (Fig. 1a). The relationship between the fluorescence properties of oils and the gross chemical composition was tested with a Zeiss fluorescence micro-spectrometric system using a set of 15 Canadian oils which were trapped as synthetic hydrocarbon fluid inclusions in NaCl crystals (Stasiuk and Snowdon, 1993). The test results confirmed that with increasing saturate to aromatic ratios and decreasing asphaltenes and resins, there is a progressive blue shift in the spectra to Lmax values of shorter wavelengths.

Fluorescence micro-spectrometry can conceivably be used to demonstrate correlations between crude oils and hydrocarbon fluid inclusions when dealing with samples from source rocks, reservoir rocks, and carrier beds which are part of the same oil system. The relationship between fluorescence properties of oils and hcfi from the Upper Devonian of southeastern Saskatchewan and from the Late Jurassic to Early

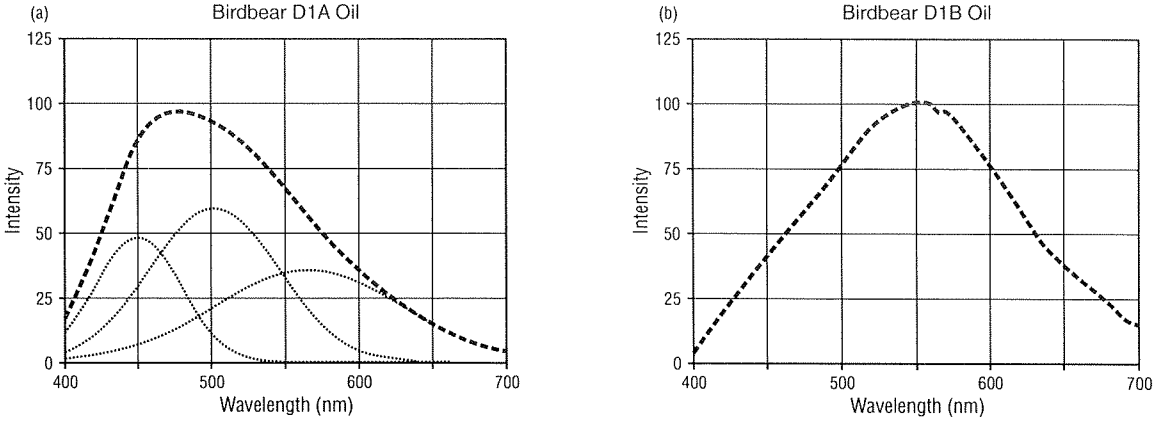

Figure 1. *Examples of fluorescence spectra of Family D1 crude oils (Osadetz et al., 1992) from Birdbear Formation: (a) D1A oil: Lmax = 475, Q = 0.15; Dome Kisbey 7-27-7-6W2; (b) D1B oil: Lmax = 555 nm, Q = 0.49; 10-26-2-19W2. The curve in (a) has been de convoluted into 3 components.*

Cretaceous of the Jean d'Arc Basin, offshore Newfoundland, is currently being tested for: (i) identification of hydrocarbon migration pathways; (ii) comparison of crude oil composition with hydrocarbon fluid inclusion composition from the same reservoir rock (are they significantly different ?); and (iii) determination of whether there is a relationship between oil type and specific diagenetic events which affected reservoir facies. In an attempt to achieve these goals, fluorescence spectra were obtained from: (i) oils trapped as inclusions in reservoir and carrier beds; (ii) crude oil samples from a reservoir; (iii) oils rapidly extracted by acetone from pulverized rock sample; and (iv) oils extracted by epoxy resin. Measurements are carried out following a standard protocol using the following: (i) for crude oil, micro-droplets are spread on a standard petrographic glass and excited at 365 nm under a H_2O immersion objective; and (ii) for hydrocarbon inclusions, doubly polished thin sections and polished block samples are scanned under H_2O immersion.

RESULTS AND DISCUSSION

Two examples are presented to illustrate the application of fluorescence micro-spectrometry to studying petroleum migration. The first example, from the Upper Devonian of the Williston Basin in southeastern Saskatchewan, is an attempt to define the pathway of hydrocarbon migration. The second example, from the Jeanne d'Arc Basin offshore Newfoundland, attempts to resolve whether the reservoired crude oils are of the same chemistry/maturity as hydrocarbon fluid inclusions in the reservoir sandstones.

Example 1: Birdbear Formation, Saskatchewan

In this example the micro-fluorescence properties of hydrocarbons from whole rock samples (i.e. fluid inclusions from potential carrier beds and reservoir rocks) are correlated to reservoired crude oil samples. The crude oils were previously evaluated by oil-source rock geochemical biomarker correlations (Osadetz et al., 1992). Fluorescence spectra were determined for Family D1 crude oils (possible Winnipegosis source; Osadetz et al. 1992) from Birdbear Formation reservoir facies at five locations in southeastern Saskatchewan. The Birdbear reservoir oils are divisible into two Types (Fig. 1). Type D1A crude (e.g., 5-33-10-32W1 and 7-27-7-6W2) has a Lmax ranging from 475 to 485 nm and Q ranging from 0.15 to 0.26 (Fig. 1a). Type D1B crude (e.g., 10-26-2-19W2 and 4-21-6-19W2) has a Lmax ranging from 550 to 560 nm and a Q ranging from 0.49 to 0.56 (Fig. 1b). These "spectral signatures" were used as the basis for recognizing potential hydrocarbon migration pathways of Family D1 crudes through potential Birdbear carrier beds.

A set of 100 samples (70% core, 30% cuttings) from suspected carrier beds, stylocumulates, fracture zones and organic-rich lithologies were collected from some 30 locations across southeastern Saskatchewan (20 x 20 Townships). Three main types of fluorescence spectra were obtained from Birdbear hydrocarbon inclusions (and rapid acetone and epoxy extracts). Two spectral types (Fig. 2a, 2b) match spectra obtained from reservoired crude oils (i.e., Type D1A oils and Type D1B oils). In addition, a third population of very high maturity, "blue-region" oil was identified at several locations (Fig. 2c, 2d); the spectral properties of these

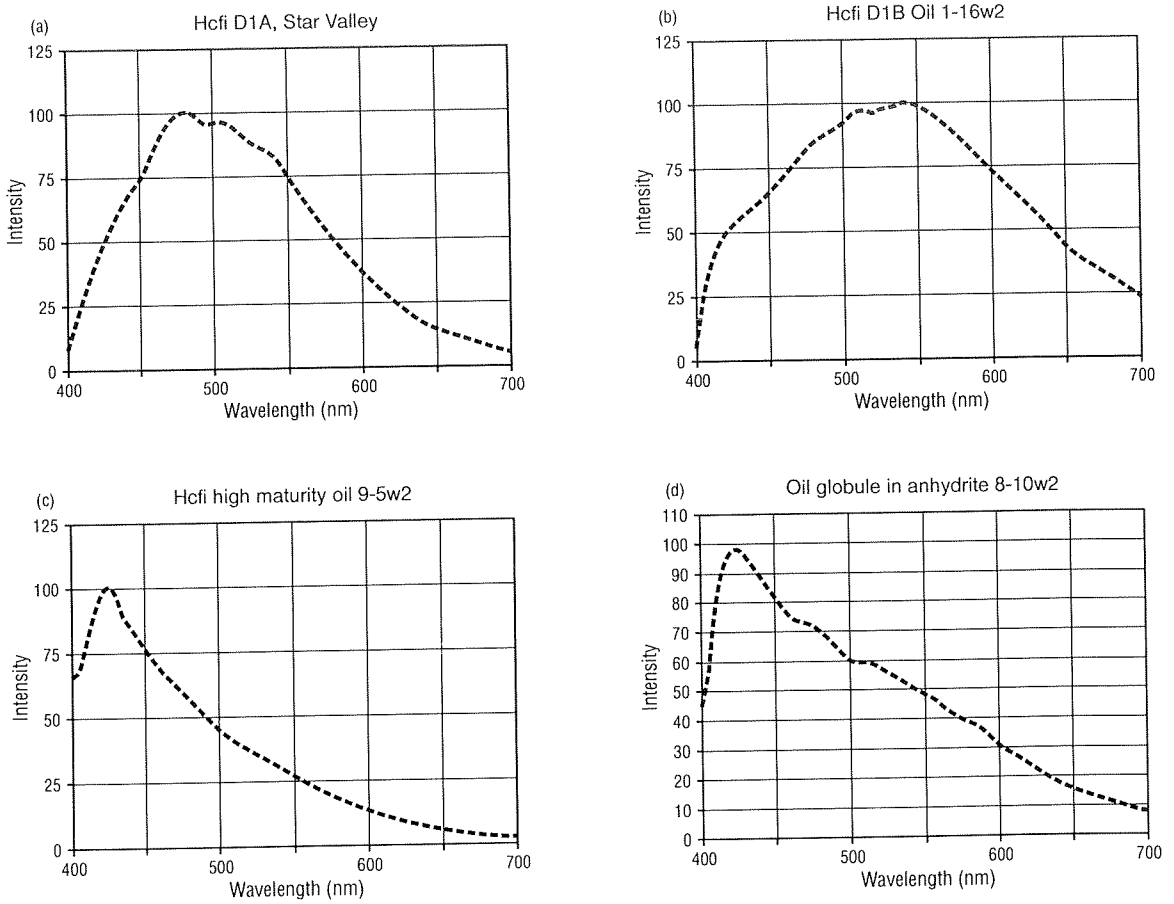

Figure 2. *(a) Example of hcfi spectra (3-19-9-5W2) which matches spectra of Birdbear D1A oil.(b) Example of hcfi spectra (10-15-1-16W2) which matches spectra of Birdbear D1B oils. (c, d) Examples of spectra of very high maturity Bbear oil: (c) is from 3-19-9-5W2, and (d) is from 5-6-8-10W2.*

oils (Lmax = 415–430 nm, $Q \leq 0.10$) suggest that the °API is probably >45.

Example 2: Jeanne D'Arc Basin, Offshore Newfoundland

The fluorescence spectra of hydrocarbon fluid inclusions within quartz overgrowths and cements, annealed fractures and authigenic kaolinite from seven sandstone reservoirs have been compared with crude oils derived from the same reservoir rock in the Jeanne d'Arc Basin (Hebron I-13, Hibernia K-18, Terra Nova K-08 and Fortune G-57, see Fowler and Brooks, 1987; Williamson, et al., 1993). Figure 3a presents examples of fluorescence spectra of a relatively low maturity and a high maturity crude oil, respectively, from sandstone reservoirs at Hibernia K-18 and Hebron I-13. A plot of Lmax and Q versus depth (Fig. 4a, 4b) for several crude oils reflects the general increase in thermal maturity and gravity (from ≈35 to 45 °API; Riecker, 1962; Stasiuk and Snowdon, 1993) of the reservoir crudes with increasing depth.

A distinctly different population of hcfi's are trapped in quartz cements/overgrowths compared with the population associated with annealed fractures (Fig. 3b). The fluorescence properties for the primary (Lmax = 500–530 nm, Q = 0.28–0.67) and secondary (Lmax = 425–475 nm; Q = 0.15–0.26) hcfi within most of the reservoir samples indicate that a relatively low maturity oil (Type A) was probably "in place" during quartz grain overgrowth and quartz cementation, whereas a relatively high maturity oil (Type B) was "in place" during later fracturing and annealing of quartz grains. Similar high maturity Type B oil "inclusions" have also been noted within kaolinite at some locations (e.g., Terra Nova H-99, 3226 m).

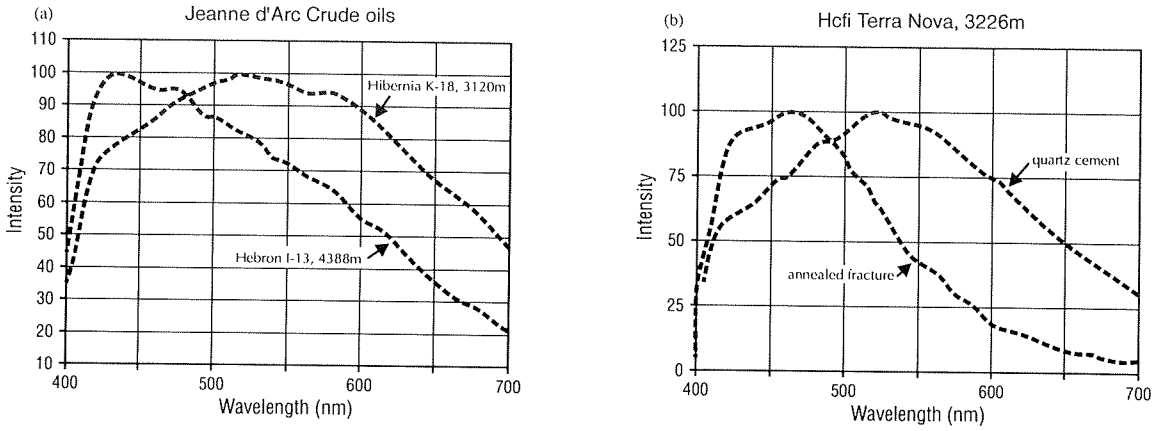

Figure 3. *(a) Examples of fluorescence spectra from relatively low (Hibernia K-18) and high maturity (Hebron I-13) crude oils from Jeanne d'Arc basin reservoirs. (b) Hydrocarbon fluid inclusion spectra of low maturity Type A oils (quartz cements and overgrowths) and high maturity Type B oils (fracture-related, kaolinite "trapped" oils).*

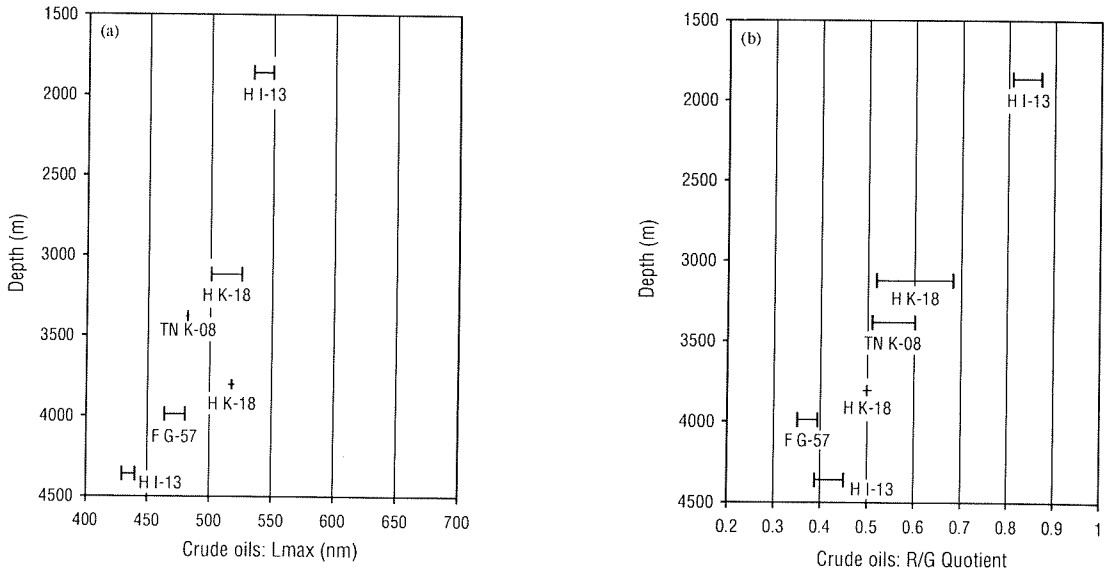

Figure 4. *Depth versus range of Lmax (a) and Q (b) for crude oils, Jeanne d'Arc basin.*

CRUDES AND hcfi: ARE THEY THE SAME OILS?

An initial comparison of the Lmax of hcfi within quartz cements and the Lmax of crude oils from reservoir sandstones suggests a similarity between the 2 oils at some locations: (i) the range of Lmax (535–550 nm) for the crude oil from Hebron I-13 at 1863–1876 m is similar to the Lmax (525 nm) for hcfi within quartz cements at 1895 m depth; (ii) the Lmax range (500–525 nm) of crude oil from Hibernia K-18 at 3120–3130 m depth compares well with Lmax (525–530 nm) for hcfi in quartz cements at 3132 m. Further comparison of the spectra from these two samples, however, reveals that even though the Lmax values are similar, the crude oil contains additional blue region and red region components in its spectra which are not present in the spectra of the quartz cement hcfi. At other locations (e.g., Fortune G-57), a difference in the hydrocarbon fluid inclusion fluorescence spectra (Fig. 5a; Lmax = 425 nm and 500–510 nm) compared with the crude oil fluorescence parameters (Fig. 5b; Lmax = 465–485 nm) is more obvious with the Lmax and spectral distribution for the crude "falling between" the Lmax and spectral distribution of the Type A and Type B oil inclusions.

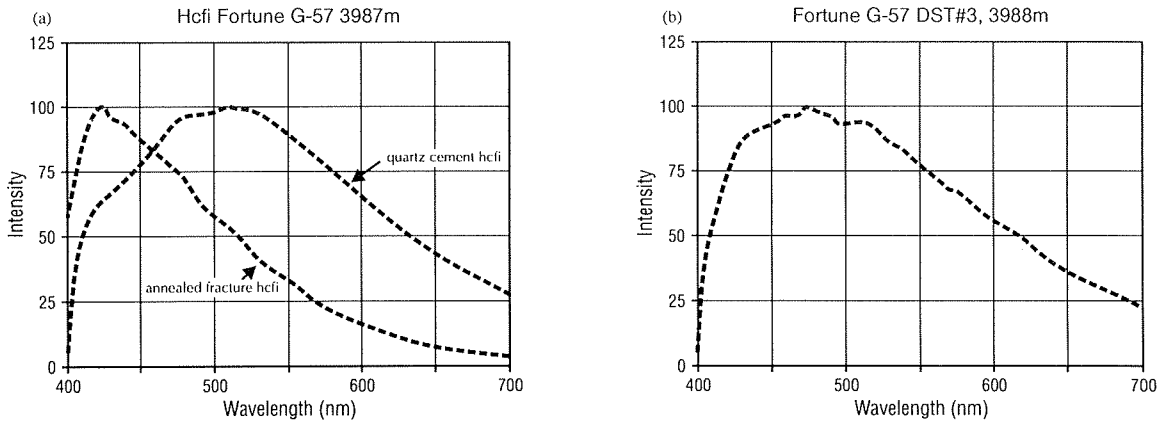

Figure 5. *Spectra of low (quartz cement) and high (annealed fracture) maturity hydrocarbon fluid inclusions (a) and crude oil (b) from Fortune G-57, Jeanne d'Arc basin.*

The discrepancies noted above strongly suggest that the crude oils must represent a mixture of oils of different maturities. The crude oils in the Jeanne d'Arc examples must represent a mixture of low and high maturity oils which are represented by Type A and Type B oils trapped in quartz cements and overgrowths (Type A oil), annealed fractures (Type B) and as "inclusions" in kaolinite (Type B).

ACKNOWLEDGEMENTS

Rick Steedman of PanCanadian Petroleum provided Birdbear core and cutting samples and is an active participant in this project. Hibernia crude oils and core samples were provided by M.G. Fowler, Institute of Sedimentary and Petroleum Geology, Calgary, and M.A. Williamson of the Atlantic Geoscience Centre, Dartmouth.

REFERENCES

Bertrand, P., Pittion, J.-L., and Bertnaud, Ch.
1986: Fluorescence of sedimentary organic matter in relation to its chemical composition. Organic Geochemistry, v. 10, p. 641–647.

Fowler, M.G. and Brooks, P.W.
1987: Organic geochemistry as an aid in the interpretation of the history of oil migration into different reservoirs at the Hibernia K-19 and Ben Nevis I-45 wells, Jeanne d'Arc Basin, offshore Newfoundland. Organic Geochemistry, v. 16, p. 461–485.

Hagemann, H.W. and Hollerbach, A.
1986: The fluorescence behavior of crude oils with respect to their thermal maturation and degradation. Organic Geochemistry, v. 10, p. 473–480.

Khavari-Khorasani, G.
1987: Novel development in fluorescence microscopy of complex organic mixtures: application in petroleum geochemistry. Organic Geochemistry, v. 11, p. 157–168.

Osadetz, K.G., Snowdon, L.R., and Brooks, P.W.
1992: Oil families and their sources in Canadian Williston Basin (southeastern Saskatchewan and southwestern Manitoba). Bulletin of Canadian Petroleum Geology, v. 40, p. 254–273.

Riecker, R.E.
1962: Hydrocarbon fluorescence and migration of petroleum. Bulletin of American Association of Petroleum Geologists, v. 46, p. 60–75.

Stasiuk, L.D. and Snowdon, L.R.
1993: Fluorescence microscopy of hydrocarbon fluid inclusions: correlation with oil chemistry, diagenesis and thermal maturity. *In* Geological Association of Canada, Program with Abstracts, v. 18, p. A99.

Van Gijzel, P.
1981: Applications of the geomicrophotometry of kerogen, solid hydrocarbons and crude oils to petroleum exploration. *In* Organic maturation studies and fossil fuel exploration, J. Brooks (ed.). Academic Press, London, p. 351–377.

Williamson, M.A., DesRoches, K., and King, S.
1993: Overpressures and hydrocarbon generation in the Hibernia-Jeanne d'Arc Basin, offshore Newfoundland. Bulletin of Canadian Petroleum Geology, v. 41, p. 373–388.

MODELS FOR ORIGIN OF PYROBITUMENS WITHIN DEVONIAN STRATA OF ALBERTA AND BRITISH COLUMBIA: THE APPLICATION OF REFLECTED LIGHT MICROSCOPY

L.D. Stasiuk

Geological Survey of Canada, 3303-33rd Street N.W., Calgary, Alberta T2L 2A7

SUMMARY

Preliminary results of organic petrological studies of kerogen and pyrobitumen within the Beaverhill Lake sequence of Alberta and British Columbia, and the Leduc Formation of Alberta (Strachen–Ricinus gas field) are presented. The findings indicate that certain pyrobitumens formed from thermal cracking of graphitizing medium gravity crude oils while other pyrobitumens may be derived from thermal alteration of nongraphitizing, NSO-rich, heavy bitumens and/or indigenous organic matter. Organic-rich intervals in the lower part of immature to marginally mature Beaverhill Lake strata, Drumheller area, contain biofilm-algal "mats"; some display vertical micro-zonation while others are associated with stromatoperoids. It is proposed that with increasing thermal maturation, primary textures in these "mats" are obliterated (overprinted) and the kerogen is transformed into a pyrobitumen-like residue with fine grained mosaic textures (gas zone). Some of the "pyrobitumen" within overmature, dark, stromatoperoid-bearing calcilutites from the Slave Point Formation in northwestern Alberta and northeastern British Columbia may be derived from similar "mats". Pyrobitumens in the Leduc Formation gas reservoirs at Strachen-Risinus were derived from two main sources of organic material, graphitizing (e.g., medium crude oil) and nongraphitizing "petroleum" fractionation products (e.g., NSO-rich, S-rich petroleums). Pyrobitumens derived from the former are characterized by high-reflecting (%Ro) coarse grained flow to domain mosaic textures whereas the latter are characterized by low-reflecting, isotropic to fine grained mosiac textures. Pyrobitumen bireflectance (%Romax - %Romin) and strong deformation textures within the upper Pool A for Leduc reservoirs strongly suggest that anomalous pressures were created during gas generation. Textural evidence also suggests that more than one phase of pyrobitumen formation probably occurred, perhaps reflecting more than one oil charge to the reservoir.

INTRODUCTION

Kerogen, bitumen and pyrobitumen from organic-rich intervals and reservoir rock in the Beaverhill Lake sequence of Alberta and British Columbia and the Leduc Formation of west central Alberta have been examined using incident light microscopy. The long term objective of the study is to understand the origin and conditions of pyrobitumen formation; whether the pyrobitumens been derived from: (i) thermal maturation of primary organic matter and/or; (ii) thermal alteration of petroleum (e.g., cracking to gas). Polished, particulate core samples of kerogen-rich Beaverhill Lake and pyrobitumen-rich Slave Point and Leduc formations were examined using white and fluorescent incident light microscopy. Maximum in oil ($\%Ro_{max}$) and minimum ($\%Ro_{min}$) reflectance in oil were determined for pyrobitumens whereas random reflectance in oil was determined for isotropic bitumens. Textures in the pyrobitumen were classified using semi-coke terminology (White, 1976; Grint and Marsh, 1981).

RESULTS AND DISCUSSION

Beaverhill Lake–Slave Point

Primary organo-sedimentary textures

Immature to marginally mature, kerogen-rich intervals (total organic carbon up to 3.71%; hydrogen index up to 415) within approximately the lower 40 m of the Beaverhill Lake in the Drumheller area contain excellent examples of organic "mats" (filamentous alginite to very thin biofilm coatings) intertwined with mineral grains (e.g., Gerdes et al., 1993). Some of the "mats" are associated with stromatoperoids whereas others display stromatolitic, vertical micro-zonation of organic and inorganic components. The "mats" were probably preserved under a limited suboxic zone

within a shallow water carbonate platform-lagoonal environment. The association of algal mats and stromatoperoids has been previously reported, although not with the same degree of preservation as noted in these Beaverhill Lake samples. Pressure solution alteration and overprinting of primary textures by stylo-cumulate textures is an important diagenetic feature in most of the samples.

Pyrobitumen derived from sedimentary "biofilm-mats"?

Early alteration of amorphous kerogen into a "softened", slightly anisotropic kerogen product has been noted at an abrupt thermal maturity anomaly in the Beaverhill Lake at 16-27-32-24W4 (2431.2 m; %Rovitrinite equivalent near 1.1; Rock Eval: Tmax = 452°C for Type II kerogen). It is proposed that with increasing diagenetic alteration and thermal maturity, the primary textures are completely destroyed (e.g., stylolitization, fracturing, extensive anhydritization etc.) and the "hydrogen-rich" components are transformed into a pyrobitumen residue with fine grained mosaic semi-coke textures.

Pyrobitumens within Slave Point rocks from the deep basin of Alberta and British Columbia (e.g., Yoyo, Shekelie, Clarke Lake) are generally considered to be products of thermally altered oil. Preliminary investigations of lithologies such as dark, stromatoperiod-bearing calcilutites (Cameron, 1969) suggest that some of the pyrobitumen may be derived from primary organic matter such as the "algal-biofilm" mats described from marginally mature Beaverhill Lake from the Drumheller area. The partially, but not severely oxidized "mats" (S-rich?) in the Drumheller samples should transform into a "pyrobitumen-like" residue with a very fine to fine grained mosaic texture (see discussion of nongraphitizing material in a later section). Additional work is underway testing the validity of this hypothesis.

Leduc Formation

Petrographic model for pyrobitumen formation

Pyrobitumens from isolated buildups of the Leduc Formation, Strachen-Risinus gas field, are texturally complex and have a wide range of reflectance values (Fig. 1). The anisotropic pyrobitumen textures are classified according to: (i) the size of individual anisotropic units; and (ii) the "mosaic" geometric pattern formed by the anisotropic units. Pyrobitumen in

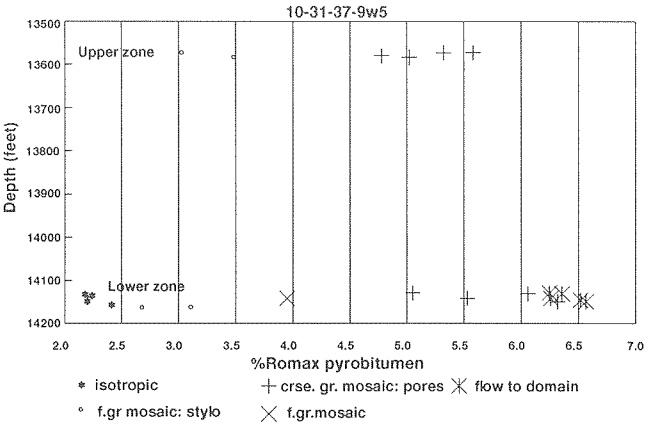

Figure 1. *Distribution of mean $\%Ro_{max}$ for the different types of pyrobitumen textures in Leduc Formation, 10-31-37-9W5.*

the Leduc buildups is divisible into two textural categories: (i) Group A: isotropic (%Ro <2.4) to very fine and fine grained mosaic (<2 μm mosaic units; $\%Ro_{max}$ <3.5) (Fig. 2a); and (ii) Group B: coarser grained mosaics (>5 to 100 μm units; $\%Ro_{max}$ 5 to 7%) with flow and domain mosaic textures (Fig. 2b). Group A pyrobitumens dominate with generally only minor amounts of Group B pyrobitumens.

Graphitizing and nongraphitizing sources

Semi-coke products (~pyrobitumen) formed during technological carbonization (e.g., refining of crude oils) provide a basis for understanding pyrobitumen formation in geological environments. The type of pyrobitumen textures produced is dependent on the chemical composition of the parent material and the reactivity of its components (e.g., Marsh and Cornford, 1976). Organic source materials vulnerable to carbonization fall into two main categories, graphitizing (e.g., petroleum pitch, medium gravity crude) and nongraphitizing (e.g., heteroatomic NSO-rich, low aromaticity bitumen; Patrick et al., 1983). Pyrolysis experiments and refinery residues (e.g., White, 1976) from graphitizing source materials produce textures similar to those in Leduc Formation Group A pyrobitumens whereas nongraphitizing source material produce textures similar to those in Leduc Formation Group B pyrobitumens. This relationship suggests that the two Groups of pyrobitumen textures in the Leduc Formation were derived from two different types of source material.

A graphitizing source (e.g., medium gravity crude) undoubtedly produced the coarse grained semi-coke

pyrobitumens in the lower zone of Pool A at 10-31-37-9W5 (Strachen) and at 10-33-36-10W5 (Ricinus). At 15-2-38-10W5 and in the upper zone of Pool A at 10-31-37-9W5, the pyrobitumens are characterized by significant proportions of both Group A and B pyrobitumen textures indicating both a graphitizing and nongraphitizing source. The source for Group B pyrobitumens was probably a heterocyclic, NSO-rich fraction or a S-rich fraction of a petroleum substance.

S-rich components and fractionation

S-rich bitumens (e.g., >4% S; H/C >1.6) are very unreactive during pyrolysis (Khorasani and Michelson, 1993). As a result they remain mainly isotropic and are relatively low-reflecting. The isotropic, low-reflecting bitumens in the Leduc buildups (Fig. 2a) may thus represent: (i) an NSO-rich (asphaltene) fractionation product produced by gas deasphalting during the initial stage of oil cracking (e.g., Tissot and Welte, 1984); (ii) a S-rich fractionation product; or (iii) a later charge of S-rich heavy oil. The former is supported by isotropic "incompatible" bitumen trapped as "islands" between coalesced mesophase in the Leduc. The later is supported by massive, isotropic bitumen infilling large voids within globular, highly anisotropic pyrobitumens to infillings and coatings of brecciated, gas-bubble deformed, anisotropic pyrobitumens.

Medium crude oil + heat ► mesophase + gas ► gas + pyrobitumen

During carbonization of materials such as crude oils, a "plastic" state molecular transformation results when large planar aromatic molecules align into parallel "sheets" and form anisotropic, spherical liquid crystals called *mesophase*. With increasing temperature the liquid crystals grow in size and ultimately coalesce to form semi-coke (≈pyrobitumen). In addition to the direct control of the starting material on pyrobitumen textures, other factors such as the presence of solids within the system and physical disturbances produced during carbonization (e.g., convection currents from gas evolution) also affect pyrobitumen textures.

Fine and coarse deformed lamellar pyrobitumen textures (Fig. 2c) from the lower zone of Pool A at 10-31-37-9W5 and at 10-33-36-10W5 are identical to textures produced during delayed (gas) coking of medium crude oils (see White, 1976). The deformation textures formed during the delayed coking process in refineries and those encountered in pyrobitumens in some parts of the Leduc reservoirs at Strachen and Ricinus resulted from the interaction between flows of liquid and evolved gas. Such oriented and fine lamellar, plastic deformation microstructures result from the nucleation, growth and percolation of gas bubbles within the mesophase (White, 1976).

Overpressuring during cracking of oil?

A plot of $\%Ro_{max}$ versus $\%Ro_{min}$ for the coarsest grained mosaic pyrobitumen in the Leduc Formation, Strachen and Ricinus, defines two clusters of data (Fig. 3). The two groups are particularly well defined for the upper and lower zones of Pool A at 10-31-37-9W5 (Fig. 3). The upper zone of Pool A has significantly higher bireflectance (bireflectance = $\%Ro_{max}$ - $\%Ro_{min}$) than the lower zone of Pool A (Fig. 3). The former also contains pyrobitumen with intense deformation textures.

The difference in the pyrobitumen bireflectance for upper Pool A at 10-31-37-9W5 and the reservoir at 10-33-36-10W5, compared with the bireflectance for lower Pool A at 10-31-37-9W5 and the reservoir at 15-2-38-10W5, is probably an indication of a pressure (and possibly temperature) difference during pyrobitumen formation, with higher pressures resulting in the highest $\%Ro_{max}$ and greatest bireflectance (Khorasani and Michelson, 1993).

Immiscibility during pyrobitumen formation

Evidence for immiscible flow during pyrobitumen formation is rather compelling. The persistent thin coatings of pyrobitumen with anisotropic lamellae oriented perpendicular to vugs and fracture walls (Fig. 2d) may have formed as a result of polarized alignment of hydrophobic and hydrophilic molecules on the condensed aromatic systems (mesophase). Gize (1986) suggests that these textures form when mesophase is in contact with an aqueous solution, becoming ordered perpendicular to the organic-aqueous contact.

REFERENCES

Cameron, E.M.
1969: Regional geochemical study of the Slave point carbonates. Canadian Journal of Earth Sciences, v. 6, p. 247–268.

Gize, A.P.
1986: The development of a thermal mesophase in a bitumen from high temperature ore deposits. *In* Proceedings of the Denver Region Exploration Geologists Society Symposium, Organics and Ore Deposits, W.E. Dean (ed.), p. 137–150.

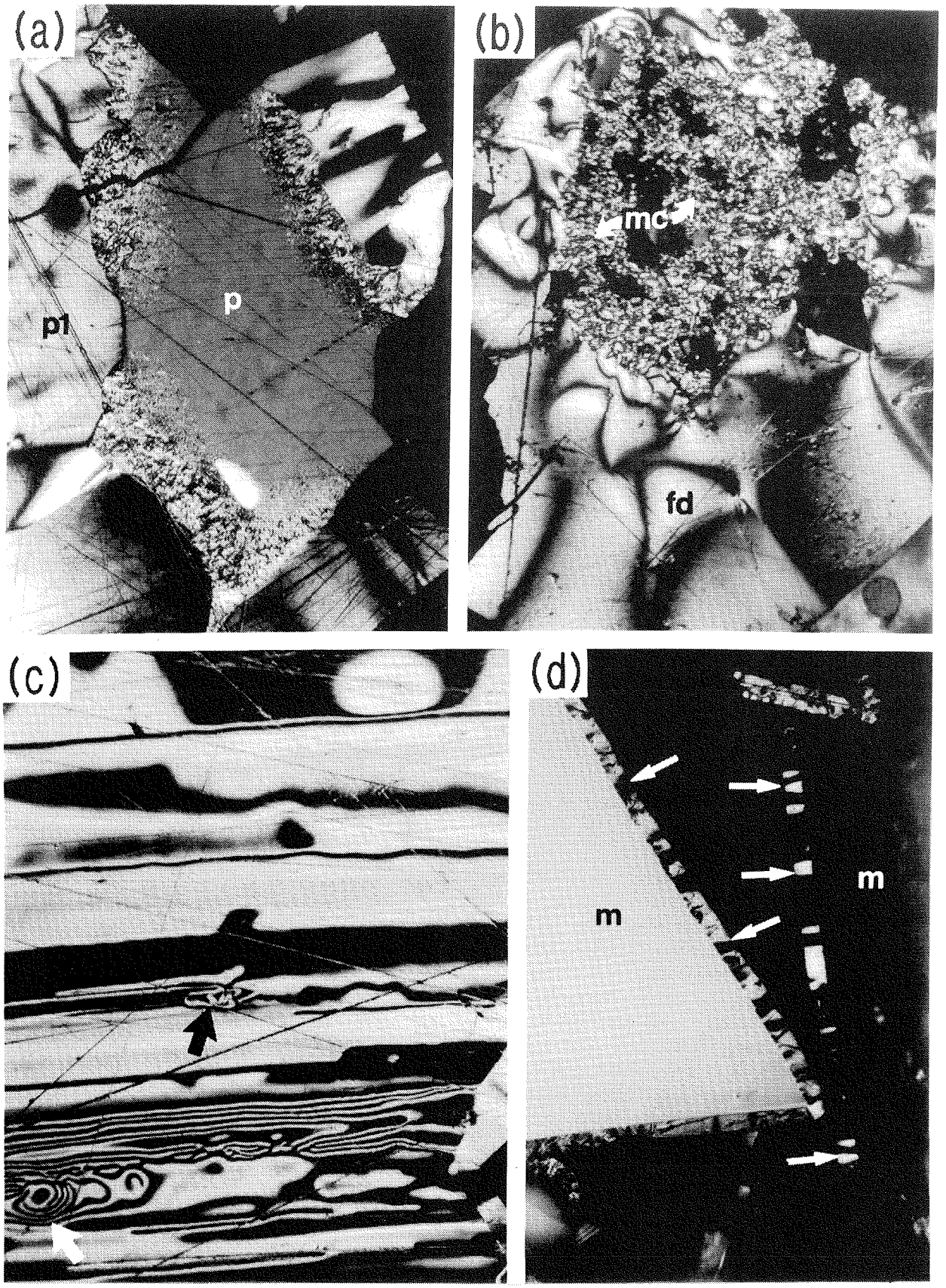
(a)
p
p1
(b)
mc
fd
(c)
(d)
m
m

Figure 2. Photomicrographs of pyrobitumens from Leduc Formation, Strachen-Ricinus gas field.; oil immersion objective, cross-polars; scale 3.2 cm = 50 μm.

a. Late stage (second oil charge? fractionation product?), isotropic to fine grained mosaic pyrobitumen (p; NSO-rich ?) coating an earlier, crude oil-derived pyrobitumen (p1).

b. Anisotropic medium to coarse grained mosaic (mc) and flow domain (fd) pyrobitumen.

c. Highly deformed lamellar pyrobitumen texture with gas bubble collapse features (indicated by arrows).

d. "Striped" coarse flow mosaic pyrobitumen (arrows) with anisotropic units perpendicular to mineral face (m).

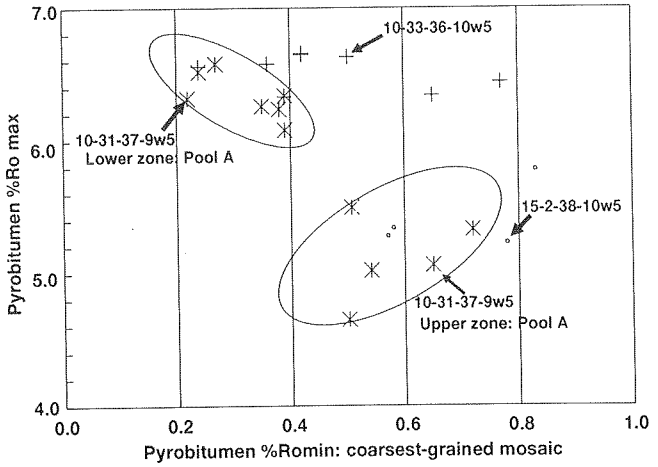

***Figure 3.** Plot of $\%Ro_{max}$ versus $\%Ro_{min}$ for the most coarse grained mosaic pyrobitumens in Leduc Formation, Strachen–Ricinus. The data for the upper zone of Pool A at 10-31-37-9W5 and parts of 10-33-36-10W5 suggest formation under anomalous pressure.*

Gerdes, G., Claes, M., Dunajtschik-Piewak, K, Riege, H., Krumbein, W.E., and Reineck, H.-E.
1993: Contribution of microbial mats to sedimentary surface structures. Facies, v. 29, p. 61–74.

Grint, A. and Marsh, H.
1981: Carbonization of coal blends: mesophase formation and coke properties. Fuel, v. 60, p. 1115–1120.

Khorasani, G.K. and Michelson, J.K.
1993: The thermal evolution of solid bitumens, bitumen reflectance and kinetic modeling of reflectance: application to petroleum and ore prospecting. Energy Sources, v. 15, p. 181–204.

Marsh, H. and Cornford, C.
1976: Mesophase: the precursor to graphitizable carbon. *In* Petroleum derived carbons, American Chemical Society, p. 266–280.

Patrick, J.W., Reynolds, M.J., and Walker, A.
1983: Carbonization of coal-tar pitches: effect of rank of parent coal. Fuel, v. 62, p. 129–130.

Tissot B.P. and Welte D.H.
1984: Petroleum formation and occurrence. Springer-Verlag, Berlin, 699 p.

White, J.L.
1976: Mesophase mechanisms in the formation of the microstructure. *In* Petroleum derived carbons, American Chemical Society p. 282–314.

IMAGE ANALYSIS IN THE STUDY OF HYDROCARBON SOURCE ROCKS

L.D. Stasiuk and K.C. Pratt

Geological Survey of Canada, 3303-33rd Street N.W., Calgary, Alberta T2L 2A7

INTRODUCTION

An automated, image analysis system is being used to generate composite and mosaic digital micrographs of microscopic images of hydrocarbon source rocks in white and fluorescent reflected light. These images are used to supplement the study of: (i) kerogen networks, (ii) primary and secondary inorganic-organic textural relationships and; (iii) the vertical distribution of alginite macerals (phytoplankton-derived organic matter). The system (see Pratt, 1993) provides a microscopic mapping tool at a level of characterization essential for the study of source rock textural features, maceral distribution and kerogen networks in relation to paleoenvironment and hydrocarbon migration networks. The image analysis system coupled with an automatic scanning stage allows for images to be captured along a vertical or horizontal traverse (e.g., 500 μm x 16 cm strip perpendicular to bedding). Primary textural features (e.g., algal mat brecciation, pinnacles, crenulation) in organic-rich laminites for example, are easier to identify and thus interpret upon examination of mosaic/composite images. Such features are commonly very difficult to recognize following normal microscopic examination procedures.

Reflected light microscopy coupled with the image analysis system allows for unique data acquisition where by thousands of microscopic images can be composed into a mosaic, highlighting, otherwise difficult to characterize, organic-inorganic micro-fabrics in fine grained sedimentary rocks. Of particular interest is the arrangement of kerogen networks in relation to the host mineral matrix; this is one of several important factors controlling hydrocarbon explusion from source rocks (e.g., Bertrand et al., 1987). One of the long term objectives of studying the spatial arrangement of organic and mineral matter in source rocks it to determine whether the hydrocarbons were expelled from the source rock system as part of the kerogen network (diffusion), through a permeable system more related to the mineral network (i.e., fractures, porosity) or as a combination of both. The degree of lateral and vertical continuity or discontinuity of a kerogen network has been proposed as having a significant impact on the efficiency of primary migration (Stainforth and Reinders, 1990; Belin, 1992). A mosaic image of an inorganic-organic migration network from the Middle Devonian, Winnipegosis Formation, Saskatchewan are presented in this summary.

Organic-inorganic textures and the distribution of alginites in a source rock provide information relating to the paleodepositional and paleoecological conditions. It would clearly be an asset to the geologist knowing whether a set of organic-rich laminites resulted from benthic mat growth within a shallow photic zone (e.g., Ordovician Yeoman Formation kukersites, Stasiuk et al., 1993), periodic algal bloom episodes or simply from normal productivity (e.g., Chow et al., in prep.). An image analysis method using polished core sections to construct vertical columns showing vertical variations in size and density of oil-prone algal bodies (alginites and acritarchs) has been developed. The method also quantifies the relative proportions of fluorescing components. Image analysis combined with traditional organic petrology, sedimentology and stratigraphy holds tremendous potential for enhancing the interpretation of source rock paleoenvironments. Examples of primary textures and the vertical distribution of oil-prone alginites from two source rock intervals (Upper Devonian, Duvernay Formation, Alberta and Middle Devonian, Lower Keg River Formation, La Crete Basin, Alberta) are used to illustrate the potential of using image analysis for supporting paleoenvironmental studies of source rocks.

EXAMPLES OF COMPOSITE MICROSCOPIC IMAGES OF SOURCE ROCKS

Organic-inorganic networks

Evidence for hydrocarbon migration through a stylocumulate (inorganic-organic) network in the Winnipegosis Formation of southern Saskatchewan has been captured in a mosaic image, perpendicular to bedding (Fig. 1). The distribution and association of organo-cumulates with residual migra-bitumen, hydrocarbon fluid inclusions and blue-shifted

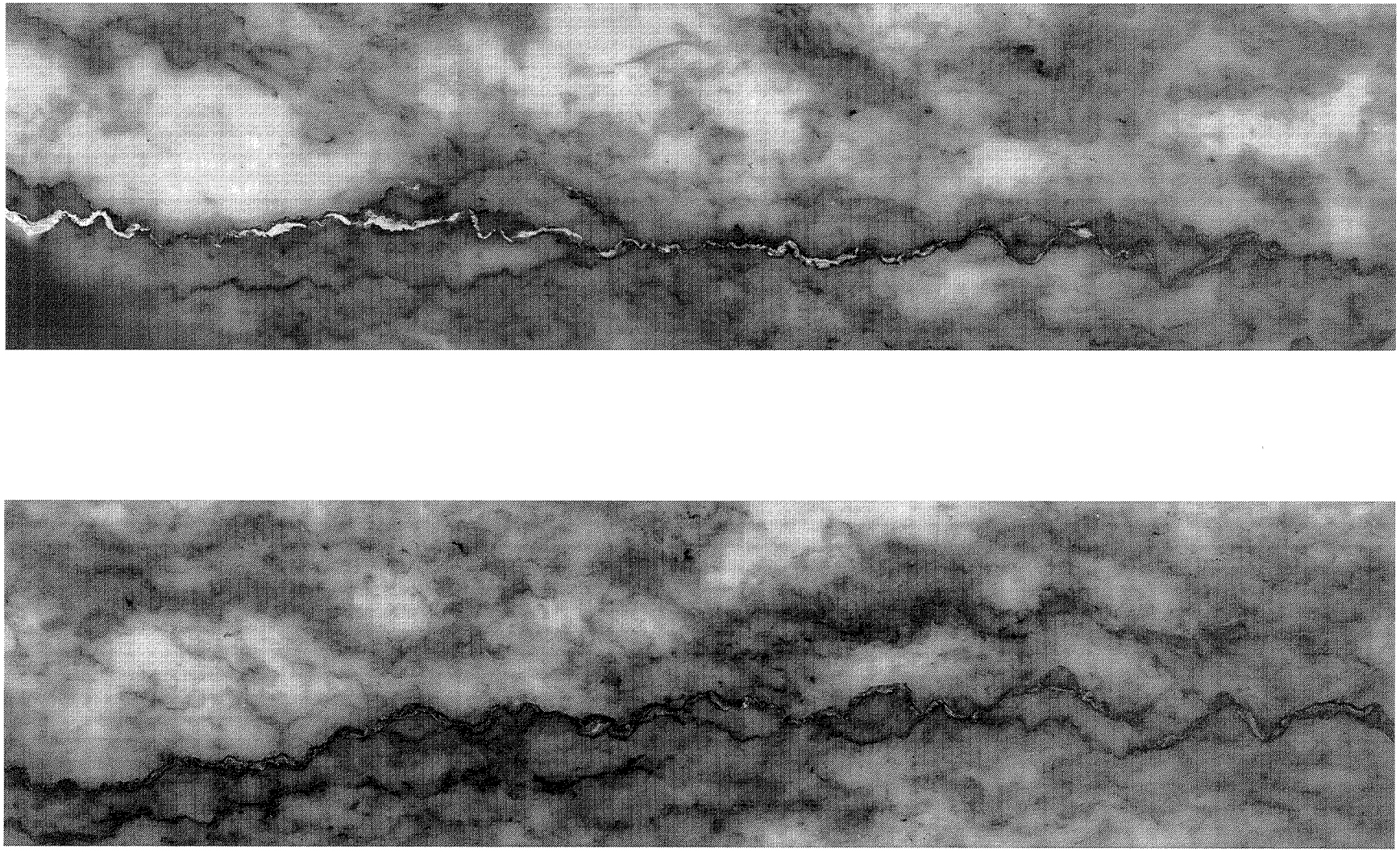

Figure 1. *Inorganic-organic network with stylocumulate textural organization. Mosaic image of organo-cumulate hosting migra-bitumen, blue-shifted alginite and hydrocarbon fluid inclusion (not visible at this scale) in the Winnipegosis Formation, Saskatchewan (10-20-6-13W2).*

Prasinophyte alginite (oil-absorbed) clearly illustrates the importance of stylocumulates (organic network) in certain aspects of hydrocarbon migration.

Primary textures

During petrographic examination of the upper Keg River Formation laminites from the La Crete Basin (14-3-93-3W5, 1256.0 m) it was noted that particular laminations, probably represent, when viewed as a composite, algal mat laminations with significant hydrocarbon source rock potential. A mosaic image of the potential stromatolites was digitized to scrutinize the microtextural arrangement of the organic-inorganic network. The composite digital image strongly suggests that the laminations and textures are derived from algal mats (Fig. 2).

VERTICAL DISTRIBUTION OF ALGINITE MACERALS

The vertical distribution of alginites (inc. acritarchs) in polished blocks of organic-rich laminites from the Duvernay Formation, Redwater, Alberta and the Keg River Formation, La Crete Basin, Alberta, was assessed in terms of total number of alginite bodies ("density"), average size of each body (area) and total area of all alginite bodies (Fig. 3). These profiles have been used to supplement petrologic, sedimentologic and stratigraphic data from the two formations to argue that the Duvernay source rocks, Redwater, Alberta, accumulated mainly as the result of normal phytoplankton productivity (i.e., preservation controlled) whereas the Keg River laminites accumulated mainly as the result of high productivity (algal blooms; Chow et al., in press).

Duvernay Formation

Within the two finely laminated, lowermost organic-rich zones of the Duvernary laminite, the alginite density, and to a lesser degree the total alginite area, increase upward to a maxima/peak, then decrease to a minimum to form two "cycles" (Fig. 3a, c). These alginite-rick zones are overlain by an interval with a marked decrease in alginite density through a central carbonate-rich zone and finally through an upper

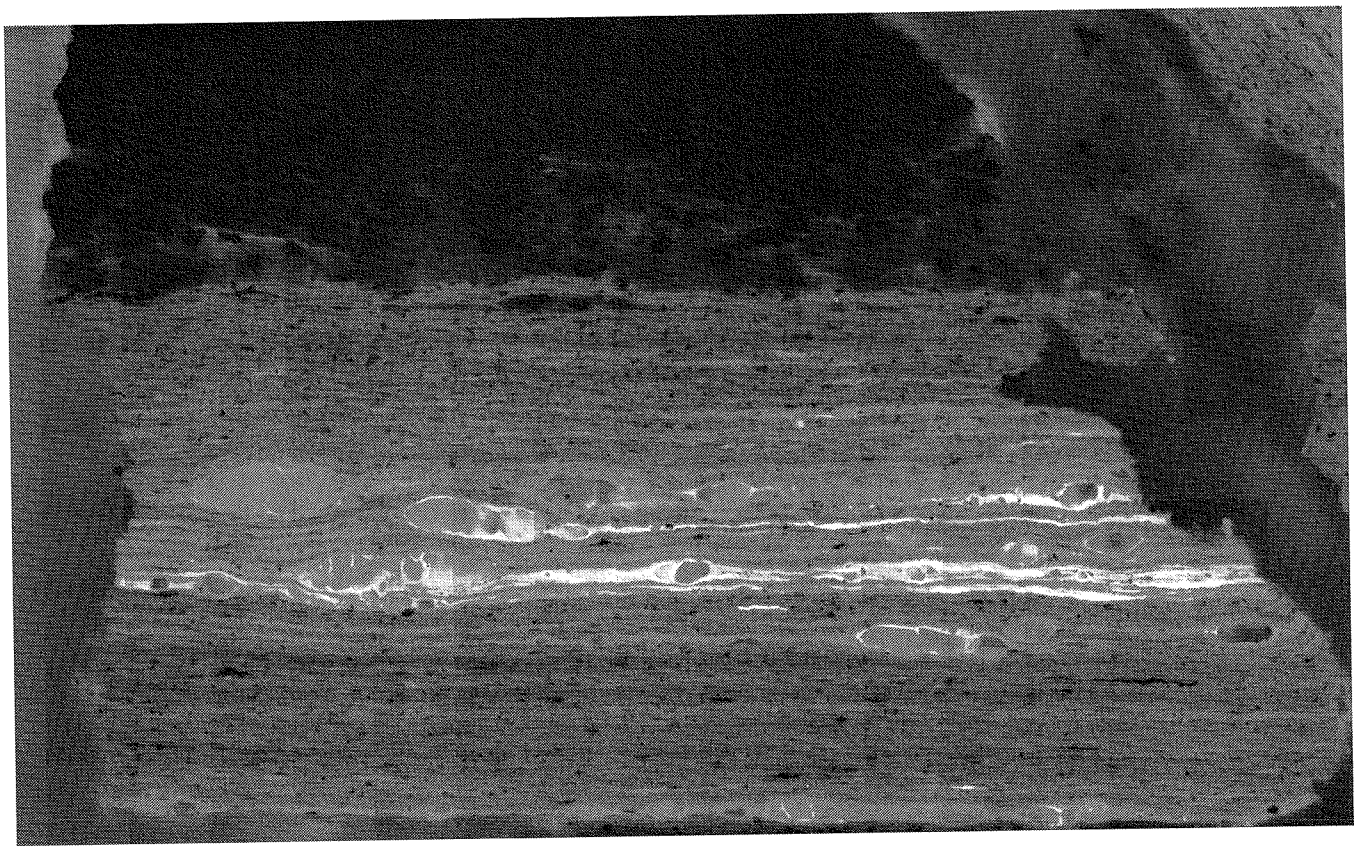

Figure 2. *Mosaic image of primary, stromatolite-algal mat textures from the upper Keg River Formation laminites, La Crete Basin (14-3-93-3W5, 1256.0 m).*

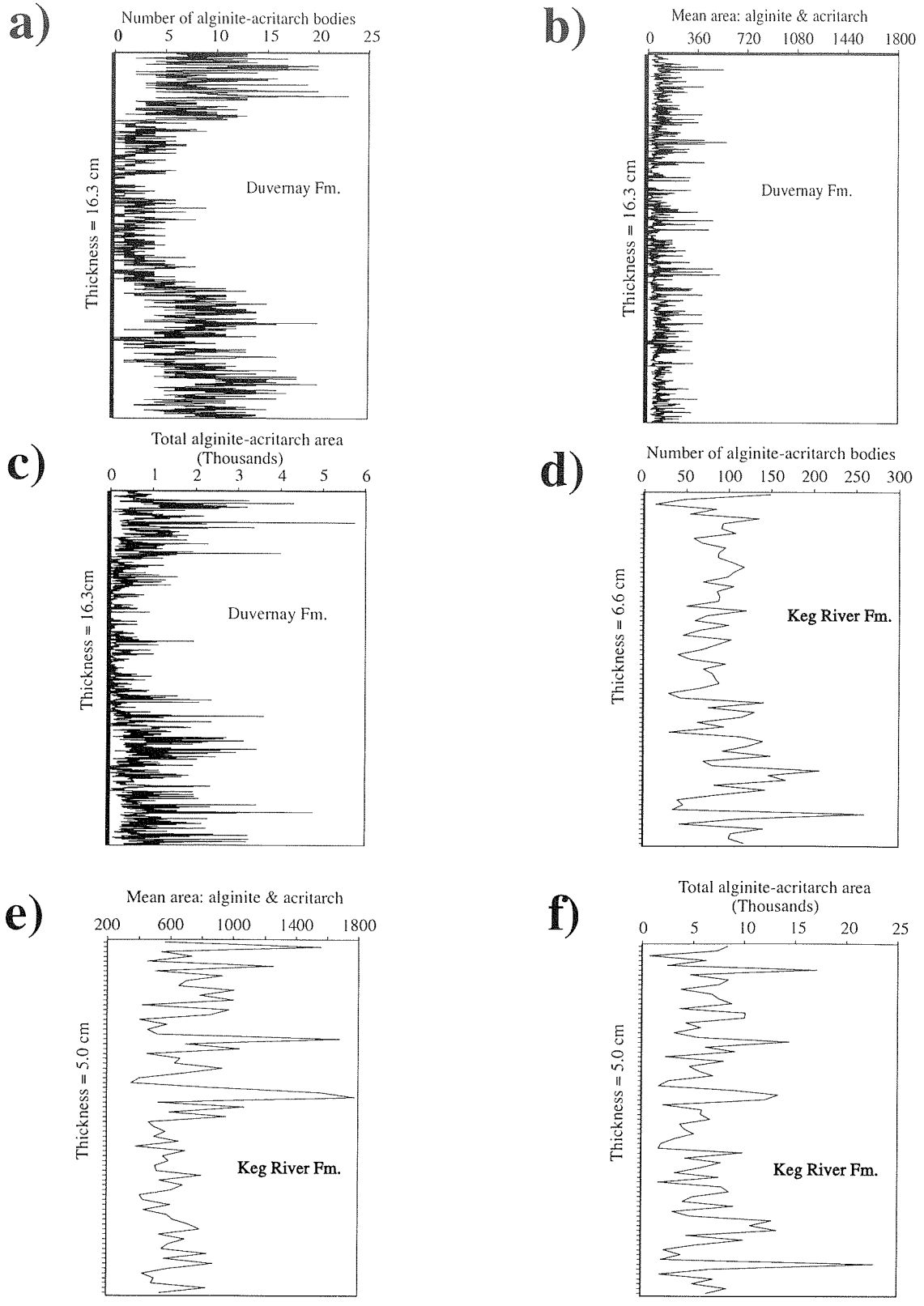

Figure 3. *Semi-quantitative assessment of alginite-acritarch macerals in organic-rich laminites of the Upper Devonian Duvernay Formation (10-28-57-21W4, 1203.85 m), Redwater Reef Complex (Figs. 3a-c), and the Middle Devonian, lower Keg River Formation (Fig. 3d-f; 3-30-109-3W5, 704.5 m), La Crete Basin.*

organic-rich zone where the number of alginites progressively increases upward. This harmonic, vertical distribution in the Duvernay laminites is probably a reflection of increasing and decreasing reefal sediment supply to the off-reef, anoxic depositional basin (J.C. Wendte, pers. comm.). The average area of the alginite bodies is quite consistent throught the organic-rich and the organic-lean zones ranging from approximately 50–500 arbitrary units with a mean on the order of 100 (Fig. 3b).

Keg River Formation

The vertical distribution of alginite bodies within a laminite of the lower Keg River Formation (3-30-109-3W5, 704.32–704.48 m depth) is illustrated in Figure 3d-f. Unlike the Duvernay laminite, the alginite body density and total alginite area plots for the Keg River does not show any systematic increasing and decreasing vertical pattern (Fig. 3d, f). The average area for the alginite bodies (mainly Prasinophytes) ranges from just under 400 to near 1800 arbitrary units (Fig. 3e). The maximum and minimum ends of the range are approximately 8x greater than the average area for the Duvernay alginite bodies.

REFERENCES

Bertrand, P., Martinez, L., and Pradier, B.
1987: Petrologic study of primary migration by hydrous pyrolysis. *In* Thermal modeling in sedimentary basin, B. Doligez (ed.). IFP Research conferences in exploration, Editions Technip, Paris, p. 633–647.

Belin, S.
1992: Application of backscattered electron imaging to the study of source rocks microtextures. Organic Geochemistry, v. 18, p. 333–346.

Chow, N., Wendte, J.C., and Stasiuk, L.D.
in prep.: Comparison of two organic-rich facies in the Devonian of the Western Canada Sedimentary Basin. Submitted to the Bulletin of Canadian Petroleum Geology.

Pratt, K.C.
1993: The use of composite and mosaic imaging of polished surfaces to enhance petrographic analysis of coal by image analysis. Organic Geochemistry, v. 20, p. 759–768.

Stainforth, J.G. and Reinders, J.E.A.
1990: Primary migration of hydrocarbon by diffusion through organic matter networks, and its effect on oil and gas generation. Organic Geochemistry, v. 16, p. 61–74.

Stasiuk, L.D., Kybett, B.D., and Bend, S.L.
1993: Reflected light microscopy and micro-FTIR of Upper Ordovician *G. prisca* alginite in relation to paleoenvironment and petroleum generation. Organic Geochemistry, v. 20, p. 707–719.

PRELIMINARY 2-D MODELS OF HYDROCARBON MIGRATION IN THE JEANNE D'ARC AND SABLE BASINS, OFFSHORE EASTERN CANADA

M.A. Williamson, Z. Huang, and P.N. Moir

Atlantic Geoscience Centre, P.O. Box 1006, Dartmouth Nova Scotia B2Y 4A2

J. Liu, C.O. Leonard, and J.E. Leonard

Platte River Associates Inc.

BACKGROUND

Hydrocarbons are distributed in sedimentary basins in response to unique combinations of physical, chemical, geologic/tectonic processes. Semiquantitative to quantitative reconstructions of such processes through *Basin Modelling* increases our understanding of these petroleum systems. This provides a powerful petroleum exploration method which finds maximum utility when used with other tools, such as, 3-D seismic interpretation. In the 1990s the levels of sophistication of basin modelling ranges from relatively simple, single point (often a well), 1-D reconstructions of burial, thermal and maturity histories to fully integrated, dynamic, multiphase migration models in 2-D. *Basin Modelling* in support of the Hydrocarbon Charge Modelling Project (HCMP) has evolved from 1-D point reconstructions to map based reconstructions involving numerous 1-D locations (based on wells and pseudo-wells) to our current efforts that reconstruct multiphase fluid generation and flow in 2-D. Each level of sophistication has provided insight into specific inadequacies in our understanding of some key subsurface geological parameter assumptions. This has in several instances driven our efforts to better constrain the subsurface parameters (Huang and Williamson, 1994; Williamson, this volume) and served to define the principal petroleum defining events of the basins of interest to HCMP.

The basin modelling component of the HCMP currently uses the BasinMod™ 2-D software of Platte River Associates, Denver, Colorado. Preliminary 2-D, 3 phase migration solutions are presented for test lines in both the Jeanne d'Arc and Sable basins. (Space limitations of this abstract limits our discussion to the Jeanne d'Arc Basin test line.)

MODELLING PROCEDURES

Only an overview of the 2-D modelling process can be presented here, however the complexity of the modelling process and calculation procedures employed by 2-D BasinMod™ should not be understated. Four basic steps (Fig. 1) are involved. **Step 1** requires the construction of a representative cross-section. This is best obtained from a suitable seismic line but can be a line drawing of an interpreted cross-section. This represents the *geological* framework which will be decompacted back through time and within which subsurface fluids will be generated and moved. An important part of this step is ensuring that the general geological framework includes sufficient information regarding lithology types (e.g., source rocks, reservoirs, seals, etc., including such parameters as permeability, porosity, kerogen type, etc.) that as far as possible are based on actual well information and measurements from the area. **Step 2** involves model

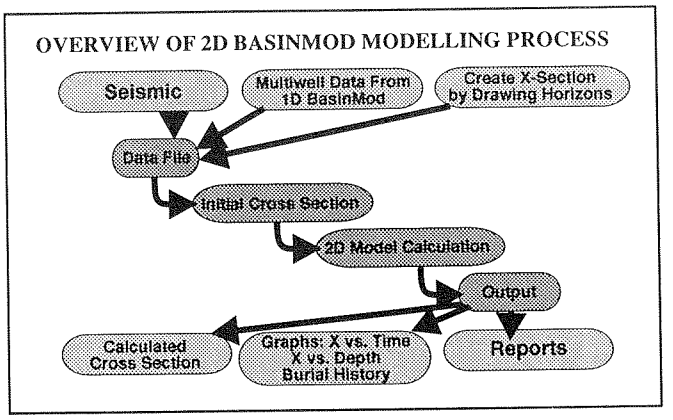

***Figure 1.** Overview of 2-D BasinMod™ modelling process.*

construction which defines model horizons, events and boundaries together with fault definition, cell information and general parameter setting. **Step 3** proceeds with the model calculations (Fig. 2). **Step 4** provides results, either as reports or graphic output.

The principal feature of the approach is that it is dynamic. That is, most of the parameters or physical/chemical variables are intrinsically related, which requires that a model be comprehensive and include as many physical/chemical properties in the calculation as possible. The cross examination of these properties will lead the modelling results toward a more realistic conclusion. The framework for the dynamic thermal, hydrocarbon generation and migration modelling is provided by the fluid flow/compaction calculations which combine the mass conservation equation, state equations of mass, and the equation of transportation. This model shows how the amount, rate and direction of fluid flow, and the porosity, permeability, fluid density, viscosity etc. vary with time.

JEANNE D'ARC TEST LINE

Figures 3 and 4 are the Jeanne d'Arc test line (from interpreted seismic) and equivalent model cross-section. The test line is from an area just north of the Terra Nova oil field. Also shown are the principal source rock, seal and reservoir intervals and present day distribution of pooled hydrocarbons and major structural features (faults). Figure 3, together with lithology information from the 3 wells shown, formed the basis for the model cross-section shown in Figure 4. Note that the structural complexity of the model section has been reduced due

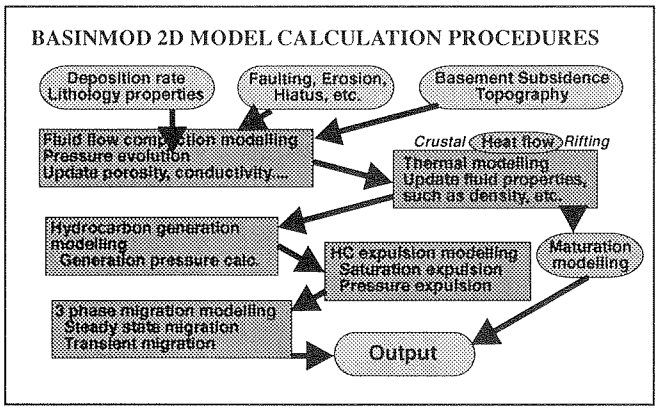

Figure 2. *Model calculation procedures.*

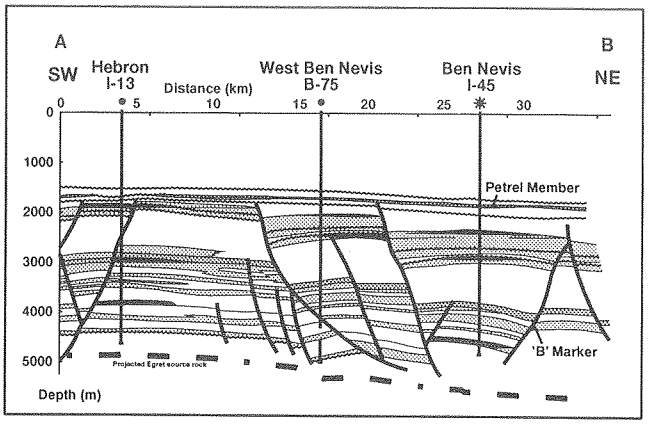

Figure 3. *Cross-section interpretation (from seismic) of the Hebron to Ben Nevis area. Shaded lithologies = porous/sandy units; non shaded = shale/silts.*

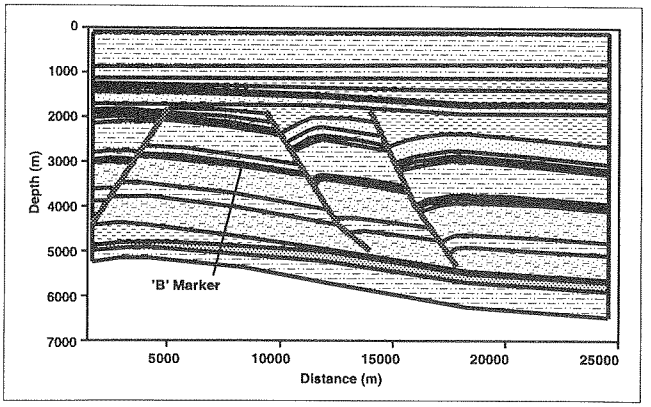

Figure 4. *Framework cross-section based on line interpretation (Fig. 3).*

to computational limitations. This particular line is being modelled (Williamson et al., this volume) as part of the effort to constrain pool filling histories of the Hebron accumulation and in particular, the post filling biodegradation history of the accumulation.

THREE PHASE MIGRATION

The modelling process employed in the HCMP is iterative, and so the results shown here represent a snap-shot, or the current best model, the only certainty about which is that it will change as a result of either better constraints becoming available for some of the

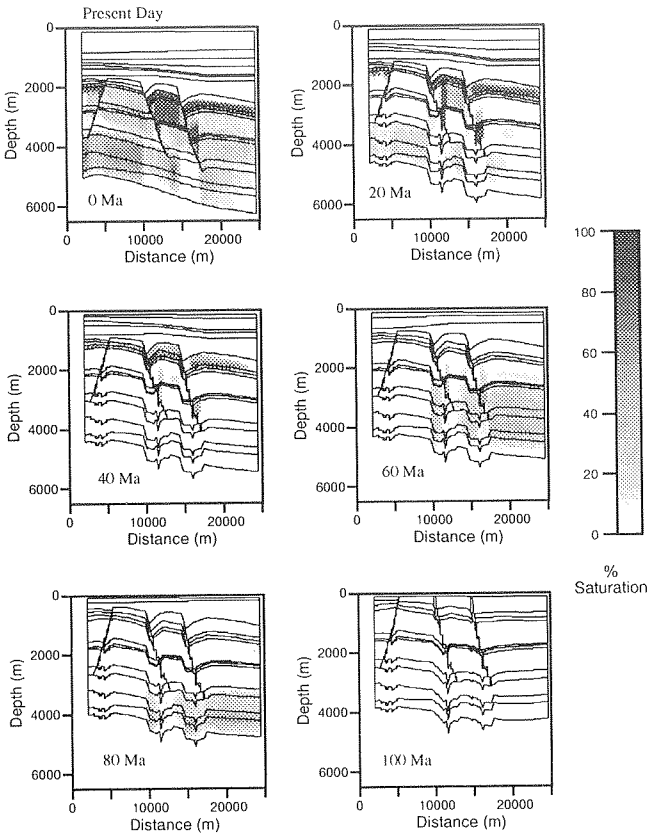

Figure 5. *Oil saturation throughout modelled cross-section from 100 Ma to present day.*

assumptions (i.e., results of other projects in progress; Williamson, this volume) or as a result of further parameter sensitivity analyses. Figure 5 shows oil saturation throughout the model cross-section at 20 Ma time steps, from 100 Ma to present day. Other reconstructions from this particular model run show gas saturation, excess fluid pressures, and levels of organic maturity (i.e., vitrinite reflectance), space limitations however preclude their inclusion in this abstract. The 2-D model shown in Figure 5 suggests that oil generation began in the deeper part of the basin around 80 Ma. This intensified around 60 Ma with apparent widespread vertical migration throughout the rock column, but also with some degree of focusing along the major fault conduits. By 40 Ma the source interval underlying the deeper part of the cross-section was no longer generating hydrocarbons and vertical migration was more or less complete with pooling of oil seen beneath a regional shale seal. Noticeable at this time step is a degree of updip lateral migration beneath the shale with oil pooling at the Hebron location (the regional high for this cross-section) as early as 40 Ma. Renewed subsidence at 40 Ma began a second phase of generation from the source interval, not only from the deeper part of the section but also from source rock underlying the shallower (Hebron block) part of the section. The faults again appear to provide important conduits to oil migration at this time. At the present day, generation and vertical migration is in full stream from beneath the Hebron block and is contributing oil vertically through the rock column and through the main Hebron fault. Clearly, the oil saturation distribution for the present day indicates an over supply (i.e., as compared to what has actually been found). This is a parameter adjustment problem and/or a boundary condition effect. This preliminary model is reasonably able to reconstruct the present day distribution of oil throughout the modelled section and provides the basis for further examination of the pool filling history of the region.

The oil saturation history of the test cross-section is a relatively simple result of an extremely complex, dynamic series of formulations and assumptions, discussion on which is beyond the scope of this paper. Several activities reported elsewhere in this volume address some of the parameter assumptions and in the long term will increase confidence in the veracity of our models. By way of example, Figure 5 clearly indicates two important controls on oil migration within the cross-section framework. These are: lateral and vertical permeability properties of the rock matrix, and, the fluid transmissive properties of the major fault conduits. The activities reported by Huang et al., Shimeld et al., Katsube et al., and Desroches et al. (this volume) represent efforts to better understand and represent these controls.

MODELLING EXPECTATIONS

The HCMP uses a basin modelling approach to derive clues as to how source, reservoir and seal systems have dynamically interacted throughout a basin's history. Much of the HCMP activity centres around the provision of key subsurface parameter information required for accurate basin models and increasing our knowledge base on specific basin processes important to the generation, expulsion, migration and entrapment of hydrocarbons. In performing *basin modelling* in this way it is important to have realistic expectations as to what a basin modelling approach provides. There are many misconceptions regarding the utility of basin modelling as an exploration tool, some of these are presented in Table 1 together with a listing of what appropriate expectations might be.

Table 1

Expectations from Basin Modelling

EXPECT TO:	DON'T EXPECT TO/THAT:
Examine scenarios – what if?	Derive unique solutions .... Drill here!!
Use as a ranking tool	End up with less questions
Continually improve input data	Use default values
Develop understanding of data and assumption weakness	Use the same approach for basins, plays, prospects
Examine drilling failures as well as success	Predicted = observed = unique solution
Use the best available data	Modelled volumes = discovered volumes
Spend lots of time to derive the best data	Use basin modelling on its own
Be provided with clues to combine with other information	Axiomitizations are correct
Place model's results into context	Perform predictions only ... Post mortems important
Simplify incredibly complex dynamics	The more sophisticated models are the most accurate
Recognize important gaps in data and knowledge	Ever understand all the complexities
Use as predictive tool in new basins with little data	
Re-evaluate appropriateness of scale	
Learn about basin processes	

HYDROCHEMICAL AND HYDROGEOLOGICAL INVESTIGATION OF A POTENTIAL COALBED METHANE AREA, SOUTHEASTERN BRITISH COLUMBIA

S.M. Harrison

SMH Environment
202, 2307-17A Street S.W., Calgary, Alberta T2T 4S3

H.J. Abercrombie

Geological Survey of Canada, 3303-33rd Street N.W., Calgary, Alberta T2L 2A7

J.F. Barker, D. Rudolph, and R. Aravena

Waterloo Centre for Groundwater Research
University of Waterloo, Waterloo, Ontario N2L 3G1

INTRODUCTION

The Institute of Sedimentary and Petroleum Geology of the Geological Survey of Canada, the University of Waterloo, and Norcen Energy Resources Limited have undertaken a program to investigate the environmental geochemistry and hydrogeology of coalbed methane (CBM) exploration and development, with particular reference to CBM resources in southeastern British Columbia. Interest in coalbed methane in the Western Canada Sedimentary Basin has increased and the coals of southeastern British Columbia are among the coals being evaluated for CBM resources in Western Canada.

Production of water during CBM recovery is an important issue in assessing the environmental impact of CBM development. The principle risks to the hydrogeologic regime include: (1) the hydrodynamic effects of depressuring the coalbed and adjacent strata, and (2) deterioration of surface water quality.

The objective of the current research is to: (1) characterize and assess the hydrochemistry/water quality, and (2) characterize the flow system of a 15 km^2 area in the Elk River Valley, near Weary Creek. The study area lies approximately 45 km north of the town of Elkford, British Columbia. Although two CBM test wells have been drilled within the Weary Creek exploration block, currently the area is inactive.

PHYSICAL SETTING

Physiography/Climate

The immediate study area is characterized by a broad, relatively flat-bottomed valley approximately 1 km wide. Elevations along the valley bottom range from about 1550 to 1600 m. The valley is flanked to the east and west by moderately steep dip slopes. Prominent ridges attain elevations of 2000 m and the more easterly and westerly peaks that define the limits of drainage basins along the Elk River attain elevations up to 2600 m.

Regionally, the Elk Valley is characterized by short, cool summers and long severe winters. Precipitation generally increases with elevation and with distance westward into the Foothills and Front Ranges. Mean annual temperature generally decreases with increasing elevation and latitude. Maximum discharge from the rivers and streams occurs during the spring melt in May and June.

GEOLOGY

Stratigraphy

Geology of the coal fields of southeastern British Columbia has been described most recently by Smith (1989), and Johnson and Smith (1991) summarized the

stratigraphy (Table 1) and discussed the coalbed methane potential of southeastern British Columbia. Morris and Grieve (1988) compiled the geology of the Elk Valley coalfield.

Table 1
Generalized stratigraphy of the Elk Valley area

AGE	GROUP	FORMATION	DESCRIPTION
CRETACEOUS	ALBERTA	Wapiabi	marine shale and siltstone
		Cardium	sandstone and shale
		Blackstone	marine shale, siltstone and sandstone
	BLAIRMORE	Beaver Mine/Mill Creek	non-marine sandstone and minor conglomerate
		Gladstone	non-marine siltstone, sandstone and minor conglomerate
		Cadomin	non-marine pebble conglomerate and sandstone
	KOOTENAY	Elk	non marine sandstone, siltstone, shale; thin coal; local conglomerate
		Mist Mountain	non marine siltstone, shale, sandstone, coal; local conglomerate
JURASSIC		Morrisey	marine sandstone
		Fernie	shale and minor sandstone and limestone grading upward to interbedded shale and sandstone
MISS/PERM			undifferentiated limestone

The CBM target beds lie within the late Jurassic/early Cretaceous Mist Mountain Formation. The Mist Mountain Formation consists of 450–550 m of nonmarine mudstone, siltstone, and sandstone with interbedded coal seams up to several meters thick. Lateral and vertical facies changes and lithological variations are characteristic of the formation.

The structural geology of the immediate study area is complex but comparatively well defined (Grieve, 1985; Morris and Grieve, 1988). The Elk Valley coalfields lie within the Alexander Creek Syncline. The Alexander Creek syncline plunges 2-5° north and ranges from overturned in the north and central parts to open in southerly parts. Regionally, the rocks are thrust and transverse faulted, repeating sections and thickening coal seams. The western boundary of the Alexander Syncline is defined by the Bourgeau Thrust which superimposes Triassic carbonates on Jurassic/Cretaceous clastics in the study area.

HYDROCHEMISTRY

Water sampling

Approximately 50 water samples were collected from sampling points in areas of outcrop and subcrop of the coal-bearing Mist Mountain Formation. The waters were collected from (1) open wells, (2) seeps/ponds, (3) streams/Elk River and (4) piezometers. Standard methods were used to sample and preserve the waters. Routine field analyses included pH, conductivity, temperature, and acid/base neutralizing capacity (ANC/BNC). Laboratory analyses are listed in Table 2.

RESULTS

Water Chemistry

Waters collected within the Weary Creek exploration block are characterized by pH ranging from 6.50 to 8.36. Conductivities range from 0.258 to 1.988 mS/cm reflecting low total dissolved solids (TDS) content. Dominant cations include Na, Ca, K, Mg and Fe. Bicarbonate (determined from ANC) is the dominant anion. The waters generally are dilute and major cation and anion concentrations generally increase with sample depth.

Analysis for regulated hydrocarbons indicated the waters are devoid of BTEX (benzene, toluene, ethyl benzene, xylene) and PAHs (polycyclic aromatic hydrocarbons). In general, metals show an increase in concentration with depth.

Oxygen and hydrogen isotopic signatures generally trend along the global meteoric water line. Tritium

Table 2

Chemical parameters, Elk River valley samples

Measured parameters			
Inorganic	**Organic**	**Dissolved gas**	**Isotopes**
• anions, cations, trace constituents	• polycyclic aromatics (PAH) • monocyclic aromatics BTEX • organic acids	• C_{1-4}	• $\delta^{18}O$, $\delta^{2}H$, ^{3}H, $\delta^{13}C$ gas; ^{13}C DIC

concentrations ranged from 0.8 TU (+/-0.3 TU) in open wells to 20.3 TU (+/-1.4 TU) in stream waters. High tritium concentrations in near-surface waters (seeps and shallow wells) indicate relatively rapid recharge and flow in the upper part of the system.

Isotopic compositions of dissolved inorganic carbon (DIC) in samples collected from open wells and piezometers are enriched in ^{13}C ($\delta^{13}C$ up to +34‰) which is characteristic of groundwaters with biogenic methane production. Carbon isotopic compositions of DIC become progressively enriched in ^{13}C with increasing DIC concentration suggesting that CO_2 is being produced biogenically.

PHYSICAL HYDROGEOLOGY

Hydrostratigraphy

To date the physical hydrogeological work has focused largely on the Mist Mountain Formation. Point hydraulic conductivities (Hvorslev tests) for coal, sandstone and siltstone range from approximately 10^{-7} to 10^{-9} m/sec. Previous results from pumping tests (Golder Associates, unpublished report, 1980) suggest that the transmissivity and storativity of coal, sandstone and siltstone beds range from about 10^{-4} to 10^{-5} m^2/sec and from about 10^{-3} to 10^{-5}, respectively.

CONCEPTUAL FLOW SYSTEM

The study area is characterized by two components of groundwater flow from (1) upland to lowland positions with discharge common along lower slopes and the valley bottom and (2) parallel to the valley bottom (Figs. 1a, b).

SUPPORTING EVIDENCE

$\delta^{18}O/\delta^2H$ and tritium distribution

Active discharge in seeps and wells in the valley bottom supports the conceptual flow system. Discharge of low salinity waters in seeps and shallow open wells in the lower slopes supports the existence of a shallow flow component (Group A; Fig. 3). Integrating $\delta^{18}O$, δ^2H and tritium data with physical indications of flow defines a lower, older and more evolved flow system (Group B; Fig. 3), and further constrains the upper, shallow system.

Regression analysis of more than sixty $\delta^{18}O$ and δ^2H analyses of water samples collected along an east–west trending transect of southern British Columbia (Yonge et al., 1989) show a linear depletion of δ^2H and $\delta^{18}O$ as a function of increasing elevation (Figs. 2a, b).

The effect of elevation on the isotopic compositions of baseflow waters (Fig. 2) is indicative of variations

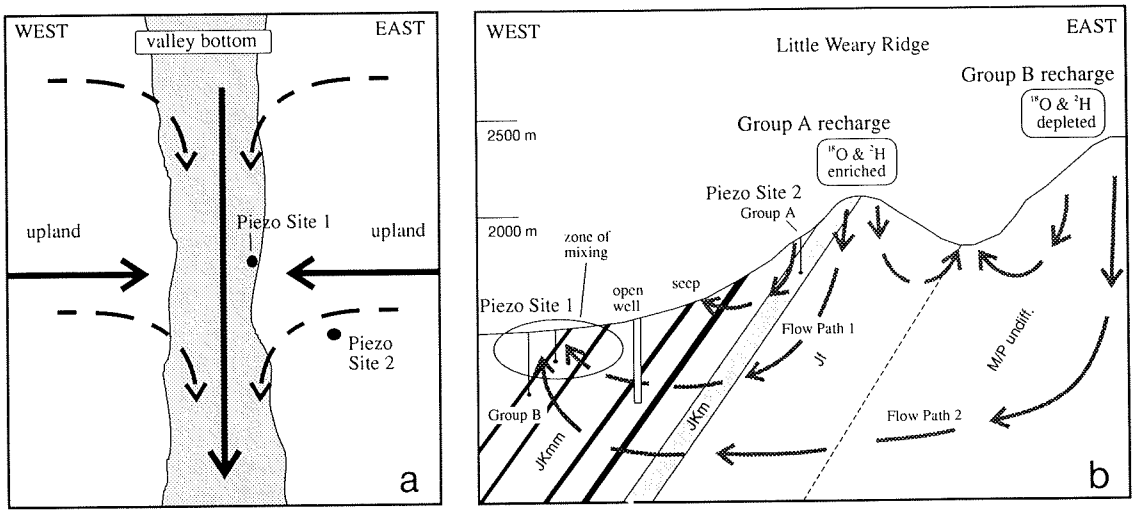

Figure 1. *Schematic flow system (a. plan and b. cross-sectional views; not to scale) for Elk Valley study area, southeastern British Columbia. Bold arrows show dominant flow components. JKmm = Mist Mountain Formation; JKm = Morrisey Formation; JF = Fernie Formation; M/P undiff. = undifferentiated Mississippian and Permian limestone.*

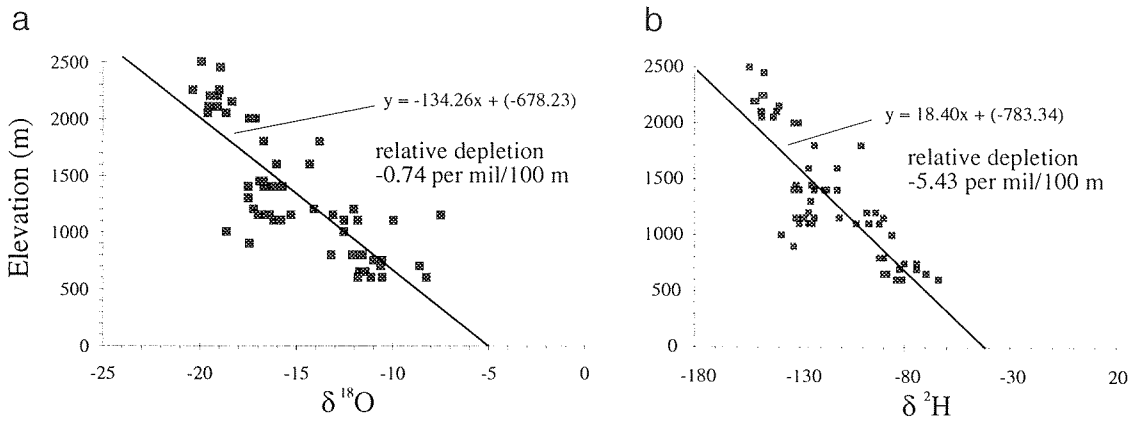

***Figure 2.** Effect of elevation on a. $\delta^{18}O$, and b. $\delta^{2}H$ of baseflow waters, southern British Columbia. Data from Yonge (1989).*

with elevation of the isotopic composition of recharge waters. The two distinct $\delta^{18}O$, $\delta^{2}H$, and tritium groundwater populations evident in the Elk Valley are postulated to reflect relative recharge position (Fig. 3). Group A groundwaters, collected along the mid to upper slope of Little Weary Ridge, show higher $\delta^{18}O$ and $\delta^{2}H$ isotopic signatures, higher tritium concentrations, and low concentrations of inorganic species suggesting proximity to recharge position and recharge at lower elevation (i.e., along Little Weary Ridge). Open wells downslope of Site 2 (Fig. 1) with similar isotopic signatures are probably also recharged along Little Weary Ridge (Flow Path 1; Fig. 1).

Significantly lower $\delta^{18}O$ and $\delta^{2}H$ isotopic signatures, lower tritium concentrations, and higher concentrations of inorganic species in Group B groundwaters suggest recharge at relatively higher elevations, slower flow, and/or a longer flow path (Flow Path 2; Fig. 1). Intermediate $\delta^{18}O$ and $\delta^{2}H$ isotopic signatures plotting between groups A and B reflect either a transitional flow system or mixing of Group A and Group B waters in the discharge area. Selected seep, stream, and pond waters plot along a local evaporation line (LEL) which intersects the global meteoric water line (GMWL) at Group A suggesting these waters are also part of flow from Little Weary Ridge.

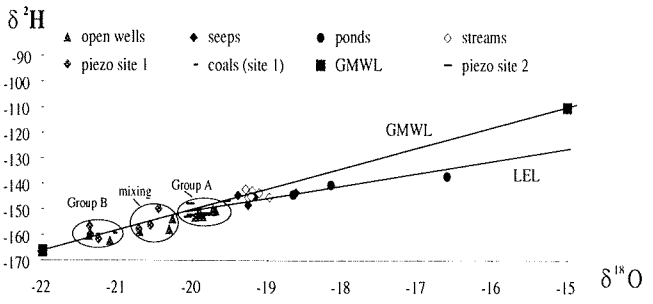

***Figure 3.** $\delta^{18}O$ and $\delta^{2}H$ for surface and subsurface waters, Elk Valley, southeastern British Columbia. GMWL = global meteoric water line; LEL = local evaporation line. Results reported relative to SMOW.*

SUMMARY

Hydrochemistry

- The waters sampled are generally dilute and devoid of BTEX and soluble PAHs. The dominant cations include Ca, Na, Mg, and Fe. The dominant anion is bicarbonate (HCO_3^-).
- Major cations concentrations and in particular Ca, Na, Mg, and Fe tend to increase with depth and residence time.
- Enriched (heavy) ^{13}C DIC signatures indicate an active biological population is producing CO_2, and probably methane, as a metabolic product in the Elk Valley flow system.

FLOW SYSTEM

The distribution of $\delta^{18}O$ and $\delta^{2}H$ isotopic signatures, and tritium concentrations define two distinct groundwater populations within the study area:

- An active, shallow flow system is defined by the comparatively higher $\delta^{18}O$ and $\delta^{2}H$ signatures, elevated tritium concentrations, and lower TDS

characteristic of Group A groundwaters. The recharge position of this system is inferred to be along Little Weary Ridge (Flow Path 1; Fig. 1).

- A deep, more evolved flow system is defined by comparatively lower $\delta^{18}O$ and $\delta^{2}H$ signatures, low tritium concentrations, and higher TDS characteristic of Group B groundwaters. The recharge position is at higher elevation and more distant from the Elk Valley (Flow Path 2; Fig. 1).

FURTHER WORK

Further work will include a more detailed compilation and interpretation of the chemical and physical data. Computer simulation of flow will be undertaken to assess the hydrogeological and environmental impact of depressurization and drawdown of the groundwater system. Geochemical modeling will be done to assess the potential for damage to the formation as a result of depressuring waters enriched in DIC (possibility of calcite precipitation in near wellbore region). Although the results of this study are not directly applicable, the methods and principles used can be extended to the plains region where more evolved waters and the presence of liquid hydrocarbons can be expected, altering organic and inorganic hydrochemical factors.

REFERENCES

Canadian Council of Resource and Environment Ministers
1992: Canadian Water Quality Guidelines.

Golder Associates
1980: Report to ELCO Mining on the 1980 Geotechnical Investigation on the Elk River Coal Project.

Johnson, D.G.S. and Smith, L.A.
1991: Coalbed Methane in southeast British Columbia. British Columbia Ministry of Energy, Mines and Resources, Petroleum Geology Branch, Special Paper 1991-1.

Morris, R.J. and Grieve, D.A.
1988: Geology of the Elk Valley Coalfield north half (Henretta Creek to Elk Lakes). British Columbia Ministry of Energy, Mines and Petroleum Resources, Preliminary Map 68.

Smith, G.G.
1989: Contributions to Canadian Coal Geoscience. Geological Survey of Canada, Paper 89–8.

Yonge, C.J., Goldenberg, L., and Krouse, H.R.
1989: An isotope study of water bodies along a traverse of southwestern Canada. Journal of Hydrology, v. 106, p. 245–255.

ARCHITECTURE OF THE SOUTHERN ALBERTA NATMAP DIGITAL FILES

D. Lebel

Geological Survey of Canada, 3303-33rd Street N.W., Calgary, Alberta T2L 2A7

INTRODUCTION

The Southern Alberta Foothills NATMAP project (1993–1998) will produce a new digital geoscience database for the eastern edge of the Cordillera in Southern Alberta, comprising new bedrock geological maps and new cross-sections of subsurface structure established in cooperation with the petroleum industry using proprietary seismic information. New maps of the Quaternary geology will also be produced. Field observations have been gathered with the building of such a digital database in mind, using a comprehensive data collection system including coded information about surveyed outcrops, rock lithologies (including composition, grain size, colour, sedimentary structures and bed thickness), and structural measurements. This information will be available in the future interactively through the graphical interface of a GIS (Geographical Information System) product or as separate datasets. Additional databases will include data about exploration wells, thermal maturation, fossil collections, till geochemistry, mineral deposits, rock analysis, measured stratigraphic sections and areal limits of previous work with bibliographical references.

DEVELOPMENT OF THE NATMAP GIS SYSTEM

Aim of NATMAP GIS Database

Several NATMAP projects are currently under way in Canada. The NATMAP program has been conceived as a way to update the geology of a particular area while upgrading the tools and skills of the geoscientists facing the increasingly convoluted GIS research and application fields. The aim of each NATMAP project being to produce digital maps and databases, all projects use some form of computer system to either gather or compile field data. Because of the multiple research interests and scientific backgrounds of the researchers involved in the various projects, it was decided to take a 'bottom up' approach to the whole issue of digital data (Broome et al., 1994). This means that each project is responsible for developing new tools or adapting tools already available from other sources. However, each project team is also responsible for translation of these data and submission at the end of the project to the central NATMAP database. Each project's database ought to share a common data dictionary with the other NATMAP projects.

The Southern Alberta NATMAP GIS

The flexible approach of the NATMAP program to digital data models has permitted the development of a GIS system which best suits the particular needs and constraints of the Southern Alberta NATMAP project: 1) simultaneous display and editing of large graphical files for each map sheet (>30 Mb DXF per map sheet); 2) production of preliminary Open Files for each geology map comprising complex displayable line attributes and symbols (thrust faults, geological contacts with four or more types of dashing, multiple structural symbols); 3) integration of 3D well and seismic data; and 4) availability of alphanumerical database query. Intergraph's MicroStation was chosen as the 'CAD engine' because it satisfies these needs. Substantial advancements in the elaboration of the GIS system were obtained through a joint agreement with the Ministère des Ressources Naturelles of Québec (MRNQ). This agreement has made available, from MRNQ, a comprehensive library of geological symbols and a GIS based system of field data gathering called Geofile, in exchange for present and future technological advancements provided during the course of the NATMAP project.

The first step in the development of the NATMAP GIS was the preparation of a prototype in 1993–94. Conclusive results have permitted further elaboration of the system, which is still under development. The architectecture of the GIS system was outlined and the structure of the graphical files and alphanumerical database was determined (Fig. 1). Cartographic tools and a customized user-interface were built to support any kind of geological linework in MicroStation (cells, custom linestyles, etc). Translation of the Geofile

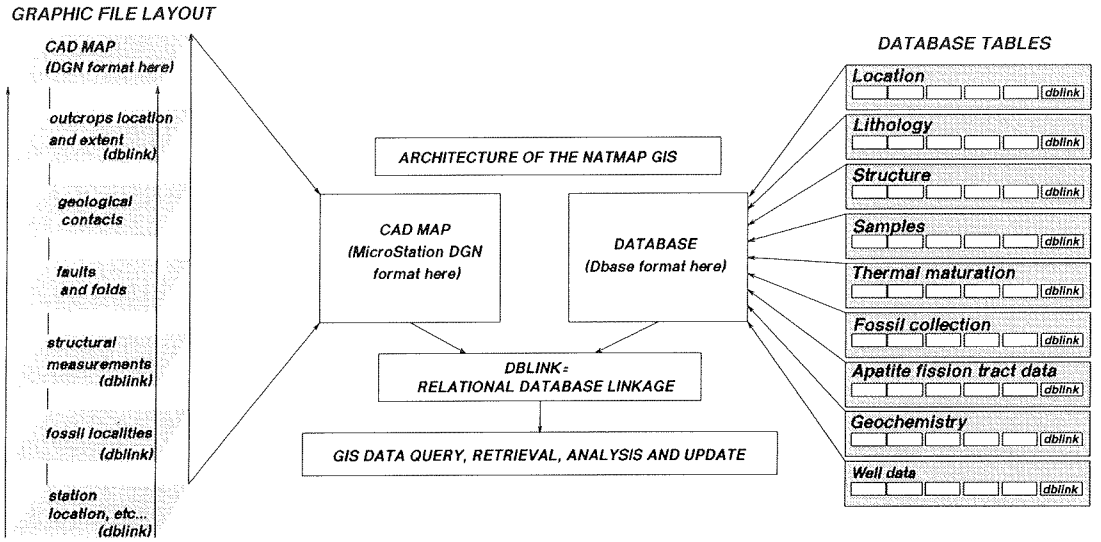

THE DIGITAL GEOLOGICAL MAP

Geology maps of the Southern Alberta NATMAP are constructed completely using a CAD program (Intergraph MicroStation). Information collected in the field using airphotographs was transferred directly within the digital map file. The graphical elements present within the digital map are distributed on a series of layers corresponding to each type of information (e.g. geological contacts, faults, bedding measurements, outcrop, observational stations, fossil localities, etc...).

THE ALPHANUMERICAL DATABASE

A database consisting of series of data tables conforming to the Xbase standard (i.e. dBase IV) is linked to each geological map. These tables comprise information in a series of data fields relating to geological field observations, oil and gas exploration wells, thermal maturity data, fossil collection, apatite fission track data, and compiled geological information

Figure 1. *Outline of the data architecture of the Southern Alberta NATMAP GIS.*

system from French to English was accomplished and a manual for users compiled (Lebel, in prep.). Field notebooks made of standardized forms and code tables were printed (Figs. 2, 3). The system was used by NATMAP participants during the 1994 field season. Other tables in the database comprise compiled nongraphical information (mineral deposit descriptions, geochemical analyses, fossil collections, thermal maturity, apatite fission track data, etc.) some of which are in turn plotted by location within MicroStation graphic files. Well information is plotted in 2-D or 3-D from the ERCB main database. Some of these data are used to issue a preliminary geological map as an Open file within a few months after the field season. Final map production will include balanced cross-section and integration of all data sets. Construction of regional balanced cross-sections uses such tools as multi-lines (used by architects to draw walls but easily adapted to draw stratigraphic units). Intergraph's I/RAS B is used to display and scale line drawings of seismic lines donated by the industry. At the final stage of production of each map sheet, the ISPG cartographic unit will build topology and produce final full-coloured A-Series maps using ArcInfo. Our end products will comprise multi-format digital files (ArcInfo, AutoCad, DXF, MicroStation, Raster images, Xbase, Ascii) and hard copy maps.

REFERENCES

Broome, J., Broderic, B., Viljoen, D., and Baril, D.
1994: The NATMAP digital geoscience management system. Computers and Geosciences, v. 19, p. 1501–1516.

Lebel, D.
in prep.: The Geofile guidebook. Geological Survey of Canada Open File.

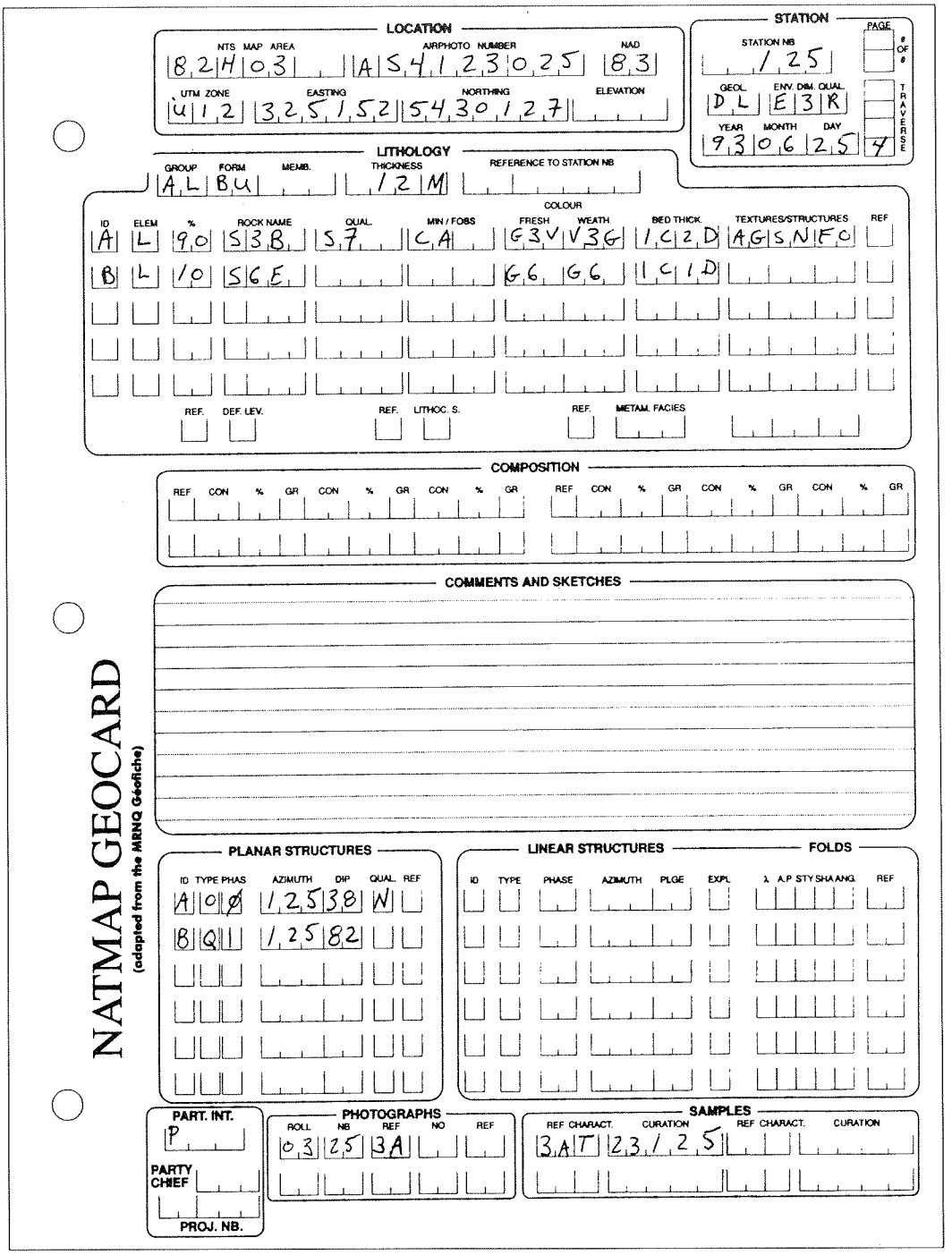

Figure 2. *Field form for the Geofile notation system. A paper form is used by the geologist during field work to compile observations relating to each outcrop, its location, rock lithologies observed, rock unit, structures and/or textures, individual mineral components, fossils, and structural measurements. The use of systematic codes for each type of information permits faster outcrop description and prevents the tedious step of data translation into a format usable by the Foothills GIS.*

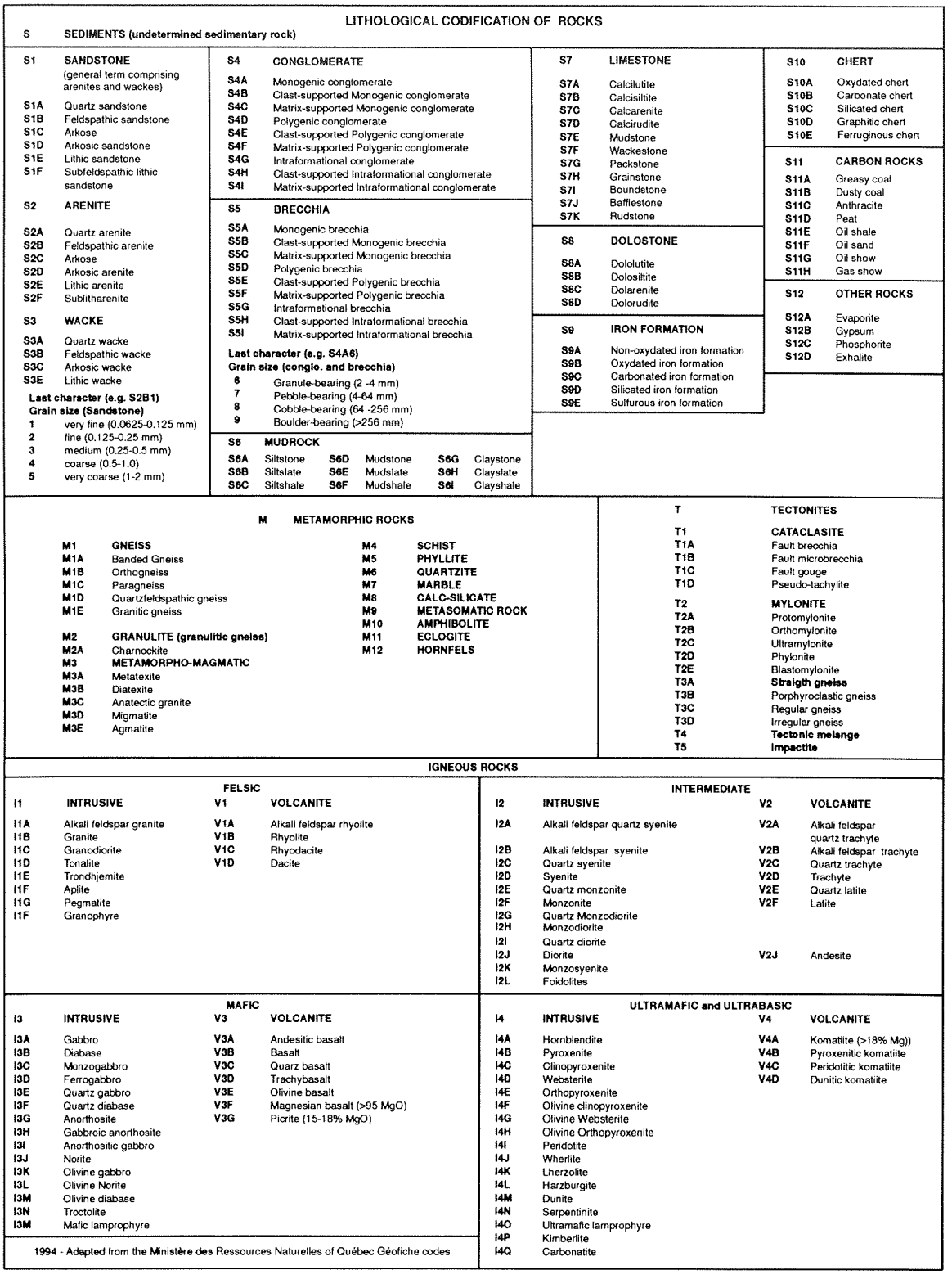

LITHOLOGICAL CODIFICATION OF ROCKS

S SEDIMENTS (undetermined sedimentary rock)

S1 SANDSTONE (general term comprising arenites and wackes)
- S1A Quartz sandstone
- S1B Feldspathic sandstone
- S1C Arkose
- S1D Arkosic sandstone
- S1E Lithic sandstone
- S1F Subfeldspathic lithic sandstone

S2 ARENITE
- S2A Quartz arenite
- S2B Feldspathic arenite
- S2C Arkose
- S2D Arkosic arenite
- S2E Lithic arenite
- S2F Sublitharenite

S3 WACKE
- S3A Quartz wacke
- S3B Feldspathic wacke
- S3C Arkosic wacke
- S3E Lithic wacke

Last character (e.g. S2B1)
Grain size (Sandstone)
1 very fine (0.0625-0.125 mm)
2 fine (0.125-0.25 mm)
3 medium (0.25-0.5 mm)
4 coarse (0.5-1.0)
5 very coarse (1-2 mm)

S4 CONGLOMERATE
- S4A Monogenic conglomerate
- S4B Clast-supported Monogenic conglomerate
- S4C Matrix-supported Monogenic conglomerate
- S4D Polygenic conglomerate
- S4E Clast-supported Polygenic conglomerate
- S4F Matrix-supported Polygenic conglomerate
- S4G Intraformational conglomerate
- S4H Clast-supported Intraformational conglomerate
- S4I Matrix-supported Intraformational conglomerate

S5 BRECCHIA
- S5A Monogenic brecchia
- S5B Clast-supported Monogenic brecchia
- S5C Matrix-supported Monogenic brecchia
- S5D Polygenic brecchia
- S5E Clast-supported Polygenic brecchia
- S5F Matrix-supported Polygenic brecchia
- S5G Intraformational brecchia
- S5H Clast-supported Intraformational brecchia
- S5I Matrix-supported Intraformational brecchia

Last character (e.g. S4A6)
Grain size (conglo. and brecchia)
6 Granule-bearing (2 -4 mm)
7 Pebble-bearing (4-64 mm)
8 Cobble-bearing (64 -256 mm)
9 Boulder-bearing (>256 mm)

S6 MUDROCK
- S6A Siltstone
- S6B Siltslate
- S6C Siltshale
- S6D Mudstone
- S6E Mudslate
- S6F Mudshale
- S6G Claystone
- S6H Clayslate
- S6I Clayshale

S7 LIMESTONE
- S7A Calcilutite
- S7B Calcisiltite
- S7C Calcarenite
- S7D Calcirudite
- S7E Mudstone
- S7F Wackestone
- S7G Packstone
- S7H Grainstone
- S7I Boundstone
- S7J Baffiestone
- S7K Rudstone

S8 DOLOSTONE
- S8A Dololutite
- S8B Dolosiltite
- S8C Dolarenite
- S8D Dolorudite

S9 IRON FORMATION
- S9A Non-oxydated iron formation
- S9B Oxydated iron formation
- S9C Carbonated iron formation
- S9D Silicated iron formation
- S9E Sulfurous iron formation

S10 CHERT
- S10A Oxydated chert
- S10B Carbonate chert
- S10C Silicated chert
- S10D Graphitic chert
- S10E Ferruginous chert

S11 CARBON ROCKS
- S11A Greasy coal
- S11B Dusty coal
- S11C Anthracite
- S11D Peat
- S11E Oil shale
- S11F Oil sand
- S11G Oil show
- S11H Gas show

S12 OTHER ROCKS
- S12A Evaporite
- S12B Gypsum
- S12C Phosphorite
- S12D Exhalite

M METAMORPHIC ROCKS

M1 GNEISS
- M1A Banded Gneiss
- M1B Orthogneiss
- M1C Paragneiss
- M1D Quartzfeldspathic gneiss
- M1E Granitic gneiss

M2 GRANULITE (granulitic gneiss)
- M2A Charnockite

M3 METAMORPHO-MAGMATIC
- M3A Metatexite
- M3B Diatexite
- M3C Anatectic granite
- M3D Migmatite
- M3E Agmatite

M4 SCHIST
M5 PHYLLITE
M6 QUARTZITE
M7 MARBLE
M8 CALC-SILICATE
M9 METASOMATIC ROCK
M10 AMPHIBOLITE
M11 ECLOGITE
M12 HORNFELS

T TECTONITES

T1 CATACLASITE
- T1A Fault brecchia
- T1B Fault microbrecchia
- T1C Fault gouge
- T1D Pseudo-tachylite

T2 MYLONITE
- T2A Protomylonite
- T2B Orthomylonite
- T2C Ultramylonite
- T2D Phylonite
- T2E Blastomylonite

T3A Straigth gneiss
- T3B Porphyroclastic gneiss
- T3C Regular gneiss
- T3D Irregular gneiss

T4 Tectonic melange
T5 Impactite

IGNEOUS ROCKS

FELSIC

I1 INTRUSIVE	V1 VOLCANITE
I1A Alkali feldspar granite	V1A Alkali feldspar rhyolite
I1B Granite	V1B Rhyolite
I1C Granodiorite	V1C Rhyodacite
I1D Tonalite	V1D Dacite
I1E Trondhjemite	
I1F Aplite	
I1G Pegmatite	
I1F Granophyre	

INTERMEDIATE

I2 INTRUSIVE	V2 VOLCANITE
I2A Alkali feldspar quartz syenite	V2A Alkali feldspar quartz trachyte
I2B Alkali feldspar syenite	V2B Alkali feldspar trachyte
I2C Quartz syenite	V2C Quartz trachyte
I2D Syenite	V2D Trachyte
I2E Quartz monzonite	V2E Quartz latite
I2F Monzonite	V2F Latite
I2G Quartz Monzodiorite	
I2H Monzodiorite	
I2I Quartz diorite	
I2J Diorite	V2J Andesite
I2K Monzosyenite	
I2L Foidolites	

MAFIC

I3 INTRUSIVE	V3 VOLCANITE
I3A Gabbro	V3A Andesitic basalt
I3B Diabase	V3B Basalt
I3C Monzogabbro	V3C Quarz basalt
I3D Ferrogabbro	V3D Trachybasalt
I3E Quartz gabbro	V3E Olivine basalt
I3F Quartz diabase	V3F Magnesian basalt (>95 MgO)
I3G Anorthosite	V3G Picrite (15-18% MgO)
I3H Gabbroic anorthosite	
I3I Anorthositic gabbro	
I3J Norite	
I3K Olivine gabbro	
I3L Olivine Norite	
I3M Olivine diabase	
I3N Troctolite	
I3M Mafic lamprophyre	

ULTRAMAFIC and ULTRABASIC

I4 INTRUSIVE	V4 VOLCANITE
I4A Hornblendite	V4A Komatiite (>18% Mg))
I4B Pyroxenite	V4B Pyroxenitic komatiite
I4C Clinopyroxenite	V4C Peridotitic komatiite
I4D Websterite	V4D Dunitic komatiite
I4E Orthopyroxenite	
I4F Olivine clinopyroxenite	
I4G Olivine Websterite	
I4H Olivine Orthopyroxenite	
I4I Peridotite	
I4J Wherlite	
I4K Lherzolite	
I4L Harzburgite	
I4M Dunite	
I4N Serpentinite	
I4O Ultramafic lamprophyre	
I4P Kimberlite	
I4Q Carbonatite	

1994 - Adapted from the Ministère des Ressources Naturelles of Québec Géofiche codes

Figure 3. *Table of Geofile codes for rocks. The notation is arranged for systematic GIS query of rock types.*

HOLDINGS OF THE NATIONAL AEROMAGNETIC AND GRAVITY DATA BASES OVER WESTERN CANADA

W. Miles

Geological Survey of Canada, 1 Observatory Crescent, Ottawa, Ontario K1A 0Y3

POSTER

Outline: Aeromagnetic and gravity data covering most of Western Canada are stored in the National Aeromagnetic and Gravity Data Bases. The data are available from the Geophysical Data Centre, Geological Survey of Canada in digital and map form. Both observed and gridded data are available in a number of formats and on a variety of media. Posted data, black line contour, and colour plots are produced for Open File publications and to client specifications. Data processing and filtering services are also provided.

Please direct any correspondence to:

Warner Miles
Geophysical Data Centre
Geological Survey of Canada
1 Observatory Crescent
Ottawa, Ontario K1A 0Y3
Telephone: 613-992-6634, FAX: 613-992-2787
E Mail: miles@agg.emr.ca

GIS: DATA INTEGRATION FOR SUBSURFACE GEOLOGICAL ANALYSIS

B.R. Palmer and T.R. Myers

Geological Survey of Canada, 3303-33rd Street N.W., Calgary, Alberta T2L 2A7

A geographic information system (GIS) is a powerful software concept for spatial analysis. The GIS concept is often misunderstood, leading to unrealistic expectations of both technical users and management. The goal of this paper is to elucidate some of these potential misunderstandings and to review some considerations in building and using a subsurface GIS. This paper is not intended to be an exhaustive treatise on the subject of subsurface GIS.

A GIS is a tool to directly link data to visualizations and provide not only traditional statistical analysis of those data sets, but also for spatial analysis (i.e., gridding, contouring, etc.), particularly, analysis of topological relationships. Aside from the actual software and hardware, the GIS consists of three components: the data, the data model, and the spatial topology. Topological analysis provides a powerful tool to the geoscientist far beyond the scope of simply posting data on a map. A functional GIS is one which allows the user to quickly load pertinent data sets and initiate the modelling process with a minimum amount of effort or technical support from information systems personnel. However, GIS software is sophisticated and often requires substantial training to operate effectively.

There are numerous development and implementation considerations which may impact on the ultimate performance of the GIS. The expense of running and maintaining a GIS is often greater than the high priced software and hardware. Many companies have avoided these costs simply by allowing the software to sit idle. The thrill and ego-warming buzz of new technology is too often dulled by the reality of actually working in the cyber environment. Utilizing the power of GIS takes commitment from management to support the geoscientists through training and realistic performance expectations of both the software and the user. Geoscientists must be willing to immerse themselves in the technology, a commitment which is often challenged by the realities of other professional duties and the misconception that the GIS will make their job easier.

The GIS allows for a modelling process and, as such, requires intellectual input from the geoscientists. The concept of GIS requires significant upfront time to determine what hypothesis the model is intended to test or what function it is to fulfil. The modelling process is subject not only to conceptual error, but, it is also dependent on the quality and quantity of the input data sets. This iterative process requires verification, analysis and refinement. Because the data sets are not static, the model may require updates and further analysis as new data are added. One essential characteristic of the data model should be the ability to track various iterations of the GIS model.

Developing an understanding of the data context prior to initiating the modelling process can save the user a lot of frustration and effort. With the volume of data available today, it is to easy to assemble large data sets without consideration of validity. The model may look elegant and provide an interesting answer, but have no basis in reality. Scalability of the data is one test for data validity. A subcrop edge or reef initially mapped at 1:5 000 000 may not be valid when placed in a 1:10 000 prospect map. Well and seismic picks should also be tested for validity, the interpreter name or a formal reference should be included in the data model for the benefit of both the modelling geoscientist and subsequent users.

Building a functional GIS is dependent on developing a functional data model which can readily be integrated into a GIS project at any scale. The scope of data model design is typically greater than that of a single user, crossing departmental boundaries to enterprise level modelling. An engineer's or accountant's view of well data may be at variance with those of the geoscientist. Therefore, it is essential that geoscientists have the opportunity to participate in the data modelling process, or at the very least have some understanding of how the data model works and knowledge of what data is actually contained within the model.

A data model is a physical and logical model which describes the underlying relationships between data sets and maps these characteristics to the structure of a relational data base. Additionally, in the context of GIS, these data must be further mapped out to define the

data structures and relationships within the GIS spatial environment. Storing bibliographic information and references to data ensures that the data have context that can live beyond the limited life span of any particular GIS model. Terms and definitions for data entities should be clearly described so as to reduce ambiguity and encourage consistency within the data sets. A common example of ambiguity in many databases occurs when defining well picks. Well picks are often stored in formation tables. These tables include not only formation picks, but also period, group, member and marker picks. Although, this may be a de facto standard for some, it is clearly not correct and can lead to unforseen problems down the road. Imagine trying to digitally construct a stratigraphic correlation chart using a formation picks table which includes picks that are not formations and are not referenced to their stratigraphic hierarchy. A pick is just not the top of the Wabamun, it may also be the base of the Exshaw, the top of the Devonian, the base of the Mississippian, the top and/or base of a stratigraphic sequence, a pick from core, a log pick, a measured depth in a bore hole, a true vertical depth in bore hole, or a pick from the ERCB or any one of number of commercial data vendors. These pick attributes should be spelled out explicitly in the data model.

Data models for GIS should include spatial primitives that fully describe a data object in three dimensional space. A pick is often described by a single point in a well bore, but it may be traversed by the well bore where structural deformation has occurred or in the case of horizontal drilling, requiring a linear two dimensional description. Core and drill stem test data are two dimensional having both top and base locations. Outcrop data may be a two dimensional line of section or may be described more fully in three dimensional terms. The data model should be robust enough to accommodate and describe this variety.

A stratigraphic correlation chart is a set of two dimensional models used to describe regional geology. These two dimensional models can be further mapped out into three dimensions to describe more locally the stratigraphy and nomenclature that is generally recognized. Stratigraphic modelling can incorporate the characteristics of both chrono and lithostratigraphy which are not often reflected by a simple picks table. An advantage of this type of modelling is that it encourages internal consistency of pick nomenclature within multiuser databases. This can prove a valuable asset when "guerilla mapping", as often done by exploration geologist chasing land sales, by providing a measurable confidence to the picks data.

Subsurface data are mostly point data. As a consequence, most geoscientists model with small volumes of data and large volumes of interpretations and interpolations by creating traditional contour or facies maps. This traditional approach does not require the spatial analysis of GIS. The GIS environment presents opportunities to integrate a greater variety of data sets to further interrogate and test or develop new geologic models. Satellite imagery, potential field data, hydrocarbon pool distributions, fracture vectors, hydrography, and digital terrain models are excellent examples of data sets which can be incorporated into GIS spatial models.

Geoscientists are well trained to interpret three-dimensional geology with two-dimensional tools. The challenge is to find new ways to map which analyse the spatial distribution of geologic characteristics. Is there a measurable or definable relationship between basement magnetic anomalies and hydrocarbon pool distributions? Is there a relationship between distribution of the Lower Mannville or Upper Devonian carbonate buildups or salt dissolution and basement magnetic anomalies? The GIS not only provides the ability to overlay these maps, but the ability to measure statistical relationships between the maps.

The effort taken to design good GIS data models will yield rewards beyond the scope of GIS. There are a growing number of software programs which can utilize these structures to model, in three dimensions, both geologic and geophysical rock properties, including seismic, log, core and fluid characteristics of reservoir properties. Multi-log multi-well log analysis software may be integrated with GIS to further enhance the log interpretations with respect to other geological data. Although there may be no limits to what the imagination can conceive, there are many practical limitations to building and utilizing a sophisticated GIS data model. There are a number of data models available, such as the Public Petroleum Data Model (PPDM), Petrotechnical Open Software Corporation (POSC), a merged PPDM/POSC model and numerous models from commercial data vendors and software consultants. It is a difficult task to determine which model is best for the varied needs of subsurface data users, however, the benefits of a good model quickly become apparent when measured against the ad hoc chaos of no model.

AEROMAGNETIC SURVEY EXCHANGE
Who holds what coverage across Canada?

J. Tod, G. Boyce, F. Dostaler, J. Janveau, R. Kane, L. Lawley, and W. Miles

Geophysical Data Centre, Geological Survey of Canada
1 Observatory Crescent, Ottawa, Ontario K1J 0Y3

A database of information on aeromagnetic surveys flown in Canada, is being compiled by the Geophysical Data Centre. The intent is to facilitate the exchange of information on private sector surveys.

Contained in the database are details of location, survey parameters, and who to contact for the data or for further details about the survey. Access to the database is free of charge. This tracking of private sector surveys will help ensure that these data (and the millions of dollars spent acquiring them) will not be lost as exploration shifts from one region of the country to another.

The Geophysical Data Centre (GDC) maintains the National Aeromagnetic and Gravity Data Bases. It distributes this data to scientists and private sector companies engaged in mineral and oil exploration. Digital data is available on a variety of media: CD, EXABYTE, 9-track, cartridge, diskette, and through Internet. Colour plots are customized to user specifications.

Geophysical Data Centre
Geological Survey of Canada
1 Observatory Crescent, Ottawa, Ontario K1J 0Y3
Tel: 613-995-5326, FAX: 613-992-2787
Internet: infogdc@agg.emr.ca

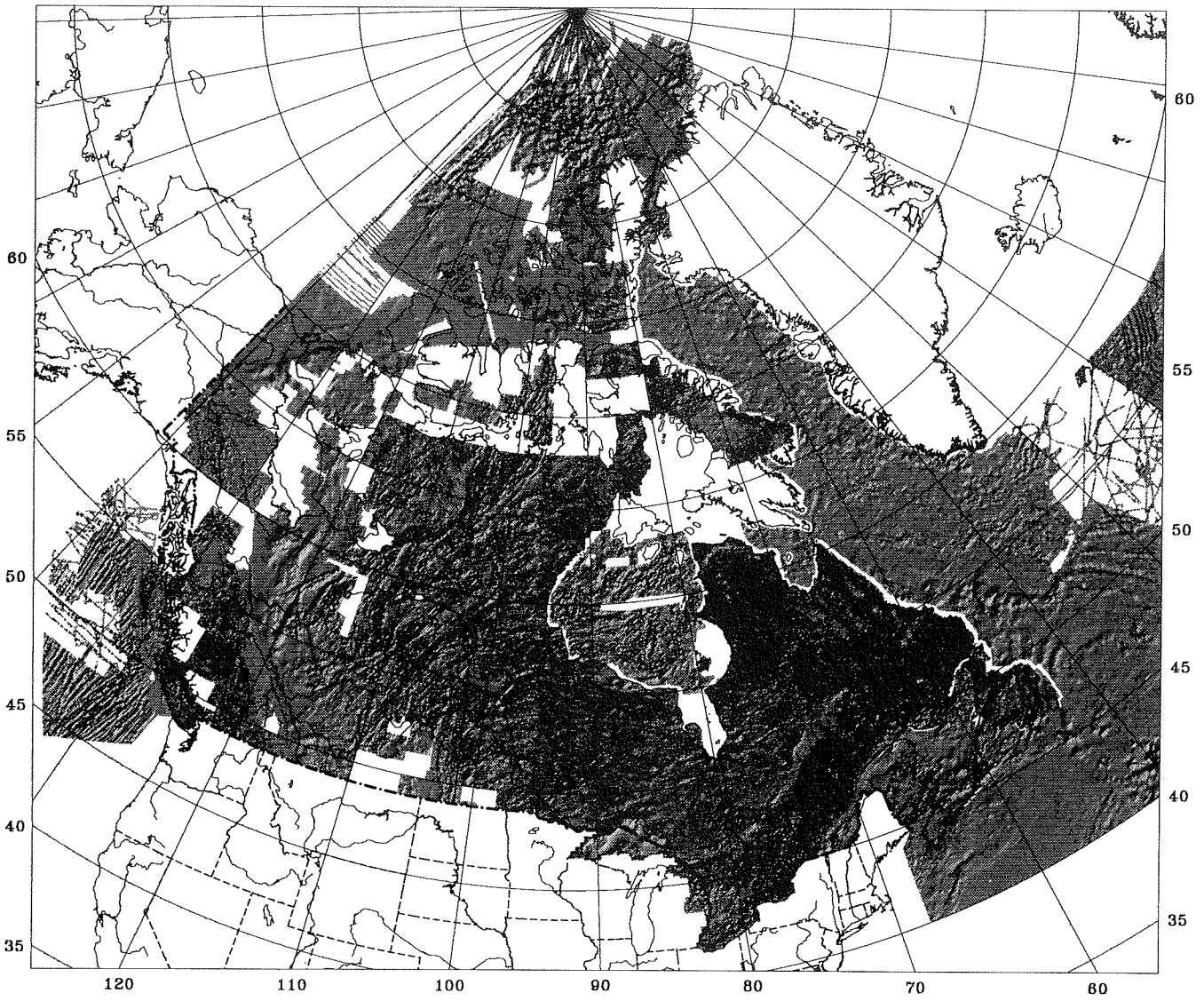

Plot 1

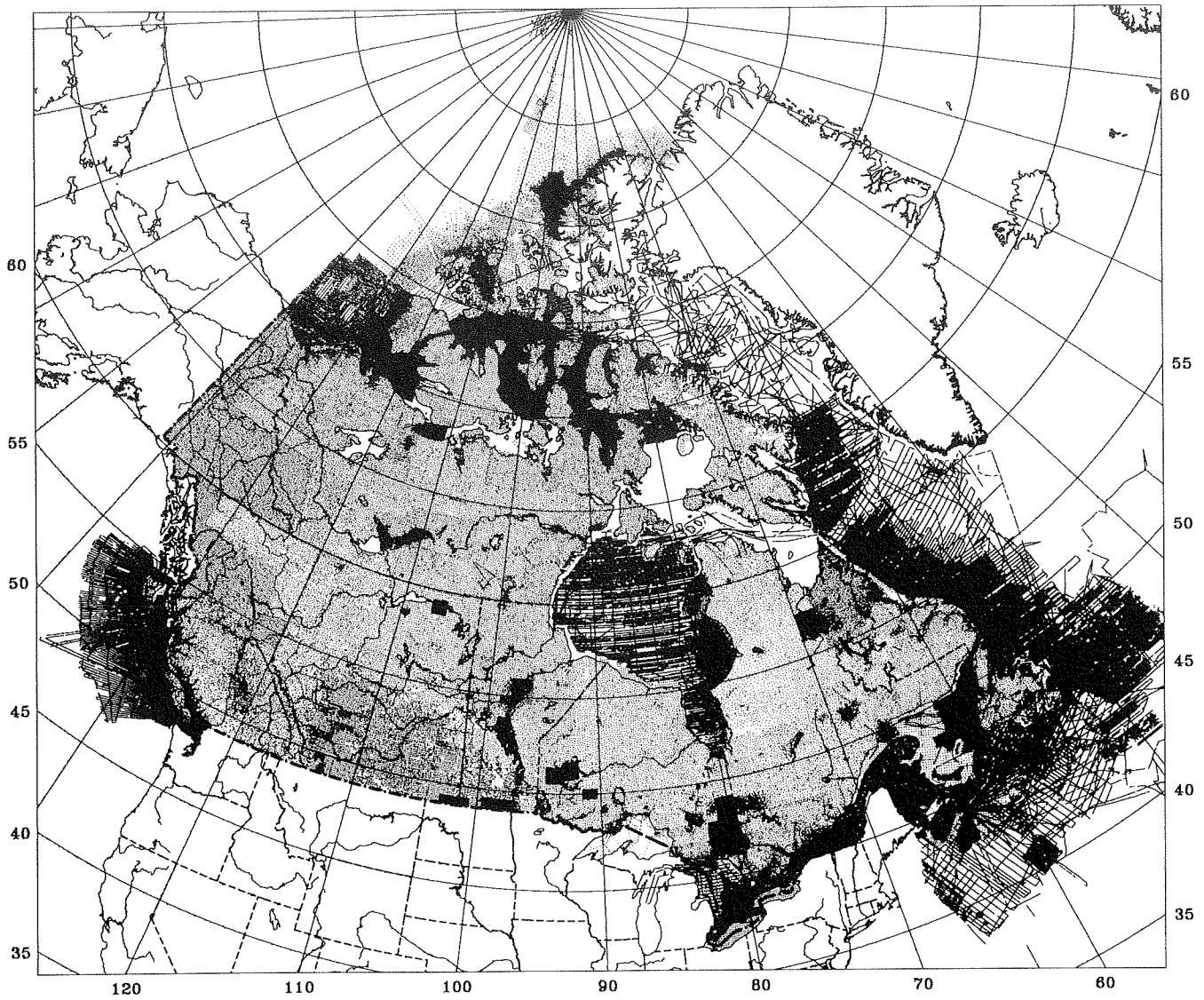

Plot 2

UPDATE OF THE NATIONAL DIGITAL GEOSCIENCE DATA LIBRARY: INITIATIVES IN DIGITAL SEISMIC INTERPRETATION, PROCESSING AND ARCHIVING

K.C. Coflin and K.D. McAlpine

Atlantic Geoscience Centre, P.O. Box 1006, Dartmouth, Nova Scotia B2Y 4A2

THE LIBRARY

In 1993, the Atlantic Geoscience Centre (AGC) was the proud recipient, on behalf of the Geological Survey of Canada (GSC) and the people of Canada, of more than $100,000,000 worth of petroleum industry geophysical and geological digital data. The information covers most of Canada's offshore (and some onshore) sedimentary basins from eastern Canada to the Arctic, including Scotian Shelf, Gulf of St. Lawrence, Grand Banks, Labrador Shelf, Hudson Bay, Baffin Bay, Arctic Islands and Ocean, Beaufort Sea and Yukon/NWT (Fig. 1).

The largest portion of these data was donated by Husky Oil and Petro-Canada in recognition of an effective and continuing scientific collaboration that has evolved between the petroleum industry and the GSC and, particularly, in acknowledgement of the expert capability for seismic data interpretation and processing that has been developed at AGC. This gift of scientific data, unprecedented in magnitude and genre in Canada or elsewhere in the world, combined with state-of-the-art workstation technology, places the GSC at the forefront of marine seismic research and basin analysis capability.

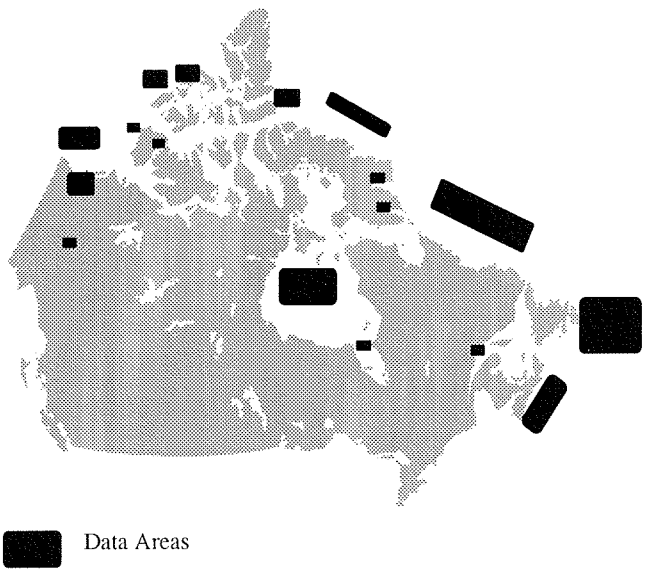

Figure 1. *Map showing areas with data available in the National Digital Geoscience Data Library.*

Appropriate curation of the data, and encouragement of collaborative use of the data for research purposes are specific terms of the donation agreements. The agreements allow access to the data not only by the GSC, but also by other research and academic organizations across Canada and world-wide. The data are stored on over 65,000 half-inch, 9-track magnetic tapes (Fig. 2), and consist mainly of field and stack (processed) multi-channel seismic lines. Also included are high resolution well-site surveys, side-scan data and refraction and potential field data. To store the information on behalf of the Survey, AGC has established a partnership with the National Archives of Canada (Heritage Canada).

INTERPRETATION AND PROCESSING FACILITY

To assist clients and collaborators within the petroleum industry, universities and the international geoscience community, AGC has established a geoscience information facility (Client Facility) to encourage research into the formation and evolution of sedimentary basins, including their oil and gas potential. The system includes a state-of-the-art CAEX workstation with mapping, seismic processing and 3-D interpretation capabilities. This facility makes it possible to integrate the comprehensive data bases of geological information already available within the GSC with the newly acquired digital seismic data. At present, this type of fully integrated system is not available at any other division within the GSC and is rare outside of the petroleum industry. The goal of the Facility is to utilize

Figure 2. *The Husky Oil tape storage facility in Calgary showing some of the 65,000 magnetic tapes before they were moved to Dartmouth.*

fully the digital data held in the library to ensure maximum realization of the benefits described above, and to allow the technology that has been confined to large commercial organizations to be used by a much broader group of researchers and students.

The Client Facility consists of a Sun SPARC 10/51 workstation including two 19" monitors, approximately 16 gigabytes of disk storage, a CD-ROM reader, a high-density 8 mm helical scan tape drive, a 22" black and white Versatec plotter and access to a ½ inch 9 track tape drive. The system is networked to a 44" colour Versatec plotter. The system software comprises Landmark Graphics SeisWorks 2-D and 3-D interactive multi- and single channel seismic reflection interpretation software, Insight 1 (a full function 2-D seismic processing package), and Zycor Z-Map Plus mapping software. Also online is Landmark's StratWorks geological interpretation software. This software is designed to manipulate petrophysical and geological information in an interactive environment, in the same way the seismic interpretation software works with seismic profiles. The software is fully integrated around a single data base which enables nearly seamless exchange of information between individual modules and packages.

CURRENT WORK

Even though these software packages were designed by and for the petroleum industry (Fig. 3), they can also be used for nonconventional applications such as processing and interpreting the high resolution seismic data frequently collected in environmental studies (Fig. 4). This is providing AGC environmental marine geologists with a technology that has been previously unavailable to them.

FUTURE

The large volume of data and varied data types in the National Digital Geoscience Data Library presents some problems in searching for specific data in a particular area of interest. To overcome these problems, we are developing a GIS-based interface for accessing the data. This interface will give users a geographic view of where data exist and a visual key as to the type of data available. When this is linked with other existing GIS information at AGC, a powerful tool will exist to gather quickly and efficiently the information necessary to address specific geological and environmental issues.

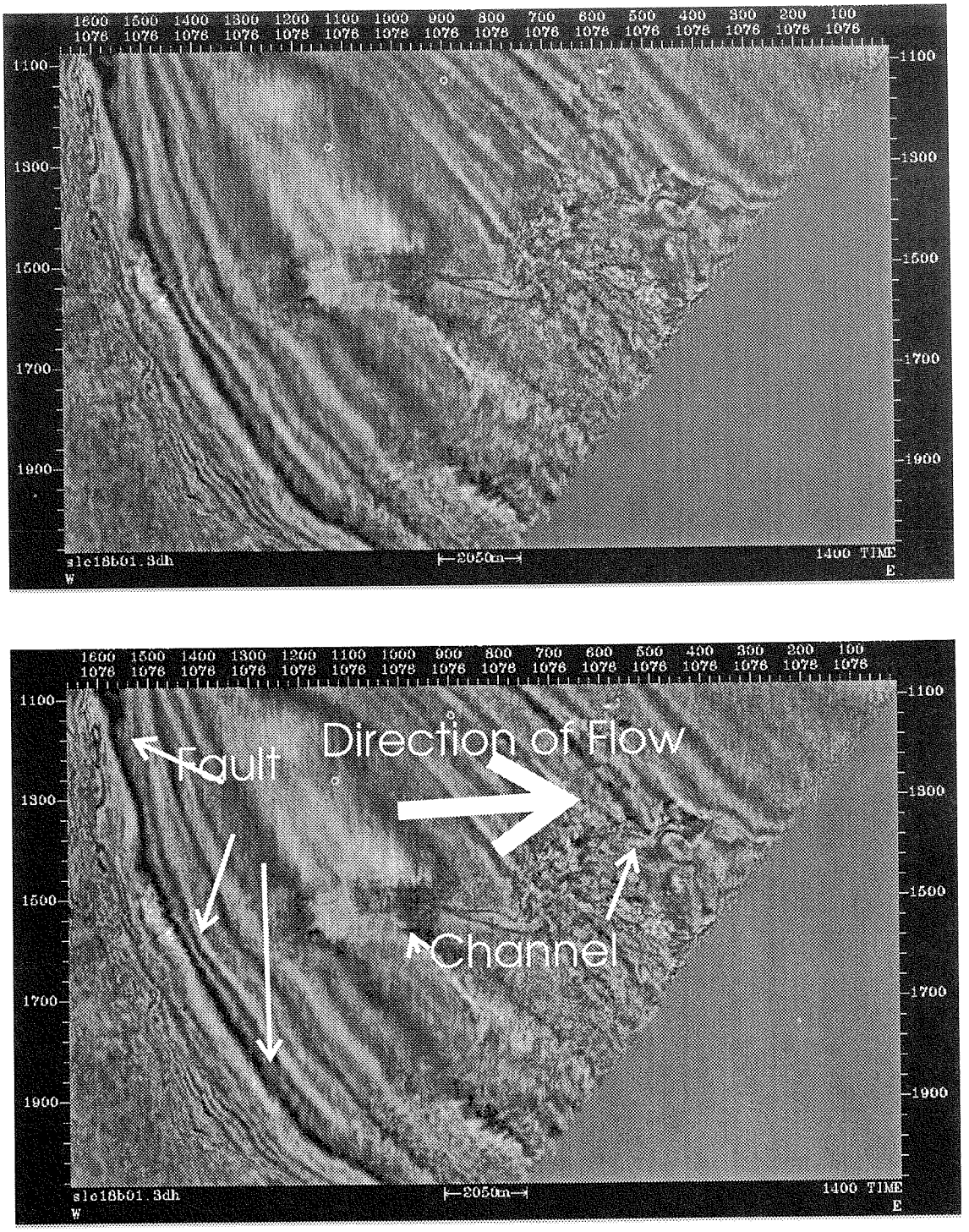

Figure 3. *Horizontal time slice from a 3-D survey showing the location of a Cenozoic channel. A collection of these time slices when animated makes it possible to image the development of this channel through time.*

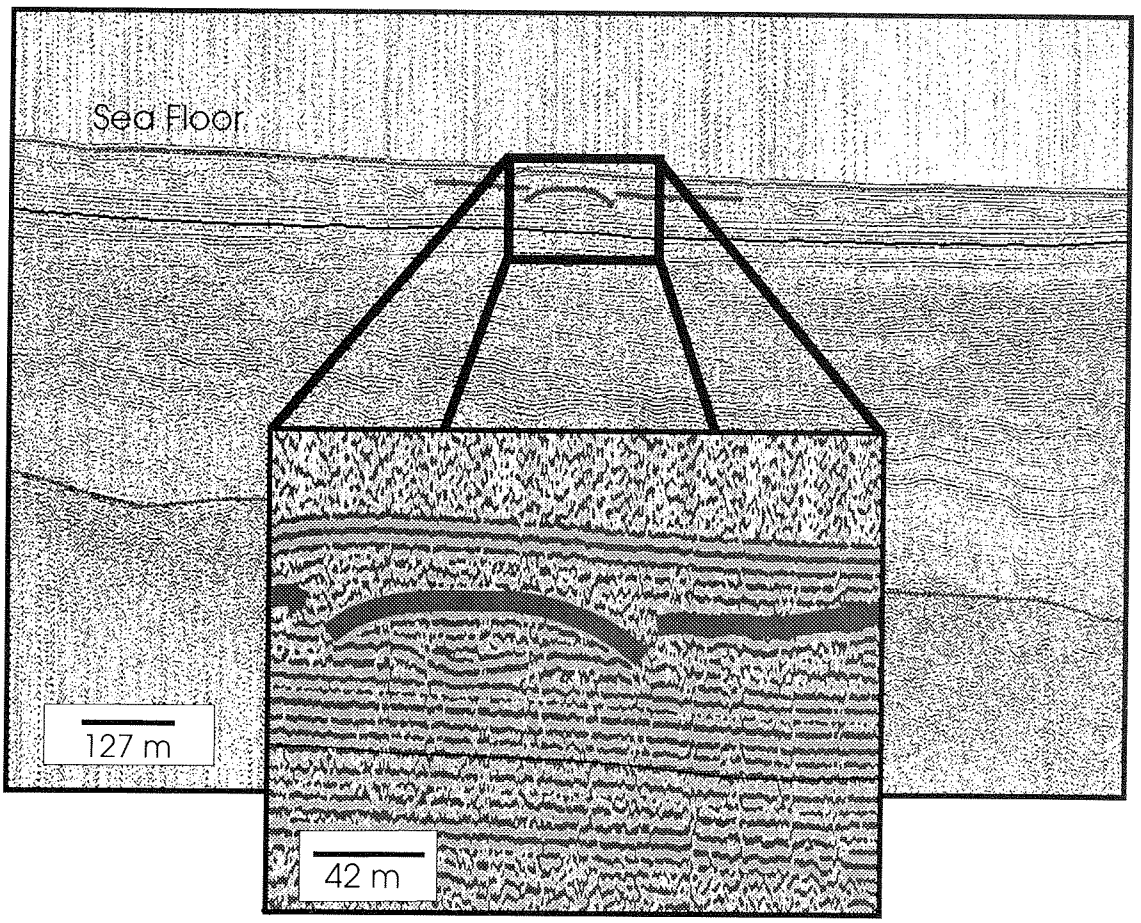

Figure 4. *High-resolution single channel seismic record from the Great Lakes being interpreted and displayed on the Client Facility hardware and software. Displays such as these increase the marine geologist's ability to interpret and map very small structures and stratigraphy.*

LOGMAP–A MULTIPLE WELL PROGRAM FOR DIGITAL LOG, MAP AND CROSS-SECTION ANALYSIS

J.R. Hitchner

Hitchner Exploration Services Ltd., 120-1035-7th Avenue S.W., Calgary, Alberta T2P 3E9

J.D. Hughes

Geological Survey of Canada, 3303-33rd Street N.W., Calgary, Alberta T2L 2A7

I.A. McIntyre

PerArdua Consulting Ltd., 439 Parkview Crescent S.E., Calgary, Alberta T2J 4N8

POSTER

LOGMAP provides a comprehensive suite of tools that allows the geologist to analyse multiple well data sets incorporating digital logs, core descriptions and analyses, drill stem tests, perforations and production histories to develop predictive map and cross-section displays that can assist in finding oil, gas and other deposits. LOGMAP incorporates an easy to use, mouse driven, graphical user interface that simpifies basic tasks such as data import and depth correction, and employs a unique interactive cross-section module that can reduce correlation times on major projects by two thirds. The program has also integrated well log analysis directly to mapping, which allows trends of data established through analysis of multiple well cross plots to be displayed on maps as scaled log traces with shading to show lithologic trends or as conventional contour maps. LOGMAP is one of the only log analysis systems that allows interactive manipulation of core analysis data in concert with digital log data.

One of the most powerful strengths of LOGMAP is its capability for interactive cross plot analysis and normalization of log data. This allows variations in log response due to well vintage, differing logging companies, borehole rugosity etc. to be reduced to a minimum prior to formal well log analysis. Contoured frequency cross plots of normalized multiple well data can be used to predict lithology, porosity, permeability and other parameters for which analytical "training sets" are available.

LOGMAP has been researched, developed and tested over the past eight years. The production version of the DOS resident program has been in intensive use for the past four years on projects ranging from 50 to 1100 wells. Both carbonate and sandstone reservoirs have been successfully analyzed, including a large coalbed methane project (Fig. 1).

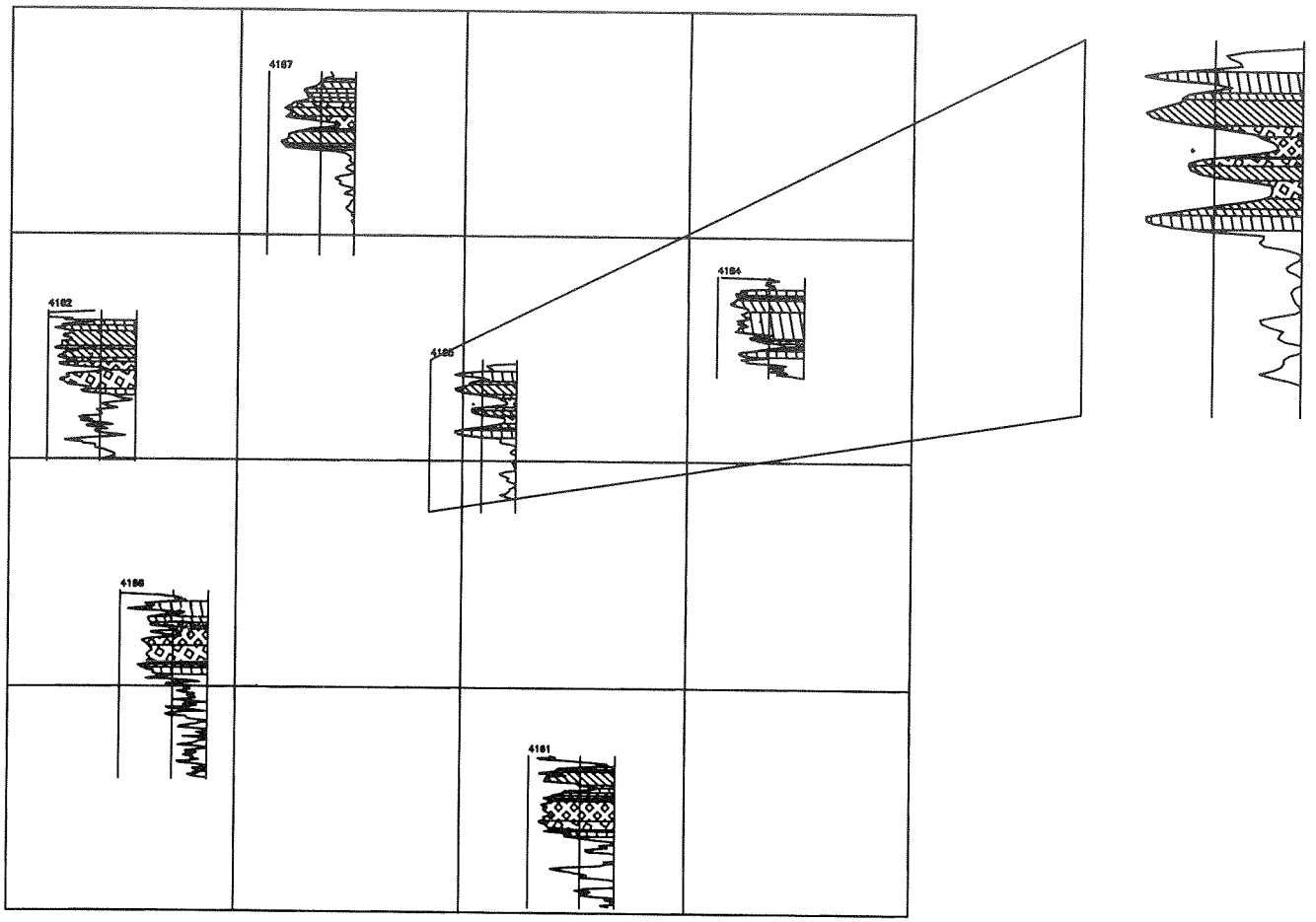

Each Shade represents a distinct facies

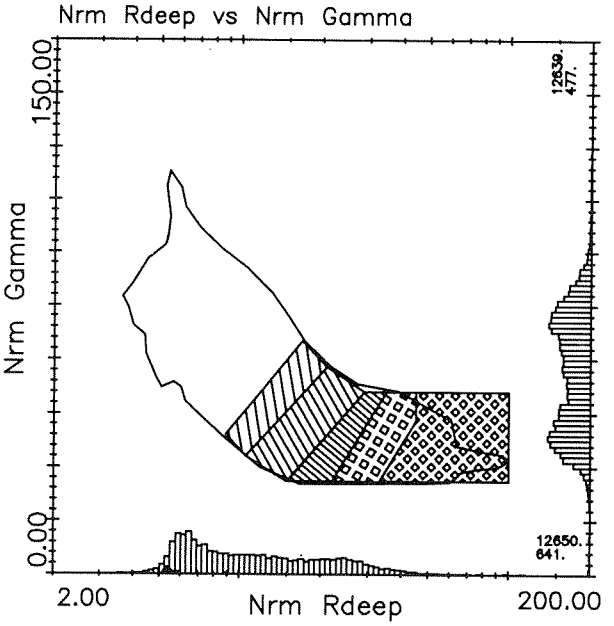

Figure 1. *Illustration of LOGMAP's capability to display the results of multi-well log analysis in map format. Polygons, interactively defined on a normalized gamma versus resistivity cross plot, are mapped against shale corrected porosity determined from log analysis. Resistive strata defined by the small square hatch pattern indicate hydrocarbon production potential where porosity is high.*

3-D COMPUTER MODELLING TECHNOLOGIES UTILIZED IN GSC'S NATIONAL COAL INVENTORY

J.D. Hughes and W.J. McDougall

Geological Survey of Canada, 3303-33rd Street N.W., Calgary, Alberta T2L 2A7

Canada's abundant coal resources offer a stable source of low cost energy for domestic electricity production and revenue from exports to Pacific-Rim and other nations. Domestic production is forecast to double by 2020 to meet expanding energy requirements and increased international demand. Concern about the environmental impact of greenhouse gas and trace element emissions from coal use, coupled with the need to optimize mining of a nonrenewable resource in the face of international competition, is the rationale behind the development of a comprehensive National knowledge base on coal resources known as the National Coal Inventory (NCI).

GSC's NCI has defined National standards for the computerization of historical coal exploration data and the integration of modern analytical information on toxic elements in coal. Computer databases have been developed for coal deposits in Nova Scotia, Saskatchewan, Alberta and British Columbia which incorporate private sector exploration data and analytical information collected by other GSC scientists. A unique suite of software tools developed for the NCI is utilized to develop comprehensive 3-D models using these databases to define the configuration, technological and environmental attributes of coal resources. Resources available given specific mining scenarios can be rapidly determined using these tools, together with constraints to development including surface land use and toxic element concentrations. Third party Geographical Information Systems (GIS) and Computer Aided Design systems (CAD) are utilized to transfer the results of geological/economic analyses in industry standard formats and to provide additional data visualization capabilities. Integration with Image Analysis Systems (IAS) allows satellite and other remotely sensed imagery to be incorporated into the geological and land use assessment of surface mineable deposits. The integrated computer models developed through the NCI provide a rational basis for assessing the economic and environmental merits of coal deposits which will have to be developed to meet expanding coal production in Canada.

The 3-D modelling tools developed for the NCI can be applied to any stratified deposits. Recent applications include assessments of potable water resources in Manitoba, hydrocarbon resources in central Alberta and Saskatchewan, and coalbed methane resources in Nova Scotia and Alberta (Fig. 1).

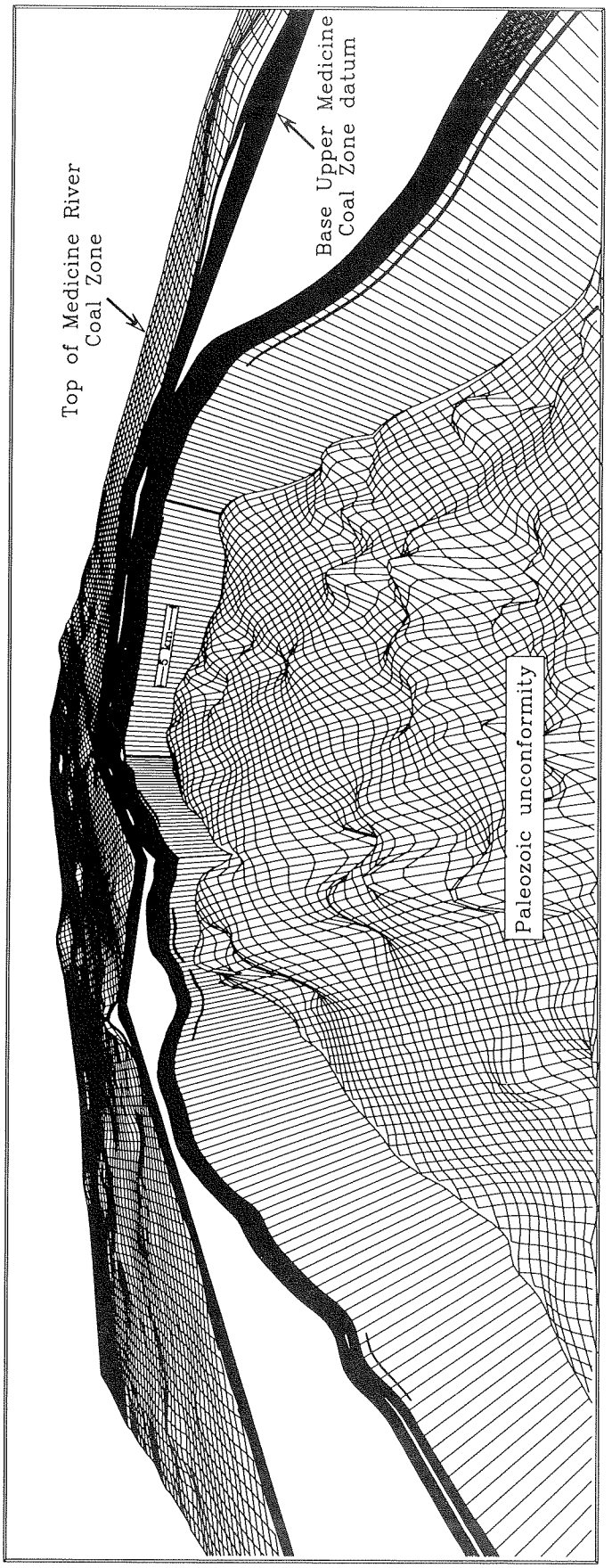

Figure 1. *Integrated display of map and 3-D cross-section information from a computer model of the Medicine River Coal Zone in the Mannville Group of central Alberta. The 3-D cross-section traverses a high on the underlying Paleozoic unconformity surface which has controlled the geometry and thickness of the Medicine River coal. The surface in the foreground is the Paleozoic unconformity restored to a Medicine River Coal Zone datum, and the surface in the background defines the top of the Medicine River coal relative to the same datum.*

COALBED METHANE RESEARCH IN CANADA

F.M. Dawson

Geological Survey of Canada, 3303-33 Street N.W., Calgary, Alberta T2L 2A7

INTRODUCTION

Coalbed methane is rapidly becoming a major hydrocarbon resource in the United States. Cumulative annual gas production was in excess of 550 BCF (end of 1992) and coal bed gas accounted for up to 20 per cent of the State of New Mexico's hydrocarbon production. Technically recoverable resource estimates for the United States are placed at 62 to 135 TCF (GRI, 1993).

Canada also contains abundant coal resources spread throughout numerous basins in British Columbia, Alberta, Saskatchewan, the Maritimes, Yukon and Northwest Territories. Many of these basins contain coal of suitable quality and at sufficient depth to be considered for coalbed methane reservoirs. In most of the coal-bearing basins, the distribution of the coals is well defined near surface, as a result of the historical mining of coal for domestic or export utilization. The coals that lie at depth however are poorly defined, both qualitatively and volumetrically leading to a high degree of uncertainty in coalbed methane (CBM) resource estimates. Coupled with a general lack of knowledge of actual gas contents and gas capacities of the coal and reservoir permeability, the resource base and economic potential of coalbed methane in Canada is essentially undefined. The Institute of Sedimentary and Petroleum Geology initiated a CBM research program in 1990 to study the potential for CBM in Canada and eventually to define the resource potential. This paper presents a summary of the types of CBM research studies currently ongoing under the auspices of this program.

GAS CAPACITY CURVES

In order to assess the CBM resource potential for the coal-bearing basins in Canada, two primary elements are required: coal volumes and gas content. Coal volumetrics are being acquired through deposit modelling under the National Coal Inventory and will not be addressed in this paper. Gas content data, in the form of actual desorption data or adsorption isotherms, are obtained for potential CBM reservoirs in coalbearing areas across Canada. Much of these data are acquired through joint venture projects with private industry. Most of the data are concentrated in the foothills and plains region of the Western Canada sedimentary basin, primarily as a function of where CBM exploration activities have been focused (Fig. 1).

Gas capacity curves (adsorption isotherms), and desorption data where available, provide a numerical estimate of the gas content (cc/g) of the coal at varying depths of the potential reservoir. Adsorption isotherm curves illustrate the adsorptive capacity of the coal for methane at varying pressures under controlled temperature conditions. Gas content isotherms reflect actual gas content of the coal under reservoir conditions. In many cases the gas content will be less than the gas capacity for the coal sample, suggesting the

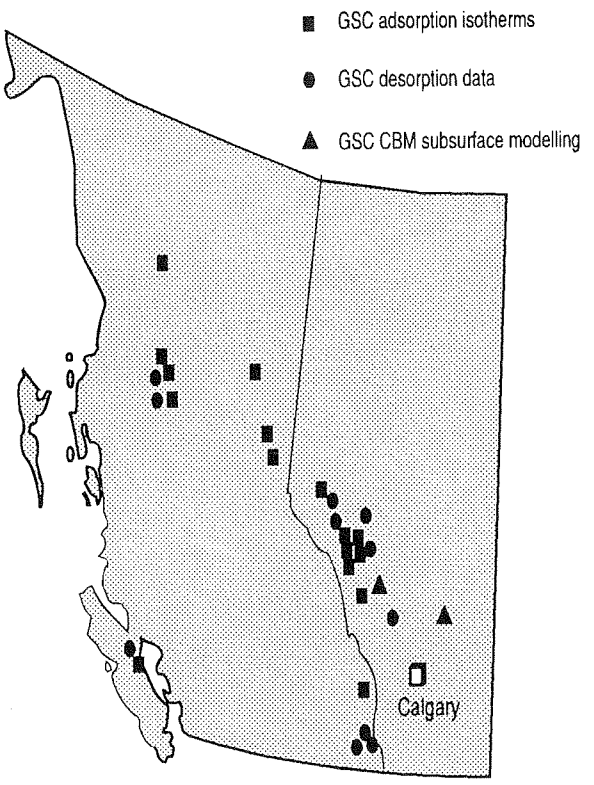

Figure 1. *Map illustrating desorption and adsorption isotherm data locations for potential coalbed methane reservoirs in Western Canada.*

reservoir may be undersaturated (Fig. 2). The shape of the adsorption/desorption curves are also used to determine the diffusion rate of the coal sample and assist in production modelling of the reservoir.

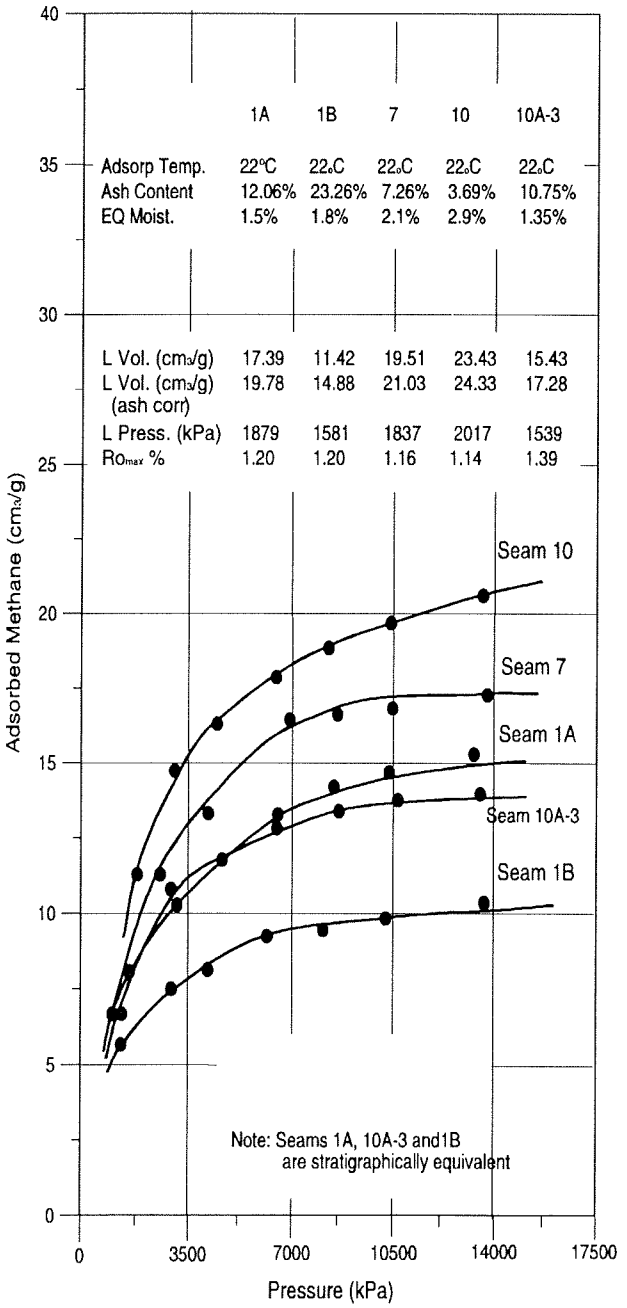

Figure 2. *Adsorption isotherm for coal samples from the Mist Mountain Formation, southeastern British Columbia.*

COAL CHARACTERIZATION

Maceral and mineral matter distribution of the coal itself play an important role in gas capacity and diffusion rate. Previous studies by other researchers have suggested that vitrinite content is the major controlling factor toward gas capacity within the coal sample (Lamberson and Bustin, 1993). Sample analyses of adsorption isotherms and maceral distributions using multivariate analyses indicate that vitrinite and inertinite and mineral matter all contribute to control the adsorptive capacity of the coal and that it is difficult to separate the individual relationship of any given component (Dawson et al., unpublished, 1994). Joint research projects undertaken with B.D. Ryan of the B.C. Geological Survey Branch have determined that the mineral matter (ash) component of the coal serves not only as a diluent (i.e., negative gas adsorptive capacity) but also damages the adsorptive capacity of the coal. Figure 3 illustrates an ash versus gas capacity curve for coal samples from the Mist Mountain Formation of southeastern British Columbia. The steeper portion of the curve occurs where the ash content is less than

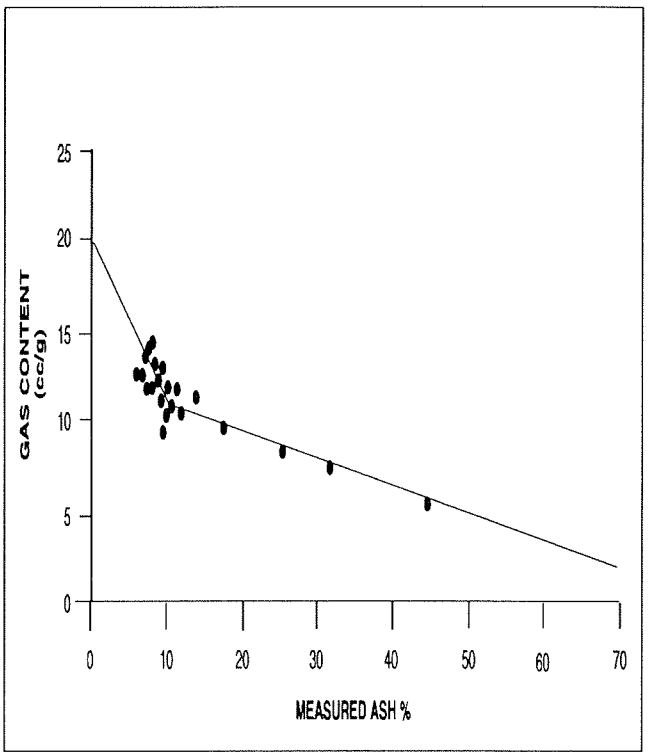

Figure 3. *Ash versus gas capacity curve for coal samples from the Mist Mountain Formation, southeastern British Columbia. Note the two slope shape of the curve and its effect on adsorptive capacity of the coal.*

10 per cent, indicating that the inherent ash component has a greater influence on the adsorptive capacity than the purely diluent component defined by the flatter curve and higher ash components. It is hypothesized that the inherent ash component not only acts as a diluent but also damages the adsorptive capacity of the coal by clogging the pore throats. Detailed maceral composition analyses and SEM work are being undertaken to examine this relationship further.

MICROPERMEABILITY

Permeability in the form of cleat and fracture development within the coal seam is critical to enable the desorbed methane gas to migrate to the borehole. This fracture network varies in order of magnitude between micropermeability (those fractures that are recognized using microscopic equipment) and macropermeability (those fractures visible to the naked eye). Research work conducted by the author indicates that maceral composition, rank and tectonic overprinting are the major controlling factors on cleat and fracture development. Experiments using a profile micropermeameter and image-based analyzing system have enabled detailed profiles of absolute permeability and maceral composition to be constructed on slabbed coal samples. Data from these experiments indicate that banded coals (i.e., thin bands of vitrinite and inertinite) appear to have the highest micropermeability (Fig. 4). Commonly, where coals have achieved a rank of 0.9% Ro_{max} or greater, devolatization of the coals has led to extensive cleat development, particularly in the vitrinite rich bands (Fig. 5). Inertinite rich bands tend to be poorly cleated but do display horizontal fractures at the bedding boundaries. Where the coals are of a lower rank, cleat apertures are poorly developed irrespective of vitrinite content (Dawson et al., 1994). Further research is ongoing to quantify the degree of cleat development to vitrinite form and distribution.

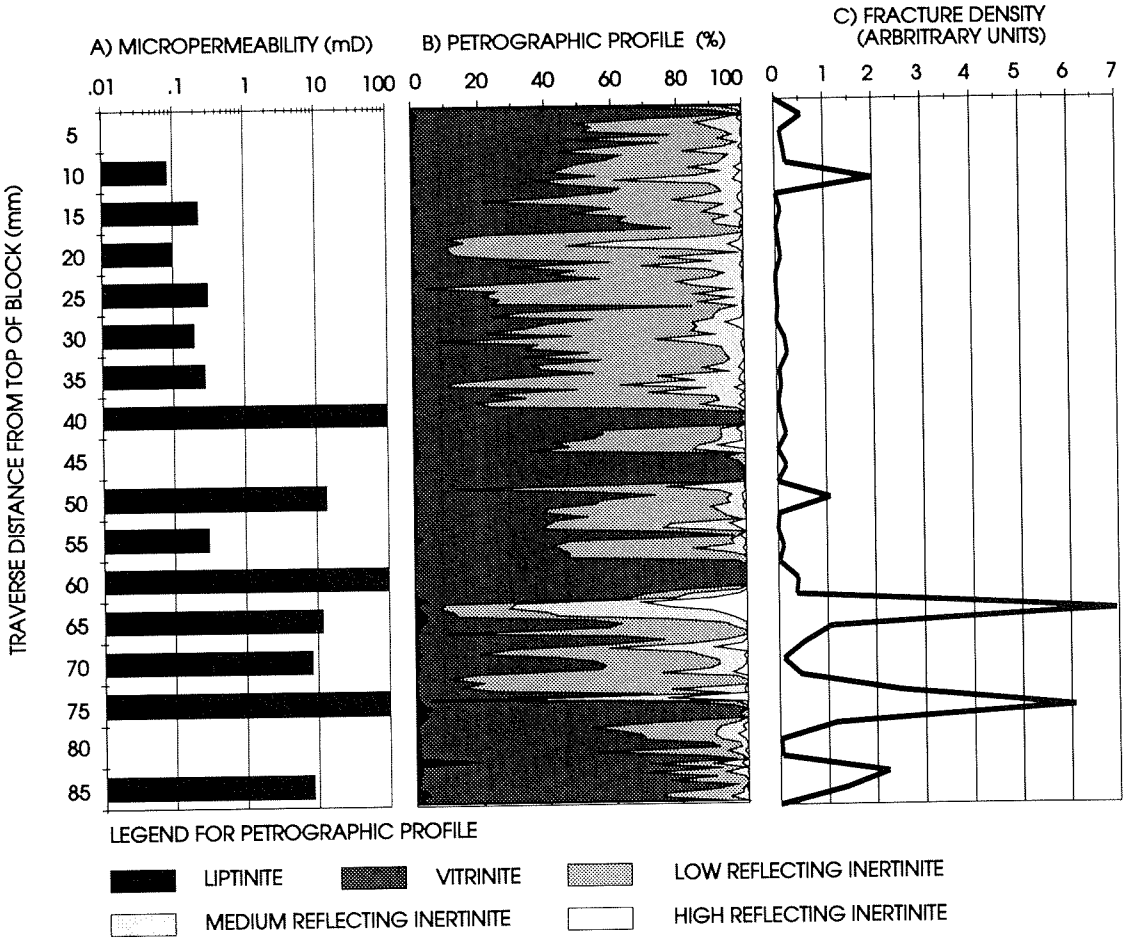

Figure 4. *Micropermeability and maceral profile for slabbed coal sample, Gates Formation, northwestern Alberta foothills.*

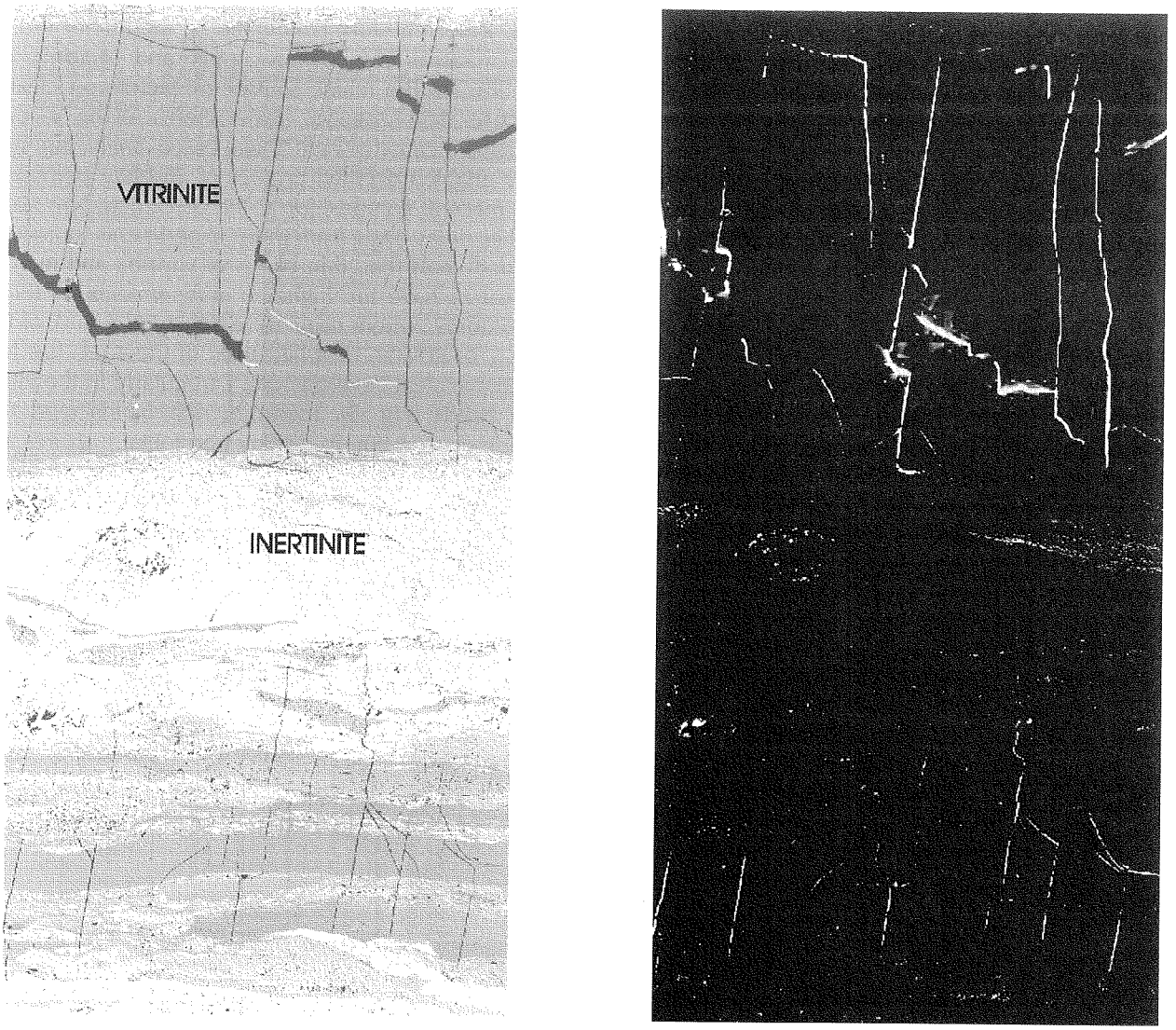

Figure 5. Digital image of maceral composition illustrating banding of vitrinite rich and inertinite rich coal bands. High fluorescence index reflects the significant cleat and fracture development vertically within the vitrinite bands.

CONCLUSIONS

Canada's abundant coal deposits present a vast potential for the development of unconventional coalbed methane resources. Exploration and development of this resource will require an understanding of the gas content of the coal and permeability of the reservoir. Research activities of the Coal Subdivision of the ISPG are addressing these variables, resulting in the presentation of data and analyses to private industry. These results are used by industry to explore and develop the coalbed methane resources of Canada in a cost effective manner.

REFERENCES

Dawson, F.M., Ryan, B.D., Clow, J.T., and Pratt, K.
1994: Coalbed Methane Micropermeability Project–Final Report. Unpublished Multi-client study, 120 p.

GRI
1993: Quarterly Review of Methane from Coal Seams Technology. Gas Research Institute, v. 11, no. 1, August, 1993.

Lamberson, M.N. and Bustin, R.M.
1993: Coalbed Methane Characteristics of Gates Formation Coals, Northeastern British Columbia: Effect of Maceral Composition. The American Association of Petroleum Geologists Bulletin, v. 77, no. 12, p. 2062–2076.

EARTHQUAKES AT THE EAGLE OIL FIELD NEAR FORT ST. JOHN, B.C.

R.B. Horner

Geological Survey of Canada
P.O. Box 6000, Sidney, B.C. V8L 4B2

J.E. Barclay

Geological Survey of Canada, 3303-33rd Street N.W., Calgary, Alberta T2L 2A7

Presently at:
Hardy Oil and Gas Canada Ltd.
1000, 530-8th Avenue S.W., Calgary, Alberta T2P 3S8

J.M. MacRae

B.C. Ministry of Energy, Mines and Petroleum Resources
1810 Blanchard Street, Victoria, B.C. V8V 1X4

R.J. Wetmiller and I. Asudeh

Geological Survey of Canada
1 Observatory Crescent, Ottawa, Ontario K1A 0Y3

ABSTRACT

Microearthquake surveys at the Eagle oil field (84-18W6M) near Fort St. John, B.C., in January–March 1993 and November 1993–March 1994 found hypocentres of low-magnitude earthquakes within a few kilometres (km) of both production and injection wells in the southern and eastern areas of the Field. Focal depths were confined to Paleozoic strata at depths of 2–3 km below sea level. This zone lies just below the producing Belloy (Permian) Formation and above the Precambrian basement at depths of about 1.2 and 4 km, respectively. A composite focal mechanism solution using all of the small earthquakes located during the latter survey indicates thrust faulting on NW–SE striking planes. That is consistent with the inferred state of stress in this region of the Peace River Arch as well as the orientation of some inferred faults in the Belloy Formation. The larger earthquakes that have occurred since January 1992 appear to lie in the areas defined by the microearthquake surveys; the 1992 and 1993 events in the south-central part of the Eagle Field and the 1994 events including a magnitude (M) 4.3 event on May 22nd, near the eastern boundary of the Field.

Water injection at the Eagle Field commenced in November 1985, prior to the first known earthquakes. Surface injection pressures of about 25 MPa are high enough to possibly induce movement on suitably oriented pre-existing faults. The occurrence of larger earthquakes in 1992-1993 and 1994 appears to coincide with increased water volumes injected at wells in those areas of the Field. As injection proceeded across the Field from SW to NE, apparently so too did the seismicity. The more accurately determined epicentres lie near the south and east edges of the reservoir where permeability would be sufficient to allow for fluid migration from the injection wells. These results support the hypothesis that water injection into the Belloy Formation for secondary oil recovery may be a trigger for this seismicity by inducing movement on pre-existing, high-angle basement-rooted faults activated mainly during Carboniferous development of the Fort St. John graben.

INTRODUCTION

Earthquakes have occurred near Fort St. John, B.C., since 1984 and show both spatial and temporal correlations with oil extraction and associated water injection for secondary recovery from the Belloy (Permian) Formation in the Eagle West and Eagle Fields (Horner et al., 1994). The first earthquakes in 1984

were relatively low-magnitude events, M <3, centred near the western boundary of the Eagle West Field. Fluid injection had been initiated there 4 years earlier. Most of the earthquakes, however, have occurred near the Eagle Field about 10 km further east in 2 distinct sequences in January–February 1992 and December 1992–January 1993. The latter sequence included events as large as M 4.0 that were felt with Modified Mercalli intensities as high as V over areas as large as 2000 km^2. Subsequently, the largest earthquake to date, M 4.3, occurred in the same area on May 22, 1994, and was followed by a M 3.1 event on August 25. In addition, 4 small events occurred between 1985 and 1989, M 2.5–3.1, but are not well located. A seismicity survey conducted in January–March 1993 found low-magnitude events exclusively in the Eagle Field and although focal depths were not accurately determined, they did appear to be consistent with reservoir depths. Fluid injection was initiated at the Eagle Field in 1985 with surface pressures of about 25 MPa. These observations along with the typically very low seismicity levels in this region of the western Canada sedimentary basin led Horner et al. (1994) to conclude that as in similar cases (e.g., Davis and Frohlich, 1993), fluid injection should be considered as a possible cause of these earthquakes.

This paper will present the results of a detailed seismicity survey conducted over the Eagle Field from November 1993 to March 1994. An earlier survey in 1993 (Horner et al., 1994) is re-evaluated and the epicentres of M 3 and larger earthquakes from 1992 to present are relocated. Water injection and pressure histories from wells in the Eagle Field are then compared with the earthquake record to assess possible correlations.

SEISMICITY SURVEYS

November 1993-March 1994

Six Scintrex PRS4 digital 3-component seismographs were deployed in an area of about 50 km^2 over the Eagle Field near the end of November 1993 (Fig. 1). The seismographs operated to the end of March 1994 and recorded several hundred very small earthquakes, all less than M 1. Thirty-five of these events were recorded at 3 or more stations and could be located. The hypocentres are plotted in Figure 1 and listed in Table 1 along with horizontal and vertical standard errors that are generally less than about 1 km.

The velocity model used to calculate these hypocentres is shown in Figure 2. RMS P-velocities

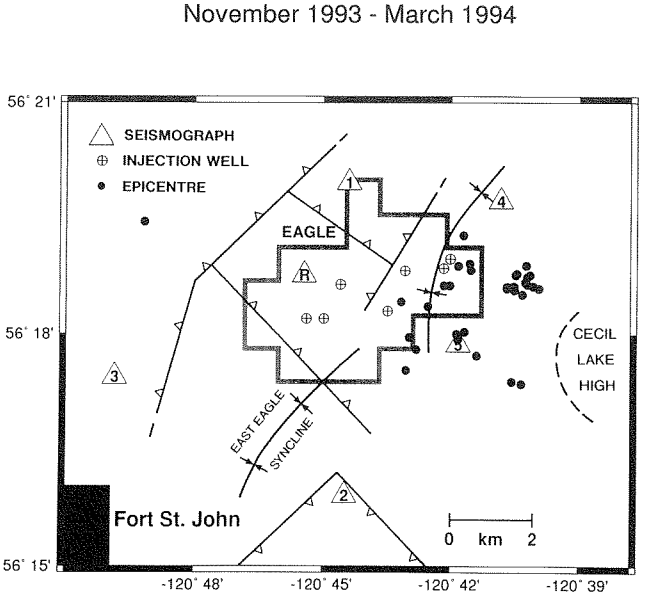

Figure 1. *Seismograph locations, injection wells in the Eagle Field (the Unit boundary is shown) and earthquake epicentres determined during the November 1993–March 1994 survey (Table 1). Oil wells are not plotted. Also shown are faults (ticks on downthrown side) and other structural elements affecting the Belloy Formation (provided by Home Oil Company Limited, Calgary).*

down to Belloy Formation depths were calculated from 4 sonic logs in the Eagle Field. Below the Belloy Formation, velocities were determined from a sonic log at a nearby well (12-10-83-17W6) that extended to near basement depth. S-velocities were calculated using a constant P:S ratio of 1.73.

The epicentres, with one exception. were all confined to near the east and southeast boundaries of the Eagle Unit. The most prominent feature is a cluster of events just east of the Unit boundary (Fig. 1). There also appear to be 2 linear orthogonal zones, one running SW–NE along the southeast side of the Unit and the other trending NW–SE through site 5. Both are about 4–5 km in length. The hypocentres are projected onto a SW–NE section through the field in Figure 3. Focal depths are confined to Paleozoic strata below the Belloy Formation and above the Precambrian basement, however, taking into account depth uncertainties of about +/- 1 km it is possible that some of the earthquakes could lie in or above the Belloy Formation, or in the basement.

One earthquake was located west of the Eagle Field (in the Eagle West Field) at a depth of about 6 km. This

Table 1

Hypocentres determined during the November 1993–March 1994 seismicity survey at the Eagle Field near Fort St. John B.C.

Date	Time	Sec	Latitude °N	Longitude °W	Depth km	St	Ph	RMS sec	MajH km	MinH km	VertE km	AzH °
1993/12/03	0525	38.44	56.2993	120.7163	2.82	4	8	0.04	0.46	0.27	0.73	006
1993/12/07	0610	58.88	56.2967	120.7135	3.52	3	6	0.03	0.55	0.32	0.91	068
1993/12/12	0917	33.68	56.3138	120.6923	2.14	3	5	0.01	0.36	0.22	1.00	118
1993/12/12	2024	21.71	56.3152	120.6927	2.14	3	5	0.02	0.36	0.23	1.00	118
1993/12/18	1121	07.29	56.3148	120.6707	2.60	4	7	0.04	0.77	0.32	0.83	112
1993/12/19	1602	02.91	56.3213	120.6952	2.49	3	5	0.05	0.68	0.80	0.97	016
1993/12/21	0052	53.37	56.3103	120.6755	2.29	4	6	0.01	0.79	0.24	0.88	105
1993/12/26	0128	34.82	56.3085	120.6722	1.99	3	5	0.00	1.64	0.25	2.14	105
1993/12/26	0206	35.34	56.3112	120.6710	3.06	5	8	0.06	0.55	0.28	0.52	121
1993/12/30	1306	41.15	56.3098	120.6658	1.67	3	5	0.01	0.95	0.25	6.57	107
1993/12/30	1547	25.62	56.3000	120.6978	3.16	3	5	0.01	1.33	0.39	0.65	097
1993/12/31	2249	37.58	56.3127	120.6747	2.12	3	5	0.01	0.78	0.24	0.84	103
1993/12/31	2249	50.59	56.3130	120.6743	2.11	3	5	0.01	1.31	0.25	1.58	107
1993/12/31	2251	0.813	56.3128	120.6747	2.21	3	5	0.01	0.78	0.24	0.82	103
1994/01/01	1415	53.57	56.3147	120.6972	2.24	3	5	0.01	0.82	0.24	1.49	104
1994/01/02	0824	09.58	56.3127	120.6692	2.21	3	5	0.01	0.72	0.26	0.83	102
1994/01/02	1137	15.63	56.3123	120.6703	1.91	3	5	0.01	0.82	0.24	1.49	104
1994/01/08	0420	0.714	56.3105	120.7005	3.12	4	7	0.01	0.38	0.30	0.57	078
1994/01/23	0932	57.84	56.3105	120.7027	3.24	4	7	0.01	0.35	0.28	0.51	060
1994/01/25	0039	50.45	56.3107	120.6703	1.99	3	5	0.01	1.66	0.25	2.24	106
1994/01/25	0158	15.22	56.3103	120.6680	1.90	3	5	0.01	0.95	0.25	2.90	106
1994/02/09	0626	49.45	56.2892	120.6725	2.24	5	8	0.03	0.46	0.23	0.64	113
1994/02/11	0626	22.09	56.3102	120.6782	2.17	4	6	0.02	0.67	0.24	0.82	109
1994/02/11	1005	56.57	56.3070	120.7195	3.03	4	6	0.02	0.80	0.37	0.52	093
1994/02/11	1014	13.92	56.3060	120.7090	3.13	4	6	0.01	0.83	0.35	0.56	094
1994/02/20	1315	53.42	56.3098	120.6782	2.11	3	5	0.01	1.04	0.24	0.59	109
1994/02/24	0038	23.28	56.3242	120.8195	5.92	3	6	0.02	0.79	0.37	0.86	150
1994/02/27	0114	22.84	56.2922	120.7175	2.82	3	5	0.01	1.77	0.38	1.83	036
1994/03/05	2000	47.24	56.2988	120.6973	3.20	4	6	0.04	0.82	0.44	0.64	140
1994/93/06	0354	19.30	56.3102	120.6778	2.84	5	7	0.03	0.64	0.28	0.71	110
1994/03/06	0426	33.35	56.3095	120.6753	2.04	3	5	0.01	0.53	0.24	1.10	112
1994/03/07	0934	23.87	56.3005	120.6948	2.92	3	5	0.01	0.48	0.35	0.69	153
1994/03/15	2337	12.23	56.2953	120.6900	2.67	3	4	0.00	1.43	0.72	1.19	076
1994/03/20	1757	30.90	56.2897	120.6762	3.36	3	5	0.03	1.51	0.59	1.42	110
1994/03/26	1407	55.34	56.2930	120.7118	2.75	3	5	0.02	1.43	0.53	0.64	090

Depth = km below sea level
St = number of stations used in the solution
Ph = number of phases used in the solution
MajH = maximum horizontal standard error (68% confidence interval)
MinH = minimun horizontal standard error (perpendicular to MajH)
VertE = depth standard error
AzH = azimuth of MajH

appears to be a somewhat unique event and is not reflected by event counts at individual stations. The highest number of events were observed at sites 5, 4 and 1 (Fig. 1) as indicated by the pattern of located earthquakes.

A composite mechanism solution (Fig. 4) was computed using a total of 74 P and 134 SH polarities from the 34 earthquakes located in or near the Eagle Field (Fig. 1). It indicates almost pure thrust faulting on NW–SE striking planes, dipping 45° either to the NE or SW. The pressure (P) axis is horizontal, oriented NE–SW and in good agreement with the direction of maximum compressive stress determined by Bell and McCallum (1990) for the Peace River Arch area. Thrust and/or strike-slip faulting would be expected in this region. Horner et al. (1994) used hydraulic fracturing data to infer that the minimum compressive stress was vertical but with a magnitude only slightly smaller than that of the horizontal minimum compressive stress.

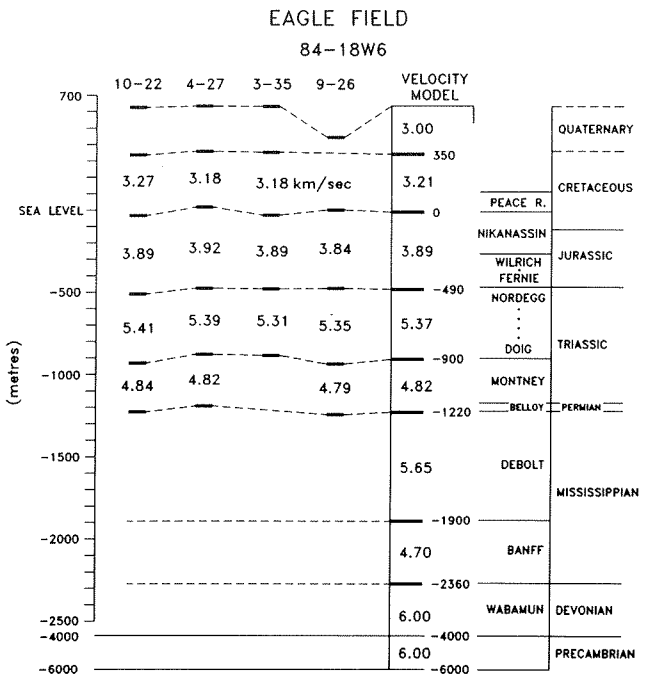

Figure 2. *Velocity model and partial table of formations for the Eagle oil Unit. P velocities were calculated from 4 sonic logs in the Unit. For depths below the Belloy Formation, a sonic log from a nearby well (12-10-83-17W6) was used.*

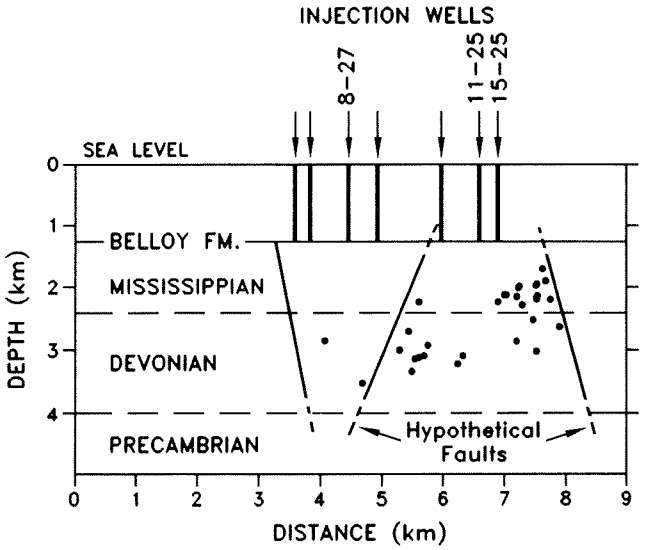

Figure 3. *Hypocentres and injection wells (Fig. 1) projected onto a SW-NE section through the Eagle oil unit. Standard errors on focal depths are about +/-1 km (Table 1). Also shown are hypothetical but typical faults in the area.*

Only 15% of both P and SH polarities are incorrect and suggest a uniform strain release mechanism in this region. The NW–SE strike of the fault plane also coincides with the NW–SE epicentre trend though site 5 as well as inferred faults in the north and southwest parts of the field (Fig. 1).

January-March 1993

Following a sequence of larger earthquakes on January 9, 1993, 5 single-component analogue seismographs were deployed in the Fort St. John area (Fig. 5) for varying time periods to the end of March 1993. Epicentres for 5 events located by Horner et al. (1994) have been relocated using the velocity model shown in Figure 2. Focal depths are fixed to 3 km because of the poor depth resolution of this network. The epicentres remain confined to the south and east areas of the Eagle Field in an SW–NE elongated zone about 4 km in length. This zone overlaps much of the same area that seismicity occurred in during the November 1993–March 1994 survey (Fig. 1), but is shifted further to the southwest.

The insert in Figure 5 shows the difference in P-arrival time at CHBC and CEBC for 11 earthquakes recorded by both seismographs. Comparison with the CHBC–CEBC P-time difference for 4 of the located events would suggest that most of the seismicity occurred in the southern part of the Eagle Field where this difference is about 1.0 sec.

EPICENTRES OF M 3 AND LARGER EARTHQUAKES 1992-1994

Epicentres of the larger earthquakes determined using the regional seismograph network cannot be considered accurate to better than about 10 km because of the wide station spacing and uncertainty in the regional velocity structure (Horner et al., 1994). The May 22, 1994 earthquake, however, was recorded by an analogue seismograph operating at site 5 (Fig. 6). An extensive aftershock sequence exhibited general event characteristics, S–P intervals and wave form appearance, that were very similar to those exhibited by events recorded at site 5 during the November 1993–March 1994 survey. S–P intervals appeared to be less than 1 second and would limit the distance from site 5 to no more than a few km. On this basis the epicentre of the M 4.3 main shock is placed near the centre of the area of seismicity shown in Figure 1, on the eastern boundary of the Eagle Field.

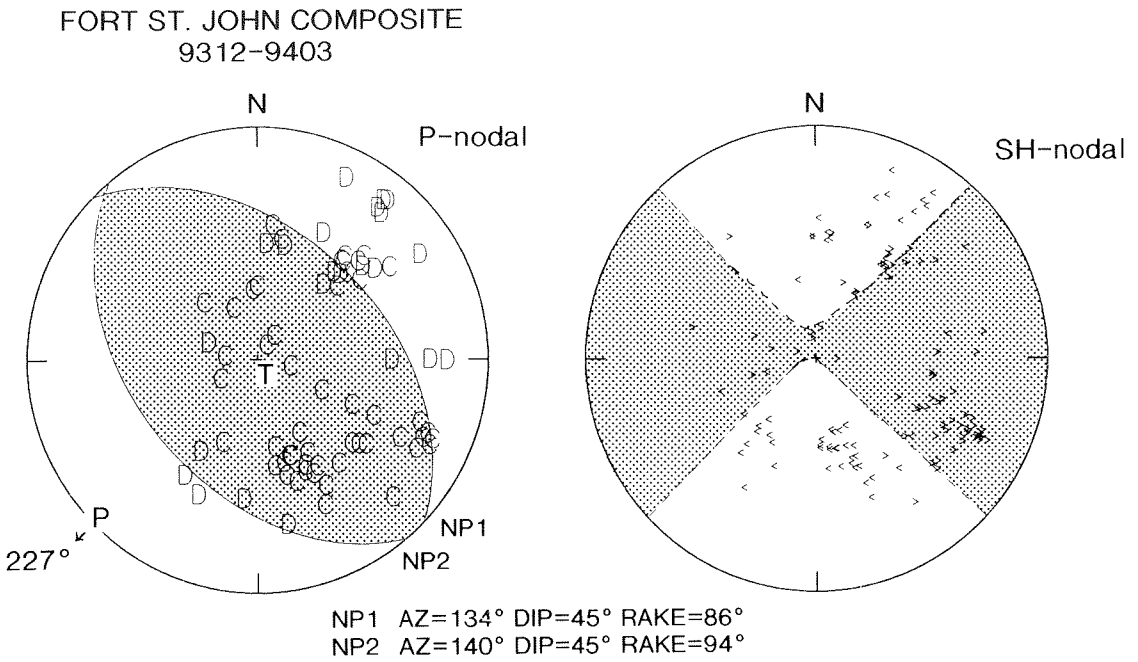

Figure 4. *Composition mechanism solution for the November 1993–March 1994 earthquakes using P and SH polarities. "C" and "D" are compressional and dilational P-first motions, respectively. ">" and "<" are positive and negative SH poloarities, respectively. The lower hemisphere of the focal sphere is shown.*

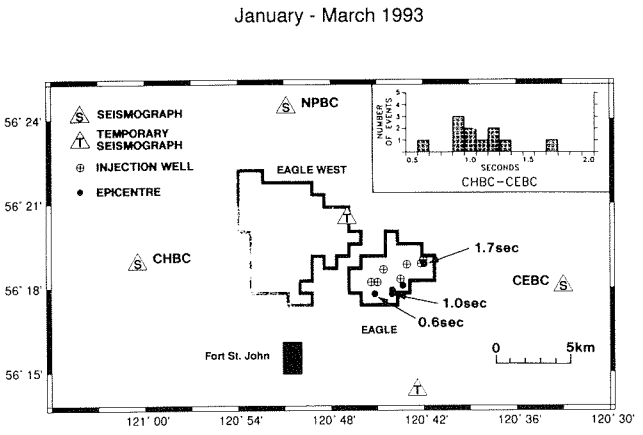

Figure 5. *Seimograph locations, injection wells in the Eagle oil unit and relocated epicentres from the January–March 1993 survey. The outlines of the Eagle West and Eagle oil units are shown. The CHBC-CEBC P arrival time difference is given for 4 of the located events. The insert shows P-arrival time differences at CHBC and CEBC for 11 common events (Horner et al., 1994).*

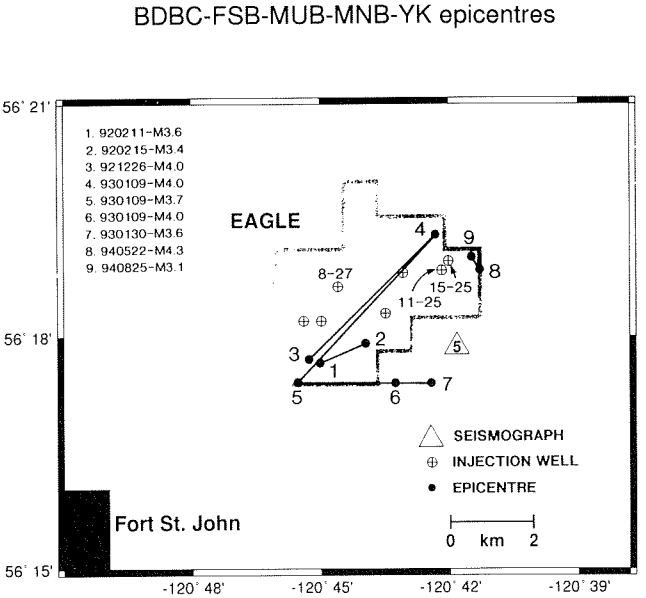

Figure 6. *Epicentre locations of M 3 and larger earthquakes since February 1992, using P arrivals exclusively from a common 5 station network (see Horner et al., 1994, for station locations). The relative locations are tied to the epicentre of the May 22, 1994 earthquake (#8) near the east boundary of the Eagle Unit (see text).*

Relative to the May 22 event, the epicentres of 8 other M 3 and larger earthquakes that occurred from February 1992 to August 1994 (Fig. 6) were determined using P arrivals exclusively, from a common 5-station network at distances ranging from about 100–800 km (see Horner et al., 1994 for station locations). The resulting accuracy of the epicentres relative to each other is estimated to be a few kilometres. The distribution suggests that the February 1992, December 1992 and January 1993 events occurred very close together and perhaps a few km southwest of the 1994 events. This location for the 1992–1993 earthquakes also corresponds closely to the area outlined by the January–March 1993 survey (Fig. 5) and suggests that the small events located during that survey could be aftershocks.

WATER INJECTION AS A TRIGGER?

Water injection was initiated at the Eagle Field in November 1985, prior to the onset of seismicity. The earliest known earthquake at the Eagle Field may have occurred in February 1986, however, this event and 3 other relatively low-magnitude events before 1992 (Fig. 7) are not well located. Water is injected into the Belloy (Permian) Formation at a depth of about 1.9 km below surface (Fig. 2). Total monthly injection rates

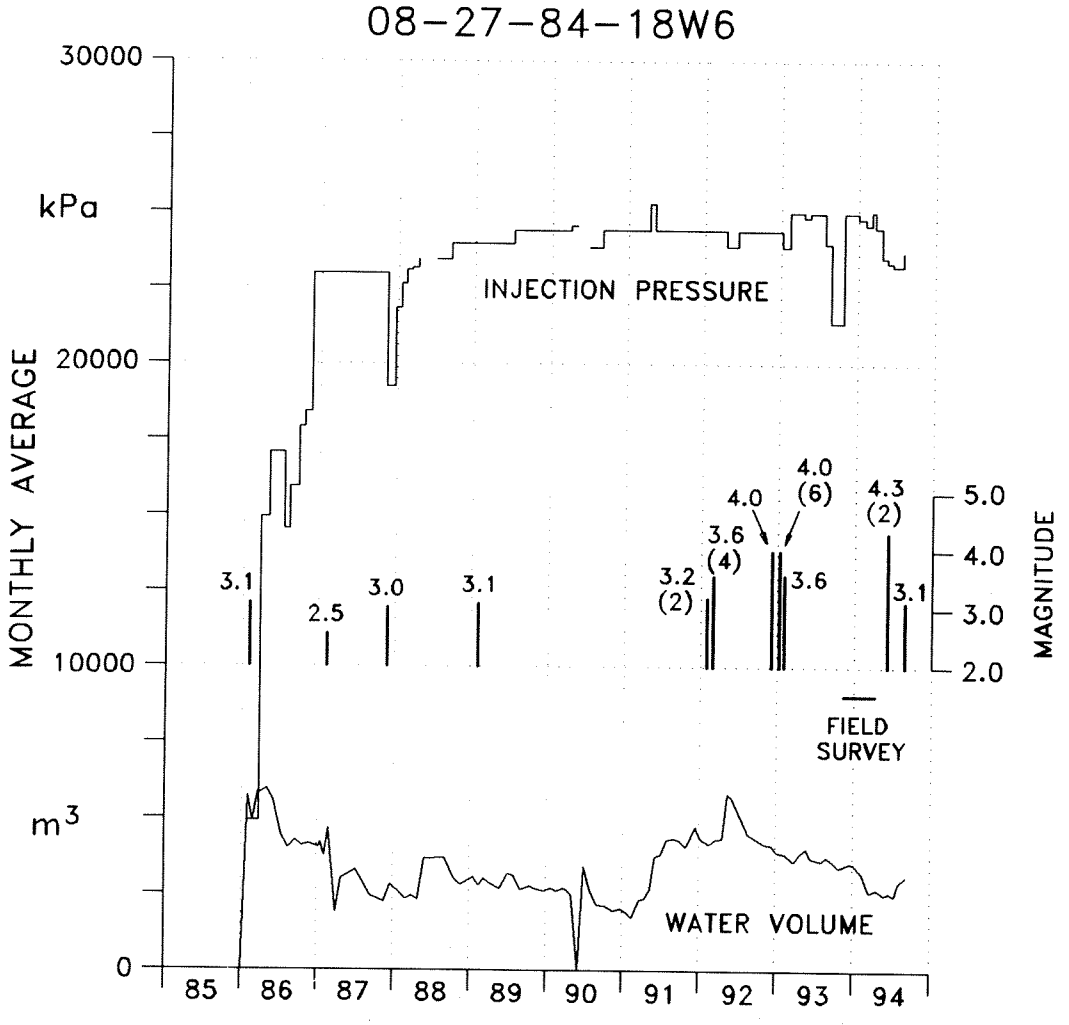

Figure 7. *Average monthly injection pressure and monthly water volumes at well 8-27-84-18W6, located near the centre of the Eagle Unit (Fig. 1), from 1985 to September 1994. The times and magnitude of earthquake activity is marked. The total number of earthquakes above about M 2.5 in each sequence is also indicated. Not shown are the 1984 earthquakes, M <3, believed associated with the Eagle West Unit.*

reached a maximum value of about 19 000 m^3/month in 1988, with maximum wellhead pressures of about 25 MPa. Horner et al. (1994) demonstrated that these pressures were possibly high enough to induce movement on suitably oriented faults according to the theory of effective stress (Hubbert and Ruby, 1959). Hypothetical but typical faults in this area are shown in Figure 3. They are basement-rooted, high-angle faults that were mainly active during Carboniferous development of the Fort St. John graben (see Barclay et al., 1990; Horner et al., 1994, and references therein). The distribution of hypocentres below the reservoir might suggest that faults like these are being re- activated. At Rangely, Colorado, where seismicity was clearly related to fluid injection (Raleigh et al., 1972), the hypocentres were also restricted to a 2 km deep zone below the reservoir.

Earthquake and injection histories are compared in Figures 7 and 8. At a well near the centre of the Eagle Field with the largest volume of water injected (8-27 in Figure 6), and presumably near the epicentres of the larger earthquakes in 1992 and 1993, water volumes were approximately doubled in 1991 to about 5000 m^3/month (Fig. 7). They peaked in 1992 to just over 6000 m^3/month before declining gradually to about 3000 m^3/month in 1994. Similarly the May 22, 1994 earthquake, presumably in the eastern part of the Eagle Field, also appears to coincide with an increase in water volume. At well 11-25 (Fig. 6) injecion volumes

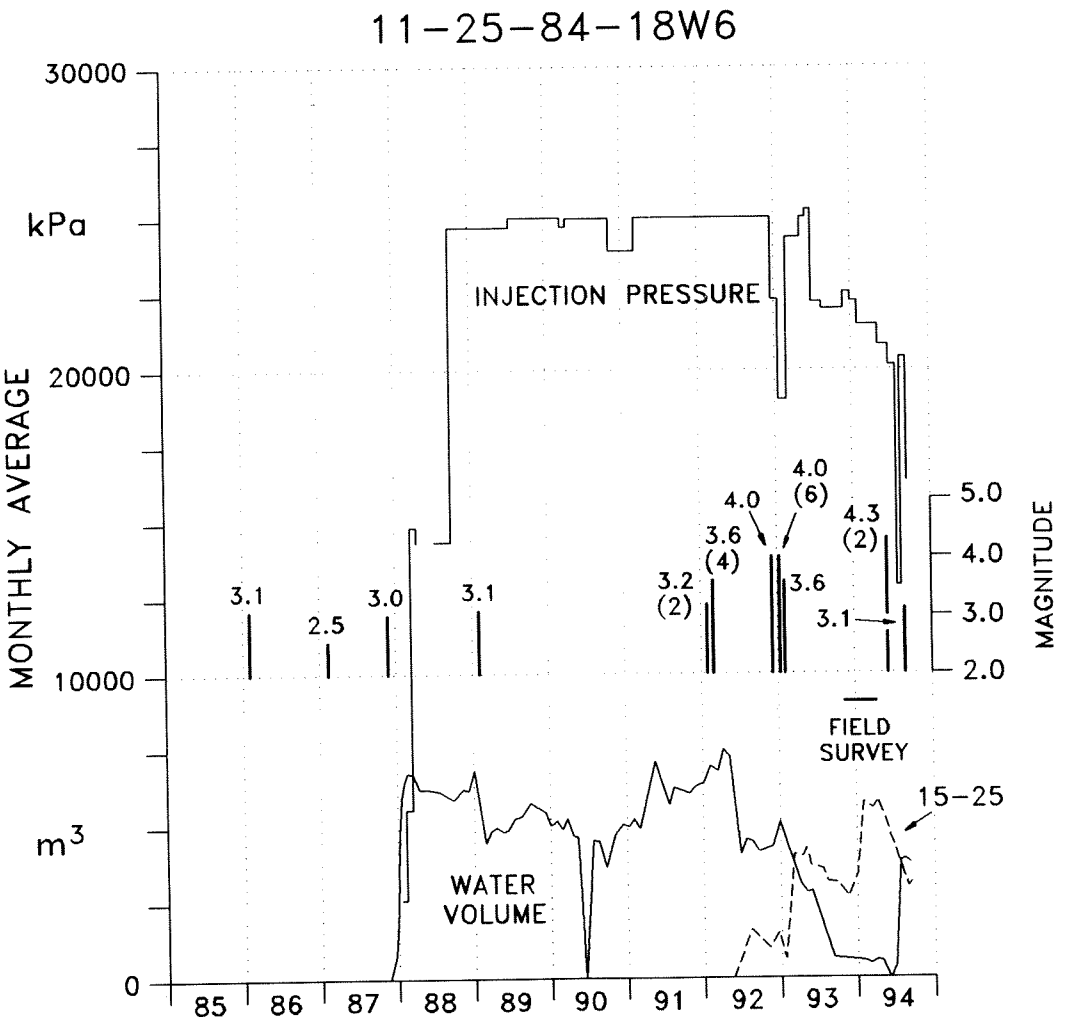

Figure 8. *Average monthly injection pressure and montly water volumes at well 11-25-84-18W6, located in the eastern part of the Eagle Unit (Fig. 1), from 1985 to September 1994. Included are the average montly water volumes injected at a nearby well (15-25-84-18W6) that started in June 1992. Earthquake activity from Figure 7 is also shown.*

of more than about 5000 m^3/month since late 1987 were decreased to under 1000 m^3/month in June 1993. Average monthly volumes remained low until June 1994 when they were increased back up to about 4000 m^3/month (Fig. 8). Combined with water injected at a nearby well (15-25 in Fig. 6) the total volume was doubled from about 4000 m^3/month in December 1993 to about 8000 m^3/month by July (Fig. 8). Although the signifigance of these observations is not clear, we also note that just as injection generally proceeded from the southwest to the northeast parts of the Eagle Field, so too did the seismicity.

The accurately determined epicentres from the two field surveys are plotted on a permeability–net pay (kh) contour map of the Eagle reservoir in Figure 9. The contours exhibit an overall SW–NE trend imprinted on a weaker NW–SE trend. These probably reflect original depositional trends. Faults restrict the reservoir to the west and southwest (Fig. 1). The SW–NE trending fault through the north part of the Field also appears to seal the west side of the reservoir from the east side. To the east, however, the reservoir appears to be mainly restricted by a thinning of the Belloy Formation toward the Cecil Lake high (Fig. 1). Faults are not mapped here but that may be mainly due to poor well control. Most of the earthquakes lie in this region on the south and east edge of the reservoir where permeability would appear sufficient to allow fluid migration from the injection wells to these sites. The apparent SE trending seismicity zone away from the field might represent a re-activated fault.

93/01-93/03 and 93/11-94/03

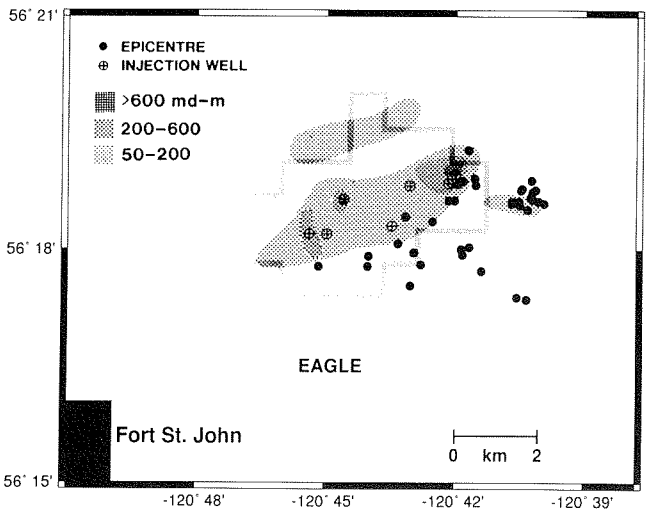

Figure 9. *Permeability–thickness (kh) contour map of the Eagle oil Unit (provided by Home Oil Company Limited, Calgary), injection wells and epicentres determined during the 2 field surveys (Figs. 1, 5).*

CONCLUSIONS

A seismicity survey over the Eagle Field from November 1993 to March 1994 found epicentres of low-magnitude events within a few km of production and injection wells, mainly near the southeast and east boundaries of the field. Focal depths of about 2–3 km below sea level appear to be confined to Paleozoic strata below the Belloy Formation. A focal mechanism solution indicates thrust faulting on NW–SE trending planes, consistent with the inferred state of stress in the region and the orientation of some inferred faults in the Belloy Formation. The epicentres of the magnitude 3 and larger earthquakes that have occurred since February 1992, appear to coincide with the areas defined by the seismicity surveys; the 1992 and 1993 earthquakes in the south-central part of the Eagle Field and the 1994 events a few km to the NE near the eastern boundary. The earthquakes show both spatial and temporal correlations with water injection. The areal extent of the seismicity also appears to be influenced by the permeability distribution. These results provide additional support for the hypothesis put forward by Horner et al. (1994) that water injection into the Belloy Formation for secondary oil recovery should be considered as the trigger for this seismicity.

ACKNOWLEDGMENTS

We gratefully acknowledge the active participation and support of Home Oil Company Limited, Calgary; in particular, Don Cairns and Dean Terrien who operated the digital seismographs during the November 1993–March 1994 survey; also Greg Kuran, Doug Uffen and Sid Leggett who provided the Eagle production and geological data used in this paper as well as much useful discussion. We also thank Mel Best and Garry Rogers for their comments. The field work also could not have been accomplished without the enthusiastic assistance of John Carter and Scott Dodd from the GSC offices in Sidney and Ottawa, respectively. Taimi Mulder assisted with the data processing. We thank Mary Wade, Neil Thompson, Terry and Carolyn Wood, and Marjorie and Leo Copes for operating the analogue seismographs and for their continuing support. We also thank Bob Lamoureux, Dick Katerberg, Steve Moore, Merle Plamondon and Leo Copes for allowing us to install seismographs on

their property during the November 1993–March 1994 survey.

REFERENCES

Barclay, J.E., Krause, F.F., Campbell, R.I., and Utting, J.
1990: Dynamic casting and growth faulting of the Dawson Creek Graben Complex: Carboniferous-Permian Peace River Embayment, Western Canada. *In* Geology of the Peace River Arch, S.C. O'Connell and J.S. Bell (eds.). Bulletin of Canadian Petroleum Geology, v. 38A, p. 115–145.

Bell, J.S. and McCallum, R.E.
1990: In situ stress in the Peace River Arch area, Western Canada. *In* Geology of the Peace River Arch, S.C. O'Connell and J.S. Bell (eds.). Bulletin of Canadian Petroleum Geology, v. 38A, p. 270–281.

Davis, S.D. and Frohlich, C.
1993: Did (or will) fluid injection cause earthquakes?-Criteria for a rational assessment. Seismological Research Letters, v. 64, p. 207–224.

Horner, R.B., Barclay, J.E., and MacRae, J.M.
1994: Earthquakes and hydrocarbon production in the Fort St. John area of Northeastern British Columbia. Canadian Journal of Exploration Geophysicists, v. 30, in press.

Hubbert, M.K. and Rubey, W.W.
1959: Role of fluid pressure in overthrust faulting. Geological Society of America Bulletin, v. 70, p. 115–206.

Raleigh, C.B., Healy, J.H. and Bredehoeft, J.D.
1972: Faulting and crustal stress at Rangely, Colorado. *In* Flow and fracture of rocks (Griggs volume), H.C. Heard, I.Y. Borg, N.L. Carter and C.B. Raleigh (eds.). American Geophysical Union Geophysical Monograph, v. 16, p. 275–284.

REGIONAL CHARACTERIZATION OF LANDSLIDE ACTIVITY, ALBERTA FOOTHILLS NATMAP

L.E. Jackson Jr.

Geological Survey of Canada, Terrain Sciences Divison
100 West Pender Street, Vancouver, B.C. V6B 1R8

GENERAL GEOLOGIC FRAMEWORK AND LANDSLIDING STYLES

Bedrock and surficial geology naturally divide the Alberta Foothills NATMAP project area (Fig. 1) into four provinces with respect to landslide activity. These are the Interior Plains and Porcupine Hills, Foothills, and glaciolacustrine fills in Foothills valleys, Rocky Mountains. Each province is characterized by a distinctive suite of slope failures.

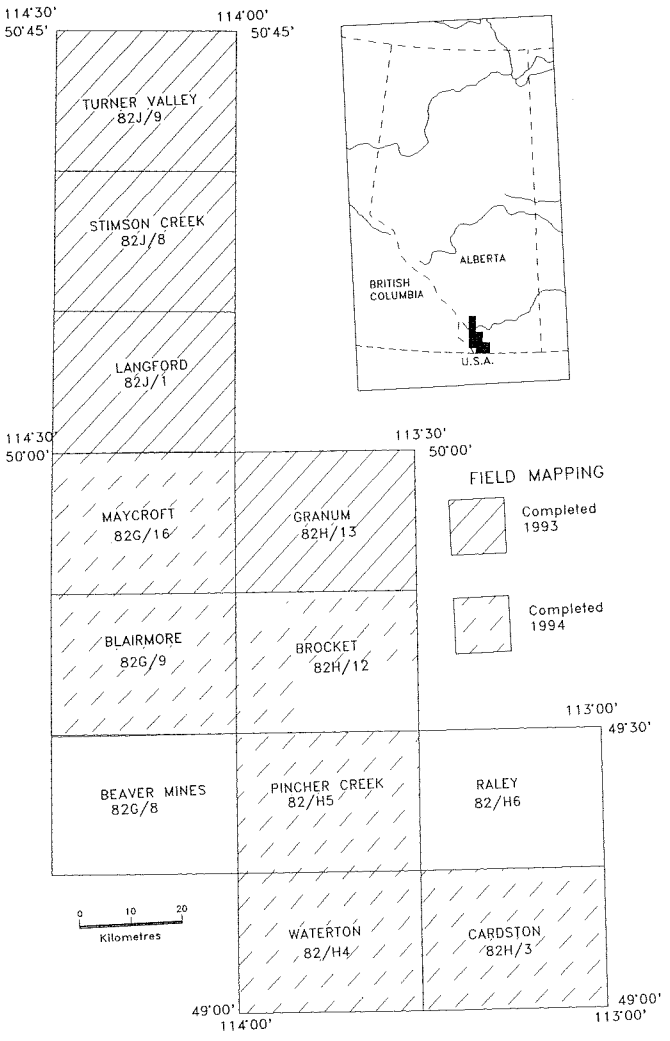

***Figure 1.** Location map showing 1:50 000 map areas for which surficial geology mapping has been completed.*

LANDSLIDE PROVINCES

Porcupine Hills and Interior Plains

Landslides are predominantly rotational slumps and earthflows that originate within shale units [Figs. 2 (indicated by diamond symbol) and 3]. They occur along valley sides within higher relief areas of the Porcupine Hills or on the outside of active contemporary stream bends or the margins of former meltwater channels such as the valley of Callum Creek and Oldman River west of Porcupine Hills. Oversteepening of valley sides, underlain by weak, expansive shales, by glaciofluvial or fluvial erosion appears to be the underlying cause of slope failures within this geologic/structural province.

Foothills

Landslides originating entirely within bedrock are relatively uncommon within this belt compared to the Porcupine Hills to the east and the Rocky Mountains to the west. The largest landslides in the Foothills are planar rockslides along dip slopes where slope angles and bedding dip angles are close in value (Fig. 4, BM). Slides also occur where bedding is intersected obliquely to dip along steep sided valleys.

Several factors account for the relatively low occurrence of landsliding in the Foothills:

1. Rocks are generally more competent within the Foothills than are younger units in the Porcupine Hills and they have not been weakened by shearing to the extent that correlative units have within the Rocky Mountains.

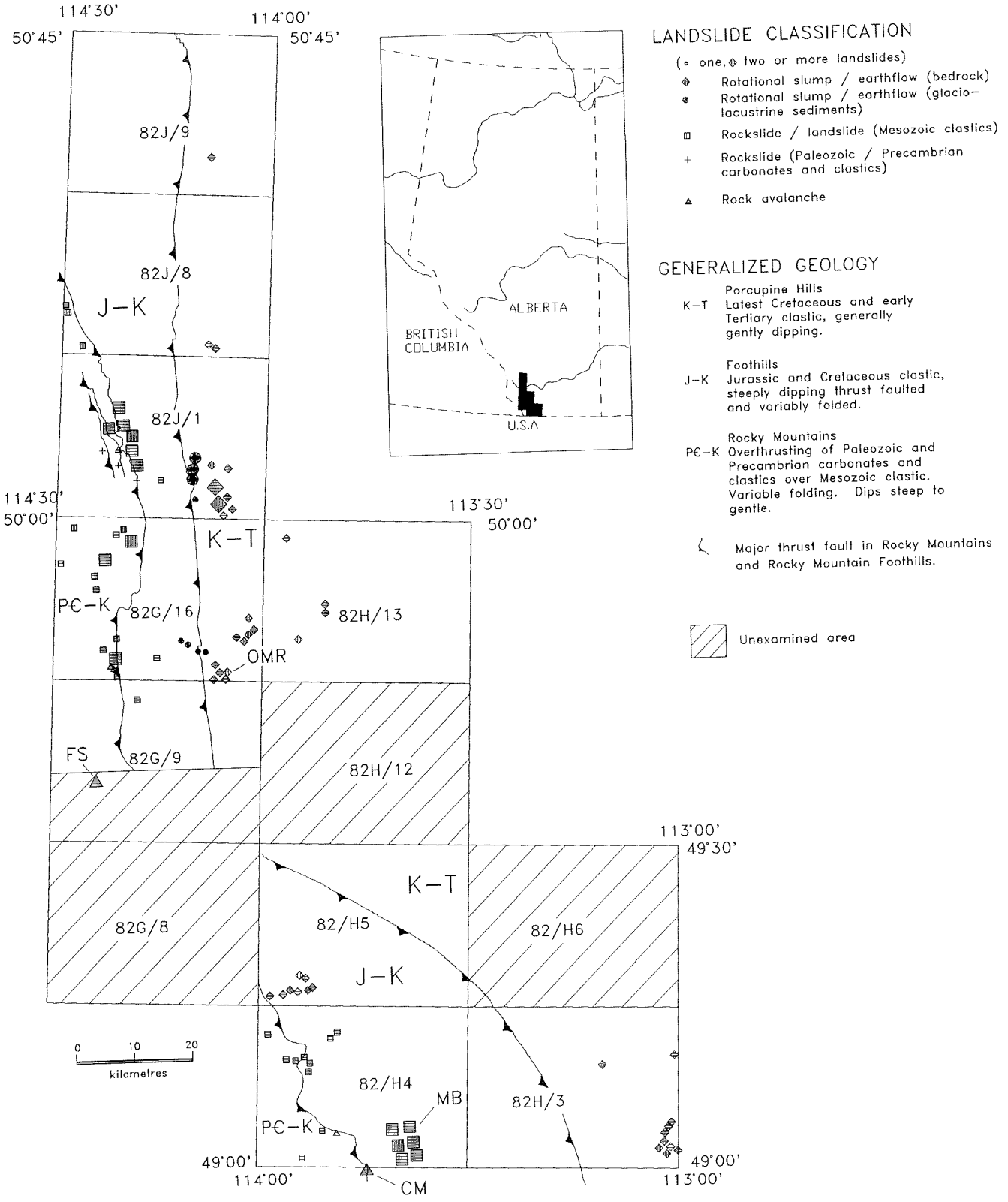

Figure 2. *Regional characterization of landslides and associated bedrock/structural provinces. Bedrock geology: CM, Chief Mountain; MB, Mokowan Butte; OMR, Oldman River between its confluences with Callum Creek (north end) and Crowsnest River (south end); FS, Frank Slide.*

2. Dip slope bedding inclinations are predominantly steeper than are slope angles. Such underdip slopes have been shown to have a low frequency of landslide activity elsewhere in the Rocky Mountains.

3. Ridges of Mesozoic clastics are not surmounted by thrust sheets of massive Paleozoic or Proterozoic rocks (as in the Rocky Mountains) which provide significant driving forces.

Glaciolacustrine Valley Fills

Glacial lacustrine sediments have mean in situ moisture contents above the plastic limit and values sometimes

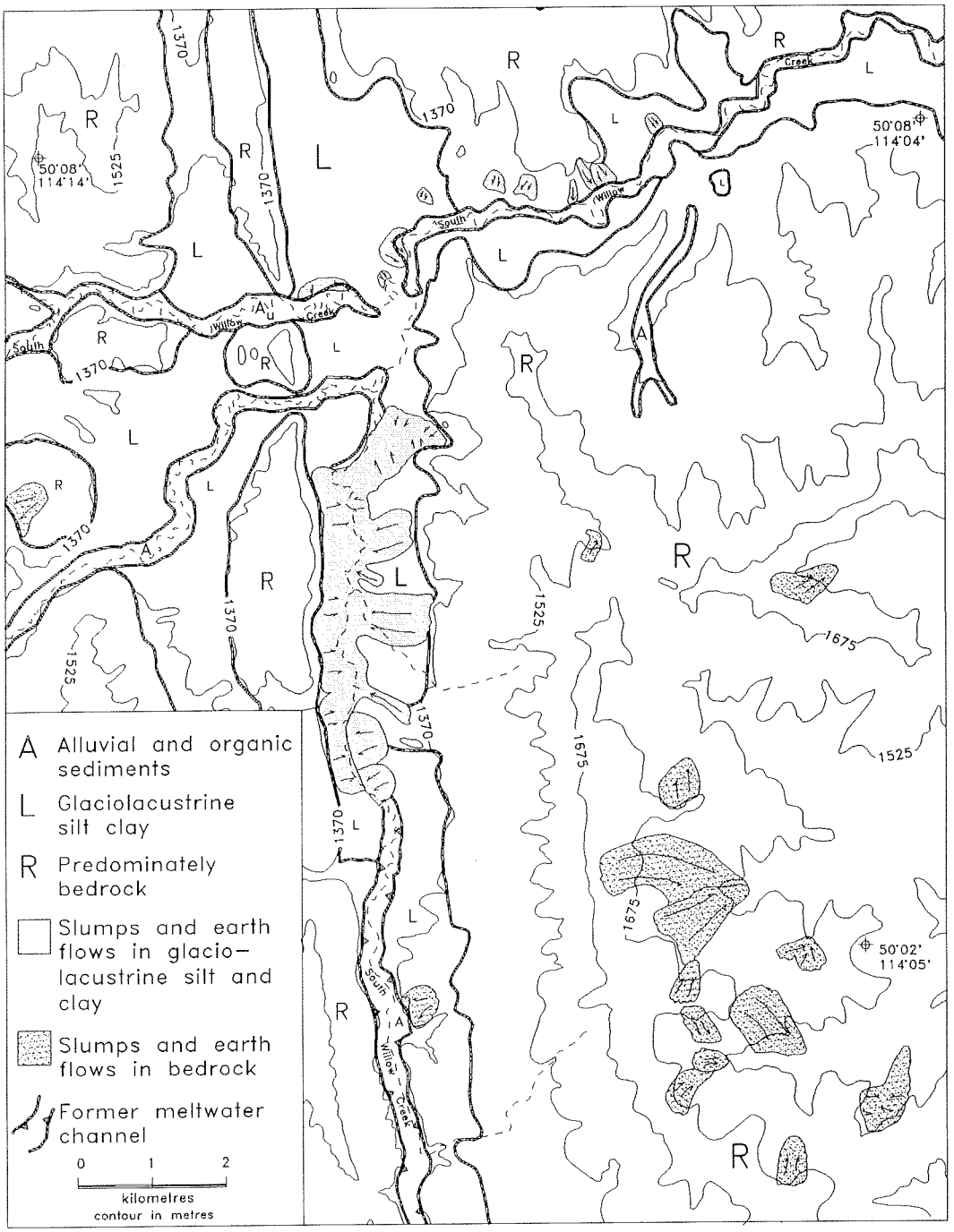

Figure 3. *Slumps and earthflows in Porcupine Hills and extensive failures in glacial lake sediments, upper reaches of South Willow Creek (SWC) and its major tributaries.*

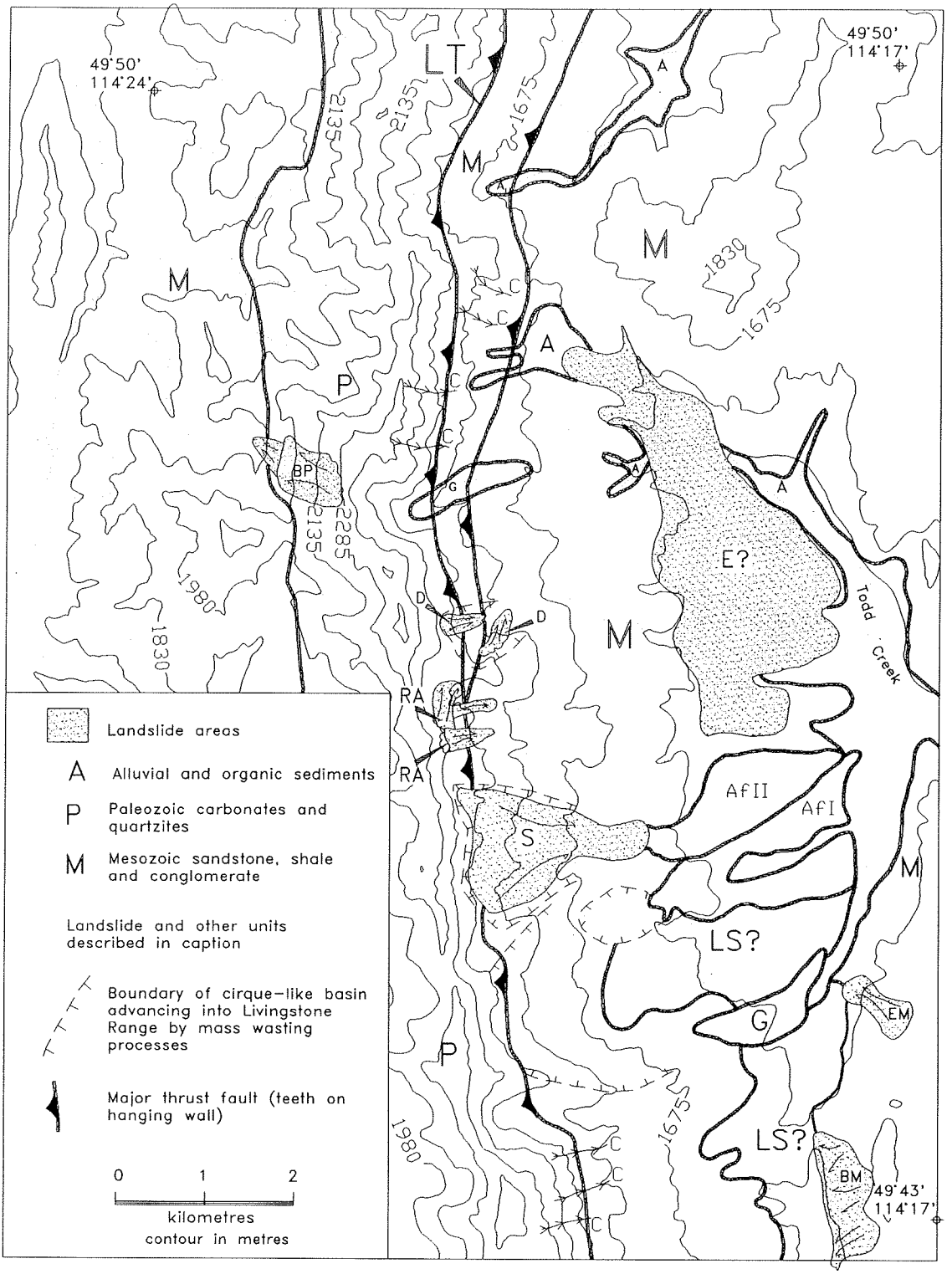

Figure 4. *Landslides and related features along the Livingstone Range in the area of Todd Creek. LT, Livingstone Thrust; BP, bedding plane rockslide in Paleozoic bedrock; RA, rock avalanche in Paleozoic bedrock; S, apparently sagging slope, terminates as an earthflow at toe; D, Rockslide in Mesozoic clastics oblique to bedding planes; E?, forested area of lobate topography without natural or artificial exposures (possibly a complex of earthflows); EM, earthflow in Mesozoic clastics; BM, bedding plane rockslide in Mesozoic clastics; AfI, AfII, succession of fans built by gravels derived from mass wasting; C, large fresh ravines actively being incised in the Livingstone Range; LS?, heavily forested area of anomalous landforms, possibly of landslide origin; G, bouldery glaciofluvial gravels.*

approach the liquid limit. They creep noticeably in many artificial cuts. They have failed massively along contemporary stream valleys and former meltwater channels. Failure apparently was initiated as rotational slumping but was transformed into mass flow (Fig. 3). Glaciolacustrine sediments and underlying upper Cretaceous bedrock commonly fail together in large slump complexes (Fig. 2, OMR).

Rocky Mountains

Two styles of failure dominate in the Rocky Mountains: rock avalanches and rockslides. Both tend to cluster above, below and across major overthrust faults in the Rocky Mountains (Fig. 2, 4–5). Rock avalanches predominantly occur in Paleozoic or Precambrian carbonates and clastics. The best known example in the region is the Frank Slide (Fig. 2, FS).

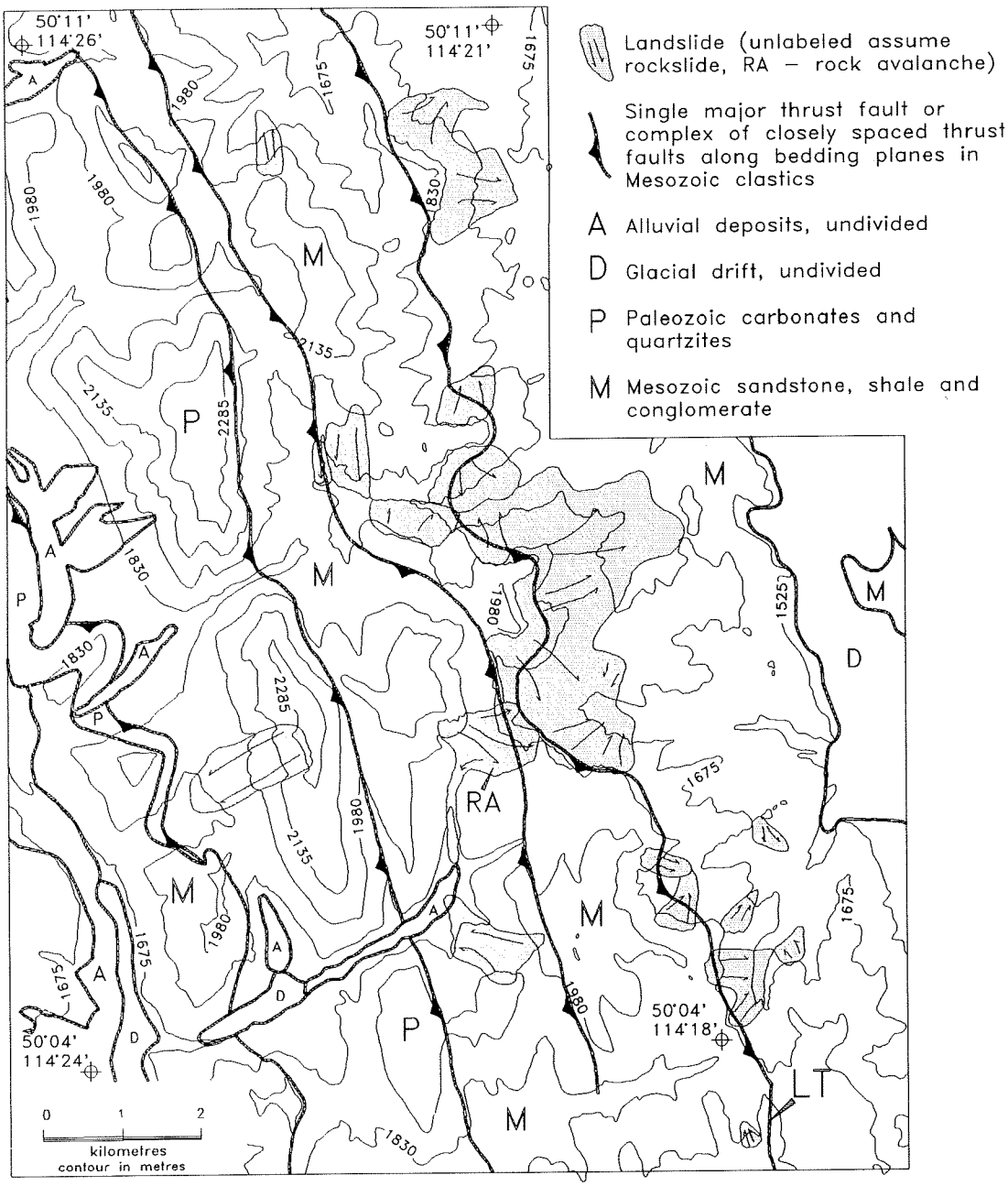

Figure 5. *Landslides and related mass wasting features and deposits, upper Willow Creek/Livingstone River basins in the area of the Livingstone Thrust (LT).*

Rockslides occur in Precambrian, Paleozoic, and Mesozoic units but the largest and greatest concentration are in Mesozoic units below and within areas of extensive thrust faulting (Figs. 2, 4, 5). I believe that these failures are due to the combination of sheared incompetent rocks within the zone of overthrusting and the driving forces exerted by the massive overlying thick carbonates and resistant clastics in the overthrust sheet. Landsliding in the Mokowan Butte area (Fig. 2, MB), although within the Foothills, was conditioned by Rocky Mountain thrust faulting. The Lewis Thrust extended over it prior to post thrusting erosion during the Tertiary. The nearly flat-lying late Cretaceous shale underlying Mokowan Butte is sheared. The combination of weak, sheared shale with low dips intersected by steep slopes creates the environment for extensive landsliding at Mokowan Butte.

REFERENCES

Jackson, L.E. Jr.
in press: Quaternary Geology ad Terrain Inventory, Alberta Foothills NATMAP, I: Regional Landslide Characterization. *In* Current Research, Geological Survey of Canada.

THERMAL ENERGY FROM ABANDONED MINES AT SPRINGHILL, NOVA SCOTIA

A.M. Jessop

333 Silver Ridge Crescent N.W., Calgary, Alberta T3B 3T6

INTRODUCTION

Coal mining began at Springhill, Nova Scotia, in 1872 and continued as the primary industry of the town until 1958, when the last of a series of rock-bursts prompted the final closing of the mines. After closure the mines were allowed to fill with water. With the main industry removed, the town entered a period of economic re-adjustment and had to strive to develop new industries. The rapidly rising cost of oil-based energy from 1973 to 1980 added a major impediment to economic recovery.

The Springhill area lies on the flanks of the Athol Syncline, (Fig. 1). The mines follow several parallel coal seams. Surface outcrops are curved, and all seams dip in a generally westerly direction, at about 30° near the surface and at an angle decreasing to about 24° at the furthest point of mining (Fig. 2). The greatest depth of the mines below the surface is about 1350 m.

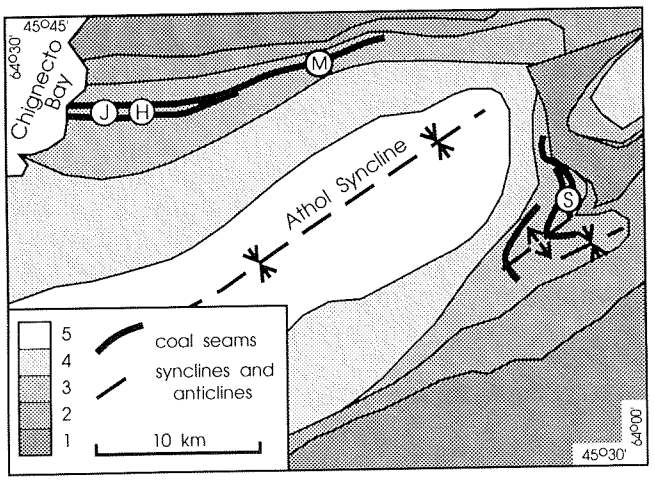

Figure 1. *Geological structure of the Springhill area. Numbers on the legend: 1, Pre-Cumberland Group; 2-5, Carboniferous Cumberland group. Major coal seams are shown by heavy lines. Locations of the main mining centres are shown by letters in circles: S, Springhill; J, Joggins; H, River Hebert; M, Maccan.*

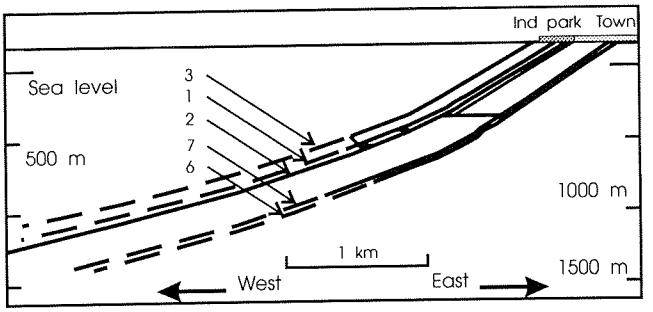

Figure 2. *Vertical section through the coal seams and Town of Springhill. Numbers are seam numbers, continuous lines indicate mined portions, and dashed lines indicate unmined extensions. Thin lines indicate connections between the levels.*

Only the western part of Springhill is located directly over mine workings (Fig. 3). The industrial park is the part best located to use the mine-water resource, having a choice of several levels of the mine from which to draw water or in which to reinject.

ENERGY CAPACITY OF THE MINES

The thermal capacity of the water in the mines depends on volume and temperature. The volume of water in the mine has been estimated to be 4 x $10^6 m^3$. Temperature of the water depends on geothermal gradient, heat exchange with the walls, and circulation. Terrestrial heat flow and geothermal gradient have been measured in the Cumberland Basin to the northeast (Fig. 4). Temperature gradients from all these sites are in the range 14 to 17 mK/m, with an average of about 15 mK/m. Equilibrium surface temperature is about 6°C. These observations imply a temperature of about 26°C at the maximum depth of the mines.

The ability of deep water to circulate widely through the mine depends on the presence of connecting channels and the driving influence of incoming water.

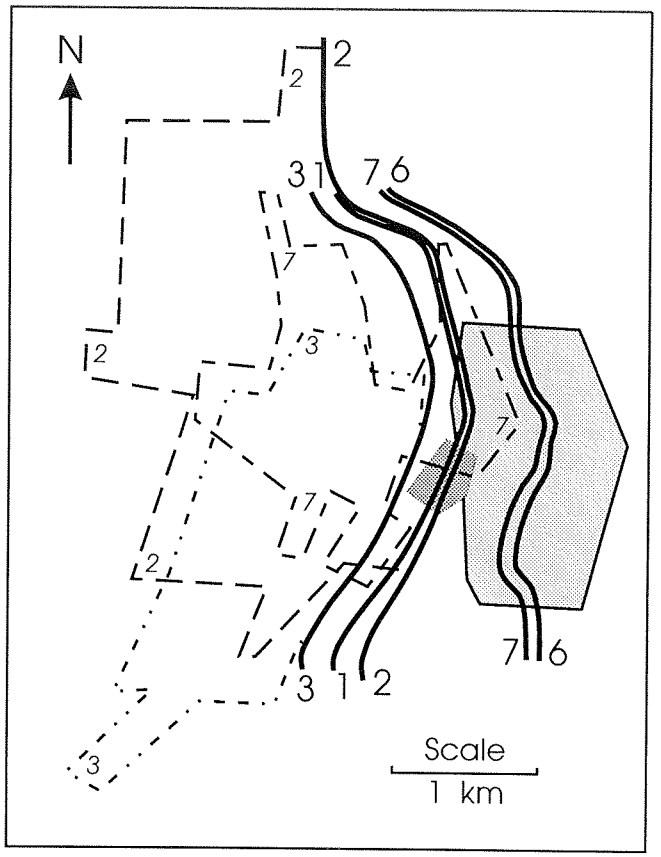

Figure 3. *Map showing the relative position of the town over the mines. Coal outcrops are shown by heavy lines, the extent of mining operations in three of the seams is shown by dashed lines, with the numbers of the seams indicated. The Town of Springhill and the Springhill Industrial Park are indicated by light and dark shading, respectively.*

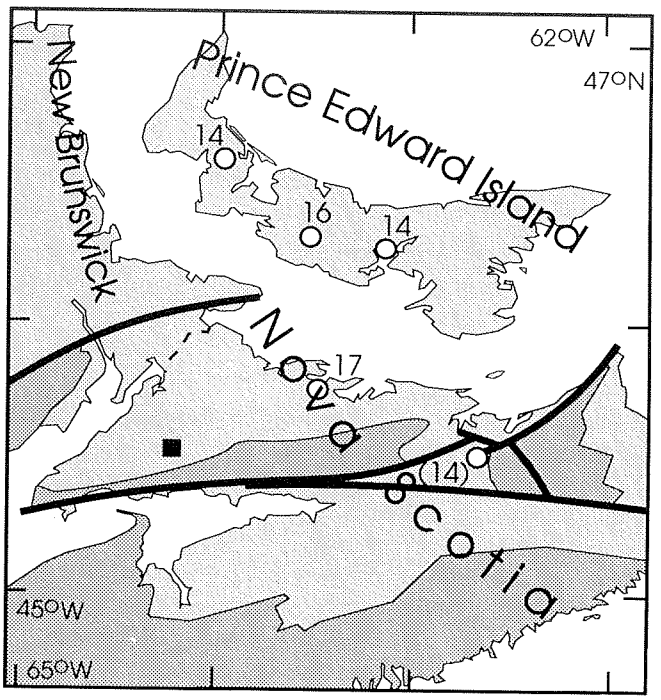

Figure 4. *Geothermal regime at Springhill. Light shading indicates areas of Carboniferous or later sedimentary rocks. The site of Springhill is shown by a black square. Sites of geothermal measurement are shown by open circles with values of geothermal gradient in mK/m.*

The several levels of the mines are known to have been interconnected, but the present state of ventilation-control doors and blockage due to roof-falls is unknown. The tunnels and mined areas probably still provide channels for water movement. Convection will occur in vertical mine shafts and in other workings provided that they are inclined by about 10° or more, and provided that obstructions such as ventilation-control doors or rock-falls do not prevent free circulation.

Water temperature up to 20°C has been observed at the surface, which is well above the ground temperature. There are two possible mechanisms that could produce this anomalous temperature-convective overturn of the water in the mines and water flow from greater depth forced by water entering the mines. It has been suggested that some of the heat in the water comes from oxidation of minerals by oxygen dissolved in the water, but this is an insignificant heat source compared with the magnitude of the observed temperature anomaly.

In the area around Springhill there are many natural springs. This shows that there is a supply of recharge water and that hydraulic potential of the area is high enough to provide a driving force for circulation in the mines. At the mine museum in Springhill, water is pumped from the mine at up to 1000 m^3/day, in order to keep a small part of the mine open and accessible to visitors. The water level is kept at 50 m below the local surface. This water is replaced in the mines by water entering from fractures in the rock. The level maintained at the museum probably controls the level in the entire mine system.

Convection alone tends to produce a water temperature approaching an average value, between the temperatures at the deepest and shallowest parts and weighted by the relative volume of the workings throughout the depth range. The median temperature is

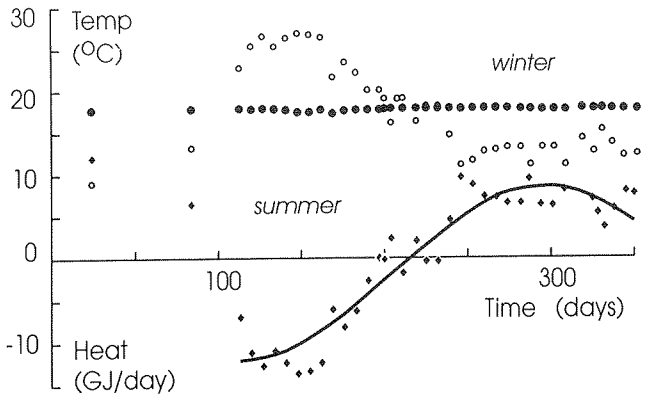

***Figure 5.** Plot of temperatures and energy use at the Ropak Can-Am building. Inlet and outlet temperatures are indicated by solid and open squares respectively. Energy taken from the mine water is indicated by solid diamonds. The two vertical scales have the same numerical values.*

about 17°C, and water is expected to approach this temperature throughout the mine after an initial period of convective adjustment. This temperature is close to the 18°C observed by Ropak Can-Am in the first year of operation.

The estimated volume of water, 4 x $10^6 m^3$, if cooled by 15 K, would yield 250 x 10^{12} J or 70 GWh. This temperature drop implies the return of water to the mine at 3°C and thus represents the total heat reasonably accessible to heat pumps. This result takes no account of recharge of water or of heat exchange from the rock to the water. The transfer of heat from the walls of the mines is a slow process and will maintain the heat content of the water over a long period of time, perhaps hundreds of years.

DATA FROM THE FIRST APPLICATION

Ropak Can-Am Ltd. have supplied detailed information for 1989, the first year of operation of the geothermal system, and some further data on total energy usage. The building has a total area of 8300 m^2, and is used for plastic moulding manufacturing, storage for raw materials or completed goods awaiting shipment, and small office area. The heat pumps are suspended from the ceiling, and so do not take up floor space. The pipes for water intake and outlet, with associated meters and controls, take up a space of about 1 m by 4 m, adjacent to one wall. Each heat pump has a motor rated at 5 horse-power (3.73 kW).

Temperature of the intake and outlet water streams were recorded over a period from 22 March 1989 to 6 March 1990, and the heat drawn from the mine water has been calculated (Fig. 5). Regular weekly measurements were made from 11 July 1989, day 113, to 6 March 1990, day 352. The inlet temperature of the water is constant at 17.9°C. The outlet temperature varies through the year, from a minimum of 11.1°C in the winter heating cycle to a maximum of 26.7°C in the summer cooling cycle. The data have been extrapolated to a period of one year by fitting a sine curve. The result of this analysis is a draw on the mine of 890 GJ and a return to the mine of 1550 GJ, for a total of 2440 GJ exchanged and a net heat input to the mine of 660 GJ.

Records in the first year show electrical power consumption of 259 MWh over a period of 239 days, a rate of 395 MWh/year. If we take the median figure of 550 kWh/day for uses other than the heat pumps, the balance left for the heat pumps is 128 MWh (460 GJ) and the coefficient of performance is 3.6. The figures on which these calculations are based are for a short period of time, and estimates derived from them are subject to errors of up to 25%.

Net heat exchange with the mine water by the Ropak Can-Am system over the first year of operation is small compared with the total amount of heat exchanged by the system. Thus the water in the mine workings acts more in the manner of a large reservoir of heat that is drawn on and replenished seasonally, rather than as a depletable resource.

The net annual heat drain by Ropak Can-Am is negative and is about 660 GJ. The accessible heat in the water of the mines has been estimated earlier to be 250 TJ, based on a temperature change of 15 K. The annual exchange of this installation is thus less than the accessible heat by a factor of 400. This present heat exchange and several others of similar magnitude could be supported for long periods in comparison with the life of the buildings.

ECONOMIC BENEFITS

Annual Costs for heating the Ropak Can-Am building of 1989 were expected to be about $125,000 per year for the total 8300 m^2. The capital cost of the heat pump system and the two wells was $110,000, 20% higher than the estimated cost of conventional oil furnaces. However, the maintenance costs are considerably lower. Good temperature and humidity control provided by the heat pump system removes the need for dehumidifiers on each of the moulding machines, at

a capital cost of $15,000 for each of twelve machines. Thus in this particular application the entire capital cost of the heating system, not just the incremental cost of the heat pumps, is more than compensated by this saving alone.

The data for the 239 days in the first year of operation show a total cost of electrical power of $16,400. If we divide this cost in the proportion for heat pumps and other uses as derived above for the electrical energy, we find that the heating cost is $11,840 for the 239 days or $18,000/year.

In the complete building of 1991, with sixteen heat pumps, and a total area of 14,000 m^2, the company estimates that the geothermal system saves $160,000 per year over the equivalent oil-fired furnace system. Disregarding the saving associated with the de-humidification, the pay-back period of the extra capital cost was thus well under one year for this installation. If the conventional dehumidification costs are also included in the calculation, the payback period is virtually instantaneous.

There are non-monetary benefits in addition to the savings in energy costs: the clean operation now permits the company to make food containers; and working conditions are much better than before, particularly in the summer, because of the cooling provided by the geothermal system. The carbon dioxide emissions necessary to provide the same benefits are thus 370 Tonnes/yr for the geothermal system and at least 740 Tonnes/yr for a system of oil heating and conventional air conditioning. Although this is a very small quantity in comparison with the national emission of gas into the atmosphere, it is small contribution to environmental responsibility that is profitable for the operator, and it is reproducible in many other locations.

POTENTIAL FOR OTHER LOCATIONS

An inventory of abandoned mines in the provinces of Nova Scotia and Quebec has been performed under contract to the Geological Survey of Canada and CANMET. It was found that much of the requisite information already exists in provincial records, but not necessarily in a form readily applicable to the assessment of geothermal resources. Only Nova Scotia has legislation to define and regulate low-temperature geothermal resources. The absence of current legislation inhibits potential developers. A clear definition of ownership of a resource and the regulations under which it may be developed are much preferred to a situation where these matters are undefined and where other, possibly multiple and conflicting, sets of regulations must be observed. Furthermore, the enactment of legislation prior to development is desirable since otherwise the developer runs a risk that regulations may be changed after considerable time and money has been expended.

FOSSILS FROM DIAMONDIFEROUS KIMBERLITES AT LAC DE GRAS, N.W.T.: BIOSTRATIGRAPHIC, PALEOGEOGRAPHIC AND THERMAL IMPLICATIONS

W.W. Nassichuk, D.J. McIntyre, and L.D. Stasiuk

Geological Survey of Canada, 3303-33rd Street N.W., Calgary, Alberta T2L 2A7

TIME OF EMPLACEMENT OF KIMBERLITE PIPES

Diamond exploration in the Slave Province has led to the discovery of Mesozoic (Cretaceous) and Tertiary (Paleocene) fossils preserved within xenoliths of sedimentary strata in the crater and diatreme facies of 13 kimberlite pipes. Samples from most of these pipes in the Lac de Gras area were provided by the BHP-DiaMet Joint Venture, but samples from a few other pipes closer to Yamba Lake (Fig. 1) were provided by the Mill City–Tanqueray Joint Venture. The authors first indicated that fossil dinoflagellates, pollen, spores and teleost fish remains ranging in age from latest Early Cretaceous (Albian) to early Tertiary (Paleocene) were recovered from pipes in the Lac de Gras area in a report in the Northern Miner (Sept. 20, 1993). Thus, emplacement of the pipes had to post-date the youngest fossils in the pipes and probably occurred between late Paleocene and early Eocene time according to the time scale of Harland et al. (1989). In the same Northern Miner report, R.O. Moore from BHP Minerals Canada indicated that rubidium-strontium data from mica (phlogopite) and whole rock samples from a pipe in the Lac de Gras area suggest eruption 52 ± 1.2 million years ago; that is, in early Tertiary (Eocene) time. Accordingly, paleontological and rubidium–strontium data for the time of emplacement (age) of the pipes appear to be mutually supportive.

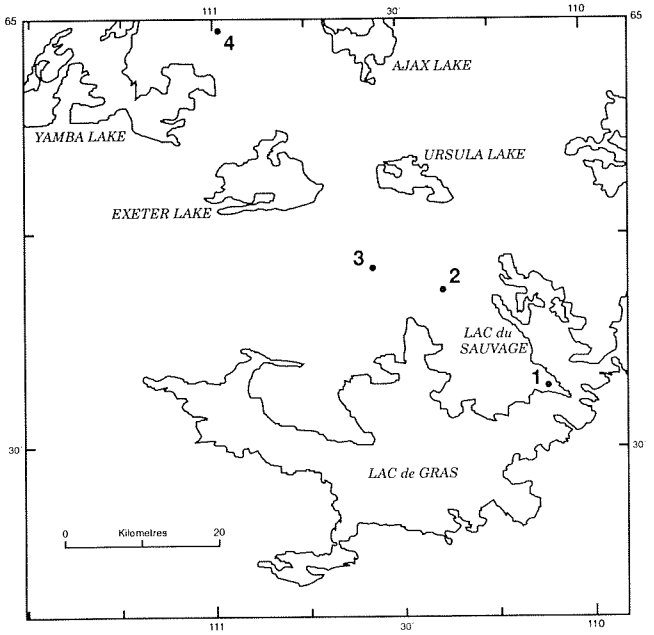

Figure 1. *Map of Lac de Gras area showing the positions of kimberlite pipes containing fossils that were referred to by Nassichuk and McIntyre (1995) and by Stasiuk and Nassichuk (1995). 1) BHP-Dia Met Point Lake pipe, 2) BHP-Dia Met "Hawk" pipe, 3) BHP-Dia Met Koala pipe, 4) Mill City Tanqueray Torrie pipe.*

BIOSTRATIGRAPHY AND PALEOGEOGRAPHY

In a preliminary report, Nassichuk and McIntyre (1995) recorded marine Cretaceous and nonmarine Tertiary (Paleocene) fossils from kimberlites in the Slave Province to advise that several research activites on the fossils are underway. Fossils will facilitate biostratigraphic correlation with Cretaceous and Tertiary successions elsewhere in northern and western Canada. The newly discovered Cretaceous and Tertiary fossils are essential for refining the paleogeography of those systems in northern Canada. Further, it is hoped that the time of emplacement of kimberlites in the Slave Province will be even more precisely determined from fossil data to assist in regional geotectonic interpretations.

Fossils from the Lac de Gras area are of extraordinary importance in defining the distribution of Lower Cretaceous (Albian) to lower Tertiary (Paleocene) strata in northern Canada. Prior to the discovery of kimberlites in the area, no data had ever been presented to prove that Mesozoic and Cenozoic rocks had been deposited above Precambrian rocks in the Slave Province. Indeed, the nearest Cretaceous exposures are several hundred kilometres to the west of Lac de Gras.

Now, it is clear that much of the Slave Province must have been covered by a veneer of Cretaceous and lower Tertiary strata, long since eroded away by river systems and glacial action. An important idea initated by McMillan (1973) is that from late Paleocene to Pliocene time a major anastomosing river system carried sediments from the eastern Cordillera and Canadian shield areas (including the Slave Province) eastward to the Labrador Sea. New data supporting this concept of easterly flow in Tertiary time was provided by Duk-Rodkin and Hughes (1994).

The discovery of marine strata of uppermost Early Cretaceous and Late Cretaceous age (Albian–Maastrichtian) in the Slave Province necessitates revision to paleogeographic reconstructions of the Western Interior Seaway. Several authors have reviewed Late Cretaceous connections between the Seaway and the Sverdrup Basin. Lac de Gras data show that Albian–Maastrichtian strata were more widespread and the Cretaceous Seaway was correspondingly wider than previously thought.

THERMAL DATA FROM ORGANIC MATTER

Wood fragments have been recovered from boreholes in the crater and diatreme facies of pipes in the Lac de Gras area. They are most abundant in the crater facies at borehole depths less than 50 m but they have also been recovered from the diatreme facies at depths exceeding 120 m. In the crater facies, wood fragments up to 12 cm long appear "fresh" and internal structures are clearly visible. In the deeper diatreme facies, wood fragments are often in direct contact with kimberlite grains. There, they are generally smaller than fragments in the crater facies, and somewhat more coalified; cellular structures, however are still clearly discernible.

Stasiuk and Nassichuk (1995) presented petrographic information on wood and other organic matter recovered from several pipes to determine the thermal history of the samples. They showed the maximum mean temperature (coal rank equivalent) that the samples must have been exposed to following original deposition and ultimate incorporation in kimberlite pipes. To do that, they analysed the samples petrographically using incident light microscopy in order to assess the general maceral composition and to determine optical properties in terms of per cent reflectance in oil (%Ro) for rank assessment. Their data are of considerable importance in evaluating temperatures in the crater and diatreme facies of kimberlite pipes shortly after emplacement.

The huminite macerals associated with the kimberlitic intrusions do not show any direct evidence of having been severely altered by a pyrometamorphic event (i.e., temperatures $>250°C$). This is not at all surprising since it has been suggested previously that fragments of country rock in the Bachelor Lake kimberlite breccias, South Africa, were only metasomatically altered, show no pyrometamorphic effects indicative of relatively high temperatures during or subsequent to their incorporation, and were probably emplaced at low temperatures (Clement, 1975).

Two groups of coal ranks were identified based on reflectance values. The low %Ro values of Group A samples ($\leq 0.20\%$Ro) are typical for values of lignitic (peatified) woods which have only been buried to very shallow depths (Stout and Spackman, 1989). The maximum average temperature for Group A samples in the crater facies must have been less than 30°C during a burial time of 50 million years to maintain the low measured reflectance values (based on time-temperature-%Ro coalification relationship; Bostick, 1979).

The range of %Ro values for most Group B diatreme samples fall within the range of reflectance for coals of lignitic to subbituminous "C" rank. Since the diatreme samples have significantly higher reflecting huminite than the shallower crater samples, a different coalification history must be involved. Further to this, the petrography suggests that the huminite macerals in the diatreme facies may be primary. This is supported by the lack of oxidation features and the distinct early compactional features (contorted appearance) indicating that the huminites were "soft wood" at the time of inclusion in the shale clasts. Barring further evidence to the contrary, it is assumed that the huminites are primary in the diatreme facies. The petrography also shows that the huminite macerals (coalified woody remains) in Group B samples did not experience pyrometamorphism (i.e., temperatures $>250°C$), otherwise gas release devolatization structures from the release of CO_2 and CO would be evident. The presence of unaltered, primary asphalt bitumen (exsudatinite) without flow textures in some Group B samples (huminite $\%Ro = 0.39$) suggests that the maximum temperature was less than 104°C, the temperature at which micro-flow begins in asphalt bitumens under atmospheric conditions.

REFERENCES

Clement, C.R.
1975: The emplacement of some diatreme facies kimberlites. *In* Physics and Chemistry of the Earth, L.H. Ahrens, F. Press, S.K. Runcorn, and H.C. Urey (eds.), v. 9, p. 51–60.

Duk-Rodkin, A. and Hughes, O.L.
1994: Tertiary-Quaternary drainage of the pre-glacial Mackenzie Basin. Quaternary International, v. 22/23, p. 221–241.

Harland, W.B., Armstrong, R.L., Cox, A.V., Craig, L.E., Smith, A.G., and Smith, D.G.
1989: A geological time scale 1989. Cambridge University Press, 263 p.

McMillan, N.J.
1973: Shelves of Labrador Sea and Baffin Bay, Canada. *In* The Future Petroleum Provinces of Canada-their Geology and Potential, R.G. McCrossan (ed.). Canadian Society of Petroleum Geologists, Memoir 1, p. 473–517.

Nassichuk, W.W. and McIntyre, D.J.
1995: Cretaceous and Tertiary fossils discovered in kimberlites in the Slave Province at Lac de Gras, Northwest Territories. *In* Current Research, 1995-B, Geological Survey of Canada.

Stasiuk, L.D. and Nassichuk, W.W.
1995: Thermal history of wood and other organic matter in kimberlites pipes at Lac de Gras, Northwest Territories. *In* Current Research, 1995-B, Geological Survey of Canada.

THE BELL RIVER SYSTEM: TERTIARY DRAINAGE FROM THE EASTERN CORDILLERA TO THE LABRADOR SEA

N.J. McMillan and A. Duk-Rodkin

Geological Survey of Canada, 3303-33rd Street N.W., Calgary, Alberta T2L 2A7

The Bell River is a name assigned to a river system that drained from the eastern Cordillera to the Labrador Sea during Tertiary and most of Quaternary time. This drainage followed the general piedmont slope that was formed during the uplifting of the Rocky and Mackenzie mountains in early Tertiary. The regions affected by this drainage were the Western Interior Plain, Hudson Bay and parts of the north Atlantic slopes (Fig. 1).

Great volumes of sediments from the eastern slopes of the Cordillera, the Interior Plains and the Canadian Shield, were transported by this drainage system to the Labrador Sea. This accounts for the enormous volume of Tertiary sediments found in the Labrador Sea. Tertiary clays, muds, silts and fine sands were derived from central and western Canada according to Hiscott (1984). This conclusion is based on the clay mineral suites in the sediments found under the Labrador and

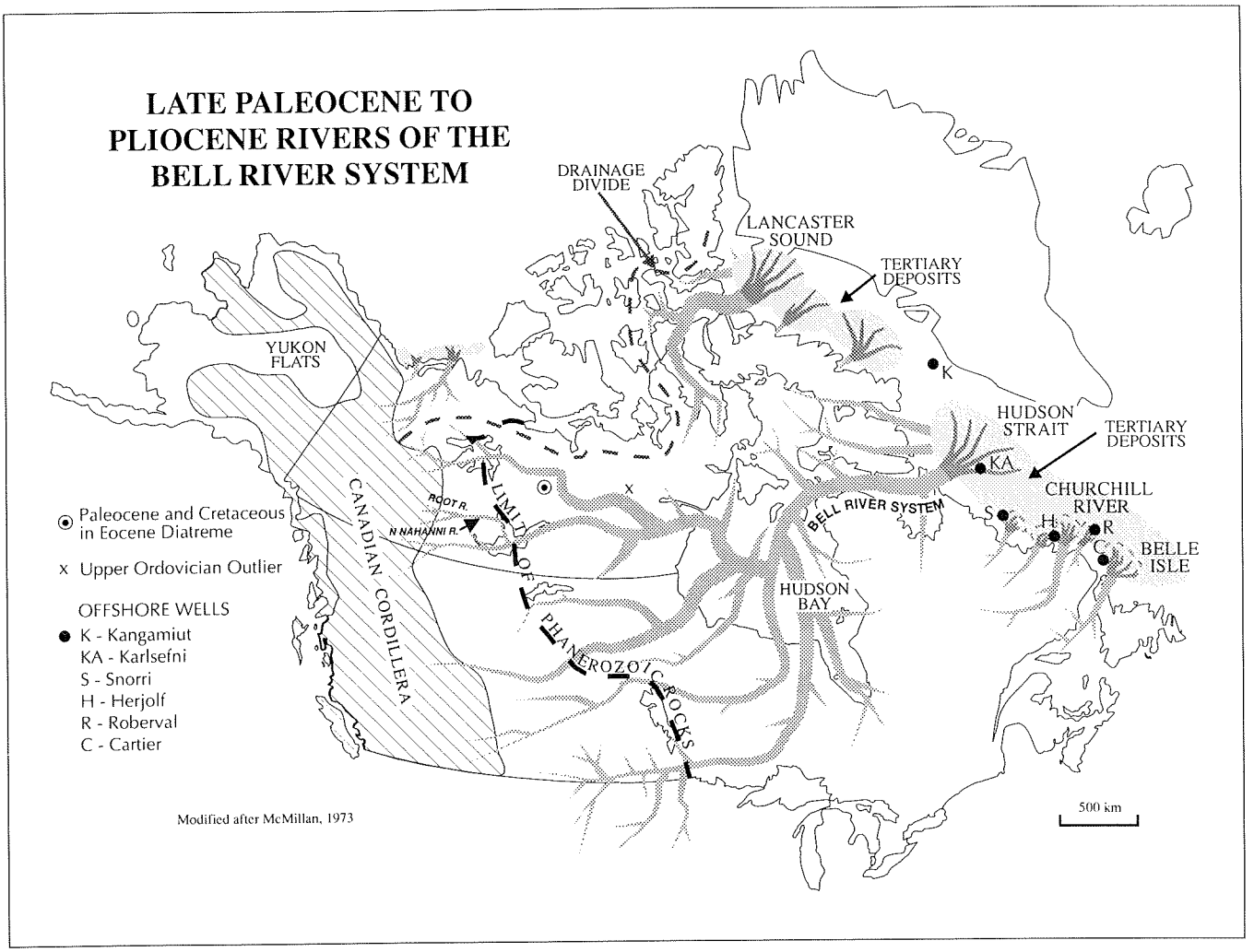

Figure 1. *Schematic map of the Tertiary drainage of the Bell River System.*

Baffin Island shelves. Later Williams (1986) conducted a thorough palynological study of rocks in the Labrador Sea and found that a substantial quantity of palynomorphs in Tertiary rocks are Cretaceous or Jurassic. Further, some of the reworked palynomorphs, including *Wodehousia spinata, Aquilapollenites amplus* and *Balmeisporites* spp. are of Late Cretaceous age but do not occur in situ in Labrador. They do, however, occur in Upper Cretaceous strata in western Canada. Nassichuk and McIntyre (1995) showed that kimberlite pipes penetrated Upper Cretaceous and Lower Tertiary (Paleocene) strata in the Slave Province north of Yellowknife when they erupted to the surface in late Paleocene or Eocene time. All of these strata have long since been eroded away, possibly by the Bell River System but xenoliths within the kimberlite pipes have yielded Upper Cretaceous and Lower Tertiary palynomorphs. It is possible, then that some of the reworked Upper Cretaceous fossils that have been recovered from Tertiary strata in the Labrador Sea might have originated in the Slave Province as well as farther west in the eastern Cordillera.

Geomorphic and stratigraphic evidence for a southeastern drainage in the Mackenzie region indicate that the northwestern tributaries of the Bell River system extended as far north as the Great Bear Lake region. Glacial diversion of rivers draining east by the late Pleistocene Laurentide Ice Sheet, formed the Mackenzie River system draining north to the Arctic Ocean.

Calculations reveal that approximately 2.5 x 10^6 km^3 of clastics belonging to the Tertiary occurs in the Labrador Sea between the shore and its mid-ridge. This volume could be derived from a 1.7 x 10^6 km^2 wedge of older rocks in western Canada (49° to Great Bear Lake and east to Winnipeg). In addition to the supply from the plain's wedge, the actively rising Eocene Rocky Mountains are considered to have been a substantial source of debris. The northern branch of the Bell River System has probably stripped unknown volumes of sediments east of the present limit of Phanerozoic rocks originally occurring in a paleo-trough extending in an east-west direction and now only known by samples from diatremes and an Ordovician outlier.

The Bell River System drained 7 000 000 km^2. This ranks it with the Amazon River which is the largest river system today – being 7 000 000 km^2.

REFERENCES

Bell, R.
1895: A great Pre-glacial River in Northern Canada. Scottish Geographical Magazine, v. 11, p. 368.

Bluemle, J.P.
1972: Pleistocene drainage development in North Dakota. Geological Society of America Bulletin, v. 83, p. 2189–2194.

Cumming, L.M.
1968: Rivers of the Hudson Bay Lowlands. *In* Earth Science Symposium of Hudson Bay, P.F. Hood (ed.). Geolological Survey of Canada, Paper 68–53, p. 144–168.

Duk-Rodkin, A. and Hughes, O.L.
1994: Tertiary-Quaternary drainage of the Pre-glacial Mackenzie Basin. Quaternary Journal, v. 22/23, p. 221–241.

Fortier, Y.O. and Morley, L.W.
1956: Geological unity of the Arctic Islands. Royal Society of Canada Transactions, Series III, v. L, p. 3–12.

Hiscott, R.N.
1984: Clay mineralogy and clay-mineral provenance of Cretaceous and Paleogene strata, Labrador and Baffin Shelves. Bulletin of Canadian Petroleum Geology, v. 32, p. 272–280.

McMillan, N.J.
1973: Shelves of Labrador Sea and Baffin Bay, Canada. *In* The Future Petroleum Provinces of Canada, R.G. McCrossan (ed.). Canadian Society of Petroleum Geologists, Memoir 1, p. 473–517.

Nassichuk, W.W. and McIntyre, D.
1995: Cretaceous and Tertiary fossils discovered in kimberlites in the Slave Point at Lac de Gras, Northwest Territories. *In* Current Research, 1995-B, Geological Survey of Canada.

Nelson, S.J.
1970: The face of time, the geological history of Western Canada. Alberta Society of Petroleum Geologists, 133 p.

Pelletier, B.R.
1968: Submarine physiography, bottom sediments and models of sediment transport in Hudson Bay. *In* Earth Science Symposium of Hudson Bay, P.F. Hood (ed.). Geological Survey of Canada, Paper 68–53, p. 100–136.

Williams, E.V.
1986: Palynological study of the continental shelf sediments of the Labrador Sea. Ph.D. thesis, University of British Columbia, Vancouver, British Columbia, 214 p.

PALYNOLOGY: PRINCIPLES AND APPLICATIONS

J. Jansonius and D.C. McGregor
(editors)

Published by the American Association of Stratigraphic Palynologists

---

Palynology, like the rest of paleontology, is under assault. Ironically, this comes when palynology has entered one of its most exciting and transformative periods, and when its usefulness is greater than it has ever been. ***Palynology: principles and applications***, to be published in two volumes in the spring of 1995, shows that palynology is a highly analytical discipline with much to offer to a wide spectrum of potential clients.

By virtue of the wide range of organisms it deals with, palynology has many interdisciplinary applications. For stratigraphers it provides an environmental perspective and temporal resolution unattainable by other means, and virtually the only way to determine the ages of nonmarine strata. Chitinozoans and dinoflagellates now rival graptolites and ammonites for regional and long-distance correlation in marine facies. Computer programs for manipulating huge palynological data sets have revolutionized their potential for interpretations and predictions of climatic change, and facilitate assessment of beds earmarked for disposal of toxic waste. Spores and pollen are even being applied in archeology, medicine, forensics and agriculture. In situ and reworked palynomorphs aid in the understanding of paleogeography, source and direction of sediment supply, determination and dating of sedimentary cycles and environments, locating primary and strata-bound ore deposits, and determining timing and pathways of migration of hydrocarbons.

CONTENTS

Volume One

13D	Microforaminiferal linings	R.P.W. Stancliffe
13E	Invertebrate cuticular fragments	M.A. Miller
13F	Older plant macerals	D. Edwards and C.H. Wellman
14	In situ pollen and spores in plant evolution	T.N. Taylor
14A	In situ spores in early land plants	D. Edwards and J.B. Richardson
14B	Angiosperm pollen in situ	E.M. Friis and K.R. Pedersen
14C	The importance of in situ pollen and spores in understanding the biology and evolution of fossil plants	T.N. Taylor, J.M. Osborne and E.L. Taylor
14D	Exine origin, development and structure in pteridophytes, gymnosperms and angiosperms	J.R. Rowley

Volume Two

15	Introduction to biostratigraphy and time scales	R.A Christopher and D.K. Goodman
16	Paleozoic phytoplankton	S.G. Molyneux, A. Le Hérissé and R. Wicander
17	Chitinozoa	F. Paris
18	Paleozoic spores and pollen	K. Higgs
18A	Early and Middle Paleozoic records of terrestrial palynomorphs	J.B. Richardson
18B	Middle and Upper Devonian miospores	M. Streel and S. Loboziak
18C	Mississippian miospores	G. Clayton
18D	Upper Carboniferous miospores	B. Owens
18E	Permian	G. Warrington
19	Mesozoic–Tertiary dinoflagellates, acritarchs and prasinophytes	L.E. Stover, H. Brinkhuis, S.P. Damassa, L. de Verteuil, R.J. Helby, E. Monteil, A.D. Partridge, A.J. Powell, J.B. Riding, M. Smelror and G.L. Williams
20	Mesozoic–Tertiary spores and pollen	D.J. Batten
20A	Trias	G. Warrington
20B	Argentinian spores and intercontinental correlation	M. Zavattieri and D.J. Batten
20C	Lower-Middle Jurassic spore zonation, northwestern Europe	E.B. Koppelhus and D.J. Batten
20D	Uppermost Triassic–Jurassic miospores in northwestern Europe	D.J. Batten and E.B. Koppelhus
20E	Upper Jurassic–Cretaceous miospores	D.J. Batten
20F	Latest Cretaceous and Tertiary spore/pollen biostratigraphy	N.O. Frederiksen
21	Aquatic Quaternary	P.J. Mudie and R. Harland
22	Non-aquatic Quaternary	G.M. MacDonald
23	New frontiers in palynology	V.M. Bryant Jr.
23A	Archaeological palynology	V.M. Bryant Jr. and R.G. Holloway
23B	Pollen analysis of underwater sites	E. Weinstein
23C	Pollen as a guide to prehistoric diet reconstruction	K.D. Sobolik
23D	Melissopalynology	G.D. Jones and V.M. Bryant Jr.
23E	Entomopalynology	M.W. Pendleton, V.M. Bryant Jr. and B.B. Pendleton
23F	Medical palynology	M.K. O'Rourke
23G	Forensic studies in palynology	V.M. Bryant Jr., J.G. Jones and D.C. Mildenhall
24	Data organization and computers	J.K. Lentin
24A	Biostratigraphic information programs	J.K. Lentin
24B	PalynoData	K. Piel

NEOGENE AND QUATERNARY CLIMATE AND BIOSTRATIGRAPHY: WHY SHOULD THE OIL AND GAS INDUSTRY CARE?

J.M. White and D.R. Issler

Geological Survey of Canada, 3303-33rd Street N.W., Calgary, Alberta T2L 2A7

Any traveller knows that changing vegetation is evidence that one is traversing climatic zones. Likewise, the fossil record of vegetation is a proxy record of the warm and then cooling climates of the Middle Miocene to Pleistocene. 'Snapshots' of vegetation and climate in the Neogene at high latitude have been provided by studies of sections in northern Yukon and Alaska (Fig. 1). This biostratigraphic and climatic record has implications for basin subsidence and thermal maturity modelling, for understanding gas hydrate formation, and for testing Global Circulation Models (GCMs) which predict the climatic effects of human industry.

The Method

Various analyses of past vegetation yield paleoclimatic information. A pollen analysis from the Ramparts Canyon, Alaska (White and Ager, 1994) dated by $^{40}Ar/^{39}Ar$ at 15.2 Ma (Kunk et al., 1994), shows the presence at high latitude of trees such as redwood, beach, oak, sweet gums, basswood and water tupelo, which require a warm climate (Fig. 2).

Many plants found in Neogene rocks at high latitude have generic relatives which grow today at much more southerly latitudes (Fig. 3); for example *Liquidambar*, or sweet gum, is found in southeastern United States (Fowells, 1965). Also, floral diversity has been shown to correlate positively with available energy (Currie and Paquin, 1987), expressed as potential annual evapotranspiration (Fig 4). The early Middle Miocene flora at high latitude was more diverse than subsequent floras.

Wolfe (1979) has argued that the modern subtropical and temperate forests of east Asia are more appropriate analogues for Tertiary high-latitude forests than the forests of North America, which are subject to periodic fluxes of Arctic air. The pollen flora from the Ramparts Canyon site on the Porcupine river shows floristic similarities to the Mixed Northern Hardwood Forest and the Mixed Mesophytic Forest of east Asia. The climatic inferences are that, at 15.2 Ma, the Mean Annual Temperature (MAT) was ca. 9°C, the Cold Month Mean Temperature (CMMT) was ca. -2°C, and the Warm Month Mean Temperature (WMMT) ≥20°C

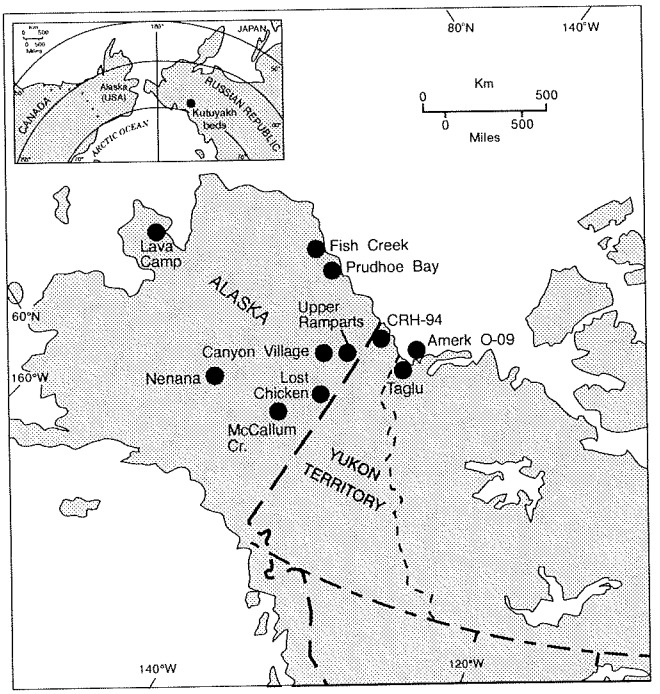

Figure 1. *Neogene biostratigraphic and paleoclimatic interpretations are based on a study of several sections in Yukon and Alaska during a joint GSC–USGS project with contributions from many other workers. The sections and their estimated ages are: Taglu borehole, 0–2.4 Ma (H. Jéttè, pers comm.); CRH-94, 2.4 Ma (C. Schweger, pers. comm.); Fish Creek, 2.4–3.0 Ma (Carter et al., 1986); Kutuyakh beds, 2.5 Ma (cited by Repenning and Browers, 1992); Lost Chicken Mine, 2.9 Ma (D. Adam, in prep.); Lava Camp, 5.7 Ma (Hopkins et al.,1971); Canyon Village, 6.57 Ma (Ager et al., in prep.); Nenana Coalfield, 7.0–16 Ma (Leopold and Liu, 1994); Ramparts Canyon, 18 and 15.2 Ma (White and Ager 1994), Amerk O-09 well, this paper.*

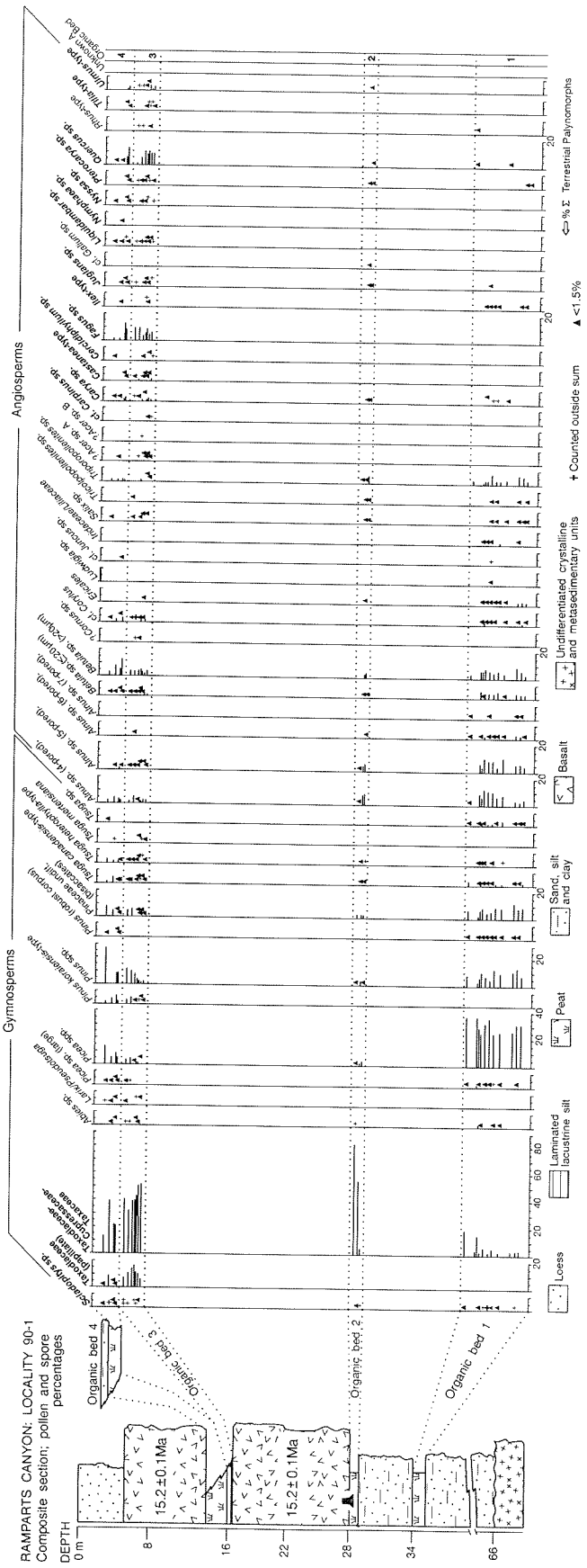

Figure 2. *Truncated pollen diagram from Ramparts Canyon site, Alaska (Fig. 1), from White and Ager (1994). The basalts which engulfed the forest floor of organic bed 2, and enclosed organic beds 3 and 4 are dated at 15.2 Ma. Organic bed 1 is of Early Miocene or early Middle Miocene age. The taxa which indicate a warmer climate than present are in bold face: i.e., Taxodiaceae (redwood), Taxodiaceae–Cupressaceae–Taxaceae (redwood, cypress or yew), cf.* ***Carpinus*** *(hornbeam),* ***Carya*** *(hickory),* ***Castanea****-type (chestnut),* ***Cercidiphyllum*** *(katsura),* ***Fagus*** *(beach),* ***Ilex****-type (holly),* ***Juglans*** *(walnut),* ***Liquidambar*** *(sweet gums),* ***Nymphaea*** *(pond lily),* ***Nyssa*** *(tupelo),* ***Pterocarya*** *(wing nut),* ***Quercus*** *(oak),* ***Tilia*** *(basswood) and* ***Ulmus****-type (elm).*

(White and Ager, 1994) (Fig. 5). In contrast is the Canyon Village site, dated to 6.57 Ma by $^{40}Ar/^{39}Ar$ (Kunk et al., 1994). Its palynoflora is relatively impoverished, conifer-dominated, and with few frost intolerant taxa. The MAT was probably in the range of 5°C, CMMT <-2°C, and WMMT ≥15°C and <20°C (Ager et al., in prep.)

Studies which relate leaf morphology to climate (Wolfe, 1993) and leaf stomatal density to atmospheric CO_2 concentration (Van Der Burgh et al., 1993), and which enhance resolution of the climatic tolerances of modern taxa will contribute to paleoclimatic interpretation.

Figure 6 compiles some paleovegetation and paleoclimatic interpretations derived from the studies of several workers (Hopkins et al., 1971; Carter et al., 1986; Repenning and Browers, 1992; Leopold and Liu, 1994; White and Ager, 1994; White et al., 1994; Adam, in prep.; Ager et al., in prep.; H. Jéttè, pers. comm.; C. Schweger, pers. comm.), which are shown with the North Atlantic paleotemperature reconstructions from Miller et al. (1987). Significant vegetation events, driven by climatic change, occurred ca. 15 Ma, ca. 12 Ma, ca. 6 Ma. and 2.6 Ma. The mean annual temperature at high latitude has dropped from ca. 9°C at 15 Ma (Ramparts Canyon) to -13°C today (Alaskan Arctic coast) and may have averaged as low as -16°C over the last 2.5 Ma (Carter et al., 1986). The first record of permafrost in sediment is from the Kutuyakh Beds near the Kolyma River (Repenning and Browers, 1992), estimated to be ca. 2.5 Ma. [Dates are adjusted to fit the Matuyama/Gauss magnetic polarity chron boundary (2r.2r/2An1n) age estimate of 2.6 Ma (Cande and Kent, 1992)].

Implications for Thermal History Modelling

The delineation of geologic vegetation change simultaneously produces continental biostratigraphy for differentiating surface and subsurface rock units. An example from the offshore Beaufort–Mackenzie Basin (Fig. 7) shows that it is the most recent stages of burial that control hydrocarbon generation (see also Issler and Snowdon, 1990) and thus, refined Neogene age control is important for basin modelling. Furthermore, this region is characterized by thick (~600 m) zones of permafrost (PF) which influence the interpretation of the heat flow history.

Figure 7 shows how two different models of permafrost development affect calculated thermal histories and organic maturation for the Amerk O-09 well (Fig. 1). In the long term PF model, the onset of PF was at 1.6 Ma; in the short term PF model, PF initiated at 0.1 Ma. The long term PF model produces a higher temperature history with a temperature maximum at 1.6 Ma, prior to the onset of cooling to present temperatures (Fig. 7a). These higher temperatures are necessary because the model is constrained to match present temperatures which are the result of long term cooling. Cooling from maximum temperatures is most pronounced in the upper part of the sediment column (~15°C at 1 km) and decreases with depth (~10°C at 4 km). In contrast, the effects of cooling over the last 0.1 Ma for the short term PF model are only significant at shallow depths (~15°C at 1 km versus ~1°C at 4 km).

The differences between PF models can be assessed by following a selected Eocene (49 Ma) layer (bold line) through its burial history (Fig. 7a). For the long term PF model, the layer undergoes a continuous temperature increase to a maximum at 1.6 Ma (153°C), followed by cooling to 146°C at present. For the short term model, the layer undergoes continuous heating to the present temperature of 142°C. If a maturity level of 0.9 %Ro represents peak hydrocarbon generation, then for the

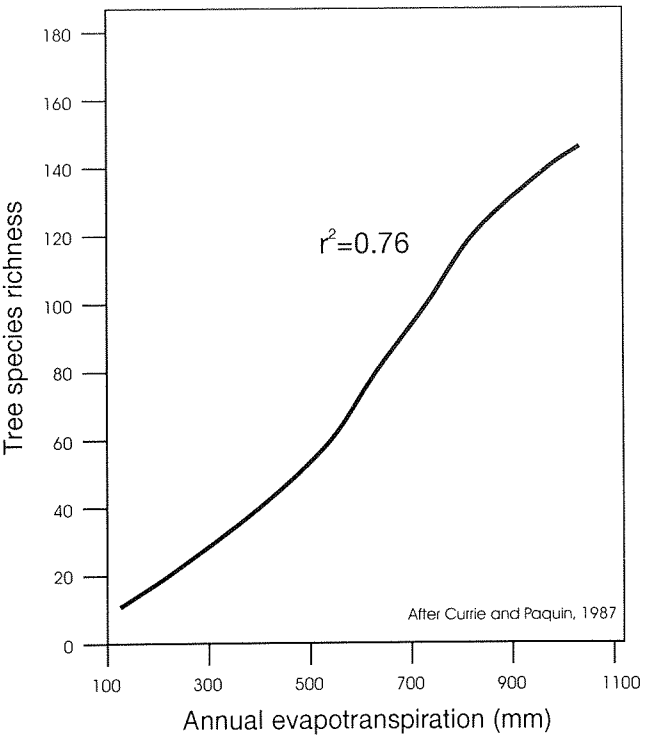

Figure 4. *Currie and Paquin (1987) have shown that there is a good correlation between modern tree species richness and available energy (measured as annual evapotranspiration). Past species diversity can only be estimated by the fossil record, but this diversity-energy relationship can be used to evaluate trends in paleotemperatures. The loss in plant diversity that took place at high latitude during the late Neogene is evidence of climatic cooling.*

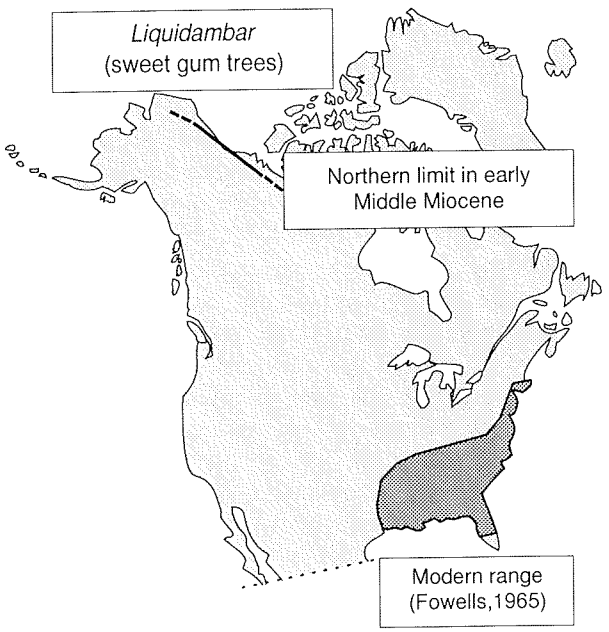

Figure 3. *The modern geographic range of* ***Liquidambar*** *(sweet gums) in North America is in southeastern United States (Fowells, 1965). Sweet gum pollen has been found in early Middle Miocene sections in northern Yukon and Alaska (White and Ager, 1994), indicating a warmer than modern climate.*

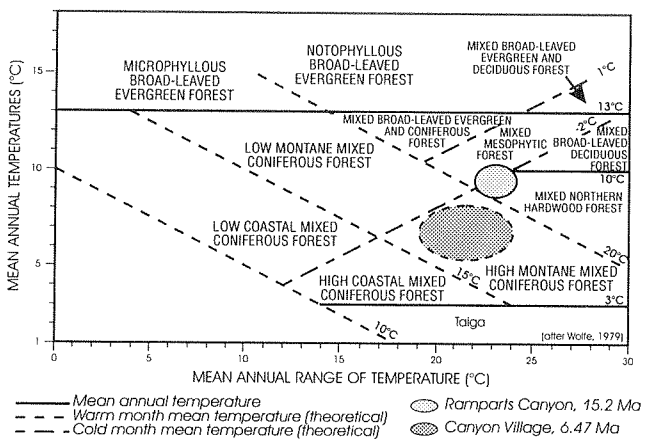

Figure 5. *The Middle and latest Miocene forests of Ramparts Canyon and Canyon Village (respectively) are shown with their apparent closest comparisons in the modern vegetation of eastern Asia. The classification of the east Asian forests, with climatic parameters, is from Wolfe (1979). The Ramparts Canyon assemblage (15.2 Ma) is species-rich. Comparison with modern forests suggests that the Mean Annual Temperature (MAT) was ca. 9°C, the Cold Month Mean Temperature (CMMT) was ca. -2°C, and the Warm Month Mean Temperature (WMMT) ≥20°C (White and Ager, 1994). A modern comparison for the more species-impoverished Canyon Village (6.57 Ma) assemblage is less clear, but the MAT was probably in the range of 5°C, CMMT <-2°C, and WMMT ≥15°C and <20°C (Ager et al., in prep.)*

case of the long term model, this layer entered the main phase of hydrocarbon generation at approximately 11 Ma (Fig. 7b). In contrast, for the short term PF model, the sediment layer is approaching peak hydrocarbon generation today. The short term PF thermal history provides a closer fit to observed %Ro data (Fig. 7c). In spite of this, surface geological evidence favours the long-term PF model (above).

The history of PF development is important for understanding the present thermal regime of the Beaufort–Mackenzie Basin. Present downhole temperatures are unable to determine which PF model is more appropriate for modelling the thermal history of this region (Fig. 8a). If the long term PF model is appropriate, then temperatures are in approximate equilibrium with the base of the PF (0°C at 650 m). Under these conditions, heat flow can be estimated by drawing a linear temperaure gradient from the base of the PF through the measured downhole temperatures (Majorowicz et al., in press) (Fig. 8b). Conversely, if PF development is recent, the temperature regime is in a transient state (nonlinear geotherm) and only the deepest measured temperatures may give a representative average geothermal gradient and heat flow (Fig. 8b). These uncertainties can produce differences in present heat flow estimates of 15% (excluding errors associated with thermal conductivity estimates).

Gas Hydrates

The temperature and pressure regime in permafrost regions is suitable for the formation of gas hydrates,

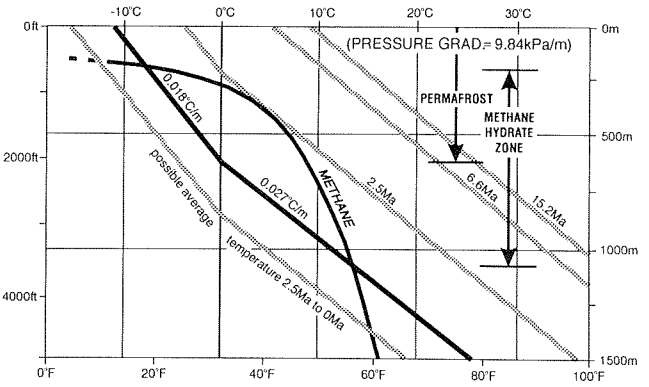

Figure 6. *Significant changes in late Neogene paleovegetation, with paleoclimatic interpretations, are shown with the North Atlantic paleotemperature curve from $\delta^{18}O$. The early Middle Miocene, ca. 15 Ma., had a warm flora at high latitude, with a Mean Annual Temperature (MAT) estimated at 9°C. Significant reduction in warm-loving taxa had taken place by 12 Ma. Peat forming plants with grasses and sedges became more abundant at ca. 6 Ma, indicating climatic cooling, with a MAT at about 5°C. Between 2.6 and 2.7 Ma, the nearshore Arctic Ocean temperature was at most 5°C. Increasing abundance of sages and asters at ca. 2.5 Ma probably indicates greater dryness and the loss of trees, and is coincident with ice-rafted detritus in the North Atlantic (Shackleton et al., 1984). The earliest evidence of permafrost is in Yakutia. Amino acid diagenesis in molluscs suggests that the effective diagenetic temperature since the Fishcreekian transgression in Alaska (ca. 2.5 Ma) has been -16°C; 7°C colder than the modern temperature.([1]Carter et al., 1986; [2]Repenning and Browers, 1992; [3]Ager et al., in prep.; [4]White and Ager, 1994; [5]White et al., 1994; [6]Miller et al., 1987).*

whose presence has been demonstrated in the Mackenzie River delta (Bily and Dick, 1974). Global onshore reserves of gas range between 1.4 x 10^{13} to 3.4 x 10^{16}, with 1.0 x 10^{12} to 1.2 x 10^{12} m^3 in the Prudhoe Bay area (Collett, 1993). Gas hydrates constitute a drilling hazard and a potential seal for conventional gas reserves (Kvenvolden and McMenamin, 1980). On Figure 9, geothermal gradients are shown from reconstructed surface temperatures at 15.2, 6.6 and 2.5 Ma. The latter surface temperature assumes that the early evidence of permafrost in the Kutuyaka beds represents a MAT of -4°C which is the southern limit of widespread permafrost today (National Atlas of Canada, 1973), and uses the temperature gradient in and below permafrost of Bily and Dick (1974). Using these gradients, we have also shown the temperature profile implied by Carter et al.'s (1986) amino acid diagenetic temperature estimate of -16°C over the last 2.5 Ma. Gas hydrates may have begun to form in permafrost at ca. 2.5 Ma. Knowledge of the subsequent late Pliocene and Pleistocene temperature history, with its high amplitude fluctuations, is crucial to understanding the formation of gas hydrates.

Future Climates

Without geological evidence of the variability of global climates, it is doubtful that climatic change could have been seriously considered as a possible effect of human industry. Far-reaching decisions about the use of fossil fuels may be made on the basis of Global Circulation Model (GCM) predictions of future climates under different greenhouse gas parameters, such as CO_2 levels. But if a stock analyst presented a predictive model of stock fluctuations, a smart investor would want to test it – could it simulate the conditions of 1929, the 1950's, the 1980's, and 1987. Paleoclimatic data is needed to test the ability of GCMs to simulate global climates.

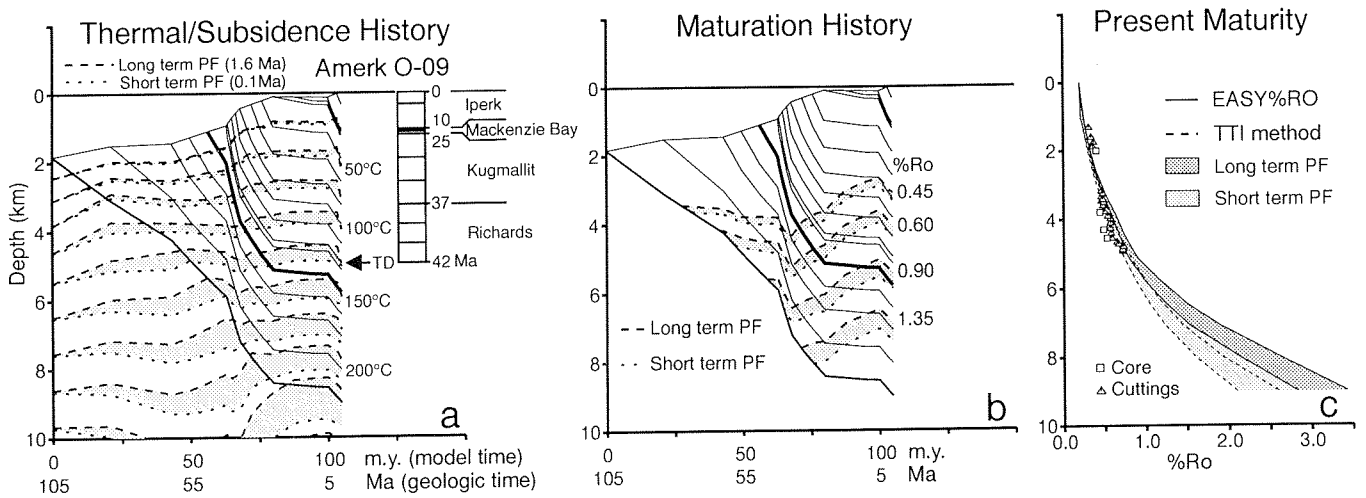

Figure 7. *Results of finite-element thermal modelling for the Amerk O-09 well, Beaufort–Mackenzie Basin. The depth-dependent stretching model assumes heat conduction and includes sediment compaction and variable thermal properties for the sediment and underlying lithosphere (Issler and Beaumont, 1989; Issler and Snowdon, 1990). Models were run assuming that the present base of permafrost (PF) (650 m; assumed to be 0°C) developed: 1) during the Quaternary period (1.6 m.y.) (long term PF model), and 2) during the last 100,000 years (short term PF model).* **a)** *Plot of sediment burial history (solid curves) and superimposed temperature variation (dashed isotherms) through time. Bold curve shows burial history for an Eocene (49 Ma) sediment layer. Both the long term (long dashes) and short term (short dashes) PF models were constrained to match present day temperatures. The stratigraphic column on the right shows the total drilled sequence. Note that the divergence in thermal predictions (shaded regions) between the long term and short term PF models increases with time and depth.* **b)** *Plot of burial history with superimposed predicted variation in selected iso-vitrinite reflectance (%Ro) levels. %Ro values were calculated using the thermal histories from panel (a) and the TTI-%Ro calibration of Issler (1984). Note that the zone of mature sediments is deeper (by ~200 m) and thicker (by ~370 m) and the onset of maturity is later (by up to ~10 m.y.) in the case of the short term PF model.* **c)** *Computed and observed vitrinite reflectance variation with depth for the Amerk O-09 well. The shaded regions represent the difference in calculated maturity using the TTI (dashes) and %EASYRO (solid lines) (Sweeney and Burnham, 1990) %Ro models for the short term (light shading) and long term (darker shading) PF thermal histories. Note that the best fit to the data is achieved using the TTI model (Issler, 1984) with the short term PF thermal history.*

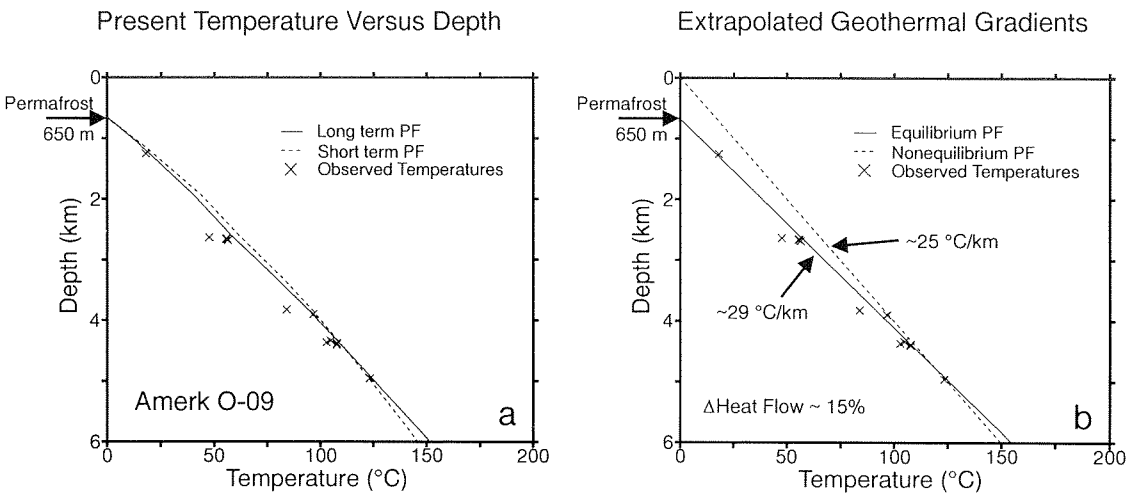

Figure 8. a) *Comparison of observed temperatures (DSTs, corrected BHTs) and the calculated temperature variation with depth for the long term (solid) and short term (dashed) PF models for the Amerk O-09 well. The long term model shows an approximately linear temperature change with depth whereas the short term model is curvilinear. Present temperature data cannot discriminate between models.* ***b)*** *Same temperature data as panel (a) but with two alternate interpretations: 1) if temperatures are in equilibrium with the PF (long term model), the best-fitting linear geothermal gradient is 29°C/km; and 2) if the geotherm is in a transient state (short term model), then only the deepest temperatures are unaffected by recent cooling and an estimated linear geothermal gradient is 25°C/km. The estimated difference in heat flow between interpretations 1) and 2) can have a significant effect on calculated maturity.*

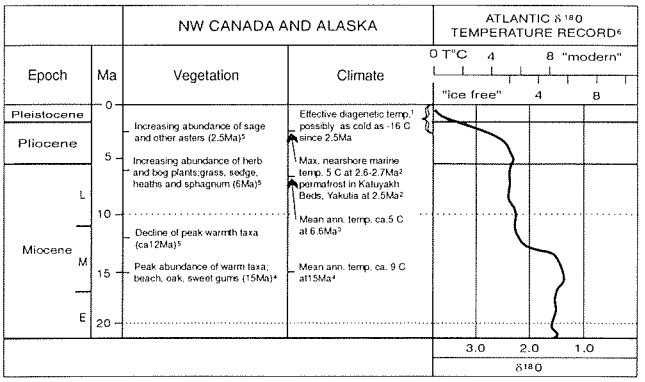

Figure 9. *The zone of modern gas hydrate stability is between the intersection of the temperature and pressure gradients for hydrate stability, and the geothermal gradients (shown in solid line, after Bily and Dick, 1974). Approximate temperature gradients (shown in toned line) for 15.2 and 6.6 Ma have been added using estimated MATs of 9°C and 5°C (respectively) and a 0.027°C/m geothermal gradient. Also marked is a temperature gradient for the time of the first evidence of permafrost (2.5 Ma), assuming that it represented the temperature of the southern limit of widespread permafrost of -4°C (25°F) (National Atlas of Canada, 1973), and using Bily and Dick's (1974) temperature gradients within (0.018°C/m) and below modern permafrost. Resolution of the late Pliocene–Pleistocene temperature history is necessary to model subsequent formation of gas hydrates. The effective diagenetic temperature of amino acids from molluscs from Fish Creek, Alaska, may have been as low as -16°C since the Fishcreekian transgression (ca. 2.5 Ma) (Carter et al., 1986), implying conditions favourable for extensive formation of gas hydrates.*

REFERENCES

Adam, D.
in prep.: Palynology, vegetation history and climatic reconstruction of the Late Pliocene Lost Chicken Placer Mine, east-central Alaska.

Ager, T.A., White, J.M., and Matthews, J.V., Jr.
in prep.: Palynology and paleoenvironments of late Miocene lake deposits near Canyon Village, Porcupine River, northeastern Alaska.

Bily, C. and Dick, J.W.L.
1974: Naturally occurring gas hydrates in the Mackenzie Delta, Northwest Territories. Bulletin of Canadian Petroleum Geology, v. 22, no. 3, p. 340–352.

Cande, S.C. and Kent, D.V.
1992: A new geomagnetic polarity time scale for the Late Cretaceous and the Cenozoic. Journal of Geophysical Research, v. 97, p. 13917–13951.

Carter, L.D., Brigham-Grette, J., Marincovich, L., Jr., Pease, V.L., and Hillhouse, J.W.
1986: Late Cenozoic Arctic Ocean sea ice and the terrestrial paleoclimate. Geology, v. 14, p. 675–678.

Collett, T.S.
1993: Natural gas production from Arctic gas hydrates. *In* United States Geological Survey, Preofessional Paper 1570, p. 299–311.

Currie, D.J. and Paquin, V.
1987: Large-scale biogeographical patterns of species richness of trees. Nature, v. 329, no. 6137, p. 326–327.

Fowells, H.A.
1965: Silvics of forest trees of the United States. United States Department of Agriculture, Handbook 271, Washington, D.C.

Hopkins, D.M., Matthews, J.V., Wolfe, J.A., and Silberman, M.L.
1971: A Pliocene flora and insect fauna from the Bering Strait region. Paleogeography, Paleoclimatology, and Palaeoecology, v. 9, p. 211–231.

Issler, D.R.
1984: Calculation of organic maturation levels for offshore eastern Canada - implications for general application of Lopatin's method. Canadian Journal of Earth Sciences, v. 21, p. 477–488.

Issler, D.R. and Beaumont, C.
1989: A finite element model of the subsidence and thermal evolution of extensional basins: application to the Labrador continental margin. *In* Thermal History of Sedimentary Basins – Methods and Case Histories, N.D. Naeser and T.H. McCulloh (eds.). New York, Springer-Verlag, p. 239–267.

Issler, D.R. and Snowdon, L.R.
1990: Hydrocarbon generation kinetics and thermal modelling, Beaufort–Mackenzie Basin. Bulletin of Canadian Petroleum Geology, v. 38, p. 1–16.

Kunk, M.J., Rieck, H., Fouch, T.D., and Carter, L.D.
1994: $^{40}Ar/^{39}Ar$ Age constraints on Neogene sedimentary beds, Upper Ramparts, Halfway Pillar and Canyon Village sites, Porcupine river, east-central Alaska. Quaternary International, v. 22/23, p. 31–42.

Kvenvolden, K.A. and McMenamin, M.A.
1980: Hydrates of Natural Gas: A Review of Their Geologic Occurrence. Geological Survey Circular 825, United States Department of the Interior.

Leopold, E.B. and Liu, G.
1994: A long pollen sequence of Neogene age, Alaska Range. Quaternary International, v. 22/23, p. 103–140.

Majorowicz, J.A., Jessop, A.M., and Judge, A.S.
in press: Geothermal Regime. *In* Geological Atlas of the Beaufort–Mackenzie Area, J. Dixon (ed.). Geological Survey of Canada, Miscellaneous Report.

Miller, K.G., Fairbanks, R.G., and Mountain, G.S.
1987: Tertiary oxygen isotope synthesis, sea level history, and continental margin erosion. Paleoceanography, v. 2, no. 1, p. 1–19.

National Atlas of Canada
1973: The National Atlas of Canada. Surveys and Mapping Branch, Department of Energy, Mines and Resources. Ottawa, Canada.

Repenning, C.A. and Browers, E.M.
1992: Late Pliocene–Early Pleisotocene Ecologic Changes in the Arctic Ocean Borderland. United States Geological Survey, Bulletin 2036.

Shackleton, N.J., Backman, J., Zimmerman, H., Kent, D.V., Hall, M.A., Roberts, D.G., Schnitker, D., Baldauf, J.G., Desprairies, A., Homrighausen, R., Huddleston, P., Keene, J.B., Kaltenbach, A.J., Krumsiek, K.A.O., Morton, A.C., Murray, J.W., and Westberg-Smith, J.
1984: Oxygen isotope calibration of the onset of ice-rafting and history of glaciation in the North Atlantic region. Nature, v. 307, p. 620–623.

Sweeney, J.J. and Burnham, A.K.
1990: Evaluation of a simple model of vitrinite reflectance based on chemical kinetics. American Association of Petroleum Geologists Bulletin, v. 74, p. 1559–1570.

Van Der Burgh, J., Visscher, H., Dilcher, D.L., and Kürschner, W.M.
1993: Paleoatmospheric signatures in Neogene fossil leaves. Science, v. 260, p. 1788–1790.

White, J.M. and Ager, T.A.
1994: Palynology, paleoclimatology and correlation of Middle Miocene beds from Porcupine River, (Locality 90-1), Alaska. Quaternary International, v. 22/23, p. 43–77.

White, J.M., Adam, D.P., Ager, T.A. , Jéttè, H., Leopold, E.B., Liu, G., and Schweger, C.E.

1994: Neogene and Quaternary palynostratigraphy of northern Yukon Territory and Alaska. Abstract, American Association of Stratigraphic Palynologists, Annual Meeting, College Station, Texas, November 2-5, 1994.

Wolfe, J.A.

1979: Temperature parameters of humid to mesic forests of eastern Asia and relation to forests of other regions of the Northern Hemisphere and Australasia. United States Geological Survey, Professional Paper, v. 1106, 37 p.

1993: A method of obtaining climatic parameters from leaf assemblages. United States Geological Survey Bulletin, v. 2040, 71 p.

THERMAL MATURITY AT THE APPALACHIAN STRUCTURAL FRONT, PORT AU PORT PENINSULA, WESTERN NEWFOUNDLAND: IMPLICATIONS OF INVERSION OF APATITE FISSION TRACK DATA

G.S. Stockmal and D.R. Issler

Geological Survey of Canada, 3303-33rd Street N.W., Calgary, Alberta T2L 2A7

L.A. Quinn

Department of Geology, Brandon University, Brandon, Manitoba R7A 6A9

A. Slingsby

Norcen Energy Resources Limited, 715-5th Avenue S.W., Calgary, Alberta T2P 2X7

INTRODUCTION

Offshore and onshore regions at and adjacent to the Appalachian structural front, western Newfoundland, comprise a frontier area being actively explored for significant petroleum resources. The structural front in this area is primarily a submarine feature (Fig. 1), but the upper detachment of a triangle zone at the leading edge of the orogen is exposed on Port au Port Peninsula (Figs. 1, 2; Stockmal and Waldron, 1990). The triangle zone, which contains rocks of the Humber Arm Allochthon (HAA), is disrupted by a major, transversely striking Devonian reverse fault (the Round Head Thrust) which carries the HAA, an inverted graben containing Middle Ordovician foreland clastics shed from the HAA, Cambro-Ordovician platformal rocks, and probable Grenville crystalline basement in its hanging wall (Fig. 2; Waldron and Stockmal, 1991; Stockmal and Waldron, 1993). Late Ordovician to Devonian(?) foreland strata within the Anticosti basin are tilted westward above the upper detachment of the triangle zone and have been structurally exhumed as a consequence of triangle zone advance (Stockmal and Waldron, 1990).

To assess the thermochronology of the deformation front, we sampled siliciclastic rocks at eight localities in the hanging wall and footwall of the Round Head Thrust (Fig. 2) for analysis of fission tracks in apatite. Stratigraphically, the sample sites include Early Cambrian platformal sediments, Middle Ordovician foreland basin sediments corresponding to the Taconian orogeny, and Siluro–Devonian(?) foreland basin sediments corresponding to the Salinic and Acadian orogenies (Fig. 3).

BACKGROUND AND METHODOLOGY

Apatite fission tracks (AFTs) are produced through the spontaneous fission decay of ^{238}U, which results in zones of linear crystal damage. The density of fission tracks is a measure of the fission track age, whereas the length distribution of confined tracks (wholly within the mineral) provides thermal history information because AFT length reduction (annealing) is a temperature-dependent process. Under most geologically acceptable heating and cooling rates, AFTs anneal over a temperature range of 60–120°C. Therefore, AFT analysis can be very useful for constraining the thermochronology of areas prospective in petroleum.

The complex geological history of western Newfoundland requires that we use an inverse model to fully assess the range of possible time–temperature solutions permitted by the data (see Issler and Stockmal, this volume). The inverse model runs a very large number of forward track annealing models which are compared statistically to observed track lengths. Through a constrained random search procedure (see Willet, in press, and Issler, in press), the program progressively builds a set of statistically acceptable thermal histories.

Thermal histories for Port au Port Peninsula, generated by the inverse model, are constrained by; (1) the known ages of deposition of the sediments; (2) the known proximity of the present-day surface to an Early Carboniferous (Visean) erosion surface; (3) conodont-alteration index values (Nowlan and Barnes, 1987); (4) geologically reasonable maximum heating and cooling rates; and (5) the known geological history which precludes heating after ~250 Ma.

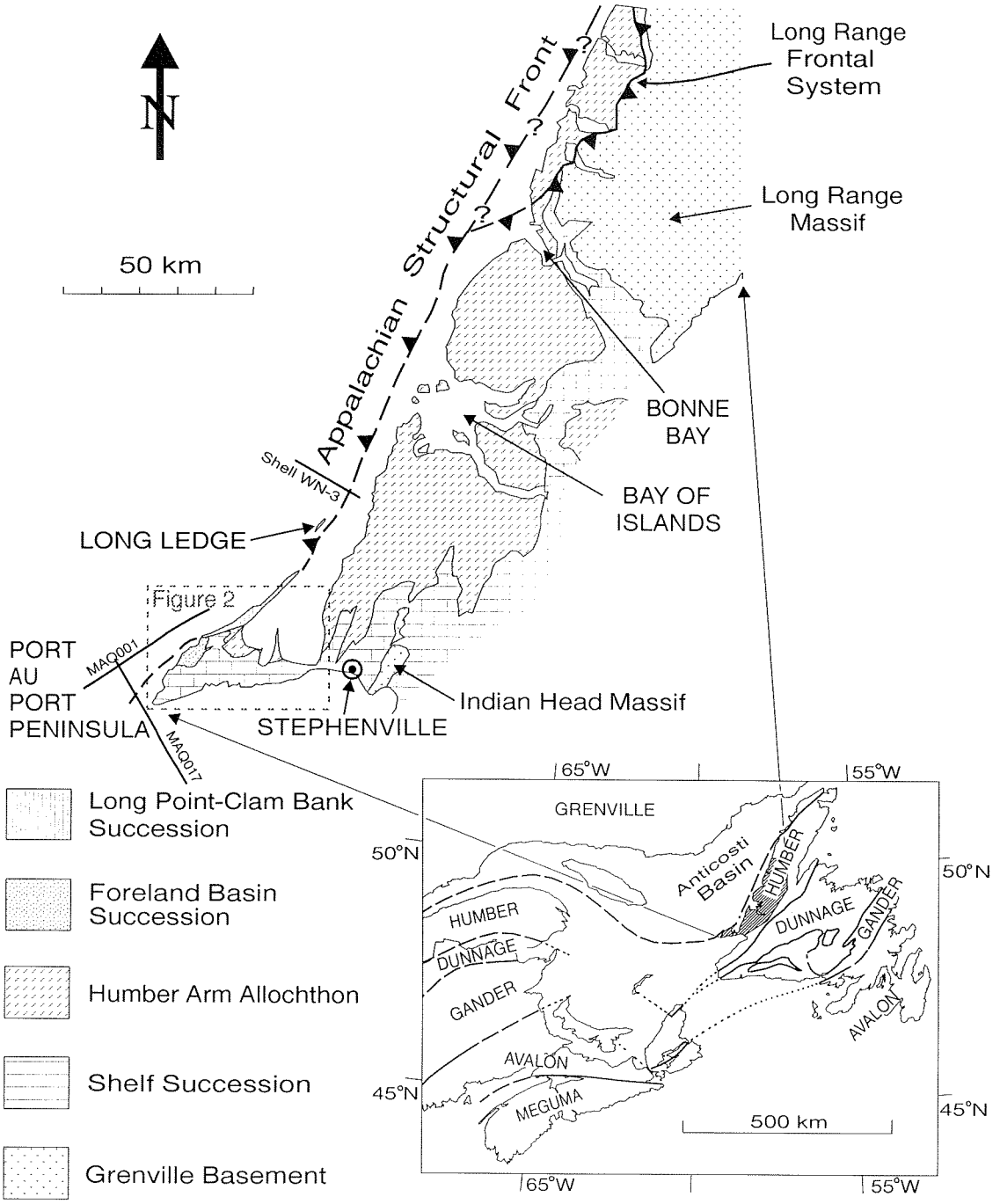

Figure 1. *Regional location map, Atlantic Canada and western Newfoundland. The triangle zone marking the Appalachian structural front extends north of the Bay of Islands, possibly to Bonne Bay. Locations of significant marine seismic reflection lines in the public domain are shown. Figure 2 location as indicated.*

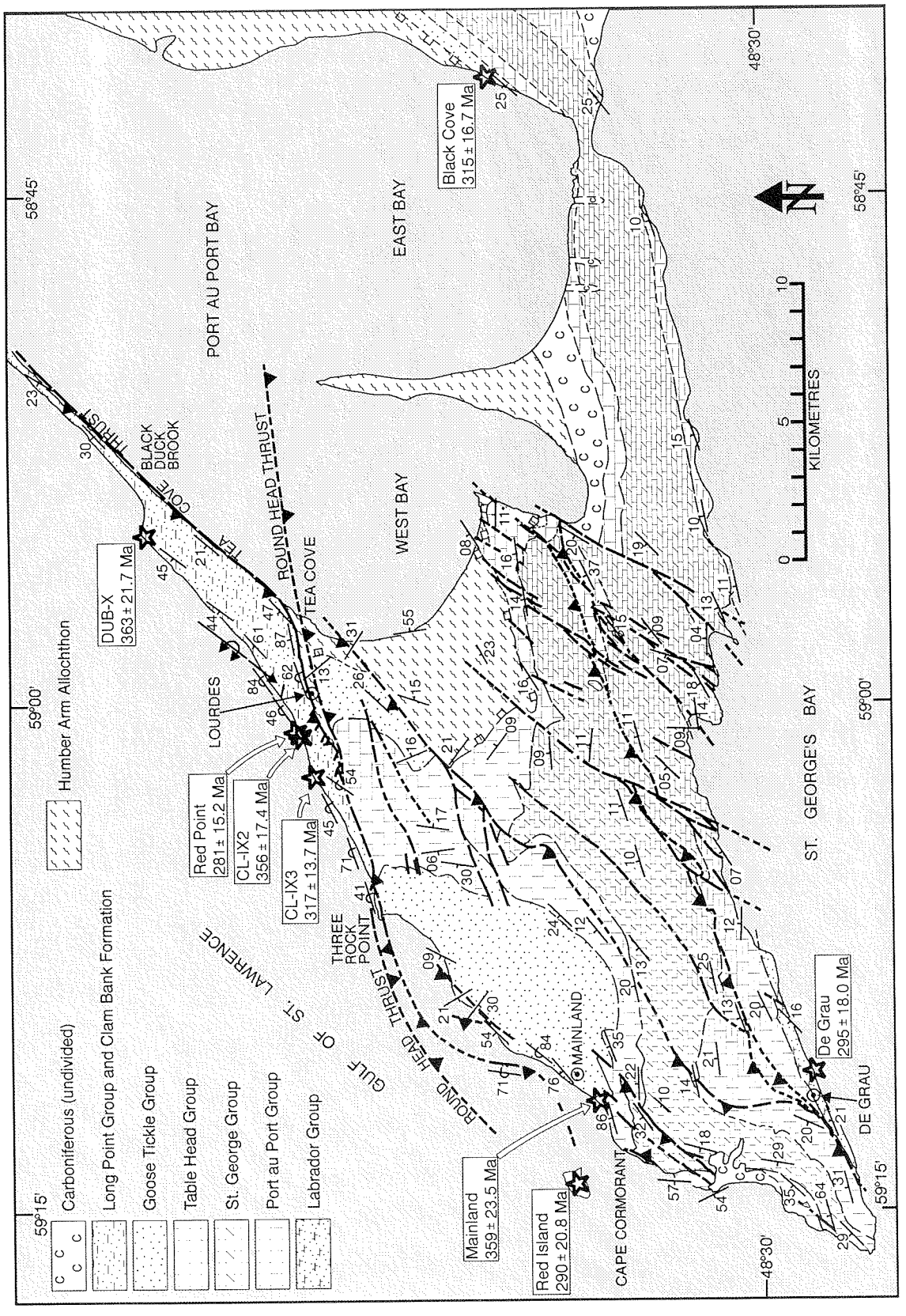

Figure 2. *Locations of AFT sample sites (stars) and age results (boxes). Geology simplified after Stockmal and Waldron (1993).*

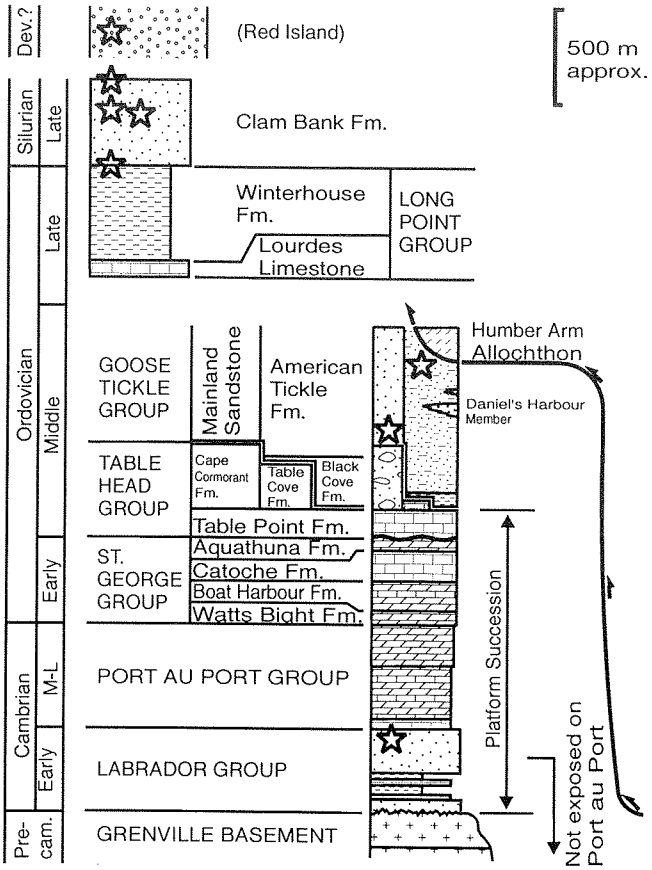

Figure 3. *Schematic stratigraphic column, Port au Port Peninsula and western Newfoundland. Positions of AFT samples noted by stars. Age of sample from Red Island (west of Mainland, Fig. 2) is unknown.*

OBSERVATIONS AND MODEL RESULTS

All eight samples yielded excellent results with respect to errors in the fission track ages and numbers of measured track lengths per sample (only the Mainland Sandstone had fewer than 100 measured lengths). Measured ages range from 363±22 Ma to 281±15 Ma (1σ errors; Fig. 2). For the purposes of this abstract, we concentrate here on two samples: CL-IX2 and Mainland, from the footwall and hanging wall of the Round Head Thrust, respectively. The poster presentation will present results from all sample sites.

Figure 4 presents inverse model results for the footwall sample, CL-IX2, from the middle of the Late Silurian (Pridolian) Clam Bank Formation (Figs. 2, 3). The left-hand plot summarizes 250 acceptable thermal histories derived from the inversion model. The heavy solid line is the exponential mean solution, and the dashed lines are envelopes on the set of solutions; note that the envelopes are not solutions themselves. The right-hand plot shows the measured track length distribution in histogram form, overlain by the computed distribution function for the exponential mean solution (heavy solid line) and the envelopes on the distribution functions for the set of 250 solutions. Figure 5 presents similar model results for the hanging wall sample, Mainland, from near the base of the Middle Ordovician Mainland Sandstone (Figs. 2, 3).

Inverse model results for both samples show similar features, and differ primarily in that the Mainland sample is inferred to have experienced somewhat higher temperatures than CL-IX2 (~90°C *versus* ~70°C) following deposition but prior to Visean

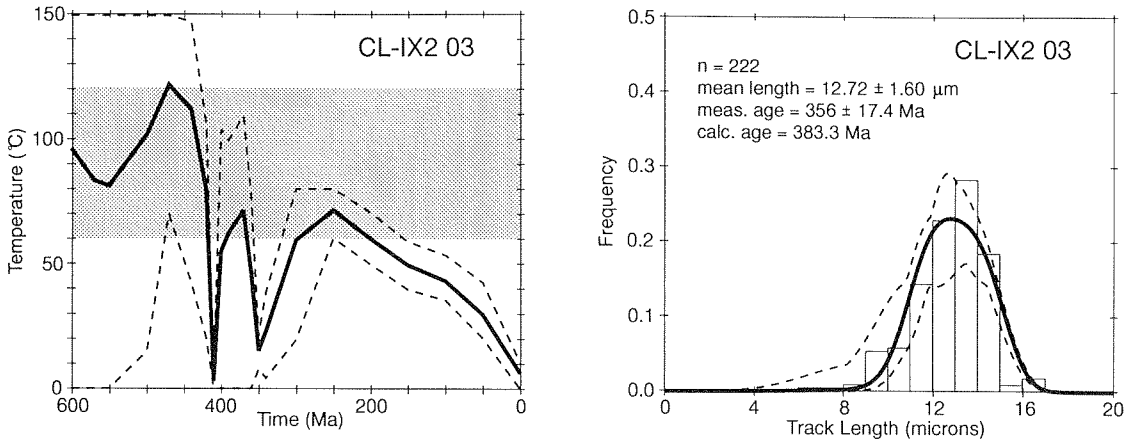

Figure 4. *Inverse model results for Clam Bank Formation sample CL-IX2. Annealing window for AFTs is shaded. See text for discussion.*

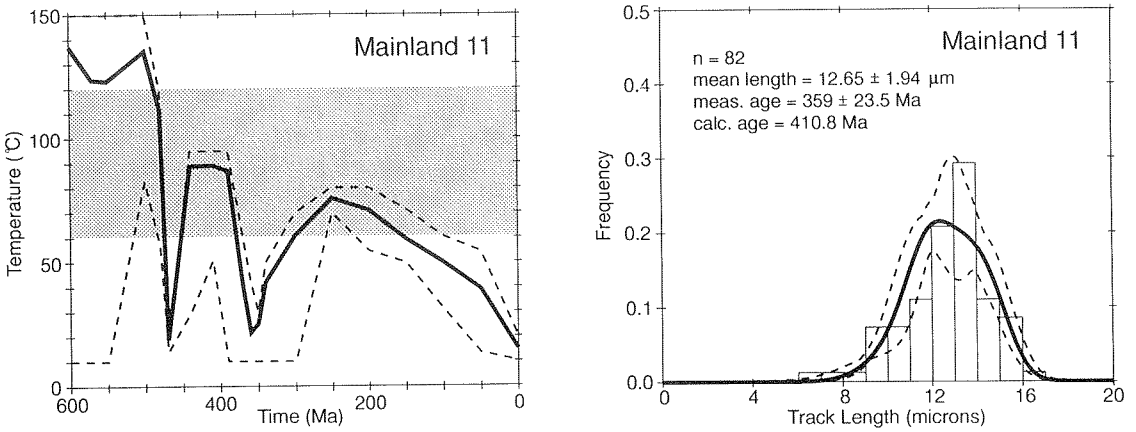

***Figure 5.** Inverse model results for Mainland Sandstone sample. Annealing window for AFTs is shaded. See text for discussion.*

exhumation. Note that some solutions for CL-IX2 indicate temperatures in excess of 100°C over this interval (upper dashed line, Fig. 4 left), but the bulk of the solutions did not reach such high temperatures. Peak pre-Carboniferous temperatures for CL-IX2 coincide with encroachment of the triangle zone in Devonian time, whereas those for the Mainland sample appear to coincide with the Salinic-Acadian orogenic period.

DISCUSSION AND CONCLUSIONS

The results from the two samples considered here are consistent with the observation of nearby oil seeps (on Shoal Point, the peninsula between West Bay and East Bay, Fig. 2), and the immature nature of black shales within the Humber Arm Allochthon along West Bay (M. Fowler, pers. comm., 1994). Previous AFT work on Port au Port Peninsula (Stockmal et al., 1994) indicated that rocks above the upper detachment of the triangle zone (the Red Point sample site, Fig. 2) suffered significantly higher temperatures than those below, which implied that the autochthonous platformal succession in the offshore to the west might be overmature with respect to oil. Resampling, however, indicates that this is probably not the case, since the results of CL-IX2, as well as those of DUB-X, refute our earlier conclusion. Interestingly, the inversion results for CL-IX3, sampled at the highest exposed level of the Clam Bank Formation (Figs. 2, 3), suggest high (~120°C) pre-Carboniferous temperatures, similar to the Red Point sample. One obvious solution is to appeal to warm fluids percolating upward along and adjacent to the Round Head Thrust through isolated zones.

Our results indicate that from a thermochronological point of view, prospectivity is good for liquid hydrocarbons at depth within the platformal succession, both in the offshore autochthonous succession, and where involved with structures at the Appalachian structural front.

REFERENCES

Issler, D.R.
in press: Optimizing time step size for apatite fission track annealing models. Computers and Geosciences.

Issler, D.R. and Stockmal, G.S.
1995: Pitfalls of apatite fission track modelling and interpretation: examples using forward and inverse techniques. This volume.

Nowland, G.S. and Barnes, C.R.
1987: Thermal maturation of Paleozoic strata in eastern Canada from conodont colour alteration index (CAI) data with implications for burial history, tectonic evolution, hotspot tracks, and mineral and hydrocarbon exploration. Geological Survey of Canada, Bulletin 367, 47 p.

Stockmal, G.S. and Waldron, J.W.F.
1990: Structure of the Appalachian deformation front in western Newfoundland: Implications of multichannel seismic reflection data. Geology, v. 18, p. 765–768.

1993: Structural and tectonic evolution of the Humber zone, western Newfoundland, 1: implications of balanced cross sections through the Appalachian structural front, Port au Port Peninsula. Tectonics, v. 12, p. 1056–1075.

Stockmal, G.S., Slingsby, A., and Issler, D.R.
1994: Analysis of apatite fission track data, external Humber zone, western Newfoundland: Implications for petroleum exploration. Exploration Update '94, Joint National Convention of the Canadian Society of Petroleum Geologists and the Canadian Society of Exploration Geophysicists, Calgary, Alberta, Program, Expanded Abstracts and Biographies, p. 228–229.

Waldron, J.W.F. and Stockmal, G.S.
1991: Mid-Paleozoic thrusting at the Appalachian deformation front: Port au Port Peninsula, western Newfoundland. Canadian Journal of Earth Sciences, v. 28, p. 1992–2002.

Willet, S.D.
in press: Inverse modeling of apatite fission track data 1. American Journal of Science.

SHARING OF RESOURCE ASSESSMENT AND ENERGY RELATED DATA: A NATIONAL MEMORANDUM OF UNDERSTANDING BETWEEN PROVINCIAL AND FEDERAL GOVERNMENT AGENCIES

T.D. Bird

Geological Survey of Canada, 3303-33rd Street N.W., Calgary, Alberta T2L 2A7

J. Rowling

Ministry of Energy, Mines and Petroleum Resources, Province of British Columbia
1810 Blanshard Street, Victoria, British Columbia V8V 1X4

INTRODUCTION

In 1994, the Canadian Council of Energy and Mines Ministers signed a Memorandum of Understanding which defines principles for intergovernmental energy resource assessment information sharing. This initiative was introduced by the British Columbia Ministry of Energy, Mines and Petroleum Resources, which started the process toward this multilateral agreement.

BACKGROUND

For strategic and regulatory purposes, various provincial and federal agencies produce assessments of the energy resources under their jurisdiction. The data that is collected, compiled and held by these agencies across Canada is important for developing energy resource assessments and methodologies. This information is often compiled in the form of published reports widely used by oil and gas exploration companies. A need for exchange of assessment data, results and ideas on methodologies is recognized.

- Standardization of data input and reporting of results will enable industrial clients the benefit of better access to raw data and published assessments (e.g., publishing a bibliography of resource assessments).
- This information sharing and collaboration will avoid duplication of effort.
- An interagency dialogue will facilitate the nationwide context use of assessment information.
- The energy resource assessment results will be more accurate and will have greater ease of comparison across territorial and provincial boundaries.

For the purpose of this arrangement, "energy" is defined to include oil, gas, coal, coalbed methane, tar sands, and gas storage, and excludes hydro, geothermal, solar, wind power, tidal energy, or minerals.

PRINCIPLES FOR INTERGOVERNMENTAL COOPERATION

- Formal cooperation should achieve cost effective compilation, analysis, retrieval and exchange of oil and gas information currently gathered or held by individual agencies.
- In order to facilitate data exchange, agencies agree to examine ways to standarize energy resource assessment information definitions and data bases.
- As permitted by the appropriate Freedom of Information legislation, all signatory agencies will provide reasonable access to nonproprietary information to all other signatory agencies, including information relevant to further engineering and economic analysis of resource assessment information. This information may include cost, production, exploration and development practice data.
- An Interagency Working Group will compile, distribute and maintain a listing of available energy resource information across Canada, and will examine additional opportunities for information sharing.

SIGNATORY AGENCIES:

Department of Natural Resources Canada

Geological Survey of Canada, Department of Natural Resources Canada

National Energy Board of Canada

Canada-Newfoundland Offshore Petroleum Board

Newfoundland Department of Mines and Energy

Canada-Nova Scotia Offshore Petroleum Board

Nova Scotia Department of Natural Resources

New Brunswick Department of Natural Resources and Energy

Quebec Ministere de l'Inergie et des Ressources

Ontario Ministry of Energy and Environment

Manitoba Department of Energy and Mines

Saskatchewan Ministry of Energy and Mines

Alberta Department of Energy

Alberta Energy Resources Conservation Board

Northwest Territories Ministry of Energy, Mines and Petroleum Resources

Yukon Department of Economic Development

British Columbia Ministry of Energy, Mines and Petroleum Resources

The following partial bibliography is an example of the resource assessment information to be shared by the GSC in the intergovernment working group

PETROLEUM RESOURCES ASSESSMENTS

Forthcoming GSC Bulletins

Barclay, J.E., Holmstrom, G.D., Lee, P.J., Campbell, R.I., and Reinson, G.E.,
Carboniferous and Permian gas resources of the western Canada sedimentary basin interior plains: Part I: Geological play analysis.

Hamblin, A.P. and Lee, P.J.
Uppermost Cretaceous, Post-Colorado gas resources of the western Canada sedimentary basin interior plains.

Osadetz, K.G., Lee, P.J., Hannigan, P.K., and Olsen-Heise, K.
Natural gas resources of the foreland belt of the Cordilleran orogen in Canada.

Reinson, G.E., Lee, P.J., Olsen-Heise, K., Campbell, R.I., and Holmstrom, G.
Geological play definitions and gas resources, Lower cretaceous Colorado Group, Western Canada interior plains.

Warters, W.J., Cant, D.J., Tzeng, H.P., and Lee, P.J.
Mannville Gas Resources of the western Canada Sedimentary Basin.

Published articles and GSC bulletins

Bird, T.D., Barclay, J.E., Campbell, R.I., and Lee, P.J.
1994: Triassic gas potential seen high in western Canada plains region. Oil and Gas Journal, December 5, 1994, p. 70–74.

Bird, T.D., Barclay, J.E., Campbell, R.I., Lee, P.J., Waghmare, R.R., Dallaire, S.M., and Conn, R.F.
1994: Triassic gas resources of the western Canada sedimentary basin, interior plains; Part I: Geological play analysis and resource assessment and Part II: Economic analysis. Geological Survey of Canada, Bulletin 483, 96 p.

Dixon, J., Morrell, G.R., Dietrich, J.R., Taylor, G.C., Procter, R.M., Conn, R.F., Dallaire, S.M., and Christie, J.A.
1994: Petroleum resources of the Mackenzie Delta-Beaufort Sea, Part I: Basin analysis, Part II: Resource assessment, and Part III: Economic potential. Geological Survey of Canada, Bulletin 474, 52 p.

Dietrich, J.R.
1995: Petroleum resource potential of the Queen Charlotte Basin and environs, west coat Canada. Canadian Society of Petroleum Geologists, Bulletin, v. 43, no. 1, March issue.

Energy, Mines and Resources Canada
1973: An energy policy for Canada: Phase 1, Volume I – Analysis. Energy, Mines and Resources Canada, Ottawa, Ontario, p. 84–98.

1975: Conventional petroleum resources of Canada 1975 estimates. A report to the EMR (Energy, Mines and Resources) Petroleum Resources Committee, Energy, Mines and Resource, Ottawa, Ontario.

1977a: Oil and natural gas resources of Canada. Energy, Mines and Resources Canada, Report EP 77-1.

1977b: Oil sands and heavy oils: the prospects. Energy, Mines and Resources Canada, Ottawa, Ontario, Report EP 77-2.

McCrossan, R.C., Procter, R.M., and Ball, N.L.
1972: An evaluation of the petroleum potential of Canada. Institute of Sedimentary and Petroleum Geology, Calgary, Alberta, p. 1–7.

Podruski, J.A., Barclay, J.E., Hamblin, A.P., Lee, P.J., Osadetz, K.G., Procter, R.M., Taylor, G.C., Conn, R.F., and Christie, J.A.
1988: Conventional oil resources of Western Canada. Geological Survey of Canada, Paper 87-26, Part I. Resource Endowment and Part II: Economic analysis.

Procter, R.M., Lee, P.J., and Skibo, D.N.
1981: Canada's conventional oil and gas resources. Geological Survey of Canada, Open File 767.

Procter, R.M., Taylor, G.C., and Wade, J.A.
1984: Oil and natural gas resources of Canada – 1983. Geological Survey of Canada, Paper 83-31.

Reinson, G.E., Lee, P.J., Warters, W., Osadetz, K.G., Bell, L.L, Price, P.R., Trollope, F., Campbell, R.I., Barclay, J.E., Dallaire, S.M., Waghmare, R.R., and Conn, R.F.
1992: Devonian gas resources of Western Canada Sedimentary Basin. Geological Survey of Canada Bulletin 452, 157 p.

Reinson, G.E. and Lee, P.J.
1993: Study finds Devonian gas resources of western Canada attractive target. Oil and Gas Journal, September 13, 1993, p. 80–93.

Reinson, G.E., Lee, P.J., Barclay, J.E., Bird, T.D., and Osadetz, K.G.
1993: Western Canada basin conventional gas resource estimated at 232 tcf. Oil and Gas Journal, October 25, 1993, p. 92–95.

Sinclair, I.K., McAlpine, K.D., Sherwin, D.F., McMillan, N.J., Taylor, G.C., Best, M.E., Campbell, G.R., Hea, J.P., Henao, D., and Procter, R.M.
1992: Petroleum resources of the Jeanne d'Arc Basin and environs. Part I and II. Geological Survey of Canada, Paper 92-08.

Wade, J.A., Campbell, G.R., Procter, R.M., and Taylor, G.C.
1989: Petroleum resources of the Scotian Shelf. Geological Survey of Canada, Paper 88-19.

Methods for estimating undiscovered petroleum resources

Lee, P.J.
1983: A discovery model for petroleum exploration. *In* Conventional and Unconventional World natural gas resources. Proceedings of the fifth IIASA Conference on Energy Resources, C. Delahaye and M. Grenon (eds.). International Institute for Applied Systems Analysis, Laxenburg, Austria, p. 171–178.

Lee, P.J.
1993: Two decades of Geological Survey of Canada petroleum resource assessments. Canadian Journal of Earth Sciences, v. 30, p. 321–332.

Lee, P.J.
1993: Oil and gas pool size probability distributions - J-shaped, lognormal, or Pareto? *In* Current Research, Part E. Geological Survey of Canada, Paper 93-1E, p. 93–96.

Lee, F.C. and Lee, P.J.
1994: Petroleum resource assessments – a fractal approach. *In* Current Research 1994-E, Geological Survey of Canada, p. 265–270.

Lee, P.J. and Price, P.R.
1991: Successes in 1980s bode for W Canada search. Oil and Gas Journal, April 22, 1991, p. 92–97.

Lee, P.J., Qin, R., and Shi, Y.
1989: Conditional probability analysis of geological risk factors. *In* Statistical Applications in the Earth Sciences. F.P. Agterberg and G.F. Bonham-Carter (eds.). Geological Survey of Canada, Paper 89-9, p. 271–276.

Lee, P.J. and Singer, D.A.
1994: Using PETRIMES to estimate mercury deposits in California. Nonrenewable Resources, v. 3, no. 3, p. 190–199.

Lee, P.J. and Tzeng, H.P.
1993: The petroleum exploration and resource evaluation system, (PETRIMES/PC): Working reference guide. Geological Survey of Canada, Open File 2703, Calgary, Alberta.

Lee, P.J. and Wang, P.C.C.
1983a: Probabilistic formulation of a method for the evaluation of petroleum resources. Mathematical Geology, v. 15, p. 163–181.

1983b: Conditional analysis for petroleum resource evaluations. Mathematical Geology, v. 15, p. 353–365.

1984: PRIMES: A petroleum resources information management and evaluation system. Oil and Gas Journal, October, 1, 1984, p. 204–206.

1985: Prediction of oil or gas pool sizes when discovery record is available. Mathematical Geology, v. 17, p. 95–113.

1986: Evaluation of petroleum resources from pool size distribution. *In* Oil and gas assessment methods and applications. D.D. Rice (ed.). American Association of Petroleum Geologists, Studies in Geology, no. 21, p. 33–42.

1990: An introduction to petroleum resource evaluation methods. Canadian Society of Petroleum Geologists, Short Course, SC-2.

Procter, R.M. and Taylor, G.C.
1984: Evaluation of oil and gas potential of an offshore westcoast Canada play – an example of Geological Survey of Canada methodology. *In* Petroleum Resources Assessment, C.D. Masters (ed.), International Union of Geological Sciences, Publication no. 17, p. 39–62.

Roy, K.J.
1979: Hydrocarbon assessment using subjective probability and Monte Carlo methods. *In* First IIASA Conference on Methods and Models for Assessing Energy Resources. M. Grenon (ed.). Pergamon Press, New York, p. 279–290.

Roy, K.J., Procter, R.M., and McCrossan, R.G.
1975: Hydrocarbon assessment using subjective probability. *In* Probability Methods in Oil Exploration. *Convenors* Davis, J.C., Doveton, J.H., and Harbaugh, J.W. American Association of Petroleum Geologists Research Symposium.

PITFALLS OF APATITE FISSION TRACK MODELLING AND INTERPRETATION: EXAMPLES USING FORWARD AND INVERSE TECHNIQUES

D.R. Issler and G.S. Stockmal

Geological Survey of Canada, 3303-33rd Street N.W., Calgary, Alberta T2L 2A7

Purpose: Some common (though not necessarily obvious) pitfalls of apatite fission track (AFT) modelling and interpretation will be examined using computer programs which generate theoretical fission track ages and track length distributions. We compare these outputs with observed data from samples whose stratigraphic ages range from late Tertiary to early Paleozoic. We explicitly consider the consequences of performing forward models only, as well as examining the range of thermal histories permitted by the data, as elucidated by an "inverse" or optimization approach. The demonstration will use a PC running the software, with the screen projected using an overhead projector adapter, as well as slides of results which cannot be run in real time during the demonstration. Here, we illustrate only two of a number of samples and situations to be discussed.

INTRODUCTION

AFT analysis is a powerful technique for reconstructing the thermal histories of sedimentary basins. It can provide important thermochronological information that cannot be obtained using more traditional paleotemperature methods. For example, unlike vitrinite reflectance (%Ro), which records the cumulative effects of time and temperature, AFT data allow for the partial resolution of time and temperature in the thermal history of a sample. In addition, AFTs are more sensitive to temperature than vitrinite reflectance and may record rapid temperature changes that may otherwise be unresolved by %Ro data. For these reasons, given an appropriate context and sampling methodology, the AFT method has the potential to provide answers to questions of relevance to the petroleum industry. For example, when did motion take place along a specific fault? What is the maximum paleotemperature and when did it occur? What is the timing, rate and magnitude of erosion/tectonic exhumation? Have these rocks been a conduit for the migration of warmer fluids?

APATITE FISSION TRACK METHOD

Fission tracks in apatite are linear regions of crystal damage which form by the spontaneous fission of ^{238}U through geologic time. The density of fission tracks intersecting a polished mineral surface is a measure of the fission track age. The length distribution of horizontal "confined" (below mineral surface) tracks provides a record of paleotemperatures because AFT length reduction is a temperature-dependent process. The shortest tracks are the oldest and have experienced the longest portion of the sample thermal history, whereas the longest tracks have formed most recently. Above the temperature for total annealing of AFTs (T_a; 110-120°C for typical heating rates), all pre-existing tracks are annealed and the fission track clock is reset. Only under conditions of cooling below the T_a does the AFT age record a geologically meaningful "event" (i.e., time of cooling below the *cooling rate-dependent* T_a). If the AFT sample experiences subsequent heating at temperatures below T_a, further age reduction occurs and the AFT age becomes a "mixed" age that does not date a discrete event. The interpretation of these partially annealed samples forms the basis for thermal history reconstruction.

LIMITATIONS OF THE METHOD

Like all paleotemperature techniques, AFT analysis has its limitations and may not be suitable for some problems. Some of the reasons for this include: (1) a lack of dateable apatite (absence of the mineral or a low uranium content), (2) poorly chosen samples, or (3) an unfavourable geological history. For example, AFT data cannot constrain events which occur at temperatures greater than the T_a. To avoid disappointment, it is necessary for users to undertake a carefully planned sampling strategy to identify intervals where AFT data could be most useful. This can be done with the aid of maturity or other paleotemperature data, if available, or with present temperature data if samples are collected

from wells. Maturity data can help distinguish whether AFTs have been partially or completely reset, an important factor for determining the significance of AFT ages. The exact relationship between %Ro and AFT annealing is poorly understood because both methods respond differently to changes in temperature and because the T_a also depends on apatite composition. However, for average situations, complete AFT annealing is likely for maturity levels >0.7%Ro.

Samples which have spent a considerable fraction of their geological history at temperatures where partial annealing is significant (typically ~60°C to 120°C; the exact temperature range depends on the rate of temperature change and apatite composition) may contain a valuable record of the thermal history. Samples that have remained below these temperatures provide information concerning the source of the apatites (e.g., prior to deposition for detrital apatites) but few details concerning the thermal history. Samples at temperatures significantly greater than T_a through most of their history may reflect only recent cooling. In this latter case, the cooling age may be of limited significance if the onset of cooling was significantly earlier. Therefore, samples must be carefully selected with specific questions in mind.

Thermal modelling of fission track annealing is a valuable means to extract time–temperature information from measured fission track parameters, particularly for samples with a complex history of heating and cooling. However, even with good quality AFT data, interpretation may not be straightforward, particularly in poorly understood geological settings. Solutions are nonunique and AFT data are best interpreted within the appropriate geological context. Below, we discuss two different modelling strategies: forward and inverse modelling. Forward models may be useful in simple, well-constrained settings but we recommend the inverse approach, which is a generalization of the forward modelling technique, because it is more objective and gives the user a better appreciation of the variability in thermal histories allowed by the data.

FORWARD MODELLING

Models for temperature-dependent AFT annealing have been developed using data from laboratory heating experiments (Laslett et al., 1987; Carlson, 1990; Crowley et al., 1991) and have been incorporated into forward models for thermal history reconstruction (e.g., Green et al., 1989; Willett, 1992; Crowley, 1993). At present, no universally accepted model exists for AFT annealing (for example, the effect of compositional variation has not been adequately quantified), but most applications use the Laslett et al. (1987) or Crowley et al. (1991) model for Durango apatite based on the data of Green et al. (1986). In forward modelling, users specify a time–temperature history which is used to calculate AFT age and track length distributions for comparison with measured values. The user modifies the trial solution until an acceptable fit is obtained. Generally, the user is guided by available geological data (e.g., burial history, present geothermal gradients, other paleotemperature data) but in the absence of any constraints, a unique solution may not be possible from AFT data alone.

Figure 1 illustrates how forward models may suffer from the nonuniqueness problem. Panels a and c each show an acceptable time–temperature history that was used to calculate AFT age and length parameters for comparison with measured values (Fig. 1b, d). The sample AFT age (66 Ma) is significantly older than its (~30 Ma) stratigraphic age, indicating that it preserves a record of cooling prior to deposition during the Oligocene. In models A and B, the post-30 Ma thermal history as estimated from the sample burial history, is identical. However, prior to 30 Ma, model A has a protracted period of cooling from temperatures above the T_a whereas model B shows moderate heating from surface temperatures to 80°C followed by cooling. Both models produce virtually identical AFT age and length parameters (Fig. 1b, d) but have vastly different geological implications. Model A suggests that the apatite may have been derived from disparate sources which experienced complete AFT annealing, that it cooled during Late Cretaceous-early Tertiary regional exhumation, and that it was redeposited during the Oligocene. Model B suggests a more discrete source such as a volcanic ash which formed at the surface and experienced moderate burial temperatures (80°C) followed by erosion and redeposition. Other geological criteria are needed to choose between these and other possible models.

INVERSE MODELLING

Although forward modelling can be useful for estimating thermal histories in well constrained settings, it does not give the user a sense of the variation in thermal histories permitted by the data. A more general approach is to find a range of solutions which give an acceptable fit to the AFT data. The value of this approach is that it can indicate which portions of the thermal history are well resolved by the data and which parts are poorly constrained. A number of inverse

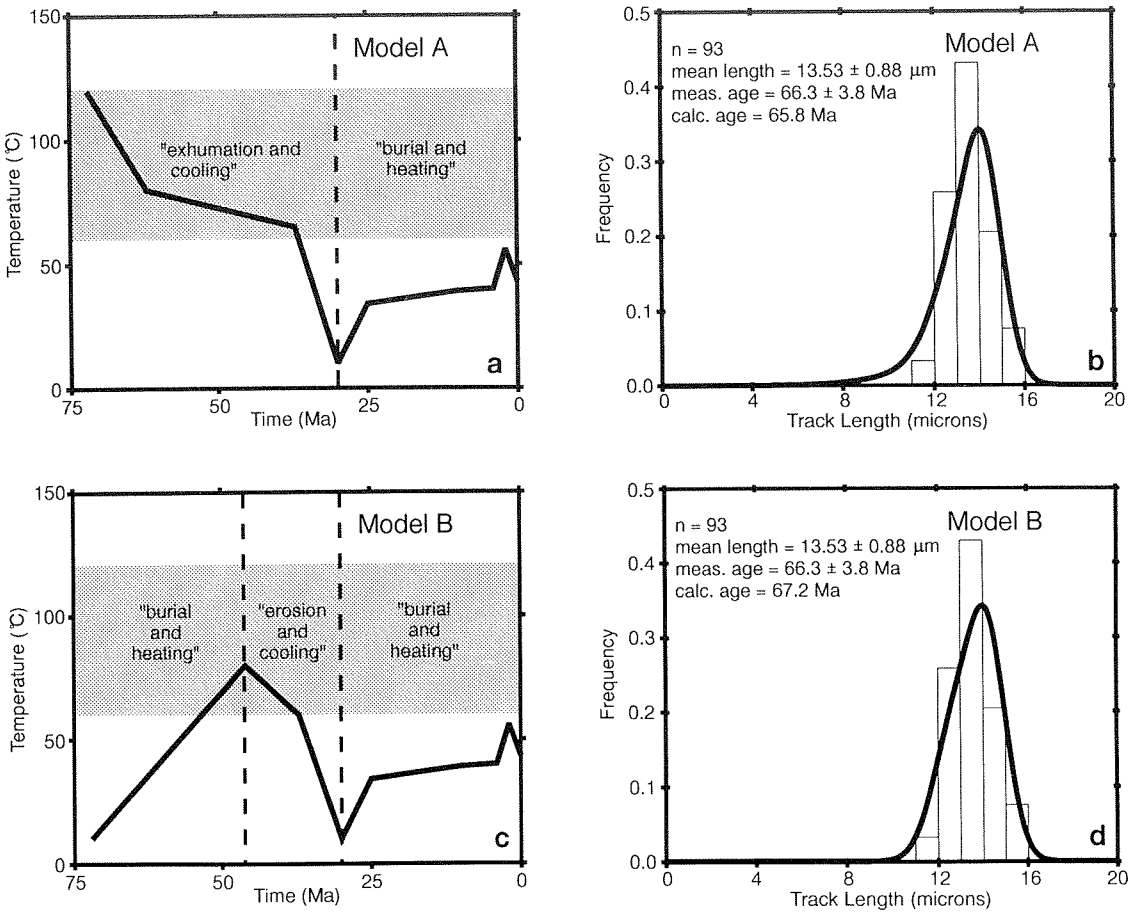

Figure 1. *Forward model thermal histories (panels a and c) and corresponding measured (histogram) and calculated (bold curve) track length distributions (panels b and d) for two different models (A and B) of the same AFT data set. A modified version of the forward model of Willett (1992), which uses the Durango annealing model of Crowley et al. (1991), was used to calculate AFT parameters. AFT data are for detrital apatite from an Oligocene (~30 Ma) subsurface sample with a present temperature of approximately 43°C. In panels a and c, the post-30 Ma thermal history, as inferred from the sample burial history, is the same for both models A and B. Cooling over the last 2 m.y. is related to permafrost development. The shaded regions in panels a and c mark the approximate zone where AFT annealing is significant. Note that calculated AFT age and length distributions are essentially identical for both models A and B (panels b and d) although the pre-30 Ma portions of the thermal histories are significantly different. A common feature of both models is that most apatite annealing occurs within the 60° to 80°C temperature range.*

models, which adopt this general philosophy, have been developed to recover thermal history information from AFT data (e.g., Issler et al., 1990; Corrigan, 1991; Lutz and Omar, 1991; Willett and Issler, 1992; Gallagher et al., 1994). We use a modified version of a program initially developed by S.D. Willett (in prep.) and applied to problems in the Western Canada Sedimentary Basin (Issler et al., 1990; Willett and Issler, 1992; Ravenhurst et al., 1994). The program has been modified to run interactively and includes a time step predictor function for numerical integration of the AFT annealing equation (Issler, submitted).

The inversion program, using a constrained random-search algorithm, finds a set of 250 forward models which statistically fit the observed fission track age and track length distribution. Figure 2 shows results of the inversion program for a sample of the Middle

Ordovician Mainland Sandstone from western Newfoundland (Stockmal et al., 1994). The Mainland Sandstone was derived from the Humber Arm Allochthon, and is interpreted to represent the foreland basin fill deposited during the Taconian orogeny. Two sets of model results are shown to illustrate some of the differences that can result given additional independent constraints. These differences illustrate the importance of incorporating all available information. Only selected results of the inversion model are shown, due to space limitations.

The depositional age (modelled as 470 Ma) and known proximity to a Carboniferous (Viséan) erosional surface (modelled as 350 Ma) are used as temperature constraints in both models, resulting in the very low temperature portions of the time–temperature curves at these times. Model "Mainland 12" incorporates these constraints only, whereas model "Mainland 11" has additional constraints stemming from Conodont Alteration Index (CAI) values (observed CAI value of 1), geologically reasonable upper limits to heating and

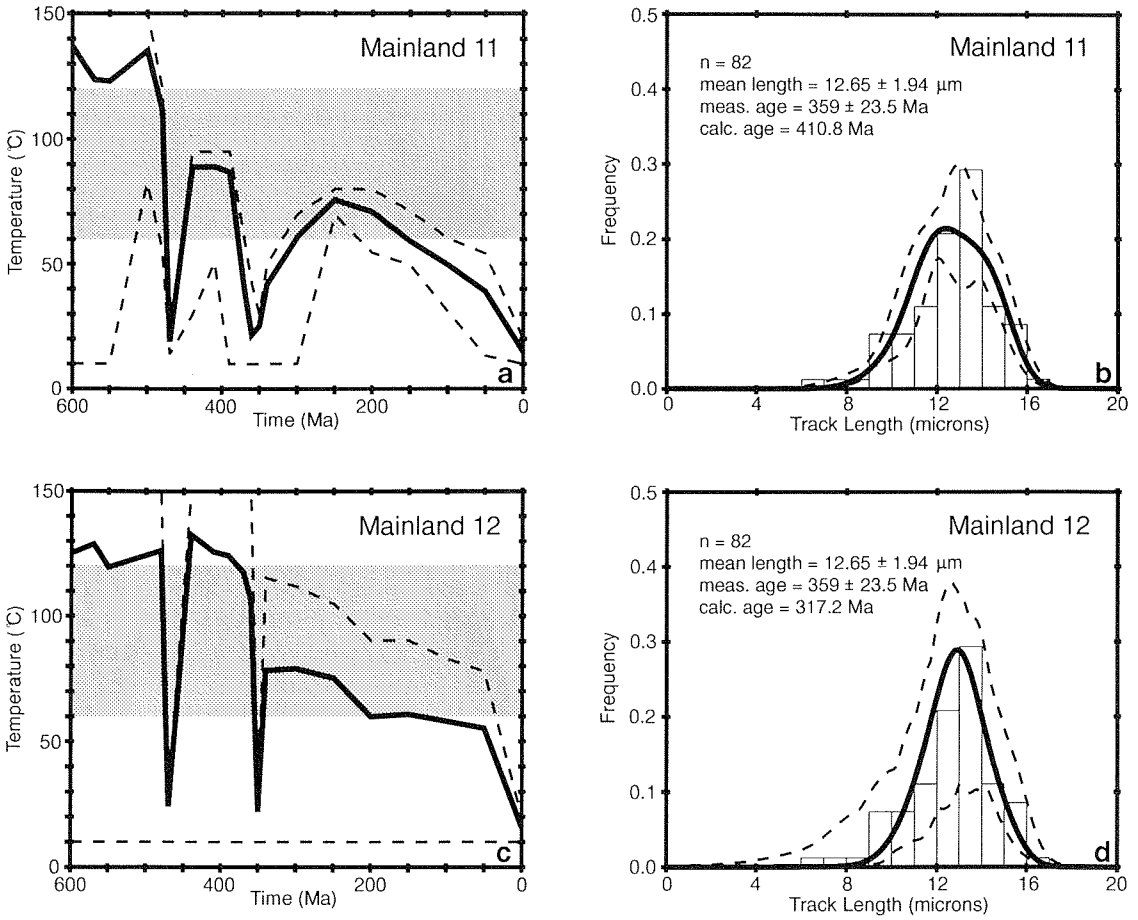

Figure 2. *Inverse model thermal histories showing the exponential-mean (bold curve) and range of 250 acceptable solutions (dashed envelope) (panels a and c) that satisfy the observed AFT ages and length distributions (histogram) (panels b and d). Note that the dashed envelopes are not solutions themselves, but define the limits of solutions which may have many more oscillations than the mean solutions. In panels b and d, the bold curve is the calculated track length distribution for the mean thermal history (panels a and c) and the dashed envelope defines the range of track length distributions for 250 statistically acceptable thermal histories. As for the time–temperature history plots, the dashed lines define a range but are not solutions themselves. Mainland 11 incorporates significantly more geological constraints than Mainland 12 which results in a significantly lower temperature history (compare panels a and c). For Mainland 12, the inverse program achieved 250 acceptable models after generating less than 4000 forward models, whereas for Mainland 11, it required more than 40,000 forward models.*

cooling rates, and cooling only after 250 Ma (known from the regional history). Clearly, there are significant differences between these two sets of calculations, most notably the differences in timing and magnitude of temperature maxima. Such differences could have great significance in determining the petroleum prospectivity of the area.

REFERENCES

Carlson, W.D.
1990: Mechanisms and kinetics of apatite fission track annealing. American Mineralogist, v. 75, p. 1120–1139.

Corrigan, J.
1991: Inversion of apatite fission track data for thermal history information. Journal of Geophysical Research, v. 96, p. 10,347–10,360.

Crowley, K.D.
1993: Lenmodel: a forward model for calculating length distributions and fission track ages in apatite. Computers and Geosciences, v. 19, p. 619–626.

Crowley, K.D., Cameron, M., and Schaefer, R.L.
1991: Experimental studies of annealing of etched fission tracks in fluorapatite. Geochimica et Cosmochimica Acta, v. 55, p. 1449–1465.

Gallagher, K., Hawkesworth, C.J., and Mantovani, M.S.M.
1994: The denudation history of the onshore continental margin of southeast Brazil inferred from apatite fission track data. Journal of Geophysical Research, v. 99, p. 18,117–18,145.

Green, P.F., Duddy, I.R., Gleadow, A.J.W., Tingate, P.R., and Laslett, G.M.
1986: Thermal annealing of fission tracks in apatite 1. A qualitative description. Chemical Geology (Isotope Geoscience Section), v. 59, p. 237–253.

Green, P.F., Duddy, I.R., Laslett, G.M., Hegarty, K.A., Gleadow, A.J.W., and Lovering, J.F.
1989: Thermal annealing of fission tracks in apatite 4. Quantitative modelling techniques and extension to geological timescales. Chemical Geology (Isotope Geoscience Section), v. 79, p. 155–182.

Issler, D.R., Beaumont, C., Willett, S.D., Donelick, R.A., Mooers, J., and Grist, A.
1990: Preliminary evidence from apatite fission track data concerning the thermal history of the Peace River Arch region, Western Canada Sedimentary Basin. Bulletin of Canadian Petroleum Geology, v. 38A, p. 250–269.

Laslett, G.M., Green, P.F., Duddy, I.R., and Gleadow, A.J.W.
1987: Thermal annealing of fission tracks in apatite 2. A quantitative analysis. Chemical Geology (Isotope Geoscience Section), v. 65, p. 1–13.

Lutz, T.M. and Omar, G.
1991: An inverse method of modelling thermal histories from apatite fission track data. Earth and Planetary Science Letters, v. 104, p. 181–195.

Ravenhurst, C.E., Willett, S.D., Donelick, R.A., and Beaumont, C.
1994: Apatite fission track thermochronometry from central Alberta: Implications for the thermal history of the Western Canada Sedimentary Basin. Journal of Geophysical Research, v. 99, p. 20,023–20,041.

Stockmal, G.S., Slingsby, A., and Issler, D.R.
1994: Analysis of apatite fission track data, external Humber Zone, Western Newfoundland: Implications for petroleum exploration. *In* Exploration Update '94, Joint National Convention of the Canadian Society of Petroleum Geologists and the Canadian Society of Exploration Geophysicists, Calgary, Alberta, Expanded Abstracts, Program and Biographies, p. 228–229.

Willett, S.D.
1992: Modelling thermal annealing of fission tracks in apatite. *In* Low Temperature Thermochronology, M. Zentilli and P.H. Reynolds (eds.). Mineralogical Association of Canada, Short Course Handbook, v. 20, p. 43–72.

Willett, S.D. and Issler, D.R.
1992: Apatite fission track thermochronometry applied to the Western Canada Sedimentary Basin - a case history from the Peace River Arch region. *In* Low Temperature Thermochronology, M. Zentilli and P.H. Reynolds (eds.). Mineralogical Association of Canada, Short Course Handbook, v. 20, p. 157–185.

EXPLOITATION AND MEASUREMENT OF IN SITU STRESSES IN SEDIMENTS

J.S. Bell

Geological Survey of Canada, 3303-33rd Street N.W., Calgary, Alberta T2L 2A7

Contemporary stress orientations can be inferred from various geological phenomena and, as well, can be measured. Table 1 summaries the main sources of stress orientation information that can be obtained in sedimentary basins. There are also a number of practices which are inferential. They require certain conditions to be fulfilled to provide reliable contemporary stress orientations (Table 2). Relative stress magnitudes can be inferred from geological phenomena, but absolute magnitudes require measurements (Table 3). The latter are often difficult to justify because of costs and logistical requirements. Fortunately, leak-off tests, and other data sources, can be used to provide reasonable estimates of the smaller

Table 1

Geological phenomena which can be used to diagnose horizontal stress orientations in sedimentary basins, together with methods of measurement, classified according to depth of application

NEAR SURFACE INFORMATION	
Phenomena	**Mechanism**
Neotectonic fractures	Stress relief following unloading
Pop-ups	Stress relief following unloading
Updip bed slip	Stress relief, lateral load removal
Active Fault offsets	Stress relief
Active Fold growth	Stress relief
Measurement method	**Constraints**
Overcoring	Requires elastic properties
Flat-jack tests	Surfaces only
INTERMEDIATE DEPTH INFORMATION (100 m to 6 km)	
Phenomena	**Mechanism**
Borehole breakouts	Stress amplification/fracturing in wells
Earthquakes	Stress relief in sediment sequence
Drilling-induced fractures	Drilling mud compression, ?weight on bits
Active faults	Stress relief
Borehole closing	Usually an elastic response to stress
Induced earthquakes	Artifical pore pressure changes
Core discing	Stress relief
Centre-line fractures in cores	Stress relief
Measurement method	**Constraints**
Hydraulic fractures	Need to record fracture orientation
Anelastic strain release	Need newly-recoverd oriented cores
Differential strain analysis	Need oriented cores
Holographic distortions	Technology lagging
DEEP (BASEMENT AND CRATONIC) INFORMATION	
Phenomena	**Mechanism**
Volcanic alignments	Stress-controlled extension
Plucking fractures	Unloading and glacial scouring
Earthquakes	Stress relief

Table 2

Techniques used to infer stress orientations in sedimentary basin

INFERENTIAL PRACTICES	
Technique	**Assumptions**
Shear wave splitting	Aligned microcracks in plane of S_v, SH_{max}
Kaiser Effect	All aligned cracks are caused by stres relief
Core anisotropy	Anisotropy mirrors today's stresses
Stoneley Wave polarization	Cracks are aligned with today's stresses
Basin scale inferences	Tectonics are compatible with today's stresses

horizontal principal stress, and overburden load estimates will approximate SH_{min}, the vertical stressS_v.

This demonstration will review current approaches to assembling in situ stress information in sedimentary basins and will discuss how these data need to be interpreted in terms of the structure and tectonic history of the individual basin. Anomalous stress orientiations can usually be explained as resulting from contrasts in geomechanical properties that are manifested in terms of geological structure, whereas anomalous magnitudes generally reflect basin history. Both orientations and magnitudes (in combination with pore pressures) can be used to assist in achieving borehole stability, hydraulic fracturing and reservoir production. The stress regime in a basin is also of interest to explorationists because it controls some aspects of fluid migration and trapping and because it plays a role in determining which fracture sets remain open.

Table 3

Methods for stress magnitude measurement in sedimentary basin

NEAR SURFACE INFORMATION	
Measurement method	**Constraints**
Overcoring	Requires elastic properties
Flat-jack tests	Surface measurements only
INTERMEDIATE DEPTH INFORMATION (100 m to 6 km)	
Measurement method	**Constraints**
Hydraulic fracturing	SH_{min} measured, SH_{max} calculated
Leak-off tests	SH_{min} estimated
Anelastic strain release	Need newly-recovered oriented cores
Differential strain analysis	Need oriented cores
Holographic distortions	Technology lagging

FOSSILS AND FUELS – HOW PALEONTOLOGICAL RESEARCH AT THE GSC SERVES THE RESOURCE INDUSTRY

T.P. Poulton and J.S. Bell

Geological Survey of Canada, 3303-33rd Street N.W., Calgary, Alberta T2L 2A7

Paleontology was one of the fathers of the science of geology that we practice today. Fossils large and small spawned biostratigraphy, the best technique ever developed for dating ancient rocks. The inter-related concepts of geologic time, the evolution of life, global mass extinctions, and interdependent earth systems rank among the most fundamental and awesome scientific contributions of all time. Paleontology is so central to these themes that it surely is more critical to geological training and general life-appreciation skills now than it has ever been. Paleontology is the study of nothing less than the entire history of past animal and plant life on this planet that we call home. The geologic time scale does not exist without this core discipline of geology, and any interpretation deriving from it, such as geologic maps and cross sections in Phanerozoic terranes, are only as good as the age data that they imply.

With fossil zones averaging less than 1 my in duration for many geologic systems (e.g., Callomon, 1984; Cope, 1993) and becoming more refined with each passing year of research, no other component of ancient sedimentary rocks offers anything close in time stratigraphic resolution. What this means is that all attempts to reconstruct paleogeographies without paleontology are doomed to be inaccurate, often grossly so. In particular, paleofacies maps based on log correlations that purport to portray former land and seascapes generally do not. What they do show are areal configurations of rock units that are determined by the correlation of petrophysical measurements, tempered in some cases by core and cutting descriptions. Shaw (1964) has shown best the contradictory transgressive-regressive histories that result from recognition of diachronous facies equivalents contrasted with those derived from the more commonly generated lithofacies maps alone.

Fossils are unequalled tools for understanding the sedimentary rock record and what has happened to it, for several reasons. Because of uni-directional organic evolution and extinction events, empirical successions of fossils can be recognized, making them unrivalled time indicators. This process is **BIOSTRATIGRAPHY**. Because animals and plants lived in equilibrium with their environment, fossils found in their original setting provide valuable data regarding that environment, including its chemical characteristics. Where they have been transported from their living environment, they provide data regarding that transport and the factors relating to it. These various studies are mutually interrelated and comprise **PALEOECOLOGY, PALEOBIOGEOCHEMISTRY**, and **TAPHONOMY**. They are closely linked with their companion discipline that studies the host sediments, sedimentology.

Animal and plant species are not generally spread across the globe, but live in particular regions, to which they are restricted by living conditions, competition and predation, and within which they evolved distinctive traits. Fossils therefore serve as indicators of ancient biotic provinces, and their study is **PALEOBIOGEOGRAPHY**. Similarities from one area to another indicate connections, such as similar climates, or connecting seaways or landmasses, powerful tools in the construction of paleogeographic maps. Together with paleoecologic characteristics, these data are a basis for the interpretation of ancient climates and depositional conditions that might have produced hydrocarbon-generating source rocks or reservoirs.

Most fossils are composed of carbonate or phosphate combined with organic material. They are affected by heat, pressure, surrounding fluid composition and all the other agents that change the character of sedimentary rocks after they are deposited. Thus fossils are sensitive indicators of **THERMAL ALTERATION**, a powerful tool in predicting hydrocarbon generation potential.

All these topics contribute fundamental data to the analysis of sedimentary basins, and to exploration for coal, oil and gas, which themselves are the remains of ancient life.

BIOSTRATIGRAPHY

The oldest, and still most important, use of fossils is in biostratigraphy.

The importance of fossils for the correct identification of rock units was recognized late in the seventeenth century. Early applications of biostratigraphy to road and canal construction in areas of shallow bedrock in England were employed empirically well before the major features of evolution were stated by Darwin, Wallace and others. A vastly expanded knowledge base, backed by a sound theoretical framework, ensures that paleontology continues to play a major role in sedimentary basin studies. With continuing study, not only are the ranges of useful fossils becoming finer, more certain, and applicable across broader areas, but a larger number of fossil groups are becoming useful.

Hydrocarbon and mineral exploration are expensive operations, involving many sophisticated techniques, and deserving of the most reliable data available. Imprecise data and inaccurate correlations cannot be used to identify inconsistencies in interpretations, and can only sustain meaningless speculation. Without precise, biostratigraphically-based correlations, you cannot recognize mistakes, or confirm true relationships and their implications. Paleontology provides a risk-reduction tool, as well as a source of critical primary data for sedimentary basin interpretations. Lateral continuity of units is a primary exploration concern that can be addressed by biostratigraphic studies.

It is a basic truth in stratigraphy that shifting depositional environments produce lithological units that are diachronous (e.g., "Walther's Law"). Correlation of lithological units or their subsurface indicators on the basis of their physical characteristics results in conceptual models which often do not reflect the actual spatial distribution of ancient sedimentary systems at particular moments of geological time, even if the rock correlations are accurate. Time correlations provided by fossils permit the spatial relationships of differing environments and lithologies to be recognized and allow paleogeographic reconstructions to be drawn.

Progress in biostratigraphy requires continuing development of its techniques and tools. Principal among them is taxonomy, the documentation of the similarities and differences between different fossil species and higher taxa, leading to the differentiation of their relative stratigraphic positions. As taxonomic research continues, taxa are either subdivided or grouped to reflect current views and enhance their usefulness, and examples of homeomorphy and evolutionary lineages and extinction events become better understood.

Modern approaches tend to emphasize the development of zonations in previously poorly known taxonomic groups, such as Radiolaria, the integration of zonations based on different fossil groups, correlations among different basins and fossil provinces, between nonmarine basinal and shelf successions, and between surface and subsurface sections. International programs, where reconstructions and correlations are supra-regional in scale, especially demonstrate the need for more refined and voluminous paleontological data.

Even in thoroughly collected, relatively well known areas of Europe, new biostratigraphic data are constantly being unearthed, and the geological interpretations deriving from them are undergoing constant revision. Current workers worldwide continue to be excited by important fossil finds, and by modern multitaxial correlation projects. The importance of such new discoveries are all the more applicable to the vast terranes of countries such as Canada, where our knowledge of the basic geology and paleontology is to a large extent still in the reconnaissance stages, the latter even in the subsurface of the western Canada Sedimentary Basin. Curtailing biostratigraphic studies is a fine way to minimize stratigraphic surprises in these areas.

SEQUENCE STRATIGRAPHY

With modern high-definition seismic techniques and processing capabilities, it is no problem to identify seismic sequences. The principles of seismic, or any other sequence analysis are simple but they can include mechanisms that ensure apparent internal consistency but shield us from knowledge of the errors that would be recognized if other appropriate tools were applied. With a modicum of sedimentological data, appropriate facies can be assigned. Add the three dimensional component and we've not only mapped the depositional units and facies, but we've also revealed the accretionary processes in time and space! If only it were that easy. The enormous power and potential of sequence stratigraphy can be properly harnessed only if we know with precision the geological ages of the rocks within and around our proposed sequences. Only then do we have evidence of the validity of the sequences themselves, their temporal relation with other sequences above and below them, and their relation

with apparently equivalent sequences elsewhere (e.g., Poulton, 1988; Sageman, 1992). Much has been written about the circular reasoning inherent in the concept of correlating imprecisely dated sequences globally, and then using the interpreted correlations as a dating tool in their own right. Clearly any proliferation of sequence stratigraphic studies should be accompanied by the required paleontological studies.

Why then are so few stratigraphic sequence studies supported by paleontological data? Two explanations suggest themselves: 1) many earth scientists have been seduced by persuasive diagrams into believing that sequences represent the ultimate revelations of basinal truth; 2) the effort required to substantiate a sequence with biostratigraphy is large and time-consuming, and it involves considerable professional collaboration. Too often, the tools by which interpretations can be verified and refined are judged to be simply not worth the effort, and too often where they have been applied after a sequence model has already been developed, they have destroyed entirely the model they were meant to support. Paleontology serves less than optimally as a late-stage add-on to formulated models. It does not often comfort those most in needs of its services, particularly when it is applied too late. To be most effective, paleontology must be fully integrated into a stratigraphic project from the initial planning stages.

There are no short cuts. Biostratigraphic correlation does not come cheap. It is labor intensive, although this is compensated by its lasting value. Acquiring sufficient background knowledge can involve the systematic collection, separation and identification of huge numbers of fossils. It is built on an edifice of descriptive taxonomy with foundations stretching back through decades of specialized literature international in scope.

PALEOECOLOGY

Animals and plants are adapted to environments to a high degree, and the relation of ancient organisms to their environments is a highly complex, multi-disciplinary subject. Thus many fossils and assemblages have proven to be sensitive indicators of depositional environment, paleobathymetry, water temperature, salinity, etc. Such interpretations often depend on comparisons with relevant living species and communities and on relating the fossils to the rocks in which they occur. Paleoecologic interpretations derived from fossil distributions clearly must not conflict with paleoenvironmental interpretations based on other data. The data to be derived from paleoecology are vast. Applied in collaboration with other data, they can enhance enormously any paleoenvironmental or paleogeographic reconstruction (e.g., Smith, 1989). It is to be overlooked at peril. Reefs, lagoons, deltas, estuaries, inner and outer shelves – these are just a few examples of paleontologically determinable geologic features. A quick initial analysis of fossil assemblages is a time-saving first step in the identification of potential hydrocarbon source rocks.

HYDROCARBON GENERATION

Several fossil groups record the thermal conditions which affected the rocks containing them, and therefore lead to understanding of the hydrocarbon generation potential of source rocks. These fossils darken in colour depending on how much heat they have been subjected to. Some techniques, such as the variation with temperature of the colour of conodont or palynomorph fossils, are cheaply and easily acquired by-products of taxonomic and biostratigraphic research. New techniques permitting graptolites, scolecodonts, and foraminifera have been developed at the Geological Survey of Canada, to extend the range of conditions where paleontological thermal maturity studies can be applied.

The fact that the fossil specimens also provide dates which permit reworked material to be disregarded, allows colour alteration to be used as a check on vitrinite reflectance and mass geochemical techniques of organic maturity, and a refinement of the results from these tools. The palynologist's ability to interpret both age and thermal characteristics of each palynomorph in a preparation can help to resolve problems arising from reworked material.

Thermal maturation studies contribute powerfully to regional geological and tectonic interpretations as well. Regional trends and local anomalies in maturation patterns provide constraints on regional geological histories. Among the questions are those relating to the significance of unconformities in the histories of basins; thickness of overburden, which is in turn related to burial/subsidence characteristics of a basin or orogenic terrane; and variations in heat flow characteristics which relate to rate of burial, fluid flow, and local intrusives.

REWORKED FOSSILS

Reworked fossils can be valuable provenance indicators. Sometimes, their message is almost unbelievable. For just one example, reworked

palynomorphs in Cretaceous sediments of the Labrador Shelf are identical to species found in older rocks in western Canada (Williams, 1986). Recent geomorphological studies have identified unequivocal evidence of a vast west-east drainage system that stretched across Canada and carried these tiny specimens to their final depositional site (A. Duk-Rodkin, pers. comm.), confirming and refining the model proposed by McMillan (1973).

Within the Middle Devonian of Alberta, fossils of pre-Devonian age indicate reworking from distantly located sequences, suggesting important paleogeographic and uplift histories which we are just starting to recognize, but are far from understanding. The implications of such paleogeographic insights are profound and may well spawn future successes in exploration ventures. Reworking of fossils bedevils paleontologists who work in the Beaufort Basin, yet the recognition of such assemblages offers huge opportunities to involve paleontology with reflection seismology and sedimentology in a multidisciplinary effort to unravel the evolution of structures that cannibalized and buried each other as they deformed. The insights gained from such an exercise reveal a changing geometry of possible fluid migration paths during burial that could strongly influence prospect recognition. If every clastic deposit is represented by an unconformity somewhere else, then paleontology provides a reliable key to that somewhere else.

GSC PALEONTOLOGY EVOLVING

This report outlines only a few of the practical applications of paleontology, out of a much larger number, among which contributions to the history of life and the biosphere, as well as touristic and aesthetic sectors, are not insignificant economic contributors. Nowlan (1993) has outlined some of the trends in which paleontology is heading as a research discipline. They include greater collaboration with geochemistry to understand some of Earth's major biotic and environmental crises, and the variation in biodiversity through time.

It is ironic that public interest in paleontology is at an all time high at the same time as the practical application of paleontology in geoscience industries and universities has decreased to perhaps critical levels. It is no less ironic that the reduced investment in paleontology in the fossil fuel industry coincides with a blossoming in paleontological tools and applications available to unravel geoscience questions. Large numbers of former practitioners are either retiring or treading other paths, as paleontology is viewed by some as yesterday's tool. Vast quantities of hardwon knowledge are being lost annually. In the lean and mean world of electronic working speeds, short-term profit production, and retirement of excess capacity, paleontology can be slow and difficult to digitize, its contributions so fundamental that they are transparent in the geological interpretations that come before colleagues and managers.

It is inconceivable that such a vast and variously applicable discipline as paleontology not contribute its full potential to the future of a country like Canada with its huge landmass, dependence on natural resources, and relatively little explored sedimentary basins, tectonic belts, and paleontological database. The difficulties of reconciling the conflicting challenges of this essential discipline with the fast pace of modern geoscience activities have generated a great deal of recent discussion and proposals for carrying paleontology forward (e.g., Allmon, 1993; Economist, 1988; Leffingwell, 1994; Shirley, 1994). GSC Paleontology is heeding the collective wisdom of the day, and responding to ensure the continuing application of an essential science to its objectives. It is mandatory to do this because, unless equivalent time-determining methods emerge, PALEONTOLOGY remains the ESSENTIAL reliable discipline for sedimentary basin analysis. Paleontology takes away a large part of the uncertainty from geological interpretations in Phanerozoic terranes and therefore reduces the element of luck or chance in mineral and hydrocarbon exploration. To ignore it is to give earth scientists rein to chase all kinds of wild geese up intellectual cul-de-sacs, wasting a great deal of effort and expense.

In a field where the published and unpublished knowledge bases are so vast, the potential for computer software to speed up data access and interpretation is huge. GSC is attempting to accelerate its ongoing program to store fossil distribution data digitally for ready access, is continuing to encourage attempts (mainly housed elsewhere) to deal with taxonomy and morphology digitally, and is experimenting with digital image capture, recognition and manipulation. Today there is no reason for an organization's corporate memory to reside only inside its employees' heads. Heads (and eyes) of paleontologists will always be needed to describe, identify and interpret fossil assemblages, but much of the data storage and manipulation can be assigned to machines, so that the slow and labor-intensive aspect of paleontology can be partially overcome.

Paleontology is an international discipline, and around the world specialists are becoming fewer by the year. GSC is therefore encouraging efforts to enhance electronic communication between specialists, and between specialists and their potential users internationally, in order to optimize what resources are available around the world (e.g., O'Neill, 1994).

In part, communicating with potential clients in the geosciences involves adopting more business-like attitudes than have been traditionally in place, including greater client sensitivity, and more accessible communication of results and requirements (e.g., Leffingwell, 1994). Itself inherently multi-disciplinary, it is essential to integrate paleontology at early planning stages into a multitude of projects aimed at a great variety of other goals.

The Geological Survey of Canada is the only organisation in the country that maintains a wide in-house expertise in paleontology as applied to regional geoscience needs. It is essentially the national custodian of Canada's geological time scale. This is a uniquely Canadian situation, as large national museums play similar roles in other countries. The GSC collections and cumulative knowledge are an invaluable source of information that can provide inexpensive data prior to further investment in exploration prospects in many areas. Enhanced collaboration among paleontologic and other geoscience colleagues within GSC and beyond can only result in a better understanding of Canada's geology and resource potential. Proportionately greater efforts are being concentrated in economically important sedimentary basins, in particular the Western Canada Sedimentary Basin. We look forward to many exciting opportunities for collaboration, in a variety of different working modes, with our colleagues in the Canadian oil and gas industry.

REFERENCES

Allmon, W.D.
1993: In defense of Paleontology. Geotimes, v. 38, no. 11, p. 5.

Callomon, J.H.
1984: The measurement of Geological time. Proceedings of the Royal Institution of Great Britain, v. 56, p. 65–99.

Cope, J.C.W.
1993: High resolution biostratigraphy. *In* High resolution stratigraphy, E.A. Hailwood and R.B. Kidd (eds.). Geological Society Special Publication, no. 70, p. 257–265.

The Economist
1988: Fossils – the story-telling science. The Economist, Dec. 18, 1988 issue, p. 101–106.

Leffingwell, H.A.
1994: Reinvigorating industrial micropaleontology. American Paleontologist, v. 2, p. 1–4.

McMillan, N.J.
1973: Shelves of Labrador Sea and Baffin Bay, Canada. *In* The Future petroleum provinces of Canada, R.G. McCrossan (ed.). Canadian Society of Petroleum Geologists, Memoir 1, p. 473–517.

Nowlan, G.S.
1993: The Ancient Biosphere. Geoscience Canada, v. 10, p. 113–122.

O'Neill, B.J.
1994: Toward a paleontological network. American Paleontologist, v. 2, p. 2, 3.

Poulton, T.P.
1988: Major interregionally correlatable events in the Jurassic of western interior, arctic, and eastern offshore Canada. *In* Sequences, Stratigraphy, Sedimentology: Surface and Subsurface, D.P. James and D.A. Leckie (eds.). Canadian Society of Petroleum Geologists, Memoir 15, p. 195–206.

Sageman, B.
1992: Paleoecology – a cure for sequence syndrome? Palaios, v. 7, no. 5, p. i, ii.

Shaw, A.B.
1964: Time in Stratigraphy. McGraw-Hill Book Company, New York, 365 p.

Shirley, K.
1993: Good ol' paleo never looked so new. American Association of Petroleum Geologists, Explorer, April 1993 issue, p. 42, 43, 45.

Smith, P.L.
1989: Paleobiogeography and plate tectonics. Geoscience Canada, v. 15, no. 4, p. 261–279.

Williams, E.V.
1986: Palynological study of the continental shelf sediments of the Labrador Sea. Ph.D. thesis, University of British Columbia, Vancouver, British Columbia, 214 p.

GEOLOGICAL SURVEY OF CANADA AUTHORS

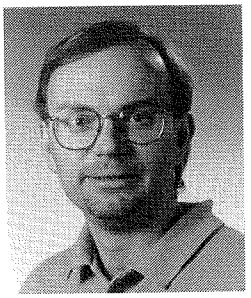

ABERCROMBIE, Hugh J.
Inorganic Geochemist
GSC-Calgary
Tel: 403-292-7106,
FAX: 403-292-5377

Research Activities:
Sedimentary basin fluid-rock interactions, hydrochemistry, and hydrogeology
Low temperature ore deposition
Environmental geochemistry

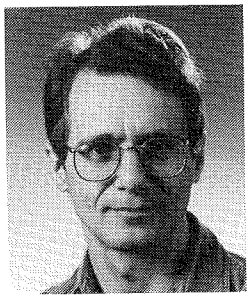

ABRAHAMSON, Byron
Geologist
GSC-Calgary
Tel: 403-292-7009,
FAX: 403-292-5377

Research Activities:
Regional Devonian and Cretaceous stratigraphic studies

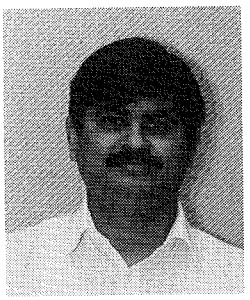

AGRAWAL, A. (Abinash)
Post Doctorate Fellow
GSC-Dartmouth
Tel: 920-426-4627,
FAX: 902-426-4465
E Mail: agrawala@agc.bio.ns.ca

Research Activities:
Seismostratigraphy
Environmental geochemistry
Hydrocarbon biodegradation

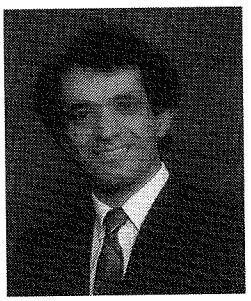

ASUDEH, I.
Research Scientist
GSC-Ottawa
Tel: 613-996-5757,
FAX: 613-992-8836
E Mail: asudeh@cg.emr.ca

Research Activities:
Seismic refraction
Earthquakes studies
Seismic instrumentation
Field data management

Photo Unavailable

BAMBER, W.
Research Scientist
GSC-Calgary
Tel: 403-292-7095,
FAX: 403-292-5377
E Mail: bamber@gsc.emr.ca

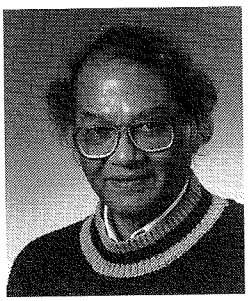

BANERJEE, Indranil
Research Scientist
GSC-Calgary
Tel: 403-292-7147,
FAX: 403-292-5377
E Mail: ibanerjee@gsc.emr.ca

Research Activities:
Stratigraphy and sedimentology of the Mannville Group
Sequence stratigraphy in coal

BATES, J.L.
Editor
GSC-Dartmouth
Tel: 902-426-4386,
FAX: 902-426-4848
E Mail: bates@agc.bio.ns.ca

Research Activities:
Digital and on-line publishing
Basin atlases
Geoscience education
Mesozoic volcanics

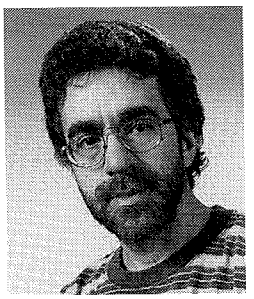

BEAUCHAMP, Benoit
Research Scientist
GSC-Calgary
Tel: 403-292-7190,
FAX: 403-292-5377
E Mail: bbeauchamp@gsc.emr.ca

Research Activites:
Late Paleozoic stratigraphy of Sverdrup Basin, Canadian Arctic

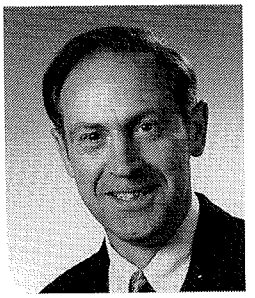

BELL, J.S. (Sebastian)
Research Scientist
GSC-Calgary
Tel: 403-292-7157,
FAX: 403-292-5377
E Mail: sbell@gsc.emr.ca

Research Activites:
Stress regimes of sedimentary basins
Basin Atlases
Overpressures

BEST, M.E. (Mel)
Research Scientist
GSC-Sidney
Tel: 604-363-6526,
FAX: 604-363-6565
E Mail: Best@pgc.emr.ca

Research Activities:
Basin modelling
Fluid flow in rocks
Geophysics (seismic and electro-magnetic)
Groundwater studies

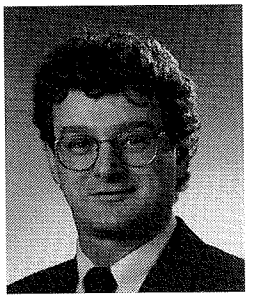

BIRD, Timothy D.
Petroleum Geologist
GSC-Calgary
Tel: 403-292-7017,
FAX: 403-292-5377
E Mail: tbird@gsc.emr.ca

Research Activities:
Petroleum geology and resource assessment
Triassic of Western Canada
Northwest Territories and Yukon

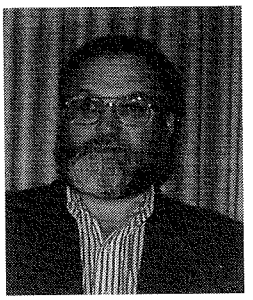

BLASCO, S.M. (Steve)
Physical Scientist
GSC-Dartmouth
Tel: 902-426-3932,
FAX: 902-426-4104
E Mail: blasco@agc.bio.ns.ca

Research Activities:
Marine and lacustrine environmental and engineering geology: Arctic offshore and Great Lakes

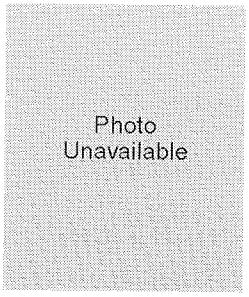

BOYCE, G.
Research Scientist
GSC-Ottawa
Tel: 613-992-6408

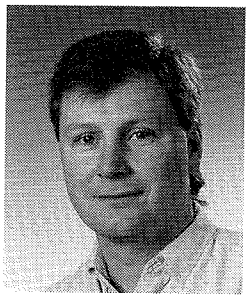

BRENT, T.A. (Tom)
Physical Scientist
GSC-Calgary
Tel: 403-292-7105,
FAX: 403-292-4961
E Mail: tbrent@gsc.emr.ca

Research Activities:
Regional geology
Reflection seismic processing and interpretation
Regional geophysics
Economic geology

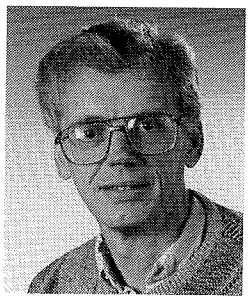

CANT, Doug
Research Scientists
GSC-Calgary
Tel: 403-292-7007,
FAX: 403-292-5377
E Mail: cant@petrol@gsc.ca

Research Activities:
Mannville Sequence, stratigraphy and sedimentology

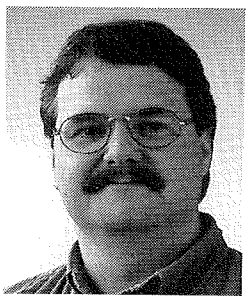

COFLIN, K.C. (Kevin)
Petroleum Geophysicist
GSC-Dartmouth
Tel: 920-426-7694,
FAX: 902-426-4465
E Mail: coflink@agc.bio.ns.ca

Research Activities:
Structural and stratigraphic interpretation of seismic data resolution seismic processing

CONN, Robert F.
Chief, Petroleum Resource Analysis Section
GSC-Ottawa
Tel: 613-995-5602,
FAX: 613-996-7837

Research Activities:
Resource economics
Resource assessments

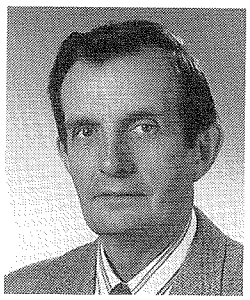

COOK, Donald G.
Research Geologist
GSC-Calgary
Tel: 403-292-7134,
FAX: 403-292-5377
E Mail: dcook@gsc.emr.ca

Research Activites:
Proterozoic stratigraphy and tectonics, Northwest Territories
Structural geology of Mackenzie Mountains, Franklin Mountains and Colville Hills

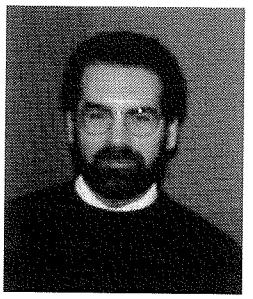

DALLAIRE, S. Mark
Senior Resource Engineer
GSC-Ottawa
Tel: 613-996-7836,
FAX: 613-996-7837

Research Activities:
Oil and gas cost estimating and costing models
Oil and gas risk analysis
Resource assessments and techniques
Resource economics

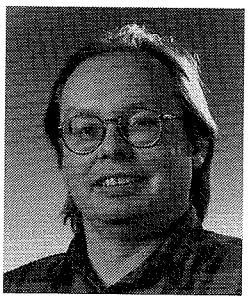

DAWSON, F.M. (Mike)
Coal Geologist
GSC-Calgary
Tel: 403-292-7115,
FAX: 403-292-5377
E Mail: dawson@coal@gsc.calgary

Research Activities:
Coalbed Methane in Canada
Coal Resource Assessment

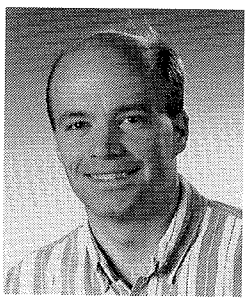

DE FREITAS, T. (Tim)
Research Scientist
GSC-Calgary
Tel: 403-292-7135,
FAX: 403-292-4961
E Mail: tfreitas@gsc.emr.ca

Research Activities:
Regional geology
Stratigraphy and sedimentology
Tectonics
Economic geology
Paleontology

DICKIE, K. (Kate)
Industry Research Associates Contractor
GSC-Dartmouth
Tel: 920-426-6759,
FAX: 902-426-4465
E Mail: dickiek@agc.bio.ns.ca

Research Activities:
Seismostratigraphy

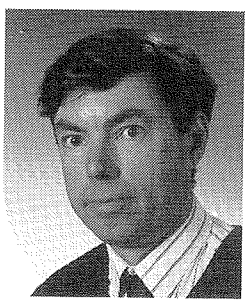

DIETRICH, Jim
Petroleum Geophysicist
GSC-Calgary
Tel: 403-292-7016,
FAX: 403-292-7034

Research Activities:
Seismic reflection studies/ petroleum assessments in western Arctic and west coast basins
Seismic studies in Western Canada Sedimentary Basin (SE Saskatchewan/SW Manitoba and east-central Alberta)

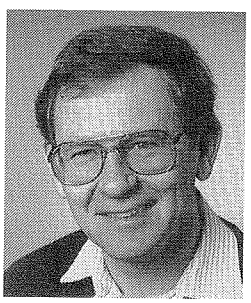

DIXON, Jim
Research Scientist
GSC-Calgary
Tel: 403-292-7136,
FAX: 403-292-5377
E Mail: Jim Dixon@carto@GSC Calgary

Research Activities:
Permian to Tertiary stratigraphy
Sequence stratigraphy
Sedimentology in mainland N.W.T., Beaufort Sea and northern Yukon

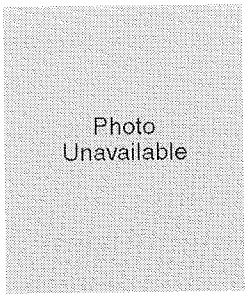

DOSTALER, F.
Research Scientist
GSC-Ottawa
Tel: 613-995-5326
E Mail: fdostaler@gsc.emr.ca

DOUGHERTY, B.J. (Jean)
Geologist
GSC-Ottawa
Tel: 613-995-8746,
FAX: 613-952-8784
E Mail: jdougherty@gsc.emr.ca

Research Activities:
Curator of the National Type Collection of Invertebrate and Plant Fossils
Database design

DUK-RODKIN, Alejandra
Research Scientist
GSC-Calgary
Tel: 403-292-7188, FAX: 403-292-5377
E Mail: aduk-rodkin@gsc.emr.ca
Research Activities:
Studies related to Quaternary and Tertiary geology Yukon-western N.W.T.
Surficial geology mapping and terrain evaluation
Reconstruction of glacial history
Quaternary stratigraphy
Tertiary-Quaternary drainage systems

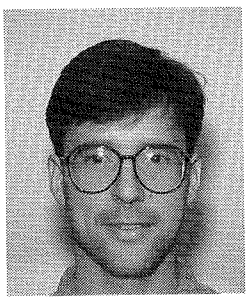

EATON, David W.
Research Scientist
GSC-Ottawa
Tel: 613-947-2783,
FAX: 613-992-8836
E Mail: eaton@cg.emr.ca

Research Activities:
Reflection seismology
Seismic modelling applied to mineral exploration
Alberta Basement Transects and Abitibi Grenville-Lithoprobe

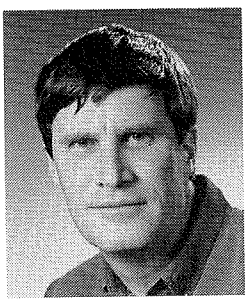

EMBRY, Ashton F.
Research Scientist
GSC-Calgary
Tel: 403-292-7125,
FAX: 403-292-4961
E Mail: embry@gsc.emr.ca

Research Activities:
Sequence Stratigraphy
Clastic Sedimentology
Arctic Stratigraphy and Tectonics
Petroleum Geology, Arctic Islands

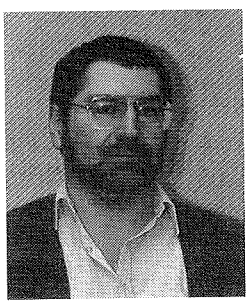

FENSOME, R.A. (Rob)
Research Scientist
GSC-Dartmouth
Tel: 902-426-2732,
FAX: 902-426-4465
E Mail: rf@agcban1.bio.ns.ca

Research Activites:
Mesozoic-Cenozoic dinoflagellates
Triassic-Cretaceous spores
Biodiversity

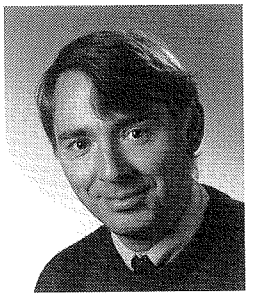

FOWLER, Martin G.
Research Scientist
GSC-Calgary
Tel: 403-292-7038,
FAX: 403-292-5377
E Mail: fowler@gsc.emr.ca

Research Activities:
Petroleum Geochemistry, especially of eastern Canada and Western Canada
Sedimentary Basin
Environmental Geochemistry

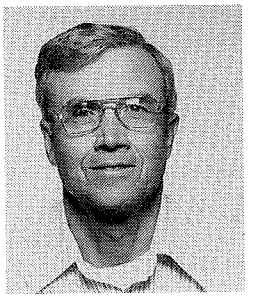

FRITZ, W.H.
Research Scientist
GSC-Calgary
Tel: 613-996-6416,
FAX: 613-952-8784
E Mail: fritz@gsc.emr.ca

Research Activities:
Cambrian biostratigrapher
Canadian Cordillera

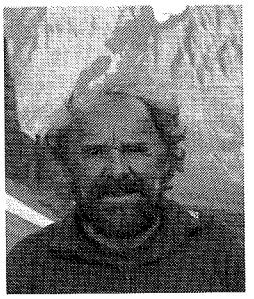

GELDSETZER, H. (Helmut) H.J.
Research Scientist
GSC-Calgary
Tel: 403-292-7155,
FAX: 403-292-7355
E Mail: hgeldsetzer@gsc.emr.ca

Research Activities:
Devonian stratigraphy of southern Rocky Mountains
Extinction boundaries
Isotope geochemistry of sediments

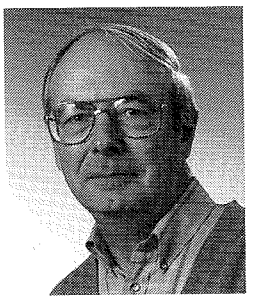

GIBSON, D.W. (Dave)
Research Scientist
GSC-Calgary
Tel: 403-292-7149,
FAX: 403-292-5377
E Mail: dgibson@gsc.emr.ca

Research Activities:
Triassic stratigraphy and sedimentology of the Western Canada Sedimentary Basin

GOODARZI, F. (Fari)
Principal Research Scientist
GSC-Calgary
Tel: 403-292-7116,
FAX: 403-292-5377
E Mail: fgoodarzi@gsc.emr.ca
Research Activities:
Organic petrology
Basin analysis
Inorganic geochemistry, environmental studies of fossil fuels
Thermal maturity
Environmental studies
Fossil fuel exploration

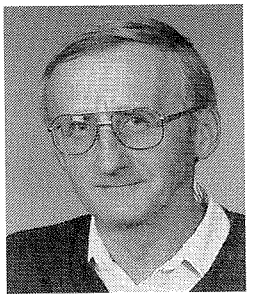

GRANT, Alan C.
Physical Scientist
GSC-Dartmouth
Tel: 902-425-4799,
FAX: 902-426-4465
E Mail: algrant@agcbanl.bio.ns.ca

Research Activities:
Palaeozoic basins
Coal bed methane
Pockmarks

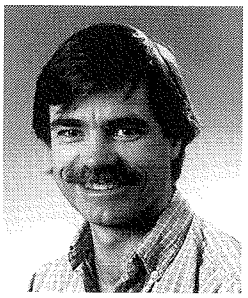

HAMBLIN, A.P. (Tony)
Research Scientist
GSC-Calgary
Tel: 403-292-7020,
FAX: 403-292-5377
E Mail: hamblin@gsc.emr.ca

Research Activities:
Upper Cretaceous-Tertiary sequences WCSB
Paleozoic Basins, Eastern Canada

Photo Unavailable

HAMILTON, T.S.
Research Scientist
GSC-Sidney
Tel: 604-363-6423,
FAX: 604-363-6565
E Mail: hamilton@pgc.emr.ca

Research Activities:
Seismic stratigraphy
Neogene volcanism
Nuclear fallout stratigraphy and active sedimentology
Regional geology of west coast and offshore

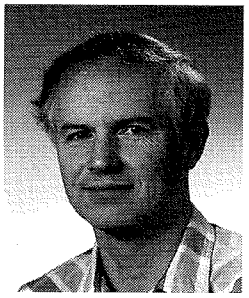

HANNIGAN, P.
Physical Scientist
GSC-Calgary
Tel: 403-292-7022,
FAX: 403-292-7034
E Mail: Peter Hannigan@gsc.emr.ca

Research Activites:
Hydrocarbon Assessment
Petroleum Geology

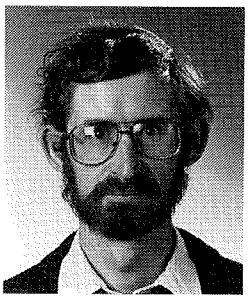

HARRISON, J.C. (Chris)
Research Scientist
GSC-Calgary
Tel: 403-292-7137,
FAX: 403-292-4961
E Mail: charrison@gsc.emr.ca

Research Activities:
Regional geology
Structural geology
Salt tectonics
Economic geology

Photo Unavailable

HORNER, R.B.
Research Scientist
GSC-Sidney
Tel: 604-363-6432,
FAX: 604-363-6565
E Mail: horner@pgc.emr.ca

Research Activites:
Cordilleran seismicity
St. Elias seismotectonics
Oil field induced earthquakes

HUANG, Zehui
Industry Research Associates Contractor
GSC-Dartmouth
Tel: 920-426-7348,
FAX: 902-426-4465
E Mail: huangz@agc.bio.ns.ca
Research Activities:
Basin Analyses
Basin Modelling
Geological application of computer neural networks and fuzzy logic
Source rock/reservoir characterization
Well log analysis

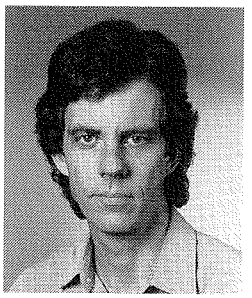

HUGHES, J.D. (Dave)
Coal Geologist/Computer Application Specialist, GSC-Calgary
Tel: 403-292-7117,
FAX: 403-292-5377
E Mail: dhughes@gsc.emr.ca
Research Activities:
Sedimentology
Structural analysis
Computer modelling
Geographic information systems
Image processing
Currently working on National Coal Inventory

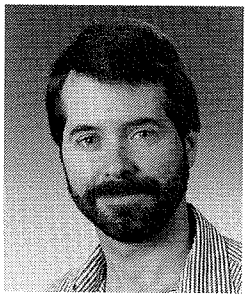

ISSLER, D.R. (Dale)
Research Scientist
GSC-Calgary
Tel: 403-292-7172,
FAX: 403-292-5377
E Mail: dissler@gsc.emr.ca

Research Activities:
Quantitative basin analysis
Thermal/subsidence modelling
Apatite fission track studies
Hydrocarbon generation kinetics
Compaction studies

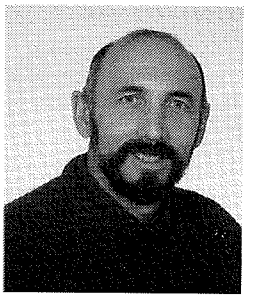

JACKSON, Lionel E., Jr.
Research Scientist
GSC-Vancouver
Tel: 604-666-3409,
FAX: 604-666-1124
E Mail: ljackson@gsc.emr.ca

Research Activities:
Regional Quaternary Geology, Yukon Territory and Alberta Foothills
Debris flow and landslide hazards in the Canadian Cordillera

Photo Unavailable

JANEAU, J.
Research Scientist
GSC-Ottawa
Tel: 613-992-6270
E Mail: jjaneau@gsc.emr.ca

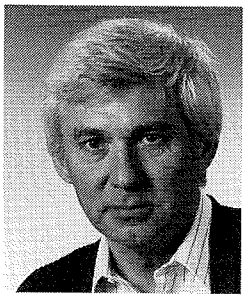

JERZYKIEWICZ, Tomasz (Tom)
Research Scientist, GSC-Calgary
Tel: 404-292-7118,
FAX: 403-292-5377.
E Mail: tjerzykiewicz@gsc.emr.ca
Research Activities:
Stratigraphy and sedimentology of the Upper Cretaceous-Paleocene of the WCSB
Geology of the Cretaceous basins of Poland
Sedimentology of the Cretaceous dinosaur-bearing strata of China and Mongolia

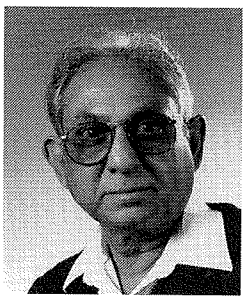

KALGUTKAR, Ramakant M.
Research Scientist, GSC-Calgary
Tel: 403-292-7099,
FAX: 403-292-6014
E Mail: Kalgutkar@gsc.emr.ca

Research Activities:
Fossil Fungi: MorphologyTaxonomy, Biostratigraphy, Paleoenvironment, Cretaceous-Tertiary
Western and Northern Canada
Currently working on the Digital atlas and keys of fossil fungal palynomorphs

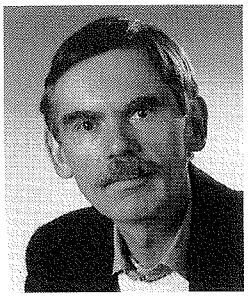

KALKREUTH, Wolfgang D.
Research Scientist
GSC-Calgary
Tel: 403-292-7199,
FAX: 403-292-5377
E Mail: wkalkreuth@gsc.emr.ca

Research Activities:
Coal petrology of Canada's coal deposits
Organic petrology and petroleum source rock characteristics
Basin Analysis

Photo Unavailable

KANE, R.
Research Scientist
GSC-Ottawa
Tel: 613-992-0980
E Mail: rkane@gsc.emr.ca

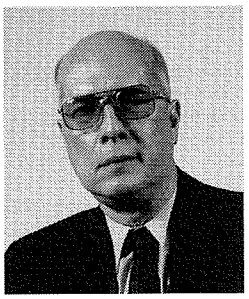

KATSUBE, T.J. (John)
Research Scientist, GSC-Ottawa
Tel: 613-995-5239, FAX: 613-992-2468
E-Mail:JohnKatsube
ELEC-401@GSC OTTAWA
Research Activities:
Tight rock (shales, crystalline rocks) petrophysics
Pore structure modelling
Electrical measurements
Low permeability and porosity measurements
Application to shale seal quality, waste barrier quality and deep con tinental structure studies

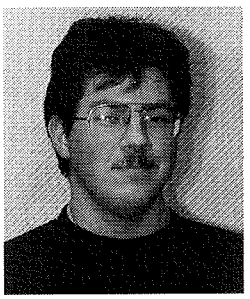

KING, G.S. (Scott)
Industry Research Associates
Contractor
GSC-Dartmouth
Tel: 920-426-3126,
FAX: 902-426-4465
E Mail: kings@agc.bio.ns.ca

Research Activities:
System Administration
Basin Modelling
Seismic interpretation

Photo Unavailable

KJARSGAARD, Bruce
Research Scientist
GSC-Ottawa
Tel: 613-995-5705,
FAX: 613-995-7997
E Mail: kjarsgaard@gsc.emr.ca

Research Activities:
Igenous petrology, regional mapping, mantle
Diamonds and kimberlites

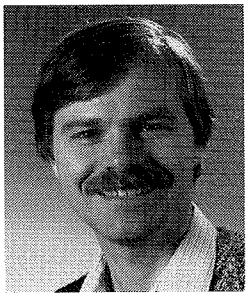

LANE, Larry S.
Research Scientist
GSC-Calgary
Tel: 403-292-7131,
FAX: 403-292-4961
E Mail: lane@gsc.emr.ca

Research Activities:
Geological mapping, structural geology, crustal structure, and tectonics, of the Beaufort Sea
Continental margin and northern Yukon

Photo Unavailable

LAWLEY, L.
Research Scientist
GSC-Ottawa
Tel: 613-992-8465
E Mail: llawley@gsc.emr.ca

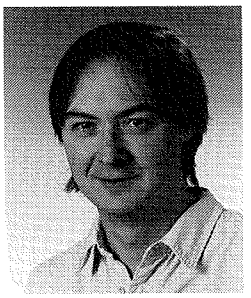

LEBEL, Daniel
Research Scientist
GSC-Calgary
Tel: 403-299-3540,
FAX: 403-292-5377
E Mail: dlebel@gsc.emr.ca
Research Activities:
Bedrock geological mapping
Structure of the Rocky Mountains Foothills and Front Ranges, and Canadian Appalachians
NATMAP Geographical (Geological) Information System

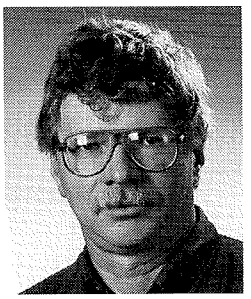

LECKIE, Dale A.
Research Scientist
GSC-Calgary
Tel: 403-292-7146,
Fax: 403-292-5377
E Mail: leckie@gsc.emr.ca

Research Activities:
Hydrocarbons, diamonds and gold in sediments
Clastic sedimentology, basin analysis
Cretaceous of Western Canada
Mannville Group, Colorado Group

LEE, P.J.
Petroleum Geologist
GSC-Calgary
Tel: 403-292-7014,
FAX: 403-292-7034
E Mail: plee@petrol.gsc.emr.ca

Research Activities:
Methods for estimating undiscovered resources
Computer applications to subsurface mapping

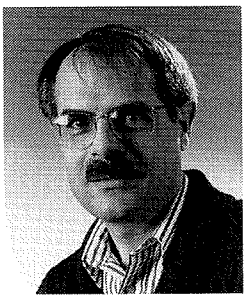

MacLEAN, Bernard C.
Research Geologist
GSC-Calgary
Tel: 403-292-7142,
FAX: 403-292-5377
E Mail: bmaclean@gsc.emr.ca

Research Activites:
Proterozoic stratigraphy and tecton ics, Northwest Territories

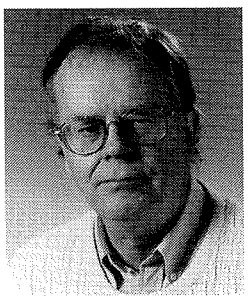

MACQUEEN, R.W. (Roger)
Research Scientist
GSC-Calgary
Tel: 403-292-7145,
FAX: 403-292-5377
E Mail: macqueen@gsc.emr.ca
Research Activites:
Mineral deposits hosted by sedimen tary rocks, particularly Mississippi Valley-type lead-zinc deposits, char- acter and origin of oil sands, heavy oils and bitumen, Western Canada Basin

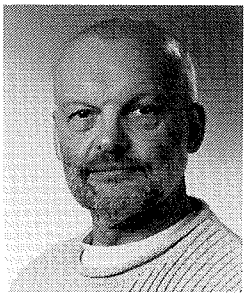

MAYR, Ulrich
Research Scientist
GSC-Calgary
Tel: 403-292-7144,
FAX: 403-292-4961
E Mail:umayr@gsc.emr.ca

Research Activities:
Regional geology
Stratigraphy and sedimentology
Tectonics
Economic geology

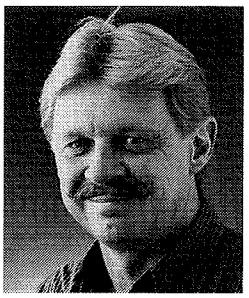

McALPINE, K.D. (Don)
Research Manager
GSC-Dartmouth
Tel: 920-426-2730,
FAX: 902-426-4465
E Mail: mcalpine@agc.bio.ns.ca

Research Activities:
Basin Atlases
Mesozoic stratigraphy of eastern Canada

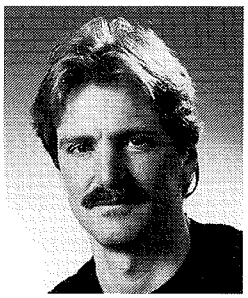

McDONOUGH, Michael R.
Research Scientist
GSC-Calgary
Tel: 403-292-7151,
FAX: 403-292-5377
E Mail: mrm@gsc.emr.ca

Research Activities:
Structural geology, regional geology
Digital geological
Remote sensing

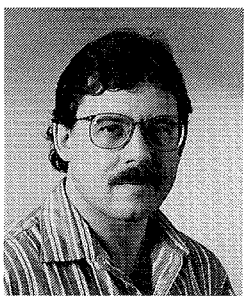

McDOUGALL, William J.
Coal Geologist
GSC-Calgary
Tel: 403-292-7117,
FAX: 403-292-5377

Research Activities:
Coal geology, computer modelling
Coal petrology, geographic information systems
Currently working on National Coal Inventory

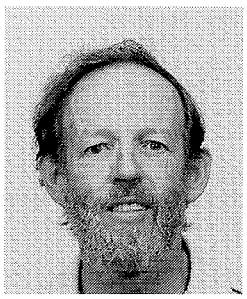

McGREGOR, D.C.
Research Scientist
GSC-Ottawa
Tel: 613-995-4680,
FAX: 613-952-8784
E Mail: mcgregor@gsc.emr.ca

Research Activities:
Paleozoic palynology and biostratigraphy
Editing

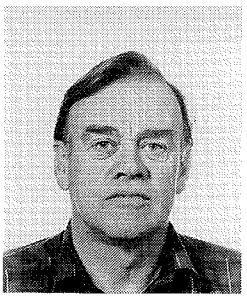

McINTYRE, D.
Research Scientist
GSC-Calgary
Tel: 403-292-7089,
FAX: 403-292-5377
E Mail: dmcintyre@gsc.emr.ca

Research Activities:
Cretaceous and Early Tertiary Palynology (dinoflagellates, pollen and spores) Western and Northern Canada

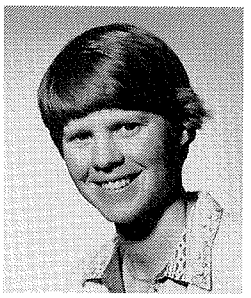

McMECHAN, M.E. (Margot)
Structural Geologist
GSC-Calgary
Tel: 403-292-7154,
FAX: 403-292-5377
E Mail: mmcmechan@gsc.emr.ca

Research Activities:
Structural geology, tectonics, Upper Proterozoic stratigraphy, thermal maturation, Canadian Rocky Mountains

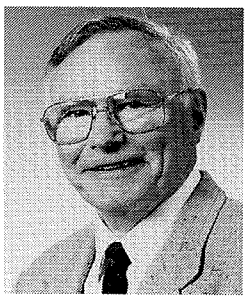

McMILLAN, N.J. (Jack)
Senior Research Scientist-Emeritus
GSC-Calgary
Tel: 403-292-7021,
FAX: 292-5377

Research Activites:
Basin analysis
Habitat of oil

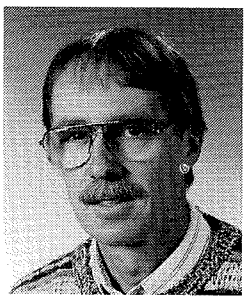

McNEIL, D.H. (Dave)
Research Scientist
GSC-Calgary
Tel: 403-292-7087, FAX: 403-292-6014
E Mail: dmcneil@gsc.emr.ca
Research Activities:
Micropaleontology, Mesozoic-Cenozoic
Foraminifera
Thermal maturation and burial diagenesis of microfossils
Sequence stratigraphy, Western Canada Sedimentary Basin, Beaufort-Mackenzie Basin

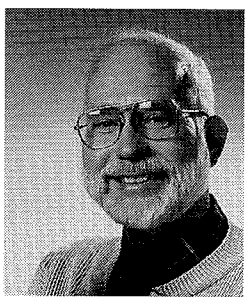

MEIJER DREES, N.C. (Nick)
Subsurface Stratigrapher
GSC-Calgary
Tel: 403-292-7152,
FAX: 403-292-5377
E Mail: nmeijer-drees@gsc.emr.ca

Research Activities:
Devonian studies, Western Canada Basin
Subsurface stratigraphy

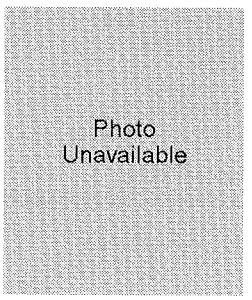

MILES, Warner
Research Scientist
GSC-Ottawa
Tel: 613-992-6634,
FAX: 613-992-2787
E Mail: miles@agg.emr.ca

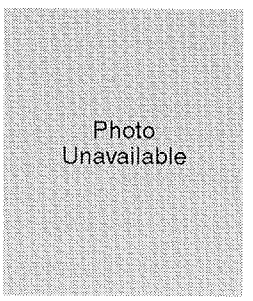

MILKEREIT, B.
Research Scientist
GSC-Ottawa
Tel: 413-995-5490,
FAX: 613-992-8836
E Mail:

Research Activities:
Reflection seismology
Application of reflection seismology to the mineral industry
Alberta Basement Transects and Abitibi Grenville-Lithoprobe

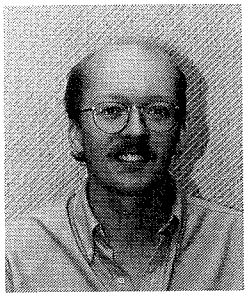

MOIR, P.N. (Phil)
Geologist
GSC-Dartmouth
Tel: 920-426-7639,
FAX: 902-426-4465
E Mail: moirp@agc.bio.ns.ca

Research Activities:
Basin Atlases
Hydrocarbon charge modelling
Geomatics and databases

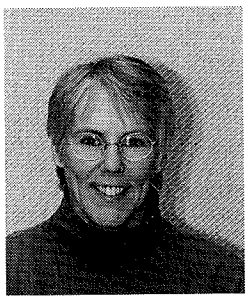

MORAN, K. (Kate)
Marine Geotechnical Engineer
GSC-Dartmouth
Tel: 920-426-8159,
FAX: 902-426-4104
E Mail: morank@agc.bio.ns.ca

Research Activities:
Sediment deformation
Physical properties of rocks

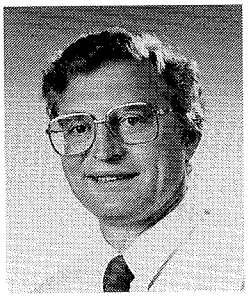

MORROW, D.W. (Dave)
Research Scientist
GSC-Calgary
Tel: 403-292-7143,
FAX: 403-292-5377
E Mail: dmorrow@gsc.emr.ca

Research Activities:
Lower Paleozoic stratigraphy
Thermal History of Basins
Dolomitization

NASSICHUK, W.W. (Walter)
Paleontologist, GSC-Calgary
Tel: 403-292-7150,
FAX: 403-292-5377
E Mail: wnassichuk@gsc.emr.ca
Research Activites:
Biostratigraphy of Carboniferous and Permian strata in western and northern Canada
Time of emplacement and thermal regime
of kimberlites in western and northern Canada
Arctic Ocean sea-bed contaminants

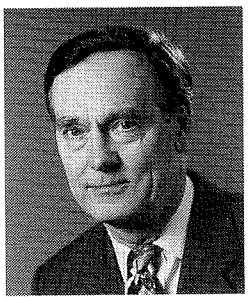

NORFORD, B.S. (Brian)
Geologist
GSC-Calgary
Tel: 403-292-7097,
FAX: 403-292-5377
E Mail: briannorford@gsc.emr.ca
Research Activites:
Stratigraphy and biostratigraphy of the Lower Paleozoic sedimentary rocks of western and northern Canada, their industrial and metallic minerals, and their potential for petroleum resources

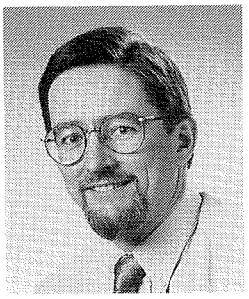

NOWLAN, G.S. (Godfrey)
Research Scientist
GSC-Calgary
Tel: 403-292-7079,
FAX: 403-292-6014
E Mail: nowlan@gsc.emr.ca

Research Activities:
Conodont biostratigraphy (Precambrian-Silurian)
Stratigraphy
Thermal maturity

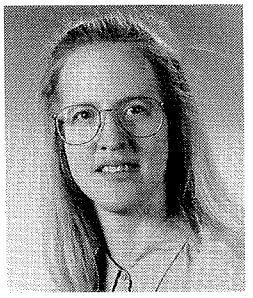

OLSEN-HEISE, Katrina E.D.
Petroleum Geologist
GSC-Calgary
Tel: 403-292-7026,
FAX: 403-292-7034
E Mail: kolsen-heise@gsc.emr.ca

Research Activities:
Integrated geological/geophysical regional studies
Carbonate sedimentology
Petroleum Resource Assessment

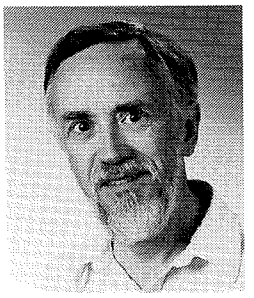

OKULITCH, Andrew V.
Research Scientist
GSC-Calgary
Tel: 403-292-7132, FAX: 403-292-5377
E Mail: aokulitch@gsc.emr.ca
Research Activities:
Coordination and compilation of the Geological Atlas of Canada
Development of digital mapping, database management and cartographic systems
Geology and geophysics of Arctic margins
Geology of the Shuswap Complex, British Columbia

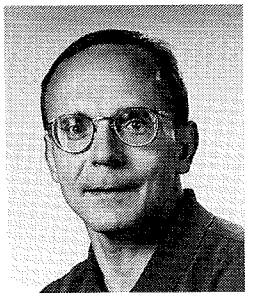

OSADETZ, Kirk
Physical Scientist and
Acting Head of Petroleum Resources Subdivision
GSC-Calgary
Tel: 403-292-7022,
FAX: 403-292-7034
E Mail: osadetz@gsc.emr.ca

Research Activites:
Hydrocarbon Assessment
Petroleum Geochemistry
Thermal History Analysis

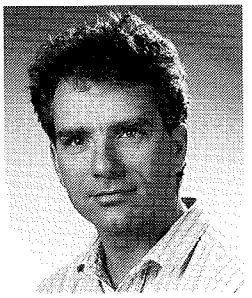

PALMER, Bruce R.
Petroleum Geologist
GSC-Calgary
Tel: 403-292-7148
E Mail: bpalmer@gsc.emr.ca

Research Activites:
Subsurface geological mapping and analysis
Geographical information systems applications
Subsurface mapping of the Western Canada Sedimentary Basin relating to the Lithoprobe project

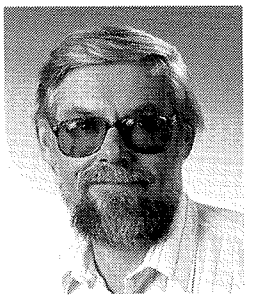

POULTON, T.P. (Terry)
Head, Paleontology Subdivision
GSC-Calgary
Tel: 403-292-7096,
FAX: 403-292-6014
E Mail: poulton@gsc.emr.ca

Research Activities:
Jurassic molluscan biostratigraphy
Jurassic regional stratigraphy and tectonics, western and northern Canada

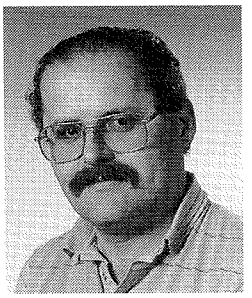

PRATT, K.C. (Ken)
Image Analyst-Quantitative digital microscopy
GSC-Calgary
Tel: 403-292-7121,
FAX: 403-292-5377
E Mail: kpratt@gsc.emr.ca
Research Activities:
Image analysis of coal and hydrocarbon source rocks
Regional coalification, relationship between coal compositional, coal seam fracture patterns and coal bed methane potential

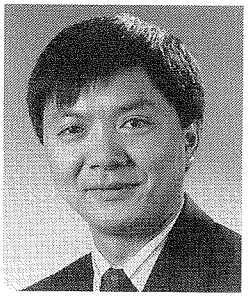

QING, Hairuo
Post-doctoral Fellow
GSC-Calgary
Tel: 403-292-7197,
FAX: 403-292-5377
E Mail: qing@gsc.emr.ca

Research Activities:
Diagenesis of carbonate rocks
Formation of dolomite reservoirs
Characterization of heterogeneous carbonate reservoirs and low-temperaturem geochemistry

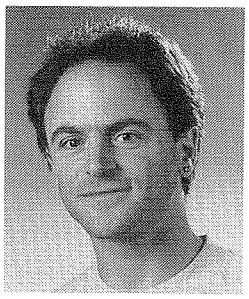

ROSS, G.M. (Gerry)
Research Scientist
GSC-Calgary
Tel: 403-292-7156,
FAX: 403-292-5377
E Mail: gerry@earth.geo.ucalgary.ca
Research Activities:
Alberta Basement Transects-Lithoprobe
Precambrian evolution of western Canada
Application of stable and radiogenic isotopes to problems of basin evolution

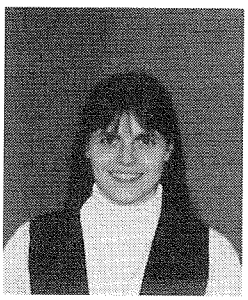

ROUX, Louise
Petroleum Cost Engineer
GSC-Ottawa
Tel: 613-996-0721,
FAX: 613-996-7837

Research Activities:
Oil and gas cost models
Oil and gas economics

SKIBO, Donald K.
Physical Scientist
GSC-Calgary
Tel: 403-292-7174,
FAX: 403-292-5377
E Mail: dskibo@gsc.emr.ca

Research Activites:
Kinematics of oil and gas generation
Radionuclide pollution in the Arctic Ocean
Hydrocarbon resource assesssment

Photo Unavailable

SNOWDON, Lloyd R.
Head, Geochemistry Subdivision
GSC-Calgary
Tel: 403-292-7035,
FAX: 403-292-5377
E Mail: snowdon@emr1.nrcan.gc.ca

Research Activities:
Exploration geochemistry
Engineering geochemistry
Environmental geochemistry
Hydrocarbon generation kinetics
Oil-source rock systems

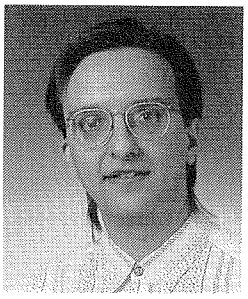

STASIUK, L.D. (Vern)
Organic Petrologist
GSC-Calgary
Tel: 403-292-7199,
FAX: 403-292-7034
E Mail: lstasiuk@gsc.emr.ca

Research Activities:
Source rocks: organic facies, thermal maturity
Oil migration, pyrobitumen

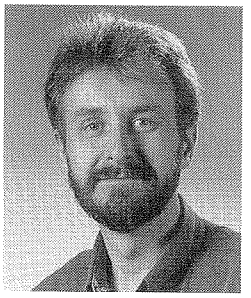

STOCKMAL, Glen S.
Research Scientist, GSC-Calgary
Tel: 403-292-7173, FAX: 403-292-5377
E Mail: gstockmal@gsc.emr.ca
Research Activities:
Structural geology and regional tectonics of foreland thrust*f* and *f* fold belts and passive and active margins
Geodynamic modelling of sedimentary basins
Overthrust belts and accretionary wedges
Conventional and deep seismic reflection interpretation
Apatite fission track thermochronology

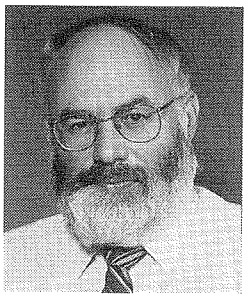

SWEET, Arthur R.
Palynologist
GSC-Calgary
Tel: 403-292-7092,
FAX: 403-292-6014
E Mail: asweet@gsc.emr.ca

Research Activities:
Late Mesozoic and Paleogene terrestrial palynology of western Canada basins

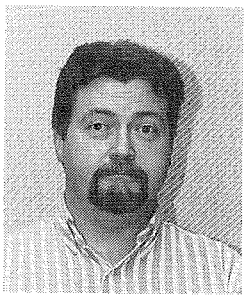

THOMAS, F.C. (Frank)
Micropaleontological Technician
GSC-Dartmouth
Tel: 920-426-1682,
FAX: 902-426-4465
E Mail: thomasf@agc.bio.ns.ca

Research Activities:
Cenozoic biostratigraphy

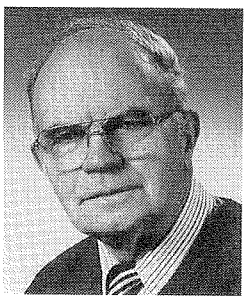

THORSTEINSSON, Ray
Research Scientist-Emeritas
GSC-Calgary
Tel: 403-292-7135,
FAX: 403-292-4961

Research Activities:
Regional geology
Paleontology
Stratigraphy
Tectonics
Economic geology

Photo Unavailable

TOD, Joan
GSC-Ottawa
Tel: 613-995-5326,
FAX: 613-992-2787
E Mail: infogdc@agg.emr.ca

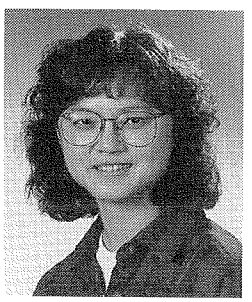

TZENG, Hsin-Ping
Petroleum Assessment Specialist
GSC-Calgary
Tel: 403-292-7015,
FAX: 403-292-7034
E Mail: ptzeng@gsc.emr.ca

Research Activities:
Applications of petroleum information system to subsurface mapping
Petroleum Resource Assessments
Petroleum information data base design

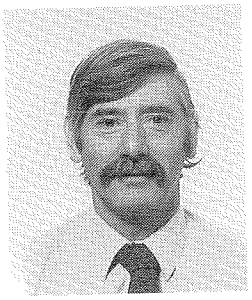

UTTING, John
Research Scientist
GSC-Calgary
Tel: 403-292-7093,
FAX: 403-292-6041
E Mail: utting@gsc.emr.ca

Research Activities:
Palynology of upper Paleozoic and Lower Triassic
Thermal maturity

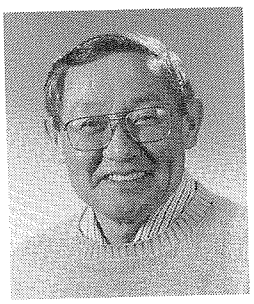

UYENO, T.T. (Tom)
Research Scientist
GSC-Calgary
Tel: 403-292-7084,
FAX: 403-292-6014
E Mail: uyeno@gsc.emr.ca

Research Activities:
Devonian conodont biostratigraphy, taxonomy, and paleoecology, thermal maturation study of conodonts

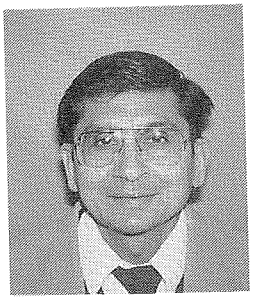

WAGHMARE, Ramesh R.
Senior Economist
GSC-Ottawa
Tel: 613-996-0237,
FAX: 613-996-7837

Research Activities:
Resource economics
Transporation economics

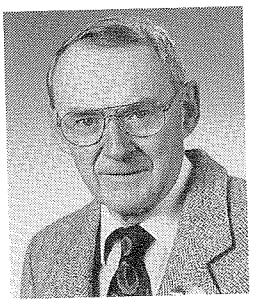

WALL, J.H. (John)
Research Scientist-Emeritus
GSC-Calgary
Tel: 403-292-7086,
FAX: 403-292-6014

Research Activities:
Micropaleontology
Mesozoic Foraminifera and Ostracoda
Western Canada Sedimentary Basin
Sverdrup Basin

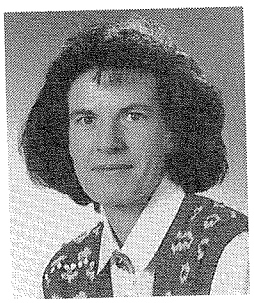

WARTERS, W. (Wendy)
Research Scientist
GSC-Calgary
Tel: 403-292-7025,
FAX: 403-292-5377
E Mail: wwarters@gsc.emr.ca
Research Activities:
Regional stratigraphic and sedimento-logical subsurface study, Lower Cretaceous and Jurassic, northwest Alberta and northeast British Columbia
Petroleum resource assessments

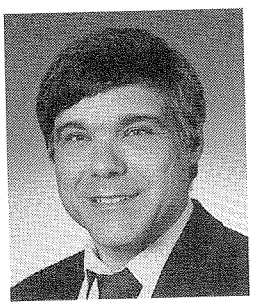

WENDTE, J.C. (Jack)
Geologist
GSC-Calgary
Tel: 403-292-7011,
FAX: 403-292-7034

Research Activities:
Devonian carbonate sedimentology, diagenesis, and stratigraphy, Western Canada Sedimentary Basin

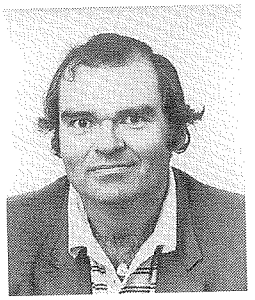

WETMILLER, R.J.
Research Scientist
GSC-Ottawa
Tel: 613-995-5548,
FAX: 613-992-8836
E Mail: bobw@seismo.emr.ca
Research Activities:
Documentation of earthquake activity in Canada
Emergency response to damaging earthquakes
Information services with regard to earthquake activity
Analysis of earthquake mechanisms

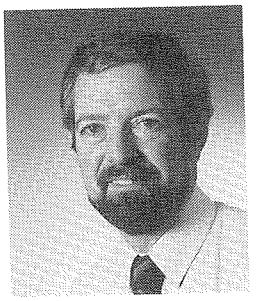

WHITE, J.M. (James)
Research Scientist
GSC-Calgary
Tel: 403-292-7085,
FAX: 403-292-6014
E Mail: white@gsc.emr.ca

Research Activities:
Mesozoic and Cenozoic palynology
Biostratigraphy
Paleoenvironments
Paleoclimatology

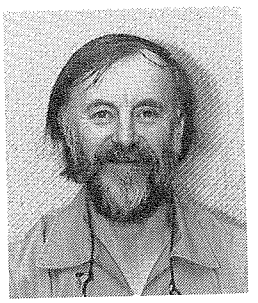

WILLIAMS, G.L. (Graham)
Research Scientist
GSC-Dartmouth
Tel: 902-426-5657,
FAX: 902-426-4465
E Mail: glw@agcban1.bio.ns.ca

Research Activities:
Mesozoic-Cenozoic palynology
Sequence stratigraphy
Databases

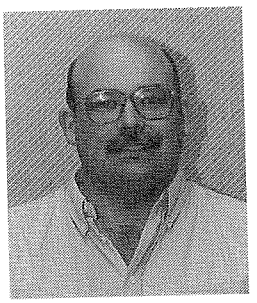

WILLIAMSON, M.A. (Mark)
Research Scientist
GSC-Dartmouth
Tel: 920-426-3126,
FAX: 902-426-4465
E Mail: willm@agc.bio.ns.ca

Research Activities:
Petroleum Systems
Basin Processes